

**ABSTRACTS OF THE TWENTY-NINTH ANNUAL  
MIDWINTER RESEARCH MEETING**

# **ASSOCIATION FOR RESEARCH IN OTOLARYNGOLOGY**



**February 5-9, 2006**

**Baltimore Marriott Waterfront  
Baltimore, Maryland, USA**

**ABSTRACTS OF THE TWENTY-NINTH ANNUAL  
MID WINTER RESEARCH MEETING  
OF THE**

---

**A**ssociation for  
**R**esearch in  
**O**tolaryngology

---

**February 5-9, 2006**

**Baltimore, Maryland, USA**

**Peter A. Santi, Ph.D.**  
*Editor*

Association for Research in Otolaryngology  
19 Mantua Road, Mt. Royal, NJ 08061 USA

## CONFERENCE OBJECTIVES

After attending the Scientific Meeting participants should be better able to:

1. Understand current concepts of the function of normal and diseased ears and other head and neck structures.
2. Understand current controversies in research methods and findings that bear on this understanding.
3. Understand what are considered to be the key research questions and promising areas of research in otolaryngology.

ISSN-0742-3152

The *Abstracts of the Association for Research in Otolaryngology* is published annually and consists of abstracts presented at the Annual MidWinter Research Meeting. A limited number of copies of this CD and previous books of abstracts (1978-2005) are available.

Please address your order or inquiry to:  
**Association for Research in Otolaryngology**  
19 Mantua Road  
Mt. Royal, NJ 08061 USA

**General Inquiry**  
Phone (856) 423-0041 Fax (856) 423-3420  
E-Mail: [headquarters@aro.org](mailto:headquarters@aro.org)

**Meetings**  
E-Mail: [meetings@aro.org](mailto:meetings@aro.org)

This book was prepared from abstracts that were entered electronically by the authors. Authors submitted abstracts over the World Wide Web using Mira Digital Publishing's PaperCutter™ Online Abstract Management System. Any mistakes in spelling and grammar in the abstracts are the responsibility of the authors. The Program Committee performed the difficult task of organizing the abstracts into sessions. The Program Committee Chair, Dr. John Middlebrooks and the President, Dr. Lloyd Minor constructed the final program. Mira electronically scheduled the abstracts and prepared Adobe Acrobat pdf files of the Program and Abstract Books. These abstracts and previous years' abstracts are available at: <http://www.aro.org>.

Citation of these abstracts in publications should be as follows:

**Authors, year, title, Assoc. Res. Otolaryngol. Abs.: page number.**

For Example:

Fettiplace, R., 2005, Ion Channel Properties and the Second Filter, Assoc. Res. Otolaryngol. Abs.: 747.



*General Chair*  
Lloyd B. Minor, MD (2005-2006)

*Program Organizing Committee*  
John C. Middlebrooks, PhD, *Chair* (2005-2008)

John P. Carey, MD (2004-2007)  
J. David Dickman, PhD (2005-2008)  
Ruth Ann Eatock, PhD (2005-2008)  
Andrew K. Groves, PhD (2004-2007)

Leonard Kitzes, PhD (2004-2007)  
Sharon G. Kuiawa, PhD (2005-2008)

Alan Palmer, PhD (2003-2006)  
Kevin Ohlemiller, PhD (2003-2006)

Joseph R. Santos-Sacchi, PhD (2004-2007)

Karen Steel, PhD (2004-2007)

Xiaoqin Wang, PhD (2005-2008)

Tom C.T. Yin, PhD (2005-2008)

Peter Santi, PhD, *ARO Editor, Council Liaison, ex officio*  
Lloyd Minor, MD, *President, Council Liaison*

*Program Publications*  
Peter A. Santi, PhD, *Editor* (2000-2009)

*Animal Research*  
Jo Ann D. McGee, PhD, *Chair* (2001-2004)

Paul J. Abbas, PhD (2002-2005)

Michael Church, PhD (2003-2006)

Meredith M. Garcia, PhD (1998-2004)

Bradley Goldstein, MD, PhD (2003-2006)

Henry E. Heffner, PhD (1998-2004)

Leonard Kitzes, PhD (2002-2005)

David B. Moody, PhD (2002-2005)

*Award of Merit Committee*  
Peter Dallos, PhD, *Chair* (2003-2006)

Ellen Covey, PhD (2002-2005)

Ruth Anne Eatock, PhD (2004-2007)

Broyna J. B. Keats, PhD (2004-2007)

Lloyd Minor, MD (2003-2006)

Alan R. Palmer, PhD (2004-2007)

Historian David Lim, MD, *Council Liaison* (2005-2009)

*Diversity & Minority Affairs*  
Ann M. Thompson, PhD, *Chair* (2002-2005)

Henry J. Adler, PhD (2003-2006)

Ricardo Cristobal, MD, PhD (2002-2005)

Xiaohong Deng, MS (2003-2006)

Jagmeet Kanwal, PhD (2003-2006)

Vishakha W. Rawool, PhD (2003-2006)

Duane Simmons, PhD (2003-2006)

Steven Rauch, MD, *Council Liaison* (2005-2006)

*Editor Advisory*  
Peter A. Santi, PhD, *Chair* (2000-2006)

Gerald Popelka, PhD, *Past Editor*

John C. Middlebrooks, PhD, *Program Committee Chair*

Darla M. Dobson, *Executive Director*

*Education Committee*  
Alan G. Micco, MD *Chair* (2005-2008)

Carey D. Balaban, PhD (2002-2005)

Ann Clock Eddins, PhD (2002-2005)

Robert D. Frisina, PhD (2002-2005)

Maureen Hannley, PhD (2003-2006)

Timothy E. Hullar, MD (2005-2008)

Robert Wickesberg, PhD (2003-2006)

David Witsell, MD (2003-2006)

*Government Relations Committee*

Patrick E. Brookhouser, MD, *Chair* (2003-2006)  
Ilsa R. Schwartz, PhD, *Vice Chair* (2003-2006)  
Ruth Y. Litovsky, PhD (2000-2003)  
George A. Spirou, PhD (2002-2005)  
Nigel K. Woolf, ScD (2001-2004)  
William A. Yost, PhD (2001-2004)  
David J. Lim, MD, *Council Liaison, ex officio* (2005-2006)

*Graduate Student Travel Awards*

Douglas A. Cotanche, PhD, *Chair* (2002-2005)  
Laura Hurley, PhD (2003-2006)  
Mathew W. Kelley, PhD (2002-2005)  
Nathaniel T. McMullen, PhD (2002-2005)  
Jennifer S. Stone, PhD (2002-2005)

*International Committee*

Karen B. Avraham, PhD *Chair* (2005-2008)  
Bernhard Gaese, PhD, Germany (2002-2005)  
Carole M. Hackney, PhD, UK (2002-2005)  
Eleonore Katz, PhD, Argentina (2003-2006)  
Takeshi Kubo, MD, Japan (2001-2004)  
Mauricio Kurc, MD, PhD, Brazil (2003-2006)  
Alan R. Palmer, PhD, UK (2002-2005)  
Jean-Luc Puel, PhD, France (2003-2006)  
Hamlet Suarez, MD, Uruguay (2001-2004)  
Hiroshi Wada, PhD, Japan (2003-2006)  
Shu Hui Wu, MD, Canada (2002-2005)  
Floris Wuyts, PhD, Belgium (2003-2006)  
William E. Brownell, PhD, *Council Liaison* (2005-2006)

*JARO Editorial Board*

Eric D. Young, PhD, *Editor-in-Chief* (2004-2007)  
Barry W. Ache, PhD (2000-2006)  
Kate F. Barald, PhD (2003-2006)  
David P. Corey, PhD (2000-2005)  
Kathleen E. Cullen, PhD (2003-2006)  
Ruth Anne Eatock, PhD (2000-2005)  
Jos J. Eggermont, PhD (2003-2006)  
Jeffrey P. Harris, MD, PhD (2000-2005)  
Matthew C. Holley, PhD (2004-2007)  
Gary D. Housley, PhD (2004-2007)  
Broyna J. B. Keats, PhD (2000-2005)  
Armin Kohlrausch, PhD (2002-2005)  
Christine Koepl, PhD (2003-2006)  
Douglas Oliver, PhD (2003-2006)  
Jay T. Rubinstein, MD, PhD (2004-2007)  
Mario A. Ruggero, PhD (2004-2007)  
Bradley A. Schulte, PhD (2003-2006)  
Robert J. Wenthold, PhD (2000-2005)  
Tom C.T. Yin, PhD (2004-2007)

*JARO (Publications CMTE)*

Gerald R. Popelka, PhD, *Co-Chair* (2004-2007)  
Arthur N. Popper, PhD, *Co-Chair* (2004-2007)  
Richard A. Chole, MD, PhD (2005-2008)  
Ellen Covey, PhD (2003-2006)  
Charley C. Della Santina, MD, PhD (2004-2007)  
Richard R. Fay, PhD (2004-2007)  
Keiko Hirose, MD (2004-2007)  
Matthew Kelley, PhD (2003-2006)  
Marlies Knipper, PhD (2004-2007)  
Jian-Dong Li, MD, PhD (2005-2008)  
Miguel Merchan, MD, PhD (2003-2006)  
John Oghalai, MD (2004-2007)  
Remy Pujol, PhD (2003-2006)  
Edwin W. Rubel, PhD (2004-2007)  
Hinrich Staecker, MD (2003-2006)  
Joseph Syka, MD (2003-2006)  
Ebenezer Nketia Yamoah, PhD (2004-2007)  
Eric Young, PhD, JARO Editor, *ex officio*  
Jasmine Ben-Zvi, Springer Representative, *ex officio*

*Long Range Planning Committee*

Robin L. Davis, PhD *Chair* (2005-2008)  
Barbara Canlon, PhD (2005-2008)  
Margaretha L. Casselbrant, MD, PhD (2003-2006)  
Judy R. Dubno, PhD (2004-2007)  
Paul A. Fuchs, PhD (2005-2008)  
Steven H. Green, PhD (2005-2008)  
Linda Hood, PhD (2003-2006)  
J. Christopher Post, MD, PhD (2005-2008)  
Dan H. Sanes, PhD (2005-2008)  
Debara Tucci, MD (2003-2006)  
Amy Donahue, PhD - NIDCD Rep.  
Robert V. Shannon, PhD, *Council Liaison* (2005-2006)  
Karen B. Avraham, PhD, *Chair, International Cmte* (2005-2008)

*Media Relations*

Maureen Hannley, PhD (2003-2006)  
M. Christian Brown, PhD (2002-2005)  
Judy Dubno, PhD (2003-2006)  
Marlies Knipper, PhD (2001-2004)  
Motoi Kudo, MD, PhD (2001-2004)  
Anil Lalwani, MD (2003-2006)  
James O. Pickles, PhD (2001-2004)  
Susan E. Shore, PhD (2003-2006)  
Karen P. Steel, PhD (2001-2004)  
Edward J. Walsh, PhD (2003-2006)  
John Williams, *Ex officio AAO-HNS Dir. Congr. Rel.*  
Steven Rauch, MD, *Council Liaison* (2005-2006)

*Membership Committee*

Douglas A. Girod, MD, *Chair* (2002-2005)  
Paul Abbas, PhD (2003-2006)  
Diana Lurie, PhD (2003-2006)  
Jeffrey J. Wenstrup, PhD (2002-2005)

*Nominating Committee*

William E. Brownell, PhD, *Chair* (2005-2006)  
Richard A. Chole, MD, PhD (2005-2006)  
Andrew K. Groves, PhD (2005-2006)  
Sharon G. Kujawa, PhD (2005-2006)  
Jay T. Rubinstein, MD, PhD (2005-2006)

*Patient Advocacy Group Relations*

Peter S. Steyger, PhD, *Chair* (2003-2006)  
Helen Cohen, EdD (2003-2006)  
Kim Gottshall, PhD (2003-2006)  
Margaret Kenna, MD (2003-2006)  
Alan Langman, MD (2003-2006)  
Charles J. Limb, MD (2005-2008)  
Alan G. Micco, MD (2003-2006)  
J. Tilak Ratnanather, DPhil (2005-2008)

*Physician Research Training*

Hilary A. Brodie, MD, PhD, *Chair* (2002-2005)  
Carol A. Bauer, MD (2001-2004)  
Holly H. Birdsall, MD, PhD (2001-2004)  
Marc Coltrera, MD (2003-2006)  
Diane Durham, PhD (2003-2006)  
Bruce J. Gantz, MD (2002-2005)  
Larry Lustig, MD (2003-2006)  
Michael J. McKenna, MD (2001-2004)  
Alan G. Micco, MD (2001-2004)  
J. Gail Neely, MD (2002-2005)  
Debara Tucci, MD (2003-2006)  
James F. Battey, MD, PhD, *NIDCD Director ex-officio*  
Maureen Hannley, PhD, *Exec VP Rsch, ex-officio*  
P. Ashley Wackym, MD, *Council Liaison* (2005-2006)

*Research Forum Co-Chairs*

John S. Oghalai, MD (2005-2008)  
J. Christopher Post, MD (2004-2007)

## President's Message

Welcome to Baltimore and to the 29<sup>th</sup> Annual MidWinter Meeting of the Association for Research in Otolaryngology. Our path to Baltimore for this year's meeting has been complicated and merits some review. In March of 2005, the ARO and the Pyramid Management Group reached an agreement that released the ARO from returning to the Adam's Mark (now Hilton) Hotel in Daytona Beach, Florida. As we have described in previous email messages to the membership, the ARO is making payments to the Pyramid Group as a part of this agreement. Our 2005 meeting at the Fairmont Hotel in New Orleans was successful, and evaluations of the hotel and the conference facilities were very positive. We had hoped to return to the Fairmont in New Orleans for the 2006 MidWinter Meeting. The tragic events surrounding hurricane Katrina forced a change in these plans. Staff members from the ARO Headquarters were in contact with representatives of the Fairmont Hotel soon after the hurricane. We wanted to return to New Orleans for the 2006 MidWinter Meeting to show our support for the people of the city who have endured so much hardship. As events unfolded in September of 2005, it became clear that it would be impossible for us to have our 2006 meeting in New Orleans, and the Fairmont Hotel released us from our contract. We are fortunate that the Waterfront Marriott in Baltimore had availability and appropriate facilities for our meeting.



The program committee under the leadership of John Middlebrooks has done excellent work in putting together an exciting scientific program. Special thanks also go to Bob Shannon who, although he officially rotated off the committee last year, provided valuable insight and advice in the organization of the program. The meeting begins with the presidential symposium on Sunday morning entitled "Vestibular Mechanisms: Achieving Balance in the Ear". Speakers in this symposium will explore aspects of vestibular function from sensory transduction in the periphery to vestibular disorders in patients. Other symposia in the meeting cover molecular biology of ear development, efferent innervation of hair cell systems, protein-protein interactions, toll-like receptors, and activity-dependent plasticity in the auditory brainstem. The workshop addresses topics in adult-onset hearing loss.

Robert Fettiplace has been selected by the Award of Merit Committee and the ARO Council to receive this year's Award of Merit. The title of Robert's Presidential Lecture is "Ion Channel Properties and the Second Filter". We will have the opportunity to celebrate Robert's accomplishments and those of other award recipients at the reception that will follow his lecture.

Eric Young has done wonderful work in leading the *Journal of the Association for Research in Otolaryngology* on a path of excellence. Eric has decided to step down as the editor of *JARO*. Under the guidance of Art Popper and Jerry Popelka, the Publications Committee conducted a thorough search for a new editor and presented recommendations to the ARO Council. The interest expressed by a number of highly qualified scientists in the editorship of *JARO* provides strong evidence of the important

place that the journal holds in our scientific community. We are pleased that Ruth Anne Eatock has accepted the position of editor. Ruth Anne and Eric are working together on the transition process.

Travel awards provide support for research trainees to attend the MidWinter Meeting. We are grateful for the generosity of the NIDCD, Deafness Research Foundation, American Academy of Otolaryngology—Head & Neck Surgery Foundation, and American Academy of Audiology/American Academy of Audiology Foundation (AAAF). The support from these organizations enables the ARO to provide travel awards and to hold the Travel Award Luncheon and Program which honors the recipients of the travel awards and their mentors.

Exhibitors at our MidWinter Meeting keep us informed about products that may benefit our research. They also provide us with information about publications and grants. In some cases they sponsor special receptions and events. Their participation helps us to keep our meeting costs down. Please show your support by visiting their exhibits.

Members of the ARO Council deserve special thanks for their role in organizing this meeting: Bob Shannon (president elect), Bill Brownell (past president), Steve Rauch (secretary treasurer), Peter Santi (editor), David Lim (historian), Ashley Wackym, Doug Cotanche, and Karen Steel. On behalf of all of us, I want to extend very special thanks to Bill Brownell who did enormously important work for the ARO during the interactions with the Pyramid Management Group.

The ARO continues to benefit from the expert organizational activities of the Talley Management Group. Darla Dobson and Lisa Astorga provide outstanding guidance and support for the ARO. We are very fortunate to have them as a part of our team. Members of the Council are working with Lisa Astorga on identification of future meeting sites. We want to keep room prices and expenses down so that as many people as possible can participate in the meeting. At the same time, we want to select cities and hotels that will be pleasant for our meetings.

These next few years are going to be especially critical for the ARO. The finances of our organization are challenged by our exodus from Daytona Beach. The support of every ARO member is vital. During these times, it is especially important for each of us to think about how much the ARO means to us. Our strength lies in the character and the commitment of our members. These attributes will enable us to meet our current challenges and move the organization forward to new levels of excellence.

**Lloyd Minor**



**Robert Fettiplace, PhD**  
**2006 Award of Merit Recipient**

Robert Fettiplace, PhD  
2006 Recipient of the Award of Merit

In a remarkable series of papers over the past 25 years, Robert Fettiplace has provided enormous insights to how sound is transduced by hair cells in the cochlea. He began this work when the first functional studies of hair cells were just beginning to be made and with a series of studies that followed logically one from another, elucidated many fundamental issues of cochlear transduction. Again and again he developed adventuresome new approaches with which he could address questions as directly as possible, even when they were technically difficult. The rigor with which results are analyzed makes compelling his interpretations of how features of hair cell function underlie cochlear transduction. Fettiplace's work shows a keen appreciation for how details in the function of hair cells are suited to the task they perform. His work elucidates many of the mechanisms that determine how vertebrates hear: how hair cells contribute to sharp tuning and frequency resolution, how adaptation of transducer channels makes hair cells sensitive to weak sounds while also tracking the amplitude of sounds that are orders of magnitude larger, how sound is conveyed by hair cells to the nervous system, and how the nervous system can affect transduction through efferent innervation.

Fettiplace received both his undergraduate and graduate training at the University of Cambridge in England. His first scientific studies were of the thickness, capacitance and water permeability of lipid bilayers. He showed that the specific capacitance of lipid bilayers is  $0.7 \text{ } \mu\text{F}/\text{cm}^2$ . He found that lipid composition determines the water permeability of membranes, with greater unsaturation increasing and cholesterol and sphingolipids decreasing water permeability over a 100-fold range. The water permeability could be directly understood by the partitioning of water in the lipid phase (Fettiplace, 1978; Fettiplace and Haydon, 1980). The discovery of aquaporins, much later, confirmed the prediction that biological membranes with proteinaceous water pores can have a high permeability to water while still having low permeability to ions (Fettiplace, Andrews and Haydon, 1971).

Fettiplace then crossed the Atlantic to work on the turtle retina with Denis Baylor, first in the Physiology Department at the University of Colorado, then in the Neurobiology Department at Stanford University. In 1975, Baylor and Fettiplace showed with recordings from photoreceptors that cones are tilted so that their axes are aligned with the pupil at an angle at which they are most efficient. Then, to determine how visual information is transferred across the retina, Fettiplace made simultaneous recordings from photoreceptors and retinal ganglion cells. These recordings revealed how well the physiology matches the needs of the visual system. Like visual transduction itself, synaptic transfer across at least two synapses was remarkably sensitive but also remarkably slow (Baylor and Fettiplace, 1977a,b). Others later showed that metabotropic glutamate receptors mediate transmission across those synapses.

Having gained an appreciation for the turtle, whose adaptations for diving make it relatively resistant to anoxia, Fettiplace returned to England and began, with Andrew Crawford, the earliest studies of cochlear hair cells *in vitro*. The first series of studies examined how hair cells are tuned. Crawford and Fettiplace (1980, 1981) showed that the electrophysiological properties endow hair cells with electrical tuning. This work initially was greeted with scepticism not only by those who had concluded that tuning arose from the mechanics of the



motion of the basilar membrane but also by those who realized that impalement with a microelectrode could introduce artifacts to the measurement of tuning. Over succeeding years the validity of those initial findings has been confirmed repeatedly by others with different types of measures, showing how high was the quality of those early recordings.

The finding that hair cells are electrically tuned requires that hair cells vary systematically in the properties of their voltage-sensitive currents as a function of position in the cochlea. On the basis of noise and single-channel recordings from isolated hair cells Fettiplace, with Jonathan Art, showed that the tonotopic differences were the result of an intrinsic difference in the kinetics of calcium-sensitive, voltage-gated potassium channels (Art and Fettiplace, 1987).

It was widely appreciated that a “cochlear amplifier” was required for tuning to be as sharp as it is. The work on electrical tuning provided a clue about how a cochlear amplifier might work but did not explain how those features that enabled tuning to be sharp also affect the mechanical properties of the cochlea. Fettiplace, again together with Crawford, therefore measured the mechanical properties of the hair bundle to determine whether membrane potential affects those mechanical properties. They pioneered methods to measure the mechanical properties of hair bundles over displacements of only a few nanometers. They perfected the use of a fine glass fiber of known stiffness whose movements are monitored with a photodiode array. These experiments showed that hair bundles are not just passive transducers of mechanical force but that they also generate force (Crawford and Fettiplace, 1985).

Fettiplace and his colleagues also examined how efferent innervation influences hair cells. Histochemical studies had indicated that the innervation was cholinergic but efferent function could not be accounted for by what was known about nicotinic or muscarinic synaptic function. Fettiplace and his colleagues thus recorded responses of hair cells to shocks of the efferent nerve bundle. They found that cholinergic efferent innervation causes hair cells to hyperpolarize by a previously unknown mechanism, that efferents produce biphasic responses that involve an inward calcium current and a later, larger outward potassium current that is mediated by calcium-activated potassium channels (Art, Fettiplace and Fuchs, 1984). Efferent cholinergic inhibition reduced the sensitivity and sharpness of tuning of the hair cell and consequently improved temporal resolution (Art, Crawford, Fettiplace, and Fuchs, 1984).

The kinetics of the mechanoelectrical transducer current is a critical feature for the ability of hair cells to encode frequency. To make such measurements it was necessary to be able to measure accurately the rate and amplitude of hair bundle displacement, for which Fettiplace and his colleagues developed a line-scan camera. This series of experiments not only revealed the kinetics of the transducer channels but also showed that calcium plays a role in determining the kinetics of the channel (Crawford, Evans, and Fettiplace, 1989). There is no better way to examine the function of transducer channels than to record from them directly. It is also especially challenging, however, because transducer channels must be mechanically connected to other cellular components to function; they cannot be plucked out of the cell to be studied in isolation. Fettiplace and his colleagues managed this feat too. Building on the observation that when the extracellular calcium concentration was lowered,

transducer channels were irreversibly lost, they removed calcium from the bath to leave only a single transducer channel which could then be studied in isolation (Crawford, Evans and Fettiplace, 1991).

In 1990, Fettiplace moved to the University of Wisconsin in Madison where he began systematically to study the role of calcium in hair cells. Fettiplace had long been aware of the profound implications of the calcium-sensitivity of the transducer currents. Transducer channels are not simply passive reporters of the position of stereocilia but through their calcium-sensitivity are linked to the biological activity of hair cells. The influence of calcium helps hair cells to set the dynamic range of transduction currents so that they are maximally sensitive to small changes in the position of the hair bundle, independent of the resting position of the hair bundle. Furthermore, calcium is not only involved in hair cell mechanotransduction; voltage-gated calcium influx supports transmitter release in the synaptic pole of hair cells. First, Fettiplace and his colleagues measured voltage-gated calcium currents in hair cells and related them to the tonotopic location. There are roughly twice as many calcium channels as potassium channels in each hair cell, with the numbers of both calcium and potassium channels varying systematically with the tonotopic position (Art, Fettiplace and Wu, 1993). Then with Tom Tucker he measured calcium currents; one ingenious measure of local calcium concentration made use of calcium-activated potassium channels as bioassays. Fettiplace also became a pioneer in using real-time confocal microscopy to examine the spatial spread of calcium through the cytoplasm. Fettiplace and Tucker found that calcium enters hair cells in the basolateral wall at microdomains but that it is rapidly buffered and transported out of the cytoplasm into intracellular stores and out across the plasma membrane (Tucker and Fettiplace, 1995, 1996). The measured calcium and potassium currents, together with an inward rectifier were then shown to account quantitatively for electrical resonance. These measurements predicted that the tonotopic arrangement of electrical resonance is established by a systematic difference in numbers and proportions of at least two variants of calcium-activated potassium channels whose speed of activation varies (Wu, Art, Goodman and Fettiplace, 1995). Characteristically, the results were summarized quantitatively (Wu and Fettiplace, 1996).

To probe the question how a tonotopic gradient is established in the cochlea, Fettiplace turned to molecular biological techniques. Jones, Laus and Fettiplace (1998) examined the regulation of the expression of variants of calcium-activated potassium channels and showed that hair cells contain six alternatively spliced variants of the  $\beta$  subunit of the potassium channel that are unevenly distributed along the cochlea. By expressing various combinations of the different forms of the  $\beta$  subunit with and without a  $\alpha$  subunit, Jones, Gray-Keller and Fettiplace (1999) described the calcium-sensitivity, voltage-sensitivity and kinetics of these isoforms of the calcium-activated potassium channel.

Examination of hair cells in the excised but intact cochlear epithelium opened the way to study mechanoelectrical transducer channels more thoroughly. Transducer channels are present only in tens or hundreds of molecules per cell and their function is critically dependent on the integrity of the epithelium in which they reside. Consequently, patch-clamp recordings from hair cells in the intact cochlear epithelium revealed transducer currents that were ten times as large as those recorded from isolated hair cells. Measuring the proportion of the mechanotransducer current that was carried by calcium in this intact preparation, again

using the combination of electrophysiological and calcium imaging techniques, Fettiplace and Tony Ricci demonstrated that sufficient calcium enters hair cells to regulate transduction even under physiological conditions when mechanosensitive channels are bathed in endolymph (Ricci and Fettiplace, 1998). Ricci and Fettiplace also showed that the transducer currents in hair cells are modulated by cyclic nucleotides and therefore that mechanosensitive transducer channels resemble cyclic nucleotide gated channels in olfactory neurons and photoreceptors. In 1999, Fettiplace renewed his productive collaboration with Andrew Crawford to examine the mechanical properties of the hair bundles and to show how the mechanotransducer channels and their adaptive properties produce active hair bundle motion (Ricci et al., 2000, 2002). To disentangle how the magnitude and kinetics of macroscopic transducer currents vary as a function of extracellular calcium as well as along the tonotopic gradient, Ricci, Crawford and Fettiplace (2003) made detailed measurements of the conductance of individual transducer channels from various parts of the cochlea and measured the influence of calcium on their function. These measurements led to two further fundamental findings. First, these measurements showed that extracellular calcium reduces the (very large) conductance of transducer channels. Second, independent of whether channels were blocked or unblocked by calcium, their conductance varied as a function of the tonotopic map, being smaller at the low frequency end of the cochlea. On the basis of these observations, Ricci et al. suggested that the mechanotransducer channels were encoded by members of the TRP gene family, a conclusion that has received considerable support since then.

As the evidence accumulated that intracellular calcium plays a key role in hair cells, it became increasingly clear that intracellular calcium concentrations have to be regulated. Once again Fettiplace, with Carole Hackney, developed a new approach. They used immunohistochemistry to obtain quantitative measures of calcium buffers that in turn made it possible to calculate free calcium concentrations in hair cells.

Fettiplace's work has long been aimed at understanding mammalian hearing. Fettiplace therefore recently turned to studying the cochlea in rats. In the rat, as in the turtle, transducer channels are sensitive to calcium and differ in their kinetics as a function of their position in the tonotopic array (Ricci, Kennedy, Crawford and Fettiplace, 2005). The kinetics of the transducer channels impose a bandpass filter whose center frequency matches the frequency to which the hair cell is tuned. Calcium buffers regulate the intracellular calcium concentration differently in inner and outer hair cells; inner hair cells contain ten-fold less calcium buffers than outer hair cells (Hackney et al., 2005). Also as in turtle hair cells, stereocilia generate force. It is the conformational change of the transducer channels themselves that generates the force (Fettiplace, Crawford and Kennedy, 2005). This force-generating mechanism is fast enough to amplify movements of the basilar membrane even at high frequencies.

In summary, Robert Fettiplace's accomplishments are remarkable. His studies have described how the interplay between the mechanical and electrical properties of hair cells serves to convert sound into electrical signals that transmit to the brain acoustic information that is sharply resolved in the frequency domain. His work has revealed how individual cochlear hair cells become tuned to a small range of frequencies. He has elucidated how mechano-electrical transducer channels sense and adapt to movements of the stereocilia.

Each of Fettiplace's papers uses direct experiments, many exceptionally technically challenging, and quantitative analyses to tell a complete story. Fettiplace has done much of the work with his own hands.

Fettiplace is a valued and respected colleague and teacher. The graduate students whom he teaches consider his course among the best they have had. He has attracted strong collaborators. Many became long-standing friends and have continued to return to Madison to work together with him during long and intensive visits. Fettiplace has influenced his field not only with his written work but also with eloquent talks and vigorous discussions at national and international meetings. He is known (and appreciated by some more than others) for being forthright about his judgments. Fettiplace has been honored for his accomplishments. He was elected a Fellow of the Royal Society at a very early age, was invited to present the Distinguished Lecture at the Acoustical Society of America, received a Claude Pepper Merit Award from the NIH, and holds a Steenbock Professorship from the University of Wisconsin. Robert Fettiplace is a most deserving recipient of the Award of Merit from the Association for Research in Otolaryngology.

*Donata Oertel*  
*Paul A. Fuchs*

# Association for Research in Otolaryngology

## Executive Offices

19 Mantua Road, Mt. Royal, NJ 08061 USA  
Phone: (856) 423-0041 Fax: (856) 423-3420  
E-Mail: [headquarters@aro.org](mailto:headquarters@aro.org) Meetings E-mail: [meetings@aro.org](mailto:meetings@aro.org)

## *ARO Council Members 2005-2006*

President: Lloyd B. Minor, MD

Johns Hopkins University School of Medicine  
Department of Otolaryngology  
601 North Caroline Street, Room 6253  
Baltimore, MD 21287-0910

Secretary/Treasurer: Steven Rauch, MD

Harvard Medical School  
Massachusetts Eye and Ear Infirmary  
243 Charles Street  
Boston, MA 02114

President-Elect: Robert V. Shannon, PhD

House Ear Institute  
Auditory Implant Research  
2100 West Third Street  
Los Angeles, CA 90057

Editor: Peter A. Santi, PhD

University of Minnesota  
Department of Otolaryngology  
Lions Research Bldg., Room 121  
2001 Sixth St. SE  
Minneapolis, MN 55455

Past President: William E. Brownell, PhD

Baylor College of Medicine  
Department of Otolaryngology  
& Communicative Sciences  
Houston, TX 77030

Historian: David J. Lim, MD  
House Ear Institute  
2100 W. Third St., Fifth Floor  
Los Angeles, CA 90057

## *Council Members at Large*

Douglas A. Cotanche, PhD  
Lab for Cellular & Molecular  
Hearing Research  
Dept. of Otolaryngology  
Childrens Hospital  
300 Longwood Avenue  
Boston, MA 02115

Karen P. Steel, PhD, FMed, Sci  
Wellcome Trust Sanger Institute  
Wellcome Trust Genome Campus  
Hinxton  
Cambridge CB 10 1SA, UK

P. Ashley Wackym, MD  
Medical College of Wisconsin  
Dept. of Otolaryngology &  
Comm. Sciences  
9000 West Wisconsin Avenue  
Milwaukee, WI 53226

## **Past Presidents**

1973-74 David L. Hilding, MD  
1974-75 Jack Vernon, PhD  
1975-76 Robert A. Butler, PhD  
1976-77 David J. Lim, MD  
1977-78 Vicente Honrubia, MD  
1978-80 F. Owen Black, MD  
1980-81 Barbara Bohne, PhD  
1981-82 Robert H. Mathog, MD  
1982-83 Josef M. Miller, PhD  
1983-84 Maxwell Abramson, MD  
1984-85 William C. Stebbins, PhD  
1985-86 Robert J. Ruben, MD  
1986-87 Donald W. Nielsen, PhD  
1987-88 George A. Gates, MD  
1988-89 William A. Yost, PhD  
1989-90 Joseph B. Nadol, Jr., MD  
1990-91 Ilsa R. Schwartz, PhD  
1991-92 Jeffrey P. Harris, MD, PhD  
1992-93 Peter Dallos, PhD  
1993-94 Robert A. Dobie, MD  
1994-95 Allen F. Ryan, PhD  
1995-96 Bruce J. Gantz, MD  
1996-97 M. Charles Liberman, PhD  
1997-98 Leonard P. Rybak, MD, PhD  
1998-99 Edwin W. Rubel, PhD  
1999-00 Richard A. Chole, MD, PhD  
2000-01 Judy R. Dubno, PhD  
2001-02 Richard T. Miyamoto, MD  
2002-03 Donata Oertel, PhD  
2003-04 Edwin M. Monsell, MD, PhD  
2004-05 William E. Brownell, PhD

## **Award of Merit Recipients**

1978 Harold Schuknecht, MD  
1979 Merle Lawrence, PhD  
1980 Juergen Tonndorf, MD  
1981 Catherine Smith, PhD  
1982 Hallowell Davis, MD  
1983 Ernest Glen Wever, PhD  
1984 Teruzo Konishi, MD  
1985 Joseph Hawkins, PhD  
1986 Raphel Lorente de Nó, MD  
1987 Jerzy E. Rose, MD  
1988 Josef Zwislocki, PhD  
1989 Åke Flöck, PhD  
1990 Robert Kimura, PhD  
1991 William D. Neff, PhD  
1992 Jan Wersäll, PhD  
1993 David Lim, MD  
1994 Peter Dallos, PhD  
1995 Kirsten Osen, MD  
1996 Ruediger Thalmann, MD & Isolde Thalmann, PhD  
1997 Jay Goldberg, PhD  
1998 Robert Galambos, MD, PhD  
1999 Murray B. Sachs, PhD  
2000 David M. Green, PhD  
2001 William S. Rhode, PhD  
2002 A. James Hudspeth, MD, PhD  
2003 David T. Kemp, PhD  
2004 Donata Oertel, PhD  
2005 Edwin W. Rubel, PhD  
2006 Robert Fettiplace, PhD

# Table of Contents

	Abstract Number
<b>Presidential Symposium</b>	
<b>Symposium</b>	
A: Vestibular Mechanisms: Achieving Balance in the Ear .....	1-9
B: Molecular Biology of Ear Development: From Molecules to Application .....	10-17
<b>Podium</b>	
C: Genetics: Animal Models 1 .....	18-28
<b>Poster</b>	
D1: Inner Ear: Mechanisms of Noise Injury .....	29-42
D2: Stereocilia .....	43-51
D3: Otoacoustic Emissions .....	52-69
D4: Inner Ear: Mechanics 1 .....	70-92
D5: Auditory Prosthesis: Binaural Implants and Alternative Prosthetics .....	93-101
D6: Auditory Brainstem: Physiology A .....	102-118
D7: Auditory Brainstem: Ascending and Descending Anatomical Projections .....	119-136
D8: Auditory Midbrain: Physiology .....	137-154
D9: Auditory Cortex: Structure and Function 1 .....	155-163
D10: Sound Localization Physiology .....	164-178
D11: Psychophysics: Procedures and Training .....	179-184
D12: Psychophysics: Grouping, Scenes and Pitch .....	185-191
D13: Vestibular: Central .....	192-209
D14: Clinical Audiology 1 .....	210-222
D15: Otitis Media .....	223-232
D16: Speech Production .....	233-235
D17: Taste and Smell .....	236-238
<b>Workshop</b>	
E1: NIDCD Workshop .....	239-239
<b>Patient Advocacy Group Workshop</b>	
E2: Adult-Onset Hearing Loss: What's the Damage? .....	240-245
<b>Symposium</b>	
F: Activity Dependent Plasticity in the Auditory Brainstem .....	246-252
<b>Podium</b>	
G: Hair Cells .....	253-267
<b>Symposium</b>	
H: Imaging Protein-Protein Interactions .....	268-273
<b>Podium</b>	
I: Drug/Gene Delivery to the Inner Ear .....	274-283
<b>Poster</b>	
J1: Inner Ear: Genetics .....	284-294
J2: Development 1 .....	295-319
J3: Regeneration 1 .....	320-338
J4: Human Genetics .....	339-353
J5: Inner Ear: Morphological Analysis .....	354-367
J6: Prestin .....	368-380
J7: Hair Cell Mechanics .....	381-394
J8: Aging: Hearing Loss in Animal Models .....	395-404
J9: Auditory Prosthesis: Elements of Speech Processing and Practical Considerations .....	405-417
J10: Auditory Cortex: Imaging and Human Studies .....	418-433
J11: Sound Localization Psychophysics .....	434-446
J12: Vestibular Periphery: Structure and Function .....	447-460
J13: Clinical Vestibular .....	461-479
J14: Inner Ear: Infection and Inflammation .....	480-487
J15: Clinical Audiology 2 .....	488-499

<b>Symposium</b>		
<b>K:</b>	Efferent Innervation of Hair Cell Systems.....	500-507
<b>Podium</b>		
<b>L:</b>	Auditory Cortex: Structure and Function 2 .....	508-520
<b>M:</b>	Development 2 .....	521-531
<b>N:</b>	Aging in Animal Models .....	532-538
<b>Poster</b>		
<b>O1:</b>	Genetics: Animal Models 2.....	539-548
<b>O2:</b>	Inner Ear Damage and Protection: Afferent Neuronal Survival .....	549-557
<b>O3:</b>	Inner Ear: Prevention/Treatment of Noise Injury .....	558-569
<b>O4:</b>	Mechanisms of Ototoxic Injury .....	570-584
<b>O5:</b>	Inner Ear: Homeostasis .....	585-604
<b>O6:</b>	Inner Ear: Development.....	605-615
<b>O7:</b>	Inner Ear: Synapses and Ion Channels .....	616-634
<b>O8:</b>	Middle Ear Models and Measurements .....	635-650
<b>O9:</b>	Auditory Prosthesis: Models and Acoustic Simulation .....	651-660
<b>O10:</b>	Auditory Brainstem: Molecular Aspects.....	661-672
<b>O11:</b>	Auditory Brainstem: Physiology B .....	673-688
<b>O12:</b>	Auditory Midbrain: Pharmacology, Plasticity and Tinnitus.....	689-702
<b>O13:</b>	Auditory Cortex: Structure and Function 3 .....	703-712
<b>O14:</b>	Psychophysics: Spatial and Binaural Hearing.....	713-720
<b>O15:</b>	Vestibular Periphery: Damage, Assessment and Treatment.....	721-730
<b>O16:</b>	Speech: Cortex .....	731-735
<b>O17:</b>	Speech: Phoneme Recognition and Degraded Speech.....	736-746
<b>Presidential Lecture</b>		
<b>P:</b>	Presidential Lecture and Award Ceremony .....	747-747
<b>Symposium</b>		
<b>Q:</b>	In Defense of the Ear: Toll-Like Receptors .....	748-752
<b>Podium</b>		
<b>R:</b>	Psychophysics .....	753-764
<b>S:</b>	Auditory Brainstem and Midbrain Physiology .....	765-775
<b>T:</b>	Vestibular: Receptors and Signals.....	776-786
<b>Poster</b>		
<b>U1:</b>	Genetically-Related Hearing Loss .....	787-798
<b>U2:</b>	Inner Ear: Intrinsic Protective/Repair Mechanisms.....	799-810
<b>U3:</b>	Inner Ear: Ischemia/Metabolic Inhibitors .....	811-814
<b>U4:</b>	Prevention/Treatment of Ototoxic Injury .....	815-827
<b>U5:</b>	Inner Ear: Ototoxicity and Metabolism .....	828-836
<b>U6:</b>	Regeneration 2.....	837-853
<b>U7:</b>	Development 3 .....	854-879
<b>U8:</b>	Inner Ear: Functional Analysis.....	880-893
<b>U9:</b>	Auditory Nerve.....	894-911
<b>U10:</b>	Aging: Deficits in Animal Models .....	912-924
<b>U11:</b>	Aging: Human Studies.....	925-931
<b>U12:</b>	Auditory Prosthesis: Residual Hearing and Preservation of Auditory Neurons .....	932-939
<b>U13:</b>	Auditory Cortex: Plasticity, Development and Hearing Loss .....	940-957
<b>U14:</b>	Animal Psychophysics.....	958-968
<b>U15:</b>	Psychophysics: Development, Aging and Hearing Loss.....	969-977
<b>U16:</b>	Clinical Otolaryngology.....	978-992
<b>Podium</b>		
<b>V:</b>	Inner Ear: Mechanics 2 .....	993-1003
<b>W:</b>	Auditory Prosthesis.....	1004-1010

## **1 Vestibular Mechanisms: Achieving Balance in the Ear**

**Lloyd B. Minor<sup>1</sup>**

<sup>1</sup>*Johns Hopkins University School of Medicine*

The vestibular receptors are located in the labyrinth of each inner ear. These receptors transduce information related to angular motion of the head (semicircular canals) as well as to translational motion and the orientation of the head with respect to gravity (otoliths). This information from the vestibular endorgans is used to control reflexes that provide stabilization of the eyes, neck, and body.

Presentations in this symposium will discuss 8 aspects of vestibular function.

Dr. Ruth Anne Eatock will discuss processes of sensory transduction in the labyrinth. The role of specific conductances and of differing morphological specificities of hair cells will be described. The discharge properties of vestibular-nerve afferents provide the sensory signal that encodes motion. Dr. Lloyd Minor will review the physiological properties of these afferents and will discuss theories concerning the diversity of afferent response dynamics. Dr. Kathleen Cullen will discuss the processing of these vestibular signals by neurons in the central pathways and the role of these neurons in the control of gaze. Dr. Dora Angelaki will describe the integration of canal and otolith signals by central vestibular neurons and will review the neural mechanisms that appear to be involved in distinguishing translations from tilts.

The motor responses controlled by vestibular reflexes are modifiable and can change to meet altered demands on their compensatory function. Dr. Stephen Highstein will discuss these adaptive processes that are particularly evident in the vestibuloocular reflex. Vestibular hair cells in birds can regenerate following ototoxic injury. Dr. David Dickman will describe the temporal sequence of these regeneration processes and will discuss regeneration in terms of the ultrastructure of the sensory epithelia and the recovery of posture and head stability.

There is a close relationship between basic vestibular research and studies of disorders of vestibular function in humans. Dr. John Carey will describe the ways in which physiological principles derived from basic research have improved the diagnosis and treatment of patients with vestibular disorders. Dr. Charles Della Santina will discuss the effects of electrical stimulation on vestibular endorgans and will describe work towards the development of a vestibular prosthesis.

## **2 Type I Hair Cells in Vestibular Epithelia: Why a Big Synapse?**

**Ruth Anne Eatock<sup>1</sup>**

<sup>1</sup>*Baylor College of Medicine*

The vestibular epithelia of reptiles, birds and mammals have two hair cell types distinguished by the form of the afferent contact. Type II hair cells, like auditory hair cells and the vestibular hair cells of fish and amphibians, are contacted by knob-like bouton endings. In contrast, type I cells are enveloped by cup-shaped endings, the only known postsynaptic calyces. Type I cells/calyces are

associated with central zones of vestibular epithelia, which differ functionally from peripheral zones. This distinctive morphology and spatial distribution suggests that the type I/calyx complex evolved to satisfy vestibular functions that are highly evolved in amniotes.

Vestibular afferents feed head motion signals to reflexes that control eye, head and body position. Unlike anamniotes, amniotes move through air and move their eyes and heads independently of their bodies. This may permit faster head motions in the form of both high-frequency motions and large low-frequency motions. Compensation for fast motions requires a fast reflex pathway. Several properties of type I cells and calyx afferents may enhance fast signaling: Hair bundles may be passively tuned to high frequencies; cells have fast voltage responses and low gains by virtue of a large, very negatively activating, noninactivating K conductance; calyx endings, neuronal processes and cell bodies are large, for rapid transmission and conduction. Distinct patterns of ion-channel and calcium-binding protein expression may also shape transmission and conduction in calyx endings and afferents.

Comparable specializations in modern amniotes – including large synaptic endings and noninactivating K conductances in central-zone hair cells – suggest their origins in a common ancestor. Parallels can also be drawn with an auditory pathway for which speed is critical: The brainstem timing pathway has calyces (presynaptic), large axons, and negatively activating K conductances.

*Supported by DC02290*

## **3 Physiology of Vestibular-Nerve Afferents**

**Lloyd B. Minor<sup>1</sup>**

<sup>1</sup>*Johns Hopkins University School of Medicine*

Hair cells in the sensory epithelia of the vestibular endorgans are innervated by vestibular-nerve afferents. These afferent fibers have their cell bodies in Scarpa's ganglion and project to the vestibular nuclei in the brainstem. Most vestibular afferents in mammals have a resting discharge rate that can range between 40 – 100 spikes/s. Studies of the responses of vestibular-nerve afferents to motion have provided valuable insights into the information transmitted from the labyrinth to the central vestibular pathways. As described by Goldberg and Fernandez, discharge regularity (defined by the distribution of interspike intervals) provides a reliable marker for response properties. Regularly discharging afferents have tonic response dynamics that resemble those expected from the mechanics of the endorgan. Irregularly discharging afferents have phasic-tonic dynamics that include a sensitivity to the velocity of cupular or otolith displacement in addition to the magnitude of this displacement.

The vestibular sensory epithelia of reptiles, birds, and mammals have Type I and Type II hair cells. For the semicircular canals, the central zone of the crista ampullaris contains almost exclusively Type I hair cells that are innervated by calyx endings. These calyx-only afferents and the adjacent dimorphic afferents that innervate both Type I and Type II hair cells are irregularly



discharging. The dimorphic afferents located in the more peripheral regions of crista as well as the bouton-only afferents are regularly discharging. Previous studies of the responses of these afferents to lower frequency rotations had indicated that the 'calyx-only' afferents had lower sensitivities to rotation. More recent work extending these investigations to higher rotational frequencies (4- 15 Hz) has revealed that the sensitivity of these 'low-gain' afferents rises with frequency to reach values comparable to the dimorphic afferents.

The significance of this diversity in afferent response properties in terms of central vestibular mechanisms remains an area of active investigative interest. Several possibilities have been suggested. Afferent responses could be matched to the dynamic loads of different vestibular reflexes. Convergence onto central vestibular neurons of otolith inputs differing in response dynamics and directional properties could confer two-dimensional sensitivity. Gating of inputs from irregularly discharging afferents onto central vestibular neurons could rapidly modify signals along reflex pathways.

Supported by NIH R01 DC02390

#### **[4] Role of the Vestibular System in Control of Gaze and Active Movements, Central Neuron Physiology**

**Kathleen E. Cullen<sup>1</sup>**

<sup>1</sup>*McGill University*

This lecture will address how the vestibular system processes head-in-space velocity during passively applied rotations versus actively generated movements. Head velocity information is similarly processed by vestibular afferents during passive rotations and voluntary behaviors such as combined eye-head gaze shifts, but marked differences are observed at the level of the vestibular nuclei. For example, one class of neurons in vestibular nuclei, which receives direct inputs from semicircular canal afferents, is substantially less responsive to active head movements than to passively applied head rotations. The projection patterns of these neurons strongly suggest that they are involved in generating head stabilization responses as well as shaping vestibular information for the computation of spatial orientation. In contrast, a second class of neurons in the vestibular nuclei which mediate the vestibulo-ocular reflex process vestibular information in a manner that depends principally on the subject's current gaze strategy, rather than whether the head movement was self-generated or externally applied. The implications of these results will be discussed in relation to the status of vestibular reflexes (i.e. the vestibulo-ocular, vestibulo-collic, and cervico-ocular reflexes) and implications for higher-level processing of vestibular information during natural behaviours.

#### **[5] Vestibular Function as an Inertial Sensory Detection System**

**Dora Angelaki<sup>1</sup>**

<sup>1</sup>*Washington University Medical School*

For creatures who live in a gravitational environment, the force of gravity represents an important variable for both

spatial perception and motor control. On one hand, the direction of gravity provides a veridical, allocentric frame of reference, important for identifying our own motion relative to inertial (i.e., world-centered) space. On the other hand, we constantly experience components of linear acceleration, the signal detected by primary otolith afferents, that are either due to our translation through space or to changes in head orientation relative to gravity. In addition, because the peripheral vestibular organs are fixed to the head, semicircular canal afferents can only measure the relative rotation of the endolymph within the canal ducts, providing no information about how the head moves in space. As a result, the unprocessed output of the peripheral vestibular sensors neither distinguishes attitude (orientation) from inertial (translational) motion nor signals the true rotation of the head in space. We will summarize recent theoretical and experimental work that has set the stage for a better understanding of how vestibular information from the different peripheral sensors is centrally processed to solve or, at best, approximate a solution to the inertial motion detection problem. We show that, although each of the vestibular sensors alone is ambiguous, appropriate vestibular convergence can lead to improved estimates of inertial motion and spatial orientation. A neural correlate of such otolith/canal convergence is found in brainstem (vestibular nuclei) and midline cerebellum (fastigial nucleus and nodulus) motion-sensitive neurons. In particular, Purkinje cells in the cerebellar nodulus encode both a space-referenced angular orientation and inertial velocity signals.

#### **[6] Evaluation of Sites Storing Novel Memories of Adapted VOR Gains**

**Stephen M. Highstein<sup>1</sup>**

<sup>1</sup>*Washington University School of Medicine*

Learning experiments can be divided into those evaluating the acquisition of new memories, and those designed to evaluate the storage of these memories. The cerebellar cortex and its target neurons in the deep cerebellar nuclei and brainstem (FTN) are candidates for this storage aspect. A model system for motor learning is the vestibulo-ocular reflex (VOR) that generates compensatory eye movements during head turns. To evaluate the storage of motor learning, we recorded the activity of Y neurons, a type of FTN that participates in vertical eye movements, before and after motor learning. Y neuron discharge was compared with that of Purkinje cells in the cerebellar flocculus. Comparison illustrates that the changes observed in the eye velocity sensitivity of Purkinje cells following motor learning are not directly transferred to Y neurons, suggesting an additional plastic site, possibly the synapse between the Purkinje cell and Y neuron. We quantified changes in the head velocity pathway to Y neurons using multiple regression models. This quantification was later employed to build model simulations that account for changes in parallel pathways to Y neurons and to explain the role of the cerebellum in VOR memory. Our results suggest that low gain adaptation results in more drastic changes than high gain adaptation. Low gain adaptation causes increases in the head velocity sensitivity in parallel pathways. Model

simulations suggest that cerebellar and brainstem plasticity are necessary for chronic memory storage. Further, we posit that results obtained following cerebellar flocculus lesion are the product of different mechanisms than those operating during memory storage in the intact animal.

## **[7] Recovery of Afferent Innervation, Motion Detection, and Gaze Stabilization During Avian Vestibular Regeneration**

**J. David Dickman<sup>1</sup>, Mridha Zakir<sup>1</sup>, Asim Haque<sup>1</sup>, Insook Lim<sup>1</sup>, David Huss<sup>1</sup>**

<sup>1</sup>*Dept. Anatomy & Neurobiology, Washington University*

Regeneration of vestibular receptor cells and subsequent functional recovery following damage is well established. However, virtually nothing is known about the spatiotemporal characteristics of regenerating vestibular afferents and whether neural regeneration in the vestibular otolith system recapitulates the topographic phenotypic expression observed during normative development. We utilized an ototoxic agent to produce complete vestibular receptor cell loss and epithelial denervation, then quantitatively examined regeneration at discrete periods up to one year. Here we report that the two hair cell (type I and II) and three afferent types (bouton, dimorph, calyx) regenerate slowly at different rates through a progressive temporal sequence. Our data suggest that both hair cells and afferents trans-differentiate through advancing forms during regeneration. We also show that regenerated afferent innervation patterns are significantly different from those developed through normative morphogenesis, so adaptive plasticity in the central neural processing of motion information should be expected during functional recovery. How does morphological regeneration correlate with recovery of afferent responsiveness and gaze stabilization? Here we report that prior to 4 weeks regeneration, functional vestibular recovery was absent. No afferent responsiveness or eye/head control during motion was observed, accompanied by severe postural ataxia and loss of spatial navigation. Between 4 – 12 weeks regeneration, afferent responses returned, but only filtered to high frequency motion. Gaze stabilization was largely under compensatory, but more stable during high frequency motion and consisted of a larger eye (VOR) component than is present in normal birds. As gaze stabilization improved, ataxia diminished and learned spatial navigation through a simple maze recovered last.

Supported by NIH DC003286 and NASA NNA04CC52G.

## **[8] Clinical Manifestations of Vestibular Pathology**

**John P. Carey<sup>1</sup>**

<sup>1</sup>*Johns Hopkins University School of Medicine*

There has been a rich interaction between the basic sciences and clinical practice in the vestibular system. Peripheral vestibular disorders have demonstrated some of the fundamental principles of vestibular physiology. For example, Ewald's first law, that stimulation of an isolated semicircular canal produces eye movements in the plane of that canal, was demonstrated in humans by posterior

canal benign paroxysmal positioning nystagmus. In turn, that principle guided the search for the cause of a syndrome of pressure- and sound-induced nystagmus in the plane of the superior canal, leading to the discovery of superior canal dehiscence syndrome. The excitation-inhibition asymmetry of peripheral vestibular responses brought about the elegantly simple head thrust test for the diagnosis of vestibular hypofunction. But pathologies of the vestibular system pose many unanswered questions. What is the underlying molecular disorder in Ménière's disease? Does hydrops cause vertigo, or is it simply an epiphenomenon in Ménière's disease? What causes vestibular neuritis, and why does it preferentially affect the superior division of the vestibular nerve? Is the vertigo that accompanies migraine due to spreading electrical depression in central structures, trigeminal efferent stimulation of the labyrinth, or some other mechanism? Such questions can only be solved by continued collaboration between basic scientists and clinicians.

## **[9] A Multi-Channel Prosthesis for Restoration of the 3-Dimensional Vestibulo-Ocular Reflex**

**Charley C. Della Santina<sup>1</sup>, Americo A. Migliaccio<sup>1</sup>, Amit H. Patel<sup>1</sup>, John P. Carey<sup>1</sup>, Hong Ju Park<sup>2</sup>, Lee-Ching W. Anderson<sup>1</sup>, Lloyd B. Minor<sup>1</sup>**

<sup>1</sup>*Johns Hopkins University, Baltimore, Maryland,* <sup>2</sup>*Konkuk University, Seoul, Korea*

Bilateral loss of vestibular sensation and consequent failure of vestibulo-ocular and postural reflexes can be disabling. There are no adequate treatment options for people who, despite rehabilitation, fail to compensate for this loss. An implantable vestibular prosthesis that encodes head movement in all 3 dimensions (3D) and conveys that information via electrical stimulation of the vestibular nerve could significantly improve quality of life for these patients. We describe animal studies supporting this approach, discuss design considerations, and present a new multi-channel vestibular prosthesis that encodes head movement in 3D.

To develop an assay of stimulus selectivity for subsequent experiments, we used 3D scleral search coils and 3D binocular video-oculography to examine eye movements in response to canal-plane-specific head rotations of awake chinchillas in darkness. Normal chinchillas (N=8) exhibited responses like those of normal humans, with gain (eye/head acceleration) near -1 in each canal plane. Chinchillas treated unilaterally with intratympanic gentamicin (N=8) exhibited findings typical of similarly treated humans, with decreased gain for head movements exciting each canal of the treated labyrinth. Single-unit recording and histologic exam confirmed persistence of viable vestibular nerve afferent fibers in treated cristae.

In chinchillas made vestibular deficient through semicircular canal plugging and otolith disruption or bilateral gentamicin treatment, biphasic current pulse trains delivered via an electrode in a horizontal canal ampulla and pulse-frequency-modulated (PFM) by head rotation in the horizontal plane elicited a compensatory 1D VOR in that plane. However, 3D oculography revealed evidence of current spread to other nerve branches,

indicating a need to increase selectivity. Similar results were noted for electrodes in other canals.

Drawing on these findings, we constructed and tested a head-mounted, multi-channel vestibular prosthesis comprising 3 MEMS gyroscopes, a microcontroller, a current source and 8 electrodes. The device encodes 3D head rotation as PFM and/or amplitude-modulated, biphasic pulsatile stimulation of three or more vestibular nerve branches. In bilaterally gentamicin-treated chinchillas, multi-channel prosthetic stimulation restored a partly compensatory 3D vestibulo-ocular reflex.

Supported by NIDCD K08-DC006216 and R01-DC002390

## **[10] The Role of Fgf-Receptors and Dlx3b/4b in Regulating Competence for Otic Placode Induction and Development**

**Andreas Fritz<sup>1</sup>, Robert Esterberg<sup>1</sup>**

<sup>1</sup>*Emory University*

In vertebrates, the inner ear arises from the otic placode. Otic placodes develop from an ectodermal thickening that lies adjacent to the neural plate. Development of the otic placode requires both intrinsic and inductive factors. Molecular mechanisms that direct the induction and early development of sensory placodes, and the otic placode specifically, in zebrafish will be reviewed. The main inducers of the otic placode are fgf ligands, which are likely to exert their influences over a prolonged period of development. The signaling molecules Fgf3 and Fgf8 have been implicated in the induction and specification of the zebrafish inner ear. fgf3 and fgf8 are expressed in early mesendoderm as well as the hindbrain and act redundantly in inner ear formation.

To begin to understand the nature of competence in otic placode formation we are focusing on the role of fgf receptors. There are four known fgf receptors in zebrafish. We are using genetic interaction analyses and morpholino knock-down to determine which receptors are necessary to specify competence to otic precursor cells. Using strains of fgf3 or fgf8 null fish, we propose that it may be possible to dissect ligand-receptor interactions.

Several placode intrinsic factors, notably foxi1 and dlx genes, appear to mediate the response to Fgf signaling. Their potential roles in providing competence of placodal ectoderm to respond to inducing signals will be discussed, with emphasis on the regulation of fgf-receptor expression as a molecular indicator for competence. In particular, dlx3b/4b are expressed throughout the nonneural ectoderm bordering the neural plate beginning in mid-gastrulation. Their expression is progressively restricted during somitogenesis to the otic and olfactory placodes. This expression pattern suggests a role in providing competence to the otic placode. We show that loss of Dlx3b/4b blocks ear development by reducing expression of the four Fgf receptors throughout the embryo. This widespread loss of Fgf receptor expression is caused by a transient misexpression of bmp2b/4/7 that returns to normal during late somitogenesis. Overexpression of bmp2b or bmp4 alone or loss of function of chordin in mutant embryos is sufficient to reduce Fgf receptor expression and provide a similar pattern of expression to

dlx3b/4b compromised embryos. Our results provide evidence that dlx3b/4b function to provide extended competence to otic cells, and restrict BMPs from dorsal structures that would normally adopt a neural fate.

## **[11] From Otocyst to Ear: The Molecular Basis of Ear Morphogenesis**

**Doris K. Wu<sup>1</sup>, Weise Chang<sup>1</sup>**

<sup>1</sup>*NIDCD*

The vertebrate inner ear is a structurally intricate organ that is derived from a hollow tear-drop shaped epithelial cyst known as the otocyst. Cells within this epithelial sheet eventually develop into either neural, sensory or non-sensory tissues. Neural-fated cells delaminate from the otic epithelium to form the neurons of the vestibular-cochlear ganglion, whereas sensory-fated cells develop into sensory hair cells and supporting cells. The non-sensory cells develop into a host of specialized structures, including the three semicircular canals and the endolymphatic duct. While genes such as Neurogenin1 and Math1 have been shown to be important for the formation of neurons and sensory hair cells, respectively, the molecular mechanisms that lead to the specification of the three primary fates and the relationship among the three fates remain unclear. This presentation will summarize our current understanding of the relationship between specification of sensory and non-sensory fates. Using development of the cristae and their associated non-sensory structures, the semicircular canals, as an example, we will illustrate how sensory tissues coordinate the development of their associated non-sensory structures. The coordinated development of the two tissues may be a fundamental principle underlying the development of such an intricate organ.

## **[12] Biasing of Cell Fate in Developing Vestibular Sensory Epithelia: The Coordinated Activities of Ngn1 and Math1**

**Steven Raft<sup>1</sup>, Andrew Groves<sup>1</sup>, Segil Neil<sup>1</sup>**

<sup>1</sup>*House Ear Institute*

In animal development, multipotent progenitor cells give rise to various differentiated cell types in a temporally regulated manner. This problem may be addressed by studying the developing inner ear, which first generates precursors of VIIIth ganglion afferent neurons and later generates the mechanosensory hair cells that synapse with VIIIth ganglion afferents. Recent studies show that these two processes overlap for a period of time in the developing vestibular system. We have used this feature as an opportunity to explore potential regulatory interactions between Ngn1 and Math1, two genes that are essential for the generation of inner ear neurons and hair cells, respectively. I will review evidence supporting the hypothesis that VIIIth ganglion neurons and some mechanosensory hair cells are clonally related. I will then describe work demonstrating that growth and differentiation of vestibular maculae are tightly linked to inhibition of neurogenesis. Evidence suggests that the coupling of these processes is mediated by the interdependent regulation of Ngn1 and Math1.

### **13 Connecting Sensory Neurons to Hair Cells and Epithelia**

**Donna Fekete<sup>1</sup>**

<sup>1</sup>*Purdue University*

Mechanisms that may regulate axon guidance of afferent and efferent fibers to the correct sensory epithelia of the inner ear will be reviewed. At the molecular level, axon guidance and fasciculation are likely to involve the spatial and temporal regulation of attractants, repellants and/or cell adhesion molecules. Efferents are generally guided to the inner ear along the afferents, although the molecular basis of this guidance mechanism is still under investigation. The differential projections of auditory vs. vestibular fibers are likely to require distinct guidance cues in the neurons themselves and/or in their target tissues. Evidence for such molecular differences will be summarized.

### **14 Neurosensory Transformation of the Otic Ectoderm**

**Bernd Fritzsch<sup>1</sup>, Sarah Pauley<sup>1</sup>**

<sup>1</sup>*Creighton University, Omaha, NE*

Ear development converts a simple epithelium into a three dimensional labyrinth with four major cell types: hair cells, supporting cells, sensory neurons and general otic epithelium. To achieve this, specific precursors have to be selected for neuroepithelial fate acquisition and have to increase in numbers through regulated proliferation and cell death to achieve adult ear numbers. We will provide a general perspective of how epithelia are converted to a neuronal fate in vertebrates, specifically addressing neuronal induction of the CNS and placodes. Such neuronal transformation of ectodermal tissue critically depends on the interaction of FGF's with BMPs, the latter being factors that promote epithelial formation. Formally, cell fate assignment and morphogenesis can be viewed as distinct processes in the ear, each involving their own discreet set of genes. However, genetic engineering of a number of genes, thought to be primarily involved in cell fate selection, turned out to have additional morphogenetic defects. Such defects may be linked to altered patterns of proliferation or may be linked to signaling mediated from differentiating sensory epithelia. We will present several examples of Tbx1, Neurog1, Shh, FGF's Foxg1, GATA3, Six1, Eya1 mutants that highlight this intersection of histo- and morphogenesis. For example, Neurog1 absence causes loss of hair cells through premature cell cycle exit. Alteration of the cell cycle as a basis for morphogenetic defects appears also to be an essential effect in Foxg1 null mice. Finally, we will present a working model how these factors might interact in a given epithelial cell to influence fate from epidermal toward neuronal, resulting in topologically restricted altered proliferation followed by histo- and morphogenesis, a hallmark of ear development.

### **15 Regulation of Cell Proliferation and Differentiation in the Developing and Postnatal Organ of Corti**

**Neil Segil<sup>1,2</sup>, Feng Liu<sup>1,2</sup>, Yun-Shain Lee<sup>1</sup>, Angelika Doetzlhofer<sup>1</sup>, Patricia White<sup>1</sup>, Andrew Groves<sup>1,2</sup>**

<sup>1</sup>*House Ear Institute*, <sup>2</sup>*University of Southern California*

Coordinating cell proliferation with growth and differentiation remains a poorly understood aspect of embryonic development, as well as postnatal regeneration. In this presentation I will discuss new results concerning the interplay of transcriptional and post-transcriptional mechanisms involved in regulating p27Kip1-dependent cell cycle exit during organ of Corti development. Specifically, we have analyzed the consequences of the loss of the gene Skp2, which is a component of a ubiquitin ligase involved in regulating p27 protein turnover. In addition, I will present data relevant to the question of hair cell regeneration and the mechanisms regulating the postmitotic state of postnatal supporting cells.

### **16 Patterning and Polarity of the Organ of Corti**

**Matthew W. Kelley<sup>1</sup>**

<sup>1</sup>*NIH, Bethesda, MD*

The mammalian organ of Corti exhibits one of the most striking examples of cellular patterning in any vertebrate system. A tightly regulated number of hair cells and supporting cells are arranged in an invariant mosaic that extends along the length of the basal-to-apical axis of the cochlear duct. In addition, all hair cells and supporting cells are polarized within the plane of the epithelium, such that the stereociliary bundles located on each outer hair cell are oriented uniformly. The cellular and molecular factors that orchestrate the development of this structure remain largely unknown, however recent results have begun to identify some of the genes that are required for these events. In particular, recent results from our laboratory suggest that members of the bHLH and FGF families function as positive regulators of hair cell and supporting cell development, respectively, while Wnts and Hedgehogs act as negative regulators of hair cell development that apparently play key roles in cellular patterning. Finally, Vangl2, Celsr1 and Scrb1, members of a conserved signaling pathway that regulates uniform cellular orientation, polarize cells within the cochlear duct.

### **17 Stem Cells in Inner Ear Cell Regeneration**

**Stefan Heller<sup>1</sup>**

<sup>1</sup>*MEEI/Harvard*

In this presentation, I will introduce different populations of stem cells from embryonic and adult sources and describe the potential of these stem cells to differentiate into inner ear cell types in vitro and in vivo. In particular stem cells isolated from the inner ear appear to be quite potent to give rise to inner ear cell types after transplantation. I will introduce and compare different sphere-forming stem cells and progenitor cells isolated from different parts of the inner ear. Experimental approaches to replace lost hair cells and spiral ganglion neurons in mouse and gerbil model systems will be discussed. Finally, I will focus on

the use of genetically modified stem cells for high-throughput screening for compounds that are effective in inner ear cell regeneration.

### **18 The Type I Transmembrane Serine Protease, TMPRSS1, Is Required for Normal Hearing**

**Justin Tan**<sup>1</sup>, Michel Guipponi<sup>2</sup>, Qingyu Wu<sup>3</sup>, Robert Shepherd<sup>1</sup>, Scott Hamish<sup>2</sup>

<sup>1</sup>Bionic Ear Institute, Melbourne, Australia, <sup>2</sup>Walter and Eliza Hall Institute of Medical Research, Melbourne, Australia, <sup>3</sup>Berlex Biosciences

Mutations in one type of transmembrane serine proteases (TMPRSS), TMPRSS3, have been identified in both familial and sporadic cases of non-syndromic sensorineural recessive deafness, DFNB8/10. The molecular mechanism in which these proteases affect deafness could only be recently understood with the availability of mouse mutants lacking these genes. Here we show that homozygous mutants lacking TMPRSS1 serine protease (TMPRSS1<sup>-/-</sup>), are profoundly deaf while their heterozygous litter mates display normal hearing thresholds. In analyzing the expression of different transmembrane serine proteases TMPRSS1 and TMPRSS3 proteins in the adult mouse cochlea, we found a mutually non-overlapping pattern of expression. TMPRSS1 is expressed in soma of spiral ganglion neurons and their fibres while TMPRSS3 is expressed strongly in inner hair cells and soma of spiral ganglion neurons, but not their fibres. In TMPRSS1<sup>-/-</sup> mice, we could not detect morphologically any degeneration of spiral ganglion neurons and hair cells of the organ of Corti. However, the tectorial membrane is abnormally enlarged in TMPRSS1<sup>-/-</sup> postnatal pups and the abnormality persists during maturation. In contrast, bipolar fibres projecting from the spiral ganglion neurons to the organ of Corti and the cochlear nucleus of these mutant mice appear thinner and less compact than their wild-type counterparts, suggesting a biochemical defect in the composition of these neuronal fibres. Using markers for myelin proteins, we showed by immunohistochemistry that expression of both peripheral myelin and myelin basic proteins are down-regulated in fibres of TMPRSS1<sup>-/-</sup> mice. In contrast, potassium channel Kv 1.1 expression in spiral ganglion neurons is strongly up-regulated, suggesting that the reduction of myelin proteins is specific. These data show for the first time, in a mouse model, that the transmembrane serine protease TMPRSS1, similar to its TMPRSS3 counterpart, is required for the development of normal hearing.

Supported by the National Institute on Deafness and Other Communication Disorders N01-DC-3-1005 (JT and RS), the Garnatt Passe and Rodney Williams Memorial Foundation (MG), the National Health and Medical Research Council Fellowship 171601 and Program Grant 257501 (HS); JT and MG contribute equally to this work.

### **19 Connexin Gap Junction-Mediated Hearing Controls in the Cochlea**

**Hong-Bo Zhao**<sup>1</sup>, Ning Yu<sup>1</sup>, Carrie Fleming<sup>1</sup>

<sup>1</sup>University of Kentucky Medical School

Connexin gap junctions play a crucial role in hearing function. However, how connexin channels affect hearing

function still remains unclear. Connexins in the cochlea are only expressed in supporting cells; no connexin is expressed in hair cells. In this experiment, the effect of connexin function on outer hair cell (OHC) electromotility was investigated. We first studied the connexin hemichannel ATP release under the physiological condition. We found that similar to ATP release under the low Ca<sup>++</sup> condition, connexin hemichannels in cochlear supporting cells could release ATP under mechanical stimulation. The release corresponded to physiological levels measured in vivo, and was in nanomolar levels were it released into the endolymph and perilymph. We further found that the nanomolar ATP can significantly affect the OHC electromotility; extracellular ATP reduced the nonlinear capacitance and the slope factor of voltage dependence, and shifted the operation points of OHC electromotility. ATP also reduced the distortion products of OHCs in responses to two sinusoidal voltage stimuli. Moreover, this effect was identified through activation of P2 receptors on the OHC surface. Immunofluorescent staining shows that the P2x7 purinergic receptors were expressed on the surface of the OHC lateral wall. Blockage of P2 receptors negated the effect of ATP on OHC electromotility. The data revealed a connexin hemichannel-mediated purinergic intercellular signaling pathway between supporting cells and hair cells in the cochlear to regulate hearing function. The data also provide a source of ATP in the cochlea.

Supported by NIH DC 05989.

### **20 A Mutation in the F-Box Gene, Fbxo11, Causes Otitis Media in the Jeff Mouse**

Rachel E. Hardisty-Hughes<sup>1</sup>, Hilda Tateossian<sup>1</sup>, Susan A. Morse<sup>1</sup>, Rosario Romero<sup>1</sup>, Alice Middleton<sup>1</sup>, Terry Hacker<sup>2</sup>, Zuzanna Lalanne<sup>1</sup>, A. Jackie Hunter<sup>3</sup>, Michael Cheeseman<sup>2</sup>, **Steve D.M. Brown**<sup>1</sup>

<sup>1</sup>MRC Mammalian Genetics Unit, Harwell, UK, <sup>2</sup>MRC Mary Lyon Centre, Harwell, UK, <sup>3</sup>GlaxoSmithKline Pharmaceuticals, New Frontiers Science Park, Harlow, UK

Otitis media is the most common cause of hearing impairment in children and is the most common cause of surgery in children in the developed world. This condition is primarily characterised by inflammation of the middle ear mucosa. Prolonged stimulation of the inflammatory response and poor mucociliary clearance can lead to the persistence of middle ear fluid giving rise to the clinical presentation of otitis media with effusion (OME). Recent evidence indicates that genetic factors play a very significant role in the development of OME in the human population (Casselbrant et al. 1999, 2004; Daly et al., 2004). As part of the UK mouse mutagenesis programme we have identified a novel deaf mouse mutant, Jeff (Jf) and described its phenotype as having chronic proliferative otitis media (Hardisty et al 2003). The Jeff mouse carries a mutation in an F-box gene, Fbxo11, a member of the E3 ubiquitin ligase family located on distal mouse chromosome 17 (human chromosome 2), which is expressed in the mucin secreting cells of the developing middle ear cavity. This is one of the first molecules to be identified, obviously contributing to the genetic etiology of

this complex disorder and potentially offers a new target for the screening and treatment of otitis media.

Casselbrant ML, Mandel EM, Fall PA, Rockette HE, Kurs-Lasky M, Bluestone CD, Ferrell RE (1999) The heritability of otitis media. A twin and triplet study. *J. Am. Med. Assoc.* 282: 2125-2130.

Casselbrant ML, Mandel EM, Rockette HE, Kurs-Lasky M, Fall PA, Bluestone CD, Ferrell RE. (2004). The genetic component of middle ear disease in the first 5 years of life. *Arch Otolaryngol Head Neck Surg.* 130(3):273-8.

Daly KA, Brown WM, Segade F, Bowden DW, Keats BJ, Lindgren BR, Levine SC, Rich SS (2004). Chronic and recurrent otitis media: a genome scan for susceptibility Loci. *Am J Hum Genet.* 75(6):988-97

Hardisty RE, Erven A, Logan K, Morse S, Guionaud S, Sancho-Oliver S, Hunter AJ, Brown SD, Steel KP. (2003). The deaf mouse mutant Jeff (Jf) is a single gene model of otitis media. *J Assoc Res Otolaryngol.* 4(2):130-8.

## **[21] Genetic Modulators of Aminoglycoside-Induced Hair Cell Toxicity in Zebrafish Lateral Line**

**Kelly N. Owens**<sup>1,2</sup>, Brock Roberts<sup>1,2</sup>, Edwin W. Rubel<sup>2,3</sup>, David W. Raible<sup>1,2</sup>

<sup>1</sup>Dept. of Biological Structure, <sup>2</sup>V.M. Bloedel Hearing Research Center, <sup>3</sup>Dept. of Otolaryngology-HNS, University of Washington

Loss of mechanosensory hair cells in the inner ear is a leading cause of hearing and balance impairment. Ototoxic drugs, e.g. aminoglycoside antibiotics, are a tractable approach for inducing hair cell loss. In wildtype zebrafish, *Danio rerio*, lateral line hair cells are killed by aminoglycosides in a dose-dependent manner. To identify factors that affect hair cell death or survival, we screened zebrafish for mutations that modulate aminoglycoside-induced lateral line hair cell death *in vivo*. Five day old larvae were exposed to neomycin, stained with the vital dye DASPEI and evaluated for the presence of hair cells. Animals were screened with high (200  $\mu$ M) or low (25  $\mu$ M) doses of neomycin to identify mutations conferring protection or sensitivity, respectively. To date, we have identified four protective mutations and one susceptibility mutation. One mutation, *agent smith*, has a semi-dominant phenotype, while the remainder are recessive. Complementation analysis is underway to determine the number of mutated genes.

We have recently identified the gene altered in the *sentinel* mutant, which modulates aminoglycoside sensitivity leading to neomycin resistance. Analysis of *sentinel* indicates that lateral line development is normal, and that mechanotransduction and aminoglycoside uptake can occur. The *sentinel* mutant has a wildtype response to cisplatin, indicating that altered aminoglycoside response is not due to disruption of general cell death components used by both ototoxins. These features suggest that absence of the *sentinel* product affects action of aminoglycosides or early events in aminoglycoside-induced cell death. The *sentinel* gene encodes a large novel transcript with homologs in other vertebrates, including humans. No functional information is known as

yet about the *sentinel* gene or its homologs. Thus, the *sentinel* product is a novel molecular component affecting aminoglycoside response. (Supported by NIH grants DC05987, F32 DC006998-01, and P30 DC04661)

## **[22] The Role of Genetic Background in Impulse Noise-Induced Hearing Loss in Mice**

Busheng Tong<sup>1</sup>, Göran Laurell<sup>1</sup>, Malou Hultcrantz<sup>1</sup>, Maoli Duan<sup>1</sup>

<sup>1</sup>Karolinska Institutet

Impulse noise may cause hearing injury in persons working in industrial environments and to people exposed to explosions and rock music. It is well known that there is an individual susceptibility to noise. A certain percentage of the population may have increased risk for developing hearing loss after impulse noise trauma. There is no method available to identify persons at risk. One major concern is the genetic background to impulse noise-induced hearing loss (INHL).

The aim of present study was to test the susceptibility to INHL in two different strains of mice, the CBA/CA and C57/6J. Each animal was bilaterally exposed to noise at 160 dB pSPL for 50, 100 and 150 impulses. Hearing threshold sensitivity was measured during four weeks after noise exposure. Preliminary results indicate that there was a significant difference between two strains of mice. The C57/6J mouse seemed to be more sensitive to impulse noise as compared to the CBA mouse indicating that genetic factors play a critical role in INHL.

## **[23] Creation and Characterization of GLUT5 Conditional Knockout Mice**

Xudong Wu<sup>1</sup>, Jiangang Gao<sup>1</sup>, Xiang Wang<sup>2</sup>, David Z.Z. He<sup>2</sup>, Jian Zuo<sup>1</sup>

<sup>1</sup>Dept. of Developmental Neurobiology, St. Jude Children's Research Hospital, Memphis, TN, <sup>2</sup>Dept. of Biomedical Sciences, Creighton University, Omaha, NE

GLUT5 is a fructose transporter expressed in outer hair cells (OHCs) and may modulate their electromotility. The developmental expression profile of GLUT5 in OHCs is later than the acquisition of the electromotility of the OHCs. It remains enigmatic how GLUT5 is involved in electromotility and whether it affects the cochlear amplifier. Here we successfully created a floxed GLUT5 mouse model. By crossing the floxed GLUT5 mouse with the EIIA Cre mouse, we obtained a complete GLUT5 knockout mouse line. Southern blot and PCR genotyping proved that GLUT5 gene is deleted in those mice. Realtime-PCR confirmed the disrupted transcript of GLUT5 mRNA in the GLUT5<sup>-/-</sup> kidneys and immunostaining revealed the deletion of GLUT5 in kidney and testes in the GLUT5<sup>-/-</sup> mice. Preliminary analyses indicated that no significant threshold elevation was detected using ABR assays in GLUT5<sup>-/-</sup> mice. Preliminary morphological analyses

showed no obvious abnormality in the cochlea and lateral walls of OHCs from GLUT5<sup>-/-</sup> mice. Immunostaining of prestin, Myosin1c, Myosin7A, synaptophysin did not reveal any obvious differences between the GLUT5<sup>-/-</sup> mice and wildtype littermates. Further morphological and cellular characterizations are in progress. Our preliminary data

support the prestin as the primary component of the OHC motor and suggest that GLUT5 may only modulate the electromotility under certain conditions. (Supported by 1 R01DC006471 and 5R21DC005168, Cancer Center Support Grant CA21765 and ALSAC)

## **[24] Generation and Characterization of a Prestin Knockin Mouse with the C1 Mutation**

Jiangang Gao<sup>1</sup>, Mary Ann Cheatham<sup>2</sup>, David Z.Z. He<sup>3</sup>, Kristin Huynh<sup>2</sup>, Xiang Wang<sup>3</sup>, Xudong Wu<sup>1</sup>, Jing Zheng<sup>2</sup>, Peter Dallos<sup>2</sup>, Jian Zuo<sup>1</sup>

<sup>1</sup>Dept. of Developmental Neurobiology, St. Jude Children's Research Hospital, Memphis, TN, <sup>2</sup>Dept. of Communication Sciences and Disorders, Northwestern University, Evanston IL, <sup>3</sup>Dept. of Biomedical Sciences, Creighton University, Omaha, NE

Local mechanical amplification is required for normal sensitivity and frequency selectivity in the mammalian cochlea. Using a knockout mouse, we showed that prestin, the outer hair cell (OHC) motor protein, is required for somatic electromotility and cochlear amplification. Unfortunately, the OHC lengths in mice lacking prestin were ~2/3 those of wildtype controls, which may have compromised auditory function. To test this possibility, a knockin prestin mouse model was developed. This effort was based upon previous *in vitro* data (Oliver et al. 2001) indicating that the voltage dependence of C1 mutated prestin is shifted in the negative direction such that motor action should be reduced at the OHC's *in vivo* membrane potential. Hence, introduction of the C1 mutation into the endogenous prestin gene was undertaken to produce a mouse model in which OHCs should theoretically be of normal length but have reduced motor function.

To this end, a targeting construct was made containing the C1 mutation in exon 7 and a Neo cassette flanked by two loxP sites inserted into intron 6. Southern blots with BamHI digestion and an external probe were used to screen for homologously recombined ES cells. F1 mice, heterozygous for the C1+Neo allele, were crossed with Cre mice to excise the DNA between the two loxP sites, thereby deleting the Neo marker. The successful introduction of the C1 mutation into the *prestin* gene was confirmed by genomic PCR and sequencing.

Preliminary characterization of C1 knock-in mice demonstrates that homozygous C1 mutants display correctly targeted mutant prestin in the OHC lateral wall, and normal OHC lengths. Further measurements of C1 mutants are in progress.

(Supported by R01 grants DC006471, DC04696 and DC00089, Cancer Center Support Grant CA21765 and ALSAC).

## **[25] The Stria Vascularis from Alport Mice Is a Hypoxic Microenvironment**

Michael Anne Gratton<sup>1</sup>, Velidi Rao<sup>2</sup>, Gautam Bhattacharya<sup>2</sup>, Amy Liao<sup>1</sup>, Dominic Cosgrove<sup>2</sup>

<sup>1</sup>University of Pennsylvania, <sup>2</sup>Boys Town National Research Hospital

Alport syndrome is a basement membrane disease in which the resultant kidney disease is associated with

hearing loss and lens abnormalities. The causative genetic defects are found in any of three type IV collagen genes, COL4A3, COL4A4, or COL4A5. In earlier work we have shown that the stria capillaries of Alport mice become thickened (Cosgrove et al, Hear. Res., 121, 84-98 1998). More recently we demonstrated that stria capillary basement membrane (SCBM) homeostasis is altered in the stria of Alport mice, in part, via dysregulation of matrix metalloproteinases (Gratton et al., Am. J. Pathol. 166, 1465-74). We surmised that the thickening of the SCBM might influence the flow of nutrients and oxygen to the stria cells, creating a hypoxic environment. Under hypoxia, most tissues respond by upregulating expression of genes involved in angiogenesis, often referred to as hypoxia-related factors. In this study, stria isolated from Alport mice and wild type littermates was subjected to RT-PCR analysis for transcripts encoding hypoxia-related factors VEGF, HIF1- $\alpha$ , HIF2- $\alpha$ , Neuropilin-1, Flt-1 (VEGF receptor-1) and Flk-1 (VEGF receptor 2). The striae from each mouse were analyzed independently to assure reproducibility, which was highly consistent across test groups. VEGF mRNA was 20-fold higher in Alport stria, HIF1- $\alpha$  mRNA was 10-fold higher in Alport stria, Neuropilin-1 mRNA was 5-fold higher in Alport stria; HIF2- $\alpha$  mRNA was 3-fold higher in Alport stria, Flk-1 mRNA was 5-fold LOWER in Alport stria, and Flt-1 mRNA levels did not vary significantly in Alport stria relative to wild type stria. Immunohistochemical staining of cochlear sections from wild type and Alport mice confirmed these data; showing substantially increased staining for VEGF and the HIF proteins in the Alport stria vascularis. Combined, these findings suggest that the thickened stria capillary basement membranes in Alport mice are creating a hypoxic microenvironment in the stria vascularis. Upregulation of these hypoxia-related angiogenic factors likely impacts downstream effector functions in the Alport inner ear.

Supported by DC006442, DC04844, and DK55000

## **[26] Genes Encoding for Cytokines and Their Receptors Differentiate Otic Capsule from Bones Formed by Endochondral or Intramembranous Ossification**

Konstantina Stankovic<sup>1,2</sup>, Arthur Kristiansen<sup>1</sup>, Joe Adams<sup>1</sup>, Michael McKenna<sup>1</sup>

<sup>1</sup>Massachusetts Eye and Ear Infirmary, <sup>2</sup>Harvard Medical School

Otic capsule is unique for many reasons: its rate of remodeling is minimal, it does not heal when broken, it is uniquely resistant to tumor invasion, it is the densest bone in the body, and it encase the most sensitive sensory organ in the body. The long term goal of our research is to understand biological mechanisms that make otic capsule unique. Such understanding will provide the foundation for developing rational treatment strategies for bone disorders that lead to hearing loss, such as otosclerosis.

To understand the molecular basis for the uniqueness of otic capsule, we compared expression levels of 61 genes in otic capsule with those in parietal bone and femur, which exemplify bones formed by intramembranous or



endochondral ossification, respectively. We focused on genes that play roles in bone remodeling, genes that encode structural bone proteins, and genes that mediate inflammatory reactions. We used real-time quantitative RT-PCR to analyze individual gene expression levels, followed by genomic techniques of unsupervised and supervised learning to analyze collective expression levels. By comparing molecular signatures of the bones we studied, we identified differentially expressed genes. We found that small sets of genes encoding for cytokines and their receptors reliably distinguish among these bone types. Out of the genes we studied, the bone morphogenetic protein receptor 1b, BMPR1b, is the most robust predictor of otic capsule.

RO1DC03401 (MJM), Safford grant (KMS, MJM).

## **[27] New Enu Mouse Mutants: Models for Human Hearing Impairment**

**Karen B. Avraham**<sup>1</sup>, Ronna Hertzano<sup>1</sup>, Hashem Shahin<sup>1</sup>, Ella Shalit<sup>1</sup>, Amiel A. Dror<sup>1</sup>, Orit Hermesh<sup>1</sup>, Amy E. Kiernan<sup>2</sup>, Charlotte R. Rhodes<sup>2</sup>, Agnieszka K. Rzadzinska<sup>3</sup>, Helmut Fuchs<sup>4</sup>, Karen P. Steel<sup>3</sup>, Martin Hrabé de Angelis<sup>4</sup>

<sup>1</sup>Dept. Human Molecular Genetics & Biochemistry, Sackler School Medicine, Tel Aviv U, Tel Aviv, Israel, <sup>2</sup>MRC Institute of Hearing Research, Nottingham, UK, <sup>3</sup>The Wellcome Trust Sanger Institute, Wellcome Trust Genome Campus, Hinxton, Cambridge, UK, <sup>4</sup>GSF Research Center for Environment and Health, Institute of Experimental Genetics, Neuherberg, Germ

N-Ethyl-N-Nitrosourea (ENU) mutagenesis screens provide new mouse models for human hearing impairment, a requisite for studying the complexity of inner ear development and mechanisms of human mutations. The mouse mutants often appear to have similar phenotypes on a superficial level, but upon closer examination, it becomes clear that the phenotypes are indeed very different. This reflects the difficulties in determining the genotype-phenotype correlations when examining audiograms and other clinical characteristics from patients with hearing loss. The variety of ENU phenotypes reflects this phenomenon. We are studying six ENU mutants. The loop (*loop*) mouse is a recessive mouse mutant and auditory brainstem response (ABR) demonstrates that these mice are profoundly deaf with vestibular dysfunction. The phenotype of Forera (*Frfr*) mice is due to a dominant mutation, leading exclusively to vestibular dysfunction due to an abnormal lateral semicircular canal. The Tailchaser (*Tlc*) mouse is a dominant mouse mutant with defects affecting the inner ear hair cell stereociliary bundle arrangement and maintenance. The Headbanger (*Hdb*) dominant mouse mutant has low frequency hearing loss and vestibular dysfunction, with elongated vestibular hair-cell stereocilia. Headchuck (*Hdck*) is a dominant vestibular mutant. Sourd (*Srd*) mice, with a dominant mutation, are deaf with extra inner hair cells. Complete characterization of the phenotypes by scanning electron microscopy, paint fill analysis, immunofluorescence with various cell markers, behavioral testing, and auditory testing, as well as identification of the causative mutation by positional-

candidate cloning, will shed light on genes essential for the function of the inner ear.

Research supported by the European Commission FP6 Integrated Project EUROHEAR LSHG-CT-20054-512063 and The German Israeli Foundation for Scientific Research and Development (GIF).

## **[28] MicroRNA Expression in the Mouse Inner Ear**

Michael D. Weston<sup>1</sup>, Sonya M.S. Rocha-Sanchez<sup>1</sup>, Kirk W. Beisel<sup>1</sup>, Bernd Fritzsch<sup>1</sup>, **Garrett Soukup**<sup>1</sup>

<sup>1</sup>Creighton University, Omaha, NE

Recent studies have emphasized the importance of understanding how biology is impacted by the transcription of noncoding RNAs, which comprise the vast majority of products from mammalian genomes. MicroRNAs (miRNAs) are small regulatory RNAs that are processed by and function through the RNA interference pathway to mediate post-transcriptional silencing of complementary target messenger RNAs. MiRNA genes are evolutionarily conserved among multi-cellular eukaryotic organisms, supporting the view that miRNAs are part of an ancient and crucial genetic regulatory program. Mammalian genomes each contain at least 200 miRNA genes, and certain miRNAs are known to effect cell proliferation, differentiation, or morphological development. However the biological functions of most miRNAs are unknown, and little is known about the developmental expression patterns and biological significance of miRNAs in the mammalian ear. We have examined miRNA expression in the postnatal mouse inner ear from P0 to P37 using microarray, northern blot, and RT-PCR analyses. Nearly half of the known miRNA genes are detected in the whole inner ear, where a number exhibit significant up- or down-regulation throughout inner ear maturation. Further analysis by in situ hybridization demonstrates that certain of these miRNAs exhibit tissue-specific expression patterns in the mouse inner ear. Moreover, a recent study of miRNA expression in the zebrafish demonstrated that three coordinated miRNAs are expressed specifically in hair cells of the ear and neuromasts. Importantly, our in situ hybridization analysis of the orthologous mouse miRNAs likewise shows their expression in the mouse inner ear to be hair cell-specific in both the auditory and vestibular organs. These results demonstrate that miRNA expression in the mammalian inner ear is both temporally and spatially defined, suggesting that miRNAs might influence the development, maintenance, or function of specific cell types crucial to inner ear functions.

## **[29] Pericyte Distribution in the Capillaries of the Cochlear Lateral Wall and Change Induced by Noise Exposure**

**Weiju Han**<sup>1,2</sup>, Xiao-Rui Shi<sup>1</sup>, Alfred L. Nuttall<sup>1,3</sup>

<sup>1</sup>Oregon Health & Science University, <sup>2</sup>Chinese PLA General Hospital, Dept of Otolaryngology Head/Neck Surgery, <sup>3</sup>Kresge Hearing Research Institute, The University of Michigan, Ann Arbor, MI, USA

The alteration of cochlear blood flow caused by loud sound is an important pathological factor in noise induced hearing loss. Pericytes, surrounding blood microvessels, play



important roles for many organs in the regulation of endothelial proliferation and differentiation. They function as progenitor cells. They synthesize and secrete a wide variety of vasoactive autoregulating agonists and synthesize and releasing structural constituents of the basement membrane and extracellular matrix. Little is known about the distribution and actions of pericytes in the cochlea. In this study, we investigated the distribution and change of pericytes in the capillaries of the cochlear lateral wall in the control and noise exposure mice with fluorescent immunohistochemistry method and confocal microscope. Experimental groups of mice were exposed to broadband noise at 120 dB SPL for 2 days (4h/d). Pericytes were identified using monoclonal anti- $\alpha$ -smooth muscle actin and anti-desmin antibody. Endothelial cells were visualized with FITC conjugated to anti-mouse CD45. Vasculature was visualized with anti-collagen type VI whole tissue preparations. We found in control tissues that the distributions of pericytes were occurred on capillaries of both the stria vascularis and spiral ligament. The pericytes wrapped around capillaries in close contact with endothelial cells. Their long processes extended along and around the surface of micro-vessels. The ratio of pericytes to endothelial cells in the cochlear microvessels is around 1:2. Noise stimulation caused the regional increase in the population of pericytes on the vessels of the stria vascularis. The results indicated that pericytes are dynamic cellular population that may play a key role in the change of cochlear blood flow caused by loud sound.

**Acknowledgment** This work was supported by NIH NIDCD grant R01 DC00105.

### **[30] Expression of Monocyte Chemoattractant Proteins (MCPs) in Mouse Cochlea Exposed to Acoustic Trauma**

**Elizabeth Shick<sup>1</sup>, Richard Ransohoff<sup>1</sup>, Keiko Hirose<sup>1</sup>**

<sup>1</sup>*Cleveland Clinic Foundation*

Acoustic injury results in cochlear monocyte/ macrophage migration into the spiral limbus and spiral ligament of the mouse cochlea, but the signals that induce monocyte migration into the cochlea are unknown (Hirose et al, 2005). Chemokines are small secreted peptides that mediate leukocyte recruitment and activation during inflammation. Based on studies conducted in knockout mice, the chemokine monocyte chemoattractant protein (MCP)-1 (Ccl-2 in the systematic terminology) plays a critical role in monocyte migration to the brain, whereas in the cochlea, Ccl-2 is not necessary for monocyte migration (Sautter and Hirose, abstract ARO 2006). This study was designed to examine gene expression of other MCPs that might exert redundant function with Ccl-2 for monocyte migration to the noise-exposed cochlea. We exposed 8-9 week old Ccl-2 knockout mice to 112dB octave band noise for 2 hours, using non-noise-exposed littermates as controls, harvested cochleas at 24, 48, and 96 hours post noise exposure and analyzed gene expression of MCP-2/Ccl-8, MCP-3/Ccl-7, and MCP-5/Ccl-12 by quantitative real time RT-PCR. Ccl-7 was substantially upregulated in the Ccl2<sup>-/-</sup> mice, peaking at 48 hours post exposure. Ccl-8 expression was slightly upregulated, again peaking at 48-

hour post exposure. There was no change in Ccl-12 expression between 24 and 96-hour post exposure. Our data point towards shared mechanisms for upregulation of Ccl-2 and Ccl-7, but not Ccl-8 or Ccl-12 following acoustic trauma and this issue can be addressed in part by comparing gene expression in wild-type and Ccl-2<sup>-/-</sup> mice. Our results leave uncertain what role MCPs play in response to acoustic trauma: Ccl-2 does not appear implicated in monocyte recruitment but may be involved in macrophage activation. The function(s) of Ccl-2 and Ccl-7 can be examined in knockouts for the common MCP receptor, CCR2.

### **[31] Chemokine Upregulation Following Acoustic Trauma**

**Stephen Tornabene<sup>1</sup>, Liem Pham<sup>1</sup>, Peter Billings<sup>1</sup>, Jeffrey Harris<sup>1</sup>, Elizabeth Keithley<sup>1,2</sup>**

<sup>1</sup>*UC San Diego*, <sup>2</sup>*Department of Veterans Affairs Research Service, San Diego*

Following noise-induced trauma, inflammatory cells are present in the inner ear. To examine potential mechanisms for active recruitment of cells, gene array analysis and reverse transcriptase polymerase chain reaction (RT-PCR) were performed on cochlear tissue. NIH-Swiss mice were exposed to 118 dB octave band noise for two hours and sacrificed at 2, 18, and 48 hours post-exposure. Gene array (SuperArray, Inc.) analysis indicated increased expression of several members of the CC chemokine family including monocyte chemoattractant protein 5 (MCP-5), monocyte chemoattractant protein 1 (MCP-1), and macrophage inflammatory protein 1-beta (MIP-1b). The cell adhesion molecule ICAM was also upregulated. RT-PCR was then performed using primers for the individual mRNA sequences. This confirmed the increased expression of MCP-1, MCP-5, MIP-1b, and ICAM relative to non-exposed control mice. This study demonstrates that several members of the CC chemokine family and the cell adhesion molecule ICAM are upregulated following acoustic trauma. The early nature of this expression implies chemokine production by cochlear tissue rather than infiltrating inflammatory cells. These data provide evidence in support of the idea that a cochlear inflammatory response is initiated in response to acoustic trauma and involves the recruitment of circulating leukocytes to the inner ear.

### **[32] Cochlear Distribution of Small Focal Lesions Following Exposure to a 4-kHz or a 0.5-kHz OBN**

**Gary W. Harding<sup>1</sup>, Barbara A. Bohne<sup>1</sup>**

<sup>1</sup>*Washington University School of Medicine*

An octave band of noise (OBN) delivers fairly uniform energy over a specific range of frequencies (3-6 kHz for 4-kHz OBN & 0.375-0.750 kHz for 0.5-kHz OBN). Above & below these ranges, energy is at least 50 dB less than that in the OBN. Hair-cell loss often occurs outside the exposure OBN. The frequency location of hair-cell loss is evident when the % location of small focal lesions is analyzed. Data sets were assembled from our permanent collection of noise-exposed chinchillas using the following criteria: 1) The sum of exposure duration & recovery time

was less than or equal to 10 days; 2) The exposure level was less than or equal to 108 dB SPL; & 3) Focal lesions were less than 1.5 mm in size. The data sets included a variety of exposures ranging from those that were high-level, short duration to those that were moderate-level, moderate duration. The % location of the center of each focal lesion was determined. Means, SDs & medians were calculated for lesion size for each OBN. Histograms were then constructed from the % location data using 2.0% bins & the counts were graphed relative to total number of lesions. For the 4-kHz OBN, 94% of the lesions were in the basal half of the OC & 6% were in the apical half. For the 0.5-kHz OBN, 29% of the lesions were in the apical half of the OC & 71% were in the basal half. The mean lesion size was 1.48% & 0.68% for the 4-kHz & 0.5-kHz OBN, respectively, with medians of 1.10% & 0.50%. The mean lesion size (in mm) for the 0.5-kHz OBN was less than half that for the 4-kHz OBN. For the 4-kHz OBN, a histogram of the % location of lesions showed that most occurred in the 5-7-kHz region, at & just above the upper edge of the OBN. Clusters of lesions were also found around 8 & 12 kHz. A cluster was present at & just below the lower edge of the OBN, as well as in the 1.5-kHz region. For the 0.5-kHz OBN, a histogram of the % location of lesions showed clusters at 0.25, 0.75 & 1.5 kHz in the apical half. In the basal half, the pattern was very similar (Pearson's  $r=0.69$ ) to that seen with the 4-kHz OBN. The distribution of basal-turn lesions suggests that the 4-kHz & 0.5-kHz OBN are damaging that region of the cochlea in the same way.

### **[33] Histopathological Changes in the Cochlea Following Exposure to Low-Frequency Noise**

**Steve Lee<sup>1</sup>**, Barbara A. Bohne<sup>1</sup>, Gary W. Harding<sup>1</sup>

<sup>1</sup>*Washington University School of Medicine*

Thirteen chinchillas were exposed for 24 h to a 0.5-kHz OBN at 95 dB SPL. The cochleae of 8 animals were fixed at 0-d post-exposure; 5 were fixed after 1-2 wks of recovery. To keep cellular debris from washing away, all cochleae were plastic-embedded before being dissected into flat preparations. By phase-contrast microscopy, hair-cell losses were determined from apex to base. Damage consisted of scattered loss of OHCs in the apical half of the organ of Corti (OC) & small focal lesions (i.e., > 50% hair-cell loss over at least 0.03 mm) in the basal half. These specific patterns of loss suggest that noise damaged the apex & base by different mechanisms. In

order to estimate the timing of cell loss, differential counts of missing & severely injured cells were performed. The presence of immature phalangeal scars & necrotic, oncotic & apoptotic hair cells indicates a recent loss while mature phalangeal scars indicate a long-standing loss. In the apical half of the OC in both groups of animals, many of the phalangeal scars replacing the missing OHCs were immature. Cellular debris was seen in the OC fluid spaces beneath these scars. By TEM, the debris was found dispersed in the Nuel spaces & consisted of vesicles of various sizes, small granules, shrunken & swollen mitochondria &, rarely, fragments of plasma membrane. TEM also revealed the presence of cellular debris in the endolymphatic space near the reticular lamina. This latter finding indicates that the barrier function of the reticular

lamina broke down temporarily when the hair cells degenerated, before phalangeal scars formed. Debris in the Nuel spaces was not surrounded by plasma membrane as would be the case if the hair cells had been apoptotic before they died & then formed apoptotic bodies. In the basal half of the OC, focal lesions were found in 2 of eight 0-day & 3 of five 1-2 wk animals. In the 0-day ears, oncotic OHCs were found at the edges of the basal-turn lesions. In the 1-2 wk ears, the basal-turn lesions primarily consisted of immature phalangeal scars. The appearance of debris in the apex & base suggests that many of the OHCs were oncotic rather than apoptotic before they disappeared.

### **[34] Intense Noise Causes Damage to the OHC Lateral Wall Leading to Hearing Loss**

**Guang-Di Chen<sup>1</sup>**

<sup>1</sup>*SUNY at Buffalo*

The cochlear active process results in a 40-60 dB cochlear amplification. Outer hair cells (OHCs) constitute an important part of cochlear micro-mechanics and are believed to be the driving force of the cochlear active process by way of their electromotility. The OHC membrane skeleton, consisting of F-actin and spectrin, maintains the unique OHC cylindrical shape and provides stiffness to the cell. In addition to its well known basic functions, the OHC plasma membrane is a main contributor to OHC axial stiffness. Prestin, a membrane protein, has been recently recognized as the OHC motor protein. Changes in the OHC lateral wall may affect OHC electromotility and/or cochlear micromechanics and, subsequently cochlear sensitivity. In this report OHC membrane fluidity (by laser bleach approach), gene expression of beta-actin, beta-spectrin, and prestin were determined after noise exposure. The noise exposure caused a reduction of OHC membrane fluidity and a time-dependent gene expression of the proteins in the OHC lateral wall. The noise-induced changes were associated with permanent threshold shifts. The motor protein appeared to be the most sensitive to noise trauma among the three proteins. The data suggest that non-lethal injuries in the OHC lateral wall may cause loss of the OHC electromotility or the cochlear micromechanics leading to a reduction of cochlear amplification and then cochlear sensitivity.

### **[35] Mechanisms of Oxidative Stress in the Potentiation of Noise-Induced Hearing Loss by Acrylonitrile**

**Benoit Pouyatos<sup>1</sup>**, Laurence Fechter<sup>1</sup>

<sup>1</sup>*Loma Linda VA Medical Center*

Acrylonitrile (ACN), one of the top 50 chemicals produced in the world, is a very powerful pro-oxidant compound whose metabolism leads to a profound glutathione (GSH) depletion and to a production of cyanide (CN) which, in turn, can inhibit superoxide dismutase (SOD). ACN, by itself, is not ototoxic, but we have shown that it can strongly promote noise-induced hearing loss (NIHL), even at noise levels that do not produce auditory impairment. The mechanism by which ACN renders the cochlea more

vulnerable to noise damage is still unknown, but we hypothesize that the decrease of GSH and/or the inhibition of SOD reduce the cochlear intrinsic anti-oxidant defenses and ultimately create oxidative stress.

In this study, we investigated in adult Long-Evans rats the effect of the alteration of CN production through the ACN metabolism on the promotion of NIHL by ACN. For this purpose, two different drugs were used: (1) Sodium thiosulfate (STS), a CN antidote commonly used in humans in case of CN poisoning and (2) 4-methylpyrazole (4MP) which blocks ACN metabolism through the oxidative pathway, preventing CN formation.

We observed that, while both STS and 4MP drastically reduced CN production by more than 80%, they did not protect against the potentiating effect of ACN. This result suggests that CN is not implicated in the potentiation of NIHL by ACN. Further studies are proposed to determine the role of GSH depletion in the increase of vulnerability to noise induced by ACN.

(supported in part by VA grant C3575R and NIOSH grant OH03481).

Key words: cochlea, noise, oxidative stress, acrylonitrile, superoxide dismutase, glutathione, cyanide.

### **[36] Nuclear Factor-Kappa B Nuclear Translocation in the Cochlea of Mice Following Acoustic Overstimulation**

**Masatsugu Masuda<sup>1</sup>**, Reiko Nagashima<sup>2</sup>, Sho Kanzaki<sup>1</sup>, Masato Fujioka<sup>1</sup>, Kiyokazu Ogita<sup>2</sup>, Kaoru Ogawa<sup>1</sup>

<sup>1</sup>Keio University, <sup>2</sup>Setsunan University

The mechanisms of noise trauma include mechanical damage, ischemia, excitotoxic damage, metabolic exhaustion, or perturbation of cochlea fluid ion homeostasis. There is increasing evidence to suggest that expression of many molecules in the lateral wall of the cochlea plays important roles in noise-induced stress responses. Since a variety of stress responses occur, there is a possibility that simultaneous modulation of multiple mechanisms can lead to better outcomes of treatment for the hearing impairment resulting from noise trauma than modulation of a single mechanism. This may be provided by modulation of transcription factors, because one transcription factor regulates the expression of many genes in response to a single stimulus that induces tissue damage. In this study, activation of the nuclear transcription factor nuclear factor-kappa B (NF- $\kappa$ B) was investigated in the cochlea of mice treated with intense noise exposure. To assess effects of noise exposure on NF- $\kappa$ B/DNA binding activity in the cochlea, we prepared nuclear extracts from the cochlea at different time points after noise exposure and carried out electrophoretic mobility shift assay. NF- $\kappa$ B/DNA binding was significantly enhanced in several hours after noise exposure. Supershift analysis demonstrated that enhancement of NF- $\kappa$ B/DNA binding was at least in part due to nuclear translocation of p65. An immunohistochemical study also showed that nuclear translocation of p65 was observed in the lateral wall after noise exposure. These results suggest that NF- $\kappa$ B may be involved in expression of genes in response to acoustic

overstimulation in the cochlea of mice. Some reports suggest that NF- $\kappa$ B acts as a protective role in the cochlea. However, some reports suggest that it acts as a cytotoxic role. Future research will be necessary to reveal whether NF- $\kappa$ B serves in protecting, killing, or both.

### **[37] A BAD Link to Mitochondrial Cell Death in Noise-Induced Hearing Loss**

**Maria Angeles Vicente-Torres<sup>1</sup>**, Su-Hua Sha<sup>1</sup>, Jochen Schacht<sup>1</sup>

<sup>1</sup>Kresge Hearing Research Institute, The University of Michigan, Ann Arbor, MI, USA

In outer hair cells (OHCs), acoustic overstimulation induces calcium overload and activation of mitochondria-mediated death pathways but it remains unknown whether these are interrelated or independent events. We have recently reported that calcineurin is activated (Minami et al., 2004) and total BAD (Bcl-2-associated death promoter) decreased (Vicente-Torres et al., 2005) in the cochlea following noise exposure. We now postulate that the calcium overload associated with acoustic overstimulation can trigger mitochondria-mediated death pathways through the dephosphorylation and, therefore activation of BAD, by the calcium-dependent phosphatase calcineurin and subsequent translocation to the mitochondria.

To explore this hypothesis, CBA/J mice were exposed to a broadband noise (2-20 kHz) causing a permanent threshold shift of about 40 dB at 12 and 20 kHz indicative of damage to the middle and upper basal turns respectively. Widespread loss of OHC was apparent in the basal turn of the cochlea. In unexposed controls, BAD immunostaining showed an essentially cytoplasmic distribution in the cells of the organ of Corti, the lateral wall and the spiral ganglion. Five hours after acoustic overstimulation, mitochondria and BAD were redistributed to the perinuclear region of OHCs in the basal and middle turns while BAD in the apical turn remained unaffected. Furthermore, upregulation of total BAD and the non-apoptotic phospho-BAD (Ser 112) were detected in the stria vascularis and the supporting cells of the organ of Corti.

Our data establish a connection between calcium and mitochondria-mediated death pathways in OHCs and also suggest a dual role for BAD. The translocation of BAD to the mitochondria in degenerating cells is indicative of the activation of the pro-apoptotic capacity of BAD while upregulation of phospho-BAD is consistent with a non-apoptotic role of BAD in these less vulnerable cells.

This work was supported by research grant DC-06457 and core center grant DC-05188 from the National Institute on Deafness and other Communication Disorders, NIH.

### **[38] The Effect of Acoustic Trauma on VR1 Expression in Rat Spiral Ganglion and Cochlear Nucleus**

**Kristin Myers<sup>1</sup>**, Thomas Brozoski<sup>1</sup>, Carol Bauer<sup>1</sup>

<sup>1</sup>SIU School of Medicine

The vanilloid receptor type 1 (VR1) is one of several members of a family of non-specific cation ion channels

that modulate nociception and inflammation within sensory pathways. VR1 has been demonstrated in multiple sensory regions through out the peripheral and central nervous system including spiral ganglion (SpG), vestibular ganglion, dorsal root ganglion (DRG) and trigeminal ganglion. The receptor is responsive to heat, protons and endogenous ligands derived from the inflammatory arachidonic acid pathway. Functionally, the VR1 receptor may mediate the acute sensation of nociception after local trauma, and the sensation of hyperalgesia associated with chronic pain. Balaban demonstrated upregulation of the VR1 receptor in mouse spiral ganglion after ototoxic damage from chronic kanamycin. If the VR1 channel modulates neural protection after local damage, we hypothesized that the receptor may play a role in mediating the development of tinnitus after acoustic damage.

The objective of this study was to quantify VR1 expression in the cochlea and auditory brainstem after acute acoustic trauma. A time series design was employed to establish the time course for upregulation of the VR1 receptor after acoustic trauma. Long-evans rats were unilaterally exposed to a 116 dB SPL 16 kHz octave band noise for one hour under ketamine-xylazine anesthesia. Rats were sacrificed at 30 min, 2 hrs, 24 hrs and 120 hrs post-exposure. Ipsilateral and contralateral SpG and cochlear nucleus were examined for VR1 expression using immunohistochemistry. DRG were used for positive controls. The effect of acute acoustic trauma on VR1 expression will be presented.

### **[39] Differential Gene Expression in the Cochlea Following Exposure to Intense Impulse Noise**

**Mette Kirkegaard**<sup>1,2</sup>, Norihiko Murai<sup>3</sup>, Mårten Risling<sup>4,5</sup>, Leif Järleback<sup>1,2</sup>, Mats Ulfendahl<sup>1,2</sup>

<sup>1</sup>Center for Hearing & Communication Research and Dept. of Clinical Neuroscience, Karolinska Institutet, <sup>2</sup>Dept. of Otolaryngology, Karolinska University Hospital, SE-171 76 Stockholm, Sweden, <sup>3</sup>Dept. of Otolaryngology, Matsue City Hospital, Matsue, Japan, <sup>4</sup>Division of Neuronal Regeneration, Dept. of Neuroscience, Karolinska Institutet, <sup>5</sup>Swedish Defence Research Agency (FOI), Karolinska Institutet, Stockholm, Sweden

Noise exposure damages the sensory hair cells of the inner ear leading to cell death and consequently hearing loss. In order to develop a treatment for noise-induced hearing loss in the future, it is necessary to have a detailed understanding of the complete repertoire of genes expressed in the inner ear and their regulation in response to noise exposure. This knowledge can be used to deduce the molecular pathways involved and identify new target genes for therapy.

We used the Affymetrix Rat 230 GeneChip for gene expression analysis to detect genes that are differentially expressed after intense impulse noise exposure. Rats were anaesthetized, exposed to a single blast wave (194 kPa/199 dB) and the cochleae were removed at 3, 24 and 72 hours following exposure. RNA from a single cochlea was hybridized to each chip in order to minimize inter-animal variation and the signals were normalized using the

robust multi-array average (RMA) approach. Changes in gene expression between control and exposed rats were compared using a t-test. Regulated genes were confirmed by real-time PCR and pathway-based analysis of the data was performed using GenMAPP ([www.genmapp.org](http://www.genmapp.org)).

At 3 hours after exposure to the blast wave, a number of genes showed a significant up-regulation. These include immediate early genes known to be involved in the immediate stress response of the tissue and other transcription-related genes. Also, genes involved in growth/differentiation responses and oxidative stress were up-regulated. At 24 hours following the exposure, the majority of the significantly regulated genes are part of the inflammatory response of the tissue or genes encoding antioxidants.

The present project has successfully implemented the GeneChip technology to detect differentially expressed genes in a rat model for noise-induced hearing loss. We have shown that it is possible to extract enough RNA from single-cochlea preparations for microarray analysis and even with a rather conservative statistical analysis, several genes of biological relevance can be identified.

### **[40] Auditory Thresholds Among Self-Reported Noise-Exposed and Non-Noise Exposed**

**Freshman**

**Vishakha Rawool**<sup>1</sup>, Lynda Colligon<sup>2</sup>

<sup>1</sup>West Virginia University, <sup>2</sup>Princeton Otolaryngology Associates

This study was designed to evaluate the effects of self-reported noise exposure on young adults within the age-range of 18-24 years. A questionnaire was administered to a college freshman class to determine history of noise exposure and history of ear infections. Based on the answers provided to the questions in the questionnaire, subjects who had no history of ear infections were selected and placed into two groups. Subjects who indicated that they were exposed to noise were placed in the 'noise-exposed' group. Those subjects whose answers to the questions were consistent with little or no hobby or work related noise exposures were placed in the 'non-exposed' group. The mean age of participants was 18.4 years. The 'noise-exposed' group consisted of 14 men and 6 women. The 'non-noise exposed' group consisted of 2 men and 18 women. Auditory thresholds for each ear were obtained from all 40 participants in a sound-attenuated booth using conventional clinical procedures. Multivariate analyses of variance (MANOVA) revealed no significant difference ( $p > 0.22$ ) in auditory sensitivity across the noise-exposed and non-exposed groups. The averaged thresholds were actually worse in the non-exposed group than those who reported exposure to noise, although this difference was not statistically significant. The MANOVA also revealed a significant ( $p = 0.0000$ ) frequency effect. Overall the thresholds were worse at 6 and 8 kHz. In addition, the analyses revealed a significant ( $p < 0.0009$ ) 'ear' and 'frequency' interaction. Right ear thresholds were worse than the left ear thresholds at 0.5, 1, 6 and 8 kHz. Left ear thresholds were worse than the right ear thresholds at 0.25 kHz. There were no other significant

interactions. Sixty nine (28%) of the 246 students surveyed reported working in noisy environments. The duration of noise exposure in these students ranged from 2 months to 4 years. Of the 69 that were exposed to noise, 10 reported wearing ear protection.

#### **41 Effects of Environmental Noise on Hearing Capabilities of Fish**

**Lidia E. Wysocki<sup>1</sup>**, Michael E. Smith<sup>2</sup>, Arthur N. Popper<sup>1</sup>, John Davidson<sup>3</sup>, Adam Frankel<sup>4</sup>, William Ellison<sup>4</sup>, Fred Ford<sup>3</sup>, Julie Bebak-Williams<sup>3</sup>

<sup>1</sup>University of Maryland, <sup>2</sup>University of Kentucky,

<sup>3</sup>Freshwater Institute, <sup>4</sup>Marine Acoustics Inc.

Interest in the effects of environmental noise on fish have has grown considerably over the past several years. Potential impacts on fish may range from subtle behavioral changes to more dramatic impacts that could include deafness or death. While most of the concerns have been related to the impact of intense sources such as sonar, pile driving, and seismic air guns, there is growing concern that exposure to lower level, but longer duration, sounds may also affect fish. One area of increasing interest lies with aquaculture facilities where fish are raised with a substantial background noise produced by aerators, pumps, filtration systems, and other devices. Consequently, fish are chronically subjected to noise and questions have been raised regarding negative impacts such as impairment of sensory systems, increased stress, and reduced growth rates.

Several studies have shown that high intensity noise can induce temporary hearing loss in fishes, and that lower intensity sounds, for days or weeks can also produce hearing loss. However, no study has examined the effects of noise exposure that continues throughout the life cycle of fish, as occurs in aquaculture facilities. Thus, the objective of this ongoing study is to investigate whether rainbow trout (*Oncorhynchus mykiss*) cultured in tanks with different sound pressure levels (150 vs. 115 dB re 1  $\mu$ Pa RMS) differ in their hearing sensitivities.

Auditory thresholds were evaluated for 16 to 17 weeks post hatching trout (weight: 12 - 46 g) using the auditory evoked potential technique. Prior to examination, animals were cultured under 150 or 115 dB noise regimes for about four weeks. Comparison of hearing thresholds at each test frequency revealed no statistical difference in hearing sensitivity between animals cultured under the two noise regimes. The study will be continued in order to assess potential long term effects of aquaculture noise on hearing and samples of the inner ear sensory epithelia will be analyzed.

#### **42 Ultrastructural Analysis of the Tegmentum Vasculosum After Intense Sound**

**Charles Askew<sup>1</sup>**, James C. Saunders<sup>1</sup>, Michael Anne Gratton<sup>1</sup>

<sup>1</sup>University of Pennsylvania

Ultrastructural damage and repair of the tegmentum vasculosum (TV) in the young chick following acoustic over-stimulation might contribute to the loss and recovery

of the endocochlear potential. This study explores this possibility by examining the ultrastructure of the TV dark cells in chicks exposed at two different ages. Transmission electron microscopy was used to evaluate the TV along the length of the cochlear duct in 5 groups of chicks. Two groups (1 or 12 days after birth) were exposed to an intense pure tone (0.9 kHz) for 48 hours and the TV was harvested immediately afterward. A third group exposed 1 day after hatching was allowed 6 days of recovery before the TV was harvested. The TV was also evaluated in age matched non-exposed control groups. It was found that the sound exposure caused a consistent reduction in the dark cell area in the 1-3 day old group, which appeared to exhibit repair after 6 days of recovery. This damage to the dark cells was restricted to the 0.9 kHz region of the cochlear duct. The 12-14 day old group showed little or no structural change after the exposure. These results suggest a period during early development, between 0-6 days, where the chick exhibits greater susceptibility to TV damage caused by acoustic over-stimulation. It remains to be determined if this damage alters the ionic environment of the scala media.

#### **43 Depolarization of Outer Hair Cells Evokes Active Hair Bundle Motion by Two Mechanisms**

**Robert Fettiplace<sup>1</sup>**, Helen Kennedy<sup>2</sup>, Michael G. Evans<sup>3</sup>, Andrew Crawford<sup>4</sup>

<sup>1</sup>University of Wisconsin-Madison, USA, <sup>2</sup>Bristol University, UK, <sup>3</sup>Keele University, UK, <sup>4</sup>Cambridge University, UK

There is current debate about the mechanism of the cochlear amplifier, a process originating in outer hair cells that endows the cochlea with sensitivity and sharp frequency tuning. Alternative hypotheses attribute force generation to somatic contractions underpinned by prestin or to hair bundle motility resulting from mechanotransducer (MET) channel gating. Voltage pulses applied across the organ of Corti have been used to examine the mechanism but this maneuver affects both outer hair cell processes: depolarization directly activates prestin and also alters the calcium influx through the MET channels, thereby changing their open probability. To distinguish contributions to force production from somatic motility and the MET channels, we measured hair bundle motion during depolarization of individual outer hair cells in cochlear explants from neonatal (P6 to P14) rats. Motion of free-standing hair bundles was detected by imaging on dual photodiodes mounted on a piezoelectric bar to supply the calibration. Depolarization evoked rapid positive bundle deflections that were sensitive to extracellular calcium and were reduced by perfusion with the MET channel blocker dihydropyridine with no effect on the non-linear capacitance reflecting prestin driven somatic motility. However, they were also diminished by 10 mM Na salicylate and depended on the intracellular anion, implying involvement of the prestin motor. Furthermore, depolarization of one outer hair cell caused motion of neighboring hair bundles indicating overall motion of the reticular lamina. Depolarization of solitary rat outer hair cells elicited cell-length changes whose voltage-activation range depended on the intracellular anion, but were insensitive to dihydropyridine. These results imply

that both the MET channels and somatic motor participate in hair bundle motion evoked by depolarization.

#### **[44] An Investigation of the Properties of Stereociliary Rootlets**

**Michael G. Evans**<sup>1</sup>, U. Guha<sup>1</sup>, Shanthini Mahendrasingam<sup>1</sup>, S. Dallender<sup>1</sup>, David N. Furness<sup>1</sup>, Carole M. Hackney<sup>1</sup>

<sup>1</sup>*ISTM and Life Sciences, Keele University, UK.*

During displacement stereocilia flex at their ankles just above the point of attachment to the cuticular plate. Each stereocilium has a central rootlet in this region that penetrates the cuticular plate, appearing to anchor it. We have investigated this region in outer hair cells (OHCs). The stereocilium shaft narrows at the ankle and widens again just before its membrane joins the apical membrane. Serial sections for transmission electron microscopy show that dense rootlet material fills most of the diameter of the ankle region. The mean gap between the rootlet and the stereocilium membrane is 23 nm in tall and intermediate stereocilia and 15 nm in short stereocilia. Links between the core and the membrane occur in the ankle region. Immunocytochemical data indicate that diffusible calcium buffers such as calretinin (22 kDa) are reduced in the stereocilium shaft, suggesting lower calcium buffering due to the filtering of large molecules. We assessed this by imaging the cells with a confocal microscope and following the passage of inert fluorescent molecules (dextran) into the cell body of isolated OHCs via a glass pipette during whole-cell recording. Small dextrans (3 kDa) enter the stereocilia within a few minutes. A larger dextran (40 kDa) causes stereocilia to fluoresce very weakly after a longer period of time, indicating it may enter the stereocilia slowly, but because it sticks to extracellular debris this result may represent extracellular binding rather than intrastereociliary accumulation. Unlike the smaller dextran, the 40 kDa dextran is partially excluded from the cell nucleus indicating that differential subcellular compartmentalisation may occur on the basis of molecular size. We have shown that the gap between the rootlet complex and the membrane in the ankle region is very narrow, although further experiments are required to verify the passage of large dextrans into the stereocilium shaft.

Supported by Deafness Research UK.

#### **[45] Structure and Composition of the Stereociliary Rootlets of Rat Cochlear Hair Cells**

Shanthini Mahendrasingam<sup>1</sup>, David N. Furness<sup>1</sup>, James R. Bartles<sup>2</sup>, **Carole M. Hackney**<sup>1</sup>

<sup>1</sup>*School of Life Sciences, Keele University, Keele, Staffordshire, UK,* <sup>2</sup>*Cell & Molecular Biology, Northwestern University, Chicago*

The stereociliary bundle of rat hair cells generates active forces that could contribute to the cochlear amplifier (Kennedy et al., 2005, *Nature* 433: 880-883). Stereocilia contain parallel actin filaments that contact an electron-dense region in the shaft which extends down into the cuticular plate to form rootlets. They also have a reduced level of calcium buffering proteins compared with the cytoplasm (Hackney et al., 2005, *J. Neurosci.*, 25: 7867-

7875). We have investigated the structure and composition of the rootlets because they are likely to influence the mechanical properties and chemical composition of the hair bundle.

For ultrastructure, post-hearing rat (P16 and P26) cochleas were fixed in glutaraldehyde and osmium tetroxide, embedded in Spurr resin and serial sectioned. For immunocytochemistry, they were fixed in 4% paraformaldehyde either with or without 0.1% glutaraldehyde and labeled by immunofluorescence or embedded in LR White or HM 20 resin for immunogold labeling.

The rootlets can extend beyond the cuticular plate and in outer hair cells may contact the lateral membrane. Their length correlates with the height of the stereocilium, but is relatively shorter in inner than outer hair cells. The rootlet is thickest in the narrowest region of the stereocilium and almost completely fills the shaft. Rootlets are immunoreactive for both  $\beta$ - and  $\gamma$ -actin and tropomyosin, but not espin, the latter being in the shaft of the stereocilia, mainly in the periphery. Immunofluorescence for troponin-C (identified in a cDNA library of the mouse organ of Corti; Pompeia et al., 2004, *Genomics* 83:1000-1011) also occurs in inner and outer hair cells and in pillar cells. These observations are consistent with the rootlet containing muscle-like proteins suggesting a stiffening and/or motile function, perhaps modulated by calcium. The rootlet structure may prevent diffusible buffers from entering the stereocilium.

Funded by Deafness Research UK and NIH DC0004314

#### **[46] Myh9 in the Mammalian Cochlea: Localization Within the Stereocilia**

**Anand N. Mhatre**<sup>1</sup>, Yan Li<sup>1</sup>, Graham Atkin<sup>1</sup>, Abdel Maghnouj<sup>1</sup>, Anil K. Lalwani<sup>1</sup>

<sup>1</sup>*NYU School of Medicine*

Mutations of non-muscle myosin type IIA or MYH9 are linked to syndromic or nonsyndromic hearing loss. Despite its widespread expression in the body, it is unclear why clinical symptoms associated with Myh9 dysfunction are restricted to specific cell types and target organs. The mouse represents an excellent model for investigating the biological role of Myh9 in the cells and tissues affected by its dysfunction. A first step in this process is to localize Myh9 expression within the organs affected by its mutation and to probe these targets for presence of potential splice variants. Herein, we describe distribution and localization of Myh9 in the mouse cochlea, specifically within the sensory hair cells and analysis of Myh9 splice variants. Mouse Myh9 was detected using a polyclonal anti-Myh9-antibody, generated against a 22 amino acid long peptide at the C-terminus of mouse Myh9. The anti-Myh9 antibody identified a single, specific, immunoreactive band of 220 kDa in immunoblot analysis of homogenate from variety of different mouse tissues. The Myh9 antibody cross-reacts with the rat but not the human orthologue. Myh9 is expressed predominantly within the spiral ligament as well as in the sensory hair cells of the organ of Corti. Confocal microscopy of cochlear surface preparations, identified Myh9 within the stereocilia of the inner and outer hair cells.

This localization raises the possibility that mutations of MYH9 may exert their pathogenic effect of hearing loss through disruption of the structure/function of the stereocilia. Screening of the EST database for potential variants and their validation through RT-PCR analysis did not identify splice variants of Myh9.

#### **[47] Adaptive Shift in the Domain of Negative Stiffness During Spontaneous Oscillation by Hair Bundles from the Internal Ear**

Loïc Le Goff<sup>1</sup>, Dolores Bozovic<sup>1,2</sup>, A.J. Hudspeth<sup>1</sup>

<sup>1</sup>HHMI at the Rockefeller University, <sup>2</sup>UCLA, Department of Physics

When a hair cell of the bullfrog's sacculus is maintained in vitro under native ionic conditions, its mechanosensitive hair bundle may oscillate spontaneously. Such active hair-bundle motility is a manifestation of the active process that amplifies mechanical inputs, tunes responsiveness, and produces compressive nonlinearity. Spontaneous oscillations have been hypothesized to result from the interaction of a hair bundle's negative stiffness, which creates a region of mechanical instability, with a myosin-based adaptation mechanism that continually repositions the bundle there (Martin, P., Mehta, A. D., Hudspeth, A. J. [2000] Proc. Natl. Acad. Sci. USA 97: 12026-12031).

To test this proposition, we designed an experimental paradigm in which a bundle was permitted to oscillate freely, then was subjected to brief periods of displacement-clamping to determine its state. More precisely, a digital signal processor was used to monitor spontaneous oscillations in real time and to trigger measurements at particular phases of the movement cycle. We used a flexible stimulus fiber in an analog feedback loop to measure a hair bundle's displacement-force relation.

By comparing the displacement-force curves obtained at the two extremes of a hair bundle's oscillation, we demonstrated a shift in the negative-stiffness region whose direction, orientation, magnitude, and kinetics agreed with the predictions of the gating-spring theory. The results accord with the idea that adaptation underlies spontaneous hair-bundle oscillation, and therefore powers the active process that also amplifies, tunes, and shapes the hair cell's mechanical responsiveness.

This research was supported by grant DC00241 from the National Institutes of Health.

#### **[48] Identification of the Ankle Link Antigen as the Usher 2c Protein, VLGR1, a Protein Required for Cochlear Hair Bundle Development**

Richard J. Goodyear<sup>1</sup>, JoAnn McGee<sup>2,3</sup>, Michael D. Weston<sup>3</sup>, P. Kevin Legan<sup>1</sup>, Gautam Bhattacharya<sup>2</sup>, Dominic Cosgrove<sup>2</sup>, D. Randy McMillan<sup>4</sup>, Perrin C. White<sup>4</sup>, Edward J. Walsh<sup>2,3</sup>, Guy P. Richardson<sup>1</sup>

<sup>1</sup>University of Sussex, UK, <sup>2</sup>Boys Town National Research Hospital, <sup>3</sup>Creighton University, Omaha, NE, <sup>4</sup>University of Texas Southwestern Medical Center, Dallas

The ankle link antigen (ALA, Goodyear & Richardson, *J. Neurosci* 19:3761-72, 1999) is a BAPTA- and subtilisin-sensitive epitope associated with the ankle links of sensory

hair bundles and the calycal processes of photoreceptors. It was originally defined by a mAb and identified as a large, Con A-reactive protein that can be immunoprecipitated from TX-100 extracts of the avian retina (Goodyear & Richardson, *J Neurosci* 23:4878-87, 2003). The ALA was immunoprecipitated and analysed by MALDI-TOF spectrometry. A single peptide with a mass identical to that of a unique peptide from the predicted sequence of VLGR1 identified the ALA as the avian orthologue of the very large G-protein coupled receptor, VLGR1, product of the *USH2C* locus (Weston et al., *Am J Hum Genet* 74:357-66, 2004). Mice homozygous for a deletion of the transmembrane and cytoplasmic domains of Vlgr1 (McMillan & White, *Mol Cell Neurosci* 26:322-9, 2004) have disorganised cochlear hair bundles, elevated ABR thresholds, and an absence of DPOAEs (Walsh et al., ARO abstract #1358, 2005). Antibodies to the intracellular domain of Vlgr1 were used to examine the distribution of Vlgr1 in the mouse inner ear. At P2, staining was observed around the base of the hair bundles in both the auditory and vestibular organs. As expected from studies showing ankle links are only transiently expressed during mouse auditory hair-bundle development (Goodyear et al. *J Comp Neurol* 485:75-85, 2005) immunoreactivity was no longer detected in the cochlea by P16 (see also Weston et al., ARO meeting 2006). Immunogold labelling of P2 cochlear cultures revealed the anti-Vlgr1 antibodies stained the ankle links. Immunostaining was not observed in homozygous Vlgr1 mutant mice, and ankle links were absent from the hair bundles. Unexpectedly, immunostaining was not observed in hair cells that had been treated with subtilisin prior to fixation, and immunogold labelling was found to be present on the extracellular surface of the hair bundle.

Supported by The Wellcome Trust, NIH NIDCD DC04662 and NEI EY016247. MDW is supported by a grant from the Deafness Research Foundation. The authors would like to thank Dr. Kathryn Lilley, Cambridge Centre for Proteomics, UK for her invaluable assistance.

#### **[49] The Usher Syndrome Type II Associated Protein, VLGR1, Localizes to Developing Mouse Inner Ear Stereocilia**

Michael D. Weston<sup>1</sup>, Sonya M.S. Rocha-Sanchez<sup>1</sup>, Dominic Cosgrove<sup>2</sup>, Kirk W. Beisel<sup>1</sup>

<sup>1</sup>Creighton University, Omaha, NE, <sup>2</sup>Boys Town National Research Hospital

Usher syndrome type II combines congenital hearing loss with progressive retinitis pigmentosa. *USH2C* loss of function mutations in the *VLGR1* gene suggests a critical role for the protein in development and homeostasis of the affected sensory organs. Vlgr1 mutant mice (BUB/BnJ) develop immature and splayed stereocilia bundles, consistent with its early onset of hearing impairment and increased susceptibility to audiogenically induced seizures (Johnson, Zheng et al. *Genomics* 85:582-590, 2005). We sought to elucidate the spatial and temporal expression of Vlgr1 in embryonic and postnatal FVB/N mice by whole mount *in situ* hybridization and immunohistochemistry. GST-Vlgr1 fusion constructs were used to raise rabbit polyclonal antibodies to the thrombospondin (TspN,



aa1433-1516, 84aa) and the entire cytoplasmic tail (aa6153-6298, 146aa). In P0 FVB/N mice, Vlg1 localizes to developing stereociliary bundles of inner ear hair cells, consistent with the mutant mouse phenotype (see also Goodyear et al, ARO midwinter meeting 2006). Vlg1 specific immunoreactivity displays both a radial and longitudinal gradient in the cochlea. Specific immunoreactivity to hair bundles was undetectable in *Vlg1<sup>Fringes</sup>* mutants, providing validation of Vlg1 antibody specificity. Vlg1 transcript levels decreased during maturation of the cochlea and corresponded to diminishing Vlg1 immunoreactivity in stereociliary bundles around P9. Both transcripts and protein are undetectable by P20. These data provide strong evidence suggesting a transient role for Vlg1 during stereocilia development. This is the first Usher type II protein localized to the sensory cells of the cochlea and vestibule and correlate with the stereocilia localizations of Usher type I associated proteins. We have also identified a novel tissue specific Vlg1 transcript lacking exon 26 which is unique to mouse inner ear mRNA. This novel isoform may influence interactions with other proteins. Such knowledge will be necessary to determine the biologic function of Vlg1 and how its dysfunction leads to the manifestation of Usher syndrome. Supported by a grant from the Deafness Research Foundation (MDW) and NIH NIDCD DC04844 (DC).

## **[50] Calcium Signals in the Stereocilia of Isolated Outer Hair Cells**

Csaba Harasztosi<sup>1</sup>, Barbara Müller<sup>1</sup>, Rajesh Ramaswamy<sup>1,2</sup>, **Anthony W. Gummer<sup>1</sup>**

<sup>1</sup>Department Otolaryngology, University Tuebingen, Tuebingen, Germany, <sup>2</sup>Graduate School of Neural and Behavioural Sciences, Max Planck Research School, Tuebingen, Germany

Entry of Ca<sup>2+</sup> ions into the stereocilia (SC), and their intracellular regulation, is crucial for mechanoelectrical transduction in outer hair cells (OHCs). The goals of the present study were to investigate the origin of Ca<sup>2+</sup> signals and localise transduction channels in the hair bundle of freshly isolated OHCs from an adult mammalian hearing organ, the guinea-pig cochlea.

OHCs were mechanically isolated from the adult guinea-pig cochlea. Ca<sup>2+</sup> transients were evoked by positive deflection of the SC using a fluid-jet stimulator. To facilitate Ca<sup>2+</sup> entry into the hair bundle, Ca<sup>2+</sup> concentration in the fluid-jet solution was 4 mM (extracellular 100 µM). Intracellular Ca<sup>2+</sup> changes were monitored using the acetoxymethyl ester form of the fluo-3 dye. The fluorescence signals were detected using a confocal laser-scanning microscope adopting framescan (1 s/frame) and linescan (2 ms/line) methods.

Cells could be classified into two subgroups - one, where the Ca<sup>2+</sup> signal could be evoked in the longest and the shortest SC, and the second group, where the Ca<sup>2+</sup> signal in the longest SC was almost negligible compared with the signal in the shorter one. In the first group of cells, we averaged the fluorescence signals in the whole hair bundle and recorded stimulus-evoked Ca<sup>2+</sup> transients with onset time constant ( $\tau$ ) of 0.26±0.19 s. To investigate the location

of mechanoelectrical transduction channels, the open channel blocker dihydropyridine (DHSM, 100 µM) was applied. DHSM significantly increased the time constant to  $\tau = 2.14 \pm 1.36$  s. The effect was essentially reversible ( $\tau = 0.75 \pm 0.24$  s) after washout. The onset of the Ca<sup>2+</sup> signal was consistently delayed at the apical area relative to the basal area (< sample time of 1 s). This delay was absent in the presence of DHSM. For the second cell group, Ca<sup>2+</sup> signals from the tip-link region in all the three rows of SC were obtained using the linescan method. Although, the fluorescence signal was at the same level before stimulation in all the three rows, the signal was faster and larger in the shortest row by a factor of 1.4±0.5 and 2.3±1.8, respectively.

The results suggest that transduction channels are located at only one end of the tip link, namely at the lower end. However, Ca<sup>2+</sup> entry into the SC of isolated OHCs is not restricted to the transduction channels.

## **[51] Inner Hair Cell Stereocilia Micromechanics**

Jessica Levi<sup>1</sup>, Jacob Kopperman<sup>1</sup>, Peter Dallos<sup>1,2</sup>, Claus-Peter Richter<sup>1</sup>

<sup>1</sup>Northwestern Feinberg School of Medicine,

<sup>2</sup>Northwestern University Department of Communication Sciences and Disorders

Outer hair cell stereocilia bundles are firmly embedded into the tectorial membrane (TM). Therefore, relative movements between reticular lamina (RL) and TM deflect outer hair cell stereocilia bundles. In contrast to outer hair cell stereocilia, inner hair cell stereocilia are weakly or not attached to the TM. Complex hydromechanical interactions between the inner hair cell stereocilia, the surrounding fluid, and the tectorial membrane deflect the bundle. We performed experiments in order to determine stereocilia motion, vis-à-vis TM and RL, in the gerbil hemicochlea at basal and middle turn locations.

Gerbil hemicochleae were placed on the stage of an upright microscope. While cochlear partition movements were induced via a paddle immersed in the fluid below the basilar membrane, magnified images of the TM, stereocilia bundles, and RL were captured during one stimulus cycle. Using a video flow technique, displacements of selected structures were measured. Vibration magnitudes and phases were determined from Lissajous figures.

TM movements were mostly transversal (perpendicular to the RL) above the outer hair cells and at the Hensen's stripe, whereas RL vibrations were predominantly radial at the pillar heads, becoming increasingly transversal towards the third row of outer hair cells. At the Hensen's stripe, movements at the TM and at the tip of the inner hair cell stereocilia bundle were almost perpendicular to each other. Moreover, movements at the stereocilia bundle tip were larger in comparison to those obtained from the inner hair cell cuticular plate. No phase differences between TM and the RL were observed for the transversal movements. However, for radial movements (parallel to the reticular lamina) phase differences are present between TM and inner hair cell stereocilia bundles. The phase differences change with frequency.



## **[52] Do Short-Wave Effects Suppress the Reflection of Cochlear Traveling Waves?**

**Christopher A. Shera**<sup>1</sup>, Arnold Tubis<sup>2</sup>, Carrick L. Talmadge<sup>3</sup>

<sup>1</sup>*Eaton-Peabody Laboratory, Boston, MA*, <sup>2</sup>*Institute for Nonlinear Science, La Jolla, CA*, <sup>3</sup>*National Center for Physical Acoustics, University, MI*

Existing theory suggests that wave reflection by mechanical perturbations or other rapid spatial variations in the partition impedance is strongly suppressed in the short-wave regime near the peak of the traveling wave (Zwislocki 1983, 2002; de Boer 1983). If so, current understanding of OAE generation---based largely on the 1d long-wave model of cochlear mechanics---needs substantial revision. To understand how the short-wave behavior near the peak of the traveling wave modifies the predictions of the long-wave theory, we solve the scattering problem in a 2d cochlear model that supports both long waves and short waves and the transition between the two. Contrary to existing theory, reflection from the peak region is actually significantly enhanced by the short-wave hydrodynamics. We discuss the implications of these results, both for the generation of reflection-source otoacoustic emissions and for the nature of the cochlear amplifier.

## **[53] Do Different SFOAE Measurement Methods Yield Equivalent Results?**

**Radha Kalluri**<sup>1,2</sup>, Christopher A. Shera<sup>2</sup>

<sup>1</sup>*Massachusetts Institute of Technology, Cambridge, MA*,

<sup>2</sup>*Eaton Peabody Laboratory of Auditory Physiology, Boston, MA*

Stimulus-frequency otoacoustic emissions (SFOAEs) have been measured using methods based on (1) suppression, (2) compression, and (3) spectral smoothing. Each of these methods exploits a different cochlear phenomenon to extract the emission. The suppression technique (e.g., Shera and Guinan, 1999) makes use of cochlear two-tone suppression. The SFOAE is defined as the complex (or vector) difference between the probe-frequency ear-canal pressure measured first using the probe tone alone and then remeasured in the presence of an additional "suppressor" tone. The suppressor tone is assumed to eliminate all or part of the emission evoked by the probe. The compression technique (e.g., Kemp and Chum, 1980) makes use of the OAE's compressive growth with stimulus level. The SFOAE is defined as the complex difference between the probe-frequency pressure measured at one probe level and a linearly scaled-down version of the pressure measured at a higher probe intensity. The spectral-smoothing technique (e.g., Shera and Zweig, 1993) makes use of the time delay between the stimulus and the emission. The SFOAE is defined as the complex difference between the probe-frequency pressure spectrum and a smoothed spectrum obtained using signal-processing techniques. The method is equivalent to time-domain windowing (i.e., IFFT analysis). Although it is

generally assumed that these various techniques for measuring SFOAEs all yield equivalent results, this equivalence has never been established. We report, compare, and contrast the SFOAEs measured in humans using each of these three techniques.

## **[54] Local and Propagating Components of Stimulus Frequency Otoacoustic Emissions** **Jonathan Siegel**<sup>1</sup>

<sup>1</sup>*Northwestern University, Hugh Knowles Center, Dept. Of Communication Sciences and Disorders*

Stimulus frequency otoacoustic emission (SFOAE) evoked by a low level probe tone  $f_p$  can be demonstrated by using a suppressor tone to separate the stimulus and emission pressures in the ear canal. If  $f_p$  is changed in small steps and SFOAE demonstrated using a moderate-level suppressor tone ( $f_{sn}$ ) close in frequency to  $f_p$ , then the phase of the emission changes relatively rapidly with  $f_p$ , indicating a relatively long delay. However, if a suppressor tone ( $f_{sh}$ ) is presented an octave or more higher than  $f_p$ , then the slope of the emission phase is much shallower, indicating a relatively short delay (Siegel et al., ARO Abst. 26: 172, 2003).

These results could be explained if  $f_{sn}$  acts primarily on SFOAE generators near the peak of the response to  $f_p$ , while  $f_{sh}$  acts primarily on generators basal to the peak where the phase of the mechanical response to  $f_p$  varies slowly with distance. But the phase of SFOAE demonstrated by  $f_{sh}$  typically shows quasiperiodic variations around the trend that correspond to similar variations in magnitude, suggesting interaction between emission components with different delays. Although the primary region of interaction between  $f_p$  and  $f_{sh}$  is presumably in the basal region effectively stimulated by  $f_{sh}$ , it appeared that the component with longer delay might originate near the peak region for  $f_p$  where there is no significant response to  $f_{sh}$ .

To test this hypothesis,  $f_p$  was always presented in combination with a suppressor of similar frequency ( $f_{sn}$ ) in an attempt to selectively remove generators from near the  $f_p$  place and so reduce their contribution to the SFOAE demonstrated by  $f_{sn}$ . The phase variations evident when presenting  $f_{sh}$  alone were reduced considerably in the presence of  $f_{sn}$ .

These results suggest that  $f_p$  initially excites basal SFOAE generators which subsequently induce apical propagation to the region of the place of  $f_p$  and secondary excitation of generators in this region. This scenario is similar to the two-source model proposed for DPOAE (Brown, et al., JASA, 100: 3260, 1996). But there is no evidence in basilar membrane measurements for suppression of a low-level tone  $f_p$  near the place of a much higher-frequency suppressor tone, so the suppression of  $f_p$  by  $f_{sh}$  in our experiments presumably originates in and propagates directly from the hair cell stereocilia bundles.

Supported by NIH grant DC-00419 and Northwestern University.

## **[55] Changes 2f<sub>2</sub>-F<sub>1</sub> Amplitude and Phase When the Level and Frequency of the Primaries Are Manipulated**

**Glenis Long**<sup>1</sup>, Carrick L. Talmadge<sup>2</sup>, Changmo Jeung<sup>1</sup>

<sup>1</sup>Graduate Center CUNY, <sup>2</sup>NCPA, University of Mississippi

Examination of the level and phase 2f<sub>2</sub>-f<sub>1</sub> generated by logarithmically sweeping f<sub>2</sub> from 1000-4000 Hz (f<sub>2</sub>/f<sub>1</sub>=1.22) reveals that 2f<sub>1</sub>-f<sub>2</sub> is larger at the lowest frequencies tested, a pattern of amplitude maxima is seen which differs from the fine structure seen in 2f<sub>1</sub>-f<sub>2</sub>. At low levels, the phase decreases rapidly with increasing frequency, but the phase becomes more gradual at the highest stimulus levels tested (L<sub>1</sub>=L<sub>2</sub>=75 DB SPL. We hypothesize that 2f<sub>2</sub>-f<sub>1</sub> is generated at the overlap region near f<sub>2</sub>, and leaks evanescently to its own best frequency place. Once it is at its own place it acts as an ordinary source for linear place-fixed retrograde waves with rapidly sloping phase. A portion of the signal reaching the base is reflected back apically, producing an interference pattern. When the f<sub>2</sub>-generation region is broader (low frequencies or higher stimulus levels), more 2f<sub>2</sub>-f<sub>1</sub> leaks into the 2f<sub>2</sub>-f<sub>1</sub> propagating region. At higher 2f<sub>2</sub>-f<sub>1</sub> levels, the nonlinear reflection dominates and the slope of the phase decreases.

## **[56] Controlling Reflected Contributions to Ear-Canal DPOAEs in Humans**

**Tiffany Johnson**<sup>1</sup>, Judy Kopun<sup>1</sup>, Stephen Neely<sup>1</sup>, Michael Gorga<sup>1</sup>

<sup>1</sup>Boys Town National Research Hospital

As typically recorded in the human ear canal, distortion product otoacoustic emissions (DPOAEs) may contain contributions from two different cochlear sources, a distortion source and a reflection source. The interaction of these sources produces the microstructure that is often observed in DPOAE responses. The reflection-source contribution may be reduced or eliminated by presenting a suppressor tone near the 2f<sub>1</sub>-f<sub>2</sub> frequency. In this study, we evaluated the relationship between suppressor level (L<sub>s</sub>) and L<sub>2</sub> in order to determine the L<sub>s</sub> that is most effective at reducing microstructure (and the reflection-source contribution). The influence of L<sub>s</sub> on DPOAE microstructure was evaluated in 1/3-octave bands with f<sub>2</sub> centered at 2 and 4 kHz. L<sub>2</sub> ranged from 20 to 80 dB SPL. L<sub>s</sub> was set according to the relation L<sub>s</sub>=0.75\*L<sub>2</sub>+C. Multiple values of C were tested, resulting in L<sub>s</sub> conditions ranging from -20 to +40 dB re: L<sub>2</sub>, depending on L<sub>2</sub>. Data were collected around both f<sub>2</sub>'s from four normal-hearing ears. The results indicated that one or more L<sub>s</sub> at each L<sub>2</sub> were effective at reducing or eliminating DPOAE microstructure without reducing the overall level of the distortion. However, no single L<sub>s</sub> could be chosen that achieved this in all subjects. Stated another way, a single L<sub>s</sub> could not be chosen for each L<sub>2</sub> that would result in reflection-source suppression without also suppressing the distortion-source contribution. In addition, the prevalence of microstructure (peak-to-valley ratio ≥ 10 dB in one cycle) varied across the two f<sub>2</sub> frequency regions. Of 12 subjects screened at 2 kHz, 11 exhibited microstructure. However, of 22 subjects screened at 4 kHz, only 5 exhibited microstructure. The

relative paucity of subjects exhibiting microstructure at 4 kHz suggests that uncontrolled cochlear-source contribution may not play a major role in limiting DPOAE test performance, at least not at 4 kHz. [Work supported by the NIH – NIDCD F32-DC007536, R01-DC02251, P30-DC04662].

## **[57] A Harmonic Difference-Tone Component in Low-Frequency Human DPOAEs?**

Deanna Meinke<sup>1</sup>, Glen Martin<sup>2</sup>, Barden Stagner<sup>2</sup>

<sup>1</sup>Audiology and Speech-Language Sciences, University of Northern Colorado, <sup>2</sup>Research Service, Jerry Pettis Memorial Veterans Medical Center

Distortion-product otoacoustic emission (DPOAE) level/phase maps similar to those described by Knight and Kemp (2000) were collected with the DPOAE frequency range extended to lower frequencies in 20 normally hearing subjects. To construct the DPOAE ratio vs level and phase plots, DPOAEs were measured in DPOAE frequency steps of approximately 44 Hz from 0.5-6.0 kHz in response to primary-tone sweeps at three levels (80,80; 75,75; 65,55 dB SPL), using constant f<sub>2</sub>/f<sub>1</sub> ratios incremented in 0.025 steps from 1.025-1.5. DPOAE level was directly plotted while the phase was corrected for primary-tone phase variation and unwrapped before plotting. The 2f<sub>1</sub>-f<sub>2</sub> DPOAEs showed "wave-fixed" phase patterns at standard f<sub>2</sub>/f<sub>1</sub> ratios of 1.21 and "placed-fixed" phase behavior for closely spaced f<sub>2</sub>/f<sub>1</sub> ratios. The 2f<sub>2</sub>-f<sub>1</sub> DPOAE, when present, showed place-fixed behavior. A large low-frequency 2f<sub>1</sub>-f<sub>2</sub> DPOAE component at DPOAE frequencies between 0.5 and approximately 1.36 kHz was apparent. This component was present across all f<sub>2</sub>/f<sub>1</sub> ratios greater than approximately 1.28 and in many subjects DPOAE levels reached 20-24 dB SPL. This emission showed wider phase banding than a similar component at f<sub>2</sub>/f<sub>1</sub> ratios less than approximately 1.28. Group delay derived from f<sub>1</sub> sweeps at constant f<sub>2</sub> frequencies of 1.5 and 2.0 kHz indicated that this wide-ratio component had a shorter group delay (3.6 ms) than the component present (4.0 ms) at more traditional f<sub>2</sub>/f<sub>1</sub> ratios. In suppression-tuning curve studies in humans (Martin et al., 2003) regions of suppression/enhancement were observed above f<sub>2</sub> that were most prominent for f<sub>2</sub> frequencies near 1.1 and 2.2 kHz. This phenomenon might in some circumstances involve a harmonic of f<sub>1</sub> interacting with f<sub>2</sub> to produce a difference tone at the 2f<sub>1</sub>-f<sub>2</sub> frequency that coincides with the measured DPOAE frequency (Fahey et al., 2000). The phase and latency of the low-frequency DPOAE component is consistent with this hypothesis. (NIDCD DC000613, DC003114).

## **[58] Upper and Lower DPOAE Sidebands Don't Play the Same Tune**

**Barden Stagner**<sup>1</sup>, Glen Martin<sup>1</sup>, Paul Fahey<sup>2</sup>

<sup>1</sup>Research Service, Jerry Pettis Memorial Veterans Medical Center, <sup>2</sup>Dept. of Physics/Electrical Engineering, University of Scranton

It is well established that there are significant differences in the behavior of the lower sideband (LSB) 2f<sub>1</sub>-f<sub>2</sub> DPOAE as compared to the upper sideband (USB) 2f<sub>2</sub>-f<sub>1</sub> DPOAE in

both humans and animals. Thus, DPOAE suppression tuning curves (STCs) of the  $2f_1$ - $f_2$  DPOAE tune near the  $f_2$  place whereas STCs of  $2f_2$ - $f_1$  tend to tune at or above the DPOAE frequency. Latencies of  $2f_1$ - $f_2$  DPOAE are longer than latencies of the  $2f_2$ - $f_1$  DPOAE. Finally, phase of the  $2f_1$ - $f_2$  DPOAE behaves like a "wave fixed" or nonlinear distortion source at its optimal ratio while phase of  $2f_2$ - $f_1$  DPOAEs behaves like a "place fixed" or linear reflection source. These findings suggest that there are fundamental differences in the generation and/or reemission of LSB as compared to USB emissions. To determine if the above differences apply in general to all LSBs as compared to USB DPOAEs as many LSB ( $2f_1$ - $f_2$ ,  $3f_1$ - $2f_2$ ,  $4f_1$ - $3f_2$ ,  $5f_1$ - $4f_2$ ) and USB ( $2f_2$ - $f_1$ ,  $3f_2$ - $2f_1$ ,  $4f_2$ - $3f_1$ ,  $5f_2$ - $4f_1$ ) DPOAEs that could be reliably detected above the noise floor were studied in awake rabbits. Harmonic otoacoustic emissions (HOAEs) of single tones (2f, 3f) were also included. Group delays, high resolution STCs and detailed DPOAE level/phase maps were collected for the four LSB and USB DPOAEs. Overall, the findings confirmed previous studies in that as a class, LSB emissions had longer group delays than USB emissions. STC findings revealed that all LSB DPOAEs tended to tune near  $f_2$  while USB DPOAEs and HOAEs exhibited complex tuning at and above the DPOAE or HOAE frequency. The possible role of evanescent excitation in the generation of USB emissions will be related to the different phase and suppression characteristics of USB versus LSB emissions. (Supported by NIDCD DC000613, DC003114).

#### **[59] Modulation Contours of Low-Frequency Biased DPOAEs** **Lin Bian<sup>1</sup>**

<sup>1</sup>*Speech and Hearing Science, Arizona State University*

Distortion products (DPs) in cochlear responses are indicators of inner ear function since they are generated from the nonlinearity in cochlear transduction. A low-frequency bias tone can modulate cochlear gain by shifting the operating point (OP) along the sigmoid-shaped transducer function. Therefore, the modulation of DP otoacoustic emissions (DPOAEs) due to low-frequency biasing reflects the nonlinear characteristics of the transducer curve at varying OPs. Previous studies showed that a bias tone at 20 Pa was effective in modulating DPOAEs, however, effects of lower level bias tones are not yet known. One way to evaluate the effect of low-frequency modulation is to measure the sidebands of the DPs, because low-frequency biasing produces an amplitude modulation of DPOAEs in time domain. Magnitudes of the multiple sidebands in frequency domain are directly related to the temporal modulation patterns of the DPs. To explore the variation of DP sidebands, DPOAEs evoked with a range of primary levels were recorded in gerbils while stepping the bias tone level from 20 to 0 Pa. A DPOAE modulation contour was constructed for various sidebands of different DPs. The absolute sideband amplitudes grew with both primary and bias levels and expanded beyond the signal limits. Another measure was the sideband magnitude relative to that of the corresponding DP that reflected the nonlinear interactions between the bias tone and primaries. The modulation contours of the relative sideband amplitudes

demonstrated limited areas of plateau indicating the optimal modulation conditions. The primary levels for maximal modulation ranged from 50 to 60 dB SPL for odd order DPs and 60 to 70 dB SPL for even DPs. Whereas the bias tone levels for a full modulation of various DPs tended to be just above 8 Pa (112 dB SPL). The modulation contour is useful in determining the lowest effective signal levels for recording low-frequency modulation of DPOAEs to avoid over-suppression.

*Supported by NIH/NIDCD grant: R03 DC006165*

#### **[60] Transducer Operating Point Changes During Endolymph Volume Manipulations Detected by Low-Frequency Biased F2-F1 Acoustic Emissions** **Alec Salt<sup>1</sup>, Shane Hale<sup>1</sup>**

<sup>1</sup>*Department of Otolaryngology, Washington University School of Medicine, St. Louis, MO*

Previous studies have shown that even order distortions generated by the ear ( $2f$ ,  $f_2$ - $f_1$ ) are sensitive to disturbances of the resting position of the cochlear transducer. At the level of the cochlear microphonics (CM),  $2f$  distortion changes were shown to be almost totally accounted for by operating point (resting position) changes during endolymph volume manipulations (Sirjani et al. JASA 115, 1219, 2004). At the level of the ear canal, a number of studies have shown that treatments that disturb endolymph volume induce greater changes in  $f_2$ - $f_1$  distortion than  $2f_1$ - $f_2$ . However, a quantitative interpretation of these  $f_2$ - $f_1$  distortion changes has not so far been possible. Low frequency biasing of the  $f_2$ - $f_1$  acoustic emission provides a tool to extract operating point data that aid in the interpretation of distortion changes. In the present study, CM and acoustic emissions were measured simultaneously to a variety of stimulus combinations, specifically 500 Hz 90 dB SPL without bias; 4000 Hz, 4800 Hz 80 dB SPL without bias and 4000 Hz, 4800 Hz 80 dB SPL 80 with low frequency bias at 4.8 Hz, 110 dB SPL. Responses were monitored sequentially during endolymph volume manipulations. Injections of artificial endolymph were performed in the second turn of the guinea pig cochlea at 100 nl/min for 10 min. A second injection at the same rate was performed at various times after the first. During the initial injection, operating point derived from CM recordings moved positive in most animals while operating point derived from low frequency biased emissions moved negative in all animals. During the second injection, operating point derived from CM and emissions measurements both moved positive. These data show that operating point changes can be resolved from  $f_2$ - $f_1$  emissions in the ear canal, but operating point changes are complex and may vary in different locations along the cochlea.

*Supported by grant NIH/NIDCD RO1 DC01368*

#### **[61] High-Frequency Click-Evoked Otoacoustic Emissions and Behavioral Thresholds in Humans** **Shawn S. Goodman<sup>1</sup>, Denis F. Fitzpatrick<sup>1</sup>, John C. Ellison<sup>1</sup>, Walt Jesteadt<sup>1</sup>, Douglas H. Keefe<sup>1</sup>**

<sup>1</sup>*Boys Town National Research Hospital*

The relationships at high frequencies between click-evoked (CE) otoacoustic emissions (OAEs) and behavioral

thresholds are poorly understood. CEOAEs are typically measured up to 5 kHz, and standard test procedures for behavioral thresholds are lacking above 8 kHz. A long cylindrical tube of 8-mm diameter served as a reflection-less termination over the finite measurement duration, and was used to calibrate audiometric stimuli and design a CEOAE stimulus with flat acoustic power. Stimuli were presented using earphones and acoustic responses measured using a microphone (Etymotic ER-2 and ER-10B+). Audiometric calibrations in a 2 cm<sup>3</sup> coupler and the reflection-less termination were compared to assess the effects of local acoustic coupling between earphone and microphone. Measurements were made using variable extensions of the earphone capillaries beyond the probe face. CEOAE responses to 4000 repetitions of the stimulus were recorded at 9 probe levels. A suppressor click was presented 15 dB above the probe click level, and CEOAEs were extracted over a 0.5-16 kHz bandwidth using a residual procedure. Synchronous spontaneous OAEs were also recorded to help interpret CEOAEs. Audiometric thresholds were measured from 0.5-16 kHz using a computer-controlled maximum-likelihood method modified from that of Green (1993). Subject inclusion criteria included age from 10-30 years and hearing within normal limits up to 8 kHz. CEOAE responses were obtained in some ears up to 16 kHz. Some third-octave filtered CEOAE responses showed evidence of multiple internal reflections above 6 kHz. Input/output functions of CEOAE level and delay as a function of click stimulus level were constructed. At higher probe levels, CEOAEs were present at shorter time delays than expected for round-trip travel times associated with reflection-source emissions. Results on the relationships between CEOAE level and behavioral thresholds at frequencies up to 16 kHz will be presented. Supported by grants DC07023, DC03784, DC04662

**[62] Pure-Tone Threshold Estimation from Distortion Product Otoacoustic Emissions Measured as Vibration of the Human Eardrum**  
Diana Turcanu<sup>1</sup>, Ernst Dalhoff<sup>1</sup>, Anthony W. Gummer<sup>1</sup>

<sup>1</sup>*Department Otolaryngology, University Tuebingen, Tuebingen, Germany*

Distortion product otoacoustic emissions (DPOAE) were measured as vibration on the eardrum of normal hearing subjects, using a highly sensitive custom-built laser Doppler interferometer. Sound pressure was recorded with a probe-tube microphone within 4 mm of the eardrum.

We tested the hypothesis that being less dependent on the tympanic membrane as well as the ear-canal transfer characteristics, information about the physiological state of the ear can be disclosed more reliably than with conventional acoustic techniques.

For this purpose, we examined if the estimation of hearing threshold by means of extrapolating vibration DPOAE growth functions gives a better correlation in the vibration measurements than in the acoustic ones.

We found that the standard deviation of the estimates obtained with the laserinterferometric measurements (8.7 dB) was much smaller than that obtained for the classical

acoustic measurements (18.8 dB). This supports the hypothesis of better reliability of the vibration technique. Supported by the German Research Council, DFG GU 194/6-1.

**[63] Hybrid DPOAE/ASSR Measurements Using a Modified DPOAE Stimulus Setting**

Thomas Janssen<sup>1</sup>, Johann Oswald<sup>1</sup>, Thomas Rosner<sup>1</sup>

<sup>1</sup>*Technical University Munich*

Distortion product otoacoustic emissions (DPOAEs) and auditory steady state responses (ASSRs) both provide frequency specific and quantitative assessment of hearing capability. The high discrepancy in recording time (seconds for a DPOAE, minutes for an ASSR) arises the question: why wasting time, why not recording DPOAEs during ASSR measurements? The present study therefore addressed the question whether ASSRs and DPOAEs can be recorded simultaneously using a modified DPOAE stimulus setting in which one of the primary-tone is amplitude-modulated.

DPOAEs of frequency  $2f_1-f_2$  and ASSRs of modulation frequency 40 Hz were measured in 10 normal hearing subjects at test frequency  $f_2$  between 0.5 and 8 kHz ( $f_2/f_1=1.2$ ). Additionally, 80 Hz ASSR were measured binaurally with two tone pairs per ear. Primary-tone  $f_2$  was amplitude-modulated for eliciting ASSR. Primary-tone level  $L_2$  was fixed (54 dB SPL) whereas primary-tone level  $L_1$  was varied between 54 and 75 dB SPL for searching for the optimal primary-tone level ratio at which DPOAE level was highest. Average decrease in DPOAE level was 2.60 dB SPL (SD=1.38 dB) that one in ASSR amplitude 1.83 dB SPL (SD=2.38 dB) for the 40 Hz ASSR and 2.36 dB (SD=2.91 dB) for the 80 Hz ASSR, respectively, when comparing single and hybrid mode. ASSR amplitude considerably decreased for  $L_1$  exceeding 69 dB SPL.

Findings suggest simultaneous DPOAE and ASSR measurements to be feasible at primary-tone levels of up to 65 dB SPL. For compensating loss in amplitude and thus yielding single mode test quality, recording time has to be increased. However, longer recording time is only necessary at close-to-threshold responses where the signal-to-noise ratio is low. The advantage of a DPOAE stimulus setting in which one of the primary tone is amplitude- modulated over a stimulus setting with unmodulated tones is that optimal stimulation and thus maximum response amplitudes can be reached independent on test frequency for both ASSRs and DPOAEs.

**[64] Comparison of the Effects of Negative Middle-Ear Pressure and Ear-Canal Pressure Variation on Distortion Product Otoacoustic Emissions**

Xiao-Ming Sun<sup>1</sup>, Mark D. Shaver<sup>1</sup>

<sup>1</sup>*Wichita State University*

The measurement of otoacoustic emissions (OAEs) is susceptible to middle-ear pressure (MEP) variation since it requires the forward and backward transmission of acoustic signals through the middle ear. Systematic

investigation has not been conducted on the effect of actual negative MEP on OAEs. In previous studies, MEP variation was usually simulated by introducing a positive or negative air pressure into the ear canal or by varying ambient pressure in a pressure chamber. However, equivalency of the ear-canal pressure (ECP) to the MEP effects needs to be substantiated because they may exert different effects on the cochlea. In this study, the 2f1-f2 DPOAE was measured for the f2 frequencies from 0.6 to 8 kHz ( $f2/f1 = 1.20$  and  $L1=65$  dB and  $L2=50$  dB SPL) in 22 human ears with normal hearing. Negative MEP at six levels from -40 to -230 daPa was achieved by performing the Toynbee maneuver or sniffing with the nostrils held shut. Positive and negative ECPs were achieved at six levels by applying air pressure into the ear canal with the absolute values equal to those of the negative MEPs. The results displayed a substantial reduction of DPOAEs in the ears with negative MEPs, particularly for the frequencies of 1 kHz and below. Even in the MEPs of -40 to -65 daPa, the reduction was about 5 dB while it reached around 10 dB in the MEPs of -190 to 230 daPa. In general, DPOAE reduction decreased with increasing frequency with a minimal value for 2 kHz but increased for 3 kHz. Comparing to a corresponding negative MEP, a positive ECP caused a similar amount of reduction as the pressure was below 100 daPa. For higher pressures, positive ECP resulted in less reduction of DPOAEs particularly for 1 kHz and below. Negative ECPs caused significantly less reduction of DPOAEs for the frequencies below 4 kHz but greater reduction for higher frequencies. Preliminary data analyses suggested that both eardrum position and actual MEP determined sound transmission through the middle ear.

#### **[65] Predicting Cochlear Vulnerability in Humans by Means of Contralateral DPOAE Suppression**

**Susanne Dietrich<sup>1</sup>**, Joerg Mueller<sup>1</sup>, Thomas Janssen<sup>1</sup>

<sup>1</sup>*Technical University Munich*

The vulnerability to noise-induced hearing loss has long been known to be highly variable across subjects. A screening tool which distinguishes between "tough" and "tender" ears would be useful for preventing noise-induced hearing loss. Maison and Liberman (2000) found the reflex strength of the medial olivocochlear system, evaluated by ipsilateral DPOAE adaptation measurements, to be inversely correlated to the degree of noise-induced hearing loss in guinea pigs. Recent findings in humans (Müller and Janssen 2005) have shown that similar changes in DPOAE level also occur for contralateral DPOAE suppression at frequencies which are located in dips of the DPOAE fine-structure.

The purpose of the present study was to find out whether there is a correlation between noise-induced hearing loss and the magnitude of contralateral DPOAE suppression. High-resolution behavioral thresholds, DPOAE fine-structure, and contralateral DPOAE suppression using broadband noise (60 dB SPL) were measured in 16 volunteers who were exposed to noise in a discotheque. Exposure time was 3 hours. Maximum noise level was 106 dB(A).

When comparing data obtained before and directly after noise exposure, a temporary threshold shift (TTS) in the audiogram and DPOAE fine-structure could be observed. The degree of the TTS varied highly across subjects. However, there was a weak correlation between individual hearing loss and decrease in DPOAE level. Roughness of both audiogram and DPOAE fine-structure decreased with increasing hearing loss. Large DPOAE suppression effects were found in all subjects. However, in our subject sample magnitude of DPOAE suppression and thus efferent reflex strength was not correlated to the degree of the TTS, as it was observed by Maison and Liberman (2000) in guinea-pigs.

Further studies are necessary for answering the question whether contralateral DPOAE suppression may serve as a clinical tool for predicting cochlear vulnerability to sound overexposure.

#### **[66] Effects of Anaesthetic Type and Middle Ear Muscle Sectioning on Contralateral Suppression of DPOAE in the Guinea Pig**

**William Azeredo<sup>1</sup>**, Charles Woods<sup>1</sup>

<sup>1</sup>*SUNY Upstate Medical U*

The guinea pig is a commonly used species in studying the efferent auditory system, including those experiments involving the contralateral suppression of DPOAEs. Anaesthesia has previously been seen to affect medial olivocochlear activity. This is not uniform across anaesthetic types, but most cause some degree of dampening relative to the awake state. The question of possible middle ear effects has also been raised in other species. In the guinea pig, the middle ear reflex is not believed to contribute significantly based on the continued effects after paralysis, and the negation of effects after sectioning the olivocochlear bundle.

We have previously used ketamine/xylazine and acepromazine/ketamine as anaesthesia in chinchillas and rats prior to studying contralateral suppression of DPOAEs. We now examine the effect of ketamine/xylazine vs acepromazine/ketamine, on the contralateral suppression of DPOAEs. With each anaesthetic type, we then compare contralateral suppression across DP frequencies before and after sectioning the middle ear muscles.

#### **[67] Noninvasive Detection of Changes in Intra-Cranial Pressure Using Distortion-Product Otoacoustic Emissions**

**Susan Voss<sup>1</sup>**, Nicholas Horton<sup>1</sup>, Taronne Tabucchi<sup>2</sup>, Fopefolu Folowosele<sup>3</sup>, Christopher A. Shera<sup>4</sup>

<sup>1</sup>*Smith College*, <sup>2</sup>*Cornell University*, <sup>3</sup>*Johns Hopkins University, Baltimore, Maryland*, <sup>4</sup>*Massachusetts Eye and Ear Infirmary*

Intracranial pressure (ICP) monitoring is currently an invasive procedure that requires access to the intracranial space through an opening in the skull. Noninvasive monitoring of ICP via the auditory system is theoretically possible because changes in ICP transfer to the inner ear through connections between the cerebral spinal fluid and

the cochlear fluids. In particular, low-frequency distortion-product otoacoustic emissions (DPOAEs), measured noninvasively in the external ear canal, have been shown to have magnitudes that depend on intracranial pressure. Postural changes in healthy humans cause systematic changes in ICP. Here, we quantify the effects of postural changes, and presumably ICP changes, on DPOAE magnitudes while simultaneously monitoring the middle-ear static pressure and intra-subject variability over five measurement sessions per subject. DPOAE magnitudes were measured on seven normal hearing, healthy subjects at four postural positions on a tilting table (angles 90, 0, -30, and -45 degrees to the horizontal). At these positions, it is expected that ICP varied from about 0 to 22 mm Hg. DPOAE magnitudes were measured for a set of frequencies  $750 < f_2 < 4000$ , with  $f_2/f_1=1.2$ . For the low frequency range of  $750 < f_2 < 1500$ , the differences in DPOAE magnitude between upright and -45 degrees were highly significant (all  $p < 0.01$ ), and above 1500 Hz there were minimal differences between magnitudes at 90 degrees versus -45 degrees. There were no significant differences in the DPOAE magnitudes with subjects at the 90 and 0 degree postures. Changes in ICP can be detected using DPOAE magnitudes. In particular, changes are largest at low frequencies. Although this approach does not allow for absolute measurement of ICP, it appears that measurement of DPOAE magnitudes may be a useful means of monitoring ICP noninvasively.

#### **[68] Measurement of Distortion Product Otoacoustic Emissions (DPOAEs) in Immature Mice**

Yuya Narui<sup>1</sup>, Akira Minekawa<sup>1</sup>, Takashi Iizuka<sup>1</sup>, Katsuhisa Ikeda<sup>1</sup>, Takuji Koike<sup>2</sup>

<sup>1</sup>Juntendo University, <sup>2</sup>The University of Electro-Communications

**Objectives:** In recent years many studies regarding the measurement distortion product otoacoustic emissions (DPOAEs) in mice were performed for researching inner ear functions (outer hair cell functions). However, in small animals such as mice, their external auditory canal (EAC) is very narrow and their auditory frequency threshold level is very high. Therefore by using existent measuring instruments it is very difficult that we measure DPOAEs precisely. In this study, we developed the new system that could measure DPOAEs in mice easily and precisely to solve these problems. DPOAEs were measured in immature mice (14-21-day-old) with this system.

**Methods:** First, the new probe with two earphones and a microphone was designed and frequency characteristics of the probe were evaluated by using an EAC model and the reference microphone in order to prove whether it could measure DPOAEs precisely.

Second, immature mice were measured by the newly developed system. Two primary tones at frequencies  $f_1$  and  $f_2$  ( $f_2/f_1=1.20$ ) with the same SPL were emitted to the EAC by the two speakers. The computer program extracted the spectral component at  $2f_1-f_2$  from the acoustic sound pressure detected by the microphone of the probe.

**Results and Conclusions:** Frequency characteristics detected by the microphone of the probe were almost the same as that detected by the reference microphone. This result suggests that our probe can apply the correct DPOAEs.

And the input/output (I/O) functions of  $2f_1-f_2$  DPOAEs were recorded at 8, 20 and 30 kHz from 14-21-day-old mice. There were little individual difference in DPOAE I/O function at 8 kHz ( $f_1=10$  kHz,  $f_2=12$  kHz) and 20 kHz ( $f_1=25$  kHz,  $f_2=30$  kHz). By contrast, the individual difference at 30 kHz ( $f_1=37.5$  kHz,  $f_2=40$  kHz) was significant. The younger the mice were the more I/O function curves at 30 kHz tended to shift to the right i.e., to higher sound pressure level, compared with other frequencies. This result suggests that the cochlear functions at high frequencies have not yet matured in younger mice.

#### **[69] DPOAEs in the Locust Depend on the Integrity of the Sensory Organ**

Doreen Möckel<sup>1</sup>, Ernst-August Seyfarth<sup>1</sup>, Manfred Kössl<sup>1</sup>

<sup>1</sup>University Frankfurt am Main, Germany

The tympanal organs of insects emit distortion-product OAEs that are indicative of nonlinear ear mechanics. To test if the sensory neurons or their accessory cells are involved in DPOAE-generation, we used the ear of *Locusta migratoria*. The organ comprises ca. 80 scolopidia gathered in a peripheral sensory ganglion (Müller's organ). Each ciliated bipolar sensory neuron is coupled to the

tympanum via a cap (= accessory) cell. Within the organ, 3 groups of neurons are distinguished based on the exact attachment of their dendrites to the tympanum and on their frequency tuning.

(i) Mechanical ablation of high-frequency scolopidia (d-cells located in "pyriform vesicle") caused a selective drop (> 30 dB) of the DPOAE-level that is evoked by stimulus frequencies above 15 kHz. After ablation of the central part of Müller's organ (containing the somata of all 3 neurons groups), DPOAEs were no longer measurable across the entire frequency range tested here (5 to 30 kHz). The results demonstrate that the sensory neurons and/or their accessory structures are critically involved in frequency-specific generation of DPOAEs.

(ii) Electrical stimulation of the intact auditory nerve (short current pulses 4 to 10  $\mu$ A or DC-currents of 0.5  $\mu$ A) caused a decrease of DPOAEs by as much as 30 dB. The strength of the effect depended on current intensity. The decrease was reversible, and DPOAE-levels re-gained control values within 1 min after the end of electrical stimulation. Similar effects were seen following electrical stimulation via the cut end of auditory nerve preparations that had been severed from the central nervous system. The results suggest that the receptor neurons themselves are the source of a nonlinear amplification mechanism and hence of the production of otoacoustic emissions.

Supported by the DFG

## **70 A Comparative Study of Stimulus-Frequency Otoacoustic Emissions in Geckos and Humans**

**Christopher Bergevin<sup>1</sup>**, Christopher A. Shera<sup>2</sup>, Dennis M. Freeman<sup>3</sup>

<sup>1</sup>*Speech and Hearing Biosciences and Technology, MIT, Cambridge, MA*, <sup>2</sup>*Eaton-Peabody Laboratory of Auditory Physiology, MEEI, Boston, MA*, <sup>3</sup>*Dept of Electrical Engineering and Computer Science, MIT, Cambridge, MA*

Models of otoacoustic emission (OAE) generation mechanisms often attribute important features of OAEs to waves traveling along the cochlear partition. Since the lizard basilar papilla manifests no obvious analog of the mammalian traveling wave, detailed comparisons between lizard and mammalian OAEs offer an important opportunity to test and extend our knowledge of emission mechanisms. We report a comparison of the frequency and intensity dependence of human and leopard-gecko stimulus frequency emissions (SFOAEs). In both species, SFOAE amplitude-vs-frequency functions (measured at fixed level) and amplitude-vs-level functions (measured at fixed frequency) manifest pronounced notches. The characteristics of these notches suggest that they result from interference between two out-of-phase components. Preliminary data indicate that a subset of these notches in frequency and level space can be strongly correlated. We interpret the data in light of existing models and the known anatomical and functional differences between the two species.

Supported by grants T32 DC00038, RO1 DC003687 (CAS), and RO1 DC0023821 (DMF) from the NIDCD.

## **71 Examining the Basis of Cochlear Tuning with Measurements of Basilar Membrane Motion**

**Ombeline de La Rochefoucauld<sup>1</sup>**, Elizabeth Olson<sup>1</sup>

<sup>1</sup>*Columbia University*

The mechanism of passive cochlear tuning still raises questions. Early models of cochlear tuning consider the organ of Corti complex (OCC) as a succession of spring-mass resonators. Every segment of the OCC has a particular stiffness, mass and resistance and resonates at a given frequency. Later models show that the organ of Corti does not need to be resonant. Then the OCC is treated as a simple stiffness and tuning arises through the interaction of the 3-dimensional fluid (which plays the role of mass) and the stiffness of the OCC. The aim of this project is to see whether the mechanical response relies upon OCC mass. To answer this question the variation with frequency of the longitudinal curvature of the wave (inverse wavelength) is considered.

Curvature ( $k$ ) is found experimentally from measurements of basilar membrane (BM) vibrations by taking the difference in the phase of two closely spaced locations and dividing by the longitudinal distance between the measurements ( $k = -\Delta\phi/\Delta x$ ). The curvature gives robust results as it depends only on the phase of the response, which is not very sensitive to cochlear condition (as opposed to amplitude which varies greatly depending on the cochlear condition). BM vibrations in the basal region of a gerbil cochlea were measured using a heterodyne

interferometer coupled to a confocal microscope. As expected, the curvature increased (i.e. wavelength decreased) as the wave approached its best place. The experimental curvature-vs-frequency curve can be directly compared with modeling predictions to better understand the role of the OCC mass. The theoretical curvature is a solution of the dispersion relation of a 3D cochlear model developed by de Boer, where the mass and stiffness values of the OCC are treated as free parameters. The stiffness values of the model are consistent with independent BM point stiffness measurements. Theoretical curves with significant OCC mass are compared to the ones in which the OCC mass is negligible. When OCC mass is included in the theoretical curvature, the curvature grows more rapidly than it does when only the fluid has significant mass. Based on these preliminary results, the experimental data are better fit by the model that includes OCC mass.

Supported by the NIDCD and the Emil Capita Foundation

## **72 Measurement of Reverse Traveling Wave in the Gerbil Cochlea**

**Wei Dong<sup>1</sup>**, Elizabeth Olson<sup>1</sup>

<sup>1</sup>*Columbia University*

Sound enters the cochlea and is carried along the sensory tissue of the cochlear partition as a forward traveling wave. Sound can also emerge from the cochlea to the ear canal, being detected as an otoacoustic emission (OAE). However, how the sound travels out of the cochlea remains unclear. The concept of backward traveling waves has been well developed in the cochlear mechanics literature. Intracochlear disturbances that result in OAEs are thought to travel backwards along the basilar membrane (BM) in the form of intracochlear pressure difference waves (i.e., exactly the reverse of forward traveling waves). However, based on his measurements, Ren (2004) argued that OAEs travel out of the cochlea directly through the cochlear fluids, rather than as a reverse wave along the cochlear partition. It is not a simple matter to relate intracochlear measurements to emissions in order to explore the properties of, or even to clearly detect, backward traveling waves. This is in part because the intracochlear sound source for an OAE is not a well defined point, and it likely moves along the sensory tissue as the frequency of the stimulus changes. This is in contrast to inward traveling waves, in which the source is located at the stapes. The verified presence of reverse waves would advance our understanding of cochlear operation.

In this contribution we report a direct measurement of reverse traveling waves using an intracochlear pressure sensor. The pressure sensors have been used in past measurements to study cochlear wave mechanics and nonlinearity. Pressure responses were recorded simultaneously in scala tympani (ST) close to the BM in the basal turn of gerbil cochlea, and in the ear canal (EC). Current stimuli were delivered at the round window in some experiments; in others two tones were delivered to the ear canal. In all experiments single tone stimuli provided a measure of forward transmission. The new



development of these measurements is that the sensor introduced into ST close to the BM apparently served as a fixed intracochlear reflection, which sourced an OAE. The pressure measured in ST was compared with the pressure measured in the EC. By analyzing the relative phases, reverse traveling waves were detected.

### **[73] Compressibility of the Cochlea** **Tianying Ren<sup>1</sup>**

<sup>1</sup>*Oregon Health & Science University*

One fundamental assumption in cochlear mechanics is that the fluid-filled cochlea is incompressible. This implies that the speed of sound in the cochlea is the same as that in water, or is 'infinite'. In spite of its fundamental importance and wide applications this assumption has not been satisfactorily tested experimentally. This study investigated the compressibility of the living cochlea by measuring the phase relationship between the stapes and round window membrane vibrations. Young, healthy gerbils with normal hearing were used in this study. The magnitudes and phases of the stapes and round window membrane responses to tone stimulation were measured as a function of frequency using a laser interferometer. The group delay from the stapes to the round window membrane was calculated based on the phase difference of the two window vibrations as a function of the frequency. The data show that the group delay from the stapes to the round window membrane is more than 15  $\mu$ s. Considering the physical dimensions of the cochlea, the data indicate that speed of sound in the cochlea is much slower than that in water. This indicates that the cochlea is more compressible than water.

Supported by NIH-NIDCD and VA RR&D Center Grant, Portland, VAMC.

### **[74] Mechanism of a Cochlear Fluid Compression Wave in Otoacoustic Emission Generation** **Tianying Ren<sup>1</sup>, Wenxuan He<sup>1,2</sup>**

<sup>1</sup>*Oregon Health & Science University*, <sup>2</sup>*Xian Jiaotong University*

It has been recently demonstrated that the backward propagation of the otoacoustic emission is much faster than the forward propagation of sounds in the cochlea, which indicates that the emission reaches the cochlear base through the cochlear fluids as a pressure wave rather than through the basilar membrane as a backward traveling wave. This study investigates how the proposed cochlear compression wave works by observing the relationship between the stapes and the round window membrane vibrations. Cubic distortion product otoacoustic emissions (DPOAEs) were evoked by f1 and f2 primary acoustic tones and measured in the ear canal in the gerbil. The magnitude and phase of the round window membrane and stapes vibration at the DPOAE frequency were measured as functions of emission frequency at different intensities, and at different f2 frequencies. It was found that near the f2/f1 ratio of 1.2, at which the maximum DPOAE is generated, the phase difference between the round window membrane and stapes footplate vibration is approximately 180 degrees. This phase difference became

smaller as f2/f1 decreased. When f2/f1 is close to one, the round-oval window phase difference trends toward zero. As f2/f1 increases from 1.2, the phase difference increases. This f2/f1-dependency of the phase difference between the windows becomes more significant at lower f2 frequencies. The antiphase vibrations of the round and oval window indicate the existence of a pressure difference across the basilar membrane. Like an external sound, the antiphase vibration of two cochlear windows and pressure difference across the basilar membrane results in a forward traveling wave. However, the in-phase vibration of two windows at the f2/f1 close to one indicates a different fast transmission mechanism in the cochlea.

Supported by NIH-NIDCD and VA RR&D Center Grant, Portland, VAMC.

### **[75] Baseline Shifts Measured in the Human Ear Canal Related to Distortion Product Generation and Two Tone Suppression**

**Eric LePage<sup>1</sup>, Narelle Murray<sup>1</sup>, John Seymour<sup>2</sup>**

<sup>1</sup>*OAEricle Laboratory*, <sup>2</sup>*National Acoustic Laboratories*

Recently we demonstrated the results of a two-tone experiment which resulted in baseline movements of ear canal pressure, and suggestive of two-tone suppression at the cochlear mechanical level. These "dc-shifts" evident in the otoacoustic waveform did not appear to be due to middle ear muscle effects, which could be demonstrated separately. We here show the relationship between these baseline shifts and the resulting distortion products generated. Two tones bursts were delivered as a masker type experiment -- a 25 ms long probe tone of fixed frequency (3kHz) and level (70dB SPL) plus a "masker" tone burst of 7 ms which varied over a grid from 0.5 octaves above and below the probe tone, and from 50 to 90 dB SPL. We show the pattern of baseline shifts towards rarefaction and condensation according to the masker parameters for different subjects. Also shown are how the distortion products vary with the baseline variation and separation of the primaries (i.e. the probe and masker) while both tones are present. These baseline shifts constitute "infrasonic" otoacoustic products, and, because of their relationship to the distortion products derived from the same records, are associated with cochlear mechanical generation.

### **[76] Intracochlear Pressure from a Three-Dimensional Linear Model**

**Yongjin Yoon<sup>1</sup>, Sunil Puria<sup>1,2</sup>, Charles Steele<sup>1</sup>**

<sup>1</sup>*Stanford University, Department of Mechanical Engineering*, <sup>2</sup>*Department of Otolaryngology-HNS*

A physiologically based three dimensional cochlear model is developed. The model includes the three-dimensional viscous fluid effects and the pectinate zone of the Basilar Membrane (BM), which is represented as an elastic orthotropic plate with dimensional and material property variation along its length. Active mechanics is represented by adding the Outer Hair Cell (OHC) motility to the passive model with linear feed-forward mechanism of organ of Corti. A hybrid WKB asymptotic and numerical method



combined with Fourier series expansions is used to provide a fast and efficient iterative procedure.

First, the passive model is in excellent agreement with the cochlear Characteristic Frequency (CF) map from Eldredge et al. (1981, JASA). Second, the BM amplitude and phase for the passive model at 3.5 mm from the base is compared with the measurements of the chinchilla's cochlea (Ruggero et al. 1997, JASA) and shows a good agreement in both magnitude and phase. Third, the BM amplitude and phase for the feed-forward linear active model is compared with the experimental results (Ruggero et al. 1997, JASA) with 0.17 feed-forward gain factor. The BM amplitude for the linear active model shows 28 dB amplification.

The pressure response for the slow traveling wave is calculated at 3.5 mm from the base. The pressure on the BM from the active model shows 12 dB amplification, which is 16 dB less than the amplification of the amplitude response. Additionally, the intracochlear pressure, 50  $\mu$ m away from the BM, at 3.5 mm from the base with the 80 dB input SPL shows 4 dB amplification effect which is observed in the Dong and Olson's current experiments (2005, JASA)

Additional complexity will be added to the current three-dimensional cochlear model. These include (1) compressive fast waves, (2) reverse traveling waves, and (3) nonlinear feed-forward active model (Lim and Steele, 2002, HR). The BM amplitude, phase and intracochlear pressure for the nonlinear active model with fast wave will be calculated and the simulation result will be compared with intracochlear pressure and Distortion Product OtoAcoustic Emissions (DPOAE) measurements for the gerbil cochlea from Dong and Olson (2005, JASA).

## **[77] Active Bidirectional Coupling by Outer Hair Cells Realizes the Cochlear Amplifier**

**Bo Wen<sup>1</sup>, Kwabena Boahen<sup>1</sup>**

<sup>1</sup>*University of Pennsylvania*

Cochlear models yield insight into cochlear micromechanics if they produce responses comparable to physiological measurements. A current focus of cochlear modeling is to better understand the role outer hair cells (OHCs) play in the cochlear amplifier. Taking into account cochlear microanatomy, we have modeled the transmission of outer hair cell motile forces to the basilar membrane (BM) through Deiters' cells (DCs) and their phalangeal processes (PhPs). We proposed that, due to the longitudinal tilt of the OHC towards the base and the oblique orientation of the PhP towards the apex, each BM segment receives feed-forward and feed-backward forces, from upstream and downstream segments, respectively. Through these bidirectional forces, the otherwise weakly coupled BM transverse fibers are actively coupled longitudinally, included in a cochlear model for the first time here.

Active bidirectional coupling (ABC), when added to a passive cochlear model, boosts frequency-selective amplification of BM responses, sharpening frequency tuning as well as increasing sensitivity. When saturation of OHC forces is included as well, the model produces

physiologically comparable responses, exhibiting compressive growth near the characteristic place (CP) at high sound levels. In addition, when two tones are present, the louder one suppresses the other, to a larger extent when their frequencies are similar. To obtain insight into how ABC realizes the cochlear amplifier, we analyzed the traveling wave at low sound levels, revealing that ABC leads to negative damping right before the CP, where the shortening traveling wave becomes comparable to the OHC and PhP tilt distance. In summary, our simulations and analysis show that ABC amplifies the traveling wave around the CP, resulting in large gain, sharp tuning, high sound-level compression, and two-tone suppression.

## **[78] The Dynamics of Medial Olivocochlear Efferent Fast Effects on Basilar Membrane Motion**

**Nigel Cooper<sup>1</sup>, John J. Guinan, Jr.<sup>2</sup>**

<sup>1</sup>*School of Life Sciences, Keele University, Keele, Staffordshire, UK,* <sup>2</sup>*Eaton-Peabody Lab., Mass. Eye & Ear Infirmary*

Activity in medial olivocochlear (MOC) efferent neurons decreases the cochlea's sensitivity to sound. At least some of this effect is caused mechanically, by decreasing the gain of the cochlear amplifier. We sought to determine the dynamics of this mechanical inhibition by measuring tone-evoked basilar membrane (BM) motion in the basal turn of the cochlea in anesthetized guinea pigs and chinchillas, at the same time as stimulating the MOC efferents with electrical shocks (e.g. 200 shocks/sec for 100 ms of every 330 ms). We found that both the onset and offset of efferent-evoked inhibition had approximately exponential time courses that varied with MOC shock level and sound pressure level. The attack time constant increased from ~30 ms at low sound levels to ~100 ms at high sound levels, and decreased slightly with increasing MOC shock level. The decay time constant (governing the BMs recovery from inhibition) decreased from ~80 ms to less than 20 ms with increasing sound level, and increased considerably (e.g. from 30 to 60 ms) with increasing MOC shock level. We also explored the effects of individual MOC shock-pulses by varying the duration of the shock trains. We observed that the potency of individual shocks increased substantially (e.g. by a factor of at least 2-3) with increasing "shock number", where potency was measured as either amplitude or duration of the inhibition produced by each shock. The individual shock data are consistent with the idea that presynaptic facilitation plays an important role in adult mammalian MOC to outer-hair-cell (OHC) synapses, as it does in developing inner hair cell synapses (cf. Goutman et al., 2005, J. Physiol. 566: 49-59) and in the turtle cochlea (cf. Art et al., 1984, J. Physiol. 356: 525-50). However, the dependence of the time constants on sound level indicates that post-synaptic factors in OHCs also play an important role in shaping the dynamics of MOC fast effects.

Supported by NIDCD RO1DC00235.

## **[79] An Isolated Gerbil Cochlea Preparation for Measuring Sound-Induced Micromechanical Motions**

**Scott Page**<sup>1</sup>, A.J. Aranyosi<sup>1</sup>, Dennis M. Freeman<sup>1</sup>

<sup>1</sup>MIT

The mechanical processes at work within the organ of Corti can be greatly elucidated by measuring both radial motions and traveling-wave behavior of structures within this organ in response to sound stimuli. To enable such measurements, we have developed a new preparation for observing three-dimensional motions of micromechanical structures in the apical region of an isolated gerbil cochlea. The cochlea is submerged in a low-chloride, low-calcium artificial perilymph solution and cemented to the bottom of a petri dish at an angle. The bone above scala vestibuli of one half of the apical turn is removed to allow optical imaging with a 40x, 0.8 NA water-immersion objective. Reissner's membrane is left intact. Illumination is provided with a blue LED coupled to an optical fiber. The fiber is positioned next to the bone surrounding scala tympani of the apical turn, so that the organ of Corti is illuminated from below. The resulting optical access allows imaging of a variety of structures that have been proposed to play a role in cochlear mechanics, including inner and outer hair cell bundles, the tectorial membrane, Deiters cells, inner and outer pillar cells, and efferent fibers in the tunnel of Corti. In some preparations, individual stereocilia of inner hair cell bundles can be resolved. Motions are stimulated by driving the stapes with a piezoelectric probe, and are measured using a stroboscopic computer microvision system. Preliminary measurements show that sub-micrometer motions of key structures in three dimensions can be quantified. This system enables quantitative studies of both the relative motions of structures within the organ of Corti in response to sound and the propagation of traveling waves along structures within the organ of Corti.

## **[80] Mutation in TECTA Alters the Fixed Charge Concentration of the Tectorial Membrane**

**Roosbeh Ghaffari**<sup>1,2</sup>, Kinuko Masaki<sup>1,2</sup>, Guy P. Richardson<sup>3</sup>, Dennis M. Freeman<sup>1,2</sup>

<sup>1</sup>Harvard-MIT HST Speech & Hearing Biosciences & Technology Program, <sup>2</sup>Massachusetts Institute of Technology, <sup>3</sup>University of Sussex, UK

The tectorial membrane (TM) is a critical mechanical structure in the cochlea. It contains an abundance of charged macromolecules, which are likely to contribute to the mechanical properties of the TM, as they do in similar tissues such as cartilage. To investigate the role of fixed charge, we excised TMs from a mouse model of a missense mutation in *Tecta* (a gene that encodes alpha-tectorin in the TM), which causes 50-80 dB hearing loss (Legan et al., 2005). We measured the fixed charge concentration (cf) of these TMs using a novel microfabricated planar patch clamp technique (Ghaffari & Freeman, 2005; Sigworth & Klemic, 2002). We found that the cf in mutant TMs was around 2.13 +/- 0.15 mmol/L, which is significantly smaller than the cf measured in normal mice (7.80 +/- 0.52 mmol/L). Based on a continuum model that relates electrostatic repulsion of fixed charge to

mechanical stiffness (Ghaffari & Freeman, 2005), we estimate that 2.13 mmol/L of negative fixed charge will contribute 0.026 kPa to the TM bulk modulus in *Tecta* mice. This is approximately a 25-fold reduction in the contribution of fixed charge to TM's bulk modulus in *Tecta* mice compared to the normal mice. Therefore, a decrease in the fixed charge concentration can reduce the TM's compressive mechanical rigidity and is a candidate for the functional basis of hearing loss in *Tecta* mice.

## **[81] TECTA Mutation Decreases the Shear Impedance of the Tectorial Membrane**

**Jianwen Gu**<sup>1</sup>, Kinuko Masaki<sup>1</sup>, Guy P. Richardson<sup>2</sup>, Dennis M. Freeman<sup>1</sup>

<sup>1</sup>Massachusetts Institute of Technology, <sup>2</sup>University of Sussex, UK

The shear impedance of the tectorial membrane (TM) plays a critical role in the interaction between the TM and the hair bundles. To determine whether a change in shear impedance is the underlying cause of the 50--80 dB hearing loss associated with a Y1870C missense mutation in *TECTA* (Legan et al. 2000, Lukashkin et al. 2004), we measured the shear impedance of TMs from normal and mutant mice using the microfabricated shearing probe (Gu et al. 2005). The magnitude of radial shear impedance fell with a slope of -16 dB/decade over the measured frequency range for TMs from both normal and mutant mice. The phase was near -80 degrees for both groups. However, the overall magnitude was about 4--8 dB lower for TMs from mutant mice. Results for longitudinal shear impedance were similar except that the slope fell with a slope of -19 dB/decade. The frequency range probed was 10--800 Hz in the radial direction and 10--9000 Hz in the longitudinal direction. These results show that one effect of the mutation is to alter the viscous and elastic components of TM shear impedance in equal proportion. Moreover, the results provide important constraints on the role of the TM in cochlear mechanics, suggesting two possible interpretations: The first is that this small change in shear impedance is sufficient to cause a 50--80 dB hearing loss, which implies that the shearing response of the TM is intimately involved in cochlear amplification. The second is that the hearing loss seen in the *TECTA* mutant is due to something other than a change in shear impedance, which points to the possibility of a second role for the TM in cochlear mechanics.

## **[82] Novel Contact Model Provides New Insights Into Tectorial Membrane Elasticity**

**Brett Shoelson**<sup>1</sup>, Richard S. Chadwick<sup>1</sup>

<sup>1</sup>Section on Auditory Mechanics, NIDCD

Shoelson et al. [1] previously reported measuring a significant radial gradient in the elasticity of the tectorial membrane (TM). These measurements were shown to correlate well with the gradient in Type A collagen fibril density [2]. Nonetheless, our conclusions were based on Hertzian-type models of contact that explicitly assume isotropy, and that thus do not take into account the presence of fibers. Moreover, they left unexplained the observed differences in elastic moduli when indenting on

the scale of a hair bundle and on the scale of an individual stereocilium [1, 3]. In a new series of computations, the TM is modeled as a Winkler (or mattress) foundation, with vertical springs extending from the bottom to the top surface. Indentation is modeled for a variety of tip shapes and sizes, and springs are permitted to change length and orientation; by minimizing the energies associated with these conformational changes, we compute relative elastic moduli that model our atomic force microscopy (AFM) data remarkably well, and that provide new insights into the shapes of force-distance curves obtained by compressing with the AFM fibrous materials like the TM. Furthermore, the Winkler model will facilitate a comprehensive analysis of the significance of tip and indentation-depth length scales on the deformation of the TM.

References: 1. Shoelson, B., et al. *Biophys J.*, 87: 2768-2777, 2004. 2. Weaver, SP., Schweitzer, L. *Hear. Res.*, 76:1-6, 1994. 3. Shoelson, B. et al. ARO abstract 1306, 2005.

### **[83] Hydrodynamics of Inner Hair Cell Bundle Mechanics**

**Sonya Smith<sup>1,2</sup>**, Richard S. Chadwick<sup>2</sup>

<sup>1</sup>Howard University, <sup>2</sup>Section on Auditory Mechanics, NIDCD

Oscillatory endolymphatic flow in the sub-tectorial space is the driving force for inner hair cell bundle deflection and subsequent mechano-transduction. This flow can arise from either a radial pressure gradient between the inner sulcus and the scala media, or from shearing of the tectorial membrane relative to the reticular lamina. The role of Hensen's stripe on bundle mechanics is also unclear. We are developing a computational approach to investigate these mechanisms. We will analyze sub-tectorial flow seen in video images of the hemicochlea using our Lagrangian optical flow method [1], and model the flows with hydrodynamic simulations using the immersed boundary method [2]. The optical flow method allows determination of fluid velocity fields without the need of seeding the flow with particles, which anyway would have difficulty following the flow at acoustic frequencies. The hydrodynamic simulations will allow us to model, on a rectangular grid, and eventually with realistic bundle geometry, the fluid interaction with the bundle structure. We report preliminary results showing the response of a single stereocilium having both bending and stretching elastic energy to fluid oscillations at frequencies characteristic of various locations of the cochlea.

References: 1. Cai, H., Richter, C.-P., Chadwick, R.S. Motion analysis in the hemicochlea. *Biophys. J.* 85:1-8, 2003. 2. Peskin, C.S., The immersed boundary method. *Acta Numerica* 11: 479-517, 2002.

### **[84] Calcium, Streptomycin, and Neomycin Change Tectorial Membrane Stiffness**

**Claus-Peter Richter<sup>1</sup>**, Geoffrey S. Getnick<sup>1</sup>, Alicia M. Quesnel<sup>1</sup>, Jessica Levi<sup>1</sup>

<sup>1</sup>Northwestern University

It has been shown that the tectorial membrane (TM) is essential for the mammalian inner ear's sensitivity and

frequency selectivity. Hereby, it is assumed that the TM mechanically interacts with the outer and inner hair cell stereocilia bundles. Consequently, changing the material properties of the TM by altering the ion composition of its bathing solution may affect cochlear function. The objective of this study was to investigate the effects of calcium, streptomycin, and neomycin on TM stiffness. TM stiffness changes are likely to alter cochlear mechanics and may suggest an additional mechanism of aminoglycoside ototoxicity.

TM stiffness was measured in gerbil hemicochleae, using a piezoelectric sensor. Measurements were made in artificial endolymph, Hank's Balanced Salt Solution, artificial endolymph with 0.02-5 mM calcium, artificial endolymph with 0-6.2 mM neomycin, and artificial endolymph with 0-6.2 mM streptomycin. The locations at which measurement were made, named the basal, upper basal, middle, upper middle, and apical turns, were 2.9 mm, 5.5 mm, 7.3 mm, 8.5 mm, and 9.8 mm from the basal end of the cochlea, respectively.

In all solutions, a TM stiffness gradient was identified along the cochlea, decreasing from base to apex. TM stiffness did not change when artificial endolymph was replaced by Hank's Balanced Salt Solution. Addition of calcium or streptomycin to artificial endolymph, however, increased TM stiffness at each location. Differences were significant at basal cochlear locations. Finally, in the presence of neomycin, TM stiffness increased at the base and decreased at the apex.

A TM stiffness gradient exists along the cochlea and is maintained for each solution. Furthermore, elevated calcium concentration, streptomycin, and neomycin alter TM stiffness and may account for immediate changes of cochlear function following the application of these drugs.

Supported by the NSF (IBN-0415901)

### **[85] Effects of Stimulus Intensity on Phase and Amplitude Characteristics of Low-Frequency Auditory Nerve Fibers**

**Marcel van der Heijden<sup>1</sup>**, Philip X. Joris<sup>1</sup>

<sup>1</sup>Laboratory of Auditory Neurophysiology, K.U.Leuven, Leuven, Belgium

We used a low-frequency (<5 kHz) counterpart of the zwuis method which we introduced previously and studied the effects of sound pressure level (SPL) on tuning of auditory nerve (AN) fibers. Data from 522 fibers from 7 cats demonstrated, with increasing SPL: 1) widening filters; 2) shifts in best frequency toward ~1 kHz; 3) reduced group delays; 4) small phase effects (<0.2 cycles) at low/moderate SPLs; 5) occasional dramatic phase effects at high SPLs (>70 dB).

These findings generally concur with common views of AN tuning derived from tonal responses and RevCor. Additional observations, however, show that these common views need refinement or revision: 1) no obvious systematic relation exists between amplitude and phase effects; 2) variation across individual animals is large; 3) some, but not all, sensitive ears showed level-dependent interactions between multiple response components (interference effects).

Apart from their obvious use in improving models of AN responses, our data achieve a detailed quantitative description of nonlinear frequency selectivity in the apex of the cochlea, a topic that is exceedingly hard to study by direct cochlear-mechanical measurements.

Supported by the Fund for Scientific Research - Flanders (FWO G.0083.02 and G.0392.05) and Research Fund K.U.Leuven (OT/01/42 and OT/05/57).

## **[86] Blood Flow Disturbance and Vascular Endothelial Growth Factor in the Stria Vascularis**

**Hiroshi Yamamoto<sup>1</sup>, Tsutomu Nakashima<sup>1</sup>**

<sup>1</sup>*Nagoya University of Medicine*

This study was performed to elucidate the relationship between the cytological changes in the stria vascularis and the vascular endothelial growth factor (VEGF) under hypoxic conditions. We made inner ear blood flow disturbance models of Spague-Dawley rats by occluding the right anterior inferior cerebellar artery (AICA) selectively for three hours and evaluated the autoregulation of cochlear blood flow (CBF) using laser-Doppler flowmetry (LDF) and the cochlea (especially the stria vascularis) histriologically. Upon the release following the three hours occlusion of the AICA, CBF moved to the previous level. However, rebound phenomeon, which is of autoregulation of blood flow, was not observed. VEGF in the stria vascularis was decreasing after the occlusion of AICA. The role of VEGF influencing upon the stria vascularis is discussed.

## **[87] Short-Arm BPPV. Does It Really Exist?**

**Neil Cherian<sup>1</sup>, John Oas<sup>2</sup>**

<sup>1</sup>*Cleveland Clinic Foundation*, <sup>2</sup>*Ohio Head and Neck Institute*

Benign paroxysmal positional vertigo (BPPV) is a common yet under recognized otologic syndrome. Controversy exists whether certain subtypes exist. The literature has discussed variants such as cupulolithiasis, sacculolithiasis and short-arm BPPV (also referred to as ampullolithiasis). Short-arm is ultimately a provable subtype based on a basic understanding of canal mechanics and observation of the response to the treatment of refractory cases of BPPV. A series of ten patients with refractory BPPV was reviewed.

BPPV is thought to be a consequence of an injured utricular macula (by infection or trauma) or by deranged otoconial metabolism. BPPV is ultimately a disorder of "otoconial destination" and how to return the otoconiae to the utricle. In theory, any area within the endolymphatic space of the labyrinth may harbor stray otoconiae.

Patients with complaints of positional vertigo were selected. The trend of the symptoms tended to be persistent over the course of weeks to months. Many of these patients failed typical canalith repositioning maneuvers. Dix-Hallpike and supine positional testing were performed. Eye movement data was captured with infrared videonystagmography and analyzed using commercial vestibular laboratory software (Micromedical Technologies). Particle repositioning maneuvers (modified Epley) were attempted for the posterior semicircular canal

of interest. A 72 hour vibration-assisted protocol was followed by the patient at home.

Upon review of the eye movement data, a few patterns were observed. An ipsidirectional low-grade torsional nystagmus was seen at times with supine positional testing with the affected ear down (head up 30 degrees). The duration, velocity and intensity of nystagmus was not always helpful in discriminating canalolithiasis (long-arm) versus short-arm. Upon sitting from Dix-Hallpike testing, the typical reversal of nystagmus was not seen and either no nystagmus was seen or an oblique nystagmus with a low-grade contradirectional torsional nystagmus was seen. Finally, with attempted particle repositioning, the nystagmus did not resolve and a similar nystagmus was often seen.

In conclusion, short-arm BPPV of the posterior semicircular canal appears to be a real and treatable form of positional vertigo. Short-arm should be considered in refractory cases of BPPV and may coexist with other variants including that of the same canal.

## **[88] The Cochlear Spiral and Its Effect on**

### **Cochlear Mechanics: Analytical Results**

**Daphne Manoussaki<sup>1</sup>, Emiliós K. Dimitriadis<sup>2</sup>, Richard S. Chadwick<sup>3</sup>**

<sup>1</sup>*Dept. of Mathematics, Vanderbilt University, Nashville, TN*, <sup>2</sup>*DBEPS/OD, NIH, Bethesda, MD*, <sup>3</sup>*Section on Auditory Mechanics, NIDCD, NIH, Bethesda, MD*

Cochlear curvature affects the mechanics of hearing, particularly for low frequencies. As wave energy propagates along the length of the cochlear spiral, a continually increasing curvature redistributes the wave energy density across the duct width, so that it is greatest at the outer wall of the spiral. By assuming the classical impedance model of cochlear mechanics, we have previously shown that this energy density redistribution causes a radial tilt for the basilar membrane and that the tilt induces a radial motion of the reticular lamina, that is inversely proportional to the radius of curvature [1]. Our result involved a number of simplifications, inherent in the impedance model. With our current work we discuss the effect of these simplifications on the mechanics of the cochlea, suggest model extensions, and show preliminary findings concerning the influence of curvature in a model with a more realistic cochlear cross-section.

[1] The cochlea's graded curvature effect on low frequency waves, D. Manoussaki, E.K. Dimitriadis, R.S. Chadwick, submitted.

## **[89] Nitric Oxide (NO)/cyclic Guanosine Monophosphate (cGMP) Pathway Induced Modulation of Cochlear Sensitivity**

**Xingqi Li<sup>1</sup>, Xuebin Jia<sup>2</sup>, Rong Wang<sup>3</sup>, Ying Zhang<sup>2</sup>**

<sup>1</sup>*The Institute of Otolaryngology, PLA General Hospital*, <sup>2</sup>*Department of Otolaryngology, Affiliated Hospital of Kunming Medical University*, <sup>3</sup>*Department of Otolaryngology, The Second Clinical Hospital of Beijing University*

This study aims to investigate the effect of nitric oxide (NO)/cyclic guanosine monophosphate (cGMP) pathway

on cochlear sensitivity. Ten groups of guinea pigs were treated with the following solutions by whole cochlear perfusion for 2 hours: (1) artificial perilymph; (2) L-arginine; (3) Ca<sup>2+</sup>-ATPase inhibitor; (4) Ca<sup>2+</sup>-ATPase inhibitor+ L-arginine; (5) Ca<sup>2+</sup>-ATPase inhibitor+cGMP; (6) Ca<sup>2+</sup>-ATPase inhibitor+ L-arginine+Non-selective NOS inhibitor; (7) eNOS inhibitor; (8) eNOS inhibitor+ Ca<sup>2+</sup>-ATPase inhibitor; (9) eNOS inhibitor+ Ca<sup>2+</sup>-ATPase inhibitor+ L-arginine; (10) eNOS inhibitor+ Ca<sup>2+</sup>-ATPase inhibitor+ L-arginine+nNOS inhibitor. The compound action potential (CAP) and cochlea microphonics (CM) were measured to assess the changes of cochlear sensitivity. After the perfusion, the cochleae were harvested and prepared for transmission electron microscopy. The average threshold shift (TS) of CAP after perfusion was 1.5dB in group 1, 3.5 dB in group 2, and 28.5dB in group 3. Groups 4 and 5 showed less TS than that of group 3 by 9 dB and 11.5 dB respectively ( $P<0.01$ ). The average CAP TS in groups 6, 7 and 8 was 29.5dB, 14.5 dB and 42.5dB respectively. The average TS of group 9 was less than that of group 8 by 7dB ( $P<0.01$ ), while that of group 10 was greater than group 9 by 6.5dB ( $P<0.01$ ). Transmission electron microscopy showed that Ca<sup>2+</sup>-ATPase inhibitor + L-arginine combined administration resulted in less severe vacuolization in OHC than that treated with Ca<sup>2+</sup>-ATPase inhibitor only. These findings suggest that: (1) The NO/cGMP pathway can regulate cochlear sensitivity; L-arginine may improve the function of Corti's organ via nNOS. (2) Being the ultimate acting enzyme of the NO/cGMP pathway, sGC (soluble guanylyl cyclase) and cGK (cyclic GMP-dependent kinase) were expressed in the supporting cells, suggesting a role for supporting cells in the modulation of cochlear function.

Supported by the National Natural Science Foundation of China (No.80070812)

## **[90] The Effect of Nitric Oxide Pathway on Slow Adaptation of Cochlear Operating Point**

Yuan Zou<sup>1</sup>, Jiefu Zheng<sup>1</sup>, Tianying Ren<sup>1</sup>, Alfred L. Nuttall<sup>1,2</sup>

<sup>1</sup>Oregon Hearing Research Center, Oregon Health & Science University, Portland, OR, <sup>2</sup>Kresge Hearing Research Institute, The University of Michigan, Ann Arbor, MI, USA

When a constant force is applied to the surface of the otic capsule, the cochlear microphonic (CM) is reduced and a slow adaptation toward the initial level occurs. We have observed that this CM change is associated with a shift of the outer hair cell (OHC) stereocilia operating point (OP) (Zou Y., et al, 2005). After applying a constant force to the bone shell over scala tympani (ST) in guinea pigs, the OP undergoes a change as if the organ of Corti moved toward the scala vestibuli (SV) direction. The OP then partially recovered toward the initial level with a time constant (TC) of  $9.2 \pm 3.5$  s. Removing the force induced overshoot of CM. In the current work, we investigate whether the operating point adaptation can be modulated by nitric oxide (NO). In the sensitive animal, L-arginine (5mM, an NO substrate) but not D-arginine (5mM) enhanced the CM overshoot following removal of force; however, a NO synthase inhibitor N(G)-nitro-L-arginine methyl ester (L-

NAME, 5mM) did not have an effect on the adaptation. Similarly, the membrane permeant cGMP analog, 8-bromo-guanosine 3':5'-cyclic monophosphate (3mM) increased the CM overshoot recovery; but the cGMP antagonist, 8-bromo-guanosine 3':5'-cyclic monophosphate Rp' did not have the effect on the OP adaptation. When the cochlea is insensitive, L-arginine (5mM) or 8-bromo-guanosine 3':5'-cyclic monophosphate (3mM) increased the cochlear sensitivity and OP adaptation; L-NAME (5mM) or 8-bromo-guanosine 3':5'-cyclic monophosphate Rp' (cGMP antagonist) decreased the cochlear sensitivity and OP adaptation. Our data demonstrate that NO/cGMP pathway is involved in OHC transduction modulation via change of the OP.

## **[91] Relationship Between Basilar Membrane Vibration and Otoacoustic Emissions**

Wenxuan He<sup>1,2</sup>, Edward Porsov<sup>1</sup>, Alfred L. Nuttall<sup>1</sup>, Tianying Ren<sup>1</sup>

<sup>1</sup>Oregon Health & Science University, <sup>2</sup>Xian Jiaotong University

Cubic distortion product otoacoustic emissions (DPOAEs) have been believed to be generated in the cochlea at the two primary-tone-overlapped locations and propagate backward to the cochlear base along the cochlear partition as a reverse traveling wave. Although this theory has been challenged by newly published data, vigorous debates on this topic remain. This study investigated the mechanism of the backward propagation of the DPOAE by observing the relationship between the basilar membrane vibration and the emission measured in the ear canal. The working hypothesis is that the basilar membrane vibration at the emission-generation site has a positive relationship with the DPOAE in the ear canal although other mechanisms may be involved. To test the hypothesis, two primary tones at frequencies  $f_1$  and  $f_2$  ( $f_1 < f_2$ ) were presented into the external ear canal in the gerbil at different intensities. The magnitudes and phases of the DPOAE and the basilar membrane vibration at the emission generation site were measured as a function of the frequency  $2f_1-f_2$ , which was varied by changing the  $f_1$  with  $f_2$  fixed. At a low and intermediate primary tone level, the maximum emission was observed when  $f_2/f_1$  was near 1.2. As  $f_2/f_1$  increased from 1.2 both the emission in the ear canal and the basilar membrane vibration decreased. As  $f_2/f_1$  decreased from 1.2 and approached one, the emission decreased. Oppositely, the basilar membrane vibration dramatically increased when  $f_2/f_1$  was close to one. The data challenge the above hypothesis and indicate that the backward traveling wave may not be the dominating mechanism for emission backward transmission. A mechanism based on the cochlear compression-wave theory will be proposed to interpret the observed data.

Supported by NIH-NIDCD and VA RR&D Center Grant, Portland, VAMC.

## **[92] Dynamic Imaging of Mammalian Stereociliary Motion In-Vitro**

**Igor Tomo**<sup>1</sup>, Jacques Boutet de Monvel<sup>1</sup>, Mats Ulfendahl<sup>1</sup>, Anders Fridberger<sup>1</sup>

<sup>1</sup>*Center for hearing and communication research & ENT Dept. Karolinska Institutet, Stockholm, Sweden*

Vibratory motion of the cochlear partition triggers conversion of mechanical stimuli into electrical signals. This transduction process depends on deflection of stereocilia atop the hair cells, which then gate mechanically sensitive ion channels. The ratio between the hair bundle deflection and sound evoked vibration of the organ of Corti is critical for further mechanical and neural events underlying sound perception.

Precise mechanisms of this complex micromechanic interaction, as it occurs during sound stimulation, are yet not fully understood due to a lack of direct measurements.

A new method for confocal imaging of rapidly moving structures was developed to image stereocilia during simultaneous sound stimulation at the apical region of guinea pigs cochlea. Custom data acquisition programs were used, to assign a phase value for each pixel within the stack of images. Corresponding pixels were then rearranged into image sequences and further processed using an optical flow computation method. High resolution images were thus acquired from outer and inner hair cells moving at several hundred Hz, which would otherwise create major motion artifacts using conventional confocal microscope solely.

Results show, that under passive conditions, outer hair cell stereocilia deflect by approximately a third of the displacement of the hearing organ. A smaller value was found in inner hair cells. Phase relations were consistent with the idea that stimulation of inner hair cells occur through the surrounding fluid drag, but maximum hair bundle deflection occurred at a different phase of the stimulus then generally presumed. The small deflection amplitudes that we measured in both hair cell types suggest a need for active amplification mechanisms present not only in the outer hair cells but also in the inner ones.

## **[93] Using ABR to Match Interaural Electrode Pairs with Bilateral Cochlear Implants**

**Zachary Smith**<sup>1,2</sup>, Bertrand Delgutte<sup>1,3</sup>

<sup>1</sup>*Eaton-Peabody Laboratory, Massachusetts Eye & Ear Infirmary, Boston, MA*, <sup>2</sup>*Harvard-MIT Division of Health Sciences and Technology, Cambridge, MA*, <sup>3</sup>*Research Laboratory of Electronics, Massachusetts Institute of Technology, Cambridge, MA*

Bilateral cochlear implantation seeks to restore the advantages of binaural hearing to the profoundly deaf by giving them access to binaural cues normally important for accurate sound localization and speech reception in noise. Psychophysical data suggest that a key issue for the implementation of a successful binaural prosthesis is the ability to match the cochlear position of stimulation channels in each ear. This may not only be important for binaural hearing, but also for the fusion of speech information across ears. We used a cat model of bilateral

cochlear implants with 8-electrode intracochlear arrays implanted in each ear. The arrays allowed the cochlear location of stimulation to be independently varied in each ear in order to test how binaural interactions change with interaural electrode separation. The binaural interaction component (BIC) of the electrically-evoked auditory brainstem response (ABR) was used as an assay of binaural processing. BIC amplitude peaked for matched interaural electrode pairs and dropped with increasing cochlear separation in either direction. Surprisingly, the widths of BIC-separation functions were roughly equal for monopolar and bipolar electrode configurations. To test the hypothesis that BIC amplitude peaks when electrodes from the two sides activate the same neural population, we measured multi-unit neural activity along the tonotopic gradient of the inferior colliculus (IC) with 16-channel recording probes and determined the extent of IC activation for each stimulating electrode. We found that the interaural electrode pairings that produced the maximal overlap in IC activation were also those that yielded maximum BIC amplitude. These results suggest that ABR measurements may provide a novel method for assigning frequency-channel mappings in bilateral implant recipients, such as pediatric patients, for which psychophysical measures of pitch ranking or binaural fusion are unavailable.

Supported by NIH grants DC05775 and DC05209.

## **[94] Bilateral Cochlear Implantation in the Ferret (*Mustela putorius*)**

**Douglas Hartley**<sup>1</sup>, Jin Xu<sup>2</sup>, Akhil Shial<sup>1</sup>, Maria Clarke<sup>2</sup>, Bashir Ahmed<sup>1</sup>, Jan W.H. Schnupp<sup>1</sup>, Robert Shepherd<sup>2</sup>, Andrew King<sup>1</sup>

<sup>1</sup>*University Laboratory of Physiology, University of Oxford, Parks Road, Oxford, U.K.*, <sup>2</sup>*Neurobiology Laboratory, The Bionic Ear Institute, Melbourne, Victoria, Australia*

Our long-term aim is to develop a behavioral animal model of bilateral cochlear implantation (CI) to maximize binaural hearing in humans, whilst using cochlear implants to study binaural system development and plasticity. Ferrets will be used since they have a relatively late onset of hearing and are highly suitable for behavioral studies. Since CI has not previously been attempted in ferrets, we have developed a new surgical technique using custom-made bipolar single-channel electrode assemblies. This surgical approach minimizes the risk of facial nerve damage, which would result in failure to thrive post-operatively. Radiological analysis showed that three active electrodes (0.3mm diameter) could be consistently implanted into the basal turn via a cochleostomy. We found that the inclusion of two 'dummy rings' in the distal part of the array facilitated a uniform insertion depth into both cochleas. Again, radiological evidence supported this observation and suggested that interaural cochlear positions of stimulation will be closely matched ( $\pm 0.2\text{mm}$ ). This is well within the range in which human psychophysical studies suggest that binaural sensitivity is preserved. Because CI trauma is associated with poor hearing outcomes, particular attention was paid to the extent of any damage caused by this technique. Four implanted cochleas were harvested for histological analysis. Subsequent microscopic

examination revealed no insertion trauma in any specimen, excluding the cochleostomy site. The effectiveness of CI was assessed by measuring electrically evoked auditory brainstem responses (EABRs) in two anesthetized bilaterally-implanted ferrets. EABRs were measured following bipolar stimulation with optically isolated biphasic current pulses (50µs/phase). EABR thresholds, defined as the lowest current level for which the mean amplitude of wave IV was  $\geq 0.2\mu\text{V}$ , were, on average, 288µA (range 125–425µA; n=4 ears). Thus, bilateral CI in ferrets is a safe and effective technique.

Acknowledgements:

Supported by the Sir Peter Morris Surgeon Scientist Programme, the Wellcome Trust and NIDCD N01-DC-3-1005

## **[95] Sensitivity of the Primary Auditory Cortex to Binaural Cues in Congenitally Deaf Cats**

Jochen Tillein<sup>1,2</sup>, Rainer Hartmann<sup>1</sup>, Silvia Heid<sup>1</sup>, Andrej Kral<sup>1,2</sup>

<sup>1</sup>*Institute of Sensory Physiology and Neurophysiology, J.W. Goethe University Frankfurt am Main*, <sup>2</sup>*Labs. of Integrative Neuroscience, University of Hamburg*

Congenitally deaf white cats (CDCs) are a model of human congenital deafness. Functional deficits in the auditory system of these adult and developing animals have been demonstrated (e.g. Kral et al., *Cereb Cortex* 10:714; *Cereb Cortex* 15:552). Here, binaural representation at the level of the auditory cortex was investigated in adult CDCs and hearing cats. Hearing cats were deafened at the beginning of the experiment. Both groups of animals were electrically stimulated with biphasic pulses (200µs/phase, monopolar) via electrodes implanted in the scala tympani of both ears. The auditory cortical field AI was mapped using local field potentials (LFPs) under separate stimulation of each ear. In contrast to hearing cats, the responses to ipsilateral and contralateral stimulation had a similar morphology in the most active area of the cortex in CDCs. In single units recordings with binaural stimulation, electrical thresholds to ipsi- and contralateral stimulation were determined first. Then, sensitivity to interaural time differences (ITDs) in the range of 0-1000 µs were tested with single pulses and pulse trains (500 Hz, 3 pulses) at intensities of 0–10 dB above unit's threshold. Finally, sensitivity to interaural level differences (ILD) 2-6 dB above threshold were tested using a constant average binaural intensity. Units sensitive to a similar range of ITDs and ILDs were found in hearing and deaf cats. In both groups of animals units with two peaks in post stimulus time histograms were found with binaural stimulation. The first peak was in a latency range of 8-35 ms after onset of the stimulus, the second peak in the range of 35-50 ms. The first and the second response were complementary in ITD sensitivity. The second responses were often sharply tuned to ITDs in both hearing and deaf animals. These results demonstrate a sensitivity of the auditory cortex to binaural cues in CDCs.

*Supported by Deutsche Forschungsgemeinschaft and MedEl Company Innsbruck.*

## **[96] Selectivity of Optical Stimulation in the Auditory System**

Agnella Izzo<sup>1</sup>, Jyoti Pathria<sup>2</sup>, Eul Suh<sup>2</sup>, Joseph T. Walsh, Jr.<sup>1</sup>, E. Duco Jansen<sup>3</sup>, Claus-Peter Richter<sup>2</sup>

<sup>1</sup>*Biomedical Engineering, Northwestern University*, <sup>2</sup>*Dept. of Otolaryngology, Northwestern University*, <sup>3</sup>*Biomedical Engineering, Vanderbilt University*

We have investigated an alternative method to stimulate the auditory neurons in the gerbil cochlea in vivo using a laser, rather than electrical current. It is known that electrical current injected from cochlear implant contacts spreads within the cochlea, causing overlapping stimulation fields and possibly limiting the performance of cochlear implant users. The potential benefit of using a laser is the ability to direct the light to a specific, known volume of tissue that is smaller than the electrically stimulated population of cells. Our data demonstrate direct stimulation of spiral ganglion cells by a laser, with a usable energy range of at least 30dB. Extended periods of optical stimulation do not result in changes in cochlear function, indicating that this is a feasible alternative method of stimulation. Immunohistochemical staining for c-fos in the cochlea shows a drastically smaller area of optical stimulation as compared to electrical stimulation. Additionally, data from tone on light masking experiments indicate that the laser can stimulate a small population of cells, similar to an acoustic toneburst. Smaller populations of stimulated cells could reduce the amount of overlap in stimulation fields, potentially leading to more discrete stimulation and the ability to utilize more stimulation contacts in a neuroprosthesis.

This work was supported by the E.R. Capita foundation.

## **[97] Effect of Stimulation Rate and Modulation Rate on ITD Sensitivity in Bilateral Cochlear Implant Users**

Gary L. Jones<sup>1</sup>, Ruth Y. Litovsky<sup>1</sup>, Smita S. Agrawal<sup>1</sup>, Richard van Hoesel<sup>2</sup>

<sup>1</sup>*University of Wisconsin-Madison, USA*, <sup>2</sup>*CRC HEAR, Melbourne, Australia*

We are investigating the range of rates for which electrical fine-timing and envelope modulation can convey ITD cues in adult bilateral cochlear implant users (BICI-N24). Current clinical sound processing strategies rely on high stimulation rates, but preserve only envelope ITD cues. As the field advances, it is important to establish whether patients are sensitive to binaural cues at high rates. Findings in this area can influence decisions about whether and how to incorporate ITD cues in speech processing strategies for BICI users.

Previous work in this field showed that ITD sensitivity with simple pulse trains is poor above a few hundred Hz. However, the lower levels that were used at higher rates to preserve constant loudness may have influenced sensitivity. In addition, 50 Hz envelope modulation was found to restore ITD sensitivity in an 800pps pulse train. Higher carrier and modulation rates were not tested.

The current study examined ITD discrimination at fixed stimulation levels using: a) simple electrical pulse trains between 100 and 1000 pps, and b) 6000 pps pulse trains,



modulated over the range 100 to 1000 Hz. Subjects were the 8 best performers from a previous study of ITD sensitivity for 100 pps. Direct control of stimulation parameters on at least two pairs of pitch-matched sites along the cochlea was enabled using a CRC SPEAR 3 processor. Results: 1) ITD discrimination thresholds generally deteriorated with increasing rate, 2) most subjects had some ITD discrimination at pulse rates up to 1000 pps or modulation rates up to 1000 Hz at one or more sites, 3) inter-subject variability was high, 4) 100 pps thresholds did not predict performance at higher rates, 5) pulse rate and modulation rate ITD thresholds were weakly correlated, and 6) modulated thresholds were typically better at 600 Hz than at 300 Hz. We will also present data on the contribution of onsets to ITD sensitivity at high rates.

Work supported by NIH-NIDCD (R01 DC 003083 and R21 DC 006641)

### **[98] Perceptual Adaptation to a Binaurally-Mismatched Frequency-to-Place Map**

**Catherine Siciliano<sup>1</sup>, Andrew Faulkner<sup>1</sup>, Stuart Rosen<sup>1</sup>, Lucinda Saul<sup>1</sup>**

<sup>1</sup>UCL

It has been well documented that both normal hearing listeners and implant users are able to adapt to an upward spectral shift of the cochlear frequency-to-place map. Recent reports of success with bilateral cochlear implants and single implants used in conjunction with a hearing aid in the contralateral ear imply that listeners are also able to adapt to frequency-place maps that most likely differ between the two ears. The present investigation examined what normal hearing listeners learned after a period of training with mismatched frequency-place maps. A dichotic sine-carrier vocoder was used to simulate cochlear implant processing, with a spectral resolution of 6 adjacent bands. From apex to base, bands 1, 3 and 5 were presented to one ear with a 6 mm basalward shift, while bands 2, 4 and 6 were presented to the contralateral ear without a shift. Listeners were trained with this processor using auditory and auditory-visual connected discourse tracking. Subjects showed significant post-training improvements with the dichotic shifted processor in both sentence intelligibility and vowel identification. However, intelligibility in the trained dichotic shift presentation never exceeded that obtained when listeners heard only the three unshifted component bands. The results suggest that users learn to attune to just the unshifted frequency bands rather than integrate the matched and mismatched frequency maps from the two ears. However, some learning of the mismatched frequency map is possible. Although the extent to which users will continue to adapt beyond acute training remains uncertain, the findings imply that in optimizing the use of bilateral hearing devices for speech recognition, consideration should be given to keeping the frequency-to-place maps similar in both ears. Work supported by the EU project HEARCOM FP6-004171.

### **[99] Bilateral Benefit in Adult Users of the HiRes 90K Bionic Ear System**

**Dawn Burton Koch<sup>1</sup>, Mark Downing<sup>1</sup>, Gulam Emadi<sup>1</sup>, Mary Joe Osberger<sup>1</sup>**

<sup>1</sup>Advanced Bionics Corporation

A University of Iowa study has reported that bilaterally implanted adults demonstrated significant improvement in speech-in-noise scores with HiRes sound processing after only one month of use compared to their scores after long-term experience with CIS. This multicenter study aims to replicate these findings in a larger group of newly implanted postlinguistically deafened adults who receive two HiRes 90K implants during the same surgery. A prospective counterbalanced between- and within-subjects design is used to evaluate bilateral listening benefits and to compare sound processing modes (CIS vs. HiRes). The study uses a six-month crossover design (three months with each processing mode) with an additional one-month period in which subjects re-evaluate the two processing modes (two weeks with each mode) and indicate a preference. Subjects then are evaluated at one and four months after using their preferred mode.

A unique aspect of the study is use of a direct-connect system for postimplant testing. The system was developed by Sigfrid Soli and colleagues at the House Ear Institute and is designed to eliminate the need for a sound booth or a speaker array, thereby allowing speech recognition and localization tests to be administered quickly and easily. The direct-connect system is based upon a family of head-related transfer functions (HRTFs) measured with KEMAR at source locations corresponding to loudspeaker positions appropriate for unilateral or bilateral testing. Left-ear and right-ear HRTFs appropriate to the selected source location are applied to the selected signal and presented via direct connection to the auxiliary input of the Auria sound processor at a specified level.

Initial study data indicate that bilateral implantation is advantageous and that sound processing may have a significant effect on bilateral benefit, consistent with the Iowa results. These early trends await verification from a larger group of study participants.

### **[100] Acoustic-Electric Interactions in the Inferior Colliculus**

**Jihwan Woo<sup>1</sup>, Paul Abbas<sup>2</sup>, Heil Noh<sup>2</sup>, Charles Miller<sup>2</sup>, Kirill Nourski<sup>2</sup>, Barbara Robinson<sup>2</sup>, Sung Hwa Hong<sup>3</sup>, In Young Kim<sup>1</sup>**

<sup>1</sup>Department of Biomedical Engineering, Hanyang University, Seoul, Korea, <sup>2</sup>Department of Otolaryngology, University of Iowa, Iowa city, IA, <sup>3</sup>Department of Otolaryngology, Samsung Medical Center, Seoul, Korea

Combined electric and acoustic stimulation of the auditory system is a new therapy for patients with severe-to-profound high- and mid-frequency hearing loss, but with remaining low-frequency hearing. Speech perception data indicate synergistic benefit with such combined stimulation. This study investigates acoustic-electric interactions in the inferior colliculus (IC, central nucleus) obtained from 7 acute guinea pig preparations.



Two different studies, 1) monaural acoustic-electric, and 2) binaural (across-ear) acoustic-electric interactions, are described. Both approaches used thin-film multi-channel electrode to record either field potentials or multi-unit activity from the IC. Electric stimuli were delivered by a minimally invasive monopolar electrode in the basal turn of the cochlea. Masking electric pulses were followed by monaural acoustic probes; masking acoustic clicks were followed by binaural electric pulse with varied masker-probe interval (MPI).

Acoustic frequency tuning curves obtained for each recording site confirmed the electrode array placement along the IC tonotopicity. Both monaural and binaural masking effects were observed. The amount of masking decreased with MPI.

The results demonstrate that electric stimulation affects the monaural IC responses evoked by acoustic stimuli in a level- and time-dependent manner. Also, acoustic stimulation affects the binaural IC responses evoked by electric stimuli.

Supported by NIH N01-DC-2-1005, MOST 2004-02186.

### **101 Temporal Bone Studies of a Round Window Implantable Hearing Device**

**Jonathan Spindel<sup>1</sup>, Geoffrey Ball<sup>2</sup>**

<sup>1</sup>College of Integrated Science and Technology, James Madison University, <sup>2</sup>Institute for Applied Physics, University of Innsbruck

Research and development over the past two decades has been directed at defining implantable hearing devices that can be used to circumvent issues associated with conventional acoustic amplification. As a result of these efforts a variety of implantable transducers have been developed, tested and applied clinically for the rehabilitation of hearing loss. Within the context of these efforts, debate continues to focus on the site of implantation that can maximize the transfer of vibrational energy to cochlea.

The objective of the current study is to investigate the response of a round window implantable hearing device. Potential advantages of a round window-based implant could include increased efficiency for delivering energy to the cochlea, use in treating conductive or mixed losses and an ability to treat patients with middle ear abnormality.

Ten fresh frozen human temporal bones were implanted with floating mass transducers (FMT; Vibrant Med-El, Innsbruck, Austria). These bones were tested in three stages of implantation: (a) un-implanted, (b) implanted with a standard incus FMT placement (I-FMT), (c) implanted with an FMT placed on the round window membrane (RW-FMT). Derived measurement of induced displacement provided objective measurement of the vibratory input to cochlea and throughout the middle ear. These data indicate that that for a similar electric signal, the RW-FMT provides 10-15 dB greater linear displacement than the I-FMT. Continuing studies in patients will provide greater insight into perceived loudness differences between these two methods of cochlear stimulation and help define surgical technique and clinical applicability of the round window approach.

### **102 Neural Responses in the Ventral Nucleus of the Lateral Lemniscus**

**David Nayagam<sup>1,2</sup>, Janine Clarey<sup>2</sup>, Antonio Paolini<sup>3</sup>**

<sup>1</sup>Department of Otolaryngology - The University of Melbourne, <sup>2</sup>The Bionic Ear Institute, <sup>3</sup>School of Psychological Science - La Trobe University

The function of the ventral nucleus of the lateral lemniscus (VNLL), a secondary processing site within the auditory brainstem, is unclear. Several studies have suggested that it plays a role in coding the temporal aspects of sound, such as the onsets and periodic components of animal vocalisations. In our study, a sample (n=283) of intracellular (n=168) and extracellular (n=115) responses to dichotically presented noise or tone bursts has been collected from the VNLL of urethane anaesthetised rats (2.6g/kg i.p.) *in vivo*. These data have provided the basis of a detailed examination of the basic neurophysiology and functional organisation of VNLL neurons. We have created a 3D reconstruction of the VNLL showing the spatial distribution of various physiological response properties, including unit response type, laterality, characteristic frequency and binaural influences. The VNLL contains units, distributed throughout the structure, that receive both monaural (51%) and binaural (49%) inputs. The majority (81%) of VNLL units are excited by contralateral stimulation. There are also VNLL units that are excited by the ipsilateral side (5%), by both sides (9%) or not excited at all (5%). Inhibitory inputs also play a large role, with units inhibited by the contralateral (8%), ipsilateral (32%) or by both (2%) sides dispersed throughout the VNLL. The dorsal VNLL, sometimes named the intermediate nucleus of the lateral lemniscus, contains the majority (67%) of units with ipsilateral inhibition and contralateral excitation. Powerful, fast inhibition within the VNLL delays spike timing in a subset (14.3%) of local neurons and may influence responses in higher centres. 3D reconstructions of intracellular recording sites did not reveal the presence of any distinct tonotopic arrangements within the VNLL. This finding is in agreement with previous extracellular and tract tracing studies and supports the notion that the VNLL is unique amongst auditory brainstem nuclei.

### **103 Binaural Interaction in the 80-Hz Auditory Steady-State Response**

**Fawen Zhang<sup>1,2</sup>, Flint Boettcher<sup>2</sup>**

<sup>1</sup>The University of Iowa, <sup>2</sup>University of South Alabama

Auditory steady-state evoked responses (ASSRs) are scalp-recorded potentials elicited by transient acoustic stimulation or modulated sounds. For example, the 80-Hz ASSR is elicited by transient stimuli presented at a rate of 80/s and primarily reflects neural activity from the auditory brainstem. ASSRs display the binaural interaction (BI) component, which is the difference between the response to binaural stimuli and the sum of the responses to monaural stimulus presented to the left ear and the right ear. This study examined the coding of binaural cues, interaural time difference (ITD) and interaural level difference (ILD), with the BI of the 80-Hz ASSR. Sixteen young human subjects with normal hearing were tested for the 80-Hz ASSR under monaural or binaural conditions. In

the binaural conditions, the ITD and ILD were manipulated from -1.6 ms to +1.6 ms and from 0 to 12 dB, respectively. Values of the BI below 0 represented suppression and above 0 represented facilitation. The ITD function of the BI in the 80-Hz ASSR displayed a wide "V" shape in individual participants. The mean ITD function of the BI normalized at the most prominent dip of the ITD function also showed a "V" shape, with both suppression and facilitation. For ILD conditions, the BI displayed suppression and its amplitude became more suppressed as the ILD was increased. The BI of the 80-Hz ASSR displayed a large intersubject variability. The difference in the ITD and ILD functions of the BI in the 80-Hz ASSR indicated that the ITD and ILD coding of clicks may be processed in different pathways. The current study suggested that, if the intersubject variability of the BI is controlled, the 80-Hz ASSR provides an objective means for evaluating binaural functions in patient such as central auditory processing disorders.

#### **104 Role of Inhibition for Coincidence Detection in MSO Neurons**

**Roberta Donato<sup>1</sup>**, David McAlpine<sup>1</sup>

<sup>1</sup>*UCL - Ear Institute*

Guinea pigs are born following a long gestational period (68-72 days) compared to other rodents, rendering them relatively mature at birth. Moreover, they are sensitive to a range of sound frequency, including low frequencies at which interaural time differences are used in sound localization tasks. We have developed a guinea pig slice model to study the role of synaptic inhibition and the cellular mechanisms involved in the coincidence detection task that neurons in the medial superior olive (MSO) perform in sound localization. Under whole cell- patch clamp configuration, synaptic current and potentials (respectively in the voltage or current clamp mode) were recorded upon stimulation of the fibres of the trapezoid body with pulse trains. With an intracellular solution containing a low concentration of Cl<sup>-</sup>, excitatory or inhibitory synaptic events displayed an opposite polarity at resting potential (~-60mV). Stimulation intensity was varied to recruit from a minimum to a maximum number of fibres, hence resulting in a combination of pure inhibitory, pure excitatory or mixed responses. For each intensity of stimulation the frequency of the train and the number of pulses was varied (10-500 Hz range, 10-100 pulses) in order to explore the dynamic properties of the synapses involved and postsynaptic characteristics of the MSO cell membrane when subjected to repeated stimuli at low or high frequency. Preliminary data indicate basic properties of principal and non principal neurons to accord with those previously described. Non-principal neurons fired upon stimulation once at threshold, whilst principal neurons never did so. At low stimulus levels principal neurons responds with inhibitory potentials only, with a mixture of inhibitory and excitatory potentials at higher intensities. The time course of excitatory and inhibitory post-synaptic potentials suggests that inhibition dominates the time course of neural events in MSO neurons.

#### **105 Response Properties of Presumed Principal Cells in DCN Following Acoustic Trauma: Inhibition, Spontaneous Activity, and Tuning**

**Wei-Li Ma<sup>1</sup>**, Eric D. Young<sup>1</sup>

<sup>1</sup>*Johns Hopkins University, Baltimore, Maryland*

The nature of central auditory transformations in sensorineural hearing loss are not well understood. Some changes in tuning are expected due to peripheral damage; other attributes, including strength of inhibition, have been shown to differ. Here we describe single unit response properties in dorsal cochlear nucleus (DCN) following acoustic trauma. The DCN has been well studied in normal animals and has an extensive inhibitory circuitry, so it is a natural site for the study of central plasticity. In addition, it has been implicated in tinnitus production by Kaltenbach and colleagues. We exposed cats to 10 kHz noise at levels sufficient to produce sharp losses up to 80 dB at high frequencies. Acute recording experiments were done 1-2 months after exposure. Peripheral hearing loss was characterized using compound action potential audiograms. Single units were characterized in terms of response maps and spontaneous activity.

All unit types described in normal animals (types I/III, II, III, IV-t, IV) are seen in exposed animals. Additionally, a new unit type, the "tail" unit is seen. These units have broadly-tuned excitatory responses with little or no inhibition under single tone stimulus paradigms; most have a sharply tuned low-pass shape at BF with a broad tail extending toward low frequencies. A small group, found exclusively at the low frequency edge of the lesion, has additional weak excitatory responses extending above BF at moderate to high levels. Another group has no spontaneous activity and significant inhibition under two tone stimulus paradigms. This latter group also shows the highest thresholds suggesting the possibility of a different origin for these units.

Spontaneous rates (SR) were compared to normals for type III, IV-t and IV units. No significant change was observed for any unit type; SR in tail units are similar to principle unit types in normal animals.

Supported by NIDCD grants R01-DC00109, T32-DC000023, and a grant from the Tinnitus Consortium

#### **106 Time Course of Neural Adaptation to Stimulus Statistics**

**Isabel Dean<sup>1</sup>**, Nicol Harper<sup>1</sup>, David McAlpine<sup>1</sup>

<sup>1</sup>*University College London*

We have shown previously that neurons in the guinea pig inferior colliculus adjust their responses according to the distribution of sound levels with which the animal is presented. These adjustments alter the coding properties of the neural population, such that coding accuracy is increased near to the most commonly-occurring sound levels. Here we present an analysis of the time course of the neural adaptation.

Extracellular recordings were made from single neurons in the inferior colliculi of anaesthetised guinea pigs. Diotic white noise stimuli were presented, the level of which was randomly selected every 50 ms from a defined distribution.

The full range of levels presented was 21-90 dB SPL. Each distribution of levels was characterised by a distinct region of more probable levels, from which levels were selected with 0.8 probability; thus, the mean sound level differed between distributions. In a switching experiment, the stimulus periodically alternated between two level distributions.

We plotted rate-level functions from the responses immediately preceding and immediately following a switch to a new distribution of levels. For most neurons, the rate-level function begins to adjust as rapidly as we can measure it: within 300 ms of the change to a new level distribution, the function differs from that immediately preceding the switch. Following this rapid initiation of the change in the rate-level function, the function continues to be adjusted in many neurons, until it reaches a steady-state, typically within 1 s. Finally, the time course of the adaptation appears to depend upon the switching period of the stimulus: preliminary results indicate that increasing the switch period, between 2.5 s and 10 s, is associated with more rapid adaptation.

### **107 Challenges to Inter-Spike Interval Models of Pitch: The Responses of Cochlear Nucleus Neurons to Band-Pass Filtered Pulse Trains** **Stefan Bleack<sup>1</sup>**

<sup>1</sup>*Institute of Sound and Vibration Research*

Carlyon et al. (J Acoust Soc Am 112: 621-33, 2002) found that a pulse train with alternating inter-pulse intervals between 4 and 6 ms ("4-6 stimulus") is perceived as having a periodicity of 5.7ms. Using a model that relies on neuronal first order intervals (FOIs) for pitch perception, they showed that the recovery of the auditory nerve from adaptation is not sufficient to explain this effect and suggested that a weighting function that favours longer FOI intervals was needed to account for the perceived pitch. Here we investigate whether there are neurons, or populations of neurons, at the next stage of processing, the cochlear nucleus (CN), that give greater representation to longer intervals. We measured the responses of single neurons in the ventral CN of anaesthetised guinea pigs to isochronous and anisochronous pulse trains. Pulse trains were band-pass filtered between 3900 Hz and 5300 Hz. Isochronous pulse trains had interpulse intervals of 3, 4, 5, 6 and 7 ms. Anisochronous pulse trains had alternating interpulse intervals between 4 and 6 ms. The results are based on the responses of 58 units, classified by the shape of their post stimulus time histograms as Primary with notch (PN, 9), transient chopper (CT, 22), sustained chopper (CS, 10) and onsets (ON, 17). PN and CT units showed a recovery behaviour that is quantitatively similar to the auditory nerve. ON and CS units showed a faster recovery between 4 and 6 ms, but not enough to account for the size of the psychophysical effect. The average of FOI distributions for single units generally has too many long intervals to account for the observed pitch of the 4-6 stimulus. When sequentially interleaving the spikes from all units the average FOI distribution contains more shorter intervals, but, by interleaving spikes from just 2 to 4 units the average FOI becomes small enough to explain the

observed pitch of the 4-6 stimulus. The location of units that may participate in such an analysis remains obscure.

### **108 Neurons in the Medial Nucleus of the Trapezoid Body and Superior Paraolivary Nucleus of the Rat Respond to Short Gaps in Tones and Noise**

**Alexander Kadner<sup>1,2</sup>**, Albert S. Berrebi<sup>1,2</sup>

<sup>1</sup>*Depts. Otolaryngology, Neurobiology & Anatomy, Sensory Neuroscience Research Center,* <sup>2</sup>*West Virginia Univ. School of Medicine*

We studied two populations of neurons in the superior olivary complex of the rat that produce responses to the offset of a sound stimulus and may be capable, therefore, of detecting gaps. Neurons of the Medial Nucleus of the Trapezoid Body (MNTB) display high rates of spontaneous activity and produce sustained responses to the stimulus onset. These responses are followed, about 5 ms after the stimulus offset, by a period of suppression of spontaneous activity. Neurons of the Superior Paraolivary Nucleus (SPON), which receive strong glycinergic inhibitory input from the MNTB, show little or no spontaneous activity and typically respond transiently to the stimulus offset.

We presented MNTB and SPON neurons with two identical stimuli (either characteristic frequency (CF) pure tones, amplitude modulated CF tones or broad band noise bursts) separated by gaps ranging from 0 to 30 ms in duration. All stimuli were 50 ms in duration, contained 2 ms on-off ramps, and were presented at 20 dB above threshold. We varied the gap duration to determine the minimum gap required for the neurons to respond to each stimulus separately.

When gaps of 5-10 ms or longer were presented, all MNTB neurons responded to 1) the offset of the first stimulus, as described above, as well as 2) to the onset of the second stimulus. In some cases, the 0 ms gap (i.e., the mere presence of the ramps) was sufficient to elicit one or both of these responses. Similarly, with minimum gaps of 5-10 ms, all SPON neurons responded to the offset of the first stimulus, and some SPON units displayed this response to stimuli separated by 0 ms gaps. We observed no systematic variation of the gap thresholds between the various types of stimuli in either nucleus. Thus, the phase information contained in CF and amplitude modulated tones does not appear to play a role in the gap detection.

The results indicate that both MNTB and SPON neurons are sensitive to relatively short gaps in sounds.

Supported by RO1 DC-02266 (ASB)

### **109 The Magnitude of Forward Masking and the Time Course of Its Recovery as a Function of Unit Type in the Ventral Cochlear Nucleus**

**Neil Ingham<sup>1</sup>**, Stefan Bleack<sup>1,2</sup>, Ian Winter<sup>1</sup>

<sup>1</sup>*Cambridge University, UK,* <sup>2</sup>*ISVR, Southampton University*

Most neurons in the auditory pathway decrease their response during the presentation of a tone. The change is often referred to as adaptation. To understand the representation of complex time varying stimuli a

knowledge of the time course of recovery from adaptation is essential. However, while several studies in the cochlear nucleus (CN) have measured adaptation and recovery from adaptation (Boettcher et al., *Hear Res* 48: 125-144, 1990; Shore, *Hear Res* 82: 31-43, 1995; Shore, *J Acoust Soc Am* 104: 378-389, 1998), they have not quantified the magnitude of masking in dB. We used a physiological two interval forced choice threshold tracking algorithm (Relkin & Pelli, *J Acoust Soc Am* 82: 1679-91, 1987) to investigate the magnitude of forward masking and the time course of recovery from forward masking of different unit types in the ventral CN of anaesthetised guinea pigs. The masker stimulus was a 100ms Best Frequency (BF) tone. We measured the threshold of a probe stimulus (25ms, BF tone) as a function of masker-probe interval at a fixed relative masker level (BF threshold +20dB), and as a function of masker level at a fixed interval (2.8ms). Neuronal threshold recovered from forward masking with an exponential time course. Primary-Like (PL), Primary-with-notch (PN), Transient Chopper (CT), Sustained Chopper (CS) and Low Frequency (LF) units produced very similar recovery functions, with a maximal masking effect of 7.9 – 9.2 dB. The average recovery time constant for these units was 31 ms. Onset (ON) units showed a higher masking effect of 23.2dB and a time constant of 14 ms. To estimate growth of masking we measured probe thresholds as a function of masker level (again using a fixed interval of 2.8ms). Onset units demonstrated the steepest growth of masking (0.6 dB/dB) whereas PL, PN, CT, CS and LF units demonstrated greater compression of growth of masking, varying between 0.16 and 0.32 dB/dB. Supported by the Wellcome Trust and BBSRC.

#### **110 Spectro-Temporal Receptive Fields of MNTB Principal Cells**

**Bernhard Englitz**<sup>1,2</sup>, Sandra Tolnai<sup>2</sup>, Cornelia Kopp-Scheinflug<sup>2</sup>, Rudolf Rübsamen<sup>2</sup>, Jürgen Jost<sup>1</sup>

<sup>1</sup>*Max-Planck Institute for Mathematics in the Sciences,*

<sup>2</sup>*University of Leipzig, Institute for Biology II*

As has recently been demonstrated spectrally tuned inhibition acts in the Medial Nucleus of the Trapezoid Body (MNTB). The temporal interaction of this inhibition with the prominent calyceal excitation determines the transfer properties of MNTB principal cells. Since the spectro-temporal content of naturally occurring stimuli can be richly structured we employed a more general method to investigate the cell's tuning properties. Using TORC stimuli (Klein et al., 2000) we determined spectro-temporal receptive fields (STRFs) and measured spectro-temporal location, size and shape of excitation and inhibition. Results from STRFs and both regular and two-tone tuning-curves were consistent. In a companion work (see Abstract Tolnai et al. 2006) we demonstrated that the temporal fidelity of inhibition is comparable to the fidelity of the excitation, thus enabling the use of TORC containing high amplitude modulation rates which yield a high temporal resolution in the STRF, i.e. about 1 ms. Independent of the desired resolution and smoothness of the tuning-properties, a major reduction in the required time for data-collection was achieved.

#### **111 Adaptive Auditory Processing in the Dorsal Cochlear Nucleus**

**Patrick Roberts**<sup>1</sup>, Christine Portfors<sup>2</sup>

<sup>1</sup>*Neurological Sciences Institute, Oregon Health & Science University,* <sup>2</sup>*Washington State University*

The dorsal cochlear nucleus (DCN) is a cerebellum-like structure that integrates auditory nerve input with multimodal inputs conveyed by parallel fibers. In vitro studies in mouse DCN have demonstrated spike-timing dependent plasticity between parallel fiber and cartwheel cell synapses, suggesting that adaptive mechanisms in the DCN cancel predictable stimuli. We paired in vivo recordings of cartwheel cells with mathematical models to test the hypothesis that plasticity between parallel fibers and cartwheel cells leads to the cancellation of predictable auditory patterns. Our spike-timing dependent plasticity model of cartwheel responses to auditory stimuli predicted that pairing two sounds causes cartwheel cells to change their response to each individual sound such that the response to one sound cancels the effect of adding the second sound. We recorded 77 single units in the DCN of awake mice. Twenty-one units were classified as cartwheel cells based on their firing of complex spikes followed by simple spikes. To test our model's prediction, we recorded spikes from cartwheel cells during pairing of two tones. Stimulus-1 was not the best frequency, but acted as a reference with the intent to activate a population of granule cells. Stimulus-2 was a best frequency tone that evoked a strong excitatory response. After repeated pairing of the 2 stimuli (about 5 min), the spike response to stimulus-2 was reduced; in particular, the simple spikes were reduced. After stimulus-2 was terminated, the simple spike response to stimulus-1 was reduced during the interval when stimulus-2 was presented. Thus, we have empirically confirmed our model-driven hypothesis that the pairing of 2 tones reduces the response of cartwheel cells to individual tones. This finding suggests that plasticity between parallel fibers and cartwheel cells may function to predict auditory stimulation patterns that are expected, similar to the mechanism found in other cerebellum-like structures.

#### **112 Pitch Encoding of Dynamic Iterated Rippled Noise in the Human Brainstem Is Sensitive to Language Experience**

Ananthanarayan Krishnan<sup>1</sup>, Jayaganesh Swaminathan<sup>1</sup>, Jackson Gandour<sup>1</sup>

<sup>1</sup>*Purdue University*

Pitch encoding of dynamic iterated rippled noise in the human brainstem is sensitive to language experience

Our earlier research has shown that pre-attentive pitch encoding of Mandarin tones embedded in *speech stimuli* is sensitive to language experience at the level of human auditory brainstem (Krishnan, Xu, Gandour & Cariani, 2005). The aim of this crosslanguage (Chinese, English) study is to determine whether early, pre-attentive stages of pitch encoding of Mandarin tones embedded in *nonspeech stimuli* is similarly influenced by language experience. By using iterated rippled noise (IRN) stimuli, we were able to remove any potential confound of lexical-semantic

information. IRN stimuli were made up of broad band noise with temporal regularities that can yield a pitch percept. Their pitch to noise ratio was varied as a function of iteration number; the gain was set to a constant value. Using a  $F_0$  contour representative of the high rising tone in Mandarin Chinese, time varying IRN stimuli were created by increasing the iteration number steps (4, 8, 16, 32, 64). FFRs, human frequency following response, were extracted from the rostral brainstem in response to the IRN stimuli presented to native speakers of Mandarin and English for each iteration step. Pitch strength and accuracy of pitch tracking were measured from the FFR's using autocorrelation analysis. Our preliminary results reveal that greater pitch strength and smoother pitch tracking emerges at a lower iteration number (8) for Chinese listeners compared to English listeners. English listeners, on the other hand, show only irregular pitch tracking even at the highest iteration number (64). These findings provide evidence in support of neural plasticity at the brainstem level induced by long-term exposure to linguistically relevant parameters of an auditory signal.

### **113 Temporal Effects of Trigeminal Input on Acoustic Responses in the Dorsal Cochlear Nucleus**

**Seth Koehler<sup>1</sup>**, Paul Manis<sup>2</sup>, Susan Shore<sup>1</sup>

<sup>1</sup>University of Michigan, <sup>2</sup>University of North Carolina Chapel Hill

The principal neurons of the dorsal cochlear nucleus (DCN), the pyramidal cells, receive auditory input on their basal dendrites, and input from the trigeminal system via granule cells on their apical dendrites (Zhou and Shore, J. Neurosci. Res., 2005; Haenggeli et al., J. Comp. Neurol., 2005). DCN cells integrate information from auditory and trigeminal inputs nonlinearly, consistent with higher multisensory centers. Preceding acoustic with trigeminal stimulation suppresses response rate to sound (Shore, Eur. J. Neurosci., 2005), regardless of whether trigeminal stimulation alone excites or inhibits unit activity. Here, we explore the effects of trigeminal stimulation on temporal properties of unit responses to sound. In vitro studies suggest that the temporal response pattern of pyramidal cells depends on the prior membrane potential (Manis, J. Neurosci. 1990). Thus, preceding acoustic with trigeminal stimulation should change the temporal response pattern of DCN pyramidal cells.

Unit responses were recorded with multichannel electrodes placed into the DCN of ketamine anesthetized guinea pigs. Units were sorted using the Plexon Offline Sorter. First spike latency (FSL), first interspike interval (FSI), and shuffled autocorrelation (SAC; Louage et al., J. Neurosci, 2004) were used to reveal temporal properties of responses to a broad band noise (BBN) stimulus alone, and BBN preceded by shocks to the trigeminal ganglion (TG) or trigeminal nucleus (TN). FSL, FSI and SACs showed significant changes when BBN was preceded by TG or TN stimulation. SACs usually had a larger central peak, indicating more consistent spike timing across trials in response to sound. SACs also showed stronger side lobes, indicating greater response regularity. These results demonstrate that not only rate, but also the temporal

patterns of DCN units in response to sound are modulated by trigeminal input.

Supported by P01 DC00078, R01 DC004825 to SES and R01 DC00425 to PBM.

### **114 Electrically Evoked Auditory Brainstem Response (EABR): Site-Specific Waveforms from Focal Stimulations in Cochlear Nucleus**

**Ryuji Suzuki<sup>1</sup>**, M. Christian Brown<sup>2,3</sup>

<sup>1</sup>Speech and Hearing Bioscience and Technology, Harvard-MIT Division of Health Sciences and Technology, <sup>2</sup>Dept. of Otology & Laryngology, Harvard Medical School, <sup>3</sup>Eaton Peabody Laboratory, Massachusetts Eye and Ear Infirmary

This study examined whether the EABR elicited by focal electrical stimulation of the cochlear nucleus depended on the site of stimulation. Stimulation sites were in the dorsal, posteroventral or anteroventral subdivisions of cochlear nucleus (DCN, PVCN, and AVCN, respectively) in anesthetized guinea pigs. A 50  $\mu$ s single phase shock was used to evoke the EABR, which was measured with epidural vertex electrode against neck muscle reference. DCN stimulation produced one broad wave lasting for about 3 ms. PVCN stimulation produced three distinct peaks within 2 ms after the shock, while AVCN stimulation produced four peaks. For comparison, acoustic click-evoked ABR waveform was more complex, containing more waves than any of the EABR's obtained with electric stimulation. Our results suggest that the EABR waveform can be used as a physiological assay to determine the site of stimulation within cochlear nucleus, a result that may be useful for guiding placement and interpreting responses from auditory brainstem implants in humans.

### **115 Frequency Following Response: Neural Correlates of Cochlear Distortion at 2f1-f2 to Tonal Sweeps**

Ananthanarayan Krishnan<sup>1</sup>, Vidya Ganesh<sup>1</sup>

<sup>1</sup>Purdue University

Fine changes in frequency of primaries results in pseudo-periodic amplitude and phase variation of the distortion product otoacoustic emissions, termed as fine structure. Fine structure is reported to reflect the presence of multiple sources, contributing to the acoustic distortion product recorded in the ear canal. Fixed and variable primary ratios are used to study fine structure in acoustic distortion products. Although fine structure has been reported to high frequency primaries for the distortion product otoacoustic emissions, it is not known if such information is preserved at lower frequencies. The distortion product at 2f1-f2 is well preserved in the scalp recorded frequency following responses (FFR-DP) for low frequency primaries. Of interest here is to determine if fine structure information is preserved in the neural version of the acoustic distortion product elicited by low frequency primaries. Frequencies following responses were recorded in normal hearing subjects using primaries consisting of tonal sweeps with both constant and varying f2/f1 ratios. While the FFR-DP amplitude for stimuli with fixed ratio

exhibited little or no modulation in amplitude, response amplitude using varying ratio showed a broad modulation. These results suggest that fine structure information is present for low frequencies, albeit not as robust as observed for the acoustic distortion products at higher frequencies. These initial results appear to suggest that the neural version of the distortion product at  $2f_1-f_2$  may be utilized to evaluate the nature of fine structure for low frequency stimuli given that the scalp recorded frequency following responses are robust at frequencies below about 1000 Hz.

### **[116] The Control of Call Frequency and Temporal Call Parameters in the Brainstem of Echolocating Horseshoe Bats**

**Kohta Kobayashi<sup>1</sup>**, Jie Ma<sup>1</sup>, Michael Smotherman<sup>2</sup>, Walter Metzner<sup>1</sup>

<sup>1</sup>*UCLA*, <sup>2</sup>*Texas A&M University*

Echolocating Greater horseshoe bats, *Rhinolophus ferrumequinum*, adjust their call parameters, such as the frequency, duration, and emission rate depending on the auditory feedback provided by the returning echo signal. We used this "Doppler-shift compensation" (DSC) behavior to investigate how the brainstem controlled these call parameters in response to different auditory feedback cues using a combination of behavioral and pharmacological approaches. Previously, we demonstrated that within the parabrachial nucleus (PB), auditory feedback controls call frequencies via a push-pull organized glutamatergic excitatory and GABAergic inhibitory feedback mechanism, whereas temporal call parameters appear to be affected mostly by GABAergic auditory feedback. Here, we show how the motor nucleus of laryngeal control, the nucleus ambiguus (NA), which receives input from PB, was involved in this differential control of spectral and temporal call parameters. To investigate those functions in relation to neural transmitters, we applied various inhibitory and excitatory transmitter agonists and antagonists, such as Muscimol, Bicuculline, AMPA, CNQX, and kynurenic acid, into the NA and adjacent regions of the brainstem while monitoring the animal's DSC behavior. Preliminary results indicate that (1) the feedback control of call frequencies, which was operated in a push-pull mode within the PB by both excitatory and initiatory mechanisms, was combined into a single "pull-down" mechanism mediated by GABAergic mechanism and restricted to the anterior portion of NA. Glutamatergic drugs did not have any effects on call frequencies within the anterior NA. (2) In contrast, both GABAergic and glutamatergic drugs controlled temporal call parameters within the more posterior portions of NA.

Supported by NIDCD.

### **[117] Responses to Dichotic Broadband Noise Stimulation in Chinchilla Ventral Cochlear Nucleus**

**U-Cheng Leong<sup>1</sup>**, Ann Eddins<sup>2</sup>

<sup>1</sup>*University at Buffalo*, <sup>2</sup>*University of Rochester*

Contralateral broadband noise (BBN) stimulation has been shown to inhibit spontaneous and driven activities of

ipsilateral VCN neurons in guinea pigs (Shore et al., 2003; Sumner and Shore, 2004). In the present study, dichotic stimuli were used to investigate binaural responses of single and multi-units in chinchilla VCN recorded with a multi-channel recording probe. Stimuli were composed of 50-ms BBN bursts that varied in interaural time difference (ITD,  $\Delta T = -60$  to  $+60$  ms re: ipsilateral stimulus onset in 10-ms steps) and interaural level difference (ILD,  $\Delta L = -10$  to  $+40$  dB re: ipsilateral level in 5-dB steps). Similar to data from the guinea pig, contralateral rate-intensity functions were monotonic with stimuli at 0-ms  $\Delta T$ . The effect of inhibition was the strongest at  $+30$  to  $+40$  dB  $\Delta L$ , and the magnitude of reduction in spike count was as great as 70% in some units. The ITD functions were non-monotonic, with a systematic decrease in firing and a gradual recovery as  $\Delta T$  increased. The maximum reduction was consistently observed at 0-ms  $\Delta T$ . As suggested in anatomical circuitry, these data provide further support of binaural processing in the VCN.

### **[118] GABAergic Regulation of Suprathreshold Cartwheel Cell Responses**

**Jian Zhou<sup>1</sup>**, Scott Molitor<sup>1</sup>

<sup>1</sup>*University of Toledo*

Cartwheel cells (CWCs) are a population of interneurons in the dorsal cochlear nucleus that receive multimodal sensory input and provide inhibition to pyramidal cells that project to the inferior colliculus. In many in vivo and in vitro preparations, CWCs respond to suprathreshold stimuli with complex spikes, a rapid burst of fast  $\text{Na}^+$ -mediated action potentials superimposed upon a slow underlying depolarization. However, CWCs can also respond to suprathreshold stimuli with simple spikes followed by characteristic afterdepolarizations (ADPs); the inhibition of their postsynaptic targets will be determined by whether CWCs respond to excitation with simple or complex spikes. One source for regulating the suprathreshold responses of CWCs may be provided by the inhibitory neurotransmitter  $\gamma$ -amino butyric acid (GABA): previous work has shown that GABA can depolarize and evoke suprathreshold responses in CWCs at rest, whereas depolarized CWCs are inhibited by these neurotransmitters.

During whole cell recordings from CWCs in the presence of kynurenic acid and strychnine, activation of  $\text{GABA}_A$ Rs via the pressure application of GABA or muscimol to visualized dendrites produced a sustained depolarization that was partially blocked by picrotoxin and completely blocked by the  $\text{GABA}_A$ R antagonist SR95531. Despite this depolarization, GABA or muscimol application typically produced simple spikes in CWCs that responded with complex spikes to brief depolarizing current pulses, and reduced ADP magnitudes in CWCs that responded with simple spikes to these brief stimuli. Pressure application of the  $\text{GABA}_B$ R agonist baclofen also reduced the ability of CWCs to produce complex spikes by evoking a small hyperpolarization that was blocked by the  $\text{GABA}_B$ R antagonist CGP54626. Therefore GABAergic neurotransmission plays a dual role during the inhibition of complex spiking, via a shunting inhibition produced by the

activation of GABA<sub>A</sub>Rs and a hyperpolarization produced by the activation of GABA<sub>B</sub>Rs.

## **119 Development of Auditory Hindbrain**

### **Neurons In Vitro**

**Thomas Kuenzel<sup>1</sup>, Jörg Mey<sup>1</sup>, Hermann Wagner<sup>1</sup>, Harald Luksch<sup>1</sup>**

<sup>1</sup>*Institut für Biologie 2, RWTH Aachen*

The time-coding pathway in the avian auditory hindbrain consists of nucleus magnocellularis (NM) and nucleus laminaris (NL). The system is highly adapted for faithful and fast transmission of precisely timed electrical activity. Because function, anatomy and physiology of NM/NL are well understood in vivo, it is an attractive model system to study functional development of neuronal circuitry. We plan to reconstruct the NM/NL circuitry as a biohybrid system in vitro, which will allow long-term monitoring of network development. As an initial step we were interested in the development of physiological properties of dissociated hindbrain neurons in a serum-free primary culture system.

The neurons survived for over 15 days and rapidly grew neurites in serum-free conditions. The number of cells showing expression of the calcium-binding protein calretinin increased with time of cultivation. We found expression of calretinin in all culture timepoints, beginning with acutely dissociated cells explanted from HH30 embryos. After about 7 days in vitro (DIV) neurons formed terminal-like structures that stained positive for the presynaptic marker synapsin I. Specialised ion-channel immunoreactivity (Kv1.1, Kv3.1b) could be found in vitro. It is unclear whether this expression was on a functionally sufficient level.

The physiological development of the hindbrain neurons was analysed with whole-cell patch recordings. We recorded from 96 neurons that were up to 15 DIV. Thirteen percent (n=12) of all cells showed spontaneous action potentials, a total of 70% (n=68) of all cells fired action potentials after current injection. A significant decrease in resting membrane potential with culture time (<DIV8: -46mV +/- 13mV vs. >DIV13: -59mV +/- 13mV; p<0,05) demonstrated functional maturation, but other properties (e.g. AP firing patterns after current injection) seemed to indicate failure to develop characteristic specialisations. Only 14% of the cells firing APs displayed a phasic firing pattern as is known for auditory hindbrain neurons.

Taken together we found a mixture of constitutive properties and properties that failed to develop in vitro. These findings may partly be due to the fact that the cell culture consisted of a mixture of neuronal subtypes.

## **120 Multi-Day Imaging of Regenerating Axons in the Auditory Brainstem**

**Armin Seidl<sup>1</sup>, Edwin W. Rubel<sup>1</sup>**

<sup>1</sup>*University of Washington*

A main feature of the developing vertebrate nervous system is preservation of neighbor relationships of receptor cells in the sensory epithelium in the topography of projections throughout the nervous system, in both ascending and descending pathways. The lateral superior

olive (LSO) is part of the sound localization mechanism in the mammalian brainstem and is well suited for a detailed investigation of the establishment of neuronal maps. The LSO receives tonotopically organized projections from both ears; excitatory ipsilateral projections from the cochlear nucleus and inhibitory glycinergic inputs from the contralateral ear, via the medial nucleus of the trapezoid body (MNTB). This tonotopy is preserved in organotypic slice cultures from neonatal animals and can regenerate after it has been disrupted (Lohmann et al., 1999, J Neurobiol, 41:596-611).

Slice cultures were prepared from the auditory brainstem of 3 or 4 day old mice (Stoppini et al., 1991, J. Neurosci Methods, 37:173-82). In some cases we lesioned the axonal projections between MNTB and LSO completely. After 1-4 days in vitro, MNTB cells were transfected with a GFP-plasmid single-cell electroporation (Haas et al., 2001, Neuron 29:583-591). After 12 hrs, labeling of single neurons and their projections could be detected. Cultures and labeled neurons remained viable for up to 10 days in culture and could be imaged over a period for up to 6 days. Viability of single neurons was not affected by axotomy, nor by time-lapse imaging over 25 hours (15-30 min interval). Single MNTB neurons in slice cultures, whose axons to LSO had been lesioned, could be imaged before and during their axonal projections did regenerate.

This preparation allows us to study the detailed dynamics of regenerating MNTB neurons into LSO. Furthermore, it enables us to address multiple questions about the mechanisms of axonal map formation on a single cell level.

## **121 Cochlear Nucleus Interneurons of the Rat Middle Ear Muscle Reflex Pathway**

**Daniel J. Lee<sup>1,2</sup>, Ronald K. de Venecia<sup>1,3</sup>, John J. Guinan, Jr.<sup>1,3</sup>, M. Christian Brown<sup>1,3</sup>**

<sup>1</sup>*Eaton-Peabody Laboratory, Massachusetts Eye & Ear Infirmary, Boston, MA*, <sup>2</sup>*Dept. of Otolaryngology, UMass Memorial Medical Center*, <sup>3</sup>*Department of Otolaryngology and Laryngology, Harvard Medical School, Boston, MA*

The middle ear muscle (MEM) acoustic reflex is a major efferent system to the auditory periphery. Sound presented to one ear can trigger the contraction of the MEMs in the same ear (uncrossed reflex) and opposite ear (crossed reflex). Although the afferent pathways (cochlea to cochlear nucleus) and efferent pathways (motoneuron to MEM) are known, the interneurons have not been identified. Previous work by our group and Relken et al have determined that distortion product otoacoustic emission (DPOAE) suppression, primary tone level changes, and ipsilateral DPOAE adaptation are sensitive measures of the rat MEM acoustic reflex. Utilizing these reflex assays, manipulations of the auditory brainstem were performed to localize the MEM reflex interneurons in the cochlear nucleus. In our 2005 ARO poster, we presented preliminary data suggesting that the crossed MEM reflex interneurons were localized to the ventral cochlear nucleus. We now present additional data from a total of 12 rats using kainic acid to selectively lesion portions of the cochlear nucleus. In three cases, lesions of the posteroventral cochlear nucleus (PVCN), but not the



DCN, nerve root, or caudal AVCN, reduced the strength of the crossed reflex. Surgical cuts of the DAS and IAS did not alter the crossed reflex. Finally, we will also correlate our lesion data with changes in the uncrossed reflex pathway. Taken together, these data indicate that the interneurons of the crossed reflex are located in the posteroventral CN and project out the ventral acoustic stria. Supported by the NIDCD 1 K08 DC06285-01 and DC 01089.

**122 Anatomical Identification of Cochlear Interneurons Controlling the Tensor Tympani Muscle in Rats: A Pseudorabies Virus Study**  
**Matthew S. Yeager<sup>1</sup>, Yael Raz<sup>1</sup>, Athanasios Blikas<sup>1</sup>, Isabelle Billig<sup>1</sup>**

<sup>1</sup>*University of Pittsburgh School of Medicine*

The middle ear muscle (MEM) reflex is often assessed in the audiological evaluation of hearing impairment. This feedback inhibition is thought to modulate auditory input, as with speech discrimination in noise, and may protect the inner ear from acoustic trauma. Although prior studies have delineated the brain structures involved in auditory pathways in various mammals, the organization of interneurons in the cochlear nuclear complex innervating the MEMs has not been fully elucidated. This study used the retrograde transsynaptic transport of pseudorabies virus to identify the topographical organization of cochlear interneurons controlling the tensor tympani (TT) muscle in the rat. A survival time of 72 hours consistently produced labeled cells and dendritic arbors bilaterally in the dorsal and dorso-medial regions of the anterior ventral cochlear nucleus (VCN), and in the entire dorso-ventral extent of the dorsal cochlear nucleus (DCN). Labeling was scattered within both posterior VCNs. Fewer labeled cells and collateral branches were also present bilaterally in the ventral part and at mid-level of the dorso-ventral extent of the anterior VCN. In agreement with prior studies, labeled TT motoneurons were located ipsilaterally in an area immediately ventral to the trigeminal motor nucleus and extended rostrally towards the lateral lemniscus. In very few cases, labeled motoneurons were also observed in the ventral and ventro-lateral borders of the trigeminal motor nucleus itself. In the superior olivary complex, transsynaptically-labeled neurons were present in the periolivary and medio-trapezoid regions, with an ipsilateral propensity. In most cases, labeling was also observed in the lateral superior olive, with a contralateral predominance. These anatomical data provide the first direct evidence that motoneurons controlling the TT muscle in the rat are influenced by cochlear interneurons located bilaterally in different parts of the DCN and VCN. These regional differences in the cochlear nuclear complex may account for multifunctional roles of the TT muscle.

**123 Thalamic Descending Projection to Non-Olivocochlear Neurons in the Gerbil**  
**Nobuyuki Kuwabara<sup>1</sup>**

<sup>1</sup>*University of Louisville School of Medicine, Louisville, KY*

Projections from the medial geniculate body in the auditory thalamus to non-olivocochlear neurons were examined.

Descending projections from auditory thalamus to olivocochlear (OC) neurons were demonstrated previously (Kuwabara et al., '03, ARO Abstr., 26:87). Some of the thalamic descending axons take the form of a collateral of the inferior colliculus (IC)-bound axon while others project directly to OC neurons without projecting to the IC (Kuwabara, '05 ARO Abstr., 28:243). Projections from thalamic descending axons to non-OC neurons in the SOC, however, have not been well demonstrated. In gerbils, some areas of SOC receive cortical descending projections, which are largely ipsilateral (Kuwabara and Schofield, '04, ARO Abstr., 27:121). In this study anterograde axonal labeling was combined with retrograde prelabeling of OC cells both in vivo specimens and uniquely cut slices to examine the projections of MGB cells to non-OC cells in the auditory brainstem.

OC neurons were prelabeled using a retrograde tracer (Fluoro-Gold, Fast blue or HRP) injected in the cochlea to discriminate OC cells from non-OC cells. IC and lateral lemniscus (LL) were also given a large injection of a fluorescent tracer that was not used in labeling OC cells to prelabel major SOC cell groups that had ascending projections. Biotinylated dextran amine (BDA) was injected in the MGB stereotaxically. Angled parasagittal brain slices containing ipsilateral auditory cell groups ranging from the thalamus to the lower brainstem that had prelabeled OC cells were also made in some specimens in which visually guided focal injections of biocytin were made in the subdivisions of the MGB.

BDA-labeled axons with terminals and en passant varicosities were found in close apposition to the cell body and proximal dendrites of prelabeled OC neurons, as predicted. Labeled terminals were also found in many other areas of the SOC: lateral superior olive (LSO), superior paraolivary nucleus (SPN), non-OC area of the ventral nucleus of the trapezoid body (VNTB) and the area between the ventral nucleus of the LL and the SOC. In some slice specimens with MGB focal injection, discrete biocytin labeling of axonal projections to the SOC, although not large in number, was found. These results suggest that the thalamic descending axons project to a wide range of brainstem cells along with OC cells.

(Supported by NSF-IBN9987660)

**124 Organization of the Human Superior Olivary Complex: Principal Nuclei**  
**Randy Kulesza<sup>1</sup>**

<sup>1</sup>*Lake Erie College of Osteopathic Medicine*

The Superior Olivary Complex is an ensemble of mammalian brainstem nuclei within the auditory pathway and involved in the processing of auditory information. This region of the auditory pathway is generally conserved across species and typically includes between seven and thirteen distinct cell groups. Evidence suggests that each of these cell groups contributes a unique circuit within the auditory pathway and a potentially unique functional role in processing sound. The complex includes two prominent and highly conserved cell groups, often referred to as principal nuclei: these are the medial superior olive (MSO) and the lateral superior olive (LSO). The entire complex,



but especially the principal cell groups, have been studied extensively in laboratory animals. Unfortunately, many questions remain regarding the detailed organization of the human Superior Olivary Complex. A detailed understanding of the neurons, neurotransmitters and circuits involved in the human auditory brainstem is necessary for the continued evolution of hearing prostheses and prevention of presbycusis; moreover it will permit the extension of current models of sound source localization to the human auditory pathway.

The principal nuclei of the Superior Olivary Complex were examined in Neutral Red stained and Geimsa stained tissue sections from post-mortem human specimens. Preliminary studies based on examination of three brainstems indicate the general location of the Superior Olive within the medulla and pons is in general agreement with previous studies of human material. The human MSO spans nearly the entire Superior Olive and exists as dorso-ventrally elongated column of densely packed cells, very much resembling the MSO seen in low frequency hearing animals. The human LSO, is much more restricted in distribution and in many sections, appears as a rounded mass of loosely packed cells. However, examination of a complete rostro-caudal series through the nucleus demonstrates a main body and a smaller medial limb. A morphometric analysis provides evidence that both human principal olivary nuclei include multiple neuronal populations and that these neurons have preferential orientations within the contours of the MSO and LSO.

#### **[125] The Effect of Slice Orientations on the Imaging of Subcortical Auditory Activity with fMRI**

**Lavinia Slabu<sup>1</sup>, Remko Renken<sup>1</sup>, J. Esther C. Wiersinga-Post<sup>1</sup>, Hans Hoogduin<sup>1</sup>, Hendrikus Duifhuis<sup>1</sup>**

<sup>1</sup>*Dept. of Biomedical Engineering, University of Groningen, BCN Neuroimaging Centre, The Netherlands*

Although auditory information is processed in several subcortical nuclei, most auditory fMRI studies focus on the auditory cortex and ignore the brainstem responses. Functional imaging of the brainstem is complicated due to heart beat related motion. The subcortical areas involved in auditory information processing are: the inferior colliculus, the medial geniculate body, the superior olivary complex and the cochlear nucleus.

The aim of this study is to investigate the effect of the slice orientation when the subcortical auditory areas are imaged using fMRI. Motion of the brainstem has two origins: gross head motion and cardiac pulsation. Heart beat related motion of the brainstem is in the superior-inferior and anterior-posterior directions.

Auditory activation was measured using the BOLD effect. Sparse sampling was used (12 s) to minimize the influence of the echoplanar noise. The stimuli consisted of pink noise modulated in the temporal and spectral domain. BOLD contrast images were acquired at a 3 Tesla MRI system with gradient echo planar imaging. The phase encoding was always in the right-left direction. Three different slice orientations were used: approximate parallel, under 45 degrees and orthogonal to the brainstem.

On the activated voxels, we calculated the standard deviation of the residual, mean t-statistic and the number of active voxels to quantify variability in activation between orientations and subjects.

Our results indicate that a parallel imaging plane should be preferred when acquiring brainstem fMRI. From the literature is known that the brainstem motion in the superior-inferior direction is stronger than in the anterior-posterior. The effect of the strongest motion is minimized using parallel slices with the brainstem.

#### **[126] Cholinergic Cells Have Branching Projections to Multiple Brainstem Auditory Nuclei in Guinea Pigs**

**Susan D. Motts<sup>1,2</sup>, Brett R. Schofield<sup>2</sup>**

<sup>1</sup>*Kent State University, <sup>2</sup>Northeastern Ohio Universities College of Medicine*

The inferior colliculus (IC) and cochlear nucleus (CN) receive cholinergic input from two nuclei in the dorsolateral pons, the pedunculo-pontine (PPT) and laterodorsal (LDT) tegmental nuclei. The PPT and LDT project to many brainstem regions and play an important role in arousal. Studies in other (non-auditory) systems show that PPT and LDT cells commonly send axonal branches to two targets. We used multiple fluorescent retrograde tracers and immunohistochemistry for choline acetyltransferase (ChAT, a cholinergic marker) to identify cholinergic cells that project to multiple auditory nuclei in guinea pigs.

Injection of different retrograde tracers into each IC produced a large number of cells that contained both tracers. Immunohistochemistry for ChAT yielded many triple-labeled cells (both tracers plus ChAT) in PPT and LDT, indicating that many of these cells are cholinergic. Triple-labeled cells were limited to the PPT and LDT, with the majority of such cells in the PPT.

Injection of tracers into one IC and one CN also produced triple-labeled cells in PPT and LDT, including cells that projected to two ipsilateral nuclei, two contralateral nuclei, or one of each. In some cases, different retrograde tracers were injected into 3 regions (e.g., both ICs and one CN), and quadruple-labeled cells (all three tracers plus ChAT) were observed in PPT. The results suggest that cholinergic cells can send axon branches to 3 nuclei.

The results indicate that cholinergic cells in PPT and LDT that innervate IC or CN commonly send axon branches to two or more nuclei. The prominence of axonal branching in these projections is similar to that of cholinergic projections to other systems. These axonal branching patterns may allow a relatively small number of cholinergic cells to activate a large part of the brainstem auditory pathways in response to an arousing stimulus.

Supported by NIH DC 04391.

**127 Auditory Brainstem Responses in a Rhesus Macaque Model of Opiate Dependence and Neuro-AIDS**

**Mariam Riazi**<sup>1,2</sup>, Joanne Marcario<sup>1,2</sup>, Frank Samson<sup>3,4</sup>, Himanshu Kenjale<sup>2,5</sup>, Istvan Adany<sup>2,5</sup>, Opendra Narayan<sup>2,5</sup>, Paul Cheney<sup>1,2</sup>

<sup>1</sup>*Department of Molecular & Integrative Physiology,*

<sup>2</sup>*University of Kansas Medical Center,* <sup>3</sup>*Department of*

*Physiology,* <sup>4</sup>*Universidad del Mar,* <sup>5</sup>*Department of*

*Microbiology, Molecular Genetics & Immunology*

It is well established that auditory brainstem response (ABR) abnormalities occur in symptomatic and asymptomatic HIV-infected human subjects, but the causes of these deficits are poorly understood. The nonhuman primate model allows a means of examining AIDS-related auditory neuropathology on a compressed disease time course. The general objective of our work is to characterize the electrophysiological consequences of opiate (morphine) dependence in a nonhuman primate model of neuro-AIDS produced by bone marrow injection of simian immunodeficiency virus (SIVmacR71/E17). Combined HIV infection and opiate dependence is a common problem, particularly among intravenous drug users. The co-existence of drug abuse with HIV infection raises important questions about the potential interaction between the two. Limited studies of the effects of opiates on AIDS severity and progression have been inconclusive. Results from this study are intended to clarify whether morphine is potentially protective, or if it exacerbates SIV-related ABR peak and interpeak latency shifts. The electrophysiological integrity of the brainstem auditory relay system was assessed by recording ABRs in a cohort of 17 male, Indian origin rhesus macaques (*Macaca mulatta*). The cohort was divided into 3 groups: morphine only (n=5), SIV only (n=5), and SIV + morphine (n=6). ABR latencies were highly reproducible across five control sessions performed over a period of one year. Two ABR sessions were collected during the morphine dependency period (26 weeks). Eight ABR sessions were recorded during the post-inoculation period (33 weeks). Viral load, CD4+/CD8+ cell counts and white blood cell counts were obtained monthly from blood samples. Viral RNA was recovered from plasma and CSF samples of all inoculated subjects (n=11) indicating productive infection. Preliminary results suggest that the SIV + morphine group shows the greatest ABR abnormalities. (Sponsored by NDA12827 and HD02528)

**128 Multipolar Neurons in the Ventral Cochlear Nucleus: Somatic Innervation of Cells That Project to the Contralateral Cochlear Nucleus**

**John Doucet**<sup>1</sup>, Nicole Lenihan<sup>1</sup>

<sup>1</sup>*Otolaryngology-H&N Surgery, Johns Hopkins University*

In rats, two classes of multipolar neurons in the ventral cochlear nucleus (VCN) project their axons to the contralateral CN (Doucet et al. [2003] ARO abstracts). (1) Radiate-commissural (RC-) multipolar neurons have large cell bodies (250 - 700µm<sup>2</sup>), dendrites that traverse VCN isofrequency planes, and a collateral axon that innervates the ipsilateral dorsal CN (DCN). RC-multipolar neurons are

comparable to D-stellate cells in mice and Type II multipolar cells in cats. (2) Commissural multipolar neurons have smaller cell bodies (100 - 300µm<sup>2</sup>) and do not innervate the ipsilateral DCN. We are interested in the structural mechanisms that govern the responses to sound of these two cell classes. In this study, we examined the proportion of their respective cell bodies opposed by synaptic terminals - a feature known to correlate with physiological unit type (Smith and Rhode [1989] J. Comp. Neurol. 282:209-225).

Experiments began by injecting Fluorogold in the CN of albino rats to retrogradely label neurons in the contralateral CN. Synaptic terminals were labeled by immunostaining sections through the CN using an antibody against SV2 - a ubiquitous synaptic vesicle protein. SV2-labeling was visualized with AlexaFluor 488. With this protocol, the soma of labeled RC- and commissural multipolar neurons fluoresce gold whereas synaptic terminals opposed to their somata fluoresce green. Soma size was used to classify the labeled cells. Somatic innervation was studied by viewing thin (0.7µm) optical sections through each labeled cell using a confocal microscope. As expected, the somata of RC-multipolar cells were covered with SV2-labeled terminals. In contrast, the cell bodies of most commissural multipolar neurons were opposed by very few SV2-labeled terminals. These results provide additional evidence that direct projections linking the cochlear nuclei derive from at least two types of multipolar cells. They also suggest that these two structural classes have different responses to sound and play distinct roles in the auditory pathway.

This work was supported by NIH/NIDCD grants R01DC006268 and P30 DC05211.

**129 Apoptosis in the Inferior Colliculus of the Jaundiced Gunn Rat Model of Auditory Neuropathy/Dys-Synchrony (AN/AD)**

**Ann C. Rice**<sup>1</sup>, **Steven M. Shapiro**<sup>1</sup>

<sup>1</sup>*Virginia Commonwealth University*

The Gunn rat model is a good model of AN/AD due to hyperbilirubinemia. While previous studies have documented abnormalities in brainstem auditory pathways, spiral ganglia, auditory nerve, basal ganglia and cerebellum of sick rat pups and suggested apoptosis as the mechanism of cell death, the histopathology has not been well characterized. Methods: We treated 15-day-old jaundiced (jj) Gunn rat pups with 200 mg/kg sulfadimethoxine to displace bilirubin from serum albumin into brain. At 48 hrs rats were videotaped and ranked on a clinical rating scale (CRS). Replicated brainstem auditory evoked potentials (BAEPs) were performed in 56 animals under anesthesia at 4 intensities and scored on a scale from normal to abnormal based on objective criteria by one of the authors blinded as to group and clinical information. Twenty-five additional brains were processed for histological analysis. Cresyl violet and TUNEL staining were performed on sagittal sections. Results: CRS in jjs correlated significantly ( $p < 10^{-6}$ ) with abnormalities of BAEP waves II and III (corresponding to human waves III and V) but not with BAEP threshold. In sulfa-treated jjs, the

inferior colliculus in jj-sulfa group overall had 21±22% (mean±SD) TUNEL positive (TUNEL+) cells indicating apoptosis versus 0% in 7 jj-saline and 9 nonjaundiced sulfa or saline-treated animals ( $p < 0.02$ , ANOVA); five of nine jj-sulfa had 36±21%, whereas four of nine had 0% TUNEL+ cells. No other areas of basal ganglia or auditory areas had significant numbers of TUNEL+ cells. Conclusions: We have identified apoptosis in the inferior colliculus 48 h after acute bilirubin toxicity; studies at other times may reveal abnormal TUNEL+ staining in other brainstem (cochlear nucleus, superior olivary complex) areas known to be affected. We suggest that that apoptosis in the inferior colliculus may contribute to the central auditory dysfunction in AN/AD due to hyperbilirubinemia.

**[130] Contralateral Excitation of Cochlear Nucleus Neurons Following Conductive Impairment May Involve Olivocochlear Pathways**  
**Debara L. Tucci<sup>1,2</sup>, Karin Halsey<sup>3,4</sup>, David Dolan<sup>3,4</sup>, Susan Shore<sup>3,4</sup>**

<sup>1</sup>Duke University Medical Center, USA, <sup>2</sup>Division of Otolaryngology, <sup>3</sup>University of Michigan, <sup>4</sup>Kresge Hearing Research Institute, The University of Michigan, Ann Arbor, MI, USA

Unilateral conductive hearing loss (CHL) alters the responses of ventral cochlear nucleus (VCN) neurons to contralateral sound: In normal guinea pigs, contralateral sound inhibits the activity of ~30% of VCN units but excites few of these neurons (Shore et al., Exp. Br. Res., 2003). CHL results in an immediate and sustained increase in the proportion of units with *excitatory* responses, with no persistent changes in the percentage of units inhibited by contralateral sound (Sumner et al., J. Neurophysiol., 2005). The decreased ascending output from the CN ipsilateral to the CHL would be expected to alter the drive of both medial and lateral efferent neurons in the brain stem, which are activated by CN projection neurons. This could explain the previous results in which CHL resulted in a decrease in the auditory nerve activity measured at the ipsilateral round window (RWN, Cook, et al., Hear. Res., 2002). Since olivocochlear pathways are both crossed and uncrossed, we wished also to explore the effects of CHL on the responses of the auditory nerve activity *contralateral* to the CHL.

RWN and compound action potentials (CAPs) were measured bilaterally with chronic RW electrodes before and after unilateral CHL. Control baseline information was obtained from all experimental animals as well as two control animals. Experimental animals underwent surgical disruption of the ossicular chain to create either a mild to moderate (Group 1, n=4) or severe to profound (Group 2, n=5) hearing loss. Compound action potential (CAP) responses were obtained to air and bone conduction stimuli, and RW responses measured immediately and on day 1, 7 and 14 following CHL.

The results indicate that CHL can produce increases in the contralateral RWN and CAP responses in the ear contralateral to the CHL, suggesting that alterations in

olivocochlear pathways play at least a partial role in compensatory excitatory responses following CHL.

Supported by NIH R01 DC005416 and P30 DC05188

**[131] Contralateral Excitation of Cochlear Nucleus Neurons Following Cochlear Damage Is Mediated by Peri-Olivary Nuclei**

**Susan Shore<sup>1</sup>, Colleen LePrell<sup>1</sup>, Seth Koehler<sup>1</sup>**

<sup>1</sup>University of Michigan

Contralateral sound stimulation inhibits the activity of about a third of ventral cochlear nucleus (VCN) neurons, but, in the normal guinea pig, excites few of these neurons (Shore et al, Exp. Br. Res., 2003). On the other hand, there is a large increase in the number of VCN neurons excited by contralateral stimulation after conductive hearing loss (Sumner et al., J. Neurophysiol., 2005). This "compensatory" excitation may be mediated by cholinergic neurons in the ventral nucleus of the trapezoid body (VNTB) (Sherriff and Henderson, Neuroscience, 1994) that send excitatory projections to the VCN (Fujino and Oertel, J. Neurosci., 2001; Mulders et al., Hear. Res., 2003).

Using multichannel electrodes, unit responses were recorded from the ipsilateral VCN of anesthetized guinea pigs after unilateral cochlear damage. Responses to ipsilateral and contralateral tone and broadband noise stimuli were characterized. Following confirmation of contralateral excitation, the effects of VNTB melittin lesions (Le Prell et al., J. Assoc. Res. Otolaryngol., 2003) on responses were assessed. Histological confirmation of lesion location was obtained *post mortem*.

Cochlear ablation resulted in a complete loss of responses to ipsilateral sound but a dramatic increase above normal in the number of units excited by contralateral sounds. The contralateral stimulation elicited sharply tuned responses with monotonic rate-level functions. Lesions of the VNTB on both sides of the brain eliminated the contralateral excitation, while lesions of the VNTB contralateral to the cochlear damage only partially eliminated the excitation.

These findings suggest that cholinergic neurons arising in the VNTB are involved in compensatory excitation following hearing loss.

Supported by RNID and NIH P30 DC05188.

**[132] Postnatal Development of the Calyx of Held**  
**Brian Hoffpauir<sup>1</sup>, George A. Spirou<sup>2</sup>**

<sup>1</sup>WVU School of Med, Sensory Neuroscience Research Center, <sup>2</sup>WVU School of Med, Sensory Neuroscience Research Center, Dept. of Otolaryngology/HNS

Studies of adult rodents indicate that the vast majority of principal cells in the medial nucleus of the trapezoid body (MNTB) receive glutamatergic input from only one calyx of Held terminal. Here, we combine serial electron microscopy and electrophysiology to better understand the developmental profile of this giant nerve terminal and look for evidence of synaptic competition between multiple inputs during the early phases of calyx formation in mice. Observations of serial ultrathin sections indicate that the protocalyces observed at P2 rapidly expand into immature cup-like calyces by P4. Complete 3-D reconstructions and

analyses of MNTB neurons and their associated inputs (contained within 306 serial sections) reveal that the majority of MNTB neurons receive one large calyx at P4, while very few cells receive multiple, although significantly smaller, inputs. In order to study the physiological development of the calyx of Held, we recorded whole cell currents from MNTB neurons in response to midline stimulation. For these experiments, coronal slices were prepared and candidate MNTB neurons were selected using a  $\text{Ca}^{2+}$  sensitive dye (Fura 2). Average EPSC amplitudes recorded from cells held at  $-70$  mV increased from  $-0.44 \pm 0.07$  nA to  $6.73 \pm 0.65$  nA from P2-P4. Currents recorded at  $-75$  and  $+75$  mV were blocked by CNQX and AP5, indicating that these EPSCs were mediated by AMPA and NMDA receptors. At these ages, the NMDA and AMPA mediated-components were of similar amplitude (at  $+75$  mV). At P4, minimal stimulation protocols indicated that 25 of 29 cells were innervated by a single large input, with the mean midline-evoked EPSC measuring  $-6.73 \pm 0.65$  nA. The four remaining cells had response properties indicative of two inputs, although the amplitudes were noticeably smaller (mean =  $-1.37 \pm 0.16$  nA). These results suggest that, by P4, competition among globular bushy cell axons is essentially complete as the majority of MNTB neurons receive only one calyceal input.

### **[133] Central Pattern of Neurodegeneration After Frequency-Restricted Acoustic Trauma**

**Jose Juiz<sup>1</sup>**, Jose Moncho<sup>2</sup>, Marco A. Izquierdo<sup>3</sup>, Manuel S. Malmierca<sup>3</sup>, Miguel A. Merchán<sup>3</sup>

<sup>1</sup>*Centro Regional de Investigación Biomédica. Universidad de Castilla-La Mancha*, <sup>2</sup>*Dpto. de Ciencias Médicas. Universidad de Castilla-La Mancha*, <sup>3</sup>*INCyL. Universidad de Salamanca*

The consequences of acoustic overstimulation and trauma on cells of the organ of Corti are well known. However, the effects on central auditory neurons have received comparatively less attention. It is important to fill this gap because the final success of recovery strategies relies on the state of adult central auditory neurons and circuits.

Young adult Long-Evans rats with normal auditory nerve CAP recordings were free-field stimulated with an 105 dB, 8 KHz tone for four hours during two consecutive days. Twenty four hours, 10 days, 30 days or 90 days after stimulation, animals were tested again for CAP recordings. They were further sacrificed and processed for Fluoro-Jade immunocytochemistry to evaluate neurodegeneration.

Abnormal CAP recordings, with increased thresholds centered at 8 KHz were obtained, regardless time after stimulus delivery. Fluoro-jade labeling showed a distinct progressive and topographic pattern of fiber degeneration in the cochlear nucleus. Traces of terminal degeneration were seen already 24 hours after stimulation. Fiber degeneration increased dramatically from 10 to 90 days after stimulation, but maintaining a topographic arrangement. No evidence of transneuronal degeneration was found, at least up to 30 days after stimulus delivery.

Therefore, frequency-restricted acoustic overstimulation causes neurodegeneration which affects at least auditory

nerve fibers in a progressive and topographic fashion. The pathophysiological impact of such neurodegeneration in the natural history and recovery from acoustic damage needs to be further evaluated.

*Supported by MCyT BFI 2003-09147-C0202 and PAI-03-015*

### **[134] Relation Between Hyperactivity in the Hamster Dorsal Cochlear Nucleus and Outer Hair Cell Loss Induced by Intense Sound Exposure**

**Michael Carron<sup>1</sup>**, James Kaltenbach<sup>1</sup>, Jinsheng Zhang<sup>1</sup>

<sup>1</sup>*Wayne State University*

Intense sound exposure causes increased spontaneous activity (hyperactivity) in the dorsal cochlear nucleus (DCN), a phenomenon that may contribute to the experience of noise-induced tinnitus. In this study, we examined the relationship between the level of hyperactivity in the DCN and the amount and type of hair cell loss following intense sound exposure. Hamsters were exposed to an intense 10 KHz tone (120-130 dB SPL) for periods ranging from 1 to 4 hours. Spontaneous activity was measured on the DCN surface 1-2 weeks following exposure. Cochleas were then removed, dissected and studied histologically using a scanning EM. Our preliminary analysis, based on a qualitative evaluation of spontaneous activity profiles and visual inspection of cochlear micrographs, yielded three groups of animals: One group showed normal levels of spontaneous activity throughout the DCN and normal hair cell populations throughout the cochlea. The second group showed major increases in spontaneous activity over broad areas of the DCN. Most of the animals in this group also showed loss of OHCs over broad regions of the cochlea containing intact IHCs. A few animals in this group, however, showed no significant loss of hair cells. The third group showed marginally elevated spontaneous activity. In most of these animals, OHC lesions were present, but these were often accompanied by IHC damage. Two animals in this group displayed no obvious hair cell loss. These results suggest that OHC loss may trigger the development of hyperactivity. However, it also seems apparent that OHC loss is not the only trigger of hyperactivity after intense sound exposure, and that the effect of OHC loss may be offset when there is accompanying loss of IHCs. A quantitative analysis of these results will be presented to directly test the relationship between the type and amount of hair cell loss and the level of activity in the DCN. (Supported by NIDCD grant RO1 DC03258).

### **[135] The Cell Types and Connections of the Cochlear Nuclei in the Tokay Gecko**

**Yezhong Tang<sup>1</sup>**, Jakob Christensen-Dalsgaard<sup>1</sup>, Catherine E. Carr<sup>1</sup>

<sup>1</sup>*Department of Biology, University of Maryland*

The cochlear nuclei of lizards show a great deal of interspecific variation. In many lizards, four nuclear populations that receive primary auditory inputs have been recognized: a medial and lateral nucleus magnocellularis (NM) and a medial and lateral angularis (NA). Only some lizards have a distinct pathway from the nucleus

magnocellularis to the nucleus laminaris similar to the pattern found in turtles, crocodilians and birds.

We have begun an analysis of the lizard cochlear nuclei with a study of the Tokay gecko (*Gekko gecko* L.). These geckos produce stereotyped vocalizations for intraspecific communication and threat (Werner et al., 1978), and have a well-developed auditory system. Their basilar papilla is also characterized by a reversed tonotopic arrangement, with the low best frequency hair cells located at the base and the high best frequency hair cells at the apex of basilar papilla (Manley et al., 1999).

These unique features led us to investigate the cell types and connections of the cochlear nucleus of the Tokay gecko. Nissl and Golgi staining were combined with immunohistochemistry and with tract tracing experiments. The cochlear nuclei were identified by both location and by projections from the papilla. Cholera toxin, dextrans and Dil were used to label the eighth nerve.

The eighth nerve formed bouton terminals throughout NM and NA. In NM, Golgi analysis revealed large neurons with large oval cell bodies and few or no dendrites in caudal NM and smaller multipolar neurons in the rostral NM. SV2 immunohistochemistry in NM revealed perisomatic synapses around NM cells. In NA, Nissl staining revealed medium and small size neurons. NA contained two major cell types in NA; bipolar neurons and multipolar neurons. Bipolar neurons had dendrites that were parallel to the incoming auditory nerve fibers, while multipolar neurons had two or more branching dendrites.

Supported by the University of Maryland Center for Neuroscience, and by NIDCD 000436 to CEC

### **[136] Direct Projections from the Superior Olivary Complex to the Medial Geniculate Body in Rats**

Yong-Ming Jin<sup>1</sup>, Albert S. Berrebi<sup>1</sup>

<sup>1</sup>*Sensory Neuroscience Research Center, Health Sciences Center, West Virginia University*

In order to fully understand the functional role of any auditory brainstem cell group, it is necessary to determine all of its sources of input and projection targets. We have previously shown that the Superior Paraolivary Nucleus (SPON), a prominent nucleus of the superior olivary complex, is a major source of GABAergic inhibitory inputs that innervate the inferior colliculus. Recently, we have undertaken a series of tract-tracing studies to reveal the ascending and descending projections of this structure in rats, using the sensitive retrograde tracer Fluoro-Gold. In the first studies, large iontophoretic deposits of Fluoro-Gold were placed into the medial geniculate body (MGB). After a survival period of seven days, the animals were perfused and their brains processed by immunohistochemistry using an antiserum directed against the tracer. Retrogradely labeled neurons were found ipsilaterally in the SPON, medial superior olive (MSO) and dorsal periolivary region, as well as contralaterally in the lateral superior olive (mainly in its medial limb). Labeled neurons were not observed in the medial or lateral nuclei of the trapezoid body (MNTB or LNTB). We also confirmed the previous finding that neurons in the dorsal cochlear nucleus and small cell cap region of the ventral cochlear

nucleus project to MGB (Malmierca et al., 2002). Further studies, using both anterograde and retrograde tracing approaches, will serve to identify subdivisions of the MGB that are preferentially targeted by these brainstem projections. Although it is premature to speculate on the potential significance of these direct brainstem--thalamic pathways, it is interesting to note that so-called  $i_{off}$  responses, which are the dominant response of SPON neurons to characteristic frequency pure tones, have also been recorded in the MGB.

Supported by NIDCD grant DC-02266 to A.S.B.

### **[137] Intrinsic Membrane Properties and Synaptic Response Characteristics of Neurons in the Rat's Dorsal Cortex of the Inferior Colliculus**

Hongyu Sun<sup>1</sup>, Shu Hui Wu<sup>1</sup>

<sup>1</sup>*Psychology Department, Carleton University, Ottawa, ON, Canada*

We studied intrinsic membrane properties and synaptic response characteristics of ICD neurons in brain slices obtained from P9-18 rats. Whole-cell patch clamp recordings were made from 102 ICD neurons. Seven distinct types of neurons could be distinguished by their firing profile with depolarizing and hyperpolarizing current injections. Regular, adaptation, pause and onset firing patterns were observed in 11.8%, 6.9%, 25.5% and 3.9% of the ICD neurons, respectively. Three other types of neurons shared a common feature: a broad rebound depolarization following a prolonged hyperpolarization. They were rebound-regular (8.8%), rebound-adaptation (29.4%) and rebound-pause (13.7%) types. The hyperpolarization-induced rebound was eliminated by  $Ca^{2+}$ -free perfusing solution. The afterhyperpolarization (AHP) following a single action potential was prominent in the ICD neurons. It had a duration of up to 120 ms, and a peak amplitude of about 10 mV. The AHP could be completely blocked by  $Ca^{2+}$ -free external solution and partially blocked by the  $Ca^{2+}$ -activated SK channel blocker, apamin. An inward rectification during the membrane hyperpolarization was found in many ICD neurons and was blocked by the H-current blocker, ZD7288. The silent period at the beginning part of the depolarization in the pause neurons was eliminated by application of the A-type  $K^+$  current blocker, 4-AP (2 mM). These results suggest that specific ionic currents (i.e.,  $Ca^{2+}$ -activated  $K^+$  current, H-current and A-type of  $K^+$  current) account for distinct ICD neuron firing patterns. To study synaptic responses, a stimulating electrode was placed in the central nucleus of the IC (ICC) or on the commissure of the IC (CoIC). The results showed a combination of excitatory and inhibitory responses with both stimulating conditions (n=20). But the ICD neurons had more excitatory and less inhibitory responses with stimulation from the ICC compared with stimulation from the CoIC.

Supported by NSERC of Canada to S.H. Wu

**138 Responses of Neurons in the Rat's Dorsal Cortex of the Inferior Colliculus to Monaural and Binaural Acoustic Stimulation**

Huiming Zhang<sup>1</sup>, Jack Kelly<sup>1</sup>

<sup>1</sup>*Institute of Neuroscience, Carleton University*

We made recordings from single neurons in the rat's dorsal cortex of the inferior colliculus (ICD) and examined the temporal and spectral characteristics of responses to 100 ms tone bursts presented to the ear contralateral to the recording site. We also investigated binaural interactions using 100 ms dichotic tone bursts. The temporal and spectral response characteristics of neurons in the ICD were typically quite different from those in the central nucleus of the inferior colliculus (ICC) or lower brainstem structures. A substantial number of ICD neurons showed "offset" or "on-off" post-stimulus time histograms. The latencies of many ICD neurons were much longer than those of neurons in the ICC. For ICD neurons with continuous firing during a tone burst, there was a large variation in the latency of the first spike in response to repetitive stimulation. Some neurons habituated during repetitive sound stimulation, showing strong responses to initial presentations, but little or no spiking thereafter. The responses of neurons that showed habituation could be restored by changes in sound intensity or frequency. Neurons in the ICD were typically tuned to a wide range of frequencies, showing broad tuning curves and low Q10 values. Some neurons responded to broad-band stimuli, but did not respond to tone bursts. Many ICD neurons were sensitive to interaural-level differences and displayed binaural inhibition. These physiological data suggest that the ICD may play an important role in the detection of complex and novel auditory stimuli.

Research supported by NSERC of Canada.

**139 Temporal Processing in the Auditory Midbrain of the South African Clawed Frog**

Taffeta Elliott<sup>1</sup>, Jakob Christensen-Dalsgaard<sup>2</sup>, Darcy Kelley<sup>1</sup>

<sup>1</sup>*Columbia University*, <sup>2</sup>*University of Southern Denmark*

Vocal communication requires the decoding of temporal information from sounds. How does the auditory system process temporal patterns? The South African clawed frog, *Xenopus laevis*, relies for communication on a specific temporal property, click rate. The behavioral importance of this feature appears for example in two male calls, growling and chirping. Growling, a train of clicks at a 100-Hz rate (10-ms interclick intervals), is made most often by subordinate males when clasped by another male. Chirping consists of bursts of five clicks at 80 Hz. Dominant males chirp when clasping another male. How do males establishing a hierarchy discriminate these calls? We are using neurophysiological methods to investigate how the temporal feature of click rate is discriminated psychophysically and coded by the auditory system. We recorded *in vivo* in the torus semicircularis of the auditory midbrain, in frogs stimulated with pure tones and recorded calls. To circumvent problems of underwater sound stimulation, we directly vibrated the cartilagenous tympanic disk. We found that rate sensitivity arises in the torus

semicircularis. When 161 cells in the torus semicircularis were presented with various click rates, a quarter selected for the characteristic click rates of male calls, failing to follow other rates. Click rate selection persists across sound level. The filtering boundaries fall across a range of behaviorally relevant rates. Rate selection could be involved in distinguishing calls.

**140 Limbic-Auditory Interactions: Hypothalamic Connections with the Inferior Colliculus**

Z. Tina Tan<sup>1</sup>, D.T. Larue<sup>1</sup>, J.A. Winer<sup>1</sup>

<sup>1</sup>*Department of Molecular and Cell Biology, UC Berkeley*

Prior work found significant projections between the medial geniculate body and the limbic system, suggesting that the MGB is the earliest level for auditory-limbic relations. Here, we present evidence for extensive and reciprocal hypothalamic (Hyp) connections with the inferior colliculus (IC).

Unilateral deposits of CT $\beta$  fragment or WGA-HRP were made into subdivisions of the cat IC. Labeled cells were found bilaterally in these hypothalamic subdivisions: dorsal (DH), dorsal area (HDA), lateral (HLA), ventromedial, dorsomedial, periventricular nucleus, posterior, and parvocellular area (PVH), and in the fields of Forel. Ipsilateral labeling dominated and was marked after IC dorsal cortex deposits. Clustering of cells occurred within Hyp, particularly in HLA and DH/SPFm, indicating a topographic projection. Labeling was concentrated in HLA, HPA, HDA, PVH, and DH/SPFm.

BDA (biotinylated dextran amines) deposits in IC subdivisions labeled axon terminals in HLA, DH/SPFm, and in the medial limitans nucleus. Ipsilaterally, axons stream from the lateral thalamus toward the midline in fascicles. Some ended near or on the ependymal layer of the third ventricle, especially dorsally. Others project dorsally, ending in the contralateral DH/SPFm. These axons were oriented vertically. The few HLA endings were clustered and oriented horizontally. BDA-labeled axons were mainly ipsilateral, from ~0.5 to 2  $\mu$ m thick, with variable bouton density (from 1-2 to 20-30), and heterogeneous shapes.

There are thus robust and reciprocal connections between Hyp and IC. The hypothalamic areas involved are related to appetitive and visceromotor functions and/or sleep. In particular, HLA and posterior hypothalamic regions participate in both.

Limbic-auditory interactions arising in the midbrain may have earlier, and different, roles in autonomic function than those in the auditory thalamoamygdaloid system.

Supported by USPHS grant R01DC02319-25. Thanks to Janine P. Beyer for surgical assistance.

**141 Responses in Inferior Colliculus to Dichotic Harmonic Stimuli**

Trevor M. Shackleton<sup>1</sup>, Liang-Fa Liu<sup>1</sup>, Alan R. Palmer<sup>1</sup>

<sup>1</sup>*MRC Institute of Hearing Research, Nottingham, UK*

Humans can integrate harmonics which alternate between the ears into a single percept with a pitch corresponding either to the fundamental of the entire complex or the

spacing of the harmonics in each ear, depending upon the resolvability of the harmonics (Bernstein and Oxenham, 2003, J Acoust Soc Am 113:3323-3334).

To test whether such integration takes place at or before the inferior colliculus, responses of single units to diotic and dichotic harmonic stimuli were recorded in urethane anaesthetised Guinea Pigs. A linear array of eight tungsten electrodes was positioned in the central nucleus of the inferior colliculus. Spike sorting software was used to separate the responses into single units.

Stimuli comprised all harmonics below 10 kHz with fundamental frequencies (F0) from 50 Hz to 400 Hz in half-octave steps. The level of individual harmonics was 50 dB SPL. Five conditions were presented: i) all harmonics in the left ear; ii) all harmonics in the right ear; iii) all harmonics in both ears; iv) even harmonics in the left ear and odd harmonics in the right; and v) odd harmonics in the left ear and even harmonics in the right.

Responses were recorded from 95 units with best frequencies between 0.2 and 15 kHz. 92 units phase-locked to F0s of 50 Hz or higher, 78 units to 100 Hz or higher and 37 to F0s of at least 400 Hz. The majority of units responded predominantly to the contralateral ear. These units responded at F0 for contralateral and diotic stimuli, but at 2F0 for dichotic stimuli. Other units had the same pattern of dichotic responses, although they were excited by either ear monaurally (the ipsilateral excitation was usually weaker). These responses all reflect the periodicity of the input stimulus at the dominant ear. Few units showed binaural integration, responding to F0 in all conditions. These data do not support the hypothesis that binaural integration of pitch occurs primarily at or before the inferior colliculus.

#### **[142] Response Properties of Single Units in the Dorsal Nucleus of the Lateral Lemniscus of Decerebrate Cats**

**Michael Pesavento<sup>1</sup>**, Oleg Lomakin<sup>1</sup>, Vivek Khandwala<sup>1</sup>, Kevin Davis<sup>1</sup>

<sup>1</sup>*Department of Biomedical Engineering, University of Rochester, NY*

The dorsal nucleus of the lateral lemniscus (DNLL) receives most of the same inputs that ascend to the inferior colliculus (IC) and, in turn, projects to the IC. Immunocytochemical studies suggest that the DNLL is a prominent source of inhibitory input to the IC. Despite its unique position in the auditory system, the DNLL has been the subject of relatively few physiological studies. Here we report on the monaural and binaural response properties of DNLL neurons in the decerebrate cat. The tone-driven discharge rates of single units were measured across a range of frequencies and levels to map excitatory and inhibitory response areas for contralateral monaural stimulation. To measure the sharpness of frequency tuning, the steepness of the low- and high-frequency borders of the excitatory area was determined by means of a linear regression. The nature of ipsilateral inputs was evaluated directly using frequency response maps and/or indirectly using methods that rely on sensitivity to interaural intensity differences. The results show that the

contralateral frequency response maps of DNLL units can be grouped into three types: V-shaped maps exhibit wide V-shaped excitatory areas (shallow low- and high-frequency slopes) and little inhibition; narrow maps show level-tolerant excitation (steep slopes on both edges) flanked by sideband inhibition; and closed maps display an O-shaped island of excitation at low levels (undefined slopes) with inhibition at higher levels. According to this classification scheme, 18% of units are V-shaped, 73% are narrow, and 9% are closed. Units that produce a type V map typically have a low best frequency (BF) and receive ipsilateral excitation (EE properties). Narrow and closed units have high BFs and show binaural excitatory/inhibitory (EI) interactions. All three DNLL unit types show high rates of driven activity. These results suggest that the DNLL has the potential to exert strong, differential influence on neural responses in the IC. Work supported by NIDCD grant R01 DC 05161-05.

#### **[143] Intracellular Recordings of Facilitatory and Inhibitory Combination-Sensitive Neurons in Awake Mustached Bats**

**Diana Coomes<sup>1</sup>**, Sergiy Voytenko<sup>1</sup>, Donald Gans<sup>1</sup>, Jeffrey Wenstrup<sup>1</sup>, Alexander Galazyuk<sup>1</sup>

<sup>1</sup>*Northeastern Ohio Universities College of Medicine*

Neurons in the inferior colliculus (IC) of mustached bats often exhibit facilitated or inhibited responses when two spectrally distinct sounds are presented at particular delays. These combination-sensitive responses are thought to analyze complex vocal signals used in echolocation and social communication. To examine the synaptic mechanisms underlying these responses, we recorded postsynaptic potentials in 80 IC neurons from awake mustached bats. In particular, we examined whether low frequency signals produced IPSPs or EPSPs associated with the inhibition or facilitation of responses to sounds within a unit's excitatory tuning curve.

In 58 units for which low frequency signals inhibited the response to high frequency sounds, we observed two patterns of postsynaptic responses. In the first group, low frequency signals evoked an IPSP, indicating that inhibition within the IC contributed to the combination-sensitive interaction. In the second group, low frequency signals did not elicit an IPSP. The absence of IPSPs may indicate that combination-sensitive inhibition for these cells is completely dependant on processing at a lower level of the auditory system. Both groups included low frequency responses with and without EPSPs.

We also recorded from 17 units in which low frequency signals facilitated the high frequency signal. In these units' responses no IPSPs were present, but EPSPs were frequently observed. We have previously shown that glycine (an inhibitory neurotransmitter) is essential for the expression of combination-sensitive facilitation in the IC. This observation led to the hypothesis that combination-sensitive facilitation is based on excitation activated by inhibitory input to the IC. The present data suggest that glycine's role in this form of facilitation does not occur at



the neuron's soma. We speculate that glycinergic input and rebound excitation may occur on distal dendrites.

Supported by NIH RO1 DC 00937, R01 DC005377, F32 DC007786.

#### **144 Phase-Locked Responses to Pure Tones in the Inferior Colliculus and Medial Geniculate Body**

**Mark Wallace<sup>1</sup>**, Liang-Fa Liu<sup>1</sup>, Lucy Anderson<sup>1</sup>, Trevor M. Shackleton<sup>1</sup>, Alan R. Palmer<sup>1</sup>

<sup>1</sup>MRC, Institute of Hearing Research, Nottingham, UK

The ventral division of the medial geniculate body (MGB) receives most of its auditory input from the inferior colliculus (IC) while the medial division receives major auditory inputs from other sources as well. One way of studying the sequential connections is by measuring phase locking (the ability to accurately signal the stimulus waveform in the spike timing). Within the ascending auditory pathway the upper frequency limit of phase-locking decreases while the latency of the response increases by about 1 ms for each synapse in the chain. Here we measured the upper frequency limit and the latency of phase-locked responses in the IC and compared them to those in the medial and ventral divisions of the MGB. We recorded single and multi-units in anaesthetised guinea pigs stimulated with a closed sound system. In three divisions of the IC the phase-locking limits and steady state latencies were: central nucleus – 1034 Hz, mean latency 8.8 ms (4.6 – 15.4 ms); dorsal cortex – 700 Hz, mean latency 16.5 ms (12.8 – 21.3 ms); external nucleus – 320 Hz, mean latency 13.4 ms (12.1 – 14 ms). The frequency limits and latencies for the MGB divisions were: ventral – 520 Hz, mean latency 11.3 ms (9 – 14 ms); medial – 1100 Hz, mean latency 9.3 ms (7.5 – 11 ms). Thus the upper frequency limit of phase-locking is higher in some cells of the medial MGB than in the IC. This is consistent with at least some cells in the medial MGB receiving input directly from the cochlear nucleus without a relay in the IC (Malmierca et al. 2002, J Neurosci 22:10891 – 10897).

#### **145 Organization of Excitatory and Inhibitory Frequency Response Areas in the Rat Inferior Colliculus**

**Salvatore Cristaudo<sup>1</sup>**, Marco A. Izquierdo<sup>1</sup>, Ellen Covey<sup>1,2</sup>, Manuel S. Malmierca<sup>1</sup>

<sup>1</sup>Auditory Neurophysiology Unit. Lab Neurob Hearing. University of Salamanca & INCYL. Salamanca, Spain,

<sup>2</sup>Department of Psychology, University of Washington, Seattle, WA, USA.

The spectral analysis of complex sounds is a fundamental task of the auditory system. Auditory neurons' receptive fields for pure tones can be represented in 2 dimensions (frequency and intensity) as the frequency response area (FRA). Excitatory FRAs of neurons in the inferior colliculus (IC) exhibit a variety of patterns. Several lines of evidence suggest that non-V shaped FRAs include regions of inhibition at frequencies outside the excitatory area. To evaluate the extent to which inhibition contributes to FRAs

of IC neurons, we recorded responses to a probe tone at the neuron's best frequency (BF), 10-20 dB above threshold, in the presence of a simultaneous second tone that was varied across a wide range of frequency and intensity values. Neurons with all types of FRAs showed regions of suppression, but suppression was more common in neurons with non-V shaped FRAs. The majority of suppressive areas were adjacent to the excitatory FRA, but some neurons also had non-adjacent suppressive areas. The suppressive regions often extended into the high and/or low frequency flanks of the excitatory FRA. In a few cases the combination of two tones produced facilitation. Some FRAs showed suppression areas similar to those seen in the auditory nerve, but many others were different. For example, some units had multiple discontinuous inhibitory bands on either side of the excitatory FRA, or inhibitory side bands with thresholds much lower than those reported in auditory nerve fibers. These data support the idea that the inhibitory components of FRAs in many IC neurons do not simply reflect peripheral suppressive properties, but represent the effects of synaptic inhibition operating in the IC. There appears to be extensive across-frequency integration at the level of the IC, which can take a variety of forms.

Research supported by the Spanish JCyL-UE (SA040/04, MSM), DGES (BFI-2003-09147-02-01, MSM), NIH (DC00607, EC). SC holds a fellowship from the USAL and MAI from the MEC.

#### **146 Stepwise Organization of Tonotopy in the Inferior Colliculus of the Rat: Electrophysiological Evidence**

**Manuel S. Malmierca<sup>1</sup>**, Marco A. Izquierdo<sup>1</sup>, Salvatore Cristaudo<sup>1</sup>, David Pérez-González<sup>1,2</sup>, Olga Hernández<sup>1</sup>, Ellen Covey<sup>1,2</sup>, Douglas L. Oliver<sup>1,3</sup>

<sup>1</sup>Auditory Neurophysiology Unit. Lab Neurob Hearing. University of Salamanca & INCYL. Salamanca, Spain,

<sup>2</sup>Department of Psychology, University of Washington, Seattle, WA, USA., <sup>3</sup>Department of Neuroscience, University of Connecticut Health Center, Farmington, Connecticut.

A fundamental feature of the inferior colliculus (IC) is its tonotopic organization, which is often assumed to be a continuous progression from low to high frequency. Fibrodendritic laminae have been postulated to be the anatomical substrate for the tonotopic organization, but the relation between frequency representation and laminar structure remains unclear. Two series of experiments conducted in urethane-anesthetized rats provide details about the fine-grained tonotopic progression in the IC. 1) Best frequency (BF) of multiunit clusters was measured in 25 or 50  $\mu\text{m}$  steps along dorsoventrally oriented microelectrode penetrations ( $n=28$ ). The resulting tonotopic progressions show that BF remained nearly constant (range =  $0.09 \pm 0.14$  octaves) for approximately  $199 \pm 66 \mu\text{m}$  (uncorrected for angle of penetration) before jumping by a mean interval of  $0.55 \pm 0.48$  octaves. 2) Frequency response areas of >400 well-isolated, single units in the IC were determined with automated software. The BFs of this sample showed a multimodal distribution



with 10-12 peaks occurring at  $0.53 \pm 0.19$  octave intervals. The frequencies of the peaks in the single unit data are strongly correlated ( $R=0.9988$ ) with the frequency steps in the tonotopic maps. These data provide convincing evidence that the IC comprises discrete physiological laminae, and provides an estimate of the size of the frequency step between adjacent laminae.

Research supported by JCyL-UE (SA0400/04, MSM), DGES (BFI-2003-09147-02-01, MSM), and NIH (DC00607, EC; DC00189, DLO). SC holds a fellowship from the USAL and MAI from the MEC.

#### **147 Temporal Integration of Postsynaptic Events by Inferior Colliculus Neurons**

Sergiy Voytenko<sup>1</sup>, Alexander Galazyuk<sup>1</sup>

<sup>1</sup>*Northeastern Ohio Universities College of Medicine*

The central nucleus of the inferior colliculus (IC) is a major integrative center in the central auditory system. It receives and integrates information from both the ascending and descending auditory pathways. To determine how single IC neurons integrate excitatory and inhibitory inputs over a wide range of sound frequencies and sound levels, we examined their intracellular responses to frequency modulated (FM) sounds in awake little brown bats (*Myotis lucifugus*). Postsynaptic potentials were recorded in response to downward FM sweeps of the range typical for little brown bats (80-20 kHz) and to three FM subcomponents (80-60 kHz, 60-40 kHz, and 40-20 kHz). More than half of recorded neurons responded to the 80-20 kHz downward FM sweep with a distinct response pattern; excitation preceded and followed by inhibition. Postsynaptic recordings in response to three FM subcomponents revealed that these neurons receive and integrate excitatory and inhibitory inputs on their postsynaptic membranes across a wide range of sound frequencies. Summated postsynaptic potentials to three FM subcomponents correlated well with neural responses to the entire FM sweep when these stimuli were presented at sound levels near unit threshold. At higher sound levels, however, this correlation was dramatically reduced. At sound levels close to unit threshold single IC neurons showed near linear summation of different postsynaptic events.

Research is supported by grant from the National Institute for Deafness and Other Communicative Disorders (NIH R01 DC005377).

#### **148 Projections from the Subcollicular Area to the Medullary Reticular Formation**

Nell Cant<sup>1</sup>, Christina Benson<sup>1</sup>

<sup>1</sup>*Duke University Medical Center, USA*

The midbrain tegmentum bordering the inferior colliculus can be subdivided into a number of anatomically distinct regions (Morest and Oliver, 1984). One of these regions, the subcollicular area, is made up of uncommonly large cells that occupy the space between the ventral boundary of the central nucleus of the inferior colliculus and the dorsal boundary of the dorsal nucleus of the lateral lemniscus, extending beneath the inferior colliculus

throughout most of its caudal to rostral extent. In the course of studies of the neuroanatomy of the auditory pathways in the gerbil, we made injections of a retrograde tracer (biotinylated dextran amine) into the superior olivary complex (SOC) and also into the pontine-medullary tegmentum caudal to the SOC. When the injections were caudal to the SOC, the large neurons of the subcollicular region were heavily labeled. They were also labeled when injections in the SOC included the superior paraolivary nucleus but not when the injection was centered in other olivary nuclei. Injection of an anterograde tracer (biocytin) into the subcollicular area allowed us to trace the course of the axons of the large cells. The axons coursed through the pontine reticular formation and into the medullary reticular formation, where they gave rise to thin collateral branches. The large axons continued to course caudally, possibly as far as the spinal cord.

#### **149 Ultrasonic Communication in Frogs**

Albert S. Feng<sup>1</sup>, Peter M. Narins<sup>2</sup>, Chun-He Xu<sup>3</sup>, Wen-Yu Lin<sup>1</sup>, Zu-Lin Yu<sup>4</sup>, Qiang Qiu<sup>4</sup>, Zhi-Min Xu<sup>4</sup>, Jun-Xian Shen<sup>4</sup>

<sup>1</sup>*University of Illinois*, <sup>2</sup>*University of California, Los Angeles*, <sup>3</sup>*Shanghai Institutes of Biological Sciences*,

<sup>4</sup>*Institute of Biophysics (Beijing)*

Among the vertebrates, only microchiropteran bats, cetaceans and some rodents produce and detect ultrasounds for the purpose of communication and/or echolocation, suggesting that this capacity may be restricted to mammals. Here we report the first evidence of ultrasound communication in an amphibian from China - the concave-eared torrent frog (*Amolops tormotus*). Males of *A. tormotus* produce diverse bird-like melodic calls with rising and/or falling frequency modulations, often containing spectral energy in the ultrasonic range. We conducted acoustic playback experiments and found that the audible as well as the ultrasonic components of a species call could evoke males' vocal responses. Additionally, *A. tormotus* calls, particularly their ultrasonic components, can trigger startle responses in selected local moth species, similar to the noctuid moths' reactions to bat's echolocation signals. Electrophysiological recordings from the auditory midbrain confirmed the ultrasonic hearing capacity of these frogs. This extraordinary upward extension into the ultrasonic range of both the frog's calls and the hearing sensitivity is likely to have coevolved in response to the intense, predominately low-frequency ambient noise from local streams. Because amphibians are a distinct evolutionary lineage from microchiropterans and cetaceans, ultrasonic perception in these animals represents a novel example of independent evolution.

Research is supported by grants from the NIDCD (R01-DC04998 to ASF & R01-DC00222 to PMN), a State Key Basic Research and Development grant (G1998010100; China) to CHX, and a National Natural Sciences Foundation grant (90208012; China) to JXS.

### **150 Topographic Organization of Spectrotemporal Receptive Fields in the Cat Inferior Colliculus**

Francisco Rodríguez Campos<sup>1</sup>, Heather L. Read<sup>1</sup>, Monty A. Escabi<sup>1</sup>

<sup>1</sup>University of Connecticut

The central nucleus of the inferior colliculus (ICC) has a distinct laminar organization and pattern of projecting brainstem input. Previous studies have characterized the laminar and frequency organizations using pure-tones and modulated signals. Here we hypothesize that STRF sensitivities obtained with broadband stimuli will be systematically distributed along the rostro-caudal and dorso-medial / ventro-lateral dimensions of the central nucleus. In order to characterize the ICC topography, we are presenting dynamic ripple stimuli and recording neuronal activity within the central nucleus using a 16 channel acute recording probe. The probe penetrations are referenced to three specific coordinate axes using a stereotaxic frame assembly and are aligned orthogonal to the ICC isofrequency lamina. These techniques are allowing us to quantify the organization of STRF preferences, and the global topographic organization within the central nucleus.(supported by NIDCD R01DC006397-01A1).

### **151 Information Content of Inter-Spike Interval and Modulation Transfer Functions in the Inferior Colliculus**

Yi Zheng<sup>1</sup>, Francisco Rodríguez Campos<sup>1</sup>, Eric Flynn<sup>2</sup>, Heather L. Read<sup>3</sup>, Monty A. Escabi<sup>1,2</sup>

<sup>1</sup>Biomedical Engineering Program, University of Connecticut, <sup>2</sup>Department of Electrical and Computer Engineering, University of Connecticut, <sup>3</sup>Department of Psychology, University of Connecticut

We studied the responses of neurons in the inferior colliculus (IC) of the anesthetized cat to noise bursts with various inter-burst intervals. Modulation transfer functions (MTFs) based on spike rate (rMTFs) show band-pass sensitivity whereas for vector strength (tMTFs) they are typically low-pass. A normalized MTF based on average spikes per stimulus event display low-pass shape. Neuronal responses were categorized into three groups: most units have high spikes rate and high synchrony (type I); a subpopulation of neurons have less than one spike per event but have high synchrony (type II); a few neurons had higher spontaneous activities and display band-pass tMTFs (type III). To identify differences in temporal spiking patterns between these three types, we characterized the inter-spike interval (ISI) histograms. Based on ISIs, we measure the information content of the responses and introduce a new entropy and information MTFs to characterize the coding capacity of spikes about specific stimuli. We found distinguished peaks not only at the ISI value that corresponds to the synchronized intervals of noise bursts, but also at the second-order interval bursts. This indicates that different temporal patterns of the synchronized response contribute to the temporal response. (Supported by NIDCD R01DC006397-01A1)

### **152 The Encoding of Echo Roughness in the Inferior Colliculus of the Spemann Bat *Phyllostomus Discolor***

Frank Borina<sup>1</sup>, Gerd Schuller<sup>1</sup>, Lutz Wiegreb<sup>1</sup>

<sup>1</sup>Ludwig - Maximilians - Universität

*P. discolor* travels a distance of several miles each night from its sleeping quarter to its hunting grounds. For orientation, the bat uses landmarks, presumably trees. If so, these trees need to be correctly identified by the bat using their echolocation system. However, the acoustic image of a tree is stochastic and very complex and so is the echo perceived by the bat. Nevertheless, behavioural experiments have shown that bats are able to discriminate and classify signals of different roughness. Recent cortical recordings describe a neural correlate of the psychophysical roughness sensitivity encoded as a rate code. But where is this rate code generated?

Here, the role of the inferior colliculus (IC) in the neural encoding of echo roughness is studied. Units are characterized in terms of their receptive fields, response types, binaural properties and their responses to signals of different roughness and different amplitude-modulation frequency and depth. A stereotactic device allows the spatial reconstruction of recording sites.

Data from over two hundred units in the IC have been collected so far. It is shown that about half of these units respond significantly different to signals with different roughness. Unlike in cortex, many roughness-sensitive units were found where the response strength decreases with increasing echo roughness. The relationship between the encoding of roughness and amplitude modulation will be assessed quantitatively. The spatial distribution of roughness-sensitive units within the IC will be described.

The current data indicate that the IC may play a crucial role in the conversion of the supposedly temporal roughness code in the auditory brainstem into the cortical rate code.

### **153 The Generation of Rebound Excitation in the Inferior Colliculus**

Shobhana Sivaramakrishnan<sup>1</sup>, Douglas L. Oliver<sup>1</sup>

<sup>1</sup>Dept of Neuroscience, University of Connecticut Health Center

In the auditory system, rebound excitation is a mechanism for precise temporal coding of acoustic signals. For example, auditory neurons that fire at the offset of a sound encode amplitude-modulated sounds with high synchrony and may also be tuned to sound duration. Rebound excitation is characterized by a burst of action potentials that follows inhibitory synaptic input. The inhibitory input and the subsequent rebound excitation form a temporal gate where the duration of inhibition sets the time during which excitation is enhanced. We have previously demonstrated that rebound spikes in the inferior colliculus (IC) are sodium spikes, and an intrinsic neuronal property, evoked by preceding hyperpolarization. In 50% of IC neurons, rebound spikes are due to simple anode-break, while in the remaining neurons (the "rebound neurons"), rebound excitation is evoked by a calcium-dependent

mechanism. Activation of the  $\text{Ca}^{++}$ -dependent process results in a shorter latency of onset of rebound excitation and, therefore, may be an important cellular feature of auditory processing. Here, we examine the mechanism that underlies calcium-dependent rebound excitation in the IC. Experiments were performed in IC brain slices of 3-4 week old rats. Whole-cell patch clamp techniques were used to measure neuronal responses to current waveforms that simulated inhibitory postsynaptic potentials (sIPSPs) generated by combining current steps with current ramps. We varied the number of sIPSPs, their amplitude, decay time and duration by changing the number of steps, the step size, ramp speed and duration. Our preliminary results suggest that  $\text{Ca}^{++}$ -dependent rebound excitation is preferentially evoked by rapidly decaying sIPSPs. Rebound excitation depends on the resting potential of the cell with a greater probability at more positive resting potentials. The rebound is abolished by 50  $\mu\text{M}$   $\text{NiCl}_2$ , suggesting a dependence on T-type  $\text{Ca}^{++}$  channels. Thus, the generation of rebound excitation in IC neurons may depend on the previous level of depolarizing activity as well as the timing and kinetics of the inhibitory inputs.

Supported by NIDCD grant DC00189.

#### **154 A Simple Extension to the STRF That Accounts for Rate-Level Non-Linearities**

**Peter Marvit<sup>1</sup>**, Heather Dobbins<sup>1</sup>, Barak Shechter<sup>1</sup>, Muhammad K.N. Afghan<sup>1</sup>, Yadong Ji<sup>1</sup>, Didier Depireux<sup>1</sup>  
<sup>1</sup>University of Maryland, Baltimore

The spectrotemporal receptive field (STRF) has been used as a linear characterization of auditory neural responses. It is often derived from spike rates in response to auditory grating stimuli (e.g., dynamic moving ripples) or other complex sounds with modulation depths greater than the neuron's dynamic range. Classic STRF computation assumes a completely linear relationship between deviations of the stimuli from a mean level and a unit's response. Real-world neurons, however, often show dramatically non-linear rate-level functions (e.g., saturation or contrast-selectivity), that disrupts the classic STRF's linearity assumption. We propose a simple extension to the STRF that additionally models level-specific characterizations of neural responses. This new STRF allows for richer neural characterization and prediction (e.g., to stimuli of different contrasts). We apply this new STRF to example cells from inferior colliculus recorded in awake ferret (*Mustela putorius*).

#### **155 Linearity in Primary Auditory Cortex of the Ferret**

**Bashir Ahmed<sup>1</sup>**, Akhil Shial<sup>1</sup>, Jan W.H. Schnupp<sup>1</sup>  
<sup>1</sup>Laboratory of Physiology, University of Oxford, UK

To predict feature selectivities of auditory cortical neurones (A1), a number of studies have used correlational analysis between the spectro-temporal structure of the sound and the neuronal response (e.g., deCharms et al., 1998, Science 280, 1439; Schnupp et al., 2001, Nature 414, 200). The underlying assumption in these studies has been response linearity based on stimulus-response

stationarity, and these approaches have provided indirect and qualitative estimates of neuronal linearity. However, how linear are auditory cortical cells? Here we report on a comparison between two independent measures of response linearity in A1 cells.

In anaesthetized ferrets (domitor+ketamine, iv), responses were recorded with Michigan probes (16 sites,  $\sim 2.5 \text{ M}\Omega$ , NeuroNexus Technologies). The stimuli were random chord sequences (tone pips, duration 10 ms, frequency range 0.5 - 25 kHz, sequence duration 7.6 s, 40 sequences, 5 repeats, at 75 dB), and broadband dynamic spectral ripples (sinusoidally modulated, frequency range 0.5 - 25 kHz, duration 30s, 5 repeats, randomly interleaved, varying in density 0.125 - 2 cyc oct<sup>-1</sup>, and velocity 0.5 - 16 Hz).

We examined the responses of A1 cells to spectral ripple stimuli and from the period histograms of their responses determined the  $f_1/f_0$  ratio, a quantitative estimate of linearity (Movshon et al., 1978, J Physiol 283, 53). A subdivision of A1 cells that were linear ( $f_1/f_0$  ratios > 1.0) to a wide range of spectral ripple stimuli were now examined to assess their linearity through a cross validation procedure applied to the responses from random chord sequences. These results showed that only a minority of these cells were linear and, hence, there was a poor correlation across these two measures.

Support Contributed By: BBSRC (UK) grant 43/S19595

#### **156 Neural Coding of Repetition Rate and Temporal Regularity in Auditory Cortex**

**Daniel Bendor<sup>1</sup>**, Xiaoqin Wang<sup>1</sup>  
<sup>1</sup>Johns Hopkins University, Baltimore, Maryland

In both the auditory and somatosensory systems, stimulus repetition rates can be categorically classified as either a discrete or continuous percept. Low repetition rates (<50 Hz) generate the discrete percept of flutter whereas higher repetition rates generate the continuous percept of vibration or pitch. In auditory cortex, two different populations of neurons encode fast repetition rates, pitch-selective neurons in the pitch area and non-synchronizing neurons in primary auditory cortex (A1). Pitch-selective neurons are tuned to a particular repetition rate and are sensitive to temporal regularity. In contrast, non-synchronizing neurons respond to a wider range of repetition rates with a positive monotonic encoding relationship (higher repetition rates evoke higher discharge rates) and generally do not significantly change their discharge rates when periodic stimuli are temporally jittered. These neurons appear to encode average repetition rate (related to the percept of roughness or vibration) rather than pitch. Slow repetition rates (that generate the percept of flutter) can be temporally represented in A1 by stimulus-synchronized discharges.

We have also observed two new classes of neurons in auditory cortex that respond to slow repetition rates with positive and negative monotonic discharge rate relationships, respectively, without exhibiting stimulus-synchronized firing patterns. Positive monotonic neurons respond maximally at repetition rates of  $\sim 50 \text{ Hz}$  while

negative monotonic neurons respond maximally at repetition rates of ~5-10 Hz.

These findings suggest that representations of average repetition rate are transformed into positive and negative monotonic rate codes by a subpopulation of neurons in auditory cortex, which have a much longer temporal integration window than that of neurons with stimulus-synchronized responses. Our observations parallel those of flutter frequency representations in somatosensory cortex and suggest a general neural encoding strategy used by sensory cortex.

### **157 Psychometric and Neurometric Discrimination of Non-Conspecific Vocalizations**

**Kerry Walker<sup>1</sup>, Andrew King<sup>1</sup>, Bashir Ahmed<sup>1</sup>, Jan W.H. Schnupp<sup>1</sup>**

<sup>1</sup>*University of Oxford*

We have previously demonstrated that the temporal discharge patterns of ferret A1 neurons transmit significant amounts of information about stimulus identity when tested with natural and time-reversed marmoset "twitter" vocalizations (Schnupp et al., 2005). Here, we compared the discrimination performance afforded by these spike pattern codes (a "neurometric" function) to behavioural performance (a psychometric function). Human psychophysical data were collected for a two-alternative forced-choice oddity task in which a natural twitter was presented along with twitters containing locally time-reversed bins of 10, 20, 40 or 80 ms width. Listeners' ability to distinguish locally time-reversed twitters from unmanipulated sounds was perfect when the reversed time windows were 80 ms wide, but declined dramatically for time windows of 20 ms or less. We also recorded responses of ferret A1 neurons to these twitter stimuli, and used statistical algorithms to determine if the temporal spiking patterns could discriminate between the natural and locally time-reversed twitters. We found that while no single unit neurometric matched the psychometric performance curve completely, the enveloped or pooled responses of a small subset of the few "best" units in our sample could support psychometric performance. These findings suggest that the temporal discharge patterns of small groups of A1 neurons contain sufficient information to underlie behavioural discrimination of non-conspecific vocal stimuli. Furthermore, A1 temporal discharge patterns were found to carry information most efficiently when sampled at a temporal resolution of 10 - 20 ms.

### **158 Representations of Three-Dimensional Spatial Locations in Auditory Cortex of Awake Monkeys**

**Sheng Xu<sup>1</sup>, Xiaoqin Wang<sup>1</sup>**

<sup>1</sup>*Laboratory of Auditory Neurophysiology, Department of Biomedical Engineering, Johns Hopkins Univ.*

Previous studies of auditory cortex in both anesthetized and awake animals have shown that firing rates and patterns of cortical neurons are modulated by sound location, and most neurons preferentially respond to sounds from the contralateral hemifield. Although spatial tuning is found to be sharper in awake than anesthetized

animals, spatial receptive fields are generally broad in auditory cortex. Moreover, spatial tuning tends to broaden with increasing sound level in anesthetized animals whereas less broadening has been observed in awake animals. However, most previous studies either investigated neurons' tuning properties for azimuth and elevation separately, or were restricted to the front region. In this study, we investigated spatial tuning to sounds coming from multiple free-field locations in the auditory cortex of awake marmoset monkeys (*Callithrix jacchus*). Fifteen equally-spaced speakers were placed on a semi-spherical surface centered around the animal's head and above the horizontal plane. A variety of complex sounds, including wide-band noise and species-specific vocalizations were used as stimuli. Spatial response fields of many neurons did not show significant changes across sound levels and were similar when tested by broad-band noise or vocalization stimuli. Neurons with both sharp and broad tuning were observed. Most neurons were found to respond maximally to a few (usually clustered) speaker locations. The distribution of neurons' preferred speaker locations spanned across all tested locations. Some neurons also exhibited different temporal firing patterns in response to different speaker locations. These observations suggest that neurons in auditory cortex may be tuned to specific spatial locations in three-dimensional space by combining azimuth and elevation information, as well as other spatial cues. Supported by NIH grant R01-DC03180.

### **159 Neural Representation of the Precedence Effect and Its Breakdown in Monkey Auditory Cortex**

**Yonatan Fishman<sup>1</sup>, Mitchell Steinschneider<sup>1</sup>**

<sup>1</sup>*Albert Einstein College of Medicine*

Identifying the location of a sound source is fundamental for auditory scene analysis. Stimulus onsets are a dominant feature determining sound location (i.e., precedence effect), a phenomenon crucial for sound localization in echoic environments. There are many situations, however, where the precedence effect can be overridden by ongoing stimulus cues. One behavioral paradigm that illustrates the precedence effect and its breakdown utilizes pulse trains of varying interpulse interval (IPI) (Freyman et al., 1997). When IPIs are short (e.g., 1 ms), sound localization is determined by the location of the initial pulse, regardless of whether later pulses emanate from the same or opposite hemifield. In contrast, when IPIs are long (e.g., 5 ms), sound localization is determined by the location of later pulses, regardless of the location of the initial pulse.

We investigated neural mechanisms potentially important for these effects by examining multiunit activity in monkey auditory cortex evoked by pulse trains with short and long IPIs, and when the initial and later pulses are located in either the same or opposite hemifield. Results parallel perceptual findings in humans: 1) onset responses correlate with the precedence effect, 2) total responses (onset plus sustained activity) correlate with the breakdown of the precedence effect. Specifically, onset responses are larger when the initial pulse originates from the contralateral hemifield, regardless of IPI. In contrast,

total responses are larger when the later pulses originate from the contralateral hemifield, but only for stimuli with prolonged IPIs.

We conclude that both early and later response components are important for sound localization and scene analysis. Context dependence of these components, as determined by IPI, may be partly responsible for the neural representation of the precedence effect and its breakdown. Supported by DC00657 and DC042890.

### **160 Neural Representation of Inharmonicity in Monkey Auditory Cortex**

**Mitchell Steinschneider<sup>1</sup>**, Yonatan Fishman<sup>1</sup>

<sup>1</sup>*Albert Einstein College of Medicine*

When a single component of a harmonic complex is mistuned from its harmonic value by a sufficient amount (> 3%), it is heard as a separate tone and stands out from the complex as a whole. This phenomenon exemplifies segregation based on inharmonicity, and is a fundamental cue utilized in auditory scene analysis. Two perceptual mechanisms are implicated in the detection of inharmonicity (e.g., Moore et al., 1986; Hartmann et al., 1990). For low, resolved harmonics, a mistuned component is perceived as “popping out” as a discrete tone, whereas for high, unresolved harmonics, detection of inharmonicity is facilitated by the perception of “beats” produced by amplitude fluctuation in the waveform temporal envelope.

We investigated neural mechanisms potentially important for detection of inharmonicity by examining multiunit activity evoked by harmonic and mistuned tone complexes in auditory cortex of a monkey performing a sound detection task. Inharmonicity was produced by mistuning either the 3rd (resolved) or 9th (unresolved) harmonic while maintaining a constant  $f_0$  of the complex, or by shifting the  $f_0$  and maintaining a constant frequency of the 3rd or 9th harmonic. The 3rd and 9th harmonics were placed at or near the best frequency of the recording site. Results parallel perceptual findings in humans: 1) responses are enhanced when a partial is mistuned from its harmonic relationship, 2) response enhancement increases with increases in mistuning, 3) enhanced responses are not explained by the characteristics of the pure tone tuning curves, and 4) phase-locked responses are evoked at “beat” frequencies in the mistuned complexes, especially for unresolved mistuned partials.

We conclude that both response enhancement and the generation of phase-locked responses evoked by “beat” frequencies may be important physiologic mechanisms for the detection of inharmonicity, which in turn may contribute to auditory scene analysis. Supported by DC00657 and DC042890.

### **161 Orthogonal Stimulus Features in Computational Topographies of Auditory Cortex**

**Paul V. Watkins<sup>1</sup>**, Dennis L. Barbour<sup>1</sup>

<sup>1</sup>*Washington University*

Neurons in primary visual cortex (V1) of several species exhibit a topographic representation of stimulus features,

including retinal position (retinotopy), orientation preference (OP), and ocular dominance (OD). Superimposed topographies of OD and OP show a non-random correlation, implying that these topographies do not develop independently. The self-organizing feature map (SOFM) is a dimensionality-reduction algorithm that can be applied to project an  $N$ -dimensional vector of stimulus features onto a two-dimensional grid representing a cortical minicolumn. The SOFM algorithm generates topographies well-matched to those observed experimentally in V1. Other than a topographic representation of frequency (tonotopy), auditory stimulus feature topographies in primary auditory cortex (A1) have been difficult to discern physiologically. We used the SOFM algorithm with  $N$  arbitrary uniformly distributed stimulus feature dimensions to test which conditions induce a single secondary stimulus feature to map orthogonally to the dominant stimulus feature (i.e. frequency) over the entire grid (global orthogonality). We found that: (1) under many conditions, the iso-contour lines of secondary stimulus features predominantly orient themselves at right angles to the dominant stimulus feature iso-contour lines (local orthogonality), without any single secondary stimulus feature becoming globally orthogonal to the dominant stimulus feature; (2) a tendency exists for periodicity of lesser stimulus features along the axis orthogonal to the dominant stimulus feature axis of gradation; (3) the dominant stimulus feature tends to orient its axis of gradation along the longest line segment in the grid; (4) typically within a particular small region of the grid only one secondary stimulus feature is locally orthogonal to the dominant stimulus feature, indicating that only one stimulus feature has a large gradient in any given small region.

### **162 Spectro-Temporal Tuning in Long Duration Stimuli for AI of the Awake Ferret**

**Barak Shechter<sup>1</sup>**, Heather Dobbins<sup>1</sup>, Muhammad K.N.

Afghan<sup>1</sup>, Peter Marvit<sup>1</sup>, Yadong Ji<sup>1</sup>, Didier Depireux<sup>1</sup>

<sup>1</sup>*University of Maryland School of Medicine*

Many current methods that provide a spectral-temporal characterization of auditory neural responses use relatively long stimuli, lasting seconds to minutes. However, neurons in the central part of sensory pathways tend to adapt in their response to stimuli presented over extended periods of time. We have previously shown that auditory cortical neurons display a second order of adaptation, whereby the characteristics of their adaptation to the presentation of repeated long stimuli change with each presentation; in other words, the rate of cortical adaptation decreases across multiple long stimuli. Methods have been developed which provide a joint spectro-temporal characterization of neural responses in the auditory pathway. In particular, the auditory grating method, known as moving ripple method and its extensions, have proven to be well correlated with the more classic tone pip methods of response area characterization. But the ripple and other related stimuli are periodic, introducing the possibility of adaptation as the receptive field is being measured. Computation of the spectro-temporal receptive field (STRF) using the response to these ripple

combinations assumes stationarity in the neural input/output function. We will demonstrate dynamic changes in tuning during the measurement of the STRF over a period of seconds, even absent a relevant behavioral task. Research supported by NIH/NIDCD

### **163 Neuronal Responses in Auditory Cortex to Phonemes in Natural Speech**

**Nima Mesgarani<sup>1</sup>, Stephen David<sup>1</sup>, Shihab Shamma<sup>1</sup>**

<sup>1</sup>*University of Maryland College Park*

We examined the responses of neurons in primary auditory cortex (A1) of awake ferrets to phonetically labeled speech stimuli. Sentences were taken from the TIMIT database and chosen to represent a diversity of male and female speakers. We presented these stimuli to awake ferrets while recording the activity of isolated A1 neurons. For analysis, we segmented the continuous speech samples into sequences of phonemes, which represent the smallest significant units of speech. We characterized the response properties of each neuron as a vector of the mean response to each phoneme. Across a population of A1 neurons, we observed distinct patterns of phoneme selectivity that may provide a neural basis for low-level phoneme discrimination.

In order to test linearity of cortical processing of natural speech sounds, we estimated spectro-temporal receptive fields (STRFs) for each neuron using normalized reverse correlation of the response to the speech stimuli. We used these STRFs to predict the response to each phoneme, which we compared to the observed phoneme responses. Differences between the observed and predicted responses may reflect non-linear processes.

We also compared neural phoneme selectivity to known human psychoacoustic data. We measured the discriminability of phoneme pairs using a distance metric based on the responses of the neural population to each phoneme. We used the population-derived distances to construct a neural phoneme confusion matrix, which we compared to a psychoacoustically derived phoneme confusion matrix (Allen, 2005). This comparison provides insight into the relationship between neural representation and perception of complex natural stimuli.

### **164 Representation of ITD in the Human Midbrain**

**Sarah Thompson<sup>1,2</sup>, Katharina von Kriegstein<sup>1,3</sup>, Adenike Deane-Pratt<sup>1</sup>, Timothy Griffiths<sup>1,3</sup>, Torsten Marquardt<sup>1</sup>, David McAlpine<sup>1</sup>**

<sup>1</sup>*UCL*, <sup>2</sup>*Cambridge University, UK*, <sup>3</sup>*Newcastle University*

Humans make use of small differences in the timing of a sound at the two ears to determine the location of low-frequency (<1500 Hz) sound sources. The neural representation of auditory space based on these interaural time differences (ITDs) is presumed to be one in which sounds leading in time at one ear activate maximally neural centres in the opposite side of the brain. An outstanding issue concerns the representation of ITDs in the human brain, particularly the range of ITDs encoded, where "range of ITDs" is taken to be synonymous with "range of delay lines". Here, we examine the

representation of ITDs in the human inferior colliculus. Using functional magnetic resonance imaging and headphone presentation of interaurally-delayed bands of noise centred at 500 Hz, we test the hypothesis that ITD processing in the inferior colliculus is achieved using a restricted range of ITD detectors; specifically, ITDs greater than half the period of the stimulus frequency are not explicitly encoded in the brain. All noises were of 400-Hz bandwidth with ITDs of  $\pm 0.5$  ms or  $\pm 1.5$  ms. ITDs of +0.5 and +1.5 ms were reliably perceived on the left, and ITDs of -0.5 and -1.5 ms on the left. We find that ITDs of  $\pm 0.5$  ms generate greater activity on the side contralateral to the perceived lateral image of the sound, but that ITDs of  $\pm 1.5$  ms generate greater activity on the side ipsilateral to the perceived lateral image. Our data are consistent with physiological evidence showing a lack of detectors in mammals explicitly tuned to ITDs beyond about half the period of the centre frequency of a sound. They are also consistent with the notion that any specific mechanisms that extrapolate constant ITDs across sound frequency channels reside at least above the level of the auditory midbrain in humans. Thus, sensitivity to ITDs in humans, at least at the level of the midbrain, is best considered in terms of the pattern of activity across both sides of the brain, rather than a contralateral representation.

### **165 Auditory Extinction as a Question of Right Space Left in Time: Spatial Segregation Deficits vs. Simultanagnosia After Right- vs. Left-Hemisphere Lesions**

**Claudia Schubert<sup>1</sup>, Manon Grube<sup>2</sup>, D. Yves von Cramon<sup>3</sup>, Rudolf R  bsamen<sup>1</sup>**

<sup>1</sup>*University of Leipzig*, <sup>2</sup>*University of Newcastle*, <sup>3</sup>*MPI for Human Cognitive and Brain Science*

The present study approached auditory extinction in bilateral simultaneous recognition under free-field conditions with specific respect to dependencies of stimulus laterality. Results were obtained in a considerable number of patients suffering from right- (RH) or left-hemisphere (LH) subcortical and/or cortical lesions, diagnosed with contralesional (RHC, LHC) or bilateral (RHB, LHB) headphone deficits, which are psychoacoustically related to auditory cortex and further extended, less specific damage, respectively.

Bilateral recognition was impaired in both RH and LH patients. Extinction was more frequent and more severe in the RH patients. Deficits were thereby more pronounced for smaller stimulus lateralities in RH patients. In LH patients in contrast, there was no consistent laterality effect observed. Another hemispheric asymmetry lay in almost equally frequent contra- and ipsilesional omissions in LH patients as opposed to nearly exclusively contralesional ones in RH patients.

The occurrence of extinction-like deficits in both patients with contralesional as well as bilateral headphone deficits, related to auditory cortex and further extended damage, respectively, supports the hypotheses of two different levels of the emergence extinction, i.e. a sensory and a higher-level form. More importantly, the interhemispheric asymmetries pointed to two different natures of extinction. The pronounced deficits in RH patients resumed the right-

hemisphere role in spatial awareness of concurrent sound sources, with the poor contralesional recognition reflecting the right-hemifield bias in the left intact hemisphere. The newly-revealed laterality-dependency points to an underlying disturbance in segregation of sound sources rather than to a mere spatial bias. In LH patients, the absence of hemifield-specific or laterality-dependent effects hints to a different deficit related to simultaneity rather than spatial perception.

### **166 Hemispheric Distribution of the Mismatch Negativity and the Representation of Interaural Time Difference**

**Adenike Deane-Pratt<sup>1</sup>, David McAlpine<sup>1</sup>**

<sup>1</sup>*University College London Dept. Physiology and UCL Ear Institute*

Interaural time difference (ITD) is the main cue used to localise low frequency (<1500 Hz) sound-sources. The mismatch negativity (MMN) evoked potential signals automatic detection of rare deviations from a series of otherwise similar sounds, and is sensitive to ITD. We used MMN to measure the response to 400 Hz-wide, bursts of binaural noise centred at 500 Hz in four deviant ITD conditions:  $\pm 500 \mu\text{s}$  ( $\frac{1}{4}$  of the period of 500 Hz) and  $\pm 1500 \text{ Hz}$  ( $\frac{3}{4}$  of the period). These stimuli had perceived lateral positions on the left or right compared to the standard condition which had 0  $\mu\text{s}$  ITD and is perceived in the centre of the head. Sounds were presented via headphones. In the case of  $\frac{1}{4}$  cycle deviants, MMN was greater over the hemisphere contralateral to the perceived position, consistent with previous data. However, a novel finding was that  $\frac{3}{4}$  (far) deviants elicited greater fronto-central negativity ipsilateral to the sound-source. This suggests that stimulus pairs with  $+\frac{1}{4}$  and  $-\frac{3}{4}$  delays, and vice versa, share a similar neural representation. Our data cannot be predicted by place-code models of ITD encoding as these require a full-range of ITD detectors, including long delays, beyond  $\frac{1}{2}$  a cycle of the period of the centre frequency of any auditory channel. Rather, our results are consistent with electrophysiological recordings in animals that suggest a restricted-range – within  $\pm \frac{1}{2}$  a cycle – model.

### **167 Directionality of the Pressure-Difference Receiver Ears in the Northern Leopard Frog, *Rana pipiens pipiens***

**Calvin C.K. Ho<sup>1</sup>, Peter M. Narins<sup>1</sup>**

<sup>1</sup>*Department of Physiological Science, UCLA*

We studied the directional response of the coupled-eardrum system in the northern leopard frog, *Rana pipiens pipiens*. Eardrum behavior closely approximates a linear time-invariant system, with a highly correlated input-output relationship between the eardrum pressure difference and the eardrum velocity. Variations in the eardrum transfer function at frequencies below 800 Hz indicate the existence of an extratympanic sound transmission pathway which can interfere with eardrum motions. The eardrum velocity was shown to shift in phase as a function of sound incident angle, which was a direct result of the phase-shift of the eardrum pressure difference. We used two laser-Doppler vibrometers to measure the interaural

vibration time difference (IVTD) and the interaural vibration amplitude difference (IVAD) between the motions of the two eardrums. The coupled-eardrum system enhanced the IVTD and IVAD by a factor of 3 and 3 dB, respectively, when compared with an isolated-eardrum system of the same size. Our findings are consistent with the time-delay sensitivity of other coupled-eardrum systems such as those found in crickets and flies.

(Supported by NIH grant no. DC00222 to PMN)

### **168 Role of Auditory Cortex and Descending Corticocollicular Projection in Adaptation to Altered Binaural Cues by Adult Ferrets**

**Victoria Bajo<sup>1</sup>, Fernando Nodal<sup>1</sup>, David R. Moore<sup>2</sup>, Andrew King<sup>1</sup>**

<sup>1</sup>*University of Oxford, <sup>2</sup>MRC Institute of Hearing Research, Nottingham, UK*

In adult ferrets, plasticity of spatial hearing has been demonstrated by the finding that stimulus-specific training can lead to a reacquisition of accurate auditory localization after manipulating binaural cues by occluding one ear. Lesion studies indicate that auditory cortex is required for adaptation, but it is not known which region of the cortex is involved or whether this is mediated by descending projections, which have been implicated in learning-induced plasticity in other studies. To investigate these issues, we have examined the behavioral consequences of manipulating the auditory cortex in various ways in adult ferrets trained to localize sound in the horizontal plane. Three experimental conditions were used: 1) mechanical lesions of primary auditory cortex (A1), 2) reversible inactivation of A1 by sub-dural placement of an inert sustained-release polymer containing the GABA<sub>A</sub> receptor agonist muscimol, and 3) selective ablation of layer V pyramidal cells projecting back to the inferior colliculus by chromophore-targeted neuronal degeneration. The ability of the ferrets to localize broadband sounds of different duration (40-2000 ms) and level (56-84 dB SPL) was measured before and after each cortical manipulation. At longer sound durations (1000 ms) sound localization accuracy was unaffected in any animal, although all groups exhibited a significant impairment in their ability to adapt to the altered spatial cues produced by occluding one ear. Ferrets with bilateral lesions of A1 or with selective lesions of the descending cortico-collicular pathway showed no improvement in performance in the presence of a unilateral earplug, whereas reversible inactivation of A1 resulted in slower and less complete adaptation than in normal controls. These results reveal a role for A1 in training-induced plasticity of auditory localization, which could be mediated by descending cortical pathways.

### **169 Neuronal Sensitivity to Virtual Acoustic Space in the External Nucleus of the Gerbil Inferior Colliculus**

**Katuhiko Maki<sup>1</sup>, Shigeto Furukawa<sup>1</sup>**

<sup>1</sup>*NTT Corporation*

The external nucleus of the inferior colliculus (ICx) is thought to be involved in coding sound-source directions.



However, few studies have investigated the representation of auditory space in the mammalian ICx. The present study investigated the neuronal spatial sensitivities in the ICx of anesthetized gerbils, specifically the topographical distribution of the spatial-response properties. The stimuli were 50-ms white-noise burst that varied in azimuth on the horizontal plane in the virtual acoustic space (VAS). The VAS stimuli were synthesized by convolving the noise burst with the quasi-individualized head-related impulse response [Maki and Furukawa, J. Acoust. Soc. Am.

118(2), 872-886; 118(4), 2392-2404, 2005] and were presented to the animal binaurally through earphones. Two stimulus levels, namely 5 and 25 dB above unit threshold, were tested. Units that showed spatial selectivity at either sound level generally exhibited preference to the contralateral hemisphere. The unit's preferred azimuth was evaluated in terms of the centroid of the rate-versus-azimuth function. For the higher-level stimuli, the spatial-response properties of the units varied somewhat systematically along the rostra-caudal dimension of the ICx. Units located rostrally tended to exhibit sharper spatial tuning and to prefer rear stimulus directions. The units' response properties, however, depended markedly on the stimulus level: As the stimulus level decreased, in general, the firing rate decreased, the spatial tuning narrowed, and the preferred azimuth shifted by a significant amount. For 50% of the units, the preferred azimuth shifted to frontal directions by  $>25^\circ$  with the 20-dB decrease of the sound level, and fewer units (20%) showed small shifts ( $<10^\circ$ ) of the preferred azimuth.

#### **[170] Azimuth Tuning Properties of Cortical Neurons in the Awake Ferret**

**Andreas Schulz<sup>1</sup>**, Fernando Nodal<sup>1</sup>, Andrew King<sup>1</sup>

<sup>1</sup>University of Oxford

We examined the spatial tuning properties of neurons in the auditory cortex of both hemispheres in head-restrained awake ferrets. Stimuli were 100 ms broadband noise bursts presented at two different sound levels (56 dB SPL and 84 dB SPL) in  $20^\circ$  steps in the azimuth plane. According to the sulcal pattern observed through the recording chambers and the frequency tuning of the units, most of the recordings were made in primary cortex, with some in surrounding belt areas. We have so far focused only on the onset response of the units, which had a latency of 10-20 ms and duration of 30-40 ms. For most units, this onset response was strongest for sounds presented in the contralateral hemifield. Because we recorded from slightly different areas in each hemisphere, comparisons between the two sides have to be treated with caution. Nevertheless, the range of best azimuths was smaller in the left than in the right hemisphere. In the right cortex, the best azimuths were distributed over almost the entire contralateral side, whereas, in the left cortex, they were clustered in the frontal hemifield from the midline to  $100^\circ$  contralateral. This hemispheric difference was also apparent in the centroid vectors. The vector lengths, which provide a measure of spatial selectivity, were significantly smaller for units recorded on the right than on the left side of the brain. Best azimuths shifted with sound level but remained on the contralateral side. The centroid vector length for the population of the units was significant

smaller at the higher sound level, indicating that, overall, the units became less sharply tuned for sound direction with increasing level. It remains to be seen whether the difference in azimuth tuning observed between units recorded on each side of the brain represents a genuine hemispheric specialization or variations in spatial response properties between different cortical areas.

#### **[171] Interaural Time Sensitivity to Tones in Noise** **Ida Siveke<sup>1</sup>**, Christian Leibold<sup>2</sup>, Benedikt Grothe<sup>1</sup>

<sup>1</sup>Division of Neurobiology, Biocenter of the Ludwig Maximilians University Munich, Germany, <sup>2</sup>Institute for Theoretical Biology, Humboldt-Universität zu Berlin, Germany

The ability to localize and detect a target signal in front of masking noise has been studied in various psychoacoustic, physiological, and theoretical studies and it has been found to depend upon the relative interaural time differences (ITD) of the target and the masker. The neuronal mechanisms underlying the localization of the tone in background noise, however, are still unclear.

In this study we investigated the influence of wide-band Gaussian noise on the ITD sensitivity to pure tones of low frequency neurons in the dorsal nucleus of the lateral lemniscus (DNLL). This nucleus receives direct inputs from the superior olivary complex, the initial site of ITD processing.

We found, that most of the neurons responded to binaural pure tones as well as to noise. Comparing the ITD sensitivity for pure tones in the presence of noise we found two conspicuous features; first the response of the neurons to tones with a favorable ITD decreased by additional presentation of a noise even if the ITD of the noise was favorable. Second, in contrast to the peaks of the ITD functions (maximal responses), the troughs (minimal response) were comparatively unaffected.

Our results therefore contradict a linear superposition of tone and noise ITD tuning curves. In particular, adding a pure tone with an unfavorable ITD to masking noise leads to a suppression of the response that would be evoked by the noise. This finding indicates that the troughs of the pure tone ITD tuning curves might be generated by an inhibitory mechanism - a hypothesis that is corroborated by a model of ITD processing in the medial superior olive, which is based on the assumption that fast contralateral inhibition precedes excitation.

We hypothesize, that for localization in noise it is imported that the minimal response of the neurons stays constant in order to conserve the ITD sensitivity to the front signal. This is likely to be achieved by inhibition at the level of the ITD detector itself.

#### **[172] Binaural Processing in the Brain Stem of Lizards**

**Jakob Christensen-Dalsgaard<sup>1,2</sup>**, Yezhong Tang<sup>2</sup>, Catherine E. Carr<sup>2</sup>

<sup>1</sup>University of Southern Denmark, <sup>2</sup>Department of Biology, University of Maryland

It has been shown recently that lizard ears are highly directional, and that the directionality is created by



acoustical coupling of the eardrums (Christensen-Dalsgaard and Manley, *J Exp Biol* 208:1209-1217, 2005), but the subsequent neural processing of directional information is unknown. In order to investigate whether the strong peripheral directionality is reflected in the central processing, we recorded the response properties of brainstem neurons in the Tokay gecko (*Gekko gecko*) stimulated by dichotic sound.

Gekkos were anesthetized by isoflurane inhalation (3% in 98% O<sub>2</sub>) and a part of the cranial roof overlying the brain stem at the entry of the eighth nerve was removed. The exposure was sealed using a gelatine sponge and the animal allowed to recover for two days. On the day of experiment, the animal was re-anesthetized and the brain stem was exposed. The acoustical coupling between the two ears was reduced by opening the mouth. Dichotic stimuli were presented using two earphone couplers sealed over the eardrum. Neural responses were recorded using high-impedance electrodes. To delineate the auditory centers we also applied dextran amine dyes and cholera toxin in the papilla and in the torus semicircularis in the midbrain.

The auditory nerve projected to the medial and lateral nucleus magnocellularis and to the medial and lateral angularis. Cells in both the nucleus angularis and the superior olive projected to the torus.

Binaural units were found in the brain stem at the entry level of the VIIIth nerve, approximately 1200  $\mu$ m below the dorsal surface (in the vicinity of the superior olive). These cells were excited by both ipsi and contralateral monaural stimulation with lowest thresholds to contralateral stimulation, and the response could be suppressed by binaural stimulation at a characteristic ITD and IID range.

Supported by the University of Maryland Center for Neuroscience, by the Danish National Science Foundation and Science Research Council (JCD) and by grant NIDCD 000436 (CEC)

### **173 Are Descending Instructive Signals from the Forebrain Needed for Manifestation of Adulthood Plasticity of the Tectal Auditory Space Map in the Midbrain?**

**Duck O. Kim<sup>1</sup>**, Andrew Moiseff<sup>2</sup>, Christopher Lee<sup>1</sup>

<sup>1</sup>University of Connecticut Health Center, <sup>2</sup>University of Connecticut

In barn owls, both the forebrain and midbrain contain spatially-tuned neurons and the two sets of space-processing neurons have been found to work in parallel (Knudsen et al., 1993). Their relative roles and interactions, however, need further elucidation. The present research seeks to test the following hypothesis: Manifestation of adulthood plasticity of the tectal auditory space map in the midbrain requires descending instructive signals from the forebrain gaze field, the auditory arcopallium (AAR). This hypothesis was motivated by the observation that, in ferrets, a bilateral lesion of the auditory cortex leads to disruption of adulthood adaptive plasticity of sound localization (King et al., ARO 2003).

In the behavioral part of this study, each adult owl undergoes a period of wearing 17-degree prisms. The

owl's head-orienting behavior is measured using a magnetic coil system before and during the prism period. Subsequent to the behavioral study, we conduct a physiological study of neurons in the owl's midbrain optic tectum. Adaptive plasticity is quantified by measuring how closely the behavioral and physiological responses to sound correspond to the responses to light altered by the prisms. The Hypothesis is tested by comparing the results from intact owls with those from owls whose bilateral forebrain AAR fields are electrolytically lesioned at an adult age prior to the prism period. All of the owls are allowed to actively hunt live prey to enhance the adulthood plasticity (Bergan et al., Soc Neurosci Abst 2004; Kim et al., ARO Abst 2005).

The positive outcome of this study will be significant because it will raise important questions to address. What is the nature of the instructive signal transmitted from the forebrain to the midbrain? How does the forebrain compute the proper instructive signal when there is persistent sensory discordance? What are the cellular mechanisms whereby a forebrain instructive signal produces the midbrain adaptive plasticity?

### **174 Contribution of Binaural Difference Cues to Azimuth Tuning of Neurons in Cat Auditory Cortex**

**Ewan A. Macpherson<sup>1</sup>**, Ian A. Harrington<sup>1,2</sup>, G. Christopher Stecker<sup>1,3</sup>, Chen-Chung Lee<sup>1</sup>, John C. Middlebrooks<sup>1</sup>

<sup>1</sup>Kresge Hearing Research Institute, The University of Michigan, Ann Arbor, MI, USA, <sup>2</sup>Department of Psychology, Augustana College, <sup>3</sup>Department of Speech and Hearing Sciences, University of Washington

We examined the contributions of interaural time and level differences (ITD and ILD) to the rate-based azimuth tuning of neurons in four areas of cat auditory cortex: the primary (A1) and anterior (AAF) auditory fields, plus the dorsal zone (DZ) and posterior auditory field (PAF), two non-primary areas that may be more specialized for spatial processing. We recorded extracellularly using multi-channel, silicon-substrate probes in  $\alpha$ -chloralose-anesthetized cats. Wideband, 80-ms noise bursts were presented from various locations in the horizontal plane either in the free field or in virtual auditory space (VAS). VAS presentation used a transaural delivery system that interfered minimally with free-field conditions, and permitted *in situ* measurement of, and synthesis with, each cat's individual head-related transfer functions. VAS stimuli carried either natural binaural cues or cues biased by delaying (by up to 300  $\mu$ s) or attenuating (by up to 15 dB) the signal at one ear or the other. Azimuth tuning was quantified by the variation in spike count with stimulus azimuth, and the contribution of ITD or ILD was determined by the extent of systematic shifts in azimuth tuning in the biased conditions. In the present sample, ILD-sensitive neurons outnumbered ITD-sensitive neurons, although both were found in each cortical field. In A1 and AAF, ITD sensitivity was generally restricted to neurons with frequency response areas (FRAs) below ~5 kHz, and ILD sensitivity to units with FRAs above ~3 kHz. Individual

units in those fields were rarely sensitive to both ITD and ILD. In DZ and PAF, more units simultaneously sensitive to ITD and ILD were observed. Those units tended to have broad or multi-peaked FRAs that included both high and low frequencies; we did not observe ITD sensitivity in units lacking low-frequency components in their FRAs. This suggests that units sensitive to high frequencies alone were not sensitive to any envelope-based ITD present in our stimuli.

### **175 Biophysical Reasons for Computational Advantages of Passive Soma Structure in Owl's Auditory Coincidence Detector Neurons**

**Go Ashida**<sup>1,2</sup>, Kousuke Abe<sup>1</sup>, Kazuo Funabiki<sup>2</sup>

<sup>1</sup>Graduate School of Informatics, Kyoto University,

<sup>2</sup>Graduate School of Medicine, Kyoto University

In the previous report presented in the 28th ARO midwinter meeting (2005), we studied the advantages of the uncommon 'passive soma' structure of the owl's nucleus laminaris (NL) neuron, which is known to act as a coincidence detector for the detection of interaural time difference (ITD). The results of our numerical simulation was that a model neuron with a passive cell body always achieved higher ITD sensitivity with lower energy costs than a neuron with an active cell body. We concluded that the owl's NL neuron uses that unusual 'passive soma' design for computational and metabolic reasons. Although this conclusion itself was clear, the underlying mechanism of the computational advantages was not sufficiently explained. Here, we put a step forward and examine the properties of the model neuron in detail.

Analysis in the subthreshold regime reveals that increasing somatic sodium conductance monotonously decreases the neuronal impedance of high frequency (>2kHz) AC signals and declines the transfer performance of AC signals from the soma to the first node. In the 'passive soma' condition, the ratio of the AC component in the nodal potential to that in the somatic potential is larger than the ratio calculated with a simple integrated-and-fire model. This result implies that the shape and the Na channel distribution of the NL neuron enhance AC signals to improve its ITD computation performance. Analysis in the suprathreshold regime shows that the after-effect of spike generation upon the neural impedance of AC signals lasts longer in a neuron with active soma than that with a passive soma. This means that the 'passive soma' structure is suitable for recovering from spikes and enables the neuron to handle high frequency signals. The results obtained by our analysis gives an explanation for the computational advantages of the NL neuron's 'passive soma' structure.

### **176 Non-Additive Signal Processing in an MSO Neuron Model, a "Neural Computational" Role for $I_{KLT}$**

**Mitchell Day**<sup>1</sup>, Brent Doiron<sup>1,2</sup>, Gytis Svirskis<sup>1</sup>, John Rinzel<sup>1,2</sup>

<sup>1</sup>Center for Neural Science, New York University, <sup>2</sup>Courant Institute of Mathematical Sciences, New York University

Neurons in the medial superior olive (MSO) participate in the neural computation of localizing a sound source. A

low-threshold potassium current ( $I_{KLT}$ ) endows MSO cells with exceptional temporal precision. Reducing  $I_{KLT}$  by DTX (*in vitro*, gerbil) switches neural firing from phasic to tonic mode (ages P14-P17), decreases phase-locking, and decreases signal-to-noise ratio with EPSG stimuli. Similar behaviors are seen in an idealized leaky integrate-and-fire model with a nonlinear low-threshold conductance.

For this simple biophysical model we use two methods to investigate how  $I_{KLT}$  may affect the "neural computation" that an MSO neuron performs. Method one involves driving the model (with, then without  $I_{KLT}$ ) with a stochastic stimulus of biophysically-relevant statistical structure in the presence of synaptic noise. We extract the time courses of stimuli that elicit spikes (spike-triggered ensemble, STE). Then we use a pattern discrimination function to identify differences between the STE in the presence of  $I_{KLT}$  and the STE in the absence of  $I_{KLT}$ . We find that differences between STEs with and without  $I_{KLT}$  are significant for stimuli in a subset of the full stimulus space. Method two involves computing the stimulus-response (SR) spectral coherence function for a stochastic stimulus and a response spike train from our model. The stimulus contains either separate or mixed low and high frequency components. In the absence of  $I_{KLT}$ , the SR coherence remains the same regardless of whether the stimuli are separate or mixed. In the *presence* of  $I_{KLT}$ , however, high frequency components enhance the SR coherence at low frequencies.

Both of these results show that the transfer function of an MSO neuron may not be independent of the stimulus it is driven with, but that the presence of  $I_{KLT}$  makes MSO computation stimulus-dependent.

Supported by NIH/NIMH Grant # MH62595-01

### **177 Juvenile *Kcna1* -/- Mice Lacking Kv1.1 Channel Subunits Discriminate Sound Source Location Poorly, But *Kcna2* -/- Mice Lacking Kv1.2 Channel Subunits Perform as Well as Control +/+ Mice**

**Helen Brew**<sup>1</sup>, Paul Allen<sup>2</sup>, Alison St. John<sup>2</sup>, Alaina Muldrow<sup>2</sup>, Bruce Tempel<sup>1</sup>, James Ison<sup>1,2</sup>

<sup>1</sup>Univ. Washington, <sup>2</sup>Univ. Rochester

Low-threshold voltage-gated Shaker potassium ion channels (Kv1) are expressed strongly in CN bushy cells and MNTB neurons. Kv1.1 and Kv1.2 channel subunits are present in different ratios as heteromers in Kv1 channels, and channel voltage-sensitivity increases with the proportion of Kv1.1 subunits. These threshold-graded channels are thought to be responsible for the high temporal acuity of neural firing necessary for spatial localization, by virtue of their adaptive regulation of baseline membrane potential. *In vitro* recordings support these ideas, but nothing is known of their relative contributions to auditory processing. Juvenile C3HeB/FeB mice were tested from PND 12 to PND 16 with reflex modification audiometry, to determine the inhibitory effect (PPI) on the acoustic startle reflex (ASR) of changing the location of a noise variously from 15 to 180 degrees apart in front of the mouse, using a modified method of limits. We tested 4 Kv1.1 null mutants (*Kcna1* -/-) and 5 +/+

littermates; 8 Kv1.2 null mutants (*Kcna2*  $-/-$ ) and 7  $+/+$  littermates. The Kv1.1  $-/-$  mice (presumed to have a high ratio of Kv1.2 subunits) show little PPI when the sound shifted by 90 degrees, and none for 45 degrees. The Kv1.2  $-/-$  mice (presumed to have high ratio of Kv1.1 subunits) inhibit at 45 degrees, sometimes at 22 degrees, as do the  $+/+$  littermates. The Kv1.1  $-/-$  mice (with normal ABR thresholds) weigh the same as the  $+/+$  littermates, but have reduced ASR and more random activity; the Kv1.2  $-/-$  weigh less than the  $+/+$  littermates, but are equal in ASR and activity. PPI is present in the majority of  $+/+$  and Kv1.2  $-/-$  mice at PND 12 and initially increases with age, as does the ASR; however, while the ASR continues to increase with age, PPI for changed location drops in some mice,  $+/+$  and  $-/-$ , by PND 16. Overall, these data suggest that the Kv1.1 subunit makes the greater contribution to precise auditory function: however, we note that the *Kcna2* deletion is more quickly lethal. Support: AG09524 and DC03805; DC05409 and DC04661

### **178 Network Model of Auditory Space Map in Barn Owl ICx**

**Yoojin Chung<sup>1</sup>**, H. Steven Colburn<sup>1</sup>

<sup>1</sup>*Biomedical Engineering, Boston University*

In this study, we used neural networks to model the processing of interaural time difference (ITD) and interaural level difference (ILD) in barn owl's external nucleus of inferior colliculus (ICx). The inferior colliculus (IC) is a midbrain nucleus where different pathways of auditory processing converge. In barn owls, a nocturnal predator with precise sound localization, there are two separate parallel pathways processing ITD and ILD. The ITD pathway primarily encodes azimuth information and the ILD pathway mainly encodes elevation information. These two pathways converge in the lateral shell of central nucleus of inferior colliculus (ICcl), and ICcl projects to the ICx which contains a map of auditory space. Neurons in ICx are tuned to specific combinations of ITD and ILD cues, and unlike the neurons in the ICcl and other nuclei before ICcl in the ascending auditory pathway, ICx neurons have broadband frequency tuning. Our model consists of peripheral auditory filters, ITD and ILD processing units for each frequency band, and ITD/ILD interaction. A feed-forward model with topological information and non-linear ITD/ILD interaction captures broad-band properties of the ICx auditory space map. In addition, an extended version of this model is used to explore the plasticity of the auditory space map induced by visual feedback, and the roles of excitatory and inhibitory projections in the plasticity. [Supported by NIH grant DC 00100]

### **179 Different Influences of Varying the Number of Daily Training Trials on Learning on Frequency- and Temporal-Interval Discrimination**

**Beverly A. Wright<sup>1</sup>**, Andrew T. Sabin<sup>1</sup>, Jeanette A. Ortiz<sup>1</sup>, Christopher C. Stewart<sup>1</sup>, Matthew B. Fitzgerald<sup>1</sup>

<sup>1</sup>*Northwestern University*

If you want to be better at a perceptual skill tomorrow, how much must you practice today? To investigate this

question, we examined how varying the number of training trials per day affected learning over multiple days on two auditory discrimination tasks: frequency discrimination and temporal-interval discrimination. For each task, we compared learning between different groups of listeners who were trained for either 360 or 900 trials per day for six days. The training consisted of repeated threshold measurements using an adaptive (3-down/1-up), two-interval forced-choice procedure with a standard stimulus composed of two 15-ms, 1-kHz tone pips separated by 100 ms. For frequency discrimination, listeners who were trained for 360 trials/day did not improve significantly ( $p > 0.39$ ), while those who were trained for 900 trials/day did ( $p < 0.01$ ), regardless of whether performance for both groups was assessed over the same number of days (six) or the same total number of trials (2460). Thus, improvement on frequency discrimination required  $>360$  trials of training per day. In contrast, for interval discrimination, the daily mean performance of both groups improved significantly and similarly over the six days (all  $p < 0.001$ ). This result indicates that 360 training trials per day was sufficient for learning on the interval task, and that training more than 360 trials per day did not increase the amount of improvement. Taken together, it appears that improvement on auditory discrimination tasks may require some critical amount of training per day (frequency-discrimination results), that training beyond that critical amount yields no additional learning on the trained condition (interval-discrimination results), and that the critical amount of training needed varies across tasks. [Work supported by NIH.]

### **180 Contribution of Passive Stimulus Exposures to Learning on Auditory Frequency Discrimination**

**Andrew T. Sabin<sup>1</sup>**, Beverly A. Wright<sup>1</sup>

<sup>1</sup>*Northwestern University, Department of Communication Sciences and Disorders*

Can passive exposure to a stimulus contribute to improvement on a perceptual task? There is considerable evidence supporting the idea that stimulus exposures alone do not yield learning; learning on a given perceptual task only occurs if the participant actively practices that task. However, this idea is based only on the extreme cases in which the participant either always, or never, actively practiced the target task throughout the entire training period. Here we instead asked whether passive exposures to a target stimulus, when mixed with active practice on a target task, can lead to perceptual learning on that task. During each of 7 daily sessions, two groups of listeners practiced both a task known to require active participation for learning, frequency discrimination, and an unrelated written task. While practicing the written task, one group was passively exposed to repetitions of the standard stimulus (passive group;  $n=8$ ), while the other group practiced the written task in silence (silent group;  $n=7$ ). Listeners alternated between the two tasks every  $\sim 5$  min (120 trials of frequency discrimination) for a total of 30 min/session. When compared to untrained controls ( $n=10$ ), the passive group improved significantly on frequency discrimination ( $p=0.01$ ), while the silent group did not

( $p=0.97$ ). Thus, entirely passive exposures to a target stimulus can lead to learning on a target task when those exposures occur in the same session as active practice of that task. These data challenge the widely held view that passive stimulus exposures do not contribute to perceptual learning. Instead, we suggest that active practice on a target task initiates a period of time during which subsequent passive exposure to the standard stimulus can contribute to learning. On a practical level, the current results raise the possibility that passive stimulus exposures can be incorporated into perceptual training regimes to make learning less effortful. [Work supported by NIH.]

### **181 Day-To-Day Variability of Absolute Thresholds Is a Major Cause of Day-to-Day Variability of Simple Reaction Times**

**Peter Heil<sup>1</sup>**, Heinrich Neubauer<sup>1</sup>, Andreas Tiefenau<sup>1,2</sup>

<sup>1</sup>Leibniz Institute for Neurobiology, <sup>2</sup>Exp. Audiology & Medical Physics, Otto-von-Guericke University Magdeburg

Reaction times constitute an important source of information in animal and human psychophysics, in cognitive neuroscience, and in the clinic. Simple reaction time (SRT) to auditory stimuli, in particular, is thought to be a measure of loudness and is frequently used to study loudness perception in normal or hearing-impaired subjects. SRT may also serve as an indicator of simulated hearing loss or of tinnitus. SRT and associated reaction probability (SRP) are also used to derive detection and difference thresholds.

SRT is a random variable. Therefore, many trials are necessary to obtain reliable estimates of location and other parameters of SRT distributions and to study the relationships of these parameters with stimulus parameters of interest. Often, this is impossible to achieve on a single day, so data are accumulated over several days spread over some period of time. There is considerable danger that some of the subject's parameters may vary and that such variation, if ignored or unknown, leads to wrong conclusions about the mechanisms underlying SRT distributions and their relationships with stimulus parameters.

We observe, in humans, considerable day-to-day variability of SRT and SRP to auditory stimuli of different sound pressure levels. Close examinations revealed that SRT – level functions and SRP – level (i.e. psychometric) functions measured on different days are of essentially identical shape but are displaced along the level axis to various degrees. We show that these displacements can be fully accounted for by day-to-day differences in a subject's absolute threshold, which was measured alternately with SRT.

Our data emphasize that variability in absolute sensitivity needs to be properly accounted for before the "true" dependencies of SRT measures on stimulus parameters emerge. In addition, our data point to intimate links between SRT, SRP and absolute threshold which we explore further.

Supported by grants of the DFG to P.H.

### **182 Modeling Psychometric Functions for Detection in Electric Hearing**

**Vasant Dasika<sup>1,2</sup>**, Lynne Werner<sup>1,3</sup>, Jeff Longnion<sup>1,2</sup>, Jay T. Rubinstein<sup>1,2</sup>

<sup>1</sup>University of Washington, <sup>2</sup>Dept. of Otolaryngology,

<sup>3</sup>Dept. of Speech & Hearing Sciences

The psychometric function for detection (PMFD) is a measure of basic auditory capacity. It represents the probability of detecting a stimulus as a function of the sound-level of the stimulus. PMFDs have been measured in normal and electric hearing adults, as well as normal hearing children and infants. This study uses modeling to predict how the inclusion of a conditioning stimulus in a cochlear implant (e.g., Hong and Rubinstein, 2003, JASA 114:3327-42), which adds randomness to the periphery, affects the PMFD in electric hearing. Moreover, the influence of "internal noise" (e.g., Werner and Boike, 2001, JASA 109:2103-11), which has been hypothesized to be due to central processing limitations that decrease the slope of the PMFD, is also investigated. A simple computational model is constructed that consists of three parts: 1) a decision rule that produces a detection if the hypothetical input variable, spike count, is greater than a given threshold value and no response if below, 2) an internal noise factor specified by an additive gaussian random variable that has been "discretized" and adds to the input spike count, and 3) a conditioner factor specified by a poisson random variable. Spike count represents the number of discharges in an array of auditory nerve fibers and is assumed to be proportional to the sound-level of the stimulus. Without the presence of either the internal noise or the conditioner, the PMFD is a step-function that equals chance for spike counts below threshold and equals 100% detection for counts above. Adding just the internal noise decreases the slope of the PMFD, while the threshold is unchanged. Adding the conditioner alone has two consequences, decreasing the slope and the threshold of the PMFD. When both the conditioner and internal noise are included, the PMFD translates to the left so the slope does not decrease, while the threshold does, compared to when just internal-noise alone was added. As the strength of the conditioner increases, the PMFD slides further left so that the threshold decreases further, while the slope remains essentially unchanged. These findings suggest that complete PMFDs for detection in electric hearing should be measured as opposed to measuring only the threshold in order to more completely assess the consequences of conditioning stimuli. The model predicts that the variability of the threshold will not increase when a conditioner is added, which is consistent with psychophysical data from Hong and Rubinstein (2003). [Supported by NIH: T32DC000018; R01DC007525; R01DC000396-19]

### **183 Effect of Psychophysical Procedure on Measurement of Temporal Integration of Loudness**

**Ikaro Silva**<sup>1,2</sup>, Mary Florentine<sup>2,3</sup>

<sup>1</sup>*Northeastern University - Dept. of Electrical and Computer Engineering*, <sup>2</sup>*Institute of Hearing, Speech, and Language*, <sup>3</sup>*Northeastern University - Dept. of Speech-Language Pathology and Audiology*

Large differences in the amount of temporal integration of loudness have been observed across studies. It is unclear to what extent this variability is a result of differences in procedures and/or differences across listeners. Little is known about how specific changes in the order of presentation of the stimulus affects the measured amount of temporal integration. This study measured the across-procedure variability of loudness matches obtained by using adaptive 2I,2AFC procedures with different paradigms for controlling the stimuli level from trial to trial. Equal-loudness matches between 5-ms and 200-ms tones were collected from six listeners tested under four different procedures. The procedures differed primarily in the sequence in which the stimuli were presented. The variations tested were the ordering of stimuli by amplitude across blocks of trials (both increasing and decreasing amplitudes), randomizing the order across those blocks, and randomizing the order within blocks. The random-within-block procedure, which sought to randomize any inter-trial information, yielded a significantly greater amount of temporal integration—defined as the difference in level between equally loud 5-ms and 200-ms tones—than the other three procedures. Overall, the results indicate that sequential effects, resulting from the choice of paradigm for controlling the stimuli order, directly affect the amount of temporal integration measured at moderate levels. Therefore, it is likely that previously reported differences in the amount of temporal integration measured using different procedures are a result of intertwined contextual biases.

### **184 Optimising Auditory Learning for Variable Training Stimuli**

**David R. Moore**<sup>1</sup>, Sygal Amitay<sup>1</sup>, Emilie Vavasour<sup>1</sup>, Amy Irwin<sup>1</sup>

<sup>1</sup>*MRC Institute of Hearing Research, Nottingham, UK*

A major issue in auditory perceptual learning is the benefit gained from the use of training stimulus sets of variable complexity. While it may be desirable to train with a variable stimulus set to promote transfer of training, a more limited set may increase learning of the elements in that set. Previously (Percept Psychophys 2005 67 691) we found that frequency discrimination training around a fixed, standard stimulus (1 kHz) promoted greater and more rapid learning than training around a standard that varied (900, 950, 1000, 1050, 1100 Hz) from trial to trial. Here we asked whether varying the standard every block of 100 trials would improve the efficiency of variable stimulus training. Adult listeners ( $\leq 20$  dB HL 0.5-4 kHz) performed a 2I-2AFC adaptive (2D:1U) frequency discrimination task over 5 days (4400 trials in 5-10 x 100 trial blocks/day) using the fixed (n=15) or block-wise variable (n=15)

standard tone, as above. Results from the first 8 listeners in each group show that performance on the block-wise variable task produced learning that was near identical to that on the fixed task, both as used here and in our previous study. Frequency difference limens (DLF) decreased from  $0.75 \pm 0.17\%$  (fixed) and  $0.79 \pm 0.20\%$  (variable) on the first block to  $0.36 \pm 0.09\%$  (fixed) and  $0.51 \pm 0.13\%$  (variable) on the seventh block. The difference between the fixed and (block) variable mean DLF from 0.04-0.15% compared with a difference between the fixed and (trial) variable mean DLF from our previous study of 0.32-0.23%. The poorer training found with trial-by-trial stimulus variation is thus due to the pattern of stimulus presentation rather than to the use of variable stimuli per se. Stimuli that vary on each trial appear to impose a cognitive load that may inhibit the listener's ability to perceive or remember the standard stimulus.

### **185 Across-Frequency Interactions in Pitch Perception**

**Christophe Micheyl**<sup>1</sup>, Andrew Oxenham<sup>1</sup>

<sup>1</sup>*MIT Research Laboratory of Electronics*

Recent results have revealed that the ability to perceive changes in the pitch of a target harmonic complex tone (HCT) could be dramatically affected by the simultaneous presentation of another HCT (interferer), even when there was no peripheral interaction between target and interferer. So far, such detrimental across-frequency interactions in pitch perception have only been demonstrated using target HCTs containing in their passband only high-rank, unresolved harmonics. Here, the demonstration of pitch discrimination interference (PDI) is extended to the case of a resolved-harmonic target. The results demonstrate significant PDI effects between two simultaneous groups of resolved harmonics, irrespective of whether the target group occupies a higher or a lower spectral region than the interferer. The effects are at least as large as those measured in the same listeners using an unresolved target and a resolved interferer. These findings argue against the view that PDI is generally caused by the interferer pitch being more salient than that of the target. In addition, the data suggest that PDI is mediated by different mechanisms depending on the F0 separation between target and interferer. [Support by NIDCD R01DC05216]

### **186 Signal Detection in Comodulated Noise: Modeling Fundamental Aspects of CDD and CMR**

**Michael Buschermöhle**<sup>1</sup>, Jan A. Freund<sup>1</sup>, Jesko L. Verhey<sup>1</sup>, Ulrike Feudel<sup>1</sup>

<sup>1</sup>*Carl-von-Ossietzky University Oldenburg*

Many natural sounds share the property of having common amplitude modulations across different frequency regions. Examples of these kinds of sounds are the masking noises used for experiments concerning comodulation detection differences (CDD) and comodulation masking release (CMR). Typical stimuli for these experiments consist of one or more masking noise bands and a signal that is either a pure tone or a noise band as well. Previous research in humans and other vertebrates has shown that in CDD and CMR experiments

signal detection thresholds vary depending on the correlation structure of the envelopes of the constituting noise bands. Based on neurophysiological data using similar stimuli as in psychophysics, we propose a simple model that is capable of reproducing important features of psychophysical signal detection thresholds in response to CDD and CMR stimuli. The model is based solely on peripheral processing and has the following stages: The incoming stimulus is frequency filtered, its envelope is extracted, followed by a compressive nonlinearity. In a last stage the temporal average is computed. Signal detection is realized by registering changes in the mean compressed envelope of the filtered stimulus. Many aspects of CMR and CDD can be accounted for by this largely analytically tractable model. Threshold differences between various correlation conditions can be understood by considering the beating of the noise bands within the filter at the signal frequency (i.e. they result from a within-channel effect).

### **187 The Detection of Across-Frequency Differences in Fundamental Frequency**

**Christophe Micheyl<sup>1</sup>, Andrew Oxenham<sup>1</sup>**

<sup>1</sup>*MIT Research Laboratory of Electronics*

Across-frequency differences in fundamental frequency (F0) are believed to provide an important cue for the perceptual segregation of simultaneous harmonic sounds, such as vowels or musical notes. This study measured the auditory system's sensitivity to F0 differences ( $\Delta F_0$ s) between groups of resolved harmonics occupying non-overlapping spectral regions under different experimental conditions. The main finding was that performance was dramatically reduced by onset-offset asynchronies between the two groups of harmonics, suggesting that the detection of  $\Delta F_0$ s across spectral regions is mediated to a large extent by segregation/grouping cues. Two unexpected outcomes were that, in the synchronous condition, performance a) was higher when the higher-F0 group was filtered into the lower spectral region than when it was filtered into the higher region, and b) decreased for  $\Delta F_0$ s above about 7% before increasing again at larger  $\Delta F_0$ s. Additional experiments, including the collection of pitch-matches, are currently being performed to clarify these two unexpected outcomes, which reveal that sensitivity to across-frequency  $\Delta F_0$ s may involve more complex mechanisms than were suggested by the results of earlier studies. [Supported by NIH grant R01DC05216.]

### **188 Simple Visual Cues Enhance the Identification of Target Sounds in Complex Auditory Scenes**

**Erol Ozmeral<sup>1</sup>, Virginia Best<sup>1</sup>, Barbara G. Shinn-Cunningham<sup>1</sup>**

<sup>1</sup>*Hearing Research Center, Boston University*

We investigated the extent to which non-auditory cues for directing auditory attention improved the ability to identify an acoustic target embedded in a complex auditory scene. Two types of stimuli were used: 1) sequences of spoken digits with reversed digits as distracters and 2) familiar Zebra Finch songs with unfamiliar songs as distracters. Subjects were seated in front of five loudspeakers (-45° to 45° azimuth, 1 m distance), each mounted with an LED.

Five different streams played simultaneously from the five loudspeakers. The listener identified a target, which occurred from one of the loudspeakers at a random time. There were four conditions: 1) all LEDs turned on during the target time-slice ("when" cue), 2) the target LED remained on throughout the trial ("where" cue), 3) the target LED turned on during the target time-slice only ("when and where" cue), and 4) no LEDs turned on ("no cue"). "When and where" cues yielded the best performance; "no cue" produced the worst; the other conditions were intermediate. The results demonstrate that in a complex auditory scene, a simple visual cue can improve the ability of listeners to extract information about an auditory target.

[Work supported by grants from AFOSR & ONR]

### **189 Informational and Energetic Masking of Speech: Psychometric Functions for Speech, Reversed Speech, and Noise Maskers**

**Nicole Marrone<sup>1</sup>, Christine R. Mason<sup>1</sup>, Gerald Kidd, Jr.<sup>1</sup>**

<sup>1</sup>*Department of Speech, Language, and Hearing Sciences and Hearing Research Center, Boston University*

One factor contributing to the difficulty in understanding a target speech signal in the presence of one or more masking speech signals is the similarity of the target speech to the masker speech. This effect can be difficult to isolate when energetic masking is the predominant factor determining performance. Sentences from the Coordinate Response Measure were digitally processed into sets of narrow frequency bands. The degree of energetic masking was varied by choosing masker bands to be the same (overlapping) or different (mutually exclusive) from the target bands. Within the same-band and different-band masker groups, the target-masker similarity was varied using three types of maskers: noise, reversed speech, and speech. Psychometric functions were measured using an identification task, with the midpoints and slopes estimated from best-fit logistic functions. Results indicated that the same-band maskers were always more effective than the different-band maskers. Also, there was a systematic ordering of masker effectiveness based on the (presumed) degree of target-masker similarity, with a more dramatic effect of masker type within the different-band masker group than in the same-band group. Finally, the slopes of the psychometric functions were steeper when more energetic masking was present (same-band conditions). These results suggest that both target-masker similarity and degree of spectral overlap contribute to the amount of masking and the slope of the psychometric function in speech masking conditions. [Work supported by NIH/NIDCD and AFOSR]

### **190 Simultaneous Two-Channel Signal Detection, Revisited**

**Gerald Kidd, Jr.<sup>1</sup>, Virginia Richards<sup>2</sup>, Christine R. Mason<sup>1</sup>, Frederick J. Gallun<sup>1</sup>, Rong Huang<sup>2</sup>**

<sup>1</sup>*Department of Speech, Language and Hearing Sciences, Boston University*, <sup>2</sup>*Department of Psychology, University of Pennsylvania*

This study examined the ability of listeners to monitor events occurring simultaneously in two widely spaced

frequency regions. The task was to detect the presence of a low frequency (558 Hz) tone and a high frequency (1791 Hz) tone presented in a 2-interval 4-alternative forced-choice procedure. On every trial, each signal was presented in either the first or second interval independently and the listener was required to indicate the interval of presentation for each signal. The level of each signal was varied separately according to an adaptive tracking procedure to obtain threshold estimates. As a control, thresholds for both signals were also obtained for single-signal presentation. Comparison of thresholds in single- and dual-signal presentation conditions provided an estimate of the costs of monitoring and responding to events in two frequency channels. Signal thresholds were obtained in quiet, in double-notch-filtered Gaussian noise, and in random-frequency multitone maskers. Much larger costs (difference between dual- and single-tone tasks) were found for the masked conditions, especially for the multitone masker. These results suggest that the costs of dividing attention along a particular stimulus dimension depends on both the resources required to solve the task in each signal channel and also the resources required to ignore competing stimuli in nonsignal channels. [Work supported by AFOSR and NIH/NIDCD]

#### **[191] Temporal Integration in Pitch Perception**

**Alain de Cheveigné**<sup>1</sup>, Daniel Pressnitzer<sup>1</sup>, François Parmentier<sup>2</sup>, Clément Gandon<sup>2</sup>

<sup>1</sup>CNRS / ENS / Université Paris 5, <sup>2</sup>ENS, Paris, France

Pitch perception improves with stimulus duration. One hypothesis is that a longer stimulus allows measurements across multiple periods. Within the context of an autocorrelation model, this amounts to taking into account higher-order peaks of the autocorrelation function (ACF). The hypothesis is investigated here using stimuli with ACFs that either have or lack higher-order peaks. Stimulus (1) consisted of a harmonic complex tone in noise at 0 dB SNR. Its ACF has peaks of amplitude 0.5 at the period and all multiples. Stimulus (2) consisted of rippled noise (noise added to itself after a one-period delay). Its ACF has a peak at the period (also with amplitude 0.5), but no higher-order peaks. Stimuli were synthesized with periods of 2, 4, 8 and 16 ms (F0s of 62.5 to 500 Hz) and durations of 192 ms. In a first task, subjects discriminated periods in an adaptive three-interval forced choice procedure. In a second task, white noise was added to the stimulus and subjects discriminated stimulus+noise from noise. At all periods, period discrimination thresholds were lower for (1) than for (2), suggesting that period discrimination indeed involved higher-order peaks of the ACF. A similar relation was found for thresholds in noise, but only for short periods. At longer periods (8 and 16 ms) thresholds for (1) and (2) were similar, suggesting that for that task subjects relied only on the first order peak. A third stimulus type, consisting of period-sized chunks of white noise assembled in pairs according to the pattern AABCC, was included to investigate temporal integration strategies. Finally, several high-pass filtered conditions were included to evaluate alternative, spectrum-based explanations. Results are consistent with a model based on an

autocorrelation statistic integrated over a limited time interval and with lags that span a relatively long range.

#### **[192] Adaptation Due to Repeated Exposure to Parabolic Flight of Static Torsional Alignment and the Pitch Vestibuloocular Reflex**

**Faisal Karmali**<sup>1</sup>, Ondrej Juhasz<sup>2,3</sup>, Mark Shelhamer<sup>1</sup>

<sup>1</sup>Johns Hopkins University School of Medicine, <sup>2</sup>Johns Hopkins University Whiting School of Engineering, <sup>3</sup>Johns Hopkins University, Baltimore, Maryland

During parabolic flight on a NASA KC-135 aircraft that provided alternating levels of reduced (~0 g) and enhanced (~1.8 g) g levels, large sensorimotor deficits initially occur. Rapid neurological adaptation improves these sensorimotor function over the course of hours or days. Here we report on adaptation of ocular control in two naïve subjects, using observations made PRE-flight, EARLY in flight (first 12 of 40 parabolas), LATE in flight (last 10 parabolas), and POST-flight, over three days of flying.

In a study of static alignment, hi-resolution full-face images were acquired every 4 seconds. 7 facial landmarks were used to align successive images to a common orientation to correct for relative motion of the subject and camera. To measure torsional position of each eye in each image, an operator interactively rotated iral images to orient them with a reference image. Torsional disconjugacy, an inappropriate response to non-terrestrial g levels, was computed as the difference between the left and right positions (+CCW). In both subjects for 0 g, disconjugacy was present EARLY (4.2° and -2.9°) but diminished by LATE day 1 (less than 2°). Disconjugacy was constant between LATE day 1 and LATE day 2. On day 3, disconjugacy had abated in both subjects. For subject A in 1.8 g, disconjugacy was 3.5° in day 1 EARLY which decreased to less than 1° for day 2 & 3. Subject B was similar, with an increase to 3° on day 2 which diminished to nearly 0° in day 3 (t-tests, p<0.05). These results show that torsional disconjugacy is initially high but is reduced within the first flight, and the adaptation that occurs is recalled at the start of subsequent flights.

In a study of the pitch (vertical) VOR, subjects made active sine-like head movements (~0.9 Hz, 20°) while their eye movements were recorded with a head-mounted video system. Gain was computed as the total eye excursion divided by head excursion, for each movement. In subject A, relative to PRE measures, gain in day 1 was reduced EARLY in 0 g and increased in 1.8 g. Relative to day 1 & 2 PRE, gain increased in day 2 EARLY. Relative to day 1 PRE, gain reduced in day 2 & 3 PRE. In day 2 & 3, gain increased from PRE to POST (t-tests, p<0.001). These results show that initially pitch VOR gain was different in 0 g, 1 g and 1.8 g, but that after day 1, the differences were no longer significant, showing the brain has adapted a response to all contexts.



### **193 Kinematics and Dynamics of Leg Movement During Treadmill Walking in Humans**

Yasuhiro Osaki<sup>1</sup>, Mikhail Kunin<sup>2</sup>, Bernard Cohen<sup>1</sup>, Theodore Raphan<sup>2</sup>

<sup>1</sup>Mount Sinai School of Medicine, <sup>2</sup>Brooklyn College, City University of New York

The aim of this study was to determine the three-dimensional kinematics and dynamics of the thigh, shank and foot as the body was propelled forward. Six subjects were tested using a video-based motion detection system (Optotrak), while they walked on a treadmill at velocities between 0.6 – 2.1 m/s. Movement parameters were normalized relative to leg length to simplify inter-subject comparisons. The stance and swing durations became shorter along hyperbolic curves as subjects walked faster. When the leg was modeled as an equivalent rigid bar pivoting about the hip, the effective radius of the leg in the stance phase varied with time and the peak pivot point lay above the hip, with little forward or lateral variation. The leg also rotated in yaw (horizontal) as well as in pitch (sagittal) and roll (coronal) during the stance phases. The combination of yaw rotation of the leg and pelvis moved the pivot point of the leg above the hip joint and extended the effective length of the leg, presumably for more efficient walking. During the swing phase, the leg segments moved forward with their peak velocities increasing linearly as a function of walking velocity. The phase plane trajectories of the swing followed concentric curves and peak velocity increased with size of movement forming a characteristic main sequence. Toe clearance relative to ground occurred in the middle of the swing phase and aligned the foot in space independent of walking velocity. A model was formulated that simulated the dominant kinematic and dynamic features of the foot trajectory. The model suggests that the locomotion cycle behaves as a dynamical system, which switches between stance and swing phases, but whose swing phases and heel contact are determined by desired walking velocity and foot orientation at toe-off. This would optimize foot placement and induce efficient stable walking.

Support: DC05222, DC05204, EY01867

### **194 Convergent Neurons in the Vestibular Nuclear Complex: A Comparative Analysis**

Kimberly McArthur<sup>1</sup>, Zakir Mridha<sup>1</sup>, Jacob Nadler<sup>1</sup>, Dora Angelaki<sup>1</sup>, J. David Dickman<sup>1</sup>

<sup>1</sup>Washington University

Responses of non-eye movement related cells in the vestibular nuclear complex (VNC) of adult homing pigeons (*Columba livia*) were examined during sinusoidal rotation and translational stimuli. Unit responses were recorded extracellularly with tungsten microelectrodes, then analyzed off-line using custom software in Matlab. We recorded VNC neurons that received convergent inputs from multiple vestibular afferents with different response characteristics. For each cell that received otolith input, we used linear motion at various angles relative to the naso-occipital head axis to characterize spatial sensitivity in the earth-horizontal plane. One-half of these cells' spatial sensitivity functions were described well by simple cosine

tuning, while the other one-half cells displayed spatio-temporal convergence (STC). Axes of maximum sensitivity to linear motion in the horizontal plane were distributed about the interaural axis. Temporal sensitivity functions for these cells along the preferred linear axis were generally flat gains as a function of frequency, but some cells showed high-pass or low-pass characteristics. For each cell that received input from the semicircular canals, we used a series of rotations around non-coplanar axes in space to determine its rotational axis of maximum sensitivity in three dimensions, under the assumption of cosine tuning. These maximum rotational sensitivity vectors reveal that most cells receiving convergent semicircular canal and otolith inputs are optimally activated by rotations that combine yaw, pitch, and roll components, and that the relative magnitude of these components in the maximum sensitivity vector varies from cell to cell. We compare our results in pigeons with previous results in rats (Angelaki, Bush & Perachio *J Neurosci* 1993) and monkeys (Dickman & Angelaki *JNP* 2002), and we discuss the implications of this comparison for oculomotor processing and spatial orientation across these species.

Supported in part by funds from NIH DC003286 and NASA NNA04CC52G.

### **195 Serotonergic Projections from Dorsal Raphe Nucleus to the Vestibular Nuclei**

Adam Halberstadt<sup>1</sup>, Carey Balaban<sup>2</sup>

<sup>1</sup>University of Pittsburgh, Neurobiology, Pittsburgh, PA,

<sup>2</sup>University of Pittsburgh, Otolaryngology, Pittsburgh, PA

The dorsal raphe nucleus (DRN) contains both serotonergic and nonserotonergic projection neurons, and both classes of DRN cells project to the vestibular nuclei (VN). The object of this investigation was to identify the terminal distribution of the serotonergic DRN-to-VN projections. The serotonin (5-HT) neurotoxin 5,7-dihydroxytryptamine (5,7-DHT; 10 µg free base in 0.5 µL 0.2% ascorbic acid) was administered by intra-DRN microinjection to 16 adult male Long-Evans rats in order to selectively lesion serotonergic projections from the DRN. After survival times of 18 h, degenerating fibers and terminals were visualized using the amino-cupric silver staining technique (DeOlmos et al., *Neurotoxicol Teratol* 16:545, 1994). In order to verify the placement of the 5,7-DHT injection site within the DRN, alternate sections were immunostained for 5-HT. Degenerating terminals and fibers were observed throughout the VN of 5,7-DHT-treated rats. Staining within the VN was densest along the border of the fourth ventricle within the ventricular plexus, and declined in more lateral regions of the vestibular nuclear complex. In the most rostral part of VN, large numbers of degenerating fibers and terminals were found in a region extending laterally from the fourth ventricle to encompass the rostral pole of the superior vestibular nucleus (SVN). Further caudally, relatively dense degenerating fibers were observed in SVN, lateral vestibular nucleus, and in the dorsal part of rostral medial vestibular nucleus (MVN). Caudal regions of the VN, including the inferior vestibular nucleus and caudal MVN contained relatively few degenerating axons. The overall topography of degenerating terminals was consistent with



the distribution of 5-HT transporter (SERT)-positive axons within the vestibular nuclear complex.

*Supported by R01 DC00739 and F31 DC006772.*

### **[196] Distribution of Saccular and Utricular Afferent Fibers and Terminals in the Vestibular Nuclei of the Hatchling Chicken**

**Anastas Popratiloff<sup>1</sup>, Kenna Peusner<sup>1</sup>**

<sup>1</sup>*George Washington University Medical Center*

The distribution of gravity-sensing, otolith afferent fibers and terminals was studied in the vestibular nuclei of 5 day old chickens using single or double labeling of fibers and terminals with biocytin/AlexaFluor, and confocal imaging. In these preparations, the vestibular nucleus neurons were immunolabeled with MAP2, and compared to vestibular nucleus neurons stained with reduced silver and rapid-Golgi.

The saccular fibers entered the medulla oblongata posterior to and at the level of the posterior tangential nucleus, coursed through ventral parts, and produced ascending and descending branches. Small saccular terminals contacted a few dendrites in the tangential nucleus, and numerous dendrites and cell bodies in the lateral part of the superior vestibular nucleus (vestibulocerebellar nucleus), and dorsal parts of the ventrolateral and descending vestibular nuclei.

The utricular fibers coursed through ventral parts of the central tangential nucleus, where they formed a few large axosomatic terminals, a few small terminals on dendrites, and then bifurcated into ascending and descending branches. Numerous utricular-fiber terminals were formed on dendrites and cell bodies in the ventral part of the superior vestibular nucleus (vestibulocerebellar nucleus), and ventral parts of the ventrolateral and descending vestibular nuclei. Thus, the otolith fibers followed discrete pathways through the vestibular nuclei, forming terminals in regions known to receive input from the ampullary fibers (Cox and Peusner, 1990). Altogether, these findings suggest that some neurons in the chick vestibular nuclei process convergent inputs from fibers concerned with graviception and angular acceleration.

### **[197] Dorsal Raphe Nucleus Projections to the Origin of the Coeruleovestibular Tract**

**Carey Balaban<sup>1</sup>, Adam Halberstadt<sup>1</sup>**

<sup>1</sup>*University of Pittsburgh*

The coeruleo-vestibular tract originates from the caudal part of nucleus locus coeruleus (LC) and provides relatively dense innervation to superior vestibular nucleus and lateral vestibular nucleus neurons, regions involved in vestibulo-ocular and vestibulo-spinal reflexes (Schuerger and Balaban, Brain Res Rev 30:189, 1999). The dorsal raphe nucleus (DRN) contains both serotonergic and nonserotonergic projection neurons; we have shown previously that the vestibular nuclei are innervated by DRN (Halberstadt and Balaban, Neuroscience 120:573, 2003); approximately 25% of these DRN neurons send collaterals to the central amygdaloid nucleus. The purpose of this investigation was to determine if the caudal LC is

innervated by projections from the DRN. The first experiment involved anterograde tracing with biotinylated dextran amine (BDA). Iontophoretic BDA injections (7.5% in 0.5 M NaCl, 4  $\mu$ A, 15 min) were confined within the DRN of seven adult male Long-Evans rats. After survival times of 5 days, BDA-labeled processes were visualized in frozen sections with standard Vectastain ABC peroxidase methods. Relatively large numbers of BDA-labeled axons bearing varicosities were found to ramify within the caudal LC. This innervation originated both medially, from within the ventricular plexus, and ventromedially, from the medial longitudinal fasciculus. For the second experiment, we examined the terminal distribution of serotonergic projections from DRN caudal LC. The serotonin (5-HT) neurotoxin 5,7-dihydroxytryptamine (5,7-DHT; 10  $\mu$ g free base in 0.5  $\mu$ L 0.2% ascorbic acid) was administered by intra-DRN microinjection to 16 adult male Long-Evans rats in order to selectively lesion serotonergic projections from the DRN. After survival times of 18 h, degenerating fibers

and terminals were visualized using the amino-cupric silver staining technique (DeOlmos et al., Neurotoxicol Teratol 16:545, 1994). Relatively large numbers of degenerating fibers and terminals were found within the caudal LC. As both DRN and caudal LC are sources of input to the VN, they may be integrally involved in linking the motor and affective components of vestibular processing. Furthermore, these findings suggest that the DRN plays an additional role in modulating the linkage between vestibular dysfunction and anxiety disorders by a direct influence on the coeruleovestibular pathway.

*Supported by R01 DC00739 and F31 DC006772.*

### **[198] The Translational Vestibuloocular Reflex: A Linear System Analysis**

**Trecia Brown<sup>1</sup>, R.D. Tomlinson<sup>1,2</sup>**

<sup>1</sup>*Department of Physiology, <sup>2</sup>Department of Otolaryngology – Head & Neck Surgery, University of Toronto, Ontario, Canada*

The translational vestibuloocular reflex (TVOR) produces an eye movement response to linear head acceleration detected by the otolith organs in the inner ear. The TVOR has been modeled as a linear control system for low to midrange accelerations (Israël and Berthoz 1989). However, no studies to date have explicitly examined the linearity of the TVOR. This study assesses the compliance of the TVOR with the superposition and homogeneity properties inherent in a linear system. If a system produces a set of responses for a given set of inputs, the superposition property will be satisfied if the system response to a linear combination of these inputs is equal to the same linear combination of the system responses to each input. To satisfy the homogeneity property, any scaling of a system input must result in the identical scaling of the corresponding output. The TVOR response to a transient sum-of-sinusoids stimulus will therefore be compared with the responses to each sinusoid component of the sum to characterize the system behaviour.

A head-fixed rhesus monkey was translated in the dark in an upright position along its interaural axis using sinusoidal and transient motion stimuli. The transients were

constructed from a sum of 2 – 4 sinusoidal waveforms with a frequency range of 0.5 – 7 Hz and an amplitude range of 0.5 – 8 cm. Eye movements were recorded using the magnetic search coil technique (Robinson 1963).

The results of this study indicate that the TVOR system displays primarily linear characteristics during interaural translation. The system satisfies the superposition and homogeneity criteria required for a linear system for 0.5 – 7 Hz stimuli. The eye response to sinusoidal stimuli is also consistent across the entire stimulus frequency range. However, the eye response to transient stimuli starts to exhibit a frequency-dependent trend at the higher frequencies thus suggesting that nonlinearities in the TVOR may exist for frequencies above 7 Hz.

### **[199] An Internal Model of Head Kinematics Predicts the Influence of Head Orientation**

**Lionel H. Zupan<sup>1,2</sup>, Daniel M. Merfeld<sup>1,2</sup>**

<sup>1</sup>Massachusetts Eye and Ear Infirmary - Jenks Vestibular Physiology Lab, <sup>2</sup>Harvard Medical School - Dept of Otolaryngology

Our sense of self-motion and self-orientation results from combining information from different sources. We hypothesize that the central nervous system (CNS) uses internal models of the laws of physics to merge cues provided by different sensory systems. Different models that include internal models have been proposed; we focus herein on the one referred to as the sensory weighting model (Zupan et al. 2002). For simplicity, we isolate the portion of the sensory weighting model that estimates head angular velocity: it includes an inverse internal model of head kinematics and an "idiotropic" vector aligned with the main body axis. For sensory inputs, we only consider the three-dimensional physical variables measured by the vestibular system: head angular velocity measured by the semicircular canals and gravito-inertial force measured by the otolith organs. Following a post-rotatory tilt in the dark, which is a rapid tilt following a constant-velocity rotation about an earth-vertical axis, the inverse internal model is applied to conflicting vestibular signals. Consequently, the CNS computes an inaccurate estimate of head angular velocity that shifts toward alignment with an estimate of gravity. Since three-dimensional reflexive eye movements known as vestibulo-ocular reflexes (VOR) compensate for this estimate of head angular velocity, the model predicts that the VOR rotation axis shifts toward alignment with this estimate of gravity and that the time constant of the VOR component compensatory for the rotation preceding the post-rotatory tilt depends on final head orientation. These predictions are consistent with experimental data in both rhesus monkeys and humans.

This research was supported by NASA grants NNJ04HF79G (LHZ) and NNJ04HB01G (DMM).

Bibliography: Zupan LH, Merfeld DM, and Darlot C (2002). Using sensory weighting to model the influence of canal, otolith and visual cues on spatial orientation and eye movements. *Biol Cybern* 86: 209-230.

### **[200] Investigation of Effect of BrainPort Balance Device Training on Performance in Subjects with Chronic Balance Dysfunction Due to Vestibulo-Cerebellar Damage**

**Mitchell Tyler<sup>1,2</sup>, Kim Skinner<sup>3</sup>, Yuri Danilov<sup>3</sup>**

<sup>1</sup>Wicab, Inc, <sup>2</sup>University of Wisconsin-Madison, Dept. of Biomedical Engineering, <sup>3</sup>Wicab, Inc.

**Objective:** To investigate and quantify changes in balance and functional performance in response to BrainPort device training, as measured by Computerized Dynamic Posturography (CDP) Sensory Organization Tests (SOT's), Activities-specific Balance Confidence Scale (ABC), Dynamic Gait Index (DGI), and Dizziness Handicap Inventory (DHI).

**Methods:** Sixteen subjects with chronic balance dysfunction due to either peripheral or central vestibulo-cerebellar pathology completed 8-10 BrainPort device training sessions over a 5-day period. The BrainPort converts head-tilt data from an oral MEMS accelerometer into a position signal presented via an electrotactile array to the superior, anterior region of the subject's tongue. Subjects use this input to correct head and body posture and achieve improved balance. Training sessions consisted of progressively challenging postural tasks while using the BrainPort, ending with a 20-minute trial. Subjects were tested before the first and after the last BrainPort training session.

**Results:** All subjects exhibited acquisition of the postural signal, retention of improved balance and postural stability, and transfer to a more stable gait and dynamic balance that persisted for up to 6 hours after training. All subjects had statistically significant improvements in the average score on all post-training tests, specifically: a 16 point increase on SOT composite scores; a 2-fold decrease on SOT's; an 18 point increase on ABC; a 40 point decrease on DHI. Subjects with low initial function had an average increase of 6 points on DGI.

**Conclusions:** The BrainPort Balance Device training produced both immediate and retained improvements in balance and the ability to perform functional activities in subjects with chronic balance dysfunction, regardless of etiology. We believe this retention effect is unique and has important potential for vestibular rehabilitation in a broad range of general balance problems.

### **[201] The Effect of Somatosensory Input on Subjective Visual Vertical in Normal Subjects**

**Dae Bo Shim<sup>1</sup>, Hong Ju Park<sup>1</sup>, Jung Eun Shin<sup>1</sup>, Hyang Ae Shin<sup>1</sup>, Jin Suk Yoo<sup>1</sup>**

<sup>1</sup>Konkuk University Hospital

We tested 34 normal subjects in their ability to set a straight line to the perceived gravitational vertical using a plain pre-programmed computer system. Measurements were taken in static conditions, sitting upright, head tilted (HT) 15°, body tilted (BT) 15°, and head lateral positions (90°) on the right or left sides with or without physical support under the head. Aims of the study were to determine if the neck somatosensory input influences on vertical perception by comparing the results with the head

or body tilted (15°), and to examine the influence of tactile sensation in the perception of verticality in head lateral positions. In the positions of -15° BT, -15° HT, and 15° HT, the mean values showed smaller errors with an opposite sign (referred to as E-effect). There was a significant difference in the subjective visual vertical (SVV) results between the upright position and the head tilt positions ( $p < 0.05$ ), but not the body tilt positions. The mean values showed large errors to the same direction (A-effect) for head lateral paradigms ( $p < 0.05$ ), which are opposite direction to the minor errors at small head tilts (E-effect). No significant difference was observed for the SVV between the actively and passively-tilted head lateral paradigms. Our results support that neck somatosensory plays a part in the perception of verticality (E-effect). In contrast, tactile sensation of the head had no effect on the settings of a visual line to subjective visual vertical in head lateral positions.

## **[202] Effects of Semicircular Canal Activation on Perceived Head Orientation**

**Richard Lewis**<sup>1,2</sup>, Csilla Haburcakova<sup>2</sup>, Wangsong Gong<sup>2</sup>, Daniel M. Merfeld<sup>1,2</sup>

<sup>1</sup>Harvard Medical School, <sup>2</sup>Massachusetts Eye and Ear Infirmary

We investigated if percepts of head orientation in the roll plane are affected by semicircular canal activity. Two rhesus monkeys were trained to indicate the perceived direction of the earth-vertical in the roll plane using a task derived from the subjective visual vertical (SVV) test commonly used in human subjects. SVV responses and eye movements were measured while afferents from one posterior canal were activated with an electrode implanted near the canal ampulla. We found that SVV responses deviated by as much as 50 deg during electrical stimulation, consistent with an illusory estimate of roll tilt towards the stimulated ear. The SVV deviation was always substantially larger than the torsional offset of the eyes, indicating that this effect was not purely visual in origin. In addition to the vertical and torsional eye movements produced by posterior canal activation, transient horizontal eye movements were also recorded. These horizontal eye movements were consistent with a "induced" translational VOR response produced by a discrepancy between the actual and estimated orientation of gravity relative to the head. These results suggest that rotational information derived from the semicircular canals contributes to the brain's estimate of head orientation in the roll plane, and that aberrant estimates of linear acceleration are produced by dissociating the actual and estimated orientation of the head.

## **[203] The VOR Elicited by a Prosthetic Semicircular Canal Does Not Engage Velocity Storage**

Csilla Haburcakova<sup>1</sup>, Richard Lewis<sup>1,2</sup>, Wangsong Gong<sup>1</sup>, Daniel M. Merfeld<sup>1,2</sup>

<sup>1</sup>MEEI, <sup>2</sup>Harvard Medical School

Eye movements are elicited by optokinetic stimulation and rotation. At low frequencies, the axis of eye rotation for

these responses shifts toward alignment with the gravito-inertial force (GIF) in primates. These axis shifts have been linked to the central velocity storage mechanism, which also prolongs the vestibulo-ocular reflex (VOR) time constant (circa 10-20 s) in primates relative to the dominant peripheral canal time constant (circa 5 s). We examined the relationship between velocity storage and these axis shifts in two squirrel monkeys. Lateral canals were plugged bilaterally with a stimulating electrode placed in one lateral canal near the ampullary nerve. The electrode was activated chronically using a semicircular canal prosthesis attached to the animal's head.

In both monkeys the prosthetic stimulation applied to the ampullary nerve had a time constant of 5 seconds; the VOR, however, had a time constant of 2-4 seconds. When the time constant of the prosthesis was increased to 80 seconds for one monkey, the VOR time constant increased to 12-14 seconds. These results imply that the velocity storage mechanism, which normally extends the VOR time constant beyond that of the cupula, was not activated by the electrical stimulation.

We also found that the eye movements produced by stimulation trapezoids with the animal tilted in roll demonstrated an axis shift which served to align the eye movement response with gravity. Similar results were obtained from the monkey tested with optokinetic stimuli, with the OKAN response aligned with the GIF. These data demonstrate physiologic shifts in the eye responses elicited by the prosthesis, with the axis of eye rotation aligning with the GIF. This occurred despite the finding that the VOR time constant was substantially shorter than time constant of the input stimulation, which suggests that the neural processes that prolong the VOR are not identical to the processes that align the axis of eye rotation with the GIF.

## **[204] The Conjugacy of the Vestibulo-Ocular Reflex (VOR) Responses to Single Labyrinth Stimulation in Trained Monkeys**

**Xuehui Tang**<sup>1,2</sup>, Youguo Xu<sup>1</sup>, Ivra Simpson<sup>1</sup>, Alexander Shelukhin<sup>1</sup>, Ben Jeffcoat<sup>1</sup>, Wu Zhou<sup>1</sup>

<sup>1</sup>ENT, University of Mississippi Medical Center, <sup>2</sup>Jinan University, Guangzhou, China

The organization of the unilateral horizontal VOR pathways is not symmetrical for the two eyes. During a single labyrinth stimulation, the VOR responses of the eye ipsilateral to the stimulation are driven by the neural innervations from three sources: the medial rectus muscle is contracted by excitatory innervations from both the ipsilateral vestibular nuclei and the abducens interneurons on the other side, and the lateral rectus muscle is relaxed by inhibitory innervations from the ipsilateral vestibular nuclei (Scudder and Fuchs, 1992; Highstein and Baker, 1978; Baker and Highstein, 1978). The VOR responses of the contralateral eye, however, are driven by the neural innervations from two sources: the medial rectus muscle is relaxed by inhibitory innervations from the abducens interneurons on the other side, and the lateral rectus muscle is contracted by excitatory innervations from the ipsilateral vestibular nuclei. Since the ipsilateral eye

receives an extra input, it seems that single labyrinth stimulation may generate disconjugate VOR responses with larger eye movements in the ipsilateral eye. An earlier study using electrooculography (EOG) suggested that nystagmus to unilateral caloric stimulation was disconjugate (Wolfe, 1979). Because of the known limitations of EOG for its nonlinearity and baseline drifts, the conjugacy of the unilateral VOR responses needs to be re-examined. In the present study, we employed search coil technique to record binocular eye position signals during both cold and warm water caloric stimulation in awake monkeys. Our preliminary results suggested that caloric nystagmus was primarily conjugate, indicating that the net innervations received by the two eyes were roughly equal during unilateral vestibular stimulation. This balanced innervation in an asymmetrical organization can be achieved through continuous calibration and motor learning (du Lac et al., 1995).

### **[205] Eye Velocity Asymmetry, Ocular Orientation and Convergence Induced by Angular Rotation in the Rabbit**

**Jun Maruta<sup>1</sup>**, Theodore Raphan<sup>2</sup>, John Simpson<sup>3</sup>, Hamish MacDougall<sup>1</sup>, Bernard Cohen<sup>1</sup>

<sup>1</sup>Mount Sinai School of Medicine, <sup>2</sup>Brooklyn College, City University of New York, <sup>3</sup>NYU School of Medicine

We studied ocular asymmetries and orienting responses induced by angular rotation in three rabbits with binocular video recordings. Each eye responded to steps of velocity with a peak slow phase velocity that varied approximately linearly between 10 and 90°/s. The movements of the two eyes were not conjugate; the gains at each stimulus speed were greater when the eyes were moving in temporal-to-nasal than in nasal-to-temporal directions. Average gains in the nasal-to-temporal direction were 0.83 and in the temporal-to-nasal directions were 0.95, a statistically significant difference ( $p < 0.05$ ). The eyes also converged and pitched down during rotation, unrelated to the direction of movement. The mean peak vergence increased from 1.8° at 10°/s to 5.8° at 90°/s, and the mean peak pitch increased from 1.0° at 10°/s to 6.4° at 90°/s. The vergence and pitch increased and refocused binocular overlap in the visual fields.

At rest, each monocular field extends medially over the midline, giving a binocular overlap of 24° in front and 30° overhead. Rotation at 60°/s evoked 4° of vergence and 5.4° of pitch, which would increase the binocular overlap from 24° to 30° in front of the animal, giving better visual acuity of the ground when it turned its head or moved in a circular pattern. Vergence and pitch outlasted the nystagmus induced by rotation, suggesting that they were generated by separate vestibulo-oculomotor subsystems. A similar temporo-nasal preponderance is present in the OKR of the rabbit (Collewijn and Noorduyn, 1972) and the VOR of the goldfish (Pastor et al. 1992) and squirrel monkey (Paige, 1983). Thus, the asymmetry in the velocities induced in the two eyes by the aVOR appears to be widely distributed across species. This preponderance would increase compensatory eye velocity in the eye that leads into the direction of rotation, while the vergence and pitch orient the eyes to enhance binocular vision.

Support: EY11812, DC05204, EY04148, NS13742, EY01867

### **[206] Relationship Between Global Orientations and Incremental Rotations of the Head in Three Dimensions**

**Mikhail Kunin<sup>1</sup>**, Yasuhiro Osaki<sup>2</sup>, Bernard Cohen<sup>2</sup>, Theodore Raphan<sup>1</sup>

<sup>1</sup>City University of New York (Brooklyn College), <sup>2</sup>Mount Sinai School of Medicine

Looking around while walking requires global changes in head position, while the periodic motion of stepping induces incremental rotations of the head. Head orientations in three dimensions obey Donders' law, such that axes representing head rotation relative to some primary position are confined to a two-dimensional surface (Glenn and Vilis, 1992). In this study, we examined the global rotation axes of the head and compared them to the incremental rotation axes using an Optotrak system, which monitors head rotations in three dimensions. The algorithms for computing incremental rotation axes in three dimensions were based on obtaining sequences of homogeneous transformations associated with head orientation. The results indicate that head roll computed as an axis-angle component is approximately inversely proportional to the product of head yaw and pitch over a wide range of head orientations. This implies that the global rotation axes of the head follow Fick-like gimbal behavior (Ceylan et al, 2000). The incremental axes of yaw rotation over the same range of head orientation, however, behave in accordance with a Helmholtz-like gimbal and are related to the anatomical properties of the dens and condyles (Kunin et al, 2004). The incremental axes of pitch rotation on the other hand are rotated in accordance with a Fick-like gimbal, such that the pitch axis is rotated in yaw by the same amount as the head. Thus, the gimbal characteristics were dependent on the direction of incremental rotation. The data are consistent with the hypothesis that there are fundamental coordinate axes tied to the anatomy of the spinal column that govern the incremental rotations of the head. However, when the head is oriented in three dimensions, additional constraints are imposed on yaw head rotations due to the muscles that appear to roll the head as it is moved in yaw, transforming its three-dimensional rotations so they have Fick-like properties.

Support: DC05222, DC05204, EY01867

### **[207] Spatial Temporal Characteristics of Central Vestibular Neurons Related to the Velocity Storage**

**Sergei B. Yakushin<sup>1</sup>**, Bernard Cohen<sup>1</sup>, Theodore Raphan<sup>2</sup>

<sup>1</sup>Mount Sinai School of Medicine, <sup>2</sup>Brooklyn College, City University of New York

We studied the spatial characteristics of 57 vestibular-only (VO) and vestibular-plus-saccade (VPS) neurons using angular rotation and static tilt in two cynomolgus monkeys. The purpose was to determine the contribution of canal and otolith-related inputs to central vestibular neurons

whose activity is associated with the central velocity storage integrator. A majority of cells received convergent canal and otolith input, which was in orthogonal planes in some neurons. In general, the canal input dominated the otolith input in these cells. When they were tested by rotation about spatial horizontal axis at 0.2 Hz with the animals in different orientations re the axis of oscillation, some units had spatial-temporal convergent (STC) characteristics. That is, the sensitivity was approximately the same in all head orientations, but the temporal phases varied from being in-phase with stimulus velocity to in-phase with stimulus position depending on the head orientation to the axis of rotation. More of these cells had STC properties at lower frequencies of rotation. We hypothesize that the STC behavior of the VO and VPS units that received canal and otolith input in orthogonal planes does not become apparent until the otolith input becomes manifest at low frequencies when the strength of the canal input is reduced by decreasing the frequency of rotation. The STC behavior of VO and VPS units was modeled as approximately orthogonal inputs from the otolith organs and semicircular canals whose sensitivity is frequency-dependent. The model predictions were well correlated with the actual data. We propose that this orthogonal convergence on VO and VPS neurons could provide the basis for gravity-dependent eye velocity orientation induced through velocity storage.

Supported by NIH Grants: DC04996, DC05204, EY11812, EY04148, and EY01867

**[208] Gaze Stabilization in Pigeons Undergoing Sensory Regeneration After Ototoxic Damage**  
**Asim Haque<sup>1</sup>**, Mridha Zakir<sup>1</sup>, Dora Angelaki<sup>1</sup>, J. David Dickman<sup>1</sup>

<sup>1</sup>Washington University School of Medicine

Head movements are thought to play a significant role in the reflexive stabilization of gaze in many avian species. Gaze is mathematically defined as eye-in-space and is the complex sum of the eye-in-head and the head-in-space. In addition, gaze stabilization involves important contributions from the vestibuloocular (VOR), vestibulocollic (VCR), and cervicocollic (CCR) reflexes and head inertia responses. Previously published work from our laboratory showed that pigeons (*Columba livia*) had undercompensatory VOR (head-fixed) responses and subsequently relied quite heavily upon movements of the head for stabilization under head-free conditions, especially during high-frequency rotations. Since gaze stabilization reflexes depend, in large part, on input from the vestibular system, elements of gaze stabilization behavior can be used as important barometers for the functional viability of the vestibular system after damage or injury. Insults to hair cells and vestibular afferents, such as ototoxic damage from aminoglycosides, have been shown to elicit a repair and regeneration response in various submammalian classes such as avians. The effects of these agents on the central neuronal populations subserving eye and head movements is not fully understood. In the present study, we applied the aminoglycoside streptomycin directly to the oval window and the vestibule of two groups of pigeons,

one followed longitudinally and the other examined after 6 months of recovery. Three-dimensional magnetic search coil techniques were employed to obtain eye and head movements under both head-fixed and head-free conditions in response to rotational stimuli (yaw, 0.01-2Hz, 20°/s; roll, 0.02-4Hz, 20°/s). No gaze stabilization responses were present initially after the insult, coinciding with observed ataxia. Throughout the recovery period, however, responses became more similar to those seen in normal animals.

*This study was supported by funding from HHMI, AOS, NIH, and NASA.*

**[209] Complex Responses of Parabrachial Nucleus Neurons to Static Tilt, Dynamic Reorientation of Tilt Axis and Off-Vertical-Axis Rotations**

**Cyrus McCandless<sup>1</sup>**, Carey Balaban<sup>1</sup>

<sup>1</sup>University of Pittsburgh

Neurons in the vestibulorecipient region of the parabrachial nucleus (PBN) respond to off-vertical axis rotation (OVAR) and to brief tilt and yaw trapezoids (McCandless & Balaban: ARO 2005, Soc. Neurosci. 2004). PBN units respond also to the direction of OVAR stimulation with high-amplitude firing rate bias responses as well as directionally-asymmetric modulation responses (McCandless et al.: ARO 2004, Soc. Neurosci. 2003). Further, responses to OVAR cannot be explained by simple linear summation of responses to brief tilt trapezoid stimuli.

We have tested PBN units with long-duration off-vertical-axis position-step stimuli, where the direction of tilt was varied by stepwise rotation (45° increments, 45sec static epoch, 40°/s rotational velocity) about a tilted axis in either the CCW or CW directions. Unit responses to this stimulus were compared to the responses to OVAR and brief tilt trapezoid stimuli. Responses to stepwise reorientation of the tilt axis were often surprising. For example, some units responded to a particular direction of tilt differentially depending on whether that orientation was produced by CCW or CW rotation. In addition, per-rotational yaw-velocity responses during stepwise OVAR could vary with direction of tilt. These responses indicate a complex dynamic interplay between otolith- and canal-derived inputs in the vestibulorecipient portion of PBN. It further suggests that the PBN contains a sophisticated representation of dynamic whole-body orientation and motion in space.

Supported by: R01 DC00730; F31 DC006321-01

**[210] Speech Understanding in Noise and Temporal Processing: A Frequency-Specific Investigation**

**Candice Costa<sup>1</sup>**, Mary Florentine<sup>1</sup>, Ikaro Silva<sup>1</sup>

<sup>1</sup>Northeastern University

There has been a constant quest for a simple clinical test that correlates a psychophysical procedure with a speech in noise task. This is because many people with sensorineural hearing loss experience problems

understanding speech in the presence of background noise, even when effects of audibility are taken into account. These problems are thought to partly result from temporal processing deficits. If reduced temporal resolution contributes to hearing-impaired listeners' difficulty understanding speech in background noise, then a correlation between impaired listeners' speech-recognition performance and psychophysical measures of temporal resolution should be observable. In fact, some studies report a correlation between speech-reception thresholds and gap-detection thresholds, whereas others do not. However, all of these studies measured speech-recognition performance with broadband speech. The use of broadband speech in these experiments does not take into consideration the fact that speech can be understood when only a portion of the speech spectrum is audible and that temporal processing may vary across frequency. In a broadband condition, it is possible that listeners decode the speech signal using only the channels in which they have good temporal processing, which could weaken the correlation between speech-recognition performance and gap-detection thresholds. In the present study, a significant correlation between narrow-band gap detection and narrow-band speech discrimination in noise was found for frequency regions around 1 and 2 kHz in the 11 normal hearing listeners, but not for frequency regions around 0.50 and 4 kHz or in a broadband condition. No correlations were found at any frequency region for 11 hearing-impaired listeners. [Work supported by NIH-NIDCD grant no. DC001087]

## **[211] Electrophysiological Correlates of Modulation Detection Interference**

**Shaum Bhagat<sup>1</sup>, Sid Bacon<sup>2</sup>**

<sup>1</sup>*University of Memphis*, <sup>2</sup>*Arizona State University*

Evidence from behavioral studies suggests that modulation detection interference (MDI) may be attributed to masker-probe interactions within a peripheral auditory channel or across peripheral auditory channels. Within-channel interactions between the masker and probe carriers could decrease the depth of modulation of the probe, increasing the difficulty of detecting amplitude modulation [Bacon and Moore, 1993]. Alternatively, a modulation detection process dependent on across-channel comparisons might be compromised if the modulation envelopes of the masker and probe were similar [Yost and Sheft, 1994]. Insight into the physiological mechanisms responsible for MDI in humans is provided by investigating the auditory steady-state response (ASSR) to multiple amplitude-modulated stimuli. Three ASSR experiments were designed to approximate conditions evaluated in the behavioral MDI paradigm. The subjects were 32 normal-hearing adults. During each experiment, probe and interfering tones were paired to record electrophysiological responses. The effects of carrier frequency, modulation depth and modulation rate of the interfering tone on ASSR amplitudes were evaluated. Experiment 1 revealed that ASSR amplitudes were reduced when a higher frequency interfering tone was paired with the probe tone, and when the interfering tone was modulated at a lower modulation depth than the probe

tone. Experiment 2 revealed that ASSR amplitude reductions were dependent on the spectral proximity of the probe and interfering tones. Experiment 3 indicated that ASSR amplitude reductions were greater when the probe and interfering tones were modulated at different rates. Analogous findings of this investigation and previous behavioral evaluations are supportive of within-channel contributions to MDI.

## **[212] Evoked Potential Measures of Binaural Enhancement in Quiet and Noise**

**Jeffrey Weihing<sup>1</sup>, Jennifer Paulovicks<sup>1</sup>, Frank Musiek<sup>1</sup>**

<sup>1</sup>*University of Connecticut*

It is well known that individuals hear better binaurally than monaurally especially in noise. However, there are few measures of this binaural enhancement phenomena. In this study the goal was to create an electrophysiological index that reflects binaural enhancement in quiet and in noise. The auditory brainstem response (ABR) and middle latency response (MLR) were selected as both of these responses can be recorded simultaneously. Suprathreshold ABR and MLR measures were obtained in three conditions. Condition 1 included individual measurements of left and right ears as well as binaural measurements in quiet. Conditions 2 and 3 included the same measures as condition 1 except for the introduction of broadband noise in the sound field at two different levels. Subjects were individuals with normal hearing sensitivity and no significant otologic or neurologic history. Results indicated that the binaural amplitudes of both the later waves of the ABR and the Na-Pa complex of the MLR were greater than individual monaural recordings, however they were less than the monaural recordings summed. This finding is similar to the classic binaural interaction phenomena that has been previously reported. This binaural enhancement of both the ABR and MLR was maintained for both noise levels, although the overall amplitudes of both the ABR and MLR responses were reduced. The MLR appeared to be proportionally more affected by noise than the ABR. These findings were susceptible to variability across subjects. The present results could have implications to the clinical setting. It may provide an objective measure that will help in identifying individuals who have severe difficulty hearing in noise.

## **[213] Developmental Changes in Auditory Discrimination in Children**

**Alexandra Ludwig<sup>1</sup>, Angela Friederici<sup>2</sup>, Rudolf Rübsamen<sup>1</sup>**

<sup>1</sup>*University of Leipzig*, <sup>2</sup>*MPI for Human Cognitive and Brain Science*

This study is based on the hypothesis that there are noticeable developmental changes in central auditory processing during childhood. It is assumed that specifically the ability to discriminate spectral and temporal signal structures is improved. We report on psychoacoustic tests for evaluating signal processing at different levels in the central auditory system. They allow a differentiation between signal processing in I) the auditory brainstem and

II) diencephalic or telencephalic auditory areas. Emphasis is laid on the computation of the psychometric functions, which allow to acquire not just a single threshold value but to evaluate different threshold criteria. Normative data on age-dependent performance in auditory processing was gathered from 146 normal hearing children and young people between 6 and 19 years of age. The integrity of auditory brainstem processing was evaluated by quantifying interaural frequency, intensity, signal duration and phase discrimination, which cause lateralized auditory percepts. Diencephalic/telencephalic processing was tested by varying similar acoustic parameters (frequency, intensity, signal duration and in addition signals with sinusoidal amplitude modulation) but presenting the test signals in conjunction with noise pulses to the other ear (dichotic signal/noise stimulation). This presentation facilitates the study of auditory signal processing in each of the two cortical hemispheres. The discrimination limens for the abovementioned parameters improved with age. The results implicate a prolonged development of the discrimination ability of basic acoustic parameters and suggest that our tests provide a useful tool for examining central auditory processing.

#### **[214] Optimizing Cochlear Microphonic Recording Parameters in Humans**

**Mariam Riazi**<sup>1,2</sup>, John Ferraro<sup>1,2</sup>, Anupa Gaddam<sup>1,2</sup>, Gouthami Erra<sup>1,2</sup>

<sup>1</sup>*Department of Hearing and Speech, <sup>2</sup>University of Kansas Medical Center*

It has recently been reported that the cochlear microphonic (CM) may play an important role in the diagnosis of Auditory Neuropathy (AN) in newborns, a disorder characterized by dysynchrony of auditory neural firings from Cranial Nerve VIII leading to central auditory processing disorders (Deltenre et al., 1999; Rance et al., 1999; Starr et al., 2001). However, since the CM waveform tends to mirror that of the acoustic stimulus, conscientious recording methodology must be applied to separate true response from artifact. This feature has played a major role in limiting the clinical usefulness of the CM, since failure to separate it from stimulus artifact leads to misinterpretation of the response and inaccurate diagnoses. This study examined CM recordings from an electrode placed in the ear canal of newborns and adults under a variety of "shielding" conditions that were aimed at inhibiting/reducing artifactual contamination of the electrophysiological waveform. Preliminary results suggest that electromagnetic shielding of both the electrode cables and the acoustic transducer are necessary to reduce electromagnetic stimulus artifact. The ultimate goal of this research is to improve the diagnostic utility of the CM in the diagnosis of AN and other hearing-related disorders.

This research was supported by grants from the Hall Foundation of Kansas City, and the Deafness Research Foundation.

#### **[215] Extremely Low Gestation Infants Are at High Risk for Auditory Neuropathy**

**Lynn Iwamoto**<sup>1,2</sup>, Konstantine Xoinis<sup>2</sup>, Yusnita Weirather<sup>2</sup>, Hareesh Mavoori<sup>3</sup>, Steven Shaha<sup>3</sup>

<sup>1</sup>*University of Hawaii Dept of Pediatrics, <sup>2</sup>Kapiolani Medical Center for Women and Children, <sup>3</sup>Hawaii Pacific Health Center for Health Outcomes*

In auditory neuropathy (AN) neural transmission of auditory information is abnormal. It is characterized by abnormal brainstem evoked responses (ABR) with normal otoacoustic emissions (OAE) or normal cochlear microphonics. Speech perception is impaired and management strategies are controversial, in part because little is known about this disorder. Sensorineural hearing loss (SNHL) is ten times more prevalent in high risk vs normal term infants, but the rate of AN is unclear. If newborns are screened with only OAE, those with AN can be missed. At our institution, high risk nursery infants are screened using ABR, followed by OAE and diagnostic ABR prior to discharge if the screening is abnormal. In this retrospective study, we characterized infants with AN who were admitted to the high risk nursery at Kapiolani Medical Center for Women and Children between 1999-2003. Hospital courses of 24 AN and 95 SNHL infants were reviewed. Compared to SNHL, infants with AN were significantly more premature (GA 28.3±4.8 AN vs 32.9±5.4 wks SNHL, p<0.0001) and smaller (BW 1318±894 AN vs 1995±1031g SNHL, p<0.01). The prevalence of SNHL was 21/1000 high risk infants, with a rate for AN of 5.3/1000. Two thirds of the AN infants were born at 23-28 wks and had significantly longer hospital stays compared to SNHL infants of the same GA. Exposure to furosemide and vancomycin were also positively correlated with AN vs SNHL; while gentamicin, dexamethasone, and peak bilirubin were not. In summary, infants with AN were more premature, smaller, hospitalized longer, and more likely to be exposed to furosemide or vancomycin. Thus, we speculate that AN may be, in part an acquired disorder in extremely low gestation infants. Those infants born at 23-28 wks GA should be routinely screened by ABR and OAE before hospital discharge. Early identification of AN holds the promise of developing earlier intervention strategies with improved speech-language and cognitive outcomes.

#### **[216] Risk Factors for Slight-Mild Sensorineural Hearing Loss Among School-Aged Children**

**Barbara Cone-Wesson**<sup>1</sup>, Sherryn E. Tobin<sup>2</sup>, Melissa Wake<sup>2,3</sup>, Zeffie Poulakis<sup>2,3</sup>

<sup>1</sup>*University of Arizona, <sup>2</sup>Centre for Community and Child Health, Royal Children's Hospital, Victoria, Australia,*

<sup>3</sup>*University of Melbourne and Murdoch Children's Research Institute*

Slight or mild hearing loss has been posited as a factor affecting speech, language, learning and academic outcomes. An epidemiological study of the prevalence and outcomes of slight-mild sensorineural hearing loss (SNHL) in elementary school children was undertaken (Wake et al, NIH R01 DC05662-01). As part of this investigation, the risk factors for slight-mild SNHL were ascertained. A cross-sectional cluster sample survey of 6581 children



(85% response; 3367 Grade 1, 3214 Grade 5) attending schools in Melbourne, Australia was performed. All children were invited to undertake screening for slight-mild SNHL defined as a low- and/or high-frequency pure tone average of 16-40 dB HL in the better ear, with air-bone gaps <10dB. Parents completed a questionnaire that included items pertaining to parental concerns regarding their child's hearing and their child's health history, including the presence of neonatal risk factors for hearing loss, history of noise exposure, and parent hearing status. Slight-mild SNHL was detected in 55/6240 (0.88%) children. Risk factor data were analysed for the 6068 children with both audiological and parent questionnaire data. Sensitivity, specificity and positive and negative predictive values for slight-mild SNHL were calculated for each of three questions regarding parental concern for their child's hearing. These items showed low sensitivity and very low positive predictive values, moderate specificity and high negative predictive values. Of eight neonatal risk factors, "abnormality of the head or neck" and "discharged on O2" had the highest odds ratios at 4.2 and 9.1, respectively, which were statistically significant at the  $p < .05$  level. Reported use of personal stereos was also a significant risk factor.

There was a remarkable congruence between the neonatal risk factors for more severe forms of SNHL (Cone-Wesson et al, 2000) and those for slight-mild SNHL. The association between slight-mild SNHL hearing loss and parent report of personal stereo use suggests that this type of noise exposure may cause permanent threshold shifts. This appears to be the first documentation of such an association in a large sample of young children. The results also suggest that parental concern about the child's hearing ability is not a sensitive indicator for slight-mild SNHL.

## **[217] Harmful Effects of Perinatal Omega-3 Fatty Acid Deficiency and Excess on the Auditory Brainstem Response (ABR)**

**Michael Church<sup>1</sup>**, K.-L. Catherine Jen<sup>2</sup>, Brittany Adams<sup>1</sup>, John Hotra<sup>1</sup>, Tina Stafferton<sup>2</sup>

<sup>1</sup>Wayne State University SOM, <sup>2</sup>Wayne State University COS

**Problem & Hypothesis:** It is well known that perinatal omega-3 fatty acid ( $\omega$ -3) deficiency can cause neurodevelopmental and growth impairments. It is less well known that perinatal  $\omega$ -3 excess can have similar effects. Whereas large  $\omega$ -3 doses will be given clinically to prolong gestation in pregnant women at risk for preterm delivery, it is important to know more about the beneficial and harmful effects on the offspring. Our objective was to compare perinatal  $\omega$ -3 deficiency and excess on offspring outcome, using the ABR as a measure of brain development and auditory function. We hypothesized that both  $\omega$ -3 deficiency and excess will have harmful effects on the offspring. **Method:** Three diets were used: Deficient  $\omega$ -3 (safflower oil,  $\sim$  0%  $\omega$ -3 fatty acids), Excess  $\omega$ -3 (Menhaden oil,  $\omega$ -3/ $\omega$ -6 ratio  $\sim$  14.5) and Control  $\omega$ -3 (soybean oil,  $\omega$ -3/ $\omega$ -6 ratio  $\sim$  0.14). The dams were started on their diets one week before mating and were kept on

their diets throughout pregnancy and lactation. One male and one female offspring per litter were ABR tested at the postnatal age of 24 days. Results: To date, 9 of 42 (21%) Deficient  $\omega$ -3 offspring, 7 of 26 (27%) Excess  $\omega$ -3 offspring, and 0 of 27 (0%) Control  $\omega$ -3 offspring had abnormal ABRs ( $P < 0.025$ ). Fourteen of these 16 abnormal ABRs in the Deficient and Excess  $\omega$ -3 groups were indicative of prolonged brainstem neural transmission times (i.e., P1-P4 interpeak latencies  $> 2$  SD above norms). The two other abnormal ABRs were indicative of 15-20dB high-frequency sensorineural hearing losses (SNHL). Both animals with SNHL were from the Excess  $\omega$ -3 group. It is uncertain at this point in our study whether the SNHL is due to permanent damage or due to a developmental delay. The Deficient and Excess  $\omega$ -3 groups showed reduced growth weights. Some pups in the Excess  $\omega$ -3 group had alopecia (sparse fur). There are strong trends for increased pup and young adulthood mortalities in the Excess  $\omega$ -3 group with the young adulthood mortalities due to chronic renal failure. **Conclusion:** These preliminary results suggest that perinatal  $\omega$ -3 deficiency and excess cause similarly harmful neurological and developmental effects. Giving large doses of perinatal  $\omega$ -3 in clinical trials seems inadvisable because of the potential for adverse health effects on the offspring. (Supported by NIH grant GM58905-7 and a Gerber Foundation grant).

## **[218] Chemotherapy and Cochlear Function in Children**

**Grazyna Lisowska<sup>1</sup>**, Grzegorz Namyslowski<sup>1</sup>, Agata Hajduk<sup>1</sup>, Renata Tomaszewska<sup>2</sup>

<sup>1</sup>ENT Dept., Medical University of Silesia, <sup>2</sup>Dept. of Pediatric Hematology and Oncology, Medical University of Silesia

Chemotherapy is associated with an increased risk of ototoxic changes. The predictive value of pure-tone audiometry on early detection of ototoxicity has been questioned. Otoacoustic emissions appear to be more sensitive to cochlear insult than the conventional pure-tone audiometry. The purpose of our study were: 1) investigate the clinical usefulness of Distortion Product Otoacoustic Emissions (DPOAEs) as early indicator of chemotherapy-induced ototoxicity, 2) determine which of the protocols of chemotherapy is most ototoxic as measured by DPOAEs, 3) compare of the short-term and long-term effects of chemotherapy on DPOAEs. Tonal audiometry, impedance audiometry and DPOAEs were measured in 10 children with acute lymphoblastic leukemia (ALL). Measurements were performed before and after each protocol of chemotherapy (ALL IC-BFM2002): during the 1st protocol vincristine, L-asparaginase, daunorubicin, cyclophosphamide, cytarabine, 6-mercaptopurine and methotrexate were used; during the 2nd protocol vincristine, doxorubicin, L-asparaginase, cyclophosphamide, cytarabine, thioguanine and methotrexate were used; during the 3rd protocol similar drugs were used. DPOAEs were measured using ILO292 Otodynamics Analyser. Cochlear activity was evaluated by recording 2f1-f2 DPOAEs with L1=65 and L2=60 dB SPL. The baseline audiometric and DPOAE evaluations were



performed just before the 1st protocol of chemotherapy. On all subsequent visits the tests of tonal audiometry, immittance audiometry and DPOAEs were repeated with procedures that were identical to those used during collection of the baseline data. Comparisons were performed between baseline measurements and those recorded before and after each protocol of chemotherapy. The chemotherapy-induced alterations in DPOAEs were defined as > 5 dB shift in > 4 consecutive frequencies. Our results indicate that: 1) the DPOAEs monitoring is valid and sensitive technique for the clinical assessment of chemotherapy-induced ototoxicity, 2) the first two months of the ALL chemotherapy show the greatest ototoxicity, 3) cochlear impairment following the ALL chemotherapy in children is in general mild, subclinical and reversible, 4) the long-term DPOAEs monitoring is needed to report reversibility of ototoxicity. In conclusion, DPOAEs measurements are very sensitive on early detection of the changes in cochlear function and are recommended for monitor hearing in patients during the chemotherapy.

### **219** Hearing Impairment and Sensitivity to Sound in Williams Syndrome

**Mazal Cohen**<sup>1</sup>, Josephine Marriage<sup>2</sup>, Stuart Rosen<sup>3</sup>, Mayada Elsabbagh<sup>3</sup>, Annette Karmiloff-Smith<sup>3</sup>

<sup>1</sup>University of Manchester, <sup>2</sup>University of Cambridge,

<sup>3</sup>University College London

Williams syndrome (WS) is a rare developmental genetic condition affecting around 1:20,000 people. Almost all people who have WS have excessive sensitivity to sounds, broadly termed hyperacusis. Individuals diagnosed with the condition rarely complain about hearing problems, however, recent reports suggest that some are hearing impaired. Accurate information on the incidence and nature of hearing impairment (HI) in WS has not been clearly defined due to small sample sizes. The aim of this work is to present the audiometric findings in a large sample of people diagnosed with WS and explore whether it impacts on hyperacusis in WS.

A measure of the severity of hyperacusis, on a scale of 0 to 10, where 10 is the most severe, was obtained from a questionnaire, completed by the participants and/or their families. 63 participants (27 male, 36 female, mean age 17.2 years, range 6 to 55 years) had an otoscopic examination, pure-tone audiometry (PTA) and impedance audiometry in an audiological clinic. PTA was not completed in 7 ears.

The thresholds in 83/119 ears tested were classified as normal (5 frequency average < 20 dB), 29 were mild (20-40 dB) and 9 were moderate (41-70 dB). The HI type was classified as conductive in 13 ears, sensorineural in 13, mixed in 5 and undetermined in 7 ears. Conductive types were associated with mild or moderate severity, and half of the conductive cases were children (< 12 years). Excluding all conductive and mixed HI, we found that the magnitude of HI increased both with age and frequency of pure tone thresholds, suggesting that the HI may be progressive.

Hyperacusis was reported in 97% of cases with mean severity of 5.78 (SD 2.6). Neither the severity of HI nor the type had a significant effect on hyperacusis. Our findings

indicate that a third of people with WS are hearing impaired, the majority have mild impairment, and that hyperacusis in WS is largely independent of the HI.

### **220** Ototoxicity of Burow's Solution

**Mayumi Sugamura**<sup>1</sup>, Takafumi Yamano<sup>1</sup>, Tetuko Ueno<sup>1</sup>, Takashi Ichbangase<sup>1</sup>, Morimich Miyagi<sup>1</sup>, Akihide Imamura<sup>1</sup>, Toshihiko Kato<sup>1</sup>, Tetsuo Morizono<sup>2</sup>

<sup>1</sup>Fukuoka University, <sup>2</sup>Nishi Fukuoka Hospital

**Purpose:** Burow's solution (13% aluminum acetate) has been increasingly recommended as a topical otologic solution for the treatment of active mucosal chronic supportive otitis media, including methicillin resistant *S. aureus*, *P. aeruginosa*, and fungal infections. The ototoxicity of this solution, however, has not been reported to date. The purpose of this study is to evaluate the toxic effect of this solution.

**Material and Methods:** Ototoxicity was evaluated in the guinea pigs using the eighth nerve compound action potentials (CAP) with an electrode on the round window. The stimulus consisted of click sounds, and tone burst of 4 and 8 kHz. The middle ears of the animals were filled with Burow's solution at several dilutions, ranging from full-strength to 1/8 strength and the reduction in the CAP was measured at 30 minutes.

The bacteriostatic activity of the solution was also studied in two kinds of MRSA isolated from ears of patients in our clinic.

**Results:** Burow's solution was found to be extremely ototoxic when applied at the original concentration, moderately toxic with one half dilutions, mildly toxic with one quarter dilution, but it showed little toxicity with one-eighth concentration.

The reduction in bacteriostatic activity correlated well with the degree of dilution.

The results were compared with our previous data on the ototoxicity of Povidone iodine solution, which was found to be far less ototoxic while being more effective in arresting bacterial growth.

**Conclusions:** The thinner round window membrane found in guinea pigs to likely be a factor that could increase the observed ototoxic effects of Burow's solution than would be expected to be seen in humans. However, these results warrant extreme caution in the use of Burow's solution.

### **221** Characteristics of ABR and FNC-ASSR in Temporary Threshold Shift by Noise Exposure in Rats

**Kwon See Youn**<sup>1</sup>, Hee Yeon Shim<sup>2</sup>, Sung Hwa Hong<sup>2</sup>, In Young Kim<sup>1</sup>

<sup>1</sup>Department of Biomedical Engineering, Hanyang University, Seoul, Korea, <sup>2</sup>Department of Otolaryngology, Samsung Medical Center, Seoul, Korea

We hypothesized that by ASSR with wider carrier frequency, ranging from 0 – 50 kHz, we can get more information from the cochlea in rats than by 100 microsecond click-evoked auditory brainstem response (C-ABR) which has 0 – 10 kHz stimulating frequency range. In our previous report, it was confirmed that thresholds of

flat-noise carrier auditory steady-state response (FNC-ASSR) were quite similar to those of C-ABR (abstract number: 503, 2005 ARO) with rats with normal hearing, even though the range of stimulation within the cochlea were different. The objective of this study is to compare the characteristics of ABRs (C-ABR and frequency specific ABRs) and FNC-ASSR with temporary threshold shift by noise exposure in rats. Sixteen SD (Sprague Dawley) rats, ranging from post natal day (PND) 44 to 58, were exposed to white noise at 125dB SPL for 4 hours a day (group 1, n=13) and 8 hours (4 hours a day, two times) (group 2, n=3) in a commercially designed noise exposure chamber. Sixteen left ears were tested for hearing thresholds with ABR (click, 8k, 16k and 32k) and FNC-ASSR using TDT neurophysiology workstation. ABR and FNC-ASSR threshold shift (TS) was determined at pre- and post-exposure up to 14 days. Hearing thresholds were elevated in all subjects just after noise exposure, and recovered to normal hearing within 2 weeks after exposure. In both groups, the amount of TS with FNC-ASSR ( $57.5 \text{ dB} \pm 25.17$ ) was a little higher than C-ABR ( $50.9 \text{ dB} \pm 20.18$ ) ( $p = 0.085$ ) just after noise exposure, but there was no significant difference. In group 2, noise exposure on the second day did not cause further elevation of thresholds comparing with the thresholds after noise exposure for 4 hours. These results suggested that FNC-ASSR could be used for hearing threshold measurement in a certain ototoxic condition in rats. Supported by R01-2005-000-10739-0, MOST 2004-02186

## **[222] Tinnitus and Normal Hearing Thresholds: Relations Between Minor Cochlear Lesions and Possible Causative Factors**

**Ann-Cathrine Lindblad<sup>1</sup>, Ulf Rosenhall<sup>1,2</sup>**

<sup>1</sup>Karolinska Institutet, <sup>2</sup>Karolinska University Hospital, Sweden

Increasing numbers of patients seek consultations for tinnitus. It is well known that tinnitus is often correlated to hearing impairment. However, it has been reported that 1/4 of those with continuous tinnitus perceive their hearing as normal. Minor, functionally important lesions might occur without elevated auditory thresholds, and thus remain undetected. The aim of the present study was to study patients with normal hearing thresholds and tinnitus. Tests of the inner ear and the efferent system were performed to see if certain possible causative factors give specific types of cochlear lesions that might cause the symptoms.

Fortyone patients were included, 14 women and 27 men, between 18 - 60 years of age, mean 36 years. Tentative causative factors were identified. For each subject the involvement of the following causative factors was judged on a four-grade scale: 1) acute acoustic trauma; 2) music; 3) genetics, and 4) non-auditory factors, e.g. muscular tension, odontological problems and stress.

Among other measurements transient evoked otoacoustic emissions, TEOAEs with and without contralateral noise, were used to test outer hair cells, OHCs, and the efferent control system. Thresholds for brief tones at the peaks and in the valleys of 100 % intensity-modulated noise,

psychoacoustical modulation transfer function, PMTF, were also used to test OHCs and possibly IHCs and the ipsilateral control system. Statistical analyses were made of the judged degree of the four causative factors versus the test results of OHC function and function of the efferent control system.

So far we have found characteristic results for tinnitus subjects having suffered acute acoustic trauma from shots and explosions, and most likely also for subjects with genetic factors. The ultimate goal of this ongoing investigation is to create a diagnostic evaluation scheme to be able to choose the best treatment for the individual patient.

## **[223] Cytokine Expression by a Human Middle Ear Epithelial Cell Line Following Parainfluenza Virus Infection**

**William Leight<sup>1</sup>, Robert Antoniou<sup>1</sup>, Joshua Surowitz<sup>1</sup>, Liquan Zhang<sup>2</sup>, Raymond Pickles<sup>2</sup>, Scott Randell<sup>2</sup>, Craig Buchman<sup>1</sup>**

<sup>1</sup>UNC Chapel Hill Department of Otolaryngology-Head and Neck Surgery, <sup>2</sup>UNC Chapel Hill Cystic Fibrosis/Pulmonary Research and Treatment Center

Background: Recent clinical and animal studies have highlighted the importance of respiratory viruses in the development of acute otitis media. While parainfluenza virus is commonly isolated from middle ear effusions and is ubiquitous in the pediatric population, its role in the development of acute otitis media remains unclear. It has been postulated that viral infection primes the innate host immune response to a secondary or concomitant bacterial infection. The present study examines the innate immune response of human middle ear epithelial cells to parainfluenza virus infection.

Methods: A human middle ear epithelial cell line, HMEEC-1, was used for experimentation. Cells were plated on 96 well culture dishes at 75% confluence. Cultures were inoculated with a recombinant type 3 parainfluenza virus, rgPIV3. Tumor necrosis factor alpha, TNF, phosphate buffered saline, and a UV-inactivated virus, uvPIV3, were used as controls. Media was collected and the levels of IL-8, RANTES, and IP-10 were measured using ELISA. Additionally, cells were collected at each timepoint and mRNA levels for all three cytokines were measured using real-time polymerase chain reaction.

Results: HMEEC-1 cells infected with rgPIV3 exhibited GFP expression as early as 24 hours after infection. HMEEC-1 produced significant accumulations of RANTES and IP-10 by 48 hours after infection. IL-8 accumulation was not statistically significant at 48 hours. By 72 hours, all 3 cytokines were significantly increased over baseline. All 3 mRNA transcripts were significantly increased over baseline by 72 hours; RANTES and IP-10 were 15 and 19 fold increased over baseline, while IL-8 was 1.6 fold increased.

Conclusions: Parainfluenza virus actively infects middle ear epithelial cells in a manner similar to RSV. This model produces results similar to PIV infection in well-differentiated airway systems and is therefore useful for further studies investigating the inciting events in viral-induced otitis media.

**224 Cytokine Induction by Respiratory Syncytial Virus and Streptococcus Pneumoniae in Well-Differentiated Human Airway Epithelial Cells**

Joshua Surowitz<sup>1</sup>, William Leight<sup>1</sup>, Amanda Poston<sup>1</sup>, Liqun Zhang<sup>2</sup>, Raymond Pickles<sup>2</sup>, Scott Randell<sup>2</sup>, Craig Buchman<sup>1</sup>

<sup>1</sup>UNC Chapel Hill Department of Otolaryngology-Head and Neck Surgery, <sup>2</sup>UNC Chapel Hill Cystic Fibrosis/Pulmonary Research and Treatment Center

Background: Respiratory syncytial virus (RSV) and Streptococcus pneumoniae (SPne) are important pathogens in otitis media. RSV pathogenesis is classically thought to be due to a combination of viral cytopathic effects and host immune response. Recent evidence suggests that secondary bacterial infection may play an important role in this disease process. This study investigates the innate immune response of human airway epithelial cells to RSV infection and secondary SPne exposure. Methods: Tracheobronchial epithelial cells were harvested from healthy donors and grown at air-liquid interface until well differentiated. Select cultures were exposed to green fluorescent protein-expressing RSV for two hours. At 72 hours post-infection, select cultures were challenged with tumor necrosis factor  $\alpha$  (TNF $\alpha$ ) or live SPne. Media was collected daily. IL-6, IL-8, and RANTES were quantified by ELISA. Results: Control cultures showed minimal morphological changes. Sequential infection with RSV and SPne induced dramatic morphologic changes. RSV-infected cultures showed significantly elevated levels of IL-6, IL-8, and RANTES when compared to controls. Secondary TNF $\alpha$  challenge resulted in amplification of IL-6, IL-8, and RANTES. In RSV-infected cultures secondarily challenged with SPne, IL-8 production increased while IL-6 and RANTES production decreased. Conclusions: RSV infection of well-differentiated airway epithelial cells significantly increases IL-6, IL-8, and RANTES. As previously shown by our group, secondary proinflammatory challenges using TNF $\alpha$  amplify this response. RSV-infected cultures exposed to SPne demonstrated a significant shift in the cytokine response profile. These findings support the hypothesis previously proposed by our group that airway epithelial cells similarly infected with parainfluenza virus shift from a TH-1 to TH-2 immune response in a pathogen-dependent fashion.

**225 Activation of Transforming Growth Factor Signaling Pathway in Rat Middle Ear with Otitis Media**

Yun-Woo Lee<sup>1,2</sup>, Yunju Chung<sup>1,2</sup>, Quang-An Zhang<sup>1,3</sup>, Steven K. Juhn<sup>1</sup>, Qing Yin Zheng<sup>4</sup>, Youngki Kim<sup>5</sup>, Patricia Ferrieri<sup>5</sup>, Diego Preciado<sup>1</sup>, Robert Margolis<sup>1</sup>, Jizhen Lin<sup>1</sup>

<sup>1</sup>Otitis Media Research Center, University of Minnesota, <sup>2</sup>Kosin University Hospital, Korea, <sup>3</sup>Jiao Tong University, China, <sup>4</sup>The Jackson Laboratory, Bar Harbor, ME, USA, <sup>5</sup>Department of Pediatrics, University of Minnesota

Tissue remodeling is a key step for the development of granulation tissue and subsequent destruction of the middle ear cavity. Transforming growth factor (TGF) plays a role in this process. Here we characterized the expression profile of TGF signaling pathway in the middle

ear mucosal tissue of rats with experimental otitis media. Rat bulli were challenged with one dose of *S. pneumoniae* type 6A (Pn6A  $10^{-7}$  cfu/bulla), non-typable *H. influenzae* (NTHi,  $5 \times 10^{-7}$  cfu/bulla) or with Eustachian tube obstruction (ETO), and harvested for microarrays and histopathology in a time-dependent manner. Bulli challenged with phosphate-buffered saline (PBS) served as controls. It was demonstrated that the activities of the TGF ( $\alpha$ & $\beta$ ), TGF- $\beta$  receptor (type I, II, and III), Smad2, collagen/tenascin/fibronectin pathways were highly regulated in the diseased mucosa compared with controls. In the Pn6A-infected ears from 3 to 7 days, the TGF- $\beta$ 1 and fibronectin-1 genes were down-regulated whereas in the NTHi-infected ears from 3 to 7 days, collagen (COL2A1) and fibronectins (FN & FN-1) were highly up-regulated. It suggests that NTHi is a relatively potent pathogen for middle ear fibrotic disorders in comparison with Pn6A. In the ETO-treated ears, from 7 to 30 days, the activity of the TGF pathway and effectors was down-regulated, suggesting that ETO itself does not contribute to fibrotic disorders of the middle ear mucosa.

This study is in part supported by the NIDCD R01DC03433, R21 DC005846, and P30DC04660, the Multiple Districts (5M) Lions Hearing Foundation, and the National Organization for Hearing Research.

**226 Effect of Locally Injected Dexamethasone, Dexamethasone Sodium Phosphate and Hydrocortisone on LPS-Induced Otitis Media in Chinchilla**

J. Courtney French<sup>1</sup>, Timothy T.K. Jung<sup>1,2</sup>, Choong-Won Lee<sup>1</sup>, Tammy Pham<sup>1</sup>, Stanley Allen<sup>1</sup>, Mark Nicosia<sup>1</sup>, Derick Ly<sup>1</sup>, Jerry Nguyen<sup>1</sup>, Earnest O. John<sup>1,2</sup>

<sup>1</sup>Loma Linda University, <sup>2</sup>VA Medical Center, Loma Linda

Objective: Otitis media (OM) is one of the most common pediatric diseases. Our previous studies showed that treatment with systemic antibiotics and corticosteroids were more efficacious than antibiotics alone. The purpose of this study was to determine effectiveness of topically applied corticosteroids on the outcome of OM. The long-term goal of this study is to find a better method of OM treatment using local therapy to avoid systemic side effects.

Study Design and Methods: This study involved 8 groups, 2 control and 6 experimental groups. Control groups contained a saline and a common vehicle group (12 animals in each). The 6 experimental group test substances were; 1% dexamethasone (12 animals), 0.1% dexamethasone (12 animals), 1% dexamethasone sodium phosphate (12 animals), 0.1% dexamethasone sodium phosphate (12 animals), 1% Hydrocortisone (12 animals), and 0.1% Hydrocortisone (11 animals). The control groups served as a positive control receiving 0.3mL of lipopolysaccharide (LPS, 1mg/mL) two hours after the first injection of test substances (saline and common vehicle) into the bulla. The two control groups also received 0.2cc of saline and common vehicle substances at 24 and 48 hours after injection of LPS. The experimental groups received LPS at 0 hours, and 0.2 mL of experimental test substances at -2, 24 and 48 hours after LPS injection. At

96 hours, the animals in each group were euthanized and studied for the presence or absence and volume of middle ear fluid.

Results: At the end of 4 days, in 11 ears the fluid diminished to the point of being unobservable (1/24 vehicle, 2/24 0.1% dexamethasone sodium phosphate, 3/24 1% dexamethasone sodium phosphate, 2/24 0.1 dexamethasone, 1/24 1% dexamethasone, 1/22 0.1 % hydrocortisone, 1/24 1% hydrocortisone). As expected, with the exception of the vehicle control group, the volume of middle ear fluid was significantly less in all groups compared to the saline control.

Conclusion: Topical corticosteroid treatment is effective in resolving LPS induced OM in experimental animals. Dexamethasone and its derivatives appears to be more effective than hydrocortisone in reducing the volume of middle ear fluid.

### **[227] Effect of Dexamethasone and Rimexolone on Morphology of the Round Window Membrane in LPS Induced Otitis Media**

Earnest O. John<sup>1,2</sup>, Stanley Allen<sup>1</sup>, Choong-Won Lee<sup>1</sup>, J. Courtney French<sup>1</sup>, Mark Nicosia<sup>1</sup>, Timothy T.K. Jung<sup>1,2</sup>, Derick Ly<sup>1</sup>, Jerry Nguyen<sup>1</sup>, Tammy Pham<sup>1</sup>, Michael Wall<sup>3</sup>

<sup>1</sup>School of Medicine Loma Linda, <sup>2</sup>VA Medical Center, Loma Linda, <sup>3</sup>Alcon Laboratories

Background: The round window membrane is the only soft tissue barrier separating the middle ear from the inner ear and appears to be the main portal for passage of toxic substances into labyrinth. Many human and animal studies have demonstrated that the architecture of the round window membrane alters in diseased conditions such as otitis media. The morphological changes in the round window membrane influence its permeability as a defense mechanism.

Purpose: To determine effect of topical treatment of dexamethasone and rimexolone on the thickness of round window membrane (RWM) in LPS induced experimental otitis media with effusion in chinchillas.

Methods: Experimental otitis media with effusion was induced in twenty chinchillas by inoculating with lipopolysaccharide (LPS) into the bullae at 0 hour. Three control and four treatment groups were studied: saline (control, n=2), dexamethasone vehicle (control, n=3), rimexolone vehicle (control, n=3), 1% dexamethasone (treatment, n=3), 0.1% dexamethasone (treatment, n=3), 1% rimexolone (treatment, n=3), 0.1% rimexolone (treatment, n=3). Seven test substances (saline, dexamethasone vehicle, rimexolone vehicle, 1% dexamethasone, 0.1% dexamethasone, 1% rimexolone, 0.1% rimexolone) were inoculated at -2, 24, and 48 hours. After 96 hours the temporal bones were extracted, fixed, and sectioned for histological analysis. Light microscopy with calibrated ocular units was used to measure the thickness of the RWM. Left and right RWM thicknesses were measured at the midpoint in each histological section.

Results: Both the control (29.57 ±6.45, 26.75± 4.46, 28.76±6.13  $\mu$ m) and treatment groups (18.07± 3.54, 21.27± 4.64, 19.96 ± 4.08, 20.12 ± 4.20  $\mu$ m) showed a mean

membrane thickness greater than normal (13.7 ±2.9  $\mu$ m). All treatment groups demonstrated a statistically significant reduction in thickness when compared to the saline control. A significant reduction in thickness was also noted in all treatment groups when compared to their respective vehicle groups.

Conclusion: Topical treatment of dexamethasone and rimexolone reduced inflammation and thickness of the RWM in LPS-induced experimental otitis media with effusion.

### **[228] Regulation of Intercellular Communication Through Gap Junction Protein, Connexins in Immortalized Human Keratinocytes Cells (HaCaT Cells)**

Yun-Hoon Choung<sup>1</sup>, Keehyun Park<sup>1</sup>, Jung-whan Song<sup>1</sup>, Hison Kahng<sup>1</sup>

<sup>1</sup>Department of Otolaryngology, Ajou University School of Medicine, Suwon, Republic of Korea

Background and Objectives: Middle ear cholesteatoma needs intercellular communication through gap junctions connexins (Cx) as well as intracellular signal pathway for hyperproliferation. The objectives of this study are to identify regulating materials to control intercellular communication through gap junction proteins Cxs, and to provide basic information to help making in-vitro models for the formation and prevention of middle ear cholesteatomas using immortalized human keratinocytes cells (HaCaT). Materials; H<sub>2</sub>O<sub>2</sub>, acetic acid (AA), dexamethasone, all-trans-retinoic acid (RA), and green tea extracts - epicatechin (EC) and epigallocatechin gallate(EGCG) were used for Cx controlling substances. Methods; To evaluate cytotoxicity of controlling substances, we performed neutral red uptake test. Reverse transcription-polymerase chain reaction (RT-PCR), Western blot, and immunocytochemistry staining were done to identify the change of the connexin (Cx26, 30, 31, 43) expression. Scrape load dye transfer assay (SLDTA) was done to evaluate the intercellular communication of HaCaT cells. Results; Cx26, Cx30, Cx43, and Cx31 in that order were expressed well in HaCaT cells. Through RT-PCR, substances that up-regulated the expression Cx26 mRNA were EGCG(50 $\mu$ g/ml), EC, and RA, and the substances that down-regulated Cx26 were AA, H<sub>2</sub>O<sub>2</sub>, EGCG(100 $\mu$ g/ml). In Western blot, EGCG(50 $\mu$ g/ml) up-regulated Cx26 protein, and AA, H<sub>2</sub>O<sub>2</sub>, and dexamethasone down-regulated it. Immunocytochemistry of HaCaT cells showed decreased expression and abnormal location of Cx26 and Cx43 under AA, H<sub>2</sub>O<sub>2</sub>, and EGCG(50 $\mu$ g/ml). SLDTA for functional study showed that acetic acid, H<sub>2</sub>O<sub>2</sub>, and dexamethasone down-regulated intercellular communication, while EC upregulated it. Conclusion; The intercellular communication through gap junction proteins, connexins in HaCaT cells can be easily controlled by several substances. Acetic acid, H<sub>2</sub>O<sub>2</sub>, dexamethasone are considered to be useful substances to inhibit the advancement of middle ear cholesteatomas, and EC may be useful when we are making in vitro cholesteatoma models using HaCaT cells.

## **229 Mucin Gene Exploration and Identification in Middle Ear Epithelium**

**Joseph Kerschner**<sup>1,2</sup>, Amy Burrows<sup>1</sup>, Joseph A. Cioffi<sup>1</sup>, Paul Popper<sup>1</sup>, J. Christopher Post<sup>3,4</sup>, Garth Ehrlich<sup>3,4</sup>

<sup>1</sup>Medical College of Wisconsin, <sup>2</sup>Children's Hospital of Wisconsin, <sup>3</sup>Drexel University College of Medicine, <sup>4</sup>Center for Genomic Sciences

Otitis media is the most common diagnosis in pediatric patients who visit physicians for illness in the United States. Mucin production in response to otitis media causes significant sequelae including hearing loss and the need for surgical intervention. Because mucins play an integral role in the mechanisms of otitis media, investigating the expression of mucin genes in this tissue is vital to the understanding of the pathophysiology of otitis media.

We investigated the expression of several novel mucin genes not previously identified in middle-ear tissue both in vivo, and in an in vitro model of immortalized human middle ear epithelium. Human tissue obtained from children at the time of tympanostomy tube placement was investigated to determine the level of expression for mucin genes MUC12, MUC13, MUC14, MUC15 and MUC16 using RT-PCR and Real Time RT-PCR. Immortalized human middle-ear epithelial cell cultures were also investigated for expression of these mucin genes. Mucin gene expression was verified in both explants and immortalized cells and sequencing of the cDNA demonstrated correlation between the two tissue types.

This study demonstrates the expression of several recently identified mucin genes in the human middle ear. Further studies are ongoing within our laboratory, to examine the implications of this mucin gene expression, their function in the physiology and pathophysiology of the middle ear as well potential modulations of this gene expression in response to inflammatory conditions such those that exist in otitis media.

## **230 Attempts of Healing Chronic Tympanic Membrane Perforation Using Stem Cells Both In Vivo and In Vitro**

**Anisur Rahman**<sup>1,2</sup>, Malou Hultcrantz<sup>2</sup>, Petri Olivius<sup>2</sup>, Magnus von Unge<sup>2</sup>

<sup>1</sup>Center for Hearing & Communication Research and Dept. of clinical Neuroscience, Karolinska Institutet, <sup>2</sup>Dept. of Otolaryngology, Karolinska University Hospital, SE-171 76 Stockholm, Sweden

Chronic tympanic membrane (TM) perforation commonly arises as a result of either trauma or otitis media resulting in conductive hearing loss and chronic infection. The only available treatment is the surgical closure using different graft materials. A large number of patients doesn't have access to this surgical treatment. We intend to develop a simple treatment which could replace surgery so that the patients could be treated with a simple office technique. In recent year's stem cells have gained interest for its tremendous capability to mature into different specific cell types.

Human mesenchymal stem cell treatment: Myringotomy was made on 12 rat's TM using a laser beam of 0.2mm

diameter. A solution of cortisone was instilled on both TMs for ten consecutive days. The perforations were still open after 1 month of cortisone instillation. The border of the perforation edge was refreshed by a needle and a 0.5 ml solution of mesenchymal stem cells (MSC) was applied around the perforation of the right TMs. A saline solution was applied on the left TMs, for control. 4/10 MSC treated TMs had closed perforations as compared with 2/10 saline treated control TMs. The number of MSC treated ears showed better healing although the total number of studied animals was small.

In vitro culture of TM with perforation and application of stem cells: The TMs of rat pups between 13 and 15 days of age were isolated and placed on special membrane-coated petri dishes with nourishing media. Perforations were made by needle and mouse embryonic stem cell (sox1) were applied to the perforations of half of the specimens and the rest left as a control and the explants were incubated. The perforations were no longer visible at 3 days after the perforation was made. The TMs looked apparently healthy at the end of 2nd week of culture. Stem cell colonies were proliferated well. Further improvement on localizing the stem cells over perforations is needed.

## **231 An Injectable Form of Esterified Hyaluronic Acid Gel (Sepragel®) Is a Safe and Effective Packing Material for Middle Ear Wound Healing in the Guinea Pig**

Simon Angeli<sup>1</sup>, **Brian Gibson**<sup>2</sup>, Ali Ozdek<sup>3</sup>, Sara Connell<sup>1</sup>, John Mc Elveen<sup>4</sup>, Thomas Van De Water<sup>1</sup>

<sup>1</sup>University of Miami Ear Institute, Dept. of Otolaryngology,

<sup>2</sup>Florida State University College of Medicine, <sup>3</sup>Ankara Research & Training Hospital, Dept. of Otolaryngology,

<sup>4</sup>Carolina Ear & Hearing Clinic

Objective: Investigate the efficacy and safety of a hyaluronic acid gel preparation (Sepragel®) as packing material in middle ear (ME) surgery. Design: Two types of experiments: 1) long-term- Sepragel® compared to Gelfoam® in an animal model of ME wound healing, postoperative hearing loss recovery, and amount of packing remaining at the end of 6 weeks; and 2) short-term- retention of Sepragel® in the ME. Material: 30 pigmented guinea pigs (Elm Hill Labs, Chelmsford, MA). Intervention: *Long-term experiment*: Group 1, Sepragel® treated animals (n = 8), standardized bilateral wounding of ME mucosa, contralateral ears were unpacked controls. Group 2, Gelfoam® treated animals (n = 6), same as group 1, contralateral ears were unpacked controls. Group 3, contralateral controls with ME wounding minus the packing material (n = 14). DPOAE and ABR tests performed: pre-operatively, 5 days, 2 weeks, and 6 weeks post-operatively. Animals sacrificed after 6 weeks post-operative had microscopic analyses. *Short-term experiment*: retention of packing material in ME at: 1) group 1- 1 week; and 2) group 2- 2 weeks. Results: *Long-term*: DPOAE testing at 6 weeks post-operative showed no significant difference between use of either packing material or between packing material and controls. ABR testing showed lower ABR thresholds for Sepragel® than Gelfoam® at all frequencies at all dates post-operative. The Gelfoam® group showed significant persistent hearing

loss at all dates post-operatively at all frequencies tested. The Sepragel® group returned to near pre-operative ABR thresholds by 2 weeks post-operative with significant hearing loss only at 1 kHz with the latter returning to pre-operative levels by 6 weeks post-operative. Sepragel® resulted in better microscopic findings in the ME, however, only shown to be *significantly* better was the lower magnitude of residual packing left behind in the Sepragel® group than the Gelfoam® group. *Short-Term:* At 1 week post-operative, 85 % of original Sepragel® packing remained while 71.25 % remained after 2 weeks. Sepragel® caused no eardrum perforations or ME edema and effusions in the ME were minimal and insignificant from week 1 to week 2 post-operative. Conclusion: Sepragel® is shown to be safe to wound healing and remains in the ME long enough to be effective for use as a packing material during ME surgery in the guinea pig. Supported by grants from Carolina Ear Institute and Genzyme Biosurgery

### **[232] Otitis Media in Inbred Mouse Strains and Hyp-Duk Mutant**

**Qing Yin Zheng<sup>1</sup>**, JiangPing Zhang<sup>1,2</sup>, Belinda S. Harris<sup>1</sup>, Christopher M. McCarty<sup>1</sup>, Heping Yu<sup>1</sup>, Patricia Ward-Bailey<sup>1</sup>, Kenneth R. Johnson<sup>1</sup>

<sup>1</sup>The Jackson Laboratory, Bar Harbor, ME, USA, <sup>2</sup>Xi'an Jiaotong University School of Medicine

Otitis media is the most common cause of hearing impairment in children and is primarily characterized by inflammation of the middle ear mucosa. In this study, we first investigated the incidence of chronic otitis media in inbred mice strains and mutants. Secondly, we found mice with the hypophosphatemia-Duke (*Phex<sup>Hyp-Duk</sup>*) mutation, presented a high incidence of chronic otitis media with effusion. Lastly, this mouse model is being evaluated using histological pathology, FACS analysis, immunohistochemistry and real time PCR. In conclusion, the mouse can be a good model for research on the hereditary factors that contribute to otitis media. Supported by NIH NIDCD DC005846.

### **[233] Dynamics of Speech and Swallowing**

**Gerald Popelka<sup>1</sup>**, Raymond Kent<sup>2</sup>

<sup>1</sup>Stanford University, <sup>2</sup>University of Wisconsin

Both speech and swallowing are complex overlapping movements of many shared oral structures. An understanding of the movement sequences of these structures for each function individually, and whether they differ for the two functions, is critical to basic knowledge of oral motor control. Existing testable hypotheses include that the tongue functions as a muscular hydrostat, that basic movements and interarticulator coordination of the shared oral structures differ between speech and swallowing, and that oral structure movements during swallowing are staged rather than continuous. Previous attempts to test these hypotheses have been limited and inconclusive because the existing technology either restricted the amount of data that could be collected or involved measurement apparatus that may perturb the behavior being measured. Real-time magnetic resonance imaging is a new technology that is highly promising for

resolving these issues because it does not rely on ionizing radiation, requires no measurement components applied to the oral structures and allows the simultaneous observation of all of the oral structures with the subject in a natural upright position. Several experiments were conducted to determine the adequacy of this new technology for testing these hypotheses. Results show that in spite of high level scanning noise, acoustic recordings of speech can be processed with a linear algorithm to lower scanning noise by 33 dB and allow adequate spectral analysis of the speech signal, that acoustic recordings can be synchronized with the moving images, and that image quality is sufficient to allow analysis algorithms for quantifying tongue cross-sectional area, lateral asymmetry and other measures, dynamically over time. Temporal resolution is sufficient for measuring vowels and liquid phonemes. A range of natural food was measured for image brightness and clearance and it was determined that several natural foods high in manganese content would be adequate for multiple swallowing measures including two liquids (blueberry or pineapple juice) and a solid food (tofu). A video and audio demonstration will be available at the presentation. Our overall goal is to apply real-time magnetic resonance imaging to answer several basic questions about the patterning of movements of oral structures during speech, swallowing and chewing.

### **[234] Electromyography in Guiding Botox Treatment for Spasmodic Dysphonia**

**Yongbing Shi<sup>1</sup>**

<sup>1</sup>Oregon Health & Science University

Spasmodic dysphonia (SD) is a form of focal dystonia affecting intrinsic laryngeal muscles. Adductor SD is characterized by strangled, broken and hoarse voice, as a result of spasmodic activities of adductor muscles in the larynx. Patients with SD have difficulties with verbal communication. Botox is a commercial preparation of botulinum toxin type A. It significantly improves voice in SD patients when administered in intrinsic laryngeal muscles by partially blocking neuromuscular transmission. Botox is routinely injected into the thyroarytenoid (TA) muscle for patients with adductor SD. However, some adductor SD patients do not benefit from TA muscle injection and some lose benefits after receiving good results for some time. This may be due to spasmodic activities from muscles other than the TA muscle. Information about these muscles will help improve treatment results. Laryngeal electromyography (EMG) provides information on neuromuscular activities in laryngeal muscles. Laryngeal EMG was performed in seven patients with adductor SD who had experienced decreased benefits from Botox injection into the TA muscle. In addition to the TA muscle, other adductor muscles including the lateral cricoarytenoid (LCA) and cricothyroid (CT) muscles were studied. Typical SD-related EMG findings included increased spontaneous activities, high-level recruitment and spikes associated with voice breaks. Botox treatment was redesigned for these patients, based upon laryngeal EMG information. Redesigning involved dose adjustment and injection into the LCA and CT muscles when indicated. Follow-up data are available for four of the seven patients. Significant improvement in overall voice quality and voice symptom

subscales was reported by all four patients. Side effects either remained virtually unchanged or reduced following treatment modification. Laryngeal EMG is a valuable tool in guiding Botox treatment for SD.

### **[235] Development of a Retrocricopharyngeal Surgical Implant to Prevent Laryngopharyngeal Reflux by Increasing Resistance to Retrograde Flow of Gastric Contents**

**Michael Lipan<sup>1</sup>, Joy Reidenberg<sup>1</sup>, Jeffrey Laitman<sup>1</sup>**

<sup>1</sup>*Mount Sinai School of Medicine*

Laryngopharyngeal reflux (LPR) is a clinical entity resulting from exposure of laryngeal and pharyngeal mucosa to gastric secretions. Patients who fail medical treatment or who have life threatening LPR are increasingly treated with anti-reflux surgery at the lower esophageal sphincter. In contrast, surgical intervention at the upper esophageal sphincter (UES) has not been attempted. The objective of this study is to determine the efficacy of a retropharyngeal implant at the UES to augment this anti-reflux barrier. Cadaveric heads (n=13) were harvested and the distal end of the esophagus was tied over a catheter for water infusion. Implants were made of silicone rubber in various widths and either cylindrical (diameters: 0.4, 0.45, 0.6, 0.8, 0.9 cm) or half-cylindrical (radii: 0.3, 0.4, 0.45, 0.6 cm) in shape. Implant length exceeded the width of the esophagus when inserted behind the cricopharyngeus. Maximal intraesophageal pressure during water infusion was measured with a water manometer in each specimen with no implant and then with each implant in place. Paired t-test was used for statistical analysis. Results show that each implant increased pressure compared to using no implant ( $p < 0.05$ ). Increasing width of the implant correlated with increasing maximal pressure among same shape implants (range: cylinders 32.3–74.0 cmH<sub>2</sub>O and half-cylinders 32.0–81.4 cmH<sub>2</sub>O). For implants of the same width (i.e., diameter of cylinder = radius of half-cylinder), half-cylinder implants achieved higher pressures ( $p < 0.05$ ). In conclusion, statistically significant resistance to liquid flow past the level of the UES can be achieved using any of the implants tested. Increased resistance correlated with increased width of the implant for those of the same shape only. Half-cylindrical implants achieved greater resistance than cylindrical implants of the same width. The initial success of this method shows promise for future development of an implant for patients with LPR.

### **[236] New Analysis of Olfactory Behavior**

**Aigo Yamasaki<sup>1</sup>, Hiroshi Yamashita<sup>1</sup>, Kazuma Sugahara<sup>1</sup>, Tsuyoshi Takemoto<sup>1</sup>**

<sup>1</sup>*Yamaguchi University*

The conventional analysis of olfactory behavior is complicated and takes much time. We report a new trial for analysis of olfactory behavior using video cameras and NIH imaging. We observed that mice avoided cotton balls including acetic acid placed in a corner of a square cage, and recorded that behavior with video cameras. Motion pictures were loaded onto a personal computer and analysis using NIH imaging. The cage was divided into 4 areas and time mice remained in each area was calculated. Mice were evenly distributed in area without

the cotton ball with acetic acid. The staying time was significantly shorter in Acetic acid area than in the other areas. Results suggest that this new analysis may be useful for studying olfactory behavior in mice.

### **[237] The Therapeutic Effect of the Co-Administration of Immunostimulatory DNA Sequence with Allergen Extract on Allergic Inflammation in Animal Model of Timothy Allergy** **Jun Woo Kim<sup>1</sup>, Jaechun Lee<sup>1</sup>, Brandon D. Hill<sup>1</sup>, Tai June Yoo<sup>1</sup>**

<sup>1</sup>*Division of Allergy & Immunology, Department of Medicine, University of Tennessee*

Despite a number of effective pharmacological options for the prevention and treatment of the anaphylactic activity that occur in sensitized individuals on allergen exposure, the termination of allergic hypersensitivities remains an elusive therapeutic goal. By allergen specific immunotherapy (SIT) with allergen extracts, allergy can be treated with the polarization of immune response to Th1 type cells, however it has a limited scope of efficacy. Recently, immunostimulatory oligodeoxynucleotide sequences (ISS-ODN) have been discovered that act as strong T helper 1 response inducing adjuvants in mice and DNA based vaccination might be an effective therapeutic option for the treatment of allergic inflammation. We present a novel immunotherapeutic strategy to evaluate the polarization of the immune responses induced by ISS-ODN with timothy allergen.

Experiments were performed in four groups of mice which designed to develop timothy allergy with sensitization and aerosol challenge with timothy extract. Group 1 received 100 µg of ISS-ODN with 110 µg of timothy allergen as a therapeutic group, Group 2, ISS-ODN with bovine serum albumin, Group 3, C-ODN (control ODN) with timothy allergen, Group 4, ISS-ODN alone. Cytokine profiles of IL-4, IL-5, IL-10, IL-13, IFN-γ, and TGF-β, degree of inflammation in lung histology, and differential counts of bronchoalveolar lavage cells were measured. Histologic studies showed a significant reduction of mononuclear cell infiltration in lung tissue of mice treated with ISS-ODN with timothy allergen and ISS-ODN without allergen in comparison with controls. IFN-γ was significantly increased in ISS-ODN with allergen group and ISS-ODN alone group comparing to control group.

These results suggest that immunization with ISS-ODN with allergen effectively inhibits allergic responses in mice and might be a new model of immunotherapy in human timothy allergy.

### **[238] Local Administration of IL-21 Suppresses Nasal Allergic Reaction in a Murine Model**

**Yayoi Hiromura<sup>1</sup>, Osam Mazda<sup>2</sup>, Tsunao Kishida<sup>2</sup>, Takemitsu Hama<sup>1</sup>, Yasuo Hisa<sup>1</sup>**

<sup>1</sup>*Department of Otolaryngology, Kyoto Prefectural University of Medicine, Kyoto, Japan,* <sup>2</sup>*Department of Microbiology, Kyoto Prefectural University of Medicine, Kyoto, Japan*

Introduction: Interleukin-21 (IL-21) is a cytokine belonging to the common gamma-chain receptor cytokine family.



Earlier studies indicated that IL-21 regulates growth and function of T and NK cells, while immunoglobulin production is influenced by IL-21. We hypothesized that this cytokine is capable of controlling IgE-mediated allergy. Here we examined the effect of IL-21 on an allergic rhinitis model of mice.

**Methods:** To induce allergic rhinitis in mice, a mixture of ovalbumin (OVA) and Al(OH)<sub>3</sub> as adjuvant was intraperitoneally administered. A group of mice was given into the nostrils with a solution containing OVA and recombinant IL-21 daily for 7 days, while control mice were given OVA alone. The mice were then challenged with the OVA solution and number of sneezes was counted during the following 10 min. Two hours later sera were collected, and the levels of total IgE, total IgG2a, and OVA-specific IgE were evaluated by enzyme-linked immunosorbent assays.

**Results and discussion:** The allergic symptom was remarkably inhibited by the nasal IL-21 administrations, as revealed by the decrease in the number of sneezes. The IL-21-treated group showed a significant reduction in total and OVA-specific IgE titers in comparison with untreated controls, while serum IgG2a level was not affected by the cytokine treatment. The results indicated that IL-21 nasal administration was effective in ameliorating allergic rhinitis.

### **239 NIDCD Research and Training Workshop for New Investigators**

**Nancy Freeman<sup>1</sup>**, Lynn Luethke<sup>1</sup>, Bracie Watson<sup>1</sup>, Roger Miller<sup>1</sup>, Christopher Platt<sup>1</sup>, Daniel A. Sklare<sup>1</sup>, Ling Chin<sup>1</sup>

<sup>1</sup>*National Institutes of Health, Bethesda, MD*

The NIDCD workshop will focus EXCLUSIVELY ON NEW INVESTIGATORS. The goal of the workshop is to provide information for the successful transition from trainee/new investigator status to an independent investigator (R01). Following a brief overview of NIH funding mechanisms and the new electronic submission process, attendees will choose one of four breakout sessions:

1. NIH 101: How does NIH work? This session will provide practical information on how the NIH/NIDCD works. Discussion will include application timelines, peer review assignments, Advisory Council activities, and the roles of NIH extramural staff throughout this process.

2. Training and Career Development (Fs and Ks): What do I need to know? The breakout session will describe the research training and career development mechanisms appropriate for new investigators, including the individual fellowship awards (F30, F31 and F32) and the career development mechanisms for clinically trained investigators scientists and clinicians (K01, K08 and K23). New initiatives will be underscored. The NIH programs providing repayment of educational loans will also be covered.

3. Transitioning to Independence: Should I apply for an R03 or an R01? The session will provide guidance on the appropriate grant mechanisms for early career stages, and will focus on the NIDCD Small Grant Award (R03) and the New Investigator R01. This session will also include a discussion of how to avoid mistakes commonly observed in the review process.

4. Clinical and Translational Research: Is my research defined as translational and what should I know about the process of submitting a clinical trial application. This session will describe the expansion of translational research at the NIDCD, the clinical trials program, and issues specific to applications in this area.

The breakout sessions are intended to allow ample time for questions and answers. A combined handout containing information from all breakout sessions will be available.

### **240 Adult-Onset Hearing Loss: What's the Damage?**

**Terry Portis<sup>1</sup>**

<sup>1</sup>*Self-Help for Hard-of-Hearing People, Inc.*

ARO members are developing new genetic and cellular therapeutic mechanisms for diagnosing and rehabilitating hearing loss. For decades, they have developed standard diagnostic tools to determine the degree of hearing loss, yet our ever-improving knowledge of the etiology of hearing loss, its epidemiology and, more practically, its effect on people's lives remain unheard in the wider healthcare environments, in society at large, and at national and international policy-making levels.

The rate of hearing loss increases from 1 in 20 for children (under 18 years old) to nearly 1 in 8 adults, and 1 in 2 individuals over 65 years old, making hearing loss the most-common sensory disorder. It still remains uncertain is the etiology and epidemiology of the myriad causes of adult-onset hearing loss (AOHL), and its impact on the everyday lives of those who experience AOHL. The following speakers, each with a national reputation in their respective fields of AOHL, will present and discuss with the whole ARO membership:

- (i) The impact of AOHL on an individual's life;
- (ii) The psychological impact of AOHL;
- (iii) The epidemiology and etiology of noise induced hearing loss;
- (iv) The epidemiology and etiology of reversible hearing loss;
- (v) The epidemiology and etiology of genetic and degenerative hearing loss in adults.

Each speaker will also introduce the problems for investigating AOHL of their respective fields, and the areas where new and innovative research for rehabilitating AOHL are urgently needed.

### **241 Living with Adult-Onset Hearing Loss**

**Denise Portis<sup>1</sup>**

<sup>1</sup>*SHHH*

Hearing loss can have a dramatic impact on a person's life, from their family relationships, work experiences and social interactions. People with hearing loss often struggle with isolation, depression and frustration. It is important for health care professionals and researchers to hear from someone who has lived with the impact of hearing loss, and found positive ways to cope.



## **[242] Psychological Aspects of Hearing Loss**

**Michael Harvey**

Unlike many congenitally hearing-impaired persons whose level of hearing has become an integral facet of their identity, persons who lose their hearing as teenagers and adults frequently experience trauma. That experience is strongly influenced by psychological, social and spiritual factors. This talk describes how these factors are interwoven to shape the psyches and life-stories of persons with acquired hearing loss, including how they affect the relationship between the hearing care professional and patient.

## **[243] New Concepts in Noise-Induced Hearing Loss**

**Michael Hoffer<sup>1</sup>**

*<sup>1</sup>Department of Defense Spatial Orientation Center*

Hearing loss has become the most frequent sensory disorder in the world's population. Recent statistics indicate that over 50% of individuals over the age of 65 suffer from some form of hearing loss. Moreover, the incidence of early adult-onset hearing loss has dramatically increased over the last several years. In this presentation we will focus on noise-induced hearing loss (NIHL) and presbycusis. After reviewing the epidemiologic data, we will discuss the mechanisms of NIHL at the cellular level, highlighting the newest information and knowledge gaps that need further research. We will then discuss the current diagnosis and treatment of these disorders, potential new treatments, and emphasizing where more work needs to be done. After this presentation the audience will have a better understanding of the etiology of NIHL, diagnostic and treatment strategies, and where future work is necessary to better treat these increasingly common disorders.

## **[244] New Concepts in Reversible Hearing Loss**

**Steven D. Rauch<sup>1</sup>**

*<sup>1</sup>Harvard Medical School*

It is widely accepted dogma that sensorineural hearing loss (SNHL) is irreversible. In fact, there are many causes of reversible SNHL, including acoustic trauma, idiopathic sudden SNHL, ototoxicity, Meniere's disease, and autoimmune inner ear disease. This presentation will focus on Meniere's syndrome and idiopathic sudden SNHL. Sudden SNHL and Meniere's syndrome each have an incidence of 15-50/100,000 pop./yr. Sudden SNHL has a spontaneous recovery rate of 25% and, with oral steroid therapy, a recovery rate of 50-60%. The cause is controversial but may be due to viral or inflammatory changes in the cochlea. Meniere's syndrome of fluctuating progressive SNHL and episodic vertigo probably arises from instability of the homeostatic systems that regulate inner ear function. It is likely that many different insults can lead to this clinical "phenotype." In both Meniere's and sudden SNHL, the essential pathophysiology remains unknown. There are multiple treatments, each with no more than modest success. There are no effective animal models, and clinical presentation exhibits wide variability that can confound diagnosis, making good clinical

research extremely difficult. While these two disorders are not the most common causes of SNHL, they are disproportionately important to researchers because they are natural experiments that provide unique opportunities to explore basic mechanisms in hearing and inner ear pathology.

## **[245] Rehabilitating Degenerative, Adult-Onset Hearing Loss**

**Lawrence Lustig<sup>1</sup>**

*<sup>1</sup>University of California, San Francisco*

Hearing loss is the most common sensory disorder among adults in the United States, affecting about 31 million people (15% of the population). About 1/2 of adults over 65 have hearing loss, making it the 3rd most prevalent condition of the elderly. This broad overview will discuss what is known about genetic and idiopathic forms of degenerative forms of hearing loss in adults, including the epidemiology of degenerative hearing loss, as well as what is currently known regarding their etiology. In addition, current experimental approaches addressing these forms of hearing loss will be discussed, as well as potential future therapies resulting from these research endeavors. This presentation will also emphasize what future research is required to address this clinically important topic.

## **[246] Is There Activity Dependent Plasticity in the Auditory Brainstem?**

**Manuel S. Malmierca<sup>1</sup>, Douglas L. Oliver<sup>2</sup>**

*<sup>1</sup>Auditory Neurophysiology Unit. Lab Neurob Hearing. University of Salamanca & INCYL. Salamanca, Spain,*

*<sup>2</sup>Department of Neuroscience, University of Connecticut Health Center, Farmington, Connecticut.*

This symposium will present exciting new data on how function in the central auditory system may be modified by activity. Both normal sound stimulation and pathology may alter the activity of the auditory system.

There is growing evidence that activity in the central auditory system may change the responses of neurons. The presentations by Kacemarek and Tzounopoulos demonstrate some of these phenomena. Sound evoked activity changes the phosphorylation state of potassium channels and alters a neuron's ability to phase-lock to high-frequency sounds. Sound evoked activity may also change the strength of synapses in different cells, and such changes could be important for directing the flow of information in the auditory pathways.

Deafness represents the most extreme and permanent loss of activity. Even though deafness may be caused by pathology restricted to the ear, it may initiate changes in the central auditory system, and this symposium will address these changes. It has been known for some time that there is a reorganization of the tonotopic map in the auditory cortex after partial hearing loss. However, changes at the cortical level could reflect reorganization at lower auditory centers. In this symposium, leading scientists will review their recent work from different levels in the brainstem – the cochlear nuclei to the inferior colliculus. The studies by Holt, Altschuler, Manis, Wang,

Forsythe, and Rubio will show molecular and physiological evidence that the brainstem auditory system does not remain static after deafness.

#### **[247] Plasticity of Cochlear Neurons in Response to Changes in the Levels of the Auditory Nerve Synaptic Activity**

**Maria Rubio<sup>1</sup>**

<sup>1</sup>*University of Connecticut*

Activity-dependent synaptic plasticity underlies many diverse processes in the central nervous system (CNS), including development, learning and memory, and pathological disorders. One component of the response to changes in afferent activity affects number and/or distribution of neurotransmitter receptors. Given the well-known CNS changes induced by deafness, there may likely be accompanying changes in receptor expression. It is undetermined whether these changes in receptor activity are as result of reorganization of central synapses. Any reorganization is hypothesized to be associated with differences in the expression and/or localization of excitatory (glutamate) and/or inhibitory (glycine and gamma-amino-butyric acid: GABA) neurotransmitter receptors.

To understand the potential changes associated with hearing impairment, this paper will discuss how alterations in the levels of the auditory nerve synaptic activity control the expression and subunit composition of excitatory and inhibitory receptors in postsynaptic neurons in the cochlear nucleus.

#### **[248] Effects of Postnatal Deafness on Synaptic Transmission at Central Eighth Nerve Synapses**

**Paul Manis<sup>1</sup>, Yong Wang<sup>1</sup>**

<sup>1</sup>*UNC Chapel Hill*

Neurons of the central auditory system respond to changes in the status of the auditory periphery with multiple cellular adjustments of both ion channels and receptors. We have been exploring the effects of high frequency hearing loss on synaptic transmission at the end bulbs of Held in the anterior ventral cochlear nucleus (AVCN). DBA/2J mice exhibit normal hearing thresholds shortly after the onset of hearing, but by 5 weeks of age thresholds are elevated by 20-40 dB for high frequencies, with little change at low frequencies. To examine the consequences of the hearing loss, we recorded from bushy cells in slices of the AVCN of DBA/2J mice, in both high frequency (HF, > 22 kHz) and low frequency (LF, < 8 kHz) regions, in P20-25 mice with normal hearing thresholds and in P45-60 mice with elevated thresholds. Comparison recordings were made from normal hearing CBA mice of the same ages. A number of changes in synaptic transmission were associated with the hearing loss in the old DBA mice, including: a decreased frequency of spontaneous miniature EPSCs (sEPSCs), smaller sEPSC amplitudes, slower sEPSC decay time constants, decreased release probability, and decreased polyamine-dependent rectification. None of these changes were seen

in CBA mice. Our results show that both pre- and postsynaptic aspects of transmission at end-bulb synapses are affected by hearing loss.

Although spike shapes and did not change, a subset of HF bushy cells in DBA mice began firing small, repetitive action potentials during 300 pA, 100 msec long current pulses, a phenomenon rarely seen in young DBA mice, or young or old CBA mice. This firing pattern could be reproduced in normal cells by subtracting 10-20 nS of the low voltage-activated potassium conductance using dynamic clamp. Thus hearing loss in DBA mice produces multiple changes in central auditory synaptic transmission and small changes in intrinsic excitability. (Supported by NIDCD R01 DC04551 and F32 DC04909.)

#### **[249] Mechanisms Underlying Cell-Specific Synaptic Plasticity in the Dorsal Cochlear Nucleus**

**Thanos Tzounopoulos<sup>1</sup>**

<sup>1</sup>*OHSU*

The dorsal cochlear nucleus (DCN), a brainstem, cerebellum-like structure, integrates acoustic with multimodal sensory inputs from diverse areas of the brain. Pathways through the DCN are thought to detect spectral cues for sound localization. Excitatory parallel fibers carry descending, sensory inputs to the apical, spiny dendrites of fusiform and cartwheel cells, while auditory nerve fibers carry acoustic inputs to the basal dendrites of fusiform cells. We have demonstrated that parallel fiber synapses exhibit opposing forms of spike timing-dependent synaptic plasticity (STDP) in cartwheel cells and fusiform cells. Convergence of different signaling mechanisms may determine the sign and the kinetics of the synaptic plasticity observed at different cell types

#### **[250] Regulation of Auditory Neurons by Phosphorylation of Potassium Channels**

**Leonard Kaczmarek<sup>1</sup>**

<sup>1</sup>*Yale University School of Medicine*

Many auditory neurons fire action potentials at high rates with high temporal precision. In part, this property can be attributed to the presence of high levels of the Kv3.1b potassium channel, which allows neurons to follow synaptic stimuli at high frequencies. Nevertheless, high levels of Kv3.1b current degrade the accuracy of action potential timing at lower frequencies of firing. Direct phosphorylation of Kv3.1b protein by protein kinase C suppresses Kv3.1 currents. In a quiet auditory environment, Kv3.1b is basally phosphorylated by this enzyme, providing maximal timing accuracy at low firing frequencies. In vivo acoustic stimulation of animals results in a rapid and reversible decrease in the level of phosphorylation, permitting neurons to fire at higher rates, albeit with lower temporal accuracy. Phosphorylation of Kv3.1b and other channels appears to be a mechanism that rapidly adjusts the intrinsic electrical properties of neurons to the pattern of incoming auditory stimuli.

## **251** Tonotopic Gradients and the Regulation of Intrinsic Neuronal Excitability in the Superior Olivary Complex

Ian Forsythe<sup>1</sup>

<sup>1</sup>University of Leicester

It is clear that the intrinsic excitability of neurones in the auditory brainstem is differentially regulated across the tonotopic axis. In the medial nucleus of the trapezoid body (MNTB) the most medial neurones express higher densities of high voltage-activated currents (Kv3) and have short duration action potentials. Low voltage-activated potassium channels (Kv1) which regulate action potential threshold are expressed in an activity-dependent manner, in that MNTB neurones from deafness (dn-/dn-) mice are more excitable than control CBA mice. In addition the principle neurones of the lateral superior olive (LSO) differentially express Kv1 currents, serving to generate a spectrum of firing phenotypes; from single spiking neurones expressing high levels of Kv1 currents in the lateral limb to multiple firing neurones expressing lower levels of Kv1 in the medial limb. Our objective is to explore the cellular basis of these tonotopic gradients and determine the functional consequences of differential potassium channel expression and modulation in the auditory brainstem.

## **252** Activity Dependent Plasticity: Deafness-Related Changes in Amino Acid Transmitters and Receptors

Avril Genene Holt<sup>1</sup>, Richard Altschuler<sup>1</sup>

<sup>1</sup>University of Michigan

Deafness can induce changes in the balance between neuronal excitation and inhibition in the central auditory pathways. There are dramatic deafness associated changes in excitatory and inhibitory amino acid transmitters and their receptors. Gene microarrays and quantitative real-time PCR were used to examine changes in gene expression in the cochlear nucleus and inferior colliculus following bilateral deafening. There were significant changes in synthesizing enzymes (e.g. GAD), vesicular transporters (e.g. vGlut1,2) and in glutamate, GABA and glycine ionotropic receptor subunits as well as metabotropic receptors (e.g. GABA-B receptor). Some changes were transient while others were more persistent (3 months) following deafening. Immunocytochemistry following deafening also revealed decreases in glycine immunolabeling in the cochlear nucleus and superior olivary complex as well as decreases in GABA immunolabeling in the inferior colliculus. Deafness-related changes were also seen in neuromodulators such as dopamine, serotonin and their receptors as well as in ion channels. These studies show that there is a protein synthesis dependent component to activity-dependent plasticity following deafness with changes across a number of neurotransmitters, transporters and receptors.

Supported by NIDCD grant DC00383 and core center grant P30 DC05188

## **253** Motility-Associated Hair Bundle Motion of Outer Hair Cells

David Z.Z. He<sup>1</sup>, Shuping Jia<sup>1</sup>

<sup>1</sup>Creighton University, Omaha, NE

It is a common assumption that mammalian hearing owes its remarkable sensitivity and frequency selectivity to a local mechanical feedback process within the cochlea. Cochlear outer hair cells (OHCs) function as the key elements in the feedback loop in which the fast somatic motility of OHCs is thought to be the source of cochlear amplification. An alternative view is that amplification arises from active hair bundle movements, similar to that seen in non-mammalian hair cells. We measured the voltage-evoked hair bundle motions in the gerbil cochlea to determine if such movements were also present in mammalian OHCs. The OHCs displayed a voltage-evoked hair bundle movement with peak response as large as 830 nm. The bundle movement was not sensitive to manipulations that would normally block mechanotransduction in the stereocilia, and was not present in either neonatal OHCs before the onset of somatic motility or prestin knockout OHCs. These results suggest that the bundle movement was not based on mechanotransducer channels but originated in somatic motility. We also questioned whether hair bundle motion could generate a radial TM motion. For this purpose, the gerbil hemicochlea was used to examine TM radial motion driven by OHC bundle motion. Significantly, bundle movements were able to generate radial motion of the TM in situ. This result implies that the motility-associated hair bundle motion may be a part of the cochlear amplifier. (Supported by NIH grant R01 DC006496 to D.H.)

## **254** Identification of Hair Bundle Proteins Using Mass Spectrometry

Jung-Bum Shin<sup>1</sup>, Debra McMillen<sup>2</sup>, Cory Bystrom<sup>2</sup>, Peter Gillespie<sup>1</sup>

<sup>1</sup>Oregon Hearing Research Center & Vollum Institute, Oregon Health & Science University, <sup>2</sup>Proteomics Shared Resource, Oregon Health & Science University

We have begun to systematically catalog the proteins present in vertebrate hair bundles using a proteomics approach. We purified hair bundles from more than 400 chicken vestibular organs using the twist-off method (Gillespie and Hudspeth, 1991). Mass spectrometry (MS) analysis used two approaches. In the first, we melted agarose containing isolated bundles, allowed it to resolidify, and digested the entire mixture of bundle proteins with trypsin. In the second approach, we separated proteins by one-dimensional gel electrophoresis, cut strips of the gel, and digested with trypsin in the acrylamide gel matrix. In both cases, tryptic peptides were separated by micro-liquid chromatography-tandem mass spectrometry ( $\mu$ LC-MS/MS). MS spectra of fragmented peptides were compared to conceptual digests of open reading frames of the chicken genome database or the nonredundant GenBank database using the Global Protein Machine (GPM) or Mascot algorithms, respectively. Several classes of proteins were identified, including known cytoskeletal proteins (actin, fimbrin,

radixin, tubulin) and mobile  $\text{Ca}^{2+}$  buffers (calretinin, calreticulin, calmodulin). A particularly prominent class of proteins were those involved in energy metabolism, such as glycolytic enzymes (glyceraldehyde-3-phosphate dehydrogenase, enolase, pyruvate kinase, triosephosphate isomerase) and creatine kinase, which may transport high-energy phosphate bonds to the stereocilia. Localization to bundles of several of these proteins, as well as others identified by the MS approach, has been confirmed using immunocytochemistry or immunoblotting.

### **[255] Aminoglycoside Ototoxicity Depends on Drug Entry Through the Hair-Cell Transducer Channels**

**Cornelis Kros**<sup>1</sup>, Walter Marcotti<sup>1</sup>, Sietse Van Netten<sup>2</sup>

<sup>1</sup>University of Sussex, UK, <sup>2</sup>University of Groningen

A serious side effect of aminoglycoside antibiotics is irreversible hair-cell damage. This ototoxicity depends on drug entry into the hair cells by means of an uptake mechanism that has long remained unresolved (Forge & Schacht 2000, *Audiol Neurotol* 5:3-22). The aminoglycosides are known to block mechano-electrical transduction but entry of these large polycationic molecules through the transducer channel pore was thought unlikely (Kroese et al. 1989, *Hear Res* 37:203-218). When dihydrostreptomycin (DHS) was applied extracellularly, transducer currents of mouse OHCs were blocked in a voltage dependent manner, most effectively at about -80 mV. The block was much reduced at positive membrane potentials as described before, but we also found a (less pronounced) reduction of the block at -150 mV, the approximate transmembrane potential across the apical surface of the OHCs *in vivo*. In response to rapid excitatory force steps the block developed with time constants in the order of one ms, speeding up as the extracellular concentrations of DHS were increased or those of  $\text{Ca}^{2+}$  were decreased. Intracellular DHS also blocked transducer currents, but at positive membrane potentials and requiring 100-fold higher drug concentrations.

All these observations could be quantitatively explained by assuming that DHS not only blocks but also permeates the open transducer channel pore, encountering two energy barriers near the extra- and intracellular sides of the membrane and a binding site about 80% into the pore from the extracellular side (Marcotti et al. 2005, *J Physiol* 567:505-521). At therapeutic concentrations some 10,000 molecules of DHS are estimated to enter each OHC per second *in vivo*, with the exit rate being so much slower that the transducer channels act as one-way valves, trapping the drug inside the cells. Experiments with neomycin and gentamicin yielded qualitatively similar results, suggesting that permeation through the transducer channels is the likely entry route of all aminoglycoside antibiotics.

Supported by the MRC

### **[256] Phase of Power Delivery by Active Hair Bundles During Responses to Small Mechanical Stimuli**

**Dolores Bozovic**<sup>1</sup>, A.J. Hudspeth<sup>2</sup>

<sup>1</sup>University of California, Los Angeles, <sup>2</sup>Rockefeller University

When placed in an appropriate ionic environment, a hair cell of the bullfrog's sacculus may exhibit spontaneous hair-bundle oscillations. These motions, which significantly exceed thermal fluctuations, have been shown to require the presence of an active process. Furthermore, it has been demonstrated that the naturally noisy oscillations can be entrained by a small sinusoidal stimulus, leading to amplification of the applied signal. To understand how amplification is accomplished, it is useful to compare the phase at which a hair bundle delivers power to its external load with the predictions of models for the amplification process. In the experiments presented here, we have entrained the spontaneous oscillations of an individual hair bundle and measured the force that it exerts as a function of time. By analyzing these results, we are able to quantify the delivery of power by the active process at various phases of the oscillation cycle.

This research was supported by grant DC00241 from the National Institutes of Health.

### **[257] Effects of Thyroid Hormone Deficiency on $\text{Ca}^{2+}$ and $\text{K}^{+}$ Channel Expression and Neonatal Spiking Activity in Rat Inner Hair Cells**

**Niels Brandt**<sup>1,2</sup>, Stephanie Kuhn<sup>1,2</sup>, Stefan Münkner<sup>1,2</sup>, Claudia Braig<sup>2,3</sup>, Harald Winter<sup>2,3</sup>, Marlies Knipper<sup>2,3</sup>, Jutta Engel<sup>1,2</sup>

<sup>1</sup>University of Tuebingen, Institute of Physiology II, <sup>2</sup>Tuebingen Hearing Research Centre, <sup>3</sup>University of Tuebingen, ENT Clinic, Molecular Neurobiology

Thyroid hormone (TH) is essential for a normal hearing function. Lack of TH in the critical developmental period between E17 and P12 leads to morphological and functional deficits in the organ of Corti and the auditory pathway. To investigate the effects of TH on inner hair cells (IHC) we used hypothyroid rats treated with the thyreostatic drug methimazol (MMI) during pre- and postnatal life.

Using the whole-cell patch clamp method we measured spontaneous and evoked  $\text{Ca}^{2+}$  action potentials (AP) and  $\text{K}^{+}$  and  $\text{Ca}^{2+}$  currents in hypothyroid animals (P2-P34) and euthyroid controls.  $\text{Ca}^{2+}$  APs are assumed to play a crucial role for differentiation of IHCs and the auditory pathway. APs were present in control IHCs from P3-P11 and abruptly vanished in parallel with the expression of a rapidly activating big  $\text{K}^{+}$  conductance (BK conductance). No APs could be elicited with current injection beyond P12 in IHCs of control animals while in IHCs of hypothyroid rats, APs persisted until at least P20. Peak frequencies of spontaneous APs in IHCs of hypothyroid rats were considerably higher than in control animals (10-25 Hz versus 0.5-3.5 Hz).

IHCs of hypothyroid rats did not express the BK conductance until P25, a finding that was confirmed by

immunocytochemistry. The Ca<sup>2+</sup> channel current (charge carrier: 10 mM Ba<sup>2+</sup>), which in IHCs of control rats peaked around P9 and declined to about 250 pA at P15, stayed 3fold elevated in hypothyroid IHCs until P25.

In conclusion, (i) IHCs of hypothyroid rats generate Ca<sup>2+</sup> APs in the first three weeks; (ii) they are unable to generate graded receptor potentials after the onset of hearing in control rats which explains deafness on the level of the IHCs; (iii) both the expression of the BK channel and the reduction of the Cav1.3 Ca<sup>2+</sup> channel expression are regulated by TH.

Supported by DFG En 294/2-4, DFG Kni-316/3-1; 4-1, Fortüne 1446-0-0

**[258] Studies on the Domain-Specific Targeting, Scaffolding and Functions of the Hair Cell Plasma Membrane Proteins Cadherin 23, TRPA1 and Prestin Using the CL4 Epithelial Cell Model**  
Lili Zheng<sup>1</sup>, Jing Zheng<sup>2</sup>, Keiichi Nagata<sup>1</sup>, Gagan Kumar<sup>1</sup>, Anne Duggan<sup>1</sup>, Jaime Garcia-Anoveros<sup>1</sup>, **James R. Bartles<sup>1</sup>**

<sup>1</sup>Northwestern University Feinberg School of Medicine,

<sup>2</sup>Northwestern University

Studies of hair cell plasma membrane (PM) proteins have been hindered by the difficulties inherent in examining these cells. Although hair cell PM proteins have been expressed in transfected cells, these cells do not generally express the apical-basolateral polarity characteristic of hair cells or other epithelial cells. We are using CL4 epithelial cells, which derive from proximal tubule, to examine the targeting, scaffolding and functions of hair cell PM proteins. CL4 cells were used in our earlier studies on the effects of espins on the length and dynamics of microvillar parallel actin bundles. We have determined that, unlike other cells used in studies of PM protein targeting, such as MDCK cells, CL4 cells establish apical-basolateral PM polarity when cultured on glass coverslips, without the need of prolonged culturing, medium supplements or permeable membrane supports. Accordingly, when we expressed hair cell PM proteins in CL4 cells by transient transfection, they faithfully recapitulated the domain-specific targeting observed in situ: prestin-GFP became highly enriched in the basolateral PM domain, whereas FLAG-cadherin 23 became highly enriched in the microvillar PM that constitutes the apical PM domain. Through a systematic comparison of the targeting and dynamics of wild-type and mutated versions of these and other hair cell PM proteins, including TRPA1, we are mapping the motifs required for targeting and scaffolding. For example, we have determined that the apical targeting of cadherin 23 does not require large segments of its extracellular domain or the exon 68 peptide and that the basolateral targeting of prestin is likely to be independent of its tyrosine-based motifs. Cadherin 23 was also targeted to the apical PM domain in CL4 cells with extra-long microvilli as a result of cotransfection with espin, suggesting that espin-expressing CL4 cells can serve as a model system for reconstituting selected aspects of stereociliary structure and function.

**[259] Conductance and Activation Properties of the Acetylcholine Receptor in Outer Hair Cells**

Pascal Darbon<sup>1</sup>, Daniel Wright<sup>1</sup>, **Michael G. Evans<sup>1</sup>**

<sup>1</sup>CNS and ISTM, Keele University, UK

Outer hair cells (OHCs) have an ACh receptor that is thought to be composed of  $\alpha 9$  and  $\alpha 10$  subunits. When expressed in oocytes, this AChR gives responses similar to those found in OHCs (Elgoyhen *et al.* (2001) PNAS 98, 3501-3506). The OHC response includes a calcium activated potassium current, as calcium flows in through the AChR. In order to examine the OHC AChR current and facilitate comparison with the  $\alpha 9/\alpha 10$  AChR, we blocked the potassium current in whole-cell voltage clamp of isolated guinea pig OHCs, by removal of external calcium, increasing internal Ca buffering with BAPTA (5-10 mM), and/or depolarisation to positive voltages. ACh (0.1 mM) was applied from a pipette.

ACh evoked a rapid inward current at -50 mV (~ 0.1s to peak) that was blocked by  $\alpha$ -bungarotoxin and reversed close to 0 mV. I-V plots of the peak current exhibited outward and inward rectification. The AChR current was sensitive to external Ca: it was reduced in amplitude in 0 Ca, but was potentiated by a partial reduction (0.2 mM Ca / 0 Mg) compared to controls (1.3 mM Ca / 0.9 mM Mg). The I-V relation maintained its rectification. Occasionally ACh application produced a much slower current (especially with low external Ca and K-based internal solutions), activating over about 1 s after a 0.5 s delay, either on its own or in addition to the faster potassium current. This current was larger in amplitude than the fast AChR current, it was inwardly rectifying, reversed close to 0 mV and was blocked by  $\alpha$ -bungarotoxin. Exposure to SERCA blockers thapsigargin (1-5  $\mu$ M) or BHQ (100  $\mu$ M) did not reveal the slow ACh-sensitive current. The fast AChR current is similar to the  $\alpha 9/\alpha 10$  AChR, suggesting that this type of AChR is present in OHCs. The slow current has clearly different characteristics, and might represent a slower kinetic version of the AChR current, although we cannot yet rule-out an involvement of Ca stores.

Supported by The Wellcome Trust and British Tinnitus Association

**[260] Loss of Cholinergic Response in SK2 Knockout Cochlear Hair Cells**

Jee-Hyun Kong<sup>1</sup>, Chris T. Bond<sup>2</sup>, John Adelman<sup>2</sup>, Paul Fuchs<sup>3</sup>

<sup>1</sup>Neuroscience, Johns Hopkins, Baltimore, MD, <sup>2</sup>The Vollum Institute, OHSU, Portland, OR, <sup>3</sup>Center for Hearing and Balance, Oto-HNS, Johns Hopkins, Baltimore, MD

ACh inhibits vertebrate hair cells through the activation of small conductance calcium-activated (SK) potassium channels. Here we report studies on cochlear hair cells from wild-type and SK2 knockout (*sk/sk*) mice. As in other hair cells, SK currents could be activated by prolonged (3 s) depolarization, due to calcium entry through voltage-gated calcium channels. The SK component was a slowly-rising outward current, distinct from the much faster delayed-rectifier that dominates the IV relation at shorter times. The SK component also was evident as outward

tails that decayed over 1-3 seconds at -44 mV. The SK currents were blocked selectively by 300 nM apamin, by 100  $\mu$ M curare, or by blocking L-type  $\text{Ca}^{2+}$  channels with 50  $\mu$ M nifedipine. The slow outward current was seen reliably in 46 wildtype IHCs but was absent from 39 *sk/sk* IHCs (P6-11). These results confirm that the SK2 gene encodes SK channels in cochlear hair cells. ACh was applied to both IHCs and OHCs from the apical turn of *sk/sk* cochleas. Neither IHCs (n = 33, P6-11), nor OHCs (n = 12, P10-17) showed any sensitivity to applied ACh (though wildtype cells did so reliably), indicating a loss of cation current through AChRs as well as loss of SK current. In addition, 6 *sk/sk* OHCs from the middle turn (10 kHz region) were unresponsive to ACh. Further, no spontaneous or potassium-evoked cholinergic synaptic currents were observed in any *sk/sk* cells, though common in wildtype hair cells. Other features of the *sk/sk* hair cells appeared normal. As usual, *sk/sk* IHCs acquired an iberiotoxin-sensitive 'BK' current at the onset of hearing. Younger neonatal *sk/sk* IHCs generated calcium action potentials like those of wildtype IHCs. However, while 100  $\mu$ M ACh could halt wildtype action potentials, those of *sk/sk* IHCs were unaffected by the presence of 1 mM ACh. Thus, the absence of SK2 channels resulted in specific functional loss of associated ACh receptors. Supported by NIDCD R01DC01508 and R01DC05211.

## **[261] Otoferlin, Defective in DFNB9 Human Deafness, Is Necessary for Sensory Hair Cells Ribbon Synapses Exocytosis**

Isabelle Roux<sup>1</sup>, Saaid Safieddine<sup>1</sup>, Regis Nouvian<sup>2</sup>, Ghislaine Hamard<sup>3</sup>, Paul Avan<sup>4</sup>, Morgane Le Gall<sup>3</sup>, Isabelle Perfettini<sup>1</sup>, M'hamed Grati<sup>1,5</sup>, Philippe Rostaing<sup>6</sup>, Antoine Triller<sup>6</sup>, Marie-Christine Simmler<sup>7</sup>, Tobias Moser<sup>2</sup>, **Christine Petit**<sup>1,8</sup>

<sup>1</sup>*Institut Pasteur, INSERM U587, Paris, France*, <sup>2</sup>*University Goettingen, Germany*, <sup>3</sup>*Institut Cochin, Paris, France*,

<sup>4</sup>*Faculte de Medecine, Clermont-Ferrand, France*,

<sup>5</sup>*NIDCD, Bethesda, MD*, <sup>6</sup>*ENS, Paris, France*, <sup>7</sup>*UPMC-P6, Paris, France*, <sup>8</sup>*College de France*

We previously identified OTOF, encoding a predicted transmembrane C2-domain protein belonging to the FER-1 family, as defective in an auditory neuropathy, DFNB9. We have obtained ample evidence indicating that otoferlin is a vesicle-associated protein of the IHC (inner hair cell) synaptic machinery. Its developmental expression pattern in the mouse hair cells, analysed by immunofluorescent labelling, parallels their afferent synaptogenesis. Using immunoelectron microscopy, we localised otoferlin to the synaptic vesicles tethered to ribbons and to the presynaptic plasma membrane of the IHCs. Otoferlin interacts with syntaxin-1 and SNAP25, two proteins of the SNARE complex, in a  $\text{Ca}^{2+}$ -dependent manner. Furthermore, in order to address the in vivo physiological role of otoferlin, we generated otoferlin knockout mice. These mutant mice have an auditory defect that entirely mimics the auditory defect of DFNB9 affected patients. Morpho-functional analyses of these mutants demonstrate that otoferlin is required for synaptic exocytosis.

## **[262] Regulation of Releasable Vesicle Pools in Inner Hair Cells of the Mammalian Cochlea** **Claudius Griesinger**<sup>1,2</sup>, Christopher Richards<sup>2</sup>, Jonathan Ashmore<sup>2,3</sup>

<sup>1</sup>*Institut für Physiologie II, Universität Freiburg*,

<sup>2</sup>*Department of Physiology, UCL London*, <sup>3</sup>*UCL - Ear Institute*

Hearing shows some unique properties among our senses including exquisite temporal precision and a literal indefatigability which enables ongoing and consistent signalling throughout our entire life. Both properties reflect the exquisite synaptic performance of inner hair cells (IHCs) which encode sound through fast release and rapidly replenish their vesicles from cytoplasmic pools at about 2 vesicles per ms (Griesinger et al., *Nature* (2005) 435,212-215). How these cytoplasmic pools are regulated is however unclear. We performed two-photon imaging in the intact cochlea to study dynamics of FM 1-43 labelled vesicles at individual release sites during and after release elicited by transepithelial stimulation. Line scans at 500 Hz revealed fast release and replenishment components. Train stimulation (> 1 second) identified an additional slow pool of releasable vesicles that was already exhausted after the first train and took several minutes to recover. Vesicle replenishment occurred during stimulation but was reduced in IHCs that were treated with an inhibitor of kinesin transport. The extent of this reduction was dependent on the incubation time, supporting our previous finding that cytoplasmic vesicle pools are filled by kinesin-dependent trafficking. To test whether PKC plays a role in vesicle pool regulation in IHCs, we used the PKC activator PMA (12-myristate 13-acetate). PMA increased both release site diameter and apparent vesicle number at the release sites by 1.5 suggesting a PKC-dependent mobilisation of vesicles towards release sites. Moreover PMA induced an obligatory slow component without affecting release probability. These results suggest that the pool size of releasable vesicles in IHCs is regulated by PKC and it is not the fast pool but a secondary slow pool which is affected.

Supported by the Wellcome trust and a BBSRC imaging grant to C.D.R.

## **[263] Hair Cell Ribbon Synapses Are Tuned to Enhance Frequency Selectivity in the Auditory System**

**Mark Rutherford**<sup>1</sup>, William Roberts<sup>1</sup>

<sup>1</sup>*University of Oregon*

Auditory systems use diverse mechanisms to decompose complex sounds into separate frequency channels. The frog (*Rana pipiens*) sacculus is a low-frequency detector, most sensitive to sounds and seismic stimuli at 50 Hz. We now show that the afferent synapses in frog saccular hair cells are specialized to maximize exocytosis at this frequency. Neurotransmitter release was measured as the increase in membrane capacitance that occurs when synaptic vesicles fuse with the plasmalemma. For small sinusoidal stimuli ( $\pm 5$  mV centered at -60 mV), the capacitance increase was greatest at 50 Hz. Strong depolarization evoked an exocytic burst that lasted 10 ms

and corresponded to the predicted capacitance of all docked vesicles at synapses, followed by a delay before additional vesicle fusion. Interrupting a depolarization with a brief hyperpolarization increased exocytosis. Intrinsic synaptic tuning thus depends on the temporal pattern of calcium entry and is distinct from the other known mechanical and electrical tuning mechanisms in hair cells.

## **264 Increased Efferent Activity Decreases Afferent Transmission from Neonatal Inner Hair Cells**

**Lisa Grant<sup>1</sup>**, Rich Helyer<sup>1</sup>, Helen Kennedy<sup>1</sup>

<sup>1</sup>*Department of Physiology, University of Bristol, Bristol, UK*

Inner hair cells (IHCs) of the developing mammalian cochlea are transiently innervated by medial olivocochlear efferent fibres, which depress the spontaneous calcium action potentials characteristic of developing neonatal IHCs [1]. This feedback circuit is thought to be important in maturation of the cochlea and tonotopic auditory cortex. We present evidence that increasing the degree of efferent activity decreased IHC calcium current (ICa) amplitude and transmitter release quantified by changes in membrane capacitance ( $\Delta C_m$ ) in response to depolarising stimuli. Correspondingly, blocking efferent activity increased  $\Delta C_m$ .

Whole cell recordings were carried out in IHCs of acutely excised organ of Corti preparations of neonatal (P6–8) CD-1 mice. Mean peak ICa amplitudes in response to depolarisation to a nominal  $-5$  mV every second were calculated. External ryanodine ( $Ry_o$ ) increased frequency of events and area under post-synaptic currents in a concentration dependent manner ( $P < 0.001$ ). This did not occur with ryanodine applied directly to IHCs in the pipette. The degree of efferent activity over 5 or 10 s was calculated as event frequency  $\times$  area (FA). Increased efferent activity depressed peak ICa amplitude ( $P < 0.001$ ). Series of depolarisations were repeated in the same cell and  $\Delta C_m$ s compared where efferent activity (FA) differed.  $\Delta C_m$  was significantly depressed when efferent activity increased ( $P = 0.0036$ ,  $n = 6$ ). To corroborate depression of  $\Delta C_m$  with increased efferent FA, IHC  $\Delta C_m$ s were recorded where FA was stimulated with  $20 \mu M Ry_o$ .  $100$  nM strychnine was then perfused onto the IHCs to block the  $Ry_o$  stimulated efferent FA and the series of depolarisations repeated. When efferent activity was blocked,  $\Delta C_m$  responses increased in amplitude by  $20\%$  and  $12\%$  ( $n = 2$ ). This provides an insight into the mechanism by which efferent feedback in the developing cochlea modulates IHC afferent signalling.

1. Glowatzki, E. & P.A. Fuchs *Science*, 2000. 288(5475): p. 2366-8

## **265 Prestin Is an Anion Transporter**

**Dhasakumar Navaratnam<sup>1</sup>**, Jun-Ping Bai<sup>1</sup>, Peter Aronson<sup>1</sup>, Joseph Santos-Sacchi<sup>1</sup>

<sup>1</sup>*Yale University*

Prestin is a recently identified protein responsible for electromotility in outer hair cells. Although its sequence

placed it in the anion transporter family SLC26, prestin was thought not to have the ability to transport anions. In fact, it has been argued that an arrested movement of anions results in charge movement within the membrane that is measured as its signature non-linear capacitance.

Here we show that CHO cells transfected with prestin are able to take up  $[^{14}C]$ formate in the presence of an outward Cl gradient. The uptake of formate in prestin transfected cells was 2-3 fold that of baseline. This uptake was inhibited by  $1$  mM DIDS, and by extracellular Cl. Furthermore, the uptake of formate was also inhibited by  $10$  mM salicylate.

Assuming that the observed Cl-gradient stimulated formate uptake represents exchange for intracellular Cl, we identified a sequence GLLPP (aa324-328) at the N terminal end of a predicted alpha helix that has the signature GXXXP sequence of a chloride binding site. We mutated each of these residues to an alanine residue and ascertained its electromotility (non-linear capacitance) and ability to mediate Cl-gradient stimulated formate uptake. Mutation of the first glycine and last proline residues resulted in a complete loss of NLC. Mutation of the residues 325-327 did not affect NLC. In contrast, mutation of these 5 residues resulted in formate uptake that was  $8\%$  (G324A),  $4\%$  (L325A),  $15\%$  (L326A),  $82\%$  (P327A) and  $0\%$  (P328A) of uptake by normal prestin. We determined by FACS of live cells stained with an antiprestin antibody, and by fluorescence microscopy of YFP tagged protein, that the two mutants lacking NLC (G324A and P328A) were expressed on the plasma membrane at levels comparable to normal prestin. Two of the mutants with diminished formate uptake (L325A, L326A) had normal NLC, suggesting that these mutations too allowed surface expression, and yet had a differential effect on anion exchange.

We conclude that prestin can function as an anion exchanger and that there are different structural requirements for its ability to mediate non-linear capacitance and anion exchange

## **266 Electrogenic Anion Transport by Prestin**

**Jonathan Ashmore<sup>1</sup>**, Jason Mikiel-Hunter<sup>1</sup>, Marisol Sampedro-Castaneda<sup>1</sup>

<sup>1</sup>*University College London*

Implicated in outer hair cell electromotility, prestin is member A5 of the family SLC26 of bicarbonate transporter polypeptides. Although members of this family possess a range of different anion-substrates, radioactive flux measurements and expression studies indicate that at least some members (e.g. A6) act as electrogenic antiporters whereas others (e.g. A7) can under, some conditions, behave like an ion channel. We have developed a system for recording from adult guinea pig OHCs in cochlear coils which allows stable whole cell recordings for periods in excess of  $1$  hr. Such periods permit exchange of external solution to necessary to study the small currents (ca  $100$  pA) which would be expected from the transport of ions across the basolateral membrane. Replacement of external control anion (chloride) with gluconate, led to a reduction of inward slope



conductance compatible with outward chloride movement. Replacement of external buffer with bicarbonate produced currents compatible with the presence of an electrogenic bicarbonate transport mechanism. The data also showed that outward (and apparently K) currents were chloride sensitive. As found in other but non-sensory cell types, the finding restricts the identity of the K channel type expressed in apical outer hair cells. When expressed in HEK293 cells, GFP tagged rat prestin (a gift of B Fakler) showed many of the electrical properties exhibited in OHCs. Although recorded currents were much smaller (as a result of expression levels between  $2.5\text{-}5 \times 10^5$  prestin copies per cell measured by nonlinear capacitance) the chloride-bicarbonate exchange and reversal potential were consistent with an electrogenic 1:2 ratio. There was limited evidence for this system acting as an efficient sulphate exchanger. Taken together, the data suggest that prestin is likely to play a role in acid-base regulation in OHCs. *Supported by the Wellcome Trust and the Physiological Society.*

### **267 Electrogenic Properties of Non-Mammalian Prestin Homologues**

Thorsten Schaechinger<sup>1</sup>, Dominik Oliver<sup>1</sup>

<sup>1</sup>*Dept. of Physiology, University of Freiburg, Germany*

Prestin is a member of the SLC26 family of anion transporters and generates the fast voltage-driven motility of mammalian outer hair cells. Although the underlying molecular mechanisms are only incompletely understood, it is clear that voltage dependence is mediated by transmembrane movement of electrical charge – possibly monovalent anions – which in turn triggers a conformational reorientation of the molecule. Charge translocation corresponds to a voltage-dependent non-linear capacitance (NLC), the electrical signature of prestin.

Recently, homologues of Prestin have been identified from zebrafish ('zPres') and drosophila. By amino acid sequence comparison, the zebrafish SLC26 member is the closest homologue of mammalian prestin known so far.

We have analyzed the electrophysiological properties of these prestin-relatives. When GFP-fusion constructs of zPres and the drosophila homologue were transfected transiently into CHO or OK cells, both showed robust plasma membrane targeting. In cells expressing zPres, voltage jumps elicited capacitive currents, resembling the voltage dependent charge movement characteristic for mammalian prestin. Charge transfer could be reasonably described by a 2-state Boltzmann function; however voltage dependence was more shallow and voltage at half-maximum charge transfer was more positive than observed with mammalian prestin. Kinetics of charge transfer were voltage dependent and slower than charge movement by mammalian Prestin. When assayed with a lock-in method, zPres generated NLC with properties corresponding to those of the charge transfer. Similarly, capacitive currents and NLC were detected in cells expressing the drosophila SLC26 protein.

Charge transfer in the non-mammalian prestin homologues may relate to, as yet hypothetical, anion

transport properties of these SLC26 members. The similarity to charge transfer by prestin suggests that prestin-driven electromotility may have evolved from anion transport and may be mechanistically related to a transport cycle.

(Supported by EC FP6 funding, contract no.512063, EuroHear)

### **268 FRET Microscopy and Its Application to the Study of Protein:Protein Interactions**

V. E. Centonze<sup>1</sup>, R.V. Krishnan<sup>1</sup>, J-H Zhang<sup>1</sup>, B. Herman<sup>1</sup>

<sup>1</sup>*University of Texas Health Science Center at San Antonio*  
Fluorescence Resonance Energy Transfer (FRET) microscopy is an optical technique that enables the detection of molecular interactions at a resolution beyond the normal limits of the light microscope. Resonance energy transfer is a process by which a fluorophore (the donor) in the excited state transfers its energy to a neighboring fluorophore (the acceptor) non-radiatively through dipole-dipole interactions. Since the efficiency of energy transfer varies as the inverse of the sixth power of the distance separating the donor and acceptor chromophores, FRET may only occur if the distance between the two molecules does not exceed 10 to 100 angstroms (1 to 10nm). Through the microscope one may detect FRET by an overall decrease in fluorescence emission of the donor with a concomitant increase in fluorescence emission of the acceptor. Besides proximity of the fluorophores, successful FRET also requires that the donor emission spectrum substantially overlap with the acceptor absorption spectrum, that the donor have sufficiently long lifetime in order to "excite" the acceptor, that the ratio and concentration of donor and acceptor fluorophores be optimized to encourage FRET interactions but discourage self-quenching, and that unintentional photobleaching be minimized. Paired fluorophores may be bound to interacting molecules indirectly via antibody labeling or directly via chemical derivatization or recombination with fluorescent proteins. Optical imaging systems such as conventional epi-fluorescence, confocal and multiphoton microscopes can all be configured to optimize the acquisition of FRET data. Various approaches for the acquisition and analysis of FRET such as sensitized emission, spectral detection, acceptor photobleaching and Fluorescence Lifetime Imaging Microscopy (FLIM) will be introduced.

### **269 FRET Microscopy in Membranes: Theory and Practice**

Anne Kenworthy<sup>1</sup>

<sup>1</sup>*Vanderbilt School of Medicine*

FRET is a strongly distance-dependent phenomenon that reports on the proximity of two fluorescently labeled molecules when they are separated by  $<100 \text{ \AA}$ . When performed using a fluorescence microscope, FRET can be used to detect protein-protein interactions in living cells as well as to investigate the spatial organization of molecules in membranes. Through our use of FRET to study a class of membrane microdomains known as lipid rafts we have learned a number of lessons about the theory and practice



of FRET. I will discuss several of these issues, including the contribution of "random" proximity effects to FRET measurements between membrane proteins and ways to accurately measure FRET efficiencies using acceptor photobleaching approaches. I will also discuss current efforts in our laboratory to optimize the design of FRET measurements with the help of computer modeling.

## **[270] FRET Reveals the Organization of Different Receptor-Ligand Complexes in Endocytic Membranes**

Horst Wallrabe<sup>1</sup>, Ronak Talati<sup>2</sup>, Ammasi Periasamy<sup>1</sup>, Margarida Barroso<sup>2</sup>

<sup>1</sup>University of Virginia - Keck Center for Cellular Imaging,

<sup>2</sup>Albany Medical Center

A Fluorescence Resonance Energy Transfer (FRET)-based assay determines the organization of receptor-ligand complexes (polymeric IgA-receptor, pIgA-R; transferrin receptor, TFR; low-density lipoprotein-receptor, LDL-R) in endocytic membranes of MDCK cells. Differently-fluorophore labeled (Donor -D- or Acceptor -A-) pIgA-R ligands, holo-transferrin (Tfn) and/or LDL were internalized into polarized or non-polarized epithelial MDCK cells, imaged using confocal microscopy and processed for FRET analysis. A two-parameter FRET assay demonstrates whether receptor-ligand complexes are randomly distributed or clustered: Acceptor's positive impact on E% signifies random distribution; E% being independent of acceptor indicates clusters. A second parameter for clustering is E%'s negative dependence on D:A. Our results show that TFR-Tfn complexes assemble as dimers as expected, whereas pIgA-R-pIgA-R ligand complexes form higher-order clusters. Furthermore, hetero-clusters containing TFR-Tfn and pIgA-R-ligand or TFR-Tfn and LDL-LDL-R complexes show different levels of clustered organization from mixed clustered/random to a clear clustered organization. Different organizations of receptor-ligand complexes may represent protein sorting as it occurs during the endosomal trafficking in polarized cells. Homo-clusters containing LDL-LDL-R undergo a clustered to random organization which may reflect the release of the LDL from its receptor. Analysis of receptor organization in endocytic membranes will provide insights into protein sorting, biogenesis of membrane microdomains and endosomal organization and dynamics.

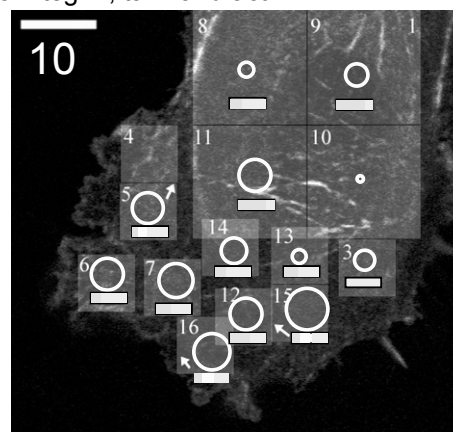
## **[271] Mapping Protein Interactions and Transport in Living Cells by Image Correlation Microscopy**

Paul Wiseman<sup>1</sup>, Jonathan Comeau<sup>1</sup>, Benedict Hebert<sup>1</sup>

<sup>1</sup>McGill University

Image correlation spectroscopy (ICS) as an imaging extension of fluorescence correlation spectroscopy (FCS). The ICS technique is ideally suited to measure transport and clustering of fluorescently tagged proteins in cellular membranes where transport is slow and static proteins abound. The image correlation methods are based on the measurement of fluorescence intensity fluctuations as a function of space and time in cells collected as image time series using a laser scanning microscope (either confocal or two-photon). Spatial and temporal variants of the basic

ICS method will be introduced and the power of these approaches to measure both aggregation and transport of cell surface proteins will be explained with the aid of computer simulations to demonstrate the measurement detection limits. The use of two-photon microscopy to perform image cross-correlation spectroscopy (ICCS) studies will also be discussed. ICCS allows direct measurement of the interactions of two co-localized proteins labeled with fluorophores having different emission wavelengths even in a high density environment. The transport properties of the co-localized proteins are also measured simultaneously by ICCS. Recent applications of the ICS and ICCS methods for characterizing the transport and clustering of GFP labeled integrin adhesion proteins in living fibroblasts will be presented. Image correlation studies which demonstrate simultaneous measurement of diffusing and flowing populations of integrin clusters, and correlated transport between the alpha-5 integrin and intracellular alpha-actinin in CHO fibroblasts at 37°C will be shown. A new full space-time image correlation approach which allows us to map directional flux (vector maps) of labeled proteins and interacting proteins will also be described. We will present transport and co-transport maps from live cell measurements of cells expressing fluorescent protein constructs of focal adhesion kinase (FAK), paxillin,  $\alpha$ -actinin,  $\alpha$ 5-integrin, talin and actin.



**Transport Map** of actinin dynamics at CHO cell basal membrane

Circles rms diffusion distance 10 min

Arrows mean flow distance 10 min

Bars fraction of proteins diffusing (green), flowing (yellow), immobile (cyan).

Scale bar 10  $\mu$ m

## **[272] Probing Interactions of Inner Ear Proteins with Acceptor Photobleach and Sensitized Emission FRET: Promises and Pitfalls**

Robert M. Raphael<sup>1</sup>

<sup>1</sup>Rice University

Intermolecular interactions play a pivotal role in many biological processes, but are only beginning to be characterized in the auditory and vestibular system. Fluorescence resonance energy transfer (FRET) is a powerful optical technique that can reveal the presence of specific protein-protein interactions on the length scale of

1-10 nm. In addition, FRET can detect changes in intermolecular interactions that occur in response to external stimuli, as well as conformational changes within the same molecule. Though FRET has enormous promise, many obstacles must be overcome in order to obtain reliable quantitative data. This talk will discuss various methods of FRET, highlighting both their pitfalls and their potential application to unresolved questions involving the molecular mechanisms underlying hearing and balance.

### **[273] Intermolecular Associations of Auditorily-Significant Membrane Proteins Studied with FRET-FLIM**

**Richard Hallworth<sup>1</sup>**, Xudong Wu<sup>2</sup>, Jian Zuo<sup>2</sup>

<sup>1</sup>Creighton University, Omaha, NE, <sup>2</sup>St. Jude Children's Research Hospital

FRET and related techniques have been used to study protein-protein interactions in a wide variety of systems in recent years. Of the available techniques, FLIM (Fluorescence Lifetime Imaging) offers relative freedom from artifacts and the possibility of imaging FRET in living cells with low photodamage. In this talk, the advantages and disadvantages of the FLIM method will be discussed and some recent results with cochlea proteins will be highlighted. Supported by DC 04761, DC 05168, and EY12950 (to J.Z.), DC 02053 (to RH), RR17417-01 (to Creighton University), and NSF-EPSCoR EPS-0346476 (to RH).

### **[274] Restoration of Immune Mediated Hearing Loss by Adoptive Cellular Gene Therapy**

**Bin Zhou<sup>1</sup>**, Mohammad Habiby Kermany<sup>1</sup>, Qing Cai<sup>1</sup>, Chun Cai<sup>1</sup>, Wenxia Liu<sup>1</sup>, Jun Woo Kim<sup>1</sup>, Patrick Kim<sup>1</sup>, Ingo Turner<sup>2</sup>, Garrison Fathman<sup>2</sup>, Tai June Yoo<sup>1</sup>

<sup>1</sup>University of Tennessee, <sup>2</sup>Stanford University

Autoimmune diseases such as autoimmune inner ear disease including Meniere's disease are common and often devastating diseases. The main feature of this disease is the development and persistence of inflammatory processes in the apparent absence of pathogens, leading to destruction of the target tissues. It may be possible to establish disease remission and to re-acquire immune homeostasis by transiently introducing immune regulatory elements by adoptive cellular gene therapy.

Mice were immunized with  $\alpha$ -tubulin and hearing loss was induced. Light microscopic images of 200 $\mu$ g and 300 $\mu$ g  $\alpha$ -tubulin-immunized mice demonstrate low density of the spiral ganglion and cochlear hair cell damage. Increased ABR thresholds were shown in BALB/c mice. Serum antibody reactivity against  $\alpha$ -tubulin was elevated. The CD4 T cells as well as Th1 cytokines mediated autoimmune response were involved. The levels of the CD4+CD25+ lymphocytes were decreased stepwise with increasing antigen dosage.

Adoptive immunotherapy via T cell delivery of the IL-12p40 subunit was performed by i.v injection of 2x10<sup>6</sup> T-cell hybridoma cells transfected with IL-12 P40 gene. ABR and DPOAE threshold for  $\alpha$ -tubulin immunized mice at 2 weeks

and 6 weeks were measured. The distortion product traces of 8, 16, 32 KHz frequency at 80 dB SPL intensity in 300 $\mu$ g  $\alpha$ -tubulin immunized were measured. DPOAE shows low responses in immunized groups. Therapeutic groups show restoration of hearing level at 6 weeks after the therapy.

Thus, we have succeeded to restore the hearing in mice with immunologically induced deafness by adoptive cellular gene therapy.

### **[275] Non Viral Delivery to the Auditory Structures**

**Mark Praetorius<sup>1</sup>**, Stefan Fink<sup>2</sup>, Kim Baker<sup>3</sup>, Ingo Baumann<sup>1</sup>, Bernhard Schick<sup>4</sup>, Peter K. Plinkert<sup>1</sup>

<sup>1</sup>University of Heidelberg, <sup>2</sup>University of Ulm, <sup>3</sup>University of Maryland, <sup>4</sup>University of Erlangen

The inner ear has been approached mainly using viral vectors in gene transfer. Recent studies suggested that gene therapy through the transfer of math1 has potential to treat sensorineural hearing loss. Non viral gene therapy as a form of gene delivery may be ideal for the cochlea. However, cochlear non viral gene delivery has been examined by several studies and found to be inefficient compared to viral vector gene transfer. Two approaches to non viral delivery to the inner ear are here discussed. We investigated delivery of silica nanoparticles and polymer based delivery. Two separate entries to the inner ear were used: Vectors were delivered via application to the round window or delivery into the cochlea via a fenestration of the utricle.

Distribution of the vehicle was assessed in the cochlea as well as in the contra lateral ear and in the brain stem. Delivery to sensory hair cells and the spiral ganglion cells was seen in the cochlear and vestibular organ on both sides, suggesting that the vector spread through the cochlea aqueduct as previously demonstrated in viral vectors. We used fluorescence microscopy and transmission electron microscopy to detect the nanoparticles. In the more distal portions of the central auditory pathway (dorsal cochlear nucleus, superior olivary complex) nanoparticles were found indicating a possible anterograde axonal transport. Non viral gene transfer using advanced non viral vectors may provide a delivery system to the sensory hair cells and spiral ganglion cells and may even be suited to transfection of neurons of the central auditory pathway.

### **[276] Localization of Hematopoietic Stem Cell-Derived Cells in the Mouse Cochlea**

**Tetsuya Tamura<sup>1</sup>**, Tomoko Kita<sup>1</sup>, Takayuki Nakagawa<sup>1</sup>, Takayuki Okano<sup>1</sup>, Ken Kojima<sup>1</sup>, Tae-Soo Kim<sup>1</sup>, Momoko Yoshimoto<sup>2</sup>, Tatsutoshi Nakahata<sup>2</sup>, Juichi Ito<sup>1</sup>

<sup>1</sup>Department of Otolaryngology, Head and Neck Surgery, Graduate School, <sup>2</sup>Department of Pediatrics, Graduate School

Recently, cell therapy has been paid considerable attention for the treatment of inner ears. Bone marrow - derived cells are included in candidates of a source for transplants, because of their multipotent and the availability of autologous cells. On the other hand, recent studies have indicated that bone marrow-derived cells play

a certain role in the cochlea. However, details of roles of bone marrow-derived cells in the cochlear have not still determined. In this study, we examined the localization and fates of hematopoietic stem cells (HSCs; Lin-c-kit+Sca-1+) at one week or six months following systemic application into irradiated mice. HSCs were collected from green fluorescent protein (GFP) transgenic mice by cell sorting on FACS Vantage. C57BL/6 mice were irradiated with 9.0Gy of gamma rays before an injection of  $5 \times 10^5$  HSCs from the tail vein. Cochleae received only irradiation exhibited normal morphology and function, suggesting that the irradiation used in this study causes no significant damage in cochleae. One week after transplantation, GFP-positive cells were found only in the vessels, not in the cochlear specimens, indicating that HSCs systemically applied did not migrate into cochlear specimens. On the other hand, numerous GFP-positive cells were located in the modiolus of cochleae and spiral ligament 6 months after transplantation. These grafted cells were exhibited the expression of CD45 or Iba-1, indicating macrophages or microglia derived from HSCs settled in the cochlea. We found no grafted cells showing the expression of  $\beta$ -tubulin, MAP2 or GFAP. These findings indicate that some population consisting of the cochlear modiolus and spiral ligament are derived from bone marrows. The location of HSC-derived cells in the cochlea suggests that bone marrow-derived cells may play a role in immunological defense in the cochlea.

#### **[277] BDNF Gene Delivery Into the Mouse Cochlea by Cell Transplantation**

**Takayuki Okano<sup>1</sup>**, Takayuki Nakagawa<sup>1</sup>, Tomoko Kita<sup>1</sup>, Juichi Ito<sup>1</sup>

<sup>1</sup>Kyoto University Graduate School of Medicine

Previous studies have indicated the efficacy of gene therapy for the treatment of the inner ear. However, various problems are still remained before clinical application. For instance, a use of viral vectors involves the risk of virus toxicity and uncontrollable gene expression, although its high efficiency for transfection. One possible strategy to resolve this problem is ex vivo gene therapy using non-virus vectors. In this study, we examined the ex vivo gene delivery to the mouse cochlea using gene transfected cells with non-virus vector. Mouse brain-derived neurotrophic factor (mBDNF) gene was used as a gene for transfer, because BDNF has various biological effects including trophic supports of neural systems, and NIH3T3 cells were used as a vehicle of mBDNF genes. The cDNA of mBDNF was inserted the pIRESneo expression vector plasmid. After transfection of the plasmid into NIH3T3 cells by a lipo-fecton method, permanent transfectants were selected by adding G418 sulfate in culture media. First, we investigated the ability of BDNF production of the mBDNF-transgenic NIH3T3 cells (NIH3T3/BDNF) in vitro. The concentration of BDNF in the culture medium following 24 h-culture was measured by ELISA. The concentration of BDNF in the culture medium of NIH3T3/BDNF is 11-fold higher than that of normal NIH3T3 cells, indicating the ability of production and secretion of BDNF protein by NIH3T3/BDNF cells. Second, we transplanted NIH3T3/BDNF cells into the inner ear of

adult C57BL/6 mice from the posterior semicircular canal. Histological analysis demonstrated the survival of transplanted cells in the cochlea. Western blotting indicated the production of BDNF in grafted cells. These findings indicate the potential of ex vivo gene therapy for the inner ear disorder.

#### **[278] Neurotrophin-3 Gene Transfection of Cochlear Cells with Hydroxyapatite Nanoparticle Vector**

**Hong Sun<sup>1</sup>**, Ming Jiang<sup>1</sup>, Guiyuan Li<sup>2</sup>, Saihong Zhu<sup>3</sup>

<sup>1</sup>Dept Oto/HNS, Third Xiang Ya Hospital, Central South University, P.R.China, <sup>2</sup>Tumor Research Institute, Central South University, P.R.China, <sup>3</sup>Dept. Surgery, Third Xiang Ya Hospital, Central South University, P.R.China

Previous studies indicate neurotrophin 3 (NT-3) and brain derived neurotrophic factor (BDNF) protect and promote the survival of cochlear hair cells and spiral ganglion neurons. Therefore, gene therapy with NT-3 or BDNF has the potential for enhancing the survival of cochlear hair cells and neurons. Viral mediated gene delivery has frequently been used to deliver therapeutically useful genes; however, immunogenicity and carcinogenicity are major disadvantages of this approach. To avoid these problems, nanoparticle mediated gene delivery has been tried; however, transfection efficiency has generally been low with this approach. To enhance nanoparticle mediated gene delivery, and to evaluate the possibilities of nanoparticles used as a vector in inner ear gene therapy, we developed a hydroxyapatite (HAT) nanoparticle vector system for cochlear NT-3 gene transfection. HAT is a calcium phosphate mineral  $[\text{Ca}_{10}(\text{PO}_4)_6(\text{OH})_2]$  found in bone and dentine. HAT nanoparticles was made from  $\text{Ca}(\text{NO}_3)_2$  and  $(\text{NH}_4)_2\text{HPO}_4$ , dried and stored at room temperature. A 25 mg/ml sterilized HAT nanoparticle suspension was made via ultrasonic treatment. Particle size was 40-50 nm determined by transmission electron microscopy. DNA (PEGFPC2-NT3) binding and protecting abilities were determined by agarose gel electrophoresis. The HAT vector produced no signs of cytotoxicity using the MTT test when applied to cultured Hela cells. When the HAT-GFP-NT3 construct was applied in vitro to Hela cell approximately 10-15% of cells were GFP positive. About 10 % of primarily cultured mice cochlear ganglion cells were GFP positive when observed under the fluorescent microscope. The HAT-GFP-NT3 construct was also infused into scala tympani of the guinea pig cochlea and GFP labeled neurons were widely expressed. The HAT nanoparticle gene vector is stable, easy to construct, shows low cytotoxicity and appears to be a promising candidate for inner ear gene therapy.

#### **[279] Sendai Virus Vector-Mediated Transgene Expression in the Cochlea In Vivo**

**Sho Kanzaki<sup>1</sup>**, Akihiro Shiotani<sup>1</sup>, Makoto Inoue<sup>2</sup>, Mamoru Hasegawa<sup>2</sup>, Kaoru Ogawa<sup>1</sup>

<sup>1</sup>Department of Otolaryngology, Keio University Medical School, <sup>2</sup>DNAVEC

Gene transfer into inner ear organs is an attractive new approach for treating hearing disorders.

Sendai virus (SeV), a member of the paramyxoviridae family, is an enveloped virus that has non-segmented, negative sense genomic RNA. SeV vectors have several advantages in gene transfer. SeV is completely free of genotoxicity and have remarkably high transfection efficiency in many tissues and cell types. There is no evidence that SeV is pathogenic in humans. We injected a recombinant Sendai virus (SeV) vector into the guinea pig cochlea using two different approaches via scala media and scala tympani.

We investigated which cell types took up the vector. The auditory brain stem responses (ABR) threshold shift and distribution of transfected cells in animals that received injections into the scala media were different compared to those in animals that received injections into the scala tympani. SeV can transfect very different types of cells, including stria vascularis, spiral ganglion neurons, and sensory epithelia of the organ of Corti (via scala media), and fibrocytes of scala tympani (via scala tympani).

Because SeV vectors potentially can deliver stimuli to the cochlea to induce hair cell regeneration, it may be a powerful tool for repairing the organ of Corti. Our data suggest that SeV vector-mediated transgene expression is a useful modality to remedy diseases affecting the cochlea.

## **[280] Inner Ear Pharmacokinetics of Dexamethasone Following Intratympanic Injection**

**Christopher Hargunani<sup>1</sup>**, Beth Kempton<sup>1</sup>, Jacqueline DeGagne<sup>1</sup>, Dennis Trune<sup>1</sup>

<sup>1</sup>*Oregon Health & Science University*

Although dexamethasone is routinely delivered intratympanically for hearing loss, we know little of its inner ear pharmacokinetics. Dexamethasone 21 phosphate (Dex-21P) is the pharmaceutical compound available for injection, but it must be converted to its biologically active form dexamethasone (Dex) to bind to the glucocorticoid receptor. This conversion from the pro-drug to its active form has not been evaluated in the ear, particularly with regard to the movement of each form through the inner ear to reach the relevant receptor. Therefore, the present study was conducted to determine the time course of Dex-21P movement from the middle ear into the inner ear, its conversion to Dex, and the distribution of both forms relative to the glucocorticoid receptor.

BALB/c mice were injected intratympanically with the prodrug Dex-21P and inner ears collected at post-injection times ranging from 5 minutes to 7 days. Ears were immunohistochemically stained for Dex-21P, Dex, and the glucocorticoid receptor. Both forms of dexamethasone were seen in the inner ear within 15 minutes, reaching their highest staining intensity at one hour. Neither drug was detected after 24 hours. The strongest staining occurred in the spiral ligament, organ of Corti, spiral ganglion, and vestibular sensory epithelia. Distribution of the drug paralleled locations of the glucocorticoid receptor except in the stria vascularis marginal cells, which stained heavily for the receptor, but not the drug. These results demonstrated that dexamethasone rapidly travels from the

middle ear into the inner ear and converts to its active form. The drug distribution matches that of the glucocorticoid receptor. However, dexamethasone probably has little impact on ear tissues after 24 hours.

(NIH-NIDCD R01 DC05593 and P30 DC005983, and VA RR&D NCRAR C2659C)

## **[281] The Effect and Elimination of Three Different Gels Injected to the Middle Ear Cavity**

**Cecilia Engmér<sup>1</sup>**, Tobias Brahmer<sup>2</sup>, Andreas Ekborn<sup>1</sup>, Hans Ehrsson<sup>3</sup>, Katarina Edsman<sup>2</sup>, Malou Hultcrantz<sup>1</sup>, Göran Laurell<sup>1</sup>

<sup>1</sup>*Department of Otolaryngology and Head & Neck Surgery, Karolinska University Hospital, Stockholm*, <sup>2</sup>*Department of Pharmacy, Uppsala University*, <sup>3</sup>*Karolinska Pharmacy, Stockholm, Sweden*

Pharmacological treatment of inner ear disorders is an expanding scientific field. Local administration of a drug might provide the inner ear with higher concentrations compared to systemic treatment. During treatment with an ototoxic drug, local administration of an antidote might protect the inner ear from injury. The goal of this project is to develop an effective and safe delivery system of providing drugs selectively to the inner ear using a slow-release vehicle instilled into the middle ear cavity by a tympanic membrane injection. Three gels, carboxy methyl cellulose (CMC), hyaluronic acid (Hya) and pluronic acid (Plu), have been identified as possible vehicles that can be loaded with pharmacological substances for intratympanic administration: The effects of the three gels on the tympanic membrane, middle and inner ear, as well as the elimination from the middle ear were studied in three groups of guinea pigs. The hearing sensitivity of the animals was determined by using auditory brain stem response (ABR) which was used as a functional measure of the elimination of the gels. In another group of animals, coal-loaded gel was injected to the middle ear cavity. Elimination rate was semi-quantified visually after opening the bulla *in vivo*. In a third group of animals, pure gel was injected, the animal decapitated on day 6 and the middle ear and cochlea fixed for morphological examinations. Preliminary data indicate that Hya was the most suitable gel for application to the middle ear cavity. In development of a novel drug delivery system to the inner ear further studies on drug-up-take, kinetics in the inner ear and drug efficacy should be undertaken.

## **[282] Cochlea Protection by Local IGF-1 Application Using a Biodegradable Hydrogel**

**Yoshinori Matsuoka<sup>1</sup>**, Takayuki Nakagawa<sup>1</sup>, Koji Iwai<sup>1</sup>, Tsuyoshi Endo<sup>1</sup>, Tomoko Kita<sup>1</sup>, Tae-Soo Kim<sup>1</sup>, Yasuhiko Tabata<sup>2</sup>, Juichi Ito<sup>1</sup>

<sup>1</sup>*Department of Otolaryngology-Head and Neck Surgery, Graduate School of Medicine, Kyoto University*, <sup>2</sup>*Institute for Frontier Medical Science, Kyoto University*

We have recently established a drug delivery system for the inner ear using a biodegradable hydrogel, which is made of porcine type-I collagen crosslinked by glutaraldehyde (Endo et al. in print). The use of a biodegradable hydrogel enables sustained release of

brain-derived neurotrophic factor into the cochlear fluid space for 7 days. The aim of this study was set to examine the efficacy of this drug delivery system for delivery of recombinant human insulin-like growth factor-1 (rhIGF-1) into the cochlea. We investigated protective effects of rhIGF-1 locally applied by a biodegradable hydrogel against noise trauma. A biodegradable hydrogel immersed with rhIGF-1 was placed on the round window membrane (RWM) of Sprague-Dawley rats, while a hydrogel immersed with physiological saline was applied to control animals. Three days after drug application, the animals were exposed to white noise at 120 dB sound pressure level for 2 h. Auditory brain stem responses (ABRs) were measured to monitor cochlear function on Day 3 and 7. The temporal bones were collected 7 days after noise exposure and the loss of hair cells was quantitatively analyzed by immunohistochemistry for myosin VIIa. There were no significant differences in ABR thresholds 3 days after noise exposure between rhIGF-1- and saline-treated cochleae. However, on day 7, rhIGF-1-treated cochleae exhibited significantly lower threshold shifts than saline-treated cochleae. Furthermore histological analysis revealed significantly higher survival rates of outer hair cells in rhIGF-1-treated cochleae compared with those in saline-treated cochleae. These findings demonstrate the efficacy of local rhIGF-1 application using a biodegradable hydrogel for protection of cochleae from noise trauma.

### **[283] A New Surgical Approach for Injections Into the Guinea Pig Cochlea**

**Donald L. Swiderski<sup>1</sup>, Matthew Johnson<sup>1</sup>, Yehoash Raphael<sup>1</sup>**

<sup>1</sup>*University of Michigan*

In this study we present a new approach to delivery of drugs or gene therapy vectors in the cochlea of the guinea pig. Previous work in our lab has demonstrated the potential of gene therapy to regenerate new hair cells in the organ of Corti. To be effective, the adenovirus vector used in these studies must be injected into the scala media. In the guinea pig, the scala media is accessible by drilling through the cochlear wall opposite the stria vascularis; however, this approach is not easily applicable to treatment of humans suffering hearing loss. In an effort to devise a surgical model that more closely approximates the approach that would be used to treat humans, we explored the feasibility of injecting an adenovirus vector into the scala media by an alternate route that passes through the round window. In this technique, a drawn glass pipette first enters the scala vestibuli through the round window, then crosses the scala vestibuli and enters the scala media through the basilar membrane in the region of the hook. To determine whether this a viable approach for administration of gene therapy vectors to treat deafness, guinea pigs were inoculated with a replication-deficient adenovirus bearing GFP four days after they had been deafened by systemic administration of kanamycin and ethacrynic acid. Successful injection of the vector into the scala media of the deafened animal resulted in expression of GFP in surviving supporting cells. In some cases, GFP was evident in supporting cells as far as the apical (fourth) turn. Expression could also be detected in cells outside of

the organ of Corti. These results suggest that the round window approach is a viable technique for evaluating therapeutic treatments in a clinically relevant manner.

This work was supported by B. and A. Hirschfield, GenVec, and NIH/NIDCD Grants R01-DC01634, R01-DC05401, R01-DC05053, T32-DC00011 and P30-DC05188.

### **[284] Functional Analysis of Protocadherin 15**

**Kumar N. Alagramam<sup>1</sup>, Qing Zheng<sup>2</sup>, Hu Yu<sup>2</sup>, Sherri M. Jones<sup>3</sup>, Karen S. Pawlowski<sup>4</sup>, Yayoi S. Kikkawa<sup>4</sup>, Charles G. Wright<sup>4</sup>**

<sup>1</sup>*Case Western Reserve University*, <sup>2</sup>*The Jackson Laboratory, Bar Harbor, ME, USA*, <sup>3</sup>*East Carolina University*, <sup>4</sup>*UT Southwestern Medical Center*

The Ames waltzer (av) mouse carries a recessive mutation, which causes deafness and vestibular dysfunction associated with degeneration of the inner ear neuroepithelia. Since the original report linking the av mutation to Protocadherin 15 (Pcdh15) was published in 2001, several mutations in the human orthologue of Pcdh15 have been linked to human syndromic (USH1F) and nonsyndromic (DFNB23) deafness. More recently, in the Ashkenazi Jewish population, the R245X mutation of PCDH15 was reported to account for 58% of USH1 cases. These studies indicate the prevalence of congenital deafness linked to mutation in PCDH15 and the importance of understanding PCDH15-associated inner ear pathology as it relates to the nature of the mutation. We have studied mice carrying different mutations (6 different alleles) in Pcdh15 over the past 6 years. Scanning and transmission electron microscopic studies of the inner ear sensory epithelia in different av alleles at various time points show that mutation in Pcdh15 affects organization of stereocilia on the sensory hair cells. Electrophysiological evaluation of av mutants shows lack of auditory and vestibular evoked potentials. Though functional abnormalities are apparent in both the cochlea and vestibular apparatus, morphologic changes in hair cells are readily observable only in the cochlea. Molecular genetic studies show that protein coded by Pcdh15 interacts with other hair-cell proteins that are necessary for normal hair cell development and function. Collectively, our study shows that Pcdh15 is necessary for the normal structural development of hair cells and it plays a functional role in mature sensory cells of the inner ear.

### **[285] A Gene Knockout Mouse Model for Usher Syndrome Type 1C**

**Denise Yan<sup>1</sup>, Qing Yin Zheng<sup>2</sup>, Xiao Mei Ouyang<sup>1</sup>, Heping Yu<sup>2</sup>, Chantal Longo-Guess<sup>2</sup>, Christopher M. McCarty<sup>2</sup>, Li Lin Du<sup>1</sup>, Kenneth R. Johnson<sup>2</sup>, Xue Zhong Liu<sup>1</sup>**

<sup>1</sup>*Department of Otolaryngology, University of Miami, FL, USA*, <sup>2</sup>*The Jackson Laboratory, Bar Harbor, ME, USA*

Mutations in the PDZ domain protein harmonin are the causes of Usher syndrome type 1C (USH1C) as well as certain forms of non-syndromic deafness. Harmonin, through its binding to four of the five USH1 proteins, is thought to play a central role in the USH1 gene network. To further understand the role of harmonin in the pathogenesis that leads to USH1, we generated a targeted

deletion of *Ush1c* in mice. Homozygous mutant mice (*Ush1c*<sup>-/-</sup>) exhibit the typical behavior associated with inner ear defects: deafness, hyperactivity, head tossing and circling. To quantitatively assess hearing loss in *Ush1c*<sup>-/-</sup> mice, we measured auditory-evoked brainstem response (ABR) thresholds to broad-band clicks and to 8, 16 and 32 kHz pure-tone stimuli on mutant and control mice of 16 and 23 days of age. *Ush1c*<sup>-/-</sup> mice (n=3) were completely deaf at all the frequencies tested, as there was no detectable ABR with 100 dB SPL stimuli, whereas age-matched *Ush1c*<sup>+/-</sup>-controls (n=4) showed ABR thresholds in the normal-hearing range. Using the LacZ reporter, we were able to study the expression of the *Ush1c* gene in the inner ear. The data showed that the *Ush1c* gene localizes in both the inner and outer hair cells in the cochlea. Histological analysis revealed that, at three weeks of age, outer hair cells of *Ush1c*<sup>-/-</sup> mice showed disorganized and splayed stereocilia in contrast to the well-organized pattern and rigid structure observed in *Ush1c*<sup>+/-</sup> littermates. Cochlear degeneration in *Ush1c*<sup>-/-</sup> mice seemed to be specific to the hair cells. The *USH1C* mouse model will be a useful tool for defining the specific pathophysiology of *USH1* in the cochlea and the retina.

(Supported by NIH DC 05575 and DC005846)

## **[286] Genomic Approaches for Pathway Identification in Regenerating Sensory Epithelia of the Inner Ear**

**David Alvarado**<sup>1</sup>, Kara Powder<sup>1</sup>, David Hawkins<sup>1</sup>, Stavros Bashiardes<sup>1</sup>, Veena Bhonagiri<sup>1</sup>, Rose Veile<sup>1</sup>, Mark E. Warchol<sup>2</sup>, Michael Lovett<sup>1</sup>

<sup>1</sup>Department of Genetics, Washington University School of Medicine, <sup>2</sup>Central Institute for the Deaf, Washington University School of Medicine

The sensory epithelia (SE) from avian cochlea and utricle were separately gene expression profiled on a custom transcription factor (TF) gene microarray at various recovery time points following damage by either laser or chemical ablation. Expression profiles for all timecourses, including numerous biological samples and hundreds of microarray comparisons, were compared to identify differentially expressed TF's. Some of these can be placed into known signaling cascades such as the *Ap1* pathway, *TGFβ* pathway, sonic hedgehog signaling and the *Pax-Eya-Six-Dach* pathway. To assess the necessity of these TF's for sensory epithelia proliferation and to identify downstream targets, >20 of these TF's were targeted for knockdown with siRNA's or pharmacological inhibitors using a 96-well SE cell proliferation assay. Targeted knockdowns of *Pax2*, *JunD* and *Cebpg*, as well as chemical inhibition of the Jun kinase (JunK) pathway, significantly inhibited SE proliferation. Several of these TF's have specific effects on proliferation in the inner ear epithelia as indicated by their failure to inhibit proliferation when targeted in avian retinal epithelia. Additionally, we identified novel epistatic relationships and pathway intersections by conducting expression profiles on SE after targeted knockdowns and/or chemical inhibitions. In one example, siRNA and profiling data demonstrate that *JunD* lies upstream of *Cebpg* and that five additional genes lie downstream of *Cebpg*: *IRX4*, *LRP5*, *TAF-172*, *RARA*, and *ZNF44*. Knockdowns of these genes indicate that *IRX4*,

*LRP5* and *TAF-172* also inhibit utricle sensory epithelial proliferation. *LRP5* is known to act as a receptor for *Wnt* signaling. Several other known effectors of *Wnt* signaling were also differentially expressed in our recovery timecourse analysis, suggesting that the JunK cascade may intersect with the *Wnt* pathway at a relatively early timepoint in avian SE regeneration.

## **[287] Age-Related Hair Cell Loss in A/J Mice**

**Qing Yin Zheng**<sup>1</sup>, Dalian Ding<sup>2</sup>, Heping Yu<sup>1</sup>, Richard Salvi<sup>2</sup>, Kenneth R. Johnson<sup>1</sup>

<sup>1</sup>The Jackson Laboratory, Bar Harbor, ME, USA, <sup>2</sup>Center for Hearing and Deafness, University at Buffalo

We previously reported that the *ahl* locus on mouse Chromosome 10 contributes to age-related hearing loss in many inbred strains, including A/J and C57BL/6J. Recent evidence demonstrates that the effects of *ahl* are caused by an inbred strain-specific 753A/G dimorphism of the *Cdh23* gene. We also previously showed that mitochondrial DNA (mtDNA) derived from the A/J strain exerts a significant detrimental effect on hearing when compared with mtDNA from the CAST/Ei strain. Our ABR data demonstrated that A/J mice start to lose hearing as early as 25 days of age. The hearing loss at such an early age is presumably due to cochlear pathology. To evaluate this hypothesis, cochleae from A/J and C57BL/6J mice were examined and compared. Surface preparations of the organs of Corti from 9-week-old A/J mice demonstrated that both inner (IHC) and outer (OHC) hair cells are lost from the basal through the apical turn; however, hair cell loss in the basal turn is much more severe than in the apex. Cochleograms for mice at ages P0, P8, P16, P27, P35, P42, P49, P63, and P140 were produced from hair cell counts along the length of the cochlear duct. Both IHCs and OHCs presented a progressive loss, but OHC loss started earlier (P16) than IHC

loss (P35). A/J mice have a full set of OHC and IHC at postnatal day 8, but by 9 weeks of age, massive OHC and IHC loss was seen in the basal 2/3rd of the cochlea. Hair cell density in the vestibular system appeared normal in 5-month-old A/J mice. Despite the massive loss of cochlear hair cells, spiral ganglion neurons and nerve fibers in the habenula perforata appeared remarkably normal. The residual IHC present in A/J could promote the survival of spiral ganglion neurons by release of neurotrophic substances such as NT-3 and BDNF. The stria vascularis also appeared normal in both strains. Thus, our preliminary results suggest that the gene(s) responsible for early onset hearing loss in A/J mice mainly affects the sensory hair cells of the cochlea. Supported by NIDCD NIH

## **[288] The Tailchaser Mutation Does Not Affect Tip Links Formation – High Resolution Scanning Electron Microscopy in the Service of Genetic Deafness Research**

**Agnieszka K. Rzadzinska**<sup>1</sup>, Karen P. Steel<sup>1</sup>

<sup>1</sup>Sanger Institute

Hearing and balance depend upon the function of hair cells equipped with highly ordered bundles of mechanosensitive stereocilia. Formation and maintenance of the

stereocilia bundle depends on several known inner ear proteins including myosin VI, VIIa, XVa, cadherin 23 and espin, as mutations in those genes specifically disrupt stereocilia organization and lead to hearing loss. However, the specific roles of those proteins in stereocilia morphogenesis remain unknown. Here we used high resolution scanning electron microscopy to analyze further the morphology of auditory hair bundles of tailchaser hetero- and homozygotes. We found that changes in stereocilia organization in these mice could be observed in outer and inner hair cells from the earliest stages of hair bundle development and was accompanied by severe deformation of cuticular plates. The extent of hair bundle abnormality was greater on the surface of outer hair cells than inner hair cells, and in the basal turn of the cochlea compared to the apex. We confirmed that stereocilia of tailchaser heterozygotes show staircase-like organization of the bundle. In contrast, this characteristic arrangement of stereocilia rows of different heights could not be observed in homozygous tailchaser hair bundles. Moreover, the stereocilia of homozygous tailchasers often fused together and formed giant protrusions on the apical surface of hair cells. Interestingly, interstereociliary links seem to be intact in both tailchaser hetero- and homozygotes.

### **[289] All Known Usher Syndrome Proteins Interact to Form an Immunoprecipitable Protein Mega-Complex Present in Hair Cells and Photoreceptor Cells**

Gautam Bhattacharya<sup>1</sup>, Michael Anne Gratton<sup>2</sup>, Neena Haider<sup>3</sup>, Daniel Meehan<sup>1</sup>, Duane Delimont<sup>1</sup>, Lauren Coffey<sup>2</sup>, **Dominic Cosgrove<sup>1</sup>**

<sup>1</sup>Boys Town National Research Hospital, <sup>2</sup>University of Pennsylvania, <sup>3</sup>University of Nebraska Medical Center

Usher syndrome is characterized by retinitis pigmentosa associated with deafness. The genes for 8 of 11 loci associated Usher syndromes have been identified, and their proteins partially characterized. We produced affinity-purified polyclonal antibodies against each of the known Usher syndrome proteins, and performed immunolocalization and co-immunoprecipitation studies. All 8 of the known Usher proteins co-immunoprecipitate from both postnatal day-2 cochlear and adult retinal extracts using antibodies directed against the carboxy-terminal cytoplasmic domain of VLGR1 (USH2C). Interestingly, only the A isoform of harmonin (USH1C) and the large (25kDa) membrane-bound isoform of clarin-1 (USH3) were found in extracts of either tissue, suggesting that they might constitute the functionally relevant protein isoforms for these genes. Both the long (450 kDa) and short (180 kDa) isoforms of usherin are present in the complex when retinal extracts are used, whereas only the long isoform of usherin co-immunoprecipitates from cochlear extracts, illustrating that the composition of the protein complex is different in retina and cochlea. Immunofluorescence immunostaining shows that all of the Usher proteins localize to the inner segments and connecting cilia of the photoreceptors, while some are in the ribbon synapse. Similarly, while all cochlear hair cells are immunopositive for all the Usher proteins, the ribbon synapse of inner hair cells is immunopositive for some.

Sucrose gradient fractionation of retinal extracts was used to show that the complex is found in microvesicles. Combined, these findings suggest that all of the Usher proteins have an interrelated function in the neuroepithelial cells of the retina and the cochlea. Further the data implicates specific isoforms of clarin-1, harmonin, and usherin as critical to the functional pathway. Vesicular localization of the complex suggests that it is being actively trafficked, possibly bi-directionally towards the synapse and stereocilia of hair cells, and the synapse and connecting cilia of rod photoreceptors. Thus, deaf/blindness in Usher syndrome likely derives from defects in the biological processes managed by this protein mega-complex, which for the moment, remain unknown. Supported by DC04844 and DC006442

### **[290] Towards the Cellular and Molecular Function of Mucolin-3**

**Margaret Atiba-Davies<sup>1</sup>**, Adam Derr<sup>1</sup>, Konrad Noben-Trauth<sup>1</sup>

<sup>1</sup>NIDCD, Bethesda, MD

The varitint-waddler mutant mouse is characterized by two spontaneous mutations (*Va* and *Va<sup>J</sup>*) in the mucolin-3 gene (*Mcoln3*). *Mcoln3* encodes a putative six-transmembrane protein with sequence and motif similarities to the family of non-selective transient-receptor-potential (TRP) ion channels. The *Va* mutation is an ala-to-pro missense mutation within the fifth transmembrane domain and *Va<sup>J</sup>* is an ile-to-thr mutation that occurs in the predicted second extracellular loop. *Va* homozygotes are most severely affected in varitint-waddler and these mice exhibit deafness, circling behaviour, sterility, and reduced viability together with an almost entirely white coat colour. Loss of hearing in *Va* and *Va<sup>J</sup>* has previously been associated with a primary defect in the sensory epithelium and patchy distribution of and reduced pigmentation in melanocytes located in the stria vascularis (Cable & Steel (1998) *Hear. Res.* 123, 125-136).

To characterize the function of *Mcoln3* we generated GFP-tagged *Mcoln3* fusion constructs and over-expressed them in COS-1 cells. Immunofluorescence showed that over-expressed *Mcoln3* becomes localized to distinct compartments or vesicles within the cytoplasm.

We have raised a *Mcoln3* specific antibody that we are currently using to define the location of the protein within the inner ear. This antibody was shown to be specific for endogenous *Mcoln3* in mouse cochlear and vestibular tissue extracts as well as heterologously expressed *Mcoln3* from COS-1 cells.

### **[291] Interaction of Myosin-1c with Other Components of the Hair-Cell Transduction Apparatus**

**Kelli R. Phillips<sup>1,2</sup>**, Guy P. Richardson<sup>3</sup>, Janet L. Cyr<sup>1,2</sup>

<sup>1</sup>Sensory Neuroscience Research Center, West Virginia University School of Medicine, <sup>2</sup>Biochemistry and Molecular Pharmacology, West Virginia University School of Medicine, <sup>3</sup>School of Life Sciences, University of Sussex  
Myosin-1c (*Myo1c*), an unconventional myosin important for adaptation of hair-cell mechanotransduction, has been shown to interact *in vitro* with both cadherin 23 (*Cdh23*), a



possible component of the tip link [Siemens *et al.*, (2004) *Nature* 428:950-955], and phosphatidyl inositol 4,5-bisphosphate (PIP<sub>2</sub>), which is present in stereociliary membranes and is necessary for transduction [Hirono *et al.*, (2004) *Neuron* 44:309-320]. We have used an *in situ* binding assay to visualize and characterize the interaction of Myo1c recombinant fragments with intracellular binding sites in hair-cell stereocilia which we term "receptors" and have found that excess calmodulin (CaM) blocks Myo1c binding [Cyr *et al.*, (2002) *J. Neurosci.* 22:2487-2495]. To investigate the role of Myo1c's highly conserved second CaM-binding IQ domain (IQ2) in receptor interactions, mutations to the IQ consensus sequence of IQ2 were made to block CaM binding. The resulting mutated Myo1c protein interacts with stereociliary receptors both in the presence and absence of excess CaM, verifying the essential role of IQ2 in the observed interaction. However, a Myo1c fragment containing only IQ2 does not bind to receptors suggesting that IQ2, when free of CaM, is necessary, but not sufficient, for receptor interaction. We next sought to determine whether the stereociliary Myo1c receptors detected in our assay were either PIP<sub>2</sub> or Cdh23.

We examined Myo1c/PIP<sub>2</sub> interactions using PIP strips, which consist of fifteen different lipids spotted on a hydrophobic membrane. We determined that Myo1c binding to PIP<sub>2</sub> on a solid support *in vitro* is also dependent upon a CaM-free IQ2 domain. To examine Myo1c/Cdh23 interactions we used tissue from mice lacking Cdh23 in our *in situ* binding assay. We detected no binding of recombinant Myo1c fragments to hair-cell receptors in homozygous Cdh23<sup>v2j</sup> mice. Moreover, hair cells from homozygous Cdh23<sup>v2j</sup> mice contain PIP<sub>2</sub> in their stereociliary membranes as evidenced by the binding of a pleckstrin homology domain-GFP fusion protein in cochlear cultures. Thus, the receptor(s) visualized in our *in situ* binding assay is not PIP<sub>2</sub> and the loss of Cdh23 coincides with a loss of Myo1c binding, suggesting that Cdh23 may be a Myo1c stereociliary receptor.

This work is supported by NIDCD predoctoral fellowship F31DC007558 (KRP), The Wellcome Trust (GPR), and NIDCD grant R01DC006402 (JLC).

## **[292] A Functional Genomics Approach to Understanding Hair-Cell Development and Operation in the Zebrafish**

**Brian McDermott**<sup>1,2</sup>, Jessica Baucom<sup>1,2</sup>, Aurelie Lechere<sup>1,2</sup>, A.J. Hudspeth<sup>1,2</sup>

<sup>1</sup>The Rockefeller University, <sup>2</sup>Howard Hughes Medical Institute

In its role as a sensory receptor that converts mechanical stimuli into electrical responses, a hair cell contains distinctive structures with specialized molecular components, including the hair bundle that mediates mechanoelectrical transduction and presynaptic active zones that permit tonic vesicular release. Because of the paucity of starting material in each vertebrate ear, on the order of tens of thousands of hair cells, and the unavailability of a pure population of hair cells, few of the hair cell's specialized molecular components have been identified and a comprehensive census of the cell's molecular constituents has yet to be accomplished.

As a starting point for an understanding of the molecular constituents of the hair cell, we have used DNA microarray technology to identify the transcripts present in adult zebrafish hair cells. Methods have been developed to rapidly isolate small, pure populations of hair cells from the lagena of the inner ear. RNA from these populations has been amplified, labeled, and hybridized to oligonucleotide microarrays. The amplification process produced greater than a million-fold increase in labeled RNA from the transcripts contained in 200 hair cells. The hair-cell transcriptome of the zebrafish includes genes involved in cytoskeletal function, vesicular fusion, transcription, and ion flow across membranes. Among these are homologs of genes that, when mutated, produce deafness in humans and mice. The transcription profile also encompasses genes of undetermined function. Using the genetic techniques applicable to the zebrafish, we have begun to investigate the roles that some of these genes' products play in hair-cell development and function.

This research was supported by grants DC00241 and F32 DC006539-01 from the National Institutes of Health.

## **[293] Identification of the Hair Cell Soma Antigen HCS-1 as Otoferlin**

**Janet L. Cyr**<sup>1,2</sup>, Mark E. Warchol<sup>2,3</sup>, Guy P. Richardson<sup>2,4</sup>, Jeffrey T. Corwin<sup>2,5</sup>

<sup>1</sup>West Virginia University School of Medicine, <sup>2</sup>Inner Ear Group, Marine Biological Laboratory, <sup>3</sup>Washington University School of Medicine, <sup>4</sup>University of Sussex, UK, <sup>5</sup>University of Virginia School of Medicine

The generation of immunological reagents against proteins present in the inner ear has proven to be extremely useful in the identification of molecules important for auditory and vestibular function. Immunization of mice with sensory epithelia from the chick utricle previously yielded an IgG2a monoclonal antibody, termed HCS-1 (for hair-cell soma 1), that recognizes an antigen specifically present in the cell body of hair cells in sharks, teleosts, amphibians and birds [Finley *et al.* (1997), *ARO abs.* #535]. The HCS-1 antibody immunoprecipitates two closely spaced protein bands with apparent molecular masses of 230- and 210-kDa from TX-100 soluble extracts of sensory organs obtained from the chick inner ear. To identify these immunoprecipitated proteins, each band was subjected to mass spectrometry. Both bands yielded a number of tryptic peptides with masses corresponding to peptides derived from the sequences for mouse and human otoferlin (Mascot scores of 420 and 390 for the 230- and 210-kDa bands respectively). Otoferlin is a protein known to be important for auditory function [Yasunga *et al.*, (1999) *Nat Genet* 21: 363-369.] and proposed to be involved in the release of synaptic vesicles from hair cells [Safieddine *et al.*, (2004) *MBHD abs* #174]. To further characterize the subcellular distribution of otoferlin in hair cells, we undertook fluorescence confocal microscopy using the HCS-1 antibody on bullfrog saccular hair cells. These studies revealed immunolabeling throughout the hair-cell soma in addition to an intense, uniform immunolabeling of the basolateral plasma membrane; immunoreactivity was absent from the stereociliary membrane. Current work is centered on characterizing the two forms of otoferlin found



in hair cells and the proteins/structures with which this protein interacts.

This work was supported by The Wellcome Trust (GPR) and NIDCD grants R01DC006402 (JLC), R01DC006283 (MEW), and R01-DC00200 (JTC). The authors would like to thank Dr. Kathryn Lilley, Cambridge Centre for Proteomics, UK for her invaluable assistance.

## **[294] The Role of BMP4 in Inner Ear Development and Function**

**Marsha Blauwkamp<sup>1</sup>**, Lisa A. Beyer<sup>1</sup>, Lisa Kabara<sup>1</sup>, Karin Halsey<sup>1</sup>, Keiji Takemura<sup>1</sup>, W.M. King<sup>1</sup>, David Dolan<sup>1</sup>, Kate Barald<sup>1</sup>, Yehoash Raphael<sup>1</sup>, Ronald Koenig<sup>1</sup>

<sup>1</sup>*University of Michigan*

Bone Morphogenetic Protein 4 (BMP4) is a member of the TGF-beta superfamily and is known to be important for normal development of the inner ear. BMP4 antagonists cause abnormalities in semicircular canal development in chick embryos. BMP4 homozygous null mice die as embryos, but BMP4 heterozygous null mice are viable and some adults exhibit a circling phenotype, which may be due to an inner ear defect. We have begun to study C57BL/6 BMP4<sup>+/-</sup> mice and their littermate controls to better understand the role of BMP4 in inner ear development and function. Paint filling studies demonstrated that there were no visible abnormalities in the semicircular canals of 4 circling BMP4<sup>+/-</sup> mice; of 16 BMP4<sup>+/-</sup> embryos analyzed, only 1 was abnormal, lacking the posterior semicircular canal. Immunostaining by the hair cell marker myosin VIIa demonstrated that the hair cells in the cochlea and the ampullae were grossly normal. However, phalloidin labelling demonstrated that while the stereocilia of the hair cells in the cochlea were normal, the stereocilia in the ampullae were greatly reduced in number. The numbers of sensory and vestibular neurons also were substantially reduced, based upon immunostaining for neurofilament. Surprisingly, quantitative testing of the vestibulo-collic reflex demonstrated that the BMP4<sup>+/-</sup> mice have better head stability in the pitch axis when compared to control mice. Auditory brainstem response thresholds at 6, 12, and 24 kHz in 4-12 week circling BMP4<sup>+/-</sup> mice (N=8) were 58±6, 46±7, and 57±8 dB SPL compared to 31±3, 23±2, and 36±5 dB SPL in age-matched control mice (N=10). These studies demonstrate the influence of BMP deficiency on several structures associated with the cochlea and the vestibular system.

Supported by NIH grants R01 DC006209 (RJK), R01 DC05053 (YR), P30 DC05188 (DFD and YR), R01 DC004184 and DC05939 (KFB).

## **[295] Role of Hindbrain in the Morphogenesis of the Inner Ear: Analysis of *Noggin* Knockout Mice**

**Jinwoong Bok<sup>1</sup>**, Lisa Brunet<sup>2</sup>, Omar Howard<sup>1</sup>, Richard Harland<sup>2</sup>, Doris K. Wu<sup>1</sup>

<sup>1</sup>*National Institute on Deafness and Other Communication Disorders, Rockville, MD*, <sup>2</sup>*University of California, Berkeley*

The development of the mammalian inner ear is dependent on tissues such as the hindbrain, mesenchyme

and neural crest. Signaling from rhombomere 5 of the hindbrain is particularly important for proper inner ear morphogenesis. In *Noggin* <sup>-/-</sup> mice, the neural tube fails to close between the diencephalon and myelencephalon and is kinked along the spinal cord region. However, gene expression analyses did not reveal a clear defect in the Anterior/Posterior or Dorsal/Ventral axial patterning of the neural tube rostral to the level of the forelimb (McMahon et al, *Genes & Dev.*, 2000). We examined the morphogenesis of *Noggin* <sup>-/-</sup> inner ears from E12.5 to E15.5 using the paint-filling technique. In general, the mutant inner ears are smaller in size and their gross patterning is distorted. Our results show that the cochlear duct of *Noggin* mutants is always shorter than wildtype and often displays aberrant coiling. Less prevalent defects include malformations of the endolymphatic duct, saccule and posterior semicircular canal. Some of the patterning defects such as the abnormal cochlear duct outgrowth are apparent before *Noggin* expression is detectable within the inner ear. These results suggest that the cause of inner ear defects lie outside inner ear tissues. We found that the relative position of the otocyst and rhombomeres in the hindbrain of *Noggin* <sup>-/-</sup> mutants is misaligned, possibly due to kinking of the neural tube. This misalignment most likely disrupts the normal signaling from rhombomere 5 and 6 that is required for inner ear patterning. We are currently testing this hypothesis by performing tissue extirpation and translocation experiments in chicken embryos.

## **[296] Lrig3: A Novel Ig-Superfamily Protein Involved in Inner Ear Development**

**Victoria E. Abraira<sup>1</sup>**, John D. Slonismky<sup>1</sup>, Andrew Tucker<sup>1</sup>, Naomi Hyun<sup>1</sup>, Rachel Berger<sup>1</sup>, Hannah Keirnes<sup>1</sup>, Lisa V. Goodrich<sup>1</sup>

<sup>1</sup>*Harvard Medical School*

Morphogenesis of the complex labyrinths of the inner ear involves precisely regulated cell proliferation, cell death, and cell-cell interactions in the epithelium and mesenchyme of the developing otic vesicle. Here, we report that the novel Ig superfamily protein Lrig3 is required for the correct formation of the vestibular system as well as proper function of the mature cochlea.

Lrig3 is a single pass transmembrane protein with 16 leucine rich repeats and 3 Ig domains in the extracellular region, and a short cytoplasmic tail with no known motifs. Lrig3 is disrupted in the gene trap line LST016 in which the wild-type transcript is truncated and replaced with beta-galactosidase and alkaline phosphatase reporter genes. Lrig3LST016 homozygous mutant mice demonstrate circling and head tossing behaviors, suggestive of inner ear defects.

Consistent with the observed behavioral phenotype, Lrig3 LST016 mutant inner ears have truncated lateral semicircular canals. Canal formation appears grossly normal until embryonic day 11.75, when the posterior portion of the lateral pouch of the mutant seems significantly reduced in size when compared to wild type littermates. By E13, the lateral canals of all Lrig3LST016 mutants end blindly and fail to form a complete structure. Lrig3 is expressed in the lateral domain of the developing

otic vesicle (OV), which eventually gives rise to the lateral semicircular canal, as well as in the surrounding mesenchyme. Although *Lrig3* expression is detected during otic vesicle patterning, mouse mutants show normal expression of all marker genes examined relative to control tissue. Thus, we conclude that *Lrig3* functions at a developmental stage after specification to influence lateral canal morphogenesis, possibly by modulating the extent of fusion in the fusion plate. In addition to vestibular deficits, *Lrig3*LST016mutant mice also demonstrate auditory deficits by 6 weeks of age as assessed by Auditory Brainstem Response (ABR) measurements. *Lrig3* expression is detected in the thickened portion of the developing cochlear epithelium, suggesting an additional role for *Lrig3* in the development or maturation of the Organ of Corti.

Current studies are aimed at understanding the molecular functions of *Lrig3* and elucidating the effects of *Lrig3* mutations in the fusion plate and in the Organ of Corti.

### **297 Anomalous Inner Ear Development of *Foxg1* Knockout Mice**

**Chan-Ho Hwang<sup>1</sup>**, Michael Mulheisen<sup>1</sup>, Eseng Lai<sup>2</sup>, Doris K. Wu<sup>1</sup>

<sup>1</sup>National Institute on Deafness and Other Communication Disorders, Rockville, MD, <sup>2</sup>Merck Research Labs

*Foxg1* is a winged helix transcription factor that is required for eye and cerebral hemisphere development in mice. During embryogenesis, this transcription factor is also expressed in some cranial placodes including the otic placode. *Foxg1* knockout mice show hypoplasia of telecephalon and anomalous development of the eye and ear. We investigated the role of *Foxg1* in inner ear development by injecting latex paint to the lumen of the mutant inner ears at 15.5 days post coitum. Inner ears of *Foxg1* mutants display an interesting phenotype of a single, anteriorly-positioned, ampulla connected by the anterior and lateral canals. In addition, the cochlear duct is shortened with only a single coil. In normal otocysts, the presumptive anterior and lateral cristae initially share a common *Bmp4*-positive domain that later splits to form two separate entities. In the *Foxg1* mutants, it is not clear whether the single crista located anteriorly represents the anterior crista alone or fused anterior and lateral cristae. Our preliminary gene expression analyses indicate that the presumptive lateral crista is initially specified in *Foxg1* mutants but disappear shortly after it separates from the anterior crista. We are currently investigating the cause for the disappearance of the lateral crista in the *Foxg1* mutants.

### **298 *Foxg1* Is Required for Morphogenesis and Histogenesis of the Mammalian Inner Ear**

**Sarah Pauley<sup>1</sup>**, Bernd Fritsch<sup>1</sup>

<sup>1</sup>Creighton University, Omaha, NE

*Foxg1* is a member of the forkhead gene family involved in patterning, morphogenesis, cell fate determination, and proliferation. Forkhead proteins contain both a DNA and a protein binding domain that interacts with various gene families, including Groucho, Hes, and Runx, to regulate

transcription of genes such as bHLH genes. *Foxi1* is essential for otic development in zebrafish but not in mammals where ears form even in the absence of *Foxi1*, but develop endolymphatic hydrops. Like *Foxi1*, *Foxg1* expression is in the developing otocyst of both zebrafish and mammals. Here we show *Foxg1* expression in later developmental stages of the otocyst and in the adult in most, but not all, cell types of the inner ear. We show that *Foxg1* mutants have both morphologic and histologic defects in the inner ear. These mice have a shortened cochlea with multiple rows of hair cells and supporting cells. Additionally, these mice completely lack a horizontal crista, although the horizontal canal forms. Anterior and posterior crista and canals are reduced to varying degrees; particularly when compounded with *Fgf10* heterozygosity. These compounding *Fgf10* heterozygotic effects suggests a molecular interaction between *Fgf10* and *Foxg1* during inner ear development, likely mediated through BMP regulation. We hypothesize that sensory epithelia formation and canal development are linked in the anterior and posterior canal systems, but are uncoupled in the evolutionarily more recent horizontal canal system. Finally, these mice demonstrate striking abnormalities in cochlear and vestibular innervation including sensory neurons that over shoot the cochlea. Most unusual are neurons from the anterior crista that do not project to the brain but to the cochlea instead, establishing an 'interepithelial connection'. As seen in the forebrain of *Foxg1* mutants, cell cycle regulation and cell fate commitment alterations may account for the loss of innervation in parts of the *Foxg1* mutant ear.

### **299 The *Fgf8* Signaling Pathway Plays an Inductive Role in Pillar Cell Development**

**Bonnie Jacques<sup>1,2</sup>**, Erynn Layman<sup>1</sup>, Mark Lewandoski<sup>3</sup>, Matthew W. Kelley<sup>1</sup>

<sup>1</sup>NIH-NIDCD, Maryland, <sup>2</sup>University of Maryland, <sup>3</sup>NIH-NCI, Maryland

Fibroblast growth factor 8 (*Fgf8*) regulates the development of many organ systems by signaling through Fgf receptor 3 (*Fgfr3*). *Fgfr3* signaling has been shown to be crucial for the development of the organ of Corti (OC), and mutations in this receptor result in profound deafness in mice. *Fgfr3* is initially expressed in a precursor pool of cells abutting the developing inner hair cells (IHCs) beginning at E15.5. At this stage, specialized cells also begin to differentiate from this pool. Directly adjacent to the IHCs are two pillar cells (PCs) followed by three rows of outer hair cells (OHCs) and underlying Deiter's cells. Given that *fgf8* is expressed exclusively by IHCs and is a secreted protein, we predicted that *Fgf8* would regulate activation of *Fgfr3* and cellular differentiation within the OC. We used a cre-lox strategy to generate an otocyst-specific knock-out of *fgf8*. PCs in mice lacking *fgf8* show a reduction in overall size and lack a characteristic pillar head extending to the luminal surface. This reduction in PC development is even more apparent in whole-organ cochlear explant cultures treated with a function-blocking antibody specific to *Fgf8*. To determine whether over-expression of *Fgf8* would positively influence PC development, an expression vector for full-length *fgf8* and GFP was electroporated into cochlear explant cultures.

Clusters of Fgf8-expressing cells found adjacent to the OC induced the formation of ectopic PCs, but only in the region of the OC which expresses Fgfr3. No PC-like cells were found in the inner or outer sulci. In contrast, electroporated cells found within the developing OC failed to express PC markers and developed as hair cells. This suggests that Fgf8 acts non-autonomously to positively induce pillar cell differentiation in cells that express Fgfr3. The gradient of Fgf8 generated by IHCs most likely acts at high levels to promote PC differentiation, which results in the positioning of PCs directly adjacent to IHCs.

### **[300] Hedgehog Signaling and GLI3 Are Required for Development of the Mammalian Cochlear Sensory Epithelium**

**Elizabeth Driver**<sup>1</sup>, Shannon Pryor<sup>2</sup>, Patrick Hill<sup>3</sup>, Joyce Turner<sup>4</sup>, Ulrich R  ther<sup>3</sup>, Leslie Biesecker<sup>4</sup>, Andrew Griffith<sup>2</sup>, Matthew W. Kelley<sup>1</sup>

<sup>1</sup>NIDCD, Bethesda, MD, <sup>2</sup>NIDCD, NIH, Rockville, MD,

<sup>3</sup>Heinrich-Heine University, D  sseldorf, Germany, <sup>4</sup>NHGRI, NIH, Bethesda, MD

Mutations in components of the hedgehog signaling pathway can cause a variety of human diseases, from sporadic cancers to severe congenital defects. Mutations in the transcription factor *GLI3*, which acts both as an activator and a repressor of hedgehog signaling, result in at least five distinct clinical phenotypes including Pallister-Hall syndrome (PHS). PHS is associated with imperforate anus, hypothalamic hamartoma, central polydactyly, and other defects. Recently, we have found that some PHS patients also exhibit mild to moderate hearing loss, primarily affecting lower frequencies. To explore the basis for this auditory defect, we examined the inner ears of a mouse model of PHS (*Gli3*<sup>Δ</sup>), which produces only the truncated, repressor form of the Gli3 protein. Although the vestibular portions of the inner ear appear unaffected in *Gli3*<sup>Δ</sup> homozygous embryos, the cochleae had a variably penetrant phenotype. Some cochleae were nearly normal, while others were much shorter and broader than wild-type. There are further defects on a cellular level, most notably large ectopic patches of hair cells in K  lliker's Organ with vestibular rather than cochlear characteristics. These ectopic hair cells appeared to be innervated, which could contribute to disruption of cochlear function. We also observed mispatterning of the endogenous hair cells; in strongly affected *Gli3*<sup>Δ</sup> mutant cochleae, there are as many as seven rows of hair cells, but the rows are disorganized and irregular. As the cellular pattern of hair cells in the cochlea is critical for sensory function, these patterning defects could lead to auditory deficits as well. The truncated Gli3 protein can act only as a repressor of hedgehog signaling, so to determine if activation of the pathway would also affect patterning, we treated cochlear explants with Sonic hedgehog protein (Shh). Consistent with an inhibitory role for hedgehog signaling in hair cell development, we found that Shh treatment represses in vitro development of hair cells relative to controls. These findings are the first to suggest both a role for hedgehog signaling in development of the cochlear sensory epithelium, and that hearing loss can result from *GLI3* mutations in PHS.

### **[301] Fgfr3 Regulates Multiple Events During Development of the Organ of Corti**

**Chandrakala Puligilla**<sup>1</sup>, Shin-Ichiro Kitajiri<sup>1</sup>, Feng Feng<sup>2</sup>, Bernd Fritzsch<sup>2</sup>, Andrew Griffith<sup>1</sup>, Matthew W. Kelley<sup>1</sup>

<sup>1</sup>NIH-NIDCD, Maryland, <sup>2</sup>Creighton University, Omaha, NE

The organ of Corti is composed of one row of inner hair cells, three rows of outer hair cells (OHCs) and at least four distinct types of supporting cells, including inner phalangeal cells, inner and outer pillar cells, and Deiter's cells. Previous results have demonstrated that the Fgf signaling pathway, and in particular Fgfr3, plays a crucial role in development of pillar cells. In particular, Fgfr3 mutant mice are deaf and pillar cell development is disrupted. However, the initial expression of Fgfr3 is not restricted to pillar cells but also includes progenitors that will develop as outer hair cells and Deiter's cells. Considering the profound loss of hearing in these animals, it seemed possible that Fgfr3 might mediate additional developmental events in the organ of Corti, in particular in outer hair cells and Deiter's cells. Analysis of the organ of Corti from Fgfr3 mutants indicated a significant increase in the number of outer hair cells with four rows of outer hair cells present from the mid-base to the apical region of the cochlea. In addition, patterning of these four rows of OHCs appeared disorganized. Development of Deiter's cells was also disrupted with decreased levels of tubulin as compared with WT, suggesting defects in differentiation. As previously reported, ABR recordings in mutant mice indicated profound hearing loss as compared with WT littermates. Finally, based on lipophilic dye tracing, there is an increase in tunnel crossing fibers forming an extra spiral bundle near what appears to be the first row of OHCs in Fgfr3 mutants. To begin to identify the downstream signaling pathways that might mediate these events, semi-quantitative PCR was used to assess changes in expression of two known targets of Fgfr3 signaling, Indian Hedgehog (Ihh) and Patched1 (ptc1). Results indicated that expression of both Ptc1 and Ihh are increased in Fgfr3 mutant cochlea, suggesting that Fgfr3 is a negative regulator of Ihh signaling in the cochlea. These results suggest that Fgfr3 mediates multiple events during development of the organ of Corti, in particular in pillar cells, OHCs and Deiter's cells.

### **[302] The Pou4f3 Transcriptional Regulation Cascade in the Inner Ear: Gfi1 and Lhx3 as Targets**

**Ronna Hertzano**<sup>1,2</sup>, Mireille Montcouquiol<sup>2</sup>, Amiel A. Dror<sup>1</sup>, Katharina Fiolka<sup>3</sup>, Buffy S. Ellsworth<sup>4</sup>, Sally Camper<sup>4</sup>, Tarik M  r  y<sup>3</sup>, Thomas B. Friedman<sup>5</sup>, Matthew W. Kelley<sup>2</sup>, Karen B. Avraham<sup>1</sup>

<sup>1</sup>Dept. Human Molecular Genetics & Biochemistry, Sackler School Medicine, Tel Aviv U, Tel Aviv, Israel, <sup>2</sup>Section on Developmental Neuroscience, NIDCD-NIH, Rockville, MD, USA, <sup>3</sup>Institut f  r Zellbiologie, Universit  tsklinikum Essen, Essen, Germany, <sup>4</sup>Department of Human Genetics, University of Michigan Medical School, Ann Arbor, MI, USA, <sup>5</sup>Section on Human Genetics, NIDCD-NIH, Rockville, MD, USA

A mutation of the gene encoding the POU4F3 transcription factor underlies human autosomal dominant non-

syndromic progressive hearing loss DFNA15. We have previously identified and validated growth factor independence 1 (*Gfi1*) as an *in vivo* target gene regulated by Pou4f3, by using Affymetrix oligonucleotide microarrays to generate expression profiles of inner ears of *Pou4f3<sup>ddl/ddl</sup>* mutant and wild type mice.

Gfi1 is a transcriptional repressor essential for hematopoiesis and hearing. Mice with a targeted deletion of *Gfi1* are neutropenic and suffer from deafness and vestibular dysfunction. Gfi1 shares with its paralogue Gfi1b, its two main functional domains: an amino terminal SNAG-repressor domain and six carboxy terminal zinc finger motifs. In order to understand the importance of each domain in the function of the protein, we generated knock-in mutants with an inactivating point mutation (P2A) in the Gfi1 SNAG domain, or a replacement of the Gfi1 coding region by Gfi1b. The mutants reveal similarities as well as cell type specific functions in the requirement of the Gfi1 functional domains in the mouse hematopoietic system and the inner ear.

Finally, we demonstrate that Lhx3 is an additional downstream target gene of Pou4f3. We first show that the levels of *Lhx3* mRNA are reduced 5-7 fold in the inner ears of the embryonic *Pou4f3* mutant mice, and we further show that *Lhx3* is a hair cell-specific gene expressed in all hair cells of the auditory and vestibular system as early as E16. We also present data demonstrating that the expression of *Lhx3* is differentially regulated in the auditory and vestibular hair cells. This is the first example of a hair cell-specific gene expressed both in auditory and vestibular hair cells, with differential regulation of expression in these two closely related systems.

Research supported by the US-Israel Binational Science Foundation (BSF) and the European Commission FP6 Integrated Project EUROHEAR LSHG-CT-20054-512063.

### **[303] Effects of Thyroid Hormone Deficiency on Cochlear Development and Function**

Mirna Mustapha-Chaib<sup>1</sup>, Qing Fang<sup>1</sup>, Lisa A. Beyer<sup>1</sup>, Jill Karolyi<sup>1</sup>, Masahiko Izumikawa<sup>1</sup>, Gary Dootz<sup>1</sup>, Tzy-Wen Gong<sup>1</sup>, Margaret Lomax<sup>1</sup>, David Dolan<sup>1</sup>, Yehoash Raphael<sup>1</sup>, Sally Camper<sup>1</sup>

<sup>1</sup>University of Michigan

Thyroid hormone (TH) insufficiency causes hearing loss and mental retardation in humans and rodents. Rodent models include pharmacological ablation of the thyroid gland and genetic disruption of endogenous TH receptors (THR). Deafness in these models is attributed to lowered endocochlear potential (EP), tectorial membrane abnormalities, delayed development of the organ of Corti, and impaired synaptogenesis. Extrapolation from these models to the human condition is limited by two confounding factors: the potential side effects of pharmacological treatment and the fact that THRs regulate transcription in the absence of TH, making it difficult to distinguish the effects of THR loss from TH loss. We selected three genetically defined strains of hypothyroid mice deficient in pituitary thyrotropin (TSH), with no measurable TH, to explore the molecular basis for deafness induced by TH insufficiency. All three strains of

TSH deficient mice have hearing loss and respond to oral TH replacement. We chose the *Pit1<sup>dw</sup>* strain for further characterization because it had the most profound deafness. DPOAEs are absent, and EP is reduced to 50 mV. Although  $\beta$ -tectorin expression is not grossly affected, mutants exhibit abnormal tectorial membrane ultrastructure and delayed development of the tunnel of Corti. Neurogenesis is delayed, although afferent and efferent innervation occurs at the base of the hair cells. Among the observed pathologies are outer hair cell (OHC) loss and alteration in the structure of pillar cells. Using light microscopy we observed no obvious morphological abnormalities in the spiral ligament and the stria vascularis. In summary, the *Pit1<sup>dw</sup>* model has both similar and unique features relative to the pharmacological and THR knockout models. We hypothesize that the permanent abnormalities in the tectorial membrane and the poor survival of OHC are likely major contributors to the profound deafness.

Supported by NIDCD R01-DC05401, R01-DC05053, P30-DC05188.

### **[304] RIBEYE-B Is Necessary for Visual Function in Zebrafish**

Yvonne Bradford<sup>1</sup>, William Roberts<sup>1</sup>

<sup>1</sup>University of Oregon

RIBEYE is a unique protein that has been shown to be associated with synaptic ribbons found at the synapses of sensory receptors and neurons of the inner ear and retina. A synaptic ribbon can be characterized as a presynaptic osmiophilic dense body, or ribbon, that is surrounded by tethered synaptic vesicles. Due to the ribbons close proximity to the active zone and synaptic vesicle associations, it has been hypothesized to be involved in synaptic vesicle cycling at the synapse. RIBEYE was initially identified in human, cow and rat by Schmitz *et al.* (2000) and further investigated in zebrafish by Wan *et al.* (2005).

RIBEYE is encoded by the *CTBP2* gene, which also encodes C-terminal binding protein 2 (CtBP2). CtBP2 acts as a transcriptional co-repressor that binds zinc finger proteins and RIBEYE is a cytoplasmic protein that appears to be a structural component of ribbon class synapses. To understand how novel developmental and physiological functions can evolve from a single gene, we have been investigating the genomic structure and embryological function of *CTPB2* in zebrafish and pufferfish. We have determined that the last common ancestor of fish and mammals already had a single copy of the *CTPB2* gene, and that a later duplication in the fish lineage generated a second copy of this and several flanking genes in pufferfish and zebrafish. This duplication resulted in the production of Ribeye-a and Ribeye-b. Characterization of Ribeye-a by Wan *et al.* (2005) shows that knockdown of Ribeye-a transcripts leads to a loss of visual function as assayed by the lack of an optokinetic response in zebrafish. To further understand the function of RIBEYE-b at ribbon synapses we are currently using Morpholinos to block translation of Ribeye-b transcripts. Initial results

suggest that knockdown of RIBEYE-b leads to loss of visual function in zebrafish as assayed by a lack of optokinetic response.

### **305 Cadherin-2 Function in Inner Ear**

#### **Development**

**Yu-chi Shen**<sup>1</sup>, Sherry Babb-Clendenon<sup>2</sup>, Qin Liu<sup>3</sup>, James Marrs<sup>2</sup>, Kate Barald<sup>1</sup>

<sup>1</sup>*University of Michigan, Departments of Cell and Developmental Biology and Biomedical Engineering,*

<sup>2</sup>*Department of Medicine, Indiana University Medical Center,* <sup>3</sup>*University of Akron, Department of Biology*

Molecular mechanisms that control inner ear morphogenesis from the placode to the three dimensional functional organ are not well understood. We hypothesize that cell-cell adhesion mediated by cadherin molecules regulates various stages of inner ear formation. To investigate the role of cadherin-2 in otic vesicle morphogenesis, a loss-of-function strategy involving cadherin-2 morpholino antisense oligonucleotide knockdown was used. The morphants were compared to wild type embryos, control MO-injected and sham injected embryos at the 1-4 cell stage and to glo mutant, a *cdh2* null mutant, embryonic zebrafish. Placode formation and vesicle cavitation occurred normally in both *cdh2* morphants and glo embryos, but morphogenesis of the otic vesicle was affected by cadherin-2 deficiency: semicircular canals (SCC) were reduced or absent. Phalloidin staining demonstrated that there was no change in hair cell number due to *cdh2* loss-of-function, but the kinocilia of hair cells in all sensory organs examined were shorter and irregularly shaped. In addition, statoacoustic ganglion (SAG) size was significantly reduced, suggesting that neuronal differentiation was affected. Significant morphological changes in the inner ear of *cdh2* morphant and glo mutants during organogenesis, as well as altered gene expression patterns examined by in situ hybridization strongly suggest that *Cdh2* is necessary for normal inner ear differentiation.

**Acknowledgements:** Two photon images were acquired at the Indiana Center for Biological Microscopy, which is partially funded by a grant (Indiana Genomics Initiative) from the Lilly Endowment to the Indiana University School of Medicine. This work was supported by a grant from the NIH to J.A.M, K.F.B and Q.L. (RO1 DC006436) and by grants from the DRF and the NIH to KFB (NIH DC05939 and DC04184) as well as NIH training grant support to Y-c Shen (T32 DC00011 University of Michigan).

### **306 Fgf-Dependant Otic Induction Requires Competence Provided by Foxi1 and Dlx3b**

**Stefan Hans**<sup>1</sup>, Joe Christison<sup>1</sup>, Dong Liu<sup>1</sup>, Monte Westerfield<sup>1</sup>

<sup>1</sup>*Institute of Neuroscience*

The inner ear arises from a specialized set of cells, the otic placode, that forms at the lateral edge of the neural plate adjacent to the hindbrain. Previous studies indicate that fibroblast growth factors (Fgfs) are required for otic induction; in zebrafish, loss of both *fgf3* and *fgf8* results in total ablation of otic tissue. Furthermore, gain-of-function

studies suggested that Fgf signaling is also sufficient for otic induction; misexpression of *fgf3* or *fgf8* leads to formation of ectopic otic tissue by cells that are competent. We previously suggested that *Foxi1* and *Dlx3b* may provide this competence because loss of both *foxi1* and *dlx3b* results in loss of all otic tissue even in the presence of a fully functional Fgf signaling pathway.

Using a transgenic approach that allows us to misexpress *fgf8* under the control of the zebrafish temperature-inducible *hsp70* promoter, we readdressed the role of Fgf signaling and otic competence during placode induction. We find that misexpression of *fgf8* fails to induce formation of ectopic otic vesicles and has different consequences depending upon the developmental stage. Overexpression of *fgf8* at early to midgastrula stages leads to formation of smaller otic vesicles. Overexpression at these stages never leads to ectopic expression of *foxi1* or *dlx3b* contrary to previous studies that indicated that *foxi1* is activated by Fgf signaling. Consistent with our results we find that pharmacological inhibition of Fgf signaling has no effect on *foxi1* or *dlx3b* expression, but instead, both *foxi1* and *dlx3b* are activated by the Bmp signaling pathway. In contrast, *fgf8* overexpression later at the end of gastrulation when otic induction begins, leads to much larger otic vesicles. We further show that a low dose of retinoic acid that does not perturb patterning of the neural plate leads to an expansion of *foxi1* in the *dlx3b* expression domain and massive *fgf*-dependant otic induction.

These results provide further support for the hypothesis that *Foxi1* and *Dlx3b* provide competence for cells to respond to Fgf and form an otic placode.

### **307 The Effect of $\gamma$ -Secretase Inhibitor or TACE Inhibitor to Hair Cell Development in Embryonic Cochlear Organ Culture**

**Shinji Takebayashi**<sup>1</sup>, Norio Yamamoto<sup>1</sup>, Daisuke Yabe<sup>1</sup>, Hitoshi Fukuda<sup>1</sup>, Ken Kojima<sup>1</sup>, Juichi Ito<sup>1</sup>, Tasuku Honjo<sup>1</sup>

<sup>1</sup>*Kyoto University*

**Introduction:** In mammals, there has been no therapeutics for hair cell damage in inner ears. To achieve regeneration of hair cells, it is first important to elucidate molecular mechanisms underlying hair cell development. Notch signaling has been shown to be involved in the development of inner ear hair cells by specifying cell fate between the hair cell and the supporting cell. The Notch signaling is activated through binding of Notch receptor to ligands. This binding initiates proteolytic cleavage of the Notch receptor by TACE and  $\gamma$ -secretase, releasing the intracellular domain of the Notch (NICD) from membrane. NICD enters the nucleus, forms a complex with a DNA binding protein RBP-J and activates target genes, thereby controlling cell differentiation. Though it was reported in vivo experiment that hair cells were increased by the deletion of genes which are involved in Notch signaling, Yamamoto, et al. showed that  $\gamma$ -secretase inhibitor, one of the drugs for the inhibition of Notch signaling, increased hair cells at postnatal mouse in vitro experiment. In order to elucidate the timing and mechanisms of the Notch signaling to hair cell development, we examined the effect of  $\gamma$ -secretase inhibitor or TACE inhibitor to hair cell development in embryonic cochlear organ culture.

Method: Mouse cochlea was prepared from embryos at embryonic day (E) 12.5, E14.5, or E17.5, and then cultured in vitro. The  $\gamma$ -secretase or TACE inhibitor was supplemented in the culture to block the Notch signaling.

Result:  $\gamma$ -secretase inhibitor or TACE inhibitor increased hair cells for E14.5 or E17.5 cochlear organ culture. But hair cells were not increased for E12.5 cochlear organ culture. BrdU uptake was seldom observed in increased hair cells. These results suggest that the effect of Notch signaling inhibitor was dependent on timing, and hair cell increase was not for cell proliferation but for cell differentiation.

### **[308] Mapping of Notch Activation During Cochlear Development in Mouse: Implications for Determination of Prosensory Domain and Cell Fate Diversification**

**Junko Murata<sup>1</sup>**, Akinori Tokunaga<sup>2</sup>, Hideyuki Okano<sup>2</sup>, Katsumi Doi<sup>1</sup>, Arata Horii<sup>1</sup>, Manabu Tamura<sup>1</sup>, Takeshi Kubo<sup>1</sup>

<sup>1</sup>*Department of Otolaryngology and Sensory Organ Surgery, Osaka University School of Medicine,*

<sup>2</sup>*Department of Physiology, Keio University School of Medicine*

Notch signaling has been shown to play context-dependent distinct roles in inner ear development based on the recent chick experiments: initially, Notch activity confers on groups of cells a prosensory character by lateral induction, subsequently, it is involved in the establishment of fine-graded patterns of hair cells and supporting cells by lateral inhibition (Daudet and Lewis, 2005). We investigated the expression patterns of activated form of Notch1 (actN1) as well as that of endogenous Notch1, Jagged1 (Jag1), and Math1 during mouse cochlear development. The activated form of Notch1 was detected by immunohistochemistry using an antibody that specifically recognizes the processed form of the intracellular domain of Notch1 cleaved by presenilin/ $\gamma$ -secretase activity (Tokunaga et al., 2004).

Between E12.5 and E14.5, actN1 was weakly observed mainly in the medial region of cochlear epithelium, where Jag1-immunoreactivity was also detected. Jag1 expression became gradually stronger in the more sharply defined area, localized in supporting cells at last, and actN1 was detected in the overlapped area. Thus a positive feedback loop was assumed to exist between the expression of Jag1 and actN1 in the medial region of the cochlear epithelium. ActN1 started to be strongly expressed in the cells surrounding Math1-positive hair cell progenitors between E14.5 and E15.5. Strong actN1-expression continued both in a supporting cell lineage and in the greater epithelial ridge (GER) during the perinatal stage but over by P7. We had already reported a part of this late embryonic and postnatal expression pattern of actN1 during mouse cochlear development in 2005 ARO MWM. These results suggest the possibility that Notch1 activation functions to demarcate a prosensory region in the cochlear epithelium at first, then it inhibits progenitor cells from becoming hair cells by classical lateral inhibition. In addition, the transient but strong activation of Notch1 in

supporting cell lineage after birth seems to play a crucial role in the terminal differentiation of supporting cells.

### **[309] Development and Retinoic Acid-Mediated Teratogenesis of the Inner Ear: A Role for Dlx5** **Dorothy Frenz<sup>1</sup>**, Wei Liu<sup>1</sup>, Lijun Li<sup>1</sup>

<sup>1</sup>*Albert Einstein College of Medicine*

Dlx constitutes a highly conserved family of homeobox genes that play a critical role in craniofacial development. Dlx5 is among the earliest genes expressed in the developing mouse inner ear. Inactivation of Dlx5 produces embryos with a complex phenotype characterized by anomalies of branchial arch derivatives, defects in osteogenesis, and inner ear dysmorphogenesis. Inner ear anomalies include absence of the anterior and posterior semicircular canals, incomplete elongation of the endolymphatic duct, and a hypoplastic, malformed otic capsule. Recent studies in our laboratory indicate that loss of Dlx5 may contribute to otic capsule anomalies by regulating expression of diffusible epithelial-derived factors that are known to play a role in otic capsule formation, including members of the transforming growth factor-beta superfamily. In utero exposure to teratogenic doses of all-trans retinoic acid (atRA), which results in inner ear and otic capsule anomalies resembling the Dlx5 phenotype, alters expression of Dlx5 in the developing inner ear. Control of Dlx5 during atRA-mediated teratogenesis is hypothesized to be regulated by upstream fibroblast growth factors 3 and 10 (FGF3, FGF10), both of which are downregulated by atRA prior to Dlx5 repression. When tested in a culture model of atRA-treated periotic mesenchyme containing otic epithelium, a combination of exogenous FGF3 and FGF10 could rescue the atRA-mediated suppression of otic capsule chondrogenesis and restore levels of endogenous Dlx5 expression. We propose a model of teratogenesis whereby modification of FGF3,-10 expression by atRA produces repression of Dlx5 expression and its downstream target genes, leading to the atRA phenotype.

(Supported by NIH/NIDCD grant R01 DC004706 and the Institute for Communicative Disorders, Albert Einstein College of Medicine)

### **[310] Ectopic Application of Sonic Hedgehog in the Developing Chick Inner Ear Leads to Reduced GATA3 Expression and Disorganization of the Vestibular Organs**

**Andrew J. Drescher<sup>1</sup>**, Jacob Kach<sup>1</sup>, Mark E. Warchol<sup>1</sup>

<sup>1</sup>*Department of Otolaryngology, Washington University School of Medicine, St. Louis, MO*

Development of the inner ear is regulated by local signaling molecules and regionalized gene expression. GATA3 is a zinc-finger transcription factor that is involved in normal inner ear development. It is expressed in the developing otic vesicle, the peri-otic mesenchyme and in a subset of sensory neurons. Within the otic epithelium, GATA3 is expressed in characteristic patterns within or adjacent to developing sensory organs. Correct expression of GATA3 is important for correct inner ear

morphogenesis, but the upstream factors regulating its expression are unclear. The morphogen Sonic hedgehog (SHH) has been shown to regulate GATA3 expression in other cell types. SHH is also secreted by the notochord and floor plate and has been shown to direct several aspects of inner ear development. Ectopic expression of SHH in the *ShhP1* transgenic mouse leads to an absence of vestibular structures (semicircular canals, utricle, and saccule) and increased neural progenitors (Riccomagno et al., *Genes Devel* 16:2365, 2002). We have studied the effect of ectopic SHH on GATA3 expression and sensory organ formation in the developing chick ear. SHH-coated beads were implanted in otic vesicles at E2.5, and embryos were then examined at E5-7. As in the *ShhP1* mouse, the SHH-treated ears lacked all three semicircular canals. Some hair cells continued to differentiate in regions where the cristae normally form, but these sensory patches were small and disorganized, and associated with decreased GATA3 expression. There was also a large, disorganized sensory patch in the central-dorsal otocyst, near the normal position of the utricle and saccule. GATA3 was expressed on both sides of this sensory region. GATA3 labeling in the cochlear duct and ventral mesenchyme was similar to that in control embryos, though the cochlear duct was shorter in length. These results further implicate SHH in vestibular development, perhaps by modifying GATA3 expression.

(Supported by NIH and NASA)

### **[311] The Role of Gbx2 and Otx2 in the Formation of Cochlear Ganglion and Endolymphatic Duct**

**Hiromitsu Miyazaki<sup>1</sup>**, Toshimitsu Kobayashi<sup>1</sup>, Harukazu Nakamura<sup>2</sup>, Jun-ichi Funahashi<sup>3</sup>

<sup>1</sup>*Department of Otolaryngology, Head and Neck Surgery, Tohoku University Graduate School of Medicine,*

<sup>2</sup>*Graduate School of Life Sciences, Tohoku University,*

<sup>3</sup>*Department of Molecular Neurobiology, Institute of Development, Aging and Cancer, Tohoku University*

Gbx2 and Otx2 are transcription factors expressed in the chick otic vesicle almost complementarily: Gbx2 expression in the dorsomedial region, which includes endolymphatic duct, and Otx2 expression in the ventral region. Between their expression boundaries, Fgf10 is expressed and cochleovestibular ganglion develops close to the medial side of Fgf10 expression domain. In the central nervous system, Otx2 and Gbx2 expression abut at the mid-hindbrain boundary, and the repressive interaction between Otx2 and Gbx2 defines the mid-hindbrain boundary. By analogy between these expression patterns, we wondered if the interaction between Gbx2 and Otx2 plays a role in the development of inner ear. To address this, we have misexpressed Gbx2 and Otx2 to the otic epithelium with in ovo electroporation. Ectopic Gbx2 and Otx2 expression could repress each other's expression, and as a consequence of their interaction, Fgf10 expression was repressed. In addition, cochlear ganglion formation was interfered by Gbx2 or Otx2 misexpression. Moreover, endolymphatic duct was severely hypomorphic in the Otx2 misexpressing embryos, which Gbx2 expression was repressed by Otx2. These results suggest

that the interaction between Gbx2 and Otx2 in developing inner ear defines the Fgf10 expression domain to induce cochlear ganglion. These results also suggest that Gbx2 expression is necessary for the formation of endolymphatic duct.

### **[312] Heterogeneous Precursors of the Mammalian Auditory Sensory Organ Are Competent for Sensory Hair Cell Differentiation**

**Dong Qian<sup>1</sup>**, Sharayne Mark<sup>1</sup>, Qin Chang<sup>1</sup>, Kristen Radde-Gallwitz<sup>1</sup>, Xi Lin<sup>1</sup>, Ping Chen<sup>1</sup>

<sup>1</sup>*Emory University School of Medicine*

The organ of Corti, the mammalian auditory sensory organ, consists of precisely patterned sensory hair cells that are separated by supporting cells. The loss of sensory hair cells in the mammalian cochlea is irreversible, leading to permanent hearing loss in humans. Identification of a bHLH gene, Math1, for hair cell differentiation provided a target for regeneration of hair cells. Here we examined the competency of supporting cells of the auditory organ, the organ of Corti, to differentiate into hair cells upon expression of Math1, and the cellular and physiological consequences of ectopic expression of Math1 in the inner ear. As revealed by both in situ and the expression of a reporter in a bacterial artificial chromosome carrying the Math1 locus, we confirmed that Math1 expression is normally restricted to the hair cell precursors in the precursor domain that gives rise to both hair cells and supporting cells. Targeted ectopical expression of Math1 in the entire precursor domain marked by the expression of a cyclin-dependent kinase inhibitor, p27Kip1, through bacterial artificial chromosome (BAC)-mediated transgenesis, resulted in the production of the hair cells at the expense of supporting cells. The extra hair cells produced, at least partially, at the expense of supporting cells survived till adulthood, and the adult animal with extra hair cells in both the cochlea and vestibule is deaf and displays circling behavior. Together, these data indicated that the precursor domain is heterogeneous but competent to become hair cells upon induction of Math1, and that precise restriction of Math1 expression is required for generation of a functional auditory organ during development and likely in regeneration as well.

### **[313] MATH1/ATOH1 Regulates a Cholinergic Subunit in the Inner Ear**

**Deborah Scheffer<sup>1</sup>**, Duan Sun Zhang<sup>2</sup>, Rachel E. Palmer<sup>3</sup>, David P. Corey<sup>2</sup>, Veronique Pingault<sup>1</sup>

<sup>1</sup>*Equipe Avenir INSERM U654, Hopital Henri Mondor, Creteil, France,* <sup>2</sup>*Department of Neurobiology, Harvard Medical School, Boston,* <sup>3</sup>*Massachusetts General Hospital, Boston*

ATOH1 is a member of the basic helix-loop-helix (bHLH) family of transcription factors which play important roles in neural development. In the developing inner ear, Atoh1 induces the differentiation of sensory hair cells of the cochlea and vestibular organs. In order to identify ATOH1 target genes in the inner ear, we set up a TET-off system in stably transfected osteosarcoma cells. We analyzed the gene expression patterns in the presence and absence of



ATOH1 using Affymetrix® microarrays. One of several genes upregulated by ATOH1 was CHRNA1 (nicotinic cholinergic receptor alpha polypeptide 1).

Nicotinic acetylcholine receptors are ligand-gated ion channels organized in pentamers. CHRNA1 encodes at least two of the five subunits of the muscle acetylcholine receptor. Outer hair cells of the cochlea receive efferent axons to provide a control of cochlear amplifier, acetylcholine being the principal neurotransmitter released by olivocochlear efferent axons. Nevertheless, Chrna1 expression and control have never been described in the inner ear.

We first confirmed Chrna1 upregulation by ATOH1 in osteosarcoma cells by semi-quantitative RT-PCR at various times after inducing ATOH1 expression. Chrna1 is upregulated as early as 2 hours, suggesting a possible direct regulation by ATOH1. We then showed expression of Chrna1 in the mouse cochlea by RT-PCR, which is lost in Atoh1 knockout mice. Because these mice seem to lack only hair cells, Chrna1 expression is apparently hair-cell specific in the auditory organ. We are thus performing immunostaining experiments to confirm that Chrna1 is expressed in mouse organ of Corti. Finally, we studied the activation of Chrna1 by ATOH1 in a luciferase assay system and determined that ATOH1 acts through regulatory regions in the proximal promoter of Chrna1. Electrophoretic mobility shift assays confirmed an identical involvement of two E-boxes located in this region.

We have therefore identified Chrna1 as the first ATOH1 target gene in the inner ear. Chrna1 is the third cholinergic subunit described in the organ of Corti, in addition to Chrna9 and Chrna10. These results could lead to a better understanding of cholinergic receptor organization in inner ear hair cells. Moreover, this work could provide more information about transcriptional control of hair cell development by ATOH1.

### **[314] MATH1/ATOH1 Regulates Expression of the Inhibitor of DNA Binding Id2**

**Veronique Pingault<sup>1</sup>, Nicole Lemort<sup>1</sup>, Duan Sun Zheng<sup>2</sup>, Amelyne David<sup>1</sup>, Zheng-Yi Chen<sup>3</sup>, Yoshifumi Yokota<sup>4</sup>, David P. Corey<sup>2</sup>**

<sup>1</sup>*Equipe Avenir INSERM U654, Hopital Henri Mondor, Creteil, France,* <sup>2</sup>*Department of Neurobiology, Harvard Medical School, Boston,* <sup>3</sup>*Department of Neurology, Massachusetts General Hospital, Boston,* <sup>4</sup>*Department of Molecular Genetics, School of Medicine, Fukui, Japan*

MATH1/ATOH1 has been found to be the major transcription factor involved so far in early differentiation of hair cells. Indeed, ATOH1 has been described as a necessary and sufficient factor to induce hair-cell differentiation. In addition, it was recently shown to allow the generation of new hair-cell-like cells in vivo, and is of interest as a possible tool for clinical hair-cell regeneration.

As no target gene of ATOH1 has been characterized so far in the inner ear, its general mode of action remains largely unknown. To better understand how ATOH1 can specifically induce hair-cell differentiation, we used the mouse OC1 cochlear cell line after transient transfection by Atoh1 and compared the pattern of mRNA expression

by using Affymetrix DNA chips. Among several genes upregulated in Atoh1-transfected cells, we found the HLH transcription factor, Id2, one of a family of Id proteins that are regulators of cell growth and differentiation.

In situ hybridization shows that Id2 is faintly expressed throughout the cochlear sensory epithelium at E13.5, while the Atoh1 transcript just starts to be detected in the basal turn. Id2 is more highly expressed in the area of Atoh1-positive cells at E14.5 and E15.5. At E16.5, hair cells are clearly positive for Id2 mRNA, as seen with on sections adjacent to those with a hair-cell marker. The supporting sensory cells are also positive.

The mouse Id2 promoter was cloned in a luciferase reporter plasmid and transfected into HeLa cells with expression vectors containing mouse cDNAs for Atoh1 and/or E47, a class I bHLH factor used to allow heterodimerization with ATOH1. The basal level of the Id2 promoter is activated by cotransfection with Atoh1 and E47. Sequentially truncated promoters and site-directed mutagenesis were used to determine which region is sensitive to ATOH1. The results indicate that ATOH1 most likely acts in a non-directed manner on the Id2 promoter.

Phalloidin staining in the cochlea of and utricle showed that homozygous Id2 knockout mice present with normal hair cells bundles and no obvious abnormalities of cell patterning or number. This absence of dramatic effect is most likely due to redundancy with other members of the Id family, as has been shown for other tissues that express Id2.

### **[315] The Establishment and Analysis of Transgenic Mice in Which the Inner Ear Cell Lineage Is Marked with GFP**

**Hiddenori Ozeki<sup>1</sup>, Kenji Kondo<sup>1</sup>, Kimitaka Kaga<sup>1</sup>**

<sup>1</sup>*University of Tokyo*

The vertebrate inner ear is derived from the otic placode and passes complicated morphogenetic process to differentiate into sensory epithelium including hair cells. Recently, we established transgenic mouse lines in which GFP expression was driven by the promoter of *ETAR* (the endothelin A receptor gene). One of the transgenic lines exhibited ectopic GFP expression in the inner ear primordium. GFP expression was first detected at E 7.5 in the ventromedial portion of the otic placode. GFP expression was detected throughout the process of ear development in the cell lineage differentiating into the sensory epithelium. This process could be visualized as a helical growth of GFP signals in otic vesicle organ culture. After birth, GFP expression was restricted to hair cells. Intense expression of GFP allowed us to isolate differentiating hair cells by FACS, which revealed the expression of *Pax2*, *Otx2* and *Myosin VIIa* in GFP-positive cells from E10.5 embryos. This population may contain inner ear stem cells as yet unknown. Furthermore, we could identify the genetic locus into which the transgene was integrated. It may lead to the identification of new genes involved in inner ear development. Thus, our mice could be useful for researches on the development and regeneration of the inner ear.



### **316 Ankrd6 as a Candidate Component of the Mammalian PCP Pathway**

**Chonnetia Jones<sup>1</sup>**, Dong Qian<sup>1</sup>, Xiaohui Zhang<sup>1</sup>, Kristen Radde-Gallwitz<sup>1</sup>, Ping Chen<sup>1</sup>

<sup>1</sup>*Emory University School of Medicine*

The organ of Corti consists of precise arrays of sensory hair cells with uniformly oriented stereocilia on the apical surfaces, displaying a distinct polarity parallel to the sensory epithelium. This type of polarity is known as planar cell polarity (PCP). Previously, we and others have shown that several mammalian homologs of the *Drosophila* PCP components are essential for the planar cell polarity in the cochlea during terminal differentiation. Here we report the identification of an additional candidate gene for the mammalian PCP pathway.

We identified the dynamic expression of the mouse *Ankrd6* in the cochlea through differential gene expression and candidate gene approaches. ANKRD6 shares homology with an essential component of the *Drosophila* PCP pathway, **Diego**, within the N-terminal ankyrin repeat domain. However, its sequence diverges from **Diego** outside the ankyrin repeat domain. The expression of *Ankrd6* in the cochlear epithelium during terminal differentiation overlaps with that of other known mammalian PCP components. In addition, *Ankrd6* is also expressed in regions with high expression levels of *Wnt* antagonists. The expression of the mammalian *Ankrd6* in the developing cochlea is consistent with the hypothesized dual role of the zebrafish *Ankrd6* in promoting PCP and inhibiting the canonical *Wnt* transduction. To determine its potential role in PCP regulation, we drove the overexpression of the mammalian *Ankrd6* by engrailed:Gal4 in the posterior region of the wing of *Drosophila*. The overexpression of the mammalian *Ankrd6* in the *Drosophila* wing leads to a PCP phenotype similar to that of over-expression and loss-of-function of *diego*, suggesting a conserved functional role of the mammalian *Ankrd6* in PCP regulation and the conservation of invertebrate and vertebrate PCP pathways. Currently, we are generating transgenic mice with loss-of-function of *Ankrd6* to determine its exact roles in mammals.

### **317 Asymmetric Localization of Vangl2 Indicates Novel Mechanisms for Planar Cell Polarity in Mammals**

**Mireille Montcouquiol<sup>1,2</sup>**, Nathalie Sans<sup>1,2</sup>, David Huss<sup>3</sup>, Jacob Kash<sup>4</sup>, J. David Dickman<sup>3</sup>, Andrew Forge<sup>5</sup>, Jennifer Murdoch<sup>6</sup>, Mark E. Warchol<sup>4</sup>, Robert Wenthold<sup>1</sup>, Matthew W. Kelley<sup>1</sup>

<sup>1</sup>*National Institute on Deafness and Other Communication Disorders, National Institute of Health*, <sup>2</sup>*Institut Francois Magendie, INSERM*, <sup>3</sup>*Department of Anatomy and Neurobiology, Washington University School of Medicine*, <sup>4</sup>*Department of Otolaryngology, Washington University School of Medicine, St. Louis, MO*, <sup>5</sup>*Centre for Auditory Research, UCL Ear Institute, London, UK*, <sup>6</sup>*University of Newcastle upon Tyne, Medical Research Council Mammalian*

The mammalian cochlea represents one of the clearest examples of planar cell polarity (PCP) within a vertebrate

system. Each mechanosensory hair cell (HC) within the cochlea contains a directionally sensitive stereociliary bundle that is oriented towards the distal side of the cell. The understanding of the molecular and biochemical bases for the development of PCP in vertebrate systems is very limited. Recent results have identified a group of mammalian PCP mutants that affect hair cells stereociliary bundle orientation, including *Vangl2*, *Scrb1*, *Celsr1*, and *PTK-7* (Montcouquiol et al., 2003; Curtin JA, et al, 2003; Lu X, et al, 2004). *Scrb1* and *PTK-7* are apparently novel vertebrate PCP genes that have no role in PCP in *Drosophila* (Montcouquiol et al., 2003; Lu et al., 2004).

Our study aims to determine the cellular interactions that mediate PCP in vertebrates through an analysis of the localization of *Vangl2* during the generation of PCP in the mammalian cochlea. We identified two binding partners for *Vangl2*, including *Scrb1*, and analyzed the different domains of interactions of these proteins through biochemistry. We identified a new role for *Scrb1* in mammalian PCP pathway. We also determined that PCP disruption in the cochlea is always concomitant with the loss of asymmetric localization of the *Vangl2*. Our data, taking together with other studies, suggest that while there has been an overall conservation of function in terms of the molecular pathways that generate PCP, significant differences exist between vertebrates and invertebrates.

### **318 Early Developmental Tonotopic Mapping of the Mouse Auditory Midbrain with Mn-Enhanced MRI**

**Xin Yu<sup>1</sup>**, Dan Sanes<sup>2</sup>, Jing Zou<sup>3</sup>, Daniel H. Turnbull<sup>1</sup>

<sup>1</sup>*New York University School of Medicine*, <sup>2</sup>*New York University Center for Neural Science*, <sup>3</sup>*University of Maryland Center for Scientific Computation and Mathematical Modeling (College Park)*

Our previous studies have established the utility of Mn-enhanced MRI (MEMRI) to detect the pattern and magnitude of sound-evoked activity within the mouse inferior colliculus (IC) (Yu et al. *Nature Neuroscience* 8:961-8, 2005). We have now extended this analysis to compare frequency-dependent activation patterns in juvenile mice. The maturation of two frequency-dependent patterns was compared in animals at postnatal (P) days 13, 16, and 19. Following Mn injections, mice were exposed 24 hours in free field of either 40 kHz or 16 kHz stimulation with amplitude modulated between 65 and 89 dB SPL. Since MEMRI produces 3-D image data, statistical analysis has enabled quantification of 3-D IC activity in the form of voxel-by-voxel comparison of the frequency dependent activity patterns. At P13, the activity patterns of the two pure tones are indistinguishable from one another. This was confirmed with a voxel-by-voxel statistical comparison of the two patterns. At P16, the activation patterns were not as distinct from one another. The voxel-by-voxel statistical comparison indicated that the two stimuli elicited different patterns of activity in the ventral IC (i.e., the presumptive 40 kHz region), but not more dorsally (i.e., the presumptive 16 kHz region). At P19, the activity patterns evoked by each tone are clearly separated. MEMRI shows that the spatial pattern of activity evoked by 40 kHz stimulation resolved to a clear ventro-

caudal contour in the IC. The spatial pattern evoked by a 16 kHz stimulus was similar in shape, but located in a more dorsal position, as expected from previous electrophysiological characterizations. Thus, MEMRI revealed a clear maturation of frequency-specific responses within the mouse IC. These results can form the basis for future analyses of altered tonotopy following genetic or environmental manipulations.

Support contributed By: NIH grants NS038461, DC006892, and DC006864

### **319 GDNF-Signaling Through GFRalpha1/Ret-Receptor Complex in Spiral Ganglion Neurons**

Kuo-Hsiung Yang<sup>1</sup>, Sara Euteneuer<sup>1,2</sup>, Kenji Kondo<sup>1,3</sup>, Lina Mullan<sup>1</sup>, Allen F. Ryan<sup>1</sup>

<sup>1</sup>UCSD, Dept. of Otolaryngology, <sup>2</sup>Ruhr-University

Bochum, Dept. of Otorhinolaryngology HNS, Germany,

<sup>3</sup>University of Tokyo, Dep. of Otorhinolaryngology, Japan

Glial cell line-derived neurotrophic factor (GDNF) has been shown to protect spiral ganglion neurons (SGN) in vivo from degeneration after inner hair cell loss in various studies. Many studies in other tissues and organs have identified GFRalpha1 as a specific receptor for GDNF. However, GFRalpha1 lacks an intracellular signaling domain. For signal transduction, GPI-anchored GFRalpha1 can dimerize with two transmembrane Ret receptors after binding of GDNF. Previous studies using different methods showed contradicting data about the presence of Ret in the inner ear. We therefore analyzed the expression of GDNF-, GFRalpha1- and Ret-mRNAs in rat SGN at different ages (P3, P5, P10, P30, and adult) using RT-PCR. Additionally we investigated the effect of GDNF with or without GFRalpha1 on the growth of neurites from neonatal (P4) SGN explant cultures.

We found that GFRalpha1- and Ret-mRNAs are expressed in SGN at all age stages while GDNF-mRNA is expressed at younger ages (P3-P20). In neonatal SGN explant cultures, supplementation with GDNF resulted in an increase of neurite number but not neurite length at the optimal concentration of 25ng/ml. However, further supplementation with soluble GFRalpha1 (10ng/ml) substantially increased the effect of GDNF.

Our data provide evidence for GDNF-signaling through a GFRalpha1/Ret-receptor complex in rat neonatal and adult SGN, and further suggest that soluble GFRalpha1 released from non-neuronal cells may play a role in inner ear GDNF signaling.

S.E. was supported by the DFG (German Research Association), grant EU120/1-1.

### **320 The Severity of Ototoxic Insult Affects Outcome of Atoh1 Treatment**

Masahiko Izumikawa<sup>1</sup>, Shelley Batts<sup>1</sup>, Donald L. Swiderski<sup>1</sup>, Mark Crumling<sup>1</sup>, Toru Miyazawa<sup>1</sup>, David Dolan<sup>1</sup>, Yehoash Raphael<sup>1</sup>

<sup>1</sup>Kresge Hearing Research Institute, The University of Michigan, Ann Arbor, MI, USA

Cochlear hair cell (HC) loss leads to permanent hearing impairment because HCs are not replaced. The bHLH

transcription factor Atoh1 (previously Math1) is essential for HC differentiation during cochlear development. We examined the outcome of *Atoh1* gene over-expression in the mature deafened cochlea. Guinea pigs were deafened by (A) unilateral (left) intracochlear neomycin, or (B) systemic kanamycin followed by ethacrynic acid. Neomycin deafening eliminates both supporting cells (SCs) and HCs in the treated ear; kanamycin-ethacrynic acid deafening eliminates HCs and leaves differentiated SCs in both ears. Four or seven days after the insult, recombinant adenovirus vector (Ad.*Atoh1*, Ad.*Atoh1-GFP*, Ad.empty or Ad.*GFP*) was inoculated into the scala media of the left cochlea. Seven days after Ad.*Atoh1-GFP* inoculation of group A animals, epifluorescence showed many GFP-positive cells in the flat epithelium. At 2 months after Ad.*Atoh1* inoculation, SEM of treated ears revealed a small number of immature looking HCs and absence of the typical organization in the organ of Corti. Some regenerated HCs attracted several neurons, suggesting convergence of innervation. No HCs were found in any control animals. In group B animals at 2 months after *Atoh1* treatment, the auditory epithelium contained numerous new cells with mature stereocilia bundles and partially restored innervation. ABR thresholds showed that treated ears were significantly better than control ears. Cross sections revealed normal appearing inner HCs, whereas new outer HCs were poorly differentiated. These data indicate that the severity of the lesion determines the responsiveness to the *Atoh1* treatment. It is possible that treatment with genes expressed earlier in development may be required to induce regeneration in the absence of differentiated SCs.

This work was supported by B. and A. Hirschfield, GenVec, and NIH/NIDCD Grants R01-DC01634, R01-DC05401, R01-DC05053, T32-DC00011 and P30-DC05188.

### **321 Prestin-Expressing Cells Generated in the Organ of Corti by Atoh1 Gene Delivery In Vivo**

Mark Crumling<sup>1</sup>, Masahiko Izumikawa<sup>1</sup>, Yehoash Raphael<sup>1</sup>

<sup>1</sup>Kresge Hearing Research Institute, The University of Michigan, Ann Arbor, MI, USA

During development of the mammalian cochlea, the transcription factor, Atoh1, induces differentiation of hair cells within the sensory primordium. Poorly understood signals cause further differentiation of the hair cells into two molecularly distinct types, inner and outer hair cells. Inner hair cells are the primary sensory transducers, while outer hair cells act mainly as signal amplifiers, relying on the membrane motor protein, prestin, for their amplifier function. In the mature guinea pig cochlea, adenovirus-mediated expression of *Atoh1* induces the formation of new hair cells. Here we examine whether *Atoh1* expression in the mature, ototoxically damaged cochlea can produce both hair cell types. Guinea pigs were systemically given kanamycin followed by ethacrynic acid to destroy cochlear hair cells. Four or five days later, the left cochlea was inoculated with Ad.*Atoh1-GFP*, Ad.*Atoh1*, Ad.*GFP*, or Ad.empty. Four to nine weeks after inoculation, the organ of Corti tissue was processed

immunohistochemically. By nine weeks after Ad.*Atoh1-GFP* treatment, some of the GFP-positive cells expressing the hair cell marker, myosin VIIa, that were located lateral to the pillar cells (the area normally occupied by outer hair cells) also expressed prestin. By eight weeks after inoculation with Ad.*Atoh1*, myosin VIIa-positive cells were found lateral to the pillar cells having similar morphology to comparably located GFP/myosin VIIa-positive cells in Ad.*Atoh1-GFP* treated ears. Some of these myosin VIIa-positive cells expressed prestin. Prestin was absent in myosin VIIa-positive and GFP/myosin VIIa-positive cells occupying normal inner hair cell positions. The data suggest that the mature, damaged organ of Corti retains the signals necessary to differentiate inner and outer hair cells in appropriate locations and that adenoviral *Atoh1* can restore components of the cochlear amplifier.

Supported by GenVec and by NIH grants R01-DC01634, T32-DC00011, and P30-DC05188.

### **[322] Viral Vector Inoculation Into the Apical Cochlear Endolymph Transduces Cells**

#### **Throughout the Auditory Membranous Labyrinth**

**Toru Miyazawa<sup>1</sup>**, Masahiko Izumikawa<sup>1</sup>, Donald L. Swiderski<sup>1</sup>, Lisa A. Beyer<sup>1</sup>, Mark Crumling<sup>1</sup>, Yehoash Raphael<sup>1</sup>

<sup>1</sup>Kresge Hearing Research, Univ. of MI

Cochlear implant patients with residual apical hair cells perform better than those with no residual sensory cells. It may therefore be beneficial to induce growth of new apical hair cells and combined them with a cochlear implant in the base. Gene transfer experiments in the guinea pig cochlea have most often been performed by inoculation of viral vectors into the 2nd or 3rd turn. Such inoculations result in maximal transduction efficiency near the site of inoculation and decreased efficiency in other areas. Therefore, it is necessary to design inoculation approaches that transduce non-sensory cells in the low frequency (apical) regions of the cochlea. To achieve this goal, we inoculated adenovirus vector with a reporter gene insert (Ad.GFP) into the endolymph of the apex after opening a discharge cochleostomy at the scala media of the second turn. Both deafened (n=8) and normal animals (n=5) were inoculated. The deafened animals were injected systemically with kanamycin and ethacrynic acid seven days before virus inoculation. All animals were sacrificed four days after viral inoculation and the cochleae were stained with GFP antibody to enhance detection of GFP and rhodamine-phalloidin to label actin. Epifluorescence revealed robust GFP expression in Deiters cells and pillar cells in the apical turn of the cochlea. Gene expression extended to lower turns of the cochlea. No transgene expression was observed in hair cells of non-deafened cochleae. The extent of transgene expression in the apical turn may allow substantial hair cell regeneration in this region, to supplement the benefits of a cochlear implant in the base.

Supported by a gift from Berte and Alan Hirschfield, GenVec, RNID, CHD and NIH/NIDCD Grants R01-DC03389, R01-DC01634, R55-DC007634, R01-DC05401, P30-DC05188, and Research account 2005 in Kanazawa Medical University.

### **[323] Prestin Transduction in the Prestin Null Mouse Cochlea *In Vitro* and *In Vivo***

**Anping Xia<sup>1</sup>**, Gentiana Wenzel<sup>1</sup>, Philip Ng<sup>2</sup>, Fred A. Pereira<sup>3</sup>, John Oghalai<sup>1</sup>

<sup>1</sup>Bobby R. Alford Dept. of Otolaryngology – Head and Neck Surgery, <sup>2</sup>Department of Molecular & Human Genetics, <sup>3</sup>Huffington Center on Aging, Bobby R. Alford Dept. of Otolaryngology – Head and Neck Surgery

The prestin protein is a key constituent of the outer hair cell lateral wall and is necessary for electromotility. The prestin null mouse has sensorineural hearing loss and outer hair cells that do not demonstrate electromotility. We sought to transduce prestin within outer hair cells from the prestin null mouse using an adenoviral vector. We created a helper-dependent adenoviral (HDAd) vector containing pCMV-HA-prestin-IRES-hrGFP. We tested the HDAd vector in cultured HEK cells and found that infected cells expressed GFP by 48 hours. We also demonstrated that GFP expressing cells co-expressed HA-prestin using immunofluorescence. We next harvested prestin null cochleae at P2 for organotypic cultures. 1.5x10<sup>10</sup> vp/ml HDAd were applied and organs cultured for 48 hours. Analysis of organs showed GFP to be expressed within outer hair cells, supporting cells as well as spiral ganglion cells. Immunostaining demonstrated HA-prestin within the lateral wall of the infected (GFP-positive) cells. HDAd was also injected into adult prestin null mice cochleae *in vivo*. After removing the bone in the second turn, 5.4x10<sup>9</sup> vp were injected through the spiral ligament into the scala media using a micropipette. Four days later, the cochleae were removed and fixed. Immunostaining revealed HA-prestin was expressed within the lateral wall of infected (GFP-positive) OHCs, IHCs, supporting cells and pillar cells. These findings indicate that HDAd can be used to transduce prestin within outer hair cells of the prestin null mouse. Prestin is expressed within the lateral wall as it is naturally in the wild-type mouse. The *in vitro* and *in vivo* expression patterns of transduced HA-prestin and GFP in the prestin null mouse organ of Corti were similar. Studies to assess the physiology of prestin null outer hair cells transduced with prestin are underway.

Supported by NIDCD grants R01 DC 04585 & DC 00354 (FAP) & DC 006671, The American Hearing Research Foundation and The Caroline Weiss Law Fund for Research in Molecular Medicine (JSO)

### **[324] Sendai Virus Vector-Mediated Transgene Expression in the Cochlea *In Vivo***

*Withdrawn*

### **[325] Strategies to Limit Host Responses Against Adenovector Mediated Inner Ear Gene Transfer**

**Hinrich Staecker<sup>1</sup>**, Mark Praetorius<sup>2</sup>, Chi Hsu<sup>3</sup>, Douglas Brough<sup>3</sup>

<sup>1</sup>Department of Otolaryngology, University of Kansas School of Medicine, <sup>2</sup>Department of Otolaryngology, University of Heidelberg, <sup>3</sup>GenVec, Inc

Adenovector mediated gene delivery has been used to alter the phenotype of the inner ear in a variety of animal

models of hearing loss. Adenovectors are versatile, easy to manufacture and modify and have a high payload capacity. We studied the immunogenicity properties of these vectors and resulting impact on gene delivery. Studies in other systems (eye and skeletal muscle) have demonstrated that immune response to adenovectors is dependent on the total dose of vector delivered. Consistent with these findings we have shown in a mouse model that we can transfect a broad range of inner ear tissues in mice pre-immunized with Ad5 without damaging hearing by limiting the total dose delivered and route/site of administration. Further refinement of enhanced delivery was gained by using a tropism enhanced Ad5 based vector with heparin binding, which allows efficient delivery of an even lower dose of vector. Vectors that preferentially bind alpha V integrin were less effective. We are also testing an additional strategy to avoid pre-existing host responses by evaluating the transfection of inner ear tissues with adenovectors constructed from different adenovirus serotypes. We demonstrated that transfection of inner ear tissue can also be accomplished by using alternative serotypes of adenovectors. Our conclusions are that development of adenovector based molecular therapeutics in the inner ear will be improved by limiting the dose of total particles delivered, by enhancing binding to target cells, by using vectors from alternative adenovirus serotypes which are not immuno-recognized and by carefully controlling the entry point to the inner ear.

### **[326] Induction of New Stereociliary Bundles In Vivo and Cellular Regeneration Using AdV Encoded shRNA Targeting P27kip1 mRNA**

Tatsuya Yamasoba<sup>1</sup>, Shin-ichi Ishimoto<sup>1</sup>, Rende Gu<sup>2</sup>, Carol Pierce<sup>2</sup>, Huy Tran<sup>2</sup>, James LaGasse<sup>2</sup>, Eric Lynch<sup>2</sup>, Jonathan Kil<sup>2</sup>

<sup>1</sup>Department of Otolaryngology – Head and Neck Surgery, University of Tokyo, <sup>2</sup>Sound Pharmaceuticals, Inc.

Improved hearing following ototoxic drug or noise exposure is linked to supporting cell proliferation and hair cell regeneration in birds. Supporting cell proliferation in wild type mice and Guinea pigs has been induced by antisense oligonucleotides (Kil ARO 2001, Gu ARO 2001) and Adenovirus (AdV) encoded shRNA targeting p27kip1 mRNA in mice (Kil ARO 2004, Gu ARO 2005). AdV p27 shRNA constructs were delivered to the scala media of adult Guinea pigs 4 days after systemic kanamycin/ethacrinic acid. Control animals were infected similarly with random sense shRNA encoding AdV. Eight weeks later, cochleae were collected and analyzed by scanning electron microscopy (SEM). AdV p27 shRNA induced new hair cell production and ectopic stereocilia production in and around the organ of Corti. These novel morphologies were observed throughout the cochlea, mainly in the second and third turns of the organ of Corti and the inner spiral sulcus. Many of these novel morphologies are reminiscent of developing and regenerating stereocilia in the vestibular organs of mammals. The novel stereocilia occurred most frequently on Deiter's cells and pillar cells. In cochleae infected with random sense shRNA encoding AdV, no novel stereocilia-like structures were observed. The AdV used also

contained a GFP reporter. GFP positive Deiter and pillar cells were present at 14d post infection. The GFP infectivity pattern is consistent with the cell types showing new hair cell bundles by SEM.

The novel induction of stereociliary bundles on supporting cells implies that these cells are able to de-differentiate following knock-down of p27 expression and express hair cell characteristics. These results support two roles for p27 in cell cycle biology and cellular regeneration: 1) p27 negatively regulates cell cycle progression, and 2) p27 maintains the non-regenerating fate of terminally differentiated cells.

### **[327] Plasticity of Synaptic Endings in the Cochlear Nucleus (CN) Following Noise-Induced Hearing Loss Is Facilitated in the Adult FGF2 Overexpressor Mouse (Tg)**

Chrystal D'Sa<sup>1</sup>, Julia Gross<sup>1</sup>, J. Douglas Coffin<sup>2</sup>, D. Kent Morest<sup>1</sup>

<sup>1</sup>Dept. of Neuroscience, University of Connecticut Health Center, <sup>2</sup>Dept. of Biomedical & Pharmaceutical Sciences, University of Montana

FGF2, an important mitogen, is also involved in innervation and synapse formation. Noise that damages hair cells may cause loss of axonal endings in the CN, followed by new growth of synapses. A role for FGF2 in these plastic changes may be seen in the FGF2 Tg, which has an excess of FGF2. Using the wildtype (Wt) for comparison, we studied the anterior part of the posteroventral CN (Ad) after noise by immunolabeling synaptic endings with anti-SV2. The endings appeared as clusters, which were quantified by size and location on somata as axosomatic endings and in the neuropil as axodendritic endings. Large perisomatic clusters mostly represent excitatory cochlear nerve endings; small clusters include inhibitory endings. In the Wt, 50% of large perisomatic clusters went away by 1 wk, underwent a small recovery at 2-4 wks, but dropped to 25% by 8 wks. In the Tg, in contrast, large perisomatic clusters increased at 1 wk, returned to control levels at 2 wks, increased again at 4 wks, and returned to control levels by 8 wks. The Wt neuropil clusters declined gradually by 30% over 8 wks. In contrast, Tg neuropil clusters dropped by 1 wk, then recovered for 2-8 wks. Thus FGF2 preserves excitatory perisomatic cochlear nerve endings and promotes recovery of neuropil clusters, including presumptive inhibitory synapses from interneurons. This raises the question of whether there was a change in the numbers of excitatory vs inhibitory synapses. Hence we are studying inhibitory and excitatory receptors in FGF2 Tg after noise. In the Wt, GABA A $\alpha$ 1 staining increased on the soma by 1 wk and stayed up for 4 wks; Wt peridendritic staining increased at 4 weeks, while neuropil SV2 declined. In contrast, Tg GABA A $\alpha$ 1 increased from 1-4 wks, while SV2 followed suit after a 1 wk delay. The finding that GABA A $\alpha$ 1 in the Wt increases in Ad soon after noise but that it decreases in Tg suggests that inhibitory activity may differ in the FGF2 overexpressor. Supported by NIDCD and a UCHC grant.

### **328** Plasticity of Synaptic Endings in the Cochlear Nucleus Following Noise-Induced Hearing Loss: Fine Structure in Adult Mice

**D. Kent Morest**<sup>1</sup>, Subramani Munirathinam<sup>1</sup>, Maya Yankova<sup>1</sup>, Julia Gross<sup>1</sup>, G. Steven Kempe<sup>1</sup>

<sup>1</sup>*Dept. of Neuroscience, Univ. CT Health Center*

Acoustic trauma not only produces hair cell loss but also synaptic degeneration and new growth in the cochlear nucleus. After noise, waxing and waning (waves) in the ratio of excitatory vs. inhibitory endings occur over time. These waves may result from neuronal modulation by synaptic nests, i.e., groups of endings not separated by glial processes, while most endings are wrapped by glia. We report here on the first two waves of ratio changes in two regions: the dorsal subdivision of the anterior part of the posteroventral cochlear nucleus (Ad), which consistently responds to noise, and the adjacent confluence of lateral and internal lamellae of the small cell shell, notable for numerous nests. F1 hybrid (C57/BxCBA/J) adults were exposed to white noise of >4kHz at 115 dB SPL for 6 hours. After 7 and 14 days, exposed and control mice were prepared for electron microscopy; hair cell and ganglion damage were mapped. Synaptic endings were classified, counted, and measured for glial coverage by image analysis and statistical programs. In Ad, significant loss of normal endings occurred at 7 and 14 days, with increases in abnormal endings. The ratio of excitatory vs. inhibitory normal endings dropped at 7 days, followed by partial recovery at 14 days, which was probably due mostly to loss of inhibitory endings. In the confluence of the shell, by contrast, a significant loss of normal endings occurred at 7 and 14 days, along with increases in abnormal endings. The ratio of excitatory vs. inhibitory normal endings increased by 7 days, but partially recovered at 14 days, probably due mostly to loss of excitatory endings. These findings suggest that the substrate for excitation is plastic and may compensate in opposing waves alternating between Ad and the small cell shell. A role of synaptic nests is seen in the decrease of their number in Ad at 7 days, with more glial coverage of endings and fewer endings per nest. In contrast the confluence does not lose nests until 14 days.

Supported by grants from NIH (R01DC000127) and UCHC.

### **329** Effect of Overexpressing the Transcription Factor E2F2 on Cell Cycle Progression in Avian Embryonic Otocyst *In Vivo*

**Xiang Wang**<sup>1</sup>, Feng Feng<sup>1</sup>, David Z.Z. He<sup>1</sup>, Kirk W. Beisel<sup>1</sup>, Bernd Fritzsche<sup>1</sup>

<sup>1</sup>*Department of Biomedical Sciences, Creighton University School of Medicine, Omaha, NE*

Recent work has demonstrated that terminally differentiated hair cells can re-enter the cell cycle when the cell cycle control gene retinoblastoma (Rb) is disrupted (Sage et al., 2005; Mantella et al, 2005). In addition, one of these papers (Mantella et al., 2005) showed that the newly formed hair cells undergo apoptosis, a well known phenomenon that is induced by overabundance of two

transcription factors, E2F1 and E2F3. Those transcription factors are normally bound by pRb, but will be free to initiate apoptosis in the absence of pRb. In contrast to E2F1 and E2F3, a third Rb-binding cell cycle initiating E2F transcription factor, E2F2, seems to be able to initiate cell cycle entry without apoptosis. Indeed, the transcription factor E2F2 has been demonstrated to induce cell proliferation in mitotically quiescent heart muscle cells without activation of apoptosis, a phenomenon much like proliferation of differentiated hair cells. Such studies suggest that overexpressing E2F2 in terminally differentiated cell types might induce a save S-phase reentry and cell division, providing a promising access to initiate regeneration on naturally non-replicative tissues. Thus far the directed E2F2 expression in auditory system has not been conducted to explore this promising new direction. In this study, we will report the effects of overexpression of E2F2 through adenovirus mediated gene transfer in chicken embryonic otocyst (E3-E6). We will report our hair cell counts using Myo6 labeling and will report on the number of TUNEL positive cells indicative of apoptosis. These findings suggested that transcription factor E2F2 overexpression in chicken embryonic otocyst increases cell cycle progression much like in other cell systems tested thus far. If our current long term experiments show that the E2F2 induced additional hair cells are viable, E2F2 may provide a potential means to improve hair cell regeneration in adult mammals.

### **330** Spatial Analysis of Supporting Cell Proliferation in the Regenerating Avian Basilar Papilla

**Luke Duncan**<sup>1</sup>, Dominic Mangiardi<sup>1,2</sup>, Jonathan Matsui<sup>1,3</sup>, Caitlin Terry<sup>1</sup>, Douglas Cotanche<sup>1,4</sup>

<sup>1</sup>*Children's Hospital, Boston*, <sup>2</sup>*Department of Biomedical Engineering, Boston University*, <sup>3</sup>*Department of Molecular and Cellular Biology, Harvard University*, <sup>4</sup>*Departments of Otology and Laryngology, Harvard Medical School, Harvard University*

The hair cells of the chick cochlea undergo apoptosis in a gradient from the proximal (high frequency) end of the epithelium towards the distal (low frequency) end, in response to a single injection of gentamicin. Following hair cell death, the neighboring supporting cells are induced to re-enter the cell cycle and produce daughter cells that will differentiate into either supporting cells or hair cells. The aim of this study was to measure the spatial progression of DNA synthesis in the supporting cells and compare this to the progression of hair cell loss. Two-week-old chicks received a single injection of gentamicin (300 mg/kg). The chicks then received a single injection of bromodeoxyuridine (BrdU) between 54 hours and 6 days after gentamicin treatment and were sacrificed 4 hours later. The cochleae were explanted, fixed, and immunohistochemically labeled with antibodies directed against BrdU and one the following hair cell markers: myosin VI, myosin VIIa, or TuJ-1 (beta-III tubulin). A continuous series of Z-stack images of the damaged sensory epithelium were collected by confocal microscopy and assembled into a single montage image of the damage lesion. The BrdU-positive nuclei were marked and

the images were cropped to include only the damaged region of the sensory epithelium. A MATLAB script was written to count and determine the location of the marked nuclei in the damage lesion. At the onset of DNA synthesis 65 hours after gentamicin, the mean position of BrdU uptake was approximately 50% down the length of the damage lesion. The center of S-phase activity progressed down the sensory epithelium to approximately 80% of the lesion's length before ceasing at 120 hours after gentamicin. The BrdU-labeled nuclei were not tightly distributed around the mean position, but extended throughout the damaged region. There was not a direct proximal-to-distal wave of BrdU labeling that matched the pattern of hair cell loss. Interestingly, the progression of BrdU uptake appeared to mirror the developmental pattern of hair cells and supporting cells in the chick embryo.

Funding for this study provided by NIH DC01689 and the Sarah Fuller Fund (DC); NIH EY14790 (JM).

### **[331] 3D Spatial Analysis of Hair Cell Regeneration in the Avian Cochlea**

**Dominic Mangiardi<sup>1</sup>**, Luke Duncan<sup>2</sup>, Caitlin Terry<sup>2</sup>, David Mountain<sup>1</sup>, Douglas Cotanche<sup>2</sup>

<sup>1</sup>*Boston University*, <sup>2</sup>*Childrens Hospital Boston*

Sensory hair cells in the cochlea convert fluid movement into neural signals that are relayed to the brain. Damage to these sensory receptors can result in permanent hearing and balance disorders in humans, while other vertebrate species such as the chicken have the capacity to regenerate lost hair cells via induction of quiescent neighboring supporting cells in the sensory epithelium to re-enter the cell cycle and produce daughter cells that can repopulate the damaged sensory epithelium. Analysis of the timing and morphology of supporting cell progression through various stages of the cell cycle has led to a 2D model of hair cell regeneration in the avian cochlea that includes the migration of progenitor cell nuclei to various depths within the sensory epithelium as the cells progress through the cell cycle and differentiation. The goal of this project is to use 3D confocal z-series stacks to extend our understanding of the re-arrangements of cells within the chick cochlear sensory epithelium during hair cell death and regeneration. Chicks were administered a single injection of gentamicin (300 mg / kg) and a separate injection of BrdU (100 mg/kg) to label progenitor cells passing through DNA synthesis. The number and position of quiescent, proliferating, and differentiating supporting cells within a designated 3D volume of the avian sensory epithelium at various stages of sensory hair cell death and regeneration was analyzed.

### **[332] Characterization of Supporting Cell Phenotype During the Early Phases of Hair Cell Regeneration in the Avian Inner Ear**

**Mark E. Warchol<sup>1</sup>**, Guy P. Richardson<sup>2</sup>

<sup>1</sup>*Dept. of Otolaryngology, Washington University, St. Louis MO*, <sup>2</sup>*School of Life Sciences, University of Sussex, Brighton UK*

The sensory organs of the avian inner ear have a remarkable ability to regenerate after acoustic trauma or

ototoxic injury. Numerous studies have demonstrated that epithelial supporting cells serve as the precursors to regenerated hair cells, either via renewed proliferation or by a direct change in cell phenotype. It is not clear, however, whether all supporting cells can participate in the regenerative process or whether regeneration is dependent on a phenotypically-distinct subpopulation of supporting cells. In this study, we have used several antibodies to characterize possible changes in supporting cell phenotype during the early phases of regeneration in cultures of the chick utricle.

In undamaged utricles, the apical surfaces of all supporting cells were immuno reactive for the Supporting Cell Antigen (SCA, a novel receptor tyrosine phosphatase – Kruger et al. *J Neurosci* 14:4815, 1999). At 0-48 hours after treatment with 1 mM streptomycin, the intensity of SCA labeling was variable, but nearly all supporting cells continued to display some level of SCA immunoreactivity. Notably, expression levels of SCA were not correlated with proliferation, and cells with distinct DAPI-labeled mitotic figures were often strongly labeled for SCA. In contrast, immunoreactivity for gm-2 (Goodyear et al., *Hear Res* 80:93, 1994) was strongly reduced in M-phase cells. Finally, we examined immunoreactivity for the PAX2 transcription factor, which is normally expressed by hair cells and supporting cells in the extrastriolar regions of the utricle. The nuclei of many S-phase supporting cells retained moderate levels of PAX2 immunoreactivity during cell cycle entry. The results suggest that avian supporting cells undergo partial dedifferentiation during the early phase of regeneration. Also, inability of mammalian supporting cells to dedifferentiate may be a key limitation on sensory regeneration.

(Supported by the NIDCD, the Wellcome Trust, and the Grass Foundation.)

### **[333] Mitogen-Activated Protein Kinases Regulate Both Wound Closure and Damage-Induced Proliferation in Epithelial Cultures of Mature Avian Utricle**

**Jonathan Bird<sup>1</sup>**, Mark E. Warchol<sup>2</sup>, Jonathan Gale<sup>1</sup>

<sup>1</sup>*Centre for Auditory Research, UCL Ear Institute, London, UK*, <sup>2</sup>*Department of Otolaryngology, Washington University, St Louis, MO, USA*.

The avian inner ear can regenerate its sensory epithelia following acoustic or ototoxic trauma. This process can be divided into an early phase of epithelial repair, followed by the production of new hair cells. Most regenerated hair cells originate from a combination of supporting cell proliferation and direct trans-differentiation. The cell signals that initiate wound closure and regulate proliferation in response to epithelial damage are poorly understood. We have used an epithelial culture model of the adult chicken utricle to investigate epithelial wound repair and cell proliferation in vitro. A laser microbeam was used to wound epithelial cultures in a precise, repeatable manner. Wounded epithelia healed over 12 hours using a combination of cell lamellipodial extension and the formation of an actin cable along the wound margin. In parallel experiments quantification of BrdU incorporation

revealed a significant increase in supporting cell proliferation within 48 hours of epithelial damage. We hypothesized that signalling from the MAP kinases p44/42<sup>ERK1+2</sup> (ERK) or c-Jun N-terminal kinase (JNK) could regulate epithelial wound closure and proliferation. ERK was transiently activated within 5 minutes of laser wounding, however inhibition using U0126 did not prevent wound healing. In contrast, JNK exhibited sustained activation and inhibition using SP600125 significantly delayed wound closure. The maintained presence of U0126 significantly reduced the damage-induced proliferation at 48 hours as did SP600125. In separate experiments, PI3K inhibition by LY294002 almost completely abolished damage-induced proliferation. Our data demonstrate that along with PI-3 kinases, the ERK and JNK protein kinases regulate key events in repair and regeneration processes in avian hair cell epithelia.

**334 Direct Supporting Cell-to-Hair Cell Conversion in the Cultured Avian Basilar Papilla**  
Jia Lin Shang<sup>1</sup>, Lowell Lombardini-Parker<sup>1</sup>, Jennifer Stone<sup>1</sup>

<sup>1</sup>University of Washington

The basilar papilla (BP) of mature birds exhibits spontaneous hair cell (HC) regeneration after experimental HC injury. New HCs are formed by mitosis of non-sensory supporting cells (SCs). Previous studies suggest new avian HCs are also created by the non-mitotic conversion of SCs into HCs, called direct transdifferentiation (e.g., Roberson et al., 1996 Aud. Neurosci. 2:195; Roberson et al., 2004, J. Neurosci. Res. 78:461). This process may also be a mechanism employed by mammals for HC regeneration (Forge et al. 1998; J. Comp. Neurol. 397:69). In this study, we analyzed mechanisms of new HC production in cochlear duct (organ) cultures from post-hatch chickens. Cultures were treated with the ototoxin, streptomycin (or SM) at 78 µM, for 2 days to kill all native HCs. Organs were cultured for additional periods in media without SM but containing 1 µM BrdU, a marker of cell division. Many MyosinVI-positive and/or HCA-positive cells were present at 8 days in vitro (2d+SM/6d-SM), indicating the differentiation of new HCs. Up to 85% of these new HCs were BrdU-negative and were thus the product of direct transdifferentiation. Several analyses, including immunohistochemistry for HC markers in whole-mounts and sections and tracing of AM143-labeled native HCs over time after SM treatment in culture, ruled out HC repair as an explanation for these observations. Further support for direct transdifferentiation of SCs into HCs was provided by treatment with the S phase-blocker, aphidicolin (25 µM). Aphidicolin treatment led to complete attenuation of SC division in the BP, as demonstrated by failed BrdU uptake. Regardless, numerous new, differentiated HCs were present throughout the BP by 8 days in vitro with continuous aphidicolin treatment, providing further support for direct SC-to-HC conversion. These studies demonstrate direct transdifferentiation is retained in organ cultures as a significant mechanism of new auditory HC production.

**335 Cath1 Protein Expression During Avian Hair Cell Regeneration**

Jon Cafaro<sup>1</sup>, Jennifer Stone<sup>1</sup>

<sup>1</sup>University of Washington

Auditory and vestibular epithelia are composed of sensory hair cells and non-sensory supporting cells. Following gentamicin-induced hair cell damage in birds, regenerated hair cells arise from surviving supporting cells via direct transdifferentiation and renewed cell division. Hair cell regeneration is rare in mammals. Characterizing the molecular signals that regulate cell fate specification and differentiation of regenerated hair cells is a crucial step in understanding regenerative processes in avian epithelia. The basic helix-loop-helix transcription factor, atonal1 (Atoh1), is critical for hair cell development in mammalian and zebrafish hair cell epithelia and therefore is an excellent candidate molecule for regulating post-embryonic hair cell production. Here, we characterize expression of chicken Atoh1 (Cath1) in quiescent and regenerating auditory and vestibular organs using immunofluorescence. Cath1 protein is not detected in the undamaged basilar papilla (BP), with no regeneration, but it is upregulated in nuclei in the basal tip of the BP as early as 1 day post-gentamicin, prior to significant supporting cell division. Expression peaks near 5 days post-gentamicin and declines steadily after that time. A few Cath1-positive nuclei are detected in the damaged region as late as 27 days post-gentamicin, but none are seen at 47 days post-gentamicin. At all times, increased cAtoh1 expression is limited to the hair cell lesion. Cath1 is detected in new hair cells as early as 3 days post-gentamicin. Dividing supporting cells are Cath1-negative. Post-mitotic hair cells upregulate Cath1 protein by 15 hours post-S phase, but post-mitotic support cells appear never to express Cath1. In the utricle, which is in a continuous regenerative state, Cath1 is expressed throughout control organs and is upregulated in the lesion after gentamicin treatment. These observations support a role for Cath1 in non-mitotic as well as mitotic hair cell regeneration in birds.

**336 Screening for Zebrafish Mutants with Defects in the Hair Cells of the Lateral Line Using Mutants with Defects in the Marginal Zone of the Retina**

Jonathan Matsui<sup>1,2</sup>, Tristan Darland<sup>1</sup>, John Dowling<sup>1</sup>, Douglas Cotanche<sup>2,3</sup>

<sup>1</sup>Department of Molecular and Cellular Biology, Harvard University, <sup>2</sup>Department of Otolaryngology, Children's Hospital, Boston, <sup>3</sup>Departments of Otolaryngology and Laryngology, Harvard Medical School, Harvard University

Sensory hair cells found in the inner ears of non-mammalian vertebrates regenerate following damage to the sensory epithelium. In many cases, adjacent supporting cells proliferate via mitosis and give rise to new hair cells and supporting cells. Recently, several mutant zebrafish were identified in a forward genetic screen in which the animals had reduced cellular proliferation in the marginal zone of the retina. The marginal zone is a retinal region that produces precursor cells that differentiate into a variety of cell types, including photoreceptors and retinal



ganglion cells throughout the lifetime of the animal. Like nonsensory supporting cells of the inner ear, these cells also rapidly proliferate following damage. The zebrafish also have a lateral line system, which is comprised of neuromasts containing a central cluster of hair cells that are capable of regenerating following laser ablation or aminoglycoside damage. Preliminary data indicate that some of these marginal zone mutants have fewer sensory hair cells in their lateral line neuromasts at 5 days post-fertilization (dpf) as assessed by phalloidin staining, and that even fewer of these hair cells are functional as assessed by FM 1-43 staining. Our results suggest that defects in proliferating retinal cells may also occur in proliferating cells giving rise to lateral line hair cells.

Funded by the National Institutes for Health EY14790 and the NOHR Foundation (JM); NIH DA016291 (TD); NIH EY00811 (JD); NIH DC01689, Deafness Research Foundation, Samuel Rosenthal and Dossberg Foundation, and the Sarah Fuller Fund (DC).

### **337 Anatomical and Functional Recovery of the Goldfish Sacculle Following Noise Exposure**

Michael E. Smith<sup>1,2</sup>, Allison B. Coffin<sup>2</sup>, Diane L. Miller<sup>2</sup>, Arthur N. Popper<sup>2</sup>

<sup>1</sup>Department of Biology, Western Kentucky University,

<sup>2</sup>Department of Biology, University of Maryland

Both the lateral line and inner ear of fishes are able to regenerate sensory hair cells that have been lost following the application of ototoxic chemicals. Questions still remain regarding whether recovery will also take place following exposure to intense sounds. Additional open questions concern the functional relationship between hair cell damage and hearing loss, and the time course of hair cell and functional recovery in fishes. To investigate these questions we performed two experiments: one examined the functional recovery of goldfish hearing and the second examined the damage and recovery of hair cells following noise-exposure. In both experiments, we exposed goldfish (*Carassius auratus*) to white noise (165 dB re: 1 µPa) for 48 h. In Exp. 1, hearing tests were performed using the auditory brainstem response on six fish for each of six time points (pre-exposure controls, immediately post-exposure, and 1, 2, 3, 5, and 8 d following exposure). Goldfish exposed to the white noise exhibited a significant temporary threshold shift (TTS; ranging from 13 to 20 dB) at all frequencies tested (from 0.2-2 kHz). After 8 d of recovery, goldfish hearing improved significantly (mean TTS < 4 dB). In Exp. 2, the sacculles of six fish were examined at the same time points as in Exp. 1. The left ears of each fish were labeled with phalloidin in order to visualize hair cell bundles and to measure hair cell bundle densities at specific points on the sacculle, while the right sacculles were used for the detection of apoptotic cells using the TUNEL protocol. Preliminary results suggest that noise-exposed fish exhibit significant loss of hair cell bundles following noise exposure. We are currently monitoring the recovery of these damaged sensory epithelia to quantify the time course of the regeneration of new and/or repaired hair cells in these areas. This is the first study to examine the relationship between hair cell damage and hearing ability in fishes.

### **338 Recovery of Mechanotransduction in Traumatized Hair Bundles of the Sea Anemone, *Haliplanella Luciae***

*Withdrawn*

### **339 A Novel DFNA36 Mutation Reveals a Critical Dominant-Negative or Gain-of-Function Mechanism Associated with Missense Substitutions of Amino Acid D572 of TMC1**

Shin-Ichiro Kitajiri<sup>1</sup>, Thomas B. Friedman<sup>1</sup>, Andrew Griffith<sup>1</sup>

<sup>1</sup>NIDCD, NIH, Rockville, MD

Dominant and recessive mutations of TMC1/Tmc1 (transmembrane channel-like gene 1) cause nonsyndromic deafness in humans and mice (Kurima et al., Nature Genetics, 2002; Vreugde et al., Nature Genetics, 2002). Heterozygous carriers of recessive mutant alleles, such as the truncation mutation R34X, have normal hearing, suggesting that a single wild type allele is sufficient for normal auditory function. Therefore, the two known dominant mutations, M412K in Beethoven mice and D572N in humans (DFNA36), must act via a dominant-negative or gain-of-function mechanism.

We have ascertained a large Caucasian family segregating autosomal dominant, progressive, sensorineural hearing loss. This phenotype co-segregated with STR markers linked to TMC1 at the DFNA36 locus. Nucleotide sequence analysis of TMC1 identified a point mutation (G1714C) predicted to result in a substitution of histidine for aspartic acid at amino acid position 572 (D572H). Interestingly, this nucleotide is the same one affected by the previously reported G1714A (D572N) mutation segregating in the original and only reported DFNA36 family. These dominant alleles must perturb some critical function associated with D572.

Both D572N and D572H cause progressive hearing loss, but the loss of hearing associated with D572N is more rapid. The hearing loss associated with D572N begins at 5-10 years of age and is profound within 10-15 years, whereas the hearing loss caused by D572H begins at 11-15 years of age and is profound by the 4th decade. This phenotypic difference may reflect a difference in genetic background, differing effects of the substitutions, or both.

### **340 Pathophysiological Role of Wolframin Mutants in Wolfram Syndrome**

Teruyuki Sato<sup>1</sup>, Kazuo Ishikawa<sup>1</sup>

<sup>1</sup>Akita University

Wolfram syndrome is an autosomal recessive disorder associated with juvenile onset non-autoimmune diabetes mellitus. The disease has been attributed to mutations in the WFS1 gene, but little is known concerning the function of WFS1 protein (wolframin). To investigate the pathophysiological roles of wolframin mutants in Wolfram syndrome, the expression vectors of wild-type WFS1 and nonsense (W648X) and missense (G695V) mutations of WFS1, both of which are found in Wolfram patients, were



transfected into clonal pancreatic  $\beta$ -cell lines HIT-T15 or MIN6 cells, and subcellular localization was determined. Wild-type and G695V wolframin proteins were co-localized with the endoplasmic reticulum (ER) marker GRP78 in a reticular pattern. In contrast, the intracellular distribution of W648X wolframin protein showed a distinct, aggregated pattern, colocalized with aggregated GRP78. However, no phosphorylation of RNA-dependent protein kinase-like endoplasmic reticulum-stress activated kinase (PERK) or activation of caspase-3 was detected in HIT-15 cells expressing W648X wolframin, indicating that neither ER stress nor apoptosis is induced by the protein. Furthermore, when endogenous wolframin was knocked down in MIN6 cells by transfecting a WFS1-specific siRNA library, caspase-3 activation was not induced. These results demonstrate that truncated W648X wolframin induces a dramatic change in the immunostaining pattern of wolframin and GRP78 and suggest that the mutation is not associated with ER stress or apoptosis in pancreatic  $\beta$ -cells.

### **[341] Nonsyndromic Dominant Hearing Loss DFNA10 Associated with a Novel Mutation of EYA4**

**Tomoko Makishima**<sup>1,2</sup>, Anne Madeo<sup>1</sup>, Carmen Brewer<sup>1</sup>, Christopher Zalewski<sup>1</sup>, John Butman<sup>3</sup>, Vandana Sachdev<sup>4</sup>, Andrew Arai<sup>4</sup>, Brenda Holbrook<sup>4</sup>, Douglas Rosing<sup>4</sup>, Andrew Griffith<sup>1</sup>

<sup>1</sup>NIDCD, Bethesda, MD, <sup>2</sup>University of Texas Medical Branch, Dept. of Otolaryngology, <sup>3</sup>CC, DRD, NIH, <sup>4</sup>NHLBI, NIH

Dominant, truncating mutations of *EYA4* have been associated with nonsyndromic hearing loss DFNA10 as well as a syndromic form of sensorineural hearing loss (SNHL) associated with dilated cardiomyopathy.

We ascertained a North American family segregating autosomal dominant, progressive, bilateral SNHL. The onset of SNHL ranged from the second to third decade of life, and appeared to be earlier in males compared to females. At onset, it primarily affected middle to high frequencies and progressed to moderate to severe levels. MRI scans revealed no inner ear structural abnormalities. Nine affected family members underwent a detailed clinical evaluation to rule out extra-auditory manifestations of a syndrome. A medical history interview, physical examination, vestibular evaluation, electrocardiography, echocardiography, and MRI evaluation of the heart detected no associated abnormalities.

Genotype analysis of microsatellite markers linked to known DFNA loci was completed in 10 affected and 6 unaffected family members. The SNHL phenotype co-segregated only with markers at the DFNA10 locus. Nucleotide sequence analysis of *EYA4* identified a novel frameshift mutation, 1489insAA, which is predicted to encode a truncated EYA4 protein with an intact N-terminal variable region, but lacking the entire C-terminal Eya domain.

The normal cardiac phenotype associated with 1489insAA is consistent with the published hypothesis that truncations affecting only the Eya domain cause nonsyndromic SNHL,

while truncations affecting the variable region cause SNHL and cardiac dysfunction (Schonberger et al., *Nature Genetics* 37: 418-422, 2005). In contrast, the auditory phenotype appears to be independent of mutation position, since the hearing loss associated with 1489insAA is similar to that reported for other *EYA4* mutations. These results should facilitate the diagnostic workup, as well as genetic, prognostic and rehabilitation counseling of patients with nonsyndromic dominant hearing loss.

### **[342] An In Vitro Model System to Study Viral-Mediated Gene Therapy in the Human Inner Ear**

**Bradley W. Kesser**<sup>1</sup>, George T. Hashisaki<sup>1</sup>, Kenneth Fletcher<sup>1</sup>, Holly Eppard<sup>2</sup>, Jeffrey R. Holt<sup>1,2</sup>

<sup>1</sup>University of Virginia Dept Oto/HNS, <sup>2</sup>University of Virginia Department of Neuroscience

To study viral-mediated gene transfer into the sensory cells of the human inner ear, we developed an in vitro preparation based on previous successful viral transfection of explant cultures from mouse auditory and vestibular organs with replication-deficient adenovirus.

Twenty-one human vestibular sensory epithelia were harvested from 5 consented patients at the time of surgery for vestibular schwannoma. The tissue was maintained in culture for up to 4 days, affixed to coverslips, and bathed in OptiMEM plus 10 mM HEPES and 0.05mg/mL ampicillin. Multiply-deleted adenoviral vectors (-E1a/b, -E3, -pol, -pTP) that carried the gene for green fluorescent protein (GFP) were added directly to the culture media at titers that ranged from 10<sup>5</sup> – 10<sup>10</sup> viral particles per mL. 24 to 72 hours post-transfection, the tissue was fixed, counter-stained with phalloidin, and imaged using confocal microscopy.

We observed numerous GFP-positive hair cells and supporting cells. As early as 24 hours post-transfection up to 72% of the cells were GFP-positive. 48 hours post-transfection, we found that the number of GFP-positive cells was correlated with viral titer with titers of 2.7 x 10<sup>7</sup> viral particles/mL corresponding to a transfection rate of 50%.

To examine the ability of adenovirus to drive expression of functionally relevant genes, we generated a vector that carried the gene for GFP and the wild-type form of KCNQ4, which when mutated causes deafness in humans. 24 to 96 hours post-transfection, the samples were fixed and stained with an anti-KCNQ4 antibody. We noted robust KCNQ4 staining in 39% of all cells examined. Of the KCNQ4-positive hair cells, 48% were GFP-negative which presumably reflected localization of endogenous KCNQ4. 52% of the KCNQ4-positive cells were GFP-positive including supporting cells and type I and type II hair cells. Much of the KCNQ4 expression in the GFP-positive cells was probably driven by adenoviral-mediated gene transfer.

### **343 A Novel Locus for Autosomal Dominant Non-Syndromic Hearing Impairment, Maps to Chromosome 2q13-Q14.2**

Huijun Yuan<sup>1</sup>, Hanjun Sun<sup>1</sup>, Ran Tao<sup>2</sup>, Wei Qin<sup>2</sup>, Denise Yan<sup>3</sup>, ShuZhi Yang<sup>1</sup>, Juyang Cao<sup>1</sup>, Guoyin Feng<sup>2</sup>, Weiyang Yang<sup>1</sup>, Xue Zhong Liu<sup>3</sup>, Dongyi Han<sup>1</sup>, Lin He<sup>2</sup>

<sup>1</sup>*Inst. Of Otolaryngology, General Hospital of Chinese PLA, Beijing, China,* <sup>2</sup>*Bio-X Life Science Research Center, Shanghai Jiao Tong University, Shanghai,* <sup>3</sup>*Department of Otolaryngology, University of Miami, FL, USA*

Hereditary non-syndromic sensorineural hearing loss is a genetically highly heterogeneous group of disorders. To date, at least 50 loci for autosomal dominant non-syndromic sensorineural hearing loss (DFNA) have been identified by linkage analysis. Here we report the mapping of a novel autosomal dominant deafness locus at 2q13-q14.2 by studying a large multi-generational Chinese family with post-lingual, high-frequency hearing loss that progresses to involve all frequencies. Onset of hearing loss in all affected subjects occurred in the second through fourth decade of life. After exclusion of the 14 known DFNA loci with markers from the Hereditary Hearing Loss Homepage (URL: <http://dnalab-www.uia.ac.be/dnalab/hhh>), a genome wide scan was carried out using 382 highly informative microsatellite markers at approximately 10 cM intervals throughout the genome. Linkage analysis was carried out under a fully penetrant autosomal dominant mode of inheritance with no phenocopies. A maximum two-point LOD score of 3.29 at theta=0 was obtained for marker D2S1277. Haplotype analysis placed the novel locus within a 8.4 cM genetic interval defined by markers D2S1888 and D2S2224 without overlapping with the other identified DFNA loci. DNA sequencing of coding regions and exon/intron boundaries of a candidate gene PAX8 in this interval did not reveal disease-causing mutation in this family.

### **344 Evaluating Suppression of Nonsense Mutations by Aminoglycoside Antibiotics as an Intervention for Vision Loss in Type I Usher Syndrome**

Annie Rebibo<sup>1</sup>, Leah Rizer<sup>1</sup>, Zubair M. Ahmed<sup>2</sup>, Julie M. Schultz<sup>2</sup>, Thomas B. Friedman<sup>2</sup>, **Tamar Ben-Yosef**<sup>1</sup>

<sup>1</sup>*Department of Genetics, Rappaport Faculty of Medicine, Technion-Israel Institute of Technology,* <sup>2</sup>*Laboratory of Molecular Genetics, NIDCD/NIH*

Type 1 Usher syndrome (USH1) is a recessively-inherited condition, characterized by profound prelingual deafness, vestibular areflexia, and prepubertal onset of retinitis pigmentosa (RP). RP is a degenerative disease of the retina, characterized by gradual restriction of the visual field, eventually leading to blindness. While the auditory component of USH1 can be treated by cochlear implants, to date there is no effective treatment for RP. USH1 can be caused by mutations in each of at least seven genes. While truncating mutations of these genes cause USH1, missense mutations of some of the same genes cause only nonsyndromic deafness. These observations suggest that partial or low level activity of the encoded proteins may be sufficient for normal retinal function, although not for normal hearing. Interventions to enable at least some

translation of full-length protein, may delay the onset and/or progression of RP in individuals with USH1 due to nonsense mutations. One such possible therapeutic approach is suppression of nonsense mutations by small molecules such as aminoglycoside antibiotics. This strategy has been previously tested for several genetic diseases with encouraging results. We are examining this approach as a potential intervention for vision loss in patients with USH1 due to nonsense mutations. We are initially testing suppression of nonsense mutations of the PCDH15 gene, underlying USH1F. Using an in vitro transcription/ translation assay of a reporter plasmid harboring various PCDH15 nonsense mutations, we demonstrated up to 91% suppression of these mutations by aminoglycosides. We are now evaluating suppression of these mutations ex vivo, using cultured cells. For future in vivo testing of this approach we are developing a mouse model. The research described here will have important implications for development of targeted interventions that are effective for patients with USH1 caused by various nonsense mutations.

### **345 Progress on Evaluating Resequencing Deafness GeneChips**

Stephanie Cox<sup>1</sup>, Prachi Kothiyal<sup>2</sup>, Jonathan Ebert<sup>3</sup>, Felisa Thompson<sup>3</sup>, Anna Frangulov<sup>4</sup>, Margaret A. Kenna<sup>4,5</sup>, Bruce Aronow<sup>2,6</sup>, John H. Greinwald<sup>3,6</sup>, Heidi Rehm<sup>1,7</sup>

<sup>1</sup>*Harvard-Partners Center for Genetics and Genomics, Boston, MA,* <sup>2</sup>*Developmental Biology/Bioinformatics, Cincinnati Children's Hospital, Cincinnati, OH,* <sup>3</sup>*Center for Hearing and Deafness Research, Pediatric Otolaryngology, Cincinnati Children's Hospital,*

<sup>4</sup>*Otolaryngology and Communication Disorders, Children's Hospital Boston, MA,* <sup>5</sup>*Otology and Laryngology, Harvard Medical School, Boston, MA,* <sup>6</sup>*University of Cincinnati College of Medicine, Cincinnati, OH,* <sup>7</sup>*Pathology, Harvard Medical School, Boston, MA, USA*

Despite the identification of 41 genes for nonsyndromic hearing loss, few tests have been developed, largely due to the high cost of sequencing. To address this problem, two Deafness GeneChips have been created, each containing 8 genes (Rehm Study: GJB2, MYO6, MYO7A, OTOF, PRES, TMIE, TMPRSS3, USH1C and Greinwald Study: GJB2, GJB6, CDH23, KCNE1, KCNQ1, MYO7A, OTOF, PDS). To validate the technology, we have developed and optimized protocols to run the chips as well as computer algorithms to analyze the data. We have also developed dideoxy sequencing assays to use for data comparison. To date we have analyzed 28 chips, 15 from patients, and obtained an average call rate of 95.9%. For 226,683 of those bases (across 9 chips), we have compared the dideoxy sequencing data to chip base calls and have obtained 99.7% accuracy. Through dideoxy sequencing, we identified 160 variants across the 9 patients, of which, 4 were not identified by the GeneChip analysis, resulting in a 2.5% false negative rate. Of the 741 possible mutations identified by the GDAS algorithm, only 133 were real variants giving a 84% false positive (FP) rate. An additional 23 variants were called "n calls" by the program (not able to be called by the algorithm). The high FP rate and "n" calls does not represent a lack of test sensitivity, as many can be manually called and all are

followed up by dideoxy sequencing; however, it creates a potential problem for the cost-effectiveness of the technology if a large amount of follow-up is required. To address this problem, we are developing novel computer algorithms to analyze the GeneChip data. Our first algorithm converts the "n" calls to a variant or wild type, depending on the associated intensity distribution. Preliminary results from 9 chips indicate that, on average, 860 out of 1090 "n" calls can be salvaged per chip, which increases our average call rate from 95.9% to 99.2%. This improvement is obtained at the cost of missing 0.3/18 variants per chip on average.

### **[346] Meniere Disease Is Associated with SNPs in KCNE1 and KCNE3 Potassium Channel Genes**

**Katsumi Doi<sup>1</sup>**, Takashi Sato<sup>1</sup>, Toshihiro Kuramasu<sup>1</sup>, Tadashi Kitahara<sup>1</sup>, Hiroshi Hibino<sup>2</sup>, Takeshi Kubo<sup>1</sup>

<sup>1</sup>Department of Otolaryngology, Osaka University Graduate School of Medicine, <sup>2</sup>Department of Pharmacology II, Osaka University Graduate School of Medicine

Although the bases for both the sporadic and inherited forms of Meniere disease (MD) remain undefined, it is likely to be multi-factorial, one of the factors being a genetic predisposition. Recently, genetic association studies on complex disease have become very popular and most of them are case-control studies using single nucleotide polymorphisms (SNPs) as markers. Mutations/polymorphisms in KCNE potassium channel genes might play causative roles in MD, because KCNE potassium channels have been suggested to be present and active in trans-membrane ion and water transports in the inner ear. In the present study, to identify MD susceptibility genes, we have conducted the genetic association study with optimized sampling, optimized phenotyping/genotyping, and a selection of KCNE genes as the candidate genes.

The SNPs analyses identified 112G/A SNP in KCNE1 gene and 198T/C SNP in KCNE3 gene in 63 definite MD cases as well as 205 and 237 non-MD control subjects. For both KCNE1 and KCNE3 genes, a significant difference in frequency of each SNP was confirmed between MD cases and non-MD control subjects. The result indicates that 112G/A SNP in KCNE1 gene and 198T/C SNP in KCNE3 gene should determine an increased susceptibility to develop MD.

### **[347] The Contribution of Connexin 26 Mutations to Slight/Mild Hearing Loss in Australian Elementary School Children**

**Hans-Henrik M. Dahl<sup>1,2</sup>**, Sherryn E. Tobin<sup>1,3</sup>, Zeffie Poulakis<sup>1,3</sup>, Field W. Rickards<sup>4</sup>, Joanne Williams<sup>1</sup>, Barbara Cone-Wesson<sup>5</sup>, Melissa Wake<sup>1,3</sup>

<sup>1</sup>Murdoch Childrens Research Institute, Royal Children's Hospital, Melbourne, <sup>2</sup>Department of Paediatrics, University of Melbourne, <sup>3</sup>Centre for Community Child Health, Royal Children's Hospital, Melbourne, <sup>4</sup>Faculty of Education, University of Melbourne, <sup>5</sup>Faculty of Speech, Language and Hearing Sciences, University of Arizona

Little is known about the genes and the mutations that cause slight/mild sensorineural hearing loss (SNHL) in

children. The aim of this study is to assess, from an unbiased population sample, the genetic contribution to slight/mild SNHL in Australian children.

We tested the hearing of 6240 elementary school children aged 6 (Year 1) and 11 (Year 5) and found that 55 (0.8%) had a slight/mild SNHL, defined as low-frequency pure tone average (LPTA) across 0.5, 1, 2 kHz and/or high-frequency PTA (HPTA), across 3, 4, 6 kHz of 16-40 dB HL in the better ear, with air-bone conduction gaps <10dB. Forty eight children with slight/mild SNHL and 90 normally hearing matched children consented to participate in a genetic study in which the connexin 26 gene was analysed for mutations and the connexin 30 gene investigated for the presence of the del(GJB6-D13S1830) and del(GJB6-D13S1854) deletions. Four of 48 children with slight/mild hearing loss were homozygous for the connexin 26 V37I change. Based on the prevalence of carriers of this change we conclude that V37I can be a causative mutation and that it often is associated with slight/mild, bilateral, high frequency SNHL. No other children in the slight/mild hearing loss group appeared to have a connexin 26 related hearing loss. A normally hearing child was homozygous for the R127H change and we conclude that this change does not cause hearing loss. The four children with homozygous V37I mutations were all of Asian ethnicity. Two children of Asian background with slight/mild SNHL were carriers of the V37I mutation. The audiological profiles of the four affected V37I homozygotes showed that the hearing losses were mainly high frequency. One V37I heterozygote had a bilateral high frequency loss, while the other had bilateral low frequency loss.

We conclude that the prevalence of slight/mild SNHL in Australian children is lower than previously reported, that mutations in the connexin 26 gene is the underlying cause in ~8% of cases and that the V37I change is a common cause of slight/mild SNHL in children of Asian ethnicity.

### **[348] Identification of a New Nonsyndromic Recessive Deafness, DFNB67**

**Zubair M. Ahmed<sup>1</sup>**, Imran Shabbir<sup>2</sup>, Shahid Khan<sup>2</sup>, Ali Waryah<sup>2</sup>, Reyna Camps<sup>1</sup>, Manju Ghosh<sup>3</sup>, Madulika Kabra<sup>3</sup>, Inna A. Belyantseva<sup>1</sup>, Thomas B. Friedman<sup>1</sup>, Sheikh Riazuddin<sup>2</sup>

<sup>1</sup>Section on Human Genetics, Laboratory of Molecular Genetics, NIDCD, <sup>2</sup>National Center of Excellence in Molecular Biology, Punjab University, Lahore, Pakistan, <sup>3</sup>Genetic Unit, Department of Pediatrics, All India Institute of Medical Sciences, New Delhi, India

We report a new locus and the identification of a gene for nonsyndromic deafness DFNB67 on human chromosome 6. DNA sequence analysis of a candidate gene revealed a frameshift mutation (246delC) and a missense mutation (Y127C) in affected individuals of two of four families. This gene encodes a protein, which is localized to hair cell stereocilia and kinocilium from development stage E16.5 to P3 in mice. Our findings establish the importance of the DFNB67 gene in human sound transduction and raise the possibility of genetic heterogeneity of recessive hearing loss in a gene rich region of human chromosome 6.

### **349** TMC1 Mutations in Pakistani Families

#### **Segregating DFNB7/B11 Deafness**

Rachel McNamara<sup>1</sup>, Tomoko Makishima<sup>1</sup>, Tayyab Husnain<sup>2</sup>, Ahmad Usman Zafar<sup>2</sup>, Zubair M. Ahmed<sup>1</sup>, Thomas B. Friedman<sup>1</sup>, Sheikh Riazuddin<sup>2</sup>, Andrew Griffith<sup>1</sup>  
<sup>1</sup>NIDCD, NIH, Rockville, MD, <sup>2</sup>Centre of Excellence in Molecular Biology, Lahore, Pakistan

Dominant and recessive mutations of *TMC1* (transmembrane channel-like gene 1) cause sensorineural hearing loss (SNHL) at the DFNA36 and DFNB7/B11 loci, respectively (Kurima et al., *Nature Genetics*, 2002). *Tmc1* mRNA is expressed in cochlear and vestibular hair cells, but its function is unknown. In this study, we performed nucleotide sequence analysis of all 24 *TMC1* exons and adjacent intronic sequence in 12 Pakistani families co-segregating recessive SNHL with microsatellite markers linked to DFNB7/B11. We identified three novel and two reported mutations in 11 of the 12 families; the family without a mutation was not large enough to support statistically significant linkage to DFNB7/B11. In each family, homozygosity for the mutation co-segregates with SNHL. None of the mutations were found in ethnically-matched normal controls. We identified the splice site mutation IVS5+1G>T in one family, missense substitutions P514L in one family, C515R in two families, and S668R in one family, and the nonsense mutation R34X in six families. All of the missense mutations are nonconservative substitutions of conserved residues (Kurima et al., *Genomics*, 2003). In combination with previous results (Kurima et al., *Nature Genetics*, 2002), we have identified *TMC1* mutations in 22 Pakistani families segregating recessive SNHL. The results confirm genetic homogeneity at this locus and our previous observation that R34X accounts for about one half of *TMC1* mutant alleles in this population. We are currently completing a haplotype analysis of R34X chromosomes to determine if it arose from a single common founder. Finally, the three additional recessive missense mutations will provide useful loss-of-function control alleles for *in vitro* studies to identify the function of *TMC1*.

10

### **350** Identification of *CHD7* Mutations in Children with Features of CHARGE Syndrome and Hearing Loss

Glenn Green<sup>1</sup>, Donna M. Martin<sup>1</sup>

<sup>1</sup>University of Michigan

Aberrant development of the inner ear, including the vestibular system, has been identified as a common cause of congenital hearing loss. CHARGE syndrome is a multiple congenital anomaly syndrome that affects development of the inner ear, eye, heart, craniofacial structures, and growth and development. Atresia of the semicircular canals has been associated with sensorineural hearing loss and is present in most individuals with CHARGE syndrome. Recently, the gene underlying much of CHARGE syndrome was identified as *CHD7*, a novel member of the chromodomain gene family (Vissers et al., 2004). The prevalence of *CHD7* mutations in individuals with atypical CHARGE or isolated features of

CHARGE (e.g. only semicircular canal dysgenesis) is not known.

We have screened DNA samples from 14 children with features of CHARGE syndrome for mutations in *CHD7*. 43 PCR primer pairs were designed to amplify the entire coding sequence and all 38 intron/exon boundaries of *CHD7*. Bidirectional sequencing of PCR products confirmed amplification of the correct target in all cases. Parental DNA was sequenced to determine whether identified mutations were *de novo*.

To date, we have identified five novel mutations in five individuals with features of CHARGE. These include three nonsense mutations, one missense mutation and one frameshift mutation. One individual who did not meet the diagnostic criteria for CHARGE but had lateral semicircular canal atresia was identified as having a *de novo* nonsense mutation. We also identified a nonpathogenic missense polymorphism present in both an affected individual and her mother.

These data suggest that mutations in *CHD7* account for a sizable portion of hearing loss associated with CHARGE. Identification of mutations in *CHD7* may aid in the diagnosis, evaluation and treatment of children with features of CHARGE.

### **351** Hereditary Hearing Loss in Israel: Genes, Prevalence and Genotype-Phenotype Correlation

Zippora Brownstein<sup>1</sup>, Orit Dagan<sup>1</sup>, Moshe Frydman<sup>1,2</sup>, Abraham Goldfarb<sup>1,3</sup>, Tom Walsh<sup>4</sup>, Jake Higgins<sup>4</sup>, Moien Kanaan<sup>5</sup>, Mary-Claire King<sup>4</sup>, Karen B. Avraham<sup>1</sup>

<sup>1</sup>Dept. Human Molecular Genetics & Biochemistry, Sackler School Medicine, Tel Aviv U, Tel Aviv, Israel, <sup>2</sup>Danek Gertner Institute of Genetics, Chaim Sheba Medical Center, Tel Hashomer, Israel, <sup>3</sup>Department of Otolaryngology/Head and Neck Surgery, Hadassah University Hospital, Jerusalem, Israel, <sup>4</sup>Departments of Medicine and Genome Sciences, University of Washington, Seattle, WA, USA, <sup>5</sup>Department of Life Sciences, Bethlehem University, Bethlehem, Palestinian Authority

Hearing loss is a highly heterogeneous genetic disorder, with over 100 genes predicted to be involved. Mutations in four genes were previously known to lead to non-syndromic hearing loss (NSHL) in the Israeli population. These include connexin 26 (*GJB2*), connexin 30 (*GJB6*), myosin IIIA (*MYO3A*), and *POU4F3*. The latter two genes were identified in two extended families only. *GJB2* mutations, however, are associated with 39% of children born with hearing loss. The del(*GJB6*-D13S1830) mutation is most often associated with a heterozygote *GJB2* mutation in deaf individuals. We have ascertained families representing new loci for deafness in the Israeli population. We report the mapping of a new otosclerosis locus, *OTSC4*, to chromosome 16q22.1-23.1. A detailed phenotypic characterization of the hearing impaired members of the family demonstrates the complex variety of hearing phenotypes within one family. Family T, with progressive NSHL, maps to chromosome 9q21 to the DFNA36 region, although we were unable to identify mutations in *TMC1* or exclude this gene. Family Z, with

recessive profound NSHL, maps to the *DFNB12* locus on 10q21-q22. We identified a novel missense mutation in a CDH23 extracellular cadherin domain. Chromosomal localization, genotype-phenotype correlations, and implications for clinical diagnosis and genetic counseling will be presented.

Research supported by NIH R01 DC005641 and European Commission FP6 Integrated Project EUROHEAR LSHG-CT-20054-512063.

### **352 Genomic Analysis of a Heterogeneous Mendelian Phenotype: Multiple Novel Alleles for Inherited Hearing Loss in the Palestinian Population**

Tom Walsh<sup>1</sup>, Judeh Abu Sa'ed<sup>2</sup>, Hashem Shahin<sup>2,3</sup>, Jeanne Shepshelovich<sup>4</sup>, Ming K. Lee<sup>1</sup>, Koret Hirschberg<sup>4</sup>, Mustafa Tekin<sup>5</sup>, **Karen B. Avraham**<sup>3</sup>, Mary-Claire King<sup>1</sup>, Moien Kanaan<sup>2</sup>

<sup>1</sup>*Departments of Medicine and Genome Sciences, University of Washington, Seattle, WA, USA,* <sup>2</sup>*Department of Life Sciences, Bethlehem University, Bethlehem, Palestinian Authority,* <sup>3</sup>*Dept. Human Molecular Genetics & Biochemistry, Sackler School Medicine, Tel Aviv U, Tel Aviv, Israel,* <sup>4</sup>*Department of Pathology, Sackler School of Medicine, Tel Aviv University, Tel Aviv, Israel,* <sup>5</sup>*Division of Pediatric Genetics, Ankara University School of Medicine, Dikimevi, Ankara*

Recessively inherited phenotypes are frequent in the Palestinian population as the result of a long tradition of marriages within extended kindreds, particularly in isolated villages. In order to characterize the genetics of inherited hearing loss in this population, we worked with West Bank schools for the deaf to identify children with prelingual, bilateral, severe to profound hearing loss not attributable to infection, trauma, or other known environmental exposure. Of 156 families enrolled, hearing loss in 17 families (11%) was due to mutations in *GJB2* (connexin 26), a smaller fraction of *GJB2*-associated deafness than in other populations. In no families was hearing loss due to previously reported Palestinian mutations in other deafness-related genes. In order to estimate how many different genes might responsible for hearing loss in this population, we evaluated ten families for linkage to all 36 known human autosomal deafness-related genes, fully sequencing genomic DNA from informative relatives for hearing-related genes at all linked sites. Four families harbored four novel alleles of *TMPRSS3*, otoancorin, and pendrin. In each family, all affected individuals were homozygous for the critical mutation. Each allele was specific to one or a few families in the cohort; none were widespread. Therefore, we used functional and bioinformatics approaches to evaluate the consequences of the mutations. In six other families, hearing loss was not linked to any known hearing-related gene, suggesting these families harbor novel genes responsible for their hearing phenotypes. We conclude that inherited hearing loss is highly heterogeneous in this population, with most extended families functioning as genetic isolates, harboring private alleles of either known or novel genes.

Research supported by NIH R01 DC005641.

### **353 GJB2 Variations in a South African Hearing Impaired Population**

**Rosemary Kabahuma**<sup>1,2</sup>, Claire Penn<sup>3</sup>, Michele Ramsay<sup>4</sup>, Jerry Sigudla<sup>1</sup>

<sup>1</sup>*Department of Otorhinolaryngology, Polokwane Provincial Hospital,* <sup>2</sup>*University of Witwatersrand,* <sup>3</sup>*Department of Speech Pathology and Audiology, University of Witwatersrand,* <sup>4</sup>*Department of Human Genetics, University of Witwatersrand*

The *GJB2* gene has been found to account for up to 50% of genetic recessive nonsyndromic hearing loss in Caucasian and Asian populations. It has been noted that there are population differences in the distribution of *GJB2* alleles in all described populations. This includes the high prevalence of 35delG in Caucasians of European descent, 235delC among Japanese and Koreans, and 167delT among the Ashkenazi Jews. A founder effect has been demonstrated in many of these populations. Data from African populations has started coming forward, such as the finding of R143W mutation in Ghana. It is important to determine the contribution of this gene to genetic hearing impairment in the African population. This will only be clarified after more population groups have been analyzed.

We assessed 184 deaf subjects with presumed genetic non-syndromic hearing loss, aged 5 to 18 years, from the Venda, Pedi and Tsonga speaking population groups of the Limpopo Province of South Africa, for mutations in *GJB2*. Using genomic DNA extracted from peripheral blood, the complete coding exon of *GJB2* was sequenced using an ABI377 sequencer. None of the reported mutations were found in the coding region. However, a high frequency of variations in the upstream (5') region, that is, C>T at -15 and C>T at -34 respectively, were found. The significance of these variations in comparison to the general population in the region is explored. It would seem that the contribution of *GJB2* to genetic nonsyndromic hearing loss in this population is minimal, leaving the way open for the search of the common gene(s) for genetic deafness in this population.

This work was supported by the MRC, South Africa, and the Mellon Foundation, South Africa

### **354 Polyester Wax: A New Embedding Medium for the Histopathologic Study of Human Temporal Bones**

**Saamil N. Merchant**<sup>1,2</sup>, Barbara Burgess<sup>1</sup>, Diane Jones<sup>1</sup>, Joe Adams<sup>1,2</sup>

<sup>1</sup>*Massachusetts Eye and Ear Infirmary,* <sup>2</sup>*Harvard Medical School*

Background: Celloidin and paraffin are the two common embedding mediums used for study of the human temporal bone (TB) by light microscopy. Although celloidin embedding permits excellent morphology, celloidin is difficult to remove with significant restrictions on success with immunostaining. Embedding in paraffin allows immunostaining but preservation of cellular detail within the membranous labyrinth is relatively poor.

Objectives/hypothesis: Polyester wax is an embedding medium that has a low melting point (37° C), is soluble in most organic solvents, is water tolerant and sections easily. We hypothesized that embedding TBs in polyester

wax would permit good preservation of morphology and allow immunostaining.

**Methods:** Nine TBs from individuals aged 1-94 years removed 2-31 hours postmortem were used. TBs were fixed in formalin, decalcified in EDTA, embedded in polyester wax and serially sectioned at 8-12 µm on a rotary microtome. The block and knife were cooled with frozen CO<sub>2</sub> (dry ice) held in a funnel above the block. Sections were placed on glass slides coated with 1% fish gelatin and 1% bovine albumin, followed by hematoxylin and eosin staining. Immunostaining was also performed on selected sections using antibodies to 200 kD neurofilament and Na-K-ATPase.

**Results and Conclusions:** Polyester wax embedded sections demonstrated good preservation of cellular detail of the organ of Corti and other structures of the membranous labyrinth, as well as the surrounding otic capsule. The protocol was reliable and consistently yielded sections of good quality. Immunostaining was successful with both antibodies. Thus, polyester wax offers the advantage of good preservation of morphology and ease of immunostaining. We anticipate that in the future, polyester wax embedding will also permit other molecular biologic assays on temporal bone sections such as the retrieval of nucleic acids and the study of proteins using mass spectrometry-based proteomic analysis.

### **[355] Hearing Loss and Amount of Spiral Ganglion Cells in Human. Is There Any Correlation?**

**Annelies Schrott-Fischer<sup>1</sup>, Mario Bitsche<sup>2</sup>, Glueckert Rudolf<sup>1</sup>**

<sup>1</sup>Research Lab. ENT Department, <sup>2</sup>ENT Department

Previous histopathological studies on temporal bones have shown that in most cases profound sensorineural hearing loss is associated with changes in the sensory epithelium of the Organ of Corti, Stria vascularis and Reissner's membrane. The degenerative behaviour of the spiral ganglion may also be of great importance in establishing criteria for selection of patient for cochlear implants. Some authors have already conducted studies on temporal bones from profound deaf patient in which the condition of the spiral ganglion and the cochlear nerve were related to the clinical diagnosis. These studies have shown an inconsistent relationship between clinical data and the number of surviving ganglion cells.

Aims of the present study was to create a data bank using the computer program MS Access to collect data of spiral ganglion counts available on human temporal bones to find similarities of all cases published so far. On the other hand we tried to evaluate the methodological aspects of quantitative analysis and compared the celloidin method with the block surface method (Spoendlin, 1987)

We correlated the total number of spiral ganglion cells with hearing thresholds in relation to age, duration of hearing loss and duration of deafness and tried to get more information of the deterioration rate of human spiral ganglion cells.

The evaluation of available data on nerve fibres, spiral ganglion cells and audiograms does not show a clear relationship. The celloidin and block surface method here show similar results.

The most significant loss of ganglion cells appears within the first 5 to 10 years. Morphological changes in long term deaf show that SGCs can persist over a long period of time, but there are no data whether these are functional. We conclude that cochlear implants should be used as early as possible to maintain functional.

### **[356] Unbiased Stereological Analysis of the Human Spiral Ligament and Stria Vascularis: A Temporal Bone Study**

**Joshua Tokita<sup>1,2</sup>, Ivan Lopez<sup>2</sup>, Gail Ishiyama<sup>3</sup>, Yong Tang<sup>4</sup>, Akira Ishiyama<sup>2</sup>**

<sup>1</sup>University of Illinois at Chicago, College of Medicine-Department of Anatomy and Cell Biology, <sup>2</sup>UCLA School of Medicine, Surgery Department-Division of Head and Neck, <sup>3</sup>UCLA School of Medicine, Neurology Department, <sup>4</sup>Department of Histology and Embryology, Chongqing University of Medical Sciences, P.R. China

The present study applies the design-based stereological Cavalieri principle to measure the volume of the stria vascularis and spiral ligament in human using post-mortem archival temporal bone specimens. Normative data was obtained from individuals with no history of audiovestibular disease, of ages ranging from 15 to 84 years old (N = 25). The effect of increasing age on stria vascularis and spiral ligament volumes was determined. The present study also used the Cavalieri principle to study the volumes of the stria vascularis and spiral ligament of subjects with histopathologically confirmed cochlear otosclerosis (N = 14, ages ranging from 60 to 87 years old) and of subjects with Meniere's disease (N = 5, ages ranging from 63 to 91 years old.) The spiral ligament and stria vascularis volumes in individuals older than 60 years were significantly less than in individuals of young adult or middle adult ages. The volume of the spiral ligament, but not the stria vascularis, from subjects with cochlear otosclerosis was significantly less than in normative age-matched controls (p < 0.0001). The stria vascularis and spiral ligament volume from subjects with Meniere's disease was significantly lower than that from age-matched normative controls. The volume of the stria vascularis and spiral ligament did not vary significantly by sex. The present study demonstrates for the first time the use of the design-based stereology – Cavalieri principle as a reliable and efficient method to estimate the volume of structures in the human temporal bone. Volumetric measurements using stereology provide a consistent method for assessing the size of a structure by avoiding assumptions associated with two-dimensional measurements. Unlike length and area measurements, the orientation of the sample when it is sectioned does not bias stereological volumetric analysis.

### **[357] Three-Dimensional Analysis of the Human Cochlea**

**Arne Voie<sup>1</sup>, Gene Saxon<sup>1</sup>, Mailee Hess<sup>1</sup>**

<sup>1</sup>Spencer Technologies, Seattle, WA

A human temporal bone specimen, harvested from a body donor and fixed in neutral buffered formalin, was prepared and imaged using the OPFOS technique (Voie, Hear Res. 171:119, 2002; Voie et al, JASA, 114 (4), Pt.2 of 2, p.

2432, 2003) producing a volumetric data set to reconstruct and analyze cochlear features in three dimensions. Using the software package Amira, full 3D reconstructions of the cochlear scalae were performed, which allow a viewer to appreciate the anatomy of the cochlea from both an external and a unique internal perspective. These data were then used to generate scalae centroid curves, which became fundamental metrics for further geometric and vector analyses. Quantities such as cross-sectional area, surface area and volume were computed for all scalae, and reported as functions of the centroid arclength and the extent of angular rotation about the cochlear axis. Further, the scalae centroids were analyzed using vector techniques to gain understanding of canal direction, curvature and torsion. A conversion from Cartesian to general cylindrical coordinates was performed, to gain further insight into canal shape and size relative to each other along the extent of the labyrinth. Results of these analyses are presented. Supported by grant NIH/NIDCD R43DC006310.

### **358 Three Dimensional Anatomy of the Helicotrema and Basal Turn of the Human Cochlea**

**Gene Saxon<sup>1</sup>**, Mailee Hess<sup>1</sup>, Arne Voie<sup>1</sup>

<sup>1</sup>*Spencer Technologies, Seattle, WA*

The complex geometry of 3D features within the human cochlea is challenging to appreciate using histological sectioning techniques which are destructive and intrinsically 2D in nature. The basilar and apical regions of an intact human cochlea were imaged for this study using the OPFOS method (Voie *Hear Res.* 171:119, 2002) and graphically rendered using Amira. The cochlear specimen was optically scanned into a series of planar images captured with inter-plane spacing of 3 microns and 2X magnification producing an image intensity data volume with 3 micron voxel edges. Features rendered in the basilar and apical turn of the cochlea were: the round window membrane, cochlear aqueduct, spiral ligament, basilar membrane, scala media, scala tympani, scala vestibuli and a portion of the vestibule. The graphical rendering further showed the close proximity of the cochlear aqueduct in relation to the round window membrane. Also clearly visualized was an almost 180 degree arc of spiral ligament which lies adjacent to the basilar portion of the round window membrane. The area of communication between the scala tympani and vestibule was discovered to be far greater than previously understood. A cul-de-sac region apical to the helicotrema was also discovered together with the helicotrema and scala media.

### **359 3-D Reconstruction of Round Window and Related Cochlear Anatomy in the Human with Implications for Cochlear Implantation**

**Haobing Wang<sup>1</sup>**, Clarinda Northrop<sup>1</sup>, Saumil N. Merchant<sup>1,2</sup>, Barbara Burgess<sup>1</sup>, Jennifer Smullen<sup>1,2</sup>, Joseph B. Nadol, Jr.<sup>1,2</sup>

<sup>1</sup>*Dept of Otolaryngology, Massachusetts Eye and Ear Infirmary*, <sup>2</sup>*Harvard Medical School*

**Goals:** To develop a 3-D virtual model of the anatomy of the round window (RW) membrane and adjacent cochlear

structures in the human. Knowledge of the spatial relationships of these structures has implications for cochlear implantation, wherein preservation of residual hearing is an important aim in some cases.

**Methods:** Archival 20 micron celloidin-embedded sections from a 14-year old male were used. Each section through the RW was stained, digitized and imported into a 3-D software program (Amira, v3.1). The 3-D model is a surface rendering of these structures of interest, including the RW, basilar membrane, osseous spiral lamina, scala media, spiral ligament, cochlear aqueduct, inferior cochlear vein, scala vestibuli, scala tympani, and the ductus reuniens.

**Results:** The scala media and basilar membrane of the hook portion of the cochlea, and the ductus reuniens were in close proximity to the posterior and superior aspect of the RW membrane (within 0.5 mm), a relationship which is generally under-appreciated by otologic surgeons. These structures are at risk for injury during cochlear implantation. Structures of relevance that were located on the cochlear side of the RW include the basilar membrane and scala media superiorly, the modiolus medially, and the inferior cochlear vein infero-medially. The shortest distance to these structures from the mid part of the RW membrane was 0.5 mm to the basilar membrane, 0.6 mm to the modiolus and 1.9 mm to the inferior cochlear vein. No critical cochlear structure was located in the area within 1.0 mm of the anterior edge of the RW membrane. A cochleostomy through the mid- and anterior part of the RW or in the otic capsule that is immediately adjacent and anterior to the RW, or through both areas would avoid injuring critical cochlear structures. The direction of placement of an implant should be anterior and slightly inferior, towards a point just medial to the carotid artery, in order to minimize trauma.

### **360 Congenital Malformations of the Cochlea: A Functional Classification System**

**Aayesha M. Khan<sup>1</sup>**, Joseph B. Nadol, Jr.<sup>2,3</sup>

<sup>1</sup>*Department of Otolaryngology Head and Neck Surgery, Saint Louis University, MO*, <sup>2</sup>*Department of Otolaryngology, Harvard Medical School, Boston, MA*,

<sup>3</sup>*Department of Otolaryngology, Massachusetts Eye and Ear Infirmary, Boston, MA*

**Introduction:** Patients with congenital malformations of the inner ear often require rehabilitation with cochlear implantation. Many classification systems for inner ear malformations have been proposed (Jackler 1987; Sennaragolu 2002; Zheng 2002). However, none of these have been shown to reliably predict clinical response after cochlear implantation. We believe a classification system that predicts the number of spiral ganglion cell counts (SGCC) may possibly also predict clinical response.

**Aim:** To develop a classification system that is predictive of SGCC in patients with congenital malformations of the cochlea.

**Methods:** This classification was based on embryological development of the inner ear (Streeter 1906) and the severity of malformations determined by histopathology. 2-D reconstruction was performed to determine the number and length of the cochlear duct (Guild 1921; Schuknecht



1993). The total SGCC were calculated (Nadol 1988) and expressed as percentage of normal age-matched controls (Otte 1978). Statistical analysis for non-parametric data was performed.

Results: The malformations were categorized as Types 0, 1, 1.5, 2 and 2.5 based on increasing number of cochlear turns, and subdivided into W: Widely patent cochleovestibular communication, S: Scala Communis and H: Hypoplasia deformities, in decreasing order of severity. Fifty seven human temporal bones with congenital malformations of the cochlea were identified from the collection at the Massachusetts Eye and Ear Infirmary. Five specimens were excluded due to absence of spiral ganglion cells leaving N=52. Spearman's Rho between SGCC expressed as percentage of normal controls and the proposed classification, was 0.813 ( $p < 0.001$ ,  $\alpha = 0.01$ ).

Conclusion: This study proposes a functional classification system that is based on embryology and histopathology. It can be used to predict the number of SGCC in patients with congenital malformations of the cochlea which may have important clinical significance.

### **[361] Morphological Observation of Human Temporal Bones with Large Vestibular Aqueduct**

**Shigeo Hirai**<sup>1,2</sup>, Sebahattin Cureoglu<sup>1,3</sup>, Patricia A. Schachern<sup>3</sup>, Mehmet F. Oktay<sup>1</sup>, Hideo Hayashi<sup>1</sup>, Michael M. Paparella<sup>4</sup>, Tamotsu Harada<sup>2</sup>

<sup>1</sup>International Hearing Foundation, <sup>2</sup>Department of Otolaryngology, Kawasaki Medical School, <sup>3</sup>Department of Otolaryngology, Otitis Media Research Center, University of Minnesota, <sup>4</sup>Minnesota Ear Head and Neck Clinic

Large vestibular aqueduct syndrome (LVA) has been reported to be one of the common ear anomalies in the evaluation of hearing loss (HL). Although many cases of LVA have been reported, the mechanism of HL associated with LVA is unclear and there is no established criterion for its diagnosis. Our objective is to determine the incidence of LVA in our temporal bone (TB) collection and its relationship to other systemic and/or otologic findings or syndromes. We measured the antero-posterior diameter of the internal and external orifices of the vestibular aqueducts (VA) of 40 normal TBs (mean age 52; range 2-93). Cases were considered as LVA if the width of the internal and external orifices were 95% greater than those of the normal VA group; greater than 0.6mm for the internal orifice and 6.25mm for the external. From 1,850 TBs, 28 TBs (21 cases) fit the criteria of LVA. Ages ranged from still born to 91 years (mean 26). There were 51 associated external and middle ear anomalies, and 48 inner ear anomalies. Congenital heart anomalies, the most commonly associated pathologic condition, were observed in 11 out of 21 cases (52%). Mondini dysplasia, the most common congenital anomaly (syndromes and dysplasia), was observed in 10 out of 21 cases (48%). Of the 21 cases, 9 had syndromes (43%) and 12 had no syndrome (57%). From these 12 cases, 10 had at least one ear anomaly which could be the cause of HL. No congenital ear anomalies except LVA were found in 2 TBs (2 cases). Although the mechanisms of HL associated with LVA are unclear, they may be attributed to other accompanying ear anomalies and pathologic conditions. LVA can also be an incidental diagnosis in patients with no HL. It is important

to investigate inner ear problems and system diagnoses that may indicate a syndrome in patients who are diagnosed radiologically as having LVA.

### **[362] SEM Analysis of Perilymph/Modiolar Communication Routes. Is Perilymph Locally Produced and Drained in the Human Cochlea?**

**Rudolf Glueckert**<sup>1</sup>, Annelies Schrott-Fischer<sup>1</sup>, Kristian Pfaller<sup>2</sup>, Helge Rask-Andersen<sup>3</sup>

<sup>1</sup>Medical University Innsbruck, Department of Otolaryngology, <sup>2</sup>Medical University Innsbruck, Institute of Anatomy and Histology, <sup>3</sup>Department of Otolaryngology Uppsala University Hospital, Sweden

We analysed the surface structure of the human cochlea using high resolution scanning electron microscopy (SEM) in macerated and freshly obtained specimens together with light microscopy of serially sectioned celloidin embedded temporal bones. Combined SEM and serial light microscopy sectioning showed that perilymph and fluid spaces in the modiolar periphery form a common system. We suggest that perilymph is mainly produced and reabsorbed by modiolar vessels. The modiolar wall of the scala vestibuli and tympani in the first and second turn is porous, forming perilymphatic communication routes to the perivascular and perineural spaces in the modiolus. A "perimodiolar lymph" or fluid space can be identified in the modiolar periphery. It communicates through a trabecular meshwork of porous membrane and web of connective tissue with the perilymph. The thin mesothelial cell sheets showed pores and displayed signs of vesicular activity. The canalicular system may play a role in the circulation of perilymph in the human cochlea and may also be a pathway for future drug and cell-based therapy to the inner ear. This meshwork showed striking similarities to the trabecular meshwork of the eye, which is known to be related to the drainage of fluid into the *canalis Schlemmi*. We suggest that this system may represent an important site for perilymph drainage, but also for perilymph production in human cochlea.

### **[363] 3D Representation of the Guinea Pig Inner Ear and the Implications for Modeling Drug Movements in the Fluids**

**Alec Salt**<sup>1</sup>, Ruth Gill<sup>1</sup>, Arne Voie<sup>2</sup>, Gene Saxon<sup>2</sup>

<sup>1</sup>Department of Otolaryngology, Washington University School of Medicine, St. Louis, MO, <sup>2</sup>Spencer Technologies, Seattle, WA

A guinea pig inner ear was fixed and prepared for OPFOS imaging based on previously-published methods (Voie Hear Res. 171:119, 2002). The initial image set including the cochlear and vestibular portions of the inner ear consisted of 862 slices, each 1380 x 1035 pixels (1.2 GB). The data were reduced to a manageable size of 345 x 258 x 215 voxels (total 19 MB) by downsampling by a factor of 4. Voxels were approximately 32  $\mu$ m on each side. The fluid and tissue compartments of the inner ear were segmented using Amira software. The compartments defined included endolymph, perilymph, the spiral ligament, the organ of Corti and vestibular sensory tissues, the round window membrane and the stapes. The volumes of each compartment, derived by total voxel count, were



perilymph: 19.7 uL; endolymph: 6.0 uL; spiral ligament 2.7 uL; organ of Corti and semi-circular canal ampullae: 1.4 uL. 3D segmentation of structures gives a unique insight into the interrelationships between compartments that are not available from histologic sections. There are two areas where visualization of the 3D structures will have a substantial impact on the way we model drug movements through the inner ear spaces. Reconstruction of the basal turn shows the spiral ligament follows the endolymphatic space as it curves around the perimeter of the round window membrane. As we know drugs pass through the spiral ligament, this provides a far more extensive communication between the basal part of scala tympani and the vestibule than has previously been recognized. This is important to our understanding of how drugs applied to the round window spread in the inner ear. Similarly, reconstruction of the cochlear apex reveals that scala tympani opens without significant constriction into an apical "cistern" that continues basally as scala vestibuli. Visualization of the 3D anatomy of the inner ear is important for teaching and for modeling the inner ear accurately.

Supported by grant NIH/NIDCD RO1 DC01368 (AS).

### **364 Development of a 3D Geometric Coordinate System for the Mouse Cochlea**

**Peter A. Santi**<sup>1</sup>, Ian Rapson<sup>1</sup>, John Purdy<sup>1</sup>, Eugene Saxon<sup>2</sup>, Arne Voie<sup>2</sup>

<sup>1</sup>University of Minnesota, <sup>2</sup>Spencer Technologies, Seattle, WA

Mouse cochleas were removed from euthanized animals and chemically fixed by immersion in 4% paraformaldehyde in the Cochlear Anatomy Laboratory. After decalcification with EDTA, dehydration with ascending concentrations of ethanol, and clearing in a solution of methyl salicylate and benzol benzoate cochleas were stained with rhodamine isothiocyanate. They were then sent to Spencer Technologies for OPFOS imaging and the serial, optical sections were returned to the Cochlear Anatomy laboratory for image processing. In order to produce a 3D coordinate system for the cochlea, similar to a stereotaxic atlas for the brain, a 3D geometric Cartesian coordinate system was chosen that referenced a B-spline curve along the length of the basilar membrane. To produce the B-spline, the basilar membrane was segmented in each optical section and a 3D reconstruction was produced. Control points at the mass center of cross-section of the basilar membrane were manually positioned along the basilar membrane. Amira then fitted the spline curve along the length of the basilar membrane using the control points. The X,Y,Z coordinates of the spline curve were exported from Amira and were used to "virtually resection" the cochlea and generate 99 orthogonal planes through the basilar membrane and the scala media. The spline was adjusted to the true mass center of the basilar membrane and the cochlea was resectioned again producing up to 500 cross sections. Since these are "true" cross sections, it is possible to obtain accurate distance and area measurements of structures in each cross section and their location along the length of the basilar membrane. Results from our method were compared to

line-segment fits to determine basilar membrane distance and width. Supported by grants to P. Santi from the Lions Hearing Foundation and the NIDCD.

### **365 Solid Modeling of the Mouse Cochlea from 3D Reconstructions Using Rapid Prototyping**

**Peter A. Santi**<sup>1</sup>, Ian Rapson<sup>1</sup>, David Hultman<sup>1,2</sup>

<sup>1</sup>University of Minnesota, <sup>2</sup>Department of Electrical and Computer Engineering

The purpose of this presentation is to describe the process and show the results of preparing solid models of the mouse cochlea from computer generated, 3D reconstructions using rapid prototyping. 3D reconstructions of mouse cochleas were prepared as previously described (Santi et al., 2004, ARO abstract #425) using the Amira program. After segmentation of all major cochlear structures, selected 3D reconstructions were combined and saved as .stl (stereolithography) files. These files were sent to the Aerospace Engineering and Mechanics shop at the UM for solid modeling using a rapid prototyping method. Reconstructions were enlarged 50X and imported into a program which orients the solid model and generates support structures for building the solid model, one layer at a time, with ABS plastic using a Dimension, fusion deposition machine (Stratasys, Inc.). Models were constructed in a few hours on a base with breakaway, support structures. A cochlea containing the three scaleas was first constructed and then individual scala were produced. External structures of the scala, such as the basilar membrane, helicotrema, and annular ligament, could be resolved on the solid models. Structures within the scala media, such as the organ of Corti, spiral limbus, and stria vascularis, could also be resolved by removing Reissner's membrane prior to solid modeling. The volume of these solid models was determined by volume displacement of water and compared with their volume as calculated by Amira. The ability to examine the relationships between different cochlear structures, tactilely as well as visually, provides a better understanding of cochlear anatomy than can be obtained by viewing 3D reconstructions on a computer display. In addition, the cost and time to produce solid models, is quite reasonable. Solid cochlear models are useful for teaching, as a presurgical experience, and to design custom cochlear implant devices. Supported by grants to P. Santi from the Lions Hearing Foundation and the NIDCD.

### **366 Great Ears: Functional Comparisons of Land and Marine Leviathan Ears**

**Darlene R. Ketten**<sup>1,2</sup>, J. Shoshani<sup>3</sup>, J. O'Malley<sup>1</sup>, J. Arruda<sup>1,2</sup>, Daphne Manoussaki<sup>4</sup>, Emiliios K. Dimitriadis<sup>5</sup>, Brett Shoelson<sup>6</sup>, Richard S. Chadwick<sup>6</sup>

<sup>1</sup>Harvard Medical School, <sup>2</sup>Woods Hole Oceanographic Institution, <sup>3</sup>University of Asmara, Asmara, Eritrea,

<sup>4</sup>Vanderbilt University, Nashville, TN, <sup>5</sup>NIH, Bethesda, MD,

<sup>6</sup>NIDCD, Bethesda, MD

Elephants and baleen whales are massive creatures that respond to exceptionally low frequency signals. Although we have many elephant and whale vocalization

recordings, nearly nothing is known about their hearing. Indirect evidence from playbacks suggests hearing of proboscideans and mysticetes is similar and is tuned primarily to low and possibly infrasonic signals.

This raises two interesting questions. First, these signals are emitted and perceived in two media, air and water, with radically different physical acoustic properties: 4.5-fold differences in sound speed; three magnitudes in acoustic impedance. For elephants and whale ears to have the same percept, whales must accommodate 60-fold acoustic pressures. Further, a commonly held tenet is that the upper limit of hearing is inversely correlated with body mass, implying there should be virtually no overlap in the hearing of these two taxa.

The goal of this study was to determine how inner ears in these Tethytherians are structured, particularly for low frequency (LF) hearing. Computerized tomography and celloidin histology preparations were analyzed in six baleen whale (n=15) and two elephant species (n=7). The data show mysticetes have a substantially greater hearing range but that coiling and apical cochlear structures are similar, suggesting common mechanical underpinnings for LF hearing.

### **[367] Otolith Crystal Type Affects Hearing Sensitivity in Chinook Salmon**

Dion Oxman<sup>1</sup>, Rachel Barnett-Johnson<sup>2</sup>, Michael E. Smith<sup>3,4</sup>, **Allison B. Coffin**<sup>4,5</sup>, Diane L. Miller<sup>4,5</sup>, Ron Josephson<sup>1</sup>, Arthur N. Popper<sup>4,5</sup>

<sup>1</sup>Alaska Department of Fish and Game, Commercial Fisheries Division, Mark, Tag, and Age Laboratory,

<sup>2</sup>National Marine Fisheries Service, Fishery Ecology Division, <sup>3</sup>Department of Biology, Western Kentucky University, <sup>4</sup>Department of Biology, University of Maryland,

<sup>5</sup>Center for Comparative and Evolutionary Biology of Hearing, University of Maryland

Teleost fishes have three inner ear otolithic end organs (sacculus, lagena, and utricle) that are used for hearing and balance. The exact contributions of different end organs to hearing are unknown in most species but the sacculus is considered the primary auditory end organ in many fishes. Each end organ contains a calcium carbonate structure, the otolith, that is similar to the otoconia found in other vertebrates. In free-ranging teleosts, calcium carbonate in the saccular otolith (the sagitta) is usually deposited as crystals of aragonite but it also occurs less frequently in a clear crystallized form called vaterite. Recent reports indicate that the frequency of occurrence of vateritic sagittae is greater in hatchery-raised salmonid and clupeid (herring-like) fishes than in their wild counterparts. Here we investigate the functional consequences of otolith composition in hatchery-raised Chinook salmon (*Oncorhynchus tshawytscha*) from the Coleman National Fish Hatchery in Anderson, CA. Of the population tested, 55% had normal (aragonitic) sagittae, 30% had vateritic sagittae, and 15% had one otolith of each crystal type. Measures of hearing using the auditory brainstem response (ABR) showed a significant 5-10 db loss in sensitivity in salmon that have at least one vaterite otolith. Analysis of inner ear structure showed no significant

difference in saccular hair bundle density or the length-to-width ratio of the sacculus between ears with different otolith types. Increased hearing thresholds in fishes with vaterite otoliths may be due to density differences between otolith types, but this hypothesis has not been investigated in detail. These results suggest that hatchery procedures may have negative consequences for fish hearing. Future studies will focus on determining if survival of salmonids is negatively correlated with the presence of vateritic otoliths.

### **[368] Assessment of Prestin-Self Association Using Acceptor Photobleach Fluorescence Resonance Energy Transfer**

Jennifer Greeson<sup>1</sup>, Fred A. Pereira<sup>2</sup>, Robert M. Raphael<sup>1</sup>

<sup>1</sup>Rice University, <sup>2</sup>Baylor College of Medicine

An active process within the cochlea is necessary to obtain the frequency sensitivity and selectivity characteristic of mammalian hearing. At present, many believe that this process is realized, at least in part, through the electromotile response seen in outer hair cells (OHCs). Electromotility requires the presence of prestin, a transmembrane protein highly expressed in the OHC lateral wall. The extent and means by which prestin participates in electromotility are unknown, but it is likely that prestin-prestin interactions play a role. We have assayed for the self-association of prestin under steady-state conditions using acceptor photobleach fluorescence resonance energy transfer (FRET). FRET is a powerful technique for studying protein-protein interactions at the molecular level. We use the HEK model cell system with the standard CFP/YFP fluorescence donor/acceptor pair and follow a method developed by Karpova et al. specifically for use on a laser scanning confocal microscopy system (Zeiss LSM 510). Careful consideration was paid to timing and noise constraints induced by the scanning system which relies on photomultiplier tubes (PMTs) as detectors. Our findings indicate the presence of prestin self-association at low levels (~6% efficiency) when CFP and YFP are both conjugated to the C-termini of prestin. Slightly higher efficiency levels are seen with a construct encoding for CFP on the N-termini and YFP on the C-termini of the same prestin molecule. These results are consistent with preliminary findings using sensitized emission FRET for both constructs. We are currently investigating mechanisms to perturb or enhance the self-association of prestin and will discuss our findings in relation to prestin activity.

### **[369] Developmental Expression of the Outer Hair Cell Motor, Prestin, in the Mouse**

Takahisa Abe<sup>1</sup>, Seiji Kakehata<sup>1</sup>, Rei Kitani<sup>1</sup>, Shin-ichiro Maruya<sup>1</sup>, Dhasakumar Navaratnam<sup>2</sup>, **Joseph Santos-Sacchi**<sup>3</sup>, Hideichi Shinkawa<sup>1</sup>

<sup>1</sup>Department of Otorhinolaryngology, Hirosaki University School of Medicine, <sup>2</sup>Neurology and Neurobiology, Yale University School of Medicine, <sup>3</sup>Otolaryngology and Neurobiology, Yale University School of Medicine

The development of motor protein activity in the lateral membrane of the mouse outer hair cell (OHC) from P5 to P18 was investigated under whole cell voltage clamp.

Voltage-dependent, non-linear capacitance (Cv), which represents the conformational fluctuations of the motor molecule, progressively increased during development. At P12, the onset of hearing in the mouse, Cv was about 70% of the mature level. Cv saturated at P18 when hearing shows full maturation. On the other hand, Clin, which represents the membrane area of the OHC, showed a relatively small increase with development, reaching steady-state at P10. This early maturation of linear capacitance is further supported by morphologic estimates of surface area during development. These results, in light of recent prestin knockout experiments and our results with quantitative PCR, show that rather than the incorporation of new motors into the lateral membrane after P10, molecular motors mature to augment nonlinear capacitance. Thus, current estimates of motor protein density based on charge movement may be exaggerated. A corresponding indicator of motor maturation, the motor's operating voltage midpoint, Vpkcm, tended to shift to depolarized potentials during postnatal development, although it was unstable prior to P10. However, after P14, Vpkcm reached a steady state level near -67 mV, suggesting that intrinsic membrane tension or intracellular chloride, each of which can modulate Vpkcm, may mature at P14. These developmental data significantly alter our understanding of the cellular mechanisms that control cochlear amplification.

(Supported by Grants-in-Aid for Scientific Research from the Ministry of Education, Culture, Sports, Science and Technology of Japan (SK, HS), NIH Grants DC00273 (JSS) and K08 DC05352 (DN).

### **[370] Search for Prestin Associated Proteins**

**Charles T. Anderson<sup>1</sup>**, Katharine Miller<sup>1</sup>, Guo-Guang Du<sup>1</sup>, Roxanne Edge<sup>1</sup>, Peter Dallos<sup>1</sup>, Jing Zheng<sup>1</sup>

<sup>1</sup>*Dept. of Communication Sciences and Disorders, Northwestern University, Evanston IL*

Hearing impairment is the most common sensory defect affecting millions of people ranging from newborns to senior citizens. Causes of hearing impairment are often associated with damage to OHCs. OHCs have a unique feature called electromotility, which is thought to provide the active mechanical amplification of the cochlear response to sound. Prestin is the molecule responsible for OHC electromotility. Substantial physiological evidence indicates that other proteins may modify electromotility, i.e., prestin's function. Currently, we know little about possible interactions between prestin and other proteins.

The yeast two-hybrid system is a powerful genetic tool for identifying protein-protein interactions. Using a key molecule like prestin as "bait" to identify its associated proteins will generate information about the function of uncharacterized proteins and their OHC interacting networks. Understanding how prestin interacts with other proteins could provide insights into cochlear physiology and perhaps lead to the identification of prestin-related inherited disorders. Yet, the conventional nucleus-based yeast two-hybrid system requires the protein-protein interactions to occur in nuclei, where membrane proteins such as prestin do not reside. Therefore, a membrane-

based yeast two-hybrid approach is used to identify prestin-associated proteins.

We have built an organ of Corti library suited for a membrane based yeast two-hybrid system. OHC specific mRNA such as prestin is present in the library. Prestin-bait was synthesized and inserted into the yeast membrane with correct orientation. Using prestin as bait, we are currently screening and analyzing prestin-associated proteins.

[Supported by Grant DC00089, DC006412 and The Hugh Knowles Center Leadership Fund)

### **[371] Prestin Lateral Mobility and the Effects of Cholesterol Depletion**

**Louise E. Organ<sup>1</sup>**, Robert M. Raphael<sup>1</sup>

<sup>1</sup>*Rice University*

The transmembrane protein prestin is crucial to outer hair cell (OHC) electromotility, which influences the micromechanics of the cochlea and is thought to be partially responsible for the sensitivity and frequency selectivity of mammalian hearing. Although the complete mechanism of electromotility remains unknown, some hypothesize that prestin alone converts changes in membrane potential to whole cell deformations. An alternate theory proposes that prestin interacts with a variety of lipids and proteins within the membrane as well as the underlying cortical cytoskeleton to axially direct force transmission. As the interactions of membrane proteins are often examined by monitoring diffusion behavior, we are using fluorescence recovery after photobleaching (FRAP) to assess lateral mobility in human embryonic kidney cells (HEKs) transfected with prestin-GFP. Additionally, since changes in the membrane environment affect non-linear capacitance thus modifying prestin behavior, we are examining the effects of cholesterol extraction with methyl- $\alpha$ -cyclodextrin (MBCD) on the mobility of both prestin and lipid analogues. For collection and analysis of FRAP data we are applying rigorous constraints and re-evaluating standard techniques to test and utilize the imaging potential of our laser scanning confocal microscope (Zeiss LSM 510). Our studies suggest prestin lateral mobility is highly restricted, with immobile fractions possibly greater than 50%. These observations are consistent with the emerging consensus that significant prestin-prestin interactions occur in the plasma membrane. Preliminary results also reveal that alteration of the membrane environment through the removal of cholesterol affects the diffusion behavior and interactions of all membrane constituents.

### **[372] Prestin, a Key Player in Outer Hair Cell Electromotility, and the $\alpha 10$ Nicotinic Cholinergic Subunit Show Positive Selection Signatures in the Mammalian Lineage**

**Lucia Franchini<sup>1</sup>**, Ana Belén Elgoyhen<sup>1</sup>

<sup>1</sup>*INGEBI (CONICET), Buenos Aires, Argentina*

The presence of outer hair cells (OHCs) only in the inner ear of mammals and of OHCs active mechanisms, makes the mammalian cochlea a unique hearing device which has the capability of detecting a wide range of frequencies

including the highest (more than 100 kHz) in the animal world. Several lines of evidence suggest that the motor protein prestin and  $\alpha 9\alpha 10$ -containing nicotinic receptors (nAChRs) are key players in the function or regulation of OHC active mechanisms. In order to understand how this system evolved in the lineage leading to mammals we performed an evolutionary molecular analysis of these proteins. We calculated the pace of protein evolution as scaled to neutral divergence by the ratio between nonsynonymous ( $K_a$ ) and synonymous ( $K_s$ ) substitution rates. Prestin underwent some dramatic changes, especially in the sulphate transporter and antisigma-factor antagonist domain, after the split between mammals and birds. In addition, in placental mammals this gene is under strong purifying selection, suggesting that its function is highly important for these organisms' fitness and adaptation. On the other hand, the  $\alpha 10$  nAChR subunit (but not  $\alpha 9$ ) shows signatures of positive selection along the lineage conducting to mammals. Detailed  $K_a/K_s$  window analysis identifies two regions that have undergone accelerated evolution in mammalian  $\alpha 10$ , part of transmembrane region I and II, two conserved regions among nAChRs. These observations suggest that mammals have evolved not only the motor protein prestin but also a nAChR at the olivocochlear efferent-OHC synapse that is highly tuned to serve its function. Some properties of this receptor might be unique to the mammalian hair cell nAChR and the  $\alpha 10$  subunit is the key component underlying its unique properties. Thus, we describe at the molecular level signatures of adaptive evolution of two OHC proteins in the lineage leading to mammals reflecting the importance of these proteins in OHC somatic electromotility.

### **[373] Upregulation of Prestin Expression in Long-Term Administration of Salicylate**

**Meng-Lei Zhu<sup>1</sup>, Ning Yu<sup>1</sup>, Hong-Bo Zhao<sup>1</sup>**

<sup>1</sup>*University of Kentucky Medical Center*

Prestin is a motor protein responsible for outer hair cell (OHC) electromotility. Salicylate can reversibly inhibit OHC electromotility and otoacoustic emission in acute application. Recently, we found that the long-term usage of salicylate can paradoxically increase DPOAEs (Huang et al, J Neurophysiol. 2005). The mechanism underlying this paradoxical increase remains unclear. In this experiment, the prestin expression and OHC electromotility-associated nonlinear capacitance was measured by real time quantitative reverse transcription-PCR and patch clamp recording after long-term administration of salicylate. The adult guinea pigs (200 - 250 g) were used and peritoneally injected with salicylate (200 mg/kg, b.i.d.) for 2 weeks. Long-term administration of salicylate could upregulate prestin expression. The level of prestin mRNA increased 3.26 fold after 2-wk administration of salicylate. The patch clamp recording also showed that nonlinear capacitance had a 20% increase. Interestingly, at the same time, the expression of Myosin VII was down-regulated. In the control animals with saline injection, there was no change in prestin expression and nonlinear capacitance. The data suggested that long-term usage of salicylate can

upregulate the prestin expression, which may be able to result in tinnitus generation.

Supported by NIH/DC 05989 and the Research Foundation of American Tinnitus Association.

### **[374] Optical Switches for the Membrane Motor of Outer Hair Cells**

**Jie Fang<sup>1</sup>, Tomoyo Sakata<sup>2</sup>, Gerard Marriott<sup>2</sup>, Kuni Iwasa<sup>1</sup>**

<sup>1</sup>*NIH, Bethesda, MD*, <sup>2</sup>*University of Wisconsin*

Electromotility in cochlear outer hair cells (OHCs), which is based on prestin, is essential for mammalian hearing [1]. The motile mechanism involves conformational transitions of the motor proteins in the membrane that couple electrical and mechanical displacements. For this reason, these transitions are most conveniently monitored as nonlinear capacitance (NLC). Here we use novel thiol-reactive spirobenzopyran probes [2] to study conformational transitions of the membrane motor. Those probes are usually in the spiro (SP) configuration and bind to cysteine residues. When they are exposed to 365 nm light, they turn into the merocyanine (MC) configuration, significantly increasing their dipole moments. Their return to the SP configuration is accelerated by the exposure to 546 nm light.

We found that the SP conjugates did not change the characteristic nonlinear capacitance of OHCs or that of prestin-transfected cells from their control conditions. However, irradiation with 365 nm light shifted the voltage dependence of NLC in the positive direction. The SP-MC transition of 4'-bromomethylspirobenzopyran, applied at 20  $\mu$ M concentration, shifted the voltage dependence of the nonlinear capacitance of OHCs by (8 $\pm$ 2) mV and that of the prestin-transfected HEK cells by (9 $\pm$ 3) mV. A shift (6 $\pm$ 1) mV in NLC of OHCs accompanied the corresponding transition of 20  $\mu$ M 8-iodomethylspirobenzopyran.

Our observations indicate that the MC configuration of the probes with larger dipole moment favors the membrane motor's expanded conformation. Since the expanded conformation is favored by hyperpolarization, the motor's interaction with the MC configuration of the probes leads to the observed positive shifts the voltage dependence of the motor. Such an effect must imply that a region close to at least one of the nine cysteine residues of prestin is important for the molecule's conformational changes and that this region's interaction energy with the probes' dipole moment is significant.

[1] Liberman MC et al. (2002) *Nature* 419: 300-304.

[2] Sakata T et al. (2005) *Proc Natl Acad Sci USA* 102:4759-4764.

### **[375] Investigations of the Functional/Structural Implications of Embedded Cysteine Residues in the Molecular Motor Protein Prestin**

**Ryan McGuire<sup>1</sup>, Fred A. Pereira<sup>2</sup>, Robert M. Raphael<sup>1</sup>**

<sup>1</sup>*Rice University*, <sup>2</sup>*Baylor College of Medicine*

Prestin is the voltage sensitive molecular motor of outer hair cells, which serves as an amplifier in the cochlea that makes hearing selective and sensitive to a wide range of frequencies. To date, little is known about its structure or

mechanism of action. Prestin (SLC26A5) is a unique member of the solute carrier family 26 (SLC26). Except prestin, all other members transport anions and thus far none of the other members exhibit prestin's unique non-linear capacitance (NLC). These striking functional differences are likely rooted within structural differences among the family members. We have compared the primary sequence of prestin to a member of the SLC26 family with which it shares high homology, PAT1 (SLC26A6), and several interesting differences were observed. Five of the six cysteine residues unique to prestin occur in locations hypothesized to be transmembrane domains. Currently, there is debate over whether prestin is a 10 or 12-pass transmembrane protein, but these results are true for both proposed topologies. These residues may participate in disulfide bonds, and therefore, we have developed a quantitative fluorescence ratioing method to detect disulfides in HEK cells. The presence of disulfide bonds in prestin is also being analyzed by gel mobility assays. Typically disulfide bonds reinforce the favored conformation of a protein to enhance its stability, but their presence and potential function in SLC26 family proteins is currently unknown. We believe that disulfide bonds could contribute to the unique character of prestin.

### **[376] Prestin Is a Cyclic Nucleotide Binding Protein**

Levente Deak<sup>1</sup>, Guo-Guang Du<sup>1</sup>, Jing Zheng<sup>1</sup>, Peter Dallos<sup>1</sup>

<sup>1</sup>*Dept. of Communication Sciences and Disorders, Northwestern University, Evanston IL*

Cyclic nucleotides (cAMP and cGMP) are second messengers that are important in intracellular signaling processes. These small molecules can modify and regulate protein function through protein phosphorylation. In addition, cAMP and cGMP can also function as ligands, which directly bind to and activate various proteins including cyclic nucleotide-gated ion channels.

A characteristic outer hair cell function, electromotility, is known to be increased by the application of cGMP. Prestin is the molecular basis of OHC's electromotility. We demonstrated, by a combination of applying different agonists/antagonists of PKG and point mutations, that prestin is a substrate of the cGMP/PKG cascade with two cGMP-dependent protein kinase phosphorylation sites. However, there are some questions that remain unresolved. For example, as expected, mutated prestin (S238A) that mimics the dephosphorylated state, loses its ability to respond to cGMP. However, mutated prestin (S238D), mimicking the phosphorylated state, still responds to cGMP stimulation. Furthermore, agonists and antagonists used previously, not only affect PKG activity, but also influence cGMP binding to certain proteins. Thus, the question is raised whether cGMP can directly bind to prestin.

In order to test this possibility, we used the inside-out patch-clamp method, in which the function of prestin can be measured without interference from other intracellular proteins and ATP. Nonlinear capacitance increased up to 3-fold after cGMP was applied to the intracellular face of

membrane-patches from prestin-expressing TSA cells. Similar result was seen with cAMP, however, the half-activating concentration was ~ 4.5 times higher than for cGMP. Since the bath solution lacked ATP, the involvement of a membrane-associated protein kinase and phosphorylation process was unlikely.

In addition, both competitive radioligand binding assay with 3H-cGMP and 3H-cGMP dissociation assay showed specific binding in membranes prepared from prestin-expressing TSA cells, but not in membranes from control TSA cells. These two independent electrophysiological and biochemical experiments demonstrate that cyclic nucleotide can directly bind to prestin and thereby increase its function. [Supported by NIH grants DC00089 and DC006412].

### **[377] MAP-1S, A Microtubule Associated Protein Interacts with Prestin and Modulates Its Activity**

Jun-Ping Bai<sup>1</sup>, Dhasakumar Navaratnam<sup>2</sup>, Joseph Santos-Sacchi<sup>1</sup>

<sup>1</sup>*Yale University, Department of Otolaryngology*, <sup>2</sup>*Yale University, Department of Neurology*

Prestin is a member of the SLC26 anion transporter family that is responsible for outer hair cell electromotility. In seeking to identify the molecular components of this the outer hair cell motor we have isolated several proteins that interact with the intracellular C-terminus of prestin. One of these proteins, microtubule associated protein-1S, is a newly identified member of the microtubule associated family of proteins. In contrast to the other members of this group of proteins however, MAP-1S has the ability to bind to both actin and tubulin.

We show here that MAP-1S interacts with prestin using immunoprecipitation. We also show that the MAP-1S is found in outer hair cells where it is concentrated along the lateral wall of the cell where the outer hair cell motor resides. Finally, when co-expressed with prestin in CHO cells (that endogenously express undetectable levels of the protein), MAP-1S causes a marked increase in non-linear capacitance, the signature of outer hair cell electromotility.

### **[378] Divergence and Homology in Mammalian Prestin Sequences**

Richard Hallworth<sup>1</sup>, Kirk W. Beisel<sup>1</sup>, Donald Sakaguchi<sup>2</sup>

<sup>1</sup>*Creighton University, Omaha, NE*, <sup>2</sup>*Iowa State University*

The appearance of the motor prestin in mammals represents a quantum jump in hair cells functionality. Thus, the presence of prestin in evolutionarily primitive mammals such as marsupials and monotremes may suggest clues to the function of prestin in placental mammals. The cochlea of the Brazilian gray short-tailed opossum (*Monodelphis domestica*) is not dissimilar to that of placental mammals. The cochlea consists of one and a half turns and has one row of inner hair cells and three rows of outer hair cells, identifiable from the configuration of their stereociliary bundles. Hearing in marsupials is comparable in threshold and frequency range to placental mammals. Amino acid sequences for marsupial prestin show greater than 90% identity to mouse and human prestin. This suggests that

the modern form and function of the mammalian cochlea was established early in the divergence of mammals from ancestral forms. We are at present obtaining prestin sequences from a monotreme for comparison. Supported by NIH DC 02053 to RH, NIH DC 05009 to KWB, NIH NS44007 to DSS, NIH RR17417 to Creighton University, and NSF-EPSCoR EPS-0346476 to RH.

### **379 Anatomy and Physiology of Prestin Knockout Mice Backcrossed to the CBA/CaJ Strain**

**Kristin Huynh<sup>1</sup>**, Roxanne Edge<sup>1</sup>, Christina Georgopoulos<sup>1</sup>, Jiangang Gao<sup>2</sup>, Jian Zuo<sup>2</sup>, Peter Dallos<sup>1</sup>, Mary Ann Cheatham<sup>1</sup>

<sup>1</sup>Northwestern University, <sup>2</sup>St. Jude Children's Research Hospital

Prestin knockout (KO) mice, on a mixed 129S7/C57BL6 background, exhibit apoptosis starting at ~3 weeks of age (Wu et al., 2004). Both inner and outer hair cells are affected, with loss beginning at the base of the cochlea and progressing towards the apex with advancing age. By ~8 weeks, all hair cells are missing from the basal 25% of the cochlea (Liberman et al., 2002). Because it is possible that removal of prestin accelerates age-related hearing loss (ARHL), the knockout was backcrossed onto the CBA/CaJ strain, which does not harbor any of the ARHL genes and has sensitive hearing well into old age. Data were obtained on N5 and N7 generation mice, when greater than 95% of the genome is that of the recipient strain, CBA/CaJ. Compound action potential (CAP) thresholds recorded at the round window demonstrate that sensitivity is reduced by ~50 dB. In addition, CAP tuning curves, obtained at 12 kHz using simultaneous masking, reveal that there is no tuning in mice lacking prestin, which was also shown in the original knockout (Cheatham et al., 2004). Anatomical data were also acquired to determine the degree of hair cell loss in the CBA/CaJ prestin KO. Following cardiac perfusion with 4% paraformaldehyde, cochleae were dissected and embedded in plastic. Whole mounts, as well as radial sections, were viewed to evaluate the extent of damage. Although hair cell loss occurs, it begins much later than that observed in the original prestin-null mouse. At 6 weeks of age, the CBA/CaJ prestin KO shows minimal hair cell damage. However, at 3 months, the loss of both inner and outer hair cells at the base of the cochlea is significant. These results suggest that the onset of hair cell loss is delayed, but not eliminated, in KO mice lacking ARHL genes.

(Work supported by The Hugh Knowles Center and by NIH grants DC00089 to P. Dallos and DC06471 and CA21765 to J. Zuo).

### **380 Biochemistry and Cellular Distribution of Prestin in Cultured Cells**

**Angela K. Sturm<sup>1</sup>**, Haiying Liu<sup>2</sup>, Donald Yoo<sup>1</sup>, William E. Brownell<sup>1</sup>, Fred A. Pereira<sup>1,3</sup>

<sup>1</sup>Bobby Alford Department of Otorhinolaryngology,

<sup>2</sup>Huffington Center on Aging, <sup>3</sup>Baylor College of Medicine

Prestin is an essential component of the molecular motor of the outer hair cells that contributes to the cochlea

amplifier, which is responsible of selectivity and sensitivity to a wide range of frequencies for hearing. In an attempt to gain insight into prestin's mechanism of action we have investigated its biochemical properties, subcellular and plasma membrane distribution in HEK cells. Using SDS- and PFO- (perfluoro-octanoic acid, a weakly denaturing reagent) gel electrophoresis and comparative analysis with native proteins of known molecular mass, we found prestin to exist in multiple protein bands. The smallest form of prestin has a relative molecular mass of 83.2 kilodaltons, which is close to the predicted mass of 81.4 kDa, based on its primary sequence. Since prestin is a glycosylated protein, we treated protein extracts with N-glycosidase F (PGNase F) and found that with increasing amounts of PGNase F, the higher molecular mass bands were lost while the band at 83.2 kDa accumulated in intensity, indicating this band as the deglycosylated form. Using gradient gels and chemical crosslinking experiments, we found prestin forms oligomers composed of at least 2 subunits and can contain multimers with 5 or more subunits. Co-immunoprecipitation studies of haemagglutinin- or GFP-tagged prestin proteins, both of which confer HEK cells with a nonlinear capacitance activity, confirmed that prestin self-associates. We also followed the synthesis and transport of prestin at the subcellular level to determine its pathway and timing of trafficking to the plasma membrane through colocalization studies with intracellular and plasma membrane markers. Prestin was seen to localize to the ER, Golgi apparatus and is expressed in the plasma membrane by 12 hours post-transfection. We also found prestin colocalized with the clathrin vesicles and in endosomes indicating prestin may participate in the clathrin endocytic pathway, which is used for transcytosis or transport of plasma membrane proteins to lysosomes. Prestin was initially dispersed in the plasma membrane but aggregates into foci by 48 h post-transfection. Some prestin foci colocalize with integrin  $\alpha 2$  proteins and cholera toxin, which binds glycosphingolipid GM1 in membrane microdomains. We continue to study conditions required for cellular distribution and the self-association activity of prestin including requirements for glycosylation and the terminal sequences. Sponsored by DC 04585 & 00354.

### **381 Electron Tomography of the Outer Hair Cell Lateral Wall**

**William Triffo<sup>1,2</sup>**, Kent McDonald<sup>3</sup>, Manfred Auer<sup>2</sup>, Robert M. Raphael<sup>1</sup>

<sup>1</sup>Rice University, <sup>2</sup>Lawrence Berkeley National Laboratory,

<sup>3</sup>Electron Microscope Laboratory, University of California at Berkeley

In the mammalian cochlea, the outer hair cell (OHC) is capable of generating axial deformations in response to variations in transmembrane potential. The cortex of the OHC, referred to as the lateral wall, can be viewed as a trilaminar composite made up of (1) the plasma membrane, (2) a network of actin and spectrin termed the cortical lattice, and (3) lamellar stacks known as the subsurface cisternae (SSC).

Previous studies of the cortical lattice using conventional TEM and AFM techniques relied on extraction protocols

that removed the lattice from its native environment. Moreover, depending on the exact fixation protocols, conflicting depictions of SSC ultrastructure have been reported. We have therefore tested a variety of sample preparation methods, including iso-osmotic fixation protocols as well as high-pressure freezing and freeze-substitution. We have succeeded in significantly improved sample preservation, allowing us to address whether the SSC is continuous or fenestrated in vivo, or whether the fenestration commonly observed results from the fixation method. Using cochlear samples from our improved preparation techniques, we have employed Electron Microscope Tomography (ET) to study the cortical lattice and its structural relationship to the plasma membrane and the subsurface cisternae.

We focus on the pillar proteins known to span the extracisternal space between the plasma membrane and cortical lattice. ET utilizes a series of TEM projections from a tilted sample to reconstruct a volume density map, allowing us to visualize macromolecular assemblies in their native cellular context. The detailed electron tomographic 3D analysis of a cellular subvolume will provide us with a more complete model of lateral wall structure, critical to understanding how forces generated in the OHC membrane are transmitted to the cytoskeleton and subsequently neighboring cells.

### **382 Cable Properties Along the OHC Cylinder**

**Lei Song<sup>1</sup>**, Joseph Santos-Sacchi<sup>1</sup>

<sup>1</sup>Otolaryngology and Neurobiology, Yale University School of Medicine

The OHC possesses a mechanically active lateral membrane which underlies mammalian cochlear amplification. The electro-mechanical activity is dependent on the motor protein prestin, which is distributed uniformly along the lateral membrane. However, the independent nature of the motors is highlighted by the existence of microdomains within the lateral membrane which can respond to forces such as tension, temperature and voltage in an autonomous fashion (Santos-Sacchi, Pflugers Archiv. 445, 331-336, 2002). Thus, it may be that differences in voltage along the lateral membrane could selectively activate the cell in a non-homogeneous manner. Here we employ double and triple electrode whole cell voltage and current clamp recordings to determine the cable properties of the OHC. We find significant differences between physical modeling of linear cabled cells and that of OHCs, indicating that the nonlinear activity of the motors' electrical response may contribute to a complex impedance along the cell length. We are currently manipulating the OHC with known blockers of its nonlinear capacitance, e.g. salicylate, altered chloride levels and gadolinium ions to dissect out the motors' contribution to voltage differences along the OHC. These data may be important in understand nonlinear mechanics in the intact organ of Corti.

(Supported by NIH DC000273 to JSS)

### **383 Outer Hair Cell Frequency Dependent**

#### **Passive Capacitance**

**Richard D. Rabbitt<sup>1</sup>**, Brenda Farrell<sup>2</sup>, William E. Brownell<sup>2</sup>

<sup>1</sup>Bioengineering, University of Utah, <sup>2</sup>Otolaryngology, Baylor College of Medicine

The stunning voltage-dependent capacitance (VDC) of outer hair cells (OHCs) is a hallmark electrophysiological feature closely associated with electromotility. VDC adds to the passive capacitance associated with the membrane permittivity. Both the VDC and passive capacitance are typically measured with interrogating sine waves superimposed on command membrane potentials in "whole-cell" mode. The OHC passive capacitance is nearly independent of the interrogation frequencies (f) used to make the measurement, at least at  $f < 1000$  Hz. This fact provides evidence that the low frequency capacitance measurement examines a constant membrane area. Frequency dependence, however, is not observed in all cell types. Cells that have a long slender geometry (e.g., axons) exhibit a frequency dependent input capacitance. At high frequencies, membrane area examined by the interrogating probe decreases and thereby decreased the input capacitance. Models of the OHC that assume the intracellular axial current is restricted to the narrow extracisterna space (ECS) between the plasma membrane and the sub-surface cisterna show similar properties, and predict that the capacitance measured at the base of the cell will decrease when measured above a critical corner frequency. A concomitant decrease in the input resistance is also predicted. The corner frequency at which this begins to occur is strongly dependent upon the axial resistance of the OHC along the ECS. We are establishing protocols to directly test this hypothesis with a two electrode approach. Preliminary data recorded from guinea pig OHCs with one electrode indicate that the apparent passive capacitance begins to decrease for interrogation frequencies above ~1kHz – consistent with the hypothesis that axial current flows along the ECS. If proven to be true, results have physiological implications regarding the role of the ECS and operation of OHCs at high frequencies in the cochlea (supported by NIDCD R01 DC04928 & DC00354).

### **384 Effect of Salicylate on Electromechanical Force Generation of Plasma Membrane Tethers**

**Linda Lee<sup>1</sup>**, Feng Qian<sup>2</sup>, William E. Brownell<sup>1</sup>, Bahman Anvari<sup>2</sup>

<sup>1</sup>Baylor College of Medicine, Bobby R. Alford Dept of Otorhinolaryngology and Communicative Sciences, <sup>2</sup>Rice University, Department of Bioengineering

Electrically-induced mechanical force (EMF) generation by cell membrane tethers has been demonstrated in many cell types, including cochlear outer hair cells, axons, and some cultured mammalian cells. We use a technique that combines optical trapping with whole-cell voltage clamping to investigate the effects of an electrically charged amphipathic agent on EMF by pulling membrane tethers. Optical trapping allows force resolution on a piconewton scale, and the patch clamp is used to control transmembrane potential. Once membrane tethers are



formed from the voltage-clamped cells, electrical excitations are delivered to the cells while recording the EMF generated by the tethers. Our preliminary results indicate that salicylate, a negatively charged amphipathic agent, which is known to cause reversible hearing loss and reduce outer hair cell electromotility, reduces the amplitude of EMF in membrane tethers. These measurements provide a basis to better understand the role of membrane surface charge in EMF.

Work supported by R01 DC02775, T32 DC007367 and R90 DK071504.

### **[385] The Voltage-Dependent Membrane Properties Affect the Sensitivity of the Outer Hair Cell Active Force**

**Zhijie Liao**<sup>1</sup>, Aleksander Popel<sup>1</sup>, William E. Brownell<sup>2</sup>, Alexander Spector<sup>1</sup>

<sup>1</sup>*Johns Hopkins University, Baltimore, Maryland*, <sup>2</sup>*Baylor College of Medicine, Houston, Texas*

The outer hair cell voltage-dependent properties associated with the molecular (motor-related) mechanism in the cell membrane are important for the cell active behavior. We present a modeling analysis of the effect of such properties on the outer hair cell active force production. The model incorporates the biophysical properties of the cell as well as the constraints imposed by the surrounding environment, and it allows analyses of high-frequency regimes of cell vibration. The biophysical properties include the elastic, piezoelectric, and viscous characteristics of the cell wall. The effect of the environment is associated with the stiffness of the constraint and the drag forces acting on the cell wall due to the interaction with the external and internal fluids. The voltage dependence enters the model via the active strain (related to the converse piezoelectric effect in the cell wall) as well as the orthotropic moduli of the cell wall. The latter moduli changes with the cell stiffness, which is voltage-dependent. We found that the cell voltage-dependent stiffness results in a shift of the active force as a function of the transmembrane potential toward the hyperpolarization range. This effect leads to a 50% increase in the active force per unit transmembrane potential in the physiological range. In addition to this, the voltage dependence of the active force in the physiological range is steeper and more nonlinear compared to that estimated on the basis of constant cell stiffness. The results obtained in a broad frequency range can be important for a better understanding of the outer hair cell active force production and the contribution of cell electromotility to the cochlear amplification, sensitivity, and nonlinearity. Supported by R01DC002775 from the NIDCD.

### **[386] Outer Hair Cell Mechanics Reformulated with Acoustic Variables**

**Jont Allen**<sup>1</sup>, Paul Fahey<sup>2</sup>

<sup>1</sup>*University of Illinois*, <sup>2</sup>*Univ. of Scranton, PA*

The electromechanical properties of the Outer Hair Cell (OHC) have been reformulated in terms of acoustic variables. It is anticipated that the acoustic variable

formulation will be more useful for incorporating OHC electromechanics into cochlear micromechanics. For guidance on the interdependency of the acoustic and electrical quantities and to aid physical intuition we also present piezoelectric circuit diagram for the OHC. These equations give specific predictions about the relationship of the nonlinear capacitance and the mechanical properties (i.e., motility and stiffness) of the cell.

### **[387] A New Strategy for Quantifying Prestin Dependency of Cochlear Outer Hair Cell Motility** **Nozomu Matsumoto**<sup>1,2</sup>, Federico Kalinec<sup>2</sup>

<sup>1</sup>*Dept. of Otorhinolaryngology, Graduate School of Medical Sciences, Kyushu University*, <sup>2</sup>*Gonda Dept. of Cell and Molecular Biology, House Ear Institute*

The motile response of isolated guinea pig outer hair cells (OHCs) was investigated using a combination of whole-cell patch clamp recording and continuous video image analysis. Electromotility of OHCs, which is associated with conformational changes in the integral membrane protein prestin, was evoked either by manipulating the membrane potential under voltage-clamp conditions or by exposing OHCs to high K<sup>+</sup> solutions. Other motile responses were investigated in voltage-clamp experiments at constant holding potential or exposing OHCs to solutions that did not affect the membrane potential. We found that electrical stimulation evoked prestin-dependent changes in OHC's length, width and longitudinal section area but not in cell volume, while prestin-independent motile responses were associated with changes in cell length, width and volume without significant changes in longitudinal section area. Moreover, we demonstrated that, if the relative change in OHC length (L) during the motile response is expressed as  $L = A^2 \times V^{-1}$  (with A and V being the relative changes in longitudinal section area and volume, respectively), A<sup>2</sup> will describe the contribution of the prestin-dependent while V<sup>-1</sup> will describe the contribution of the prestin-independent mechanisms. Thus, relative changes in any two of these cellular morphological parameters (L, A or V) would be necessary and sufficient for characterizing any OHC motile response. This simple approach provides access to information previously unavailable, and may become a novel and important tool for increasing our understanding of the cellular and molecular mechanisms of OHC motility.

### **[388] Calcium-Dependent Shortening and Volume Increase in Auditory Hair Cells of the Frog Inner Ear**

**Nasser Farahbakhsh**<sup>1</sup>, Dwayne Simmons<sup>2</sup>, Peter M. Narins<sup>1</sup>

<sup>1</sup>*UCLA*, <sup>2</sup>*Washington University School of Medicine*

In hair cells isolated from the rostral segment of the amphibian papilla (AP) of the leopard frog, *Rana pipiens*, increases in the concentration of the intracellular free calcium, induce cell-length shortening. These shortenings are composed of two partially-overlapping phases: an initial rapid iso-volumetric shortening, and a slower length decrease accompanied with swelling. Moreover, the rapid initial phase is sensitive to calmodulin inhibitor, W-7, while the osmotic phase is inhibited by quinidine or furosemide. We now show that the myosin light chain inhibitor, ML-7,



as well as the calcium-calmodulin-dependent protein kinase II inhibitors, KN-62 and KN-93, significantly diminish the iso-volumetric shortening. Furthermore, myosin VI appears to be present in the soma of AP hair cells. Finally, we report that the osmotic component of cell shortening is sensitive to the protein phosphatase inhibitor, okadaic acid. These findings suggest that at least two well-characterized  $\text{Ca}^{2+}$ -dependent kinases (MLCK and CAMKII) and a serine/threonine phosphatase participate in the signal transduction mechanism responsible for the calcium-dependent shortening in rostral AP hair cells. Such a complex regulatory mechanism might be utilized by the auditory efferent neurotransmitters for adaptive modulation of sensitivity and frequency selectivity in the amphibian papilla.

Supported by NIH grants no. DC-00222 to PMN and DC-004086 to DDS.

### **[389] Contribution of Cilia to Hair-Cell Capacitance Modulation During Mechanotransduction**

**Kathryn Breneman**<sup>1</sup>, Stephen M. Highstein<sup>2,3</sup>, Richard Boyle<sup>4</sup>, Richard D. Rabbitt<sup>1,3</sup>

<sup>1</sup>University of Utah, <sup>2</sup>Washington University, <sup>3</sup>Marine Biological Lab, <sup>4</sup>NASA Ames Research Center

The exquisite timing and temporal adaptation of hair-cell transmitter release relative to hair-bundle motion is critical to receptor-related functions such as sound source localization using inter-aural timing disparities and vestibular coding of maintained gravito-inertial stimuli. The kinetics of synaptic transmission is a key factor. Transmitter release has been studied previously using whole-cell capacitance measurements to monitor transient changes in membrane surface area associated with synaptic vesicle fusion and membrane cycling. Measurements are typically performed following depolarizing voltage steps delivered through a recording microelectrode. Presently, capacitance modulation was recorded in response to hair bundle motion in semicircular canal hair cells *in vivo*. Under voltage-clamp conditions, where tonic transmitter release and constant whole-cell impedance was expected, the capacitance decreased when the mechano-transduction channels were open and increased when they were closed. These data implicate changes in apparent capacitance associated with transduction. To interpret the results, we modeled the cilia as passive cables with mechano-sensitive transduction channels at their tips. Consistent with the data, the model predicts that the effective capacitance measured at the soma will decrease when transduction channels are open relative to when they are closed due to cable properties of the cilia. This effect is predicted to be particularly large in semicircular canal hair cells due to the long cilia. Modeling results also address the passive electrical filtering properties of hair cell cilia and may explain the correlation between cilia length and best frequency reported previously in hair cell sensory systems. Supported by NIH DC006685, NSF IGERT DGE9987616, and NASA NNA-04CK67H.

### **[390] Comparison of Cochlear Transducer Functions Derived from the Cochlear Microphonic and Summating Potential**

**Chul-Hee Choi**<sup>1</sup>, Mark Chertoff<sup>2</sup>

<sup>1</sup>Baylor College of Medicine, <sup>2</sup>University of Kansas Medical Center

The cochlear microphonic (CM) is an ac far-field electrical potential generated by the vector summation of outer hair cell (OHC) receptor currents, and originates from the nonlinearity of mechano-electrical transduction (MET). The relationship between the CM and the first derivative of the cochlear transducer function ( $f_{Tr}$ ) representing MET was first described by Nieder and Nieder (1971, JASA, 49, 478-492). The long term goal of this research is to develop a useful clinical method that is very sensitive to changes in the cochlear mechanics and physiology associated with sensorineural hearing loss. In this study, we introduce a method to derive a cochlear  $f_{Tr}$  from the CM and compare the cochlear transducer functions derived from the CM to those obtained from the summating potential (SP) previously described by Choi *et al.* (2004, JASA. 116, 2996-3007).

The CM was simulated using a Taylor series approximating a nonlinear function. Mathematical exploration suggested that the CM magnitude is essentially proportional to the first derivative of the nonlinear function when the signal level is very small. The CM magnitude was used to derive the first derivative of the  $f_{Tr}$  by using a low frequency bias tone to place a high frequency probe tone in different locations along the cochlear  $f_{Tr}$ .

Two probe tones (6 and 12 kHz) ranging from 70 to 90 dB SPL in 10 dB step and a 25 Hz bias tone with various amplitudes were presented to eight animals. The CM was recorded from an electrode placed on the round window. Results showed that the CM magnitude as a function of the bias levels has a shape similar to the first derivative of the cochlear  $f_{Tr}$  as shown in the simulation. The correlation coefficient ( $r^2$ ) between the CM magnitude and the first derivative was above .97 indicating that the CM magnitude is proportional to the first derivative of the cochlear  $f_{Tr}$ . Furthermore, the cochlear transducer functions obtained from the CM were compared to those of the SP. There were significant differences between the Boltzmann functions fitted to the CM and SP transducer function. These differences may result from different contribution of the IHCs and OHCs, suggesting that the CM and SP may be used to estimate OHC and IHC transducer functions.

Supported by NIH grants: 2 R01 DC02117

### **[391] Threshold – Reconsidering Published Data**

**George Offutt**<sup>1</sup>

<sup>1</sup>Center for Sensory Processes

It is a generally accepted assumption that cochlear receptors are only sensitive to mechanical stimulation. Doubtless some sensitivity is a result of mechanically stimulating the hair cells (HC), but consider the possibility that mechanical stimuli are not the only source of HC stimulation. For the 20 dB above threshold, BM motion is not required for cochlear activity (Offutt, 1986, Hear Res). Compound action potentials were little changed at those

levels when the cochlear microphonics (CM) and presumably the BM motion were nulled.

The inner hair cells (IHC) are about 12 dB more sensitive than the outer hair cells (OHC) as measured by intracellular recordings at ~800 Hz (Dallos, 1985, J Neurosci). How can the OHC function to mechanically stimulate the IHC close to threshold when the IHC are more sensitive than the OHC? However, the OHC have a 20 to 30 dB greater mechanical sensitivity than IHC as determined by CM (Pierson and Møller, 1980, Hear Res). These data argue against the generally accepted processes of cochlear function.

In the 1930's there were at least two opposing concepts of how the ear functioned. There were many experiments showing sensitivity to electrical stimulation and many Europeans, especially in Stockholm and Leningrad, thought the ear was an electroreceptor. In opposition were those who thought the ear was only mechanically sensitive. This assumption of total mechanical sensitivity is flawed because it is based in-part on an hypothesis using the negative argument that there were no HC known to be electroreceptors (Stevens, 1937, JASA). Now there are many HC that are known to be sensitive electroreceptors to both anodal and cathodal (e.g. to 0.01  $\mu\text{V}/\text{cm}$ ) stimuli. However the generally accepted assumption of mechanical sensitivity remains.

Responses to electrical stimuli are usually considered to be due to electrophonics (i.e. a secondary mechanical stimulation). Nevertheless, since 1970 I have been interpreting and evaluating published data using the assumption of electrical sensitivity by the IHC. It has been exciting and unanticipated how the electromodel is compatible with published data and can possibly explain the basis of many clinical problems.

### **392 Mechanoelectric Transduction and Adaptation Set Hair Cell Resting Potential and Allow an Estimate of Endolymphatic $\text{Ca}^{2+}$ Concentrations**

**Hamilton Farris<sup>1</sup>, Gregg Wells<sup>2</sup>, Anthony Ricci<sup>1</sup>**

<sup>1</sup>Louisiana St. Univ. H.S.C., <sup>2</sup>Texas A&M Health Science Center

Turtle auditory hair cells are tuned to acoustic stimuli via an electrical resonance mechanism established by the interaction of L-type  $\text{Ca}^{2+}$  channels and BK type potassium channels. Both theoretical and in vitro recordings require a DC current applied to cells to set the resting potential at a point on the I(Ca) and I(BK) activation curves where best electrical resonance (i.e., positive and negative current steps elicit symmetrical resonance) can be obtained. Because the DC current is not required in vivo (Crawford and Fettiplace, 1981), the question arises, what mechanism underlies this DC current? Data presented here test the hypothesis that current through the mechano-electric transduction (MET) channels provides such a current and that steady-state adaptation of this current dictates the hair cell resting potential. First, mechanical block of the MET current hyperpolarizes the membrane potential (from -56 mV to -70 mV in 2.8 mM  $\text{Ca}^{2+}$ ), resulting in broadband resonance (>170 Hz equivalent rectangular bandwidth (ERB)) that is limited to

depolarizing current injections, with a passive low pass response to negative current injections. Second, a direct relation was found between the amplitude of DC current injected to obtain the best resonance ( $242 \pm 77$  pA) and the resting MET current while bathed in endolymph (130mM  $\text{K}^+$ , 0.05 mM  $\text{Ca}^{2+}$ ;  $218 \pm 66$  pA). This condition elicits greater resonant tuning ( $73 \pm 17$  Hz ERB) with symmetrical resonance elicited for positive and negative current steps. Varying apical  $[\text{Ca}^{2+}]$  alters the current on at rest by resetting the position of the MET activation curve via adaptation and by altering the  $\text{Ca}^{2+}$  block of the channel, resulting in changes in hair cell resting potential and input resistance. A model based on that of Hudspeth and Lewis reproduced the effects of altering baseline leak current on membrane potential and resonance. The amount of MET current on at rest alters hair cell sensitivity by altering the input resistance of the cell and also modulates the basolateral filter by setting the resting potential. Using the sensitivity of electrical resonance to the MET current on at rest enabled the estimate of the endolymphatic  $[\text{Ca}^{2+}]$  as ~0.05 mM, similar to that measured for bulk endolymph (Crawford et al., 1991). These results demonstrate the importance of both maintaining low endolymphatic  $[\text{Ca}^{2+}]$  and emphasize the significance of adaptation in establishing hair cell resting potential. Funding: NRSA to HF, NIH RO1 to AR

### **393 Evaluation of Laser Capture Microdissection for Outer Hair Cell Collection**

**Charles T. Anderson<sup>1</sup>, Jing Zheng<sup>1</sup>**

<sup>1</sup>Dept. of Communication Sciences and Disorders, Northwestern University, Evanston IL

Outer hair cells (OHC) play an important role in frequency selectivity and signal amplification in the mammalian cochlea, making them the focus of a wide range of research projects. Because OHCs comprise a small minority of the cells in the cochlea, separating and isolating them for applications such as cDNA library creation and proteomic studies remains a challenging task. Laser Capture Microdissection (LCM) is a method for accurately isolating specific cells from large regions of tissue for RNA, DNA, and protein studies. It is designed to capture cells from very thin sections of tissue, but due to the constraints of cochlear anatomy, thin sections of the cochlea contain limited numbers of OHCs.

We have adapted the technique of LCM to isolate OHCs from organ of Corti whole mounts, each of which contain hundreds of OHCs that are simultaneously accessible and theoretically collectable. Because a large number of OHCs are harvested from each mouse, reductions in the numbers of animals used and the materials purchased provides added benefit. For comparison, we also used a more traditional mechanical dissection to collect OHCs. In this method, modified from He et al. (2000), a partial organ of Corti is removed from the modiolus, prior to the dissection of groups of OHCs from their neighboring supporting cells. The mRNA resulting from LCM isolation and the traditional method was used to create cDNA pools through the non-specific SMART PCR amplification technique. The quality of cDNA derived from the OHCs collected with LCM and the traditional mechanical method

are compared and the merits and limitations of the techniques are discussed. [Supported by NIH grants DC00089 and DC006412].

### **394 The Direct Electrical Interaction Between Deiters Cells and Outer Hair Cells**

Ning Yu<sup>1</sup>, Hong-Bo Zhao<sup>1</sup>

<sup>1</sup>University of Kentucky Medical School

In vivo, the stalk of a Deiters cell (DC) like a bow supports the outer hair cell (OHC) standing on the cup of the DC. Deiters cells have gap junctions to couple together. However, there is no gap junctional coupling between DCs and OHCs. It has been reported that the stalk of the DC is movable in responses to ATP treatment and electronic stimulation. However, its effect on OHC electromotility remains unclear. In this experiment, the electrical interaction between Deiter cells and outer hair cells were investigated by use of a double voltage clamp technique. The connected OHC and DC were separately patched by double voltage clamps under whole cell configuration. The effects of depolarization and hyperpolarization of DCs on OHC electromotility were tested, and the OHC nonlinear capacitance (NLC) and distortion products were recorded. As the membrane potential of DCs was altered from hyperpolarization (-120 mV) to depolarization (+40 mV), the OHC NLC was decreased; the reduction could be as large as 10 pF. The changes in the membrane potential of the DCs also shifted the OHC operating-point. However, the shift direction varied between the cells. The OHC distortion products in response to two sinusoidal voltage stimuli were also altered by the DC membrane potential. Similar to voltage clamp, injection of negative current in DCs under the current clamp increased OHC nonlinear capacitance, and injection of positive current inducing DC depolarization reduced the OHC nonlinear capacitance. However, no direct electric passage was found between the DCs and OHCs. The data indicated that the change in the DC membrane potential can directly modify the OHC electromotility. The data also implied that as gap junctional coupling between DCs has changes to influence their electronic synchronization and membrane potential, this could result in an apparent effect on OHC function.

Supported by NIDCD DC 05989 and American Tinnitus Associate Research Foundation.

### **395 Affects of Exposure to an Augmented Acoustic Environment in Aged CBA Mice: Cochleograms, ABR Thresholds and Behavior**

Jeremy G. Turner<sup>1</sup>, Jennifer L. Parrish<sup>1</sup>, Barbara Canlon<sup>2</sup>, Stacy Darr<sup>3</sup>, Larry F. Hughes<sup>1</sup>, Donald M. Caspary<sup>1</sup>

<sup>1</sup>Southern Illinois University School of Medicine,

<sup>2</sup>Karolinska Institutet, <sup>3</sup>Illinois College

Age-related hearing loss, presbycusis, is one of the most common ailments of the elderly. Presbycusis is often treated with hearing aids which serve to amplify some or all of the sound lost because of peripheral changes. However, hearing aids have mixed results in the elderly population because presbycusis, in addition to the peripheral hearing loss, involves age and deprivation-induced plastic changes to the central auditory system. As

a result, reintroducing sound with a hearing aid does not necessarily (or immediately) restore normal hearing to the elderly listener. Indeed, clinicians have become aware of a delay in the effectiveness of hearing aids after fitting patients (acclimatization). How acclimatization works is poorly understood, but it is likely that central plastic changes resulting from wearing hearing aids occur. The current study seeks to examine what changes occur in aged animals when missing sounds are reintroduced to a presbycusis mammal. Aged CBA mice (24 mo, n=26) with presbycusis were either exposed to 6 weeks of an augmented acoustic environment (AAE; 70 dB SPL, broadband noise stimulation, 12 hours/night) or normal vivarium conditions. The effects of the treatment were assessed by measuring behavioral gap detection and prepulse inhibition, auditory brainstem response (ABR) thresholds and cochleograms. AAE was associated with

significantly better ABR thresholds and cochleograms in aged male mice. However, female mice showed ABR thresholds and cochleograms which were significantly worse following the 6-wk treatment. AAE exposure was associated with improved behavioral prepulse inhibition and gap detection in male mice at 2 and 4 weeks after initiation of AAE exposure, whereas female mice showed little change. These findings suggest that the male and female CBA mouse auditory system responds differently to acoustic stimulation late in life. Supported by NIH grants AG023910 (JGT), DC00151 (DMC), The Swedish Research Council, Tysta Skolan, and the Karolinska Institutet.

### **396 A Comparison of Age-Related Hearing Loss in F1(CBAXC57) Mice with Their Parental Strains**

Sara Bozorg<sup>1,2</sup>, Xiaoxia Zhu<sup>1,2</sup>, Robert D. Frisina<sup>1,2</sup>

<sup>1</sup>Univ. Rochester Med. Sch., <sup>2</sup>Int. Ctr. Hearing Speech Res.

Presbycusis – age related hearing loss – is the number one communication problem of the aged. A loss of high-pitch hearing and a reduced ability to process biologically relevant acoustic signals in a noisy environment occur. A major contributor to presbycusis may be the age-dependent decline of the medial olivocochlear (MOC) efferent system. Decline of the MOC system precedes the degeneration of cochlear outer hair cells (OHCs) in human listeners as well as in animal models of presbycusis: CBA and C57 mice. The CBA strain displays a mild-to-moderate hearing loss in old age that parallels the time course of the human clinical condition, where as the C57s develop hearing loss earlier in life. The present investigation determined the time course of hearing loss in F1(CBAXC57) mice. Auditory brainstem responses (ABRs), distortion product otoacoustic emissions (DPOAEs), and contralateral suppression (CS) of DPOAEs were obtained from young (2.1-2.9 mon) and middle-age (14.0-16.4 mon) F1s, and auditory sensitivity, OHC responses, and the MOC system were evaluated, respectively. DPOAE-grams were obtained with L1=65 and L2=50 dB SPL, f1/f2 = 1.25, using eight points per octave (5.6-44.8 kHz). DPOAEs were recorded in quiet and with a contralaterally applied 3-30 kHz wideband noise at 55 dB SPL. ABR thresholds were measured for 3-48 kHz.

Analyses revealed a small decline in DPOAE levels with age. CS was present in all mice at low and mid frequencies, and declined in middle-age F1s at high frequencies. In summary, middle-aged F1 mice show a decline in MOC function at high frequencies, but the decline, at this age, does not extend significantly to the OHC system, similar to the CBA strain. So, the progression of age-related hearing loss in F1 is intermediate between the parental strains, and as in previous studies of both strains, the age-related decline in the efferent system precedes OHC declines and ABR threshold elevations.

*Work supported by NIH: NIA & NIDCD*

### **397 F1 (CBA x C57) Mice Show Accelerated Age-Related Hearing Loss Relative to Their CBA Parental Strain**

**Ameet Singh**<sup>1,2</sup>, Rahul Seth<sup>1</sup>, Xiaoxia Zhu<sup>1,2</sup>, Robert D. Frisina<sup>1,2</sup>

<sup>1</sup>Univ. Rochester Med. Sch., <sup>2</sup>Int. Ctr. Hearing Speech Res.

Two genetically inbred mouse strains have been utilized extensively to study age-related hearing loss - presbycusis. The CBA strain loses its hearing at a slow rate as a function of age, whereas the C57 strain displays a rapid, progressive sensorineural hearing loss. The medial olivocochlear efferent system (MOC) has been shown to modulate the response of the cochlear outer hair cell system. The objective of this study was to examine the differences in the MOC system between F1 (CBAxC57) mice and the parental strains by comparing the distortion-product otoacoustic emissions (DPOAEs) generated with and without contralateral white noise stimulation (CS). Twenty middle aged (14-16.4 mon) F1 (CBAxC57) mice (11 male, 9 female) were tested with DPOAEs. Recordings were obtained from individual subjects (anesthetized with ketamine/xylazine) under two conditions: 1) in quiet, and 2) in the presence of a contralaterally applied wideband noise. These measures were compared to middle aged CBA mice. DPOAE levels were decreased (mean difference 2.018 +/- 0.5955) in F1 (CBAxC57) mice when compared to CBA mice across the frequency range of 5.6 to 44.8 kHz. A greater difference in DPOAE's was noted in the higher frequency range (26-45 kHz). There was reduced contralateral suppression noted in F1 (CBA x C57) mice when compared to CBA mice. Contralateral suppression was noted in F1 (CBA x C57) mice in the low (5.6 to 12kHz) and middle (13-25kHz) frequencies with diminished suppression in the high frequencies (26-45kHz). In conclusion, F1s show greater age-related declines in hearing relative to their CBA parental strain, for middle aged mice.

*Work supported by NIH: NIA & NIDCD*

### **398 Can Diet Influence Presbycusis?**

**Sarah Hein**<sup>1</sup>, Beth Hand<sup>1</sup>, Gary Dootz<sup>1</sup>, Yehoash Raphael<sup>1</sup>

<sup>1</sup>University of Michigan

Presbycusis, also known as age-related hearing loss (AHL) is a very common form of hearing loss in the elderly

human population. The C57BL/6J (B6) mouse is an ideal model for studying AHL because they are observed to lose their hearing gradually starting at 2-3 months of age and then progressively until they are 10-12 months of age. In this study, we wish to observe the effects on AHL of altering the B6 mouse's diet. Specifically, we are testing the hypothesis that a low food intake diet will reduce or prevent AHL in the B6 mice. Mice in the experimental group (N=5) receive 90% of a normal mouse diet whereas mice in the control group (N=5) receive the normal mouse diet (ad libitum feeding). Auditory brainstem response audiometry (ABR) is used to detect changes in the B6 mouse's hearing over time. The mice are now 17 weeks old and the hearing in both groups is near normal. Behaviorally, the mice on the low food diet are more active, have a harder time responding to anesthesia, and are more adventurous than those mice on the normal diet. The mice will be maintained on their respective diets until they reach the age of 12 months, at which time we will perform a histological analysis of the cochleae. If the restricted diet yields significant protection against AHL, we will apply positive reinforcement operant conditioning to better characterize the hearing in these mice. Findings on the influence of diet on hearing preservation may help design clinical means for delay or prevention of presbycusis.

Supported by the CHD and NIH NIDCD grants R01 DC05053 and P30-DC05188.

### **399 Oxidative Stress and Age-Related Hearing Loss**

**Eric Bielefeld**<sup>1</sup>, Donald Coling<sup>1</sup>, Robert Burkard<sup>1</sup>, Bo-Hua Hu<sup>1</sup>, Donald Henderson<sup>1</sup>

<sup>1</sup>SUNY at Buffalo

The Fischer 344 rat was used to study the progression and cellular mechanisms of age-related hearing loss (ARHL) or presbycusis. The rats' hearing was measured at 3, 12, 18 and 24 months using brainstem evoked potential audiometry (ABR). At 3, 18 and 24 months the cochleae were analyzed for hair cell pathology, signs of oxidative stress, and status of mitochondrial function. Over the period of 3 to 24 months, the Fischer 344 rats developed means of 18-50 dB hearing loss at 5, 10, 20, and 40 kHz. The 24-month-old rats have no measurable DPOAE, but there are only small lesions of outer hair cells (OHC) at the base and apex of the cochlea. The discrepancy between hearing loss, as measured by DPOAEs and ABR, and the small number of OHC can begin to be reconciled by assessing the status of the mitochondria. From base to apex, the 24-month-old rat had depressed succinate dehydrogenase (SDH) labeling. In addition, throughout the cochlea, there is increased free radical labeling by dichlorofluorescein (DCF) and OHC that morphologically show signs of apoptosis. Collectively, these results suggest that ARHL, at least in the Fischer 344 rat, may be the consequence of an increase in reactive oxygen species (ROS) activity due to malfunctioning OHC mitochondria, which in turn leads to apoptosis of the sensory cells. [Research supported by grant #1R01DC00686201A1]

#### **400 Minocycline Slows the Progression of Age-Related Hair Cell Loss in DBA Mice**

Dalian Ding<sup>1</sup>, Haiyan Jiang<sup>1</sup>, Ping Wang<sup>1</sup>, Richard Salvi<sup>1</sup>

<sup>1</sup>University at Buffalo

Minocycline, a semisynthetic tetracycline derivative, is a potent antibiotic used to treat gram negative and gram positive infections. Recent findings indicate that minocycline can protect against a wide range of neurodegenerative disorders by inhibiting caspases, iNOS and the release of cytochrome c. We recently reported that minocycline also protects against aminoglycoside induced hair cell loss in vitro. Since minocycline crosses the blood brain barrier and can be administered long term without serious side effects, we hypothesized that minocycline would slow the development of hair cell loss in DBA/1J mice, a strain that develops significant hair cell loss in the base and apex of the cochlea between 1 and 2 months of age. To test this hypothesis, we compared the amount of inner hair cell (IHC) and outer hair cell (OHC) loss in untreated DBA/1J mice versus mice treated with minocycline in their drinking water (5 mg/ml minocycline in 5% sucrose) from 20 to 45 days of age. Untreated DBA/1J mice developed significant IHC loss in the basal 20% of the cochlea and significant OHC loss in the basal 35% and the apical 20% of the cochlea. DBA/1J mice treated with minocycline showed the same overall pattern of hair cell loss; however, the magnitude of IHC and OHC loss in the base of the cochlea was greatly reduced by minocycline treatment. These results suggest that minocycline, which can be absorbed into neural tissue with oral administration, may be a practical method for slowing the progression of age-related hair cell loss in the inner ear. Supported by NIH grant R01DC06630-01

#### **401 Presbycusis in CBA Mice Is Associated with an Age-Related Increase in Immune Cascade Response and Upregulation of Cochlear Casein Kappa Activity**

Mary D'Souza<sup>1,2</sup>, Martha L. Zettel<sup>1,2</sup>, Xiaoxia Zhu<sup>1,2</sup>, Martha Lynch-Erhardt<sup>1,2</sup>, Andrei Yakovlev<sup>1</sup>, Robert D. Frisina<sup>1,2</sup>

<sup>1</sup>Univ. Rochester Med. Sch., <sup>2</sup>Int. Ctr. Hearing Speech Res.

Presbycusis - age-related hearing loss, is a primary sensory problem and is one of the top three chronic medical conditions affecting the elderly. To explore the underlying cochlear gene expression changes that may predispose or cause presbycusis, a microarray study in CBA mice of different age-groups was conducted. The mice were subjected to distortion product otoacoustic emission (DPOAE) and auditory brainstem response (ABR) testing to measure hearing abilities. We measured the mRNA expression in individual mice from both (left+right) cochleae. Subject groups: Young adult (3.5 mon, N=9), middle aged (12 mon, N=17), old mild (27 mon, N=9), and old severe (30 mon, N=6). Microarray data was statistically analyzed by a novel procedure, which is a combination of search-and-testing through a multivariate methodology; and has clear advantages over univariate approaches. For this multivariate analysis, ten probe-sets

were highly statistically significant exhibiting major expression changes with age and hearing loss (ABR and DPOAE). Six of these genes are associated with immune responses (e.g., IgK variant 8). In addition, mRNA levels of genes associated with macrophage differentiation, including macrophage-expressed gene (Mpeg1), Cathepsin S, and Casein Kappa were at elevated levels in old presbycusis mice when compared to young. These age-related expression level changes present a scenario where hearing loss in old age is associated with the influx of neutrophils and the activation of macrophages. Another gene, Cyclin D2, encodes cytokines and regulates p27<sup>(KIP1)</sup>, showed decreased levels of expression in old mild and severe presbycusis mice. The increased levels of macrophage and Cathepsin S and decreased levels of Cyclin D2 gene in aging mice is worth further investigation, to highlight additional underlying molecular mechanisms in presbycusis.

Work supported by NIH: NIA & NIDCD

#### **402 Redox-Related Signal Transduction Pathways in Age-Related Hearing Loss**

Su-Hua Sha<sup>1</sup>, Andra Talaska<sup>1</sup>, Jochen Schacht<sup>1</sup>

<sup>1</sup>Kresge Hearing Research Institute, The University of Michigan, Ann Arbor, MI, USA

Research into the biological mechanisms underlying the general aging process has identified an antagonistic relationship between tissue survival and reactive oxygen species (ROS). Cells respond to oxidant stress by invoking redox-regulated signaling pathways that induce changes in gene expression determining survival or death of the cells. Maintenance of redox homeostasis is crucial for cell survival in age-related hearing loss as it is in other aged tissues.

In this study, we investigated redox-homeostasis and signal transduction pathways in the aging CBA/J mouse cochlea. Glutathione-conjugated proteins, especially the 42 kDa actin conjugate, are indicators of oxidative stress and increased at 12 and 18 months in the inner ear. Staining for 4-hydroxynonenal, a marker for lipid peroxidation, and 3-nitrotyrosine, a neurochemical marker for peroxynitrite increased at the age of 18 months and even more at 23 months in the organ of Corti, especially in the area of the phalangeal process of Deiters cells and the inner and outer pillar cells. Both markers stained weakly in spiral ganglion cells at 3, 12 and 18 months, and increased at 23 months. In contrast, the protein levels of cellular antioxidant defense systems, such as apoptosis inducing factor (AIF) and Mn-superoxide dismutase (SOD2) were reduced. Furthermore, we had previously identified the NF- $\kappa$ B pathway as a protective mechanism in the inner ear (Jiang et al., 2005). In the aging cochlea, protein levels of NF- $\kappa$ B decreased. These results shed light on redox-related homeostatic mechanisms that are compromised in the aged cochlea and may contribute to age-related hearing loss.

This study was supported by program project grant AG-025164 from the National Institute of Aging and core grant P30 DC-05188 from the National Institute on Deafness and Other Communication Disorders, NIH.

**403 The Effects of Resveratrol, Grape Skin Preparation (GSP), Red Wine and 12% Alcohol on Age-Related Changes of COX-2 and 5-LOX Expression in the Inner Ear and Brain**

Nimisha Patel<sup>1</sup>, Michael Seidman<sup>1</sup>, Francis Leong<sup>1</sup>, Hao Jiang<sup>1</sup>, Wayne Quirk<sup>2</sup>

<sup>1</sup>Henry Ford Health System, <sup>2</sup>Central Washington University

This study was designed to determine the effects of several novel antioxidants (extracted from grapes or red wine) and 12% alcohol on COX-2 and 5-LOX expression in the inner ear and brain of rat model of aging. There is compelling anecdotal and experimental evidence that moderate alcohol consumption may reduce specific mediators of inflammation. It is not known whether this effect is because of the alcohol itself or one highly studied constituent of red wine (resveratrol). It is known that COX-2 and 5-LOX (inflammatory biomarkers) are upregulated in certain traumatic events including noise induced hearing loss, myocardial infarction and cerebrovascular accidents.

Twenty nine-month old Fisher 344 rats were used for the study. Subjects were placed in one of six groups: Control; Resveratrol 43 ug/kg; Resveratrol 430 ug/kg; Resveratrol 4300 ug/kg 12% alcohol and grape seed preparation (GSP). Time-released pellets were used for the resveratrol groups, GSP subjects were fed 2.5 gms daily and the 12% alcohol subjects were gavaged 5/7 days with 3 ml of alcohol. Animals were sacrificed at 12 and 18 months and the inner ear and brain tissue were harvested for analysis.

Results demonstrate a significant upregulation of COX-2 in the 12% alcohol group and essentially no upregulation of COX-2 in the resveratrol groups. In addition to these data the 5-LOX and 18 month data will be presented. These findings support the idea that red wine, extracts of red wine and GSP can reduce age-associated upregulation of inflammatory biomarkers and that this "protection" is not observed with 12% alcohol alone. The extracts tested might protect against certain disease states and positively affect the normal aging processes.

**404 Morphological Alterations at the Peripheral Auditory Nerve Synapse in C57BL/6J Mice with Age-Related Hearing Loss**

Sofia Stamatakis<sup>1</sup>, Mohamed Lehar<sup>1</sup>, David K. Ryugo<sup>1</sup>, Howard Francis<sup>1</sup>

<sup>1</sup>Dept. Otolaryngology, Johns Hopkins University

Poor speech discrimination in noise is a significant disability associated with presbycusis yet the underlying pathology is not understood. We hypothesize that age-related changes in the ultrastructure of afferent dendrites and their synapses with inner hair cells (IHC) may be responsible, at least in part. We have conducted a morphometric study of afferent innervation in C57BL/6J mouse, an animal model of presbycusis, with the objective of identifying structural changes at the auditory nerve-IHC synapse.

Cochleae of four 2-3 month old mice with normal ABR thresholds and three 8-12 month old mice with elevated ABR thresholds were prepared for transmission electron

microscopy (TEM). Serial alternate sections of IHCs at approximately 55% distance from the cochlear apex were reconstructed in 3-dimensions using computer software.

Changes in terminal and synaptic morphology were observed in the older animals. The size of the synaptic body (SB) more than doubled to  $0.47 \pm 0.28 \mu\text{m}^2$  in the older group and was associated with an increase in the number of vesicles ( $18.3 \pm 4.4$  to  $29 \pm 8.5$ ) within 100 nm of the SB. Post-synaptic changes included increases in terminal volume ( $3.66 \pm 2.92 \mu\text{m}^3$  vs.  $1.59 \pm 1.30 \mu\text{m}^3$ ;  $t=8.5$ ,  $p<.0001$ ) and mitochondrial content ( $0.208 \pm 0.160 \mu\text{m}^2$  vs  $0.122 \pm 0.135 \mu\text{m}^2$ ;  $t=4.357$ ,  $p<.0001$ ). The post-synaptic pathology coincided with the loss of afferent synapses in animals with more advanced hearing loss and cochlear degeneration. In contrast, pre-synaptic alterations were observed in the absence of post-synaptic changes and with the least cochlear degeneration and threshold shift.

Morphological transformations may commence in the pre-synaptic IHC thereby disrupting neurotransmission and auditory nerve function. Resulting post-synaptic changes likely impact the encoding properties of the nerve, perhaps initiating a cascade of pathology that travels along the auditory pathway. Further characterization of this progression may improve our understanding of age-related changes that influence speech perception.

Acknowledgements: NIH/NIDCD grants DC05909, DC05211, DC00232, and DC00143, and grants from the DRF, AHRF and NOHR.

**405 Electromagnetic Field Distribution and SAR Evaluation in a Model of a Human Implanted Cochlea Exposed to 900 MHz**

Claudia Franzoni<sup>1</sup>, Marta Parazzini<sup>1</sup>, Gabriella Tognola<sup>1</sup>, Paolo Ravazzani<sup>1</sup>, Ferdinando Grandori<sup>1</sup>

<sup>1</sup>Istituto di Ingegneria Biomedica Consiglio Nazionale delle Ricerche

As mobile phones have become part of daily life, possible risks related to exposure to their radiofrequency electromagnetic fields (EMF) have been studied from several aspects. However few studies have focused on the their interaction with cochlear implants and, in any case, only analyzing electromagnetic interference or compatibility.

Since these metallic implants may cause local enhancement of the EMF near the implant, leading also to stronger energy absorption, i.e. increase of specific absorption rate (SAR, W/kg), in this study the effects of the presence of a cochlear implant (and particularly the electrode array) on the EMF distribution and energy absorption in cochlear tissue exposed to an external source of EMF have been estimated using numerical methods and modelling.

EMF calculations were carried out using commercial software (CST Microwave) based on the Finite Integration Technique (FIT), using two different types of cochlear models. The first was a synthetic geometric model resembling the true shape of human cochlea obtained by the segmentation of an histological section made by microscope; the second was obtained by the segmentation of CT images of an implanted patient. For both the models,

the geometry of the electrode array was modeled according to the size, shape, and materials of a real cochlear implant array and then inserted in the cochlear model.

In all simulations the EMF source was modeled as a plane wave with  $E=1$  V/m and the electrode array was turned off.

Data from this study show that the electrode array inside a cochlea exposed to an external radiofrequency EMF source produced some peaks on the amplitude of the electric and magnetic fields near the implant and a consequent local increase of the absorbed power and tissue temperature. Moreover, peaks of current density upon the electrodes array were noted. However, at the typical power levels of mobile phones the enhancement is unlikely to be problematic.

#### **406 A Practical Method of Predicting the Loudness of Amplitude Modulated Electrical Stimuli in Cochlear Implants**

Colette McKay<sup>1</sup>, Katherine Henshall<sup>2</sup>

<sup>1</sup>Aston University, <sup>2</sup>University of Melbourne

The aim of this study was to test the validity of a simplified method of predicting the loudness of electrical stimuli for the particular case of amplitude modulated stimuli. A loudness model by McKay et al. [2003, J Acoust Soc Am **113**: 2054-2063] proposed a practical method of predicting the relative loudness of arbitrary current pulse trains. In brief, the method involves applying a current-to-loudness function for each pulse, and adding up the loudness contributions within a temporal integration window of several milliseconds. The loudness model has been validated with arbitrary steady-state electrical stimuli.

Six users of the CI24M or CI24R implants participated in the study. The amplitude modulated stimuli had three carrier pulse rates (500, 1000, and 8000 Hz), two modulation rates (250 and 500 Hz), four modulation depths (5, 10, 15, & 20 current steps), and at three levels within the dynamic range (threshold, 60%DR and 90%DR). Subjects loudness balanced the stimuli to fixed-current pulse trains. The loudness model was used to predict the current of the fixed-current pulse train that was of equal loudness to each amplitude modulated stimulus.

The results were consistent with the predictions of the loudness model. That is, at low current levels (near threshold at all carrier rates, and at all levels of the high carrier rates) the current of the balanced fixed-current pulse train was close to the RMS current of the modulated stimuli. As the current level increased (i.e. as rate was decreased, or the level in the dynamic range was increased for lower carrier rates) the current of the balanced fixed-current pulse train moved from the RMS level towards the peak level. The adjustment required to loudness balance the modulated stimuli was dependent on the absolute current level, rather than the level within the dynamic range, in keeping with the predictions of the loudness model.

Support provided by the Australian National Health and Medical Research Council

#### **407 Pattern of Facial Nerve Stimulation in Children with Cochlear Implants**

Sharon Cushing<sup>1</sup>, Blake Papsin<sup>2</sup>, Karen Gordon<sup>2</sup>

<sup>1</sup>University of Toronto, <sup>2</sup>Hospital for Sick Children

##### **BACKGROUND**

Electrical stimulation from a cochlear implant can spread beyond the auditory nerve causing unwanted sensations and interfering with hearing.

##### **OBJECTIVES**

The aims of this study were to describe the pattern of stimulation across the main branches of the facial nerve in paediatric cochlear implant users with objectively documented facial nerve stimulation.

##### **STUDY DESIGN**

A prospective study of a randomized sample of 41 paediatric implant users. Facial nerve responses were evoked by 3 electrodes along the implant array. In addition to midline EABR, surface electromyography (EMG) of frontalis, orbicularis oculi, orbicularis oris/mentalis, and platysma muscles was performed. All recordings were performed in awake children

##### **RESULTS**

EMG responses from the facial nerve were recorded in more than 56% (23/42) of implant users (Nucleus 24) and in most cases occurred when levels were perceptually loud but comfortable. When present, uniform activation across all branches of the facial nerve was not observed yet a clear myogenic response was always found in the EABR channel. Myogenic responses were most commonly seen by electrodes placed over the orbicularis oculi and orbicularis oris/mentalis. More occasional responses were recorded from electrodes overlying frontalis and platysma. The threshold for activation of each facial nerve branch was likewise not uniform.

##### **CONCLUSIONS**

1. The non-uniform pattern of facial nerve stimulation demonstrated in this study, suggests that clinicians should concentrate on orbicularis oculi, oris and mentalis muscles when monitoring for signs of facial nerve stimulation.
2. The non-uniform pattern of activation of facial nerve branches may reflect variable thresholds for nerve branches or muscle groups within the face.

#### **408 Interactions Between Acoustic Signal Level, Microphone Sensitivity and Signal Compression for Speech Recognition in Noise by Cochlear Implant Users**

Geraldine Nogaki<sup>1</sup>, Qian-Jie Fu<sup>1</sup>, John J. Galvin, III<sup>1</sup>, Sherol Chinchilla<sup>1</sup>

<sup>1</sup>House Ear Institute

For cochlear implant (CI) users, speech perception is strongly affected by interactions between the acoustic signal level, microphone sensitivity setting, automatic gain control (AGC) and acoustic input dynamic range (IDR). To examine these interactions, sentence recognition thresholds (SRTs) were adaptively measured in 6 Nucleus-22 patients using their clinically assigned speech processors, in quiet and noise, for a range of signal levels



and microphone sensitivity settings. First, SRTs in quiet (i.e., audibility) were measured as function of the sensitivity setting. Results showed that higher speech levels were required at low sensitivity settings. Next SRTs in noise were measured for two fixed speech levels (55, 65 dBA), as function of the sensitivity setting. Results showed that, for low sensitivity settings, performance was better at 65 dBA; as the sensitivity was increased, performance at 55 dBA was equal to or better than that at 65 dBA. Finally, SRTs in noise were measured for 5 fixed noise levels (30, 40, 50, 60, 65 dBA), for a fixed sensitivity setting (4; corresponding to acoustic inputs between 40 and 70 dBA).

At low noise levels, speech levels needed only to be adjusted for audibility, as the noise level was center-clipped by the IDR. Medium noise levels provided the best performance, as both speech and noise were optimally mapped onto the IDR for the fixed sensitivity setting. At high noise levels, performance worsened, most likely due to peak clipping caused by interactions between the sensitivity setting, IDR and AGC. The results showed clear effects of signal audibility and distortion due to interactions between signal level, microphone sensitivity, AGC and IDR. The results suggest that these parameters require careful attention when testing patient performance with clinically assigned speech processors. The results also suggest that these parameters need optimization for the variety of listening environments typically encountered by CI patients.

#### **[409] Do Higher Pulse Rates Improve the Detection of Slow Amplitude Modulations in Cochlear Implants?**

**Tim Green<sup>1</sup>, Stuart Rosen<sup>1</sup>, Andrew Faulkner<sup>1</sup>, Nicholas Hamilton<sup>1</sup>**

<sup>1</sup>UCL

Recently developed cochlear implant (CI) systems can deliver pulses to the auditory nerve at much higher rates than was previously possible. It has been suggested that higher stimulation rates may allow an enhanced representation of temporal envelope information, and produce patterns of neural response more closely resembling those found in normal hearing. However, studies assessing speech perception at different pulse rates have provided no consistent evidence of benefits from high rates.

Our approach to this issue focuses on basic auditory abilities underlying speech perception, such as the detection of slow amplitude modulation (AM). Adaptive testing was used to find the minimal modulation depth detectable at AM rates of 2-16 Hz. CI users (Clarion C1 and C2) were tested with biphasic pulses on a single electrode. Simulations in normal listeners used narrow acoustic pulses high-pass filtered at 9 kHz, presented with a low-pass noise to mask low frequency spectral components. The relatively wide auditory filtering at high frequencies minimizes the temporal smearing of pulses.

For normal listeners pulse rate varied in octave steps between 101.6 and 812.5 Hz. Performance increased with rate, especially at lower rates, with a tendency for pulse rate effects to be greater for higher modulation rates. It

appears that more frequent sampling of the envelope is beneficial, even when sampling rates are 50 times higher than the frequencies present in the modulation.

Initial results from CI users show a highly variable pattern. One C1 user (tested with rates between 102 and 3250 Hz) showed substantially better AM detection as rate increased, while two others showed little effect of rate. In contrast, for the only C2 user of three tested to show a substantial effect of rate (between 482 and 5787 Hz), performance declined as rate increased.

Supported by the RNID, and a Wellcome Trust Vacation Scholarship (VS/05/UCL/A3).

#### **[410] Use of Prosodic Components of Speech in Pediatric Cochlear Implant Recipients' Utterances** **Shu-Chen Peng<sup>1,2</sup>, J. Bruce Tomblin<sup>1</sup>, Linda J. Spencer<sup>1</sup>**

<sup>1</sup>Department of Speech Pathology and Audiology, University of Iowa, <sup>2</sup>Department of Hearing and Speech Sciences, University of Maryland

Cochlear implants (CIs) have been shown to be limited in encoding fundamental frequency information that is important for the recognition of lexical tones, speech intonation and other prosodic features of speech. Hence, the acquisition of prosodic components of speech in children who must develop a spoken language system via a CI can greatly be impacted. The purposes of this study were: (a) to compare the performance of pediatric CI recipients' use of prosodic cues pertaining to speech intonation in signifying utterance types (questions vs. statements) to that of their NH peers, and (b) to quantify how each of the acoustic properties, i.e., F0, intensity, and duration cues is utilized by individuals with a CI or with NH in contrasting utterance types in their production. Twenty-five prelingually deafened individuals with a CI (ranging from 7 to 21 years of age) and 16 age-matched children and young adults with normal hearing (NH) served as participants. All CI participants had a minimum of five years of device experience. Ten pairs of declarative and interrogative utterances matched for their phonemic structures were elicited from each participant using a set of pictures. All utterances were then acoustically analyzed and perceptually judged by eight NH listeners. The results from perceptual judgments showed that the proportion of utterances (specifically questions) of the CI group was considerably lower than that of the NH group. Acoustic results indicated some acoustic properties present in the utterances of the CI group followed similar patterns to those in the utterances of the NH group. However, certain acoustic properties, such as the amount of voice pitch rise at the utterance-final word in questions of the CI group showed significant reductions in magnitude than that in those of the NH group. The present results suggested pediatric CI users may show limited mastery over the use of prosodic components of speech in their production. A detailed comparisons of the acoustic properties in the utterances produced by the CI and NH participants will be presented. These results have implications for a need of improving CI technology and for the development of adequate speech intervention and aural (re) habilitation strategies to facilitate the acquisition of intonation and other prosodic aspects of speech in pediatric CI users.

#### **411 Electrode Discrimination in Children with Cochlear Implants**

**Jonathan Kopelovich**<sup>1,2</sup>, Marc Eisen<sup>3</sup>, Kevin Franck<sup>1</sup>

<sup>1</sup>Children's Hospital of Philadelphia, <sup>2</sup>NIDCD, <sup>3</sup>Johns Hopkins University School of Medicine, Department of Otolaryngology - Head & Neck Surgery

Our goal is to define how objective measures of electrode interaction at the auditory nerve level relate to the perception of channel independence in congenitally deaf children with cochlear implants. Here we seek to define how stimulus intensity and electrode position effect the perception of electrode discrimination.

Twenty-five congenitally deaf children (4.0 - 17.7 yrs.) with >3 months experience with their implants participated. Electrode discrimination was measured as a difference limen (DL) of inter-electrode distance. DLs were determined using an adaptive two-interval forced-choice psychophysical task presented on an animated, interactive videogame platform. Stimuli were monopolar 500 ms trains of biphasic 25 us pulses on individual electrodes, and position of the test electrode was varied with a one-up, two-down procedure. DLs were calculated as the mean of the last four reversals achieved during a 25-trial run. Stimulus intensity, probe electrode position, and direction of differential electrode stimulation were varied between runs.

Four reversals were achieved in 161 of 204 completed runs. Among the subjects, DLs showed considerable variability (range 0.34 – 8.55 mm). Older subjects tended to have lower DLs ( $\rho = -0.34$ ,  $p < 0.01$ ). Neither probe location nor direction of test electrode from the probe co-varied with DL. Pairwise comparison demonstrated improved electrode discrimination with higher versus lower stimulus intensity (mean improvement 0.62 mm  $\pm$  0.21 S.E.M,  $n = 55$ ). These results are surprising based on our previous findings that electrode interaction increased with increasing stimulus intensity and apical electrode position (Eisen and Franck, JARO 6:160, 2005). These results suggest that electrode interaction alone is insufficient to predict electrode discrimination and imply that cues other than the degree of overlap in stimulated auditory nerve fiber populations are used to perceive different channels among electrodes.

#### **412 Combined Acoustic and Electric Hearing: Pitch Matches as a Predictive Factor for Device Performance**

**Lina Reiss**<sup>1</sup>, Christopher Turner<sup>1</sup>, Sheryl Erenberg<sup>1</sup>, Bruce Gantz<sup>1</sup>

<sup>1</sup>University of Iowa

For patients with severe high-frequency hearing loss, a short-electrode cochlear implant (Iowa/Nucleus Hybrid Implant) was recently developed to preserve residual acoustic low-frequency hearing (Gantz and Turner, 2003). Speech recognition scores using combined acoustic-electric hearing improved for all subjects over pre-operative, acoustic-alone scores, with improvements ranging from 5-70% (mean 38%). The residual acoustic hearing also improved speech recognition in a background of other talkers as compared to traditional cochlear implants (Turner et al., 2004).

However, there is a large variability in performance among short-electrode subjects that is unexplained by differences in residual acoustic hearing. This variability may be due to differences in nerve survival, electrode insertion geometry, and central influences. Study of these variables will help to predict patient benefit. Here we focus on pitch matches as an indirect, behavioral measure of nerve survival. Pitch matches were conducted by comparing sequential presentations of an acoustic tone to the contralateral ear and electrical stimulation at a single electrode in the implanted ear.

Results from 13 subjects show pitch matches to be highly variable, ranging from 400 Hz to 2500 Hz for the most apical electrode (~10 mm insertion). These pitch matches are also much lower than predicted by the Greenwood map (~4400 Hz) based on electrode depth in the cochlea. This variability may be in part due to different degrees of neural survival, i.e. the lowest pitch match cases may be the result of few, if any, surviving spiral ganglion neurons in the base of the cochlea, such that the response to the electrical stimulation at the base actually comes from surviving apical neurons. Preliminary findings suggest modest correlations between the pitch match frequency of the most apical electrode and the speech recognition in quiet and with background talkers, with the lowest pitch match cases tending to perform more poorly.

#### **413 Physiological Measures of Cochlear Prosthesis Channel Interaction**

**Ben Bonham**<sup>1</sup>, Russell L. Snyder<sup>1,2</sup>, John C. Middlebrooks<sup>3</sup>, Stephen J. Rebscher<sup>1</sup>, Alexander Hetherington<sup>1</sup>

<sup>1</sup>Epstein Laboratory, UCSF, <sup>2</sup>Utah State University,

<sup>3</sup>Kresge Hearing Research Institute, The University of Michigan, Ann Arbor, MI, USA

Contemporary human cochlear implants (CIs) are multichannel devices. Each of these channels is thought to excite a unique restricted and tonotopically appropriate population of auditory nerve fibers, similar to populations excited by spectrally limited acoustic stimuli. This is the basis for current processing strategies used in CIs. Psychophysical and clinical studies indicate that these devices provide many users with open-set speech reception. Our animal studies seek to understand the physiological mechanisms that underlie this performance.

Using deaf animal models and intracochlear electrodes that approximate commercial CI electrodes, we have shown that many factors influence the spatial (spectral) and temporal distribution of neural activity evoked in the central auditory system by CI stimulation. Among these factors are: the amplitude of stimulus pulses, the pulse waveform (symmetric biphasic or pseudomonophasic), the orientation and separation of the electrode contacts, the mode of stimulation (monopolar, bipolar, or tripolar), the relative location and timing of concurrently activated channels (auditory nerve populations), and the relative location and timing of previously activated channels. This poster describes the effects of cochlear electrode position and stimulating mode on the distribution of neural activity in the inferior colliculus. In some cases, the patterns of activation approximate those that are evoked by tonal acoustic stimuli, while in other cases they are significantly

different. As an example, stimulation of widely spaced longitudinal bipolar electrode pairs using symmetric biphasic current pulses results in patterns of activation with two clearly resolvable peaks, one peak corresponding to each electrode site. As bipolar spacing is decreased the distance between these peaks decreases and the peaks eventually coalesce.

#### **[414] Estimating Represented Frequencies for Cochlear Implant Electrodes in Human Temporal Bone and Imaging Studies**

**Patricia A. Leake<sup>1</sup>**, Olga Stakhovskaya<sup>1</sup>, Divya Sridhar<sup>2</sup>

<sup>1</sup>*Dept. Otolaryngology-HNS, Univ. of California San Francisco*, <sup>2</sup>*University of Miami School of Medicine*

Greenwood's frequency-position function (Greenwood, 1990, JASA 87) has been used to estimate frequencies of cochlear implant (CI) stimulation sites both in temporal bone studies and in imaging studies of living CI recipients. This function calculates frequency as percent of organ of Corti (OC) length, but at present there is no accurate method for estimating OC length in such studies. Also, many CIs place electrodes near the modiolus to target the spiral ganglion (SG), and the SG frequency map is different from that of the OC (Sridhar et al, ARO 2005). Our goal is to develop better methods for estimating frequencies of CI electrodes.

Cadaver cochleae (n=9) were fixed <24 hrs postmortem, stained with osmium tetroxide, microdissected, decalcified briefly, embedded in epoxy resin and examined in surface preparations. In digital images, the OC and SG were measured and radial nerve fibers were traced to define frequency-matched points along the two structures. Expressed as percent of length, the data sets were highly correlated and best fit by a cubic function that allows derivation of SG frequency from Greenwood's equation.

The mean OC length was 33.13 mm, but the mean SG length (center of Rosenthal's canal) was only 13.69 mm, and that of the modiolar wall adjacent to the SG (optimum position of CI electrode) was 15.49 mm. Both OC and SG lengths were correlated ( $r^2=0.78$  and  $0.88$ , respectively;  $p<0.005$ ) with cochlear size (average of the maximum basal coil diameter and the orthogonal diameter). This finding may allow estimation of OC and SG length in imaging studies. Data also suggest that frequency vs. angular position is relatively constant, but insertion distance is correlated with cochlear size (e.g.,  $450^\circ$  from the round window the mean OC frequency is 604 Hz with a range of only 0.4 octave, but insertion distance at  $450^\circ$  varied from 20.9 to 24.8 mm). Accurate frequency maps for the OC and SG should allow better matching of CI processor filter bands to stimulation sites.

*Work supported by NIDCD Contract N01-DC-3-1006*

#### **[415] Intensity Discrimination in Single and Multi-Electrode Patterns in Cochlear Implants**

**Ashmita Gaur<sup>1,2</sup>**, Robert V. Shannon<sup>1</sup>

<sup>1</sup>*House Ear Institute, Department of Auditory Implants and Perception, Los Angeles, California*, <sup>2</sup>*University of Southern California*

In multi-channel cochlear implants, an electrode array is inserted in the cochlea so that different auditory nerve

fibers can be stimulated at different places in the cochlea. Extensive psychophysical studies have mostly shown a poor correlation with speech recognition performance. One possible reason for this lack of correlation is that the psychophysical tests are typically performed on single electrodes whereas speech presents a dynamically changing stimulus across the entire electrode array. It is possible that psychophysical performance is quite different for single electrodes compared with multi-electrode activation, due to peripheral interactions between electrodes or to central interactions or both. The present experiments measured intensity discrimination on single electrodes and in multi-electrode stimulation as a function of level. Stimuli were presented at 250 pulses/sec/electrode or 1000 pulses/sec/electrode on single electrodes and on 5, 10 and 15 electrode clusters, stimulated with interleaved biphasic pulses. Intensity discrimination on a single target electrode was measured as a function of level and as a function of the amplitude of the other electrodes in the multi-electrode complex. Differences in intensity discrimination for single and multi-electrode complexes presumably reflect a combination of peripheral interactions between electrodes and central integration of information across electrodes (profile analysis). The relevance multi-electrode measures of psychophysical capabilities for speech pattern recognition will be discussed. [Funded in part by NIDCD]

#### **[416] Multi-Channel Loudness Perception in Cochlear Implant Listeners**

**Kara Schvartz<sup>1</sup>**, Monita Chatterjee<sup>1</sup>, Monica Dade<sup>1</sup>

<sup>1</sup>*Hearing and Speech Sciences, University of Maryland at College Park*

In normal hearing listeners, the loudness of a two-tone complex is known to increase with frequency separation between stimuli (loudness summation). Relatively little is known about loudness summation in cochlear implant listeners other than the common observation that the loudness of multi-channel stimuli is often greater than that of a single-channel stimulus. Previous investigations have provided mixed evidence for across-channel loudness summation effects. The aim of this study was to quantify the dependence of two- and three-channel loudness perception on the spatial separation between component channels. Effects of stimulation mode (bipolar, monopolar) were also investigated.

A double-staircase adaptive method was used for all loudness-balancing procedures. First, all single-channel stimuli were loudness-balanced to the 50% dynamic range point of a reference channel. Next, the loudness of a multi-channel reference stimulus containing two or three interleaved pulse trains, R1, R2 and R3, was compared with the loudness of a fixed single-channel stimulus. In the two-channel paradigm R1 remains at a constant apical, basal or medial position while R2 varies from most basal to most apical. In the three-channel paradigm R1 and R2 are fixed in location and R3 is varied.

Results obtained with four adult CI listeners (one Nucleus-22, three Nucleus-24) show large and significant increases in perceived loudness with increasing number of stimulated channels. Significant inter-subject variations in

patterns of across-channel loudness summation were observed. Relationships observed with the duration of profound deafness, measures of electrode discrimination, and measures of perceptual distance between component stimuli suggest that these factors interact with loudness summation to produce the multi-channel loudness percept. [Work supported by NIDCD RO1DC04786]

#### **[417] Effects of Electrode Location, Stimulation Mode and Stimulation Rate on Pitch Discrimination by Cochlear Implant Users**

**John J. Galvin, III<sup>1</sup>, Qian-Jie Fu<sup>1</sup>**

<sup>1</sup>House Ear Institute

In cochlear implants (CIs), an electrode's pitch is largely determined by the excitation pattern produced by stimulation. While the place of stimulation (electrode location) is the dominant source of pitch information for CI patients, the spread of excitation (stimulation mode) and the stimulation rate may also influence pitch percepts. If these parameters give rise to distinctly different pitch percepts, the number of spectral channels may be increased beyond what is afforded by a fixed stimulation rate and/or mode. In the present study, pitch discrimination was measured in 5 users of the Nucleus CI device, as functions of electrode location, stimulation rate and stimulation mode. First, pitch discrimination was measured for 4 evenly spaced probe electrodes, relative to a reference set of 7 evenly spaced electrodes with a fixed stimulation rate (250 pulses-per-second, or pps) and mode (BP+1). For each probe electrode, the stimulation rate was varied between 250 and 2000 pps and the stimulation mode was varied between BP+1 and monopolar (Nucleus-24 patients) or "pseudo-monopolar" (Nucleus-22 patients). Results showed that electrode location contributed most strongly to pitch perception; for most subjects, stimulation rate and mode also significantly contributed to relative pitch perception. Next, pitch percepts were directly compared for fixed probe electrodes by varying the stimulation rate, mode, or both parameters. Results showed that, for most subjects, pitch percepts were significantly influenced by stimulation rate and mode. These results suggest that, because stimulation rate and mode contribute to pitch perception, acoustic frequency-to-electrode assignments should accommodate these pitch differences. The results also suggest that by varying the stimulation rate and mode, more spectral channels may be transmitted by the fixed number of implanted electrodes.

#### **[418] Cerebellar Activity During Passive Perception of Rhythm Increases According to Temporal Irregularity**

**Charles Limb<sup>1,2</sup>, Allen Braun<sup>1</sup>**

<sup>1</sup>NIDCD, NIH, Rockville, MD, <sup>2</sup>Dept. Otolaryngology-Head and Neck Surgery and Peabody Conservatory of Music, Johns Hopkins Hospital

While the cerebellum is known to play a fundamental role as a timekeeper in the active production of rhythmic patterns, its contribution to passive perception of auditory rhythm is not well understood. We used functional MRI (3 Tesla) to study rhythm perception in musically untrained

individuals. Ten normal-hearing, right-handed subjects (mean age 27.3  $\pm$  6 years; 7 males, 3 females) listened passively to a series of rhythms presented at an underlying tempo of 120 beats per minute over 6 minutes. The rhythms varied according to temporal regularity, and were classified as quantized, irregular, or random. All patterns utilized a percussive drum sample as the unit of sound and contained the same number of notes within a 30 second block, with the only differences being the temporal onset of each note. Following the passive listening scan, subjects underwent an active paradigm to measure their ability to classify rhythmic patterns according to regularity. Subjects were able to identify the relative degree of regularity between rhythmic stimuli accurately (85%  $\pm$  12.3). Blood oxygen level-dependent contrast images of the cerebellum were analyzed using Statistical Parametric Mapping 99. Random effects analysis ( $p < 0.005$ ) revealed significant levels of cerebellar activity during passive perception of rhythm patterns in comparison to the resting baseline, particularly in left hemisphere lobule VI (maxima at  $x = -20.8$ ,  $y = -59.5$ ,  $z = -24.8$  in Talairach space). Furthermore, the intensity of activation increased according to the degree of randomness of the rhythm stimulus, such that the least regular pattern exhibited the most intense cerebellar activation. Increased levels of activity during perception of highly irregular rhythms may reflect an increase in cerebellar demands required to assess deviations from an implicit temporal clock.

#### **[419] The Effects of Attentional Load on Auditory ERPs Recorded from Human Electrocorticograms**

**Michael Neelon<sup>1</sup>, Justin Williams<sup>2</sup>, P. Charles Garell<sup>1</sup>**

<sup>1</sup>Department of Neurological Surgery - University of Wisconsin, <sup>2</sup>Department of Biomedical Engineering, University of Wisconsin

Responses to acoustic input were recorded from human temporal cortex using subdural electrodes implanted in four epileptic patient-volunteers in order to investigate how attentional load modulates auditory neural response. Patients performed a dichotic listening task in which they listened for rare frequency deviants in a series of tones presented to both ears at interstimulus intervals of 400, 800 and 2000 msec. Across all ISIs, stimuli presented contralateral to electrode location produced the strongest deflections in the averaged ERP at approximately 90 and 176 msec post-stimulus on average (labeled N90stg and P170stg). Maximal recording sites for these peaks most often occurred over the Sylvian fissure or the upper bank of the posterior superior temporal gyrus. Neither ISI nor selective attention exhibited substantial effects on peak latencies. However, overall ERP amplitudes declined significantly as ISI increased, and attending to the contralateral stimulus significantly increased both the N90stg and P170stg peaks for most patients as ISI decreased. This effect of attention increased with decreasing ISI for both components most clearly in the difference between the grand-average ERPs for attending to vs. ignoring the contralateral stimulus, and even more dramatically in the percentage ratio of that difference over the mean peak amplitude. These general amplifying effects of attention along with its peak anatomical location

suggest that attention can modulate exogenous sources in auditory cortex.

**420 Effects of Amplification and Stimulus Intensity on Cortical Auditory Evoked Potentials**  
**Curtis Billings<sup>1</sup>, Kelly Tremblay<sup>1</sup>, Pamela Souza<sup>1</sup>**

<sup>1</sup>*University of Washington*

To date, little is known about the effects of amplification on the neural representation of auditory stimuli. For the unaided ear, increasing the intensity of a stimulus alters the N100 evoked potential, resulting in increased peak amplitudes and decreased peak latencies. Whether or not these latency and amplitude changes occur when stimuli are presented through a hearing aid is currently unknown. Therefore, we examined the effects of stimulus intensity change on the N100 evoked potential for both aided and unaided conditions. We set out to determine if: 1) increasing stimulus intensities resulted in decreased latencies and increased amplitudes in both unaided and aided conditions, and if 2) aided and unaided intensity functions differed from each other.

A 1000 Hz tone was presented at seven stimulus intensity levels (30, 40, 50, 60, 70, 80, and 90 dB SPL). To eliminate effects of hearing impairment, 8 normal-hearing adults were tested. Participants were fit monaurally with a mild gain hearing aid with the volume control deactivated. A Repeated-Measures ANOVA revealed a main effect of intensity, meaning regardless of condition (unaided or aided), N100 amplitudes increased and latencies decreased as the stimulus presentation level increased. However, there was no main effect of amplification and no intensity x amplification interaction, suggesting that aided and unaided intensity functions did not differ significantly from one another.

These results raise new questions about the effects of amplification on auditory evoked potentials. Hearing aids increase the intensity of a signal through amplification; therefore, when compared with unaided responses, we might have expected to see larger N100 amplitudes and shorter N100 latencies in the aided conditions. Possible reasons for not seeing this effect, including hearing aid circuitry, will be discussed. (Funded by: National Institutes of Health training grant T32-DC05361 and American Federation for Aging Research)

**421 Modulation-Encoding and Co-Representation of the Acoustic Envelope and Carrier in Human Auditory Cortex**

**Huan Luo<sup>1,2</sup>, Yadong Wang<sup>1,3</sup>, David Poeppel<sup>1,2</sup>, Jonathan Z. Simon<sup>1,3</sup>**

<sup>1</sup>*Neuroscience and Cognitive Science Program, University of Maryland*, <sup>2</sup>*Department of Biology, University of Maryland*, <sup>3</sup>*Electrical and Computer Engineering Department, University of Maryland*

The acoustic envelope and its carrier are two key features of ecologically relevant natural sounds. To test that both may be co-represented in human auditory cortex, we designed and played stimuli for which both the envelope and carrier are modulated, and recorded the resulting

neural activity via magnetoencephalography (MEG). Our preceding study found that human auditory cortex uses modulation encoding to co-represent both envelope and carrier dynamics; specifically, phase modulation (PM)

encoding is used for slower (0.3-3 Hz) carrier dynamics, i.e., the phase of the auditory Steady State Response (aSSR) at the envelope modulation frequency (here 37 Hz) tracks the carrier dynamics. To test the robustness of this encoding, and to explore the possibility of a change in coding for stimuli with faster carrier dynamics, we have used the same experimental design but with frequency modulation frequencies (*f*FM) of 2.1 Hz to 30 Hz. Results show that modulation encoding persists up to *f*FM of 20 Hz. At intermediate rates, there is a transition from (two-sideband) PM encoding to single-sideband modulation encoding. This is consistent with an additional contribution from a neuronal population using amplitude modulation (AM) encoding: that is, using amplitude, not phase, of aSSR to track the carrier change.

**422 Human Auditory Cortical and Behavioral Sensitivity to Transitions Between Order and Disorder**

**Maria Chait<sup>1</sup>, Jonathan Z. Simon<sup>1</sup>, David Poeppel<sup>1</sup>**

<sup>1</sup>*University of Maryland*

Sensitivity to changes in ongoing sounds plays a key role in auditory scene analysis and detection of new objects in the environment. An important issue is whether this sensitivity depends on attention or is driven by bottom-up processes. Here we use the high temporal resolution of magnetoencephalography (MEG) to explore the neural mechanisms that underlie listener's ability to detect changes in ongoing stimuli, and compare these with psychophysically derived behavior. In particular we study the temporal dynamics of the process by which listeners detect transitions from "disorder", modeled here as a sequence of tones with random frequency, to "order", a constant tone, and vice versa. Signals are 1440 ms in duration, consisting of a 840 ms reference section (either random or constant as defined above) immediately followed by a 600 ms change section (either random or constant). Controls are 1440 ms long, fully random or constant signals. Random sections consist of a sequence of tone pips (pip duration *T* = 60, 30, or 15 ms is constant within each block). Frequencies are randomly drawn between 222-2000 Hz. In the behavioral experiment listeners are required to respond as fast as they can when they detect a change in the stimulus. In the MEG experiment, naïve listeners passively listen to the same stimuli (while performing an irrelevant task). The neural response to the change is recorded. Constant-to-random responses are faster than random-to-constant responses, as predicted theoretically. Focusing on the size of the integration window used to detect the change, we show that listeners adjust the integration window to the statistical properties of the signal even when not actively attending to the changes. This performance is compared to the theoretically optimal limit.

This work was supported by R01 DC05660 to DP.

#### **423 Interregional Connectivity Between Primary Auditory Region and Early Visual Cortex Predicts Successful Recovery Following Cochlear Implant in Congenital Deaf Children**

Eunjoo Kang<sup>1</sup>, Hyejin Kang<sup>2</sup>, Hyo-Jeong Lee<sup>3</sup>, **Seung-Ha Oh<sup>4</sup>**, Simon B. Eickhoff<sup>5</sup>, Dong Soo Lee<sup>2</sup>, Chong-Sun Kim<sup>4</sup>

<sup>1</sup>*Department of Psychology, Kangwon University in Chuncheon, Korea,* <sup>2</sup>*Department of Nuclear Medicine, Seoul National University College of Medicine in Seoul, Korea,* <sup>3</sup>*Inserm U742, University of Pierre and Marie Curie (Paris 6) in Paris, France,* <sup>4</sup>*Department of Otolaryngology, Seoul National University College of Medicine in Seoul, Korea,* <sup>5</sup>*Institute of Medicine, Forschungszentrum Jülich in Jülich, Germany*

Previous studies indicated that individual differences in brain physiology determine successful development of auditory-language capacity following cochlear implantation (CI) in congenital deaf children. In this study, we investigated if differences exist in functional connectivity patterns of primary auditory cortex (A1) between the deaf children with good CI outcome and those with poor outcome.

<sup>18</sup>F-FDG-PET scan was performed preoperatively in a group of 33 congenital deaf non-signers (1.5~11 yrs, mean: 6.2), who underwent pediatric CI surgery. Based on their postsurgical auditory speech perception measured at 2 years after the CI surgery, i.e., correct repetition of auditory sentences without viewing lip-movement (0 ~ 100%, median: 67%), GOOD (n=17, mean: 83.9%) and POOR (n=16, mean: 28.3%) groups were categorized. A mean FDG-uptake of each participant was obtained from the A1 probabilistic cytoarchitectonic map provided with SPM Anatomy toolbox (Eickhoff et al., Neuroimage 2005). This value served as a covariate to elucidate the regions showing significant functional correlation with A1 in a given group.

Although, no group difference was found in the mean FDG level of A1, the interregional connectivity differs greatly between the two groups. Metabolic activity in A1 was correlated with early visual regions ( $P < 0.0001$ , uncorrected) in GOOD group, whereas it was with the frontal regions and cingulate instead in POOR group. These results suggest that the cross-modal functional connectivity between the primary auditory and early visual region developed in some but not all congenital deaf children underlies successful recovery of auditory function, good enough to gain auditory speech perception following gaining of auditory sensation after CI.

\* This research was supported by Korean Ministry of Science and Technology (R01-2002-000-00346-0).

#### **424 Neuroimaging Markers for Human Primary Auditory Cortex: Physiologic and Anatomic Candidates**

**Jennifer Melcher<sup>1,2</sup>**, Irina Sigalovsky<sup>1,3</sup>, Michael Harms<sup>4</sup>

<sup>1</sup>*Massachusetts Eye and Ear Infirmary,* <sup>2</sup>*Harvard Medical School,* <sup>3</sup>*Speech and Hearing Bioscience and Technology Program, Harvard-MIT Div. of Health Sciences and Tech.,* <sup>4</sup>*Pfizer*

In auditory neuroimaging, functional activation is typically assigned to cortical architectonic areas by mapping

imaged brains onto atlases. However, variability across brains makes this approach highly approximate and a poor replacement for direct localization of cortical areas in individuals. The possibility of direct localization has been opened with the recent identification of two potential markers for primary auditory cortex (PAC). Here we compare these candidate markers to previous histological localizations of PAC and to each other. One candidate, identified by Seifritz et al (Science 297:1706-1708,2002) and elaborated on by us (Harms et al., J Neurophysiol 93:210-222,2005), comes from spatial mappings of the time course of fMRI responses to sound. Responses to some sounds are more sustained on Heschl's gyrus and more transient in surrounding cortex. This pattern resembles the primary/non-primary organization of primate auditory cortex, suggesting that more sustained responses may mark PAC. Using structural MRI, we identified a second candidate marker in spatial mappings of an imaging parameter sensitive to myelin content (longitudinal relaxation rate, R1; Sigalovsky et al., NeuroImage 26:S101,2005). A region of high R1 (indicating heavy myelination) was identified within the gray matter of Heschl's gyrus. It was proposed that this region corresponds to PAC, known to overlap Heschl's gyrus and to be heavily myelinated. In the present study, we found that the regions of high R1 and more sustained response always overlapped Heschl's gyrus. However, the disposition of the high R1 region relative to the gyrus more closely resembled that of PAC in histological studies. When measured in the same subjects, the regions of high R1 and more sustained response only partially overlapped. Thus, they cannot both coincide with PAC. We suggest the high R1 region is a more likely marker of PAC because of its closer correspondence to the known neuroanatomy of auditory cortex.

NIH R21DC006071,P30DC005209

#### **425 Asymmetry in the Laminar Structure of the Planum Temporale**

**Anqi Qiu<sup>1</sup>**, Clare Poynton<sup>1</sup>, Patrick Barta<sup>1</sup>, J. Tilak Ratnanather<sup>1</sup>, Michael Miller<sup>1</sup>

<sup>1</sup>*Center for Imaging Science, Johns Hopkins University*

The functional difference between the left and right human auditory cortices may be due to the asymmetry of the underlying laminar structure of the planum temporale (PT). Located on the superior temporal plane posterior to the Heschl's gyrus (HG) and extending to the posterior ramus, the PT is believed to be responsible for speech and language processing. Morphometric measures from recent post-mortem and neuroimaging studies suggest that the left PT is thinner and larger than the right PT.

In a neuroimaging study of auditory hallucination in schizophrenia, we have quantified the laminar structure of the PT and studied its asymmetry in a population of 20 healthy subjects (age: 36.5 ± 11.2). We obtained scalar quantitative measurements (surface area and gray matter volume) and cortical thickness maps from MRI using computational anatomy methods (Ratnanather et al., NeuroImage, 20, 359, 2003). Regions enclosing the superior temporal gyrus were masked, segmented into gray (GM) and white (WM) matter tissues that were used

to generate the GM/WM surface. Distances of GM voxels closest to the delineated PT surface were collected to give the PT GM cortical mantle. Labeled cortical mantle depth maps (LCDMs) associating a distance with each GM voxel (Miller et al., PNAS, 100, 15172, 2003) were generated. Volumes were calculated by summing the histogram. Cortical thickness was locally estimated based on labeled cortical depth maps (LCDMs) and superimposed on the PT surface.

Results show that surface area and GM volume on the left are significantly greater than those on the right (paired t-test:  $p < 0.001$  and  $p = 0.002$ , respectively). LCDMs of the left and right PT surfaces provide additional information that thickness varies across the PT from 1.5mm to 4mm. The PT is thin along the Heschl's sulcus posterior to the HG and becomes thicker as one moves towards the STG and the posterior ramus. Permutation tests on cdfs of LCDMs indicate there is significant asymmetry ( $p < 0.034$ ). The variability of PT cortical thickness may reflect neuronal organization resulting in asymmetric hetero-modal functional parcellation.

Supported by NIH NCRR P41-RR015241 and NIMH R01-MH064838

#### **[426] Assessing Binaural Interaction in Functional Magnetic Resonance Imaging of Human Inferior Colliculus and Auditory Cortex**

**G. Christopher Stecker**<sup>1,2</sup>, Teemu Rinne<sup>2,3</sup>, Tim Herron<sup>2</sup>, Isaac Liao<sup>2,4</sup>, Xiaojian Kang<sup>4</sup>, E. William Yund<sup>2</sup>, David Woods<sup>2,4</sup>

<sup>1</sup>University of Washington, <sup>2</sup>VA Research Service, Martinez CA, <sup>3</sup>Helsinki University, <sup>4</sup>University of California, Davis

Functional MRI has become an important tool for studying the functional organization of the auditory system, from brainstem nuclei to cortical fields, and techniques for differentiating the responses of such structures have become increasingly important. Here, we investigated the binaural sensitivities of fMRI BOLD responses in human inferior colliculus (IC) and auditory cortex (AC). Stimuli were 600-ms triplets of sinusoidally amplitude modulated iterated-rippled noise bursts (16 iterations at 10 ms delay, SAM: 35 Hz @ 90%), presented 1/s at 85 dB SPL. Echo-planar imaging at 1.5 Tesla was used to acquire a single 10mm slice (1.9 x 1.9 x 10 mm resolution) oriented obliquely through IC and AC every TR of ~4.4 s, cardiac gated. The single slice and relatively long TR help reduce the acoustic noise associated with imaging. During imaging, subjects performed a difficult visual oddball detection task (to limit overt attending to auditory stimuli). Auditory stimuli were presented in 20-s "sound" blocks that alternated with 12-s "silent" blocks. Sound blocks presented diotic stimuli or monotic stimuli to the left or right ear. Nine subjects were each scanned in two separate sessions of 20 sound blocks in each condition. Differences between sound and silent blocks showed bilateral activation of AC in all conditions, strongest when the contralateral ear was stimulated. IC activations appeared strictly contralateral in monotic conditions, but bilateral in the diotic case. That is, they exhibited "E0-type" binaural interactions (monaural activation by contralateral stimulation, unaffected by ipsilateral input). This finding

contrasts with physiological data demonstrating binaural sensitivity among a majority of IC neurons. AC activations, on the other hand, were dominated by EE-type interaction as evidenced by extensive bilateral cortical activation with monotic stimulation. Restricted regions of E0-type and EI-type (where activations to monotic sound were reduced by binaural stimulation) interaction were additionally observed in analyses of individual subjects' data. Overall, the results demonstrate the dependence of fMRI BOLD responses on structure-specific patterns of binaural interaction, and thus the utility of such patterns in differentiating and identifying auditory structures.

#### **[427] The Differential Effects of High Stimulus Rates on Middle Latency Response (MLR) Components Investigated Using Continuous Loop Averaging Deconvolution (CLAD)**

**Ozcan Ozdamar**<sup>1,2</sup>, Jorge Bohorquez<sup>1</sup>, Saumitra Sinha Ray<sup>1</sup>, Tao Wang<sup>3</sup>, Marie Cheour<sup>3</sup>

<sup>1</sup>University of Miami, Dept. Biomedical Engineering, <sup>2</sup>Dept. Otolaryngology and Pediatrics, <sup>3</sup>University of Miami, Dept. Psychology

Due to overlapping problems, the adaptation properties of the primary components (Pa and P1) of the auditory Middle Latency Responses (MLRs) are not investigated thoroughly. With conventional averaging it is not possible to exceed rates of 10 Hz without generating complex overlapping waveforms or steady state responses (SSRs). With the Maximum Sequence (MLS) technique, higher rates are achievable but only with highly jittered stimulus sequences that have highly variable adaptation effects. In this study, the effects of rate on both MLR components are studied using low jitter click sequences at mean rates from 7 Hz to over 200 Hz in normal hearing awake subjects. Auditory Brainstem Responses (ABRs) are simultaneously recorded for control purposes. Recordings show that Pa can be consistently recorded at all rates up to 200 Hz. Its amplitude decreases slowly up to about 100 Hz above which a rapid decrease is observed. Pa waveshape remains fairly constant at all rates with little latency or width changes. P1 component, on the other hand, shows a variable waveshape with latencies covering a wide range (50-70ms) and amplitudes increasing and decreasing at different rates. Contrary to some reports in the literature, however, P1 component is present at high rates and can be fairly consistently recorded up to 100Hz.

#### **[428] Brain Metabolism During Speech Reading in Normal-Hearing and Profoundly Deaf Subjects – An Activation Study by 18F-FDG-PET**

**Yasushi Naito**<sup>1,2</sup>, Keizo Fujiwara<sup>1</sup>, Tomohisa Okada<sup>2</sup>, Michio Senda<sup>2</sup>, Tsunemichi Adachi<sup>1</sup>, Masahiro Kikuchi<sup>1</sup>, Shogo Shinohara<sup>1</sup>, Yosaku Shiomi<sup>1</sup>, Tomoko Manabe<sup>1</sup>

<sup>1</sup>Kobe City General Hospital, <sup>2</sup>Institute of Biomedical Research and Innovation

Children with pre-lingual deafness can acquire spoken language by cochlear implantation, of which efficacy, however, deteriorates if the children grow older and pass their critical period. Our previous PET study (Naito et al.: Adv Otorhinolaryngol (Basel), 2000) indicated that processing of visual language prevails, and networks for



spoken language processing may not develop in the superior temporal cortex if pediatric cochlear implant users do not use hearing and speech in daily life. In the present study, we examined cortical glucose metabolism of normal-hearing and profoundly deaf subjects during lip-reading by 18F-FDG-PET, to obtain basic data on the cortical processing of visual component of language and the effect of deafness on it. Six right-handed volunteers and two profoundly deaf subjects, one prelingually deafened and one postlingually deafened subject, participated in this study. The subject was instructed to watch a video of the face of a speaking person with sound deleted, between intravenous injection of 18F-FDG and PET scanning of the brain. The PET data were analyzed by SPM2. The cortical areas with significantly higher metabolism than global mean value in normal subjects were the occipital visual cortices, left angular gyrus, left middle temporal gyrus, the right hemisphere homologue of the Broca's area, supplementary motor area, and the prefrontal cortex. In the postlingually deafened subject, low metabolic area was in the left middle temporal gyrus and in prefrontal cortex. High metabolism regions in the prelingually deafened child were primarily in the visual cortices, and those in the temporal lobes were minimal, suggesting that the temporal cortices may not have become specialized region for processing visual language but may still have plasticity to develop networks for spoken language processing. 18F-FDG PET might be used as pre-operative examination of critical period of language acquisition in profoundly deaf children.

#### **429** Cortically-Evoked Responses to Gaps in Noise

**Gabriel J. Pitt<sup>1</sup>**, Jennifer Lister<sup>1</sup>, Lauren Stack<sup>1</sup>, Nathan Maxfield<sup>1</sup>

<sup>1</sup>University of South Florida

The objective of this study was to describe cortically-evoked responses to gaps in noise in a group of twelve young adults with normal hearing. Gap detection thresholds (GDTs) were obtained behaviorally using narrow band noise (NBN) markers in a standard psychophysical procedure for two "channel" conditions: 1) Within-channel, NBN markers before and after the gap were identical and 2) Across-channel, NBN markers before and after the gap were centered on different frequencies. GDTs were significantly larger for the Across-channel condition than the Within-channel condition. P1-N1-P2 responses were recorded for each participant and channel condition using four gap durations selected relative to performance on the behavioral GDT task: 1) 1 ms gap representing the standard stimulus, 2) sub-threshold gap, 3) GDT, and 4) supra-threshold gap. Responses were examined in two time windows, following the onset of the first and second markers. For the first marker, P1-N1-P2 responses were easily identified and were similar for all conditions and participants. For the second marker, P1-N1-P2 responses were identified for the Within-channel conditions for the two larger gap durations (i.e., threshold and supra-threshold gaps) and for all Across-channel conditions. P1-N1-P2 responses to the onset of second marker were not identifiable for the Within-channel conditions when the gap duration was shorter than GDT.

Second marker P1, N1, and P2 amplitudes were significantly larger for Across-channel conditions than Within-channel conditions. P2 latencies were significantly longer in the Across-channel than in the Within-channel condition. Significant effects of gap duration were observed for N1 amplitude, P2 latency, P1 amplitude, and P1 latency. These data suggest that the neural processes underlying Within- and Across-channel gap detection are different. A comparison of results from "peak picking" and principal component analysis (PCA) is also discussed.

#### **430** Auditory System Networks in Resting State fMRI Data

**Mark Eckert<sup>1</sup>**, Nirav Kamdar<sup>2</sup>, Michael Greicius<sup>2</sup>, Mengkai Sheih<sup>2</sup>, Catherine Chang<sup>2</sup>, Vinod Menon<sup>2</sup>

<sup>1</sup>Medical University of South Carolina, <sup>2</sup>Stanford University

Tonically activated "default mode" networks have been observed in functional imaging resting state data. These observations have highlighted robust coupling between homologous regions across the cerebral hemispheres. This study examined whether the cycle of activity in primary auditory cortex was coupled with activity throughout the auditory system when participants rested with their eyes closed for 4 minutes of fMRI scanning. Anatomical regions of interest (ROI) encompassing the medial Heschl's gyrus were created to extract the average time series of resting state auditory cortex activity for each of the 31 participants. The average time series from the ROIs was used as a covariate to determine which brain regions exhibited correlated activity across the 4 minute time period. Both the left and right hemisphere auditory cortex demonstrated correlated activity with the contralateral Heschl's gyrus, bilateral superior temporal gyrus, bilateral medial geniculate bodies, and bilateral anterior and posterior insula. Interestingly, significantly correlated activity with the anterior extent of the calcarine sulcus was also observed. These results demonstrate coupled activity of the auditory system during constant exposure to scanner noise. A more exciting finding was the coupled activity of visual cortex that represents the peripheral visual field. Macaque tracing studies demonstrate direct connections between auditory cortex and this visual area. We predict this finding reflects a cross-modal network that is sensitive to detecting stimuli in peripheral space.

#### **431** Interregional Connectivity of Broca's Area in Congenital Deaf Children and Cochlear Implant Outcome

**Hyo-Jeong Lee<sup>1,2</sup>**, Eunjoo Kang<sup>3</sup>, Hyejin Kang<sup>4</sup>, Seung-Ha Oh<sup>2</sup>, Simon B. Eickhoff<sup>5</sup>, Dong Soo Lee<sup>4</sup>, Chong-Sun Kim<sup>2</sup>

<sup>1</sup>Inserm U742, University of Pierre and Marie Curie (Paris 6) in Paris, France, <sup>2</sup>Department of Otolaryngology, Seoul National University College of Medicine in Seoul, Korea, <sup>3</sup>Department of Psychology, Kangwon University in Chuncheon, Korea, <sup>4</sup>Department of Nuclear Medicine, Seoul National University College of Medicine in Seoul, Korea, <sup>5</sup>Institute of Medicine, Forschungszentrum Jülich in Jülich, Germany

Individual differences in brain physiology have been reported to be associated with later successful acquisition

of auditory-language following cochlear implantation (CI). For example, in congenital deaf children the greater glucose metabolism in prefrontal cortex including Broca's area positively correlated with the positive results following CI (Lee HJ et al., 11th HBM, abstract 168). Deaf-induced plasticity also has been implicated in interregional connectivity in primary auditory cortex (Kang et al., Neuroimage 2003). In this study, we investigated whether there were differences in cortical connectivity of Broca's area in deaf children, which in turn was associated with later CI outcome.

<sup>18</sup>F-FDG-PET scan was performed preoperatively in a group of 33 congenital deaf non-signers (1.5~11 years old) who were pediatric CI candidates. Deaf children were categorized into GOOD (n=17, mean: 83.9%) and POOR (n=16, mean: 28.3%) groups based on the auditory speech performance at 2 years after CI, that was measured by sentence perception test in auditory only condition (0 ~ 100%, median: 67%). Interregional correlation analysis was performed in each group between BA44/45 and other brain regions using a mean FDG-uptake in the probabilistic cytoarchitectonic map of BA44/45 provided with SPM Anatomy toolbox (Eickhoff et al., Neuroimage 2005).

The interregional connectivity was different between two groups while mean FDG level of the area was not ( $P > 0.3$ ). In GOOD group, metabolic activity in BA44/45 of each hemisphere correlated with contralateral analogue and bilateral premotor cortex ( $P < 0.0001$ , uncorrected), whereas in POOR group, that was restricted within ipsilateral premotor cortex. This result suggests that, development of interhemispheric functional connectivity between BA44/45 and premotor cortex in the deaf children would result in the better auditory rehabilitation.

\* This research was supported by Korean Ministry of Science and Technology (R01-2002-000-00346-0).

#### **432 Contribution of Frequency Differences to Gap Evoked Cortical Event-Related Potentials in Cochlear Implant Users**

**Ming Zhang<sup>1</sup>, Steven Zupancic<sup>1</sup>, Dwayne Paschall<sup>1</sup>, Joehassin Cordero<sup>1</sup>**

<sup>1</sup>Texas Tech University Health Sciences Center

The ability to understand spoken language is critical for the traditional social aspects of life. Using spoken language as stimuli is important because it mimics the real communication environment. However, the language signal contains many physical parameters including duration, frequency, intensity, and gap. One of these parameters may contribute more to speech recognition than the others. Among all, gap detection is an important parameter for speech recognition based on the behavioral studies (Gordon-Salant & Fitzgibbons, 1993). Speech perception occurs at high levels within the central nervous system. Gaps present in speech may evoke the perception-related electrical responses such as cortical event-related potentials. It is believed that the measurement of cortical responses can be a useful method for the assessment of the electrical stimulation patterns produced by a cochlear implant in response to speech stimuli. Such studies may yield important

information for development of rehabilitation programs for the individual user (Ponton & Don, 1995). Gap detection has been found to be frequency dependent in the previous psychoacoustic research studies, though no equivalent electrophysiologic studies have been reported. However, gap detection can also be frequency dependent in electrophysiologic studies, which may be recordable as cortical event-related potentials. A gap was inserted in the middle of various carrier frequencies as stimuli to elicit the cortical event-related potentials (i.e., p300) in cochlear implant users. Our preliminary results showed that gap evoked p300 responses were frequency dependent. It may suggest that for cochlear implant processing strategies, one or two frequencies which contribute prominent p300 responses, may be selected as a dominant stimulation regardless of the signal intensity, and as certain customized rates as portion of total stimulation time. (Acknowledgement: We thank Dr. Qian-Ji Fu for his suggestions for this study.)

#### **433 Comparison of Gap Detection Ability Determined by Cortical Event-Related Potentials Between Cochlear Implant Users and Normal Hearing Individuals**

**Steven Zupancic<sup>1</sup>, Ming Zhang<sup>1</sup>, Dwayne Paschall<sup>1</sup>**

<sup>1</sup>Texas Tech University Health Sciences Center

Electrically stimulated hearing in cochlear implant users is different from the acoustically stimulated hearing in normal hearing subjects in many aspects such as spectral resolution, intensity compression, dynamic range, and the overall sensation of sound (Fu et al, 1998). Even though the obvious functional differences exist between the two types of hearing, electrophysiologic examination of similarities is evident by the presence of cortical event-related potential responses (Ponton & Don, 1995). However, there are electrophysiologic differences between the two groups (i.e., peak latency of the response). We compared gap detection ability determined by cortical event-related potentials. The existence of cortical event-related potentials is an important indication that the sound has been recognized or perceived at the cortical level. Comparison of the two types of hearing has been studied using duration and frequency differences to elicit the cortical event-related potentials, specifically mismatched negativity (MMN), to assess the subject's recognition ability. It is believed that studying the similarities and differences of the auditory evoked potentials between the two types of hearing enhances the understanding of the underlying mechanisms of electric hearing. The use of gap evoked cortical event-related potentials to assess perception ability using the p300 response has not been studied, which we believe to be recordable and to have shorter latency in implant users. In the current study, gap detection and its effect on the p300 response was evaluated. The preliminary results indicate that the gap evoked p300 can be recorded from both cochlear implant users and normal hearing subjects. Also, the latency of the p300 is different between the cochlear implant users and the normal hearing subjects. The impact of the results on cochlear implants will be discussed.

### **434 Binaural Perceptual Learning: The Effect of Training on Interaural Level Discrimination with Amplitude Modulated Tones**

**Daniel Kumpik<sup>1</sup>**, Oliver Kacelnik<sup>1</sup>, Jan W.H. Schnupp<sup>1</sup>, Andrew King<sup>1</sup>

<sup>1</sup>*Oxford University*

Recent work indicates the possibility of a dual-rate mechanism for learning to discriminate high-frequency ILDs (Wright & Fitzgerald, 2001, PNAS, 98: 12307-12312). Data indicate that rapid learning seen in the initial stages of a daily training regime immediately generalises to conditions that use a fixed standard ILD other than 0 dB for the comparison stimulus, but not to different stimulus frequencies or cue types (i.e. low-frequency ITDs). This phase was postulated to represent predominantly procedural learning. In contrast, a later, slower-improvement stage was postulated to represent perceptual modifications that are stimulus-specific and less likely to generalise to other stimulus conditions. To examine whether such training generalises to ITDs present in the same stimulus, and across hemisphere and carrier frequency, sequentially presented Sinusoidally Amplitude Modulated tones were used to assess ILD and ITD discrimination thresholds using a 2AFC adaptive staircase technique. ILD/ITD stimulus values roved around a point 30° to the left or right of the midline. Subjects were pretested to assess lateralisation performance for four different conditions, in which three variables were manipulated (lateralisation cue type (ILD/ITD); perceived origin of lateralisation cue (30° left of midline/30° right of midline), and carrier frequency (4 kHz vs 0.5 kHz). Subjects were then trained for eight days on ILD left 4 kHz (training condition) before completing the posttest. Trained listeners learned significantly more than controls between the pre- and posttests, and a one-way ANOVA with repeated measures showed a significant effect of session on threshold throughout the training period. The improvement in thresholds was seen to generalise only to ILDs with a different carrier frequency (0.5 kHz) and not to ITDs or to the other hemisphere. These data suggest that ILD processing for stimuli originating on opposite sides of the midline is functionally separate.

### **435 Speech Intelligibility Demonstrates a Spatial Gradient of Attention**

**Kachina Allen<sup>1</sup>**, Karen Froud<sup>2</sup>, David Alais<sup>1</sup>, Simon Carlile<sup>1</sup>

<sup>1</sup>*Dept. of Physiology, University of Sydney, NSW.*

*Australia, <sup>2</sup>Dept. Biobehavioural Sciences, Teachers College, Columbia University, NY, USA*

This study examined the role of the focus of spatial attention on speech intelligibility with competing, concurrent talkers. The ability to rapidly switch the spatial focus of attention necessitates targets whose correct identification involves discrimination of only the onset sound. Ongoing differences then discriminate the targets from the maskers. A new speech corpus of nonsense words was recorded consisting of targets "parg", "karg" or "targ" and two masker sets; "borg", "gorg" or "dorg" and "boog", "goog" or "doog". They were recorded by a single, female, American English speaker (44.1 kHz sampling

frequency). The masked threshold (50% correct) was measured when the target and two maskers were co-located directly in front of the subject (80% of trials). In addition, random "unexpected" trials (20%) were played with target and maskers co-located  $\pm 20^\circ$ ,  $\pm 40^\circ$  or  $\pm 60^\circ$  away from the straight ahead "expected" location. Results were pooled from corresponding locations right and left of the expected location. The threshold worsened progressively with distance from the expected location by 3 dB from directly ahead to  $\pm 60^\circ$ .

In a second condition the two maskers were symmetrically and horizontally separated from the target by  $\pm 20^\circ$  at both expected and unexpected locations as before. In this case the speech reception thresholds worsened progressively by 5 dB. These data are consistent with the view that spatial attention produces a gain in speech intelligibility in the presence of competing sounds and that this gain decreases progressively as a function of distance from the attended location.

### **436 Theoretical MAA Estimation Based on Ambiguity Information**

**Ram Krips<sup>1</sup>**, Miriam Furst<sup>1</sup>

<sup>1</sup>*Tel Aviv University*

The performance of hearing ability has been widely studied throughout the last century. One of the standard tools for the estimation of the performance is the Minimal Audible Angle (MAA). We focus on the performance results of MAA azimuth localization tests for narrow band stimuli. A major characteristic of the experimental results in this test is the deterioration in performance for frequencies above 1 KHz.

A model that includes the outer ear represented by a set of head related transfer function (HRTF), and a cochlea which is represented by a set of Gammatone filter bank followed by a probabilistic firing model for the neurons was developed in order to estimate human performance in localization tasks. Just Noticeable Difference (JND) of acoustical auditory features can be estimated by applying mathematical tools such as Cramer Rao Lower Bound (CRLB), or Barakin Lower Bound (BLB).

When CRLB is applied, MAA decreased monotonically as a function of frequency. However, the experimental data represents an increase in MAA for frequencies above 1 kHz. On the other hand when the BLB estimation is used, where the ambiguity in estimating directions is considered, the MAA performance deteriorates as a function of frequency similarly to the experimental data.

When the instantaneous rate of the neural response includes loss of synchrony in high frequencies, both CRLB and BLB estimations yield increase in MAA as a function of frequency above 1 KHz.

We thus conclude, the brain does not loose information from the loss of synchrony in high frequencies, since this information does not exist due to the ambiguity in estimating direction in high frequencies. In other words, the brain doesn't waste "energy" (complex neural mechanisms) in order to solve a problem (synchronization to high frequency data) where the information is ambiguous.

### **437 Virtual Sound Localization Using Head Related Transfer Functions Modified in the Spectral Modulation Frequency Domain**

Jinyu Qian<sup>1</sup>, David A. Eddins<sup>2</sup>

<sup>1</sup>University of Pennsylvania, <sup>2</sup>University of Rochester

Sound localization cues generally include interaural time difference (ITD), interaural intensity difference (IID) and spectral cues. The purpose of this study is to investigate the important spectral cues involved in so-called head related transfer functions (HRTFs) using a combination of HRTF analyses and a virtual sound localization (VSL) experiment. VSL allows systematic manipulation of different cues. Previous investigations have shown considerably worse VSL performance using randomly selected, non-individualized HRTFs than using individualized HRTFs. An efficient procedure for HRTF customization and subject training in a VSL task were developed in the present study to improve the VSL performance using non-individualized HRTFs. The overall baseline VSL accuracy was higher than that reported by previous studies using non-individualized HRTFs. The individually customized HRTFs were used for further investigation of the spectral cues in sound localization. Previous psychoacoustical and physiological studies have both suggested the existence of spectral modulation frequency (SMF) channels for analyzing spectral information (e.g. the spectral cues coded in HRTFs). SMFs are in a domain related to the Fourier transform of HRTFs. The relationship between various SMF regions and sound localization was tested here by filtering or enhancing HRTFs in the SMF domain under a series of conditions using a VSL experiment. Present VSL results revealed that azimuth localization was not significantly affected by HRTF manipulation. Applying notch filters between 0.1 and 0.4 cyc/oct or between 0.35 and 0.65 cyc/oct resulted in significantly less accurate low elevation responses, while spectral enhancement in these two SMF regions did not produce a significant change in sound localization. Likewise, lowpass filtering at 2 cyc/oct did not significantly influence localization accuracy, suggesting that the major cues for sound localization are in the SMF region below 2 cyc/oct.

### **438 Sound Localisation Accuracy Following Four Days of Unilateral Ear Plugging**

Samuel Irving<sup>1</sup>, A. Quentin Summerfield<sup>2</sup>, David R. Moore<sup>1</sup>

<sup>1</sup>MRC Institute of Hearing Research, Nottingham, UK,

<sup>2</sup>Department of Psychology, University of York

Unilateral and asymmetric conductive hearing losses lead to immediate impairments in the ability to understand speech in noisy environments and to localise sound. However, listeners may rapidly regain normal perception. Kacelnik and colleagues (Oxford University, unpublished) showed that azimuthal sound localisation in ferrets can return almost to pre-plug levels within a few days of unilateral ear plugging. Surprisingly, performance remained excellent immediately after removal of the plug, suggesting at least two mechanisms of perceptual learning induced by changes in the balance of binaural input.

The present study asked whether such learning is present in typically-hearing adult humans. Listeners were familiarised with a free-field localisation task over 3 x 1 hr sessions. Broadband noise bursts of 40, 100 and 500 ms and a range of intensities that were pseudorandomly interleaved (56-84dB SPL) were presented from one of 24 speakers arrayed in a circle horizontally at the level of the listener's ear. Listeners indicated the stimulus speaker via a lap-mounted touch screen. An E.A.R. Classic® plug was inserted in one ear and remained in place continuously 24 hours/day for 4 days. Localisation was tested in 1 session per day during this period and immediately after plug removal.

Preliminary data show that the hearing loss produced by the plug (20–40 dB at 64 – 8000 Hz) resulted in a large immediate decrease in localisation ability both on the side contralateral to the plug (mean unsigned error increased from 5° to 11°), and particularly on the side of the plug (mean unsigned error increased from 5° to 25°). However, performance improved over the next 4 sessions (mean unsigned error decreased to 7°). On plug removal, performance immediately returned to pre-plug levels. The results suggest that, as for ferrets, humans gradually learn to map abnormal binaural cues onto particular sound directions. However, the normal map is retained throughout the hearing loss.

### **439 Intra-Individual Shifts in the Sonar Sound Frequency of CF-FM Bats, *Hipposideros Terasensis*, Influenced by Conspecific Colony Members**

Shizuko Hiryu<sup>1</sup>, Koji Katsura<sup>1</sup>, Tsuyoshi Nagato<sup>1</sup>, Liang-Kong Lin<sup>2</sup>, Hiroshi Riquimaroux<sup>1</sup>, Yoshiaki Watanabe<sup>1</sup>

<sup>1</sup>Graduate School of Engineering, Doshisha University,

<sup>2</sup>Department of Biology, Tunghai University

We examined the intra-individual variations in the resting frequency of pulse CF2 (Frest) over four years in an artificial colony of the Taiwanese leaf-nosed bat (*Hipposideros terasensis*, CF-FM). Patterns of change in Frest were observed when individuals were added to or removed from the colony so that we investigated whether Frest was affected by neighboring colony members. Frest of each bat continually showed a long-term gradual change throughout the observed period, and all bats in the colony increased or decreased their Frest in the same direction as a group non-seasonally. The greatest short-term changes were observed when new bats with a relatively low Frest joined the colony, and Frest of new bats converged with those of the original colony members around 8 to 16 days after their introduction. Conversely, a single individual showed a sudden short-term decrease in Frest after its isolation from other colony members. It is commonly believed that Frest differs among colonies, or conspecific individuals due to physical constitution, sex or morphometric differences, but does not vary within individuals. At present, we cannot suggest a cause for such shifts in Frest. However, our findings strongly indicate that the audio-vocal feedback for conspecific pulses appears to be involved in such intra-individual shift in Frest so that Frest is flexible according to the presence of neighboring conspecific bats in a colony. For a fine analysis of Doppler-shifted echoes in cluttered

environment, the bat's auditory system is expected to have flexible adaptation whereby the frequency properties change preferentially. [The research supported by a grant to RCAST at Doshisha Univ. from MEXT, Special Research Grants for the Development of Characteristic Education from the Promotion and Mutual Aid Corporation for Private Schools Japan, Innovative Cluster Creation Project by MEXT.]

#### **440 Pinna Movement of Taiwanese Leaf-Nose Bat, *Hipposideros Terasensis***

**Tomotaka Hagino<sup>1</sup>**, Shizuko Hiryu<sup>1</sup>, Yuichi Morinaka<sup>1</sup>, Liang-Kong Lin<sup>2</sup>, Hiroshi Riquimaroux<sup>1</sup>, Yoshiaki Watanabe<sup>1</sup>

<sup>1</sup>*Graduate School of Engineering, Doshisha University,*

<sup>2</sup>*Department of Biology, Tunghai University*

Bats emit ultrasonic pulses through their mouths or noses (transmitters), and then receive the returning echoes with their ears (microphones). From our observation for the echolocation behaviors, data showed that pinna movement related to sound localization. The present study examined the pinna movements of Taiwanese leaf-nosed bat while the stationary bat executed the echolocation for a moving target. The bat was put on a perch in the center of the observation room. The emitted pulses of the stationary bat were recorded with a microphone which was set just below the bat's nose. A swung pendulum (a ball with 8 cm diameter attached to a string of 1.5 m length) was used as the target in this experiment. Pinna movements were observed by a pair of high-speed cameras. We also measured the target distance between the bat and the ball of the pendulum from the video images. Before the ball approached, each pinna had an irregular movement. Once the bat perceived the target approaching, both pinna directed toward the target and showed the alternating pinna movements in which the right pinna is moving forward and the left pinna moves in the opposite direction. These pinna movements were synchronized with pulse emission. At the timing when one pinna was directed forward and the other directed in the opposite direction, the bat received the echo from the target and then, the succeeding echo was received by the pinna at another asymmetry position. This alternating pinna movement should provide additional binaural cue in the echoes for sound localization. Based on the pinna movement, we proposed a model of sound localization. [The present study was supported by grant to RCAST at Doshisha University from MEXT of Japan, Special Research Grants for the Development of Characteristic Education from the promotion and Mutual Aid Corporation for Private Schools Japan, the Innovative Cluster Creation Project promoted by MEXT.]

#### **441 Acoustic Scanning of a Complex Auditory Scene by the Echolocating Bat, *Eptesicus Fuscus***

**Cynthia F. Moss<sup>1</sup>**, Kaushik Ghose<sup>1</sup>, Marianne E. Jensen<sup>1</sup>, Annemarie Surlykke<sup>2</sup>

<sup>1</sup>*Dept. Psychology, UMD, Maryland, USA,* <sup>2</sup>*Biology, SDU, Odense, Denmark*

Insectivorous bats can orient in complete darkness by emitting ultrasonic cries and listening to echo returns from

the surroundings. Sonar echoes convey the distance, position and identity of objects in the environment, which the bat uses to build a spatial representation of obstacles and prey. Echolocators actively control the directional aim and spectral-temporal features of the sonar cries, and therefore, the bat's vocal response to dynamic acoustic information provides a window to its spatial perception. It is not known if a bat perceives a cascade of echoes from multiple objects as a spatial auditory scene, comparable to a visual scene. To address this question, we studied the bat's active control over the spatial, temporal and spectral characteristics of its vocalizations as it negotiates obstacles and prey.

We trained bats in a dual sonar task, requiring both obstacle avoidance and prey localization in a laboratory flight room. Bats searched for a tethered insect, positioned behind one of two 15 cm diameter openings in a fine mist net that divided the flight room. The bat could only take the insect if it selected and negotiated its way through the correct net opening. As the bat performed this task, we used 2 high speed video cameras to reconstruct its 3-D flight path, and also recorded its synchronized echolocation signals and sonar beam directing behavior with a microphone array. The video and sound recordings allowed us to analyze the bat's vocal motor strategies as it performed this complex echolocation task. Our data on temporal patterning and direction of the bats' sonar signals reveal the range and azimuth of their acoustic gaze. Our results suggest that bats deal with multiple objects by sampling information sequentially from discrete locations in the environment. Our data also emphasize the importance of the bat's temporal patterning of sonar sound sequences to extract spatial detail for successful performance in this dual task.

#### **442 Adaptive Echolocation Behavior in FM Bats Foraging in Pairs**

**Chen Chiu<sup>1,2</sup>**, Amaya Perez<sup>1</sup>, Wei Xian<sup>1</sup>, Cynthia F. Moss<sup>1,2</sup>

<sup>1</sup>*University of Maryland,* <sup>2</sup>*Neuroscience and Cognitive Science Program*

Insectivorous bats use echolocation to navigate and forage in the wild, and they commonly fly in groups. Therefore, it is important for one bat to avoid interference with another bat's echolocation calls when two or more bats fly and/or forage together. Previous studies of jamming avoidance in echolocating bats (e.g. Ratcliffe, J. M., et al., *Can. J. Zool.*, 2004; Ulanovsky, N. et al., *Proc. R. Soc. Lond. B*, 2004) were conducted in the field, with many uncontrollable variables. The results showed frequency changes when two or more conspecific bats flew together in the same environment. The purpose of our study is to examine whether big brown bats, *Eptesicus fuscus*, adjust their echolocation calls to avoid interfering with each other in the laboratory, where we can carefully control conditions and monitor details of the flight path and vocal behavior as they pursue the insect prey.

A total of three *E. fuscus* (two males and one female) were successfully trained to catch a tethered mealworm in a large flight room. Baseline data were taken first when each bat flew alone to catch the mealworm. Two bats were

subsequently flown together with a single prey item. Preliminary results show that paired bats adjusted the highest and/or lowest frequencies of the FM sonar calls, as well as the sweep rate, and duration of these calls to avoid interfering with each other's echolocation. The bats were able to catch the mealworm and avoid collisions in the air. However, there was usually one bat that caught more successfully than the other. In addition, several unusual calls, distinct from regular echolocation calls found in the baseline trials, were recorded in the two bat scenario. The role of these calls still needs to be clarified.

This study provided insight into the adaptive behaviors in *E. fuscus* for successful echolocation in a dynamic environment that contains a complex mix of echoes from its own sonar cries and those from conspecifics.

#### **443 Sound Localization Using Gaze Pointing Under Different Sensori-Motor Contexts**

**Babak Razavi**<sup>1</sup>, Michael T. Rozanski<sup>2</sup>, William E. O'Neill<sup>1</sup>, Gary D. Paige<sup>1</sup>

<sup>1</sup>University of Rochester School of Medicine and Dentistry, <sup>2</sup>Syracuse University

Head pointing is often used to assess sound localization. A more accurate measure may be *gaze* (eye + head). Gaze pointing to visual targets produces different distributions of eye and head depending upon instructions and target eccentricity, but the overall accuracy of gaze pointing exceeds that of the head alone. We examined whether the same holds for sound localization, and whether the eyes correct for orienting errors in head position, making gaze a generally better measure than head for quantifying spatial localization.

Human subjects sat in a dark echo-attenuated room facing a cylindrical screen at 2 m, occluding a speaker on a robotic arm that presented auditory targets (0.1-20 kHz noise) in the horizontal plane ( $\pm 50^\circ$ ). Localization of continuous or transient (memorized) auditory targets was quantified under three conditions: *gaze pointing* with free eyes and head in darkness, *gaze-manual pointing* where gaze was guided by a joystick laser pointer, and *head-laser pointing* where the eyes were centered by fixating a head-fixed laser. Eyes, head and laser (if on) were first aligned with a central fixation spot. After the spot was extinguished, subjects localized targets by aligning their head (and laser if on) with perceived target location.

Results showed that sound localization using *head-laser pointing* (eyes centered) is very accurate (spatial gain  $\sim 1$ ). With the head and eyes free in darkness (*gaze pointing*) or guided by a joystick laser pointer, localization remains accurate, but the head generally undershoots the target and is corrected by eye position. Localization of continuous and transient targets yields similar performance. Localization of auditory and visual (LED) targets was comparable, suggesting that the two senses share common strategies during spatial localization. We conclude that during head pointing gaze is a more accurate indicator of auditory or visual target location than head position alone.

NIH grants R01-AG16319, P30-DC05409, P30-EY01319, T32-GM07356 & T32-EY07125.

#### **444 Correlates of Precedence Effect in Bilateral Cochlear Implant Users Under Conditions of Direct Electrical Stimulation and in Free Field**

**Smita S. Agrawal**<sup>1</sup>, Ruth Y. Litovsky<sup>1</sup>, Gary L. Jones<sup>1</sup>, Richard van Hoesel<sup>2</sup>

<sup>1</sup>University of Wisconsin-Madison, USA, <sup>2</sup>CRC HEAR, Melbourne, Australia

Bilateral cochlear implants (BiCIs) are being provided to a growing number of patients. Our previous study showed that sensitivity to binaural cues depends on the age of onset of deafness (Litovsky et al., 2005, ARO, Abs.:168). Many of the same patients have now also participated in studies on the precedence effect (PE). The PE refers to the fact that the auditory system lets the original source dominate a delayed replica (echo), to facilitate localization. In adults with normal hearing the PE is strongest at brief source-echo delays ( $<10$  ms), and weakens with increase in delay. Physiological and psychophysical studies suggest that the binaural system contributes significantly to the PE, making the PE a useful tool for evaluating the efficacy of BiCIs. We measured the PE in 9 adult BiCI users who acquired hearing loss either during adulthood (N=5), mid-childhood (N=3) or prelingually (N=1). In a direct stimulation (DS) study, electrically pulsed signals were manipulated at pitch-matched electrodes via a SPEAR 3 processor to simulate a source-echo pair under headphone conditions. Interaural timing (ITD) and level (ILD) cues were adjusted in separate experiments. In a free field (FF) study, the PE was investigated by varying source positions in azimuth. Results from the DS study suggest that a robust PE occurred in all subjects with adult onset and in 2/3 subjects with mid-childhood onset; there was no evidence for PE in the subject with prelingual onset. This suggests that subjects with better binaural ITD sensitivity due to later onset of hearing loss are able to capitalize on that advantage in reverberant conditions. In FF the PE was found in all 9 subjects, but results were variable, less dependent on delay and more difficult to interpret. It is very likely that when subjects are listening through their own clinical processors, resultant stimulus coding is not optimal for providing the neural circuitry with the appropriate cues to elicit the PE in free field.

#### **445 Exploration of Spatial Release from Masking in a Simulation of Cochlear Implant Listening**

**Richard Freyman**<sup>1</sup>, Uma Balakrishnan<sup>1</sup>, Karen Helfer<sup>1</sup>

<sup>1</sup>University of Massachusetts

The results of several recent speech recognition studies indicate that spatial differences between target and masker can produce greater release from masking when the masker is competing speech than when it is continuous noise. The difference has been explained by assuming that competing speech can under some conditions produce "informational" masking in addition to energetic masking, and that informational masking is released by perceived spatial differences that do not lead to energetic masking release. Informational masking is thought to occur when target and masker are to some extent confusable with one another. The current study investigated the result of increasing this confusability by

processing both target and masking stimuli to create six-channel speech-envelope-modulated (SEM) noise, which is a rudimentary simulation of processing by a cochlear implant. Target speech stimuli were nonsense sentences spoken by a female talker. Maskers were five different two-talker combinations of female speakers reciting similar nonsense sentences. Envelopes extracted from six frequency bands were used to modulate noise carriers with passbands equivalent to those frequency channels, and then the six noises were summed. The noisy target and masking stimuli appeared informally to be missing qualities that would help distinguish target and masking voices, leading to the expectation that informational masking would increase. Nevertheless, speech recognition results from normal-hearing listeners showed no signs of informational masking. In particular, there was no advantage of perceived spatial differences between target and masker (even though those perceptual differences were verified through localization measurements). Our preliminary hypothesis is that the target-to-masker ratios required for reasonable performance with these degraded nonsense sentence stimuli were sufficiently high that the simple increased loudness of the target in relation to the masker eliminated perceptual confusions between target and masker. Follow-up studies will investigate this hypothesis by using easier tasks with similarly processed stimuli. [Work supported by NIDCD #DC01625.]

#### **446 Precedence Effect with Cochlear Implants - Simulation and Results**

**Bernhard Seeber<sup>1</sup>, Ervin Hafter<sup>1</sup>**

<sup>1</sup>*University of California, Berkeley*

In recent years cochlear implants (CIs) were successful in restoring the ability in many patients to understand speech in quiet and in acoustically dry environments. However, patients still encounter great difficulties in understanding in situations of speech-in-noise. The present study investigates if CI-patients show the precedence effect, i.e. the suppression of the directional influence of the lagging sound on the localization of a leading sound. Previous studies showed that CI-patients rely on the evaluation of interaural level cues (ILDs) for localization, and interaural temporal cues (ITDs) are ignored. Since precedence is predominantly based on the evaluation of ITDs at low frequencies, it is interesting to see if the altered cues with CIs carry enough information for the precedence effect.

Experiments are done in the simulated open-field environment, a calibrated loudspeaker setup in our anechoic chamber. A burst of wide-band-noise or the speech utterance "shape" are played with equal level, but varying interstimulus-delay, from speakers at  $\pm 30^\circ$ . Subjects judge the apparent location of the sound using a movable visual pointer.

Four subjects with bilateral CIs were tested so far, of which 2 subjects showed some localization ability in the localization baseline test. None of those subjects showed the precedence effect. If sounds were played concurrently, the sound was localized in the middle between both loudspeakers, equivalent to summing localization in normal hearing. If a time delay was introduced between

lead and lag, sounds were localized at both loudspeakers separately, even for short delay times. This is surprising because we assumed summing localization to take place over an extended range of delay times. Studies with vocoder-simulations of CIs are underway to clarify if the information present in ILDs and envelope-ITDs is sufficient to evoke the precedence effect in normal hearing subjects. Support provided by NIH and NOHR.

#### **447 The Anatomy of the Vestibular Labyrinth of the Florida Manatee (*Trichechus Manatus Laterostris*)**

**Campbell Williams<sup>1</sup>, Sentiel Rommel<sup>2</sup>, Marie Chapla<sup>2</sup>, Timothy Hullar<sup>1</sup>**

<sup>1</sup>*Washington University in St. Louis,* <sup>2</sup>*Florida Department of Environmental Protection*

Aquatic mammals inhabit a unique, three dimensional world. Their ability to navigate successfully in this environment is likely to depend heavily on the vestibular system. Much research has been done on the vestibular system of terrestrial mammals, but less is known about the vestibular system of obligate marine mammals. The cetacean (whale and dolphin) vestibular system has been shown to be greatly reduced in size, but no study of the sirenian (manatee and dugong) vestibular labyrinth has been made. This study will help determine what vestibular adaptations may be shared among marine mammals and will allow a better understanding of the endangered manatee's ability to orient and navigate.

Three petriotic bones from one female and two male Florida manatees (*Trichechus manatus laterostris*) were scanned using computerized tomography (CT) and isotropic three-dimensional image sets produced. Using custom-written software, the semicircular canals were identified and traced from the dilated ampulla region until they re-entered the vestibule. The dimensions of each canal were determined and unit vectors normal to the plane of each canal were used to measure the angles between ipsilateral sister canals. The images were then registered using a computerized algorithm to a scan of an entire manatee skull, allowing orientation of each labyrinth in the frame of reference of the animal.

Measurements of the female and male animals were significantly different. In the males, the three semicircular canals spanned an average arc of  $173 \pm 4.18$  degrees. The radius of curvature of the anterior semicircular canal ( $4.92 \pm .203$  mm) was significantly greater than the radii of both the horizontal ( $4.35 \pm .181$  mm) and posterior ( $3.91 \pm .106$  mm) canals, as has been observed in most other species. Angles between canals varied by up to 22.4 degrees (anterior-posterior:  $87.47 \pm 1.77$ , anterior-horizontal:  $112.42 \pm 2.72$ , posterior-horizontal:  $96.13 \pm 2.77$ ). A similar geometry has been observed in terrestrial species. The bony anatomy of the manatee vestibular labyrinth differs from that of cetaceans but corresponds relatively closely to that of terrestrial animals.

This research was supported by the Hoopes Undergraduate Research Fund (CDW) and the Mallinckrodt Institute of Radiology (TEH) of Washington University. Thanks to Tim Holden for imaging assistance.



#### **448** MicroCT Analysis of the Dolphin Vestibular Labyrinth

Daniel Calabrese<sup>1</sup>, Timothy Hullar<sup>1</sup>

<sup>1</sup>Washington University in St. Louis

Cetaceans (whales and dolphins) underwent morphologic changes of the inner ear when they returned to the sea approximately 35 million years ago. The major radius of their semicircular canals is understood to have decreased in length at that time, but little else is known about changes in the bony anatomy of their vestibular systems accompanying this transition.

Three pairs of *Tursiops truncatus* (bottlenose dolphin) tympano-periotic complexes were scanned using high-voltage X-ray computed tomography (microCT). Each complex was registered to a conventional CT scan of an intact dolphin head and the bony canals were segmented using custom-written software. The canal planes were calculated from the digitized data using a least-squares regression analysis. The radii of curvature and the planarity of the canals were similarly calculated. Vectors normal to each plane were calculated and the angles between these vectors were determined using a simple cosine rule.

All canals were patent. The posterior canal subtended an arc of  $164.8 \pm 31.3^\circ$ , the horizontal an arc of  $129.8 \pm 20.8^\circ$ , and the anterior canal an arc of  $156.8 \pm 12.4^\circ$ . The horizontal canals were the largest, with the average radius of curvature for the right horizontal canal equal to  $0.628 \pm 0.037$  mm and for the left equal to  $0.588 \pm 0.023$  mm. The right and left posterior canal radii were the smallest, with mean radii of  $0.423 \pm 0.086$  mm and  $0.464 \pm 0.125$  mm respectively. The canals were relatively flat, with averaged deviations from planarity between  $13.4 \pm 4.6^\circ$  and  $37.1 \pm 24.0^\circ$ . Angles between the canal planes were all acute, ranging from  $62.1 \pm 3.1^\circ$  for the angle between the right horizontal canal and the right anterior canal to  $84.5 \pm 13.1^\circ$  for the angle between the left horizontal canal and the left posterior canal. Relative to terrestrial mammals, the bony canals of cetaceans have a decreased radius of curvature, reduced anterior canal size relative to the horizontal canal, and acute rather than nearly orthogonal angles among the canals. The cetacean semicircular canals appear not to be simply a "scaled-down" version of the terrestrial mammalian canals.

This research was supported by the Hoopes Undergraduate Research Grant (DRC). We thank James Mead, Charley Potter, and Dee Allen of the Marine Mammal Division at the National Museum of Natural History, Smithsonian Institution for valuable help with the specimens.

#### **449** Dendritic Architecture of Utricular Peristriolar Afferents in the Mouse

Larry Hoffman<sup>1</sup>, Timothy Jones<sup>2</sup>

<sup>1</sup>UCLA, <sup>2</sup>East Carolina University

The dendritic arbors of vestibular afferent neurons conform to three general morphologies known as calyx, dimorphic, or bouton classes. Within any of these general classes, however, is a broad diversity in architecture, which may influence the spatial and temporal signals that are transmitted by these neurons. For example, dendrites of

dimorphic utricular afferents exhibit broad architectural diversity that may be associated with innervation locus within the topography of the utricle. The specific factors that govern dendritic architecture in these neurons are not well understood. We are investigating the role of natural stimulation in shaping these architectures by comparing afferent dendrites in otoconia-deficient *head-tilt* mice (i.e. *het/het*) and their otoconia-containing heterozygous littermates (i.e. *het/+*). We are reporting here our findings for afferents projecting to the central peristriolar region of the utricle.

The superior vestibular nerves in isoflurane-anesthetized adult *het/het* and *het/+* mice were pressure-injected with tetramethylrhodamine-biocytin. Following a minimum incubation of 2 hours, anesthetized animals were decapitated, and the vestibules were rapidly exposed and infused with chilled 4% paraformaldehyde. The fixative was exchanged with phosphate-buffered saline after 3 hours. The utricles were microdissected and subjected to phalloidin histochemistry for stereocilia labeling. Labeled afferent dendrites and overlying stereocilia bundles were imaged via confocal microscopy.

At the present time we have reconstructed dimorphic afferents projecting to the central peristriolar region in *het/het* and *het/+* utricles (i.e. approx. midway along the length of the striola). These afferents from both phenotypes were found to exhibit constrained dendritic arbors, exhibiting 1-2 calyces and relatively short bouton branchlets. Afferents projecting to both the lateral and medial peristriolar regions were similar. The similarities in these dendrites indicate that natural stimulation does not play a critical role in shaping the architecture of afferent dendrites in this particular region of the macula.

Supported by DC005776.

#### **450** Longitudinal Variation in the Striola of a Turtle, *Trachemys Scripta*: Direction Is More Important Than You Think

Cole Graydon<sup>1</sup>, Jingbing Xue<sup>1</sup>, Ellengene Peterson<sup>1</sup>

<sup>1</sup>Ohio University

The activation axes of vertebrate utricular hair cells fan out radially from the medial margin of the macula. This enables utricles to detect different directions of head movement. It is generally supposed that this radial arrangement is symmetrical, i.e., that comparable populations of hair cells and afferents signal head movement in any direction. Here we present evidence for a different utricular organization. We focus on a specialized region of the macula, the striola.

The crescent-shaped striola in *Trachemys* parallels the anterior, lateral, and posterior perimeter of the macula. Type I hair cells are restricted to a 50  $\mu$ m -wide band within the striola. This band is approximately 20  $\mu$ m medial to the line of polarity reversal. A line connecting its anterior and posterior termini is nearly parallel to the mid-sagittal plane. Thus, utricular type I hair cells detect three directions of head tilt (from anterior to posterior striola: nose down, ipsilateral ear down, nose up) and three directions of linear acceleration (posterior, contralateral, anterior). How similar are the type I hair cells and calyx-

bearing afferents that signal these different directions of head movement?

We stained utricular wholemounts to visualize hair bundles, calretinin-positive ( $\text{Cal}^+$ ), and calretinin-negative ( $\text{Cal}^-$ ) calyces. Calretinin staining is believed to distinguish all-calyx or the most irregularly firing afferents. Our results suggest that the density of type I hair cells, the number of hair cells contacted by single calyceal terminals, and the frequency of  $\text{Cal}^+$  calyces are all greater in postero-lateral striola. Thus, the utricle is not radially symmetrical: the characteristics of utricular receptors and afferents vary with the direction of movement they encode. We hypothesize that this longitudinal variation in the striola reflects the functional demands of naturally occurring head movements. *Supported by NIH DC05063*

#### **451 Simulating In-Vivo Stimuli to 3-D Virtual Hair Cells in Turtle Utricle**

**Jong-Hoon Nam<sup>1</sup>**, John Cotton<sup>1</sup>, John Grant<sup>1</sup>

<sup>1</sup>VA Tech

Both head acceleration and gravity induce Otoconial layer displacement (OLD) that stimulates hair cell bundles in vivo. OLD causes shear displacement of gel layer (GL) and column filament layer (CFL). Hair cells reside in pockets of endolymph fluid (EF) within the GL and CFL. Microfluidic analysis shows the GL and CF displacement realized must push the EF, inducing flow into the bundle. We speculate in vivo hair cells are stimulated by both the OLD, via attachment to the kinocilium and by EF via drag on the whole bundle. However, in vitro experiments of hair cell mechanics have not tested such natural stimuli conditions. Further, few model studies have simulated hair cell response to in vivo stimuli.

In this study, we simulate bundles under the simultaneous stimuli of OLD and EF generated drag forces. These are inherently different signals – acceleration from the OLD, and jerk (the first time derivative of acceleration) from the EF. To achieve this, we constructed Finite Element models of striolar and extrastriolar utricular hair cell bundles reflecting the 3-D bundle structure. We collected detailed bundle morphologies from confocal, scanning, and DIC microscopic images to determine the number of stereocilia, their height, spacing, and link structure. Our model includes active channel dynamics, where each separate tip link assembly (link, gating spring, and channel) is modeled. The model also incorporates  $\text{Ca}^{2+}$  ion movement through gating channels governed by individual tip link tension and intercellular  $\text{Ca}^{2+}$  concentration.

We present individual open channel probability as a function of time from the initiation of otoconial layer movement. We show individual channel activity as well as the combined effect on inward current. In the striolar cell, we see a combined effect of the two stimuli in the first milliseconds of channel activity. This same combined effect was not seen in the extrastriolar cell. (Supported by NIH R01 DC 05063)

#### **452 Voltage-Gated Currents in Hair Cells of the Turtle Utricular Macula**

**William Moravec<sup>1</sup>**, Ellengene Peterson<sup>1</sup>, Ruth Anne Eatock<sup>2</sup>

<sup>1</sup>Ohio University, <sup>2</sup>Baylor College of Medicine

The turtle utricular macula is a good system in which to explore how hair cell specializations shape vestibular signals. It has four zones organized in bands: zone 1 is lateral extrastriola; zones 2 and 3 are in the striola; zone 4 is medial extrastriola. Type I cells, which contact calyx afferent endings, are restricted to zone 3. Type II cells differ across zones in hair bundle properties and, as we show here, basolateral conductances.

We recorded whole-cell currents from hair cells in zones 2-4 in semi-intact utricular maculae excised from the red-eared turtle. As in other vestibular epithelia, type I cells expressed a large potassium (K) conductance with a relatively negative activation range. Boltzmann fits of activation curves from tail currents at  $-40$  mV had  $V_{1/2}$  values ranging from  $-40$  to  $-70$  mV. From N-shaped current-voltage relations, we infer that some type I cells also had a Ca-dependent K conductance ( $g_{\text{K,Ca}}$ ) activated by  $\text{Ca}^{2+}$  influx. Type II cells had  $g_{\text{K,Ca}}$  plus prominent inactivating conductances ( $g_{\text{A}}$ ).  $g_{\text{K,Ca}}$  and  $g_{\text{A}}$  activated more positively than  $g_{\text{K,L}}$ ;  $V_{1/2}$  ranged from  $-20$  to  $-40$  mV. There were differences between zones.  $g_{\text{A}}$  in zone 4 was a larger proportion of peak conductance and faster to inactivate. The mean time constant at  $-24$  mV was  $20 \pm 1.6$  ms (14 cells) in zone 4 and  $34 \pm 3.4$  ms (8) in zone 2 ( $P < 0.001$ ).

In current clamp mode, depolarizing steps ( $\geq 50$  pA) evoked a single voltage peak in type I cells and damped oscillations in type II cells. The oscillations had relatively high frequencies ( $> 100$  Hz) and electrical quality factors,  $Q$ ,  $\geq 3$ . Both  $g_{\text{K,Ca}}$  and electrical tuning may have been enhanced by the light  $\text{Ca}^{2+}$  buffering of the pipette solution (0.2 mM EGTA).

$g_{\text{K,Ca}}$  is likely to comprise BK (Slo) channels. A polyclonal antibody to mouse Slo subunits (Alomone) produced punctate staining of hair cell membranes and diffuse staining of afferents, including calyces, in utricular whole mounts.

*Supported by DC05063*

#### **453 Voltage-Gated $\text{Na}^+$ and $\text{Ca}^{2+}$ Currents in Rodent Vestibular Ganglion Cells**

**Daniel Schneider<sup>1</sup>**, Karen Hurley<sup>2</sup>, Julian Wooltorton<sup>2</sup>, Ruth Anne Eatock<sup>2</sup>

<sup>1</sup>University of Texas, <sup>2</sup>Baylor College of Medicine

The firing properties of vestibular afferents vary from highly regular to highly irregular. This variation may reflect differences in Na, Ca, and K channels underlying spiking. Heterogeneity in Na and Ca channels is suggested by expression in vestibular ganglia of multiple subunits (Wooltorton et al. ARO 2005; Tsai et al. ARO 2005).

Somata were enzymatically dissociated from the anterior division of the rat vestibular ganglion (postnatal days, P, 0-8). Whole-cell recordings were made at  $22^\circ\text{C}$  from somata with capacitances from 4 to 25 pF. In current clamp mode in standard solutions, neurons produced a single spike at

the onset of depolarizing steps from hyperpolarizing prepulses. For voltage clamp recordings, K currents were eliminated by replacing K<sup>+</sup> with Cs<sup>+</sup> and external Ca<sup>2+</sup> was 5 mM. Depolarizing voltage steps activated Na currents which activated and inactivated rapidly and Ca currents which activated more slowly and did not inactivate in 10 ms.

For Na currents, activation and inactivation curves were usually fit with single Boltzmann functions.  $V_{1/2}$  values (midpoints) of inactivation ranged from -44 to -97 mV (29 neurons); S values (a measure of width) from 5 to 23 mV; maximum conductance ( $g_{max}$ ) from 7 to 51 nS (mean  $23 \pm 2.5$  nS, SEM). Activation  $V_{1/2}$  values ranged from -18 to -50 mV and S values from 2 to 10 mV. The large ranges suggest heterogeneous expression. In many neurons, 500 nM tetrodotoxin (TTX) fully blocked the Na current. In 3 neurons, 500 nM TTX blocked  $57 \pm 3.5\%$  of the current; the unblocked current had a more negative inactivation  $V_{1/2}$  than did the total current. These data are consistent with co-expression of TTX-sensitive and TTX-insensitive subunits.

Ca currents were 'HVA' ( $V_{1/2} = -10 \pm 1.3$  mV,  $S = 9 \pm 0.6$  mV,  $g_{max} = 7 \pm 1.2$  nS;  $n=19$ ), and showed run-up. Activation at -25 mV was fit with a Hodgkin-Huxley equation with a time constant of 0.5-1 ms raised to the power of 3.

*Supported by DC02290.*

#### **454 Sodium Activated Potassium Current Participates in the Action Potential Repolarization in the Vestibular Afferent-Neurons of the Rat**

**Enrique Soto**<sup>1</sup>, Blanca Cervantes<sup>1</sup>, Agenor Limón<sup>2</sup>, Rosario Vega<sup>1</sup>

<sup>1</sup>Universidad Autónoma de Puebla, <sup>2</sup>University of California, Irvine

Sodium activated potassium channels ( $K_{Na}$ ) have shown to be expressed in cardiomyocytes (Kameyana et al., 1984) and neurons (Bader et al., 1985). It has been proposed that inflow of Na<sup>+</sup> through this channels during action potential produces a transient activation of  $K_{Na}$ . The  $K_{Na}$  current contribute to adaptation of firing rate and to slow afterhyperpolarizations that follow repetitive firing (for a review see: Bhattacharjee and Kaczmarek, TINS, 28, 2005, 422-428).

In this work we studied the functional expression of  $K_{Na}$  in the primary afferent-neurons of the rat's vestibular system. Currents were recorded using whole cell voltage clamp in cultured (18-24 hrs) afferent neurons.

By using 200 nM tetrodotoxin (TTX) the peak inward Na<sup>+</sup> current was completely blocked. Outward current after TTX application was subtracted from control current showing a transient current which lasting about 20 ms and with peak current of  $2.3 \pm 0.7$  nA ( $n = 4$ ). TTX did not significantly modify the steady state outward current.

The application of anemone toxin CgNa which has been shown to slow the Na<sup>+</sup> channel inactivation (Salceda et al, 2001), increased the Na<sup>+</sup> current inactivation time constant  $128.8 \pm 19.7\%$  without significantly affecting the peak inward current, and concomitantly the outward current measured in the tail increased  $5.6 \pm 2.4\%$  ( $n = 4$ ).

We found that by replacing Na<sup>+</sup> by choline in the extracellular solution there was a complete reduction of the inward Na<sup>+</sup> current and the peak outward current decreased  $40.1 \pm 1\%$  ( $n = 5$ ). Subtraction of the current after choline application and control current shown that choline affected both a sustained and transient components thus indicating a complex action of choline on the outward currents.

These results suggest that  $K_{Na}$  is expressed in the vestibular afferent-neurons and, due to its fast and transient activation, it may contribute to enhance the repolarization process of the action potential.

#### **455 Sequence Analysis of 22,400 Clones from a Normalized Rat Vestibular Periphery cDNA Library**

**Joseph A. Cioffi**<sup>1</sup>, Christy B. Erbe<sup>1</sup>, Rebecca Eernisse<sup>1</sup>, Tina Samuels<sup>1</sup>, Sabrina Mendolia-Loffredo<sup>1</sup>, P. Ashley Wackym<sup>1</sup>

<sup>1</sup>Medical College of Wisconsin

The vestibular organs located in the inner ear sense changes in both the motion and position of the head. This is accomplished by a complex interplay of neurotransmitters, receptors, ion channels, signal transduction and other molecules in vestibular sensory epithelia. Significant gaps remain in our knowledge of the detailed molecular mechanisms and pathways subserving vestibular function. Our laboratory has initiated a systematic and comprehensive effort to characterize the vestibular transcriptome. To this end, we have thus far obtained sequence from 22,400 randomly selected cDNA clones derived from a normalized cDNA library constructed from microdissected vestibular end organs and Scarpa's ganglia in the Brown Norway rat. Sequences are trimmed of vector and poly A tails, analyzed for the presence of canonical or alternative polyA signals, and then BLASTed against the NCBI non-redundant GenBank database (<http://www.ncbi.nlm.nih.gov/>). High homology hits (>90% to rat, >80% to mouse, or human sequences over at least 100 bp) are recorded, including their GenBank ID's. The GenBank ID's are then used to search the Rat Genome Database (RGD), using the Genome Annotation Tool (<http://rgd.mcw.edu:7778/gatool/>) for rat, human, and mouse. The following information from RGD is recorded: Gene Symbol, Gene RGD ID, Human Homolog Symbol, Human Chromosome, Mouse Homolog Symbol, Mouse Chromosome, MGD ID, Disease Terms, Splice Variant Symbol, and Splice Variant RGD ID. The following information is recorded from Entrez: Gene Symbol, Official Name, Summary, Unigene ID, RefSeq, GO, Mapping, and Homologene ID. After all the sequences have been annotated, they are then parsed into the following categories: Matched Known (homology to an EST with a known function), Matched Unknown (homology to an EST with no known function), and New EST's (no high homology matches). New EST's are further analyzed using genome specific BLAST searches as well as BLAT searches. Preliminary gene expression analysis on a subset of new EST's across a variety of rat tissues revealed expression patterns consistent with neural-specific expression. A commercially available rat brain cDNA library was screened by PCR and subsequently

used to obtain additional cDNA sequences corresponding to these interesting clones.

#### **456 Characterization of a Mouse Inner Ear-Specific Collagen**

**James Davis<sup>1,2</sup>**, Miguel Guzman<sup>1</sup>

<sup>1</sup>*The Children's Hospital of Philadelphia,*

<sup>2</sup>*Otorhinolaryngology, Head & Neck Surgery, Univ. of Pennsylvania School of Medicine*

Acellular, sensory accessory membranes overlie the vestibular hair cells in the semicircular canals and the otolithic organs. These membranes are known as the cupula in the semicircular canals and the otolithic/otoconial membrane in the otolithic organs and the tectorial membrane in the cochlea. The otolithic membrane in the bluegill sunfish saccule is comprised of at least two prominent layers of matrix materials that couple the sensory epithelium to the overlying otolithic mass. We are interested in structural features of this anatomic network of endorgan structures that result in vestibular function in the sunfish inner ear.

We are investigating a unique form of collagen termed saccular collagen (SC) that we have found to be a constituent of the sunfish saccular otolithic membrane. We have identified mammalian orthologues of the fish saccular collagen molecule are currently focused on a detailed characterization of the mouse saccular collagen/otolin-1 protein and gene. We have utilized chickens to generate two polyclonal anti-peptide antibodies specific to the mouse SC protein. Characterization of the location and developmental regulation of the expression of the murine SC protein is underway. We are also using molecular biologic methods to obtain and study the murine SC transcript and gene and their associated transcriptional regulatory elements.

The mouse SC protein appears to be inner ear-specific indicating that its transcriptional regulatory elements may be also. Characterization of its putative inner ear-specific expression elements may lead to the development of a useful genetic tool for directing exogenous gene expression into the mammalian endolymphatic compartment.

We are also interested in whether the human SC protein may be involved in human inner ear disorders. Mouse mutants with mutations in this collagen may exist or may be created to facilitate the creation of murine models of human vestibular pathology associated with SC protein absence or dysfunction. This report will provide updates on our efforts to characterize the saccular collagen protein and gene in mammals.

#### **457 Loss of erbB Receptor Function in Supporting Cells of the Vestibular Sensory Epithelia Results in Progressive Macular Degeneration in Adult Mice**

**Joshua Murrie<sup>1</sup>**, M. Charles Liberman<sup>2</sup>, Gabriel Corfas<sup>1</sup>

<sup>1</sup>*The Children's Hospital Boston,* <sup>2</sup>*Mass. Eye and Ear Infirmary*

Experimental evidence indicates that supporting cells of the vestibular sensory epithelium act as precursors to hair

cells during development and after ototoxic damage. It has also been suggested that these supporting cells provide critical trophic support to hair cells in the adult, but this remains to be demonstrated. To begin to explore the function of supporting cells in the adult vestibular organs we used transgenic mice in which erbB receptor signaling in these cells is blocked by expression of a dominant-negative erbB receptor (DN-erbB4). We focused on this signaling pathway because the erbB ligand NRG1 is a potent mitogen for supporting cells in the neonate and because we have shown that erbB signaling is important for the function of supporting cells in the adult cochlea.

Mutant mice display behavioral defects consistent with severe vestibular dysfunction including ataxia, spinning behavior, and inability to swim. Histological analysis shows that animals are born with normal inner ears, but that DN-erbB4 expression in the adult vestibular system results in progressive degeneration of the saccular and utricular maculae. By 6 weeks of age, there is a 40% reduction in both the utricular and saccular maculae. After 5 months, the utricular macula is reduced by 50% while there is a 70% reduction in the saccular macula. Importantly, DN-erbB4 expression in the sensory epithelia precedes the onset of macular degeneration. Together these results suggest that NRG1-erbB signaling is necessary for the maintenance and functioning of the adult vestibular system.

#### **458 Adenylate Cyclases in the Rat Vestibular Periphery**

**Paul Popper<sup>1</sup>**, Christy B. Erbe<sup>1</sup>, Erica Samuel<sup>1</sup>, Tina Samuels<sup>1</sup>, Joseph A. Cioffi<sup>1</sup>, P. Ashley Wackym<sup>1</sup>

<sup>1</sup>*Medical College of Wisconsin*

Adenylate cyclase is a family of enzymes (AC1-AC9) that play a key role in integrating the signal transduction pathways in the vestibular periphery. We have been investigating the expression of AC1 through AC9 in the rat vestibular periphery. Using RT-PCR, all AC isoform transcripts were detected in Scarpa's ganglia and all but AC4 transcripts were detected in cristae ampullares. We are using immunohistochemistry and in situ hybridization techniques to confirm and localize AC gene expression. In addition, we are using calretinin and peripherin antibodies to characterize the neuronal elements that have AC immunoreactivity in the epithelia of cristae ampullares. AC2 hybridization and immunoreactivity was observed in both ganglion and hair cells. In addition, AC2 immunoreactivity was detected in nerve terminals partially colocalized with calretinin and peripherin immunoreactivity, indicating that AC2 is expressed in caliceal, dimorphic and bouton afferents. AC4 hybridization and immunoreactivity was detected in ganglion cells. AC4 immunoreactivity was found in all three types of afferent terminals. AC5/6 immunoreactivity in hair cells, using an antibody raised against the carboxy terminus of these isoforms appeared to be restricted to the hair bundles. Pre-absorption of the antibody with the immunizing peptide eliminated the staining suggesting the immunoreactivity may be AC5/6. Using an antibody raised against the amino terminus of the human AC6 revealed staining in nerve terminals and hair cells. The investigation of the expression of the other AC

#### **459 Recovery of Primary Vestibular Afferent Activity During Regeneration from Ototoxic Damage**

**Zakir Mridha<sup>1</sup>**, Asim Haque<sup>1</sup>, J. David Dickman<sup>1</sup>

<sup>1</sup>*Dept. of Anatomy and Neurobiology, Washington University, Saint Louis, MO USA*

The vestibular system provides for compensatory reflexive behaviors such as postural adjustments and oculomotor responses that occur as the head rotates or when the body shifts relative to gravity. Aminoglycoside antibiotics are known to produce hair cell death and afferent damage, both of which regenerate over time. The aim of this study was to determine the functional capacity of the regenerated vestibular afferents in birds that have undergone treatment with streptomycin. Neural recordings from vestibular afferents in both normal and birds those recovered for 2 to 52 weeks following ototoxic damage. Each afferent was characterized as either a semicircular canal or otolith fiber using rotations in different planes, linear motion and OVAR. Once identified, the responses to sinusoidal stimuli at different frequencies were obtained. Maximum sensitivity vectors were determined using 0.5 Hz rotations at different head orientations. For canal fibers, at 2-12 weeks recovery, the mean spontaneous discharge rates were significantly lower than those of normals. After 2 weeks of recovery, none of the 62 fibers recorded exhibited any response to motion, and at 3 weeks of regeneration, the majority (65/75) still did not respond. After 4 weeks, sensitivity returned with small gains, but most were unresponsive. Fibers at 4-12 weeks recovery exhibited gains that were similar to normal at high frequencies but were greatly reduced at low frequencies. Phase values for these afferents were much more varied but generally were advanced relative to normal. Following 24-52 weeks of regeneration, the afferent gain and phase values were not significantly different from normal. In terms of sensitivity vectors, at early regeneration time points, some afferents were less well tuned, but by 12 weeks, all afferents were oriented similar to normal vectors. Recordings from otolith afferents are still in progress.

**This work was supported in part by NIDCD DC003286 and NNA 04CC52G**

#### **460 Comparison of Physiological Responses of Vestibular-Nerve Afferents Innervating the Semicircular Canals in the Juvenile and Adult C57BL/6 Mouse**

Gyu Han<sup>1</sup>, **David Lasker<sup>1</sup>**, Hong Ju Park<sup>2</sup>, Lloyd B. Minor<sup>1</sup>

<sup>1</sup>*Johns Hopkins University School of Medicine, Department of Otolaryngology - Head & Neck Surgery*, <sup>2</sup>*Konkuk University, Department of Otolaryngology - Head and Neck Surgery*

Extracellular recordings were made from vestibular-nerve afferents innervating the semicircular canals in anesthetized C57BL/6 juvenile mice (4-8 weeks of age, n = 254) and adult mice (16 – 24 weeks of age, n = 99).

Afferents were divided into two groups, regular ( $CV^* < 0.1$ ) and irregularly ( $CV^* > 0.2$ ) discharging afferents based on a normalized measure of the coefficient variation. In juvenile mice, 196 (77%) afferents were classified as regular afferents and 33 (13%) were classified as irregular afferents. The remaining 10% were classified as intermediate afferents. In the adult mice 62 (63%) afferents were classified as regular afferents and 29 (29%) were classified as irregular afferents. The remaining 9% were classified as intermediate afferents. The average resting activity (spikes/s) of regularly discharging afferents was  $49.8 \pm 15.0$ ,  $56.5 \pm 15.5$ , and  $54.7 \pm 15.4$  in 4-6 week, 6-8 week, and 16-24 week mice, respectively ( $p < 0.05$ ). The average resting activity of irregularly discharging afferents was  $27.8 \pm 11.2$ ,  $43.8 \pm 15.1$ , and  $42.2 \pm 18.0$  sp/s in 4-6 week, 6-8 week, and 16-24 week mice, respectively ( $p < 0.001$ ). Sensitivity ((sp/s)/(°/s)) and phase (°) re head velocity were measured for regularly and irregularly discharging afferents for rotations at 2 Hz. Sensitivity for regular afferents measured  $0.12 \pm 0.04$  and  $0.16 \pm 0.07$  for juvenile and adult mice, respectively ( $p < 0.001$ ). Phase lead re velocity for these afferents measured  $4.2 \pm 7.5^\circ$  and  $0.4 \pm 7.0^\circ$  for juvenile and adult mice, respectively ( $p < 0.08$ ). Sensitivity for irregular afferents measured  $0.42 \pm 0.15$  and  $0.42 \pm 0.26$  for juvenile and adult mice, respectively ( $p > 0.9$ ). Phase lead re velocity for these afferents measured  $20.0 \pm 9.0^\circ$  and  $22.3 \pm 13.2^\circ$  for juvenile and adult mice, respectively ( $p > 0.6$ ). Although there was no difference in mean sensitivity and phase for irregular afferents, there was a greater range of sensitivities in the adult (0.12 - 0.98) versus juvenile (0.24 - 0.61) mice. We hypothesize that the reduced number of irregular afferents and smaller range of sensitivities for these afferents in juvenile versus adult mice could reflect a delayed development of the physiological properties of calyx-only afferents. Supported by NIH R01 DC02390

#### **461 Optic Flow Elicits Greater Postural Sway in Patients with Anxiety Disorders**

**Mark Redfern<sup>1,2</sup>**, Joseph Furman<sup>1,2</sup>, Rolf Jacob<sup>2,3</sup>

<sup>1</sup>*Department of Bioengineering, University of Pittsburgh*,

<sup>2</sup>*Department of Otolaryngology, University of Pittsburgh*,

<sup>3</sup>*Department of Psychiatry, University of Pittsburgh*

Patients with anxiety disorders often exhibit symptoms of space and motion discomfort (SMD), similar to those of patients with vestibular disorders. These symptoms suggest that anxiety disorders may result in increased visual dependence for standing balance. The purpose of this study was to determine the postural sensitivity to optic flow of patients with anxiety disorders during fixed floor and sway-referenced conditions. Three subject groups participated: 22 patients with panic disorder, 38 patients with non-panic anxiety, and 31 healthy controls. Subjects stood on an Equitest™ posture platform in either a fixed or sway-referenced floor condition during sinusoidal movement of the visual surround. The moving scene conditions were: no motion, 0.10 Hz sinusoid, or 0.3 Hz sinusoid for 60 s. Anxiety patients were also evaluated for SMD. Results indicated that anxiety patients swayed significantly more than controls in response to optic flow stimuli with a fixed floor, but not with a sway-referenced floor. There were no significant differences between the

panic and non-panic anxiety groups. SMD was an independent predictor of greater sway in response to optic flow in the anxiety patients; those with excessive SMD had significantly greater sway responses than those who did not have excessive SMD. These data suggest that 1) patients with anxiety disorders are more visually dependent for balance compared to controls, 2) excessive SMD is a sensitive indicator of visual dependence, and 3) anxiety patients do not use available proprioceptive information to the same extent as controls. Patients with anxiety disorders, especially those with excessive SMD, appear to be visually dependent for balance possibly as a result of impaired integration of proprioceptive, visual, and vestibular inputs to the postural control system.

#### **462 Space and Motion Discomfort (SMD) Is a Marker for Abnormal Postural Control in Anxious Patients with Height Phobia**

**Rolf Jacob<sup>1</sup>, Mark Redfern<sup>1</sup>, Joseph Furman<sup>1</sup>**

<sup>1</sup>*University of Pittsburgh*

Space and motion discomfort (SMD) is a situational symptom pattern of feelings of unease in environments characterized by unreliable visual or somatosensory cues for balance, such as heights, boats, large open spaces or crowds. Excessive SMD is often seen in patients with vestibular disorders. Height is a situation involving unreliable visual balance cues that generates a form of SMD, height vertigo. The aim of this study was to determine whether height phobia (H+) and excessive SMD (S+) have independent associations with abnormal postural sway. Subjects included 104 persons: 29 were psychiatrically normal and 47 had an anxiety disorder that included height phobia as a symptom (H+) and 28 had an anxiety disorder but no height phobia. SMD was measured using an established questionnaire. Subjects were categorized as having excessive SMD (S+) if their SMD score was >6. Postural control was assessed using Equitest™. Results indicated that 1) there was a significant but asymmetric relationship between H+ and S+ ( $\phi=0.35$ ;  $p = 0.0066$ ). Among anxiety patients with S+, 80% had H+; however, among anxiety patients with H+, only 50% had S+, thus establishing two subgroups of patients with H+, i.e. H+S+ and H+S-; 2) S+ but not H+ was significantly correlated with excessive sway during Equitest™ conditions III ( $\phi = 0.28$ ;  $p=0.03$ ) and IV ( $\phi = 0.37$ ,  $p=.003$ ). Among 21 patients with H+S+, 7 (33%) had abnormal sway on condition IV compared to only 2 of 22 H+S- patients (9%). Taken together, these results suggest that a subgroup of patients with height phobia have abnormal postural control and that these individuals can be identified by a questionnaire measure of SMD. The clinical significance of this result is that an easily identifiable subgroup of patients with height phobia may be amenable to treatment with vestibular rehabilitation.

#### **463 Otolith-Ocular Function in Anxiety Disorders**

**Joseph Furman<sup>1</sup>, Mark Redfern<sup>1</sup>, Rolf Jacob<sup>1</sup>**

<sup>1</sup>*University of Pittsburgh*

Previous studies of vestibulo-ocular function in patients with anxiety disorders have suggested a higher prevalence

of peripheral vestibular dysfunction compared to control populations, especially in panic disorder with agoraphobia. Also, our recent companion studies have indicated abnormalities in postural control in patients with height phobia who suffer from space and motion discomfort. The aim of the present study was to assess the otolith-ocular reflex and semicircular canal-otolith interaction in a well-defined group of patients with anxiety disorders. The study included 104 subjects (ages 18-55 years, 89 female) divided into three groups: 1) 25 patients had panic disorder, 2) 50 patients had non-panic anxiety, and 3) 29 were psychiatrically normal controls. The patients were further categorized based on the presence (60%) or absence (40%) of height phobia and the presence (40%) or absence (60%) of excessive space and motion discomfort (SMD). Constant velocity off-vertical axis rotation (OVAR) was used to assess the otolith-ocular reflex and sinusoidal OVAR was used to assess dynamic semicircular canal-otolith interaction. Post-rotatory responses following constant velocity earth-vertical axis rotation (EVAR) were used to assess static semicircular canal-otolith interaction by head tilts. The eye movement response to rotation was measured using bitemporal electrooculography. Results showed no statistically significant effects of panic, height phobia, or SMD on either the modulation or bias components of the response to constant velocity OVAR. Also, we found no effect of psychiatric diagnosis or SMD on semicircular canal-otolith interaction. No significant correlations were found between SMD and measures of the otolith-ocular reflex. We conclude that in contrast to reported abnormalities in vestibulo-spinal function in patients with anxiety disorders, comparable changes are not apparent in the otolith-ocular system. Differences in vestibulo-spinal versus vestibulo-ocular responses in patients with anxiety disorders may be due, in part, to greater serotonergic and adrenergic influences on the vestibular nuclear areas responsible for vestibulo-spinal function compared to vestibulo-ocular function.

#### **464 Afferent Responses to Experimentally Induced Benign Paroxysmal Positional Vertigo**

**Suhrudd Rajguru<sup>1</sup>, Marytheresa Ifediba<sup>1</sup>, Richard D. Rabbitt<sup>1</sup>**

<sup>1</sup>*University of Utah*

Benign paroxysmal positional vertigo (BPPV) is commonly attributed to the gravity dependent movement of loose calcium carbonate particles located within the lumen of the semicircular canal. Fluid drag caused by the velocity of the particles within the duct induces pressure across the cupula that ultimately leads pathological afferent responses. To quantify the relationship between particle movement and afferent discharge modulation, we introduced spherical glass beads into the canal lumen and recorded modulation of single and multi-unit afferent discharge as the beads moved under the action of gravity toward the ampulla. Experiments were done in the oyster toadfish, *Opsanus tau*, using glass beads selected to mimic the specific gravity and size of human otoconia. The dynamic responses of afferents were characterized prior to introduction of the beads using head rotation and/or

mechanical indentation. These control experiments provided the frequency-dependent gain (spikes/sec per deg/sec) and phase (deg re: peak stim) of afferents. The same afferents were recorded during gravity-induced movement of the beads. Results clearly show the onset latency, magnitude and long-lasting afferent responses during bead movement. A linear model was used to combine results of the control and bead-moving conditions to determine the equivalent angular head movements associated with movement of beads. These equivalent head movements were then used to estimate compensatory pathological eye movements associated with the particle movements. Results further show that afferent responses occur when the particles are sliding along the inside lumen of the canal wall and are consistent with clinical observations and the canalithiasis mechanism of BPPV. [Supported by NIDCD RO1-DC006685]

#### **465 Investigations of the Orientation of Nystagmus Maxima in Cupulolithiasis Disorders Using a Multi Axis Positioning Chair**

Erik Viirre<sup>1</sup>, John Epley<sup>2,3</sup>, Jon Bircck<sup>3</sup>, Hitendra Babaria<sup>3</sup>

<sup>1</sup>UC San Diego, <sup>2</sup>Portland Otolologic Clinic, <sup>3</sup>Vesticon

**Introduction.** Treatment of lithiasis-based disorders of the inner ear has been greatly improved by the development of canalith repositioning maneuvers. More complex maneuvers require a precise knowledge of the orientation of the cupulae of the semicircular canals. However, manually executed procedures lack the degree of precision and repeatability necessary to acquire this knowledge. The computerized, multi-axial Omniax positioning chair, developed by Vesticon, Inc., provides precision serial positioning in any plane. Video-oculography "rides along" with the chair, providing nystagmus quantification in three dimensions. With this technology, one can achieve repeatable head orientations with an angular resolution on the order of 1 degree. Determination of the points of maximal slow phase velocity of nystagmus in cupulolithiasis demonstrates the optimal gravitational vector acting upon a weighted cupula.

**Methods.** As part of an ongoing study, two subjects with persistent ageotropic horizontal nystagmus, nystagmus sampling was carried out in serial positions proximal to the anticipated points of maximum deflection of the horizontal canal cupulae. A datum line of 0 degrees was established from external canthus to the tragus. Samples were acquired at 5-degree increments from supine to 45 degrees toward the active side, as well as 180 degrees inverted from these, parallel and perpendicular to the plane of the datum line.

**Results.** In both subjects, peak nystagmus velocity was calculated automatically and determined to occur at discrete positional points relative to the gravitational vector. A hysteresis factor was noted.

**Conclusions.** The multi-axial rotation chair was demonstrated to provide precision positioning in multiple planes. Functionally important pathophysiology in cupulolithiasis was demonstrated with implications for diagnosis and treatment.

#### **466 A New Method to Determine the Causing Site of Horizontal Canal Benign Paroxysmal Positional Vertigo; Bowing and Leaning Nystagmus**

Yun-Hoon Choung<sup>1</sup>, Keehyun Park<sup>1</sup>, Jung-whan Song<sup>1</sup>, Hison Kahng<sup>1</sup>, Yu Ri Shin<sup>1</sup>

<sup>1</sup>Department of Otolaryngology, Ajou University School of Medicine, Suwon, Republic of Korea

**Objectives:** The cure rate of benign paroxysmal positional vertigo (HC-BPPV) by otolith repositioning maneuver is about 60-90% less than those of posterior canal BPPV. One of causes of this low rate is the difficulty of determining the exact causing site for HC-BPPV using Ewald's second law. The purpose of this study is to develop the new method which can easily determine the causing site of HC-BPPV and evaluate its efficiency. **Materials and Methods:** Twenty eight patients with HC-BPPV were included in this study. The classical method for determining the site is based on comparing the intensity of positioning nystagmus or symptoms in the head positioning test (Ewald's second law). The new method is following. After we confirm whether the type of HC-BPPV is canalithiasis or cupulolithiasis on supine position, we check the direction of nystagmus when the patient bows the head over 90° (bowing nystagmus) and leans the head backward over 45° (leaning nystagmus) on sitting position. For canalithiasis, the causing site is determined as the same direction as that of bowing nystagmus and the opposite direction to that of leaning nystagmus. For cupulolithiasis, the causing site is determined as the opposite direction to that of bowing nystagmus and same direction as that of leaning nystagmus. we compared the efficiency of two methods using Barbecue maneuver (BM). **Results:** In 28 patents (16 canalolithiasis, 12 cupulolithiasis), the patients showed the different causing site between two methods were 11 cases including 7

cases of canalolithiasis and 4 cases of cupulolithiasis. Three of these 11 patients were not completely treated by BM based on the causing site following the Ewald's law, and then cured by just one trial of BM (opposite direction) based on the new method. The rest 8 cases were easily treated by BM based on the direction following the new method. Just one case did not show any bowing or leaning nystagmus. Comparing the treatment results between the classical method (n=20) and the new method (n=28), the cure rate of the new method (85.2%, 23/27) was significant higher than that of classical method (60%, 12/20) on first trial of BM. **Conclusions:** The bowing and leaning nystagmus (Choung's method) is a new method which can easily determine the causing site of HC-BPPV.

#### **467 Oculomotor Responses to Vertical Head Autorotation Test in Posterior Canal Benign Paroxysmal Positional Vertigo**

Jose A Lopez-Escamez<sup>1</sup>, Maria I. Molina<sup>1</sup>, Cristobal Zapata<sup>1</sup>, Maria Jose Palma<sup>1</sup>, Maria Jose Gamiz<sup>1</sup>, Manuel Gomez-Fiñana<sup>1</sup>, Antonio J. Fernandez-Perez<sup>1</sup>

<sup>1</sup>Otology & Neurotology Group CTS495, Hospital de Poniente de Almeria, El Ejido, Almeria, SPAIN

**Objective:** To evaluate the eye movement response to the head auto-rotation test (HART) in the vertical plane in



patients with benign paroxysmal positional vertigo. Patients and methods: Design: A transversal, descriptive study. Setting up: Outpatient clinic in a general Hospital. Individuals: 34 posterior canal BPPV cases with a video-oculographic diagnosis, older than 18 years old, 7 of them were not able to perform the HART. Intervention: HART was performed by a an electrooculographic system with simultaneous recording of head movement by an accelerometer in the vertical plane (Vorteq, Micromedical Instruments). The HART with eyes fixation was performed 3 times to determine its reliability. Main outcome measures: Gain, asymmetry and phase for the vertical VOR respectively. A statistical analysis was carried out to determine the test reliability and the number of individuals with an abnormal result. Results: Gain is the only variable that showed a reproducible result in the HART for the active head movement at 1-2 Hz (test-retest reliability 0,83-0,89). The values of gain showed a moderate correlation at the frequencies 1-3 Hz (correlation 0,60-0,87). Asymmetry and phase were not reproducible variables (correlation < 0,55). Thirteen of 27 (48%) patients presented a decrease of the vertical gain, another 13 showed normal values and one case showed raised values. Conclusion: Gain is the only useful variable in the vertical HART. Forty-eight percent of patients with posterior canal BPPV have a reduced vertical gain. Funded by Proyect FIS PI021394 from Health Institute Carlos III.

#### **468 Are There Any Collerations Between Oculomotor Abnormality and Gait in Patients with Spinocerebellar Degeneration?**

**Kazuo Ishikawa<sup>1</sup>**, Weng Hoe Wong<sup>1</sup>, Yan Wang<sup>1</sup>, Teruyuki Sato<sup>1</sup>

<sup>1</sup>*Akita University*

Introduction: Abnormality in the vestibular system results in oculomotor, postural and gait abnormality. If there is a certain correlation between those output abnormalities, one could give pertinent advice for patients with balance disorder to prevent from an accident in a daily life such as falls and some other accident. With these in mind, correlation between oculomotor abnormalities and gait instability was examined in patients with spino- cerebellar degeneration.

Methods: 16 patients were enrolled for this study. Standard clinical examinations to study oculomotor function by DC electronystagmography and gait analysis by the use of tactile sensors installed under both feet were performed. Regarding oculomotor function, eye tracking, saccade and optokinetic pattern tests were performed. To examine gait stability, coefficient of variation of stance, swing and double support were calculated. Also average length of trajectories of center of force (TCOF) and stability of TCOF were checked. Then those variables obtained from two different systems were comparatively examined.

Results: Those who had dysmetric saccades showed significantly greater CV value of swing with eyes open and greater instability of TCOF with eyes closed. And those who showed decreased visual suppression had a greater

CV value of stance and double support with eyes closed. However no other correlation was obtained.

Discussion and Conclusion: Although the number of cases are still limited, it appears that patients with dysmetric saccade, especially overshoot, must become more ataxic under visual deprivation. This could reflect that those patient might have some lesion at fastigial nucleus which play important roles of saccadic eye movement and control of locomotion. Also normal visual suppression plays an important role for more stable gait.

#### **469 Vestibulo-Ocular Impairment in "Pure" Cerebellar Ataxias**

**John Anderson<sup>1</sup>**, Peka Christova<sup>1</sup>, Christopher Gomez<sup>1</sup>

<sup>1</sup>*University of Minnesota*

The spinocerebellar ataxias (SCAs) are a group of neurodegenerative diseases characterized by progressive unsteadiness of posture, gait ataxia, ocular motor abnormalities, dysarthria, and motor incoordination due to degeneration of cerebellar and brainstem neurons. Some genetic subtypes have been considered to be "pure" cerebellar ataxias that lack extracerebellar deficits and clinically are difficult to distinguish. In this study the vestibulo-ocular reflex (VOR) and postural stability were examined in four such SCAs: SCA5, 6, 8, and 26. We hypothesized that analyses of visual-vestibular interactions and vestibulo-spinal contributions to the control of posture would differentiate among these SCAs and provide evidence for differential neural involvement by the disease processes. Sinusoidal rotations and ramp changes in angular velocity were used to record the VOR in the dark and during visual suppression of the VOR. Postural sway was evaluated with the Neurocom protocol. The results showed that (a) the VOR gain was normal in SCA5, 6, and 26 but was greater than normal in SCA8; (b) visual suppression of the VOR was normal in SCA5, very low for SCA6 and 8, and moderately low for SCA26. A multivariate analysis using variables for the VOR and postural stability differentiated each of the four SCAs, suggesting a differential involvement of neurons in the cerebellum by the disease processes.

#### **470 Chronic Imbalance or Dizziness and Falling: Results from the 1994 Disability Supplement to the National Health Interview Survey and the Second Supplement on Aging Study**

**Chia-wen Ko<sup>1</sup>**, Howard J. Hoffman<sup>1</sup>, Daniel A. Sklare<sup>1</sup>

<sup>1</sup>*NIDCD, Bethesda, MD*

The relationship of the symptoms of dizziness and unsteadiness (imbalance) to the risk of falling has been examined previously in clinic populations and community samples, but not in large nationally representative, population-based surveys. The 1994-95 Phase I Disability Supplement to the National Health Interview Survey (NHIS-D) interviewed 122,938 adult (20+ years), non-institutionalized subjects for chronic (3 months or longer) imbalance or dizziness and other problems. One year later, 25,371 of these subjects who met one or more disability criteria established in Phase I, were re-

interviewed with questions relating to falls and activities of daily living. Also based on the 1994 NHIS, a nationally representative sample of 9,447 subjects aged 70+ years were interviewed as part of the Second Supplement on Aging (SOA II) Study using the same questions regarding falls. Based on national sampling weights, 7.0 million (24%) of 29.4 million disabled American adults aged 20 to 69 years and 4.6 million (21%) of 21.8 million older Americans (70+ years) experienced falls during the one year follow-up period. After adjusting for age, sex, race/ethnicity, education, and family income, results indicated that older subjects with chronic dizziness or imbalance problems had a 2–3 fold increased risk of falling compared to older subjects who did not report chronic dizziness or imbalance (odds ratio [OR]=2.14, 95% confidence interval [CI]: 1.45–3.14 for dizziness only; OR=2.51, CI: 1.95–3.24 for dizziness and imbalance; OR=2.64, CI: 2.08–3.34, for imbalance only). In disabled adults, the risk of falling for people with chronic dizziness only (OR=1.28, CI: 1.01–1.62) was reduced compared to people with chronic dizziness and imbalance (OR=2.29, CI: 1.94–2.70) or chronic imbalance only (OR=2.72, CI: 2.29–3.22). Difficulty in performing one or more activities of daily living (bathing, dressing, eating, getting in and out of bed, using toilet, getting around inside home) is highly prevalent among adults with chronic imbalance or dizziness: 11.5% with chronic dizziness, and 33.4% with chronic imbalance. Chronic dizziness or imbalance in older adults is associated with many medical conditions, e.g., stroke, arthritis, diabetes, hypertension, and heart disease. Better management of medical conditions and activities of daily living is critically important to subjects with chronic imbalance or dizziness problems who are at increased risk of falls.

#### **[471] Influence of Vibrotactile Feedback on Controlling Upright Stance During Postural Perturbations**

**Scott Wood<sup>1</sup>**, Owen Black<sup>2</sup>, William Paloski<sup>1</sup>, Angus Rupert<sup>3</sup>

<sup>1</sup>NASA Johnson Space Center, <sup>2</sup>Legacy Health System, <sup>3</sup>Naval Aerospace Medical Research Laboratory

Vibrotactile feedback has been used to display orientation cues to mitigate risks associated with spatial disorientation and postural instability. The purpose of this study was to examine the influence of vibrotactile feedback on balance control during support surface perturbations. Postural equilibrium was measured with a computerized hydraulic platform in 14 healthy adults (7M, 7F, 20–63 y). A simple matrix with four electromechanical stimulators applied to the torso was triggered using real-time measures of AP sway position and velocity. Trials (100 s duration with eyes closed) were conducted with the support surface sway-referenced, during sum-of-sines perturbations (0.01, 0.15, 0.3 & 0.6 Hz, peak amplitude of 8 deg) or during a combination of the sway-referencing and sum-of-sines perturbations. Instantaneous measures of position and velocity were used to derive feed-forward projections of postural sway at 0, 500 and 1000 msec. Peak-to-peak and RMS sway during either sway-referencing or sum-of-sines perturbations were significantly lower with vibrotactile

feedback. Postural stability was greater with feed-forward projections of sway at 500 msec compared with 0 msec (no velocity used) or 1000 msec projections. These results suggest that incorporating sway velocity will optimize the effectiveness of vibrotactile feedback for balance prosthesis and vestibular rehabilitation applications.

#### **[472] Motion Sickness Sensitivity During Head Mount Visually Distorted Environments**

**Kim Gottshall<sup>1</sup>**, Robert Moore<sup>2</sup>, Michael Hoffer<sup>1</sup>

<sup>1</sup>Naval Medical Center San Diego, <sup>2</sup>San Diego State University

Visual misperception is a common cause of motion sickness in virtual environments with head mount devices. Visual-vestibular mismatch may manifest as balance disorders. The present study explored the relationship of artificially produced visual distortion on balance function and motion sickness perception. A group of 80 normal individuals wore head mount visual distortion lenses that produced a 25 degree shift to the right or left. These individuals had degradation in dynamic gait function, but slight persistent motion sickness perception. Individuals who underwent active head motion exercises recovered the gait function while distortion head mount lenses were in place with resolution of any slight motion sickness complaints. Individuals who did not participate in exercise with active head motion retained poor dynamic gait performance and slight motion sickness complaints. Next a group of subjects with either peripheral or central vestibular pathology were given the visual distortion lenses and asked to perform active head motion exercises and rate motion sickness perception. Dynamic gait tasks were again used as a functional measure. Active head motion facilitated compensation for the effect of visual distortion lenses in peripheral vestibular pathology patients with perception of motion sickness diminishing over repeated trials. Central vestibular pathology patients performing active head motion exercises retained a high perception of motion sickness regardless of improvement in dynamic gait tasks.

#### **[473] Superior Semicircular Canal Dehiscence Syndrome**

**Chunfu Dai Dai<sup>1</sup>**

<sup>1</sup>Otolaryngology Department

Superior semicircular canal dehiscence was first described by Dr. Minor in 1998. Recently, two patients presented left ear hearing loss and episode of vertigo were diagnosed as left superior semicircular canal dehiscence in Otolaryngology Department, Fudan University, Shanghai, China. Both patients are female, in her 50's year old. One patient complained of vertigo which was able to induce by loud noise and valsal action, physical exam revealed a torsional nystagmus to left, audiometric test demonstrated low frequency dominated sensorineural hearing loss, acoustic reflex was not available in the left. Caloric test showed normal response in both ears. Temporal bone coronal CT scan with superior cannal reconstruction revealed 0.3 mm dehiscence in the left superior semicircular canal. This patient underwent superior

semicircular canal dehiscence repair, partial of her symptoms were relieved. The other lady showed left conductive hearing loss, hearing threshold (500, 1000, 2000, 3000 Hz) was 53 dB, no factor was identified to induced her attack of vertigo, acoustic reflex was not available in the left ear. Caloric test showed left ear alert. Temporal bone coronal CT scan with superior canal reconstruction revealed obvious dehiscence in the left superior semicircular canal. Surgical intervention was considering by her and her family.

**474 Amplitude of Head Movement During Target Acquisition in an Optic Flow Environment Is Reduced in Persons with Vestibular Dysfunction**  
**Susan Whitney<sup>1</sup>, Patrick Sparto<sup>1</sup>, Mark Redfern<sup>1</sup>, Joseph Furman<sup>1</sup>**

<sup>1</sup>University of Pittsburgh

**Introduction:** People with vestibular disorders often experience symptoms of disorientation when exposed to moving visual environments. This is particularly true when head movements are required concurrent with optic flow. The purpose of this study was to examine natural head movement behaviors in people with and without vestibular dysfunction while visually following moving targets.

**Methods:** Seven people with unilateral vestibular hypofunction (UVH) and 7 age- and gender-matched controls (CON) participated (age range 25-77; 3 men, 4 women per group). Subjects returned for 6 sessions; during each session, a different optic flow environment was used (differences consisted of changes in velocity and contrast). Seven tasks requiring movement of head and/or eyes were performed in each session. This abstract reports on 2 of these tasks: a 70 deg gaze shift in the yaw plane after following a target moving from 10 to 60 deg from midline, and a 90 deg gaze shift in the yaw plane, originating 40 or 50 deg from midline. Four or five gaze shifts were performed in each direction. Head motion was recorded using a 6 degree-of-freedom electromagnetic tracking system at a rate of 20 Hz. The amplitude of head yaw motion from the beginning to end of the target acquisition was computed. Repeated measurements ANOVA was performed in order to determine if there were differences in the amplitude of head yaw due to subject group or direction of motion for the 2 tasks.

**Results:** During the trial requiring 70 degree gaze shifts in the yaw plane, subjects with UVH had approximately 9 degrees less head yaw motion compared with CON ( $p = 0.025$ ). Subjects with UVH had 11 degrees less head yaw motion compared with CON during the trial requiring 90 deg gaze shifts; however, this difference was not significant due to greater variance in the head movements ( $p = 0.085$ ).

**Conclusion:** Persons with unilateral vestibular hypofunction use a different target acquisition strategy than normal individuals; this strategy of reduced head motion may be adaptive as a means to decrease symptoms and improve accuracy.

This project was supported in part by funding from the National Institutes of Health (R21 DC005372, K23 DC005384, K25 AG001049, P30 DC005205) and the Eye and Ear Foundation.

**475 Comparison of Simultaneous Electronystagmography vs. Infrared Video Nystagmography in a Clinical Computerized Vestibular Laboratory Patient Population**

**Judith White<sup>1</sup>, Stacy Weisend<sup>1</sup>, Melissa Drabo<sup>1</sup>**

<sup>1</sup>The Cleveland Clinic

**Background.** Infrared video nystagmography is a newer technology utilizing computerized oculographic image analysis to measure infrared recorded eye movements and nystagmus. Simultaneous recording of electrode and infrared video eye movements is possible by applying standard skin surface electronystagmography electrodes under the goggle system used for infrared recording. It is possible to compare the eye movements recorded simultaneously in the same individual.

**Objective.** This study examines the sensitivity of computerized infrared video nystagmography vs. simultaneous electronystagmography during the spontaneous nystagmus, positional and positioning tests as part of the computerized vestibular laboratory assessment of vestibular function in a patient care setting.

**Study Design.** Patients referred for vestibular laboratory function testing at a tertiary care vestibular center were enrolled in the study after informed consent was obtained. Ten consecutive patients were included. Simultaneous electrode and infrared video nystagmography were recorded, and testing was performed by a vestibular technician with over five years of experience with each system. Commercially available (Micromedical Technologies, Chatham, Ill) comparable vestibular laboratory software was used to analyze the nystagmus.

**Results.** Nystagmus was recorded more often by the infrared video nystagmography than with electronystagmography. Nystagmus slow phase velocity was higher using infrared video nystagmography. Since both systems use X-Y axis recording, torsional nystagmus is not analyzed accurately by either system in patients with benign paroxysmal positional vertigo.

**Conclusion.** Infrared video nystagmography was more sensitive than electronystagmography in the spontaneous, positional and positioning tests used as part of clinical laboratory vestibular testing in a group of ten patients. Torsional nystagmus is not analyzed well by either computer system, although infrared video recording allows for subsequent playback and human interpretation.

**476 Normative Data for Vestibular Evoked Myogenic Potentials Induced by Air- Or Bone-Conducted Tone Bursts**

**Dietmar Basta<sup>1</sup>, Ingo Todt<sup>1</sup>, Arne Ernst<sup>1</sup>**

<sup>1</sup>University of Berlin

The motor response of the vestibulocollic reflex (VCR) can be recorded as a vestibular evoked myogenic potential (VEMP) from different muscles of the neck (e. g. sternocleidomastoid muscle, trapezoid muscle) during high-level clicks or tone bursts, by mechanically tapping on the forehead or by galvanic stimulation. The response characteristics of acoustically elicited VEMP's largely depend on the stimuli applied. A tone-burst stimulation of 500 Hz seems to be clinically most appropriate because those VEMPs can be elicited at the lowest stimulus

intensity possible. Unfortunately no gender and age related normative data for tone-burst evoked VEMP's are available till now. The aim of the present paper was therefore to describe normative data for tone-burst evoked VEMPs.

VEMPs of 64 healthy subjects were recorded ipsilaterally during air- or bone-conducted tone burst stimulation. The EMG of the tonically activated sternocleidomastoid muscle was recorded by surface electrodes. Averages were taken for the tonic muscle activity, P1/N1-latencies and amplitudes of male and female volunteers within 3 different age groups.

The latencies did not show any significant differences between female and male volunteers or between air- and bone-conducted stimulation. The latencies did also not show any significant difference among the three age groups. The limits for normal latencies (mean + 2 SD) are therefore 20.3 ms for P1 and 28.0 ms for N1. There was a clear age dependend relation between tonic muscle activity and VEMP-amplitude.

The present findings strongly suggest the evaluation of VEMP latencies and amplitudes by using normative values obtained exactly with the same stimulus parameters.

Normative data as described in the present study are required to detect isolated saccular defects which are indicative of a vestibular disorder.

Supported by the Sonnenfeld Foundation, Germany

#### **477 Test Positions in Vestibular Evoked Myogenic Potentials**

**Brandon Isaacson<sup>1</sup>**, Emily Murphy<sup>1</sup>, Helen Cohen<sup>1</sup>

<sup>1</sup>*Baylor College of Medicine*

The test, vestibular evoked myogenic potentials (VEMP), is usually performed with the patient in the supine lying position with the nose midline and the neck flexed. The response depends on the level of sternocleidomastoid contraction. To develop a paradigm to increase SCM contraction during stimulation we tested three head positions: the standard position, supine lying with head turned contralaterally to the stimulus and neck flexed, and sitting with head turned contralateral to the stimulus. Because some patients with middle ear dysfunction show no VEMP response to air-conducted sound normals and bilaterally impaired patients were also tested with the position yielding the strongest response to air- conducted sound, but using a bone conduction transducer. Preliminary results suggest that the most efficacious test position is supine lying with the head turned contralateral to the stimulus and the neck flexed.

#### **478 Vestibular Evoked Myogenic Potential (VEMP) in Meniere Patients with Drop Attacks**

**Ferdinand C.A. Timmer<sup>1</sup>**, Guangwei Zhou<sup>2</sup>, John J. Guinan, Jr.<sup>3,4</sup>, Sharon G. Kujawa<sup>2,4</sup>, Barbara S. Herrmann<sup>2,4</sup>, **Steven D. Rauch<sup>4,5</sup>**

<sup>1</sup>*Academic Medical Center*, <sup>2</sup>*Audiology Dept., Mass. Eye and Ear Infirmary*, <sup>3</sup>*Eaton-Peabody Laboratory, Mass. Eye & Ear Infirmary*, <sup>4</sup>*Harvard Medical School*, <sup>5</sup>*Otolaryngology Dept., Mass. Eye and Ear Infirmary*

The Vestibular Evoked Myogenic Potential (VEMP) is an inhibitory sacculo-collic reflex recorded in the ipsilateral

sternocleidomastoid muscle in response to acoustic stimulation of the saccule. We have shown previously that patients with Meniere's disease have poorer VEMP thresholds and altered VEMP tuning compared to normal subjects [Rauch et al. 2004]. We have interpreted these findings as evidence that changes in the VEMP are indicators of saccular hydrops. In this study we tested the hypothesis that VEMP thresholds are more often elevated or absent in Meniere patients experiencing Tumarkin drop attacks than in other patients suffering Meniere's disease. We compared VEMP thresholds (250, 500, 1000 Hz) and frequency tuning in otologically normal subjects (n=12) to those recorded for affected and unaffected ears of patients with unilateral Meniere's disease patients by AAO-HNS (1995) diagnostic criteria with (n=12) and without (n=82) Tumarkin drop attacks. VEMP responses were present at all frequencies in both ears of all normal subjects. The response showed tuning in the frequency domain, with best thresholds at 500 Hz. In unaffected ears of unilateral Meniere patients, VEMPs were undetectable in 13% of measurements attempted. This number rose to 18% in affected ears of unilateral Meniere patients and to 41% in Meniere ears suffering Tumarkin drop attacks. Frequency tuning of the VEMP response was less well defined and shifted to a higher frequency (1000 Hz) in Meniere ears.

There was a gradient of threshold elevation and altered tuning that corresponded to the gradient of worsening disease. Our findings support the hypothesis that Tumarkin drop attacks arise from advanced disease involving the saccule and that VEMP may be a clinically valuable metric of disease severity or progression in Meniere patients.

(Supported by NIH NIDCD Grant RO1 DC04425)

#### **479 Vestibular Evoked Myogenic Potential (VEMP) in Cases of Contralateral Unilateral Vestibular Deafferentation**

Guangwei Zhou<sup>1</sup>, Barbara S. Herrmann<sup>1,2</sup>, John J. Guinan, Jr.<sup>2,3</sup>, Sharon G. Kujawa<sup>1,2</sup>, **Steven D. Rauch<sup>2,4</sup>**

<sup>1</sup>*Audiology Dept., Mass. Eye and Ear Infirmary*, <sup>2</sup>*Harvard Medical School*, <sup>3</sup>*Eaton-Peabody Laboratory, Mass. Eye & Ear Infirmary*, <sup>4</sup>*Otolaryngology Dept., Mass. Eye and Ear Infirmary*

We have shown previously [Rauch et al. 2004] that approximately one third of asymptomatic ears of unilateral Meniere patients have changes in VEMP threshold and frequency tuning that are similar to those seen in symptomatic Meniere ears. There are two possible explanations for this observation: (1) a subset of asymptomatic ears has developed asymptomatic saccular hydrops and the VEMP is sensitive to these changes; or (2) the measured VEMP response is due to bilatera inputs such that relative deafferentation of one ear from advanced Meniere's disease leads to an altered VEMP response recorded from the unaffected side. We undertook to differentiate these two possibilities by measuring VEMP in the healthy ear of patients who had undergone unilateral vestibular deafferentation by surgical resection of vestibular schwannoma of their contralateral ears. We hypothesized that, if there are binaural inputs to

the VEMP response, VEMP recordings from the healthy ears of our schwannoma patients should show "Meniere-like" changes in threshold and frequency tuning. Conversely, if the VEMP is truly a single-side ipsilateral reflex, then deafferentation of one side should not affect the other side and the schwannoma patients should exhibit normal VEMPs. VEMPs were recorded from otologically-normal subjects, symptomatic and asymptomatic ears of unilateral Meniere patients, and healthy ears of unilateral vestibular schwannoma patients. VEMPs recorded from the healthy ears of the schwannoma patients were most similar in threshold and frequency tuning to those recorded from our normal subjects. We interpret these data to support the hypothesis that the VEMP is a unilateral reflex that, in unilateral Meniere's disease, is sensitive to asymptomatic saccular hydrops. This finding raises the exciting prospect of a clinically useful detector of presymptomatic inner ear changes in Meniere's disease. (Supported by NIH NIDCD Grant RO1 04425)

#### **480 The Meaning of Specific Autoimmune Antibodies in Occurrence and Prognosis of Acute Inner Ear Disorders**

**Kerstin Ratzlaff<sup>1</sup>, Mark Praetorius<sup>1</sup>, Reinhild Klein<sup>2</sup>, Peter K. Plinkert<sup>1</sup>**

<sup>1</sup>University of Heidelberg, <sup>2</sup>University of Tuebingen

Introduction:

By now the exact pathogenesis of the different forms of acute inner ear disorders like sensorineural hearing loss, sudden deafness, tinnitus and Meniere's disease is still unknown.

Disorders of inner ear blood circulation are widely discussed just like viral infections and autoimmune processes. The aim of this study is to examine specific autoimmune antibodies and their function in occurrence, therapy and prognosis of acute inner ear disorder.

Material and Methods:

Prospective clinical study with n=40 patients, among 12 female and 28 male, suffering from acute inner ear disorder without any known autoimmune disease. Average age 47.6 years. Patients underwent a therapy consisting of steroids and rheologica. Hearing was examined regularly using pure-tone audiometry. Specific autoimmune antibodies were examined at the beginning and at the end of the therapy using enzyme-linked-immunosorbent assay and immuno-fluorescence-test.

Results:

In 71% of all patients there was an occurrence of autoimmune antibodies, in 29% no autoimmune process could be provided. Antibodies against sarcolemma (ASA) and sinusoids were mostly detected (23%), followed by anti-nuclei-antibodies (ANA; 16%), antibodies against Microsomes, Phospholipids, Laminin (6.5% each), and anti-Endothelium and anti-Smooth muscle antibodies (3.2%). Hearing improvement after therapy was significantly higher in patients being negative in autoimmune antibodies compared to the positive ones.

Conclusion:

As described before we do also agree in our study that occurrence of autoimmune antibodies should be considered as one possible mechanism in the pathogenesis of acute inner ear disease. These findings do not affect the choice of therapeutic treatment.

More likely, the clinical value seems to be found especially in regard to the prognosis of disease. Studies going in depth with these findings are continued.

#### **481 Prednisolone Improvement of Cochlear Function in Mice with Chronic Otitis Media**

**Dennis Trune<sup>1</sup>, Beth Kempton<sup>1</sup>, Carol MacArthur<sup>1</sup>**

<sup>1</sup>Oregon Health & Science University

C3H/HeJ mice possess a gene defect in their TLR4 receptor that renders them unable to respond to gram-negative infections. As a result, approximately 50% develop spontaneous chronic otitis media (COM). Because the inner ear is at risk in COM, mice were evaluated to determine the impact of middle ear disease on the inner ear. Also, mice with unilateral COM were treated with glucocorticoids to determine if such steroid treatments can control either middle or inner ear pathology. Eight C3H/HeJ mice with unilateral chronic otitis media (7-12 months) were treated for 5 weeks with oral Prednisolone (10 mg/kg). Untreated mice served as controls. ABR thresholds were measured before and after treatment and histologic examination was made of middle ear and inner ear pathology. The untreated mice ears showed worsening ABR thresholds. Two of the originally clear middle ears developed OM. Inner ear disease was seen ipsilateral to two out of three OM ears and two of the originally clear middle ears. Of the 8 animals that received steroids, ears with OM (3/8) had improved ABR thresholds and 4/8 clear middle ears showed ABR improvement. All 8 middle ears clear at the onset of treatment were still clear, but 3/8 had cochlear disease in the absence of COM. Of the 8 ears with prior OM, only 1/8 cleared the middle ear infiltrate, but 6/7 had clear inner ears. Inner ear inflammation was not seen in any of the prednisone-treated ears that improved their ABR thresholds. This study demonstrated there is significant inner ear disease with COM, both ipsilateral and contralateral to the diseased middle ear. Prednisolone treatment appears to improve hearing in these animals, whether they had ME disease or not, suggesting a direct effect on inner ear inflammation.

(NIDCD R01 DC05593 and P30 DC005983, and VA RR&D NCRAR C2659C)

#### **482 Ovariectomy Prevents Hearing Loss in Autoimmune Mice**

**Dennis Trune<sup>1</sup>, Beth Kempton<sup>1</sup>, Karen Fong<sup>1</sup>**

<sup>1</sup>Oregon Health & Science University

The mechanisms of autoimmune inner ear disease are poorly understood. The incidence of autoimmune hearing loss in women is twice that of men, paralleling the greater proportion of women who suffer from systemic autoimmune diseases, such as lupus or multiple sclerosis. One current theory is that estrogen stimulates the immune system, leading to overproduction of self-recognizing

antibodies to cause systemic autoimmune disease. It has been shown that estrogen removal by ovariectomy suppresses systemic disease symptoms in autoimmune mice. Previous studies from this laboratory (Trune & Kempton, *Hear. Res.* 167:170-4, 2002) showed female autoimmune mice have worse hearing than males. Therefore, this mouse strain was studied to determine the potential role of estrogen in autoimmune inner ear disease. Systemic autoimmune disease and hearing loss begin at 3-4 months. Therefore, female mice were ovariectomized at two months of age to determine the impact of estrogen loss on hearing levels during the progression of systemic disease. Hearing thresholds were compared to unoperated autoimmune mice. ABR thresholds at 32 kHz progressively rose in unoperated mice, reaching a 20 dB loss at 5 months and 30 dB loss by 7 months. The ovariectomized mice did not demonstrate any threshold shift from baseline until 7 months, which was only 9 dB. Statistical comparison of the threshold shifts showed the two groups were different at all ages of comparison. Serum immune complexes also rose more slowly in the ovariectomized mice, lagging the development of systemic disease normally seen. These results demonstrate that estrogen may be a significant factor in the progression of autoimmune inner ear disease. Ongoing studies are being conducted to determine the effects of estrogen on inflammatory gene expression in the ear.

NIH-NIDCD R01 DC05593 and P30 DC005983, and the VA RR&D NCRAR C2659C.

#### **483 Steroid Control of Cochlear Inflammatory Factors in Autoimmune Inner Ear Disease**

**Dennis Trune<sup>1</sup>**, Beth Kempton<sup>1</sup>, Jacqueline DeGagne<sup>1</sup>, Christopher Hargunani<sup>1</sup>

<sup>1</sup>*Oregon Health & Science University*

Sensorineural hearing loss occurs with systemic inflammation, although the mechanisms causing cochlear damage are unknown. Such disorders include bacterial and viral labyrinthitis, autoimmune inner ear disease, and otitis media, as well as some cases of Meniere's disease and sudden hearing loss. Glucocorticoid therapy is presumably effective because it suppresses cochlear inflammatory processes, but this has never been directly demonstrated. These steroids suppress the immune system by preventing activation of NF- $\kappa$ B, a transcription factor that causes expression of numerous pro-inflammatory cytokines and enzymes. To better understand the role of these inflammatory processes, cochleas from autoimmune disease and normal mice were evaluated for the presence of the NF- $\kappa$ B transcription factor and some of the inflammatory products it controls, such as immunoglobulin (IgG), vascular endothelial growth factor (VEGF) and inducible nitric oxide synthase (iNOS). Mice also were treated with the glucocorticoid prednisolone to determine if directly suppresses such inflammatory gene expression in the cochlea. Following treatment with oral prednisolone for 2 months, cochleas were removed for immunohistochemical detection of NF- $\kappa$ B, iNOS, IgG, and VEGF. Additional cochleas were used for ELISA determination of activated NF- $\kappa$ B levels. All

inflammatory factors were observed in the cochlea and staining was stronger in the autoimmune mice. Steroid treatment reduced the intensity of their staining and ELISA showed reduction of activated NF- $\kappa$ B. These findings suggest a number of significant inflammatory processes occur within cochlear tissues during autoimmune inner ear disease. Furthermore, the transcription factor NF- $\kappa$ B that drives their gene expression is suppressed in cochlear tissues by oral steroid treatments.

(NIH-NIDCD R01 DC05593 and P30 DC005983, and the VA RR&D NCRAR C2659C)

#### **484 Cytokine-Mediated Strial Pathology**

**Michael Ruckenstein<sup>1</sup>**, Jeffrey Bedrosian<sup>1</sup>, Michael Anne Gratton<sup>1</sup>

<sup>1</sup>*University of Pennsylvania*

Murine models of Lupus have demonstrated idiopathic degeneration of the intermediate cell layer of the stria vascularis. This pathology is analogous to that seen in models of noise-induced hearing loss and ototoxicity. Free radical formation is felt to be the mediator of the stria pathology in these latter forms of cochlear pathology. If free radical formation is responsible for the stria degeneration observed in Lupus mice, the trigger for the formation of these cytotoxic mediators is unclear. We hypothesize that elevated levels of circulating cytokines may be responsible for triggering the stria pathology in Lupus mice. Female MRL-Fas<sup>lpr</sup> mice were observed for the development of cochlear pathology as evidenced by elevations in ABR thresholds, and systemic pathology (as evidenced by proteinuria). Animals were sacrificed, their serum sampled, and their cochleas fixed for immunohistology and transmission electron microscopy. Ultrastructural analysis confirmed the presence of stria degeneration. Serum samples demonstrated elevations in cytokines, specifically TNF $\alpha$ . Immunohistologic analysis revealed specific changes in stria cytokines and cytokine receptors. The implications of these findings are discussed in relation to the pathogenesis of stria pathology in Lupus mice.

#### **485 Endolabyrinthitis Following Perinatal Murine Cytomegalovirus (MCMV) Infection in SCID Mice**

**Nigel Woolf<sup>1,2</sup>**, Dawn Jaquish<sup>1,2</sup>, Anuradha Desai<sup>1</sup>, Fred Koehn<sup>1,2</sup>

<sup>1</sup>*UCSD Medical School*, <sup>2</sup>*Veterans Administration Medical Center San Diego*

Cytomegalovirus (CMV) is the leading cause of human congenital viral infection and the major source of human nonhereditary congenital deafness. Notably, at birth 90% of human CMV (HCMV) congenitally infected neonates have no clinical signs, but up to 15% of these asymptomatic infants later develop sensorineural hearing loss (SNHL). Perinatal HCMV infections may also cause SNHL, but a direct relationship between perinatal HCMV infection and the postnatal development of SNHL has not yet been established. Since CMV strains are species-specific, HCMV cannot be used in animal models. However, murine CMV (MCMV) infection in mice provides

a useful model for HCMV infections, and we have established that SCID (severe combined immunodeficient) mice are highly susceptible to both congenital and perinatal MCMV infections. Following intraperitoneal injection at birth (P0) with 0.01 PFU of a recombinant Smith strain MCMV expressing an EGFP reporter gene (rMCMV a gift from Drs. Stanley Henry and John Hamilton: Henry et al., J Virol Meth 89:61, 2000), 0% of P7 and 94.1% of P14 neonates developed rMCMV inner ear infections. rMCMV infection was visualized in the cochlea at P14 by EGFP expression in stria vascularis, spiral ligament, Reissner's membrane, endosteal lining cells scala tympani and scala vestibuli, and spiral ganglion and vestibular ganglion neurons. In marked contrast with the development of rMCMV endolabyrinthitis following perinatal infection, SCID mice infected either in utero or at older postnatal ages developed only rMCMV perilyabyrinthitis. In the P14 brain, perinatal rMCMV infection correlated with abnormal postnatal neuronal migration patterns and significant changes in cerebral expression of multiple pro-inflammatory cytokines, chemokines, and their receptors. Our data confirmed for the first time that, for a brief period during postnatal development, rMCMV infection in SCID mice induces an endolabyrinthitis resembling HCMV congenital inner ear infections in humans.

Supported by NIH DC00386 and DC02666, and the VA Research Service.

#### **486 Characterization of Immune Response in $\beta$ -Tubulin Induced Murine Autoimmune Hearing Loss**

**Chun Cai<sup>1</sup>**, Bin Zhou<sup>1</sup>, Jonathon Glickstein<sup>1</sup>, Tai June Yoo<sup>1</sup>

<sup>1</sup>University of Tennessee

The main feature of autoimmune disease such as autoimmune inner ear disease including Meniere's disease is the development and persistence of inflammatory processes in the apparent absence of pathogens, leading to destruction of the target tissues. Western blot analysis has shown that 59% of Meniere's disease patients produce antibodies to a 55 kD inner ear membranous and neural protein identified to be  $\beta$ -tubulin. Hearing loss in mice can be induced by immunization with  $\beta$ -tubulin using ABR and DPOAE recorder and spiral ganglion as well as hair cells damages can be observed by morphological study of temporal bones. But the precise immunological mechanism of inner ear disease remains obscure.

In the current study, BALB/c mice were subcutaneously injected with  $\beta$ -tubulin in dosage of 100, 200 and 300 ug with CFA per mouse, immunizations were boosted in IFA with varying doses of tubulin twice at one-week intervals. Control mice underwent subcutaneous injection of PBS and CFA/IFA as well. After 2 weeks of last boosting, we have found that the antibodies activity to  $\beta$ -tubulin increased in dose dependent compared with controls, all control subjects were relatively unresponsive. Moreover, IFN- $\gamma$  level was markedly increased in both serum and supernatant of lymphocytes, protein levels of, IL-4, IL-5 IL-10 and IL-13 were significantly reduced following  $\beta$ -tubulin

immunization. Interestingly, flow cytometric analysis of spleen cells from  $\beta$ -tubulin induced mice and control mice have been showed that 2.72% of total splenocytes in control mice were CD25+CD4+ regulatory T cells (Treg cells), the population of Treg cells was reduced in  $\beta$ -tubulin induced mice and followed dose dependent (such as 1.68% in 300 $\mu$ g, 2.16% in 200  $\mu$ g and 2.19% in 100  $\mu$ g), the Treg cells in naive mice is 2.6%. Moreover, IFN- $\gamma$  and IL-2 level was markedly increased in supernatant of Treg cells culture, protein levels of IL-4, IL-5, IL-10, and IL-13 were significantly reduced following  $\beta$ -tubulin immunization.

Thus, these data indicate an immune reactivity against  $\beta$ -tubulin, which might be responsible for the autoimmune inner ear hearing loss. The further study is required to elucidate the role of CD25+CD4+ T cells in the pathogenesis of this disease, which would eventually result in better therapy.

#### **487 Oral Administration of Low Dose $\beta$ -Tubulin Decreases Autoimmune Hearing Loss Lesion in the Mice**

**Qing Cai<sup>1</sup>**, Tai June Yoo<sup>1</sup>

<sup>1</sup>Medicine

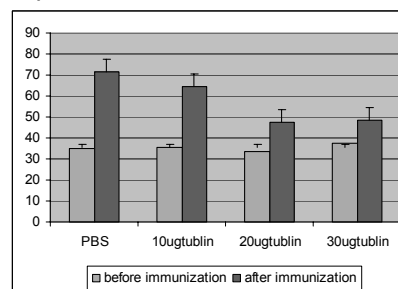
**Background:** Induction of peripheral tolerance by oral administration of antigen has been applied to the treatment of autoimmune disease such as rheumatoid arthritis. Oral tolerance to low dose  $\beta$ -tubulin is an effective antigen-specific method to suppress experimental autoimmune hearing loss. We investigated the changes of cytokine level in  $\beta$ -tubulin induced autoimmune hearing loss in mice: INF- $\gamma$ , IL-2, IL-6, IL-10 and TGF- $\beta$ .

**Method:** 20 mice were divided into 4 groups at random, one group of mice were fed with PBS as control, and the other 3 group were fed with 10 $\mu$ g, 20  $\mu$ g or 30  $\mu$ g of tubulin respectively, then they were immunized by  $\beta$ -tubulin. Before and after immunization, the hearing thresholds were measured by ABR and DPOAE.

**Result:** The PBS-fed mice were found to have severe hearing loss, but the hearing of the 20  $\mu$ g and 30  $\mu$ g  $\beta$ -tubulin fed mice were protected effectively and the threshold were much better than that of the PBS-fed mice.

The sera collected from each mouse at 3, 5 and 7 weeks after primary immunization were used to cytokine analysis by ELISA. And spleen cells are cultured and the histology of temporal bones are being examined.

**Conclusion:** These results suggest that protection from autoimmune hearing loss by oral administration of minute amounts of  $\beta$ -tubulin are observed. Therefore, this oral tolerance can be used to treat the autoimmune hearing loss in human patients.





#### **488** Course of Hearing Loss Promotes the Occurrence of Tinnitus

Ovidiu Koenig<sup>1</sup>, Roland Schaette<sup>2</sup>, Richard Kemper<sup>2</sup>, Manfred Gross<sup>1</sup>

<sup>1</sup>Charité - Universitätsmedizin Berlin, <sup>2</sup>Institute for Theoretical Biology, Humboldt University Berlin

Chronic tinnitus is very often accompanied by a hearing impairment, but it is still unknown whether hearing loss actually causes tinnitus.

We investigated the hypothesis that the development of tinnitus after hearing loss depends on the course of the audiogram. Earlier studies on the subject suffered from patient samples with mixed etiologies of hearing loss, which may have lead to inconclusive findings. We therefore analyzed a sample where all patients have noise-induced hearing loss, containing 30 patients without tinnitus, 26 patients with tone-like tinnitus, and 17 patients with noise-like tinnitus. The groups did not differ significantly in age.

All patients had moderate to severe hearing loss at high frequencies, and most had only minor hearing loss at low frequencies. We found that the three groups differ in the overall amount of hearing loss and in the steepness of the slope of the audiogram. On average, patients without tinnitus had the most severe hearing loss and the most shallow audiogram slopes, whereas patients with tone-like tinnitus had the least amount of hearing loss and the steepest slopes in the audiograms. Patients with noise-like tinnitus were intermediate. The differences in the maximum steepness between each of the tinnitus groups and the no-tinnitus group were significant ( $p=0.02$  for noise-like tinnitus and  $p=0.006$  for tone-like tinnitus). Moreover, there was a correlation between the tinnitus pitch and the edge of the audiogram for tone-like tinnitus, with tinnitus pitch being on average 1.6 octaves above the audiogram edge frequency, and 0.7 octaves above the frequency with the steepest slope.

Our results suggest that the development of tinnitus could be facilitated by a steep audiogram slope. A possible mechanism is that the steep slope causes abrupt discontinuities in the activity along the tonotopic axis of the auditory system, which could be misinterpreted as sound.

#### **489** The Effect of Intravenously Administered Mexiletine on Tinnitus - A Pilot Study

Erik Berninger<sup>1</sup>, Jan Nordmark<sup>1</sup>, Gunnar Alván<sup>2</sup>, Kjell K. Karlsson<sup>1</sup>, Esma Idrizbegovic<sup>1</sup>, Lennart Meurling<sup>1</sup>, Ayman Al-Shurbaji<sup>1</sup>

<sup>1</sup>Karolinska Institute, Stockholm, <sup>2</sup>Medical Products Agency, Uppsala

The effect of intravenously administered mexiletine on subjective tinnitus and hearing was studied in six patients, who initially responded positively to lidocaine. Distinct mexiletine-induced decreases in tinnitus loudness were demonstrated in three subjects, as reflected by maximum VAS (visual analogue scale) level reduction of 34, 95, and 100%, respectively. One subject reported change in tinnitus pitch, another one showed a slight (18% on VAS) tinnitus reduction and one subject disclosed no effect. Side effects were seen only during one of seven infusions.

Mexiletine induced shifts in pure-tone threshold, transient evoked otoacoustic emission, and acoustic reflex threshold, probably reflecting a reversible interference in the function of organ of Corti. The concentration effect relationship remained unclear and no general "therapeutic" level could be identified. This study confirms the effect of mexiletine on the auditory function and its potential as a possible therapeutic agent or a model for further development in tinnitus pharmacotherapy.

#### **490** Contribution to Tinnitus Severity by Subconscious Versus Conscious Factors

Pawel Jastreboff<sup>1</sup>, Margaret Jastreboff<sup>2</sup>

<sup>1</sup>Emory University, <sup>2</sup>Towson University

Introduction: There is a common assumption that tinnitus can be a problem only when it is perceived. The neurophysiological model of tinnitus postulates that the subconscious path, linking the auditory with the limbic and autonomic nervous systems, might be at least as important as the conscious, cognitive loop. To assess the relative importance of these loops to tinnitus severity, an analysis of the contribution of a variety of measures linked predominantly to conscious and subconscious factors was performed. Tinnitus Handicap Inventory (THI) was used as the measure of tinnitus severity. Questions from form developed for the structured initial and follow-up interviews were used to evaluate various components contributing to tinnitus severity.

Method: Over 500 patients were evaluated before and during TRT treatment utilizing THI and structured interviews. Patients were asked to provide, retrospectively as an average for the last month, an estimate of a variety of measures including % time when aware of tinnitus, % time when annoyed by tinnitus, and on scale 0 to 10 the level of tinnitus annoyance, subjectively judged loudness, and impact on life. Multidimensional regression analysis was performed utilizing THI as a dependent variable and questions from the structured interviews as independent variables.

Results: The regression analysis revealed that the information contained in structured interviews allows for predicting total THI score in a highly statistically significant manner. While other variables were significant, notably, neither subjectively judged loudness of tinnitus nor proportion of time when patients are aware of it were significantly contributing to THI score, supporting the postulate that subconscious pathways play a dominant role in tinnitus severity.

Conclusions: These results support the postulate that the subconscious connections are dominant for severity of chronic, clinically significant tinnitus.

#### **491** THI Improvement of the Severely Handicapped Tinnitus Patients Treated with Tinnitus Retraining Therapy

Isamu Yuge<sup>1</sup>, Kaoru Ogawa<sup>1</sup>, Minako Satou<sup>1</sup>, Seiichi Shinden<sup>1,2</sup>, Akihiro Kurita<sup>1</sup>, Sho Kanzaki<sup>1</sup>

<sup>1</sup>Keio Uni. School of Medicine, <sup>2</sup>Saiseikai Utunomiya Hospital

Tinnitus retraining therapy (TRT) introduced by P.J. Jastreboff has its aim on inducing and facilitating

habituation by the patient to her or his tinnitus. Two components addresses a different aspect of habituation, one is directive counseling that is a structured educational program designed to remove anxieties and another is sound therapy that is a long-term use of constant low-level sound to promote habituation. Sound therapy is proposed to be administered by using one of the following modalities that is sound generator, environmental sound enrichment or hearing aids, according to the status of the patient.

Our study was performed to retrospectively evaluate the outcome of the treatment of each sound therapy modalities in the early phase of TRT using the repetitive test of Tinnitus Handicap Inventory (THI). Since Nov., 2004 until March, 2005, 145 tinnitus patients were registered in the institution and 94 patients of these has repeatedly examined. The number of severely handicapped cases was 48, 24 for the sound generator treatment and 24 for the environmental sound enrichment therapy. After the 4 month of administration period, improvement was achieved in 62.5% of cases with the sound generator and in 58.3% of cases with the environmental sound enrichment. Although THI score improvements were significant in each groups, pre-and post-treatment score variations had not been significantly different between the two modalities. According to the results, each one of the sound therapy modality could be selected to the severely handicapped patients with the expectancy of improvement rate not significantly different, although the study needs follow up re-examination.

#### **[492] Open Ear Hearing Aid Amplification in Tinnitus Therapy**

**Luca Del Bo**<sup>1</sup>, Emanuela Domenichetti<sup>2</sup>, Matteo Bettinelli<sup>2</sup>, Enrico Fagnani<sup>3</sup>, Umberto Ambrosetti<sup>3</sup>, Alberto Scotti<sup>4</sup>

<sup>1</sup>Fondazione Ascolta e vivi, Italia, <sup>2</sup>Del Bo srl, Milan Italy,

<sup>3</sup>Fondazione Ospedale Policlinico Milano Italia, <sup>4</sup>Ospedale S. Paolo Milano Italia

**Background:** ry often tinnitus patients have a hearing loss limited to f>2 kHz; open ear hearing instruments (HI) can deliver a good gain in HF band (2-6 kHz); open ear HI doesn't introduce any insertion loss so the listening is very "transparent". Tinnitus pitch frequently is in 3 - 8 kHz area, so we can postulate that an open ear hearing instruments could deliver: a selective HF sound enrichment; a sound stimulation in high frequencies. Aim of this investigation is to assess the efficacy of tinnitus treatment after few month of TRT with open ear hearing instruments

**Methods:** 20 patients who came to our clinic and met the following requirements were recruited: tinnitus associated or not associated with hyperacusis; tinnitus associated with ski slope o mild hearing loss; disabling tinnitus (patients falling in category 0 according to Jastreboff cat. were excluded); regular follow up visits; open ear hearing instruments Gn Resound Air and Widex Elan Diva were used. For the assessment of the efficacy of tinnitus treatment with open ear hearing instruments we have collected data through Jastreboff questionnaires and Tinnitus Handicap Inventory Questionnaire (THI) presented upon the first visit and at the follow-up visit after a mean value of 4.55 months (SD= 2,61).

**Results:** Patients reported a very good comfort, an improvement of high pitch sounds detection and, in many

cases, a sudden decrease of tinnitus perception. Patients appreciate "transparency" and clarity of amplification. The following results are collected: THI questionnaire; Initial THI: 46,4; Final THI: 22,8; Tinnitus effect on the life (Jastreboff questionnaire 0-10 scale); Initial: 5.5; Final: 2.5. *Results will be presented in details.*

**Conclusion:** Open ear HI could be an effective device for sound enrichment in TRT in mild and ski slope hearing loss; open ear HI could substitute custom sound generators.

#### **[493] Auditory Behavioral and Evoked Potential Measures in Migraine Headache Sufferers Between Attacks**

**Kamakshi Gopal**<sup>1</sup>, Johanna Allport<sup>1</sup>, Mandi Baldrige<sup>1</sup>

<sup>1</sup>University of North Texas

Neurotologic symptoms are not uncommon among migraine headache sufferers. Most auditory-related complaints of migraineurs, even between migraine attacks, include increased sensitivity to sounds, difficulty processing auditory information, and hearing loss. The goal of the study was to identify if inherent differences existed in auditory measures between migraineurs not experiencing any migraine symptoms for at least a week before testing, and normal controls. Additionally, the study also intended to identify if asymmetries existed between the ears in any auditory-related behavioral or evoked potential measure. The migraine group consisted of ten female adult subjects with a history of frequent migraine headaches in the past five years. These subjects were, however, not on any prophylactic anti-migraine treatment at the time of testing. The control group consisted of ten adult female subjects with no history of migraine related disorders. Results obtained on pure-tone audiometry and immittance audiometry indicated no differences between the two groups. With auditory evoked potential measures, however, differences were observed between the groups in amplitude growth from 40 to 80 dB nHL for ABR peak V and MLR peak Na. The migraine group exhibited a more pronounced amplitude growth in both ears compared to the control group, but statistical significance was found only for the right ear. Although the mean composite scores on the SCAN-A test (a screening test of auditory processing) were within normal limits for both groups, the migraine group exhibited an overall lower mean score, and a significantly poorer score on the competing sentences subtest. It is speculated that subtle but permanent abnormalities of central auditory system may exist among the migraineurs affecting their information processing capabilities.

#### **[494] Menière's – Migraine Overlap Syndrome**

**Borka Ceranic**<sup>1</sup>, Linda Luxon<sup>2</sup>

<sup>1</sup>Department of Audiology, St. George's Hospital, London,

<sup>2</sup>Department of Neuro-otology, The Hospital for Neurology & Neurosurgery, London

Menière's disease (MD) is a clinical entity with manifestations of a dysfunctional labyrinth. Co-morbidity with migraine has been observed in a large proportion of patients and similar symptoms may occur in either condition, justifying the description "migraine of the inner ear", sometimes used for MD.

The aim of this study was to explore clinical, mainly auditory manifestations in patients affected by both MD and migraine.

Of 120 patients with MD, 65% (n=78) were affected by migraine in their lifetime and an additional 17% (n=15) had a family history of migraine, but did not suffer migrainous symptoms. A detailed clinical history and site-of-lesion auditory assessment (pure tone audiometry, otoacoustic emissions, stapedial reflexes and auditory brainstem evoked responses) were obtained in all patients (n=93).

In all patients, migraine preceded MD and in 73% an exacerbation of MD symptoms coincided with an exacerbation of migraine. In 82% of patients with haemicranial headache, MD occurred on the same side, or was worse in those with a bilateral presentation. During the acute stage of MD, 78% of patients reported oversensitivity to environmental sounds, while 42% complained of otalgia/facial pain or facial hyperaesthesia.

The maximum recorded hearing loss was 60-70 dBHL of a flat configuration and the stapedial reflexes were recorded in 95% of patients, suggesting that an almost exclusive lesion of the cochlear outer hair cells is the main pathophysiological alteration in these patients.

The possibility that MD and migraine may have a common background has been considered. This may have important implications for pharmacological treatment of MD associated with migraine.

#### **[495] Right-Left Difference in the Sensitivity of High Frequency Sounds**

**Tadashi Nishimura<sup>1</sup>, Takefumi Sakaguchi<sup>1</sup>, Hiroshi Hosoi<sup>1</sup>**

<sup>1</sup>Nara Medical University

Standard pure-tone audiometry is performed using frequencies  $\leq 8$  kHz. However, human hearing allows perception of higher frequency sounds. In some disorders causing hearing loss (age-related, noise-induced, or toxic deafness), hearing loss generally starts at high frequencies. Therefore, audiometry in the high-frequency range may be useful for the early detection of these disorders. To evaluate the clinical applicability of high-frequency audiometry, we performed audiometry in the high-frequency range in 128 ears showing a hearing threshold of  $< 30$  dB HL in standard pure-tone audiometry. As a result, high-frequency hearing depended on frequency and age. Marked dispersion of hearing threshold values was observed, particularly around the frequency showing an acute increase in the threshold. However, the right-left difference in the hearing threshold was slight in the same subjects and did not depend on frequency or age. These results suggest the usefulness of high-frequency audiometry for evaluating unilateral hearing impairment.

#### **[496] Changes in Speech Production in a Prelingually Deafened Adult Cochlear Implant User**

**Patrick Wong<sup>1</sup>, Arth Srivastava<sup>2</sup>**

<sup>1</sup>Northwestern University, <sup>2</sup>Illinois Mathematics & Science Academy

The current study is a first study reporting the speech production characteristics of a prelingually deafened adult

cochlear implant (CI) user after a course of speech-language treatment. The participant is culturally deaf and received the CI at the age of 43 years. A 24-week ABCABC single-subject treatment program was conducted addressing articulation, grapheme-phoneme conversion (printed word pronunciation), and voice production, with two four-week segments for each area. Treatment-specific progress, revealed by independent probes, was made in areas of articulation and grapheme-phoneme conversion, but not voice production. Formal measures also confirmed her progress. These results were discussed in relation to how long-term reduction of general auditory input and under-use of the speech production mechanisms can be remediated by technological and behavioral treatment.

#### **[497] Japanese Phoneme Recognition of Profoundly Deaf**

**Takefumi Sakaguchi<sup>1</sup>, Tadashi Nishimura<sup>1</sup>, Yoshiaki Watanabe<sup>2</sup>, Hiroshi Hosoi<sup>1</sup>**

<sup>1</sup>Department of Otorhinolaryngology, Nara Medical University, <sup>2</sup>Department of Electronics, Doshisha University

Although speech recognition test are usually examined in Japanese clinics using a "Japanese monosyllable list 67-S", which is authorized by the Japanese Audiological Society, only numerical scores of the test are usually focused on and, in most cases, the speech confusion analysis is not performed in order to know how and why patients fail to perceive certain sounds.

In this study, we have designed experiments to evaluate the speech confusion characteristics of the severely hearing-impaired patients using "confusion maps".

A Speech recognition tests were carried out in a sound-proof chamber using Japanese phonemes database (NTT-AT) with profoundly deaf persons and normal hearing subjects. The stimuli were presented randomly in 4 different sound levels, 10, 20, 30, 40 dBSL using a loudspeaker. Based on the confusion matrix obtained from the relationship between the stimuli and the responses, the 100 phoneme were plotted using multidimensional scaling method and showed their confusion distance.

Qualitative differences were found among subjects with the approximately equivalent monosyllabic discrimination scores that suggests the needs of different fitting strategy.

#### **[498] Low Frequency Hearing Loss in Prenatally Stressed Rats**

**Alexander Kadner<sup>1</sup>, Vanessa J. Pressimone<sup>2</sup>, Brent Lally<sup>3</sup>, Adrienne K. Salm<sup>3</sup>, Albert S. Berrebi<sup>1</sup>**

<sup>1</sup>Sensory Neuroscience Research Center, West Virginia University, <sup>2</sup>Vassar College, <sup>3</sup>Dept. Neurobiology & Anatomy, West Virginia University

The prenatally stressed (PS) rat is used as a model of both pathological anxiety and schizophrenia. As in humans with these disorders, PS rats display abnormalities in auditory processing as measured by sensory gating and prepulse inhibition (PPI) paradigms. A causative factor underlying the PS rat phenotype is exposure to elevated glucocorticoids in utero. It has been recently demonstrated that prenatal exposure to glucocorticoids also causes higher vulnerability to noise-induced trauma in adult life.

In this study we investigated the possibility of altered hearing thresholds in PS rats raised in the normal auditory environment of our medical center animal quarters. Pregnant dams were assigned randomly to PS and control groups. Between gestational days 14-21 half of the dams were subjected to the mild stressors of handling, exposure to a novel cage and saline injection at random times during lights-on daily. This protocol reliably produces offspring with behavioral and hormonal similarities to humans with pathological anxiety and schizophrenia.

Between postnatal days 74-151, hearing thresholds of male PS (n=8) and control (n=7) offspring were assessed by recording auditory evoked brainstem responses to 0.5, 1, 2, 4, 8, 16, 32 and 64 KHz pure tones presented at varying decibel intensity. The resultant audiograms showed PS offspring had significantly higher hearing thresholds than control animals at 1, 2 and 4 KHz (t-tests,  $p < 0.05$ ). The threshold shifts caused by prenatal stress ranged between 8 and 10 dB.

Hence, it appears that PS rats hear their world differently than do non-stressed offspring. These findings should be considered in interpreting behavioral studies of PS rats, particularly PPI and gating studies using low frequency auditory stimuli. These seemingly paradoxical results now suggest the testable hypothesis that a compensatory expansion of auditory maps for the spared frequencies underlies the heightened auditory sensitivity of PS rats.

Supported by DC-02266 (ASB) and SNRC SURI fellowship (VJP)

#### **[499] Air-Bone Gap in Patients with Large Vestibular Aqueduct Syndrome**

**Eisuke Sato**<sup>1,2</sup>, Makoto Sugiura<sup>1</sup>, Takahiko Yoshino<sup>1</sup>, Terukazu Mizuno<sup>1</sup>, Hironao Otake<sup>1</sup>, Ieda Maria Ishida<sup>1</sup>, Tsutomu Nakashima<sup>1</sup>

<sup>1</sup>Nagoya University School of Medicine, <sup>2</sup>Cleveland Clinic Foundation

**Objective:** To investigate the mechanism of the air-bone gap in patients with large vestibular aqueduct syndrome (LVAS). **Design:** Prospective study. **Methods:** Twenty-three patients (46 ears) with LVAS served as experimental subjects. Standard pure-tone audiometry (PTA) were performed on each ear. Magnetic-resonance imaging was used to determine the diameter of the endolymphatic duct and the volume of the endolymphatic duct and sac. The diameter of endolymphatic duct is measured at the midpoint between the common crus and its external aperture. **Results:** The audiometric configurations of the average of PTA sloped downwards from the low to the high frequencies with air-bone gaps in low frequencies. There was no correlation between the volume of endolymphatic duct and sac and the degree of air-bone gaps in low frequencies. When the diameter of the endolymphatic duct was less than 2mm, the air-bone gaps in 250Hz, 500Hz and 1kHz were recognized in 100%, 87.5%, and 50%, respectively. When the diameter of the endolymphatic duct was from 2mm to 3mm, the air-bone gaps in 250Hz, 500Hz, and 1kHz were recognized in 100%, 96.1%, and 57.7%, respectively. When the diameter of the endolymphatic duct was more than 3mm, the air-bone gaps in 250Hz, 500Hz, and 1kHz were recognized in all cases. As the diameter of the

endolymphatic duct increased, the air-bone gaps in 500Hz and 1kHz were frequently observed. **Discussion:** As the duct is wide, higher frequency sound can transmit through the duct. The enlarged vestibular aqueduct acts as pressure release point, "the third window", and produces an increase in the compressional response of the cochlea. Thereby, the sensitivity to bone conduction may be improved in these patients. **Conclusions:** Air-bone gaps in patients with LVAS depend on the width of the endolymphatic duct rather than its volume.

#### **[500] Evolution and Development of the Octavo-Lateral Efferent System**

**Bernd Fritzsche**<sup>1</sup>, Feng Feng<sup>1</sup>

<sup>1</sup>Creighton University, Omaha, NE

Efferent innervation of the ear is found in all vertebrates. Inner ear efferents (IEE) are one of three cholinergic motoneurons of the hindbrain and spinal cord; the others are somatic and visceral motoneurons. Efferent cell bodies show co-localization with facial branchial motoneurons (FBMs) in the hindbrain in many vertebrates. In some bony fish, amphibians and amniotes there is segregation of FBMs from IEEs. In contrast to almost all other motoneurons, except the oculomotor motoneurons, IEEs may have bilaterally distributed cells and axons. In addition, IEEs may have branches that connect to the lateral line system of neuromast organs, but hair cells of these organs may also be innervated by their own efferent neurons (LLEs). Common LLEs and IEEs have been exploited for physiological assessment of efferent function in salamanders. Consistent with the evolutionary segregation of IEEs from FBMs is the mammalian and avian progressive segregation of these two motoneuron populations during development. Equally consistent with the rich variety of distribution patterns found in adults is the disparity of segregation processes of these two populations during development. In chicken, IEEs segregate from FBMs through differential migration of

IEEs, in part across the midline to the contralateral side. In contrast, in mammals, FBMs migrate away from their hindbrain origin in rhombomere 4 to rhombomere 6, leaving the IEEs behind to project an axon across the floor plate and migrate laterally. One gene that may participate in this separation is GATA3. Further developmental migration segregates the mammalian IEEs into a ventrolateral olivo-cochlear and dorsolateral vestibular efferent population. Around E16.5, lateral and medial olivo-cochlear neurons begin to separate. Efferent fibers reach the inner ear as early as E12.5 in mice and have progressed to vestibular and cochlear hair cells by E14.5, prior to cholinergic receptor expression.

#### **[501] Organization of Efferent Pathways to the Cochlea: Origins, Targets, Cytochemical Subgroups and Receptor Subtypes**

**M. Charles Liberman**<sup>1,2</sup>

<sup>1</sup>Massachusetts Eye and Ear Infirmary, <sup>2</sup>Harvard Medical School

The organization of the lateral and medial olivocochlear systems in the mammalian ear will be summarized in this presentation, including anatomical and physiological

evidence for the neural circuitry that drives them, physiological studies of the acoustic stimuli that activate them, immunohistochemical and physiological evidence for functional subgroups within each major system, anatomical evidence as to the nature and number of the peripheral targets of each fiber type, and evidence from knockout mouse studies as to the receptor subtypes involved in their peripheral effects.

Research supported by NIDCD RO1 DC 00188 and P30 DC 005209

## **502 Organization of Efferent Pathways to the Vestibular Organs: Origins, Targets, and Cytochemical Subgroups**

**Anna Lysakowski<sup>1</sup>**

<sup>1</sup>*University of Illinois at Chicago*

The organization of efferent pathways to, and innervation of, the vestibular organs in mammals will be considered. Topics include 1) the origins of this pathway in the so-called "e-group", the vestibular efferent nucleus in mammals, 2) its targets in the cristae and utricular macula (based upon ultrastructural and tracer studies), and 3) cytochemical subgroups (based upon neurotransmitter receptor immunohistochemistry). The results provide evidence for a neurochemical-based division within the e-group, differences in the terminal fields of ipsilateral vs. contralateral efferents, and segregation of different receptor subtypes (cholinergic, purinergic and peptidergic) within the sensory epithelium. Cellular features of hair cells on the ultrastructural level, such as the size and number of subsynaptic cisterns, and their calcium store and calcium pump composition, also appear to vary, depending upon where they are located within the epithelium. If time permits, the mammalian pattern will be compared with that in other vertebrates.

## **503 Cellular Mechanisms of Efferent Action in the Cochlea**

**Paul Fuchs<sup>1</sup>**

<sup>1</sup>*The Center for Hearing and Balance, Otolaryngology-Head and Neck Surgery, Johns Hopkins*

Pre- and postsynaptic factors contributing to the efferent-mediated inhibition of hair cells will be considered, including recent work detailing facilitation of efferent transmitter release onto hair cells in the rat cochlea. Postsynaptically, inhibition involves the activation by intracellular  $\text{Ca}^{2+}$  of SK channels. The relative significance of  $\text{Ca}^{2+}$  influx through nicotinic channels and its release from postsynaptic (synaptoplasmic) cisterns will be discussed.

## **504 Synaptic Physiology and Pharmacology of Efferent Actions in Vestibular Organs**

**Joseph C. Holt<sup>1</sup>**

<sup>1</sup>*University of Texas Medical Branch at Galveston*

Efferent actions are more diverse in vestibular organs than in other hair-cell organs and include presynaptic (hair-cell) inhibition, presynaptic excitation, and postsynaptic (afferent) excitation. In addition, there can be both fast and

slow responses. ACh may be the primary efferent transmitter responsible for all these effects. How might ACh generate such different responses? Studies in both the frog and turtle suggest there are three main determinants: (1) The nature of the ACh receptor (2) The cellular localization of the ACh receptor. (3) The downstream involvement of additional cellular mechanisms. Efferent-mediated inhibition invariably involves the activation of  $\alpha 9$ -containing nicotinic ACh receptors ( $\alpha 9\text{nAChR}$ ) on hair cells. Calcium influx through  $\alpha 9\text{nAChR}$  then activates small-conductance, calcium-dependent potassium channels (SK) thereby hyperpolarizing hair cells and decreasing transmitter release. In contrast, efferent-mediated excitation of afferent discharge can be generated in one of three ways: (1) Activation of presynaptic receptors, without the involvement of SK, depolarizes the hair cell and increase transmitter release. (2) Activation of postsynaptic receptors depolarizes the afferent. (3) Post-inhibitory excitation mediated by the activation of a hyperpolarization-activated channel (Ih), an inward rectifier (IRK) and/or a T-type Ca channel following the hair cell hyperpolarization triggered by  $\alpha 9\text{nAChR}$  and SK. With the exception of the post-inhibitory excitation, the nicotinic receptors involved in efferent-mediated excitation of afferent discharge are pharmacologically distinct from  $\alpha 9\text{nAChR}$ . Given the kinetics of metabotropic signaling, muscarinic receptors are good candidates for mediating efferent slow responses. Understanding how these various signaling pathways can contribute to such diverse efferent responses in frog and turtle can be used to elucidate the mechanisms underlying efferent responses in mammals.

## **505 Olivocochlear Efferent Effects in Mammals**

**John J. Guinan, Jr.<sup>1</sup>**

<sup>1</sup>*Harvard Medical School, Mass. Eye & Ear Infirmary*

Medial olivocochlear (MOC) efferents, fibers that innervate outer hair cells, produce several effects in the cochlea. In a silent background, MOC activity reduces responses to low-level sound in basilar-membrane (BM) motion, otoacoustic emissions, and auditory-nerve (AN) responses. However, in a background of noise, MOC efferents can increase AN responses to transient sounds. These effects mediate two putative functions of MOC efferents: (1) adjustment of the range of hearing and (2) reducing the masking of signals by noise. In addition to these "fast" efferent effects that build up over tens to hundreds of ms, there is a "slow" efferent inhibition that builds up over tens of seconds. This "slow" inhibition is due to a different mechanical mechanism than the fast effects, probably the reduction of outer-hair-cell stiffness, and appears to be associated with at third putative MOC function, the reduction of damage due to traumatic sounds. These fast and slow efferent effects both appear to be due to an MOC-induced reduction of cochlear amplifier gain. In addition, MOC activation reduces auditory-nerve responses to the earliest peak of click responses and at certain frequencies in tuning-curve tails, effects which have not been found in basal-turn BM motion. These MOC effects are not explained by a reduction of cochlear amplifier gain and appear to be due to an MOC inhibition of a cochlear

motion that is not part of the classic BM traveling wave. Their function is unknown. Effects due to lateral olivocochlear (LOC) efferents, the fibers that innervate the dendrites of auditory-nerve fibers, are just beginning to be understood. Current evidence indicates that LOC efferents can produce inhibition and/or excitation, both on a very-slow time scale of minutes. The function of LOC efferents is unknown, but one role is probably protection from acoustic trauma.

Supported by NIDCD RO1000235, R01DC005977, P30DC005209

## **[506] Functions of the Efferent Vestibular System (EVS)**

**Jay M. Goldberg<sup>1</sup>**

<sup>1</sup>*University of Chicago*

Across the vertebrate scale, there are differences in central EVS pathways and in peripheral EVS actions. In any one species, a diversity of EVS actions target different afferent populations. These observations suggest that the EVS has multiple functions that vary across species. In any one species, it is useful to characterize how electrical EVS stimulation affects afferent discharge. In turtles, as in frogs, some vestibular afferents are excited, others are inhibited, while still others show a mixed inhibitory-excitatory response. Synaptic mechanisms responsible for this diversity have been summarized elsewhere in this symposium. Inhibition in the turtle is targeted to afferents with high gains, while excitation occurs in units with lower gains. This suggests that were the EVS activated during voluntary head movements, it could switch the vestibular organs from a postural to a volitional mode. In mammals, as in the toadfish, EVS electrical activation results in predominantly excitatory actions. Spike responses in mammals are entirely excitatory, consist of fast and slow response components, and differ across afferent populations. Those in irregular (central/striolar) afferents are large and include fast and slow components; in regular (peripheral/extrastriolar) afferents, responses are small and predominantly slow. These observations suggest that were the EVS activated in anticipation of voluntary head movements, it could prevent inhibitory silencing. Recordings in alert monkeys challenge this hypothesis: afferent rotational responses were indistinguishable for active and passive head movements. In decerebrate chinchillas, there are EVS-mediated afferent responses to vestibular (rotational) inputs from either ear resembling those obtained with electrical stimulation; the EVS in decerebrates can give rise an appreciable increase and large oscillations in background discharge. We need to determine which, if any, of these EVS effects are present in alert animals.

## **[507] Efferent Actions and Their Function in Lateral-Line Systems**

**William F. Sewell<sup>1</sup>**

<sup>1</sup>*Harvard/MEEI*

The innervation pattern and other anatomical features of lateral-line organs will be described with a particular emphasis on the *Xenopus* lateral line organ.

Pharmacological evidence will be reviewed that supports the conclusion that the nicotinic actions of efferents are mediated by the alpha 9/10 receptor. The effects of the neuropeptide, CGRP, and other neurotransmitters will be compared in lateral lines and the mammalian cochlea. Finally, the function of the efferent innervation will be considered by describing the responses of efferent neurons.

## **[508] Synaptic Components of Receptive Field Plasticity in the Adult Auditory Cortex**

**Robert Froemke<sup>1</sup>, Michael Merzenich<sup>1</sup>, Christoph Schreiner<sup>1</sup>**

<sup>1</sup>*Coleman Lab, Keck Center, Dept. Otolaryngology, UCSF*

Receptive fields (RFs) of the adult sensory cortex are plastic, capable of a high degree of reorganization. However, the mechanisms of RF plasticity are unknown. Here we examine the contributions of excitatory and inhibitory currents to long-term changes in RF structure after pairing sensory stimulation with neuromodulator release.

We made whole-cell voltage clamp recordings in vivo from neurons in the primary auditory cortex of the adult anesthetized rat. After mapping auditory RFs with tone pips of varying frequencies for 5-10 minutes, we repetitively paired tones at a certain frequency, the conditioned stimulus (CS), with electrical stimulation of the basal forebrain, the major source of cortical acetylcholine (Bakin and Weinberger, 1996; Kilgard and Merzenich, 1998). This conditioning procedure led to large, rapid increases in excitatory currents evoked by CS. Conversely, the excitatory response to the characteristic frequency (CF) was diminished after pairing, regardless of the spectral distance between CS and CF. We also observed that conditioning led to a reduction in inhibitory current evoked by CS. These changes in excitation and inhibition persisted for >20 minutes after conditioning, and were highly specific- aside from changes to CS and CF, responses to all other frequencies were generally unaltered. Excitatory and inhibitory plasticity were coordinated together, as both effects were prevented when NMDA receptors were blocked.

This specific shift in the balance of excitation and inhibition might alter the output of cortical neurons. Extracellular recordings revealed that, after pairing, there were two main changes to peristimulus time histograms of spiking responses evoked by the paired tone: an increase in peak and an increase in width. These results demonstrate that long-lasting modifications of excitatory and inhibitory inputs are rapidly induced in vivo, and can be used to control both the spectral and temporal structure of cortical receptive fields.

## **[509] Temporal Response Properties in the Auditory Cortex of the Awake Gerbil**

**Maria Ter-Mikaelian<sup>1</sup>, Dan Sanes<sup>1</sup>, Malcolm Semple<sup>1</sup>**

<sup>1</sup>*Center for Neural Science, New York University*

The temporal precision of responses to discrete or periodic stimuli is thought to be an important attribute of auditory cortical coding. Evidence derives primarily from studies of

anesthetized animals. Here, we compare temporal coding in awake and anesthetized (barbiturate-ketamine) auditory cortex of Mongolian gerbils and find substantial differences.

Minimum first-spike latency to tone pips at best frequency (BF) is 12 ms longer for single neurons recorded in awake as compared to anesthetized cortex (Mann-Whitney,  $p < 0.0001$ ,  $df = 57$ ). In addition, the standard deviation (SD) of the first-spike latency differs with anesthetic state: SD increases with latency under anesthesia, but is poorly correlated with latency in awake cortex. These observations suggest that an active process increases response latency and constrains its timing in awake cortex. Furthermore, neurons in awake cortex do not adapt as rapidly as those in anesthetized cortex (measured as time from response onset to time when spike rate decreased by 50%).

The temporal precision of the response to periodic stimuli was assessed with long (10s) sinusoidally amplitude-modulated tones (SAM, BF carrier). Vector strength is profoundly higher in awake cortex for the most effective modulation frequencies. As an additional measure of temporal precision we assessed response reliability reflected in the correlation between 10s trials. Greater response reliability is associated with high SAM synchrony cutoff frequency. Moreover, neurons with the most rapid spike rate adaptation display significantly higher SAM synchrony cutoffs. Collectively responses in the awake animal provide a substantially revised view of the temporal kinetics within auditory cortex.

#### **510** Categorical Representation of Functionally Meaningful Vocalizations in the Ventrolateral Prefrontal Cortex

Yale Cohen<sup>1</sup>, Marc Hauser<sup>2</sup>, Brian Russ<sup>1</sup>

<sup>1</sup>Dartmouth College, <sup>2</sup>Harvard University

Communication is one of the fundamental components of both human and non-human animal behavior. Species-specific vocalizations are especially important in the socioecology of several species of non-human primates, such as rhesus monkeys (*Macaca mulatta*) since they convey information about the identity and the age of the caller, often provide information about sex and emotional or motivational state, and transmit information about objects and events in the environment. While there is a rich history focusing on how the spectrotemporal features of vocalizations are represented, the neural code underlying more abstract features of vocalizations, such as their categorical representations and putative meanings, are not understood.

Here, we test whether species-specific vocalizations are categorically represented in the ventrolateral prefrontal cortex (vPFC), a cortical area thought to play an important role in the processing vocalizations. We found that the firing patterns of vPFC neurons do not provide evidence for discrimination between vocalizations that convey information about low-quality food, high-quality food, or high-quality and low-quality food. In contrast, the firing patterns do provide evidence for discrimination between those vocalizations that convey information about food (both high- and low-quality) and those conveying

information about non-food events. These data suggest that vPFC neurons categorize food-quality information at one level and non-food information at a different categorical level. Overall, these data further implicate a role for the vPFC in the categorization of socially meaningful signals and in the decoding of the meaning of these signals.

#### **511** Call Preference in Cortical Neurons May Emerge from Tuning to Multiple Acoustic Dimensions

Stuart Washington<sup>1</sup>, Jagmeet Kanwal<sup>1</sup>

<sup>1</sup>Department of Physiology and Biophysics, Georgetown University Medical Center

Neurons in the Doppler-Shifted Constant Frequency processing (DSCF) area within the primary auditory cortex (AI) of the mustached bat, *Pteronotus parnellii*, respond well to both the simplest (tone bursts) and most complex (social calls) stimuli. DSCF neurons are non-linearly facilitated by combinations of frequencies in the FM<sub>1</sub> (frequency modulation in the 1st harmonic of the pulse) and CF<sub>2</sub> (2nd harmonic, constant frequency in the echo) in the echolocation signal (Kanwal et al, 1999). This fairly uniform frequency tuning of DSCF neurons does not adequately account for any diversity in their call response profiles. To understand the computational basis for call preference in DSCF neurons, we hypothesized that they are tuned to multiple acoustic dimensions. To test this hypothesis, we recorded the responses of single DSCF neurons ( $n = 62$ ) in awake bats to the presentation of linear FMs, that are intermediate in complexity (tones versus calls) and are amenable to mathematical modeling. We paired the FM stimuli with a ~25 kHz tone burst (FM<sub>1</sub> range) to facilitate the neural response. By systematically varying the slopes, bandwidths, sweep directions, and center frequencies of FMs for stimulus levels ranging from 100 to 20 dB SPL (200 stimulus repetitions at 4/s), we defined the best FM for a neuron. Based on peak firing rates at best amplitudes (bin width = 5 ms), 77% of the neurons preferred an upward FM (UFM) and 23% preferred a downward FM (DFM). Optimal slopes for UFM ( $0.41 \pm 0.67$  kHz/ms) differed significantly ( $p < 0.05$ ) from those for DFM ( $0.20 \pm 0.13$  kHz/ms; mean  $\pm$  s.d.). Best bandwidths for UFM ( $2.53 \pm 1.01$  kHz) and DFM ( $3.94 \pm 1.68$  kHz) also differed significantly ( $p < 0.01$ ). Furthermore, we observed that changes in amplitude caused significant, non-monotonic fluctuations in peak neural responses to FM tuning, and in 8 neurons, the preference for FM direction was reversed when compared at different stimulus amplitudes. The predominance of larger magnitude responses to UFM than to DFM and tuning to shallow ( $< 1$  kHz/ms) slopes for best FMs is likely important for call processing as these types of FMs are absent in the echolocation pulse. Altogether, our results demonstrate that describing excitatory frequency tuning alone is inadequate to understand the emergence of call preference in DSCF neurons, rather auditory cortical neurons may compute combinations of several acoustic dimensions within calls.

Supported by NIDCD/NIH grants #DC02054 to J.K. and #DC007576 to S.W.



## **512 Effect of Enriched Environment on Synaptic Transmission in the Rat Auditory Cortex**

**Justin Nichols**<sup>1</sup>, Vikram Jakkamsetti<sup>1</sup>, Rajasekhar Byrapureddy<sup>1</sup>, Bryan Roof<sup>1</sup>, Huyen Bui<sup>1</sup>, Tres Thompson<sup>1</sup>, Michael Kilgard<sup>1</sup>, Marco Atzori<sup>1</sup>

<sup>1</sup>The University of Texas at Dallas

Prolonged exposure to an enriched auditory environment (EE) induces changes in the acoustically-evoked receptor potentials (ERP) in the auditory cortex (Percaccio et al. 2005). Such changes might be induced by several causes, such as 1) different thalamo-cortical input, 2) different intracortical processing, or both. In our study we used a rat auditory cortex slice preparation to test this second hypothesis.

We first investigated the possibility that EE altered the cortical capability to undergo long-term changes. Long-term potentiation induced with tetanic (100 Hz) stimulation of the afferents was not different in control vs. EE rats (amplitude after tetanus)/(amplitude in control) =  $1.30 \pm 0.33$  in EE vs.  $1.25 \pm 0.12$  in control). We then hypothesized that changes in the ERP signal were associated with postsynaptic changes at glutamatergic synapses. We selected the ratio between NMDA receptor-mediated currents and AMPAR-mediated currents (INMDA/IAMPA) as an indicator of postsynaptic function. In perforated patch-clamp recordings from cells of layer 2/3 and stimulating with extracellular electrodes in the infragranular layer, we detected no changes in INMDA/IAMPA ( $0.83 \pm 0.38$  in EE vs.  $0.79 \pm 0.22$  in control).

Finally we investigated the possibility that EE induced long-lasting alterations in short-term plasticity of glutamatergic and/or GABAergic synaptic transmission by measuring the pair pulse ratio (PPR) of postsynaptic currents. We detected a tendency of EE to induce a higher PPR for short intervals ( $1.64 \pm 0.14$  vs.  $1.31 \pm 0.12$  at 20 ms interpulse interval (i.i.),  $1.75 \pm 0.28$  vs.  $1.44 \pm 0.19$  at 40 ms i.i.,  $1.69 \pm 0.12$  vs.  $1.41 \pm 0.15$  at 50 ms i.i.). Additionally, GABAergic synaptic responses showed a trend in which EE rats displayed a higher PPR depression compared to control ones ( $0.26 \pm 0.04$  vs.  $0.43 \pm 0.10$  at 20 ms i.i.,  $0.47 \pm 0.18$  vs.  $0.79 \pm 0.30$  at 50 ms i.i.,  $0.63 \pm 0.27$  vs.  $0.75 \pm 0.21$  at 100 ms i.i.). We conclude that differences in auditory gating are associated with changes in local presynaptic properties within the auditory cortex.

## **513 Neural Correlates of Streaming Without Spectral Cues in Human Auditory Cortex**

**Alexander Gutschalk**<sup>1,2</sup>, Jennifer Melcher<sup>1,3</sup>, Christophe Micheyl<sup>2</sup>, Courtenay Wilson<sup>4</sup>, Andrew Oxenham<sup>2</sup>

<sup>1</sup>Eaton-Peabody Laboratory, Massachusetts Eye & Ear Infirmary, Boston, MA, <sup>2</sup>Research Laboratory of Electronics, Massachusetts Institute of Technology, Cambridge, MA, <sup>3</sup>Department of Otology and Laryngology, Harvard Medical School, Boston, MA, <sup>4</sup>Harvard-MIT Division of Health Sciences and Technology, Cambridge, MA

A sequence of pure tones is usually perceived as one coherent stream if the tones are all closely spaced in frequency, but as two or more streams if the frequencies

differ widely. It has been proposed that this perceptual streaming phenomenon is based on the separation of tones into different channels along the tonotopic axis of the auditory system. Using pure tones, recent functional magnetic resonance imaging (fMRI) and magnetoencephalography (MEG) studies have identified possible neural correlates of streaming in human auditory cortex. However, psychoacoustical data demonstrate that stream segregation can also occur with sequences of complex tones that differ in fundamental frequency ( $f_0$ ), but are filtered into the same spectral region, and thus excite the same peripheral channels. Here we use such stimuli to investigate whether the cortical correlates of stream segregation identified in earlier fMRI and MEG studies reflect only tonotopic differences or whether they remain the same in the absence of peripheral tonotopic cues. The stimuli were sequences of peripherally unresolved harmonic complex tones arranged into a continuously repeating ABBB pattern, with the  $\Delta f_0$  between A and B being 0, 1, 3, or 10 semitones. fMRI showed enhanced sustained activity in auditory cortex for sequences perceived as two streams (3 and 10 semitones) compared to one stream (0 and 1 semitone). This enhancement was more prominent in, but not limited to, areas outside Heschl's gyrus. In MEG, the A tone elicited a significant P1m component for the 3- and 10-semitone  $\Delta f_0$ s, but not for lower  $\Delta f_0$ s. The fMRI and MEG responses parallel the psychophysical measures of streaming, suggesting that the previously identified cortical correlates of streaming do not reflect merely tonotopy, but represent a more general code in auditory cortex.

Research supported by DFG (GU 593/2-1), NIH (P30 DC005209; R01 DC 05216), and Hertz Foundation.

## **514 Multilinear Spectrotemporal Models for Predicting Auditory Cortical Responses**

**Misha Ahrens**<sup>1</sup>, Jennifer Linden<sup>2</sup>, Maneesh Sahani<sup>1</sup>

<sup>1</sup>Gatsby Unit, UCL, <sup>2</sup>Ear Institute and Dept Anatomy, UCL

A widely-used characterisation of an auditory neuron is the STRF (spectro-temporal response function or receptive field). In one view, the STRF is a spectrotemporally-linear response model; that is, a model that predicts the firing rate of the cell as a linear function of the spectrogram of the incident sound. However, recent work (Sahani and Linden 2003; Machens et al. 2004) has shown that, for neurons in the primary auditory cortex, predictions derived from such models are not very accurate.

Here we investigate two extensions to the STRF model, using rodent auditory cortical responses to dynamic random chord stimuli. One, discussed previously (Luczak et al. 2004), incorporates a term linear in the recent spike history. While such a model did often achieve higher predictive accuracy than the simple STRF, we show that, in our data, the larger part of this increase was due to correlations in the non-stimulus-locked noise component of the activity, rather than due to history-dependent changes in the stimulus-driven response.

The second approach allows us to express broad classes of non-linear models in a novel and efficient multilinear form, facilitating efficient parameter estimation by

regularised alternating least squares. We exploit this formalism to investigate models that include non-linear transforms of input intensity, as well as non-linear stimulus-specific adaptation effects. We show that such models can predict auditory cortical responses significantly more accurately than the standard STRF.

### **[515] Auditory Information Processing During Sleep and Wakefulness**

Marisa Pedemonte<sup>1</sup>, Ricardo A. Velluti<sup>1</sup>

<sup>1</sup>*Neurofisiología, Facultad de Medicina*

The sleeping brain is a totally different brain from many viewpoints including the processing of sensory information. The auditory is the only tele-receptor relatively open during sleep, in micro-osmatics, with other particularities such as increased blood flow in nuclei and cortex, dreaming auditory images, etc. Glass micropipettes were used for auditory neuronal recordings throughout the pathway in chronically implanted restrained guinea pigs. Bioelectrical controls allowed the diagnosis of the animal state, e.g., wakefulness, slow wave or paradoxical (REM) sleep. The stimuli were: a) pure tone-bursts (50 ms, 2/s). b) pre-recorded guinea pig natural calls (700ms, every 2s).

Experimental approaches: 1. The auditory neurone's firing rate. The primary auditory cortex, the inferior colliculus, the lateral olive and the cochlear nucleus exhibited three unit's firing types on passing to sleep: increment, decrement, no-change, with different firing shifts proportions. No units were observed to stop firing on passing to sleep. 2. The discharge pattern. Auditory neurones may only change the pattern entering sleep. 3. The temporal relationship between auditory neurones firing and hippocampus theta field activity (phase-locking) is a phenomenon in the time domain observed during wakefulness and sleep. Every auditory stimulus develops in time, that is why the CNS must have a functional possibility to encode this parameter.

4. Natural call stimulation. The response of auditory cortex and inferior colliculus neurones was different when recorded during wakefulness or sleep. When the natural call was played backwards, inverted in time, the neuronal firing changed in waking or sleep. It became evident that the processing of complex sounds continues to be carried out in sleep. The auditory information processing is further demonstrated to be present during sleep.

1 We are grateful to AUDILUX-Fundación "Ricaldoni" (Montevideo) for its financial support.

### **[516] Gap Evoked Auditory Response from the Inferior Colliculus and the Auditory Cortex of Guinea Pigs**

Jian Wang<sup>1</sup>, Yanmei Feng<sup>2</sup>, Shankai Yin<sup>2</sup>

<sup>1</sup>*Dalhousie University*, <sup>2</sup>*Shanghai JiaoTong University*

Response to silent gap embedded in acoustic markers has been used to reflect the temporal processing of auditory system in both psychoacoustic and physiological experiments. In this study, the evoked potentials were recorded from electrodes implanted into the inferior colliculus and the auditory cortex of guinea pigs in responses to gaps formed by the noise bursts in four

frequency bands (0.5-8 kHz, 0.5-16 kHz, 0.5-32 kHz, and 16-32 kHz) at three levels (85, 65 and 45 dB SPL). To verify the effect of general anesthesia, the gap responses recorded in the control condition (from conscious animals) were compared with the results obtained when animals were anesthetized with two different dose of pentobarbital (30 mg/kg versus 15 mg/kg). The response to the onset of the post-gap marker was measure to establish the input-output functions for the response latency and amplitude against the gap durations, as well as the gap-response threshold. In general, the broader the gap-marker bandwidth, the larger amplitude and the shorter latency were evoked. However, the differences were not significant. General anesthesia by pentobarbital did not significantly change the gap-response amplitude for long gap durations (superthreshold gaps) in both IC and AC. However, the effect of general anesthesia was shown in AC as the elongated latency and the larger gap-response threshold. Reduced presentation level resulted in a parallel reduction in the response amplitude, but did not change the speed of recovery from the forward masking of the pre-gap marker on the response to the onset of the post-gap marker, as indicated by the identical amplitude ratio-gap duration functions obtained at different presentation levels.

### **[517] Muscarinic Acetylcholine Receptors Mediate Sound-Guide Cortical Plasticity Evoked by Electrical Stimulation of Basal Forebrain in Mice**

Ganling Chen<sup>1</sup>, Jun Yan<sup>1</sup>

<sup>1</sup>*Department of Physiology and Biophysics, Hotchkiss Brain Institute, University of Calgary*

Learning-induced or experience-dependent plasticity in primary auditory cortex is guided by acquired sound information and promoted by increased levels of cortical acetylcholine (ACh). The nucleus basalis (NB) of the basal forebrain is the major output source of cholinergic neurons and sends wide projections to the auditory cortex. In mice, electrical stimulation of NB paired with a tone (tone-ES<sub>NB</sub>) shifts frequency tunings of cortical neurons towards the frequency of the paired tone. Interestingly, tone-ES<sub>NB</sub> also leads to frequency-specific decrease in the response threshold of cortical neurons that do not tune to the frequency of the paired tone (non-PT neuron). It has been known that the global application of atropine, a muscarinic acetylcholine receptor antagonist, to the auditory cortex, eliminates cortical plasticity evoked by auditory learning or tone-ES<sub>NB</sub>. We hypothesize that the frequency-specific threshold decrease of cortical non-PT neurons evoked by tone-ES<sub>NB</sub> results from the cholinergic facilitation of collateral thalamocortical projections from tone frequency channel to non-PT neurons. To test our hypothesis, we applied microiontophoretic injection of atropine to the recorded cortical non-PT neurons during tone-ES<sub>NB</sub>. We found that tone-ES<sub>NB</sub> with microiontophoresis of atropine still elicited frequency-specific shifts in frequency tunings of cortical non-PT neurons; the shift was smaller however than that of the control group (with microiontophoresis of saline). Significantly, the frequency-specific threshold decrease was not seen in the atropine group. To further confirm our findings, we examined the changes in frequency tuning curves of cortical non-PT neurons by the

microiontophoretic injection of ACh paired with tone stimulation. We induced significant threshold decreases that were highly correlated to the tone frequency. The frequency-specific threshold decrease was blocked when atropine was applied together with ACh to cortical non-PT neurons. Our data suggest that cortical muscarinic receptors are crucial for both frequency-specific threshold decreases and the frequency-tuning shifts in order for auditory learning and experience to occur.

### **518 GABA Shapes Selectivity for the Direction and Rate of Frequency Modulated Sweeps in the Auditory Cortex**

**Khaleel Razak<sup>1</sup>, Zoltan Fuzessery<sup>1</sup>**

<sup>1</sup>*University of Wyoming*

It has been suggested that the auditory cortex does not create, but simply inherits, response selectivity for complex sounds, as selectivity is already present at the level of the inferior colliculus (IC). This assumption is mostly untested. Ionophoretic blockade of GABA<sub>A</sub> receptors is one method to explore hierarchical processing in sensory systems. However, except for frequency tuning, the role of GABA in shaping response selectivity has not been studied in the auditory cortex. Here we tested whether GABA shapes selectivity for the rate and direction of frequency modulated (FM) sweeps in cortical neurons in the pallid bat auditory cortex.

The pallid bat echolocates using downward FM sweeps (60 to 30 kHz, 2-4 msec) In both the IC and the cortex, >60% of the neurons tuned in the echolocation range are selective for FM rates and direction found in the echolocation call. In the auditory cortex, rate selectivity is created by late arriving, narrow bandwidth high-frequency inhibition, while direction selectivity is created by early arriving, broad bandwidth low-frequency inhibition. By iontophoresing bicuculline (a GABA<sub>A</sub> receptor antagonist) we asked whether auditory cortex re-creates rate and direction selectivity, properties already found in the IC. Bicuculline either eliminated or reduced direction selectivity in 91% cortical neurons tested. Rate selectivity was eliminated or reduced in 47% of the neurons. Using a two-tone over time paradigm we found that in neurons that lost direction selectivity, low-frequency inhibition was either reduced in strength or slowed down in arrival time by bicuculline, resulting in strong responses to upward FM sweeps. Similar effects with high-frequency inhibition were seen for neurons in which rate selectivity was affected. These data show intracortical inhibition is required for cortical response properties. Views about inheritance in the colliculus-thalamus-cortex pathway need to be reconsidered.

### **519 Reduction of Cell Density in the Mouse Medial Geniculate Body and Primary Auditory Cortex After Noise Exposure**

**Dietmar Basta<sup>1</sup>, Barbara Tzschentke<sup>1</sup>, Arne Ernst<sup>1</sup>**

<sup>1</sup>*University of Berlin*

The noise-induced hearing loss (NIHL) is largely characterized by cochlear damage, but this cannot fully explain the audiological symptoms in humans, e.g.

hyperacusis, tinnitus, reduced speech perception. Noise seemingly has an effect on key structures of the central auditory pathway, e.g. noise can induce apoptosis of neuronal tissue within the auditory midbrain. Higher auditory structures (e.g. medial geniculate body, auditory cortex) are characterized by metabolic changes upon noise exposure. However, little is known about the microstructural changes of the higher auditory pathway. The present paper was therefore aimed at investigating the cell density in the medial geniculate body (MGB) and the primary auditory cortex (AI) before and after noise exposure.

Normal hearing mice were exposed to noise (10 kHz center frequency at 115 dB SPL for 3 h) at the age of 21 days under anesthesia (Ketamin/Rompun 10:1). After one week, auditory brainstem response recordings (ABR) were performed in noise exposed and normal hearing

animals. After fixation, the brain was microdissected and stained (Kluever-Barrera). The cell density in the MGB subdivisions and the AI were determined by counting the cells within a grid. Noise-exposed animals showed a significant ABR threshold shift over the whole frequency range. Cell density was significantly reduced in all subdivisions (medial, dorsal and ventral) of the MGB and in layer IV-VI of AI. In contrast to this findings cell density remained unchanged in layer I-III of the AI and in the non-auditory reference area (dentate gyrus). The present findings demonstrate a significant noise-induced change of the neuronal cytoarchitecture in central key areas of auditory processing. These changes could contribute to the complex psychoacoustic symptoms of NIHL.

Supported by the Sonnenfeld Foundation, Germany.

### **520 Language-Dependent Pre-Attentive Pitch Processing in Young Adults**

**Bharath Chandrasekaran<sup>1</sup>, Ananthanarayan Krishnan<sup>1</sup>, Jayaganesh Swaminathan<sup>1</sup>, Jackson Gandour<sup>1</sup>**

<sup>1</sup>*Purdue University*

Previous research has shown that pre-attentive pitch encoding by the human auditory brainstem neurons is sensitive to linguistic experience (Krishnan, Xu, Gandour & Cariani, 2005). Whereas data are available on pre-attentive processing of consonants and vowels at the cortical level, none are yet available on lexical tones, i.e., linguistic use of pitch to convey meaning at the syllable level. The mismatched negativity (MMN), a cortical potential elicited by an odd-ball paradigm, reflects pre-attentive processing of auditory stimuli. In this study we examined scalp-distributed cortical MMNs elicited from three Mandarin Chinese tones (high level, high rising, low falling-rising) presented to 10 Mandarin Chinese and 10 English young adult speakers. Results revealed that the Mandarin tonal stimuli, irrespective of shape of the F0 contour, elicited MMNs of significantly greater peak amplitude between 200-250 ms post-stimulus in the Chinese group as compared to the English group. In addition, the width of the mismatched negativity for the Chinese group ranged from 150 to 300 ms regardless of tone. In the English group, the Mandarin tones elicited only a smaller-amplitude MMN between 100-150 ms post-

stimulus. This early MMN also exhibited a significantly smaller width as compared to the Chinese group. We infer that the early MMN reflects an auditory/acoustic level of pre-attentive processing, the late MMN, a linguistic level. Thus, an integrated MMN, larger in both width and amplitude implicates both levels of processing for Chinese listeners, whereas the smaller-amplitude, smaller-width, and earlier peaking MMN reflect an auditory level of processing only. Such findings can be accounted for by models of auditory perception that allow for top-down modulation at the earliest cortical stages of processing. Moreover, cross-language differences provide evidence in support of experience-dependent cortical plasticity in the processing of pitch in the speech domain.

## **[521] Fgfs-3, -8, and -10 in Mouse Inner Ear Development**

**Suzanne Mansour<sup>1</sup>**, Albert Noyes<sup>1</sup>, Tracy Wright<sup>1</sup>, Lisa Urness<sup>1</sup>, Ekaterina Hatch<sup>1</sup>

<sup>1</sup>University of Utah

Development of the inner ear proceeds through phases of otic placode induction, otic axis specification, vesicle formation and morphogenesis, and cell type specification. FGF signaling is required during all of these developmental events. In particular, we have shown that Fgf3 and Fgf10 or Fgf3 and Fgf8 are required redundantly to initiate mouse otic placode formation. Furthermore, we found that Fgf8 expression induces Fgf10 expression during this process. These three Fgf genes also have known or suspected roles later in otic vesicle axis formation, morphogenesis, innervation and cell type specification. These later roles, however, are obscured in global knockout mice and particularly in double mutant combinations, by lethality and/or the sequelae to abnormal induction. To achieve temporal and spatial separation of the multiple functions of these signals in otic development, we have generated CRE-dependent conditional (floxed) alleles of both Fgf3 and Fgf10 and acquired an Fgf8 conditional mutant. For both new alleles, germline deletion of the floxed exon recapitulates previously described Fgf3 or Fgf10 homozygous knockout phenotypes. Previous studies of the Fgf3 null phenotype caused by an insertion mutant have been extended by paint-filling and marker analysis of mutant ears in both the old (insertion) and new (Cre-deletion) null alleles. The results suggest that FGF3 induces dorsal development of the otic vesicle. We will also describe progress in defining the tissue origins of the FGF8 placode-inducing function and the post-induction roles of Fgf3 and Fgf10 in otic vesicle morphogenesis.

## **[522] An Integrative Role of Sox9 Genes in Fgf-Dependent Otic Induction**

**Dong Liu<sup>1</sup>**, Stefan Hans<sup>1</sup>, Monte Westerfield<sup>1</sup>

<sup>1</sup>University of Oregon

It is generally accepted that the inner ear derives primarily from ectoderm that is competent to respond to otic induction signals, although the molecular basis of otic induction is still elusive. We previously suggested that zebrafish Foxi1 and Dlx3b-Dlx4b may provide naïve ectoderm with otic competence to respond to Fgfs from the

developing hindbrain. Sox9a and Sox9b lie genetically downstream in the Foxi1, Dlx3b-Dlx4b and Fgf dependent pathways.

We find that blocking either Foxi1 or Dlx3b-Dlx4b function in *fgf8* mutants completely blocks ear formation, suggesting that Fgf8 is the major inducing signal. In support of this interpretation, implantation of Fgf soaked beads into ventral ectoderm at mid-gastrula stage shows that Fgf8 is a potent ear inducer while Fgf3 appears a much weaker one. In Foxi1 and Dlx3b-Dlx4b defective backgrounds, ear induction by Fgf8 beads diminishes. Over expression of Foxi1 and Dlx3b has little effect on ear induction by Fgf8 beads, likely because both factors are already broadly expressed in most non-neural ectoderm. In contrast, forced expression of either Sox9a or Sox9b induces multiple otic placodes, and ectopic induction requires only Dlx3b. Dlx and Sox proteins are absent from neural tissues during early stages of otic induction and Fgf8 beads are unable to induce differentiation of otic cells in these tissues even when Foxi1 and Dlx3b are over expressed. In contrast, Fgf8 beads can induce ectopic ear cells in the neural tube and spinal cord when Sox9a or Sox9b is over expressed.

Because Fgfs, Foxi1 and Dlx3b regulate expression of the *sox9a* and *sox9b* during otic development, we propose that Sox9 proteins integrate the Foxi1, Dlx3b-Dlx4b, and Fgf8 pathways to ensure that cells express the long-lasting competence factor, Dlx3b, and adopt and maintain an ear fate. (Fund from NIH)

## **[523] Ear or Skin? Wnt Signaling Mediates a Placode-Epidermis Fate Decision**

**Takahiro Ohyama<sup>1</sup>**, Othman Mohamed<sup>2</sup>, Makoto Taketo<sup>3</sup>, Daniel Dufort<sup>2</sup>, Andrew Groves<sup>1</sup>

<sup>1</sup>House Ear Institute, <sup>2</sup>McGill University, <sup>3</sup>Kyoto University

The otic placode, the anlagen of the inner ear, develops from an ectodermal field characterized by expression of the transcription factor Pax2. Previous fate mapping studies suggest that these Pax2<sup>+</sup> cells will give rise to both otic placode tissue and epidermis (Streit, Dev. Biol. 2002; Ohyama and Groves, Genesis 2004), but the signals that divide the Pax2<sup>+</sup> field into placodal and epidermal territories are unknown. We analyzed a reporter strain that carries six copies of TCF/Lef binding sites (Mohamed et. al., Dev. Dyn. 2004) which revealed that the canonical Wnt signaling pathway is normally activated in a subset of Pax2<sup>+</sup> cells. We also performed conditional inactivation of  $\beta$ -catenin in these cells and found an expansion of epidermal markers at the expense of the otic placode. Conversely, conditional activation of  $\beta$ -catenin in Pax2<sup>+</sup> cells causes an expansion of the otic placode at the expense of epidermis, and the resulting otic tissue expresses exclusively dorsal otocyst markers. Together these results suggest that Wnt signaling acts instructively to direct Pax2<sup>+</sup> cells to an otic placodal, rather than an epidermal fate, and promotes dorsal cell identities in the otocyst. Based on our present study, we propose a new model of inner ear induction that reconciles conflicting data from recent studies.

**524 The Role of Eya1 and Six1 in Mammalian Inner Ear Development: Insights Into the Developmental and Molecular Causes of Ear Defects Occurring in BOR Syndrome**

Dan Zou<sup>1</sup>, Derek Silvius<sup>1</sup>, Pin-Xian Xu<sup>1</sup>

<sup>1</sup>McLaughlin Research Institute

Eya1 encodes a transcriptional coactivator and has been shown to play an essential role during the development of mammalian auditory system. Mutations in the human EYA1 gene cause Branchio-Oto-Renal (BOR) syndrome, a congenital birth defect that accounts for as many as 2% of profoundly deaf children, and mice lacking Eya1 show an arrest of otic development at the otocyst stage. Six1, a member of the Six gene family homologous to Drosophila so, encodes a homeodomain protein and its gene product physically interacts with Eya1. During inner ear development, we found that Six1 functions downstream of and genetically interacts with Eya1. Interestingly, Six1-deficient mice show defects in all three parts of the ear similar to that observed in Eya1 mutants, and mutations in the human SIX1 gene also cause BOR syndrome. Furthermore, we have recently analyzed neurogenesis in otic placode to address whether Eya1 and Six1 are required for specifying the neuroblast precursors, for precursor cell survival or for inducing the expression of Neurog1. Our results show that neurogenesis of the inner ear is initiated normally in Eya1 and Six1 mutant embryos as judged by Neurog1 expression, but the mutant neuroblast cells that have not yet expressed SCG10 undergo abnormal cell death. Thus, during inner ear neurogenesis, Eya1 and Six1 appear to be dispensable for the initiation of neurogenesis but both may regulate the progressive differentiation of neuroblast precursor cells. Together, our analyses establish that both Eya1 and Six1 act as critical regulators for inner ear development and neurogenesis. These results provide important insights into the developmental and molecular causes of ear defects occurring in BOR syndrome.

**525 The Contrasting Roles of Two Notch Ligands in Development of the Mouse Inner Ear**  
**Rachael Brooker<sup>1</sup>, Katsuto Hozumi<sup>2</sup>, Julian Lewis<sup>3</sup>**

<sup>1</sup>Wellcome Trust Sanger Inst., <sup>2</sup>Tokai University School of Medicine, <sup>3</sup>Cancer Research UK

The sensory epithelium of the inner ear is composed of a regular array of hair cells separated from one another by supporting cells. The Notch signalling pathway is thought to control production of this pattern through a process of lateral inhibition. An additional, early role has recently been identified for Notch signalling in specifying sensory patches early in development. There are multiple Notch ligands expressed in the developing sensory patch, though the parts they play individually in patterning the inner ear are not clear. We have examined the functions of two of these Notch ligands, Delta1 and Jagged1, in the development of the inner ear using conditional knockout mice.

In the absence of Delta1, auditory hair cells are produced early and in excess, in agreement with the lateral inhibition hypothesis, but, surprisingly, supporting cells are also

overproduced. Delta1 conditional knockout mice also exhibit defects in the vestibular patches. While the cristae are present and appear normal, the maculae are lost or reduced. In the absence of Jagged1, the total number of hair cells in the cochlea is strongly reduced (although the number of inner hair cells is roughly doubled). This suggests that Jagged1 is required for the early function of Notch in establishing the sensory patches early in development. Jagged1 conditional knockout mice also exhibit a loss of several of the vestibular sensory patches, with the cristae being most severely affected.

In addition to effects on cell fate choices, it appears that each Notch ligand influences cell divisions during the development of the patch. These findings confirm that Notch signalling has two distinct functions in the inner ear, for which different ligands are primarily responsible.

**526 Noncanonical Wnt4 Signaling Inhibits Mechanosensory Hair Cell Formation in the Developing Mammalian Cochlea Through Protein Kinase C and Regulation of Math1**

Alain Dabdoub<sup>1</sup>, Erynn Layman<sup>1</sup>, Farhana Feroze-Merzouk<sup>1</sup>, Jennifer Jones<sup>1</sup>, Florence Naillat<sup>2</sup>, Seppo Vainio<sup>2</sup>, Jeffrey Rubin<sup>1</sup>, Matthew W. Kelley<sup>1</sup>

<sup>1</sup>NIH, Bethesda, MD, <sup>2</sup>University of Oulu

Normal cellular patterning in the organ of Corti is crucial for auditory function as over or under production of hair cells leads to hearing deficit. Here we identify the Wnt4 pathway as a cascade that inhibits hair cell formation in the mammalian cochlea. We analyzed Wnt4 signaling by characterizing the cochleae of Wnt4<sup>-/-</sup> mice and show an increase in the number of cells that develop as inner hair cells. In addition, in vitro studies demonstrate that application of Wnt4 protein results in inhibition of hair cell formation. The effect of Wnt4 is through the Wnt/PKC pathway as inhibition of PKC results in the formation of extra inner hair cells and PKC inhibition concomitantly with Wnt4 rescues the Wnt4 inhibitory effects. Further, by Western blot analysis we show that Wnt4 induces an increase in the phosphorylation level and hence activation of PKC thus demonstrating a direct role for Wnt4 in PKC activation in the cochlea.

Math1 has been shown to be necessary and sufficient for hair cell formation. To determine whether Math1 is a target of PKC we examined whether PKC inhibition leads to an increase in Math1 expression by quantitative RT-PCR. Expression of two supporting cell markers Hes1, expressed in inner phalangeal cells and Hes5, expressed in Deiter's cells, were also examined. Math1 and Hes1 increased by 48 hours after PKC inhibition, but not Hes5, consistent with an effect on inner, but not outer, hair cells. Also, using site-directed mutagenesis, we created a single point mutation in a PKC consensus site in Math1. We mimicked phosphorylation at the PKC consensus site by replacing threonine 197 with aspartate. We electroporated this mutated Math1 into cochlear explants and assayed its ability to induce hair cell formation. This single mutation abolished the ability of Math1 to induce hair cell formation.

We provide the first evidence for a role for Wnt4/PKC in the mammalian cochlea in regulating hair cell formation likely through modifying the activity of Math1.

### **527 Wild-Type Cells Rescue Genotypically Math1-Null Hair Cells in the Inner Ear of Chimeric Mice**

Xiaoping Du<sup>1</sup>, Patricia Jensen<sup>2</sup>, Daniel Goldowitz<sup>3</sup>, Kristin Hamre<sup>3</sup>

<sup>1</sup>University of Tennessee, <sup>2</sup>Harvard Medical School, <sup>3</sup>Univ. of Tenn. Health Sci. Center

The role of the transcription factor, Math1 in hair cell (HC) development has been considered to be a cell-intrinsic one in which only cells that express Math1 will become hair cells. We present evidence from chimeric mice that Math1 has a broader role in HC development. In chimeric mice, cells from genotypically wild-type and genotypically mutant embryos intermingle in a random fashion to form a single embryo. We examined the inner ears from Math1-null chimeric mice at various postnatal ages (P0 to P12.5). The hair cells (wild-type or mutant) were labeled by one of the hair cell-specific markers (myosin VIIa, calretinin and calbindin) while genotypically Math1-null cells were defined by beta-Galactosidase histochemistry or immunohistochemistry. The identification of Math1-null chimeras was determined by cerebellar phenotype and confirmed by PCR analysis of microdissected cells. Over 14 Math1-null chimeras were examined and in every case, genotypically Math1-null HCs were found in the cochlea and vestibular end-organs. These cells expressed appropriate HC markers providing evidence that these Math1-null cells are differentiating appropriately as hair cells. Several different genotypes were used as the wild-type component of the chimeric mice and all gave comparable results. These results suggest that the molecular pathway(s) that allow a cell to differentiate as a hair cell remain intact in genotypically Math1-null cells. Further, the presence of Math1 in the wild-type cells alters some aspect of the milieu, including cell-cell interactions, to create a permissive environment to allow these cells to differentiate as hair cells.

### **528 PCP Signaling During Inner Ear Morphogenesis**

Xiaowei Lu<sup>1</sup>

<sup>1</sup>University of Virginia

Sensory hair cells in the inner ear are polarized within the plane of the sensory epithelium, as defined by the orientation of the stereociliary bundles on their apical surfaces. In the cochlear sensory epithelium, this planar cell polarity (PCP) is coordinated among hair cells such that the stereociliary bundles adopt uniform orientation. This feature is essential for the correct perception of sound, and is regulated by an evolutionarily conserved, noncanonical Wnt signaling pathway. Recently, using a gene trap screen in the mouse, we identified PTK7, an atypical receptor tyrosine kinase, as a novel regulator of hair cell PCP. Interestingly, homologs of several vertebrate PCP genes, including PTK7, have not been implicated in PCP signaling in *Drosophila*, suggesting that vertebrates have evolved novel strategies to regulate PCP. To elucidate the precise role of PTK7 in PCP signaling during sensory hair cell development, we are trying to determine epistatic relationship between PTK7 and known PCP

genes using morphological and molecular readouts. Using immunohistochemistry, we characterized PTK7 expression pattern in the sensory epithelia during establishment of PCP. As hair cells differentiate, PTK7 is transiently enriched on the apical surface of the hair cells and subsequently become asymmetrically localized in a subset of hair cells. In addition, PTK7 appears to undergo post-translational modifications. We are investigating the functional significance and regulation of these molecular events. Details of our analysis will be presented.

### **529 EphB2 Regulates Growth of Auditory Axons at the Brainstem Midline**

Karina Cramer<sup>1</sup>, Shazia Siddiqui<sup>1</sup>

<sup>1</sup>University of California, Irvine

The control of axonal growth at the midline of the nervous system is an important aspect of circuit assembly. Several axon guidance molecules, including Eph receptors and their ligands, ephrins, play important roles in midline axon guidance. Axons emanating from neurons in the avian cochlear nucleus, nucleus magnocellularis (NM), branch and contact both ipsilateral and contralateral nucleus laminaris (NL). The ipsilateral branch contacts dorsal NL dendrites and the contralateral branch contacts ventral NL dendrites. This circuitry facilitates sound localization at low frequencies. The mechanisms that direct NM axon branches across the midline are not known. Here we examined the time course of NM axon growth at the midline and the expression of Eph family proteins at the midline during this growth. In addition, we misexpressed Eph receptors during development and evaluated the effects on axonal growth across the midline. We labeled NM cells at several ages using electroporation of GFP plasmids or in vitro dye labeling and found that NM axons reach the midline at about E4. Immunohistochemical studies showed that EphB receptors are absent at the midline at E3, and expression at the ventral margin of the midline begins at E4. Expression extends dorsally to the ventricular zone beginning at E5, but remains highest at the ventral midline. NM axons thus grow across the midline at a time when EphB receptor expression levels are low. Overexpression of EphB2 in the midline at E2 resulted in misrouted axons that deflected away from transfected midline cells. This effect suggests a predominantly non-cell autonomous reverse signaling role for EphB2. These data suggest an inhibitory role for midline Eph receptors, in which low levels at early ages permit axon growth and subsequently high levels prohibit growth after axons have crossed the midline. Supported by NIH DC005771.

### **530 A Gene Targeting Study Reveals the Mechanism That Defines the Details of Mammalian Otoconial Crystal Formation**

Hua Yang<sup>1</sup>, Xing Zhao<sup>1</sup>, Xiaona Huang<sup>1</sup>, Bernd Fritzsch<sup>2</sup>, Yesha (Yunxia) Lundberg<sup>1</sup>

<sup>1</sup>Boys Town National Research Hospital, <sup>2</sup>Creighton University School of Medicine

The presence of dense, crystallized extra-cellular matrix called otoconia is necessary for optimal stimulus input to

the sensory epithelium of the gravity receptors. In an effort to study the processes that regulate mammalian otoconia crystal growth, we employed a murine gene targeting strategy. Absence of Oc90, the main protein of otoconia, in mice lead to grossly abnormal otoconia crystallization and delayed vestibular functional development and balance deficits. Further analysis revealed the role of Oc90 in crystal seeding and in integrating a protein complex that defines the details of crystal formation including size, shape, number and stability. Initial examination showed no other histological abnormality of the inner ear in these mutant mice.

### **[531] BDNF in the Adult Auditory System**

**Marlies Knipper<sup>1</sup>**, Rama Panford-Walsh<sup>1</sup>, Wibke Singer<sup>1</sup>, José Morales García<sup>1</sup>, Lukas Ruettiger<sup>1</sup>, Iris Köpschall<sup>1</sup>, Karin Rohbock<sup>1</sup>, Ulrike Zimmermann<sup>1</sup>

<sup>1</sup>University of Tuebingen, ENT Clinic, Molecular Neurobiology

During embryonal development BDNF plays a crucial role for survival of the vestibular ganglia (Bianchi et al., 1996; Fritzsche et al., 1997, 1999; Pirvola & Ylikoski 2003). The role of BDNF for the adult inner ear, in particular for the mature cochlea is less understood. Disruption of trkB signalling pathways have been shown to lead to significant hearing loss (Schimmang et al., 2003), suggesting an important function of BDNF in the mature adult auditory system. Sensory-driven neuronal activity shapes developing circuits in sensory systems using the same key molecules and gene cascades up- and downstream of BDNF /trkB during development, experience mediated plasticity or during memory. Questioning an activity-dependent use of BDNF transcripts in the mature auditory system, we analysed BDNF expression in the peripheral and central auditory system during noise, injury and age. Surprising results became evident, which will be discussed controversially in the context of a role of BDNF for altered plasticity performance in the auditory system.

Acknowledgements: This work was supported by the Deutsche Forschungsgemeinschaft Kni 316/3-2 and Fortüne 816-0-0.

### **[532] L-NAC Does Not Protect B6 Mice from Age-Related Hearing Loss**

**Rickie Davis<sup>1,2</sup>**, Min-Wen Kuo<sup>2</sup>, Susan Stanton<sup>2</sup>, Barbara Canlon<sup>3</sup>, Edward Krieg<sup>1</sup>, Kumar N. Alagramam<sup>4</sup>

<sup>1</sup>NIOSH, <sup>2</sup>University of Cincinnati, <sup>3</sup>Karolinska Institutet,

<sup>4</sup>Case Western Reserve Medical School

The C57BL/6J mouse (aka B6) is homozygous for the age-related hearing loss allele (ahl) which causes them to begin losing hearing at about 3 months of age.

N-acetyl-L-cysteine (aka L-NAC) has been shown to protect the ear from noise-induced hearing loss in chinchillas. This is hypothesized to be due to the ability of L-NAC to cross the blood brain barrier and serve as the precursor to glutathione—the body's natural reactive oxygen species scavenger.

Twelve four-week old female B6 mice were divided into two groups—one group received a daily water change

including dissolved L-NAC (1 mg/ml) and a control group receiving just a daily water change. Water consumption was monitored.

Auditory brainstem responses for 4, 8, 16 and 32 kHz tone bursts were measured monthly until the mice were 8 months of age. Upon completion of the final ABR, mice were sacrificed, cochleae taken and prepared for quantitative whole mount morphological analysis.

Hearing loss was measurable in both groups at 16 and 32 kHz. Neither ABR thresholds nor cytochrome c oxidase differed significantly between the two groups.

We conclude that L-NAC, at the concentration used here, does not protect against hearing loss in mice from the effects of the ahl allele.

Research supported by a grant from the University Hospitals of Cleveland to KA.

"The findings and conclusions in this presentation have not been formally disseminated by NIOSH and should not be construed to represent any agency determination or policy."

### **[533] Cochlear Current Injection Restores Hearing in the Furosemide-Treated Ear**

**Richard A. Schmiedt<sup>1</sup>**, Hainan Lang<sup>2</sup>, Francis Spelman<sup>3</sup>, Tim Johnson<sup>3</sup>, Matt Carson<sup>3</sup>, Scott Corbett<sup>3</sup>

<sup>1</sup>Dept. of Otolaryngology--Head and Neck Surgery, Medical University of SC, Charleston, SC, <sup>2</sup>Dept. of Pathology and Laboratory Medicine, Medical University of SC, Charleston, SC, <sup>3</sup>Advanced Cochlear Systems

We have shown that a hallmark of the presbycusis ear is a decreased endocochlear potential (EP) in scala media (SM) caused by the degeneration of the lateral wall and stria vascularis. An animal model of presbycusis that replicates age-related EP loss uses furosemide to reversibly block the EP generator in the stria vascularis (Schmiedt et al, J Neurosci, 22:9643-9650, 2002). The furosemide can be delivered to the cochlea chronically with an osmotic pump via a cannula, or, as was done here, acutely by intraperitoneal injection. With the decreased EP, the neural audiogram in the gerbil obtained with the compound action potential (CAP) mimics the profile seen with human presbycusis: a flat 15-20 dB hearing loss at low frequencies coupled with a sloping hearing loss at higher frequencies. To ameliorate this type of stria hearing loss, we have developed a stimulating system allowing direct currents of at least 10  $\mu$ A to be injected continuously for up to 12 hours into the gerbil cochlea. One micropipette is used to measure the EP through the round window; a second micropipette placed in the first turn is used to inject the current into SM. Injecting anodal (positive) current directly into SM as referenced to body ground increases the EP and can restore neural thresholds to their pre-furosemide values. With this electrode configuration, the effective resistance describing the voltage / current relationship is typically between 2 and 5 kohms. Thus a 10  $\mu$ A current will increase the basal EP by 20 to 50 mV with corresponding improvements in neural thresholds of 10 to 20 dB at low frequencies and up to 40 dB at high frequencies. Our results also show that neural threshold shifts caused by hair cell injury during electrode placement



are not responsive to the injected current, unlike the neural shifts caused by a decreased EP as the result of strial dysfunction.

[Work supported by NIH grants R01 AG014748 and R43 DC005531.]

### **534 Age-Related Accumulation of Mitochondrial DNA Mutations Leads to Early Onset of Presbycusis in Mitochondrial Mutator Mice**

**Shinichi Someya**<sup>1,2</sup>, Tatsuya Yamasoba<sup>2</sup>, Masaru Tanokura<sup>2</sup>, Tomas Prolla<sup>1</sup>

<sup>1</sup>University of Wisconsin-Madison, USA, <sup>2</sup>University of Tokyo

Presbycusis is characterized by an age-associated progressive decline of auditory function, and is associated with inner ear pathology in mammals. Presbycusis arises mainly from the degeneration of hair cells or spiral ganglion cells in the cochlea. However, the molecular mechanisms of presbycusis remain unknown. Mutations in mitochondrial DNA (mtDNA) accumulate in tissues of mammalian species and have been hypothesized to contribute to age-associated diseases. We created *PolgA*<sup>D257A/D257A</sup> (D257A) mice which express a proof-reading deficient version of the mitochondrial DNA polymerase  $\gamma$  (POLG), accumulate mtDNA mutations during aging, and display features of accelerated aging (Science. 309, 481-484, 2005). The mutant mice had a reduced lifespan (D257A maximum survival, 460 days; median survival, 416 days; compared to maximum and median survival >850 days for WT littermates,  $P < 0.0001$ ). Presbycusis is a hallmark of aging in multiple species, including mice and humans, and has been correlated with the age-related accumulation of mtDNA mutations in auditory tissue. We conducted ABR analysis and observed no difference in auditory function between WT and D257A mice at 2 months of age, but found marked elevation of ABR thresholds at 4, 8 and 16kHz ( $P < 0.0001$ ) in D257A mice by 9 months of age, indicating severe hearing loss. Histological analysis revealed age-related loss of hair cells and spiral ganglion cells, a feature of presbycusis. Thus, accumulation of mtDNA mutations can have a causal role in presbycusis. Because the cochleae were severely affected in D257A mice, we next examined the effects of mtDNA mutations on apoptotic marker genes in the cochlea by conducting gene expression analysis using high-density oligonucleotide microarrays representing 45,037 genes and ESTs. A comparison of cochlea from WT and D257A mice revealed that 22 apoptotic marker genes were up-regulated in the D257A. We then examined the cochlea using the terminal transferase-mediated dUTP nick-end labeling (TUNEL) assay which detects apoptotic cells in situ. The 9 month-old D257A mice showed significantly more TUNEL positive cells compared to WT mice in the cochlea examined. Together, these findings suggest that loss of critical, irreplaceable cells in the cochlea through apoptosis is associated with the accumulation of mtDNA mutations. Our findings also suggest that apoptosis and subsequent loss of irreplaceable cells may be an important mechanism of presbycusis in mammals.

### **535 Accelerated Hearing Loss and Auditory Neuronal Degeneration in Mitochondrial DNA Mutator Mice**

Xianzhi Niu<sup>1</sup>, Aleksandra Trifunovic<sup>2</sup>, Nil-Göran Larsson<sup>2</sup>, **Barbara Canlon**<sup>1</sup>

<sup>1</sup>Dept. of Physiology and Pharmacology, Karolinska Institute, Sweden, <sup>2</sup>Dept. of Medical Nutrition, Novum, Karolinska Institute, Sweden

Mitochondrial DNA (mtDNA) mutations are a major cause underlying cellular respiratory chain deficiency and results in tissue pathogenesis in neurodegenerative disorders. In the present study, experimentally created knock-in mice with a proof-reading-deficient version of PolgA, the nucleus-encoded catalytic subunit of mtDNA polymerase, were used to investigate the effects of aging on the auditory system. The general aims of this project are: (1) to determine auditory function in the mtDNA mutant mice using auditory brainstem responses (ABR) and distortion product otoacoustic emissions (DPOAE); (2) to quantify neuronal loss in spiral ganglia neurons and the cochlear nucleus using stereological techniques; (3) to quantify the degree of apoptosis using activated caspase-3 immunostaining and TUNEL staining. The results show that mtDNA-mutator mice at 6 and 10 months have significantly higher ABR and DPOAE thresholds compared to their age-matched controls. The mtDNA-mutator mice have a significantly greater loss of neurons in the spiral ganglia, dorsal cochlear nucleus, and posteroventral cochlear nucleus. The activated caspase-3 and TUNEL positive neurons were more numerous in the spiral ganglia neurons in the mutant mice compared to wild type mice. Our results indicate that an increase in mtDNA mutations results in premature age-induced auditory degeneration and hearing loss.

Acknowledgments: This study was supported by grants from the Swedish Medical Research Council, and the Stiftelsen Tysta Skolan.

### **536 Growth of Neurites from Explants of Adult Rodent Spiral Ganglia**

**Marivi Bartolome**<sup>1</sup>, Kwang Pak<sup>2</sup>, Eduardo Chavez<sup>2</sup>, Stefan Dazet<sup>3</sup>, Pablo Loyzaga<sup>1</sup>, Allen F. Ryan<sup>2</sup>

<sup>1</sup>University Complutense of Madrid, <sup>2</sup>University of California, San Diego, <sup>3</sup>University of Bochum, Germany.

The reason for cochlear neuronal loss with increased age is not clear. However, it may involve reduction in trophic maintenance that is normally supplied by the hair cells to which the neurons are connected. Cochlear hair cells produce the neurotrophic factors; these factors are taken up by the dendrites of SG neurons through their specific receptors, and they mediate neuronal survival. There is very little information available on neurotrophic signaling in the aging inner ear. However, it seems possible that neurotrophin receptor expression decreases with age in these neurons, as it does in brain.

The growth of neurites from the spiral ganglion explants during cochlear rat development has been extensively studied. Spiral ganglion neurites respond to a variety of guidance and survival factors, including neurotrophic growth factors, extracellular matrix molecules. Therefore,

information based on the responses of immature neurons may not be applicable to older neurons.

The ganglion achieves adult morphology at around 20 days after birth. Initial experiments indicated that explants from 21-day-old animals failed to attach and/or to extend neurites in culture, using protocols developed for neonatal spiral ganglia. We therefore altered the extracellular matrix molecules, and used additional neurotrophic factors, in an attempt to promote improved adherence and neurite extension. With these changes, neurite extension from 21 to 30 day explants achieved. Explants obtained from 3, 5, 9, 12, 15 and 18 month old spiral ganglia were substantially less successful. Few neurites exited the explants, and remained within the borders often circling the edge. The results suggest that before older neurites can be studied in vitro, methods to allow them to exit the explant must be improved.

Supported by: Complutense University grants: Beca Amo 2004, Research Project 2005, Movilidad Profesores 2005 (Spain); NIH grant DC00139 and the Research Service of the VA (US).

### **[537] Auditory Processing Deficits in K<sup>+</sup> Channel Knockout Mice**

**Jared R. Spencer<sup>1</sup>, Xiaoxia Zhu<sup>1</sup>, Robert D. Frisina<sup>1</sup>**

<sup>1</sup>*Otolaryngology Dept., Univ. Rochester Med. Sch., Int. Ctr. Hearing Speech Res.*

Presbycusis is one of the most prevalent chronic medical conditions of our geriatric population. While presbycusis leads to raised hearing thresholds, the main complaint is difficulty perceiving speech in background noise. Recent evidence suggests that voltage-gated potassium channels (Kv) play crucial roles in the precise encoding of auditory temporal information. Kv3.1 and Kv1.1 have been found in uniquely high concentrations within the auditory brainstem, including areas of the medial olivocochlear (MOC) efferent system, presumed to play a role in preserving cochlear function and enhancing signal detection in noise. Studies have suggested a decline in expression of these channels with age and with diminished cochlear input. We hypothesize that alterations in Kv3.1 and Kv1.1 contribute to age-related sensory declines. The objective of the present study was to determine if deficiencies in Kv1.1 lead to alterations in the MOC efferent system and outer hair cell function, as measured by contralateral suppression (CS) of distortion product otoacoustic emissions (DPOAEs) and baseline DPOAEs, respectively.

Declines in the above measures have been correlated with age-related hearing loss. Kv1.1 mice were obtained at a young adult stage (1-2 mon) and divided into 3 groups, including (-/-), (+/-), and (+/+) genotypes. Auditory brainstem responses were obtained to assess overall hearing abilities. Mice were anesthetized and 2f1-f2 DPOAE recordings obtained in quiet and in the presence of a contralaterally applied wideband noise. Findings on several Kv1.1 knockout mice (-/- n=4, +/- n=6, +/+ n=4) demonstrated statistically significant reductions in DPOAE amplitude ( $P < 0.0001$ ) and CS ( $P = 0.0056$ ). Kv1.1 knockout mice show deficiencies in the MOC efferent system as well as outer hair cell function. Alterations in

Kv1.1 may spark MOC efferent system decline, leading to declines in outer hair cell function and higher hearing thresholds.

Work supported by NIH: NIA & NIDCD

### **[538] A Mouse Model of Strial Presbycusis**

**Kevin K. Ohlemiller<sup>1</sup>, Patricia M. Gagnon<sup>1</sup>**

<sup>1</sup>*Washington University Dept. of Otolaryngology*

Degeneration of stria vascularis and reduction in endocochlear potential (EP) underlie some age-related hearing loss (ARHL). Strial ARHL has resisted study because it may not promote a fixed audiogram shape and archetypal temporal bones are few. While a familial component has been speculated, there are no candidate genes. Microvascular disease is proposed to play a role. Presently there exists one well-characterized animal model, the gerbil (e.g., Schulte and Schmiedt, HR 1992; Spicer and Schulte, HR 2002). More animal models, particularly mouse models, of strial ARHL may help identify common degenerative events, and possibly candidate genes.

BALB/c mice show neither strial pathology nor EP reduction by 13 mos of age (Ohlemiller, JARO 2002). By 19 mos, however, we found that roughly half of BALBs show a 20-50 mV EP reduction. Since C57BL/6 (B6) mice show little EP reduction by 24 mos, we compared measures of stria and ligament in young (<6 mos) and old (17-24 mos) B6 and BALBs. We reasoned that age-related changes uncorrelated to EP in B6 could be ruled out as significant contributors to EP reduction in BALBs.

Marginal cell density was an excellent predictor of the EP across ages in BALBs ( $R^2 = .69$ ). Spiral ligament thickness was also correlated with EP ( $R^2 = .53$ ). Factors that poorly predicted EP included ligament fibrocyte density, basal and intermediate cell density, and vascular parameters such as capillary density/diameter and basement membrane thickness. Age-related vascular changes tended to be greater in B6 than in BALBs. Our results suggest that marginal cell pathology is the primary cause of BALB EP reduction with age. BALBs may carry one or more alleles that impact marginal cell survival or replacement. Tests in congenic mice indicate these exclude otocadherin, agouti, and tyrosinase loci. Our findings independently support recent work in gerbils (Spicer and Schulte, HR 2005) also favoring a marginal cell, not vascular, origin for some strial ARHL.

### **[539] Characterization of a New Allele of Ames**

**Waltzer, Pcdh15 Av-6J**

**Qing Zheng<sup>1</sup>, Hu Yu<sup>1</sup>, Karen S. Pawlowski<sup>2</sup>, Yayoi S. Kikkawa<sup>2</sup>, Charles G. Wright<sup>2</sup>, Jesse Washington<sup>3</sup>, Lauren Kiskey<sup>3</sup>, Kumar N. Alagramam<sup>3</sup>**

<sup>1</sup>*The Jackson Laboratory, Bar Harbor, ME, USA*, <sup>2</sup>*UT Southwestern Medical Center*, <sup>3</sup>*Case Western Reserve University*

We have characterized a new allele of protocadherin 15 gene that arose as a spontaneous mutation at The Jackson Laboratory. The new allele was shown to be deaf by ABR analysis at 4 weeks of age. The mutation was

proven to be recessive by outcross to unrelated B6 mice with a production of 21/21 normal phenotype mice. F2 progeny (n=102) were generated by intercrossing with CAST/Ei mice. The homozygous mutant F2 progeny (n=32) were used for genetic mapping. The mutation was mapped between markers D10Mit31 and D10Mit42. A complementation test with av-3J (a mutation of *Pcdh15*) confirmed allelism. The new allele has been designated *Pcdh15av-6J*. An allelic series of *Pcdh15* provides an opportunity to carry out structure-function analysis of the encoded protein. Systematic study of inner ear pathology in different alleles combined with new findings on the nature of the mutation in *Pcdh15* in those alleles will help us understand a) the function of *Pcdh15* in hair cell development and b) the cause of inner ear disorders in USH1F and DFNB23 patients.

*Pcdh15av-6J* mutants are deaf and they display circling and abnormal swimming behavior. Abnormalities of cochlear hair cell stereocilia are apparent in *Pcdh15av-6J* mutants at 5 and 10 days after birth (P5 and P10). By P20, there are clear degenerative changes involving the entire organ of Corti with loss of sizable numbers of inner and outer hair cells. These changes advance to complete degeneration of the organ of Corti over large areas of the cochlea by P40, at which time there is also significant loss of spiral ganglion cells in the most severely affected regions. Efforts are currently underway to supplement these findings with transmission electron microscopy and to identify the mutation in the *Pcdh15av-6J* allele. Results obtained thus far support our previous findings indicating that *Pcdh15* plays an important role in hair-bundle morphogenesis and maintenance of the organ of Corti. This work was supported by NIDCD grant DC05385 to KA.

#### **540 Identification of 12 Mutant Mouse Strains with High-Frequency Hearing Loss in the TMGC ENU-Mutagenesis Screen**

**Mohammad Habiby Kermany**<sup>1,2</sup>, Lisan Parker<sup>1</sup>, Yun-Kai Guo<sup>1,2</sup>, Darla Miller<sup>3</sup>, D.J. Swanson<sup>4</sup>, Tai June Yoo<sup>2</sup>, Daniel Goldowitz<sup>4</sup>, Jian Zuo<sup>1</sup>

<sup>1</sup>Dept. of Developmental Neurobiology, St. Jude Children's Research Hospital, Memphis, TN, <sup>2</sup>Dept. of Medicine, Health Science Center, University of Tennessee, <sup>3</sup>Life Sciences Division, Oak Ridge National Laboratory, <sup>4</sup>Dept of Anatomy and Neurobiology, University of Tennessee, Health Science Center, Memphis, TN, USA

Ethyl-n-nitrosourea (ENU) is a mutagen that introduces single base-pair changes in the genome. The Tennessee Mouse Genome Consortium (TMGC) employed an ENU-mutagenesis scheme to identify mouse recessive mutants with neural phenotypes. As a primary screen for auditory phenotypes in the TMGC neuromutagenesis program, we employed auditory brainstem responses (ABR) to click and 8, 16, and 32 kHz stimuli. In the past 3 years, we have screened 284 pedigrees (1,620 mice). 22 pedigrees (7.74%) showed abnormal hearing phenotypes varying from unilateral to bilateral deafness, mild to severe hearing loss in low, middle or high frequencies. For putative mutant pedigrees, we measured at least 4-6 mice per pedigree and the pedigree-average ABR thresholds needed to be larger than 1.7 x standard deviation (SD) among all offspring from the same parental strain; for mutants, we

required at least 12-18 mice of both genders in more than three generations and larger than 2.0 x SD. Using these criteria, 12 pedigrees (4.22%) have been defined as mutants. All 12 mutants displayed high frequency hearing loss. Interestingly, 2 mutants showed sex-biased hearing loss with only females being affected and 3 mutants displayed wide range frequency hearing loss. Temporal bone histology of the 12 mutants revealed different morphological defects: absence of cochlea, degenerations of outer, inner hair cells, and supporting cells, degeneration of spiral ganglia, or the smaller size of the cochlea and organ of Corti. Interspecific and intraspecific genetic crosses have been set up to map the mutant loci. In contrast to other ENU mutagenesis screens, our screen identified frequency specific as well as mild hearing defects. We also identified sex-biased defects likely due to modifiers in sex chromosomes or off-target mutations. These mutants thus serve as models for high-frequency hearing loss, one of the most common progressive hearing disorders in humans. (Supported by 5 U01MH061971 & R01DC06471).

#### **541 Intracochlear Injection of Adenovirus Vector to a Mouse Model Created by a Conditional Knockout of *Gjb2* Gene**

Takashi Iizuka<sup>1</sup>, Sho Kanzaki<sup>2</sup>, Zhen-Hua Jin<sup>1</sup>, Yuya Narui<sup>1</sup>, Osamu Minowa<sup>3</sup>, Tetsuo Noda<sup>4</sup>, Kaoru Ogawa<sup>2</sup>, **Katsuhisa Ikeda**<sup>1</sup>

<sup>1</sup>Juntendo University, <sup>2</sup>Keio University, <sup>3</sup>Mouse Functional Genomics Research Group, Riken, <sup>4</sup>Department of Molecular Biology, Cancer Institute

Hereditary deafness affects about 1 in 2,000 children and mutations in the *GJB2* gene are the major cause in various ethnic groups. *GJB2* encodes connexin26, a putative channel component in cochlear gap junction. However, the pathogenesis of hearing loss caused by the *GJB2* mutations remains obscure. The generation of a mouse model to study the function of connexin26 during hearing has been hampered by the fact that *gjb2* knockout mice are embryonic lethal. We generated targeted disruption of *gjb2* using Cre recombinase controlled by P0. We examined the potential of gene therapy in the inner ear, using the mutant mice, the control mice and wild type mice.

For the mouse, three main routes of delivery are possible, namely basal turn approaches (via a cochleostomy), semicircular canal approaches and round window approaches. We chose basal turn approaches to examine the expression in organ of Corti and lateral wall. Adenoviral vectors carrying the green fluorescent protein (GFP) gene were injected into the basal turn of cochlea. Auditory brainstem responses were measured at preoperation and postoperation.

The homozygous mutant mice had an average hearing threshold 70-80dB at 8, 12, 16, 20 kHz at preoperation, which was further elevated over 90dB after operation. Injection of vector to the heterozygous mutant mice and wild type mice resulted in 40-60dB threshold elevation.

The expression of GFP was noted in the organ of Corti of the inner ear in both the homozygous and the heterozygous mutant mice.

The injection technique for hearing preservation should be considered. However, our data suggests that the adenovirus mediated gene transduction may be successful in the inner ear of *gjb2* knockout mice.

#### **542 Mapping Quantitative Trait Loci for Hearing Loss in Black Swiss Mice**

Meghan Drayton<sup>1</sup>, Konrad Noben-Trauth<sup>1</sup>

<sup>1</sup>NIDCD

In common inbred mouse strains, hearing loss is a highly prevalent quantitative trait, which is mainly controlled by the *Cdh23*53A variant and alleles at numerous other strain-specific loci. We investigated the genetic basis of hearing loss in non-inbred strains. Outbred mice of Swiss Webster, CF-1, NIH Swiss, ICR, and Black Swiss strains exhibited distinct hearing profiles characteristic of progressive, sensorineural hearing impairment. By quantitative trait locus (QTL) mapping of backcross and intercross progeny, we identified three QTLs underlying hearing loss in Black Swiss mice: a main-effect QTL mapped to chromosome (chr) 10 (named *ahl5*, peak association 42cM) and two moderate QTLs were localized to chr 13 (*ahl6*, 24cM) and chr 18 (*ahl7*, 44cM). The *ahl6* and *ahl7* QTLs exerted a synergistic modifying effect on *ahl5* expression. Backcross progeny homozygous at all three QTLs reconstituted the parental Black Swiss phenotype. Cadherin 23 (*Cdh23*) and protocadherin 15 (*Pcdh15*), mapping near or within the 95% confidence interval of *ahl5*, bear nucleotide polymorphisms in coding exons, but these appear to be unrelated to the hearing phenotype.

#### **543 Expression of Recombinant Tectorin Fragments In Vitro and an Analysis of Their Interactions**

Gowri D. Nayak<sup>1</sup>, Hilary J. Pollard<sup>1</sup>, Yves A. Muller<sup>2</sup>, Janet L. Cyr<sup>3</sup>, P. Kevin Legan<sup>1</sup>, Guy P. Richardson<sup>1</sup>

<sup>1</sup>University of Sussex, UK, <sup>2</sup>Friederich-Alexander-Universität, <sup>3</sup>WVU School of Medicine

The tectorins, *Tecta* and *Tectb*, are major non-collagenous glycoproteins of the tectorial membrane. Together they form the striated-sheet matrix, a structure composed of alternating light and dark-staining filaments linked by cross-bridges. *Tectb* is composed of a single zona pellucida (ZP) domain, whereas *Tecta* is composed of an N-terminal entactin G1-like domain, three full and two partial von Willebrand Factor (vWF) type D repeats and a C-terminal ZP domain. ZP domains are found in a number of filament-forming proteins and we have proposed models for the structure of the striated-sheet matrix based on potential *Tecta* and *Tectb* interactions (Legan et al *J Biol Chem* 272:8791-8801, 1997). We are investigating the use of prokaryotic and eukaryotic expression systems for the production of recombinant tectorin fragments and to analyse their interactions. Bacterial expression systems have thus far failed to produce significant amounts of soluble tectorin fragments. To explore the solubility of tectorin fragments in a mammalian expression system we used pCEP-pu vectors, which use the signal peptide from BM40 to target the protein of interest to the secretory

pathway (Kohfeldt et al *FEBS letters* 414:557-561, 1997). When recombinant tectorin fragments were expressed in HEK 293 EBNA cells, high levels of soluble protein were secreted into the culture medium. SDS-PAGE of the *Tectb* ZP domain expressed in this system shows that it forms oligomers under non-reducing conditions. Inclusion of the external hydrophobic patch (Jovine et al *Proc Natl Acad Sci USA* 101:5922-5927, 2004) greatly increases the amount of monomeric protein observed. Co-transfection, followed by immunoprecipitation and western blotting shows that the *Tecta* and *Tectb* ZP domains interact and that the *Tecta* ZP domain and the vWF D1-D4 domains interact. The identification of interactions between the domains of *Tecta* and *Tectb* will allow a refinement of the models for striated-sheet matrix structure.

Supported by the Wellcome Trust and NIDCD R01DC006402

#### **544 Generation of a Mouse Knockout Allele of Transmembrane Channel-Like Gene 1 (TMC1)**

Kiyoto Kurima<sup>1</sup>, Kotaro Ishikawa<sup>1</sup>, Thom Sounders<sup>2</sup>, Andrew Griffith<sup>1</sup>

<sup>1</sup>National Institute on Deafness and Other Communication Disorders, Rockville, MD, <sup>2</sup>University of Michigan

Dominant and recessive mutations of transmembrane channel-like gene 1 (*TMC1*) cause nonsyndromic sensorineural hearing loss at the *DFNA36* and *DFNB7/B11* loci, respectively. Similarly in mice, dominant and recessive mutations of *Tmc1* cause SNHL in the Beethoven (*Bth*) and deafness (*dn*) mouse lines, respectively. These strains segregate an amino acid substitution (M415K) in *Tmc1*<sup>Bth</sup> and a deletion of exon 14 in *Tmc1*<sup>dn</sup>. We have created a *Tmc1*-knockout mouse line (*Tmc1*<sup>KO</sup>) by homologous recombination to replace exons 8 and 9 with a gene trap cassette and a beta-galactosidase reporter gene. Homozygous *Tmc1*<sup>KO</sup> mice are congenitally deaf, while heterozygous mice have no detectable hearing loss in comparison to wild-type littermates as measured by ABR threshold analysis. X-gal staining of whole-mounted inner ears from homozygous *Tmc1*<sup>KO</sup> mice revealed strong staining in inner and outer hair cells beginning at postnatal day 8 (P8). At P20, outer hair cells in the basal turn of the cochlear duct begin to fail to stain with X-gal. The loss of staining of outer hair cells and, to a lesser extent, inner hair cells then progresses toward the apical turn of the cochlear duct. The

progressive loss of X-gal staining of *Tmc1*<sup>KO</sup> outer hair cells may be due to down-regulation of *Tmc1* expression, or it may reflect the rapid degeneration of hair cells that has previously been documented for *Tmc1*<sup>dn</sup> mice, which contrasts with the progressive loss of inner hair cells in *Tmc1*<sup>Bth</sup> mice. *Tmc1*<sup>KO</sup> mice will be a useful model to investigate the basis of hair cell degeneration and hearing loss caused by *Tmc1* mutations, and to elucidate the expression and function of TMC1 protein in inner ear hair cells.

## **545 Transmembrane Topologic Organization of TMC1**

Valentina Labay<sup>1</sup>, Rachel McNamara<sup>1</sup>, Tomoko Makishima<sup>1</sup>, Andrew Griffith<sup>1</sup>

<sup>1</sup>NIH-NIDCD, Maryland

Dominant and recessive mutant alleles of trans-membrane channel-like gene 1 (TMC1/Tmc1) cause hearing loss in humans and mice. Tmc1 is expressed in cochlear and vestibular hair cells. TMC1 is the founding member of a novel gene family with seven additional members in mammals, all of which are predicted to encode proteins with 6 to 10 trans-membrane (TM) domains and a novel, conserved region termed the TMC domain. At present, little is known about the function of mouse TMC1 (mTMC1). To provide a foundation for identifying the function and potential interacting protein partners of mTMC1, we defined the trans-membrane topologic organization of mTMC1 heterologously expressed in Cos7 cells. GFP-tagged mTMC1 is expressed in Cos7 cells in a reticular pattern consistent with the location of the endoplasmic reticulum (ER). We used an established method for studying membrane protein topology in the ER of intact cells: after formaldehyde fixation, Cos7 cells were selectively permeabilized using either the mild detergent digitonin or the stronger detergent Triton X-100. Digitonin at low concentration permeabilizes only the plasma membrane whereas Triton X-100 at high concentration permeabilizes both the plasma and internal membranes. This technique allowed us to monitor the location of various antigenic sites within mTMC1 with immunofluorescence microscopy. We generated a series of Tmc1 cDNA expression constructs with a hemagglutinin (HA) epitope tag inserted in predicted hydrophilic loop regions. Using antibodies against various regions of mTMC1 and against the inserted HA tag, we defined the TM domains and topologic orientation of internal loops of mTMC1. Our model suggests that mTMC1 in the ER contains six TM domains, and the N- and C- termini of mTMC1 and a large loop containing the TMC domain are cytoplasmically oriented. We are currently repeating these experiments in an additional cell line to confirm this model of mTMC1 topology.

## **546 Characterization of Two Mouse Strains with Inherited Inner Ear Dysfunction**

Kristina L. Hunker<sup>1</sup>, Lisa A. Beyer<sup>1</sup>, Margit Burmeister<sup>1</sup>, Donna M. Martin<sup>1</sup>, Yehoash Raphael<sup>1</sup>, David C. Kohrman<sup>1</sup>

<sup>1</sup>University of Michigan Medical School

We have characterized two new strains of mice with distinct defects in inner ear structure and function. Both arose spontaneously on inbred strain backgrounds. Affected *burm* mice lack a startle reflex and auditory brainstem responses (ABRs) to pure tones, indicating profound sensorineural hearing loss. They also exhibit bi-directional circling behavior, consistent with dysfunction of the vestibular system. Gross inner ear structure is normal in affected mice. Outer hair cells are largely missing by 2 months of age; inner hair cells are intact, although stereocilia exhibit decreased actin filament content. This

pathology suggests defects in pathways critical for maturation or maintenance of normal sensory cell function. Breeding studies are consistent with a single, autosomal recessive locus as the basis for the *burm* phenotype. Mice of the *Mac* strain also exhibit circling behavior, indicating vestibular dysfunction, but retain normal ABR thresholds until at least 3 months of age. Adult *Mac* mice exhibit fusion of the cristae of the superior and lateral semicircular canals of the inner ear, indicating a likely developmental defect that contributes directly to the circling behavior. The mutant phenotype segregates as an autosomal dominant locus with reduced penetrance. Genetic linkage studies for both mutant strains are in progress. Identification of the affected genes is likely to provide new insight into genetic control of development and function of the inner ear.

Supported by NIH-NIDCD grant P30-DC05188.

## **547 Expression and Mutation Analysis of Grxcr1, the Gene Affected in the Mouse Deafness Mutant Pirouette, and a Related Gene, Grxcr2**

Kristina L. Hunker<sup>1</sup>, Lili Zheng<sup>2</sup>, Inna A. Belyantseva<sup>3</sup>, Lisa A. Beyer<sup>1</sup>, Yehoash Raphael<sup>1</sup>, Thomas B. Friedman<sup>3</sup>, James R. Bartles<sup>2</sup>, David C. Kohrman<sup>1</sup>

<sup>1</sup>University of Michigan Medical Center, <sup>2</sup>Northwestern University, <sup>3</sup>National Institutes of Health

The mouse mutant *pirouette* (*pi*) exhibits profound hearing loss and circling behavior inherited as recessive traits. Previous studies have demonstrated abnormally thin stereocilia during sensory cell maturation in the inner ears of *pi/pi* homozygotes. The defective gene in *pi* mice, *Grxcr1*, is expressed in neuroepithelial cells in the cochlea and encodes a 290 amino acid protein that contains two recognizable domains: a central region of similarity to glutaredoxins, enzymes that reduce oxidized cysteines on cellular proteins during normal homeostasis and under oxidative stress conditions; and a C-terminal cysteine-rich region.

Transfection experiments with *Grxcr1*-GFP expression constructs have demonstrated a close association of GRXCR1 with actin filament-rich structures on the dorsal/apical surface of cultured fibroblast and epithelial cells. Analysis of GRXCR1 mutant proteins indicated that the glutaredoxin and cysteine-rich domains are not required for this localization, while the novel N-terminal region of the protein is necessary and sufficient. Transfection of *Grxcr1* constructs into cochlear explants from neonatal mice indicated localization of GRXCR1 within stereocilia of inner and outer hair cells. In transfected non-sensory epithelial cells of the explants, GRXCR1 was localized in apical microvilli, which were substantially elongated compared to microvilli in untransfected cells. Along with the distinctive pathology in *pi* mutants, these studies are consistent with a role for GRXCR1 in controlling actin cytoskeletal architecture in the apical region of hair cells. A paralogous gene, *Grxcr2*, which exhibits an inner ear-specific expression pattern similar to that of *Grxcr1*, also localizes to actin filament-rich structures in transfected cells, suggesting that it may play a similar role in the inner ear.

Supported by NIH-NIDCD grants P30-DC05188, RO1-DC004314 (JRB), and RO1-DC03049 (DCK, YR, and JRB) and NIDCD Intramural 1Z01DC000039-09 (TBF).

#### **[548] A Mouse Organ of Corti cDNA Microarray**

Anne Giersch<sup>1,2</sup>, Anne Kasper<sup>1</sup>, Cynthia Morton<sup>1,2</sup>

<sup>1</sup>Brigham and Women's Hospital, <sup>2</sup>Harvard Medical School, Boston, MA

Microarrays are a powerful technique to monitor expression of thousands of genes simultaneously. Arrays may be used to study gene expression changes during development, expression differences between tissues, or for comparisons of healthy and diseased tissues. Both commercial and "home made" custom arrays are available in several different platforms, such as oligonucleotides or cDNAs. Each system has its own advantages and disadvantages, including variations in cost, reproducibility, and ease of use.

We have used the NIH mouse organ of Corti cDNA library to create a custom cDNA microarray. Representative cDNAs from each gene found in the library are included on the array, as well as additional genes known to have a role in hearing or deafness that were not among the library collection of clones. In total, over 6000 individual organ of Corti expressed genes are included on the array. Many cDNAs represent well characterized genes whereas other transcripts are completely unknown expressed sequence tags (ESTs). Data characterizing the quality of the array and results of initial studies using the mouse organ of Corti cDNA microarray array in an experimental system will be presented.

Acknowledgments: We appreciate funding from the NIDCD for support of this project and wish to thank the laboratory of Dr. Bechara Kachar for construction and donation of the organ of Corti cDNA library.

#### **[549] The GABA<sub>A</sub> Receptor Agonist Muscimol Ameliorates Kainic Acid Excitotoxicity in the Guinea Pig Cochlea**

Shuhei Sakai<sup>1</sup>, Keiji Tabuchi<sup>1</sup>, Hidekazu Murashita<sup>1</sup>, Akira Hara<sup>1</sup>

<sup>1</sup>University of Tsukuba

Previous studies have shown that the application of kainic acid to the round window membrane induces excitotoxicity of afferent dendrites and significantly decreases the amplitude of the compound action potential (CAP). On the other hand, it is known that the GABA<sub>A</sub> receptor agonist muscimol is neuroprotective in excitotoxicity in the central nervous systems. The aim of the present study is to clarify the effect of muscimol on the cochlea against excitotoxicity induced by kainic acid. Albino guinea pigs weighing 250g to 300g were used. Kainic acid (10mM) and/or muscimol (100μM) were applied on the intact round window membrane. CAP thresholds were examined before, 1, 3 and 7 days after the drug application. CAP threshold shifts following kainic acid exposure were significantly decreased by muscimol as compared with the control animals given only kainic acid. Furthermore, the protective effect of muscimol was significantly inhibited by the application of

GABA<sub>A</sub> receptor antagonist bicuculline (100μM). These results suggest that muscimol ameliorates kainic acid excitotoxicity in the cochlea by GABA<sub>A</sub> receptor activation.

#### **[550] Spiral Ganglion Cell Survival in Deafened Guinea Pigs After Delayed Neurotrophic Treatment and Brief Electrical Stimulation**

Martijn Agterberg<sup>1,2</sup>, Huib Versnel<sup>1,2</sup>, John De Groot<sup>1,2</sup>, Sjaak Klis<sup>1,2</sup>

<sup>1</sup>Dept. of Otorhinolaryngology, University Medical Center Utrecht, <sup>2</sup>Rudolf Magnus Institute of Neuroscience, Utrecht University

Cochlear hair cell loss leads to degeneration of spiral ganglion cells (SGCs). Several studies indicate that electrical stimulation and application of neurotrophic factors can reduce this SGC degeneration. We are interested in SGC survival in animals that have been deaf for a period during which a significant SGC loss occurs. Structure and function of SGCs were investigated in deafened guinea pigs treated with brain-derived neurotrophic factor (BDNF) and/or receiving daily brief electrical stimulation (BES).

Guinea pigs were deafened by co-administration of kanamycin and furosemide. Two weeks after deafening, the right cochleas were implanted with an electrode and cannula. In the BDNF-treated group the cannula was attached to a mini-osmotic pump (flow rate: 0.25 μl/h) filled with BDNF (100 μg/ml). BDNF was administered to the cochlea for 4 weeks. In the BES group, the animals received electrical stimulation approximately 30 minutes per day, 6 days a week, for 4 weeks. An additional group of animals received both BDNF and BES. In all animals, compound action potentials (CAPs) and auditory brainstem responses (ABRs) were recorded frequently. In most animals, electrically evoked ABRs (eABRs) were recorded as well. Acoustical stimuli were broadband clicks and tone pips of various frequencies (2-16 kHz). The electrical stimulus currents were 100-1000 μA, pulse width was 20 μs. At the end of the experiment animals were sacrificed for histology.

We found a significant effect of BDNF treatment: SGC densities in BDNF-treated (right) cochleas were more than 2 times greater than in untreated (left) cochleas. EABRs showed larger amplitudes in BDNF-treated animals than in untreated animals, which indicates that the SGCs which survived due to the exogenous BDNF, maintained their functionality. Preliminary findings indicated little or no effect of BES on survival of SGCs or amplitude of eABRs.

This work was funded by the Heinsius-Houbolt Foundation, The Netherlands.

#### **[551] Effects of Activity-Dependent Signals on Spiral Ganglion Neurite Growth**

Pamela Roehm<sup>1</sup>, Ningyong Xu<sup>1</sup>, Steven H. Green<sup>1,2</sup>, Marlan Hansen<sup>1</sup>

<sup>1</sup>Dept. of Otolaryngol., <sup>2</sup>Department of Biological Science, University of Iowa

The effects of activity-dependent signals carry critical implications for maintenance and regeneration of the

auditory nerve, especially in cochlear implant recipients. We have investigated the effects of membrane electrical activity on SGN neurite growth. We find that while membrane depolarization with elevated extracellular K<sup>+</sup> promotes SGN survival, it inhibits neurite growth in vitro. This effect is blocked by verapamil, thus demonstrating the role of L-type calcium channels in this process. Time-lapse imaging confirms that depolarization inhibits neurite extension. We examined the role of protein kinase A (PKA), an activity dependent kinase necessary for SGN survival benefits from depolarization, in SGN neurite outgrowth. Transfection of SGNs with constitutively active PKA isoforms tagged with green fluorescent protein (GPKA) inhibits neurite growth. This inhibition inversely correlates with expression levels and occurs whether the GPKA is excluded from or restricted to the nucleus. The cell permeant cAMP analog, cpt-cAMP, also inhibits neurite growth at 10 mM but promotes growth at 1 mM, independent of the extracellular matrix substrate. Since PKA activity inhibits neurite growth and is required for the survival-promoting effects of depolarization, we asked whether PKA inhibitors could protect SGN neurites from the effects of membrane depolarization. Neither overexpression of GPKI, a small peptide PKA inhibitor, nor treatment with RpcAMPS, a small molecule PKA inhibitor, prevented the inhibition of neurite growth by depolarization. Thus, membrane electrical activity inhibits SGN neurite growth through different mechanisms than those recruited to promote survival. Identification and manipulation of signals activated by membrane electrical activity that inhibit neurite growth may permit continued survival benefits while eliminating the potentially damaging consequences on neurites.

#### **552 cAMP-Dependent Protein Kinase (PKA) Promotes Spiral Ganglion Neuron (SGN) Survival Through Outer Mitochondrial Membrane (OMM) Signaling**

Jie Huang<sup>1</sup>, Steven H. Green<sup>2</sup>

<sup>1</sup>Department of Biological Sciences, University of Iowa,

<sup>2</sup>Department of Biological Sciences and Otolaryngology, University of Iowa

We have previously shown that cAMP is a survival-promoting stimulus for cultured neonatal (postnatal day 4-6) SGNs; membrane depolarization promotes survival in part by recruitment of cAMP signaling. PKA does not function as a prosurvival signal through actions in the cell nucleus nor via the transcription factor CREB but, rather, in an extranuclear location. By specifically targeting the PKA catalytic subunit (PKAc) or, alternatively, the PKA inhibitor protein (PKI) to the OMM, we showed that OMM localization of PKA is sufficient to promote survival and is necessary for promotion of survival by cAMP (but not BDNF). We hypothesized that this involves phosphorylation of the proapoptotic regulator Bad, which prevents its translocation to the OMM. Indeed, we now show OMM-targeted PKA can rescue SGNs from cell death caused by Bad overexpression but failed to rescue when the overexpressed Bad was mutated at certain phosphorylation sites. These data not only indicate that

Bad phosphorylation is important for the prosurvival effect of PKA but identify Ser112 and Ser136 on Bad (but not Ser155) as the critical targets. We have also shown that activation of the protein kinase Jun N-terminal Kinase (JNK) and consequent Jun phosphorylation accompanies SGN death in vitro and in vivo, is necessary for SGN death, and is suppressed by depolarization. Because PKA appears to block proapoptotic signaling at a point late in the sequence of events leading to apoptosis, we hypothesize that PKA is not a signal used by depolarization to suppress JNK. We show that PKA activation does not block Jun phosphorylation in SGNs triggered to die and that other pathways mediate this effect of depolarization. Support from NIDCD R01 DC002961.

#### **553 Innervation, Denervation and Reinnervation of Cochlear Inner Hair Cells by Spiral Ganglion Neurons (SGNs) Studied *In Vitro* in an Organotypic Culture**

Qiong Wang<sup>1</sup>, Steven H. Green<sup>1,2</sup>

<sup>1</sup>Department of Biological Sciences, University of Iowa,

<sup>2</sup>Department of Otolaryngology, University of Iowa

Type I spiral ganglion neurons (SGNs) innervate inner hair cells (IHCs). An organotypic explant culture of a segment of organ of Corti (OC) with associated SGNs (type I and type II) from neonatal (postnatal day 4-6) rat cochlea preserves the synaptic interactions between hair cells and SGNs. We have used this preparation to investigate the reinnervation of IHCs by type I SGNs following trauma to the SGN peripheral processes. Immunofluorescence (IF) imaging of NF200 shows that each peripheral axon contacts a single IHC, as is the case in vivo. IF imaging of the pre- and postsynaptic scaffolding proteins, respectively, Bassoon and PSD95, show well preserved afferent endings: in middle turn OC segments, there are 12.7 ± 2.8 PSD95 IF puncta/IHC. Treatment with glutamate receptor agonists NMDA and kainic acid (0.5 mM each) for 2 h causes degeneration of the terminals and peripheral portion of the type I SGN processes, without effect on type II SGNs, which closely mimics noise-induced damage to SGNs in vivo. Regenerating SGN axons, detected by NF200 IF, contact IHCs within 6 hours. New synapses form on IHCs within 24 hours, detectable by PSD95 labeling. The regenerating axons do not extend past an intact row of IHCs to contact outer hair cells, suggesting that a "stop" signal exists in the IHC row. A difference between regenerating axons and those in control cultures becomes apparent as more time is allowed for the reinnervation. By 72 h after reinnervation has begun, axons can be observed extending past the initially-contacted IHC and forming synapses (PSD95-immunoreactive puncta) on multiple adjacent IHCs. Thus, although specificity to IHCs is maintained in reinnervation, specificity to a particular IHC is not. This may be due to reduced competition among regenerated SGN axons which are fewer than the original (control) innervation. Current studies are focusing on molecular signals required for contact and synaptogenesis in regenerating SGN axons.



**554 The Survival and Outgrowth Effects of BDNF/GDNF on Spiral Ganglion Cells *In Vitro* by Combined Application with Dexamethasone**

Patrick Wefstaedt<sup>1</sup>, Verena Scheper<sup>1</sup>, Thomas Lenarz<sup>1</sup>, Timo Stöver<sup>1</sup>

<sup>1</sup>Medical University of Hannover

With regard towards an optimal cochlear implant performance several neurotrophic factors have been shown to improve spiral ganglion cell (SGC) survival as well as neurite outgrowth both in vivo and in vitro. Glucocorticoids like dexamethasone are interesting candidates for the reduction of connective tissue formation following electrode insertion.

The objective of the present study was to investigate the effects of BDNF/GDNF application in combination with dexamethasone treatment on survival and neurite outgrowth of SGCs in vitro.

Therefore dissociated rat spiral ganglion cells were maintained for 48h in a supplemented serum free culture medium with addition of the mentioned factors in different concentrations and combinations with each other.

The results indicate that BDNF as well as GDNF mediated effects on SGC survival are not attenuated by additional application of dexamethasone. Additionally, trophic effects could be demonstrated both for single BDNF and combined BDNF/ dexamethasone application.

We conclude that dexamethasone application exerts no toxic effects on SGCs in the examined concentrations and should be looked into further in vivo.

**555 BDNF Survival Effects on Spiral Ganglion Cells *In Vitro* Are Enhanced by Patterned Electrical Stimulation**

Timo Stöver<sup>1</sup>, Patrick Wefstaedt<sup>1</sup>, Gerrit Paasche<sup>1</sup>, Thomas Lenarz<sup>1</sup>

<sup>1</sup>Medical University of Hannover

Previous studies have been shown that depolarization is effective to promote spiral ganglion cell survival in vitro, and can be enhanced by additional application of neurotrophic factors like BDNF. In vivo intra cochlear charge-balanced stimulation of deafened guinea pigs has also been demonstrated to enhance spiral ganglion cell survival in combination with neurotrophic factors, whereas in vitro protective effects of electrical stimulation on SGC survival are unknown.

For the present study we therefore developed a stimulation device to test the effects of different stimulation parameters of a patterned electrical stimulation on dissociated spiral ganglion cells (p3-5) in vitro, with the advantage to rapidly test different stimulation setups. In initial experiments we furthermore analysed the effects of an in vitro patterned electrical stimulation of dissociated spiral ganglion cells as single treatment and in combination with the neurotrophic factor BDNF.

Our results indicate that single patterned electrical stimulation with different setups (50Hz biphasic pulses, 6 & 30V) does not enhance spiral ganglion cell survival in vitro as a single treatment, but enhances the neuroprotective effects of BDNF application on cultured spiral ganglion cells.

Overall the developed stimulation device is suitable for experiments analysing the effects of an electrical stimulation on cultivated spiral ganglion cells and provides the possibility to test various stimulation parameters for their ability to enhance SGC-survival.

**556 Auditory Nerve Survival Remains Enhanced Four Weeks Following Cessation of Treatment with Glial Cell-Line Derived Neurotrophic Factor**

Josef Miller<sup>1,2</sup>, Diane Prieskorn<sup>1</sup>, Soo Duk Lee<sup>1</sup>, Jong-Seung Kim<sup>1</sup>, Alice Mitchell<sup>1</sup>, Richard Altschuler<sup>1</sup>

<sup>1</sup>Kresge Hearing Research Institute, The University of Michigan, Ann Arbor, MI, USA, <sup>2</sup>Center for Hearing and Communication, Karolinska Institutet, Stockholm, Sweden

There is now considerable evidence that neurotrophic factors can enhance auditory nerve survival following deafness. It is hoped that such treatment may one day enhance the benefits of cochlear prostheses. There have been reports however that this enhancement may not be maintained once neurotrophin application is ended. Gillespie et al (2003) found that within two weeks of cessation of treatment, with brain derived neurotrophic factor, there was not only a rapid degeneration of SGN but that the number of surviving neurons were comparable to those found in animals with no treatment at all. We examined the effects of cessation of treatment with glial cell-line derived neurotrophic factor (GDNF, Amgen, Inc.). We assessed the effect of replacing GDNF treatment by artificial perilymph or electrical stimulation, the latter having been shown to enhance auditory nerve survival. Guinea pigs were chemically deafened bilaterally and delivery of GDNF (100 µg/ml), via cannula and osmotic pump into scala tympani, began 3 wk post deafening, with one group also implanted with intracochlear electrodes for chronic electrical stimulation (100 µA, 100 µS, 250 Hz). Group 1 was 11 wk deafened controls, group 2 received 4 wk of GDNF followed by 4 wk AP and group 3 received 4 wk GDNF followed by 4 wk electrical stimulation. Group 1 showed the lowest density of surviving SGN. Groups 2 and 3 both showed significantly enhanced auditory nerve survival compared to Group 1. The greatest survival was observed in Group 3. Thus increased auditory nerve survival by GDNF treatment is still observed at 4 wks following cessation of drug treatment and electrical stimulation following drug treatment may further enhance SGN survival. This indicates that transient treatment with neurotrophic factors may enhance the benefits of cochlear prostheses, particularly if followed by cochlear electrical stimulation.

Supported by NIH DC03820, Ruth and Lynn Townsend Professorship, UAW/GM funds

**557 TrkB and p75NTR Signaling Pathways Are Differentially Altered in Degenerating Spiral Ganglion Neurons *In Vivo***

Justin Tan<sup>1</sup>, Robert Shepherd<sup>1</sup>

<sup>1</sup>Bionic Ear Institute, Melbourne, Australia

Aminoglycosides induce sensorineural hearing loss in rodents by destroying hair cells of the organ of Corti. With prolonged deafness, there is a progressive degeneration

of spiral ganglion neurons, characterized by loss of both afferent and efferent nerve fibers to hair cells of the organ of Corti. Because recent studies suggest that neurotrophins binding to Trk receptor tyrosine kinases and the p75 neurotrophin receptor may elicit respectively pro-survival and apoptotic signals, we asked if the expression of these receptors in spiral ganglion neurons and their peripheral processes is altered in an aminoglycoside-based rodent model of sensorineural hearing loss. Using immunohistochemistry and Western blotting, we show for the first time that the expression of p75NTR is dramatically increased in neuronal fibers of spiral ganglion neurons with increasing duration of deafness implicating a novel role of p75NTR in primary auditory neuronal degeneration. In contrast, trkB expression in these fibres is down-regulated, suggesting specific changes in expression of these neurotrophin receptors. To further underline the specificity of these contrasting signalling pathways, we analyzed the expression of transcription factors which are downstream targets of p75NTR-mediated (c-Jun) and trkB-mediated signaling (CREB). We observed a strong nuclear activation of phosphorylated c-Jun protein, but a decreased expression of pro-survival phosphorylated CREB, in spiral ganglion neurons of deaf rodents. Taken together, these data suggest that aminoglycoside-induced degeneration of spiral ganglion neurons is associated with both an augmentation of pro-apoptotic signaling pathways, and a reduction of signaling pathways related to cell survival. As surviving spiral ganglion neurons are targets of cochlear implantation, understanding these pathways in degenerating spiral ganglion neurons would enable us to manipulate them with combined pharmacological intervention and electrical stimulation.

Supported by the National Institute on Deafness and Other Communication Disorders; Grant Number N01-DC-3-1005

#### **558 Blockage of Interleukin-6 Signal After Noise Exposure Ameliorated Functional Recovery in Noise Induced Hearing Loss**

**Masato Fujioka<sup>1</sup>**, Hirotaka James Okano<sup>1</sup>, Masatsugu Masuda<sup>1</sup>, Sho Kanzaki<sup>1</sup>, Masahiko Mihara<sup>2</sup>, Yoshiyuki Ohsugi<sup>2</sup>, Kaoru Ogawa<sup>1</sup>, Hideyuki Okano<sup>1</sup>

<sup>1</sup>Keio University School of Medicine, <sup>2</sup>Chugai Pharmaceutical Co. Ltd

Recent studies have revealed the involvement of inflammatory responses in noise-induced hearing loss (NIHL). We have previously reported the induction of proinflammatory cytokines, including interleukin-6 (IL-6) in the early phase of NIHL cochlea (Fujioka, et., al. in revision); within 6 hours after noise exposure in type III and IV fibrocytes of lateral wall expanding toward stria cells, at around 24 hours in spiral ganglion neurons.

In the present study, we examined the role of IL-6 in NIHL by using anti-mouse soluble-interleukin-6 receptor (sIL-6R) neutralizing antibody, MR16-1 (from Osaka University and Chugai-Roche Pharmacy Co. Ltd). To obtain NIHL model, we used 4-week-old male C57BL/6Jcl mice, exposed to one octave-band noise centered at 4 kHz with the peak at 124 dB SPL for 2 hours. The ABR threshold shift was irreversible up to 3 months, demonstrating the model was

permanent threshold shift (PTS). Systemic administration of MR16-1 (intraperitoneal injection) immediately after noise exposure suppressed the noise-induced phosphorylation of STAT3 (signal transducer activating target-3: one of the target transcription factors of IL-6 intracellular signal) in whole cochlea, suggesting the IL-6 signaling in cochlea was blocked in this treatment. The expression of phosphorylated STAT3 was detected intensively in intermediate cells and endothelial cells of stria vascularis in 12 hours after noise exposure. Next, we examined the threshold shift of each mouse by using tone-burst ABR. Surprisingly, compared with control IgG injection, ABR threshold shift was ameliorated gradually from 2 weeks after treatment.

Our data suggest that excessive inflammatory response through IL-6 signaling in lateral wall after noise exposure may be a deteriorating factor in noise-induced hearing loss. In addition, this data also showed the possibility of the clinical implication of anti-interleukin-6 therapy in NIHL.

#### **559 Therapeutic Time Window of Methylprednisolone in Acoustic Injury**

**Keiji Tabuchi<sup>1</sup>**, Hidekazu Murashita<sup>1</sup>, Keiko Oikawa<sup>1</sup>, Shuhei Sakai<sup>1</sup>, Isao Uemaetomari<sup>1</sup>, Tadamichi Tobita<sup>1</sup>, Shigeki Tsuji<sup>1</sup>, Hideki Okubo<sup>1</sup>, Tetsuro Wada<sup>1</sup>, Akira Hara<sup>1</sup>

<sup>1</sup>University of Tsukuba

Glucocorticoids have been widely used in the treatment of acoustic injury. Although several researchers have reported that glucocorticoids possess protective effects against acoustic injury in the animal experiments, the therapeutic time window of glucocorticoids in acoustic injury has never been examined. The purpose of the present study was therefore to examine the therapeutic time window of glucocorticoid. Female ddY mice of 8 weeks of age were used in this study. Animals were subjected to a 4 kHz pure tone of 128 dB SPL for 4 hours through an open field system inside a sound-exposure box. Auditory brainstem response (ABR) was examined before, immediately after and two weeks after acoustic overexposure. After final ABR measurements at two weeks after acoustic overexposure, whole mounts of organ of Corti were stained for the nucleus with propidium iodine, and missing hair cells (missing of staining with propidium iodine) were counted every 0.33 mm segments. Methylprednisolone significantly improved the ABR threshold shifts and decreased hair cell loss two weeks after acoustic overexposure when it was administrated before or immediately after acoustic overexposure but not when administrated three hours after acoustic overexposure. The present findings suggest that methylprednisolone has protective effects against acoustic injury of the cochlea with a short therapeutic time window.

#### **560 Inhibition of SDH Activity Delays the Initiation of HC Apoptosis Induced by Exposure to Intense Noise**

**Bo-Hua Hu<sup>1</sup>**

<sup>1</sup>State University of NY at Buffalo

The current study was designed to examine whether interruption of the energetic function of mitochondria shifts

hair cell (HC) apoptosis to necrosis following exposure to intense noise. 3-Nitropropionic acid (3-NP) was used to inhibit succinate dehydrogenase (SDH), a respiratory enzyme in the citric acid cycle converting succinic acid to fumaric acid. The drug (20 or 50 mM) was applied on the round window of the chinchilla cochlea and the same volume of artificial perilymph was applied to the contralateral cochlea of the same animal served as control. Sixteen hours after the drug application, the animals were exposed to impulse noise at 155 dB pSPL for 75 pairs. The cochleae were collected at 30 minutes, 3 hours and 2 weeks after the noise exposure, and stained for SDH, nuclear morphology and caspases-3, -8 and -9. The results showed that at 30 min after the noise exposure, the 3-NP-treated cochleae had significant less HC death than the control cochleae although both the 3-NP-treated and the control cochleae exhibited activation of caspase-3, 8, and 9. The 3-NP-treated ears had more HCs showing nuclear swelling. As time elapsed after the noise exposure, the cochlear lesion expanded in both the 3-NP-treated and the control cochleae. Like the control cochleae, the 3-NP-treated cochleae exhibited activation of caspase-3, 8 and 9 in the HCs having condensed nuclei. However, many HCs with strong caspase activity in the 3-NP-treated cochleae maintained a relative normal shape, suggesting a reduced pace of pathological developments in apoptotic HCs. Interestingly, there was weak caspase staining in certain dying HCs having swollen nuclei, a morphological sign of necrosis. This result suggests that certain OHCs started the death process via apoptosis, but shifted to necrosis due to the malfunction of mitochondria. At 2 weeks after the noise exposure, there was no significant difference in the threshold shifts, nor the extent of HC damage between the 3-NP-treated and the control ears. Collectively, the results of the study suggest that interruption of mitochondrial energy production does not change the eventual magnitude of the cochlear pathology, but alters the ratio of apoptotic and necrotic HCs and delays the initiation and progression of HC apoptosis. (Supported by the Grant NIDCD 1R03 DC006181-01A1)

#### **561 Protective Effect of Halothane Anesthesia on Noise-Induced Hearing Loss in Mice**

**Joong Ho Ahn<sup>1</sup>**, Joung Uk Kim<sup>2</sup>, Hyun Jung Lee<sup>3</sup>, Hun Hee Kang<sup>3</sup>, Young Jin Kim<sup>1</sup>, Tae Hyun Yoon<sup>1</sup>, Kwang Sun Lee<sup>1</sup>, Jong Woo Chung<sup>1</sup>

<sup>1</sup>*Department of Otolaryngology, Asan Medical Center, University of Ulsan, College of Medicine, Seoul,*

<sup>2</sup>*Department of Anesthesiology, Asan Medical Center, University of Ulsan, College of Medicine, Seoul,* <sup>3</sup>*Asan Institute for Life Sciences, Seoul, Korea*

The aim of the present work was to analyze the effect of halothane anesthesia on noise-induced sensorineural hearing loss.

BALB/c mice were used. The 'noise group' mice were exposed to white noise (122 dB p.e. SPL) for 3 hours per day for 3 consecutive days. A 'control group' consisted of mice kept in the noise booth for 3 hours per day for consecutive days without noise. A third experimental group, the 'anesthetized group', consisted of mice that

were anesthetized with an inspired concentration of 1.2 - 1.5 vol% halothane with 4 L/min of oxygen in the noise booth for 3 hours per day for 3 consecutive days with noise. White noise (300 -10,000 Hz) was delivered inside the noise booth.

We found that mice in the noise group experienced an increase in hearing threshold from 22.0 dB HL in pre-exposure to 75.0 dB HL one day after noise exposure. In the anesthetized group, the increase in hearing threshold was less dramatic and less sustained, being 20.0 dB HL at pre-exposure and increasing to 48.0 dB HL and 28.5 dB HL at one day and one week after noise exposure, respectively.

The survival rate for each row of hair cells gradually decreased from the apical to basal turn of the cochlea. In the anesthetized group, outer hair cells suffered significantly less noise-induced damage compared to those from the noise group. In the basal turn, 90% of hair cells survived in the anesthetized group, which was significantly greater than the 60% which survived in the noise group.

The present data indicate a protective effect of halothane anesthesia on noise-induced hearing loss and tissue damage. While identification of the mechanisms underlying these effects awaits further study, this protection may be due to the inhibitory effects of halothane on ROS-mediated damage.

This work was supported by a grant (2004-015-E00181) from the Korea Research Foundation, Seoul, Korea.

#### **562 BN82270, a Potent Calpain Inhibitors Protect Auditory Sensory Cells from Acoustic Trauma Induced Cell Death**

**Jing Wang<sup>1,2</sup>**, Bernadette Pignol<sup>3</sup>, Sabine Ladrech<sup>1</sup>, Marcel Mersel<sup>1</sup>, Jérôme Ruel<sup>1,2</sup>, Jean-Luc Puel<sup>1</sup>

<sup>1</sup>*INSERM,* <sup>2</sup>*Auris Medical,* <sup>3</sup>*IPSEN-Beaufour*

Together with caspases, calpains have been shown to be an important factor in the regulation cell death. Here we report in guinea pig that acoustic overstimulation (6 kHz, 120 dB SPL for 30 minutes) increased calpains and caspase-3 activities, activated pro-apoptotic Bax leading to cleavage of fodrin, DNA fragmentation and subsequent permanent hearing loss. Perilymphatic perfusion BN82270, a potent calpain inhibitors and a free radical scavengers via an osmotic minipump, prevents DNA fragmentation, and hair cell degeneration. This was confirmed by functional tests showing a clear dose-dependent reduction (ED<sub>50</sub> = 3.61 µM) of permanent hearing loss and complete protection at 100 µM. Although less efficient than intracochlear perfusion, the application of BN82270 onto the intact round window membrane protect and, even rescues the cochlea when applied after acoustic trauma within a therapeutic window of 24 hours. These results indicate that BN82270 may be of potential therapeutic value to prevent and rescue the cochlea from acoustic trauma.

### **563 Ebselen (SPI-1005) Provides Significant Protection from Noise Exposure in Rats by Supporting Glutathione Peroxidase Activity in the Cochlea**

**Eric Lynch**<sup>1</sup>, Rende Gu<sup>1</sup>, Carol Pierce<sup>1</sup>, Huy Tran<sup>1</sup>, Jerry Glattfelder, Jr.<sup>1</sup>, James LaGasse<sup>1</sup>, Jonathan Kil<sup>1</sup>

<sup>1</sup>*Sound Pharmaceuticals, Inc.*

Previous reports have indicated that GPx levels in the cochlea are high (McFadden 2001) and that deletion of GPx1 in mouse leads to an increased susceptibility to NIHL (Ohlemiller 2000). We determined the expression pattern of GPx1, 3, 4 in rat and mouse cochlea. Immunostaining indicates that GPx1 is the major isoform present in the cochlea and is highest in the stria vascularis, organ of Corti, and spiral ganglion. GPx2, normally restricted in its expression to the colon, has not been evaluated. We have quantified changes in the expression level of GPx1 acutely following noise exposure using immunofluorescence in placebo and ebselen treated F344 rats. Our data indicates that GPx1 levels are reduced in noise exposed rats and that these levels can be restored with ebselen.

Ebselen (SPI-1005), a small molecule GPx mimic with very low toxicity has been shown to provide significant protection from TTS and PTS in F344 rats (Lynch et al., 2004, Lynch et al., 2005) and Guinea Pigs (Pourbahkt and Yamasoba 2003, Yamasoba et al., 2005) when dosed orally at 8-10 mg/kg. In our studies, rats were dosed with 4mg/kg, ebselen bid x 3d, 7d, or 14d, p.o., starting one day before noise exposure (113 dB, 4-16 kHz OBN, 4hrs). Permanent hearing threshold shifts evaluated at time points up to 15 weeks following noise exposure, indicated that ebselen provides significant long lasting protection from PTS for all dosing regimes tested with best results obtained in the 14 d dosing group. Comparative analysis of ebselen dosing starting before versus after noise exposure has also been evaluated. Best protection from NIHL is found with dosing starting prior to noise exposure and within two days after noise. Analysis of dose response to ebselen in rats indicates no significant effect at 2 mg/kg and a plateau effect at higher concentrations.

Analysis of perilymph from ebselen dosed Guinea pigs demonstrates that the metabolites of ebselen are present in the cochlea at 2 and 4 hours post dosing using LC-ICPMS. Together, these data support the role of ebselen as an appropriate compound for the protection of auditory function.

### **564 Effect of Ebselen on Noise Induced Cochlear Damage**

**Yong-Ho Park**<sup>1</sup>, Ki-Sang Rha<sup>1</sup>, Chan-Il Park<sup>1</sup>

<sup>1</sup>*Department of Otolaryngology, Chungnam National University Hospital, Daejeon, Korea*

**Background and Objectives:** With the advancement of modern civilization and mechanical development of society, the prevalence of noise-induced hearing loss is increasing. There were some suggestions that noise-induced hearing loss may be reduced or prevented with antioxidant treatment. The purpose of this study is to evaluate the effect of ebselen as a free radical scavenger

or antioxidant in noise-induced cochlear damage. **Materials and Method:** Thirty male Sprague Dawley rats (250-300 g) with normal auditory brainstem response (ABR) thresholds were exposed for 6 h to 115dB SPL broad band noise. 10mg/kg ebselen were injected intraperitoneally at 12h before and 1h before noise exposure. After noise exposure, auditory brainstem response thresholds shift were evaluated. And a study for iNOS and nitrotyrosine expressions in cochlea were examined by immunohistochemical staining. **Results:** After noise exposure, auditory brainstem responses indicated that ebselen treatment reduced threshold shifts significantly. The expression of iNOS and nitrotyrosine were observed in hair cells, supporting cells of the organ of Corti, stria vascularis and spiral ganglion. And the expression of iNOS and nitrotyrosine were reduced in ebselen treated group compared with in non-treated group. **Conclusion:** Ebselen protects cochlea from noise by playing a role as a scavenger of reactive free radicals.

### **565 Post-Exposure Application of the Antioxidant Edaravone Reduces Noise-Induced Hearing Loss in Guinea Pigs**

**Kuniyoshi Tanaka**<sup>1</sup>, Tsuyoshi Takemoto<sup>1</sup>, Kazuma Sugahara<sup>1</sup>, Takefumi Mikuriya<sup>1</sup>, Kenji Takeno<sup>1</sup>, Hiroshi Orita<sup>1</sup>, Makoto Hashimoto<sup>1</sup>, Hiroaki Shimogori<sup>1</sup>, Hiroshi Yamashita<sup>1</sup>

<sup>1</sup>*Yamaguchi University School of Medicine*

We investigated the effects of edaravone against noise-induced hearing loss in guinea pigs. Edaravone is a free radical scavenger that is clinically used in Japan. Edaravone ( $1.722 \times 10^{-2}$  M) was infused into the right ear by an osmotic pump, and the left ear was untreated as a control. Animals received edaravone 9 h before (-9h group, n = 7) and 9 h (+9h group, n = 8), 21 h (+21h group, n = 7) and 33 h (+33h group, n = 4) after noise exposure (130 dB SPL, 3 h). Seven days after noise exposure, we examined the shift in auditory brainstem response thresholds and histopathologic characteristics of the sensory epithelia. The smallest shift in auditory brainstem response threshold and smallest proportion of missing outer hair cells were observed in the +9h group. To support this result, immunohistochemical analysis of 4-hydroxy-2-nonenal was carried out at each time point (unexposed controls, and following noise exposure: immediately, 9 h, and 21 h) after noise exposure (n=2 each). Sections from animals sacrificed immediately after noise exposure showed little immunoactivity, similar to controls. However, Sections from animals sacrificed 9 h after noise exposure showed immunoactivity in the organ of Corti. Moreover, the immunoactivity in the organ of Corti increased 21 h after noise exposure. Our data suggest that edaravone may be clinically effective in the treatment of acoustic trauma, especially if given within 21 h of noise exposure.

**566 Geranylgeranylacetone Attenuates the Cochlea Damage from Noise Injury in the Guinea Pig**

Takefumi Mikuriya<sup>1</sup>, Kazuma Sugahara<sup>1</sup>, Tsuyoshi Takemoto<sup>1</sup>, Kuniyoshi Tanaka<sup>1</sup>, Kenji Takeno<sup>1</sup>, Hiroaki Shimogori<sup>1</sup>, Hiroshi Yamashita<sup>1</sup>

<sup>1</sup>*Yamaguchi University School of Medicine*

Geranylgeranylacetone (GGA) used widely as anti-ulcer agent in Japan is known to be an inducer of heat shock proteins (Hsps) in the gastric mucosa, liver, heart, and brain, etc. It was reported that the protective effect in these tissues against various stresses. However, the effect of GGA on the inner ear has been unclear. At the last MidWinter Meeting, we showed that single oral dose of GGA could induce Hsps in the cochlea and thereby GGA protected cochlea against acoustic trauma histologically and functionally. At this meeting, we present the effect of GGA in additional experiments. We used Hartley guinea pigs. To evaluate cochlear function, we assessed thresholds of the auditory brain stem response (ABR). For histological assessment, we observed the sensory epithelium using surface preparation technique. For biochemical examination, the expression of HSP 70, 40 in the cochlea were investigated by western blot analysis. All animals were exposed to intense noise (130 dB SPL octave band noise) with a center frequency of 4 kHz for three hours. Seven days after the sound exposure, ABR threshold was recorded and the second turn of the organ of Corti was observed. After the noise exposure, there were fewer defects on outer hair cells of organ of Corti in GGA treated ears than those of the control's significantly. In addition, the threshold shifts was suppressed in pretreatment of GGA group compared with the other groups. Western blot analysis showed that the expressions of Hsp 70, 40 increased without sound exposure stress. Therefore these Hsps is likely to protect the cochlea. These result show that oral dose of GGA have potential to protect cochlea from acoustic trauma.

**567 Methionine Versus Saline for Ototoxic Protection Against Cisplatin in the Guinea Pig**

Rose Mary Stocks<sup>1</sup>, David Armstrong<sup>1</sup>, Sreekrishna Donepudi<sup>1</sup>, Herbert Gould<sup>1,2</sup>, Xiaoping Du<sup>1</sup>, Kristin Hamre<sup>1</sup>, Jonathan Hayes<sup>1</sup>, Jerome Thompson<sup>1</sup>

<sup>1</sup>*University of Tennessee*, <sup>2</sup>*University of Memphis Speech and Hearing Center*

Objective: Determine if continuous infusion of d-methionine to the round window membrane (RWM) affords protection against cisplatin ototoxicity in the Hartley albino guinea pig (HAGP) versus saline controls.

Design: Prospective Randomized Control Study

Setting: University Animal Research Laboratory

Subjects: 21 male HAGPs with initial weights between 200-250 grams.

Methods: For each HAGP, baseline hearing was measured by auditory brainstem response recordings at 2K, 8K, 16K, and 32K Hertz. Then 4% d-methionine was administered continuously via a surgically placed mini-osmotic pump (Alzet 2002) to the middle ear space. The

distal tip of each pump was placed adjacent to the RWM via a transbullar approach. The contralateral ear served as control and received a similarly placed pump primed with 0.9% isotonic saline. Three days later, subcutaneous injections of cisplatin (1.1mg/kg/day) were instituted for 8 days. On day 14, the pumps were removed. Four weeks later post treatment ABR were performed. Subsequently the temporal bones were harvested and the cochleas were histologically prepared. The remaining inner and outer hair cells were counted for selected cochleas.

Results: Using multivariate analysis, no statistical difference was found between the d-methionine and saline treated ears pre or post cisplatin administration. The condition effect of cisplatin ototoxicity was observed and hearing loss due to cisplatin proceeded in an apical fashion beginning at the highest frequency. Histologic evaluation of cochlea demonstrated partial protection of OHC's (between 3.4 and 29.5 kHz) and IHC's throughout but function could not be confirmed based on ABR data.

Conclusions: With this regimen RWM continuous infusion of d-methionine in the setting of systemically administered cisplatin does not provide preservation of hearing by ABR in comparison to saline controls. Paradoxically, structural integrity of both inner and outer hair cells is preserved to some degree in the selected cochleas.

**568 Safety of Edaravone on the Inner Ear in the Guinea Pig**

Hiroshi Orita<sup>1</sup>, Kenji Takeno<sup>1</sup>, Hiroataka Hara<sup>1</sup>, Hiroaki Shimogori<sup>1</sup>, Hiroshi Yamashita<sup>1</sup>

<sup>1</sup>*Yamaguchi University School of Medicine*

Edaravone, a free radical scavenger, has potent free radical quenching action and is used in clinical practice to treat cerebral infarction in Japan. We thought the possibility that edaravone might be a candidate for the topical treatment of inner ear pathology induced by free radical. We investigated the safety of edaravone on the normal cochlea of the guinea pig. Experiments were performed on male Hartley guinea pigs with normal Preyer's reflexes and tympanic membranes. Under xylazine (16 mg/kg, i.p.) and ketamine (16 mg/kg, i.p.) anesthesia, the mastoid bulla was opened by a postauricular incision to allow visualization of the round window under a surgical microscope. A gelatine sponge sized 2 mm<sup>3</sup> dipped 6 mg/ml edaravone was put on the round window. One week after the operation, we performed caloric test and ABR and vestibular and cochlear functions were evaluated. After physiological examination, all animals were deeply anesthetized and temporal bones were removed and examined histologically. Caloric response time and ABR thresholds were not influenced by topical application of edaravone. Histological examination showed no obvious morphological change. These results suggest that topical application of edaravone is a safety treatment for inner ear.

## **569** Difference in Recovery of Outer and Inner Hair Cells After Exposure to High Level Sound in Rats

Margaret Jastreboff<sup>1</sup>, Jianron Shi<sup>1</sup>, Pawel Jastreboff<sup>2</sup>

<sup>1</sup>Towson University, <sup>2</sup>Emory University

**Introduction:** Sound-induced damage of the cochlea is a preferable method to induce experimental tinnitus in animals, because it resembles clinical cases. Available animal models of tinnitus require days to assess the presence of tinnitus and therefore it is not certain when tinnitus emerges after sound exposure. It is recognized that recovery of hearing occurs after exposure within about two weeks, but it is not clear if this recovery is due to recovery of outer hair cells (OHC), inner hair cells (IHC) or both systems. Therefore, the total cochlear transduction and functional properties of OHC were evaluated before and after exposure to intensive sound.

**Method:** 24 pigmented rats undergoing behavioral procedures of an animal model of tinnitus were used. At the proper stage of behavioral procedures, rats were exposed unilaterally for 20 minutes to 6.8 kHz, 105 dB SPL pure tone using a closed system, with calibration performed during sound exposure. Frequency-specific auditory brainstem response (ABR) and distortion product otoacoustic emissions (DPOAE) testing were performed before, just after, and 12 days after unilateral exposure. The sound exposure and measurements were performed under Nembutal anesthesia (50 mg/kg, i.p.).

**Results:** Measurements performed just after sound exposure showed frequency-specific significant hearing loss with a maximum of 45-50 dB threshold shift. DPOAE was suppressed by in similar manner with maximum attenuation of 40 dB. Measurements performed 12 days later revealed that while ABR improved by about 20 dB, no recovery was observed for DPOAE.

**Conclusions:** The discordant damage theory postulates that the tinnitus signal might depend on the difference between functional status of OHC and IHC. Assuming correctness of this theory our results suggest that tinnitus was gradually becoming stronger during the first few days after sound exposure.

## **570** Oxidative Stress and Cell Death in Drug-, Noise-, and Age-Related Hearing Loss: One Mechanism for All, One Cure for All?

Su-Hua Sha<sup>1</sup>, Hongyan Jiang<sup>2</sup>, Jochen Schacht<sup>1</sup>

<sup>1</sup>Kresge Hearing Research Institute, The University of Michigan, Ann Arbor, MI, USA, <sup>2</sup>Sun Yat-Sen University, Guangzhou, China

Different types of auditory dysfunctions frequently show similar patterns of pathology with loss of outer hair cells as a hallmark of drug-induced, noise-induced, and age-related hearing loss. Hair cells in the base of the cochlea are more sensitive to these traumata than those in the apex. Furthermore, oxidative stress is one component common to each of these pathologies. Such parallels suggest that the underlying mechanisms may be similar and that, therefore, attempts at protection may rely on similar approaches.

Information on biochemical and molecular pathways involved in cochlear damage by noise, drugs or age has

been gathered from a variety of animal species in the past and yielded relatively coherent results. Now the CBA mouse has been established as a model for aminoglycoside-induced, noise-induced, and age-related hearing loss. Such a uniform model allows for even better comparisons of mechanisms and also enables molecular biological or genetic studies of the commonalities and differences of these pathologies.

CBA mice chronically treated with aminoglycosides, exposed to noise, or of advanced age (18 to 24 months) all exhibit the established pattern of trauma-induced hair cell loss accompanied by functional deficits as evidenced by ABR recordings. Analysis of appropriate markers provided evidence for oxidant stress in all models with variations in the nature of the stress (ROS versus RNS). Likewise, the transcription factors and apoptotic or necrotic pathways involved in cell death differed between drug-, noise- and age-related hearing loss. Comparative studies may provide further insight into trauma-specific cochlear survival and cell death mechanisms and guide the design of targeted protective interventions.

Dr. Schacht's research is supported by grants DC03685 and DC06457 and core center grant P30 DC05188 from the National Institutes on Deafness and Other Communication Disorders, National Institute of Health.

## **571** The Fate of Degenerated Outer Hair Cells: Prestin in Supporting Cells

Mark Crumling<sup>1</sup>, Karen Abrashkin<sup>1</sup>, Masahiko Izumikawa<sup>1</sup>, Tzy-Wen Gong<sup>1</sup>, Donald L. Swiderski<sup>1</sup>, Yehoash Raphael<sup>1</sup>

<sup>1</sup>Kresge Hearing Research Institute, The University of Michigan, Ann Arbor, MI, USA

Cells in epithelial sheets often phagocytose their damaged or dying neighbors, maintaining the integrity of the epithelium. As an epithelial sheet, the organ of Corti serves as a partition between the K<sup>+</sup>-rich endolymph of the scala media and the Na<sup>+</sup>-rich perilymph of the scala tympani. Integrity of the organ of Corti, therefore, is crucial to ion homeostasis and the physiology of the cochlea. In the organ of Corti, loss of hair cells could compromise the integrity of the reticular lamina, risking the survival of remaining hair cells. In this report, we track the fate of damaged outer hair cells after ototoxic or noise insult, using prestin, an outer hair cell protein, as a marker. In guinea pigs, kanamycin followed by ethacrynic acid caused extensive outer hair cell loss. Two to nine days after the ototoxic drug treatment, prestin was found inside supporting cells in areas where outer hair cells were missing. The Deiters and outer pillar cells contained intracellular prestin-positive aggregates. Seven days after a damaging noise exposure, prestin was also found in supporting cells. Four or seven days after a noise exposure that produced extensive outer hair cell loss and decreased cochlear prestin mRNA expression in mice, similar supporting cell localization of prestin was observed. After inducing a more severe lesion in which both hair cells and differentiated supporting cells were lost by intratympanic application of neomycin in guinea pigs, prestin was absent in the cuboidal epithelial cells that remained on the basilar membrane seven days after neomycin application. Taken together, the results suggest

that differentiated supporting cells phagocytose damaged outer hair cells or their contents.

Supported by NIH/NIDCD Grants R01-DC01634, R01-DC05401, R01-DC05053, T32-DC00011 and P30-DC05188.

### **[572] Expression and Induction of the Transient Receptor Potential (TRP)V1 in the Rat Cochlea by Cisplatin**

**Debashree Mukherjee**<sup>1</sup>, Craig Whitworth<sup>1</sup>, Sarvesh Jajoo<sup>1</sup>, Leonard Rybak<sup>1</sup>, Vickram Ramkumar<sup>1</sup>

<sup>1</sup>*SIU School of Medicine*

Cisplatin is a widely used in the treatment of various solid tumors. However, its utility is compromised by significant ototoxicity and nephrotoxicity. While nephrotoxicity is effectively controlled by hydration and diuretics, ototoxicity still poses a significant problem. The generation of reactive oxygen species (ROS) has been linked to cisplatin-induced nephrotoxicity and ototoxicity. In the course of our studies to identify genes associated with cisplatin ototoxicity, we observed a significant increase in the expression of transient receptor potential (TRP)V1 channel in the rat cochlea following cisplatin administration. This protein is generally expressed in small diameter neurons within the sensory ganglia comprising the pain pathway. TRPV1 is a nonselective cation channel which responds to heat (activation threshold ~43°, low pH and capsaicin). Our data indicate increased TRPV1 protein expression in the cochlea, particularly in the outer hair cells and spiral ganglion cells. Administration of cisplatin to rats (13 mg/kg, i.p.) resulted in a profound increase in TRPV1 protein in these regions and a 15±3-fold increase in whole cochlear TRPV1 mRNA by 3 days. This increase in TRPV1 mRNA was associated with increases in NADPH oxidase subunit, Rac1, and the NADPH oxidase isoform, NOX3. Using organ of Corti hair cell line (UB-OC1), we showed a similar induction of TRPV1 mRNA and protein expression by cisplatin, which was attenuated by inhibition of NADPH oxidase activity. Based on these data, we propose that TRPV1 serves as a sensor of oxidative stress in the cochlea and that its expression is closely regulated by NADPH oxidase activity. Induction of TRPV1 in the hair cells and spiral ganglion cells and activation by endogenous ligands or low pH could contribute to cisplatin damage to these cells, since activation of this receptor in peripheral neurons is linked to apoptosis. As such, antagonists of TRPV1 could serve as protective agents against cisplatin ototoxicity.

### **[573] Proteomic Identification of Cisplatin-Induced Changes in Regulatory Proteins of Rat Inner Ear**

**Donald Coling**<sup>1</sup>, Dalian Ding<sup>1</sup>, Maciej Lis<sup>2</sup>, Rebecca Young<sup>3</sup>, Elizabeth Stofko<sup>1</sup>, Kenneth Blumenthal<sup>4</sup>, Richard Salvi<sup>1</sup>

<sup>1</sup>*SUNY - Buffalo, Center for Hearing and Deafness*, <sup>2</sup>*SUNY - Buffalo, Dept of Oral Biology*, <sup>3</sup>*SUNY - Buffalo, Dept of Medicine*, <sup>4</sup>*SUNY - Buffalo, Dept of Biochemistry*

Cisplatin is a widely used chemotherapeutic agent whose use is limited by severe side effects which include

nephrotoxicity, neurotoxicity, ototoxicity and vestibulotoxicity. Recent studies suggest that new protein synthesis and protein degradation play important roles in initiating cisplatin-induced apoptosis and in protecting cells from toxic insult. To identify changes in protein expression induced by cisplatin, we have used 2 dimensional differential gel electrophoresis (2D-DIGE) and matrix-assisted, laser desorption-ionization/time of flight (MALDI-TOF) mass spectrometry to analyze cochlear sensory epithelium from a P3 rat organ culture model. Sensory epithelium was cultured for 3 h in serum free BME medium in the presence or absence of 1 mM cisplatin. Proteins from cisplatin-treated cultures, labeled with the fluorescent DIGE fluor, Cy3, were mixed with proteins from untreated cultures labeled with Cy5 and separated on the same gel by 2D-DIGE. In control, dye swapping experiments, dyes used to label proteins were switched. Equal amounts of protein from each treatment group were mixed and labeled with Cy2 for intergel controls. Gels were scanned for Cy2, Cy 3 and Cy5 by fluorescence imaging. Replicate analysis of fluorescent images from 6 gels (twelve pairs of conditions) revealed 1.3 – 2.1 fold cisplatin-induced increases in the expression of 5 proteins and 1.5 – 6.4 fold decreases in the expression of 16 proteins (p<0.01, ANOVA). Four proteins were identified by MALDI-TOF mass finger printing (p≤0.05). Nucleobindin 1, a protein involved in nuclear calcium homeostasis increased by 2.1 fold (p<0.001). Heat shock protein 70 (HSP 70), a chaperone protein involved in stress response decreased 1.3 fold (p<0.0001). Hbs 1-like protein, homologous to a yeast translation elongation factor decreased 2.2 fold (p<0.01). Finally, a novel protein tentatively named “similar to putative zinc finger protein,” and a probable DNA or RNA binding protein decreased by 1.6 fold (p<0.0001). Changes in cisplatin-induced protein expression are discussed with respect to known or hypothesized functions of the identified proteins. The authors gratefully acknowledge support from the National Organization for Hearing Research Foundation.

### **[574] Metabolic Changes in Chinchilla Inferior Colliculus Following Carboplatin-Induced Ototoxicity: An *In Vivo* Quantitative microPET Study**

**Edward Lobarinas**<sup>1</sup>, Asit K. Paul<sup>2</sup>, John C. Luisi<sup>2</sup>, Dalian Ding<sup>1</sup>, Hani A. Nabi<sup>2</sup>, Richard Salvi<sup>1</sup>

<sup>1</sup>*University at Buffalo, Center for Hearing and Deafness*,

<sup>2</sup>*University at Buffalo, Department of Nuclear Medicine*

In previous studies, we have shown that in chinchillas, high doses of carboplatin will selectively destroy inner hair cells (IHC) and type-I neurons while sparing outer hair cells (OHC) and type-II neurons. Carboplatin-induced IHC loss greatly reduces the neural output of the cochlea as reflected in the compound action potential. However, local field potentials recorded from the inferior colliculus (IC) and auditory cortex show only a slight reduction in ears with significant IHC lesions. To gain insight into the functional changes in IC as a result of carboplatin-induced IHC loss (75 mg/kg, i.p.), chinchillas were imaged using a small animal positron emission tomography (PET) scanner (Focus 120 ®, Concorde Microsystems, Inc) and a metabolic marker F-18 fludeoxyglucose (FDG). Awake-



chinchillas were injected with ~3 mCi of FDG and placed in either quiet or a moderate intensity sound (80 dB SPL NBN) condition for 1 h during FDG uptake. Chinchillas were then anesthetized and imaged across 4 conditions: baseline quiet, baseline sound, post-carboplatin quiet and post-carboplatin sound; on 4 different days. Post-carboplatin images were acquired 3 and 5 days post-treatment. FDG uptake per unit volume of IC was calculated as a fraction of injected dose based on the IC counts. In the pre-carboplatin condition, sound produced a 145% increase in activity of the IC relative to quiet. Metabolic activity in quiet was similar before and after carboplatin, indicating that carboplatin had no significant effect on resting metabolic rate. However, after carboplatin, sound produced a small, 32% increase in IC activity. These results indicate that carboplatin-induced IHC damage causes a substantial decrease in sound-evoked metabolic rate in the IC 3-5 days post-treatment. Additional studies are underway to determine if sound-evoked metabolic rate in the IC recovers to normal levels with longer post-treatment times. (Supported by NIH grant R01 DC06630-01)

### **[575] Carboplatin Induced Cochlear Hair Cell Lesion in Organotypic Cultures**

**Haiyan Jiang<sup>1</sup>**, Dalian Ding<sup>1</sup>, Richard Salvi<sup>1</sup>

<sup>1</sup>*University at Buffalo*

Carboplatin is a second-generation, antineoplastic drug that is considered to be less ototoxic and less nephrotoxic than cisplatin. In vivo studies have shown that carboplatin produces relatively little hair cell damage in guinea pigs, gerbils, rats and mice; however, when carboplatin is administered systemically to chinchillas it produces a lesion that differs significantly from other ototoxic drugs in two major respects. First, instead of damaging the outer hair cells (OHC) first, carboplatin selectively destroys inner hair cells (IHCs) and type I spiral ganglion neurons in the chinchilla. Second, instead of producing a lesion that spreads from base-to-apex, carboplatin produces a relatively uniform IHC lesion along the entire length of the cochlea. When carboplatin is administered systemically, one factor that may influence its ototoxic potential is the amount of drug uptake into the cochlea. To determine if the uptake of carboplatin into the cochlea might be responsible for the striking species differences in carboplatin ototoxicity, we prepared cochlear organotypic cultures from adult chinchillas and postnatal day 3 rat pups. When chinchilla cochlear cultures were treated with carboplatin, hair cell damage was mainly confined to the IHC as it is in vivo. In contrast, when rat cochlear cultures were treated with carboplatin, hair cell loss was first observed in OHC followed by IHC.

### **[576] Cisplatin Induced Changes in Apoptosis Related Gene Expression in Rat Cochlear Cultures**

**Richard Salvi<sup>1</sup>**, Ping Wang<sup>1</sup>, Haiyan Jiang<sup>1</sup>, Lei Wei<sup>1</sup>, Dalian Ding<sup>1</sup>

<sup>1</sup>*University at Buffalo*

Cisplatin damages the hair cells in the inner ear resulting in high frequency sensorineural hearing loss. Our previous

in vivo and in vitro studies suggest that cisplatin activates p53 signaling pathways and triggers programmed cell death by way of cell surface receptors that activate initiator caspase 8 followed by executioner caspase 3. Because the signaling pathways involved in cisplatin-induced cell death are likely to be complex, we used 96-gene apoptosis microarrays and quantitative RT-PCR to identify a subset of genes that showed significant, early changes in expression in postnatal rat cochlear cultures treated with 0.2 mM cisplatin. Cochlear cultures showed little evidence of hair cell pathology 3 h after cisplatin treatment; however, after 12 h, many hair cells appeared abnormal, but still present. Gene microarray and RT-PCR analysis showed that the expression of 4 genes in the p53 signaling pathway (Bnip3, Birc3, Mcl1, Gadd45a) increased 2-6 fold 3 h post-treatment. After 12 h, all 4 genes showed significantly reduced expression. Six genes in the tumor necrosis factor (TNF) receptor family (Bcl10, Myd88, Rad, Tnfaip2 protein, Tnfrsf12a, Tnfrsf1a) showed a 2-10 fold increase in expression at 3 h, but after 12 h, expression of nearly all of these genes had declined significantly. These results suggest that the p53 and TNF receptor signaling pathways play an important role in the early stages of cisplatin-induced ototoxicity and that modulating these pathways may provide significant protection against cisplatin-induced ototoxicity. Supported by NIH (R01 DC06630-01).

### **[577] Styrene-Induced Cochlear Damage**

**Guang-Di Chen<sup>1</sup>**, Bo-Hua Hu<sup>1</sup>, Ashley Gambino<sup>1</sup>, Robert Burkard<sup>1</sup>, Donald Henderson<sup>1</sup>

<sup>1</sup>*SUNY at Buffalo*

Styrene is an aromatic solvent widely used as a precursor for polystyrene plastics in many industrial environments. It is known to disrupt the auditory system in both humans and animals. Styrene exposure results in hearing dysfunction in the mid-frequency range. Supporting cells are the first targets of the solvent, followed by the outer hair cells of the third row (OHC3), OHC2, and OHC1. However, the cell death pathway is still unclear. In this study, Long Evans pigmented rats were exposed to styrene by oral gavage with dosages of 200, 300, and 400 mg/kg body weight. Hearing loss was assessed with auditory brainstem responses (ABR). In vivo staining of caspase-8 and caspase-9 was used to identify apoptotic cell death pathway in dying OHCs. Positive staining of caspase-8 and caspase-9 indicated that both death receptor-mediated and mitochondria-mediated apoptotic pathways are involved in styrene-induced hair cell death. The cochlear injuries were styrene dose dependent. There was little effect of 200 mg/kg on ABR threshold, but then each 100 mg styrene increase caused an additional 4-5 dB threshold shift. Interestingly, styrene first attacks the 3rd row of OHCs with relatively large lesion but may only induce minor hearing loss. Styrene and noise produce subtle but reliable differences in cochlear pathology. [Research supported by grant 1R01OH008113-01A1 from NIOSH]

### **578 Possible Mechanism of Gentamicin Toxicity in Vestibular Hair Cell with Expression of Caveolin-1 and Heme Oxygenase-1**

Kyu-Sung Kim<sup>1</sup>, Ho-Suk Choi<sup>1</sup>, Byung-Han Cho<sup>1</sup>, Byung-Rim Park<sup>2</sup>

<sup>1</sup>College of Medicine, Inha University, <sup>2</sup>College of Medicine, Wonkwang University

**Objectives:** Oxidative stress has been implicated as a mechanism of aminoglycoside-induced ototoxicity. Heme oxygenase (HO) catalyzes the rate-limiting step in oxidative degradation of heme, and to yield a carbon monoxide (CO) as byproduct exhibits potent anti-inflammatory effect. The caveolin-1 is known as a mediator of cell death or survival of injured cell and inhibitor of various signaling pathways. Some studies have suggested that caveolin-1 interacts with HO-1 at the plasma membrane caveolae, and in the absence of caveolin-1 protein, the activity of HO-1 increased suggesting inhibitory regulation of enzyme activity, cause cell damage. The present investigation was performed to identify the expression of heme oxygenase-1(HO-1) and caveolin-1 in gentamicin(GM)-induced ototoxicity. **Materials and methods:** UB/UE-1 vestibular cell line cultured 33°C for 48hours and at 39°C for 24hours for differentiation. Then, cells were treated with 0.1mM of GM, H89, an inhibitor of PKA, aminoguanine(AG), iNOS inhibitor alone or their combination. After 8hours, and 24hours after treatment, we examined HO-1, caveolin-1 expression by western blot and measured cGMP level and PKA activity. **Result:** Caveolin-1 was expressed spontaneously in differentiated UB/UE-1 cells and increased after gentamicin treatment. The gentamicin-induced caveolin-1 expression was inhibited by H89 and AG. HO-1 is induced higher in the group of both gentamicin and H89 treatment than gentamicin or H89 alone. **Conclusion:** The PKA-mediated caveolin-1 overexpression and its relation to HO-1 is a probable mechanism of GM-mediated vestibular cell damage.

### **579 Hearing Loss in Patients with Gentamicin Vestibulotoxicity**

Robert Dobie<sup>1</sup>, Owen Black<sup>2</sup>, Susan Pesznecker<sup>2</sup>, Valerie Stallings<sup>2</sup>

<sup>1</sup>UC-Davis, <sup>2</sup>Legacy Research and Tech Center

**Objective.** Determine whether patients with gentamicin vestibulotoxicity have hearing thresholds worse than predicted by distributions of better-ear hearing thresholds of people of the same age and gender in the general population and if so, the severity and audiometric pattern of that hearing loss.

**Design.** Retrospective case series from previously published prospective and retrospective studies of vestibular function in patients receiving gentamicin.

**Setting.** Tertiary neurotological practice.

**Patients.** Convenience sample of 33 consecutive patients presenting with objective evidence of vestibulotoxicity after systemic gentamicin therapy. 25 of the 33 had valid and complete audiometry.

**Interventions.** None.

**Main outcome measure.** Age- and gender-corrected better-ear pure tone thresholds, 0.5 to 6 kHz. The better ear audiogram was defined two ways: primarily, the audiogram of the ear with the better average threshold at 0.5, 1, and 2 kHz; secondarily, the composite audiogram taking the better threshold for each frequency.

**Results.** Patients exhibiting gentamicin vestibulotoxicity had hearing thresholds that were similar to those seen in the general population at 0.5, 3, and 6 kHz. Median thresholds were 6 – 7 dB worse than expected at 1 and 2 kHz (95% confidence intervals: 2 to 13 and 3 to 12 dB, respectively). The largest median difference was 15 dB at 4 kHz (95% confidence interval: 3 to 23 dB), but this difference was not significant for the more conservative composite definition of the better ear.

**Conclusions.** Patients with gentamicin vestibulotoxicity have little additional hearing loss in comparison to the general population. Treating physicians should monitor both auditory and vestibular function when aminoglycosides, especially gentamicin, must be used.

### **580 NF-κB Plays a Proapoptotic Role in Cisplatin Induced Ototoxicity in Auditory Cell Line**

Sung Hyun Boo<sup>1</sup>, So Yean Park<sup>2</sup>, Hyun-Seok Lee<sup>1</sup>, Yang-Sun Cho<sup>1</sup>, Sung Hwa Hong<sup>1</sup>, Won-Ho Chung<sup>1</sup>

<sup>1</sup>Department of ORL-HNS, Sungkyunkwan University School of Medicine, Samsung Medical Center, <sup>2</sup>Samsung Biomedical Research Institute, Sungkyunkwan University School of Medicine

Cisplatin is a commonly used chemotherapeutic agent, but ototoxicity is a major toxic side effect. Many studies have shown that the mechanism of ototoxicity by cisplatin involves apoptosis of hair cells. However, the underlying mechanism remains unclear. NF-κB is a transcription factor that regulates apoptosis in many organs and tissues. In the present study, we investigated the role of NF-κB in apoptotic pathway induced by cisplatin in auditory cell line, HEI-OC1 cells.

To identify apoptotic cell death induced by cisplatin, HEI-OC1 cells were incubated with cisplatin at different concentrations(5, 25, 50, 100μM) for 24 hours, and caspase 3 activity was assayed with Colorimetric CaspACE Assay™ kit (Promega, USA). Treated cells with 50μM of cisplatin were immunostained with anti-caspase 3 antibody(Cell signaling, USA) and anti-NF-κB p65 antibody(Santa cruz, USA). Two different NF-κB inhibitor, Bay 11-7085(Alexis biochemical, USA) and SN-50(Biomol, USA), was coincubated with cisplatin (50μM) for 24 hours and caspase 3 activity was assayed.

The results showed that cisplatin increased caspase 3 activity in HEI-OC1 cells cultured at 33°C (p<0.05) compared to normal control. The concentration of 50μM showed maximal effects. Many cells were stained with anti-caspase 3 antibody in treated cells. In normal control, NF-κB was immunohistochemically localized in cytoplasm. However, in treated cells NF-κB was translocated to the nucleus, which demonstrated activation of NF-κB. Co-treatment with Bay 11-7085 and SN-50 significantly

reduced caspase 3 activity compared to cisplatin only group.

Based on our study, NF- $\kappa$ B is activated and plays a pro-apoptotic role during cell death by cisplatin in HEI-OC1 cell line.

This work was supported by Samsung Biomedical Research Institute grant, #SBRI C-A5-331-1.

### **581 Modulation of Cytoplasmic Gentamicin Uptake by Loop Diuretics and Anti-Diuretics**

**Qi Wang<sup>1</sup>**, Bing-Cai Guan<sup>1</sup>, Zhi-Gen Jiang<sup>1</sup>, Peter Steyger<sup>1</sup>

<sup>1</sup>*Oregon Health & Science University*

Loop diuretics potentiate gentamicin uptake by hair cells and subsequent ototoxicity, yet the underlying mechanisms remain uncertain. We used MDCK cells to determine the effect of loop diuretics and anti-diuretics on the uptake of fluorescent gentamicin (GTTR), and cellular electrophysiological conditions.

Bumetanide, an inhibitor of the Na/K/Cl co-transporter, greatly enhanced GTTR uptake in MDCK cells. This enhanced uptake can be negated by pre-treating cells with lanthanum (La<sup>+++</sup>) that purges cation channels from the luminal plasma membrane. Recovery of GTTR uptake to control levels occurred within ~60 minutes following La<sup>+++</sup> treatment. The anti-diuretic vasopressin decreased GTTR uptake.

Whole-cell recordings found that the resting potential of MDCK cells was  $-22.7 \pm 1.7$  mV, with baseline membrane potential oscillations of  $0.53 \pm 0.07$  mV. Bumetanide enhanced these membrane potential oscillations to  $2.6 \pm 0.5$  mV ( $p < 0.005$ ), and hyperpolarized cells by  $10.5 \pm 1.9$  mV. The cation channel blocker La<sup>+++</sup> depolarized the resting potential by  $8.3 \pm 1.5$  mV, and reduced the amplitude of membrane potential oscillations. The anti-diuretic vasopressin also hyperpolarized cells, and induced an outward current, with increased membrane resistance, suggesting that a closure of cation channels may underlie its inhibition of GTTR uptake.

In ratiometric fluorescence pH studies, the resting pH of MDCK cells was  $\text{pH } 7.5 \pm 0.064$ . Bumetanide and La<sup>+++</sup> did not significantly change the intracellular pH, but vasopressin reduced the intracellular pH by  $0.59 \pm 0.175$  units (i.e., more acidic), conditions also known to close pH-sensitive TRPV cation channels.

As in bacteria, energy-dependent processes regulate intracellular resting potentials and pH, which modulate gentamicin uptake. Increased negative membrane potentials and  $\Delta\text{pH}$  (i.e. the intracellular environment is more basic than the extracellular environment) increases bacterial uptake of aminoglycosides. In MDCK cells, hyperpolarization increases, and reduced  $[\Delta\text{pH}]$ , induced by loop diuretics and anti-diuretics modulate gentamicin uptake, mimicking conditions that enhance bacterial aminoglycoside uptake.

*Funded by NIDCD R01 04555, P30 05983 and R21 06084.*

### **582 Transient Transfection of TRPV4 Enhances Aminoglycoside Uptake**

**Takatoshi Karasawa<sup>1</sup>**, Qi Wang<sup>1</sup>, Zachary Oestreicher<sup>1</sup>, Peter Steyger<sup>1</sup>

<sup>1</sup>*Oregon Health & Science University*

We previously demonstrated that gentamicin uptake in the cultured kidney cells is modulated by regulators of the transient receptor potential vanilloid 1 channel (TRPV1), a member of TRP family of nonselective cation channels. For gentamicin to enter the endolymph from where it can access the hair cells and cause ototoxicity, we hypothesized that a TRP channel has a role in enabling gentamicin to be transported from serum to stria fluids and endolymph. A previous report demonstrated that another member of TRP family, TRPV4, was localized in stria vascularis in the inner ear (Leidkte et al., 2000).

Immunocytochemistry for rodent TRPV4 revealed specific immunolabeling at the luminal surface of murine marginal cells, intra-stria capillaries, and in the luminal cells of the spiral prominence. In MDCK cells and murine distal tubule and collecting duct epithelial cells, TRPV4 is localized near the baso-lateral membranes. In non-polarized, transfected HEK 293T cells, TRPV4 immunolabeling was uniformly distributed near the cell membrane and within the cytoplasm.

To determine if TRPV4 is aminoglycoside-permissive or modulates aminoglycoside uptake, we: 1) overexpressed TRPV4; and will 2) knock-down, 3) activate, and 4) inhibit TRPV4 function *in vitro* using Texas Red-conjugated gentamicin (GTTR) to document enhanced or reduced cytoplasmic uptake of gentamicin. HEK 293T cells transiently transfected with a rat TRPV4 and showed enhanced GTTR uptake compared to vector-transfected and untransfected cells in assays with extracellular media at either physiological  $[\text{Ca}^{++}]$  or nominally zero  $[\text{Ca}^{++}]$ . We are now undertaking TRPV4 knock-down in cell lines developed from mouse kidney, to further investigate TRPV4 involvement in gentamicin uptake.

*Funded by NIDCD R01 04555, P30 05983, T32 DC 05945 and R21 06084.*

### **583 Prenatal Dioxin (TCDD) Exposure Impairs Cochlear Function in Mice**

Theresa M. Safe<sup>1</sup>, Lisa A. Opanashuk<sup>1</sup>, Thomas A. Gasiewicz<sup>1</sup>, **Anne E. Luebke<sup>1</sup>**

<sup>1</sup>*University of Rochester Medical Center*

2,3,7,8-tetrachlorodibenzo-p-dioxin (TCDD) is a ubiquitous and persistent environmental contaminant known to exert developmental toxicity. The aryl hydrocarbon receptor (AhR) is believed to mediate the toxic effects of dioxin and adult AhR knockout (AhR KO) mice have elevated auditory thresholds when compared to their wildtype (WT) littermates. The normal function of the AhR is poorly understood. We were interested in testing whether a single prenatal dioxin exposure or the loss of the AhR disrupts auditory system function. Cochlear function was analyzed in offspring from C57Bl/6 dams that were exposed to 500 ng/kg TCDD or olive oil (vehicle) on embryonic day 12 by measuring 1) auditory brainstem response (ABRs) to tone pips at 6 log-spaced frequencies from 5.6 to 30 kHz, and

2) distortion-product otoacoustic emissions (DPOAEs) evoked by primaries with f2 at the same 6 frequency values. Cochlear function was assessed at 1.5 months of age in 5 experimental groups: (1) vehicle-exposed male mice (2) vehicle-exposed female mice (3) TCDD-exposed male mice (4) TCDD-exposed female mice (5) AhR knock-out male mice. Cochlear threshold sensitivity was significantly elevated by prenatal dioxin exposures in both female and male mice as measured by 1) visual inspection of ABR waveforms obtained at 10 dB level increments and 2) DPOAE iso-response contours. TCDD-exposed male mice had elevated ABR thresholds at all frequencies, whereas TCDD-exposed female mice had elevated thresholds for frequencies > 16 kHz. These observations are consistent with previous studies indicating that gestational TCDD exposure produces neurotoxicity in a sexually dimorphic manner. (Supported by NIH grants RO1 003086, RO1 ES09430, R21 ES013512, P30 ES01247)

#### **584 Ultrastructural Analysis of Initial Events in Aminoglycoside-Induced Hair Cell Loss in the Zebrafish Lateral Line**

**Remy Pujol<sup>1,2</sup>**, Kelly N. Owens<sup>2,3</sup>, David W. Raible<sup>2,3</sup>, Edwin W. Rubel<sup>2,4</sup>

<sup>1</sup>INSERM Unit 583, Université Montpellier, INM, Hôpital St. Eloi, FRANCE, <sup>2</sup>V.M. Bloedel Hearing Research Center, <sup>3</sup>Dept. of Biological Structure, <sup>4</sup>Dept. of Otolaryngology-HNS, University of Washington

Loss of mechanosensory hair cells induced by aminoglycoside exposure is well documented, but the underlying etiology is poorly understood. We examined the effect of the aminoglycoside neomycin on hair cells of lateral line of the larval zebrafish, *Danio rerio*, an amenable vertebrate system for genetic and developmental analysis which allows visualization of hair cells *in vivo*. We documented the dose-dependent relationship between lateral line hair cell loss and neomycin exposure (Harris et al. 2003). Here, we determined early cellular events associated with aminoglycoside-induced hair cell damage in 5 day-old zebrafish using TEM analysis.

Ultrastructural analysis of wildtype 5 day-old larvae reveals hair cells with mature features including stair-cased stereocilia, with rootlets embedded in a dense cuticular plate, basal nuclei, and afferent and efferent innervation. At high (200  $\mu$ M) doses of neomycin, aminoglycoside-induced hair cell death is similar ultrastructurally to that of other species. We examined both short time courses and range of doses (10 – 200  $\mu$ M) of neomycin to determine the earliest cellular responses. Moderate concentrations of neomycin (50  $\mu$ M) for 15-30 minutes resulted in pronounced damage, with severe degeneration of hair cells. Thus, neomycin-induced hair cell loss can occur rapidly. We also observed other events less frequently, including degenerating hair cells, pyknotic nuclei or fusion of stereocilia. Damaged hair cells were observed residing next to hair cells with no apparent damage. At low doses of neomycin (25  $\mu$ M) for 15 minutes, we observed hair cells with initial signs of damage, of which the most

prevalent was swollen mitochondria particularly surrounding the nucleus. Concurrently, mitochondria within afferent dendrites and support cells appear normal. *Supported by Bloedel Traveling Scholars Program and NIDCD grants DC 05987, DC00018, and DC04661*

#### **585 Pharmacokinetics of Oxaliplatin in Blood, Cerebrospinal Fluid and Perilymph After Intravenous Administration in the Guinea Pig**

**Victoria Hellberg<sup>1</sup>**, Inger Wallin<sup>2</sup>, Andreas Ekborn<sup>1</sup>, Hans Ehrsson<sup>2</sup>, Göran Laurell<sup>1</sup>

<sup>1</sup>Department of Otorhinolaryngology and Head & Neck Surgery, Karolinska University Hospital, Sweden,

<sup>2</sup>Karolinska Pharmacy, Stockholm, Sweden

Introduction: Cisplatin is an anticancer drug that is used world-wide. Drug-induced hearing loss and tinnitus can be a major problem for the patient and thereby dose-limiting. Oxaliplatin is a third generation platinum anticancer drug used for the treatment of colorectal carcinoma where cisplatin is ineffective. Oxaliplatin is not reported to have any ototoxic side effects. No previous study has shown if oxaliplatin reaches the inner ear after systemic administration. Materials and methods: 16.6 mg/kg oxaliplatin was given intravenously for 15-45 s to guinea pigs. Blood samples were drawn within a time range of 1.5 to 120 minutes after administration of oxaliplatin and were ultrafiltered before analysis. Clear CSF was collected from the subarachnoid space and scala tympani perilymph was aspirated within a time range of 5 to 120 minutes. Liquid chromatography with postcolumn derivatization was used for quantitative determination of the parent drug (Ehrsson & Wallin 2003). Results: The terminal elimination half-life in blood was 12.1 min. Oxaliplatin in CSF reached a mean maximum concentration of 14.9  $\mu$ M 5.2 minutes after injection. In perilymph the peak concentration was delayed as compared to CSF. The mean maximum concentration of 4.57  $\mu$ M was seen after 14.9 min. The concentration level remained constant around 3  $\mu$ M for about 50 minutes. Discussion: Compared to an equimolar dose of cisplatin given to guinea pigs the levels of oxaliplatin was about 50% of the concentration of cisplatin both in CSF and perilymph. The elimination half-life was shorter for oxaliplatin as compared to cisplatin (Laurell et al. 1995). The lack of an ototoxic effect of oxaliplatin in humans might be related to a low permeability for oxaliplatin through the blood-labyrinth barrier.

#### **586 Intact Blood-Perilymph Barrier in the Rat After Impulse Noise Trauma**

**Göran Laurell<sup>1,2</sup>**, Marie Teixeira<sup>1</sup>, Maoli Duan<sup>2</sup>, Olivier Sterkers<sup>1</sup>, Evelyne Ferrary<sup>1</sup>

<sup>1</sup>EMI-U 0112, UFR Xavier Bichat, Paris, France,

<sup>2</sup>Department of Otolaryngology and Head & Neck Surgery, Karolinska University Hospital, Stockholm

Impulse noise trauma is reported to cause multiple effects on the cochlea including mechanical damage, oxidative stress and excitotoxicity. The aim of the study was to observe the effects of impulse noise on cochlear homeostasis. A well-established rat model was used for evaluation of the early effects of impulse noise trauma on

the blood-perilymph barrier integrity. In order to evaluate if a change of the paracellular transport properties contribute to cochlear injury after impulse noise, the paracellular transport of radioactive mannitol into scala tympani perilymph (PLT) and electrolyte concentrations in PLT were estimated. Fourteen animals exposed to synthesized impulse noise of 160 dB were designed as the experimental group and 15 rats not exposed to noise were used as a control group. After impulse noise exposure mannitol was administered and PLT samples were taken during 2 hours post-noise trauma. In the control group corresponding PLT samples were taken after mannitol injection. PLT mannitol concentration (the ratio 3H-radioactivity in perilymph over plasma) and electrolyte concentrations in PLT did not differ between the two groups. Histological evaluation was carried out by light microscopy and revealed no signs of disruption of the cochlear compartments. In conclusion, taken all together, the results of the present study do not support the hypothesis that the blood-perilymph barrier is a major target for early impulse noise-induced cochlear lesion.

#### **587 Sequential Apical Sampling from the Cochlea as a Method to Quantify Longitudinal Drug Gradients: Validation with an Ionic Marker**

Robert Mynatt<sup>1</sup>, Stefan Plontke<sup>2</sup>, Shane Hale<sup>3</sup>, Ruth Gill<sup>3</sup>, Alec Salt<sup>3</sup>

<sup>1</sup>Department of Otolaryngology, St. Louis University, St. Louis, MO, <sup>2</sup>Department of Otorhinolaryngology Head and Neck Surgery, University of Tübingen, Germany,

<sup>3</sup>Department of Otolaryngology, Washington University School of Medicine, St. Louis, MO

The most commonly used method to sample cochlear perilymph consists of the aspiration of fluid from the basal turn of scala tympani (ST). It has recently been shown that samples obtained in this manner are highly contaminated with cerebrospinal fluid (CSF) (Salt, Kellner, Hale. *Hear Res* 182, 24, 2003). Taking samples from the cochlear apex allows perilymph to be obtained at a greater distance from the cochlear aqueduct and therefore with less CSF contamination. In the present study, we evaluated a novel method in which all the fluid emerging from the cochlear apex after perforation (driven by cerebrospinal fluid pressure) was collected as sequential, 1 &#956;L samples. In guinea pigs, ST volume is approximately 4.7 &#956;L, so the collection of 10 samples ensures that all the perilymph is collected as it is "washed out" of the cochlea and replaced with CSF. To evaluate the method we applied an isosmotic 20 mM solution of the ionic marker trimethylphenylammonium (TMPA) to the round window (RW) membrane of guinea pigs for 2 hours. The RW niche was dried and ten separate, 1 &#956;L samples were then collected sequentially from the apex over a period which averaged 5.5 min (33 s per sample). Each sample was diluted in 25 &#956;L of artificial perilymph and the TMPA content measured in vitro with a TMPA-selective microelectrode. The TMPA content was relatively low in the first sample, increasing to a peak level in sample 4 or 5 and then falling progressively with later samples. The results were consistent with a basal-apical concentration gradient of TMPA occurring as a result of the local delivery protocol. Simulation of the TMPA dispersal along ST and

of the fluid movements during the sampling procedure allowed us to closely replicate the experimental sampling data. The use of sequential apical samples appears to be a valuable method for documenting the dispersal of substances along the length of ST.

Supported by grant NIH/NIDCD RO1 DC01368 (AS).

#### **588 Gentamicin Concentration Gradient Along Scala Tympani of the Guinea Pig Cochlea After Round Window Drug Administration**

Stefan Plontke<sup>1</sup>, Robert Mynatt<sup>2</sup>, Shane Hale<sup>3</sup>, Alec Salt<sup>3</sup>

<sup>1</sup>Department of Otorhinolaryngology Head and Neck Surgery, University of Tübingen, Germany, <sup>2</sup>Department of Otolaryngology, St. Louis University, St. Louis, MO,

<sup>3</sup>Department of Otolaryngology, Washington University School of Medicine, St. Louis, MO

The distribution of drugs in the ear is of scientific and clinical importance. It was shown with ionic markers that local applications to the round window (RW) membrane generate a concentration gradient along the cochlea, with lower concentrations in apical turns (Salt and Ma, *Hear. Res.* 154, 88, 2001). Calculations suggest that longitudinal gradients persist even after prolonged applications. For clinically-relevant substances, such as gentamicin, it has been predicted, based on simulations, that concentration gradients occur after RW application (Plontke, Wood and Salt, *Otology and Neurotology* 23: 967, 2002). We have now developed methods to quantify concentration gradients of drugs in the ear. Gentamicin (40 mg/ml) was administered to the RW niche of guinea pigs in vivo for 2 or 3 hrs. Perilymph was then sampled from the cochlear apex using a sequential-sampling protocol. Ten samples, each with a volume of 1µl, were taken into calibrated capillary tubes. Analysis of the samples showed the gentamicin content of the first sample in each experiment (dominated by perilymph from apical regions) to be substantially lower than that of the fourth sample (dominated by basal turn perilymph), qualitatively demonstrating the existence of a concentration gradient along scala tympani (ST). Sample data were interpreted using a finite element model (<http://oto.wustl.edu/cochlea/>), modified to incorporate fluid movements, drug diffusion and volume accumulation corresponding to those in apical sampling. By simulating the sample concentration data, it was possible to establish the drug profile along ST immediately prior to sampling. This analysis shows that drug gradients along the scala necessary to generate the observed sample concentrations are substantially higher than suggested by the raw sample concentrations. This approach permits, for the first time, the longitudinal gradient of gentamicin along ST to be measured.

Supported by grant NIH/NIDCD RO1 DC01368 (AS).

#### **589 Microarray Analysis of Ion Transport-Related Genes in Reissner's Membrane**

Nithya Raveendran<sup>1</sup>, Satyanarayana Pondugula<sup>1</sup>, Daniel C. Marcus<sup>1</sup>

<sup>1</sup>Kansas State University

Reissner's membrane (RM) is anatomically poised to play an important role in endolymph ion homeostasis;

disregulation is thought to be the cause of Meniere's disease, a syndrome that is often treated with glucocorticoids. We previously demonstrated currents across gerbil RM that could be accounted for by active absorption of  $\text{Na}^+$  from endolymph via apical epithelial Na channels (ENaC) and basolateral K channels & Na,K-ATPase [Lee & Marcus, *Neurosci.* 2003], similar to the glucocorticoid-stimulated transport in semicircular canal [Pondugula et al., *AJP* 2004]. Here we sought molecular evidence for mRNA expression of key elements of this pathway in rat and mouse RM using gene microarray and quantitative RT-PCR. Rat RM showed the same amiloride-sensitive  $I_{sc}$  as in gerbil. Dexamethasone (DEX) led to an up-regulation of  $\alpha$ -ENaC by a factor of 3 although the  $\alpha 1$  subunit of Na,K-ATPase was unchanged. Gene array showed that DEX up-regulated all 3 subunits of ENaC ( $\alpha$ : 3x;  $\beta$ : 1.2x;  $\gamma$ : 1.5x) and the  $\alpha 2$  subunit of Na,K-ATPase in mouse RM. Transcripts for  $\beta 1$ , 2 & 3-Na,K-ATPase were slightly down-regulated. Other important genes in this pathway (sgk1, glucocorticoid receptor, Nedd 4-2, 11 $\beta$ HSD-1) were also present. This Na transport function of RM was surprising in light of earlier reports suggesting a cAMP-regulated Cl transport function for this epithelium, although the two are not mutually exclusive. Indeed, we found transcripts present for anion transporters (Na/K/2Cl-cotransporter; pendrin; anion exchanger-1,-2,-3,-4; Cl channels) and cAMP regulation (PKA, cAMP-dependent GEF, adenylyl cyclase, phosphodiesterase). These results support our earlier finding of an active amiloride-sensitive Na absorptive function in gerbil RM, extend these results to rat and mouse RM, demonstrate that this pathway is under control of glucocorticosteroids and provide a molecular basis for possible Cl transport function. Supported by NIH-NIDCD grants R01-DC00212, NCR P20 RR17686 & P20 RR16475.

#### **[590] Glucocorticoid Regulation of Genes Involved in the Amiloride-Sensitive Na Transport Pathway of Rat Semicircular Canal Duct Epithelium**

**Satyanarayana Pondugula<sup>1</sup>**, Nithya Raveendran<sup>1</sup>, Zuhail Ergonul<sup>2</sup>, Lawrence Palmer<sup>2</sup>, Daniel C. Marcus<sup>1</sup>

<sup>1</sup>Kansas State University, <sup>2</sup>Weill Medical College of Cornell University

We have recently shown that glucocorticoid receptors (GR) stimulate absorption of Na by semicircular canal duct (SCCD) epithelia via amiloride-sensitive epithelial sodium channels (ENaC) [Pondugula et al., *AJP*, 2004]. We sought to determine the presence of genes involved in control of amiloride-sensitive Na transport pathway by rat SCCD epithelia and whether their level of expression was regulated by glucocorticoids using quantitative real-time RT-PCR. Transcripts were present for  $\alpha$ ,  $\beta$  &  $\gamma$  subunits of ENaC;  $\alpha_1$ ,  $\alpha_3$ ,  $\beta_1$ , &  $\beta_3$  isoforms of Na,K-ATPase; inwardly rectifying potassium channels (Kir [ $IC_{50}$  of short circuit current ( $I_{sc}$ ) for  $\text{Ba}^{2+}$ : 210  $\mu\text{M}$ ] Kir2.1, Kir2.2, Kir2.3, Kir2.4, Kir3.1, Kir3.3, Kir4.1, Kir4.2, Kir5.1 & Kir7.1; sulfonyl urea receptor1 (SUR1); GR; mineralocorticoid receptor (MR); 11 $\beta$ -hydroxysteroid dehydrogenase type1 (11 $\beta$ -HSD1) & 11 $\beta$ -HSD2; Sgk1 and Nedd4-2. On the other hand,

transcripts for  $\alpha_4$ -Na,K-ATPase; Kir1.1, Kir3.2 & Kir3.4, Kir6.1, Kir6.2 and SUR2 were absent and  $I_{sc}$  was not inhibited by glibenclamide, a blocker of Kir6.1/2-SUR. Dexamethasone ([DEX]100 nM; 24 hr) not only up-regulated the transcripts of  $\alpha$ -ENaC (~4 fold [X]);  $\beta_2$  (~2X) &  $\beta_3$  (~8X) Na,K-ATPase; Kir2.1 (~5X), Kir2.2 (~9X), Kir2.4 (~3X), Kir3.1 (~3X), Kir3.3 (~2X), Kir4.2 (~3X) & Kir7.1 (~2X); Sgk1 (~4X) and Nedd4-2 (~2X) but also down-regulated GR (~3X) and 11 $\beta$ -HSD1 (~2X). Transcript levels of GR & 11 $\beta$ -HSD1 were higher than MR & 11 $\beta$ -HSD2 in the absence of DEX. DEX altered transcript levels by selective activation of the GR and not MR. Proteins were present for  $\alpha$ ,  $\beta$  &  $\gamma$  subunits of ENaC and Sgk1 and  $\alpha$ -ENaC protein was up-regulated by DEX. These findings are consistent with the genomic stimulation by glucocorticoids of Na absorption by SCCD epithelia and provide an understanding of the therapeutic action of glucocorticoids in the treatment of Meniere's disease. Supported by NIH-NIDCD grant R01-DC00212, NCR P20 RR17686 & P20 RR16475.

#### **[591] Calcium Homeostasis by Cochlear and Vestibular Vitamin D-Responsive Epithelial Calcium Channel (ECaC1, TRPV5) Pathway**

**Daisuke Yamauchi<sup>1</sup>**, Nithya Raveendran<sup>1</sup>, Satyanarayana Pondugula<sup>1</sup>, Daniel C. Marcus<sup>1</sup>

<sup>1</sup>Kansas State University

The low luminal  $\text{Ca}^{2+}$  concentration of mammalian endolymph in the inner ear is required for normal hearing and balance. We recently reported the expression of a  $\text{Ca}^{2+}$  transport system based on the epithelial  $\text{Ca}^{2+}$  channel ECaC1 (TRPV5) in primary cultures of semicircular canal (SCCD) epithelium [Yamauchi et al., *BBRC*, 2005]. The expression of this pathway in native rat cochlear and vestibular tissues was studied with quantitative RT-PCR and Western blot. Tissue explants of stria vascularis (SV) and lateral wall (LW) from the cochlea and of SCCD were acutely cultured for 24 h in the presence or absence of 1,25-dihydroxyvitamin D3 (vitD). ECaC1 was present in all 3 tissues and was upregulated in SCCD by vitD. ECaC2 was expressed at low levels or not detected and was unaffected by vitD. Calbindin-D9k and -D28k were detected in all tissues and -D9k upregulated in SCCD and LW.  $\text{Na}^+/\text{Ca}^{2+}$ -exchangers (NCX-1,-2,-3) were expressed in all tissues and NCX2 was strongly upregulated in LW by vitD. Multiple plasma membrane  $\text{Ca}^{2+}$ -ATPase isoforms were detected. PMCA-1,-3,-4 were found in all tissues. PMCA4 was downregulated in SCCD and PMCA3 was upregulated in LW by vitD. PMCA2 was not detected in SCCD and low in SV. The vitamin D receptor was detected in all tissues, with the highest expression in SCCD; expression levels were not affected by exposure to vitD. Western blot analysis of SCCD primary culture yielded a band near the expected molecular weight for ECaC1 (ca 70 kDa). These results demonstrate the expression of all components of the vitamin D-responsive ECaC  $\text{Ca}^{2+}$  absorptive pathway in both the cochlear and vestibular organs. The ECaC pathway is likely a major mechanism involved in calcium homeostasis and mutations in these genes or chemical interference would be expected to

result in compromised hearing or balance. Supported by NIH grants R01-DC00212 and P20-RR017686.

### **592 CFTR Knockout Mice Demonstrate That CFTR Chloride Channel Mediates cAMP-Stimulated Secretion in Semicircular Canal Duct Epithelium**

Tao Wu<sup>1</sup>, Suresh B. Kampalli<sup>1</sup>, Robert C. De Lisle<sup>2</sup>, Daniel C. Marcus<sup>1</sup>

<sup>1</sup>Kansas State University, <sup>2</sup>Univ Kansas Medical School

Semicircular canal duct (SCCD) epithelia contribute to the homeostasis of vestibular endolymphatic ion composition by electrogenic Cl secretion under adrenergic control via cAMP [Milhaud et al., *Am J Physiol*, 2002]. Previous pharmacologic and electrophysiologic studies [Kampalli et al. *ARO*, 2005] suggested that secretion occurred from the cytosol across the apical membrane via the CFTR Cl channel and demonstrated the involvement of protein kinase A. It was therefore of interest to determine more directly whether CFTR carried all or part of the stimulated Cl current. Previous studies were performed on rat and gerbil SCCD. Here, we established that native canals from wild type mice express transcripts for CFTR and utilized CFTR knockout mice to determine the level of function of this channel in SCCD. A current-density vibrating probe was used to monitor transepithelial short circuit currents ( $I_{sc}$ ) from microdissected native canal ducts. Wild type mice showed a reversible robust increase in  $I_{sc}$  to isoproterenol (ISO;  $\beta$ -adrenergic agonist) and to a mixture of forskolin & IBMX (F-I; adenylyl cyclase agonist & phosphodiesterase inhibitor). Heterozygotes also responded to these stimuli by significant increases in the  $I_{sc}$  (ISO:  $6.9 \pm 3.2$ ; F-I:  $5.0 \pm 2.5 \mu A/cm^2$ ,  $n=13$ ). As seen in previous Ussing chamber measurements of  $I_{sc}$ , these responses were prevented by addition of bumetanide (inhibitor of Na-K-2Cl cotransporter) and DIOA (inhibitor of K-Cl cotransporter) ( $0.1 \pm 0.5 \mu A/cm^2$ ). By contrast, there was no significant change in  $I_{sc}$  by stimulants from SCCD of CFTR knockout mice (ISO:  $-0.9 \pm 0.8$ ; F-I:  $-0.5 \pm 0.7 \mu A/cm^2$ ,  $n=8$ ). There was again no response in the presence of bumetanide and DIOA, as expected ( $-0.7 \pm 0.8 \mu A/cm^2$ ). These findings demonstrate that cAMP-stimulated Cl secretion in SCCD is mediated by CFTR and that there is no evidence for the participation of other Cl channels in this process. Supported by NIH-NIDCD grant R01-DC00212 and NCRR P20 RR17686.

### **593 Barttin Increases Whole-Cell Conductance of CIC-K2 Channels in Cultured Type IV Spiral Ligament Fibrocytes**

Chunyan Qu<sup>1</sup>, Fenghe Liang<sup>1</sup>, Schulte Bradley<sup>1</sup>

<sup>1</sup>Medical University of South Carolina

Barttin, a protein encoded by the gene BSND, forms the  $\beta$ -subunit of CIC-Ks channels and is essential to their activity. Barttin has been suggested to increase the membrane expression and stability of transfected CIC-Ks channels. Mutations in barttin have been identified in a variant of Bartter's syndrome associated with sensorineural deafness and kidney failure. Previously, we

used immunohistochemical and RT-PCR approaches to demonstrate the expression of both CIC-K1 and CIC-K2 in types II, IV and V fibrocytes of the rodent spiral ligament. However, similar analyses of cultured type IV fibrocytes showed the presence of CIC-K2, but absence of CIC-K1. Whole-cell patch clamp studies on cultured type IV fibrocytes revealed a weak outwardly rectifying  $Cl^-$  current regulated by extracellular  $Cl^-$  and  $Ca^{2+}$ , with channel characteristics resembling those of CIC-K2. However, the  $Cl^-$  currents were much smaller than those recorded in other studies performed on freshly isolated renal tubule cells or strial marginal cells. Surprisingly, RT-PCR analysis identified barttin mRNA expression in tissue freshly isolated from the region of the spiral ligament containing mainly type IV fibrocytes but not in the fibrocytes cultured from this region, which could explain the reduced  $Cl^-$  currents. To test this possibility, cultured cells were stably transfected with a pEYFP-C1 vector containing barttin cDNA. This led to a marked increase of  $Cl^-$  currents with amplitudes two to fivefold higher than those recorded in non-transfected cells or cells transfected with empty vector. Quantitative real-time RT-PCR showed an approximate eightfold increase in the expression of mRNA for CIC-K2 in the transfected cells. However, CIC-K1 mRNA was not detected in the transfected cells. These findings suggest that a differential transcriptional effect underlies the loss of messenger RNA for CIC-K1 and barttin when type IV fibrocytes adapt to cell culture conditions. The results also indicate that up-regulated gene transcription of CIC-K2 by barttin is an alternative mechanism for barttin-mediated channel activation.

### **594 The Gap Junction Channel Systems in the Cochlea: Molecular Diversity and Redundant Functional Contributions of Various Subtypes of Connexins**

Wenxue Tang<sup>1</sup>, Shoab Ahmad<sup>1</sup>, Benjamin Stong<sup>1</sup>, Qing Chang<sup>1</sup>, Emil C. Muly<sup>1</sup>, Ping Chen<sup>1</sup>, Xi Lin<sup>1</sup>

<sup>1</sup>Emory University School of Medicine

Gap junctions (GJs) are special type of membrane channels facilitating intercellular ionic, biochemical and electrical communications. Each half of a GJ is constituted by homomeric or heteromeric assemblies of six compatible connexins (Cxs). Genetic studies have indicated that Cxs play vital roles in normal hearing. However, the functional roles of GJs in the cochlea remain unclear. Our studies suggested that there are two distinct GJ systems in the cochlea.

The first system is the GJs linking the supporting cells in the organ of Corti, fibrocytes in the lateral wall and spiral limbus. These GJs are assembled heteromerically from Cx26 and Cx30. Deletion of Cx30 gene, the co-assembly partner of Cx26, resulted in a significant reduction in Cx26 protein expression level although the Cx26 cellular distribution pattern was unchanged. Gene deletion results obtained by other groups show that a minimum of three copies of Cx26 and Cx30 genes are needed for normal hearing. However, whether three or more copies of the same Cx gene (either Cx26 or Cx30) are sufficient for normal hearing is unknown. We found that overexpressing the Cx26 by transgenic BAC expressions in the Cx30-/-



mice completely rescued the hearing of the mutant mice, suggesting that hearing loss in the Cx30-/- mice was caused by reduced overall level of Cx expressions in forming the GJs.

The second GJ system, consisted mainly of the Cx29, was found exclusively in the cochlear Schwann cells. Cx29-/- mice show a delay in the maturation of hearing thresholds, a loss of high-frequency sensitivity and distortions in auditory brainstem responses. The morphology of sensory hair cells and otoacoustic emissions were normal in Cx29-/- mice. In contrast, decreases in MAG expression and demyelination at the soma of spiral ganglion neurons were found. These data suggest that Cx29 is a novel candidate gene for studying the demyelination type of auditory neuropathy.

**[595] Probing the Regulation of Connexin26 Expressions in the Cochlea: Effects of Missing the Gap Junction Co-Assembly Partner (Cx30) and Noise Exposures**

Wenxue Tang<sup>1</sup>, Shoab Ahmad<sup>1</sup>, Qing Chang<sup>1</sup>, Xinxin Chen<sup>1</sup>, Yan Qu<sup>1</sup>, Ping Chen<sup>1</sup>, Xi Lin<sup>1</sup>

<sup>1</sup>Emory University School of Medicine

Connexins (Cxs) are a family of proteins constituting the gap junctions (GJs), which are the only known intercellular channels facilitating communication between groups of cells. Cx26 play vital functions in the cochlea, as its mutations are linked to a large number of hereditary nonsyndromic deafness cases. We are interested in investigating the regulation of Cx26 expressions, which is an important mechanism to control the GJ-mediated intercellular signaling in the cochlea.

The Cx26 expressions at the mRNA and protein levels were analyzed by cDNA macroarray hybridizations and Western blot analyses. In the absence of Cx30 (the co-assembly partner of Cx26 in the cochlea), the Cx26 expressions in the Cx30 knockout (KO) mice were not significantly different from the wild type controls until about two weeks after births. However, the Cx26 expression was significantly reduced in both the cochlea and brain of the adult Cx30KO mice. In contrast, Cx26 expressions were not notably changed in the liver of adult Cx30KO mice where the major co-assembly partner is the Cx32. In responses to noise exposures that cause temporary threshold shifts (TTS), Cx26 protein expressions were down regulated between 1-4 hours after noise was stopped and partially recovered after 24 hrs. The full recovery was typically reached two days after noise exposures. In response to noise exposures that cause permanent threshold shifts (PTSs) the Cx26 protein expressions were up regulated two hours after noise exposure. The increased Cx26 protein expression after the PTS noise exposures was maintained at least for seven days (the longest time we have measured so far). As a control, the PTS noise exposures to the Cx30KO mice, which are deaf, did not show upregulation of Cx26 at all. Our results indicated that the stable expression level of Cx26 depends on the presence of its co-assembly partner, Cx30. The Cx26 expressions are differentially regulated by noises that cause TTS and PTS.

**[596] Gap Junctions Between GLUT1-Positive and -Negative Cells in the Cochlea: Their Possible Roles in Intercellular Transport of Glucose Over the Blood-Inner Ear Barrier**

Toshihiro Suzuki<sup>1</sup>, Tatsuya Matsunami<sup>1</sup>, Yasuo Hisa<sup>1</sup>, Masahito Oyamada<sup>2</sup>

<sup>1</sup>Department of Otolaryngology-Head and Neck Surgery, Kyoto Prefectural University of Medicine, <sup>2</sup>Department of Pathology and Cell Regulation, Kyoto Prefectural University of Medicine

Despite the known importance of glucose metabolism for auditory function, the mechanisms of glucose transport in the cochlea, where the blood-inner-ear barrier is established, are not completely understood. We hypothesized that gap junctions mediate intercellular transport of glucose in the cochlea in cooperation with facilitative glucose transporter 1 (GLUT1). To test this hypothesis, we analyzed the expression and localization of GLUT1, the gap junction proteins connexin26 and connexin30, and the tight junction protein occludin in the adult rat cochlea using confocal microscopy. GLUT1 and occludin were detected in blood vessels, and GLUT1, connexin26, connexin30, and occludin were also expressed in stria basal cells and limbal fibrocytes just basal to supralimbal lining cells. Gap junctions were present among not only these GLUT1-positive stria basal cells but also GLUT1-negative stria intermediate cells and fibrocytes in the spiral ligaments. Similarly, gap junctions exist among the GLUT1-positive limbal fibrocytes and more centrally located GLUT1-negative limbal fibrocytes. In vivo glucose imaging using a non-metabolizable and fluorescent glucose analogue, 6-[N-(7-nitrobenz-2-oxa-1,3-diazol-4-yl)amino]-6-deoxyglucose, showed that glucose in the blood was rapidly distributed throughout the stria vascularis and spiral ligament, and that the gap junctional uncoupler heptanol inhibited the distribution of glucose in the spiral ligament. These findings suggest that gap junctions play an important role in the glucose transport in the cochlea, i.e., that gap junctions mediate glucose transport from GLUT1-positive cells (stria basal cells and limbal fibrocytes) to GLUT1-negative cells (stria intermediate cells and fibrocytes in the spiral ligament and spiral limbus).

**[597] Simulation of Ion Transport in the Stria Vascularis**

Imran Quraishi<sup>1</sup>, Robert M. Raphael<sup>1</sup>

<sup>1</sup>Rice University

Ion transport by stria marginal cells and vestibular dark cells, which are believed to operate similarly, has been implicated in a variety of genetic and drug-induced forms of deafness and imbalance disorders. These cells appear to work by inward transport of potassium through Na<sup>+</sup>,K<sup>+</sup> ATPase and a passive Na<sup>+</sup>,K<sup>+</sup>,2Cl<sup>-</sup> cotransporter (NKCC) and out of the luminal surface through an outward rectified conductance. We have constructed a numerical model of a generic marginal cell epithelium at steady state. The model validates the putative location of transport proteins and demonstrates how different parameters affect the cell's function. It is based on experimentally derived kinetics of

ion channels and transporters. Numerical results demonstrate that the cell is able to transport  $K^+$  into the endolymph despite a lower  $[K^+]$  inside the cell than in the endolymph by maintaining a positive apical transmembrane potential. In the case of a significant load resistance, counter-ion flow is necessary to maintain transcellular  $K^+$  transport, but this is unnecessary in the absence of such a load. Additionally,  $Na^+, K^+$  ATPase and NKCC are shown to act synergistically, regardless of the load resistance. The model is useful for determining the sensitivity of the system to the properties of the different transporter and channel proteins, and can be extended to predict the transport of drugs into the endolymph. We are extending the model to include the electrophysiological properties of the basal and intermediate cells in stria vascularis.

### **[598] Functional Consequences of a Tyrosinase Promoter for Diphtheria Toxin**

**Michael Anne Gratton**<sup>1</sup>, Liping Nie<sup>2</sup>, Charles Askew<sup>1</sup>, Ebenezer Yamoah<sup>2</sup>

<sup>1</sup>University of Pennsylvania, <sup>2</sup>University of California-Davis

Dysregulation of homeostasis in the stria vascularis has a profound effect upon the transduction of auditory signals within the cochlea. We hypothesized that the endocochlear potential is generated and maintained by a cadre of potassium channels in the plasmalemma of the intermediate and marginal cells in conjunction with potassium transporters. Here we report the consequences of a strategy to cripple a specific cell in the stria vascularis. A tissue specific promoter, tyrosinase, which drove expression of a suicide gene, diphtheria toxin, was used to eliminate or halt differentiation of neural crest melanocytes following migration to the stria vascularis in C57 mice. Functionally, elevated auditory brainstem responses as well as a greatly diminished endocochlear potential were measured. Ultrastructural examination revealed that at 3 weeks of age, the stria vascularis was slightly thicker than age-matched wild-type C57 mice. However, by 4 months of age, the stria was significantly thinner due to the absence of intermediate cells. Immunohistochemistry indicated that from 1-3 weeks of age, intermediate cells begin to express potassium channel proteins followed by a downregulation in the level of expression. The downregulation occurs in spite of the continued expression of melanocyte markers. By 7 weeks of age, no reactivity is noted for the melanocyte markers. The role of the intermediate cell in cochlear homeostasis will be discussed.

This work was supported by grants to MAG (NIH-DC006442) and ENY (NIH-DC03828, DC04523).

### **[599] Developmental Change of Purinergic Receptors in Cochlear Outer Sulcus Cells**

**Jun-Ho Lee**<sup>1</sup>, Jeong-Wha Huh<sup>1</sup>, Chong-Sun Kim<sup>1</sup>, Sun-O Chang<sup>1</sup>, Seung-Ha Oh<sup>1</sup>

<sup>1</sup>Department of Otolaryngology Seoul National University College of Medicine

Purpose: P2X2 receptors are dominant and P2Y4 receptors are exclusively expressed in the stria vascularis.

The outer sulcus cells (OSC) are located between spiral prominence and basilar membrane and they contribute to endolymphatic homeostasis. P2X2 purinergic receptors are found to be expressed in OSC by immunohistochemistry in adult species (Jarlebak et al, 2000) and by functional characterization (Lee et al, 2001). However, little is known in developing age.

Methods: The vibrating probe technique was chosen to measure transepithelial currents under short circuit conditions due to the small extent of the OSC epithelial domain. The vibrating probe technique was identical to that previously described (Marcus and Shipley, 1994; Marcus, 1996). Immunohistochemical stainings were performed using P2Y4 antibody (Alomone Lab, Jerusalem, Israel) since our preliminary results showed that P2Y4 receptors were functionally expressed in neonatal OSC. The secondary antibody was anti-rabbit fluorescence-labeled Alexa 488 (Molecular Probes, Eugene). Sections were observed with a Confocal microscope using a 40x and 100x oil objectives.

Results: Application of adenosine, ADP, and UDP (100  $\mu$ M, each) did not change the Isc in OSC at all ages, which indicates that P1, P2Y1, and P2Y6 were not expressed. However, the Isc increased by application of UTP, ATP, 2'- & 3'-O-(4-benzoyl-benzoyl)adenosine 5'-triphosphate (BzATP), and alpha,beta-methyleneadenosine 5'-triphosphate (alpha,betamethylATP) (100  $\mu$ M, each) depending on the ages. Surprisingly, the response to UTP was most prominent at PD 1, and gradually disappeared until PD 21 when hearing function was fully achieved. The UTP response on neonatal OSC was blocked by reactive blue 2 (100  $\mu$ M), an inhibitor of P2Y4 receptor, which indicates that P2Y4 receptors are functionally expressed in neonatal OSC. In contrast, functional contribution of P2X2 receptors in OSC were found to be weak at early neonatal period, and gradually increased as P2Y4 receptors decreased. Immunohistochemical staining was consistent with the electrophysiological recordings that P2Y4 receptors in OSC were down-regulated as the age increased.

Conclusion: P2Y4 receptors were transiently expressed in OSC during development. The developmental change of P2X2 and P2Y4 receptors in OSC may contribute to establish normal ionic environment during development. (This study was supported by Seoul National University Hospital grant # 03-2004-032).

### **[600] TNF $\alpha$ Modulates Spiral Modiolar Artery Tone via Regulation of the Endogenous Sphingosine Kinase 1**

**Elias Q. Scherer**<sup>1,2</sup>, Darcy Lidington<sup>2</sup>, Bernhard Friedrich Peter<sup>2</sup>, Stuart M. Pitson<sup>3</sup>, Wolfgang Arnold<sup>1</sup>, Ulrich Pohl<sup>2</sup>, Steffen-Sebastian Bolz<sup>2</sup>

<sup>1</sup>ENT-Department, Technical University of Munich, Germany, <sup>2</sup>Institute of Physiology, Ludwig-Maximilians University, Munich, Germany, <sup>3</sup>Institute of Medical and Veterinary Science, Adelaide, Australia

Blood supply to the inner ear is entirely dependent on adequate blood flow through the spiral modiolar artery (SMA). Consequently, even minor constriction of this artery can cause inner ear ischemia. Despite its potential

clinical importance, our knowledge regarding the endogenous tone- and resistance-regulating mechanisms of the SMA is limited. We have previously shown that sphingosine-1-phosphate (S1P) induces strong vasoconstriction of the SMA. We proposed (i) that endogenous S1P (generated by sphingosine kinase 1; Sk1) is a key regulator of SMA tone; and (ii) that TNF $\alpha$ , an inflammatory cytokine associated with several inner ear pathologies, potentially activates Sk1 in the SMA.

Gerbil SMA were isolated, cannulated (25mmHg transmural pressure) and cultured for 19-21h with plasmids encoding green fluorescent protein (GFP), GFP-tagged Sk1 (hSk1-GFP) or a catalytically inactive mutant of Sk1 (hSk1<sup>G82D</sup>).

Compared to non-transfected vessels, GFP expression did not alter vasoconstriction induced by exogenously applied S1P (n=5) or the diameter-Ca<sup>2+</sup><sub>i</sub> relationship (Ca<sup>2+</sup>-sensitivity). Expression of hSk1<sup>G82D</sup> (n=7) significantly shifted the diameter/Ca<sup>2+</sup><sub>i</sub> relationship to the right. In contrast, treatment of the SMA with 1nM TNF $\alpha$  (2h, n=6) left-shifted this relationship, an effect that could be prevented by the expression of hSk1<sup>G82D</sup> (n=7) or by treatment with the TNF $\alpha$  receptor antagonist Ethanercept (1 $\mu$ g/ml, n=4). TNF $\alpha$  was also observed to stimulate the translocation of Sk1-GFP to the plasma membrane, indicative of Sk1 activation.

We conclude that Sk1/S1P contributes to the physiological tone regulation of the SMA, primarily by a mechanism involving the modulation of Ca<sup>2+</sup> sensitivity. TNF $\alpha$  activates Sk1 in the SMA, leading to enhanced Ca<sup>2+</sup> sensitivity. Thus, TNF $\alpha$  could be a primary mediator of several inner ear pathologies (e.g., sudden hearing loss) via S1P-mediated augmentation of SMA contractile apparatus Ca<sup>2+</sup> sensitivity and hence, vessel tone.

### **[601] Ca<sup>2+</sup> Spark Frequency in the Spiral Modiolar Artery Is Increased by Depolarization and Decreased by Ryanodine**

**Keil Regehr<sup>1</sup>**, Casey Devore<sup>1</sup>, Chengya Liang<sup>1</sup>, Philine Wangemann<sup>1</sup>

<sup>1</sup>*Anatomy & Physiology Dept., Kansas State University*

Ryanodine receptors (RyR) have been shown to mediate dilation in arterial smooth muscle via sudden Ca<sup>2+</sup>- and ryanodine-sensitive Ca<sup>2+</sup> release (Ca<sup>2+</sup> sparks) from the sarcoplasmic reticulum. Ryanodine at 1  $\mu$ M concentration is known to promote a subconductance state with high open probability. In the gerbil spiral modiolar artery (SMA), 1  $\mu$ M ryanodine causes vasodilation. The goal of this study was to determine whether 1  $\mu$ M ryanodine and membrane potential depolarization increases spark frequency and/or amplitude. Vessel diameter was monitored by video microscopy, and Ca<sup>2+</sup> sparks were visualized with fluo-4 microfluorometry. Sparks in the SMA had a frequency of 2.7  $\pm$  0.3 Hz, a rise time (0-100%) of 16.6  $\pm$  0.8 ms and a half-decay time of 22  $\pm$  2 ms (n=25). By 100 s, 1  $\mu$ M ryanodine reduced spark frequency from 2.4  $\pm$  0.4 to 0.6  $\pm$  0.2 Hz (n=11) with no effect on rise or half-decay time. Incremental increases of [K<sup>+</sup>]<sub>o</sub> from 3.6 to 75 mM caused a vasodilation at low and a constriction at high concentrations. Increases from 3.6 to 38 mM K<sup>+</sup> caused a vasoconstriction consistent with membrane depolarization

and an increase in spark frequency from 2.3  $\pm$  0.3 to 3.5  $\pm$  0.3 Hz (n=21) with no effect on rise or half-decay time. These findings suggest that the ryanodine-induced high open probability subconductance state of the RyR causes Ca<sup>2+</sup> to leak from the sarcoplasmic reticulum into the subsarcolemmal space where it may accumulate to sufficiently high concentrations to activate BK K<sup>+</sup> channels. Activation of the BK K<sup>+</sup> channels can be expected to cause hyperpolarization of the plasma membrane, closure of L-type Ca<sup>2+</sup> channels, and a decrease in the global Ca<sup>2+</sup> concentration that mediates the observed ryanodine-induced vasodilation. Further, these findings suggest that K<sup>+</sup>-induced membrane depolarization elevates spark frequency by opening L-type Ca<sup>2+</sup> channels, elevating Ca<sup>2+</sup> influx and loading of the sarcoplasmic reticulum leading to an activation of the RyR. NIH-R01-DC04280

### **[602] Serotonin Induces Hyperpolarization via Endothelial Release of Nitric Oxide in Guinea Pig Spiral Modiolar Artery**

**Yu-Qin Yang<sup>1</sup>**, Alfred L. Nuttall<sup>1,2</sup>, Zhi-Gen Jiang<sup>1</sup>

<sup>1</sup>*Oregon Hearing Research Center, Oregon Health & Science University, Portland, OR,* <sup>2</sup>*Kresge Hearing Research Institute, The University of Michigan, Ann Arbor, MI, USA*

Serotonin (5-HT) is a recognized neurotransmitter in central and peripheral nervous system and a local hormone (e.g., it may be released from blood platelets), thus it plays multiple pivotal functions in mammals, including a role in systemic and local circulation control (Doggrell, 2003; Sachanska, 1999). It has also been implicated in the pathophysiology of tinnitus and Meniere's disease (Blazso et al., 1997; Liu et al., 2003; Nikolaev et al., 1976; Sachanska, 1999; Salvinelli et al., 2003; Simpson et al., 2000). However, the cellular actions of 5-HT in inner ear vasculature remain unexplored. Using the spiral modiolar artery (SMA) *in vitro* preparation and intracellular recording techniques, we found: 1) 5-HT (0.1-30  $\mu$ M) concentration-dependently caused a 1-30 mV hyperpolarization in the great majority of cells that had a low resting potential (RP,  $\sim$ -40 mV) but no effect or rarely a small depolarization in high RP ( $\sim$ -75 mV) cells. 2) 5-HT-induced hyperpolarization was completely blocked by 10  $\mu$ M clozapine, an antagonist for 5-HT<sub>7</sub>, 5HT<sub>3</sub> and 5-HT<sub>6</sub> receptors, and which sometimes unmasked a depolarization (2-4 mV). The latter was sensitive to 1  $\mu$ M ritanserin. 3) 5-HT-hyperpolarization was suppressed by 100  $\mu$ M N<sup>G</sup>-Nitro-L-arginine-methyl ester (L-NAME), a NO-synthase inhibitor, and 3  $\mu$ M glipizide, a K<sub>ATP</sub> channel blocker, but not affected by 100  $\mu$ M Ba<sup>2+</sup>. 4) 18 $\beta$ -glycyrrhetic acid (30  $\mu$ M, a gap junction blocker) suppressed 5-HT-hyperpolarization in smooth muscle (SMC) but not that in the endothelial cells (EC). We conclude that, in the SMA, serotonin mainly acts on 5-HT<sub>1</sub>-like receptors in the EC membrane to cause a release of NO, the latter in turn induces an opening of the ATP-sensitive potassium channel and thus a membrane hyperpolarization in endothelial cells, and also in smooth muscle cells via gap junction electric coupling. Supported by NIH NIDCD DC 004716 (ZGJ) and DC00141 (ALN).

### **603 Inward Rectifier Potassium Channel Is the Key Component for the Conduction of Hyperpolarization in Guinea Pig Spiral Modiolar Artery**

Zhi-Gen Jiang<sup>1</sup>, Yu-Qin Yang<sup>1</sup>

<sup>1</sup>Oregon Hearing Research Center, Oregon Health & Science University, Portland, OR

Focal application of a vasoactive agent, e.g., acetylcholine (ACh) induces a membrane hyperpolarization and dilation that can conduct along the vessel axis. Such conducted dilation contributes to the coordination of blood flow within microvascular resistance networks (Emerson et al., 2000; Welsh et al., 1997), thus forming a basis for the rheology in the microvessel. The conductive feature of the dilation and the associated membrane hyperpolarization is unique and interesting because an inhibitory signal in all other excitable tissues is generally non-conductive and the ionic mechanism for this conductive inhibition remains unclear (Figueroa et al., 2004). Using intracellular recording and cell labeling techniques and an *in vitro* preparation of guinea pig spiral modiolar artery (SMA), we explored the mechanism in question. We found: 1) The initial resting potentials (RP) in sampled cells showed a mixture of two Gaussian distribution peaked near  $-75$  and  $-40$  mV. Cells having a RP near  $-60$  mV were rare. 2) A cell initially having a low RP (near  $-40$  mV) often swiftly shifted its RP level to high RP (near  $-75$  mV) spontaneously or after a hyperpolarizing treatment such as with  $10$  mM  $K^+$  or  $3$   $\mu$ M ACh. A reversal shift from high to low RP was also observed spontaneously or after a depolarizing treatment. 3)  $Ba^{2+}$  ( $1$ - $100$   $\mu$ M) always caused a shift from high RP to low RP by its wash-in and a reversed shift by its wash-out. An overshoot was often seen in the end of fast shift in both directions. 4) ACh-induced a robust hyperpolarization in nearly all low RP cells. The hyperpolarization in the smooth muscle cells (SMC), but not that in the endothelial cells (EC), was blocked by 84% by a gap junction blocker  $25$   $\mu$ M  $18\beta$ -glycyrrhetinic acid (GRA) and near completely blocked by GRA plus  $100$   $\mu$ M  $Ba^{2+}$ . 5) Dual cell recording and  $K^+$ -induced hyperpolarization measurement indicated a heterogeneous electrocoupling among cells and a macroscopic myoendothelial coupling efficiency of  $0.49$ . We conclude that the vascular smooth muscle cells express abundant inward rectifier  $K^+$ -channels ( $K_{ir}$ ); the ACh-induced hyperpolarization originates in the EC, electrotonically spreads to the muscular layer and in turn disinhibits the  $K_{ir}$  in the SMCs; the intercellular electrocoupling and the positive feed back by the loop of hyperpolarization $\rightarrow K_{ir}$  disinhibition $\rightarrow$  further hyperpolarization in muscle cells form the cellular basis for the conductive inhibition. Supported by NIH NIDCD DC004716.

### **604 Whole-Cell Recording of Smooth Muscle Cells in Guinea Pig *In Vitro* Spiral Modiolar Artery**

Bing-Cai Guan<sup>1</sup>, Alfred L. Nuttall<sup>1</sup>, Zhi-Gen Jiang<sup>1</sup>

<sup>1</sup>Oregon Hearing Research Center, Oregon Health & Science University, Portland, OR

We demonstrated previously that the smooth muscle cells (SMC) and endothelial cells (EC) are heterogeneously

coupled in the guinea pig spiral modiolar artery, which makes an important way of intercellular communication but a great difficulty for single-cell voltage clamping studies, the latter is a key method to elucidate ionic mechanisms of many unique features of this vessel, which could not be studied in dissociated or cultured cells. Whole-cell voltage-clamp recording from intact vessel segments has been conducted only in a few other small arteries, probably due to its technical difficulties. Here we report a use of this method on cochlear spiral modiolar artery (SMA) that has rich connective and nerve tissues in adventitial layer. The SMA was dissected from the cochlea and manually cleaned off the surrounding tissue. A segment ( $300$ - $500$   $\mu$ m in length) of the SMA was placed in a recording dish and incubated in HEPES-buffered physiological solution containing collagenase A ( $0.75$  mg/ml) at  $37^\circ\text{C}$  for  $20$ - $30$  min. The adventitial tissue was further cleaned carefully using fine tweezers under stereoscope. Cells in the preparation were then visualized under an inverted microscope in DIC mode. Conventional whole-cell recording was conducted using a high  $K^+$ -solution containing micropipette having a tip size  $\sim 1$   $\mu$ m and a resistance of  $3 - 5$  M $\Omega$ . We found that a good seal resistance could reach  $2$ - $5$  G $\Omega$  and a post-rupture access resistance  $\sim 20$  M $\Omega$ . The capacitive current showed a relaxation fitted well with a double exponential function, with time constants ( $\tau$ ) about  $2$  and  $25$  ms. The input conductance was  $\sim 1.6$  nS near the holding potential of  $-40$  mV. The I/V relation showed an outward rectification along depolarization steps up to  $+40$  mV but little inward rectification upon hyperpolarization steps down to  $-170$  mV. ACh ( $3$   $\mu$ M) induced an outward current that was always blocked by  $30$   $\mu$ M  $18\beta$ -glycyrrhetinic acid ( $18\beta$ -GRA), a gap junction blocker, suggesting that the recorded cells was usually the SMC. Application of  $18\beta$ -GRA increased the input resistance from  $100$ - $600$  M $\Omega$  to the order of G $\Omega$ . The capacitive current relaxation became very fast and single exponential ( $\tau \approx 0.66$  ms). The I-V relationship in  $18\beta$ -GRA showed an inward rectification upon hyperpolarization, which was abolished by addition of  $100$   $\mu$ M  $Ba^{2+}$ . The data suggest that 1) whole-cell recording of smooth muscle cells in the SMA was feasible, 2) gap junction blockade is required to obtain good space clamping of a single cell, 3) ACh-induced outward current occurred in the ECs, not in the SMCs, and 4) inward rectifier potassium channels do express rich in the SMCs. Supported by NIH NIDCD DC 004716 (ZGJ) and DC00141 (ALN).

### **605 Hair Cell Loss in Postnatal Conditional Rb-Knockout Mice**

Thomas Weber<sup>1</sup>, Mary Corbett<sup>1</sup>, Yong Tian<sup>1</sup>, Lionel Chow<sup>1</sup>, Suzanne Baker<sup>1</sup>, Jian Zuo<sup>1</sup>

<sup>1</sup>St. Jude Children's Research Hospital

Recent studies showed that the retinoblastoma protein (pRb105) is required for the normal development of inner ear sensory epithelia (Sage et al. 2005, Mantela et al. 2005). Loss or absence of Rb in the developing otocyst leads to the production of supernumerary hair cells in the vestibular and cochlear system, consistent with Rb's role as cell cycle regulator. There is increasing evidence that in

addition to its traditional role, Rb is also required for cell differentiation and maintenance of postmitotic cells. In this study we investigated whether Rb might also play a role during the postnatal maturation of inner ear hair cells. We crossed conditional Rb knockout mice with two mouse-lines expressing Cre-recombinase in cochlear and vestibular hair cells. The first line starts expressing Cre around P6; in the second line Cre-expression was induced by injecting tamoxifen at P0 and P1. The mice we obtained were viable and reached adulthood. They behaved normally in rotor-rod tests, indicating that ongoing expression of Rb in postmitotic hair cells is not critical for the maintenance of the vestibular system. ABR-measurements revealed severe deafness of homozygous Rb-knockout mice of both lines. Heterozygous and Cre-negative littermate controls had normal hearing. Whole mount preparations of the cochleae showed that significant hair cell loss had occurred in both lines, which could explain the observed hearing phenotype. In the remaining hair cells, the expression of prestin and myosin VII appeared to be normal, suggesting that these cells had undergone normal development. It seems that hair cells had been lost from an organ of corti with three rows of OHCs and one row of IHCs.

This is the first study analyzing Rb's function in the postmitotic, adult mouse inner ear. Our results reveal a critical role of the tumor-suppressor Rb for hearing function which is apparently different from its role as cell cycle regulator.

Supported by ALSAC, NIH Cancer Center Support CORE grant (CA21765), and NIH grants to J.Z. (DC05168, DC06471) and to SB (CA096832).

Mantela J. et al. (2005) The retinoblastoma gene pathway regulates the postmitotic state of hair cells of the mouse inner ear. *Development*, 132

Sage C. et al. (2005) Proliferation of Functional Hair Cells in Vivo in the Absence of the Retinoblastoma Protein, *Science*, 307

#### **606 Differential Expression of Cdh23 and Pcdh15 Isoforms in the Cochlea and Retina of Wild Type and Waltzer Mice**

Ayala Lagziel<sup>1</sup>, Zubair M. Ahmed<sup>1</sup>, Linda M. Peters<sup>1</sup>, Thomas B. Friedman<sup>1</sup>, Robert J. Morell<sup>1</sup>

<sup>1</sup>NIDCD, NIH, Rockville, MD

Mutant alleles of *CDH23* and *PCDH15* are associated either with deaf-blindness and vestibular dysfunction (Usher syndrome type 1D, and 1F, respectively), or isolated deafness (DFNB12 and DFNB23). In *waltzer* (*v*) mice, mutant alleles of *Cdh23* (predicted null alleles and therefore thought to model USH1D) cause deafness and vestibular dysfunction but not blindness. Cadherin 23 and protocadherin 15 are members of a family of adhesion glycoproteins and both are associated with links which interconnect stereocilia throughout development. We recently reported the spatiotemporal expression pattern of cadherin 23 during development of the inner ear in wild type and in *v<sup>6J</sup>* *waltzer* mice (Lagziel et al., 2005). In addition we reported several short isoforms of *CDH23/Cdh23* in the wild type, which are also present in

the homozygous *v<sup>6J</sup>* mouse mutants and are unaffected by this mutant allele. Here we report an analysis of the relative expression levels of alternative transcripts of *Cdh23* and *Pcdh15* in wild type and *v<sup>6J</sup>* mice using semi-quantitative real time PCR assays and RNA from cochleae and retinae from different developmental time points. We found that the *Cdh23* isoforms differ in their temporal and spatial patterns of expression, and that certain isoforms of the *v<sup>6J</sup>* allele were down-regulated, while other isoforms were up-regulated. We also found that *Pcdh15* regulation was affected by the *v<sup>6J</sup>* allele. The pattern of up or down-regulation was dependant on the tissue examined (retina or cochlea), and on the developmental stage. The results of this study suggest that a correlation of mutant genotype to phenotype in mice and humans might not depend on a model of a single cadherin 23 isoform, but on the resolution of function for each of the *Cdh23* isoforms, and possibly the relationship between the transcription regulation of the *Pcdh15* and *Cdh23* genes.

#### **607 Persistence of Cav1.3 Ca<sup>2+</sup> Channels in Mature Outer Hair Cells Suggests Afferent Function of Type II Fibers**

Martina Knirsch<sup>1,2</sup>, Niels Brandt<sup>1,2</sup>, Claudia Braig<sup>2,3</sup>, Nicola Schug<sup>2,4</sup>, Stephanie Kuhn<sup>1,2</sup>, Stefan Münkner<sup>1,2</sup>, Marlies Knipper<sup>2,3</sup>, Jutta Engel<sup>1,2</sup>

<sup>1</sup>University of Tuebingen, Institute of Physiology II,

<sup>2</sup>Tuebingen Hearing Research Centre, <sup>3</sup>University of Tuebingen, ENT Clinic, Molecular Neurobiology,

<sup>4</sup>University of Tuebingen, ENT Clinic, Molecular Genetics

Outer hair cells (OHC) are innervated by type II afferent fibres of as yet unknown function. If these fibres indeed relayed afferent information from the OHCs, presynaptic Ca<sup>2+</sup> channels would be required. By using the whole cell patch clamp technique we recorded Ca<sup>2+</sup> channel currents with 10 mM Ba<sup>2+</sup> as a charge carrier in OHCs and IHCs of mice and rats between P1 and P32. L-type Ca<sup>2+</sup> channel currents showed developmental peak values of 165 pA (mouse) and 188 pA (rat) at P2, respectively. Currents declined upon further OHC maturation in parallel to the acquisition of a mature OHC phenotype. Mouse OHC I<sub>Ba</sub> decreased to <20 pA at P19, probably due to the poor metabolic state of the cells, whereas average I<sub>Ba</sub> in the more robust rat OHCs amounted to 66±18 pA (n=13; P28). Properties of rat IHC and OHC currents were similar to those of neonatal mouse IHC/OHC Ba<sup>2+</sup> currents carried by the Cav1.3 subunit (Platzer et al. Cell 2000; Michna et al. J. Physiol. 2003). Whole-mount in situ hybridisation, RT-PCR from selected IHCs and OHCs and immunostaining confirmed the presence of Cav1.3 in mature IHCs and OHCs. Mature rat OHCs showed 3.3fold smaller Ba<sup>2+</sup> currents compared to IHCs (219 ± 26 pA, n=6, P30). Assuming that rat OHCs are innervated by about 3 type II afferent fibers and IHCs by about 12 type I afferent fibers, the amount of I<sub>Ba</sub> per afferent fiber would be of the same size in OHCs and IHCs (22 pA vs. 18 pA, respectively) which strongly suggests that OHCs are capable of exocytosis. The presence of the synaptic vesicle protein otoferlin and the presynaptic protein CtBP2 add further pieces of evidence for an afferent function of OHCs.

### **608 Spontaneous Action Potential Activity in Immature Inner Hair Cells Varies with Cochlear Position**

Stuart Johnson<sup>1</sup>, Walter Marcotti<sup>1</sup>, **Cornelis Kros<sup>1</sup>**

<sup>1</sup>*School of Life Sciences, University of Sussex, Falmer, Brighton, UK*

Immature mammalian cochlear inner hair cells (IHCs) fire spontaneous Ca<sup>2+</sup>-dependent action potentials (APs) up to around 7 days after birth (P7) (Marcotti *et al.* 2003, *J Physiol* 548:383-400). Spontaneous AP activity plays a major role in the development of many mammalian sensory systems (Katz & Shatz 1996, *Science* 274:1133-1138) and is believed to be either a permissive signal, promoting the survival of newly formed neurones, or an instructive signal that is able to guide specific neuronal development (Crair 1999, *Curr Opin Neurobiol* 9:88-93). However, the nature and function of AP activity in immature cochlear IHCs remain unknown.

Spontaneous AP activity was studied, at body temperature, using both whole-cell and cell-attached patch clamp recording from IHCs of the apical and basal coils of the immature mouse cochlea (P2-P4). Both methods of AP recording indicated position-dependent differences in the firing frequency and patterning of spontaneous activity that was revealed by analysis of interspike intervals from recordings of up to 30 s in duration. Basal IHCs had higher firing frequencies than apical cells. The coefficients of variation from the interspike intervals of each cell showed that the spontaneous AP pattern was regular in basal cells, compared to the more irregular or bursting pattern of apical cells. Therefore, these results indicate that the spontaneous AP activity of IHCs appears to contain two components that indicate their location within the immature cochlea.

We conclude that the differences in the frequency and pattern of spontaneous action potentials between apical and basal IHCs could instruct the tonotopic organization of neural connections in the auditory pathway, as previously suggested for the auditory brainstem of the chick (Lippe 1995, *Brain Res* 703:205-213), and also play more intrinsic roles such as promoting the position specific expression of ion channels or other molecules involved in the transduction of sound.

*Supported by the MRC*

### **609 Expression of Voltage-Gated Currents in Cochlear Inner Hair Cells of nAChR $\alpha$ 10 'Knockout' Mice During Development**

**María Eugenia Gómez-Casati<sup>1</sup>**, Julián Taranda<sup>1</sup>, Marcela Lipovsek<sup>1</sup>, Jessica Savino<sup>1</sup>, Douglas Vetter<sup>2</sup>, Jim Boulter<sup>3</sup>, Ana Belén Elgoyhen<sup>1</sup>, Eleonora Katz<sup>1</sup>

<sup>1</sup>*INGEBI (CONICET), Buenos Aires, Argentina*, <sup>2</sup>*Tufts Univ. School of Medicine*, <sup>3</sup>*Univ. of California*

Cochlear inner hair cells (IHC) release neurotransmitter onto afferent auditory nerve fibers in response to sound

stimulation. During early development, synaptic transmission is triggered by spontaneous Ca<sup>2+</sup> spikes, which are modulated by an efferent cholinergic innervation to IHCs. This synapse is inhibitory and mediated by the  $\alpha$ 9 $\alpha$ 10 nAChR. After the onset of hearing, large-conductance Ca<sup>2+</sup>-activated K<sup>+</sup> channels are acquired and both spontaneous action potentials and the efferent innervation disappear from IHCs.

We are studying the developmental changes in membrane properties in cochlear IHC of nAChR  $\alpha$ 10 'knockout' mice in order to evaluate whether there are changes in the functional expression pattern of the different channels during development due to the lack of the  $\alpha$ 10 subunit.

Electrophysiological properties of IHCs were studied by whole cell recordings in acutely excised apical turns of the organ of Corti. Before the onset of hearing, IHCs from wild type and heterozygous mice have slow voltage responses and fire spontaneous action potentials. Preliminary experiments in IHCs from  $\alpha$ 10 knockout mice, show there are no changes in the peak amplitude ( $3909 \pm 722$  pA

[+/-],  $3468 \pm 404$  pA [+/-] and  $2923 \pm 642$  pA [-/-]), voltage sensitivity and reversal potential ( $-64 \pm 6.5$  mV [+/-],  $-67 \pm 1.8$  mV [+/-] and  $-72 \pm 5.1$  mV [-/-]) of the total K<sup>+</sup>-currents after the onset of hearing with respect to their wild-type and heterozygous littermates. Moreover, outward currents have the additional fast component ( $\tau$ ,  $0.23 \pm 0.06$  ms at 46 mV) indicative of a functional BK channel as previously documented (Kros *et al.*, 1998). We are now evaluating whether there are changes in the expression and kinetics of Ca<sup>2+</sup> and K<sup>+</sup> channels before the onset of hearing and their impact on spontaneous action potentials.

### **610 Differentiation of Cochlear Progenitor Hair Cells from Mouse Bone Marrow Stem Cells**

Feng Ling<sup>1</sup>, Masahiro Komori<sup>1</sup>, Yuehua Jiang<sup>2</sup>, Walter Low<sup>3</sup>, John Anderson<sup>1</sup>, Catherine Verfaillie<sup>2</sup>, **Jizhen Lin<sup>1</sup>**

<sup>1</sup>*Department of Otolaryngology, University of Minnesota*, <sup>2</sup>*Stem Cell Institute, University of Minnesota*, <sup>3</sup>*Department of Neurosurgery, University of Minnesota*

Embryonic stem cells, capable of self-renewal and differentiation into multilineages, are excellent for development of therapeutics. However, their actual use in the clinic is not acceptable due to ethical reasons. Bone marrow stem cells (referred as to multipotent adult progenitor cells, MAPCs), similar to embryonic stem cells in nature, hold promises for therapeutic use in human diseases. Here we demonstrated that MAPCs differentiated into cochlear progenitor hair cells *in vitro*, under the influence of cochlear tissue-related growth factors and differentiation factors, namely, epidermal growth factor (EGF) at 10 ng/mL+basic fibroblast growth factor (bFGF) at 10 ng/mL+retinoic acid (RA) at 10<sup>-9</sup>M, and brain-derived neurotrophic factor (BDNF) at 10 ng/mL. Primitive mouse MAPCs (Oct4 positive) were cultured in DMEM/F12 supplemented with N2 (a selective growth medium for neuronal culture) with the above growth and differentiation factors in combination for 18 days followed by DMEM/F12 supplemented with N2 for additional 7 days. Cells were harvested for evaluation of the hair cell marker expression (myosin VIIa, Brn3.1, *Math1*, and *Espin*) by reverse transcription polymerase chain reaction and/or

immunohistochemistry. MAPCs without the treatment of EGF, bFGF, RA, and BDNF served as controls. It was found that differentiated MAPCs expressed multiple hair cell markers, namely, myosin VIIa, Brn3.1, *Math1*, and Espin whereas MAPCs without the induction of EGF+bFGF+RA+BDNF were weak or negative with the expression of myosin VIIa, Brn3.1, *Math1*, and Espin. It suggests that MAPCs are capable of differentiating into cochlear progenitor hair cells under the influence of cochlear tissue-related growth and differentiation factors and are potential stem cells for cell therapy of deafness.

This study is in part supported by NIDCD P30DC04660, University of Minnesota Academic Health Center seed grant, and Multiple Districts (5M)Hearing Foundation.

### **[611] Adeno-Associated Viral Serotype 2/1 Is a Highly Efficient Vector for in Utero Gene Transfer to Hair Cell Precursors**

**Jeffrey Bedrosian<sup>1</sup>**, Michael Anne Gratton<sup>1</sup>, Tang Waixing<sup>2</sup>, Jessica Landau<sup>1</sup>, Jean Bennett<sup>2</sup>

<sup>1</sup>*University of Pennsylvania School of Medicine: Department of Otolaryngology*, <sup>2</sup>*University of Pennsylvania School of Medicine: Department of Ophthalmology*

Gene transfer during gestational development represents a promising gene therapy strategy for correction of congenital developmental anomalies. Congenital hearing deficits may one day be treated in this manner, as gene transfer to precursor hair cells may prove to be a highly efficient means of generating transgene expression in a high percentage of mature hair cells. Through *exo-utero* and transuterine microsurgical approaches, we tested delivery of lentivirus and an array of recombinant adeno-associated viral serotypes (rAAV) expressing enhanced green fluorescent protein (eGFP) to the E11-12.5 developing mouse otocyst. We examined the ability of these viral vectors to successfully infect hair cell precursors and to express eGFP by post-natal day 0 (P0). We noted successful infection of hair cells and eGFP expression from lentivirus, AAV 2/1 and AAV 2/8. We then studied the longer term expression of these viral vectors and found AAV 2/1 to be a highly efficient vector for transduction of both inner and outer hair cells. The hearing thresholds of mice injected with these viral vectors were tested by ABR response and with the exception of the lentivirus injected group, were found to be unchanged from uninjected controls. Thus, *in utero* microinjection of rAAV, especially AAV 2/1, into the developing mouse otocyst represents an exciting and highly efficient new approach to gene delivery to murine hair cells.

### **[612] Functional Consequences of Expression of Multiple KCNQ4 Channels in the Mouse Inner Ear**

**Liping Nie<sup>1</sup>**, Tonghui Xu<sup>1</sup>, Jiling Mo<sup>1</sup>, Yi Zhang<sup>1</sup>, Weihong Feng<sup>1</sup>, Ana Vazquez<sup>1</sup>, Ken Morris<sup>2</sup>, Kirk W. Beisel<sup>2</sup>, Ebenezer Yamoah<sup>1</sup>

<sup>1</sup>*Department of Otolaryngology, University of California, Davis*, <sup>2</sup>*Department of Biomedical Sciences, Creighton University School of Medicine, Omaha, NE*

Four different isoforms of KCNQ4 channels, v1-v4, were identified and cloned from the mouse inner ear. These

channels are alternative splice variants derived from the same gene. v1-v3 include exon9, exon10 and exon11 respectively; however, in the case of v4, all of these three exons are excluded. As a result, these channel isoforms have identical protein sequences except the proximal region of the C- terminals between two putative calmodulin-binding domains (CaMBD). It has been demonstrated that Ca<sup>2+</sup>/calmodulin regulates KCNQ4 channels by reducing the magnitude of the current. Most importantly, KCNQ4\_v1-v4 are differentially expressed at distinct developmental and adult stages with both longitudinal and radial differences in the mouse cochlea. Thus, the functional studies on these channel isoforms are providing novel insights to the molecular mechanisms of hearing, which would be difficult to obtain by other means.

Our experiments demonstrated that the sequence differences in different variants result in significant changes in channel properties. Potassium permeation of the channels varies remarkably from one isoform to another. In the heterologous expression system, the current density of four channels is v4> v2 v3> v1. v4 has permeation properties that will confer enhanced K efflux under conditions of reduced driving force; thus, it serves as the predominant channel in controlling the membrane potential of hair cells. Indeed, these KCNQ4 channels are modulated differentially by Ca<sup>2+</sup>/calmodulin, which is consistent with the fact that alternative splicing introduces the variations in CaMBD and phosphorylation sites. In contrast, the putative tetramerization assembly domain in the distal C terminals is unperturbed in all four variants. A dominant negative mutation, G285S, in one of four isoforms has the same effect on the other three when co-expressed in CHO cells. More detailed functional studies on these channel isoforms are currently in progress.

### **[613] Developmental Expression of Voltage Gated Calcium Currents in Chicken Inner Ear Hair Cells**

**Snezana Levic<sup>1</sup>**, Liping Nie<sup>1</sup>, Ebenezer Yamoah<sup>1</sup>

<sup>1</sup>*Department of Otolaryngology and Center for Neuroscience, University of California, Davis*

Calcium influx through Cav1.3 channels in hair cells mediates neurotransmitter release and is necessary for normal hearing. In addition, there is evidence to suggest that calcium influx through voltage-gated calcium channels plays a role in hair cell development. We demonstrate the functional expression of multiple voltage-gated calcium channels in the developing hair cells in chicken basilar papilla. Specifically, there is a transient expression of transient calcium current that may play a role in the development of hair cells. Calcium currents were recorded using extracellular solution, (in mM) NaCl 110, KCl 6, 4-AP 5, CaCl<sub>2</sub> 5, TEA-Cl 25, D-glucose 10, HEPES 10; and intracellular solution (in mM) NMG 70, CsCl 75, Na<sub>2</sub>ATP 5, MgCl<sub>2</sub> 2, HEPES 10, EGTA 10, D-glucose 10. Calcium currents were present at all ages examined (E6-P3) and underwent most dramatic changes at ~ E12-E16. Most notably, the calcium current density was markedly increased at these stages (E12-E16; ~14 pA/pF at E12 vrs ~7 pA/pF at P3). In addition, there was a developmental decline of calcium currents sensitivity to holding potential (-90 vs. -50 mV; ~60% at E12 (n=32), <2% at P2 (n=9)).



The transient component which was activated from -90 mV was observed only in embryonic stages (~75% of cells at E12 (n = 53)). Kurtosin, nickel and mibefradil reduced the amplitude of the embryonic calcium currents activated preferentially from -90 mV. We will present data that demonstrate: 1. Functional presence of multiple voltage-gated calcium channels 2. There is developmental up-regulation of transient calcium currents. Calcium influx through different voltage-gated calcium channels may confer multiple functions during development. Indeed, development of synapses, hair cell morphology, and regulation of membrane excitability may be determined by the functional expression of different calcium channels.

#### **614 Functional Maturation of Mouse Cochlear Hair Cells Requires *Tmc1***

**Walter Marcotti**<sup>1</sup>, Alexandra Erven<sup>2</sup>, Stuart Johnson<sup>1</sup>, Karen P. Steel<sup>2,3</sup>, Cornelis Kros<sup>1</sup>

<sup>1</sup>University of Sussex, UK, <sup>2</sup>MRC Institute of Hearing Research, Nottingham, UK, <sup>3</sup>Wellcome Trust Sanger Institute

DFNA36, a form of progressive hearing loss and DFNB7/B11 which lead to profound congenital deafness are due to dominant and recessive mutations of the human trans-membrane cochlear-expressed gene 1 (*TMC1*) (Kurima et al. 2002, Nat Genet 30:277-284), for which *Beethoven* (*Bth*) and *deafness* (*dn*) are mouse models (Vreugde et al. 2002, Nat Genet 30:257-258), respectively. *TMC1* is a member of a novel gene family that encodes a transmembrane protein of unknown function. In the mouse its expression in both IHCs and OHCs in early postnatal development (from postnatal day 5 (P5), where the day of birth is P0) suggests that it might play a role in the normal maturation of these cells. We therefore looked for any effects of *Tmc1* mutations on the structural appearance and biophysical properties of immature and mature cochlear hair cells.

Gross cochlear physiology (compound action potential and endocochlear potential) and cells morphological appearance (scanning electron microscopy) was investigated at P15, P30 and P60 in *Bth* and *dn* mutant mice. Single-cell electrophysiology was performed using the patch clamp technique from apical-coil hair cells (P6-P58) in acutely dissected organs of Corti. While immature hair cells of mutant mice appear to develop normally in both ultrastructural appearance and biophysical properties, mature cells lack (*dn*) or have a reduced expression (*Bth*) of the membrane currents that characterize the adult phenotype. Moreover, the exocytotic machinery in *Bth* and *dn* mutant IHCs appears to remain at an immature stage of development. Mutant mice also showed progressive cell damage, mainly in the basal turn of the cochlea.

The results obtained in this study suggest that *Tmc1* could either be involved in the trafficking of molecules to the plasma membrane or serves as an intracellular regulatory signal implicated in the differentiation and maturation of immature hair cells.

*Supported by the MRC. WM is a Royal Society University Research Fellow*

#### **615 Metabotropic Glutamate Receptors Modulate Efferent Inhibition of Immature Inner Hair Cells**

**Juan Goutman**<sup>1</sup>, Gaston Sendin<sup>2</sup>, Tobias Moser<sup>2</sup>, Elisabeth Glowatzki<sup>1</sup>

<sup>1</sup>Johns Hopkins University School of Medicine,

<sup>2</sup>Department of Otolaryngology - University of Goettingen

Inner hair cells (IHC) in the mammalian cochlea receive transient efferent innervation that disappears after the onset of hearing. These efferent synapses activate inhibitory postsynaptic currents (IPSCs) through acetylcholine receptor and sK potassium channel. Quantal parameters of these synapses were studied by electrical stimulation of efferent axons and whole cell recordings from IHCs in excised apical turns of the rat cochlea (P7-12) (Goutman et al., 2005). At a holding potential of -90 mV, a quantal size of -18 pA was estimated from the amplitude distribution of spontaneous IPSCs, and a quantum content of 1 was calculated for evoked IPSCs by different methods including failures and coefficient of variation. The amplitude distributions for evoked IPSCs showed multiple peaks following Poisson statistics, suggesting that more than one vesicle could be released. The low probability of release observed in stimulation protocols with frequencies between 0.25 – 1 Hz was increased by the application of metabotropic glutamate receptor (mGluRs) agonists, either the non-subtype specific t-ACPD (100  $\mu$ M, n = 7), or the mGluR type I specific DHPG (50 and 100  $\mu$ M, n = 4). A clear reduction in the failure rate and a shift to higher values in the amplitude distribution of evoked IPSCs was observed, while the quantal size remained constant. The mean IPSC amplitude was more than 200% larger during the application of the mGluR agonists compared to control. These results suggest a presynaptic locus of action for the mGluRs agonists. Application of the glutamate transporter blocker TBOA (200  $\mu$ M) increased spontaneous efferent release, raising the possibility that spilled-over glutamate released at the IHC afferent synapse might activate mGluRs (n = 4). Our results suggest that glutamate released at the IHC afferent synapse may activate a feedback loop that strengthens the action of transient efferent synapses onto IHCs through the activation of mGluRs. Supported by NIDCD DC00646 (EG), HFSP RGY-19/2004 (EG and TM).

#### **616 Role of Synaptic Ribbons in Auditory Nerve Response: Recordings from Mice Lacking the Synaptic Scaffolding Protein Bassoon**

**Bradley Nicholas Buran**<sup>1</sup>, Tobias Moser<sup>2</sup>, Eckart Gundelfinger<sup>3</sup>, M. Charles Liberman<sup>4,5</sup>

<sup>1</sup>Speech and Hearing Bioscience and Technology, Harvard-MIT Division of Health Sciences and Technology,

<sup>2</sup>Department of Otolaryngology, University of Goettingen, Goettingen, Germany, <sup>3</sup>Dept of Neurochemistry and Molecular Biology, Leibniz Institute for Neurobiology,

Magdeburg, Germany, <sup>4</sup>Eaton-Peabody Laboratory, Massachusetts Eye & Ear Infirmary, Boston, MA,

<sup>5</sup>Department of Otolaryngology and Laryngology, Harvard Medical School, Boston, MA

The synaptic ribbon is an electron-dense structure surrounded by synaptic vesicles, which is found at hair cell

afferent synapses. The function of the ribbon in synaptic transmission remains the subject of ongoing research. In a knockout mouse with a targeted deletion of *bassoon*, the gene for a synaptic scaffolding protein, synaptic ribbons are no longer tethered to the presynaptic membrane. This loss of active-zone anchored ribbons coincided with a strong reduction of synchronous hair cell exocytosis *in vitro*. [Khimich et al., Nature 434:889-894, 2005].

To further study the function of synaptic ribbons in the mammalian cochlea *in vivo*, we compared spontaneous and sound-evoked activity from auditory nerve (AN) fibers in bassoon-null mice and their wild-type littermates. Techniques for recording single-fiber activity in mice are described elsewhere [Taberner and Liberman, J. Neurophys. 93: 557-69, 2005]. DPOAE thresholds were similar in mutants and wild-types, except at the highest test frequencies. Selective elevation of ABR thresholds was observed in mutants, consistent with anomalies in synaptic transmission.

AN tuning appeared normal in mutants except at high frequencies. AN discharge retained the normal stochastic pattern seen in interval histograms of spontaneous activity. However, average spontaneous rates were reduced: the maximum was 30 sp/sec in mutants vs 180 sp/sec in wildtypes. Sound-evoked discharge was assessed by post-stimulus time histograms to tone bursts at 30 dB re threshold. Although mutant fibers showed sustained responses, even to 5 sec stimuli, both steady-state and onset rates were reduced. Onset reductions were more striking than steady-state reductions; correspondingly, the time constants for post-onset adaptation were altered. Data suggest that a key role of the synaptic ribbon is to support the high rates of discharge normally seen in the AN.

### **[617] Role of Synaptic Ribbons in Sound Coding: Hair Cell Transmitter Release in Mice Lacking the Presynaptic Scaffolding Protein Bassoon**

**Darina Khimich**<sup>1</sup>, Juan Goutman<sup>2</sup>, Eckart Gundelfinger<sup>3</sup>, Elisabeth Glowatzki<sup>2</sup>, Tobias Moser<sup>1</sup>

<sup>1</sup>University of Goettingen, <sup>2</sup>Johns Hopkins University, Baltimore, Maryland, <sup>3</sup>IfN Magdeburg

The synaptic ribbon is an electron-dense structure found at hair cell afferent synapses as well as at retinal synapses. A previous study on mutant mice for the synaptic scaffolding protein Bassoon, whose hair cells mostly lack synaptic ribbons, showed a reduction of the hair cell readily releasable pool of synaptic vesicles and a synaptic hearing impairment (Khimich et al., Nature 434:889-894, 2005). To further study the function of synaptic ribbons in the mammalian cochlea we performed patch-clamp studies of presynaptic hair cell exocytosis and excitatory postsynaptic currents of afferent dendrites in Bassoon mutant mice and their wildtype littermates.

Unlike normal hair cells, the ribbon deficient hair cells of 1- and 3-week-old mice almost entirely lost fast exocytosis when dialyzed with the slow Ca<sup>2+</sup> chelator EGTA. This suggests that the remaining readily releasable vesicles are not properly colocalized with the sites of Ca<sup>2+</sup> entry in the absence of the ribbon and/or Bassoon. Augmentation of

Ca<sup>2+</sup> current by BayK8644 did increase but failed to fully recover fast exocytosis in ribbon deficient hair cells. Sustained exocytosis was nearly normal. Endocytic membrane retrieval following exocytosis occurred even somewhat faster in mutant hair cells. Early endosomal antigen 1, an endosomal marker, was similarly distributed in WT and mutant hair cells. Potassium currents (BK, KCNQ4 and KV) and membrane potentials were found to be normal in ribbon deficient hair cell.

The data suggest that the synaptic ribbon supports faithful auditory signaling by placing a sufficient number of readily releasable vesicles close to the sites of Ca<sup>2+</sup> entry at the active zone.

Supported by the Human Frontier Science Program RGY19/2004 to EG and TM, the European Commission grant "Eurohear" to TM and the NIDCD, R01 DC06476 to EG.

### **[618] Contribution of the Synaptic Ribbon to Temporal Reliability of Hair Cell Exocytosis**

**John Wittig, Jr.**<sup>1</sup>, Rony Weisman<sup>1</sup>, Sachin Puranik<sup>1</sup>, Thomas D. Parsons<sup>1</sup>

<sup>1</sup>University of Pennsylvania

Phase-locking of the auditory nerve to a periodic acoustic stimulus requires the hair cell afferent synapse to release vesicles with marked temporal precision. We have developed a computational model of the hair cell pre-synaptic active zone to study the timing of exocytosis down to the resolution of single vesicle fusions. Our biophysically detailed model is fully stochastic and composed of several stages: gating of calcium channels, buffered diffusion of individual calcium ions, and fusion of synaptic vesicles. The model parameters are derived from experimental findings on the distribution of synaptic vesicles (Lenzi et al., 2002), activation of calcium channels (Armstrong et al., 1998), and kinetics of exocytosis (Beutner et al., 2001).

In order to better understand what limits the temporal precision of this synapse, we investigated possible sources of exocytic variability. Each stochastic step in the synaptic cascade introduces another potential source of variability and contributes to the total variance in the hair cell's response. The model allows us to freeze individual stochastic elements in the cascade and assess their relative contribution. Both the response amplitude and synaptic latency exhibited a coefficient of variation (CV) of around 0.2 in the fully stochastic model. However compared to amplitude, the timing of neurotransmitter release is relatively insensitive to model perturbations. Freezing the number or location of synaptic vesicles reduced the CV of the response amplitude by ~50% while having no effect on the CV of the synaptic latency. We interpret these preliminary studies to suggest that while there is significant temporal jitter in individual vesicle fusions, the large number of fusiogenic vesicles present at the synapse insures temporal response fidelity and supports a role for the synaptic ribbon in the precise timing of hair cell neurotransmitter release.

## **619 Synaptic Vesicle Recycling in Vestibular Hair Cells of Rodents**

**Sophie Gaboyard-Niay<sup>1</sup>**, Steven Price<sup>1</sup>, Anna Lysakowski<sup>1</sup>

<sup>1</sup>*University of Illinois at Chicago*

Synaptic transmission in vestibular hair cells is characterized by tonic and graded transmitter release through persistent exocytosis. Consistent with the large amount of vesicle trafficking needed, hair cells harbor a peculiar synaptic structure called a ribbon, a dense structure surrounded by synaptic vesicles. It is thought to facilitate constant vesicle release. This synaptic vesicle cycle was followed in vestibular hair cells of rats and mice over time (10, 30, 90 and 180 min) using intraperitoneal injection of AM1-43. This fixable styryl dye fluoresces when taken up by membranes during endocytosis. Confocal microscopy and 3D reconstruction showed loading in the basolateral membrane of hair cells up to 90 min but not for the 180 min injection. In addition, there were bright "spots", peculiar structures located between the cuticular plate and vestibular hair cell nuclei. They were observed at any time after injection: from 10 to 180 min. Photoconversion of AM1-43 and electron microscopy showed label in the basolateral membrane and in synaptic vesicles surrounding ribbons, and revealed the "bright spots" in the upper part of the cells to be multivesicular bodies (MVBs). This suggests that a proportion of synaptic vesicles will rapidly refill the readily releasable pool of synaptic vesicles by endocytosis, while others will fuse into MVBs not involved in synaptic vesicle refilling. Some AM1-43-labeled MVBs were apposed to the nuclear membrane after 3 hrs. As with neurons, MVBs may function as an endosome carrier vehicle or "retrosome" (Weible and Henri, 2004). The retrosomes may enable molecules to be transported intact to the nucleus and thus receive a snapshot of the synaptic activity of the sensory cell occurring at the time the "retrosome" is formed.

Supported by the NSBRI through NASA NCC 9-58 and by NIH grant DC-02521.

## **620 Neural Adaptation of the Hair Cell Afferent Synapse Following Increases in Acoustic Stimuli**

**Lauren Tang<sup>1</sup>**, Adam C. Furman<sup>1</sup>, James C. Saunders<sup>1</sup>, Thomas D. Parsons<sup>1</sup>

<sup>1</sup>*University of Pennsylvania*

Adaptation is a common feature of sensory systems, including the auditory system. A decrement in neural activity in the face of a maintained sound reduces redundant sensory input and perhaps fosters the detection of novel stimuli. However, the cellular mechanisms that allow an adapted sensory system to respond to a novel stimulus are poorly understood. We have undertaken *in vivo* single-unit recording of cochlear nerve activity in the chick to study what happens to the steady state adapted response when the stimulus suddenly undergoes an intensity change. The stimulus was set to the characteristic frequency of each unit. In this intensity change paradigm, the intensity of the first segment ranged from 0 to 35 dB SPL above threshold in 5 dB increments for the first 100 ms, and then increased to 40 dB SPL above threshold for

a second 100 ms. Following the step increase in sound intensity was a range of transient increases in discharge rate exhibiting an adapting response at sound onset. Parameters of this transient response were measured and compared across the varying intensity levels. Analysis revealed that as the initial intensity increased, both the onset peak and percent adaptation of the first segment increased. However, the onset peak and percent adaptation of the second segment decreased, despite a constant level of stimulation. The adapted level for the first segment also increased, whereas the adapted level for the second segment remained relatively constant. The time constant of adaptation exhibited no significant difference across intensity. We interpret the transient discharge activity at sound onset to result from the exhaustion of a functional pool of synaptic vesicles in the cochlea hair cell. Consistent with that, the magnitude of the second response was inversely related to the magnitude of the first response, suggesting cross-depletion of a vesicle pool. Surprisingly, the size of this apparent functional pool scaled with intensity.

## **621 Immunofluorescence Co-Localization of PACAP and Receptor PAC1-R with Neuronal Markers Within the Organ of Corti: Implications for Efferent Modulation of Afferent Signaling**

**Marian J. Drescher<sup>1</sup>**, Khalid M. Khan<sup>1,2</sup>, Neeliyath A. Ramakrishnan<sup>1</sup>, James S. Hatfield<sup>3</sup>, Dennis G. Drescher<sup>1,4</sup>

<sup>1</sup>*Department of Otolaryngology, Wayne State University School of Medicine, Detroit, MI, USA*, <sup>2</sup>*Department of Biological and Biomedical Sciences, Aga Khan University, Karachi, Pakistan*, <sup>3</sup>*Electron Microscopy Laboratory, Veterans Affairs Medical Center, Detroit, MI, USA*, <sup>4</sup>*Department of Biochemistry and Molecular Biology, Wayne State University School of Medicine*

In the investigation of neuromodulation by pituitary adenylyl cyclase-activating polypeptide (PACAP) in the rat cochlea, we previously identified the expression, in cochlear subfractions, of six splice variants of the PACAP receptor, PAC1-R, including two new splice variants (ARO Abstr. 28: 226, 2005). Possible mechanisms for neuromodulation can now be suggested from immunofluorescence co-localization of neuropeptide and receptor with neuronal markers. In addition to co-localization in afferents and efferents, we investigated whether the organ of Corti receives direct adrenergic innervation, representing a site of PACAP action, given the close association in the CNS of PACAP and catecholaminergic neurotransmission. PACAP has now been found to co-localize with ChAT, one of six neuronal markers, both in intraganglionic efferent fibers within the spiral ganglion as well as in the efferent cups beneath inner hair cells and in small (but not large) efferent fibers at the base of outer hair cells for all cochlear turns. PAC1-R co-localized with the afferent GluR 2/3, with immunoreactivity overlapping basal and apical sites of inner and outer hair cells in the organ of Corti for all three cochlear turns, also evident in the non-sensory Hensen's cell region of the apical turn. Adrenergic marker dopamine  $\beta$ -hydroxylase is expressed in nerve fibers overlapping

outer hair cells and Hensen's cells in the apical turn, with some fibers also expressing PAC1-R. Overall, we have obtained evidence that PACAP constitutes an efferent neuromodulator with its effects mediated by PAC1-R on afferent and adrenergic nerve fibers within the organ of Corti. PAC1-R receptors on type I afferents beneath the inner hair cell may thus respond to PACAP originating from lateral olivocochlear efferents, resulting in potentiation of nicotinic acetylcholine receptors/neuroprotection of glutamate-induced toxicity on/in the type I afferents.

Supported by NIH RO1 grants DC000156 and DC004076.

## **[622] Overexpression of SK2 Channels Enhances Classic Efferent Suppression Without Enhancing Noise Resistance**

**Lisan Parker<sup>1</sup>**, Stéphane F. Maison<sup>2</sup>, Lucy Young<sup>1</sup>, M. Charles Liberman<sup>2</sup>, Jian Zuo<sup>1</sup>

<sup>1</sup>*St. Jude Children's Research Hospital*, <sup>2</sup>*Harvard Medical School and Eaton-Peabody Laboratory, Massachusetts Eye & Ear Infirmary*

Outer hair cells (OHCs) express SK2, small-conductance  $\text{Ca}^{2+}$  activated  $\text{K}^{+}$  channels, at synapses with olivocochlear (OC) efferents. Acetylcholine release from OC terminals activates SK2 via  $\text{Ca}^{2+}$  entry through the  $\alpha 9/\alpha 10$  cholinergic receptor complex also at the synapse. To investigate the role of SK2, we examined shock-evoked OC effects, the density of OC innervation, and resistance to acoustic injury in mice overexpressing SK2 channels.

Baseline thresholds (ABR and DPOAE) were normal in SK2 overexpressors. OC-mediated suppression was quantified via DPOAEs with shocks to the OC bundle at the floor of the IVth ventricle. SK2 overexpressors exhibited enhanced OC suppression. Cochlear wholemounts and sections were immunostained for synaptophysin to assess OC innervation. Efferent terminals on OHCs were reduced in the SK2 knockouts at ages as early as 1 month (see also Vetter et al., ARO 2005), but appeared normal in overexpressors. Resistance to acoustic injury was assessed in overexpressors by measuring threshold shifts (ABR and DPOAE) 1 wk after exposure to a noise band at 100 dB for 2hrs. No difference in the magnitude of permanent noise-induced hearing loss was observed.

Overexpression of the  $\alpha 9$  subunit in OHCs leads to enhanced shock-evoked OC effects and increases the ear's resistance to acoustic injury (Maison et al., 2002); loss of  $\alpha 9$  abolishes shock-evoked OC effects (Vetter et al., 1999), and neither mutant line shows dramatic changes in the density of efferent innervation. Comparing these results with previous work from Vetter et al. (ARO 2005) and this present study suggests that 1) protection from acoustic injury arises downstream of the  $\text{Ca}^{2+}$  entry through the  $\alpha 9$  channel but does not require the OHC potential changes coupled to SK2 activation, and 2) SK2 channels are important in the development or maintenance of cochlear efferent innervation.

Research supported by RO1DC0188/06471, P30DC05209, ALSAC, CA21765, and UNCF/Merck.

## **[623] Postulated Genesis of Cytosolic Vesicles in Cochlear Hair Cells from Segmented Cisternae Contacting Mitochondria**

**Samuel S. Spicer<sup>1</sup>**, Bradley A. Schulte<sup>1</sup>

<sup>1</sup>*Medical University of South Carolina*

Numerous vesicles presumably synaptic in nature largely fill the basal compartment of inner hair cells (IHCs) whereas spheroidal collections of vesicles of undetermined function comprise the Hensen bodies in outer hair cells (OHCs). The cytologic mechanism for biosynthesis of these unique vesicle populations was investigated here by electron microscopy. The vesicles in basal cytosol of IHCs and Hensen bodies lay associated spatially with linear cisternae. These cisternae revealed disassembly into aligned, dense walled segments where contacting clustered mitochondria. Their colocation with mitochondria implied that the segmenting cisternae utilize ATP and contain an ATPase. Vesicle genesis occurring during endocytosis is mediated by the action of type IV ATPases or flippases. These Ptype ATPases translocate aminophospholipids from the external to the internal leaflet of the phospholipid bilayer and thereby establish in the cell membrane a lipid asymmetry essential to budding of endocytic vesicles from the plasmalemma. It can be postulated then that the mitochondria associated cisternae in IHCs and Hensen bodies analogously possess a type IV ATPase. This flippase hypothesized to exist in segmented cisternae contacting mitochondria would translocate aminophospholipid to the inner monolayer of the cisternae thereby inducing their segmentation and genesis of cytosolic vesicles.

## **[624] In Vitro Analysis of Direct Interaction of the L-Type Calcium Channel $\text{Ca}_v1.3$ Subunit and Gas/olf Expressed in Saccular Hair Cells**

**Neeliyath A. Ramakrishnan<sup>1</sup>**, Marian J. Drescher<sup>1</sup>, Dennis G. Drescher<sup>1,2</sup>

<sup>1</sup>*Department of Otolaryngology, Wayne State University School of Medicine, Detroit, MI, USA*, <sup>2</sup>*Department of Biochemistry and Molecular Biology, Wayne State University School of Medicine*

Vertebrate hair cells predominantly express the L-type  $\text{Ca}_v1.3$  subunit of the voltage-gated calcium channel (VGCC). L-type channels are typically modulated via phosphorylation, and few studies exist reporting their direct interaction with G-protein subunits such as  $\text{G}\alpha_s$ . However,  $\text{G}\alpha_s$  is known to co-immunoprecipitate with  $\text{Ca}_v1.1$  (skeletal muscle L-type calcium channel), and expression of  $\text{G}\alpha_s$  with  $\text{Ca}_v1.2$  (cardiac L-type calcium channel) activates channel conductance, without an increase in VGCC expression and without dependence on PKA phosphorylation. Previously, we detected by RT-PCR and immunohistochemistry the expression of  $\text{G}\alpha_s/\text{olf}$  in a trout saccular hair-cell preparation (ARO Abstr. 27: 239, 2004). Currently, using the  $\text{Ca}_v1.3$  II-III loop as bait in yeast two-hybrid protocols, we obtained prey clones from a trout saccular hair-cell cDNA library possessing sequence identical to that of trout saccular hair-cell  $\text{G}\alpha_s/\text{olf}$ -2. Pull-down assays using immobilized II-III loop fusion protein

specifically precipitated Gas/olf from a trout brain lysate. Similarly, immobilized anti-Gas/olf affinity-purified antibody immunoprecipitated II-III loop fusion protein, an interaction significantly blocked by the antigen. Thus, these several tests of specificity demonstrate that the II-III loop of Ca<sub>v</sub>1.3 binds the Gas/olf subunit. Gas/olf-specific immunoreactivity has also been localized to sites both apical (stereocilia) and basal in the saccular hair cells, the latter corresponding to hair cells sites for neural inputs, both efferent and afferent. The Gas/olf affinity-purified antibody yields a major band at 46 kDa on western blots, predicted for saccular hair-cell Gas/olf-2. We hypothesize that at the base of the hair cell, Ca<sub>v</sub>1.3 is modulated by Gas/olf, released upon Gas/olf-receptor interaction, impacting influx of calcium and release of hair-cell transmitter.

Supported by NIH R01 grants DC000156 and DC004076.

## **625 Calcium Buffering of BK Channels and Exocytosis in Hair Cells**

**Matthew Giampola**<sup>1</sup>, Thomas D. Parsons<sup>2</sup>

<sup>1</sup>*University of Pennsylvania School of Medicine,*

<sup>2</sup>*University of Pennsylvania School of Veterinary Medicine*

Calcium modulates neurotransmitter release and calcium-activated potassium channels such as BK channels necessary for resonance. Intracellular calcium buffers localize calcium signaling within cellular regions but also affect functionality of calcium-dependent processes. Various buffering capacities may contribute to the ability of cells to respond precisely at particular stimulation frequencies. We explored calcium buffering in isolated cochlear tall hair cells of White Leghorn chickens (8-21 days old). We approximated endogenous calcium buffering properties by comparing recordings in the presence of endogenous buffer (perforated patch: Nystatin, 200µg/ml) to recordings in the presence of various calcium buffers with known properties and concentrations (whole cell). We monitored both calcium-triggered vesicle fusion (capacitance changes) and calcium-activated potassium currents as dependent measures.

For capacitance measures, cells were depolarized with voltage clamp from a holding potential of -81 mV to a testing potential of -21 mV for durations ranging from 50 ms to 500 ms. Endogenous calcium buffering capacity was better mimicked by millimolar concentrations of a fast buffer (1.6mM BAPTA) than by submillimolar concentrations of a slow buffer (0.2mM EGTA).

To explore calcium buffering over smaller time scales, we measured BK potassium current under various calcium-buffering conditions. Cells were voltage clamped to a holding potential of -81 mV and then clamped to testing potentials (-111 to 79 mV) for 3 ms. I<sub>k</sub> remaining in the presence of Iberitoxin is subtracted from I<sub>k</sub> measured under control conditions, revealing the portion of the current attributable to BK channels. BK tail currents were analyzed for shifts in current/voltage relationship under buffering conditions. Weak buffering was seen to shift resonance activation to lower voltages while strong buffering shifted activation to higher voltages.

## **626 Structural and Functional Evidence for BK**

### **β1 Subunits in Chick Hair Cells**

**R. Keith Duncan**<sup>1</sup>, Yi Li<sup>1</sup>, Alan Evans<sup>2</sup>, Karolina Wesolowski<sup>1</sup>, Kewa Mou<sup>1</sup>

<sup>1</sup>*University of Michigan,* <sup>2</sup>*Howard University*

Large-conductance, calcium-activated potassium (BK) channels play an important role in the excitability of hair cells, particularly in lower vertebrates where they contribute to an electrical tuning mechanism. We have previously shown that BK properties (e.g. calcium affinity and kinetics) vary tonotopically in the chick cochlea. These functional variations seemingly fit known molecular variations, namely the graded expression of BK β1 transcripts from high in the cochlear apex to low in the base. However, the kinetics of native BK channels from the chick cochlea are 10-fold faster than cloned channels co-assembled with β1. To determine whether β1 has a functional role in the cochlea, we created a custom antibody to the chicken β1 subunit. Preliminary characterization of immune sera suggests an asymmetric distribution of BK β1 in tall hair cells rather than short, but a tonotopic gradient remains unclear. Cells within the tegmentum vasculosum (i.e. analog to mammalian stria vascularis) were also brightly labeled by this antibody. To correlate structure with function, we analyzed single channel recordings from chick hair cells. BK channels often exhibit prolonged openings, called bursting, during which there are many, brief transitions to the closed state. Mean burst durations for native channels (200 nM Ca<sup>2+</sup> and Popen = 0.5) ranged from 1 to 26 ms. The shorter burst durations are similar to data reported for α-only BK channels, whereas the longer burst durations are similar to data reported for α+β1 BK channels at a 1:1 stoichiometry. Mean burst durations between these extremes may result from intermediate stoichiometries. These data provide further evidence for BK β1 effects in the cochlea. Altered β1 expression has been tied to vascular problems in aged animals, leaving open the possibility that BK β1 contributes to auditory deficits in some cases.

Supported by a grant to R.K.D. from the American Hearing Research Foundation

## **627 TRPA1, a Hair Cell Channel with Unknown Function?**

**Ruben Stepanyan**<sup>1</sup>, Erich T. Boger<sup>2</sup>, Thomas B. Friedman<sup>2</sup>, Gregory I. Frolenkov<sup>1</sup>

<sup>1</sup>*University of Kentucky, Lexington, KY,* <sup>2</sup>*National Institute on Deafness and Other Communication Disorders, Rockville, MD*

TRPA1, an ion channel activated by pungent compounds and cold temperatures, has been recently suggested to be a mechanotransduction channel of vertebrate hair cells (Corey et al., *Nature*, 432:723-30). TRPA1 was shown to express in nociceptive neurons and vertebrate hair cells. Among several localizations within a hair cell, immunostaining revealed TRPA1 in the stereocilia. Heterologously expressed TRPA1 is activated by allyl isothiocyanate (AITC) and icilin suggesting that these

agonists are likely to interact directly with this channel (Nagata et al., J Neurosci., 25:4052-61, 2005). The goal of our study was to test whether AITC and icilin activate putative TRPA1 channels in hair cells of the mammalian organ of Corti. Whole cell patch clamp recordings were obtained from outer hair cells of cultured mouse organ of Corti. Both agonists of TRPA1 evoked prominent inward currents, which developed to a maximal effect on average within eleven (AITC, 10  $\mu$ M) or six (icilin, 100  $\mu$ M) seconds. These currents represented an inward rectifying conductance with almost no effect of agonists at positive holding potentials. This strong inward rectification was very different from the voltage dependence of mechanotransduction current in the same cells. Prolonged application of AITC or icilin produced complete desensitization of the response. After desensitization, when subsequent applications of TRPA1 agonists did not produce anymore cell current responses, a mechanical stimulation of stereocilia with a water jet evoked a prominent mechanotransduction current in the same outer hair cell. The amplitude of mechanotransduction current did not noticeably decrease after AITC or icilin-evoked desensitization. We concluded that the TRPA1 agonists, AITC and icilin, activate in mouse outer hair cells a channel or channels that are likely unrelated to the mechanotransduction complex.

#### **628 Characterizing the Internal Face of the Turtle Auditory Hair Cells Mechanotransducer Channel**

**Anthony Ricci<sup>1</sup>, Jessica Waguespack<sup>1</sup>**

<sup>1</sup>*Louisiana State University*

Recent investigations found that the met single channel conductance increased when external calcium was lowered (Ricci et al., 2003). Removing the calcium block of the met channel by depolarization did not increase the conductance thus discounting the hypothesis that flicker block of the channel by calcium was responsible for the increased conductance, leaving the mechanism for the different conductance to be explored.

Lowering external calcium resulted in rectification of the macroscopic met current, with currents increasing at negative potentials but remaining constant at positive potentials, in agreement with the single channel recordings. Previous work identified curare as an open channel blocker and methylene blue as a permeable blocker when placed in the external solution (Farris et al., 2004). When applied internally these agents had no effect. To demonstrate that diffusion barriers were not limiting access of drugs into the stereocilia, fluorescent dextrans of different molecular weights (up to 40 kD) were tracked into the sensory hair bundle. This data suggest the inner face of the met channel differed from the external face, and that permeation through the channel may be limited.

To directly assess permeation, internal solutions containing different sized monovalent ions were used. By plotting the relative current at positive potentials against the radius of these ions the pore diameter was estimated to be about half that estimated from the external face of the channel thereby demonstrating the channel is intrinsically rectified. This may suggest a conformational

change resulting in a subconductance state of the channel at positive potentials.

Work was supported by RO1 to AJR.

#### **629 Two Classes of Outer Hair Cells Along the Tonotopic Axis of the Cochlea**

**Jutta Engel<sup>1,2</sup>, Claudia Braig<sup>2,3</sup>, Lukas Rüttiger<sup>2,3</sup>, Stephanie Kuhn<sup>1,2</sup>, Stefan Münkner<sup>1,2</sup>, Marlies Knipper<sup>2,3</sup>**

<sup>1</sup>*University of Tuebingen, Institute of Physiology II,*

<sup>2</sup>*Tuebingen Hearing Research Centre, <sup>3</sup>University of Tuebingen, ENT Clinic, Molecular Neurobiology*

Recently it has been shown that OHCs exhibit a surprising sensitivity for deletion of ion channels that thus far had been assigned to play a decisive role in inner rather than outer hair cells. The voltage-gated L-type Ca<sup>2+</sup> channel with the pore-forming  $\alpha$ 1 subunit Cav1.3 (formerly  $\alpha$ 1D) is expressed in IHCs (Platzer et al., 2000; Michna et al., 2003). Cav1.3-deficient mice (Cav1.3<sup>-/-</sup>) are deaf due to the complete absence of L-type currents in IHCs, but most surprisingly degeneration of OHCs was observed in the 3rd postnatal week, soon after the onset of hearing in wildtype mice (Platzer et al., 2000; Glueckert et al., 2003).

The predominant K<sup>+</sup> current of IHCs is the voltage- and Ca<sup>2+</sup>-activated K<sup>+</sup> current IK<sub>f</sub> carried by BK channels (Dulon et al., 1995; Kros et al., 1998; Marcotti et al., 2003). Recently the deletion of the BK $\alpha$  gene in the mouse was shown to result in progressive high-frequency hearing loss that surprisingly similar to Cav1.3 mouse mutants was associated with a loss of outer rather than inner hair cells (Rüttiger et al., 2004). We compared both knockout mouse models on the level of the expression pattern of ion channels, phenotype and function and found interesting differences. The results are discussed on the level of the existence of two classes of OHCs differing with respect to their sensitivity to gene deletion of either Cav1.3 or BK and their expression of pre- and postsynaptic proteins for OHC afferent transmission.

Supported by DFG En 294/2-4, DFG Kni-316/3-1; 4-1

#### **630 BK Channels (Slo) Interact with CDK5 Kinase in Chick Hair Cells – Implications to Tuning**

**Jun-Ping Bai<sup>1</sup>, Alberto Ortega<sup>2,3</sup>, Joseph Santos-Sacchi<sup>1</sup>, Dhasakumar Navaratnam<sup>1</sup>**

<sup>1</sup>*Yale University, <sup>2</sup>Yalu University, <sup>3</sup>University of California*

Large conductance K channels encoded by the Slo gene are the chief determinant of electrical resonance in hair cells of the inner ear. These channels show varying kinetics in hair cells along the tonotopic axis. In exploring how these varying kinetics are brought about two mechanisms, alternative splicing and association with the beta-1 subunit, have been identified as contributory mechanisms. However, neither of these two mechanisms could explain the range of kinetic properties demonstrated by BK channels in hair cells.

In attempting to elucidate other mechanisms for the heterogeneity in hair cell BK channel properties we have used the yeast two-hybrid technique to isolate proteins that interact with Slo and modulate its kinetics by allosteric and

other means. One of the proteins we identified using such a screen was CDK5 kinase, a serine threonine kinase that is enriched in the nervous system. This kinase has been implicated in controlling numerous processes including neuronal migration, degeneration and synaptic function.

We show here that CDK5 is found in chick cochlea hair cells, and that it interacts with Slo using immunoprecipitation and FRET assays. Furthermore, in heterologous systems the addition of the CDK5 activator p35 increases open probability of BK channels by causing a left shift in the voltage-P0 relationship. The implications of these results to electrical tuning will be discussed.

### **631 BK Channels Regulation in Rat Inner Hair Cells**

**Emilie Hoang Dinh<sup>1</sup>**, Maryline Beurg<sup>1</sup>, Didier Dulon<sup>1</sup>

<sup>1</sup>INSERM U587 et Université de Bordeaux 2

Inner hair cells (IHCs) display a complex set of K<sup>+</sup> currents: IKf, IKs and IKn carried by BK, Kv and KCNQ channels, respectively. In mature rat IHCs (with careful series resistance correction), a rapidly activating current with partial inactivation was directly recorded when blocking IKs and IKn with 4-AP and XE991 or linopirdine. This current is believed to be IKf since it was largely blocked by paxilline and iberiotoxin (IbTX). However, under these conditions, a slowly activating non-inactivating voltage-dependent current still remained. This residual slow current appeared not to be carried by SK channels since it was not dequalinium-sensitive. We believe that this slow current resistant to 4-AP, XE991 and paxilline is at the basis of a large underestimation of the inactivating phase of IKf. Inactivation was found in both apical and basal IHCs and in 10 mM intracellular BAPTA conditions. Paxilline (5  $\mu$ M) was more efficient than IbTX (250 nM) in blocking IKf suggesting the implication of beta subunits known to confer resistance to the peptide toxin. The addition of intracellular trypsin (0.5 mg/ml) did not significantly suppress IKf inactivation, excluding an N-type beta2 mechanism. RT-PCR experiments using beta3 specific primers suggested the expression of such regulatory subunits in the organ of Corti. W7 (100  $\mu$ M) a strong calmoduline inhibitor modified IKf (amplitude reduction and slower activation kinetics) but inactivation was conserved. Beside beta auxiliary subunits, these results imply another possible regulatory mechanism of IKf through a CaMkinase pathway.

### **632 Expression, Alternative Splicing, and Localization of KCNQ Potassium Channels in the Mammalian Cochlea**

**Zhe Jin<sup>1</sup>**, Guihua Liang<sup>1,2</sup>, **Leif Järleback<sup>1</sup>**

<sup>1</sup>Center for Hearing & Communication Research, Karolinska Institutet, Stockholm, Sweden, <sup>2</sup>Department of Neurology, The 1st Affiliated Hospital, Guangxi Medical University, Nanning, PR China

Voltage-gated potassium channels containing KCNQ1 and KCNQ4 subunits play key roles in hearing; gene disruption results in deafness associated with Jervell and Lange-Nielsen syndrome, and non-syndromic autosomal dominant sensorineural hearing loss DFNA2, respectively.

Other members of this gene family (e.g. *KCNQ2*, *KCNQ3*) also encode slow, low voltage-activated K<sup>+</sup> currents, i.e. M currents, which regulate neuronal excitability. We have recently described the presence of M-like K<sup>+</sup> currents in sensory hair cells, as well as the expression of the underlying *Kcnq2* and *Kcnq3* genes in the cochlea (Liang *et al*, ORL, 67, 75-82, 2005).

Here, the aim was to further characterize the genetic correlates of cochlear M currents, and to localize *Kcnq* gene expression and distribution of M channel subunits KCNQ2 and 3 in the cochlea.

All members of the *Kcnq* family were expressed in guinea pig and rat cochlea. Cochlear expression of *Kcnq2* exhibited five alternatively spliced forms with a developmental expression pattern. By using RT-PCR, we found expression of *Kcnq2* and *Kcnq3* transcripts in total RNA isolated from micro-dissected cochlear sub-regions; this was supported by immunolocalization of KCNQ2 and 3 subunits in fixed, cryo-sectioned cochleas from mouse, rat, and guinea pig. Expression of *Kcnq2* splice variants was found in modiolus and organ of Corti, while *Kcnq3* expression was also detected in the cochlear lateral wall. KCNQ2 immuno-reactivity was observed in auditory neurons of the spiral ganglion, and in hair cell synaptic regions. KCNQ3 immuno-reactivity was similar, but in addition, satellite cells in the spiral ganglion and the lateral wall showed immuno-labeling.

These findings provide further evidence for cochlear M channels in key structures for auditory pathophysiology; important roles in regulation of cellular excitability in the auditory system, and hearing disorders related to (hyper)excitability, e.g. tinnitus and hyper-acusis, are implied.

### **633 Localization of Pre- and Post-Synaptic Proteins at the Chick Cochlear Hair Cells-Afferent Fiber Synapse**

**Shunda Irons-Brown<sup>1</sup>**, J. Andrew Dziewit<sup>2</sup>, Thomas D. Parsons<sup>1</sup>

<sup>1</sup>University of Pennsylvania, <sup>2</sup>Temple University

We employed immunocytochemistry and fluorescent laser scanning confocal microscopy to localize putative epitopes of the pre-synaptic ribbon protein, RIBEYE, C-terminal binding protein (CtBP), the post-synaptic glutamate receptor, (GluR2), and afferent fibers (NF-200) in the avian cochlea. Anti-GluR2, CtBP, RIBEYE staining exhibited a punctate, patch-like pattern concentrated at the base of the hair cell. Three-dimensional reconstruction of serial image stacks confirmed that the apparent receptor patches lie along the hair cell's baso-lateral surface. A marked gradient in GluR2 patch staining was observed along the radial axis from the neural to abneural edge of the cochlear duct, consistent with the labeling of synaptic contacts between the hair cell and its afferent fibers. A noted co-localization of the synaptic ribbon to the glutamate receptor patches was observed when the cells were double-labeled cells with both anti-GluR2 and anti-RIBEYE antibodies. Approximately 80% of the receptor patches examined in each tissue section overlapped with aggregates of RIBEYE staining. At 2 days of age post-



hatch, 83+/-5% (7 sections from 4 birds), and at 6 days, 78 +/- 9% (9 sections from 4 birds) of receptor patches were co-localized with a synaptic ribbon. After 14 days of incubation (E14, 7 embryos), afferent fiber staining showed a mature gradient label along the radial axis. Ongoing studies are focused on the development sequence of the synaptic ribbon-glutamate receptor morphological complex formation and distribution.

#### **634 Diversity of Ca<sup>2+</sup>-Activated K<sup>+</sup> Channels in the Mouse Cochlea**

**Sonya M.S. Rocha-Sanchez<sup>1</sup>**, Sylvia Ziegenbein<sup>1</sup>, Ken Morris<sup>1</sup>, Chikatoshi Kai<sup>2</sup>, Jun Kawai<sup>2,3</sup>, Piero Carninci<sup>2,3</sup>, Yoshihide Hayashizaki<sup>2</sup>, Robin L. Davis<sup>4</sup>, Kirk W. Beisel<sup>1</sup>

<sup>1</sup>Creighton University, Omaha, NE, <sup>2</sup>RIKEN Genomic Sciences Center, <sup>3</sup>Genome Science Laboratory, Discovery Research Institute, <sup>4</sup>Rutgers University

The BKCa channels are comprised of four alpha subunits (Kcnma1) and accessory beta subunits (Kcnmb1-4) and diversity is BKCa generated by the alternative splicing of the KCNMA1 gene and combinatorial usage of the beta subunits. The goal of our studies was to examine the variability and potential diversity of BKCa channel expression in mouse inner ear hair cells and relate this diversity to evolutionary conservation of the associated electrophysiological and tonotopic properties. Bioinformatic analyses allowed the examination of genomic sequences and comparisons of the genomic exon-intron structure organization of mouse, rat, human, opossum, chicken, frog and zebrafish KCNMA1 orthologs. These data suggested that the KCNMA1 alternative splicing was highly conserved with 6-7 splice sites being utilized in all species.

Data derived from the RIKEN mouse transcriptome base along with RT-PCR experiments using murine gene-specific oligonucleotide primers analyzed the scope and extent of Kcnma1 and Kcnmb1-4 variation to identify if alternative splicing generated additional transcript variants in the inner ear hair cells. The murine Kcnma1 utilized 6 out of 7 potential splice sites. In the cochlea splice variants were present representing sites 3, 4, 6, and 7, while site 1 was insertionless and site 2 utilized only exon 10. Site 5 was not present. Whole mount confocal immunofluorescence analyses showed that KCNMA1 exhibited a quantitative longitudinal gradient with a reciprocal gradient found between inner and outer hair cells. A differential expression was also observed in usage of the long form of the C-terminus tail. KCNMB1 also exhibited a quantitative longitudinal reciprocal gradient between inner and outer hair cells. Spiral ganglia neurons exhibited a base to apex longitudinal gradient for KCNMA1, KCNMB1 and KCNMB4. Since KCNMA1 has extensive heterogeneity in the number of possible splice variants, it provides a "functional" paradigm by which the gene expression pattern of other alternative spliced transcripts can be analyzed.

This work was supported in part by National Organization of Hearing Research (SMRS) and NIH Grants (KWB) DC4279 and DC5009.

#### **635 Tympanic Membrane Model**

**Pierre Parent<sup>1</sup>**, Jont Allen<sup>1</sup>

<sup>1</sup>University of Illinois at Urbana-Champaign

Various models have promoted better understanding of the ear mechanics. In this study, a middle ear model is designed in the time domain to simulate the propagation of a sound wave along the hearing system. For that purpose, fixed samples are distributed along the whole path and periodically updated to represent volume velocity amplitude values at their position. Interactions between the different system parts and reflections are computed at each point along the path to ensure proper representation of the traveling wave. The ossicles chain is represented by a lumped-parameter elements (mass/stiffness) circuit, the cochlea by a resistor and the ear canal by a simple delay line. The gist of the study is modeling the tympanic membrane: the drum is discretized into concentric annuli, each one with its own impedance and reflection coefficient. Taking into account the differences in speed of sound between the canal and the membrane on the one hand, and between the membrane and the middle ear cavity on the other hand, the discretized eardrum model is interfaced with those models. The whole system is implemented in a signal processing computer language, Matlab, and simulations are run to test its consistency. For several physical measures, derived from the canal input impedance computation, comparisons with experimental data -human ears and artificial couplers- are carried out. In both cases, simulations underline a good match between model predictions and experimental data along the whole range of audible frequencies: typical high-frequency behaviors are even better captured than with some mechanical couplers. Future work could include modeling of several middle ear diseases to understand them better and help clinical diagnosis from reflectance measurements.

#### **636 A Nonlinear Finite-Element Model of the Newborn Ear Canal**

**Li Qi<sup>1</sup>**, Justyn Lutfy<sup>2</sup>, W. Robert J. Funnell<sup>3</sup>

<sup>1</sup>Biomedical Engineering, McGill University, <sup>2</sup>Anatomy & Cell Biology, McGill University, <sup>3</sup>BioMedical Engineering & Otolaryngology, McGill University

Tympanometry in newborns may provide important clinical information about the middle ear, but the measurements are difficult to interpret. This may be due in part to the compliance of the newborn external ear canal; however, it is unclear how the newborn ear-canal wall moves under high static pressures. In this study, a nonlinear finite-element model is being developed in order to study the mechanical behaviour of the ear canal. The geometry of the model is based on a clinical X-ray CT scan of a 22-day-old newborn. The nonlinear hyperelastic Mooney-Rivlin constitutive law is applied to model soft tissues undergoing large deformations. Plausible ranges for material-property values are based on data from the literature. Results of the model are compared with available experimental measurements.

### **637 Analysis of a Technique for Measuring the Transmission Matrix of the Middle Ear**

**Antonio Miller**<sup>1,2</sup>, Christopher A. Shera<sup>2,3</sup>, Susan Voss<sup>3,4</sup>

<sup>1</sup>*Speech and Hearing Bioscience and Technology Program, Harvard-MIT Div. of Health Sciences and Tech.,*

<sup>2</sup>*Eaton-Peabody Laboratory, Massachusetts Eye & Ear Infirmary, Boston, MA,* <sup>3</sup>*Department of Otology and Laryngology, Harvard Medical School, Boston, MA,* <sup>4</sup>*Picker Engineering Program, Smith College*

We analyze a published model of the cat middle ear [Puria & Allen (1998), *J Acoust Soc Am*, 104(6)] to find the optimal combination of experimental measurements for determining the acoustic transmission matrix of the cat middle ear. The technique builds on previous work [Voss & Shera (2004), *J Acoust Soc Am*, 116(4)] which exploits the properties of distortion-product otoacoustic emissions (DPOAEs) to drive the middle ear "in reverse". A 2-port transmission matrix description of middle-ear mechanics is developed assuming that the input-output response at the tympanic membrane and stapes is linear, one dimensional, and time invariant. Model assumptions and approximations are then discussed and justified. The experimental procedure requires the near simultaneous measurement of ear-canal acoustic pressure, middle-ear input impedance, stapes footplate velocity, and DPOAEs. Measurements on the intact ear provide 3 of the equations needed to determine the 5 unknown system parameters. Two additional equations are obtained by draining the cochlea and measuring the forward transfer function and middle ear input impedance. One additional constraining equation comes from fixing the stapes footplate and measuring the middle-ear input impedance. Model results validate the derived system equations and suggest improvements to the experimental method.

### **638 Characterization of the Chinchilla Middle-Ear as a Two-Port Using Transmission Matrix Analysis**

**Jocelyn E. Songer**<sup>1</sup>, John J. Rosowski<sup>2,3</sup>

<sup>1</sup>*MIT-Harvard,* <sup>2</sup>*MIT,* <sup>3</sup>*Harvard Medical School*

In order to develop a mathematical model of the effects of Superior Canal Dehiscence (SCD) on the physiology and mechanics of the chinchilla ear, a complete characterization of the chinchilla middle ear is necessary. Despite the common usage of the chinchilla as an animal model in studies of auditory physiology, the middle-ear transfer characteristics of the chinchilla have not been established. We will present a two-port model of the middle ear that relates the input variables of the sound pressure at the tympanic membrane and the volume velocity of the tympanic membrane to the output variables of the sound pressure in the vestibule and the stapes volume velocity. The values of the four parameters of the two-port's transmission matrix (A, B, C, and D) and the cochlear input impedance are defined from measurements of middle-ear input admittance and stapes velocity in normal, cochlear drained and stapes-fixed conditions. With these parameters in hand, we can describe both the forward and reverse sound transmission through the middle ear with normal and modified cochlear loads. The matrix characterization then acts as the input stage of a model of

SCD and allows predictions of the effects of introducing a hole or dehiscence into the superior semicircular canal on middle- and inner-ear sound transmission. [Supported by NIDCD]

### **639 Vibrations of the Stapes and the Long and Lenticular Processes of the Incus in the Chinchilla Middle Ear**

**Luis Robles**<sup>1</sup>, Andrei Temchin<sup>2</sup>, Yun-Hui Fan<sup>2</sup>, Hongxue Cai<sup>2</sup>, Mario Ruggero<sup>2</sup>

<sup>1</sup>*Universidad de Chile, Santiago,* <sup>2</sup>*Northwestern University*

Last year we presented measurements of ossicular vibrations in the chinchilla middle ear showing that transmission is boosted by a peak in the transfer function at the incudo-stapedial joint (L. Robles et al., *ARO MWM Abstracts* 28: 321, 2005). However, we reported the boost as occurring between the incus and the head of the stapes. In fact, our measurements were made at the long and lenticular processes of the incus (W. R. Funnell et al., *JARO* 6: 9-18, 2005). We have now extended the measurements to ascertain that this boost is also present between the long process of the incus and the head of the stapes. This study, as the previous one, has been motivated by a review that disputed the commonly held notion that middle-ear vibrations restrict the bandwidth of hearing (M. A. Ruggero and A. N. Temchin, *P.N.A.S. USA* 99: 13206-13210, 2002). The vibratory responses to tones of the long and lenticular processes of the incus and the head of the stapes were measured using a laser velocimeter and a wide-band acoustic-stimulus system. The velocity magnitudes of the vibrations of the lenticular process of the incus and the head of the stapes were very similar, relatively constant (~0.1 mm/s/Pa) up to 32 kHz and decreasing at a rate of ~20 dB/oct at higher frequencies. In both cases the phase lags relative to pressure in the external ear canal increased approximately linearly, with slopes equivalent to a pure delay of about 70-80  $\mu$ s. The already wide frequency response of the long process of the incus is enhanced by a broad peak in magnitude of the transfer function between the long and the lenticular processes of the incus, that is accompanied by a phase lag. The magnitude peak boosts the vibrations of the lenticular process of the incus and the stapes head up to 20 dB at frequencies in the range of 20 to 30 kHz, further flattening the magnitude of the middle-ear transfer function. These results support the contention that the chinchilla middle ear behaves as a wide-band pressure transformer which transmits acoustic signals into the cochlea even at frequencies far exceeding the cut-off of hearing (Ruggero and Temchin, op. cit.).

Work supported by NIH Grant DC-00419.

### **640 The Sound Inputs to the Pressure-Difference Ear of Lizards**

**Geoffrey Manley**<sup>1</sup>, **Jakob Christensen-Dalsgaard**<sup>2</sup>

<sup>1</sup>*Lehrstuhl für Zoologie, Technische Universität München, Germany,* <sup>2</sup>*Institute of Biology, University of Southern Denmark, DK-5230 Odense M, Denmark*

The lizard eardrum exhibits a robust directionality, with more than 20 dB differences between ipsilateral and

contralateral stimulation. Furthermore, the directivity of the eardrum is asymmetrical across the midline and will therefore be sharpened by binaural comparisons in the CNS (Christensen-Dalsgaard and Manley, *J Exp Biol* 208:1209-1217, 2005). The directionality is created by acoustical coupling of the eardrums and interaction of the direct and indirect sound components on the eardrum. The ensuing pressure-difference characteristics generate the highest directionality of any terrestrial vertebrate ear. The aim of the present study was to measure the gain of the direct and indirect sound components.

We investigated the directionality of eardrum vibrations of three lizard species: *Anolis sagrei* and *Basiliscus vittatus* (iguonids) and *Hemidactylus frenatus* (gekkonid) by laser vibrometry, using either free-field sound or a headphone and coupler for stimulation. The directionality of the ear of these lizards is pronounced in the frequency range from 2 to 5 kHz. The directivity is ovoidal, asymmetrical across the midline, but largely symmetrical across the interaural axis (i.e. front-back). Occlusion of the contralateral ear abolishes the directionality.

To measure the gain of the sound pathways, we stimulated the two eardrums with local sound sources (a coupler close to the eardrum). Within the frequency range of maximal directionality, the contralateral gain (compared to sound arriving directly) is close to 1, indicating a pronounced acoustical transparency of the lizard head that may even exceed 1 due to resonances in the interaural cavities.

Our results show that the directionality of the lizard ear is caused by the acoustic interaction of the two eardrums. Thus, the lizard ear is not only a very clear example of a two-input pressure-difference receiver, but is also largely explained by a simple acoustical model based on an electrical analog circuit.

#### **[641] Measurements of Stapes Velocity in Live Human Ears**

**Wade Chien**<sup>1,2</sup>, John J. Rosowski<sup>1,2</sup>, Michael E. Ravicz<sup>2</sup>, Saumil N. Merchant<sup>1,2</sup>

<sup>1</sup>*Department of Otology and Laryngology, Harvard Medical School, Boston, MA,* <sup>2</sup>*Eaton-Peabody Laboratory, Massachusetts Eye & Ear Infirmary, Boston, MA*

While the mechanical properties of the live human middle ear at its input, e.g., middle-ear admittance and sound-induced umbo velocity, have been characterized reasonably well, few measurements of middle-ear output, e.g., stapes velocity, have been reported in live humans. Consequently, our understanding of human middle-ear transmission has come mostly from studies in animal and cadaveric ears. In this study we measured sound-induced stapes velocity intra-operatively in 8 patients undergoing cochlear implantation. These patients had no history of middle-ear pathology, and their ossicular chains appeared normal on intra-operative inspection and palpation. The mean velocity magnitude was stiffness-dominated at frequencies below 1 kHz, continued to increase up to ~4 kHz, and then decreased at higher frequencies. The phase of the velocity led sound pressure by 0.2 periods at 0.3 kHz, but gradually became a phase lag of 0.2 periods at 2 kHz. The mean of our stapes velocity measurements is

similar to the mean of 7 ears in the only other published live measurements [Huber et al. *Ann. ORL* 110: 31-35, 2003]. Like the Huber et al. data, our live measurements are on average 3–6 dB lower in magnitude than similar measurements in cadaveric temporal bones at frequencies below 2 kHz. A large part of this difference may be attributed to variations in angle of measurement [Chien et al., *ARO* 2005]; the laser-measurement angles (with respect to the axis of piston-like stapes motion) possible in the live ear are more oblique than those in cadaveric ear.

[Supported by NIDCD]

#### **[642] Anatomy and the Effect of Aging on the Distal Incus in Human**

**Wade Chien**<sup>1,2</sup>, Clarinda Northrop<sup>3</sup>, Stephen Levine<sup>3</sup>, William Peake<sup>4</sup>, Saumil N. Merchant<sup>1,2</sup>

<sup>1</sup>*Eaton-Peabody Laboratory, Massachusetts Eye & Ear Infirmary, Boston, MA,* <sup>2</sup>*Department of Otology and Laryngology, Harvard Medical School, Boston, MA,* <sup>3</sup>*The Temporal Bone Foundation, Boston, MA,* <sup>4</sup>*Massachusetts Institute of Technology, Cambridge, MA*

The ossicular chain couples the tympanic membrane to the inner ear and transmits acoustic signals from the outer to the inner ear. Examination of the anatomy and mechanical properties of the ossicular chain can provide insights into sound transmission from the tympanic membrane to the inner ear. In this study, the anatomy of the distal incus, including the lenticular process, was examined using histologic preparations from 102 normal temporal bones aged between less than 1 month and 100 years. In agreement with Funnell's data in cat (*JARO*, 2005 Mar;6(1):9-18), we found that the bony lenticular process has a proximal narrow "stem" and a distal flattened "cap" that forms one side of the incudo-stapedial joint. The joint capsule extends from the stapes head to cover the stem portion of the lenticular process on all sides; the capsule is considerably thickened at the level of the stem. Three-dimensional reconstructions made from sections of selected bones convey the complexities of the anatomy of this region.

Measurements of the bony architecture of the distal incus in all 102 temporal bones were made, including lengths and cross sectional areas, estimates of number of lacunae filled with osteocytes, and the degree of bone resorption. These measurements, analyzed as a function of age, provide an anatomic description that spans a large age range, which can serve as a normal baseline against which structural pathology can be identified. The results have implications for basic mechanisms of sound transmission through the middle ear, and provide insights regarding bone resorption at the level of the distal incus, which occurs clinically in some patients with chronic otitis media or after stapedectomy.

#### **[643] A Detailed 3D Model of the Incudostapedial Joint**

**Clarinda Northrop**<sup>1</sup>, Stephen Levine<sup>1</sup>, Collin Karmody<sup>1</sup>

<sup>1</sup>*Temporal Bone Foundation*

**Goal:** To make an accurate detailed image of the incudostapedial joint based on serial histological sections

using computer technology. Each anatomical structure was segmented out and rendered into a 3D model where they can be viewed individually or in relation to each other. The structures detailed include the lenticular process of the incus, the head of the stapes, the ligamentous joint capsule, the two joint spaces and the intervening meniscus.

**Methods:** The 20 micron celloidin serial sections of an 80 year old male were scanned into the computer and aligned in Photoshop and Maya. The incus, stapes, capsular ligaments, fibers of the stapedius tendon, and the joint meniscus were segmented into individual layers and made into a 3D image using Maya Software.

**Results:** This 3D model clearly reveals the fine details of the incudostapedial joint, demonstrating that this is a bichambered joint with a dividing meniscus. It also clarifies the dynamics between form and function.

#### **644 Real-Time Opto-Electronic Holographic Measurements of the Sound-Induced Displacements of Tympanic Membranes**

Furlong Cosme<sup>1</sup>, Michael E. Ravicz<sup>2</sup>, Matthew T. Rodgers<sup>1</sup>, **John J. Rosowski<sup>2</sup>**

<sup>1</sup>Worcester Polytechnic Institute, <sup>2</sup>Massachusetts Eye and Ear Infirmary

A fiber-optic based opto-electronic holographic system [C. Furlong and R. J. Pryputniewicz, "Determination of surface shape and deformation using electro-optic holography methods," SPIE, 3478:86-97, 1998] has been applied to the study of the sound-induced displacements of tympanic membranes (TM). One version of the system is capable of calculating and producing a continuously updated display of time-averaged holograms of the displacement of the surface of the TM at rates of up to 250 frames per second. This display allows observations of the development of nodal fringe patterns of displacements while the amplitude and/or frequency of a stimulus sound frequency are swept. Such observations lead to easy identification of the nodal frequencies. A second version of the system allows measurement of the magnitude and phase of displacements of the entire membrane surface. The applications of these techniques include the identification and measurement of standing and traveling waves on the surface of the normal tympanic membrane, investigations of inter-specific differences in TM motion, and tests of hypothesis concerning the sensitivity of membrane displacement patterns to TM perforations, as well as the motion of various TM graft configurations in surgical reconstructions of the ear.

[Supported by NIDCD and NSF]

#### **645 Measurements of the Effects of Middle Ear Fluid on Acoustic-Mechanical Transmission in Human Ear**

Rong Gan<sup>1</sup>, Chenkai Dai<sup>1</sup>, Don Nakmali<sup>2</sup>, Mark Wood<sup>2</sup>

<sup>1</sup>University of Oklahoma, Norman, OK, <sup>2</sup>Hough Ear Institute, Oklahoma City, OK

Fluid in the middle ear cavity is a defining symptom of otitis media with effusion (OME) and commonly associated with

conductive hearing loss. The amount and rheological property of the fluid found in OME are variable, which result in different resistance on the moving parts of the middle ear such as the tympanic membrane and ossicles, and thus, affect sound transmission through the ear. In this paper, we report our recent study on effects of amount of fluid in middle ear cavity and the middle ear air pressure on movements of the tympanic membrane (TM) and stapes footplate in human cadaver temporal bones. Displacement of the TM at umbo in response to sound pressure (90 dB SPL) at ear canal was first measured with a laser Doppler vibrometer while the middle ear air pressure was varied and saline or silicone fluids were introduced into the middle ear cavity. Next, the second laser vibrometer was employed to simultaneously measure displacement of the stapes footplate which was exposed through the middle fossa approach. The results include: 1) frequency response curves of displacements at the TM and stapes footplate at frequency range of 100 – 10k Hz in response to a change of middle ear air pressure from -20 to 20 cm H<sub>2</sub>O; 2) frequency response curves of the TM and footplate displacements in response to various amounts of middle ear fluid; and 3) effect of combined fluid and air pressure on TM and footplate movements. The results have quantitatively demonstrated how the fluid level, viscosity, and middle ear pressure affect middle ear transfer function for sound transmission. (Supported by NIH/NIDCD R01 DC006632)

#### **646 The Effect of Ear Canal Pressure on Pure-Tone Thresholds, Acoustic Conductance and Acoustic Transmittance**

**M. Patrick Feeney<sup>1,2</sup>**, Chris A. Sanford<sup>3,4</sup>

<sup>1</sup>University of Washington, Otolaryngology Head and Neck Surgery, <sup>2</sup>Virginia Merrill Bloedel Hearing Research Center, <sup>3</sup>University of Washington, <sup>4</sup>Department of Speech and Hearing Sciences

Changes in pure-tone thresholds induced by static pressure changes in the ear canal were estimated from shifts in acoustic transfer functions for 20 young adults with normal hearing. Pure-tone thresholds at 0.5 and 2 kHz were measured at ambient pressure, and at ear canal pressures of  $\pm 200$  daPa using a 2 up 1 down-3AFC procedure. The average increase in pure-tone threshold for positive ear canal pressure was around 5 dB at 500 Hz and 2 dB at 2000 Hz, which was in good agreement with changes in conductance and transmittance in dB. An ANOVA revealed a significant difference in estimates of threshold shift between the two frequencies, but no significant difference among the three estimates of threshold shift (psychoacoustic, conductance and transmittance) within each frequency. Similar findings were observed for negative ear canal pressure at 2 kHz, but at 0.5 kHz there was a smaller change in pure-tone thresholds and transfer functions. These results are in agreement with the changes in round window volume displacement with ear canal pressure previously reported for temporal bone measurements in Norwegian cattle [M. Kringlebotn. J. Acoust. Soc. Am. 107(3):1442-1450, 2000]. The results of this study suggest that changes in

middle-ear conductance and transmittance may provide an objective measure of conductive hearing loss.

#### **647 Output Vibration Measurements of Bone-Anchored Hearing Aids (BAHA)**

**Osama Majdalawieh<sup>1</sup>, Manohar Bance<sup>1</sup>, Rene Van Wijhe<sup>1</sup>**  
<sup>1</sup>*Dalhousie University*

**Objectives:** Some patients cannot use normal hearing aids, and in these we can exploit the bone conduction pathway. The BAHA stimulates the inner ear via skull vibrations using an osseointegrated titanium skull fixture. Our objectives were to determine: 1) output differences in a three commercially available BAHAs 2) output of the unloaded BAHA compared to skull vibrations when it drives the skull mass 3) fall in skull vibration amplitude with distance from the actuator. **Methods:** Four Compact, a Classic 300, and a Cordelle II BAHAs were used. Measurements were made on the unloaded BAHA vibrating stem, a plastic skull, and a real BAHA-fitted patient skull, using a laser Doppler vibrometer. The transfer functions were derived for displacement (DTF), velocity (VTF), and acceleration (ATF). **Results:** The unloaded BAHA DTF is a low pass function, the AFT is a bandpass centered around 1 kHz, and the VTF is almost flat. The Cordelle II vibration output was higher by 20-25 dB at low frequencies than other BAHA types. Amongst the four Compacts, there was a significant 10-15 dB output variance at low frequencies. Artificial skull vibrations at 1 inch from the BAHA decreased by about 6 dB compared to ½ inch. No major resonances were found. **Conclusions:** There is a significant output variation even between BAHAs of the same model. The Cordelle II provides more gain mostly at low frequencies, and not across the speech frequency bands. Vibrations of the skull were 30-40 dB below that of the unloaded BAHA. These all have clinical implications in understanding sound experience using the BAHA.

#### **648 Effect of Cochlear Implant Electrode Insertion on Middle Ear Transfer Function as Measured by Intra-Operative Laser Doppler Vibrometry**

**Neil Donnelly<sup>1</sup>, Carlo Santulli<sup>1,2</sup>, Thanos Bibas<sup>1</sup>, Dan Jiang<sup>1</sup>, Alec Fitzgerald O'Connor<sup>1</sup>**

<sup>1</sup>*Dept. of Otolaryngology Head and Neck Surgery, Guy's and St Thomas Hospitals,* <sup>2</sup>*School of Construction Management and Engineering, University of Reading, UK*

**Background:** Preservation of residual low-frequency hearing with addition of electrical speech processing can substantially improve the speech perception abilities and hearing in noise of cochlear implant users. To utilise the preserved low frequency hearing requires an intact middle ear conductive mechanism. Little is known about the effect of a cochlea implant electrode on the displacement pattern of the ossicles. The aim of this study is to investigate the impact of cochlear implant electrode insertion on middle ear low frequency transfer function.

**Patients and methods:** Stapes displacement was measured in four patients undergoing cochlear

implantation. Measurements were carried out intra-operatively before and after electrode insertion via the round window membrane. Each patient acted as their own control. Sound was delivered into the external auditory canal via a speaker and calibrated via a probe microphone. The speaker and probe microphone were integrated into an individually made ear mould. Ossicular displacement to low frequency stimuli at 80 dB SPL was measured at the head of stapes via the posterior tympanotomy using an operating microscope mounted laser Doppler vibrometry system.

**Results:** Insertion of a cochlear implant electrode into the scala tympani has a small effect on stapes displacement. At 1000 Hz, all patients showed a decrease in stapes displacement, the effect is up to 10 dB (range from 3 dB to 10 dB). The result at 2000 Hz was variable. Two patients showed a decrease in stapes displacement at 4 dB and 11 dB, whilst the other two showed a small increase up to 6 dB. The effect at 500 Hz is small, ranging from a 5dB decrease to a 6 dB increase. The averaged effect across all three frequencies is a 2.5 dB decrease in stapes displacement (SD = ±5.7).

**Conclusion:** Insertion of a cochlear implant electrode produces a small change in stapes displacement at low frequencies; this is most likely to be a reduction, with the effect being more consistent at 1000 Hz.

#### **649 Histopathology of Ossicular Grafts and Implants in Chronic Otitis Media**

**Fayez Bahmad, Jr.<sup>1</sup>, Saumil N. Merchant<sup>1</sup>**

<sup>1</sup>*Massachusetts Eye and Ear Infirmary and Harvard Medical School*

**Background:** Many different types of autograft and homograft implants, as well as synthetic ossicular prostheses have been employed in middle ear surgery for chronic otitis media. Functional hearing results after ossiculoplasty continue to be modest. The histopathologic study of ossicular implants can provide insight into some of the factors influencing functional results after chronic ear surgery.

**Methods:** Histopathologic observations were made on 45 cases in our temporal bone collection: 39 surgical specimens and 6 cases in which the graft was sectioned "in situ". The 45 cases included 19 malleus or incus grafts, 7 cortical bone grafts, 6 cartilage grafts and 13 synthetic prostheses.

**Results and Conclusions:** Autogenous malleus, incus and cortical bone grafts behaved in a similar manner and maintained their morphologic size, shape and contour for extended periods of time, up to 30 years. They did not incite formation of new bone, nor did they show excessive resorption of bone in the absence of infection. They showed varying amounts of replacement of nonviable bone by new bone through a slow process of creeping substitution that was dependent on revascularization and not on duration of implantation. Sculpturing of such grafts should be done with adequate irrigation to avoid thermal injury and subsequent necrosis. The graft should be reduced in size by sculpturing to avoid unwanted bony ankylosis to surrounding structures such as the facial

canal or promontory. These histologic observations support the continued use of autograft ossicular and cortical bone grafts for middle ear reconstruction.

Cartilage grafts showed a tendency to develop chondromalacia with resulting loss of stiffness, and a tendency to undergo resorption. These changes intensified with time. Synthetic prostheses made of plastic (Polyethylene, Plastipore) or Bioglass elicited foreign body giant cell reactions with varying degrees of biodegradation of the implants.

#### **650 Demonstration of Different Aeration Pathways to Prussak's Space in the Human Epitympanum**

Katie Kirkpatrick<sup>1</sup>, David P. Morris<sup>1,2</sup>, Rene Van Wijhe<sup>1</sup>, Manohar Bance<sup>1,2</sup>, Stephen Levine<sup>3</sup>, Clarinda Northrop<sup>3</sup>

<sup>1</sup>The Ear Lab, Department of Anatomy and Neurobiology Dalhousie University, Halifax, NS. Canada, <sup>2</sup>Division of Otolaryngology Head & Neck Surgery, QE II Health Sciences Centre, Halifax, NS. Canada., <sup>3</sup>The Temporal Bone Foundation, Boston, MA

**Aims:** Aeration of the human epitympanum is a contentious area of study with conflicting opinions being held. It is hoped that a better understanding of the aeration pathways of the epitympanum will bring some explanation of retraction pocket formation, the direction of spread of attic cholesteatoma and the development of recurrent disease after surgical treatment.

**Methods:** Histological preparations of serially sectioned human temporal bones were reconstructed in 3-D using the Amira (R) software package to show detail of Prussak's space, the associated mucosal folds and aeration pathways. This was correlated with clinical photographs from cadaveric dissections and 'injection studies' of gel introduced by needle puncture into Prussak's space to simulate an expanding cholesteatoma.

**Results:** A number of common patterns of aeration pathway were demonstrated. It is proposed that certain patterns may be more likely to give rise to retraction and may also be responsible for the direction of spread of cholesteatoma once it has formed.

**Conclusion:** These novel techniques are valuable in demonstrating attic fold anatomy and have allowed aeration pathways to be assessed in detail. It is hoped that this information will prove clinically relevant to the otologic surgeon considering tympanoplasty.

#### **651 A Biophysical Model of Auditory Nerve Response to Electrically-Encoded Speech**

Jeff Longnion<sup>1</sup>, Jay T. Rubinstein<sup>1</sup>

<sup>1</sup>University of Washington

The consistent increase in speech perception scores among cochlear implant users over the past 25 years testifies to the manifold contributions of engineering, clinical, and basic science research to our understanding of electrical stimulation and how best to encode speech via prosthetic stimulation of the auditory nerve.

Towards this effort, computational models have made valuable contributions. Specifically, previous research has

demonstrated that a stochastic model of a myelinated auditory nerve fiber has been useful in elucidating responses to both analog and pulsatile electrical stimuli. However, until now computational demands have precluded the simulation of longer duration stimuli such as speech. To address this issue we devised a parallel processing scheme allowing the computational load to be distributed among processors in a computational cluster. Also, we modified the model to include stochastic parameters of a human node of Ranvier as well as nodal slow and fast-type potassium channels which experiments suggest may be important to accurate simulation of refractory characteristics and response to repetitive stimuli. Simulations demonstrate that the updated model has jitter, relative spread, and refractory characteristics consistent with published clinical and animal model experiments. We have emulated the House single channel implant and other encoding strategies and simulated the response of the model to spondees encoded with these strategies. Preliminary analysis reveals a mostly monotonic correlation between speech envelope and average instantaneous spike rate with evidence of subthreshold inactivity, saturation, and masking effects. This initial data suggests the potential value of this model for studying and testing speech encoding techniques in cochlear implants. Ongoing research includes more sophisticated analysis of speech encoding strategies and their capacity to convey speech information. (Supported by NIH program project DC00242)

#### **652 Dynamical Chaos Produces Realistic Firing Irregularity Without Ongoing Physiological Noise**

David O'Gorman<sup>1</sup>, Christopher A. Shera<sup>2</sup>, John White<sup>3</sup>

<sup>1</sup>Speech and Hearing Bioscience and Technology Program, Harvard-MIT Div. of Health Sciences and Tech.,

<sup>2</sup>Eaton-Peabody Laboratory of Auditory Physiology,

<sup>3</sup>Department of Biomedical Engineering, Boston University

The irregularity apparent in the discharge patterns of electrically stimulated auditory-nerve fibers depends upon the stimulus rate (Moxon 1969; van den Honert and Stypulkowski 1987; Javel 1990). Moxon (1969), for example, showed that when a fiber is stimulated at the relatively low rate of 300 pulses per second it responds nearly identically to every stimulus pulse. But, when the stimulation rate is increased to 480 pulses per second, the fiber fires after "every second, third, or more stimulus pulse[s] in irregular sequences" (p. 29). The prevailing view is that this firing irregularity is a manifestation of ongoing physiological noise generated by the random opening and closing of voltage-gated ion channels embedded in the neural membrane. However, we demonstrate that at sufficiently high stimulus rates (e.g., 5 kHz), the chaotic dynamics of excitation and refractoriness suffice to account for the main features of the irregularity apparent in the measured discharge patterns (Litvak et al. 2001), even in the complete absence of ongoing noise. Specifically, the deterministic Fitzhugh-Nagumo (FN) model captures the tendency of the measured Fano factors to fall within the bounds of a dead-time modified Poisson process at low discharge rates but significantly above them at intermediate discharge rates, although this

tendency to exceed the bounds of the dead-time modified Poisson process becomes prominent at lower discharge rates in the data than in the model. Ongoing additive noise with an intensity set by measurements of the relative spread abolishes the tendency of the Fano factor to exceed the predictions of the dead-time modified Poisson process at intermediate rates, in contradiction to the experimental results, but has little effect on the Fano factor at low discharge rates. Our results demonstrate that in the FN model ongoing noise (1) is not necessary for generating realistic firing irregularity at high stimulus rates and (2) actually regularizes the response at intermediate firing rates, reducing the irregularity below what is observed in the absence of noise. We conjecture that these same conclusions apply to the electrically stimulated auditory nerve.

Supported by NIH Grant F31DC006188, an MIT-Poitras Fellowship, and the MIT-Zakhartchenko Fellowship.

### **653 Studying Electrically Evoked Activity in the Auditory Nerve Using the Earlab Simulation Environment**

**Socrates Deligeorges<sup>1</sup>**, David Mountain<sup>1</sup>

<sup>1</sup>*Boston University*

There are many factors which can affect cochlear implant performance. Some of these factors relate to hardware differences such as the pattern of electrode activation, or the acoustic preprocessing and compression implemented, as well as the methods used to modulate stimulating pulse trains. There are also factors that are biological such as individual variations in cochlear anatomy, electrode position and insertion depth, and the number and location of surviving auditory nerve fibers.

Understanding how these factors impact implant performance is challenging problem requiring integration of data from a wide variety of human and animal experiments. To assist in this effort, we have adapted the Earlab simulator for cochlear prosthetic research. The Earlab simulation environment uses a modular architecture where different anatomical structures are simulated using plug in modules. The modules are designed to use species-dependent or patient dependent parameters that can be easily manipulated to recreate psychophysical or physiological experiments. Modules are currently available that simulate auditory structures in the periphery, brainstem, and midbrain. The integrated modeling environment not only allows study of the implant processing schemes at the auditory periphery, but at high auditory centers as well simultaneously. Neural activity can be represented either as average firing rate or in terms of the individual times of occurrence of action potentials. The modular approach also allows one to upgrade specific modules as more physiologically accurate modules become available.

To study the impact of processing schemes on cochlear implant performance, we have developed three types of Earlab modules. These modules represent hardware speech processors, electrical current spread, and neural excitation. These modules are designed to replace the modules that represent middle ear and cochlear

mechanics and hair cell physiology in simulations of normal hearing. The simulation environment is designed to use standard audio files as input to facilitate the simulation of responses to standard speech and speech in noise test sets.

Simulations will be presented comparing acoustically evoked auditory nerve responses in normal ears to electrically evoked responses in implanted ears. The target stimuli are sentences from Hearing in Noise Test (HINT) lists and results for several common speech-processing strategies will be compared.

Funded by NIDCD and NIMH grant DC04731

### **654 Computer and Dynamic Testing of a Vestibular Appliance Prototype**

**Tamara Alexandrova<sup>1,2</sup>**, Vladimir Alexandrov<sup>2,3</sup>, Sergei Migunov<sup>2</sup>, Willi Guerrero<sup>3</sup>, Gonzalo Halpa<sup>3</sup>, Nency Diaz-Molina<sup>3</sup>, Rosa Tamayo<sup>3</sup>, Aida Ortega<sup>1</sup>, Enrique Soto<sup>1</sup>

<sup>1</sup>*Instituto de Fisiologia BUAP*, <sup>2</sup>*Moscow State University*,

<sup>3</sup>*Facultad Fisico Matematica BUAP*

A lot of works have appeared that are devoted to the design and implementation of appliance prototypes for the vestibular system. Clinical trials of such prototypes must be preceded by their thorough testing. In this work we consider the technology for two types of testings: a) computer testing, b) dynamic testing.

For computer testing, we model the falling and compare the reactions of mathematical model of the prototype vestibular appliance with reactions of mathematical models of a semicircular canal and of inertial mechanoreceptors. Mechanical coupling, a hair-cell and a primary afferent neuron were considered for vestibular system modelling (1). The total ionic current, the receptor potential in hair cells, synaptic transmission, and pulse generation in afferent neurons that depends on the synaptic current were modeled. We also consider a model of the prototype for the vestibular appliance (2). This study presents the first results of computer testing.

Dynamic testing of the prototype requires: a) a prototype for the vestibular appliance, b) vestibular apparatus specimen of a laboratory animal, c) a controllable dynamic simulator, d) an algorithm for dynamic simulation of falling. We present the following algorithms for dynamic simulation of falling: 1) consideration of the first stage of falling in a mechanical model of the human, 2) prototype functional scheme as a micro accelerometer and a vibrating micro gyroscope, 3) comparison of the prototype vestibular appliance with the sacculus and the frontal semicircular canal of the amphibian.

We prepared a dynamic falling simulator consisting of a platform on top of a controlled inverted pendulum (for the sacculus, the semicircular canal, the micro accelerometer, and the micro gyroscope).

1. Sadovnichii et al. Moscow University Mechanical Bulletin 2002, No 6, p.46-54.

2. Shkel, et al. IEEE, 2002, 1526-1531.

Financed by CONACyT 43433



### **655 Behavioral-Neural Model for Temporal Integration in the Deaf Cat**

**Ralph E. Beitel<sup>1</sup>**, Maike Vollmer<sup>1</sup>, Russell L. Snyder<sup>1</sup>

<sup>1</sup>*Otolaryngology-HNS, UCSF, San Francisco CA*

Temporal integration (TI) allows lower (more sensitive) detection thresholds when the duration of a stimulus is increased in normal hearing subjects. However in hearing-impaired subjects, an increase in stimulus duration has a smaller effect on threshold, i.e., there is less TI. This poster describes a model of TI based on behavioral and neurophysiological experiments in the deaf cat.

Cats (n=3) deafened neonatally by intramuscular injections of ototoxic antibiotics were trained to avoid a mild electrocutaneous shock when single or trains of electrical biphasic rectangular pulses (5.0 ms/phase) were applied to the cochlea via a UCSF feline auditory prosthesis. Psychophysical detection thresholds (50% avoidance) and reaction times were estimated as functions of stimulus duration. Electrophysiological responses of single neurons in the central nucleus of the inferior colliculus (ICC) were evoked using sinusoidal pulse trains (100 Hz), which varied in intensity and duration. Only data for neurons (n=42/76) that responded with sustained discharges to 300 ms pulse trains at +2 dB SL are presented in this poster.

The results include: 1) Psychophysical thresholds decreased by about 7 dB for the longest duration stimulus (1.0 s) compared to the shortest duration stimulus (0.01 s) for each cat (t-test;  $p < .001$ ); 2) the slope of the mean behavioral TI function was -1.2 dB/doubling of stimulus duration; 3) for each neuron, the number of spikes increased monotonically with stimulus duration (ANOVA;  $p < 0.001$ ); 4) neuronal response magnitude was dependent on stimulus intensity (ANOVA;  $p < 0.001$ ); and 5) the slopes of mean neuronal TI functions were equivalent to the slopes of behavioral TI functions in the deaf cats but were reduced compared to TI reported for normal hearing cats.

NIH/NIDCD Contract N01-DC-3-1006.

### **656 Mandarin Chinese Tone Identification in Cochlear Implant Subjects: Predictions from Acoustic Models**

**Kenneth Morton<sup>1</sup>**, Leslie Collins<sup>1</sup>

<sup>1</sup>*Duke University*

Current cochlear implants do not provide sufficient spectral information to achieve a high level of speech comprehension in tonal languages, such as Mandarin Chinese. For reliable speech perception, the four lexical tones of Mandarin Chinese must be correctly distinguished. Recent research has indicated that greater spectral resolution may be possible in cochlear implants through the use of variable stimulation rate and current steering. These stimulation techniques may provide the means of returning the auditory fine structure required for Mandarin Chinese tone recognition. The four cochlear implant signal processing algorithms examined in this study, the Continuous Interleaved Sampling (CIS) algorithm, the Frequency Amplitude Modulation Encoding (FAME) algorithm (Nie et al., 2005), the Multiple Carrier Frequency Algorithm (MCFA) (Kucukoglu et al., 2005), and the strategy proposed by Lan et al. (2004), contain

differing amounts of spectral information. Automated pattern recognition techniques applied to Mandarin Chinese tone recognition tasks using data from acoustic models can be used as a means of testing the abilities of these algorithms to transmit the changes in fundamental frequency indicative of the four lexical tones. The ability of processed Mandarin Chinese tones to be correctly classified may predict trends in the effectiveness of different signal processing algorithms in cochlear implants. The results using several tone recognition techniques will be reported as a function of noise level and comparisons will be made to a listening experiment using normal hearing subjects with acoustic models.

### **657 Evaluation of a Noiseband-Based Cochlear Implant Simulator: Consonant Perception Revisited**

**N. Ellen Taylor<sup>1,2</sup>**, Adeshola Lawal<sup>3</sup>, Karen Hardy-Bruce<sup>4</sup>, Thomas Talavage<sup>1</sup>, J. Brandon Laflen<sup>2,5</sup>, Mario Svirsky<sup>5,6</sup>, Heidi Neuburger<sup>6</sup>

<sup>1</sup>*Purdue University*, <sup>2</sup>*Rose-Hulman Institute of Technology*, <sup>3</sup>*University of Minnesota*, <sup>4</sup>*Kettering University*, <sup>5</sup>*New York University School of Medicine*, <sup>6</sup>*Indiana University School of Medicine*

In behavioral experiments, consonant identification (24 pre-recorded phonemes) was compared between 32 CI users at 1 year post-implantation, and two groups of 30 NH listeners undergoing initial exposure to an 8-channel noiseband-based CI simulator. The CI simulator was configured such that the output (synthesis) filters modeled electrode placements in a CI with incomplete insertion, while the input (analysis) filters modeled either a 0mm or 6.5mm basalward shift, relative to the synthesis filters. Confusion matrices were used to evaluate performance of both (0mm and 6.5mm shift) NH groups relative to the CI users, examining preservation of three phonemic features: voicing, place of articulation and manner of articulation. In addition to rates of correct identification, patterns of phoneme misidentification were evaluated using ANOVAs across the CI and each of the NH groups.

Performance differences across the three subject groups are expected to be useful in identifying components of speech signals that are currently over- or under-represented in acoustic simulations of CI electrical stimulation. Performance across groups varied appreciably, both on an individual phoneme and overall level. Some phonemes (e.g., /aha/, /ara/) led to equivalent performance between NH listeners and CI users, while others (e.g., /ada/, /ava/, /aza/) exhibited differences in patterns of confusion that were significant at the  $p < 0.05$  level. Detection of voicing decreased with increases in simulated basalward shift. The 0mm shift produced preservation of place of articulation more consistent with CI users than 6.5mm shift. Conversely, the 6.5mm shift produced the more consistent preservation of manner of articulation. These data support continued development of noiseband-based simulators to achieve more accurate models of the auditory nerve activity produced by CI electrical stimulation.

**658 Relationship Between Perception of Spectral Ripple and Speech Recognition in Cochlear Implant and Vocoder Listeners**

Leonid Litvak<sup>1</sup>, Anthony J. Spahr<sup>2</sup>, Aniket Saoji<sup>1</sup>, Gene Yevgeny Fridman<sup>1</sup>

<sup>1</sup>Advanced Bionics Corporation, <sup>2</sup>Arizona State University

In a previous study examining spectral resolution and speech understanding in cochlear implant (CI) listeners (Saoji et al, CIAP 2005), we reported a significant correlation between spectral modulation detection thresholds (SMDTs) for low-modulation frequencies (cycles/octave) and performance on a vowel ( $r=0.77$ ) and consonant ( $r=0.93$ ) identification tasks. We hypothesized that the spectral SMDT was determined by the activation pattern associated with electrical stimulation. Specifically, broad activation patterns would impair spectral resolution, resulting in an elevated SMDT. In the present study we simulate broad activation patterns using a multi-band vocoder to determine if similar impairments in the SMDT and speech understanding scores could be produced in normal-hearing (NH) listeners.

Tokens were first decomposed into 15 logarithmically-spaced bands and then re-synthesized by multiplying the envelope of each band by matched filtered noise. The spectrum of filtered noise had a peak at the center of the band. Various amounts of current spread were simulated by adjusting the drop-off of the noise spectrum away from the peak (40 dB/octave to 5 dB/octave).

Simulating broader activation patterns significantly degraded spectral resolution and speech understanding. The average SMDT at 0.25 cycles/octave increased from 3.5 dB to 13 dB, while vowel identification scores dropped from 91% to 25% and consonant identification scores dropped from 93% to 56%. In each condition, the impairments in speech understanding were generally similar to those found in CI listeners with similar SMDTs at 0.25 cycles/octave.

These results support the hypothesis that the different levels of speech understanding achieved by CI listeners is related to spectral resolution, and that the vocoder simulation may be a useful tool for evaluating speech processing strategies that seek to improve performance of cochlear implant listeners.

**659 Evaluation of a Noiseband-Based Cochlear Implant Simulator: Vowel Perception**

N. Ellen Taylor<sup>1,2</sup>, Adeshola Lawal<sup>3</sup>, Karen Hardy-Bruce<sup>4</sup>, Thomas Talavage<sup>1</sup>, J. Brandon Laflen<sup>2,5</sup>, Mario Svirsky<sup>5,6</sup>, Heidi Neuburger<sup>6</sup>

<sup>1</sup>Purdue University, <sup>2</sup>Rose-Hulman Institute of Technology, <sup>3</sup>University of Minnesota, <sup>4</sup>Kettering University, <sup>5</sup>New York University School of Medicine, <sup>6</sup>Indiana University School of Medicine

In behavioral experiments, vowel identification (9 pre-recorded words) was compared between 29 cochlear implant (CI) users at 1 year post-implantation, and two groups of 15 normal-hearing (NH) listeners undergoing initial exposure to an 8-channel noiseband-based CI simulator. The CI simulator was configured such that the output (synthesis) filters modeled electrode placements in

a CI with incomplete insertion, while the input (analysis) filters modeled either a 0mm or 6.5mm basalward shift, relative to the synthesis filters. Confusion matrices were used to evaluate performance of both (0mm and 6.5mm shift) NH groups relative to the CI users, examining preservation of tongue position and first formant (F1). In addition to rates of correct identification, patterns of misidentification were evaluated using ANOVAs across the CI and each of the NH groups.

Performance differences across the three subject groups are expected to be useful in identifying components of speech signals that are currently over- or under-represented in acoustic simulations of CI electrical stimulation. For both NH groups, detection of F1 was not consistent with the CI group. Preservation of tongue position was more consistent for the 0mm shift than for the 6.5mm shift. These data support continued development of noiseband-based simulators to achieve more accurate models of the auditory nerve activity produced by CI electrical stimulation.

**660 Localization and Precedence Effect in Normal Hearing Listeners Using a Vocoder Cochlear Implant Simulation**

Gonggiang Yu<sup>1</sup>, Ruth Y. Litovsky<sup>1</sup>, Soha Garadat<sup>1</sup>, Corina Vidal<sup>1</sup>, Raena Holmberg<sup>1</sup>, Fan-Gang Zeng<sup>2</sup>

<sup>1</sup>University of Wisconsin-Madison, USA, <sup>2</sup>UC-IRVINE

Vocoder simulations offer a means of assessing perceptual limits imposed by cochlear implants (CI). This study investigated sound localization and precedence effect (PE) using a bilateral CI simulation in 9 normal-hearing subjects. Stimuli were convolved through HRTFs to produce virtual sound locations. For sound localization variables were (1) the number of frequency bands (1-, 2-, 4-, 8-, 16-, and natural), (2) the presentation mode (bilateral or unilateral) and (3) in quiet or with background noise (speech sentence presented from front or right). The stimuli occurred at 24 locations with 15 degrees separation on the azimuthal plane spanning both front and back. Results from sound localization showed that (1) Background noise was not detrimental to sound localization for the natural stimuli. (2) Background noise significantly degraded performance only with 1- and 2-bands. (3) Performance was always poor under monaural conditions. For PE variables were (1) the number of frequency bands (2-, 4-, 8-, 16-, and natural) and (2) different time delays between lead and lag sources (0-, 1-, 5-, 10-, 15-, 20-, 30-, 50-, 100-ms). Results from the PE study showed a significant effect of the number of bands on listener's ability to discriminate changes in position of the echo (lag), with elevated thresholds being associated with the small number of bands. This work suggests that the simulated bilateral implant listeners can withstand a large reduction in frequency resolution before performance is significantly degraded.

**661 Suspected Genetic Drift of Auditory Phenotype in  $\alpha$ -Calcitonin Gene-Related Peptide ( $\alpha$ CGRP) Knockout Mice**

Rhiannon R. Bussey<sup>1</sup>, Anne E. Luebke<sup>1,2</sup>

<sup>1</sup>Dept of Biomedical Engineering, University of Rochester Medical Center, <sup>2</sup>Dept of Neurobiology & Anatomy, University of Rochester Medical Center

CGRP is a 37 amino acid neuropeptide immunolocalized in the unmyelinated component of the cochlear efferent innervation. In the mammalian brain, two isoforms of CGRP exist coded by different genes ( $\alpha$  and  $\beta$  CGRP). Previous work has shown that  $\alpha$ CGRP knockout mice in the C57Bl/6 background strain have reduced ABR wave I suprathreshold amplitudes at 4 months (Maison et al. 2003).  $\alpha$ CGRP knockout mice have also been generated in the 129S6/SvEv mouse strain. Cochlear function was analyzed in the offspring bred from homozygous knock-out or wild-type mice respectively by measuring 1) auditory brainstem responses (ABRs) to tone pips at 6 log-spaced frequencies from 5.6 to 30 kHz and 2) distortion-product otoacoustic emissions (DPOAEs) with secondary tones (f<sub>2</sub>) at the same 6 frequencies. Cochlear function was assessed for both the C57Bl/6 and 129S6/SvEv strains at 1 and 3 months.

Our test results differ from the previous work in two ways: 1) ABR and DPOAE thresholds were not identical between  $\alpha$ CGRP KO and age-matched controls in both strains and 2) ABR wave I suprathreshold amplitudes were not reduced for  $\alpha$ CGRP KO animals in all groups. Possible explanations for the different auditory results from previous work include: 1)  $\beta$ CGRP compensation, 2) CGRP receptor complex up-regulation, and 3) genetic variation between  $\alpha$ CGRP KO animals and the corresponding wild-type strain. No CGRP immunoreactivity was observed in the efferent innervation of  $\alpha$ CGRP KO animals. ELISA analysis will determine the molar levels of cochlear CGRP. Future work will include examining the components and integrity of the CGRP receptor complex using 2D gel analysis and immunoblotting. Additionally,  $\alpha$ CGRP knock out animals in both C57Bl/6 and 129S6/SvEv strains will be regenerated from heterozygous breeding to determine if loss of auditory phenotype was due to lack of littermate controls (Supported by NIH DC003086).

**662 Development of Synaptic Inputs to the Lateral Superior Olive in KCC2-Knockdown Mice**

Hanmi Lee<sup>1</sup>, Karl Kandler<sup>1,2</sup>

<sup>1</sup>University of Pittsburgh, <sup>2</sup>Center for the Neuronal Basis of Cognition

The lateral superior olive (LSO) receives converging, tonotopically organized, glycinergic inputs from the medial nucleus of the trapezoid body (MNTB) and glutamatergic inputs from the cochlear nucleus (CN). Before hearing onset, when immature MNTB-LSO synapses are also glutamatergic and GABAergic, glycine and GABA are depolarizing instead of hyperpolarizing. During this period, the MNTB-LSO pathway is topographically refined by synaptic elimination (silencing) and strengthening. While the functional significance of the switch from depolarization to hyperpolarization at MNTB-LSO synapses is unknown, it has been speculated that it might play a role in synaptic refinement and strengthening. To address this question,

we investigated LSO circuit development in mice in which the potassium-chloride co-transporter 2 has been genetically knocked down (KCC2-KD) which causes GABA and glycine to remain depolarizing (Balakrishnan et al., J. Neurosci., 2003).

LSO neurons were recorded in brainstem slices prepared from control and homozygote KCC2-KDs aged between P2 to P12.

From P2 to P12, synaptic responses elicited by single MNTB-fibers increased in control mice from  $29 \pm 4$  pA (n=6) to  $311 \pm 105$  pA (n=44) and in KCC2-KDs from  $55 \pm 10$  pA (n=14) to  $606 \pm 202$  pA (n=29). Maximal MNTB-responses in controls increased from  $731 \pm 147$  pA (n=3) to  $4612 \pm 957$  pA (n=27) and in KCC2-KDs from  $1130 \pm 428$  pA (n=8) to  $3781 \pm 692$  pA (n=27). Except for the single-fiber responses in newborns ( $p < 0.04$ , t-test), values were not significantly different between control and KCC2-KDs mice ( $p > 0.05$  K-S test). In addition, at P10-12, no differences were observed in the amplitude of AMPA receptor mediated responses elicited by CN inputs ( $I_{\text{AMPA}}$  at -70 mV; control:  $219 \pm 37$  pA (n=24), KCC2-KD:  $206 \pm 32$  pA (n=21),  $p > 0.5$  K-S test).

These results suggest that the switch to hyperpolarizing postsynaptic responses at glycine/GABAergic synapses is not required for the developmental strengthening of MNTB-LSO connections.

**663 Potassium Channel Gene Expression in the Cochlear Nucleus**

David Friedland<sup>1</sup>, Rebecca Eernisse<sup>1</sup>, Paul Popper<sup>1</sup>

<sup>1</sup>Medical College of Wisconsin

Potassium channels play an integral role in the transmission of signals in the central auditory system. Different potassium channels exhibit specific voltage dependencies and other electrophysiological properties that account for many of the unique firing patterns of auditory neurons. Serial analysis of gene expression (SAGE) and microarray (gene chip) were used to characterize the expression patterns of potassium channel genes in the rat cochlear nucleus subdivisions. These high-throughput methods identified mRNAs for 46 different potassium channels or channel modifying proteins, among the three subdivisions of the cochlear nucleus. Real-time reverse transcriptase PCR was performed to confirm the presence of 23 of these potassium channel transcripts and to determine the relative expression levels of these genes in the three subdivisions. Three of the potassium channel transcripts showed significant levels of differential expression by real-time RT-PCR: *Kcnc2*, *Kcnj13* and *Kcns3*. *Kcnc2* was expressed more than 20-fold higher in the DCN as compared to the AVCN and PVCN. *Kcnc2* encodes for Kv3.2, a voltage gated potassium channel, that has been shown to be critical for high-frequency firing and is associated with inhibitory interneurons. In contrast, *Kcnj13* had a 9.5-fold greater expression in AVCN, and a 14-fold greater expression in PVCN, than in DCN. *Kcnj13* encodes for Kir7.1 which is a member of the inward rectifier-type potassium channel family and seems to function in setting resting membrane potentials. Similarly, expression levels for *Kcns3* were 26.5-fold higher in AVCN when compared to DCN. *Kcns3* encodes for Kv9.3 which forms heterodimers with Kv2.1 and generates a slowly

deactivating channel. Determining the expression patterns of potassium channels in the subdivisions of the cochlear nucleus will help in understanding the electrophysiological mechanisms subserving central auditory processing. Supported by NIDCD K08DC006227.

#### **664 Morphology of MOC Central Branches and Somata Are Normal in Alpha 9 Knockout Mice**

**M. Christian Brown<sup>1,2</sup>, Douglas Vetter<sup>3</sup>**

<sup>1</sup>Dept. of Otolaryngology, Harvard Medical School, <sup>2</sup>Eaton-Peabody Laboratory, Massachusetts Eye & Ear Infirmary, Boston, MA, <sup>3</sup>Dept. of Neuroscience, Tufts University School of Medicine

Transgenic mice with deletion of the alpha 9 nicotinic acetylcholine receptor lack the cochlear effects of stimulation of the medial olivocochlear (MOC) neurons, because the receptor for the action of these neurons on outer hair cells has been deleted (Vetter et al., 1999, Neuron 23:93-103). In spite of this "de-efferentation", behavioral tests of hearing, including detection of tones in noisy backgrounds, are normal in this knockout mouse (May et al. 2002, Hearing Res. 171:142-157). A hypothesis proposed to explain the normal hearing is that of compensation by central MOC branches given off to the cochlear nucleus. The action of these central branches is preserved in the knockout because they act via an acetylcholine receptor other than alpha 9. If the central branches are involved in compensation, they may show morphological changes in the transgenic mouse. We looked for such changes using acetylcholinesterase stains of brainstems in three groups of mice: 1) knockouts, 2) wild-types of the same 129/SvEv strain, and 3) CBA strain. Histology from all mice showed dark staining of the MOC neurons, including their somata, axons, and cochlear-nucleus branches. There were no intergroup differences in the number of branches formed, the staining density of the branches, or the regions of cochlear nucleus innervated by the branches. In addition, there were no differences in the number of somata of MOC neurons (or in the number of somata of lateral OC neurons). These observations suggest that there have not been substantial morphological changes in the central branches or cell bodies of MOC neurons in the knockouts, even in the face of the deletion of the alpha 9 receptor and the substantial peripheral morphological changes reported previously (Vetter et al., 1999). Although central compensation has not been ruled out by these results, such compensation now seems a less attractive hypothesis to explain the normal hearing observed in the knockouts.

#### **665 Loss of Behavioral Ability to Track Ongoing But Not Initial SAM Envelope in Mice Lacking Kv3.1 That Have Normal Modulation Transfer Functions**

**Paul Allen<sup>1</sup>, Rolf Joho<sup>2</sup>, Alaina Muldrow<sup>1</sup>, Peter Rivoli<sup>1</sup>, Alison St. John<sup>1</sup>, James Ison<sup>1</sup>**

<sup>1</sup>Department of Brain and Cognitive Sciences, University of Rochester, <sup>2</sup>Center for Basic Neuroscience, U.T. Southwestern Medical Center

The high-fidelity transmission of temporal information by neurons in the auditory brainstem is thought to rely on their

strong expression of high-threshold Kv3 voltage-gated potassium channels that facilitate high-frequency firing by controlling the width of the action potential and the duration of the refractory period. Here we study the effects of Kv3.1 genotype on detection and discrimination of sinusoidal amplitude modulated noise (SAM). We address the hypothesis that Kv3.1  $-/-$  mice have a lower cut-off in their Modulation Transfer Function (MTF) than  $+/+$  and  $+/-$  littermates, as *in vitro* data suggest failure of fast repeat-firing in Kv3.1  $-/-$  neurons. Second we investigate the ability of these mice to encode the initial and ongoing SAM envelope, which depends on reliable phase-locking of neural responses to the stimulus. We used pre-pulse inhibition of acoustic startle (PPI), where the prepulse was the onset of 100% sinusoidal amplitude modulation of an otherwise continuous 70dB SPL broadband noise. Subjects were 2-4 month old Kv3.1  $-/-$ ,  $+/-$ , and  $+/+$  (N=8, 25, 7) mice (C57BL/129Sv/ICR background). In Experiment 1, MTFs were measured for modulation frequencies 20-2000 Hz and SAM commencing 100ms prior to the startle stimulus (ES). There was no effect of Kv3.1 genotype on MTF with all groups showing MTF maxima at 90Hz, 50% points at 600Hz, marginal detection at 1400Hz and no detection of 2000Hz SAM. In Experiment 2, SAM frequency was fixed at 100Hz, and the interstimulus interval (ISI) between onset of modulation and ES was systematically varied such that PPI was sampled at 4 different phases for the 1st, 7th, and 21st cycles. For Kv3.1  $+/+$  and  $+/-$  mice PPI was found to modulate with SAM phase, even during the 21st cycle. For Kv3.1  $-/-$  mice, only the 1st cycle yielded strong modulation. Sinusoidal curve fitting to the 7th and 21st cycle PPI data shows no effect of genotype on the baseline or phase of PPI, but a highly significant reduction of PPI modulation amplitude,  $F(2/16) = 18.51$ ,  $P < 0.001$ . Detection of very high MF is intact in Kv3.1  $-/-$  mice yet phase-locking to moderate MF appears compromised. These results suggest parallel mechanisms for modulation encoding that differ in their reliance on Kv3.1, with perhaps, differential implications for human speech detection and comprehension.

Support Contributed By: NIH grants AG09524 and NS42210 (RHJ)

#### **666 Auditory Neural Activation Is Altered in the Dorsal Cochlear Nucleus of EphA4 and Ephrin-B2 Deficient Mice**

**Ilona Miko<sup>1</sup>, Mark Henkemeyer<sup>2</sup>, Karina Cramer<sup>1</sup>**

<sup>1</sup>Department of Neurobiology and Behavior, University of California, Irvine, <sup>2</sup>Center for Developmental Biology, University of Texas Southwestern Medical Center at Dallas

The development of auditory neural circuitry depends on several factors, including the Eph receptor tyrosine kinases and their ligands, the ephrins. Alterations in Eph/ephrin expression disrupt projection patterns in chick and mouse auditory brainstem nuclei. It is not known whether these perturbations alter auditory neural activity. We addressed this question by examining activation of c-fos, an immediate early gene correlated with neural activation. We exposed 18-day old mice lacking EphA4 (EphA4 $-/-$ ) or one of its ligands, ephrin-B2 (ephrin-B2 $+/-$ ),

to 75 minutes of free field 8kHz tone pips, then processed brain sections for c-fos immunocytochemistry. Of all brainstem nuclei, the dorsal cochlear nucleus (DCN) shows the strongest c-fos activation in tone-specific cell clusters after exposure to a pure tone stimulus. We compared the number and distribution of c-fos-positive neurons responsive to 8kHz tones in the DCN of mutant and wild type mice. The mean number of c-fos-positive neurons in EphA4<sup>-/-</sup> DCN (n=3) was 40% lower than that in wild type DCN (n=3; p<0.05, Student's t-test). There was no significant difference in the mean number of c-fos positive neurons in the DCN of ephrin-B2<sup>+/-</sup> versus wild type mice. Along the dorsoventral, tonotopic axis of DCN, the mean position of c-fos positive neurons was similar for all mutant and wild type mice exposed to 8kHz tones, yet the distribution (standard deviation) of these neurons was 35% greater for ephrin-B2<sup>+/-</sup> mice (n=5) than for wild type mice (n=3; p<0.05). Along the rostrocaudal axis of DCN, the standard deviation of cell count was significantly greater in both EphA4<sup>-/-</sup> and ephrin-B2<sup>+/-</sup> than in wild type mice. These differences in distribution may be a consequence of defective axon guidance caused by the lack of normal EphA4 and ephrin-B2 expression patterns in the mutant mice. Supported by NIH DC005771 (to KSC), T32 NS045540, DC006225 (to MH) and the UCI IRU in Hearing and Speech Sciences.

#### **[667] EphA4 Is Necessary for Establishing Topography in Mouse Auditory Brainstem**

**Candace Hsieh<sup>1</sup>, Karina Cramer<sup>1</sup>**

<sup>1</sup>*University of California, Irvine*

The anteroventral cochlear nucleus (AVCN) projects tonotopically to the contralateral, but not ipsilateral, medial nucleus of the trapezoid body (MNTB). This pathway is part of a circuit that computes the location of sound sources. The mechanisms that form these precise connections are not known. Here, we investigated the role of the receptor tyrosine kinase EphA4 in establishing this pathway by characterizing the AVCN-MNTB projection in wild type and EphA4 null mice. We placed small (100-200  $\mu$ m<sup>2</sup>) pieces of NeuroVue<sup>TM</sup> Red dye into confined regions of AVCN in fixed brainstems from P10 mice. After 2 weeks of dye transport, brainstems were sectioned (100  $\mu$ m) and calyces of Held were counted in both MNTBs. A ratio of the number of ipsilateral to contralateral calyces (I/C ratio) was calculated. Additionally, we determined the position of each labeled calyx in MNTB relative to the entire mediolateral extent of MNTB (M-L ratio). Our results indicate no difference in I/C ratios between wild type ( $0.005 \pm 0.003$ , n = 4) and EphA4 null mice ( $0.011 \pm 0.006$ , n = 5; P > 0.05), indicating that the strictly contralateral projection from AVCN to MNTB was not altered by the deletion of EphA4. We next examined the topography of the AVCN-MNTB projection and confirmed in wild type mice that dye placement in dorsal AVCN labels medial MNTB while dye placement in ventral AVCN labels lateral MNTB. We then examined the pattern of topography in EphA4 null mice and found that the mean M-L ratio after ventral dye placement was significantly different from wild type mice [ $0.49 \pm 0.03$  (n = 5) vs  $0.58 \pm 0.01$  (n = 3), respectively; P < 0.05]. The data thus indicate that while

deletion of EphA4 does not affect pathfinding to the correct target on the appropriate side, it does affect termination of axons within MNTB, so that the topography of AVCN-MNTB projections is degraded. Supported by NIH DC005771, NIH DC007538, and the NOHR Foundation.

#### **[668] Changes in the Distribution of Vesicular Glutamate Transporters in the Cochlear Nucleus After Deafness: Relationship to Auditory and Non-Auditory Inputs**

**Jianxun Zhou<sup>1</sup>, Naveen Nannapaneni<sup>1</sup>, Susan Shore<sup>1</sup>**

<sup>1</sup>*University of Michigan*

The cochlear nucleus (CN) receives glutamatergic inputs from both auditory nerve and somatosensory structures. Projections of auditory and somatosensory structures to the CN are mostly nonoverlapping: type I auditory nerve fibers primarily project to the magnocellular cell areas of the CN, whereas trigeminal projections to the CN terminate in its granule cell domains (Zhou and Shore, J Neurosci Res. 2004; 78(6): 901-7). Vesicular glutamate transporters (VGLUTs) selectively package glutamate into synaptic vesicles and are excellent markers for glutamatergic neurons. Two subtypes of VGLUTs, VGLUT1 and VGLUT2 are complementarily distributed and account for the majority of VGLUTs expression in the brain. In this study, we wished first to examine the distribution of VGLUT1 and VGLUT2 in the CN as well as its association with the trigeminal-CN pathway in guinea pigs. Secondly, we wished to determine how the expression and distribution of VGLUT1 and VGLUT2 was altered after kanamycin-induced unilateral deafening. VGLUT1 and VGLUT2 immunoreactivity was found predominantly in axon terminals with nonoverlapping expression in the CN: most of the VGLUT1 immunoreactivity was in the ventral CN (VCN) and the superficial layer of the dorsal CN (DCN). Immunoreactivity against VGLUT2 was located primarily in the granule cell layer of the DCN and the small cell cap and granule cell regions of the VCN. After injections of tracers into the spinal trigeminal nucleus, co-localization of VGLUT2 with the anterogradely labeled

terminal endings was consistently found in the granule cell domains of the CN. Preliminary data indicate that, 1 week after unilateral cochlear injection with kanamycin, there was a large decrease in VGLUT1 immunoreactivity in the ipsilateral VCN and a slight increase in VGLUT2 immunoreactivity in the granule cell domains of the ipsilateral CN when compared with normal CNs. This study indicates that VGLUT1 and VGLUT2 may be differentially involved in synaptic transmission in the auditory and non-auditory pathways to the CN.

Supported by NIH grant R01 DC004825 and P01 DC00078

#### **[669] Purinergic (P2) Receptors in Spherical Bushy Cells of the Gerbil Cochlear Nucleus**

**Ivan Milenkovic<sup>1</sup>, Rudolf Rübsamen<sup>1</sup>**

<sup>1</sup>*Institute of Biology II, University of Leipzig*

The firing of spherical bushy cells (SBC) is determined by an interaction between excitatory (glutamatergic) and

inhibitory inputs (GABAergic and glycinergic) and contributes to sound localization based on interaural time differences. Based on the recent findings that ionotropic P2X receptors can modulate the neuronal activity in the cochlea and in the medial nucleus of the trapezoid body (MNTB), we conducted a whole-cell patch-clamp and a  $\text{Ca}^{2+}$ -imaging study to investigate the expression of P2 receptors in SBC. Puff applications of ATP (100 $\mu\text{M}$ ), the metabolically stable analogue ATP $\gamma\text{S}$  (100 $\mu\text{M}$ ), or the specific P2X $_7$ -receptor agonist BzATP (100 $\mu\text{M}$ ), induced strong depolarization of the plasma membrane and transient inward currents. The responses were effectively blocked by PPADS (100 $\mu\text{M}$ ) or suramin (100 $\mu\text{M}$ ), and were not affected by the blockers of AMPA/kainate receptors, CNQX and GYKI 52466, suggesting the activation of the postsynaptic P2X receptors. Furthermore, bath application of ATP (100 $\mu\text{M}$ ) increased the  $\text{K}^+$  conductance, presumably in a  $\text{Ca}^{2+}$ -dependent manner. Extracellular ATP (100 $\mu\text{M}$ ), ADP (100 $\mu\text{M}$ ), 2-methyl-thio-ADP (100 $\mu\text{M}$ ), and to a lesser extent UDP (100 $\mu\text{M}$ ), evoked rapid and transient increases in  $[\text{Ca}^{2+}]_i$ . No changes in  $[\text{Ca}^{2+}]_i$  were observed upon UTP (100 $\mu\text{M}$ ), AMP (100mM), or adenosine (100mM) application. The  $\text{Ca}^{2+}$  transients were antagonized by PPADS (100 $\mu\text{M}$ ), they were not affected by the blockers of glutamatergic neurotransmission and showed no exclusive dependence on extracellular  $\text{Ca}^{2+}$ . The experiments show that SBC respond to application of different P2 receptor agonists with alterations of the  $[\text{Ca}^{2+}]_i$  and the whole-cell currents, and point to the expression of more than one subtype of purinergic receptors. In addition to putative P2X $_7$  receptors, it is proposed that SBC express at least one subtype of metabotropic P2Y receptors as revealed by the  $\text{Ca}^{2+}$  imaging experiments. Further characterization of the P2 receptors subtypes and their physiological roles in SBC remain to be elucidated.

#### **670 Novel c-Fos Gene Response Sensitivity to Sound Pattern**

**Dean Hillman<sup>1</sup>, Alvin Htut<sup>2</sup>**

<sup>1</sup>New York University School of Medicine, <sup>2</sup>Binghamton University

Expression of the *c-fos* gene occurs in response to novel auditory stimuli as well as to a number of other activity related conditions and lasts for 4-6 hours. When rats were preconditioned in a quiet, unchanging environment for 8-12 hrs, Fos protein was lost from neuronal nuclei. We demonstrated that Fos protein appeared within 30 to 45 minutes of novel tone patterns. Furthermore, continuous stimulation of a sound pattern habituated the response in neurons so that most of the *c-fos* expression disappeared in 48 hours (Kandiel et al. Brain Res. 1999). In this study, our goal was to determine which components (intensity, frequency or pattern) of sound are discriminated as being novel for signaling *c-fos* gene expression. Stimulation of pre-conditioned "quiet" animals, with 2K Hz -3 sec on and 3 sec off- 70 dB bursts, was followed 1 hr later with fixation for immunoreactivity of Fos protein containing neurons. In a paradigm of intensity increments of 50, 60, 70 or 80 dB, the Fos protein response was near equal across the intensity range. When the 3 sec sound pattern was changed to one with 0.1 sec on/off, the short burst patterns

had much less Fos reactivity than the 3 sec pattern. These results suggest that differentiation of novelty in sounds, that gives rise to the *c-fos* gene response in dorsal cochlear nuclei, is detected in pattern. Supported by NIH grant NS13742.

#### **671 Caspase-3 Activation in NM Neurons Following Cochlea Removal and Topical Gentamicin Application**

**Christina L. Kaiser<sup>1</sup>, Douglas A. Girod<sup>1</sup>, Dianne Durham<sup>1</sup>**

<sup>1</sup>Department of Otolaryngology/Head and Neck Surgery, University of Kansas Medical Center

Cochlea removal results in the death of 30% of neurons in the avian cochlear nucleus (n. magnocellularis, NM). Prior to cell death, increased immunoreactivity for cytochrome-c and activated caspase-9 are observed (Wilkinson et al, Neurosci. 120:1071-1079; 2003), suggesting NM death occurs by apoptosis. Here, we further investigate apoptosis in NM neuronal cell death by evaluating whether caspase-3, an effector caspase located downstream of caspase-9, is activated following cochlea removal or partial deafferentation caused by topical gentamicin application. Ten day-old broiler chickens underwent either unilateral cochlea removal or topical gentamicin administration with a Gelfoam pledget soaked in gentamicin (200 mg/mL). The contralateral ear remained untreated to serve as an internal control. At sacrifice, brains were removed and prepared for cryostat sectioning and activated caspase-3 immunocytochemistry. Following cochlea removal, activation of caspase-3 in ipsilateral NM neurons was observed at 12 hours, with some caspase-3 labeling still present at 3 days. Activation of caspase-3 in ipsilateral NM neurons was also detected following topical gentamicin application but with a delayed time course. No activated caspase-3 staining was seen 12 hours after gentamicin application; however, caspase-3 label was detected at 2 1/2 days after gentamicin treatment. Activated caspase-3 immunoreactivity was not detected in contralateral NM neurons at any time following gentamicin application or cochlea removal. Qualitative analysis of both cochlea removal and gentamicin treated tissue showed activated caspase-3 in the majority of NM neurons. Despite this ubiquitous expression of activated caspase-3, not all NM neurons die, indicating that competing cell death and cell survival mechanisms must work downstream of caspase-3 to regulate NM neuronal cell death.

Supported by NIDCD R01 DC01589

#### **672 Lhx9 Is Required for Normal Development of the Cochlear Nucleus**

**Kathleen Yee<sup>1</sup>**

<sup>1</sup>Tufts University School of Medicine

The cochlear nucleus is the mandatory synaptic site in the brain of inner ear afferents. The anatomy and physiology of the mature cochlear nucleus has been studied for many years, but less is known about the molecules that control its early development.

Reported here are findings on 1) the expression of a lim-homeodomain transcription factor, Lhx9, during early

cochlear nucleus development and 2) the impact of its absence on the anatomical organization of the mature cochlear nucleus. In situ hybridization reveals that Lhx9 is expressed in the presumptive (p)DCN and pVCN as early as embryonic day (E)11.5. At E14.5, Lhx9 mRNA expression is strong in the deep region of the DCN and also expressed in the VCN but at a lower intensity. Based on these expression data, it was of interest to examine cochlear nucleus development in the absence of Lhx9 expression. In contrast to wildtype littermates, Lhx9 <sup>-/-</sup> mice (11 weeks of age) show **1**) in nissl-stained sections (40µm)

a) aberrant organization of the mature cochlear nucleus,  
b) varied thickness and cell density of the molecular layer and

c) qualitatively, a high density of cells with small somata and a lower density of cells with large somata in the fusiform layer; and

**2**) with immunohistochemical staining against the neuropeptide PEP19, cartwheel cells with smaller cell bodies and thinner caliber characteristic curved processes of cartwheel cells.

While these data show that Lhx9 is expressed during early cochlear nucleus development and that in the absence of Lhx9 function in vivo, the cochlear nucleus exhibits altered patterns of cellular organization, many questions remain to be answered. It is of interest to determine whether Lhx9 is expressed only in the embryonic cochlear nucleus or whether it is also expressed later in the more mature nucleus. Currently under investigation is whether the anatomical changes observed in the Lhx9 homozygous mutant cochlear nucleus are direct and/or indirect effects of Lhx9 function.

### **[673] Distinct Biophysical Properties of Cochlear Nucleus Neurons in the Frog Brainstem**

Sungchil Yang<sup>1</sup>, Albert S. Feng<sup>1</sup>

<sup>1</sup>*Department of Molecular & Integrative Physiology and Beckman Institute, University of Illinois UC*

The frog's dorsolateral nucleus (DLN) is the first auditory processing center in the brain, analogous to the cochlear nucleus in mammals. Previous studies have shown that, although the DLN has no anatomic subdivisions, it contains distinct morphological cell-types and neurons therein exhibit diverse temporal discharge patterns in response to tone bursts at the unit's CF, as observed in the mammalian cochlear nucleus. However, it is unclear whether the different temporal firing patterns are attributed to having different intrinsic membrane properties or to the cell's morphology and connectivity pattern, or both. The present study investigated the intrinsic firing patterns and biophysical characteristics of DLN neurons as well as their locations in the DLN, with intracellular recordings and staining (with biocytin) from brain slices in vitro. In response to injections of depolarizing currents, DLN neurons exhibit at least four distinct firing patterns: sustained-chopper, transient-chopper, onset and primary-like. The majority of DLN neurons show sustained-chopper firing patterns. These neurons (located throughout the nucleus) have the highest input resistance of all cell-types,

show saturating I-V curves and can be further subdivided into two subclasses based on the cell's input resistance and soma size. Onset neurons (at the medial border of the DLN) have the lowest impedance and linear I-V curves. Transient-chopper cells (located in the dorsal area of the DLN) show short-term regular firing of spikes in response to depolarizing currents, saturating I-V curves, and no depolarization sag during hyperpolarizing currents. Primary-like neurons show decreasing inter-spike intervals with depolarizing current injections and a linear I-V curve. These four functional cell-types bear some resemblances as well as differences to the comparable cell-types in the mammalian cochlear nucleus.

Research is supported by a grant from the National Institutes of Health (R01DC04998).

### **[674] Computational Model of Response Maps in the Gerbil Dorsal Cochlear Nucleus**

Xiaohan Zheng<sup>1</sup>, Herbert Voigt<sup>1</sup>

<sup>1</sup>*Boston University*

The neurons in the mammalian (gerbil, cat) dorsal cochlear nucleus have responses to tones and noise that have been used to classify them into unit types. These types (I-V) are based on excitatory and inhibitory responses to tones organized into plots called response maps (RMs). Type I units show purely excitatory responses, while type V units are primarily inhibited. A computational model of the neural circuitry of the mammalian DCN, based on the MacGregor neuromine, was used to investigate RMs of the principal cells (P-cells) that represent the fusiform and giant cells. In gerbils, fusiform cells have been shown to have primarily type III units response properties, however fusiform cells in the cat DCN are thought to have type IV unit response properties. The DCN model is based on a previous computational model of the cat (Hancock and Voigt, 1999) and gerbil (Zheng and Voigt, 2005) DCN. The basic model for both species is the same architecturally, and to get either type III unit RMs or type IV unit RMs, connection parameters were adjusted. Interestingly, regardless of the RM type, these units in gerbils and cats show spectral notch sensitivity and are thought to play a role in sound localization in the medial plane. In this study, further parameter adjustments were made to explore systematically their effect on the RMs. Significantly, type I, type III, type IV, type IV-T and type V unit RMs are possible to create in the model's P-cells. Thus five of the six major RMs observed in the cat and gerbil DCN are found in the model. [Work supported by Boston University's Biomedical Engineering department and Hearing Research Center.]

### **[675] The Time Course of Glycine Receptor-Mediated Currents in the MNTB**

Tao Lu<sup>1</sup>, Larry Trussell<sup>1</sup>

<sup>1</sup>*Oregon Health & Science University*

Principal cells of the rat MNTB receive both calyceal- and bouton-type synapses, the latter suggesting the presence of inhibitory inputs. The presence of inhibitory synaptic activity has been previously documented; its



pharmacology suggests the presence of both GABAergic and glycinergic synapses. The glycinergic synapses are particularly striking in their size and speed, which may be necessary to serve their physiological function (Awatramani et al, 2004, 2005). In 2-week old rats, miniature inhibitory postsynaptic currents (mIPSC), blockable by the glycine receptor antagonist strychnine, decay with a predominant single exponent of  $3.3 \pm 0.6$  ( $\pm$ SD) ms at room temperature, irrespective of peak amplitude. To explore the underlying molecular mechanisms for rapid glycinergic synapse, we excised outside-out membrane patches from MNTB neurons of 2-week old rats and applied glycine using a piezo-controlled rapid solution exchange system. This approach allowed us to apply a known concentration of the agonist glycine for brief periods, with onset and offset times of  $< 200$  microsec. The resulting currents were then compared to the time course of mIPSCs.

Surprisingly, the decay time of the response to 1 ms pulses of 1 mM glycine were almost always best fit with two exponentials of comparable magnitude, where even the faster time constant ( $14.9 \pm 16.7$  ms) was usually much slower and more variable than the decay of mIPSCs. Weighted mean exponential time constants were variable in different patches but averaged  $29.7 \pm 20.2$  ms for patches from cells in brain slices and  $21.2 \pm 10.5$  ms from dissociated neurons. Somewhat faster decay kinetics were observed when glycine was applied for periods briefer than 1 ms or at concentration lower than 1 mM, but were still much slower than mIPSCs. Modulation by either zinc or ATP could not account for the difference. Moreover, rapid application of glycine to whole dissociated neurons also gave time constants far slower than synaptic responses ( $23.9 \pm 19.7$  ms for faster exponent, and  $34.2 \pm 17.0$  ms for weighted mean time constant). We have also measured the response kinetics of other amino acid agonists of glycine receptors. Taurine and beta-alanine produced currents in patches which decayed with a weighted mean time constant similar to that of strychnine-sensitive mIPSCs ( $3.5 \pm 2.2$  ms for taurine,  $4.2 \pm 0.9$  ms for beta-alanine), and produced similar kinetics in whole cells as well. These observations suggest the possibility that the natural neurotransmitter at these inhibitory synapses may not be glycine.

Supported by DC04450

## **676 A Physiological Model of Autocorrelation**

**Lowel O'Mard<sup>1</sup>, Ray Meddis<sup>1</sup>**

<sup>1</sup>CNBH, University of Essex

A physiologically plausible computer model of pitch processing is presented. The model is based upon an earlier autocorrelation model of pitch (Meddis and O'Mard, 1997), except that, the autocorrelation function has been replaced by a simple neural circuit that extracts periodic information from auditory signals.

The Meddis and O'Mard pitch model consists of four sequential processing stages: (1) peripheral frequency selectivity, (2) within-channel half-wave rectification and low-pass filtering, (3) within-channel periodicity extraction, and (4) cross-channel aggregation of the output. The pitch

perception is represented by the aggregated periodicity function. The physiological model also contains stages (1) and (2). Stages (3) and (4) have been replaced by a neural circuit consisting of two banks of chop-S neurons with associated dendritic processing (low-pass filtering). The first bank contains ventral cochlear nucleus (VCN) chop-S cells tuned to a range of chopping frequencies. Each centre frequency channel has a VCN cell at each of the chopping frequencies. The outputs from VCN cells with the same chopping frequency are integrated by cells in the second bank representing inferior colliculus units. The pitch perception is represented by the output of the IC cells.

The model successfully demonstrates a number of experimental results related to pitch processing. These include (i) the pitch of alternating-phase harmonic stimuli (ii) the increased pitch difference threshold of harmonic complexes consisting of higher harmonics; and (iii) the influence of a mistuned harmonic on the pitch of the complex.

The model has been implemented using the development system for auditory modelling (DSAM), a computing library designed as a standard platform for producing applications to create and evaluate auditory models. It brings together many published auditory models (produced by different research groups), analysis functions and general utility functions within a flexible, stable programming platform that has been extensively tested for robustness and accuracy. DSAM has been extended to incorporate threaded parallel processing. This allows DSAM to take full advantage of the multi-processor and multi-core processor systems available today.

This study has shown that a physiological mechanism similar to autocorrelation is possible and that it can reproduce experimentally determined observations.

## **677 Voltage-Sensitive Conductances in Bushy Cells of the Ventral Cochlear Nucleus of Mice**

**Xiaojie Cao<sup>1</sup>, Donata Oertel<sup>1</sup>**

<sup>1</sup>Department of Physiology, UW-Madison

The biophysical properties of bushy and octopus cells of the ventral cochlear nucleus (VCN) allow them to receive and convey acoustic information contained in the timing of firing of small and large groups of auditory nerve fibers respectively. We have made whole-cell recordings from bushy cells in the anterior VCN in slices and compared them with recordings made under similar conditions in the posterior VCN from octopus cells. These recordings show that the properties of the low-voltage- (gKL) and high-voltage activated (gKH) potassium conductances in bushy cells resemble those of octopus cells but are 2- to 5-fold smaller. The hyperpolarization-activated conductance (gh) is not only smaller but also slower and differently modulated in bushy than in octopus cells. Under voltage-clamp gKL, gKH, and gh were measured from 18-21 day-old mice. gKL in bushy cells was similarly activated by depolarizations more positive than  $-65$  mV and similarly sensitive to (-dendrotoxin ((-DTX) but was 5-fold smaller than in octopus cells. The mean maximum gKL was  $103.5 \pm 30.6$  nS ( $n=5$ ) in bushy cells. An (-DTX insensitive,

tetraethylammonium-sensitive conductance, gKH, was activated by voltage steps positive to  $-30$  mV, as in octopus cells. The maximum conductance was  $49.1 \pm 14.7$  nS ( $n=5$ ), 2-fold smaller than in octopus cells. A ZD7288-sensitive hyperpolarization-activated conductance, gh, was activated at potentials negative to  $-50$  mV. It was half-activated at more negative potentials,  $-87$  mV, the maximum conductance was 3-fold smaller at  $44.5 \pm 11.2$  nS ( $n=6$ ), and its activation and deactivation kinetics were slower than in octopus cells. Changes in temperature affected the kinetics and the magnitude of gh in bushy cells, but did not adapt to changes in temperature. All voltage-clamp recordings were made in the presence of  $1$   $\mu$ M TTX,  $0.25$  mM CdCl<sub>2</sub>,  $40$   $\mu$ M DNQX,  $1$   $\mu$ M strychnine. This work was supported by a grant from NIH DC00176.

## **[678] Auditory Nerve First-Spike Latency and Absolute Threshold**

**Ray Meddis<sup>1</sup>**

<sup>1</sup>*University of Essex*

Behavioral absolute threshold for a pure tone stimulus in quiet can not easily be defined in physiological terms. Auditory nerve (AN) rate threshold is an inappropriate comparison because psychophysical thresholds depend on the duration of the stimuli used. Traditional temporal integration theories explain many psychophysical observations but it remains unclear where the integration takes place. This modeling project starts from the observation that auditory nerve first-spike latency is reduced as the stimulus is increased in both duration and level. This could be related to the dependence of behavioral threshold on duration because more intense stimuli can be detected at shorter durations. Unfortunately, near threshold, there is no simple way to distinguish the first spike after stimulus onset from spontaneous activity. However, if first-order relay neurons are set to respond only to coincidental AN action potentials across a number of fibers, they can be shown to have thresholds that depend appropriately on stimulus duration. A computer model of the auditory periphery is described that has realistic first-spike latency properties. It also has firing thresholds that decline with increased stimulus duration in a manner similar to psychophysical observations. This is a temporal integration model where the integration takes place using pre-synaptic calcium in inner hair cells.

## **[679] Opposite Actions of Glycine at a Mammalian Central Synapse**

**Cornelia Kopp-Scheinpflug<sup>1</sup>**, Susanne Dehmel<sup>1</sup>, Rudolf Rübsamen<sup>1</sup>

<sup>1</sup>*Department of Neurobiology, University of Leipzig, Germany*

The calyx of Held, innervating neurons of the medial nucleus of the trapezoid body (MNTB), serves as one of the most elaborate models of synaptic transmission in the mammalian CNS. In recent history, the view of the calyx-of-Held-MNTB-synapse has changed dramatically from serving a simple relay function to being modified by complex interactions of excitation and inhibition. It has been shown that responses of MNTB neurons are affected

by inhibition, which was proved to be glycinergic by studies in brain slices. Here, we report in vivo data on opposing effects of glycine in the MNTB. For single MNTB units tuning characteristics, rate-level functions, PST histograms and failure rates of synaptic transmission following sound stimulation were tested before and after application of strychnine (glycine receptor antagonist). Application of strychnine blocked inhibitory sidebands and caused significant widening in frequency tuning throughout all units tested. However, at frequencies within the excitatory response area, especially at higher sound intensities, two thirds of the units responded to the blockade of glycine with a clear decrease in sound-evoked firing rates. Blockade of glycine also caused the failure rate of synaptic transmission to increase for all activity exclusively transmitted by the calyx (spontaneous and within the excitatory response area) and to decrease in areas with additional inhibitory input (sidebands). These results indicate that glycine serves opposite functions during signal transmission at this CNS synapse: At the margins of the response area the postsynaptic discharge activity is reduced while at its center the excitatory calyceal input is amplified.

## **[680] Preliminary Study of Transmitter Release Regulation in the Guinea Pig Cochlear Nucleus**

Zhicheng Mo<sup>1</sup>, **Sanoj K. Suneja<sup>1</sup>**, Steven J. Potashner<sup>1</sup>

<sup>1</sup>*University of Connecticut Health Center*

This study was undertaken to identify regulators of transmitter exocytosis in auditory pathways. Transmitter exocytosis from presynaptic endings is known to depend on  $\text{Ca}^{2+}$  influx into the cytosol, which activates proteins that facilitate the docking and fusion of synaptic vesicles with the plasma membrane of the active zone. On depolarization of the axonal ending,  $\text{Ca}^{2+}$  may enter the cytosol via voltage-gated  $\text{Ca}^{2+}$  channels in the plasma membrane as well as inositol triphosphate ( $\text{IP}_3\text{R}$ ) and ryanodine ( $\text{RyR}$ ) receptor channels in the smooth endoplasmic reticulum. When these routes were blocked separately by extracellular  $\text{Ca}^{2+}$ -deprivation, 2-aminoethoxydiphenyl borate or tetracaine, respectively, the release of D-[<sup>3</sup>H]aspartate, evoked by electrical field stimulation of dissected samples of the anteroventral cochlear nucleus (AVCN), declined by 87%, 40%, and 65%. D-[<sup>3</sup>H]Aspartate served as a non-metabolizable marker for transmitter glutamate. Phosphorylation of the  $\text{IP}_3\text{R}$  and  $\text{RyR}$ , which increases their activities, is downregulated by protein phosphatases (PP). Block of PP-1 and PP-2A with okadaic acid had little effect on release, but block of PP-2B (calcineurin) with FK506 elevated the release 2.3 fold. These findings suggest that voltage-gated  $\text{Ca}^{2+}$  channels,  $\text{IP}_3\text{Rs}$  and  $\text{RyRs}$  contributed to transmitter release. In addition, inhibitors of protein synthesis, such as rapamycin and cycloheximide, or of vesicle trafficking, such as brefeldin A, applied to the dissected AVCN for 30-60 min reduced the electrically-evoked release by 50-70%, implying that release required continuous protein synthesis. Finally, fusion of vesicles with the plasma membrane is thought to be facilitated by phospholipase D (PLD) activity. A partial block of PLD with 1-butanol or 2,3-diphosphoglycerate inhibited release by at least 50%, consistent with a contribution of PLD activity. Taken

together, these findings demonstrate that putative regulators of transmitter exocytosis include voltage-gated  $\text{Ca}^{2+}$  channels,  $\text{IP}_3\text{R}$ ,  $\text{RyR}$ , protein synthesis and  $\text{PLD}$  (Supported by DC00199).

### **[681] Temporal Processing Models of Neurons in the Dorsal Cochlear Nucleus**

**Sharba Bandyopadhyay<sup>1</sup>**, Eric D. Young<sup>1</sup>

<sup>1</sup>*Johns Hopkins University, Baltimore, Maryland*

Auditory neurons often exhibit nonlinearities in temporal processing. The current study investigates stimulus envelope processing in the dorsal cochlear nucleus (DCN). Temporal processing models that relate the dB stimulus envelope to discharge rate over time, through gain functions, have been developed. The stimuli used are broadband noise-like stimuli made of sums of tones spaced 1/64th octave apart. Random temporal shapes (RTS, with an approximately Gaussian distribution) of varying contrasts are enforced on them. With 3 dB contrast, linear models often had good prediction performance. By allowing the linear gain function to vary with time, possibly taking into account the effect of stimulus and spiking history, the model performance often improved. Further by adding second order interactions extending over a small range back in time the model performance improved significantly. Similar models were estimated for the case of random current injections (with different degrees of contrast) into a Hodgkin-Huxley-type DCN pyramidal cell model. Prediction performance of the temporal processing model and the model itself, in such a situation, changed with changing contrasts in the random current injections. Such behavior may be expected in actual neurons as well, based on nonlinear temporal properties of DCN neurons. This allows the possibility of developing nonlinear models of temporal processing in the DCN and elsewhere in the auditory system based on locally linear or quadratic models. Supported by NIH grants DC00109 and DC00115.

### **[682] Activity-Dependent Changes in Intracellular Cl-Regulation in Developing Auditory Neurons**

**Yasuhiro Kakazu<sup>1</sup>**, Shumei Shibata<sup>1</sup>, Shi H.B.<sup>1</sup>, Matsumoto Nozomu<sup>1</sup>, Kazutaka Takaiwa<sup>1</sup>, Takashi Nakagawa<sup>1</sup>, Shizuo Komune<sup>1</sup>

<sup>1</sup>*Kyushu University*

A developmental change in GABA and glycine responses have been reported in many CNS neurons, and has been demonstrated to be due to a decrease in the  $[\text{Cl}^-]_i$ . We examined  $[\text{Cl}^-]_i$  in isolated rat lateral superior olive (LSO) neurons using gramicidin patch-clamp recordings of glycine gated  $\text{Cl}^-$  currents and by measuring intracellular  $\text{Cl}^-$  fluorescence. In neurons from 14-16-day-old rats (P14-P16), which had previously received unilateral or bilateral cochlear ablations before the onset of hearing, there was no developmental decrease in  $[\text{Cl}^-]_i$ . No significant differences in  $[\text{Cl}^-]_i$  were observed amongst rats with either ipsi- and contralateral ablations. Implanted strychnine pellets also prevented the decrease in  $[\text{Cl}^-]_i$  in most neurons. In some of these neurons in which  $[\text{Cl}^-]_i$  remained high, there was a lack of expression of the  $\text{K}^+/\text{Cl}^-$  cotransporter 2 (KCC2) mRNA. These results

demonstrate that the developmental decrease in  $[\text{Cl}^-]_i$  in LSO neurons is dependent on neuronal activity and that both GABAergic/glycinergic and glutamatergic afferent activity contribute to this maturation of the  $\text{Cl}^-$  regulatory mechanisms.

Most part of this work was previously reported by Shibata et al. (Neurosci Res. 2004 48:211-20).

### **[683] High Fidelity Action Potential Propagation in the Axons of MSO Neurons**

**Luisa Scott<sup>1</sup>**, Nace Golding<sup>1</sup>

<sup>1</sup>*Section of Neurobiology and Institute for Neuroscience, University of Texas at Austin*

Time-coding auditory neurons like principal neurons of the medial superior olive (MSO) phase-lock to sounds, firing at high instantaneous frequencies. We have shown that action potentials (APs) are initiated in the axon of MSO neurons indicating that once generated, APs backpropagate to the soma and forward propagate along the axon. To further explore the efficacy of AP propagation in MSO principal neurons we made simultaneous whole-cell somatic and loose-patch axonal current-clamp recordings (35°C) in brainstem slices from 9 P14-17 gerbils. Somatic patch pipettes contained 30  $\mu\text{M}$  Alexa 488 to visualize axons during recordings and biocytin to later confirm the location of the recording site in morphological reconstructions. Axonal APs were often too small to detect in single trials possibly due to the heavy myelination of the axons. In 3 cells, axonal signals (recorded ~100  $\mu\text{m}$  from the soma) were detectable on single trials, and a response threshold was set at 3 SD above noise. MSO neurons showed a remarkable ability to follow trains of suprathreshold somatic current injection (1 ms pulses). APs recorded at the soma and axon could follow 1000 Hz trains (5-10 stims) when current amplitudes were well above threshold (5000 pA). Generally APs detected at the soma were also detected at the axonal recording site. However, at higher frequencies (>500 Hz) and during longer trains (100 pulses) APs detected at the soma occasionally (<10%) failed to reach the axonal recording site. Surprisingly, APs were also occasionally recorded in the axon when somatic responses were subthreshold, suggesting failure in antidromic propagation. Overall, our data show principal MSO axons can maintain higher frequencies of AP firing than found in non-auditory neurons thus far (upper limit, 300 Hz). Our propagation failures in both antidromic and orthodromic directions may reflect an intervening region of high AP attenuation in the axon initial segment.

### **[684] Temporal Properties of Inhibition Acting on MNTB Principal Cells**

**Sandra Tolnai<sup>1</sup>**, Bernhard Englitz<sup>1,2</sup>, Susanne Dehmel<sup>1</sup>, Cornelia Kopp-Scheinpflug<sup>1</sup>, Jürgen Jost<sup>2</sup>, Rudolf Rübsamen<sup>1</sup>

<sup>1</sup>*University of Leipzig, Institute of Biology II*, <sup>2</sup>*Max Planck Institute for Mathematics in the Sciences*

Recent findings revealed a significant influence of spectrally tuned inhibition in the Medial Nucleus of the Trapezoid Body (MNTB). For this inhibition to be capable

of shaping responses of MNTB neurons to temporally modulated stimuli, especially natural stimuli, requires the ability to follow these amplitude modulations at high temporal precision. We investigated this hypothesis using sinusoidally amplitude modulated (SAM) single and two-tone stimuli, which allowed a quantification of the modulation transfer functions of excitation and inhibition on a cell-by-cell basis. Although stimulus-delays of excitation and inhibition varied from 2.5 to 5 ms between cells, inhibition consistently followed excitation at a delay of about 0.5 ms within a cell. Inhibition phase-locked to the SAM with VS values comparable to the respective excitation VS values, i.e. modulation rates of up to 700 Hz and VS values up to 0.9. Further the temporal shape and nonlinear-scaling of this inhibition was estimated.

### **[685] Specificity of Connections in the Dorsal Cochlear Nucleus Revealed by Dual Whole Cell Recordings**

**Jaime Mancilla<sup>1</sup>**, Paul Manis<sup>1</sup>

<sup>1</sup>UNC Chapel Hill

Pyramidal cells in the dorsal cochlear nucleus (DCN) receive direct auditory information via the eighth nerve and non-auditory information from parallel fibers synapsing onto both pyramidal and cartwheel cells. The cartwheel cell inhibitory feedforward loop is an interesting component of the DCN circuitry, because cartwheel cells show immunoreactivity for both  $\gamma$ -amino-butyric acid (GABA) and glycine, raising the possibility of transmitter co-release onto target cells. We used a brainstem slice preparation of the DCN to study the properties of cartwheel connections onto both pyramidal and other cartwheel cells. In addition, we analyzed on going inhibitory postsynaptic potentials (IPSPs) and currents (IPSCs) in cartwheel and pyramidal cells. Dual whole cell recordings in the DCN suggest that pyramidal cells do not connect to either near by cartwheel (0/15 pairs) or pyramidal cells (0/2 pairs). Cartwheel cells, on the other hand, synapse onto both near by pyramidal (10/15 pairs) and cartwheel cells (2/2 pairs). Evoked cartwheel cell IPSPs onto pyramidal cells had amplitudes of  $1.3 \pm 0.9$  mV (mean  $\pm$  SD) and times-to-peak (ttp) of  $3.7 \pm 1.2$  msec ( $n = 8$ ). The paired pulse ratio of IPSPs was  $0.5 \pm 0.2$  at an interval of 20 msec ( $n = 8$ ), indicating short-term synaptic depression. Cartwheel cell IPSPs onto nearby cartwheel cells had amplitudes of 0.2 mV and ttp of 20.6 msec ( $n = 2$ ). Analysis of voltage traces in simultaneously recorded pairs often showed correlated activity. IPSPs in cartwheel cells that were correlated with IPSPs in pyramidal cells were smaller (amp =  $0.7 \pm 0.4$  mV) and slower (ttp =  $12.3 \pm 5.7$  msec) than those occurring in pyramidal cells (amp =  $1.2 \pm 1.2$  mV; ttp =  $4.0 \pm 1.9$  msec;  $n = 85$  events in 2 pairs). Taken together these data suggest that the same inhibitory interneuron could produce IPSPs with different kinetics depending on the target cell.

Supported by DC00425 to PBM.

### **[686] A Quantitative Model of Short-Term Synaptic Plasticity in the Avian Cochlear Nucleus Angularis**

**Katrina MacLeod<sup>1</sup>**, Timothy Horiuchi<sup>2</sup>

<sup>1</sup>Dept Biology, University of Maryland, College Park, <sup>2</sup>Dept Elec. Comp. Engineering, University of Maryland, College Park

The synaptic properties of the auditory nerve inputs to neurons of the cochlear nucleus are fundamental to the transformation of auditory information. In birds, timing and intensity information used in sound localization are processed in parallel streams beginning with the two divisions of the cochlear nucleus, n. magnocellularis and n. angularis. Recent results have suggested that differences in the rapid, activity-dependent changes in synaptic strength, known as short-term synaptic plasticity, may contribute to differential transmission of timing and intensity components. To better characterize the short-term plasticity effects, we have developed a quantitative model based on several published models of synaptic transmission in other brain areas (Tsodyks and Markram 1997, Varela et al. 1997, Dittman et al. 2000). We recorded activity-dependent changes in the amplitudes of AMPA-receptor mediated EPSCs from chick embryonic brainstem slices, using constant frequency trains of stimuli evoked by extracellular stimulation of the auditory nerve tract. The model consists of a two-pool depletion component, and a facilitation component. The postsynaptic response was calculated as the fractional release of vesicles from a readily releasable pool, which is replenished from a backup pool with an exponential time constant, itself replenished from an infinite reserve. This two-pool model allows for two time constants of recovery from vesicle depletion, but can be reduced to a single pool model. Facilitation was implemented by allowing the fraction of release to be time-varying and activity-dependent. The six parameters in the model were found by calculating the best fit of the model to the full set of EPSCs in each train at 6 frequencies for each cell, using a least-squares minimization procedure implemented in MATLAB. This quantitative model can be used to predict responses on a spike by spike basis to more naturalistic stimuli.

### **[687] Short Term Synaptic Depression and Recovery at the AVCN Endbulb Synapse in Mice**

**Yong Wang<sup>1</sup>**, Paul Manis<sup>1</sup>

<sup>1</sup>UNC-Chapel Hill

The spike patterns of bushy cells in the mammalian anterior ventral cochlear nucleus (AVCN) are not a carbon copy of the activity in the auditory nerve fibers (ANFs). In vivo recordings in AVCN bushy cells have shown that a fraction of ANF spikes fails to drive bushy cells. Synaptic depression during high rates of ANF activity, and subsequent recovery during periods of lower activity, can significantly shape the functional relationship between ANFs and bushy cells. To characterize the dynamic changes in synaptic efficacy at this specialized synaptic terminal, we studied the time course of synaptic depression and recovery with high frequency shock

stimulation to the auditory nerve fibers in a slice preparation in CBA mice. We also investigated the role of AMPA receptor desensitization in synaptic depression. In contrast to the strong depression reported for young medial nucleus of the trapezoid body (MNTB) neurons, we found, at 33°C, in mature CBA mice (P21-45), that the synaptic responses to 15-20 stimuli at 100, 200 and 300 Hz were depressed by 33±6%, 55±4%, and 70±4%, respectively, at the end of the train. Higher frequency shock trains also resulted in a faster recovery of the synaptic release, consistent with the posited role of presynaptic Ca<sup>2+</sup> accumulation in the recovery process. Since cyclothiazide can not only affect presynaptic mechanisms but is also ineffective at these older synapses, we used a low-affinity competitive antagonist of AMPA receptors,  $\gamma$ -D-glutamylglycine ( $\gamma$ -DGG), to probe the role of desensitization in shaping the synaptic response. Preliminary results (n=3) suggest that AMPA receptor desensitization plays a lesser role in mature endbulb synaptic depression during high frequency stimulation compared to what has been reported at the immature calyceal synapse in the MNTB. In addition,  $\gamma$ -DGG appears to slow down recovery from depression in an activity-dependent manner.

(Supported by NIDCD grant DC04551).

#### **688 Paradoxical Control of Membrane Excitability by Hyperpolarization-Activated Cationic Channels in Principal Neurons of the Medial Superior Olive**

**Sukant Khurana<sup>1</sup>, Shanxue Jin<sup>1</sup>, Nace Golding<sup>1</sup>**

<sup>1</sup>*Section of Neurobiology and Institute for Neuroscience, University of Texas at Austin*

In many neurons, hyperpolarization-activated cationic currents ( $I_h$ ) contribute to the resting potential and may shape both the duration and amplitude of synaptic potentials. To understand the role of these channels in the medial superior olive (MSO), we made whole-cell current-clamp recordings from MSO principal neurons (17-22 days) in gerbil brainstem slices maintained at 35°C.  $I_h$  constitutes a large component of the resting membrane conductance in MSO principal neurons. In the presence of ZD7288, a blocker of  $I_h$ , the average resting potential hyperpolarized by 9.8 mV (from -53.1 to -62.9 mV), and the average membrane resistance ( $R_m$ ) increased from 8 to 24 M $\Omega$  (n=4). Trains of sub-threshold simulated EPSCs (100-500 Hz, 0.2 to 2s duration) induced increases in  $R_m$  (up to 56%) that were sensitive to stimulus amplitude and frequency. These  $R_m$  changes developed and decayed slowly, with both features following a dual exponential time course (rise = 33±19, 1080±376 ms, n=3; decay = 36±2, 425±22 ms, n=8). Train-induced  $R_m$  changes were linearly related to EPSP amplitude and frequency, and action potential generation provided additional contributions. Activity-dependent changes in  $R_m$  were largely eliminated in the presence of 50  $\mu$ M ZD7288, indicating that the primary underlying mechanism was the deactivation of  $I_h$ . Also, trains of simulated and real IPSPs induced decreases in  $R_m$ . The above results stand in contrast to those from other neuron types, where deactivation of  $I_h$  provides a powerful net hyperpolarization of EPSPs,

attenuating the amplitude and duration of excitation. The paradoxical action of  $I_h$  in MSO neurons may stem from its relatively larger contribution to the resting membrane conductance. We propose that in MSO neurons *in vivo*, cumulative activation and deactivation of  $I_h$  during repetitive binaural activity provides a means to dynamically control intrinsic membrane excitability, or neuronal gain over longer time periods.

#### **689 GABAergic Inhibition Shapes Responses of SFM Selective Neurons in the Inferior Colliculus of the Bat**

**Qi Yue<sup>1</sup>, David Pérez-González<sup>1</sup>, Ellen Covey<sup>1</sup>, John H. Casseday<sup>1</sup>**

<sup>1</sup>*University of Washington*

Previous studies have shown that some neurons in the inferior colliculus (IC) of the big brown bat (*Eptesicus fuscus*) are specialized for responding to SFM signals. SFM-selective cells do not respond to pure tones, and they also show high selectivity to at least one of four main parameters of SFM: carrier frequency, modulation rate, modulation depth and sound level. Most of the SFM-selective cells are selective for low sound levels, with an upper threshold as well as a lower one. The purpose of this study was to determine the role of GABAergic inhibition in shaping the responses of SFM-selective neurons in the IC. We recorded sound-evoked responses of SFM-selective cells before, during, and after the application of gabazine (SR-95531), an antagonist of GABA-A receptors. During gabazine application all SFM-selective cells became responsive to higher sound levels, and most completely lost their selectivity to amplitude. For cells with phase-locked responses, the phase locking was abolished during drug application. Some SFM-selective cells became responsive to pure tones, but only to tones of short duration. Gabazine application caused discharge patterns to change, increasing the number of spikes and lengthening the period over which the cell responded. The effect of gabazine on tuning to SFM modulation rate, depth and carrier frequency was variable. In most cases tuning to these parameters broadened, but selectivity was maintained. These findings suggest that GABAergic inhibition plays a role in suppressing responses to pure tones and shaping multiple response parameters of SFM-selectivity in the IC, especially amplitude selectivity and phaselocked discharge patterns. The fact that selectivity to some parameters of SFM stimuli remained suggests that part of the selectivity is either inherited from input neurons or is controlled by other factors such as glycinergic inhibition or intrinsic properties. Supported by NIDCD DC-00287 and DC-00607.

#### **690 Physiological Role of Postsynaptic GABA<sub>B</sub> Receptors in the Dorsal Cortex of the Young Rat's Inferior Colliculus**

**Hongyu Sun<sup>1</sup>, Shu Hui Wu<sup>1</sup>**

<sup>1</sup>*Psychology Department, Carleton University, Ottawa, ON, Canada*

In the present study, we used whole-cell patch clamp recording techniques to determine whether postsynaptic

GABA<sub>B</sub> receptors can modulate membrane excitability and be involved in synaptic transmission in ICD neurons. ICD neurons (n=82) were recorded in coronal brain slices from P9-18 rats. Under voltage-clamp conditions ( $V_h = -60$  mV), GABA<sub>B</sub> receptor-mediated IPSCs could be induced by repetitive stimulation (10 pulses, 200 Hz) of the commissure of the IC (CoIC). They had a mean duration of  $0.83 \pm 0.21$  s, and a peak amplitude of  $45.7 \pm 9.1$  mV at  $0.16 \pm 0.03$  s from the onset of the response, and were blocked with application of the GABA<sub>B</sub> receptor antagonist, CGP35348. The reversal potential of the IPSC was close to the expected equilibrium potential for K<sup>+</sup>. The GABA<sub>B</sub> agonist, baclofen (20  $\mu$ M), induced an outward K<sup>+</sup> current, leading to membrane hyperpolarization and a decrease in the membrane input resistance. The outward current showed an inward rectification, which was blocked by both CGP35348 and the K<sup>+</sup> channel blocker, barium. The effects of baclofen were dose dependent. Baclofen also reduced the firing rate and increased the threshold of firing. The afterhyperpolarization following a single action potential was partially blocked by baclofen. The Ca<sup>2+</sup>-mediated rebound and hyperpolarization-activated I<sub>h</sub> were eliminated by baclofen. In addition, two distinct voltage-dependent K<sup>+</sup> current components, a transient (I<sub>A</sub>) and a sustained (I<sub>K</sub>), were substantially increased by application of baclofen. Voltage-dependent Ca<sup>2+</sup> currents were slightly depressed by baclofen. These results indicate that activation of postsynaptic GABA<sub>B</sub> receptors can induce a longer lasting inhibitory postsynaptic potential in ICD neurons. The postsynaptic GABA<sub>B</sub> receptors are coupled to inwardly rectifying K<sup>+</sup> channels and play a significant role in modulating the membrane excitability of ICD neurons through regulation of voltage-dependent K<sup>+</sup> and Ca<sup>2+</sup> currents.

Supported by NSERC of Canada to S.H. Wu

#### **[691] Dominant Role of Inhibitory Inputs in Combination-Sensitive Facilitation: Comparison of Glycinergic and Glutamatergic Neurotransmission**

**Jason Sanchez**<sup>1,2</sup>, Donald Gans<sup>1,2</sup>, Jeffrey Wenstrup<sup>2</sup>

<sup>1</sup>Kent State University, <sup>2</sup>NEOUCOM

In the mustached bat's inferior colliculus (IC), *combination-sensitive* neurons display time-sensitive facilitatory interactions between inputs tuned to distinct spectral elements in complex sounds. These interactions underlie analyses of sonar and social vocalizations. This study compares the roles of glycinergic and glutamatergic neurotransmission on facilitatory combination-sensitive interactions. We recorded single unit responses before, during, and after local micro-iontophoretic applications of antagonists to AMPA, NMDA, and glycine receptors. Application of the NMDA receptor antagonist CPP alone or in combination with the AMPA receptor antagonist NBQX significantly reduced or eliminated the response to best frequency sounds across a broad range of sound levels. However, application of these glutamate antagonists did not eliminate facilitatory combination-sensitive interactions. In a majority of these units, strychnine, the glycine receptor antagonist, was subsequently applied in combination with the glutamate antagonists. The facilitatory interaction was

always eliminated by strychnine application. These results suggest that glutamate neurotransmission is not needed for facilitatory combination-sensitive interactions in the IC. Instead, the facilitation appears to depend entirely upon glycinergic inputs that are presumed to be inhibitory. We propose that glycinergic inputs tuned to two distinct spectral elements in vocal signals each activate a post-inhibitory rebound excitation. When the rebound excitations from two spectral elements coincide, the unit discharges. Excitation from glutamatergic inputs, tuned to the unit's best frequency, is superimposed onto this facilitatory interaction, presumably mediating responses to a broader range of acoustic signals. Supported by NIH grants R01 DC00937 (J.J.W) and F31 DC007298 (J.T.S) from NIDCD.

#### **[692] Activation of Serotonin 3 Receptors Changes *In Vivo* Auditory Responses in Mouse Inferior Colliculus**

**Alex Bohorquez**<sup>1</sup>, Laura Hurley<sup>1</sup>

<sup>1</sup>Indiana University, Bloomington, IN

Serotonin (5-HT) has been shown to play a major role in modulating the responses of single neurons to auditory stimuli in the inferior colliculus (IC). Further understanding the role of serotonin in the mammalian auditory system requires knowledge of which serotonin receptors are present and how they alter auditory responses. This study characterized how activating the only ionotropic serotonin receptor type, the serotonin 3 receptor (5-HT<sub>3</sub>R), changed the responses of inferior colliculus neurons to auditory stimuli. The auditory responses of 24 neurons from the IC of six male mice were recorded extracellularly, before and during the iontophoresis of mCPBG, a 5HT<sub>3</sub>R agonist. Of these 24 neurons, 10 (41.7%) showed at least a 30% change in spike count upon application of mCPBG. Decreased spike counts, seen in 5 neurons, averaged 55% of control values. Increased spike counts, seen in 4 neurons, averaged 288% of control, and one neuron responded to mCPBG biphasically, initially increasing and secondarily decreasing its spike count. Since 5HT<sub>3</sub>Rs are cation channels, such varied responses could be due to activation of intrinsic circuitry within the IC. The effects of mCPBG were usually rapid, occurring within 30 seconds of the onset of iontophoresis in six of the ten neurons, and recovering in eight neurons from 12 to 70 seconds after the halt of iontophoresis. In 4 of the 10 neurons that were responsive to mCPBG, the response desensitized during the continuing iontophoresis of mCPBG. Previous studies have shown that the 5HT<sub>3</sub>R is present in the IC and may play a role in synaptic plasticity in this nucleus. The current study suggests that this receptor can also modulate sound-evoked responses.

#### **[693] History-Dependent Firing in Neurons of the Owl's Auditory Space Map**

**Theodore Cornforth**<sup>1</sup>, Terry Takahashi<sup>1</sup>

<sup>1</sup>University of Oregon

Amplitude modulated (AM) noise is a common feature of the acoustic environment and the ability of the auditory system to encode these modulations is an important

aspect of communication. Neural encoding of AM is typically measured using modulation transfer functions (MTFs), which describe how neural activity such as spike rate varies as a function of signal modulation. An assumption inherent in using MTFs to study auditory processing is that MTFs are a static function that converts an AM signal input into a neural output. We show here that the activity of neurons in the barn owl's inferior colliculus (IC) auditory space map change in a way linearly dependent on the prior history of inputs received by the neurons, suggesting that MTFs are dynamic rather than static functions.

By analogy with the work performed by Smirnakis *et al.* 1997 using the visual system of flies, we performed an amplitude switching experiment in which the variance of a zero-mean broadband noise was alternately modulated by one of two square wave AM functions to give a low amplitude portion of the stimulus ("low") and a higher amplitude portion ("high"). The AM stimuli switched between low and high at a constant rate and were at least 10 seconds in duration. These stimuli were presented to anesthetized barn owls while extracellular recordings were made from individual IC cells.

When a switch was made from low amplitude to high, the spike rate decreased from its maximum immediately after the switch with time constant  $\tau_H$ , and when the switch was made from high to low, the spike rate increased from its minimum immediately after the switch with time constant  $\tau_L$ . During the course of the stimulus, the firing rate of the cells adapted, in the sense that the values of  $\tau_H$  and  $\tau_L$  changed from some initial value to eventually maintain a different, final value. These final values were measured under stimuli with different rates of AM modulation. Consistent with the findings of Smirnakis *et al.* 1997 and Fairhall *et al.* 2001, the final values of  $\tau_H$  were found to increase linearly as the rate of AM modulation decreased and the final values of  $\tau_L$  were found to decrease linearly as the rate of AM modulation decreased. Presumably this type of spike rate adaptation serves to optimize the encoding of the sensory input in an information-theoretic sense as was found in Fairhall *et al.* 2001 for H1 neurons in the visual system of flies. Future work will address this issue.

Fairhall, AL, GD Lewen, W Bialek, RR de Ruyter van Steveninck. 2001. Efficiency and ambiguity in an adaptive neural code. *Nature* **412**:787.

Smirnakis, SM, MJ Berry, DK Warland, W Bialek, M Meister. 1997. Adaptation of retinal processing to image contrast and spatial scale. *Nature* **386**:69.

#### **694 Plasticity of Afferent Projections from the Dorsal Nucleus of the Lateral Lemniscus to the Central Nucleus of the Rat Inferior Colliculus After Bilateral Cochlear Ablation**

Samuel R. Franklin<sup>1</sup>, Craig K. Henkel<sup>1</sup>, Judy K. Brunso-Bechtold<sup>1</sup>

<sup>1</sup>Wake Forest University School of Medicine Department of Neurobiology and Anatomy

By postnatal days 4-6 (P4-P6) in rat pups, ascending auditory projections begin organizing into a pattern of

afferent bands in the central nucleus of the rat inferior colliculus (CNIC). The segregation of afferent projections from different lower auditory sources establishes multiple synaptic compartments within each fibrodendritic layer of CNIC. We hypothesize that early competitive interactions within the CNIC influence the overall pattern of developing afferent bands in CNIC layers even before onset of hearing (approximately P12 in rat). Previous studies in our laboratory showed that unilateral cochlear ablation on either P2, before bands form, or on P9, after bands form, disrupt the development and maintenance of banded afferent projections from the dorsal nucleus of the lateral lemniscus (DNLL) to the CNIC. It still remains unclear, however, whether or not patterns of spontaneous activity in ascending auditory pathways generated by the cochlea are requisite for segregation of afferent bands. To address this, bilateral cochlear ablations (BCA) were performed in P9 rat pups when bands have already formed and are being refined. All animals were sacrificed at P12 and pins coated with the carbocyanine dye, 1,1'-diiododecyl-3,3,3',3'-tetramethylindocarbocyanine perchlorate (DiI), were subsequently placed in the DNLL commissure to label afferent axons projecting to both CNICs. DiI labeled axons distributed along layers and symmetrically filled the CNIC on each side. Analysis of the spatial distribution of the labeled DNLL afferent axons indicated a pattern of dense and light terminal fields in CNIC that varied from the regular spacing of banded label along CNIC sublayers in surgical controls. These findings suggest that just three days after BCA, plastic changes have taken place in the banded pattern of DNLL projections and, together with results of unilateral cochlear ablation in previous experiments, support the hypothesis that activity-dependent competition sculpts synaptic compartments within fibrodendritic layers in CNIC. Supported by NIH NIDCD grant DC 004412.

#### **695 Preference to Natural Sound Dynamics in the Central Auditory Pathway**

Jose Alberto Garcia Lazaro<sup>1</sup>, Bashir Ahmed<sup>1</sup>, Jan W.H. Schnupp<sup>1</sup>

<sup>1</sup>Oxford University

In a recent study (1), we showed that neurons in primary auditory cortex (A1) respond more strongly and reliably to dynamic stimuli whose statistics follow "natural"  $1/f$  distributions, than to stimuli exhibiting other statistics. In order to investigate whether this tuning to  $1/f$  dynamics is already found at lower stages of the auditory pathway, we are now extending our study to the central nucleus of the inferior colliculus (IC), an obligatory auditory relay nucleus in the midbrain. To test whether neurons in the IC exhibit tuning to  $1/f$  dynamics, we recorded responses to 10.74 sec segments of random tone complexes in which the fundamental frequency and the envelope fluctuated as a function of statistically independent " $1/f^\gamma$  random walks", with  $\gamma$  set to values between 0.5 and 2, from anaesthetized (domitor/ketamine) ferrets. Michigan probes (single shank, 16 sites, separation 150um, NeuroNexus Technologies) were used for these recordings. Our preliminary data indicate that there is a subpopulation of neurons in the IC which also responds with higher firing



rates to stimuli in which  $\gamma$  takes values near 1, although the tuning to stimulus dynamics appears less pronounced than what is typically observed in cortex. Responses from cortical (A1) neurons typically drop off rapidly for faster ( $\gamma < 1$ ) fluctuations, but decline only slowly for  $\gamma > 1.5$ , often reaching a plateau. A1 neurons often exhibited strong offset responses for stimuli with exponents  $< 1$ . Responses from IC, in contrast, decrease only slowly both for faster or slower fluctuations and they lack the offset responses seen in cortical neurons. Interestingly, we found evidence of two other subpopulations of neurons that respond in remarkably different ways to  $1/f$  stimuli: responses from one subpopulation are flat, and do not exhibit tuning to any particular stimulus dynamics. In contrast, responses of the other subpopulation, exhibit strong suppression during stimulus presentation. These results suggest that tuning to  $1/f$  dynamics becomes more pronounced on ascending levels of the auditory pathway. Taken together with recent results in primary visual cortex (2), data obtained both from primary auditory cortex and IC suggests that tuning to natural dynamics may be a general feature of sensory systems.

Supported by the BBSRC (UK) grant 43/S1959, and studentships from CONACYT and Defeating Deafness to JAGL.

#### References:

1. Garcia-Lazaro, J. A., Ahmed, B. & Schnupp, J. W. H. in *CoSyNe Abstracts 2005 (Snowbird, Utah)*. 236.
2. Yu, Y., Romero, R. & Lee, T. S. (2005) *Phys. Rev. Lett.* **95**, 108103.

### **[696] Prestin Knock-Out Mice Exhibit Temporal-Processing Deficits in the Inferior Colliculus**

**Olga Vasilyeva**<sup>1</sup>, Anne E. Luebke<sup>1</sup>, Jian Zuo<sup>2</sup>, Joseph Walton<sup>1</sup>

<sup>1</sup>University of Rochester, <sup>2</sup>St. Jude Children's Research Hospital

Active mechanical amplification of sound can occur in cochlear outer hair cells (OHCs) which change their length with oscillations of their membrane potential. Such length changes are the proposed cellular source of the cochlear amplifier, and prestin is the motor protein responsible for OHC electromotility. Previous findings have shown that mice lacking prestin displayed a loss of OHC electromotility, a 40-60 dB reduction in cochlear sensitivity (DPOAEs, ABRs, and compound action potential (CAP) thresholds, diminished frequency selectivity, and reduced CAP dynamic range. Prestin is expressed during the 1st postnatal week and rapidly reaches a mature level before the onset of hearing. We were interested in determining if the severe sensorineural hearing threshold loss associated with the loss of motor protein prestin would also impair auditory midbrain temporal-processing. Auditory midbrain temporal-processing was assessed in four experimental groups: (1) Wildtype (WT) controls, N=12, 21-34 d; (2) Prestin knockout (KO), N=15, 21-34 d; (3) WT, N= 10, 35-50 d; (4) Prestin KO, N=11, 35-50 d. To assess temporal-processing, we measured near-field auditory evoked potentials from dorsal (500 mm) and ventral (1500 mm) portions of the inferior colliculus (IC) in response to a silent

gap embedded in noise. Two intensities were used for WT mice in order to equate overall SPL (80 dB SPL carrier) and sensation level (40 dB SPL carrier). Tones (3-48 kHz) and broadband noise burst intensity growth level functions were also obtained.

Not unexpectedly, in both age groups of KO mice thresholds to tone burst and broadband noise bursts were elevated by 40 to 60 dB. In addition, there were clear differences in the amplitude by intensity functions between prestin KO and WT mice, both in terms of tone burst frequency and in depth of recording. No difference in response amplitude was found between age groups within the WT and KO mice. The prestin KO animals had a significant increase in gap thresholds, as compared to the KO animals for both age groups. The slope of the gap functions was also reduced in the prestin KO groups as compared to WT mice, indicating a prolongation in recovery from prior stimulation. Taken together, these data indicate that severe sensorineural hearing loss, following the loss of prestin, is also associated with impaired central auditory temporal processing.

Work supported by NIA PO1 AG09524, NIDCD P30 DC05409 and NIDCD DC003086

### **[697] Modelling Excitatory and Inhibitory Convergence in the Inferior Colliculus (IC): Receptive Field Plasticity**

Chris Scholes<sup>1</sup>, Russell L. Snyder<sup>2</sup>, **Christian Sumner**<sup>1</sup>

<sup>1</sup>MRC Institute of Hearing Research, Nottingham, UK,

<sup>2</sup>Department of Psychology, Utah State University

Restricted cochlear damage produces changes in the tonotopic organization and receptive field properties of central auditory neurons tuned to the damaged frequencies. Excitatory response areas of these neurons shift to frequencies corresponding to undamaged cochlear regions, while thresholds remain relatively unchanged. In the IC, this re-tuning occurs immediately after restricted spiral ganglion (SG) lesions (Snyder and Sinex, 2002), which remove inputs from a narrow best frequency (BF) range, while leaving mechanical filtering intact. One hypothesis to explain this re-tuning is that removal of peripheral inputs from a restricted BF range may also remove inhibitory influences revealing (unmasking) more excitatory inputs. Previously, Sumner (2005, ARO abstr. #488) presented a model consistent with this hypothesis. It incorporated converging excitatory inputs and 'on-BF' shunting inhibition. This model reproduced changes in IC tonotopy and receptive fields observed following small SG lesions. If SG lesions are progressively enlarged, re-tuning also expands to reveal further previously hidden excitatory inputs from an even wider range of BFs (Snyder et al., 2003, ARO abstr. #687). To model this it was necessary to expand both the excitatory and inhibitory convergence, which must be tonotopically aligned on the dendrites. When the excitatory and inhibitory receptive fields are both much wider than the lesion, the model shows reliable unmasking effects. For models with less convergence, the results depend on the source of inhibitory drive. When there is tonic inhibition, the model shows reliable re-tuning for a variety of inhibitory and excitatory arrangements. If

the inhibition is purely stimulus driven, then the inhibitory and excitatory convergences must be closely matched. These results suggest that there may be a large degree of inhibitory and excitatory convergence at the level of the IC, and that inhibitory and excitatory inputs are aligned tonotopically across dendrites.

**698** **Neuronal Processing of Cochlear Distortion Products in the Midbrain – Simultaneous Acoustic and Electrophysiological Measurements**  
**Cornelius Abel<sup>1</sup>, Manfred Kössl<sup>1</sup>**

<sup>1</sup>*Zoologisches Institut - Universität Frankfurt am Main*

Nonlinear cochlear amplification gives rise to distortion-product OAEs (DPOAE) which presumably modify the acoustic input to the auditory nerve and the ascending auditory pathway. During acoustic stimulation with two tones, we measured neuronal responses in the inferior colliculus both to the stimuli and to distortion products generated by the cochlea. Simultaneously, we recorded the acoustic magnitude of the distortion products as otoacoustic emissions in the ear channel with a sensitive microphone.

After recording the frequency tuning curves of neuronal single units or multi units we used two short pure tone pulses (with frequency/level combinations outside of the unit's excitatory response region; duration of 30-50 ms) as primary stimuli to elicit cochlear distortions. The stimuli were adjusted to obtain distortion product OAEs that were within the excitatory field of the unit. Simultaneous measurement of DPOAE levels, stimulus levels, and neuronal activity allowed us to analyse the contribution of additional frequency components generated by the inner ear for central auditory processing.

Strong responses to both quadratic or cubic cochlear distortions were recorded that were comparable to the unit's pure tone response. In some cases the units response to DPOAE was stronger than to pure tones. In other cases, inhibitory side bands effectively suppressed the neurons' response to cochlear distortion products. When two or more distortion products are within the excitatory- and/or inhibitory neuronal fields, the neuronal response to DPOAE can differ considerably from the pure tone response.

The results suggest that the modification of acoustic signals by the nonlinear behaviour of the inner ear should be taken into account when assessing neuronal processing of complex sounds.

This study was supported by the DFG.

**699** **Deafness Related Changes in the Gene Expression of 2 Pore Potassium Channels in the Inferior Colliculus**

**Avril Genene Holt<sup>1</sup>, Catherine Lomax<sup>1</sup>, Ling Tong<sup>1</sup>, Jose Juiz<sup>2</sup>, Richard Altschuler<sup>1</sup>**

<sup>1</sup>*University of Michigan*, <sup>2</sup>*Universidad de Castilla – La Mancha*

Tinnitus can be induced in animal models by exposing rats to a tone resulting in a permanent hearing loss (PTS) or to a tone that results in only a temporary hearing loss (TTS).

We hypothesized that changes in activity related genes would occur under both conditions if the gene played a role in tinnitus. We found increases in NMDA receptor subunit expression in the cochlear nucleus 5 days following noise exposure in both the PTS and TTS tinnitus models. The 2 pore potassium channels are believed to play an important role in setting the baseline activity of neurons. The current study examined the effect of noise exposures producing a PTS and TTS on the expression of nine of these channels. Five days following noise exposure, significant decreases in gene expression were seen in the inferior colliculus in TASK 1, TASK 5, THIK 2, TREK 2 and TWIK 1 in the PTS, but not the TTS condition. Interestingly these changes occur when there is no recovery of hearing and may therefore be primarily associated with deafness. Indeed we also find comparable significant decreases in these channels three weeks following bilateral cochlear ablation, supporting this interpretation.

Acknowledgements -This research was supported by a research grant from the American Tinnitus Association to AGH and core center grant P30 DC-05188 from the NIDCD, NIH

**700** **Reversible Unilateral Neural Hearing Loss Modifies Response Properties of Binaural Auditory Midbrain Neurons**

**David Gooler<sup>1</sup>**

<sup>1</sup>*Department of Speech and Hearing Science, University of Illinois*

Chronic sensorineural hearing loss typically alters frequency sensitivity and selectivity of central auditory neurons. The effect of acute neural hearing loss on the processing of acoustic signals by binaural neurons is less understood. This study evaluated the effects of acute, reversible neural hearing loss on response properties of single neurons in the frog auditory midbrain. The creation of a temporary hearing loss permitted direct measures of excitatory and inhibitory response properties in the same binaural neuron under conditions of intact hearing and unilateral hearing loss. For this purpose, unilateral neural hearing loss was induced using a cryoprobe to cool the auditory nerve and produce a reversible block of neural conduction.

The cryoprobe was constructed from two different sized syringe needles such that the barrel of one was placed coaxially inside the other with a 125  $\mu$ m silver wire forming the cooling tip of the probe. Cooled ethanol was pumped through the central barrel and exited through a port in the luer region of the outer barrel. Through a dorsal surgical approach the cryoprobe tip was positioned just above one auditory nerve. Frequency-response-areas of auditory midbrain neurons were recorded before, during, and after reversible unilateral hearing loss.

The results of this study indicated that the inactivation of the auditory nerve was acute and reversible. Repeated cooling and warming cycles required to inactivate and reactivate neural function reached stable levels within one to two minutes. Binaural auditory midbrain neurons revealed changes in frequency response properties

indicating that acute unilateral hearing loss can alter both excitatory and inhibitory properties. Monaural stimulation under temporary contralateral neural inactivation compared with intact hearing often revealed different frequency response properties.

### **701 Noise-Induced Reorganization of the Tonotopic Map in the Inferior Colliculus of the Rat**

**Marco A. Izquierdo<sup>1</sup>**, Salvatore Cristaudo<sup>1</sup>, Miguel A. Merchán<sup>1</sup>, Manuel S. Malmierca<sup>1</sup>

<sup>1</sup>*Auditory Neurophysiology Unit. Lab Neurob Hearing. University of Salamanca & INCYL. Salamanca, Spain*

It is well established that mechanical lesions of the auditory receptor produce plastic changes in the tonotopic organization of the auditory thalamus and cortex, indicating that lesion-induced plasticity in the auditory pathway is not restricted to the cortex. An important question is whether such reorganization reflects the operation of processes at lower auditory centres such as the midbrain, i.e., the inferior colliculus (IC). Thus, the aim of this study is to test the hypothesis that noise-induced lesions produce plastic changes in the tonotopic organization at the midbrain level.

We exposed hooded rats (*Rattus norvegicus*. Rj: Long Evans) to pure tones (e.g., 8 kHz at 100-115dB SPL for 8-12 hours). Following acoustic trauma, animals were kept in normal conditions. After a survival period of at least 40 days, animals were anaesthetized with urethane (1.5 g/kg, i.p.) and the acoustic lesion was assessed by measuring the compound action potential (CAP). Single- and multiunit recordings were then made in the IC using tungsten electrodes to determine whether the normal frequency organization of the IC had changed.

Our preliminary results show that the tonotopic organization of the IC undergoes changes similar to those described in the cortex and thalamus. However, the measured thresholds increase with recording depth in the IC suggesting that most of the changes in frequency organization are compatible with the residual-response hypothesis (e.g., Rajan et al., 1993; JCN 338:17-49), and plastic changes are not as obvious in the IC as in the cortex.

We thank Alan Palmer for teaching us the CAP technique. This study was supported by the Spanish JCyL-UE (SA0400/04, MSM, MAM), DGES (BFI-2003-09147-02-01, MAM, MSM). SC holds a fellowship from the USAL and MAI from the MEC.

### **702 Enhanced Excitation and Reduced Inhibition in the Inferior Colliculus After Partial Inner Hair Cell Loss in the Chinchilla**

**Ala Alkhatib<sup>1</sup>**, Désirée Biedenkapp<sup>1</sup>, Ulrich W. Biebel<sup>1</sup>, Jean W.T. Smolders<sup>1</sup>

<sup>1</sup>*J.W.Goethe-University, Physiology II, Frankfurt, Germany*

In the chinchilla, inner hair cells are more vulnerable by the ototoxic drug carboplatin than outer hair cells. With an appropriate dose (80 mg/kg) of carboplatin a partial inner hair cell (IHC) loss is obtained without damage of the outer hair cells. The partial IHC loss occurs over nearly the

whole length of the cochlear partition. We investigated the effects of carboplatin-induced partial IHC loss on response properties of neurons in the central nucleus of the inferior colliculus (ICc) in awake chinchillas. Auditory brain stem responses (ABR), local field potentials (LFP) from the ICc and stereotaxic microelectrode recordings of multi- and single-unit responses to tone stimuli were made in the same awake chronic animals before and after carboplatin treatment. After partial carboplatin-induced inner hair cell loss of less than 50%, there was a small elevation of neural thresholds at the characteristic frequency, predominantly in the upper frequency range. Excitatory regions of receptive fields of multi-units in the ICc were broadened, inhibitory regions were reduced and the sound evoked excitatory firing rate was increased. The proportion of non-monotonic rate-level functions was reduced, that of monotonic functions increased. The decrease of response rate with sound level at high stimulus levels in non-monotonic rate-level functions was reduced. Amplitudes of local field potentials (LFP) in response to CF tones the inferior colliculus were enhanced. Amplitudes of auditory brain stem responses (ABR) were reduced. Components of the ABR with latencies of 5-10 ms were the least affected. These components correspond in latency to those of the LFP recorded from the ICc. Reduced inhibition and enhanced excitation in the ICc after partial IHC loss may play a role in central compensation of moderate peripheral hearing loss.

Supported by the Deutsche Forschungsgemeinschaft (SFB 269 B1 and GRK 361)

### **703 Cortico-Cortical Connections of Ferret Auditory Cortex**

**Jennifer Bizley<sup>1</sup>**, Victoria Bajo<sup>1</sup>, Fernando Nodal<sup>1</sup>, Andrew King<sup>1</sup>

<sup>1</sup>*University of Oxford*

Here we investigate the cortical connections of the different auditory cortical fields in the ferret. Auditory cortex in this species is located on the Ectosylvian Gyrus (EG) and, based on the responses of neurons to pure tone stimuli, comprises at least 6 separate fields (Bizley et al., 2005, *Cerebral Cortex* 15:1637-1653). Primary areas are located on the middle EG (MEG) and non-primary areas on the posterior and anterior EG (PEG and AEG). Injections of neural tracers (biotinylated dextran amine, tetramethyl rhodamine and/or cholera toxin  $\beta$  subunit) were made into physiologically-defined auditory areas. The resulting patterns of retrograde and anterograde labelling were studied in order to examine the cortical inputs and outputs of the different auditory fields. Our results show that primary and non-primary auditory areas are each reciprocally connected with both primary visual and somatosensory cortex, as well as higher visual, somatosensory and multisensory areas. Primary auditory cortex appears to have more extensive connections with other primary sensory areas, rather than higher sensory areas, whereas secondary auditory areas are connected predominantly with higher, rather than primary, sensory areas. Reciprocal connections were also observed between all auditory fields and posterior parietal areas, with more labelling resulting from injections into the AEG

and PEG compared to those made in the MEG. Injections into the PEG and AEG also revealed that these regions project to and receive input from the prefrontal cortices. Similarly, injections made into primary cortex indicated that there is also a sparse, direct projection to the prefrontal cortex and provided evidence for a weaker feedback pathway. Differences in the pattern and strength of cortical connections between the various auditory fields support our physiological data that these are functionally-distinct regions.

#### **704** Cortico-Thalamic Connectivity of Ferret Auditory Cortex

**Fernando Nodal<sup>1</sup>**, Victoria Bajo<sup>1</sup>, Jennifer Bizley<sup>1</sup>, Andrew King<sup>1</sup>

<sup>1</sup>*University of Oxford*

Despite a marked increase in the use of ferrets for auditory research, there is a surprisingly fragmented description of the anatomy of its auditory pathway, especially from the midbrain upwards. Recently we have used intrinsic optical imaging (Nelken et al., *J Neurophysiol* 2004, 92:2574-2588) and electrophysiological recording (Bizley et al., *Cerebral Cortex* 2005, 15:1637-1653) techniques to characterize six different auditory cortical areas located in the Ectosylvian Gyrus (EG). Guided by this cortical parcellation, we have injected neuronal tracers into physiologically-defined regions of the EG to study their cortico-thalamic connectivity. Tracer injections covering a substantial portion of the Middle EG (MEG), where the primary fields are located, resulted in dense ipsilateral anterograde labelling, mainly in the ventral (v) and dorsal (d) divisions of the medial geniculate body (MGB). Some giant terminals were observed in the dMGB. Smaller injections in MEG resulted in more restricted labelling within the vMGB, most likely indicating that this cortico-thalamic projection is topographically organized. Injections in the posterior EG (PEG), where at least two secondary cortical fields are found, produced labelled neuronal profiles in the dorsal and medial MGB, with vMGB being practically devoid of any labelling. Lastly, injections in the anterior EG, where another two areas have been described physiologically, resulted in profuse anterograde labelling in dMGV, where giant terminals were observed, and in the supragenulate nucleus. These cortico-thalamic projection patterns provide further evidence for the existence of several distinct cortical fields in the EG and are comparable to those described in other mammalian species.

#### **705** Effects of Rapid Reversible Cortical Inactivation Upon Neurons in the Auditory Thalamus

**Simon J. Jones<sup>1</sup>**, Alan R. Palmer<sup>1</sup>

<sup>1</sup>*MRC Institute of Hearing Research, Nottingham, UK*

The functions of the profuse descending projections from the auditory cortex to the medial geniculate body (MGB) are almost unknown. Here we assess the effect of reversible cortical inactivation upon the responses of MGB neurons in urethane anaesthetised guinea pigs to sounds presented diotically and monaurally to each ear.

Responses were recorded in the MGB simultaneously via 8 microelectrodes. The primary auditory cortex was inactivated by cooling with a cryoloop and confirmed by a single microelectrode inserted at the centre of the loop. Full frequency/level response areas were measured and responses to 100 repetitions of a 50µs click were assessed from peristimulus time histograms before, during and after cortical inactivation.

Cortical inactivation resulted in facilitation and/or suppression of the MGB responses that were measured at different times on different electrodes. Four classes of effect of cortical inactivation were identified. In the first group (81/155) the MGB responses were either suppressed or facilitated for all stimulation conditions and time windows. In a second group (16/155) the facilitation and suppression was most notable within a restricted widow from 20-130 ms after the click, while the third group (12/155) showed facilitation or suppression of activity occurring at longer latency (>200 ms). The final group (46/155) showed facilitation of responses to one ear while the responses to the other were suppressed.

Similar examples of ear specific facilitation and suppression were clearly evident in the response area analyses as a result of cortical inactivation.

The descending inputs from the auditory cortex produce facilitation or suppression of the MGB responses that occur in different neurones at different times or selectively to the responses evoked by stimulation of the two ears. We do not yet know whether the different patterns of responses follow the topographic pattern of input to the MGB from different cortical areas.

#### **706** Auditory Responses in the Basolateral Amygdala of the Mustached Bat, *Pteronotus Parnellii*

**Naumann Thomas<sup>1</sup>**, Stuart Washington<sup>1</sup>, Jagmeet Kanwal<sup>1</sup>

<sup>1</sup>*Georgetown University*

Previous studies have shown that neurons in the lateral amygdala respond to both unconditioned sound stimuli and to conditioned tone bursts in anesthetized and freely-moving rats (Bordi & LeDoux, 1992; Bordi et al., 1993; Quirk et al., 1995). Pure tones are rarely, if ever, produced in a social context and have no motivational value in the absence of conditioning, yet data on amygdalar responses to species-specific calls, to which an animal is naturally conditioned during development, are conspicuously missing. We postulated that neurons in the basolateral amygdala (BLA) respond more robustly to relatively complex stimuli such as species-specific calls and frequency modulated (FM) sweeps, than to tones. To test our hypothesis, we presented awake mustached bats, *Pteronotus parnellii*, with different intensities of tone bursts (30 ms duration and 0.5 ms rise time) and with 14 species-specific simple syllabic calls and successfully recorded single unit activity and local field potentials (LFPs) with tungsten microelectrodes targeted to different regions (n = 7) of the BLA. Peak responses generally occurred at short latencies (ranging from 11 ms to 15 ms), but response latencies could be as long as 40 and even 150 ms.

Whereas short latencies overlap with those observed in the auditory cortex, the long latency responses were unique to neurons in the BLA and matched more closely those found in a frontal auditory field (Kanwal et al., 2000). LFPs recorded at two locations (bandpass filtered from 2 to 300 Hz) showed complex responses with one or more peaks to a large majority of the different call types, whereas single unit recordings exhibited call selective responses (significant response to <5 of 14 call types) that were nearly twice as big as the response to pure tones. We also observed a directional preference for FM stimuli centered on the bat's resting CF<sub>2</sub> (2nd harmonic, constant frequency component in the echolocation pulse). Regardless of stimulus type, we observed responses only at high (> 70 dB SPL) stimulus amplitudes. There was no clear evidence of a regional specificity or organization of auditory response properties within the BLA. Our data, however, suggest that the BLA exhibits a wide spectrum of auditory responses and may impart call selectivity via local networks that are receptive to behavioral conditioning. Supported in part by NIH/NIDCD research grant DC02054 to J.K.

### **707 Population Coding in Rat Auditory Cortex**

**Kenneth Harris<sup>1</sup>**, Artur Luczak<sup>1</sup>, Stephan Marguet<sup>1</sup>, Peter Bartho<sup>1</sup>, Shuzo Sakata<sup>1</sup>

<sup>1</sup>*Rutgers University*

Our present knowledge of neocortical processing in vivo is mainly based on single unit or paired recordings. What remains less known is the simultaneous response of several cells to sensory stimulation. We recorded the response of populations of 50-100 single units from the auditory cortex of anesthetized and awake rats using multiple site silicon probes. White noise, click, pure tone, and amplitude modulated stimuli were presented free field. At the level of individual cells, a mixture of excitation and inhibition was seen, the timing of which varied across neurons and stimuli, sometimes exhibiting oscillatory patterns. Analysis at the population level revealed complex stimulus-dependent activity sequences in response to stimulation. For temporally unstructured stimuli (pure tones), firing rates evolved for approximately 300ms after stimulus onset, before settling into a steady state, in which cellular firing rates could differ from background rates during silence. Similar sequences were seen after tone offsets and click stimuli. During amplitude modulated stimuli, population activity displayed continuous evolution until 300ms after stimulus offset.

Population responses were variable, even in response to repeated presentation of identical stimuli. However, apparent variability was correlated between recorded neurons. Two types of cross-correlation were observed: narrow peaks (1-2ms) likely reflected monosynaptic connections between neurons, whereas broader peaks likely reflected more complex network interactions. These observations suggest that sensory processing by auditory cortical populations reflects the dynamical evolution of activity in a complex network.

### **708 Corticofugal Modulation of the Paradoxical Response Latencies of Inferior Collicular Neurons in Bats**

**Xiaofeng Ma<sup>1</sup>**, Nobuo Suga<sup>1</sup>

<sup>1</sup>*Washington University in St. Louis*

The central auditory system creates various types of neurons which respond to acoustic stimuli differently from peripheral neurons. One of them is a "paradoxical latency-shift" neuron. The response latency of sensory neurons typically shortens with an increase in stimulus intensity. However, ~10% of inferior collicular neurons of the big brown bat show a paradoxical latency-shift: long latency for strong stimuli and short latency for weak stimuli. Paradoxical latency-shift neurons are tuned to a particular delay of a weak sound from a strong sound, so that they presumably play an important role in ranging (Sullivan 1982). The corticofugal system forms multiple feedback loops and improves and adjusts subcortical auditory signal processing in the frequency, amplitude, time and spatial domains (Suga and Ma 2003, review). However, it has not yet been examined whether the corticofugal system modulates a subcortical paradoxical latency-shift. We electrically stimulated cortical neurons and studied how collicular paradoxical latency-shifts were corticofugally modulated. We found that cortical stimulation evoked two types of changes in paradoxical latency-shift which depended on the relationship in best frequency (BF) between the stimulated cortical and recorded collicular neurons. When the BF was matched, cortical stimulation shortened the latencies of collicular neurons at high intensities, so that the paradoxical latency-shift became smaller. When the BF was unmatched, however, cortical stimulation lengthened the collicular latencies at high intensities, so that the paradoxical latency-shift became larger. Our data indicate that corticofugal feedback is involved in shaping response latencies of subcortical auditory neurons in the time domain through inhibition. (NIDCD DC 00175)

### **709 Organization of Level Dependent Intrinsic Activity in Rat Auditory Cortex**

**Heather L. Read<sup>1</sup>**, Nathan Higgins<sup>1</sup>, Monty A. Escabi<sup>2</sup>

<sup>1</sup>*Department of Psychology, University of Connecticut,*

<sup>2</sup>*Department of Electrical Engineering/Biomedical Engineering*

Primary auditory cortex (AI) and surrounding belt cortices have distinct topographies for bandwidth, level-dependence and cochlear frequency sensitivity. For example, a level-dependent decrease in single and multi-unit frequency response area to pure-tones is a prominent feature of AI and posterior auditory field (PAF) but not anterior-auditory field (AAF). The goal of this study is to quantify topographic shifts in frequency responses to pure-tones with changes in sound level. Comparisons across cortical regions are made using both Fourier intrinsic optical imaging and multi-unit recording methods (Kalatsky et al., 2005). Pentobarbital anesthesia is used to maintain stable recordings. Sounds are presented binaurally via a tube and speakers are calibrated to account for any frequency distortions. Optical activity is induced with short

duration 50 msec pure-tones presented as an ascending or descending frequency stair case and repeated over a 10 minute period. A fixed decibel level is chosen for each 10 minute imaging session. Multi-unit activity is induced with short duration 50 msec pure-tones with a pseudo-random order for tone frequency and decibel level. Small systematic shifts in frequency tuning with decibel level are observed across the entire cochleotopic map with both methods. In several regions, multi-unit frequency tuning at a given decibel level was highly predictive of the frequency tuning derived from intrinsic imaging data. Several sub-regions with non-monotonic level dependence were identified with both methods. The topographic organization of level dependence likely reflects parallel forms of encoding for this acoustic parameter in the auditory cortices. supported by NICHD: HD2080

#### **710 Local Area Network and Its Function in the Gerbil's Auditory Cortex-Reversible Focal Inactivation with Infrared Laser Irradiation Technique**

**Akira Yamamoto<sup>1</sup>, Takashi Doi<sup>1</sup>, Motoi Kudo<sup>2</sup>, Hiroshi Riquimaroux<sup>1</sup>**

<sup>1</sup>*Graduate School of Engineering, Doshisha University,*

<sup>2</sup>*Department of Anatomy, Shiga University of Medical Science*

This study investigated local area network in AI (primary auditory cortex) and AAF (anterior auditory field) by blocking neural activities with the near-infrared laser irradiation. In previous in vivo studies, the laser irradiation could focally inhibit neural activities in a few minutes after the irradiation started, while the activities recovered in a few minutes after its cessation (Riquimaroux and Kataoka, 2005). By using this technique, the present study examined corticocortical relationships in the gerbil's auditory cortex. CF (constant frequency) and FM (frequency modulated) tones were presented to anesthetized animals, and neural responses were extracellularly recorded contralaterally to the ear of stimulation. When we irradiated adjacent areas to a recorded area within AI or AAF, the neural activities of some neurons were disinhibited and the neurons started to show firings to the frequencies that had not elicited activities before the irradiation. When irradiated AAF area and recorded neural responses from AI, the irradiation changed phasic responses into tonic responses, and vice versa. These results indicate that there are functional connections within AI or AAF, and between AI and AAF, and that these connections play an important role to modify time-response patterns of neural responses. Indeed, we found neurons showing different time courses in their responses to FM tones depending on the FM direction. For instance, a neuron which elicited tonic responses to falling FMs generated phasic responses to rising FMs. Generally, BFs (best frequencies) of neurons in AI and AAF are well organized, and neighboring neurons have slightly different BFs. The present findings might explain how to create the difference in temporal firing patterns responding to different FM directions. These data suggest that neurons in the auditory cortex are

capable to modify time-response patterns of neural activities by using neighboring connections.

#### **711 Correlations of Neuronal Spectral and Temporal Response Properties with Location in the Marmoset Auditory Thalamus**

**Edward Bartlett<sup>1</sup>, Xiaoqin Wang<sup>1</sup>**

<sup>1</sup>*Johns Hopkins University, Baltimore, Maryland*

As auditory information ascends the auditory pathway, representations of sound features become parsed into several processing streams. Multiple auditory processing streams have been described in the auditory brainstem and midbrain that are involved in precise temporal coding or encoding species-specific vocalizations. Furthermore, two cortical auditory processing streams that have been described in analogy with vision are the 'what' and 'where' streams. As the information bottleneck of nearly all auditory input that reaches the cortex, the auditory thalamus is the site of convergence for subcortical auditory pathways and serves as the basis for establishing cortical processing streams. However, the types of processing streams through the primary and non-primary subdivisions of the auditory thalamus are poorly characterized. We have recorded from the single neurons in the auditory thalamus of the awake marmoset and tested their responses to modulated and unmodulated tones, modulated and unmodulated noise stimuli, and click trains. We are examining how the spectral and temporal response properties of neurons are correlated with each other and with their locations in the auditory thalamus, thereby forming the basis for parallel output channels to the cortex. Preliminary data indicate that neurons that do not synchronize to high modulation rates are found mainly caudally and medially in the auditory thalamus whereas those that are well-synchronized at high modulation rates are found rostrally and laterally.

#### **712 Topographic Organization of Sound Frequency and Intensity Across Multiple Auditory Cortical Fields in the Rat**

**Daniel Polley<sup>1</sup>, Michael Merzenich<sup>2</sup>**

<sup>1</sup>*Vanderbilt University - Department of Hearing & Speech Sciences,* <sup>2</sup>*University of California, San Francisco - Department of Otolaryngology*

The functional architecture of a single auditory cortical field arises from a 'lattice' of independent maps that code for sound frequency, bandwidth, intensity, and binaural interaction type. The position of various auditory cortical fields and their inherent organization for these response features has been extensively studied in the cat but less so in other species. The present report describes the functional layout of five tonotopically organized fields in the rat auditory cortex obtained through high density microelectrode mapping experiments: The primary auditory cortex (AI), the posterior auditory field (PAF), the ventral auditory field (VAF), the ventroanterior auditory field (VAAF), and the anterior auditory field (AAF). A topographic ordering index was calculated for a broad range of response features and applied to each auditory field. In addition to the expected cochleotopic organization,

we also observed a spatially ordered representation for preferred sound level, rate-level function monotonicity, and sharpness of tuning in AI, VAAF and AAF. The present results demonstrate that spatially ordered maps for multiple auditory feature parameters can co-exist even within the small physical scale of the rat cortex.

### **713 Which Physical Sound Unit Drives the Binaural System?**

**Lutz Wiegand<sup>1</sup>**

<sup>1</sup>*University of Munich*

The experiments and simulations of Heil and Neubauer [PNAS, 2003] have shown that both absolute psychophysical threshold and electrophysiological first-spike latency are determined by the integrated pressure envelope.

Does this finding also apply to the psychophysics of the timing of above-threshold stimuli?

We tried to measure this using an envelope ITD paradigm where we asked listeners to match the lateralisation of a diotic stimulus and a stimulus with different pressure envelopes in the two ears. Stimuli were trains of 12 temporally asymmetric tone pips (carrier = 5 kHz; 2-ms linear rise, no steady-state, 4-ms linear decay time) presented at a period of 16 ms. One interval consisted of a binaural reference and a test sound. The reference sound was always diotic with the pips having a 2-ms rise and 4-ms decay time. The test sound, whose ITD was varied to match the lateralisation of the reference sound, was presented in two different conditions: (1) pips in both ears had the 2-ms rise and the 4-ms decay time or (2), pips in the right ear were time inversed (4-ms rise, 2-ms decay). Lateralisation matches were obtained for 5 different sensation levels between 20 and 60 dB.

At 20 dB SL, listeners advanced the pips with the 4-ms rise time by about 1.1 ms relative to the pips with the 2-ms rise time to be lateralised as the diotic pips. With increasing SL, this advance decreased exponentially to about 0.58 ms at 60 dB SL.

These results are inconsistent with the hypothesis that the binaural crosscorrelation is performed at a fixed pressure-envelope integral. Instead, the crossing points of the pressure-envelope integrals increase with increasing SL.

These results question the validity of a pressure-envelope approach for the temporal coding of above-threshold stimuli. The data shed new light onto how ITD information may be integrated over time.

### **714 The Cost of Dividing Auditory Attention Between Two Spatial Locations**

**Virginia Best<sup>1</sup>, Prity Bengani<sup>1</sup>, Frederick J. Gallun<sup>1</sup>, Barbara G. Shinn-Cunningham<sup>1</sup>**

<sup>1</sup>*Hearing Research Center, Boston University*

A psychophysical experiment was conducted to measure the performance cost associated with tracking two speech sources simultaneously (dual task) compared to tracking just one source in the competing pair (single task).

Two different sentences were presented simultaneously from two loudspeakers separated about the frontal midline.

Three different spatial configurations were examined, with the sources at  $\pm 10^\circ$  (close),  $\pm 45^\circ$  (intermediate), or  $\pm 90^\circ$  (far). For each listener and each spatial configuration, an appropriate amount of noise was added to the loudspeakers to equalize the difficulty of the single task and fix performance at about 85%. Cost was calculated as the drop in performance in the dual task compared to the single tasks.

It was hypothesized that if spatial attention acts like a 'spotlight' then there should be less cost in the dual task for the close configuration. Results showed that the cost was approximately equal across the three configurations. However, when the cost was recalculated without penalizing simple confusions between the two sentences, there was significantly less cost in the close configuration. The results suggest that while spatial separation reduces confusions between competing messages, it increases the cost of attending to both messages simultaneously.

[Work supported by a grant from ONR]

### **715 Speech Recognition and Spatial Release from Masking Under Binaural and Monaural Vocoder Simulations with Variable Number of Frequency Bands**

**Soha Garadat<sup>1</sup>, Ruth Y. Litovsky<sup>1</sup>, Gonggang Yu<sup>1</sup>, Sarah Neader<sup>1</sup>, Fan-Gang Zeng<sup>2</sup>**

<sup>1</sup>*Binaural Hearing and Speech Laboratory, Waisman Center, UW-Madison, USA*, <sup>2</sup>*Hearing and Speech Research Laboratory, School of Medicine, UC-Irvine, USA*

Speech reception thresholds (SRTs) were measured using binaural vocoder simulations to assess the limits imposed by cochlear implants (CIs). Stimuli were convolved through HRTFs to produce virtual sound locations. SRTs were measured adaptively for variable frequency bands (4-, 8-, 16-, and natural) in quiet and in the presence of competing speech. Target words were at  $0^\circ$  and the competing sentences were in front ( $0^\circ$ ), right ( $90^\circ$ ) or left ( $-90^\circ$ ). Target and interfering stimuli were recorded with different male talker and presented over headphones under binaural or monaural (R ear) conditions. Nine normal-hearing adult subjects participated. Results showed that under binaural conditions performance worsened as the number of frequency bands was decreased, evidenced by increase in SRTs and also increase in masking. Binaural conditions were successful in reproducing the free-field effect of spatial release from masking (SRM; improvement in performance due to spatial separation of the target and competitors). SRM increased as the number of frequency bands was reduced. In the monaural conditions there were similar improvements in performance as a function of decrease in frequency bands, however, SRM only occurred when the competing sentences were presented from the left (ear with better signal to noise ratio). The respective contributions to performance of head shadow and binaural summation effects will be discussed. In conclusion, these findings suggest that binaural fittings of CIs may be especially critical for speech understanding in noise under conditions of reduced spectral resolution.



**716 Binaural Temporal Processing: Role of the Cochlear Phase Response and Cross-Channel Analysis**

**David Magezi<sup>1</sup>**, Katrin Krumbholz<sup>1</sup>

<sup>1</sup>*MRC Institute of Hearing Research, University Park, Nottingham, United Kingdom*

It is generally assumed that the analysis of interaural time differences (ITDs) is performed in a channel-by-channel manner and that the channels whose temporal responses are being compared originate from corresponding places along the two cochleae. Recent physiological results suggest, however, that ITD processing may involve the comparison of timing information from non-corresponding channels, i.e., channels with different characteristic frequencies. The aim of this experiment was to test whether the binaural system is able to compare temporal information from non-corresponding channels and to examine the role of the cochlear phase response in ITD processing. ITD discrimination threshold was measured for tones that were partially masked by highpass- or lowpass-filtered noises. The high- and lowpass noise maskers were designed to make the basal or apical part of the cochlear travelling-wave response to the tones inaudible. In a first condition, the spectral characteristics of the masker were the same in both ears. In a second condition, the masker in one ear was highpass filtered whereas the masker in the other ear was lowpass filtered. ITD discrimination thresholds were measured with a 2AFC procedure, in which the listener judged whether the second of two tones was lateralised further to the left or the right than the first tone. The results from the first condition suggest that the basal part of the travelling wave is more important for ITD processing than the apical part with its steeper phase gradient. Results from the second condition indicate that the binaural system can indeed extract ITDs from different parts of the cochlear response in the two ears; however, performance was much worse in this condition. These results provide important constraints for models of interaural temporal processing and would be expected to have implications for the development of spatial pre-processing strategies in hearing aids and cochlear implants.

**717 Contralateral Masking of Narrow Bands of Speech**

**Frederick J. Gallun<sup>1</sup>**, Christine R. Mason<sup>1</sup>, Gerald Kidd, Jr.<sup>1</sup>

<sup>1</sup>*Hearing Research Center, Boston University*

For listeners identifying a speech target processed into eight narrow frequency bands, performance suffers in the presence of a speech masker composed of six non-overlapping narrow frequency bands. When the two speech signals are presented monaurally, performance may be significantly influenced by the presence of noise added to the opposite ear. When the noise spectrum matches the *masker* speech bands, performance improves, but when the noise matches the *target* speech bands, performance declines (Kidd et al., JASA v. 118(2), 2005). This study examined this phenomenon further by testing the effect of contralateral noise on unmasked (no

ipsilateral speech masker) speech target bands varying in number from 2 to 8. The contralateral noise was either multiple narrow bands matched to the bands of the target or was broadband. For the multiple narrow bands of noise, performance was reduced relative to the no-noise case, but only for the fewer numbers of target bands. With broadband noise, there was no effect regardless of the number of speech bands. It appears likely that the interference caused by the contralateral noise depends on the matching, narrowband nature of the stimuli and, in some manner, the difficulty of the speech task. [Work supported by NIH/NIDCD and AFOSR]

**718 Characterizing Binaural Sensitivity to Dynamic Interaural Level Differences**

**Eric R. Thompson<sup>1</sup>**, Torsten Dau<sup>1</sup>

<sup>1</sup>*Center for Applied Hearing Research, Technical University of Denmark*

Perceptual experiments were performed with the goal of measuring the sensitivity of the binaural system to dynamic interaural level differences (ILDs). The test subjects were to identify the interval with interaurally antiphasic amplitude modulation with either unmodulated (detection task) or diotically amplitude modulated (discrimination task) reference intervals in three-interval, forced-choice tasks. High frequency pure-tone as well as diotic and uncorrelated narrowband noise carriers were used in the experiments. In addition, the amplitude modulation detection thresholds were measured in the presence of interaurally in-phase and antiphasic amplitude modulation maskers. The results showed a limited frequency resolution in the processing of interaural level fluctuations in the binaural system. These results were used to develop and test a processing model that aims at accounting for detection and masking data with monaural and binaural, static and dynamic signals. The model was based on the key stages from the monaural modulation-filterbank model from Dau et al. (1997) and the binaural processing model from Breebaart et al. (2001).

**719 Effect of Rearing in Omnidirectional White Noise on the Auditory Resolution in Azimuth Sound Localization in the Mongolian Gerbil (*Meriones Unguiculatus*)**

**Julia Maier<sup>1</sup>**, Teresa Hoeffe<sup>2</sup>, Benedikt Grothe<sup>2</sup>, Georg M. Klump<sup>1</sup>

<sup>1</sup>*Oldenburg University*, <sup>2</sup>*University of Munich*

The interaural time difference (ITD) is used by the auditory system to compute the azimuth localization of a sound source. ITD tuning of MSO-neurons is mediated by glycinergic inhibition. In an anatomical study in gerbils Kapfer et al. (2002) demonstrated that glycinergic synapses in the MSO undergo an experience-dependent refinement process. Before hearing onset, glycinergic inputs are distributed over somata and dendrites of the cells. After hearing onset, they are restricted to the somata. Seidl & Grothe (2005) reported a correlated maturation of ITD sensitivity on a single cell level. By rearing gerbils in omnidirectional white noise the refinement process can be disturbed (Kapfer et al. 2002)

having negative consequences for the ITD sensitivity (Seidl & Grothe 2005). Here we test psychophysically if rearing gerbils in omnidirectional white noise also reduces their auditory resolution in azimuth sound localization. Noise-reared gerbils (NRGs) were trained in a 2AFC paradigm with food rewards to report if stimuli were presented to them from the left or the right side by choosing the appropriate direction in a y-maze. Stimuli were 125-ms pulses of broad-band noise, 300-Hz-wide bands of noise with center frequencies 0.5 and 2 kHz, and tones of 0.5, 1, 1.5, 2, 4 and 8 kHz. Here we present minimum resolvable angles (MRAs) of NRGs (n=7) and compare these with MRAs of gerbils raised without noise treatment (n=4). Although there was no significant difference between the mean resolution in azimuth for specific stimulus types, the mean performance of the NRGs was always worse than that of untreated gerbils. The sample of NRGs always had a larger variance than that of untreated gerbils. For tones of 0.5 and 2 kHz this difference was significant ( $p < 0.05$ , Levene test) and there was a trend for tones of 1.5 kHz ( $p = 0.055$ , Levene test). The performance of individual NRGs will be compared to the distribution pattern of glycinergic synapses in their MSO.

Supported by the DFG

## **720 Interhemispheric Interplay and Asymmetries in Spatial Perception of One vs. More Than One Sound Source: A Comprehensive Analysis of Performance in Patients with Acquired Brain Lesions**

**Manon Grube**<sup>1</sup>, Claudia Schubert<sup>2</sup>, D. Yves von Cramon<sup>3</sup>, Rudolf Ruebsamen<sup>2</sup>

<sup>1</sup>Auditory Research Group, Medical School, University of Newcastle, <sup>2</sup>Institute for Biology II, University of Leipzig, <sup>3</sup>Day Clinic for Cognitive Neurology, University of Leipzig

The present study set out for a comprehensive analysis of interhemispheric differences in spatial localization, discrimination and bilateral recognition. Included patients had suffered MCA strokes or intracerebral hemorrhage, and were previously diagnosed with contralesional (LHC, RHC) or bilateral (LHB, RHB) headphone deficits associated with damage of auditory cortex and beyond, respectively. Basic localization was impaired in right- and left-hemisphere patients of both groups, exhibiting systematic contralesional compressions and overall decreased accuracy. Discrimination however, was much more affected by right-hemisphere damage, the overall smaller left-hemisphere deficits were more pronounced in LHB than in LCH patients. In bilateral recognition, right-hemisphere damage again had a more severe impact; proportions of extinction was tendentially higher in RHB vs. RCH patients and LHB vs. LHC patients. The results presented support bilaterally organized, contralaterally dominant basic sensory representations of auditory space. Right-hemisphere dominance for more complex spatial processing was evidenced in spatial discrimination, requiring the allocation of subsequently active sound sources with respect to each other, and was further corroborated in bilateral recognition. The milder yet present deficits after extended left-hemisphere damage

point to its complimenting role, in particular to right-hemifield perception. The comparative analysis revealed no systematic correlations between tasks in right-hemisphere patients, while in left-hemisphere patients deficits tended to increase together. In conclusion, the results suggest contralateral dominance for basic localization of single sound sources, followed by right-hemisphere dominance in increasingly demanding tasks involving simultaneous or subsequent allocation of more than one sound source, complimented by left-hemisphere contribution in spatio-temporal aspects.

## **721 Independent Effects of Simultaneous Inputs from the Saccule and Lateral Semicircular Canal. Evaluation Using VEMPs**

**Shotaro Karino**<sup>1</sup>, Ken Ito<sup>1</sup>, Atsushi Ochiai<sup>1</sup>, Toshihisa Murofushi<sup>1,2</sup>

<sup>1</sup>Department of Otolaryngology Head and Neck Surgery, Faculty of Medicine, University of Tokyo, <sup>2</sup>Department of Otolaryngology, Tokyo Postal Services Agency Hospital, Tokyo, Japan

**Objective:** To determine the effects of stimulation of bilateral lateral semicircular canals (LSCCs) by accelerated rotation and caloric stimulation of unilateral LSCC on vestibular evoked myogenic potentials (VEMPs) in healthy volunteers.

**Methods:** In experiment 1, VEMPs were recorded while subjects (n=11) were seated in a rotational chair and angular acceleration around the earth-vertical axis was provided. Amplitudes of p13-n23 were corrected using background muscle activities. In experiment 2, subjects (n=8) in the semi-lateral position kept the LSCC in the vertical position and activated the sternocleidomastoid muscle by twisting the neck. After irrigating the external auditory canal with ice water, VEMPs were recorded on the irrigated side. In experiment 3, the same setting as experiment 2 was applied (n=6), and hot water of 44°C was used for irrigation.

**Results:** There were no significant differences in latencies of p13 or n23, and in corrected amplitudes by either rotatory or caloric stimulation.

**Conclusions:** Simultaneous stimulation of LSCCs has little effect on VEMPs.

**Significance:** No functional interaction between the saccule and LSCC was detected in VEMPs, although convergence of semicircular canal and otolith nerve inputs onto single vestibular nucleus neurons has been demonstrated electrophysiologically in animal experiments.

## **722 Influence of Diazepam in Unilateral Vestibular Re-Input Model Using Tetrodotoxin with Osmotic Pump**

**Kenji Takeno**<sup>1</sup>, Hiroaki Shimogori<sup>1</sup>, Hiroshi Orita<sup>1</sup>, Kuniyoshi Tanaka<sup>1</sup>, Tsuyoshi Takemoto<sup>1</sup>, Takefumi Mikuriya<sup>1</sup>, Hiroshi Yamashita<sup>1</sup>

<sup>1</sup>Yamaguchi University School of Medicine

Diazepam is a medicine used in the treatment of acute vestibular vertigo. It is well known that it influences vestibular compensation process. In the past, studies investigating effect of diazepam in peripheral vestibular

destruction was reported. However, no study was reported, which investigating effect of diazepam on a model that the vestibular function recovered like recurrent vertigo such as Meniere's disease. We made peripheral vestibular re-input model by tetrodotoxin (TTX) administration to unilateral inner ear with osmotic pump and examined the influence of diazepam to the vestibular system in this model.

Hartley white guinea pigs were used in this study. TTX administration to unilateral inner ear was performed for 3 days with osmotic pump. Two groups (TTX alone administration group (n=7) and diazepam administration group (n=6)) were made. Caloric response and VOR were observed in 7 and 14 days after 3 days TTX administration finished (7 and 14 days after vestibular re-input). Statistical difference was examined between two groups.

Seven days after vestibular re-input, directional preponderance of the nystagmus(DP) to the TTX-treated side was observed in TTX alone administrated group. DP was disappeared 14 days after vestibular re-input. DP was not observed in diazepam group in each examined day.

These results suggest that diazepam may be useful for the patients in acute stage of peripheral vestibular vertigo, by decreasing vertiginous symptom.

### **723 Acute Peripheral Vestibulopathy Originated from Singular Nerve Territory**

**Ja-Won Koo<sup>1</sup>**, Jae-Jun Song<sup>1</sup>, Min-Hyun Park<sup>1</sup>, Kwang Dong Choi<sup>2</sup>, Ji Soo Kim<sup>2</sup>

<sup>1</sup>Department of Otolaryngology Seoul National University College of Medicine, <sup>2</sup>Department of Neurology Seoul National University College of Medicine

Acute peripheral unilateral vestibular loss of unknown etiology is also diagnosed as (cochleo)vestibular neuritis or labyrinthitis/neurolabyrinthitis depending on the possible extent and hearing involvement. Even though the extent of vestibular involvement can be variable, it is more likely partial rather than a complete vestibular paresis, with predominant involvement of the superior division (horizontal and anterior semicircular canal and utricle). Anatomical and embryological differences demonstrated by the temporal bone study may explain this relative vulnerability. Though the involvement of inferior division sparing superior one has been reported, isolated involvement of singular nerve territory sparing saccular function has not been demonstrated yet. We report on a case of atypical cochleovestibular functional loss in 41 year-old previously healthy woman without any cardiovascular risk factor. Cochleovestibular function was serially assessed using audiometry, caloric test, conventional rotation test, vestibulo-ocular reflex during head thrust test using scleral search coil, vestibular evoked myogenic potentials (VEMP), and fundus photograph. Initial spontaneous nystagmus was subtle down beating with counterclockwise torsional component, which was augmented by head shaking maneuver and isolated right posterior semicircular canal deficit was noted during head thrust test. VEMP thresholds and the waveforms showed symmetric and the parameters were within normal range. Serial vestibular functional evaluations are demonstrated in this atypical peripheral

vestibulopathy patient and possible mechanisms are discussed.

### **724 Effect of Local Application of Vitamin E on AMPA-Induced Vestibulotoxicity in the Guinea Pig**

**Hiroaki Shimogori<sup>1</sup>**, Kazuma Sugahara<sup>1</sup>, Takefumi Mikuriya<sup>1</sup>, Kenji Takeno<sup>1</sup>, Hiroshi Orita<sup>1</sup>, Hiroshi Yamashita<sup>1</sup>

<sup>1</sup>Yamaguchi University School of Medicine

Ischemic injury is one of the major causes of inner ear diseases. The ischemic injury induced elevation of glutamate concentration in the cochlear perilymph. Glutamate is the most likely neurotransmitter between hair cells and primary afferents in the inner ear. But excessive glutamate also has toxic effects on the inner ear. We previously reported that local application of edaravone, one of the free radical scavengers clinically used in Japan, was useful to protect vestibular periphery from AMPA-induced peripheral vestibular disorder like ischemic injury. The aim of this study was to evaluate effect of vitamin E, another kind of antioxidant, on AMPA-induced peripheral vestibular disorder.

Twenty Hartley guinea pigs with normal Preyer's reflexes and normal tympanic membranes were used in this study. Intracochlear administration of AMPA (10 mM) was performed at 0.6 ml/hr for 5 minutes by a syringe pump. Thirteen animals were treated with AMPA alone (group A). In the remained 7 animals, Vitamin E-soaked gelform was put on the round window membrane just after AMPA administration (group B).

After surgery, we measured the frequency of spontaneous nystagmus in each animal as the number of quick phase beats per minute at 6, 9, 12, 15 and 18 h after surgery. We performed caloric tests 1 week after surgery by irrigating the external auditory meatus with 5 ml ice-cold water for 10 sec in the dark. Nystagmus was recorded on videotape with an infrared charge-coupled device camera, and caloric response time was measured. We calculated the time ratio as the ratio of the treated side response time (right) to the untreated side response time (left).

No significant difference was found both in the frequency of spontaneous nystagmus and the time ratio between the group A and B.

Our results indicate that local application of vitamin E may not be so useful for treatment of vertigo induced by ischemia, compared with edaravone.

### **725 Vestibulo-Collic Reflex (VCR) as a Physiologic Tool for Evaluating Vestibular Function in Guinea Pigs**

**Ana H. Kim<sup>1,2</sup>**, Keiji Takemura<sup>1</sup>, Yehoash Raphael<sup>1,2</sup>, W.M. King<sup>1,2</sup>

<sup>1</sup>Kresge Hearing Research Institute, The University of Michigan, Ann Arbor, MI, USA, <sup>2</sup>Department of Otolaryngology, University of Michigan

The vestibulo-collic reflex (VCR), much like the vestibulo-ocular reflex, attempts to stabilize head position in space during body motion. We measured VCR in normal adult guinea pigs by attaching a loop of wire (head coil) to the

guinea pig head, and placing the animal in an electromagnetic field. The animal's body was restrained, but the neck and head were positioned to retain a relatively normal range of motion. Animals were subjected to sinusoidal (1-15 Hz) and abrupt angular accelerations ranging in both the horizontal (yaw) and vertical (pitch) dimensions. The compensatory head movement in response to this stimulus represented the VCR. Guinea pigs demonstrated greater gain in yaw ( $0.45 \pm 0.11$ ) than in pitch ( $0.26 \pm 0.11$ ). This observation may be due to their relatively heavy head and neck anatomy, hampering their motion against gravity during pitch. Vestibular lesions were induced with ototoxic drugs. Unilateral lesions resulted in reduced gain ( $0.23 \pm 0.08$ ) that were highly nonlinear on postoperative day 1, with subsequent improvement by day 7 ( $0.32 \pm 0.10$ ) in yaw, with phase leads of 4-24 degrees. Bilateral lesions resulted in an even greater reduction of gain ( $0.13 \pm 0.06$ ) on postoperative day 1 that improved by postoperative day 7 ( $0.26 \pm 0.01$ ). Unlike the unilateral lesioned animals, bilateral vestibular lesions induced larger phase leads that were more pronounced at higher frequencies. These data suggest that this novel method of assessing vestibular function in guinea pigs can be useful for research on vestibular impairment, with important implications on vestibular hair cell regeneration on balance.

This work was supported by NIH/NIDCH Grants R01-DC01634, R01-DC05401, and P30-DC05188.

#### **[726] Vergence-Mediated Modulation of the Human VOR Is Unaffected by Canal Plugging**

**Americo A. Migliaccio<sup>1</sup>, Lloyd B. Minor<sup>1</sup>, John P. Carey<sup>1</sup>**

<sup>1</sup>*Johns Hopkins University School of Medicine*

The normal angular vestibuloocular reflex (VOR) adapts with increased gain when viewing a near target. Intratympanic (IT) gentamicin not only reduces VOR gain but also abolishes this vergence adaptation. Animal studies suggest that vestibular afferent spontaneous firing continues, but modulated responses do not after IT gentamicin. It has been suggested that canal plugging should have the same effect.

The effect of anterior canal (AC) plugging on the VOR for passive head impulses in canal planes while viewing a far (124cm) or near (15cm) target was studied in 5 human subjects using scleral search coils. We tested subjects before and after AC plugging to treat vertigo caused by dehiscence of the AC. Impulses were low-amplitude ( $\sim 20^\circ$ ), high-velocity ( $\sim 150^\circ/\text{s}$ ), high-acceleration ( $\sim 3000^\circ/\text{s}^2$ ) head rotations in the planes of the canals. Targets were placed in the plane of the canal being stimulated.

Before plugging VOR gain for the ipsilateral AC went from  $0.82 \pm 0.13$  for far targets to  $0.98 \pm 0.13$  for near targets ( $+20.4 \pm 7.4\%$ ). After plugging the AC VOR gain went from  $0.51 \pm 0.12$  for far targets to  $0.61 \pm 0.13$  for near targets ( $+19.4 \pm 6.1\%$ ). There was no difference in the vergence-mediated gain increase between pre- and post-plugged conditions ( $P=0.82$ ). AC plugging also did not change the latency of the VOR for either AC.

These results are in contrast to those found in subjects treated with IT gentamicin, who have similar far-viewing ipsi-lesional VOR gains ( $0.55 \pm 0.19$ ) to AC-plugged subjects but no gain increase during near viewing. In addition, in gentamicin-treated subjects the ipsi-lesional VOR latency during both near and far viewing is significantly greater than the contra-lesional latency. We hypothesize that gentamicin may have a preferential effect on the non-linear component of the VOR, but that canal plugging does not.

#### **[727] The Fate of Calyceal Afferents in Chinchilla Semicircular Canal Cristae After a Single Intratympanic Gentamicin Injection**

**Eugene Chu<sup>1</sup>, Lee-Ching W. Anderson<sup>1</sup>, Mohamed Lehar<sup>1</sup>, John P. Carey<sup>1</sup>**

<sup>1</sup>*Johns Hopkins University, Baltimore, Maryland*

Gentamicin and the aminoglycoside class of antibiotics, while useful clinically, are known to cause nephrotoxicity, cochlear toxicity, and vestibular toxicity. The selective toxicity of gentamicin for vestibular hair cells has been exploited in the treatment of the vestibular symptoms of Ménière's disease. Nevertheless, the mechanisms by which these ototoxic effects are mediated remain unknown. Previous studies in the chinchilla have demonstrated the preferential and near complete destruction of type I hair cells and their associated nerve calyces after intratympanic gentamicin treatment. However, our laboratory has found physiologic evidence for the persistence of calyceal remnants after intratympanic gentamicin treatment based on the continued firing of very irregular units, which in controls are known to be calyx only units. Utilizing immunohistochemical techniques and antibodies selective for calyx associated proteins (tenascin) and calyx only afferents (calretinin) we provide additional morphologic evidence for the persistence of calyceal remnants. Calyx associated tenascin immunoreactivity was abolished after treatment with gentamicin, suggesting damage to the calyceal ending. However, post-gentamicin calretinin immunoreactivity persisted in thick fibers within the stroma of the crista ampullaris and in globular endings within the neuroepithelium. This suggests that afferent calyces may lose their type I hair cells and extracellular matrices but remain in the form of globular endings after gentamicin treatment. These endings may still make en face contacts with type II hair cells, which could provide the synaptic activity for continued spontaneous firing.

Keywords: aminoglycosides, vestibular hair cells, calretinin, tenascin, Ménière's disease

#### **[728] Differential Uptake May Explain Selective Toxicity of Intratympanic Gentamicin for Vestibular Type I Hair Cells**

**Sofia Lyford-Pike<sup>1</sup>, Casey Vogelheim<sup>1</sup>, Eugene Chu<sup>1</sup>, John P. Carey<sup>1</sup>**

<sup>1</sup>*Johns Hopkins University School of Medicine*

The ototoxic effect of gentamicin has been used to advantage in the treatment of intractable vertigo in

Ménière's disease. Intratympanic injections control vertigo in >90% of cases. Histological studies have found that the loss of Type I vestibular hair cells far exceeds that of Type II cells in animal models. Stereocilia and apical structures of these hair cells may be lost without complete loss of the cell body. The objective of this study was to determine whether this selective toxicity for Type I hair cells was attributable to selective uptake of the drug by these cells. The localization of gentamicin within vestibular epithelium was determined by both direct and indirect methods. Gentamicin conjugated to Texas Red was used as a direct tracer, and anti-gentamicin antibody provided an indirect means of localization. Conjugated or unconjugated gentamicin was injected into the left tympanic space of chinchillas. Animals were sacrificed and fixed prior to the onset of signs of vestibular hypofunction (typically at about 2 weeks). Confocal fluorescence microscopy was used to determine the localization of the labels. Results from animals sacrificed within one week of administration showed that numerous Type I hair cells still remained throughout the epithelium. Both methods demonstrated that gentamicin concentration was greater in Type I than Type II hair cells. Gentamicin-Texas Red labeling was restricted to the neck and apical structures of Type I cells. Anti-gentamicin antibody labeling appeared in the majority of Type I hair cells throughout their cytoplasm, but with particular intensity at the apex. Weaker anti-gentamicin antibody labeling appeared in the apices of some Type II cells. These results suggest that Type I hair cells are more susceptible to gentamicin because they more avidly take up or retain the drug in the early period after administration. Localization of the drug to apical structures of the hair cells correlates to the greater loss of these structures compared to that of hair cell bodies.

## **729 Do Vestibular Efferents Play a Role in Long-Term Vestibular Compensation Following Unilateral Labyrinthectomy in Response to Passive or Active Head Movement?**

**Soroush G. Sadeghi<sup>1</sup>**, Lloyd B. Minor<sup>2</sup>, Kathleen E. Cullen<sup>1</sup>

<sup>1</sup>*Dept of Physiology, McGill University*, <sup>2</sup>*Dept of Otolaryngology, Johns Hopkins University*

Stimulation of the primate vestibular efferent system results in an increase in the resting discharge and a decrease in the sensitivity of the afferent fibers (Goldberg and Fernandez, 1980). Based on these findings, we speculated that, following unilateral lesions, the efferent system may contribute to compensation by extending the working range of the afferents on the contralesional side. To test this proposal, we first recorded from a total of 393 canal afferents in three macaque monkeys before (total=191, horizontal (HC)=70, anterior (AC)=71, posterior (PC)=50) and from the contralesional vestibular nerve at periods of 1-12 months after (total=202, HC=89, AC=69, PC=44) unilateral labyrinthectomy. The distribution of the resting rate and  $cv^*$  of afferents before and after labyrinthectomy did not differ. Also, we saw no change ( $p>0.05$ ) in the resting rate of the regular ( $106 \pm 23$  vs.  $96 \pm 25$  sp/s), high-gain irregular ( $123 \pm 31$  vs.  $109 \pm 27$  sp/s), and low-gain irregular ( $93 \pm 46$  vs.  $85 \pm 40$  sp/s) units. The

sensitivity and phase lead of the responses to passive rotations were not different before and after the lesion for the wide range of frequencies tested (0.5-15 Hz) for velocities up to  $80^\circ/s$  ( $P>0.05$ ). A subset of neurons were further tested during voluntary head on body movements. Responses were comparable before and following labyrinthectomy. Consistent with this finding, we also saw no significant effect on afferent responses when 1) the neck proprioceptors were passively stretched by rotating the body under a stabilized head and 2) when a neck motor command was produced while the head was stabilized (mean torques =  $\sim 2$  Nm). Taken together, these findings strongly suggest that the vestibular efferents by means of their afferent connections do not play a significant role in long-term compensation following unilateral labyrinthectomy.

## **730 Age Related Changes in Gravity Receptor Function in CBA/CaJ Mice**

**Bruce E. Mock<sup>1</sup>**, Sherri M. Jones<sup>1</sup>

<sup>1</sup>*East Carolina University*

While much is known about age-related hearing loss, relatively little is known about age related functional changes in the vestibular periphery. Most studies have focused on structural changes in the end organs and eighth nerve and studies of function have used indirect measures such as vestibulo-ocular reflex. The CBA/CaJ mouse strain, in comparison to other widely used mouse strains, is known to retain good hearing sensitivity until advanced age. We were interested in determining if this strain retains gravity receptor function as well. The purpose of the present research was to characterize gravity receptor function in CBA/CaJ mice across age. To do this, linear VsEPs, a direct measure of utricular and saccular function, were recorded in mice ages 2 months to 20 months. For statistical analyses, mice were grouped into 4 age categories: 2-5 months, 6-8 months, 9-12 months, and 18-20 months. VsEP thresholds, peak latencies and peak to peak amplitudes were quantified and analyzed using ANOVA and MANOVA. VsEP thresholds for the various age groups were as follows: 2-5 months ( $-8.2 \pm 2.5$  dB re: 1g/ms), 6-8 months ( $-8.8 \pm 2.4$  dB re: 1g/ms), 9-12 months ( $-6.0 \pm 1.7$  dB re: 1g/ms) and 18-20 months ( $-3.9 \pm 2.5$  dB re: 1g/ms). On average, VsEP thresholds were significantly poorer for the oldest age group when compared to mice younger than 9 months, but were not significantly different from the 9-12 month old group. Peak latencies and peak to peak amplitudes were not significantly different across age. Latencies for P1

ranged from  $1.36 \pm 0.07$  ms to  $1.54 \pm 0.18$  ms in the youngest to oldest age groups, respectively. P2 latencies ranged from  $2.20 \pm 0.82$  ms to  $2.50 \pm 0.28$  ms. Amplitudes for the youngest to oldest groups ranged from  $0.72 \pm 0.18$   $\mu$ V to  $0.67 \pm 0.18$   $\mu$ V for P1-N1. P2-N2 ranged from  $0.79 \pm 0.27$   $\mu$ V to  $0.77 \pm 0.15$   $\mu$ V. These results suggest that CBA/CaJ mice retain good gravity receptor sensitivity until at least one year of age. At 12 months, they may begin to show a slight decline in gravity receptor sensitivity and by 18 to 20 months show a significant functional loss. The time course of age related changes in gravity receptor

sensitivity appears to be similar to that reported for auditory function in CBA/CaJ mice.

### **[731] Distinct Patterns of Cortical Hemispheric Activation Are Evident Using Speech Stimuli in Subjects with Right Ear Compared to Left Ear Unilateral Deafness**

Jill Firszt<sup>1</sup>, Wolfgang Gaggl<sup>2</sup>, John Ulmer<sup>2</sup>, Robert Probst<sup>2</sup>, Edgar DeYoe<sup>2</sup>

<sup>1</sup>Washington University School of Medicine, <sup>2</sup>Medical College of Wisconsin

Studies in animals (Kites, 1984) and humans (Ponton et al., 2001) suggest that unilateral hearing loss modifies the documented asymmetric cortical activation patterns in the auditory cortex and the effects of unilateral deafness may be ear-dependent (Khosla et al., 2003).

The purpose of the current study was to investigate the effects of ear of stimulation on hemispheric activation patterns in human adult subjects with profound unilateral hearing loss in one ear and normal hearing in the contralateral ear. To expand on previous studies, speech stimuli were presented in quiet and in noise to the intact ear. A non-speech stimulus (e.g., pulsed noise) was employed for comparison with speech stimuli results. Hemodynamic responses using functional magnetic resonance imaging (fMRI) were obtained for both hemispheres of the auditory cortex.

Results indicate a distinct difference in the hemispheric cortical activation patterns of adults with complete unilateral hearing loss that is dependent on the ear of stimulation and therefore ear of deafness (i.e., right ear stimulation-left ear deafness or left ear stimulation-right ear deafness) and whether the stimulus is speech compared to non-speech, or speech in quiet or noise.

Specifically, with left ear deafness (i.e., right ear stimulation) cortical activation is greatest in the left or contralateral hemisphere and is asymmetric. When speech is presented in noise, the asymmetry is diminished, yet the dominant hemisphere is contralateral to the ear of stimulation. In right ear deafness (i.e., left ear stimulation) cortical activation is greatest in the left or ipsilateral hemisphere and is symmetric rather than asymmetric. When noise is added, the overall activation is decreased and the asymmetric pattern is variable.

In response to a non-speech stimulus, activation was consistently greater in the contralateral hemisphere to the ear of stimulation, regardless of the ear of deafness.

Supported by NIH/NIDCD K23DC05410

### **[732] The Neural Basis of Delayed Auditory Feedback - Posterior Auditory Cortex and Right "Broca's Area"**

Sophie K. Scott<sup>1</sup>, Hideki Takaso<sup>1</sup>, Richard J.S. Wise<sup>2</sup>

<sup>1</sup>University College London, <sup>2</sup>MRC Clinical Sciences Centre

Previous PET studies have shown an important role for left posterior auditory fields and left anterior insula in speech production. Here we present a PET study of speaking under delayed auditory feedback: subjects read a story

aloud during scanning, and received DAF at 0, 50, 125 or 200ms. Subjects were able to continue speaking under all DAF conditions, although they all rated their speech as harder as the DAF increased in duration. Neural activity (as indexed by regional cerebral blood flow) increased with amount of DAF in bilateral non-primary auditory fields, running lateral and posterior to primary auditory cortex. There was also activity in a right homologue of Broca's area. This indicates that there is sensitivity not just to the existence of DAF in non-primary auditory fields, but also to the precise amount of DAF. We cannot however yet specify whether such activity relates to the processing of DAF discrepancy, control of speech output timing, or both, when the subjects speak under DAF. However it is striking that a similar right Broca's area has been shown to be suppressed during propositional speech production and is activated in the same subjects during rhythmic counting (Blank et al, 2003). We suggest, therefore, that at least some of the activation seen is associated with aspects of timing control when speaking under DAF. These results also show a linking of speech input/output systems, which have basis in the known anatomy of the primate brain. We would also like to suggest that the dominance of the left hemisphere in speech production may be modulated by the timing constraints of the speech production task.

### **[733] Feature-Based Mapping of Speech Sounds in Auditory Cortex: Common Mechanisms for Vowels and Consonants?**

Jonas Obleser<sup>1</sup>, Sophie K. Scott<sup>1</sup>, Aditi Lahiri<sup>2</sup>, Carsten Eulitz<sup>2</sup>

<sup>1</sup>University College London, <sup>2</sup>University of Konstanz

The apparently effortless identification of speech is one of the human auditory cortex' finest and least understood functions. This is partly due to difficulties to tease apart effects of acoustic and phonetic attributes of speech sounds. Here we present evidence from two magnetic source imaging experiments showing that the auditory cortex represents speech sounds (such as [g], [t], [u], [i]) in a topographically orderly fashion, which is based on the phonetic feature PLACE OF ARTICULATION.

Healthy subjects listened to a variation of natural German speech sounds edited from spoken words, while auditory evoked fields were recorded with a whole-head magnetoencephalograph (MEG). In a study on different German vowels, it was found that the origin of the most vigorous brain response after ~ 100 ms (N100m) in auditory cortex depended not on phoneme identity, but on the mutually exclusive PLACE feature assigned (front vs. back vowel) irrespective of other features such as rounding or tongue height. For vowels, this brain map could in principle be explained through quasi-linear second formant's frequency coding. However, when translating this design to a set of acoustically much more variable stop consonants, the very same mapping was found, dependent on mutually exclusive PLACE features front (alveolar) vs. back (velar), irrespective of voicing.

The consonant mapping also turned out to be speech-specific, i.e. only when consonants were identifiable as members of a native speech sound category, the

topographical spreading-out in the auditory cortex was observed. Most importantly, feature separation in cortex also varied with a listener's ability to tell these easy-to-confuse consonants from one another. In sum, our recent results demonstrate that speech-specific maps of features can be identified in human auditory cortex, and they will further help to delineate speech processing pathways based on models from functional neuroimaging and non-human primates.

### **734 Cortical Responses to Speech After Cochlear Implantation**

**Frank Eisner<sup>1</sup>**, Stuart Rosen<sup>1</sup>, Richard J.S. Wise<sup>2</sup>, Sophie K. Scott<sup>1</sup>

<sup>1</sup>University College London, <sup>2</sup>MRC Clinical Sciences Centre

We investigated the organization of the cortical speech processing system in a proficient adult cochlear implant user (BL) with positron emission tomography. Both BL and normal-hearing control listeners showed activation of the left anterior superior temporal sulcus during stimulation with intelligible speech, but not with acoustically similar, unintelligible speech. Unlike in control listeners, there was activation in visual cortex in BL in the intelligible listening conditions. Earlier reports of activity in visual areas during speech processing in cochlear implant users have been attributed to cross-modal plasticity, specifically, to a stronger association of the auditory and visual modalities that is formed as a consequence of greater reliance on lipreading. The present results suggest that visual areas in cochlear implant users may not be involved in early acoustic-phonetic analysis, but may possibly be recruited for higher levels of language processing or for the integration of contextual cues. A second finding of the present study was that anterior superior temporal regions in the right hemisphere, which were activated in control listeners when stimulation required the processing of pitch variation, did not show a response in BL. An account of this latter result is that the absence of a strong sensation of pitch from birth has led to cortical reorganization and a disengagement of these areas from speech processing.

### **735 Hemispheric Representations of Word Meaning in Tonal Language Speakers as Revealed by the Mismatch Negativity**

Hao Luo<sup>1</sup>, Jing-Tian Ni<sup>1</sup>, Da-Ren Zhang<sup>1</sup>, Fan-Gang Zeng<sup>2</sup>, Lin Chen<sup>1</sup>

<sup>1</sup>University of Science and Technology of China,

<sup>2</sup>University of California, Irvine, USA

It is controversial whether hemispheric specialization for speech is associated with acoustic attributes or with linguistic functions of auditory inputs. Advocates of acoustic association hypothesize that speech processing would be lateralized to the right brain hemisphere when input signals are variant in frequency but to the left when variant in time regardless of their linguistic functions. Advocates of functional relevancy, however, hypothesize that sounds with the same linguistic roles are preferentially processed in the same hemisphere regardless of their acoustic attributes. Mandarin Chinese, a tonal language,

provides an ideal model to test these two hypotheses because in this language spectrally variant lexical tones and temporally variant syllables have equal linguistic functions in defining word meaning. In the current study, a single-syllable Chinese word with a consonant-vowel structure was presented to the native Mandarin Chinese speaking subjects in an auditory odd-ball paradigm and the meaning of the word was deviated through changing either its consonant or its tone. Whole-head electrical recordings of the mismatch negativity and source reconstruction analysis revealed stronger automatic brain responses to changes in word meaning due to deviation in lexical tones in the right hemisphere. In contrast, the responses to changes in word meaning due to deviation in consonants were lateralized to the left hemisphere. Our results demonstrate that although syllables and lexical tones have equal linguistic functions in Chinese language, they are preferentially processed in different hemispheres. We conclude that hemispheric lateralization of speech processing depends, at least at the stage of automatic processing, on the acoustic attributes of input signals in tonal language speakers.

This work was supported by the National Natural Science Foundation of China (Grant No: 30270380, 30228021).

### **736 Learning to Discriminate Between Visually Confusable Speech Segments**

Sharon Thomas<sup>1</sup>, Michael Pilling<sup>1</sup>

<sup>1</sup>MRC Institute of Hearing Research, Nottingham, UK

When people speak, they produce distinctive facial movements (especially of the mouth, tongue, teeth and jaw), which reflect the mechanical manipulations required to produce the sounds of speech. A high degree of correlation exists between vocal-tract behavior and this visually observed facial motion. Numerous studies have shown that seeing the face of a talker can dramatically improve the intelligibility of speech sounds in quiet and noisy environments. However, despite the pervasive influence of visual speech on the perception of auditory speech, the identification of unimodal visual speech (lipreading or speechreading) is a notoriously difficult task. There are a number of factors which contribute to the difficulties of efficient speechreading, the most pertinent of which is that many English sounds look similar on people's lips, such as the bilabials /b/ and /p/. This experiment investigated the effectiveness of training to improve the ability of observers to discriminate highly confusable visual speech segments. The training task was a 2-alternative forced-choice procedure between unimodal visual presentations of the bilabial /b/ and /p/ articulations. On each trial, subjects chose which of two consecutively presented words contained the viseme /b/. The /b/ /p/ words comprised minimal pairs, differing only in their initial phoneme (e.g., bin / pin). Participants indicated whether the /b/ word was in presentation 1 or 2. During training, feedback (correct / incorrect) was given. No feedback was given during test stages. Significant improvements were observed between pre- and post-training tests. These improvements were found both on the same stimulus words as presented in the pre-training test and also in



transfer to new words and to new viewing conditions. 'Sham' training, where all stimulus items contained a /b/ phoneme resulted in performance at chance for both post-training tests. A control condition of no training also resulted in performance at chance for all tests. When the task was changed during training from a 2 alternative forced choice task to a /b/ detection task, (one video presented on each trial, with random feedback), performance was flat across test and training conditions. Results are discussed in terms of ideal learning conditions for effective discrimination between confusable visual speech tokens.

**[737] Effects of Stress Accent and Phonetic Features on the Intelligibility of Speech in Noise**  
**Pierre Divenyi<sup>1,2</sup>**

<sup>1</sup>VA Medical Center, Martinez CA, <sup>2</sup>East Bay Institute for Research and Education

It has been shown that intelligibility of unstressed syllables in sentences is a function of the signal-to-noise ratio (SNR) of the surrounding stressed syllables (P. Divenyi [2005], Proceedings of Forum Acusticum 2005, pp. 1533-1538). This effect was observed across different degrees of word entropy and for young as well as elderly listeners. The finding suggests that, in a "cocktail-party effect" (CPE) situation, information in stressed syllables facilitates the understanding of unstressed syllables even though these latter have an average SNR below that of their stressed neighbors. But how is this information propagation affected by the phonetic features either in the stressed or in the unstressed syllables? Results of the present experiments show that vowel features and the consonantal feature of voicing are transmitted already at very low SNR's regardless of stress level. In contrast, the features of place and manner of articulation in the stressed syllables appear to affect not only the transmission of information in the stressed but also in the surrounding unstressed syllables, suggesting that these two features in the stressed syllables assume the most important role in CPE performance. [Supported by Grant R01-AG07998 from the National Institute on Aging and by the Veterans Affairs Biomedical and Laboratory R&D.]

**[738] Interpreting Consonant and Vowel Confusion Functions Using Information-Theoretic Measures**

**Andrew Lovitt<sup>1</sup>, Sandeep Phatak<sup>1</sup>, Jont Allen<sup>1</sup>**

<sup>1</sup>University of Illinois at Urbana-Champaign

The classical Miller-Nicely 1955 (MN55) closed-set consonant recognition experiment of 16 consonants (C) and a vowel (V), presented with white noise, was repeated using a recorded database of CV sounds (LDC2004-E1). The results show that the consonant confusion patterns differ significantly from the patterns of MN55. A second experiment, having CVs consisting of 4 vowels (16Cx4V) and using speech weighted noise, shows that the shape of the noise spectrum can effect the consonant confusions. Consonant confusions can also correlate with the vowels. Specific spectro-temporal properties of the speech sounds,

that correlate with the confusion patterns, have been established.

**[739] Articulatory Gestures, Not Auditory Frequency Resolution, Determine Formant Frequency Discrimination Thresholds in Vowels**  
**Sadao Hiroya<sup>1</sup>, Takemi Mochida<sup>1</sup>, Makio Kashino<sup>1</sup>**

<sup>1</sup>NTT Communication Science Laboratories

The motor theory of speech perception assumes that the perception of the phonological units of speech is based on inferring the articulatory gestures of the speaker (Liberman and Mattingly 1985, Cognition 21: 1-36), but the validity of this assumption is still controversial. Here, we examined the relationship between thresholds for vowel formant frequency discrimination and articulatory gestures that produce the vowel. To quantify the non-linear relationship between articulatory gestures and formant frequencies in vowels, we simultaneously recorded articulatory gestures (e.g., the movements of the lips and tongue) using an electro-magnetic articulographic (EMA) system and acoustic signals of monophthongal English vowels. The ratio of formant change to articulatory movements was defined as the articulatory-formant sensitivity (AFS). The steady-state vowels of the stimuli were synthesized from the first four formants and fundamental frequencies. We conducted a formant frequency discrimination experiment and found that the discrimination thresholds were significantly correlated with AFS, but not with the predictions by the auditory excitation pattern model. On the other hand, discrimination thresholds for a synthesized sound consisting of four sinusoids, each of which had the same frequency as the corresponding formant of the vowel sound, were explained well by the excitation pattern model. These results are not consistent with previous findings on vowel formant discrimination (Kewley-Port and Watson 1994, JASA 95: 485-496), indicating that vowel perception involves a process incorporating the constraints of articulatory gestures.

**[740] Psychometric Per Utterance Confusion Patterns in Listening Experiments**

**Andrew Lovitt<sup>1</sup>, Bryce Lobdell<sup>1</sup>, Jont Allen<sup>1</sup>**

<sup>1</sup>Beckman Institute for Advanced Science and Technology, University of Illinois at Urbana-Champaign

Confusion matrices (CM) \$P\_{\{H|U\}}(SNR)\$ were collected in a manner similar to the Miller Nicely experiment (1955) for 286 consonant-vowel (CV) utterances (16Cx1V), as a function of signal to noise ratio (SNR) (-18 to +30 dB). We show that for a given CV there is large variability across utterances (i.e., talkers) as the SNR is decreased. Misarticulated utterances are dealt with by a simple entropy measure on the confusion matrix with no added noise. Many utterances are found to "morph" into a related sound (i.e., /ta/->/pa/) as the SNR is decreased. We believe that morphing is a useful tool in basic research on identify elemental perceptual features.

#### **[741] Comparison of Information Extracted by Normal Hearing and Hearing-Impaired Listeners from Temporally Smeared Envelopes of Syllables in Noise**

**Yang-soo Yoon<sup>1</sup>**, David Gooler<sup>1</sup>, Jont Allen<sup>1</sup>

<sup>1</sup>*Univ. of Illinois at Urbana-Champaign*

The goal of the study was to better understand differences in consonant confusions for normal listeners (NH) and hearing-impaired listeners (HI) by quantifying and comparing information extracted from confusion matrices (CMs). CMs were measured as a function of signal-to-noise ratio (SNR: -8, 0, 8, 16, 24, & Quiet) for 16 spectrally degraded consonant-vowel speech sounds. Further, the processed stimuli were temporally smeared by low-pass filtering to produce four smearing conditions: No Smearing and 4Hz, 8Hz, and 16Hz Smearing. Classical information theory was used to estimate the association between stimuli (S) and responses (R). The articulatory feature system that Miller and Nicely (1955) analyzed was applied to the theory. Total information transferred (T) from CMs was computed by subtracting stimulus entropy,  $H(S)$ , from the residual entropy,  $H(S|R)$ , in bits. In our case  $H(S)$  is 4 bits. For NH, T increased steeply with SNR, and reached its asymptote ( $\approx 3$ bits) at 8 dB SNR for each smearing condition. For HI, T increased gradually with SNR, and reached its asymptote ( $\approx 2$  bits) at 8 dB SNR. In general, the amount of information carried decreased with greater temporal smearing. However, for NH a similar amount of information was transmitted for No Smearing and 16Hz Smearing across SNRs. For HI, there was no difference in bits transferred for 16Hz Smearing and 8Hz Smearing. The proportion of T for each feature was computed by  $1 - H(S|R)/H(S)$  and partialled out to indicate the contribution of individual features. For all smearing conditions, NH received 25% more information than HI across SNRs. In particular, duration and nasality contributed the greatest amount of information for both groups. The information on affrication was the least transmitted for both groups. The analysis of the feature system also showed that the five features accounted for almost 80% of T for both groups. A detailed analysis of CMs with information theory will be presented.

#### **[742] Advantage of Noise-Vocoded Speech Sound Training with Real-Time Processor**

**Yang-soo Yoon<sup>1</sup>**, David Gooler<sup>1</sup>, Jont Allen<sup>1</sup>

**Koichi Yamanoi<sup>1</sup>**, Ryosuke Tachibana<sup>1</sup>, Hiroshi Riquimaroux<sup>1</sup>

<sup>1</sup>*Graduate School of Engineering, Doshisha University*

The noise-vocoded speech sound (NVSS) used in the present study was synthesized from natural speech sound where amplitude envelope was preserved and spectral information was replaced by four bands of noise. The short-term training dramatically improved the intelligibility of NVSS, while its intelligibility was extremely low for the first time. The purpose of this experiment was to compare the effect of the conventional training to the one with the training by using the real-time processor. The influence on intelligibility of NVSS by vocalization would be clarified. The real-time processor was a device for transforming the

natural speech sounds into NVSS. Not only the sound presented but also sound that subject vocalized were transformed into NVSS. Normal hearing people served subjects. The subjects were divided into an experimental group and a control group. Each group was trained by different conditions. The sentences were used for the training. The stimuli were presented through the real-time processor in the experimental group. The subjects were instructed to vocalize the perceived sounds. On the contrary in the control group, pre-made NVSSs were presented through a headphone and the subjects were not instructed to recite in the control group. The correct answer was presented visually after the stimulus was presented optional number of times in the both group. Each trial was repeated during the training term and novel sentences were presented in each trial. The perception test of NVSS was carried out to investigate before and after trainings to compare the conventional with the real-time training methods. Twenty sentences, fifty familiar words, and fifty unfamiliar words were used in the test. The intelligibility of familiar words was more improved from pre- to post-training test in the experimental group than the control group, while the intelligibility of sentences and unfamiliar words were not improved.

#### **[743] Adaptation to Noise-Vocoded Speech: Exploring Inter-Individual Variability**

**Carolyn McGettigan<sup>1</sup>**, Sophie K. Scott<sup>1</sup>

<sup>1</sup>*University College London*

Noise-vocoding is a method of distorting speech that simulates the transduction of the acoustic speech signal by a cochlear implant (Shannon et al., 1995). When normal-hearing English speakers hear noise-vocoded sentences, they initially find them very difficult to understand but can learn to "tune in" to the speech after a relatively short period of exposure (Davis et al., 2005). However, in previous studies, we have noticed a considerable amount of variability between individuals in the capacity to recognise and adapt to noise-vocoded speech.

Inter-individual variability in performance has frequently been described in the literature on cochlear implants (Skinner, 2003; Shannon, Fu & Galvin, 2004; Wei, Cao & Zeng, 2004). A number of studies have identified cognitive predictors of success with cochlear implants in adults (Knutson et al., 1991, Gantz et al., 1993). Pisoni and colleagues have carried out similar work in children; Cleary, Pisoni and Kirk (2002) highlighted the encoding and manipulation of phonological representations in working memory as important processes in relation to children's success or failure with their cochlear implant.

The current study investigates variability in speech perception abilities in the normal-hearing population, using noise-vocoded speech to elicit a wide range of speech recognition scores. In an approach similar to that of van Rooij and Plomp (1989, 1990, 1992), we used a battery of tests to assess the relative contributions of auditory, cognitive and demographic factors to speech perception performance. A regression analysis identified working memory, verbal IQ and rhythm perception as possible factors underlying this variation in performance.

**744 Psychoacoustic Assessment of Spectrally Degraded Speech: Comparing Naturally Produced, Sinewave Synthesized and Noise Vocoder Stimuli**

Jeremy Loebach<sup>1,2</sup>, Robert Wickesberg<sup>1</sup>

<sup>1</sup>University of Illinois at Urbana-Champaign, <sup>2</sup>Indiana University - Bloomington

Previous studies have demonstrated that speech perception can persist in the face of severe spectral degradation (Remez et al., 1981; 1994; Shannon et al., 1995); however, a direct comparison of the perceptual consequences of the different forms of spectral reduction has not yet been explored. The purpose of this study was to examine the effects of spectral reduction, by comparing the recognizability of naturally produced, sinewave synthesized and noise vocoder (Shannon) speech stimuli.

Twenty-four naturally produced nonsense syllables were re-synthesized according to the methods of Shannon and colleagues (1995) to contain 1, 2, 3 or 4-bands of envelope modulated noise, and sinewave synthesized according to the methods of Remez and colleagues (1981; 1994). The 144 stimuli were divided evenly across six blocks containing a mixture of each synthesis type, but only a single instance of each syllable. 30 normal hearing, untrained subjects listening via a tubeophone identified the stimuli by selecting one of twenty-four buttons labeled with the stimuli transcriptions that were presented on a computer screen. The responses were summed across subjects to generate a confusion matrix for each of the six synthesis types.

Percent correct identification scores indicated that subjects' performance increased as the spectral degradation of the stimuli decreased. Performance was poorest on the Shannon 1 band tokens, but improved as the number of bands increased from 1 to 4. For the sinewave tokens, performance was midway between the Shannon 2 and 3 band tokens, indicating that three narrow bands of spectral information are better than two, but not as good as three, broad bands of envelope modulated noise. More errors were made in identifying place of articulation for the Shannon tokens, whereas more voicing errors were made for the sinewave tokens. These findings suggest a tradeoff between spectral and temporal information for the features of place and voicing.

**745 Comparing the Neural Encoding and Psychoacoustics of Noise Vocoder (Shannon) Speech: A Physiological Means to a Perceptual End**

Jeremy Loebach<sup>1,2</sup>, Robert Wickesberg<sup>2</sup>

<sup>1</sup>Indiana University, <sup>2</sup>University of Illinois at Urbana-Champaign

In a previous study, we explored the representation of naturally produced and Shannon speech stimuli in the auditory nerve of the chinchilla (Loebach & Wickesberg, 2005; Loebach 2005). Temporal patterns were observed in the ensemble responses to the naturally produced tokens that provided templates for the word initial stop consonants /b/, /d/, /p/ and /t/. These patterns were also observed in

the responses to the Shannon versions of the tokens, and the degree of pattern similarity to the templates varied as a function of spectral reduction. While pattern similarity generally corresponded to past behavioral data (Shannon et al., 1995), the goal of the present study was to compare directly the physiological representations with our psychoacoustic data for these stimuli.

Ensemble responses to naturally produced and Shannon 1, 2, 3 and 4-band versions of the tokens were normalized to their peak firing rate. Dynamic time warping provided a quantitative measure of similarity. Pair-wise comparisons indicated that the degree of pattern similarity increased with the number of noise bands: 1 band stimuli required more warping to be made equivalent to the template, whereas the 4 band stimuli required less warping. Examination of the psychoacoustic data for these tokens revealed that the percent correct recognition scores also increased with the number of bands. To compare the physiological and psychoacoustic data, the warping values were plotted against the percent correct recognition scores. A regression analysis revealed a significant negative linear relationship, indicating that the warping values comparing the physiological patterns decreased as the perceptual accuracy increased. This correspondence suggests that ensemble responses provide a physiological substrate that correlates with psychoacoustic recognition of consonants, and demonstrates that stimuli that produce similar temporal patterns in the peripheral auditory system can elicit a common percept.

**746 Effect of Smoothing Filter Slope Angle on Temporal Speech Information**

Eric W. Healy<sup>1</sup>, Heidi M. Steinbach<sup>1</sup>

<sup>1</sup>University of South Carolina

Recent work has demonstrated that spectral information contained within the skirts of even relatively-steep filters can contribute substantially to narrow-band speech intelligibility. However, experiments employing low-pass filtering in the temporal domain have employed a wide range of smoothing filter slope values. In the current study, intelligibility was assessed for sentences represented by three amplitude-modulated tones as temporal smoothing slope angles were manipulated. Intelligibility by normal-hearing listeners was reduced by factors of approximately two or three as slope angles were increased within the range of commonly-employed values of 6 to 48 dB/octave, despite that the nominal low-pass cutoff value was held constant at either 100 or 16 Hz. However, significant changes in performance were not observed when smoothing slopes were increased beyond 48 dB/octave. These results indicate that especially shallow filtering in the temporal domain may allow information to be present at rates above the nominal cutoff, which may serve to underestimate the availability of higher-rate temporal information [Work supported by NIH].

## **747 Ion Channel Properties and the Second Filter**

**Robert Fettiplace<sup>1</sup>**

<sup>1</sup>*University of Wisconsin-Madison, USA*

Comparison of the sharp frequency tuning of mammalian auditory nerve activity to that of passive basilar membrane mechanics led to the idea of a second cochlear filter, the metabolic vulnerability of which implied a link to hair cell transduction. We explored this notion by recording in the turtle auditory papilla, which exhibits sharp hair cell frequency selectivity but little basilar membrane tuning. Receptor potentials of turtle hair cells were found to be electrically tuned by concerted action of voltage-dependent Ca<sup>2+</sup> channels and voltage- and Ca<sup>2+</sup>-dependent K<sup>+</sup> (BK) channels. Characteristic frequency (CF) is varied by altering the density and kinetics of the BK channels along the cochlea. Studies of single BK channels combined with modeling predicted a smooth gradation in CF using just two kinetic variants forming five heteromeric channels with overlapping distribution. In turtle and in chicken (Ramanathan et al., 1999), which also possesses electrical tuning, kinetic variation of BK channels may stem from differential expression of  $\beta$ -subunits and alternatively spliced  $\alpha$ -subunits. Electrical tuning has not been found in mammals but another tuning mechanism that has results from activation and rapid Ca<sup>2+</sup>-dependent adaptation of the mechanotransducer (MET) channels. This is a transduction filter, centered on the CF, which can drive active hair bundle motion. Changes in adaptation rate with CF occur by altering MET channel properties, especially unitary conductance and by analogy with BK channels, only a few MET channel variants may be needed to achieve a smooth CF gradient. Active hair bundle motion by multiple short hair cells could account for extension of the frequency range in birds. Moreover, this process in mammalian outer hair cells may generate sufficient force to augment passive mechanical tuning and supplement action of the prestin motor particularly at high frequencies.

I wish to thank Andrew Crawford who participated in much of the work described.

## **748 Pathogen Recognition Through Toll-Like Receptors**

**Douglas Golenbock<sup>1</sup>**

<sup>1</sup>*University of Massachusetts Medical School*

During the process of microbial invasion, the innate immune system is activated to produce protective proinflammatory molecules. Microbial products interact with the innate immune system via a variety of receptors; first and foremost in this immune recognition are the Toll-like receptors (TLRs), type I transmembrane proteins containing leucine repeat motif, necessary for ligand binding, and a Toll-interleukin 1 resistance (TIR) domain necessary for subsequent signal transduction. TLR4 activates several innate immune responses, including NF- $\kappa$ B dependent genes, type I interferons and chemokines. TLR4 is the most heavily studied TLR, and constitutes a model of how we believe the other none human TLRs function. The major ligand for TLR4 is bacterial endotoxin, or LPS, and is the central molecule that warns the host of

Gram-negative bacterial infection. Receptor activation by TLR4 involves receptor aggregation and the rapid recruitment of TIR domain containing adapter proteins. Several aspects of TLR4 activation may be unique amongst TLRs. First, TLR4 may not actually bind its ligand, but interact with a co receptor MD-2, which binds LPS directly. MD-2 binding to LPS depends on two highly charged residues, K128 and K132, which appear to flank a hydrophobic pocket in which the fatty acid residues of lipid A may fit. Secondly, TLR4 function involves all four TIR domain containing adapter molecules. TRAM appears to be the major adapter necessary for TLR4 function. Furthermore, the function of TRAM in TLR4 signaling is dependent upon N-myristoylation. Hence, TLR4 responses to endotoxin both represent a paradigm for TLR function, as well as a unique warning system to immune cells for bacterial invasion.

## **749 MyD88-Mediated Neutrophil Recruitment in Immunity Against Staphylococcus Aureus**

**Genhong Cheng<sup>1</sup>**, Lloyd S. Miller<sup>1</sup>, Ryan M. O'Connell<sup>1</sup>, Robert L. Modlin<sup>1</sup>

<sup>1</sup>*University of California, Los Angeles*

Bacterial infection remains a dangerous threat to human health on a worldwide level. Although antibiotics have traditionally been used to treat infections, the prevalence antibiotic resistant bacterial strains are on the rise. Therefore, there is a growing need to better understand the mammalian immune response against infection in hopes of designing a new generation of antimicrobial agents. We have established a bioluminescent *Staphylococcus aureus* infection model to analyze the innate immune response to bacteria in the skin. Using this model, we have found that the adaptor protein MyD88 plays a critical role in bacterial clearance. Furthermore, the MyD88-dependent immune receptors Toll-like Receptor 2 (TLR2) and Interleukin 1 Receptor (IL-1R) were also required for proper bacterial clearance. However, while IL-1R/MyD88 signaling was required for neutrophil recruitment following infection, the TLR2/MyD88 axis was dispensable for this process. Thus, our findings indicate that MyD88 mediates immune receptor specific responses to bacterial infection in the skin.

## **750 Role of TLRs in Middle Ear Inflammation, Mucosal Hyperplasia and Recovery from Otitis Media**

**Allen F. Ryan<sup>1</sup>**, Joerg Ebmeyer<sup>1</sup>, Masayuki Furukawa<sup>1</sup>, Won-Ho Chung<sup>1</sup>, Kwang Pak<sup>1</sup>, Stephen I. Wasserman<sup>2</sup>

<sup>1</sup>*ENT, UCSD and VA Medical Center*, <sup>2</sup>*Medicine, UCSD*

Members of the Toll-like receptor (TLR) family recognize pathogen-associated molecular patterns. The adaptor MyD88 mediates many downstream effects of TLR activation, and the pro-inflammatory cytokine and death ligand TNF $\alpha$  often serves as a shared end point and amplification mechanism. Otitis media (OM) was induced by middle ear (ME) inoculation with nontypeable *H. influenzae* (NTHi) in wild-type and MyD88- or TNF $\alpha$ -deficient mice. In MyD88 nulls, ME leukocyte infiltration and mucosal hyperplasia were normal for the first day after

inoculation. However, while OM peaked on day 2 and then recovered rapidly from day 3 to 10 in wild types, it continued to increase in MyD88-deficient animals until day 5, and remained present at day 10. Moreover, the ME remained culture-positive until day 10, much longer than in wild-type mice. In TNF $\alpha$ -deficient mice, leukocyte infiltration of the ME was substantially higher from day 2 onward, and had not recovered by day 10. Mucosal hyperplasia was similar to wild type until day 3, but greater afterward and had not recovered by day 10. Bacterial clearance was normal. The results suggest that while TLR signaling is involved in OM, initial ME responses to NTHi occur via MyD88- and TNF $\alpha$ -independent mechanisms. Since the time course and magnitude of OM are altered by deletion of either gene, both play a significant role later during OM. MyD88 appears to be required for normal bacterial clearance, while the dominant role for TNF $\alpha$  may be to mediate apoptosis during OM recovery.

Expression of 45,000+ transcripts representing essentially all mouse genes was compared between NTHi-inoculated and sham-inoculated MEs using gene chips. A total of 17 genes related to TLR signaling were differentially regulated at 3 hours, and 21 at 6 hours, also supporting a role for TLR signaling in OM.

(Supported by grants DC00129 and DC006279 from the NIH/NIDCD.)

## **751 Mechanisms of Toll-Like Receptor 9 Activation and Implication for Auto-Immune Diseases**

**Eicke Latz<sup>1</sup>**

<sup>1</sup>*University of Massachusetts Medical School*

Toll-like receptor 9 (TLR9) is activated by nucleic acids in a complex multi-step process. DNA traffics into endo-lysosomal compartments and TLR9 is activated after translocating from the endoplasmic reticulum to endo-lysosomal DNA containing structures. TLR9 can bind many different single stranded DNA sequences and conformations. The microenvironment and the DNA concentration inside endo-lysosomal compartments appear to be critical for TLR9 activation. TLR9 is optimally activated by low concentrations of DNA sequences resembling microbial DNA. These DNA sequences typically contain unmethylated CpG dinucleotides in a certain sequence context. However, TLR9 can additionally recognize high DNA concentrations without the same sequence stringency. In this way, TLR9 can be triggered by DNA-containing immune-complexes that are present in sera of patients with auto-immune disorders, such as systemic lupus erythematosus. These observations open the exciting possibility to pharmacologically target the TLR9 signaling axis.

## **752 TLR-Dependent Signaling Networks in Otitis Media**

**Jian-Dong Li<sup>1</sup>**

<sup>1</sup>*University of Rochester*

Although tremendous effort has been put towards identifying the surface molecules of nontypeable

*Haemophilus influenzae* (NTHi) and *S. pneumoniae* for vaccine development over the past decades, it is only recently that we have begun to appreciate the intricate host epithelial signaling networks activated by NTHi and *S. pneumoniae*, the major human bacterial pathogens causing otitis media. Upon interacting with host epithelial cells, NTHi activates multiple signaling pathways that, in turn, inadvertently contribute to the pathogenesis. Among those signaling pathways, activation of NF- $\kappa$ B leads to up-regulation of IL-1 $\beta$ , IL-8 and TNF- $\alpha$ , mucin *MUC2* and Toll-like receptor 2 (TLR2), whereas activation of p38 MAP kinase mediates not only up-regulation of inflammatory mediators and mucin *MUC5AC* but also down-regulation of TLR2. Interestingly, NTHi-induced activation of PI3K-Akt pathway, however, leads to inhibition of p38 MAP kinase. In addition, TGF- $\beta$ -Smad signaling pathway cooperates with NF- $\kappa$ B to positively mediate up-regulation of mucin *MUC2*, but acts as a negative regulator for NTHi-induced mucin *MUC5AC* transcription via a MAP kinase phosphatase-1 (MKP-1)-dependent down-regulation of p38 MAP kinase. Moreover, glucocorticoids synergistically enhance NTHi-induced TLR2 expression via specific up-regulation of the MKP-1 that, in turn, leads to inactivation of p38 MAP kinase, the negative regulator for TLR2 expression. Finally, our recent study revealed a novel autoregulatory feedback pathway through which activation of NF- $\kappa$ B by TNF- $\alpha$  and NTHi induces CYLD that in turn leads to the inhibition of NF- $\kappa$ B signaling via negative cross-talk with multiple signaling pathways. These studies may bring new insights into molecular pathogenesis of otitis media and open up novel therapeutic targets for these diseases.

(Supported by grants from NIH DC004562, DC005843 & HL070293 to J.D. Li).

## **753 New Method for Deriving Loudness Functions from Binaural Level Differences for Equal Loudness**

**Jeremy Marozeau<sup>1</sup>, Mary Florentine<sup>1</sup>, Michael Epstein<sup>1</sup>**

<sup>1</sup>*Communication Research Laboratory, Northeastern University*

This study proposes a new method to derive loudness functions for individual listeners from Binaural Level Difference for Equal Loudness (BLDEL) data by assuming that the Equal-Loudness-Ratio hypothesis (ELRH) for binaural sounds is true. The ELRH for binaural sounds states that the loudness ratio between monaural and binaural sounds, presented at the same level, is independent of level. In other words, the binaural loudness function is simply an upward vertical shift of the monaural loudness function when plotted on a log scale as a function of level in dB SPL. The vertical distance between the two functions is directly related to the ratio between the binaural and monaural functions. Because the loudness of a binaural sound is often considered to be the double of the loudness of the same monaural sound, the loudness ratio between the binaural and monaural tones was assumed to be two. The horizontal distances between the two functions were then adjusted to correspond to the level difference between equally loud monaural and binaural

tones using a least-squares fit to match with measured monaural-to-binaural equal-loudness matches. The derived individual loudness functions are in good agreement with data in the literature. The slopes of the functions are steeper under 40 dB SPL and above 90 dB SPL than in the mid-level range between 40 and 90 dB SPL. In the mid-level range, the average loudness function can be approximated by a power function of intensity with an exponent of 0.35. In order to test the Equal-Loudness-Ratio hypothesis, cross-modality matching was used to measure loudness growth for the monaural and binaural tones directly. Although there is some variability, the results show that the ratio between the two functions is constant, at least to a first approximation. These findings support the Equal-Loudness-Ratio hypothesis for binaural sounds. [Work supported by NIH-NIDCD grant R01DC02241.]

#### **754 Comparison of Adaptive Psychometric Procedures Based on the Theory of Optimal Experiments and Bayesian Adaptive Techniques** **Jeremiah Remus<sup>1</sup>, Leslie Collins<sup>1</sup>**

<sup>1</sup>*Duke University*

Recipients of cochlear implants have exhibited significant variability in tests of speech recognition, suggesting that for some implantees the percepts and responses evoked by the patterns of electrical stimuli may not adequately transmit the auditory cues necessary for distinguishing certain speech tokens. Psychophysical variables such as electrode discrimination and intensity just-noticeable-differences may help identify these psychophysics-based impediments to speech recognition, and techniques to compensate for the underlying anomalies may improve the transmission of important speech cues [e.g. Zwolan et al. (JASA 1997)]. However, procedures to measure psychophysical data that could potentially be used for tuning the speech processor can be very time consuming and clinically infeasible. In this study, four adaptive psychometric procedures based on the theory of optimal experiments and Bayesian adaptive procedures were considered for measuring the threshold for detecting a stimulus in simulated experiments. Performance was compared to that obtained with currently used procedures. The results indicate an increase in efficiency using the proposed, more sophisticated psychometric methods. Efficient procedures for quickly measuring psychophysical variables and channel interactions will allow the collection of psychophysical data that may be useful for tuning the cochlear implant speech processor for individual subjects, and thus potentially improving speech recognition.

#### **755 Reliability of Measures of Children's Auditory Processing**

**David R. Moore<sup>1</sup>, Melanie Ferguson<sup>1</sup>, Justin Cowan<sup>1</sup>, Alison Riley<sup>1</sup>, Sally Hind<sup>1</sup>**

<sup>1</sup>*MRC Institute of Hearing Research, Nottingham, UK*

The greatest challenge in assessing children's sensory capability is to dissociate their performance of the assessment task from their ability to detect or discriminate stimuli. In psychoacoustics, two general approaches have

been taken to this challenge. One is to model children's behaviour as a 'noisy operator' and to draw inferences about 'sensory' and 'non-sensory' contributions to performance. The other is to study response variability, usually between individuals as a cross-section of age. Here, we have examined variability both within and between test sessions of 6-11 y.o. children's (n=60) performance on a battery of detection (x2), auditory processing (x7) and speech-in-noise (SiN, x2) tests. Younger children performed more poorly than older children, but their pattern of variability was similar. At all ages, variability was low between successive threshold determinations within a single detection and processing test session ( $r=0.52$  to  $r=0.92$ ; all  $p<0.001$ ). However, between sessions separated by a mean of 34 days (range 7–82), variability was much greater, overall, with individual tests showing either moderate ( $r=0.48-0.68$ ) or poor ( $r=0.08-0.26$ ) test-retest correlation. Poor correlations were, for some tests, associated with tightly clustered data and/or poor performance of outliers in one session, usually the first. However, some tests, notably amplitude (AM) and frequency (FM) modulation detection, showed widely variable performance across the sample. SiN tests also showed age-related improvements and modest correlations ( $r=0.33-0.62$ ) between sessions for sentence- and syllable-in-noise and –in-quiet thresholds. Quiet-noise threshold differences, an index of the greater difficulty hearing in noise, did not change with age, but did show modest intersession correlations ( $r=0.29-0.49$ ). These results show that intrasession reliability is a poor predictor of intersession reliability when measuring children's auditory processing. Some tests commonly used to assess auditory processing (AM and FM) were found unreliable while others (masking, frequency discrimination) were more reliable.

#### **756 Efficiency Versus Precision of Adaptive Threshold Estimation in Animal Psychoacoustics: Evidence from Auditory Discrimination in Rats**

**Bernhard Gaese<sup>1</sup>, Christian Felsheim<sup>2</sup>, Isabella King<sup>3</sup>, Wolfger von der Behrens<sup>1</sup>, Joachim Ostwald<sup>2</sup>**

<sup>1</sup>*J.W. Goethe-Universität Frankfurt a.M.*, <sup>2</sup>*Universität Tübingen*, <sup>3</sup>*RWTH Aachen*

Psychoacoustical methods are used to estimate perceptual abilities in humans and in a variety of animals, very often by determining thresholds of detection and discrimination. Using methods for adaptive threshold estimation has strongly facilitated psychophysical investigations in humans, and became recently also more common in animal research. Such adaptive procedures track the presumed threshold based on the subject's previous responses. Modern versions of these are based on maximum likelihood or Bayes' estimation, thereby being optimized for speed and accuracy. In fact, normal listeners perform in many cases close to optimal performance as it is determined by computer simulations. The question is how robust these methods are against the corrupting effects of false responses, as they occur frequently in animal research or under clinical conditions. This can be measured by determining the number of trials needed to obtain reliable thresholds.

In a first experiment, we investigated the ability of rats to discriminate between upward and downward modulated FM-tones as a function of sweep speed in a two-alternative-forced-choice-paradigm. Variations of the stimulus with different FM sweep range and lower frequency boundary of FM sweeps were tested in adaptive testing procedures. Animals needed between 220 and 400 trials for reliable threshold estimation based on very conservative criteria. While thresholds after 30 trials did not correlate very well with final thresholds ( $r = 0.31$ ), data after 50 or 100 trials provided very good estimates.

Several thresholds were determined simultaneously in a second series of experiments by intermingling several adaptive procedures in one session. Experiments on free-field binaural unmasking in rats quantified the improvement in threshold when signal and masker were presented with different interaural properties. As well-trained animals were able to perform up to 3000 trials in one session, it was possible to determine thresholds for the different conditions (up to 7) with adaptive procedures in one session. Trial numbers for robust estimates of final thresholds were comparable to trial numbers in the FM experiment.

### **757 Evidence for an Effect of Attention on the Buildup of Across-Frequency Streaming**

**Adrian K.C. Lee<sup>1</sup>**, Rhodri Cusack<sup>2</sup>, Robert P. Carlyon<sup>2</sup>, Barbara G. Shinn-Cunningham<sup>3</sup>

<sup>1</sup>Harvard-MIT Division of Health Sciences and Technology, Speech and Hearing Bioscience and Technology, <sup>2</sup>Medical Research Council Cognition and Brain Sciences Unit,

<sup>3</sup>Hearing Research Center, Department of Cognitive and Neural Systems, Boston University

In everyday life, we often have to select one source from the mixture of sounds that reach our ears. To assist this selection, the auditory system segregates acoustical energy into different auditory objects or streams based on available acoustical cues. Here we investigate whether an auditory object, formed by grouping energy across frequency, is affected by attention.

The stimuli were an alternation between a pure tone (A) and a harmonic complex (B) in an ABA-ABA-ABA- pattern, with the whole sequence lasting 20 seconds. The harmonic complex was spectrally shaped to create a synthetic vowel, and repeated at half the rate of a separate, ongoing stream of pure tones. The vowel was generated such that its perceived identity depended on whether or not one particular harmonic (the "target") was perceived in the complex (shifting the vowel from /eh/ when the target was perceived in the complex to /ih/ when the target was not perceived in the complex).

Both the perceived vowel identity and the perceived rhythm of the tone sequence changed over time. To test whether the change in vowel percept was affected by attention, we presented the 20-second-long ABA-sequences to one ear and a 7-second-long series of noise bursts to the contralateral ear (with the two starting simultaneously). In one condition, subjects were asked to judge properties of the contralateral noises for their 7-sec duration, then to switch attention to the ABA- sequence and judge vowel identity. In a second condition, subjects

ignored the noise bursts and judged vowel identity throughout the entire 20 secs. Results suggest that there is a pre-attentive adaptation process akin to phonemic transformation, but that, in addition, the extent to which the target component was integrated into the vowel depends not only on the time that the ABA sequence has been presented, but also on the time over which it is attended. These results imply that attention affects auditory scene analysis in ambiguous stimuli containing a "target" that logically can fall into one of two competing auditory objects. [Portions of this work were supported by a grant from ONR N00014-04-1-0131].

### **758 The Relative Contributions of Pitch and Presentation Ear on the Perceptual Grouping of Competing Sounds**

**Nandini Iyer<sup>1</sup>**, Douglas Brungart<sup>1</sup>, Brian Simpson<sup>1</sup>

<sup>1</sup>Air Force Research Labs

While studying auditory grouping, it is not uncommon to investigate the relative salience of grouping cues by providing listeners with two or more competing cues. The aim of this experiment was to investigate the relative contribution of pitch (F0) and location as grouping cues to segregate a target and masking talker. For this purpose, the phrases in the Coordinate Response Measure (CRM) corpus were divided into short time intervals that alternated from a low to high F0 or from the left to right ear at a rate of 1 to 128 Hz. Listeners heard these sentences in three experimental conditions where the target phrase was combined with a single masker phrase that alternated in such a way that only a single talker was present in each ear at any given time: 1) Constant Pitch, where the target and masker phrases were presented at fixed F0 values but were presented to alternate ears in each time segment; 2) Constant Ear, where the target was presented to one ear and masker was presented to the other ear, but both alternated between a high and low pitch in each time segment, and 3) Alternating Pitch and Ear, where the target and masker phrases alternated from a low pitch in one ear to a high pitch in the opposite ear. Additional data was collected in a diotic control condition where the target and masker phrases alternated in pitch but were presented to both ears simultaneously. The conditions were designed so that listeners grouping the target signal on the basis of pitch would perform better in the Constant Pitch condition but poorly in the Constant Ear condition, whereas listeners grouping on the basis of ear would perform better in the Constant Ear condition but poorly in the Constant Pitch condition. Results indicated that listeners tended to group target by ear when the pitch shifts were smaller, but pitch dominated when the differences were relatively large.

### **759 Informational Masking and Spatial Asymmetry in a "Cocktail Party" Environment: Results with Children and Adults**

**Patti Johnstone<sup>1</sup>**, Ruth Y. Litovsky<sup>1</sup>

<sup>1</sup>University of Wisconsin-Madison, USA

Spatial release from masking (SRM) was studied under conditions of 'informational masking' in free field. Speech intelligibility thresholds were compared when interferers were (1) near the target speech (at 0°) or (b) spatially



separated from the target by 90° to the right or left. Participants were 30 adults and 30, 6-7 year-old children (equal numbers of males and females). Informational masking was introduced by (1) varying the interferer content (male voices, female voices or modulated noise); and manipulating uncertainty in the auditory environment (interferer type either known or randomly altered on a trial-by-trial basis).

Adult listeners demonstrated a significant spatial asymmetry of 3.5 dB for all interferer types, but only for context uncertainty. SRM was larger when the interferers were on the right side; when the left ear has a better SN/R the spatial advantage is larger than when the right ear has a better SN/R. In children there is no overall asymmetry, however, when broken down by gender it appears that while young girls perform more like adults, young boys demonstrated a reversed asymmetry of about 2.5 dB. These findings suggest that spatial asymmetry in the presence of noise is opposite to that seen under dichotic listening conditions in quiet.

Work supported by NIH-NIDCD (F31 DC 006785 and R21 DC 006642)

### **760 Effects of Signal/Masker Duration and Forward Masking Fringes on the Binaural Detection of 500-Hz Tones**

Leslie Bernstein<sup>1</sup>, Constantine Trahiotis<sup>1</sup>, Richard Freyman<sup>2</sup>

<sup>1</sup>University of Connecticut Health Center, <sup>2</sup>University of Massachusetts

Using a single-interval adaptive psychophysical procedure, we measured the detectability of 500-Hz pure tones presented in the NoS $\pi$  configuration against a background of either narrowband or broadband masking noise. The study was designed to investigate and to account for the effects on thresholds of varying the durations of the signals and maskers in both “pulsed” and “forward-fringed” masking conditions. A novel finding was that, in both broadband and narrowband masking conditions, the presence of brief forward fringes of masking noise resulted in *increases* in threshold for the shortest signal durations. Longer forward fringes led to *decreases* in threshold when the masker was broadband, replicating earlier studies. When the masker was narrowband, however, the presence of longer forward fringes did not lead to decreases in threshold. The data can be accounted for quantitatively via: 1) a “pre-detection” temporal integration associated with peripheral auditory filtering; 2) across-frequency, duration-dependent, influences that differentially affect broadband and narrowband NoS $\pi$  detection and 3) a central, i.e., “post-detection,” stage of binaural temporal integration.

### **761 A Binaural Model of Monotic Level Discrimination**

Daniel Shub<sup>1,2</sup>, H. Steven Colburn<sup>2</sup>

<sup>1</sup>Massachusetts Institute of Technology and Harvard University, <sup>2</sup>Boston University Department of Biomedical Engineering

This work explores conditions in which performance on a monaural level discrimination task is degraded by a

stimulus presented to the “other” ear with both psychophysical and modeling techniques. A one-interval, two-alternative-forced-choice paradigm was used in the psychophysical portion of the work. The target tone (600 Hz, 300 ms, 0° phase) was presented at the left ear with a level of either 50 (un-incremented) or 58 (incremented) dB SPL. A distractor tone (600 Hz, 300 ms) was simultaneously presented to the right ear. The phase and level of the distractor tone were randomized (level between 50 and 80 dB and phase between  $\pm 90^\circ$ ) on a trial-by-trial basis. In the absence of the distractor, the probability of correct was over 0.95, while in the presence of the distractor, performance was reduced to a probability of correct of 0.75. Performance was highly influenced by the distractor level and phase. For example, with the un-incremented target, when the distractor level was below 60 dB the probability of correct was over 0.8, but when the distractor level was 80 dB the probability of correct was 0.45. A detailed analysis of how performance varied with the distractor level and phase for both the un-incremented and incremented targets will be presented. A model based on the binaural level (the sum of the levels of the target and distractor) and lateral position (a weighted sum of the interaural differences in time and level) does not predict the psychophysical results; this two-dimensional model predicts a strong bias that is not observed in the psychophysics. Adding a third dimension, results in performance being limited only by internal noise. Our modeling focused on the “time-image” (based on interaural time difference) as the added dimension. Predictions of this three dimensional model are both qualitatively and quantitatively similar to the psychophysics.

[Supported by NIH grant DC 00100]

### **762 The Role of Fundamental Frequency in Segregating and Understanding a Talker Competing with Another Talker in a Reverberant Setting**

Madhusudana Shashanka<sup>1</sup>, Sigrid Nasser<sup>1</sup>, Barbara G. Shinn-Cunningham<sup>1</sup>

<sup>1</sup>Boston University

Everyday reverberation usually does not degrade speech intelligibility. Similarly, it is generally easy to understand a talker competing with one other talker. However, understanding a target talker competing with another talker in modest reverberation can be extraordinarily difficult. This study investigated whether providing a robust fundamental frequency (F0) segregation cue could improve target intelligibility.

Because F0 varies over time in natural speech, reverberation can reduce the efficacy of F0 for separating talkers (e.g., Culling et al., JASA 2003; Darwin and Hukin, JASA 2000). We manipulated the pitch contours of target (five-digit TIDIGIT strings) and masker (sentences from the TIMIT database) to produce robust monotone F0 differences ( $\Delta F0$ ) that could improve perceptual segregation of target and masker in reverberation. We compared target intelligibility for natural-F0 and monotone speech at a target-to-masker ratio of 0 dB.

In all anechoic conditions, performance was near ceiling. Reverberation degraded performance for natural-F0 speech. Compared to natural-F0 performance, intelligibility in the reverberant monotone conditions was 1) significantly better when the target was one semitone above the masker, 2) essentially equal for  $\Delta F0 = 0$  or 2 semitones, and 3) significantly worse when  $\Delta F0$  was negative.

Spectro-temporal overlap between target and masker partial explains this initially puzzling result. Compared to the natural-F0 reverberant case, the percentage of time-frequency bins in which the reverberant monotone target had more energy than the masker was higher when  $\Delta F0 > 0$ , equal when  $\Delta F0 = 0$ , and lower for  $\Delta F0 < 0$ . No such interaction between energetic overlap and pitch contour occurred for anechoic conditions.

These results suggest that both energetic masking and perceptual effects influence how F0 affects segregation and intelligibility in reverberant settings. [Portions of this work were supported by grants from CELEST & AFOSR.]

### **763 Listening Strategies Affect the Benefit of Spatial Separation in Informational Masking**

**Antje Ihlefeld<sup>1</sup>, Barbara G. Shinn-Cunningham<sup>1</sup>**

<sup>1</sup>*Hearing Research Center, Boston University*

In cocktail-party settings, target intelligibility improves systematically as the spatial separation between target and any maskers increases. Many of the factors that contribute to this spatial separation advantage (acoustic target-to-masker ratio effects at the better ear, low-level binaural processing) may not require active spatial attention from the listener. However, when informational masking is the primary form of interference, differences in target and masker attributes such as perceived location, timbre, or other cues appear to improve performance because they enable a listener to actively focus attention on the target in a top-down manner.

We explored the relative importance of perceived differences in target and masker location and/or timbre in a selective-attention task dominated by informational masking. We measured performance as a function of spatial separation between two talkers when listeners were given a priori information about target location, target timbre, or both attributes. Results show that spatial separation of the target and masker facilitates target intelligibility only if the subject is cued as to the location of the target. When subjects are provided with a priori knowledge of target timbre but no knowledge of target location, performance is independent of the spatial separation between target and masker. Furthermore, when subjects are cued to target location, the probability that subjects confuse masker content with that of the target decreases with increasing spatial separation; however, when subjects do not know target location a priori, such confusions are independent of target and masker separation. These results suggest that in informational-masking dominated tasks, spatial cues do not provide any bottom-up advantages to speech understanding. Instead, attention must be focused on spatial location in order for spatial separation advantages to be obtained.

[work supported in part by a grant from AFOSR]

### **764 Update on Infants' Increment Detection in Tones and Noise**

**Lynne Werner<sup>1</sup>, Hyunah Jeon<sup>1</sup>, Beth Kopyar<sup>1</sup>**

<sup>1</sup>*University of Washington*

Infants and adults were compared in intensity discrimination for 1000 Hz tones and for broadband noise in two conditions. In one condition the listener detected increments in a continuous sound; in the other condition the listener detected an intensity difference between gated bursts of sound. The gated stimuli and the increments were 500 ms in duration, with 16 ms rise-fall. Stimuli were presented to the listener's right ear through ER1 insert phones. Discrimination thresholds were estimated using an adaptive procedure and the observer-based method. Increment and no-increment (control) trials were presented. Three increments were presented on an increment trial. In the gated condition, bursts were repeated at 1000-ms intervals throughout a test session, and increments alternated with standard intensity bursts on increment trials; trial duration was 6 s. In the continuous condition the standard intensity was present throughout the session, and two trial formats were tested. In one, three increments were presented at 1000-ms intervals; trial duration was 4 s. In the other, three increments were presented at 1500-ms intervals; trial duration was 6 s. The results showed that adults performed better in the continuous condition than in the gated condition, for both tone and noise. Infants performed better in the continuous condition than in the gated condition for noise, but not for tones. There was no difference in performance between the two trial formats in the continuous condition. This result is consistent with the idea that adults listen selectively in frequency when processing narrow-band sounds, but that infants do not. [Supported by NIDCD - R01 DC00396 and P30 DC04661]

### **765 Intrinsic Origin of Hyperactivity in the Hamster Dorsal Cochlear Nucleus Following Intense Sound Exposure**

**Jinsheng Zhang<sup>1</sup>, James Kaltenbach<sup>1</sup>, Jie Wang<sup>1</sup>**

<sup>1</sup>*Wayne State University*

Several lines of evidence indicate that noise-induced hyperactivity in the dorsal cochlear nucleus (DCN) may represent a neural correlate of certain forms of tinnitus. The current study was designed to understand whether maintenance of DCN hyperactivity is dependent on descending input from other brain structures. We used 43 adult hamsters, among which 22 animals were exposed under anesthesia to a 10 kHz tone at 125-130 dB SPL for 4 hours, and another 21 were only anesthetized for 4 hours and served as controls. Thirty to forty days after sound exposure or control treatment, circumferential cuts around the DCN were made in an attempt to isolate the DCN from its adjacent brainstem structures. Beginning 30-40 min following this surgical manipulation, electrophysiological recordings were performed. Spontaneous multiunit activity was recorded from 3 rows of sites with 13-15 sites in each row along the medial-lateral axis of the DCN. Spontaneous events were sampled over a period of 90 sec for each recording site.

Spontaneous rates were calculated and averaged across the 3 rows of recordings in each animal. Group means were then determined by averaging across animals. Histological evaluations were performed to determine the degree to which circumferential sectioning resulted in separating the DCN from inputting fiber tracts including the acoustic striae, subpeduncular route, trapezoid body and olivocochlear bundle. Based on these results, control and exposed animals were divided into 3 subgroups: animals without sectioning, animals with partial sectioning, and animals with complete or nearly complete sectioning. The results showed that circumferential sectioning did not affect significantly the level of peak activity in either control or exposed animals. However, sectioning caused a spread of DCN hyperactivity to more lateral locations in the DCN. Taken together with our previous finding that DCN hyperactivity is independent of peripheral inputs (Zacharek et al., 2002), the current data suggests that maintenance of the magnitude of DCN hyperactivity may be intrinsic to the DCN itself, but the spatial spread of this activity may be influenced by descending inputs. The possible mechanisms related to the origin of DCN hyperactivity and its functional relevance to tinnitus are discussed.

(Supported by Tinnitus Research Consortium).

#### **766 Bilirubin Potentiates Inhibitory Synaptic Transmission in Lateral Superior Olive Neurons of the Rat**

Yasuhiro Kakazu<sup>1</sup>, Shi H.B.<sup>1</sup>, Takashi Nakagawa<sup>1</sup>, Matsumoto Nozomu<sup>1</sup>, Shumei Shibata<sup>1</sup>, Kazutaka Takaiwa<sup>1</sup>, Shizuo Komune<sup>1</sup>

<sup>1</sup>Kyushu University

Bilirubin is a well-known toxin that may result in multiple neurologic deficits. There are lots of evidences suggesting that bilirubin affect neuronal synaptic activity; however, the real-time effect of bilirubin on synaptic transmission, especially the inhibitory synaptic transmission, has been never studied. In this study, using voltage-holding whole-cell patch clamp techniques, we observed the effect of bilirubin on inhibitory postsynaptic currents (IPSC) in postnatal 13 to 15-day-old (P13-15) neurons dissociated from lateral superior olive nucleus (LSO), one of the brainstem auditory nuclei that are highly vulnerable to bilirubin toxicity. The results showed that 10mM bilirubin increased the frequency of spontaneous IPSC (sIPSC) with no change in the mean amplitude, suggesting a presynaptic locus for the action. The facilitation peaked 2 to 4 min after 10mM bilirubin application. At ten minute after the withdrawal of bilirubin, the frequency of sIPSC decreased, but sustained significantly greater rate than that before bilirubin application. Bilirubin exerted no change on the mean amplitude of glycine-evoked postsynaptic currents. In the presence of tetrodotoxin, the frequency of miniature IPSC (mIPSC) was also potentiated by 10mM bilirubin. The action of bilirubin was observed in the absence of extracellular Ca<sup>2+</sup>. Pretreatment of BAPTA-AM in Ca<sup>2+</sup>-free solution fully inhibited the bilirubin action. The facilitation of bilirubin is concentration and exposure duration-dependent. Bicuculline partially abolished the action of bilirubin, suggesting that both GABAergic and glycinergic transmissions are involved in

this facilitation. Thus, in LSO neurons, bilirubin facilitates inhibitory synaptic transmission, which is Na<sup>+</sup>, Ca<sup>2+</sup> channels independent and presynaptic [Ca<sup>2+</sup>]<sub>i</sub> dependent. The increase of inhibitory synaptic transmission shows a novel effect of bilirubin on the central nervous system.

#### **767 The Influence of 'In Vivo' Spontaneous Rates on Short-Term Plasticity in the Calyx of Held Synapse**

Joachim Hermann<sup>1</sup>, Benedikt Grothe<sup>1</sup>, Achim Klug<sup>1</sup>

<sup>1</sup>University of Munich

Neurons in the medial nucleus of the trapezoid body (MNTB) are, like most other auditory brainstem neurons, spontaneously active at certain rates. This property is largely a reflection of auditory nerve spontaneous activity. Thus, the processing of sound stimuli *in vivo* is performed by these neurons on a background of spontaneous activity. This property is lost in most *in vitro* preparations due to the absence of the sensory surface, and thus, *in vitro* studies typically assess the effects of simulated sound stimuli without the naturally present background of spontaneous activity.

The goal of our study was to assess the effect of this background activity on synaptic transmission of the Calyx of Held – MNTB synapse in brain slices of the Mongolian gerbil. This was accomplished by stimulating the afferent fibers of the Calyx with simulated 'spontaneous' activity for at least 2 minutes to pre-condition the neurons. The conditioning stimuli were modeled after *in-vivo* data and were poisson distributed pulse patterns of mean frequencies between 20 Hz and 100 Hz. Voltage clamp recordings performed during the conditioning period show that the EPSC amplitudes initially decrease very fast but then typically reach a steady-state level within the first two minutes of conditioning. At this point the EPSC amplitudes are depressed to 25% - 50% of the initial value, depending on the mean frequency of the conditioning stimulus used.

To evaluate the effect of this treatment on the processing of sound stimuli, we also recorded EPSC amplitudes in response to trains of 100 Hz to 600 Hz. Before conditioning the synapses with 'spontaneous' activity, EPSC amplitudes depress strongly, presumably due to strong synaptic depression. In conditioned synapses, the degree of depression due to the simulated sound stimuli was much smaller and showed a near linear decrease even in the case of stimulating with higher frequencies. It appears that the conditioning steps changed the interactions between effects of short-term synaptic plasticity such as depression or facilitation.

Supported by DFG Grant KL1842 to A.K.

#### **768 Encoding of Interaural Time Differences in the Nucleus Laminaris of the Chicken**

Christine Koepl<sup>1</sup>, Catherine E. Carr<sup>2</sup>

<sup>1</sup>Technical University Munich, <sup>2</sup>University of Maryland

The neurons of the avian nucleus laminaris (NL) encode interaural time differences (ITD) for sound localization. In the barn owl, NL neurons generate ITD selectivity by coincidence detection between binaural excitatory inputs

and encode ITD in a place map according to the Jeffress model. An alternative mechanism of ITD encoding, involving additional inhibitory inputs and requiring no place map of ITD has been shown for the MSO of gerbils and guinea pigs. The two scenarios have been suggested to represent competing optimal coding strategies, depending on head size or the naturally-experienced range of ITDs (Harper and McAlpine, 2004). This suggestion may be tested directly in the chicken, a bird with a head size like a gerbil.

Recording either neurophonic potentials or single units in the chicken in vivo, we characterised 44 NL sites, covering a frequency range from 80 Hz to 3.5 kHz. The majority of these were also histologically verified. Although all sites showed selectivity for ITD, we found pronounced differences between the low- and high-frequency regions of NL.

Data for CFs above 1.5 kHz were consistent with the notion of binaural excitatory inputs determining ITD

selectivity and with the Jeffress model of encoding a range of ITDs. Best ITD varied systematically along the isofrequency axis of NL. Delays to monaurally delivered clicks and tones accurately predicted the best ITD. Best ITD and characteristic delay (CD, determined by testing with a range of frequencies) also correlated well. In contrast, for sites with CF below 1.5 kHz, monaural click and tone responses did not predict best ITD; best ITD and CD did not correlate. The range of best ITDs was larger and included responses that were clearly outside the range naturally experienced by the chicken (Hyson et al., 1994), and we observed a systematic decline of best ITD with increasing characteristic frequency.

Supported by DFG KO 1143/12-2 to CK and by a Humboldt Research Award and NIHDCD 000436 to CEC.

### **769 Low-Threshold Potassium Conductance Enhances Phase-Locking by Bushy Cells in Silico** **John Wittig, Jr.<sup>1</sup>, Kwabena Boahen<sup>1</sup>**

<sup>1</sup>*University of Pennsylvania*

Globular bushy cells in the mammalian cochlear nucleus (CN) exhibit enhanced phase-locking to low frequency tones relative to their auditory nerve (AN) inputs (Joris et al. 1994). These cells are innervated by both modified endbulb and bouton-like synapses from the AN (Liberman 1991; Ostapoff and Moris 1991). Bushy cells express a potassium conductance that activates near rest (KLT; Oertel 1983, 1985; Manis and Marx 1991; Rothman and Manis 2002), which endows them with a fast membrane time constant and a solitary onset-spike response to current injection. Several modeling studies have examined the source of enhanced phase-locking by varying the strength and number of synaptic inputs onto model bushy cells (Joris et al. 1994, Rothman et al. 1993, 1996, 2002). While providing insights into how bushy cells compute, these works did not directly demonstrate the affect of KLT expression on phase-locking enhancement (see Svirskis et al. 2002 for KLT affects on MSO spike-timing).

We have implemented a silicon model of the mammalian CN with a tonotopic arrangement of 1080 globular bushy cells that have active conductances including KLT. Our

model includes four other CN neuron-types with a total of 4410 conductance-based neurons on the chip. Each bushy cell receives synaptic input from low, medium, and high spontaneous rate AN fibers, as well as from inhibitory interneurons modeled on chip (tuberculoventral and d-stellate; Wickesberg and Oertel 1990; Golding and Oertel 1997). By creating a comprehensive model of the CN, we are able to assess how membrane and network specializations within each cell type affect their ability to enhance auditory information. Here we demonstrate the necessity of KLT for phase-locking enhancement: When driven by 13 AN fibers having a collective vector strength (VS) of 0.66 our silicon bushy cells enhance VS to  $0.73 \pm 0.09$  (mean  $\pm$  standard deviation of 120 cells) with KLT enabled, though VS is degraded to  $0.55 \pm 0.12$  with KLT disabled.

### **770 In Vivo Whole Cell Recordings Reveal Patterns of Inhibitory Innervation of Neurons in the Inferior Colliculus**

**Ruili Xie<sup>1</sup>, George Pollak<sup>1</sup>**

<sup>1</sup>*University of Texas at Austin*

The inferior colliculus (IC) receives projections from the majority of lower nuclei and many of those projections are inhibitory. In this study we evaluated inhibitory innervation of IC cells with whole cell recordings in awake Mexican free-tailed bats. The majority of cells had narrow tuning curves, upper-threshold rate-level functions to BF tone bursts and were directionally selective for downward FM sweeps. The most remarkable features of these cells were that they displayed very wide subthreshold inhibitory responses (IPSPs) to tones that spanned up to 2.5 octaves. The inhibitory responses were also remarkable because they were composed of a brief IPSPs evoked by the onset and offset of the tone bursts. EPSPs were evoked but only by a small range of frequencies "sandwiched" between the on and off IPSPs evoked by frequencies above and below those that evoked the EPSPs. We propose a circuit that could explain the subthreshold responses evoked in these cells and how that circuitry could generate the discharge features evoked both by tones and FM sweeps in these cells.

Supported by NIH grant DC 00268.

### **771 New Evidence for a Pitch Helix in the Ventral Nucleus of the Lateral Lemniscus in the Gerbil**

**Gerald Langner<sup>1</sup>, Susanne Braun<sup>1</sup>, Claudia Simonis<sup>1</sup>, Christina Benson<sup>2</sup>, Nell Cant<sup>2</sup>**

<sup>1</sup>*Darmstadt University of Technology, Germany*, <sup>2</sup>*Duke University Medical Center, USA*

As reported previously (Assoc.Res.Otolaryngol. 26:Abs. 683, 2003), evidence was found for a helical organization of the ventral nucleus of the lateral lemniscus (VNLL) in the gerbil. This finding is in line with tracer studies in the rat by Merchán and Berbel (J. Comp. Neurol. 372, 1996). Furthermore, functional mapping experiments using the 2-deoxyglucose technique (2-DG) revealed a periodotopic organization in the VNLL which is reminiscent of the pitch helix known from psychophysics. We now present new

evidence for this unique functional organization of the VNLL and discuss its possible role in periodicity analysis.

Many neurons in the central nucleus of the inferior colliculus (ICC) are tuned to modulation frequencies and are arranged in periodicity maps orthogonal to the tonotopic map. In line with a model of periodicity analysis (Langner, Hearing Res. 60, 1992) we observed comb-filters in neurons of the ICC shortly after onset of their responses to periodic signals. After this initial phase, the measured transfer functions were continuously changing into band-pass filters. It is likely that the source of the underlying inhibition, which seems to be precisely synchronized to the signal periodicity, is the VNLL.

The periodotopic organization is probably created first at the level of the ICC. However, because our tracer studies have demonstrated that the VNLL receives feedback from the ICC, we also expected to find some evidence of periodotopy in the VNLL. Our new results from 2-DG experiments confirmed our previous results which showed that in the VNLL low pitch is represented dorsally and high pitch ventrally. Three-dimensional reconstructions of the VNLL gave evidence for a helical periodicity map with 7 to 8 turns.

Finally, after restricted injections of a retrograde tracer, biotinylated dextran amine, into the ICC, topographically organized labeling of both fibers and neurons in the ipsilateral VNLL was observed. The labeling patterns were in agreement with an underlying helical organization of the VNLL. This interpretation was confirmed by a three-dimensional computer reconstruction (program AMIRA).

## **772 A Comparison of Possible Neural Architectures for Tuning Curve Enhancement in the Inferior Colliculus**

Ian Bruce<sup>1</sup>, Jennifer Ko<sup>1</sup>

<sup>1</sup>McMaster University, Hamilton, ON, Canada

Some neurons in the mammalian inferior colliculus (IC) exhibit threshold tuning curves that are sharper than those of auditory nerve fibers, particularly at high intensities. The presence of inhibitory sidebands in response maps of these IC neurons has led several investigators to suggest that a lateral inhibitory network (LIN) in the IC is the neural architecture responsible for the tuning curve enhancement (e.g., Yang et al., J. Neurophysiol. 1992; Suga, Neurosci. Res. 1995). However, data from the IC of chinchilla (Palombi and Caspary, J. Neurophysiol. 1996) indicate that the majority of the inhibitory input to these neurons is aligned in frequency with the excitatory input, rather than from lateral inhibitory connections.

We have studied different neural architectures that might explain the experimental data from IC neurons. Neurons were simulated using the leaky integrate-and-fire model with conductance-based synaptic inputs, with input spike trains generated from a model of the cat auditory periphery (Bruce et al., JASA 2003). The response maps and tuning curves of a single-layer, uniform, recurrent LIN were compared to a number of different networks arrangements with feedforward inhibitory input. Feedforward inhibition was aligned with the excitatory input but had a broader frequency response due to convergent auditory nerve fiber input. While the LIN generated inhibitory sidebands around

the tip of its response map, it did not generate sharper tuning curves at higher intensities. In contrast, a network that had interneurons providing feedforward inhibitory input aligned with the excitatory input produced tuning enhancement at higher intensities, consistent with the physiological data.

[This work was supported by the Canadian Institutes of Health Research (New Emerging Teams grant 54023).]

## **773 Context-Independent Representation of Sound Frequency in the Inferior Colliculus**

Benjamin Robinson<sup>1</sup>, David McAlpine<sup>1</sup>, Isabel Dean<sup>1</sup>

<sup>1</sup>UCL

Recent data suggest that firing rates of neurons in the inferior colliculus of the anaesthetised guinea pig do not represent absolute sound levels; instead, neurons adjust their response functions in accordance with the mean sound level, so that efficient coding is maintained over a wide range of levels. We examined whether such contextual adjustment can also occur in response to changes in mean sound frequency, employing a narrow-band noise stimulus with a range of centre frequencies spanning two octaves around the best frequency of any given neuron. Within this range, a small region of frequencies was presented with high probability, whilst the rest of the range was presented at low probability. By shifting the high probability region around the range, we were able to record frequency-response functions to stimuli which varied only in their mean, not absolute, frequencies. Response functions of most neurons were altered with changes in the mean, but no consistent pattern of change emerged. Certainly, it was not the case that response functions shifted their steepest slopes to lie over high probability regions. Furthermore,  $d'$  analysis suggested a remarkably constant discriminability about neural best frequency across neurons and conditions, indicating that the representation of sound frequency might not adapt markedly to context in the IC. In revealing this invariance of sound frequency representation at the level of the IC, which contrasts with the dynamic representation of sound amplitude at this level, these data suggest that adaptation occurs in a parameter-specific hierarchy at successive points in the auditory system. Results such as these will both constrain models of collicular function and provide the tools for a close functional dissection of the pathways responsible for adaptation at successive levels of auditory processing.

## **774 Asymmetrical Facilitation Creates Direction and Velocity Selectivity for FM Sweeps in the Inferior Colliculus**

Zoltan Fuzessery<sup>1</sup>, Dustin Richardson<sup>1</sup>

<sup>1</sup>University of Wyoming

Neuronal selectivity for the direction and velocity of a frequency-modulated (FM) sweep has been modeled as a direction-dependent asymmetry in the inhibitory and/or excitatory inputs. The most commonly documented mechanism for direction selectivity is an asymmetrical inhibitory sideband that prevents responses to the sweep direction that encounters the sideband before entering the

neuron's excitatory domain. An asymmetrical facilitation has been suggested, but not demonstrated. In the pallid bat inferior colliculus, we have reported that a selectivity for downward FM sweeps is created by broadband low-frequency inhibition that arrives earlier than excitation during the course of an upward sweep. A selectivity for the velocity of downward FM sweeps is shaped by two different types of inhibition: an early on-best frequency (BF) inhibition that creates fast-pass velocity tuning, and a delayed high-frequency inhibition that can also create similar velocity tuning. Here we report that direction and velocity tuning can also be created by an asymmetrical facilitation that can be evoked even when FM sweeps remain within excitatory tuning curves. Such narrowband sweeps can evoke multiple excitatory and inhibitory inputs that summate or facilitate in one sweep direction, and either inhibit or fail to facilitate in the opposite direction. A rebound from inhibition may also contribute to facilitation. Because these events interact only over narrow time windows that will occur only during a specific range of FM sweep velocities, these interactions also shape a neuron's velocity tuning. Overall, the number of mechanisms within a single auditory processing station that may interact to shape selectivity for behaviorally relevant signals is quite remarkable.

#### **[775] Spectro-Temporal Receptive Fields Revealing Direction Selectivity of Neurons in the Inferior Colliculus**

**Sari Andoni<sup>1</sup>, Na Li<sup>1</sup>, George Pollak<sup>1</sup>**

<sup>1</sup>*University of Texas at Austin*

We used spectro-temporal receptive fields (STRFs) to evaluate how the spectral and temporal features of inhibition interact with excitation in the inferior colliculus (IC) of Mexican free-tailed bats, and how those interactions create feature selective properties. STRFs of IC neurons in our study revealed a dominance of spectrum-time inseparability. Most neurons were also direction selective favoring the downward moving ripple direction. Correlating direction selectivity with linear inseparability across all neurons showed that direction selectivity is the main contributor to inseparability in the IC. Blocking inhibitory receptors reduced both inseparability and direction selective properties of IC neurons. Since species-specific social communication calls were mostly composed of downward moving ripples, we show that IC neurons are specifically tuned to extract auditory features present in these calls by means of inhibitory innervations that shape both their inseparability and direction selectivity.

#### **[776] Ryanodine Receptors in the Frog Semicircular Canal**

**Paola Perin<sup>1</sup>, Laura Botta<sup>1</sup>, Umberto Laforenza<sup>2</sup>, Simona Tritto<sup>2</sup>, Monica Grazioli<sup>2</sup>, Giulia Gastaldi<sup>2</sup>, Ulderico Ventura<sup>2</sup>, Paolo Valli<sup>1</sup>**

<sup>1</sup>*University of Pavia - Dept. Physiology and Pharmacology,*

<sup>2</sup>*University of Pavia - Dept. Experimental Medicine*

In the frog semicircular canal, physiological data have shown the presence of a caffeine- and ryanodine-sensitive  $\text{Ca}^{2+}$  release process, which is activated by prolonged

depolarization of hair cells (Lelli et al. 2003). However, no data are available, so far, on the expression of ryanodine receptors (RyRs) in the frog inner ear.

In this study, we investigated the expression of RyR isoforms in the frog labyrinth, by performing RT-PCR on tissue homogenates, and their distribution in the semicircular canal, by immunohistochemistry on thin sections of the ampulla. RT-PCR experiments displayed the expression of mRNA for RyR $\alpha$  (the frog homologue of mammalian RyR1) but not RyR $\beta$  (homologue of RyR3) in the frog labyrinth. Immunolabeling of the crista ampullaris showed the presence of RyRs in hair cells, but not in nerve fibers or connective tissue. The observed labeling was heterogeneous: diffuse in some hair cells, patched in others, possibly reflecting different states of clustering of the receptors.

At difference with what was previously observed in mammalian IHCs (Marcotti et al. 2004), in the frog canal we did not observe any major effect of RyR activation or blockade on membrane currents. On the other hand, since afferent release was affected by ryanodine and caffeine (Lelli et al. 2003), we investigated the relative localization of RyRs and afferent synapses, by performing double immunolabeling for RyRs and the active zone protein RIM-1.

#### **[777] Semicircular Canal Dimensions Predict Afferent Sensitivity But Not Frequency Response Timothy Hullar<sup>1</sup>**

<sup>1</sup>*Washington University in St. Louis*

The geometry of the semicircular canals has been used to calculate their sensitivities to particular motions. These results have been used to estimate the behaviors of extinct animals, eliciting insights into the development of flight among reptiles, bipedal locomotion among humans, and swimming among whales and dolphins. It is not known, however, how well canal sensitivity or frequency response can be predicted from canal dimensions.

The data presented here rely on studies reporting the responses of primary semicircular-canal afferents to sinusoidal oscillations among species including fish, amphibians, reptiles, birds, and mammals. The lower corner frequencies (determined at the point where afferents phase-lead velocity by 45 deg) and sensitivities to 0.5 Hz sinusoidal oscillations of the afferent responses were compared among species. Anatomic measurements of the canals of the same species were also collected from the literature. The ability of several current models of canal hydrodynamics to relate canal anatomy and vestibular-afferent physiology was tested.

Contrary to the predictions of most models of the semicircular canals, no relationship was found between canal dimensions and the lower corner frequencies of afferent responses. However, regularly-discharging afferents showed a clear linear relationship between sensitivity and canal dimensions, such that sensitivity in spikes·sec<sup>-1</sup>/deg·sec<sup>-1</sup> = 0.05 + 0.16·radius of curvature in mm,  $r^2 = 0.88$ . These results suggest that the sensitivity but not frequency response of regular afferents may be predicted accurately from canal geometry. They further suggest that the density and specific gravity of the

endolymph may be relatively constant across a wide variety of species. Predictions of afferent responses based solely on canal anatomy, however, likely neglect significant other elements in signal transduction.

Supported by NIH NIDCD K08 DC006869 and the McDonnell Center for Higher Brain Function

### **778 KCNQ Channel Expression in Mouse Vestibular Ganglion Neurons**

Jessica R. Risner<sup>1</sup>, Jeffrey R. Holt<sup>1</sup>

<sup>1</sup>University of Virginia

Vestibular information transduced in the periphery is encoded and conveyed to the CNS by vestibular ganglion (VG) neurons. Previously, we found that VG neurons are inherently tuned to frequencies that range from <1 Hz to 44 Hz and can be categorized as low- or high-threshold based on the current required to evoke action potentials. We are interested to identify the membrane properties of VG neurons that contribute to their diverse firing properties. We hypothesize that the diversity results from expression of a heterogeneous population of voltage-gated K<sup>+</sup> conductances. We are currently investigating the molecular basis of these conductances, with particular focus on the KCNQ family of K<sup>+</sup> channels.

We used quantitative RT-PCR to examine the expression levels of KCNQ mRNA within VG harvested from P3 mice. We found that KCNQ2-5 were expressed but that KCNQ4 was most abundant, with an expression level 2 to 4 orders of magnitude greater than the other KCNQ mRNA. Using antibodies specific to each KCNQ subunit and an antibody to neurofilament 200, to identify neurons, we localized KCNQ3, 4 & 5 to VG neuron cell bodies.

To examine the influence of KCNQ channels on VG neuron function we used the whole-cell, tight-seal technique and applied 200μM linopirdine, a KCNQ family specific antagonist. Linopirdine blocked 23±14% (n=8) of the whole-cell conductance. The linopirdine-sensitive conductance had a mean G of 12±9 nS and a V<sub>1/2</sub> of -39±25 mV. To examine the contribution of KCNQ channels to the firing properties of VG neurons we characterized the responses of eight cells in current-clamp mode. Interestingly, linopirdine altered the response of VG neurons in a variety of ways. Four neurons had an increased threshold; two had a decreased threshold and two showed no change. Linopirdine also altered the frequency range to which VG neurons were tuned. Our data suggest expression of a heterogeneous population of KCNQ channels contributes to the diverse firing properties of VG neurons.

(This work was supported by NIDCD grant DC05439)

### **779 Modulation of Hair Cell Excitability in the Rat Utricle Under Specific Conditions: Organotypic Culture and After Excitotoxicity *In Vivo***

Aurore Brégeaud<sup>1</sup>, Danièle Dememes<sup>1</sup>, Cécile Travo<sup>1</sup>, Jean-Luc Puel<sup>1</sup>, Christian Chabbert<sup>1</sup>

<sup>1</sup>INSERM U583

In the rat, the maturation of synaptic contacts between utricle hair cells and afferent nerve fibres arising from the

vestibular primary neurons, occurs during the first week after birth. In that period, the percent of hair cells expressing I<sub>Na</sub>, a voltage-gated sodium current mainly carried by the Nav1.2 and 1.6 α-subunits, decreases from more than 90 % to less than 10 %. In the same time, the neonate hair cells lose their ability to trigger TTX-sensitive action potentials<sup>a</sup>. To investigate whether the setting of synaptic contacts regulates I<sub>Na</sub> expression and hair cell excitability, we used an *in vitro* model of nonafferented utricles in which no synapse formation can occur. In this model, I<sub>Na</sub> and action potentials were still present in most sensory hair cells after 10 days in culture. To check whether I<sub>Na</sub> expression and action potentials could reappear *in vivo* in mature hair cells after impairment of synaptic contacts, we induced transient and severe damages of the nerve endings by applying kainic acid directly into the inner ear<sup>b</sup>. Electron microscopy performed 48 hours after kainic acid application revealed swelling of vestibular afferent endings. No morphological damages remained one week after the pharmacological injury. Consistently, I<sub>Na</sub> were transiently recorded in 50 % of sensory hair cells in adult rats 48 hours after kainic acid application allowing the cells to trigger action potentials. This phenomenon did not occur in the presence of the glutamatergic antagonist (DNQX) and was not observed one week after, when the synapses are repaired. Altogether these results provide strong evidence that (1) damaged vestibular afferent nerve endings can recover after glutamate excitotoxicity, and (2) that I<sub>Na</sub> expression and excitability of the sensory hair cells may trigger this process. The role of transient excitability of sensory hair cells during development, and its reappearance during synaptic repair in adult will be discussed.

a. Chabbert & al, 2003 *J. Physiol.* 553:113-123

b. Puel & al, 1994 *J. Comp. Neurol.* 341: 241-256

### **780 GABAergic Hair Cells Are Present in the Posterior Canal Crista Ampullaris of the Turtle**

Stephen M. Highstein<sup>1</sup>, Jonathan Art<sup>2</sup>, Gay R. Holstein<sup>3</sup>

<sup>1</sup>Washington University School of Medicine, <sup>2</sup>University of Illinois at Chicago, <sup>3</sup>Mt. Sinai School of Medicine

Primary vestibular afferent response dynamics reside in an orderly map within the crista ampullaris of the posterior semicircular canal in the red-eared turtle, *Trachemys scripta elegans*. Moreover, turtle crista hair cell basolateral ionic currents are similar to those of other species; the effects of these currents upon receptor potentials are not sufficient to account for the deviation of nerve response dynamics from canal biomechanics. The present study was conducted to visualize the three-dimensional spatial distribution of GABA and glutamate immunolabeling in whole mounts of the vestibular labyrinth of the red-eared turtle, in order to map the regional distribution of hair cell transmitter phenotypes across the crista ampullaris. Endorgans were immersion-fixed with mixed aldehydes and then processed for immunofluorescence detection of GABA and/or glutamate using monoclonal antibodies produced in our laboratory. Concurrent control experiments included anterior and horizontal canal cristae incubated in (i) GABA antibody that was pre-absorbed with



a GABA-glutaraldehyde-BSA conjugate and glutamate antibody that was pre-absorbed with a glutamate-glutaraldehyde-BSA conjugate (double label pre-absorption control), (ii) single label pre-absorption controls, or (iii) incubation buffer with no primary antibodies (tissue auto-fluorescence control). Specimens were examined using a multiphoton/confocal laser scanning microscopy system after mounting in Petri dishes coated with 2% low melting point Agarose. Results demonstrate that GABAergic hair cells are present in the turtle crista ampullaris, and are non-uniformly distributed along the longitudinal axis of the epithelium. In contrast, glutamatergic hair cells are present throughout the sensory epithelium. These findings suggest that the convergent influence of multiple hair cell transmitter phenotypes upon a single afferent ending will contribute to shaping the dynamic response of that ending.

Support Contributed By: NIDCD grant DC006677. Multiphoton microscopy was performed at the MSSM Microscopy SRF, supported in part with a HHMI-BRSP award.

### **[781] Primary Afferent Endings Associated with GABAergic and Non-GABAergic Vestibular Hair Cells**

**Victor L. Friedrich, Jr.**<sup>1</sup>, Stephen M. Highstein<sup>2,3</sup>, Giorgio Martinelli<sup>4</sup>, James Tucker<sup>5</sup>, Sarah Clifford<sup>5</sup>, Richard D. Rabbitt<sup>3,5</sup>, Gay R. Holstein<sup>3,4</sup>

<sup>1</sup>*Dept. of Neurosci., Mount Sinai Sch. Med., NY*, <sup>2</sup>*Dept. of Otolaryngol., Washington Univ. Sch. Med., St. Louis, MO*, <sup>3</sup>*Marine Biological Laboratories, Woods Hole, MA*, <sup>4</sup>*Dept. Neurol., Mount Sinai Sch. Med., NY*, <sup>5</sup>*Dept. Biomed. Eng., U. Utah, Salt Lake City, UT*

The search for the origins of diversity in primary afferent dynamics is a dominant theme in vestibular research (Highstein et al., J. Neurophysiol. 2005). We recently showed that glutamatergic and GABAergic hair cells provide convergent synaptic input to some horizontal semicircular canal primary afferents, and that presynaptic hair cell transmitter phenotype contributes to the population diversity in afferent response dynamics (Holstein et al., PNAS, 2004). To explore further sources of this diversity, we injected axons with Neurobiotin, perfused toadfish (*Opsanus tau*) with mixed aldehydes, labeled the injected Neurobiotin with fluorescent-conjugated streptavidin, identified GABAergic hair cells using a monoclonal anti-GABA antibody and fluorescent-tagged secondary antibodies, and performed whole-mount three-dimensional volume imaging of entire cristae and labeled arbors using single and two-photon confocal microscopy. Concurrent pre-absorption, secondary antibody and tissue auto-fluorescence control experiments utilized the anterior and posterior canal cristae from the same fish. Results demonstrated a wide variety of afferent terminal morphologies in the crista. Afferents varied in numerous attributes including dendritic branching patterns, extent of the dendritic arborization field, and terminal structure. Whereas many fibers terminated exclusively around the basal surfaces of the hair cells, other fibers preferentially targeted particular lateral or perinuclear

portions of the hair cell membrane. Moreover, in addition to the bouton and "cup-like" endings described previously (Boyle et al., J. Neurophysiol. 1991), afferents terminating as elongated thorny spikes were observed in association with the lateral aspects of some hair cells. The results suggest that hair cell-afferent architecture, together with hair cell transmitter phenotype, are sources of diversity in primary afferent response dynamics.

Support contributed by: NIDCD grants DC006677 and DC006685. Multiphoton microscopy was performed at the MSSM Microscopy SRF, supported in part with a HHMI-BRSP award.

### **[782] Improved Method for Preparing Flattened Whole-Surface Mounts of Cristae Sensory Epithelium for Use in the Study of Peripheral Vestibular Efferent Projections**

**James Barrese**<sup>1,2</sup>, Anna Lysakowski<sup>1</sup>

<sup>1</sup>*Dept. of Anatomy and Cell Biology, Univ. of Illinois at Chicago, IL*, <sup>2</sup>*Univ. of Illinois at Chicago College of Medicine*

We have recently made improvements on a method for flattening the saddle-shaped structure of the sensory epithelium of the crista ampullaris. By providing us with a whole-surface mount of the entire sensory epithelium, this technique allows us more efficient study of regional variations in peripheral vestibular afferent and efferent innervation. While the method is best suited for use on freshly-fixed tissue, we have also used it successfully on cristae stored in 4% paraformaldehyde in 0.1 M phosphate buffer (PB) for up to 2-4 years. Cristae are microdissected, leaving an excess of ampulla, and rinsed in 0.1 M PB. The specimen is pinned through the ampullary membranes in a Sylgard-coated dish and stroma is gently teased away from the overlying sensory epithelium using minutiae pins and fine forceps, allowing for enzyme penetration and further microdissection. Cristae are then rinsed with saline to remove excess PB, and incubated with 20 µg/ml thermolysin (in a base of 2 mM Tris-HCl & 1 mM CaCl<sub>2</sub>) at 25 °C for ½-6 hours (dependant on the level of tissue fixation). After incubation, organs are rinsed in saline and PB to remove all enzyme. Once sufficient stroma is removed to allow flattening, the sensory epithelium is then mounted on a slide, cover-slipped, and examined with microscopy.

We are using this method to further study the peripheral distribution of anterogradely labeled efferent fibers in the crista. Our recent findings (Maksoud and Lysakowski, ARO, 2004) have been expanded by the addition of several more organs and efferent fibers reconstructed with NeuroLucida. We are also analyzing cases in which a midline brainstem incision has been made to determine the distinct contributions of ipsilateral vs. contralateral components. This method can also be combined with subsequent immunohistochemical labeling for light and confocal microscope studies.

Supported by NIH R01-02521.

### **783 Head Motion Scales Allometrically with Animal Size**

**Robert Mallery<sup>1</sup>**, Timothy Hullar<sup>1</sup>

<sup>1</sup>*Washington University in St. Louis*

The size of the semicircular canals varies allometrically with the mass of a species. Because the dimensions of the semicircular canals are believed to determine their sensitivity to different amplitudes and frequencies of rotational head motion, it has been assumed that smaller canals are found in animals with higher-amplitude, higher-frequency head motions. This assumption has not previously been tested.

We measured the frequency content, angular velocity, and angular acceleration of head motions of two rodents of different body and semicircular canal size, mouse (weight 30 g, canal radius of curvature 0.693-1.063 mm) and chinchilla (weight 600 g, canal radius of curvature 1.609-2.635 mm). Each animal was allowed to move unrestrained within an enclosure. An orthogonal pair of scleral search coils within a three-axis magnetic field coil system were used to track the motion of the mouse's head, while a proprietary-technology magnetically-based position sensor was used to track the motion of the chinchilla's head. Measurements were made in a coordinate system based on the horizontal semicircular canal of each animal.

Rotational velocities were greater in mouse than in chinchilla, especially about the roll axis. Rotational accelerations showed a similar pattern, with at least 5% of head movements exceeding 100,000 deg/sec<sup>2</sup> about the roll axis. Wavelet analysis indicated that the frequency content of head movements approached 30 Hz in the chinchilla and exceeded 40 Hz in the mouse. The difference in frequency content between the two was most significant about the roll axis. Thus the stimulus to the semicircular canals in these related species appears to scale allometrically with animal size. These results have implications for understanding the evolution of the vestibular system as well as for diagnosis and prognosis of patients suffering from imbalance disorders.

Supported by NIH NIDCD T32 DC000022 (RMM), NIH NIDCD K08 006869 (TEH), and the McDonnell Center for Higher Brain Function (TEH)

### **784 Axis of the Transient Human Vestibulo-Ocular Reflex (VOR) After Unilateral Vestibular Deafferentation (UVD)**

**Benjamin Crane<sup>1,2</sup>**, Junru Tian<sup>1,3</sup>, Joseph Demer<sup>1,3</sup>

<sup>1</sup>*UCLA*, <sup>2</sup>*Otolaryngology*, <sup>3</sup>*Jules Stein Eye Institute*

The normal VOR axis approximates the head's except for 1/4 angle dependence on gaze position. Using 3-D magnetic search coils, we examined the VOR axis in 6 humans (mean age 58 ± 16 yrs) with surgical UVD of 5 – 156 mos duration, where VOR gain remains deficient for ipsilesional rotation. Subjects underwent mechanically delivered whole body rotation in darkness about a yaw axis centered between the otoliths at peak acceleration 2800°/s/s. Prior to rotation subjects viewed a target 175 cm away centered, or 20° up or down. Within 10 ms of head rotation onset and during the initial 60 ms of

ipsilesional rotation the VOR velocity axis was shifted forward 15° relative to that for contralesional rotation in all subjects. No significant tilt asymmetry was found in control subjects. After 60 ms many subjects made saccades correcting the axis shift. During the initial 60 ms, the tilt angle ratio (TAR) of the VOR axis was 1/4 the vertical gaze angle for both ipsi- and contralesional rotation, as typical of normal subjects. After 60 ms the TAR became 1/2 angle, consistent with Listing's Law for saccades. A model is presented to describe the observed axis deviation based on the anatomic orientation of the semi-circular canals and selective silencing of horizontal but not vertical canal afferents. The 1/4 angle dependency of the VOR axis on gaze angle was not affected by UVD, and is therefore likely to be have a motor rather than sensory basis.

### **785 Synaptic Transmission Between Type I Hair Cells and Calyx Endings in the Turtle Posterior Crista**

**Jay M. Goldberg<sup>1</sup>**, Joseph C. Holt<sup>2</sup>, Shilpa Chatlani<sup>1</sup>

<sup>1</sup>*University of Chicago*, <sup>2</sup>*University of Texas Medical Branch*

There are three difficulties facing synaptic transmission between type I hair cells and calyx endings. 1) Active zones are located on the calyx inner face, which is loaded with K channels and should impede the spread of synaptic currents to the outer face where the spike generator is presumably located. 2) Neurotransmitter might accumulate in the intercellular cleft and drastically reduce quantal transmission. 3) The presence of a large, non-inactivating K channel (IKL), by lowering the input impedance of the hair cell, might prevent transducer currents from sufficiently depolarizing the hair cell to trigger quantal release. Despite these difficulties, the discharge of calyx-bearing afferents recorded extracellularly responds to head rotations and canal indentations. To study how this is accomplished, we have been comparing quantal transmission in intracellular recordings from calyx-bearing (C) and bouton (B) afferents identified by their distinctive efferent-mediated responses. While quantal rates (qrates) are similar in the two groups, quantal size (qsize) and duration (qdur) are considerably smaller in C units. The differences may be a consequence of the intracellular impalement of C units since during the first few minutes after impalement there is a drastic decline in quantal activity, which is exacerbated by Na-channel blockers and can be reversed by K-channel blockers. This suggests that a balance between active conductances, particularly a persistent Na current and K channels, shape synaptic transmission. Brief qdurs imply that homeostatic mechanisms are adequate to compensate for the effects associated with individual quanta. However, during intense synaptic activity, compensatory mechanisms can be overwhelmed as evidenced by a slow and steady depolarization evoked by prolonged high-frequency stimulation in C, but not in B, units. That quantal transmission occurs suggests that IKL is not as great an impediment as supposed. (Supported by DC02508)

## **786 Efferent-Mediated Responses in Bouton**

### **Afferents of the Turtle Posterior Crista**

**Joseph C. Holt<sup>1,2</sup>**, Jay M. Goldberg<sup>2</sup>

<sup>1</sup>*University of Texas Medical Branch at Galveston,*

<sup>2</sup>*University of Chicago*

Electrical stimulation of efferent fibers gives rise to inhibitory responses in bouton afferents innervating the torus (BT) and midportions (BM) of the turtle posterior crista. The inhibition is of presynaptic (hair-cell) origin and consists of the sequential activation of  $\alpha 9$ nAChR and small-conductance, calcium-dependent potassium channels (SK) leading first to a brief increase and then a more prolonged decrease in hair-cell quantal release. Both the  $\alpha 9$ nAChR and SK actions are smaller and briefer in BM units. In addition, the inhibition in BM units is followed by a post-inhibitory (PI) excitation. The PI excitation depends on the preceding SK inhibition as both are abolished by SK blockers. This suggests that a mechanism triggered by the SK inhibition is responsible for the PI excitation. A likely mechanism is the hyperpolarization-activated channel (Ih), which is found in hair cells residing in the midportions, but not in the torus (Brichta and Goldberg, 2002). Blockers of Ih enhance the preceding SK inhibition while abolishing the PI excitation. Other candidates, including the inward rectifier (IRK) and a T-type Ca channel, may also contribute. While recording afferent discharge, a post-train spike increase can occur in the absence of a preceding spike decrease. This is a result of the presynaptic inhibition being countered by a postsynaptic (direct afferent) excitation. Because a PI excitation is a common feature of efferent actions in lateral-line, as well as in vestibular organs, the mechanisms described here may be of general relevance. (Supported by NIH Grant DC02508)

## **787 TGF- $\beta$ and Runx2 Control of Bone Matrix Mechanical Properties in Bone Disease-Associated Hearing Loss**

**Jolie Chang<sup>1</sup>**, Jacob Johnson<sup>1</sup>, Guive Balooch<sup>2</sup>, Ryan Stern<sup>3</sup>, Anil K. Lalwani<sup>4</sup>, Lawrence Lustig<sup>1</sup>, Tamara Alliston<sup>2</sup>

<sup>1</sup>*Department of Otolaryngology - HNS, University of California San Francisco,* <sup>2</sup>*Department of Cell and Tissue Biology, University of California San Francisco,*

<sup>3</sup>*Department of Otolaryngology-HNS, University of Washington,* <sup>4</sup>*Department of Otolaryngology, New York University Medical Center*

Several bone diseases have associated hearing loss that has been attributed to defective bone matrix properties. However, the mechanism by which bone properties affect hearing is not well understood. Recently, TGF- $\beta$  was identified as the first known regulator of bone matrix mechanical properties. Mutations in TGF- $\beta$  cause Camurati Engelmann disease and may play a role in cleidocranial dysplasia (CCD), both bone diseases with associated hearing loss. Runx2 is a key osteoblast transcription factor that is mutated in CCD. TGF- $\beta$  represses Runx2 activity to inhibit osteoblast differentiation. Accordingly, CCD symptoms such as dysplastic clavicles are apparent in Runx2<sup>+/+</sup> mice and in D4 mice, which overexpress TGF- $\beta$  in bone.

We hypothesized that TGF- $\beta$  regulation of Runx2 and bone matrix quality may be critical for hearing. We first tested hearing in D4 mice which have reduced bone matrix mechanical properties, such as elastic modulus, due to TGF- $\beta$  overexpression. Auditory brainstem response (ABR) measurements revealed a significant hearing loss in D4 mice at click, 2, 8, and 32 kHz frequencies with a 10-20dB difference in threshold level compared to wild-type littermates. To determine if Runx2 was required for the TGF- $\beta$  effect on bone matrix, the elastic modulus of Runx2<sup>+/+</sup> tibial bone was measured using atomic force microscopy with nanoindentation. We found the elastic modulus of Runx2<sup>+/+</sup> bone matrix was reduced. This defect was exacerbated when Runx2<sup>+/+</sup> mice were crossed with D4 mice, and rescued by crossing Runx2<sup>+/+</sup> mice with those that had impaired TGF- $\beta$  signaling. These data strongly suggest that Runx2 is required for the effect of TGF- $\beta$  on bone matrix quality. The role of TGF- $\beta$ /Runx2 regulated bone matrix quality in hearing is under investigation. Investigation of key bone regulators and bone matrix quality in hearing may lead to the identification of therapeutic targets for the prevention or treatment of bone disease-associated hearing loss.

## **788 Hearing Loss and Inner Ear Morphology in Estrogen Receptor Alfa and Beta Knock Out Mice**

**Rusana Simonoska<sup>1</sup>**, Annika Stenberg<sup>1</sup>, Lena Sahlin<sup>1</sup>, Malou Hultcrantz<sup>1</sup>

<sup>1</sup>*Karolinska University Hospital, Sweden*

Background: Hearing loss appears to be more profound in elderly males than females. There are also well-known sex differences in the auditory brainstem response (ABR), where women have shorter latencies than men. In addition women with Turner syndrome (45,X), who are biologically estrogen deficient, have longer ABR latencies and early rapid aging of the ear (presbycusis). There are case reports that hormone replacement therapy and oral contraceptive use can lead to hearing loss, but of another type, the acute sudden deafness. Such contradictory aspects of the estrogen action are commonly found and may spring from the fact that there are two estrogen receptors, alfa and beta, both of which we have earlier showed to be present in the inner ear of mouse, rat and humans.

In previous studies with estrogen receptor beta knock-out mice (ERb<sup>-/-</sup> mice) we showed that ER<sup>-/-</sup> mouse has normal hearing and inner ear morphology at 3 months of age but at 12 months of age the ERb<sup>-/-</sup> mouse is deaf with corresponding severe loss of hair cells and ganglion cells.

Aim: The effect of aging on hearing and inner ear morphology in

estrogen receptor alfa knock out mice (ERa<sup>-/-</sup> mice) and comparison to ERb<sup>-/-</sup> mice.

Methods: Comparisons between the knock-outs and wild type controls, both males and females was done regarding hearing and inner ear morphology. Immunohistochemical and immunofluorescence techniques for visualisation of estrogen receptors and Peripherin (specific for type II spiral ganglion cells) were used for the latter.

Results: ERa<sup>-/-</sup> mice have almost the same progressive hearing loss as the ERb<sup>-/-</sup> mice, but there is a tendency for gender difference for ERb<sup>-/-</sup>.

Conclusion: No difference in the hearing between the 2 groups of knock out mice was observed, suggesting that both estrogen receptors are equally important for the hearing function. However, the gender difference may be important regarding ER beta.

### **789 DPOAE and ABR Measures of Auditory Function in ELN-Heterozygous Knockout Mice**

**Jeffrey Marler<sup>1</sup>**, Brenda M. Ryals<sup>1</sup>, Sharon G. Kujawa<sup>2</sup>, Zsolt Urban<sup>3</sup>

<sup>1</sup>James Madison University, <sup>2</sup>Massachusetts Eye and Ear Infirmary, <sup>3</sup>Washington University

Williams syndrome (WS) is a neurodevelopmental disorder involving a hemizygous deletion of 17-21 genes on chromosome 7q11.23, including the elastin gene (ELN), which encodes a key component of elastic fibers in connective tissues. Supravalvular aortic stenosis (SVAS) is a genetic disorder involving a point mutation of ELN. There are recent reports of mild-to-moderate SNHL in both clinical groups (Cherniske et al. 2004 Am J Med Genet131A, Marler et al. in press Am J Med Genet). While there has been no report of ELN in the cochlea, elastic fibers have been identified in the round window membrane of the mouse cochlea (Kitamura et al. 2002 Hear Res 174), and related proteins, elastin microfibril interface-located protein-EMILINs, reported in the basilar membrane of mice (Amma et al. 2003 Mol Cell Neurosci 23).

To explore a possible role for ELN in auditory function, we evaluated ABR and DPOAE (5.6-45.2 kHz) in ELN-heterozygous knockout mice (Li et al. 1998 J Clin Invest 102). ABR waveforms and DPOAE amplitudes were matched to wild type litter mates at post-natal week 13 and an individual adult CBA/CaJ (control). There was no significant difference in the ABR thresholds or DPOAE amplitudes between ELN +/- and litter mate controls. Both had elevated thresholds in the mid-to-high frequencies compared with the CBA/CaJ. These initial results suggest that hearing in the ELN +/- mouse are either no different from or at least as good as those of the background strain (SV129 and C57BL/6) at post-natal week 13 or that any role ELN may have in hearing may be masked by existing hearing deficits in the background strain. Further studies on the postnatal development of auditory function in ELN +/- mice are planned in order to evaluate whether ELN deficiency alters membrane remodeling, mechanical adaptation or other age-related processes which may influence auditory function later in life.

NHLBI R01 HL073703 (ZU), JMU CISAT Small Grant (JAM, BMR)

### **790 Functional and Histopathological Age-Related Changes of the Ear in the MPS-I Mouse**

**Patricia A. Schachern<sup>1</sup>**, Chester Whitley<sup>2,3</sup>, Sebahattin Cureoglu<sup>1</sup>, Vladimir Tsuprun<sup>1</sup>, Michael M. Paparella<sup>1,4</sup>

<sup>1</sup>Department of Otolaryngology, University of Minnesota,

<sup>2</sup>Department of Human Genetics, University of Minnesota,

<sup>3</sup>Department of Pediatrics/ University of Minnesota,

<sup>4</sup>Minnesota Ear Head & Neck Clinic

Mucopolysaccharidosis type I (MPS I) is an autosomal recessive disorder caused by a mutation in the gene encoding the enzyme  $\alpha$ -L-iduronidase. This enzyme is

responsible for degradation of dermatan and heparan sulfates and its deficiency results in accumulation of these glycosaminoglycans in lysosomes of virtually all organs, resulting in severe somatic and neurologic changes. Clinical findings include otitis media and a mixed hearing loss. The cellular and molecular mechanisms of ear pathology and hearing loss are not understood, however, mouse models of MPS I make such investigations possible. We present age-related audiometric and histopathological changes using homozygote (-/-), heterozygote (+/-) MPS I and wild type (+/+) mice aged 2 mo to 19 mo. Auditory brainstem responses (ABR) were obtained to clicks and tone bursts at 1-32 kHz, and pathological changes to the middle and inner ears were studied with light and electron microscopy. ABR thresholds in the +/+ and +/- animals were similar at all ages, however, hearing of -/- mice was significantly decreased at all ages compared to +/+ and +/- mice. Hearing loss progressed from a mild to moderate loss at 2 mo to total deafness by 8 mo. In the -/- mice, lysosomal storage vacuoles were observed at all ages in the spiral ligament, spiral prominence, limbus, basilar membrane, epithelial and endothelial cells of Reissner's membrane, endothelial cells of vessels, and some ganglion cells. Although storage vacuoles were seen at 2 mo, the hair cells and ganglion cells at this age appeared normal, however, by 8 mo there was total loss of all sensory structures. These progressive age-related changes suggest that early intervention using new methods of enzyme replacement and gene therapy may be necessary to prevent sensory cell damage and hearing loss.

### **791 Phenotype Assessment of Tyrosine Kinase Discoidin Domain Receptor 1 (DDR1) -/- Mice in the Inner Ear**

**Angela-Maria Meyer-zum-Gottesberge<sup>1</sup>**, Thomas Massing<sup>2</sup>, Ursula Becker-Lenzian<sup>1</sup>, Bogdan Beirowski<sup>3</sup>, Manfred Weber<sup>3</sup>, Oliver Gross<sup>3</sup>

<sup>1</sup>University of Düsseldorf, <sup>2</sup>University Duesseldorf,

<sup>3</sup>University of Cologne

Collagens I, II to IV, V and IX were detected in the inner ear in a fibrillary form or related to a basal membrane. Three different types of collagen-receptors are currently known: integrins heterodimer with beta1subunits and the tyrosine kinases Discoidin Domain Receptors DDR1 and DDR2. Aberrant expression and signaling of these receptors have been implicated in several human diseases linked to accelerated matrix degradation and remodeling including tumor invasion, atherosclerosis, liver fibrosis, and malformation of the ductal morphogenesis of the glands. Since a deficit of DDR1 leads to alteration of the glomerular basement membrane in the kidney (Gross et al. 2004) we become interested if such as deficit may cause a significant inner ear phenotype. The preliminary observation of heterozygotes of DDR1 revealed most progressive alterations in the stria vascularis, where an accumulation of the electron dense compounds in the epithelial layer occurs. The objective of this study was to characterize immunohistochemically the distribution of the DDR1-receptor in the inner ear of wild type. Furthermore, in order to understand how the inner ear phenotype of DDR-deficient mice developed, the auditory function and

ultrastructural alternation of heterozygote and homozygote DDR1-mice comparing to wild type at 4 and at 8 weeks age were examined. DDR1 immunostaining was detected mainly in the stria vascularis, in the supporting cells of the organ of Corti and less in the spiral ganglion and nerve. The most prominent otopathological changes of DDR-deficient mouse were closely related to the location of the DDR1-receptor. The most progressive structural alterations were related to the stria vascularis, where alteration of the capillary BM and an excess of an accumulation of the electron dense compounds in the epithelial cells occurred. Furthermore, additional inner ear phenotype (without an accumulation of the extracellular matrix) was identified in the outer hair cells and the spiral ganglion cells. Additionally, lack of DDR1 in the temporal bone leads also to a formation of exostosis that arises from the bony wall of the cochlea. The role of the DDR1, especially in the inner ear, is not yet fully understood, however, a severe decrease of the auditory function and the structural alterations stressed its essential role for the inner ear.

### **792 Primary Endolymphatic Duct Tumor in a Patient with Vestibular Schwannoma**

Leslie Michaels<sup>1</sup>, Sava Soucek<sup>2</sup>, Tao Upile<sup>1</sup>, Jianning Liang<sup>1</sup>, Anitha Bolanthur<sup>1</sup>, Anthony Wright<sup>1</sup>

<sup>1</sup>University College London, <sup>2</sup>St. Mary's Hospital, London

Archival temporal bones were reviewed in a patient who had been operated on in 1961 for a right-sided vestibular schwannoma, but had died soon after. At autopsy the cause of death had been infarction of the pons and midbrain. The residua of vestibular schwannoma are observed in the right temporal bone. In the left there is a primary papillary tumor of the endolymphatic duct, which has not yet spread from this situation. The finding offers the rare opportunity for studying in situ this neoplasm of the vestibular system, a lesion which is usually not detected until it has spread widely through the temporal bone. It had not yet been described in 1961 (first report: Heffner D. Cancer 1989;64:2292-2302). None of the other manifestations of neurofibromatosis 2 or von Hippel-Lindau disease had been seen at autopsy, nor was there any family history of either of the two diseases, but the association of vestibular schwannoma and endolymphatic duct tumor, respectively neoplasms characteristic of the two diseases, in the same patient, raises the possibility of a genetic relationship between those two conditions.

### **793 AUNX1, a Novel Locus Responsible for X-Linked Recessive and Early-Onset Auditory Neuropathy in an Extended 5-Generation Chinese Family, Maps to Xq23-27.3**

Qiuju Wang<sup>1,2</sup>, Qingzhong Li<sup>1</sup>, Shaoqi Rao<sup>3</sup>, Suzanne M. Leal<sup>4</sup>, Yan Shen<sup>2</sup>

<sup>1</sup>Chinese PLA Institute of Otolaryngology, <sup>2</sup>Chinese National Human Genome Centre, <sup>3</sup>Departments of Cardiovascular Medicine and Molecular Cardiology, The Cleveland Clinic Foundation, <sup>4</sup>Baylor College of Medicine, Department of Molecular and Human Genetics

Auditory neuropathy (AN) was characterised by low frequency hearing loss, normal otoacoustic emissions

(OAEs) and absent or diminished auditory brainstem responses (ABRs). Its prevalence estimates varied from 1/200 (0.5%) patients with sensorineural hearing loss (SNHL) to 15% of SNHL. AN have been described as autosomal dominant and recessive, or X-linked, based on our previous clinical investigations of the pedigree included in the present study. To date, only three genes/loci for AN were reported: the OTOF gene (2p22-p23), the AUNA1 locus and the mitochondrial 12SrRNA T1095C mutation. OTOF gene was suggested for a non-syndromic recessive auditory neuropathy (NSRAN) characterized with a set of special audiological features consistent with an autosomal recessive hearing disorder but lack of any other detectable peripheral neuropathy. AUNA1 locus reported by Kim et al (2004) was the first linkage responsible for autosomal dominant AN that maps to 13q14-21. Recently, we identified a mitochondrial variant (12SrRNA T1095C) whose mutation causes the AN symptom in a Chinese patient. The T1095C mutation is predicted to disrupt an evolutionarily highly conserved A-to-U base-pair at the P-site of 12S rRNA. Here, we describe a detailed genetic characterization of the extended 5-generation Chinese AN pedigree whose clinical features were already reported previously. This previous study gave strong evidence that the mode of inheritance for the Chinese AN pedigree (with 42 informative individuals including 7 affected males) is X-linked recessive. The ages of onset were at the adolescence (average 13 years old). The degrees of hearing impairment varied from mild to severe, with the presence of otoacoustic emissions and the absence of auditory brainstem responses. Two-point and multipoint model based linkage analysis using the MILNK and LINKMAP programs of the FASTLINK software package produced maximum two and multipoint LOD scores of 2.41 and 2.41, respectively. These findings defined a novel X-linked auditory neuropathy locus (AUNX1, Xq23-q27.3).

### **794 Generation and Characterization of Mice with Myh9 Deficiency**

Anand N. Mhatre<sup>1</sup>, Yan Li<sup>1</sup>, Kevin Wang<sup>1</sup>, Graham Atkin<sup>1</sup>, Anil K. Lalwani<sup>1</sup>

<sup>1</sup>NYU School of Medicine

Mutant alleles of MYH9 encoding a class II nonmuscle myosin heavy chain-A (NMMHC-IIA) have been largely linked to hereditary megathrombocytopenia with or without additional clinical features that include sensorineural deafness, cataracts and nephritis. These naturally occurring mutations have identified a critical biological role of this motor protein in the organs and cells that are adversely affected by its dysfunction. To assess its biological role in the affected targets, particularly the inner ear, we have generated and characterized mice with Myh9 deficiency. These mice were derived using the XA136 ES cell line (BayGenomics, <http://baygenomics.ucsf.edu/>) carrying a gene trap insertion, containing ?-gal marker gene, in Myh9, within the intron flanking exons 4 and 5. Mice carrying the Myh9 null allele display an otherwise normal phenotype including normal hearing and platelet properties as determined in young adults, despite Myh9 haploinsufficiency. Myh9 promoter-linked expression pattern of the ?-gal enzyme activity in the heterozygote

mice matches Myh9 immunoreactivity in various target organs including the cochlea. Intercross of mice heterozygous for the Myh9 null allele (Myh9<sup>-/-</sup> Myh9<sup>+/+</sup>) did not yield pups homozygous for the Myh9 null allele, indicating embryonic lethality of the Myh9 knock-out. Analysis of embryos at varying time points established that the homozygotes die in utero at E10.5. The embryonic lethality associated with the complete Myh9 deficiency establishes a critical role for this nonmuscle myosin in fetal development. The generation of mice carrying Myh9 null allele represents a critical resource for analysis of its biological role in development and in the target organs affected by its naturally occurring mutations.

#### **795 Inflammation Contributes to Damage of Stria Vascularis and Spiral Ligament in Pendred Syndrome**

**A. Oelke<sup>1</sup>**, R. Singh<sup>1</sup>, R.J. Maganti<sup>1</sup>, S.V. Jabba<sup>1</sup>, Philine Wangemann<sup>1</sup>

<sup>1</sup>Anatomy & Physiology Dept., Kansas State University

Pendred syndrome, an autosomal-recessive disorder characterized by deafness and goiter, is caused by a mutation of SLC26A4, which codes for the HCO<sub>3</sub><sup>-</sup> transporter pendrin. We are investigating the relationship between pendrin expression and deafness using adult mice that have (+/- or +/+) or lack a complete Slc26a4 gene (-/-). Previously we reported that pendrin is expressed in the cochlear lateral wall and that -/- mice have an acidified endolymphatic pH, a hyperpigmented stria with reorganized marginal cells and a loss of tissue mass in the spiral ligament. These data suggested that loss of pendrin alters the tissue pH in the lateral wall and leads to tissue damage followed by cellular reorganization. Here we test the hypothesis that inflammation contributes to tissue damage. Gene expression analysis by microarray was performed on total RNA isolated from stria vascularis of +/+ and -/- mice. A select group of transcripts was quantified by qRT-PCR in total RNA isolated from stria vascularis, spiral ligament, liver and spleen of 80 – 83 days old male +/- and -/- mice. Expression of macrophage markers including Ptprc (=Cd45), Cd68, Cd83, Lys2, Lgals3 (=Mac-2), Ms2, Ctsb, Ctss, Ctsk, C1r, C3 and C4 were significantly increased in stria vascularis of -/- mice compared to +/+ mice. No expression of markers of acute inflammation (Il1a, Il1b, Il6, Il12), T-cells (Tcra, Tcrb, Cd3, Cd4, Cd8), NK cells (Ncam1 (=Cd56), Fcgr3 (=Cd16)) or B cells (Cd19, Cd20, Sdc1 (=Cd138)) was found in stria vascularis of +/- or -/- mice. Expression of Cd83, Lys2 and C3 in -/- mice was increased 4, 122 and >30-fold in stria vascularis and 2, 9 and 7-fold in spiral ligament compared to +/- mice. No difference in expression of Cd83, Lys2 and C3 was found in liver or spleen. The data suggest that inflammation contributes to tissue damage of stria vascularis and spiral ligament and that inflammation resolves with persistent macrophages remaining in stria vascularis.

NIH-R01-DC01098, NIH-P20-RR017686 Core C

#### **796 In Vitro Functional Analysis of Human Connexin 26 Mutations, E47K and G45E, Demonstrate That Deafness Linked Mutation May Specifically Alter Gap Junction and Hemichannel Function**

**Benjamin Stong<sup>1</sup>**, Qing Chang<sup>1</sup>, Shoab Ahmad<sup>1</sup>, Xi Lin<sup>1</sup>

<sup>1</sup>Dept of Otolaryngology Head and Neck Surgery, Emory University School of Medicine

Connexin (Cx) 26 mutations are the most common cause of nonsyndromic hereditary hearing loss. Of approximately 120 mutations, over 100 are autosomal recessive. Despite these important genetic discoveries, the effect of Cx26 mutations on cochlear function is poorly understood. G45E and E47K are point substitution mutations located in the first extracellular domain that results in charge changes in the amino acid side chains. Using an in vitro expression system, we studied the effect of these two mutations on gap junction (GJ) and hemichannel (HC) functions.

When expressed in HEK 293 cells, E47K did not alter GJ plaque formation at the light microscope level. However, these GJs as well as their HCs were impermeable to calcium, propidium iodide (PI), and intercellular electric currents, consistent with interruption of biochemical and ionic intercellular communication. In contrast, G45E resulted in cell death within 24hrs of transfection. It is known that increased extracellular Ca<sup>++</sup> concentrations ([Ca<sup>++</sup>]<sub>o</sub>) drive HCs into closed states. Adding exogenous Ca<sup>++</sup> to cells transfected with G45E rescued cell viability in a dose dependent manner, resulting in normal morphology and functional GJs permeable to both ions and fluorescent tracer molecules, suggesting intact cellular GJ coupling. These results imply that dynamic calcium dependent gating is involved in wild type Cx26, and the primary effect of G45E is to shift the Ca<sup>++</sup> dose response curve resulting in leaky HCs.

Our work suggests novel mechanisms, including GJ and HC uncoupling and incompetent HCs, with resultant cell death, by which Cx26 mutations result in hearing impairment. If the G45E shift in [Ca<sup>++</sup>]<sub>o</sub> dependent gating is extrapolated to the in vivo environment, we postulate that mutations resulting in a shift in the Ca<sup>++</sup> dose response curve and incompetent HCs may result in endocochlear cell death and thus presents possible therapeutic strategies including manipulating [Ca<sup>++</sup>]<sub>o</sub> and/or binding affinity.

#### **797 Over-Expression of Connexin26 Completely Rescued the Hearing Sensitivity of Connexin 30 Knockout Mice**

**Shoab Ahmad<sup>1</sup>**, Wenxue Tang<sup>1</sup>, Xinxin Chen<sup>1</sup>, Qing Chang<sup>1</sup>, Ping Chen<sup>1</sup>, Xi Lin<sup>1</sup>

<sup>1</sup>Emory University School of Medicine

Genetic studies indicated that connexins (Cxs), the building block of gap junctions (GJs), play vital roles in the cochlea. However, molecular mechanisms of pathogenesis of deafness due to mutations in Cxs remain unknown. We and others have shown that major GJs in the cochlea are formed from heteromeric assemblies of Cxs26 & 30. In this work we investigated whether, in the absence of the Cx26

co-assembly partner (Cx30), the remaining Cx26 can still form functional GJs and whether the homomeric GJs are sufficient for maintaining normal hearing in mice.

Using a genetic approach, we over-expressed Cx26 in Cx30 knockout mice by providing extra copies of Cx26 through transgenic expressions of modified bacterial artificial chromosome (BAC). In this BAC the Cx26 was intact, but Cx30 was replaced with a reporter gene (HcRed). Pronuclear injections of the modified BAC in mice resulted in a new strain that carried two copies of BAC, and thus two extra copies of Cx26, as confirmed by Southern analyses. These normal hearing Cx26over/Cx30+/+ mice were bred with deaf Cx26+/+/Cx30-/- mice (Teubner, et al., 2003) for two successive generations resulting in Cx26over/Cx30-/- mice. Measurements of the auditory brainstem responses (ABRs) of the Cx26over/Cx30-/- mice showed hearing thresholds across a frequency range of 4-32 kHz indistinguishable from the wild type mice. Examinations of the cochlear morphology also showed complete rescue of hair cells by over expressing Cx26 in the Cx30 knockout mice (confirmed by PCR, Southern and Western blots). The complete restoration of the hearing in the Cx30 knockout mice by over expression of Cx26 suggest that the diversity of Cx expressions in forming GJs is not essential for normal functions of the cochlear GJs. Homomeric GJs consisting of only Cx26 are sufficient for maintaining the normal GJ-mediated functions in the mature cochlea.

#### **[798] Clinical Presentation of GJB2/GJB6 Mutations**

Ingo Todd<sup>1</sup>, Hans Christian Hennies<sup>2</sup>, Dietmar Basta<sup>1</sup>, Arne Ernst<sup>1</sup>

<sup>1</sup>ENT Department at the Unfallklinik Berlin,

<sup>2</sup>Department of Dermatogenetics, University of Cologne

Connexin mutations are known to be responsible for a high percentage of non-syndromic forms of SNHL. So far, more than 90 mutations have been identified for the most relevant connexin, i.e. Cx 26. Connexins are assumed to play a central role in the ionic homeostasis of the cochlea. Various types of hearing losses have been described in those patients affected by mutations of Cx 26/30. Unfortunately, there is so far no specific clinical or audio-neurological pattern available which could possibly guide the clinician to identify a mutational hearing loss without further molecular genetic screening.

In the present study, the frequency of GJB2/GJB6 mutations was investigated in two groups of patients. Group I was characterized by 300 patients with a hearing loss of more than 30 dB in two frequencies, group II by 300 patients which were counselled at the department for non-otologic reasons.

Group I had a frequency of 10 % GJB 2 mutations with a higher preference in specific clinical subgroups, but no GJB6 mutation. Interestingly, group II showed nearly the same frequency of GJB 2 mutations. Further audiological diagnostics revealed that they were affected by different types of hearing losses in all cases, too.

The analysis of specific clinical subgroups should lead to a deeper look inside the clinical pattern of connexin mutations.

Supported by a grant from the Sonnenfeld and Fritz Thyssen foundation

#### **[799] Selective Inner Hair Cell Loss Enhances Noise-Induced Outer Hair Cell Lesions**

Dalian Ding<sup>1</sup>, Bo Du<sup>1</sup>, Haiyan Jiang<sup>1</sup>, Richard Salvi<sup>1</sup>

<sup>1</sup>University at Buffalo

Outer hair cells (OHC) are especially vulnerable to acoustic overstimulation and the amount of damage is closely correlated with the exposure level and the mechanical input to the cochlea. The mechanical input to the cochlea can be modified by two sources of negative efferent feedback, the middle ear muscles and olivocochlear efferent neurons. The outputs from these two negative feedback circuits are modulated by inputs relayed to them from inner hair cells (IHC) and type I spiral ganglion neurons. Therefore, we hypothesized that selective destruction of IHC and type-I neuron was significantly enhance the amount of noise-induced OHC damage. To test this hypothesis, we compared the amount of OHC and IHC loss in three groups (5/group) of chinchillas: (1) noise-exposed group (105 dB SPL octave band noise centered at 4 kHz, 5 h), (2) carboplatin-treated group (100 mg/kg i.p.) and (3) carboplatin plus noise-exposed group (noise exposed 20 days post-carboplatin). The noise-exposed group showed approximately 60% OHC loss and the amount of OHC damage was greatest in the basal, high frequency region of the cochlea. The carboplatin-treated group, by contrast, showed minimal OHC loss; however, they developed large IHC lesions (~90%) over most of the cochlea consistent with our earlier results. Significantly, more than 85% of the OHC and ~90% of the IHC were missing in carboplatin plus noise group. The increase in OHC damage was greatest in the apical half of the cochlea. These results indicate that selective IHC/type-I spiral ganglion lesions significantly enhances noise-induced OHC damage presumably by reducing the negative feedback provided by the middle ear muscles and olivocochlear efferent neurons and possibly other mechanisms.

#### **[800] Acoustic Trauma in MCP-1/CCL-2 or CCR-2 Knockout Mice**

Nathan Sautter<sup>1,2</sup>, Richard Ransohoff<sup>1,3</sup>, Keiko Hirose<sup>1,2</sup>

<sup>1</sup>Cleveland Clinic Foundation, <sup>2</sup>Head & Neck Institute,

<sup>3</sup>Lerner Research Institute, Department of Neurosciences

Monocyte migration in the mouse cochlea has been shown after acoustic injury (Hirose et al, 2005). Monocyte chemoattractant protein 1 (MCP-1, or CCL-2 in the systematic terminology) and CC chemokine receptor 2 (CCR-2) are a ligand/receptor pair that play important roles in monocyte migration into the central nervous system in varied inflammatory processes including mechanical trauma. The roles of CCL-2/CCR-2 in the cochlea are unknown. We examined acoustic trauma in CCL-2-/- or CCR-2-/- mice, in comparison with wild-type littermate animals, to determine if absence of these molecules would



preclude monocyte recruitment to the injured cochlea. Both wild-type and non-exposed knockout mice were used as controls. ABR thresholds and histopathology of the cochlea were examined following noise exposure. The location and number of inflammatory cells in the cochlear duct were also documented. Interestingly, inflammatory cells accumulated equally in noise exposed CCL-2<sup>-/-</sup> or CCR-2<sup>-/-</sup> or wild-type mice after acoustic exposure. ABR threshold shift was also comparable to wild types in CCL-2<sup>-/-</sup> and CCR-2<sup>-/-</sup> mice. Strikingly, acoustic trauma caused significantly worse hair cell survival in CCR-2<sup>-/-</sup> cochleas, as compared to CCL-2<sup>-/-</sup> or wild type mice.

Our studies indicate that deletion of CCL-2 or CCR-2 does not alter inflammatory cell accumulation in the cochlea after exposure to damaging noise levels. However, deletion of CCR-2 increases hair cell susceptibility to injury suggesting a protective effect of CCR-2 mediated by signaling to the cochlear macrophage, or via other cells yet unidentified in the cochlea that express CCR-2.

### **[801] Akt1 Is Involved in Recovery from Temporary Noise-Induced Hearing Loss**

**Andra Talaska<sup>1</sup>, Su-Hua Sha<sup>1</sup>, María Angeles Vicente-Torres<sup>1</sup>, Jochen Schacht<sup>1</sup>**

<sup>1</sup>*Kresge Hearing Research Institute, The University of Michigan, Ann Arbor, MI, USA*

The cellular kinase Akt is an enzyme prolific in the regulation of the life and death of a cell, acting through phosphorylation of a plethora of downstream targets affecting protective homeostatic, as well as apoptotic and necrotic pathways. One of these downstream targets is NF- $\kappa$ B which we have identified as a survival pathway in cells that persist after aminoglycoside insult in a mouse model (Jiang et al. *J Neurosci Res.* 79, 2005). Conversely, aminoglycoside treatment committing cells to apoptosis decreased the activation of Akt (Guan et al. *ARO Abstract* #567, 2005). As investigation into their pathogenesis has found many similarities between noise- and drug-induced hearing loss, we have now prospected the role of Akt in inner ear stress imposed by noise. Specifically, we investigated the involvement of Akt in temporary and permanent threshold shift-models of noise-induced hearing loss using Akt1-knockout mice. In the PTS model, Akt1-knockout mice presented permanent threshold shifts of about 40 dB at 24 kHz, not significantly different from that of their wild-type littermates. However, in the TTS model, while the groups had equal initial shifts, the knockout mice showed significantly less recovery from the noise trauma from two hours to three days post-exposure as compared to wild type. By 14 days, thresholds in both wild-type and knock-out animals had returned to pre-exposure levels. Akt and related pathways, then, may be involved in an early homeostatic response to noise-induced insult.

This work was supported by research grant DC-06457 and core center grant DC-05188 from the National Institute on Deafness and other Communication Disorders, NIH.

### **[802] The Protective Effect of Restraint Stress on Noise Induced Hearing Loss Is Glucocorticoid Receptor Mediated**

**Peter Johansson<sup>1</sup>, Yeasmin Tahera<sup>1</sup>, Inna Meltser<sup>1</sup>, Anita C. Hansson<sup>2</sup>, Barbara Canlon<sup>1</sup>**

<sup>1</sup>*Department of Physiology and Pharmacology, Karolinska Institutet*, <sup>2</sup>*National Institute on Alcohol Abuse and Alcoholism, NIH*

The stress response stimulates the secretion of glucocorticoids. Previous studies have shown that acute psychological and physiological stress has protective effects on noise induced hearing loss. Our hypothesis was that these protective effects are glucocorticoid mediated.

In order to test our hypothesis CBA mice were given the glucocorticoid synthesis blocker metyrapone and the glucocorticoid receptor antagonist RU 486. After drug treatment the animals were subjected to mild physical restraint followed by noise trauma. Prior to noise trauma control animals were instead given either 1) placebo + restraint stress or 2) placebo + home cage instead of restraint stress. Auditory brainstem response (ABR) and distortion product otoacoustic emission (DPOAE) were measured in order to establish effects of noise trauma. Analysis of serum corticosterone and in situ hybridization of cochlear glucocorticoid receptor mRNA were conducted in order to assess changes in hormonal regulation.

Our results show that animals given placebo + restraint stress treatment prior to noise trauma demonstrated lower ABR-thresholds shifts compared to the other groups. There were no obvious differences in DPOAE amplitudes. Serum corticosterone levels were elevated in both the placebo + restraint stress and drug + restraint stress groups. Glucocorticoid receptor mRNA expression in the cochlea was lower in the placebo + restraint stress treated group compared to the other groups.

These results confirm that restraint stress has a protective effect on noise induced hearing loss. The lack of difference between the groups in DPOAE amplitudes suggests that the protective effects are not localized in the outer hair cells of the cochlea. We can also conclude that blocking glucocorticoid secretion and receptor binding abolishes the protective effects of restraint stress. This implies that the protective effects of restraint stress are glucocorticoid mediated.

### **[803] Restraint Stress Reduces the Damaging Effect of Acoustic Trauma by Modulating the Mitogen-Activated Protein Kinases in the Cochlea**

**Inna Meltser<sup>1</sup>, Yeasmin Tahera<sup>1</sup>, Peter Johansson<sup>1</sup>, Barbara Canlon<sup>1</sup>**

<sup>1</sup>*Department of Physiology and Pharmacology, Karolinska Institutet*

Acoustic trauma is well known to cause hearing loss, yet the mechanism underlying this damage is not well understood. The main purpose of the present study was to determine the cellular events that can occur in the cochlea following the combined treatment with physiological stressors such as restraint stress and acoustic trauma. Here we show that restraint stress decreases hearing loss

induced by acoustic trauma (100 dB SPL for 45 min). The protective effect of the restraint is mainly produced by an increase of systemic corticosterone and the activation of glucocorticoid receptors (GR) in the inner ear. Mitogen-activated protein kinases (MAPK) are involved in stress-related cellular responses and can modify the activity of GR locally in the inner ear. Using immunocytochemistry we found that all three phosphorylated MAPK (p38, ERK and in a less extend JNK) are expressed in the spiral ganglion neurons of the cochlea. Western blot analysis showed no changes in MAPK phosphorylation in the modiolus tissue in response to the acoustic trauma alone, whereas the combination of the restraint and acoustic trauma decrease phosphorylation of JNK and ERK, and increased the phosphorylation of pp38. Disruption of GR-mediated pathway by the combined systemic treatment with metyrapone and GR-antagonist RU486 abolished these changes for JNK and, partially, for ERK, but not for p38. Thus, all three MAPKs are involved in the response of spiral ganglion neurons to restraint followed by acoustic trauma, but only JNK and ERK activity is regulated by GR. These data show that GR-mediated regulation of MAPKs activity plays a role in modulating the sensitivity of the inner ear to glucocorticoids.

#### **804 Can Erythropoietin Protect the Inner Ear from Toxic Effects?**

**Arianne Monge**<sup>1</sup>, Ivana Nagy<sup>1</sup>, Sharouz Bonabi<sup>1</sup>, Max Gassmann<sup>2</sup>, Daniel Bodmer<sup>1</sup>

<sup>1</sup>Inner Ear Research, ENT Department, University Hospital Zurich, Zurich, Switzerland, <sup>2</sup>Institute of Veterinary Physiology, University of Zurich, Zurich, Switzerland

The most sensitive part in the inner ear are the hair cells, they can not regenerate and their damage leads to an irreversible hearing loss. Therefore we try to find substances that can protect the hair cells from damage. Erythropoietin (Epo) may be a possible candidate. Epo is known as the primary regulator of erythropoiesis, preventing apoptosis and promoting differentiation of the red blood cell precursors. Several new studies have shown that Epo has also a neuroprotective effect. Many in vitro studies documented an inhibition of cellular apoptosis by Epo. Different in vivo studies documented a reduction of structural damage when Epo was applied, for example in animal models for brain-, spinal cord- and retina pathology. Epo exerts its effects by binding to the Epo-Receptor. This raised the question, if the inner ear expresses the Epo-Receptor. In newborn rats we found by RT-PCR Epo and Epo-Receptor mRNA in the organ of corti, the spiral ganglion and the stria vascularis. Immunohistochemistry was performed to localize the Epo-Receptor. Outer- and inner hair cells and supporting cells of the organ of corti, the spiral ganglion cells and the stria vascularis stained for the Epo-Receptor. The presence of the Epo-Receptor in the organ of corti supports the theory that Epo may be able to prevent the inner ear hair cells from apoptosis. We will study, if Epo effects on damaged hair cells in vitro.

#### **805 Induction of Kidney Injury Molecule (KIM)-1 Expression in the Rat Cochlea by Noise**

**Craig Whitworth**<sup>1</sup>, Debashree Mukherjee<sup>1</sup>, Larry F. Hughes<sup>1</sup>, Leonard Rybak<sup>1</sup>, Vickram Ramkumar<sup>1</sup>

<sup>1</sup>SIU School of Medicine

Kidney injury molecule (KIM)-1 is a protein initially identified in the renal proximal tubular epithelium, whose expression is regulated by kidney injury. KIM-1 is believed to be involved in tissue repair and healing. We have recently identified this protein in the cochlea and in several organ of Corti hair cell lines. Exposure to cisplatin produced a substantial induction in KIM-1 expression in the cochlea *in vivo* and in an organ of Corti hair cell line, UB-OC1. Furthermore, we showed that induction of KIM-1 by cisplatin was associated with increased expression of the NADPH oxidase-associated protein, Rac1, and a novel NADPH oxidase isoform, NOX3. This induction of KIM-1, NOX3 and Rac1 by cisplatin was reduced by the antioxidant, lipoic acid. In the current study, we investigated whether noise exposure induces KIM-1 expression in the cochlea. For these studies, male Wistar rats were exposed to 90 dB SPL noise (8 kHz octave band) for 8 h while the controls were subjected to the same noise at 60 dB SPL. ABR testing was performed before and within 6 hours after noise exposure. Animals were sacrificed after the last ABR measurements and their cochleas excised and used for RNA preparation and real time PCR studies. Ninety dB noise exposure resulted in a  $42.5 \pm 2.2$  dB temporary threshold shift at 8 kHz and a  $39.2 \pm 1.9$  dB shift at 16 kHz (mean  $\pm$  SEM). In contrast, 60 dB noise exposure resulted in a  $0.8 \pm 2.2$  dB shift at 8 kHz and a  $6.7 \pm 2.6$  dB threshold shift at 16 kHz. A statistically significant increase ( $6.4 \pm 1.7$ -fold) in KIM-1 expression was seen following 90 dB noise exposure, which was associated with a  $9.0 \pm 2.6$  fold induction in NOX-3 expression and a  $7.4 \pm 1.3$  fold induction in Rac1. Co-regulation of NADPH oxidase and KIM-1 in the cochlea by noise suggests that reactive oxygen species (ROS) play a role in mediating this induction. These data suggest that induction of KIM-1 by noise could be an important step in preconditioning the cochlea against damage by ototoxic chemicals and more intense noise trauma.

#### **806 Induction of Heat Shock Proteins by Noise Stress in Normal and Hsf1 Knockout Mice**

**Tzy-Wen Gong**<sup>1</sup>, Lynne Fullarton<sup>1</sup>, Ariane Kanicki<sup>1</sup>, Gary Dootz<sup>1</sup>, David Dolan<sup>1</sup>, Richard Altschuler<sup>1</sup>, Margaret Lomax<sup>1</sup>

<sup>1</sup>University of Michigan

Our research has focused on the classic heat shock or stress response, a major protective mechanism controlled by heat shock transcription factor 1 (HSF1). Many different environmental stresses are known to activate HSF1, leading to DNA binding and induction of genes for heat shock proteins (HSPs). We have investigated the effect of acoustic stimulation on the induction of heat shock proteins, using an Hsf1 knockout mouse model that lacks functional HSF1. We previously showed that Hsf1<sup>-/-</sup> null mice do not recover completely from a mild noise exposure [98 dB broadband noise (BBN), 2-20 kHz, 2 hr]

that produces only a temporary threshold shift (TTS) in wild-type mice (Fairfield et al., 2005). In this study, we examined expression of several HSP genes in both Hsf1<sup>+/+</sup> heterozygotes and Hsf1<sup>-/-</sup> null mice following noise stress. Levels of mRNA for HSPs were measured in total RNA from whole cochlea by quantitative RT-PCR with TaqMan probes. The induction of HSPs by noise overstimulation was examined following exposure to BBN (2-20 kHz) presented for 2 hr at three different noise intensities (98 dB, 106 dB, and 120 dB SPL). In Hsf1<sup>+/+</sup> heterozygotes, we observed a 2-fold induction of the two genes for Hsp70 (Hsp70.1, Hsp70.3) at 98 dB, and a 10-fold induction at 106 dB and at 120 dB. In Hsf1<sup>-/-</sup> null mice, induction of Hsp70.1 and Hsp70.3 still occurred, but was significantly lower than in Hsf1<sup>+/+</sup> heterozygotes. These studies indicate that HSF1 is activated following noise over stimulation, leading to induction of HSPs. Induction of HSPs in the absence of HSF1, however, indicates that other signaling pathways may contribute to induction of HSPs and thus play a role in protecting the cochlea from noise overexposure. Focusing on the response of Hsf1<sup>+/+</sup> heterozygotes to 106 dB BBN, we measured auditory thresholds by ABR and determined that this noise exposure produced a permanent threshold shift (PTS) of 10 dB at 16 kHz, and a 20 dB threshold shift at 24 kHz 2 weeks following the noise exposure. Immunocytochemistry with antibodies to HSP70 indicated that exposure to 106 dB noise caused an increase in HSP70 immunoreactivity in stria vascularis and spiral ganglion neurons.

Supported by NIH grants P01 AG025164, R55 DC06290 (RA), and P30 DC005880.

### **807 Expression of Ubiquitin Ligase Ube3b in the Mouse Ear, Eye, and Tooth**

**Tzy-Wen Gong**<sup>1</sup>, Adam Mileski<sup>1</sup>, Siew-Ging Gong<sup>2</sup>, Chao Guo<sup>1</sup>, Margaret Lomax<sup>1</sup>

<sup>1</sup>The University of Michigan, <sup>2</sup>University of Toronto

Ubiquitination, addition of ubiquitin residues, targets cellular proteins for degradation by the 26S proteasome. This process is achieved by the consecutive action of three enzymes or enzyme complexes ubiquitin activating enzyme (E1), conjugase (E2), and ligase (E3). We identified a chick partial cDNA that was up-regulated after noise over-stimulation (Lomax et al., Hearing Res 147, 293-302, 2000) and subsequently cloned full-length cDNAs for human, mouse, and chick UBE3B, a novel E3 ligase with a C-terminal HECT-domain (Gong et al., Genomics 82, 143-152, 2003). Northern blot analysis indicated that UBE3B is widely expressed in many tissues. To elucidate the functional role of UBE3B, we examined expression patterns of this gene in the inner ear, eye, and tooth in the mouse. Expression was examined by in situ hybridization using a cRNA probe corresponding to UBE3B-specific sequence in the 3' UTR and by immunohistochemistry using rabbit antiserum generated against a 15-aa peptide unique to chick and mouse UBE3B. Immunohistochemical observations recapitulated those of in situ hybridization. In the inner ear, the highest

expression was observed in the Schwann cells along the axonal processes of the cochlear and vestibular nerves. UBE3B was expressed at lower levels in the spiral and vestibular ganglion cells, the sensory epithelium, and marginal cells of the stria vascularis. In the eye, UBE3B was expressed strongly in the optic nerve, with lighter, but significant expression in the photoreceptor layer, the inner nuclear layer, the inner plexiform layer, and the ganglion cell layer. In the developing tooth, UBE3B was localized to the ameloblasts of the coronal portion. Additional studies will be conducted to further understand the role of UBE3B in these cells and to identify target molecules of this ubiquitin ligase. (Supported by Deafness Research Foundation (TWG).)

### **808 WDR1 Expression in the Normal and Noise-Damaged Chick Vestibule**

**Myung-Whan Suh**<sup>1</sup>, Seung-Ha Oh<sup>1</sup>, Min-Hyun Park<sup>1</sup>, Jae-Jun Song<sup>1</sup>, Dong Hoon Shin<sup>2</sup>, Ga Hee Mun<sup>2</sup>

<sup>1</sup>Department of Otorhinolaryngology-Head and Neck Surgery, Seoul National University Hospital, <sup>2</sup>Department of Anatomy, Seoul National University College of Medicine

Introduction: Unlike mammals, the avian cochlear hair cells can regenerate even after acoustic over stimulation. WDR1 is one of the genes that is suspected to play a major role in this difference. It has been reported that WDR1 mRNA is expressed in the over stimulated cochlea. The aim of this study was to evaluate whether the WDR1 is up regulated even in the chick vestibule after acoustic over stimulation. Materials and methods: 7-day-old chicks were divided into three groups, control group (Normal), noise damaged group (Damage) and recovery group (Regeneration). The damage group was exposed to 120 dB SPL white noise for 5-6 hours and was euthanized after the noise. The regeneration group was allowed to recover for 2 days. The three ampullas of each semicircular canals, utricle and saccule were dissected and immunohistochemically stained with the anti-WD40 antibody. The intensity of staining was compared in the sensory epithelium. For quantitative analysis real time RT PCR of the WDR1 mRNA was performed. Results: As for the superior, posterior, lateral ampulla and utricle, the intensity of staining was significantly higher in the regeneration group compared to the normal group. The supporting cell layer and hair cell walls were mainly stained. Real time RT PCR was performed to confirm the higher expression of WDR1 in the regeneration group. The WDR1 mRNA expression was 1.34 times higher in the regeneration group and 1.68 times higher in the positive control, compared to the normal group. But not in accordance with the other vestibular organs, saccule did not show higher expression in the regeneration group. It was thought that the acoustic over stimulation had the greatest impact to the saccule that the excessive damage was too extensive to be recovered in the saccule. Conclusion: WDR1 was up regulated after the acoustic over stimulation in the vestibular organs except for the saccule. The chick vestibular hair cell may also have a protective mechanism, but somewhat imperfect.

### **809 WDR1 Presence in the Songbird Inner Ear**

**Henry J. Adler<sup>1</sup>**, Elena Sanovich<sup>1</sup>, Elizabeth F. Brittan-Powell<sup>1</sup>, Robert J. Dooling<sup>1</sup>

<sup>1</sup>*University of Maryland, Center of Comparative and Evolutionary Biology of Hearing*

We aim to determine the role of WD repeat-1 protein (WDR1) in hearing loss and recovery in birds following trauma for several reasons. WDR1 was first identified in the acoustically injured chicken basilar papilla, and has nine WD40 motifs, important for protein-protein interactions. WDR1 also has significant homology to actin-interacting protein-1 (AIP-1) in several species such as slime mold and earthworm. AIP-1 was shown to interact with cofilin/actin depolymerization factor, adding significance to the potential role of WDR1 in actin dynamics.

The specific goal of our present study is to demonstrate WDR1 expression in the inner ears of birds other than chicken. We target songbirds because a type of songbird, the Belgian Waterslager (BWS) canary, exhibits early onset hearing loss. We subjected RNA [isolated from the basilar papillae of chicken and three different songbirds (Gloster canary, BWS canary, zebra finch)] to reverse-transcription-PCR with a pair of oligonucleotides flanking chicken WDR1 nucleotide (nt) positions 493–778. PCR on the four bird species revealed a single 286-nt band. The DNA sequence of that band from each songbird has a 94–95% identity to the above mentioned chicken WDR1 DNA region.

We labeled avian basilar papillae with rabbit anti-WDR1 antibody that was raised against a synthetic peptide identical to the first 12 amino acids of mammalian WDR1. This staining was followed by a second round of immunolabeling with Alexa Fluor 633–conjugated goat anti-rabbit antibody. Confocal microscopy examinations of the inner ears of chicken and Gloster canary revealed WDR1 localization to hair cells, but not supporting cells. The two sets of data confirmed and extended earlier findings of WDR1 expression in the normal avian inner ear (Adler et al., *Genomics*, 1999, 56:59–69; Oh et al., 2002, *J Comp Neurol* 448:399–409).

Supported by a disability supplement (HJA) to NIDCD 000436 (Catherine E. Carr), NIH DC01372 (RJD), and NIH P30–DC04664 (C-CEBH).

### **810 Mitochondria Regulate Agonist Induced Cytoplasmic Calcium Signals in Cochlear Support Cells**

**Zoë Mann<sup>1,2</sup>**, Michael Duchén<sup>2</sup>, Jonathan Gale<sup>1,2</sup>

<sup>1</sup>*Centre for Auditory Research, UCL Ear Institute, London, UK*, <sup>2</sup>*Dept. of Physiology, UCL, London, UK*.

In eukaryotes mitochondria are the sites of oxidative phosphorylation and thus the major cellular energy producers. However, in many cell types mitochondria also play an important role in regulating cytoplasmic calcium ( $[Ca^{2+}]_c$ ). A number of mitochondrial mutations are associated with hearing loss, yet we know little about the functions of mitochondria in sensory epithelia of the inner ear.

We investigated mitochondrial regulation of  $[Ca^{2+}]_c$  in Claudius cells in neonatal rat cochlear cultures using a confocal imaging system. Indicator dyes Fura2 and Rhod2 were used to measure  $[Ca^{2+}]_c$  and mitochondrial  $Ca^{2+}$   $[Ca^{2+}]_m$  respectively. Exogenous application (20–30s) of ATP (0.1 to 50  $\mu$ M) caused dose-dependent, rapid and reversible increases in  $[Ca^{2+}]_c$  due to its action on P2 receptors on these cells (Gale et al, 2004). At 100nM ATP had little or no effect on  $[Ca^{2+}]_m$  whereas at 1  $\mu$ M ATP mitochondrial  $Ca^{2+}$  uptake was observed. Recovery of  $[Ca^{2+}]_m$  occurred within a few minutes. 50  $\mu$ M ATP caused robust mitochondrial  $Ca^{2+}$  uptake that could take as long as 45 minutes to reverse. CCCP (5  $\mu$ M), a protonophore that collapses the mitochondrial membrane potential, reduced mitochondrial  $Ca^{2+}$  uptake resulting in significant prolongation of the  $[Ca^{2+}]_c$  increase induced by ATP concentrations at or above 1  $\mu$ M. In preliminary experiments we have also observed changes in  $[Ca^{2+}]_m$  in hair cells and their immediate support cell neighbours.

Our data are compatible with mitochondria acting as spatio-temporal buffers of  $[Ca^{2+}]_c$  in the cochlea. Some of the mutations that alter mitochondrial function could elicit their effects via the disruption of cellular homeostasis described here.

*Supported by an RNID Studentship to ZM and the Royal Society.*

### **811 Cochlear Blood Flow During Occlusion and Reperfusion of the Anterior Inferior Cerebellar Artery – Effect of Topical Application of Dexamethasone to the Round Window**

**Hironao Otake<sup>1</sup>**, Hiroshi Yamamoto<sup>1</sup>, Masaaki Teranishi<sup>1</sup>, Michihiko Sone<sup>1</sup>, Tsutomu Nakashima<sup>1</sup>

<sup>1</sup>*Department of Otorhinolaryngology, Nagoya University Graduate School of Medicine*

**Objective:** Intratympanic administration of steroid has been used for the treatment of sudden sensorineural hearing loss. We attempted to investigate the effect of the topical application of dexamethasone on cochlear blood flow (CBF).

**Methods:** Sprague Dawley (SD) rats with normal Preyer reflexes were used. The animals were anaesthetized with ketamine (100 mg/kg) and xylazine (5 mg/kg) intramuscularly. To maintain the anaesthesia, ketamine (50 mg/kg) was added every 45 min. The right tympanic bulla was opened by a ventral-lateral approach, and the middle ear mucosa over the bony wall of the cochlea was gently removed with a cotton pledget. The tip of the laser Doppler probe was positioned on the basal turn of the cochlea and connected to a laser Doppler flowmeter to measure CBF. Dexamethasone (0.33% and 3.3%) dissolved in 0.5 ml saline was administered to the round window. The anterior inferior cerebellar artery (AICA) was occluded for 2 hours and then the occlusion was released. The CBF response to the occlusion and release was observed with and without the topical application of dexamethasone.

**Results:** Even if dexamethasone was administered to the round window, CBF did not change significantly. After occlusion of the AICA, CBF decreased to 50% ~ 60% and

remained at this level for 2 hours. Previous administration of dexamethasone did not change the CBF response to the occlusion.

When the occlusion was released, CBF returned to the previous level in 2 out of five rats without topical application of dexamethasone. However, the CBF returned to the previous level in 8 out of ten animals in which dexamethasone was applied to the round window prior to the occlusion of the AICA. The CBF response was not different between two concentrations of dexamethasone.

Conclusion: Topical application of dexamethasone to the round window did not exert influence on CBF. However, the topical application of dexamethasone may help function to keep autoregulation of CBF.

## **[812] The Role of D2 Autoreceptors in Cochlear Ischaemia**

**György Halmos**<sup>1,2</sup>, Gábor Polony<sup>1,2</sup>, Tamás Horváth<sup>1</sup>, Zoltán Doleviczényi<sup>1</sup>, Gábor Répássy<sup>2</sup>, Ágnes Kittel<sup>1</sup>, E. Sylvester Vizi<sup>1</sup>, Balázs Lendvai<sup>1</sup>, Tibor Zelles<sup>1</sup>

<sup>1</sup>*Institute of Experimental Medicine, Hungarian Academy of Sciences*, <sup>2</sup>*Department of Otolaryngology, head and Neck Surgery, Semmelweis University*

One possible mechanism of the ischemia-induced sensorineural hearing loss is the afferent nerve damage due to the glutamate excitotoxicity, released from the inner hair cells. The lateral olivocochlear (LOC) efferent fibers are thought to have protective role in this process, forming axodendritic synapse on the afferent nerve and by releasing dopamine, which postsynaptically inhibits the glutamate-induced firing of the cochlear nerve. D2 and D3 receptors have been detected on the afferent dendrite. In our previous studies we investigated the presence of possible dopamine autoreceptors on the LOC axon terminals, and D1 receptors have been pharmacologically identified, while the role of D2 receptors remained controversial. In the present study we investigated the effect of an in vitro ischemia model, on guinea-pig cochlear [3H]DA release by revoking oxygen and glucose from the perfusion solution (oxygen-glucose deprivation, OGD). Using in a microvolume superfusion system on isolated guinea-pig cochleae, we found that OGD alone failed to induce a detectable elevation of [3H]DA level, but in the presence of specific D2 receptor antagonists, sulpiride and L-741,626, it evoked a significant increase in the extracellular concentration of [3H]DA. D2 negative feedback receptors are involved not exclusively in the regulation of synthesis and vesicular release of DA, but also in the activation of its reuptake. Thus, D2 receptor antagonism interferes with the powerful reuptake of DA from the extracellular space. To explore the underlying mechanism of this DD-releasing effect we applied the DA-uptake inhibitor nomifensine and found that it inhibited the effect of OGD on cochlear DA release in the presence of D2 antagonists. This finding indicates that the OGD-evoked DA release was mainly mediated through the reverse operation of the DA transporter. Our results confirm the presence and role of D2 DA autoreceptors in the regulation of DA release from LOC efferents in ischemia.

## **[813] Decreased Energy Metabolism, Mitochondrial Dysfunction, and Induction of Apoptosis in the Cochlea of CBA Mouse Given Germanium Dioxide**

**Tatsuya Yamasoba**<sup>1</sup>, Chikako Yamada<sup>1</sup>, Shinichi Someya<sup>2</sup>, Masaru Tanokura<sup>3</sup>

<sup>1</sup>*Department of Otolaryngology, University of Tokyo*,

<sup>2</sup>*Departments of Genetics & Medical Genetics, University of Wisconsin*, <sup>3</sup>*Department of Applied Biological Chemistry, University of Tokyo*

It has been shown that, when chronically given to rats, germanium dioxide (Ge) induces ragged-red fibers and cytochrome-c oxidase-deficient fibers in the skeletal muscles. These pathological changes resemble those observed in patients with mitochondrial encephalomyopathy. We previously demonstrated that guinea pigs given 0.5% Ge exhibited skeletal muscle atrophy and moderate ABR threshold shifts due to degeneration of the stria vascularis and cochlear sensory epithelium that contained a lot of electron-dense mitochondrial inclusions. Immunohistochemical study showed reduction of cytochrome c oxidase activity in the skeletal muscle and kidney in these animals (Yamasoba et al. ARO abstr, 2002). These findings indicate that animals given Ge can be used to study the mechanism of cochlear damage associated with mitochondrial dysfunction.

In the current study, we examined alteration of gene expression profiles in the mouse cochlea induced by Ge application. CBA mice given 0.15% Ge exhibited skeletal muscle atrophy and profound hearing loss 3 moths later. Histopathological analysis revealed marked degeneration of stria vascularis, spiral ganglion cells, and organ of Corti, predominantly supporting cells. TEM observation revealed electron-dense mitochondrial inclusions in the degenerated tissues in the cochlea, as well as the skeletal muscles and kidney. When compared to age-matched untreated animals, there were down-regulation of genes associated with hearing function, neurotransmission, DNA repair, protective response against oxidative stress, and energy metabolism including all five mitochondrial complexes, and up-regulation of genes related to apoptosis. These findings indicate that Ge application induces down-regulation of energy metabolism due to mitochondrial dysfunction, which then triggers apoptotic cell death and results in profound deafness.

## **[814] A Mouse Model for Specific Degeneration of the Spiral Ligament**

**Shinpei Kada**<sup>1</sup>, Takayuki Nakagawa<sup>1</sup>, Juichi Ito<sup>1</sup>

<sup>1</sup>*Department of Otolaryngology-Head and Neck Surgery, Graduate School of Medicine, Kyoto University*

The spiral ligament (SL) plays essential roles in potassium ion recycling in the cochlea. SL degeneration is, thus, considered as a cause for sensorineural hearing loss due to aging (Spicer et al. 2002) or noise exposure (Hirose et al. 2003). In addition, previous studies indicated involvement of SL degeneration in the etiology of hearing loss in Meniere's disease (Merchant et al. 2005). Regeneration of the SL is, therefore, included one possible strategy for the treatment of sensorineural hearing loss.

Recently, a rat model for SL degeneration has been reported (Hoya et al. 2004). In this model, local application of a mitochondrial toxin, 3-nitropropionic acid (3-NP) is caused comparatively selective degeneration of the SL. Then, we intended to establish a mouse model for SL degeneration using 3-NP, because a mouse is a preferable animal for the availability of a source for cell transplantation. Here we used C57BL/6 mice as experimental animals. Local application of 3-NP was performed by an injection into the posterior semicircular canal (Nakagawa, et al. 2003). The left ear was locally applied 3-NP (300 mM, 1.5  $\mu$ l) and the right ear was used as a control. ABR measurements were conducted preoperatively, 1, 4, 7 and 14 d after the administration of 3-NP, and histological evaluation of the cochlea was performed. We then calculated the cell density of the SL in each turn of the cochlea. Significant elevation of ABR thresholds were observed from 1 d after the treatment, and permanent threshold shifts were identified. Cell densities of the SL significantly reduced in each turn on 14 d after the treatment. These findings indicate that this mouse model can be the basis for development of the strategy for SL regeneration.

#### **[815] Protective Effect of Sulforaphane Against Cisplatin-Induced Ototoxicity**

**Bok-Ryang Kim<sup>1</sup>**, Byung-Min Choi<sup>1,2</sup>, Sung-Min Choi<sup>1</sup>, Myung-Ryong Gea<sup>1</sup>, Kwang Lee<sup>1</sup>

<sup>1</sup>*Department of Biochemistry, School of Medicine, Wonkwang University,* <sup>2</sup>*Wonkwang University*

Cisplatin is a highly effective chemotherapeutic agent but it has a significant ototoxic side effects. In this study, we investigated the protective effect of sulforaphane (SFN), a well-known inducer of phase 2 detoxification enzymes from vegetables, on cisplatin-induced apoptosis in HEI-OC1 cells. Cisplatin induced apoptotic cell death in a dose-dependent manner, which was revealed as an apoptotic process characterized by DNA laddering, DAPI staining, and annexin-V binding. However, pretreatment of cells with SFN blocked the apoptosis induced by cisplatin in HEI-OC1 cells, efficiently. Exposure of HEI-OC1 cells to SFN resulted in the induction of antiapoptotic protein Bcl-2. SFN-pretreated HEI-OC1 cells were inhibited activation of caspase-9 and -3 by cisplatin. Also, cisplatin-induced apoptosis was blocked by caspase-9 inhibitors. The antiapoptotic action of SFN was associated with increasing expression of antiapoptotic protein Bcl-2 and decreasing activity of caspase-9. These results show that SFN may be a useful strategy to prevent harmful side effects of cisplatin-induced ototoxicity in patients having to undergo chemotherapy.

#### **[816] The Effect of 2-Aminoethoxydiphenyl Borate on Caspase-3 Activity in Gentamicin Treated Cochlear Sensory Cells**

**Jae-Yun Jung<sup>1</sup>**, Jeong-Hwan Moon<sup>1</sup>, Jin-Chul Ahn<sup>2</sup>, In-Young Baek<sup>2</sup>, Chung-Ku Rhee<sup>1,2</sup>

<sup>1</sup>*Dankook University Hospital,* <sup>2</sup>*Medical Laser Research Center*

Auditory hair cell death in response to aminoglycoside antibiotics occurs via apoptosis. Elevated intracellular

calcium level is known to play important roles in apoptotic pathway. IP3 receptor (ligand-gated channels that release Ca<sup>2+</sup> from intracellular stores) is emerging as key site for regulation of apoptosis. 2-Aminoethoxydiphenyl borate (2-APB) is one of reliable IP3 receptor antagonists. We examined the effect of 2-APB on gentamicin (GM) ototoxicity in vitro, using HEI-OC1 cell line.

HEI-OC1 cells were treated with 100  $\mu$ M GM. Using a CaspACE assay, we measured caspases-3 activity in gentamicin GM treated hair cells with and without 2-APB pre-incubation. We also observed intra-cellular calcium concentrations in HEI-OC1 cells using confocal microscopy (calcium green-1 stain).

Cytosolic calcium elevation by gentamicin was remarkably inhibited by 2-APB. Caspases-3 activities of GM treated cells were higher than those of control. After incubation with 2-APB, caspases-3 activities of GM treated cells were shown to decrease.

This result suggests 2-APB can reduce caspase-3 activity in gentamicin treated HEI-OC1 cells by inhibition of calcium increase in cytosol.

#### **[817] Kallidinogenase Protects Kanamycin-Induced Ototoxicity in the Rat Cochlea via Bradykinin-B2 Receptor**

**Takashi Sato<sup>1</sup>**, Katsumi Doi<sup>1</sup>, Toshihiro Kuramasu<sup>1</sup>, Takeshi Kubo<sup>1</sup>

<sup>1</sup>*Osaka University Graduate School of Medicine*

It is still important to prevent and reduce aminoglycoside ototoxicity because aminoglycoside remain to be one of the first-line antibiotics in gram-negative infections and the intratympanic gentamycin treatment for intractable Meniere's disease is becoming increasingly popular.

Since bradykinin is known to show a protective action against glutamate neurotoxicity in the retina and some parts of aminoglycoside ototoxicity might involve glutamate neurotoxicity through an upregulation of glutamate receptors, we investigated the effect of bradykinin on kanamycin-induced ototoxicity in the rat cochlea with an systemic application of kallidinogenase which cleaves tissue-ubiquitous kininogen into bradykinin.

RT-PCR analysis identified the expression of bradykinin-B2 receptor mRNA in the rat cochlea. Immunohistochemical study demonstrated that bradykinin-B2 receptor protein was mainly expressed in the spiral ganglion cells. Co-application of kallidinogenase together with kanamycin significantly reduced hearing impairments induced by kanamycin. Both outer hair cells and spiral ganglion cells were more preserved by an application of kallidinogenase. These protective effects were completely reversed by HOE140, a selective antagonist for bradykinin-B2 receptor. These results suggest that kallidinogenase exerts a protective action against kanamycin-induced ototoxicity through an activation of bradykinin-B2 receptor in the rat cochlea.

### **818** Flunarizine Protects Cisplatin-Induced Apoptosis of Auditory Cells Through Modulation of Proinflammatory Cytokine Production via Nrf2/HO-1 Signaling

Hongseob So<sup>1</sup>, Hyungjin Kim<sup>1</sup>, Channy Park<sup>1</sup>, Jaehyung Lee<sup>1</sup>, Jeonghan Lee<sup>1</sup>, Yunha Kim<sup>1</sup>, Sungyeol Park<sup>1</sup>, Jinkyung Kim<sup>1</sup>, Sangheon Lee<sup>2</sup>, Raekil Park<sup>1</sup>

<sup>1</sup>VCRC, Wonkwang University School of Medicine,

<sup>2</sup>Department of Otolaryngology, Wonkwang University School of Medicine

Cisplatin is a widely used chemotherapeutic agent that is also highly ototoxic. A number of evidences in cytotoxic mechanism of cisplatin, including perturbation of redox status and formation of DNA adduct, have been suggested. We previously demonstrated that cisplatin-induced apoptosis of HEI-OC1 auditory cells through secretion of proinflammatory cytokines and chemokines through NF- $\kappa$ B activation. In addition, we reported that flunarizine, known as (SibeliumTM), protected cells from cisplatin through direct inhibition of lipid peroxidation and mitochondrial dysfunction (Hearing Res. 205, 127-139, (2005). In this study, we further demonstrate that treatment of flunarizine protects cells from cisplatin through the modulation of proinflammatory cytokines, including TNF- $\alpha$ , IL-1 $\beta$ , and IL-6 and chemokine, such as CXCL10 and CCL25. Furthermore, Nrf2/heme oxygenase-1 plays a critical role in flunarizine-mediated protection of HEI-OC1 auditory cells against cisplatin.

### **819** Oral D-Methionine Provides Cisplatin Otoprotection as Effectively as Intraperitoneal D-Methionine in Rats

Michael Todd Gerber<sup>1</sup>, Sara Woodward Dyrstad<sup>1</sup>, Robert Meech<sup>1</sup>, Larry F. Hughes<sup>1</sup>, Deb L. Larsen<sup>1</sup>, Kathleen C.M. Campbell<sup>1</sup>

<sup>1</sup>Southern Illinois University School of Medicine

Cisplatin is an anti-cancer drug that can cause permanent hearing loss. The sulfur-based amino acid D-methionine (D-met) is an antioxidant that can protect against cisplatin-induced ototoxicity. Multiple animal studies have shown that systemic D-met protects the organ of Corti, and stria vascularis from cisplatin without significant interference with cisplatin's anti-tumor action or apparent side effects when administered appropriately. The goal of this study was to determine whether oral D-met is as effective as injected D-met in providing cisplatin otoprotection. Male Wistar rats were divided into 6 groups of 5 animals each. Group 1 comprised a normal control group receiving saline injection only. Group 2 comprised a treated control group given a 30-minute i.p. infusion of 16 mg/kg cisplatin. Group 3 received 1000 mg/kg (200mg/ml concentration) oral D-met delivered by gavage 2 hours before infusion of 16 mg/kg cisplatin. Group 4 received 300 mg/kg D-met delivered i.p. 30 minutes before cisplatin infusion. This i.p. D-met dose is known to fully protect against cisplatin-induced ABR threshold elevations. Group 5 received 300 mg/kg D-met delivered i.p. only. Group 6 received 1000 mg/kg (200 mg/ml concentration) D-met delivered orally by gavage. Auditory brainstem response (ABR) data collection was obtained at baseline just prior to drug

delivery and again 3 days after drug administration centered at frequencies of 4, 8, 14, 20, and 30 kHz. An intensity series was obtained for each animal from 100 to 0 dB sound pressure levels (SPL) for tone bursts in 10 dB decrements. Post-treatment ABR thresholds were significantly higher for the cisplatin alone group than for any other group, and none of the D-met groups yielded findings significantly different from those of the saline alone controls. Histology is in progress. We conclude that D-met taken orally is as effective as injected D-met at preventing cisplatin-induced ABR threshold elevation in rats.

### **820** Edaravone Protects Vestibular Hair Cells Against Neomycin Ototoxicity *In Vitro*

Tsuguyuki Arai<sup>1</sup>, Kazuma Sugahara<sup>1</sup>, Takefumi Mikuriya<sup>1</sup>, Tsuyoshi Takemoto<sup>1</sup>, Hiroaki Shimogori<sup>1</sup>, Hiroshi Yamashita<sup>1</sup>

<sup>1</sup>Yamaguchi University School of Medicine

It is well known that the product of free radicals is associated with the sensory cell death induced by aminoglycoside. Many researchers reported that antioxidant reagents could which can be used clinically in Japan. We have already reported that edaravone can protect for vestibular sensory cells *in vivo*. However, the optimum concentration of the reagent has been unclear to use the reagent for the inner ear diseases. The purpose of this study is to evaluate the optimum concentration of the reagent for sensory hair cells. Cultured utricles from CBA mice were used in this study. Neomycin was added into the medium to induce inner ear cell death. Edaravone was added into the medium an hour before the exposure to neomycin. After the experiment, sensory hair cells were labeled with anticalmodulin antibody in the cultured utricles. In addition, immunohistochemistry against 4-hydroxy-2-nonenal was performed to evaluate the product of hydroxyl radical. About 25% hair cells disappeared 24 hours after the exposure to neomycin. In contrast, the loss of sensory cells was significantly suppressed the cultured utricles with edaravone in addition to neomycin.

### **821** Alkalinized Sodium Thiosulfate as a Locally-Delivered Otoprotective Agent Against Cisplatin in the Guinea Pig

Rose Mary Stocks<sup>1</sup>, Jonathan Hayes<sup>1</sup>, Sreekrishna Donepudi<sup>1</sup>, Herbert Gould<sup>2</sup>, David Armstrong<sup>1</sup>, Xiaoping Du<sup>1</sup>, Kristin Hamre<sup>1</sup>, Jerome Thompson<sup>1</sup>

<sup>1</sup>University of Tennessee Health Science Center,

<sup>2</sup>University of Memphis

Objective: To determine the otoprotective efficacy of locally-administered alkalinized sodium thiosulfate (STS-A) versus saline (control) against cisplatin ototoxicity as measured by audiometric analysis in the Hartley albino guinea pig (HAGP).

Design: Prospective Randomized Control Study.

Setting: Animal research facility.

Methods: Twenty-three male HAGP weighing 200-250g underwent pre-treatment auditory brainstem response (ABR) measurements at 2, 8, 16, and 32 kHz bilaterally.



Each HAGP received continuous infusion of STS-A and saline to the round window membrane niches via surgically inserted mini-osmotic pumps. A retroauricular approach through the mastoid bulla was used. The assignment of agent to left versus right ear was randomized. Three days after insertion, HAGP received daily subcutaneous cisplatin injections at a dose of 1.1 mg/kg for 8 days. Mini-osmotic pumps were removed three days after completion of cisplatin regimen. Perioperative antibiotics were used for all surgical procedures. Four weeks post-removal, post-treatment ABR measurements were performed at the same frequencies. HAGP were sacrificed, and harvested cochleas were prepared for future histologic studies.

**Results:** Statistical analysis of the audiometric data revealed progressively elevated hearing thresholds at higher frequencies, consistent with ototoxicity from cisplatin. However, no statistical differences were seen in threshold shifts between the STS-A and saline treatment groups. In the post-treatment data, there were 10 absent responses out of 84 total measurements in the STS-A ears, versus 13 absent responses out of 84 total measurements in the saline ears. This difference is not statistically significant ( $p=0.65$ ); however, the large number of absent responses may be due to limitations of the equipment to measure greater hearing thresholds.

**Conclusion:** Based on audiometric data taken from a group of twenty-one HAGP (two deaths), alkalinized STS does not provide significant otoprotection against cisplatin when compared to saline. In comparison to previous studies with pH-balanced STS, alkalinized STS does not seem to provide any added benefits.

## **822 KCNMB4 siRNA Attenuates Cisplatin-Induced Apoptosis in Gerbil Spiral Ligament Fibrocyte Cultures**

**Fenghe Liang<sup>1</sup>**, Chunyan Qu<sup>1</sup>, Bradley A. Schulte<sup>1</sup>

<sup>1</sup>*Medical University of South Carolina*

Apoptotic volume decrease (AVD) mediated mainly by cellular  $K^+$  efflux is an early and reversible stage of apoptosis, occurring before cytochrome C release, caspase activation and DNA fragmentation. Thus the targeted inhibition of  $K^+$  efflux could be a useful intervention in the treatment of degenerative diseases or the side effects of chemotherapy such as ototoxicity. We have shown that over-activation of BK channels contributes to cisplatin-induced apoptosis in spiral ligament fibrocytes (SLFs). We also have identified a  $\beta_4$  subunit and its encoding gene KCNMB4, which is co-expressed with BK channels in SLFs.  $\beta$  subunits are known to increase the activity of BK channels at lower intracellular  $Ca^{2+}$  levels and membrane potentials. Here we examined the effects of siRNA knockdown of KCNMB4 on BK channel activity and cisplatin-induced apoptosis in gerbil SLF cultures. A custom designed 21 mer siRNA was transfected into gerbil SLFs and gene silencing effects were monitored by quantitative RT-PCR. Transfected and nonsilenced control cultures were incubated with 200  $\mu$ M cisplatin for 12 hrs. Apoptosis assays using Annexin V-FITC and PI flow cytometry were performed 24 hrs after cisplatin treatment. Whole-cell K currents were recorded in all control and

treatment groups. siRNA treatment decreased the cisplatin-induced apoptotic rate from 84% in the cisplatin only group to 23%. siRNA also shifted the BK channel half-maximal activation potential ( $V_{150}$ ) from 41.4 mV in non-silenced scrambled control cells ( $n=17$ ) to 132.4 mV ( $n=14$ ). Cisplatin treatment shifted the  $V_{150}$  from 40.2 mV in control cells to -19.7 mV ( $n=9$ ). The  $V_{150}$  in cells treated with siRNA and cisplatin averaged 44.2 mV ( $n=8$ ), a value comparable to that in normal cells. These data show that siRNA knockdown of KCNMB4 shifts the BK channel activation curve to a higher voltage range, effectively countering the shifts toward a lower range promoted by cisplatin treatment, and thus attenuating cisplatin-induced apoptosis in gerbil SLF cultures.

## **823 A Novel Protein Therapy to the Inner Ear. Systemic Application of PTD-FNK Prevents Hair Cell Damage Induced by Ethacrynic Acid and Kanamycin Sulfate**

**Akinori Kashio<sup>1</sup>**, Keigo Suzukawa<sup>2</sup>, Takashi Sakamoto<sup>3</sup>, Tatsuya Yamasoba<sup>4</sup>, Sadamitsu Aso<sup>5</sup>, Shigeo Ohta<sup>5</sup>

<sup>1</sup>*Dept Oto/HNS Kameda Medical Center, Chiba Japan,*

<sup>2</sup>*Dept Oto/HNS Hitach General Hospital, Ibaragi Japan,*

<sup>3</sup>*Dept Oto/HNS Sanraku Hospital, Tokyo Japan,* <sup>4</sup>*Dept Oto/HNS University of Tokyo, Tokyo Japan,* <sup>5</sup>*Department of Biochemistry and Cell Biology, Nippon Medical School, Kanagawa Japan*

Preventing massive cell death is an important therapeutic strategy for various injuries and disorders. Protein therapeutics has the advantage of delivering proteins in a short period. We have engineered a new protein called PTD-FNK. FNK, which is a protein modified from the anti-apoptotic bcl-x gene to have more powerful cytoprotective activity, is fused with protein transduction domain (PTD) of HIV/Tat protein so that it can be directly and readily introduced into cells. We investigated if this protein, PTD-FNK, was distributed in the inner ear when given systemically and if it attenuated cochlear damage induced by an aminoglycoside and a diuretic. Guinea pigs, weighing 250-300g, with normal auditory brainstem response (ABR) thresholds at 2, 4, 8 and 20 kHz were used. PTD-FNK-myc was injected i.p. to the animals and 1, 3, and 6 hours later they were euthanized under deep anesthesia. The temporal bones were dissected, fixed in paraform aldehyde, decalcified, and embedded in paraffin. Paraffin-embedded sections immunostained with antibody to myc showed that PTD-FNK was diffusely expressed in the cytoplasm of cells in the cochlea, more prominently in the lateral wall, organ of Corti, and spiral ganglions and most significantly 1 hour after the injection. Next, animals were deafened by systemic injection of kanamycin sulfate (400mg/kg, s.c.) and 2 hours later ethacrynic acid (50mg/kg, i.v). PTD-FNK or the vehicle was injected i.p. 1 hour before and several times 1 through 7 hours after the administration of kanamycin sulfate. Seven days after the ototoxic insults, ABRs were measured and animals were euthanized. The temporal bones were dissected and fixed, surface preparations of the cochlea stained with rhodamine-phalloidin, and missing outer and inner hair cells counted. In untreated controls, no ABR waveforms were elicited at

any frequencies and nearly all outer hair cells were missing. PTD-FNK significantly attenuated ABR threshold shifts and the extent of hair cell damage. These findings suggest that, when systemically applied, PTD-FNK can be successfully delivered to the cochlea and that protein therapy can be a novel therapeutic tool for inner ear disorder.

#### **824 c-Jun N-Terminal Kinase Inhibition Blocks Aminoglycoside But Not Cisplatin-Induced Hair Cell Death in the Zebrafish Lateral Line**

**Henry Ou<sup>1</sup>, Felipe Santos<sup>1</sup>, David W. Raible<sup>1</sup>, Edwin W. Rubel<sup>1</sup>**

<sup>1</sup>*University of Washington*

The c-jun N-terminal kinase (JNK) pathway has been shown to play an important role in mediating apoptosis in a number of cell types including hair cells. Jun kinase is activated in cells in response to environmental stress and is felt to be an important apoptotic signal. Despite these findings, the function of JNK remains unclear, with JNK activation antiapoptotic in some cells and proapoptotic in others. In hair cells, inhibition of JNK has been shown to block aminoglycoside-induced hair cell death in the zebrafish lateral line, cultured mouse utricles, and organ of Corti explants. In contrast, in vivo studies of guinea pigs with JNK inhibitor delivered via implanted minipumps failed to block cisplatin-induced hair cell death (Wang et al., 2004). While these experiments were done in different animal systems, they suggest that c-jun N-terminal kinase inhibition blocks aminoglycoside-induced hair cell death but not cisplatin-induced hair cell death.

In the present study we examine the differential inhibition of cell death by c-jun N terminal kinase inhibition in aminoglycoside and cisplatin exposed zebrafish lateral line hair cells. Five day post fertilization zebrafish labeled with fixable FM 1-43 were pretreated with 1 hour of 0, 10, 50, or 100 micromolar JNK inhibitor. Fish were then exposed to either 1 hour of neomycin, or 4 hours of cisplatin at doses previously demonstrated to cause equivalent degrees of hair cell death. Fish were then fixed and hair cell counts in a sample of individual neuromasts were performed using fluorescence microscopy.

Results show statistically significant protective effects of JNK inhibition in aminoglycoside exposed hair cells. In cisplatin exposed animals, no protective effect was noted with identical c-jun kinase inhibitor concentrations. These findings suggest that cisplatin and aminoglycosides induce cell death in hair cells through different pathways. Complete analysis of the two-dimensional dose-response matrix may provide insights as to the nature of these pathways and in the development of protective agents for hair cells exposed to these two compounds.

#### **825 Pifithrin-Alpha Protects Gentamicin Ototoxicity**

**Mei Zhang<sup>1</sup>, Michele Cramer<sup>1</sup>**

<sup>1</sup>*University of Florida*

Gentamicin is a widely used antibiotic with high efficacy and low cost. However ototoxic side effects limit its clinical

usage. P53, a sequence-specific DNA binding protein, plays an important role in cellular response to genotoxic stress. We reported that pifithrin-alpha (PFT), a P53 inhibitor, protected cisplatin induced hair cell loss in the organotypic cochlear and vestibular cultures of P3 rats (Zhang et al. Neurosci, 2003). In this study, we carried out experiments to determine if PFT would protect the hair cells against gentamicin ototoxicity. Cochlear cultures of middle-basal turn of organ of Corti were obtained from P3 Sprague-Dawley rats. Some cultures were treated with gentamicin alone to obtain gentamicin dose response curve. Gentamicin was administered at 100  $\mu$ M, 250 $\mu$ M, 500 $\mu$ M or 1000 $\mu$ M. To study the protective effect of PFT, some cultures were treated with 100 $\mu$ M gentamicin plus varying concentration of PFT (40 $\mu$ M, 60 $\mu$ M or 100 $\mu$ M) to obtain PFT dose response curve. Untreated control cultures were run in parallel. After 48 hours treatment, the cultures were fixed with formalin and stained with rhodamine-phalloidin. Then the tissues were mounted and observed under fluorescence microscopy. The images were processed with Adobe Photoshop software. The numbers of IHCs and OHCs per 0.25 mm length of cochlear were counted from three representative regions of each explant and the mean number was determined for each specimen. Data were analyzed by ANOVA. The results showed that gentamicin caused significant inner hair cell (IHC) and outer hair cell (OHC) loss and induced a dose-dependent damage in the organotypic cultures of organ of Corti. PFT protected the IHCs and OHCs from gentamicin damage in a dose-dependent manner. 60 $\mu$ M and 100  $\mu$ M PFT provided a significant protective effect against IHC loss ( $p < 0.01$ ,  $n = 6$ ) and OHC loss ( $p < 0.001$ ,  $n = 6$ ). Our results suggest that p53 is involved in gentamicin ototoxicity.

Supported by Deafness Research Foundation

#### **826 Salicylate Induced Increase in Cochlear Neural Activity Is Modified by NMDA Antagonist**

**Karin Halsey<sup>1</sup>, Diane Prieskorn<sup>1</sup>, David Dolan<sup>1</sup>, Tom Lobl<sup>2</sup>, Stephen McCormack<sup>2</sup>, Josef Miller<sup>1</sup>**

<sup>1</sup>*Kresge Hearing Research Institute, The University of Michigan, Ann Arbor, MI, USA,* <sup>2</sup>*NeuroSystec Corporation*

Salicylate (SA) is known to cause hearing loss and tinnitus (McFadden et al., 1984). The mechanism of the SA induced hearing loss may differ from that of SA induced tinnitus. SA disrupts arachidonic acid metabolism which may induce tinnitus by potentiation of NMDA receptor currents (Guitton et al., 2003). Round window noise (RWN) (Dolan et al., 1990), a gross measure of 8th nerve spontaneous neural activity, increases with systemic application of SA (Schreiner and Snyder, 1987; Martin et al., 1993; Cazals et al., 1998). NST-001 (1-(2-Methyl-1-thiophen-2-yl-cyclohexyl)-piperidine hydrochloride) is a NMDA receptor antagonist which may suppress tinnitus (Guitton et al., 2004). In this study, guinea pigs were chronically implanted with an intracochlear recording electrode to measure RWN and the cochlear whole-nerve action potential (CAP). The animals received either acute or daily SA injections (350 mg/kg, SQ) for 18 days. Acute SA injections typically resulted in elevated CAP thresholds

and reduced RWN. The preliminary results for chronic injections of SA showed an increase in RWN amplitude without change in CAP threshold. After determination of elevated RWN and normal CAP thresholds, animals were surgically prepared for round window application (30 min) of NST-001 in the non-implanted ear. The effects of NST-001 on the CAP and RWN were concentration dependent: 1 mM NST-001 had no effect on the CAP or RWN, 3 mM NST-001 reduced the RWN without effect on the CAP, 5 mM NST-001 elevated CAP thresholds and depressed the RWN amplitude. To the extent that increased RWN amplitude is a model of peripheral tinnitus in humans, NST-001 holds promise as a therapeutic agent in the treatment of this disorder.

This work was supported by NeuroSystec.

## **827 Drug Delivery to the Cochlea Using Poly Lactic/Glycolic Acid Nanoparticles**

**Akifumi Mizukoshi<sup>1</sup>**, Tetsuya Tamura<sup>1</sup>, Takayuki Nakagawa<sup>1</sup>, Tomoko Kita<sup>1</sup>, Tsuyoshi Endo<sup>1</sup>, Tae-Soo Kim<sup>1</sup>, Tsutomu Ishihara<sup>2</sup>, Megumu Higaki<sup>3</sup>, Juichi Ito<sup>1</sup>

<sup>1</sup>*Department of Otolaryngology-Head and Neck Surgery, Graduate School of Medicine, Kyoto University,* <sup>2</sup>*DDS Institute, The Jikei University School of Medicine,* <sup>3</sup>*Institute of Medical Science, St Marianna University School of Medicine*

This study aimed to investigate the efficacy of encapsulating therapeutic molecules in poly lactic/glycolic acid (PLGA) nanoparticles for drug delivery to the cochlea. First, we examined the distribution of rhodamine, a fluorescent dye in the cochlea following systemic or local application of rhodamine-encapsulated PLGA nanoparticles or non-encapsulated rhodamine using adult guinea pigs. Local application was performed by placing PLGA nanoparticles (140-180 nm in a diameter) on the round window membrane (RWM). After systemic application of rhodamine nanoparticles, fluorescence was identified in the liver, kidney and cochlea. The systemic application of nanoparticles had a significant effect on targeted and sustained delivery of rhodamine to the liver but not the kidney or cochlea. Rhodamine nanoparticles placed on the RWM were identified in the scala tympani as nanoparticles, indicating that the PLGA nanoparticles can permeate through the RWM. Furthermore, the local application of rhodamine nanoparticles to the RWM was more effective in targeted delivery to the cochlea than systemic application. Based on these findings, we examined protective effects of betamethasone-encapsulated PLGA nanoparticles (nano-betamethasone) against aminoglycoside toxicity. A gelfoam immersed with nano-betamethasone or non-encapsulated betamethasone was placed on the RWM of the left ear of guinea pigs after systemic application of kanamycin and ethacrynic acid. Nano-betamethasone-treated cochleae exhibited less threshold shifts of ABRs than contralateral non-treated cochleae, while no significant difference in threshold shifts was found between non-encapsulated betamethasone-treated and contralateral cochleae. These findings indicate that PLGA nanoparticles can be an useful drug carrier to the cochlea via local application.

## **828 Gentamicin Uptake Into Mammalian Cochlear Hair Cells In Vitro**

**Dalian Ding<sup>1</sup>**, Haiyan Jiang<sup>1</sup>, Richard Salvi<sup>1</sup>

<sup>1</sup>*University at Buffalo*

Aminoglycoside antibiotics selectively damage the hair cells in the cochlea in a stereotypic pattern. In vivo, hair cell loss begins in the base of the cochlea and spreads towards to the apex. Moreover, in any given region, outer hair cell (OHC) loss precedes inner hair cell (IHC) loss. There was speculation that the progression of hair cell loss might be due to a base-to-apex concentration gradient; however, the same pattern of cell loss is recapitulated in cochlear organotypic cultures where concentration gradients do not exist. An alternative possibility is that the base-to-apex and OHC-to-IHC hair cell loss gradients arise from differential rates of drug uptake. To test this hypothesis, we treated rat cochlear organotypic cultures with rhodamine-labeled gentamicin and examined the pattern of hair cell labeling and cell death in vitro. Rhodamine-gentamicin was selectively taken up by hair cells; little or no labeling was seen in supporting cells. The uptake of labeled gentamicin progressed from base-to-apex and from OHC-to-IHC. Following uptake, the hair cells degenerated along the same spatial and temporal gradients indicating that the labeled drug was still active. Thus, the spatial and temporal patterns of aminoglycoside uptake are sufficient to explain three main features of aminoglycoside damage: (1) selective damage to hair cells versus supporting cells, (2) the base-to-apex gradient and (3) greater vulnerability of OHC versus IHC. (Supported by NIH grant R01 DC06630-01)

## **829 Examining the Mechanism of Heat Shock-Induced Protection Against Ototoxic Hair Cell Death**

**Lisa L. Cunningham<sup>1</sup>**, Carlene S. Brandon<sup>1</sup>

<sup>1</sup>*Medical University of South Carolina*

Sensory hair cells are sensitive to death induced by noise exposure, aging, and some therapeutic drugs. Two major classes of ototoxic drugs are the aminoglycoside antibiotics and the antineoplastic agent cisplatin. Exposure to these drugs results in hair cell death that is mediated by the activation of specific apoptotic proteins. Aminoglycoside-induced hair cell death is mediated by the activation of c-Jun N-terminal kinase (JNK). The induction of heat shock proteins (HSPs) in response to cellular stress is a ubiquitous and highly-conserved response that can significantly inhibit apoptosis in a variety of systems by directly inhibiting the activation of apoptotic proteins, including JNK. We have previously shown that heat shock (43°C for 30 minutes) results in a robust and reliable upregulation of HSPs in the hair cells of the adult mouse utricle in vitro. In addition, this heat shock treatment results in significant protection of hair cells against both cisplatin- and aminoglycoside-induced death. Here we have begun to explore the mechanism(s) underlying heat shock-induced protection of hair cells by examining the effect of heat shock on the phosphorylation of JNK. JNK is a member of the family of mitogen-activated protein kinases (MAP kinases) that also includes extracellular signal-

related kinase (ERK) and p38. These kinases are activated in cells in response to a variety of environmental stresses. JNK is activated by dual phosphorylation at Thr and Tyr residues by MAP kinase kinases (MKKs). Inhibition of JNK has repeatedly been shown to inhibit aminoglycoside-induced hair cell death (Pirvola et al. 2000 J Neurosci. 20(1):43; Wang et al. 2003 J Neurosci. 23(24):8596; Matsui et al. 2004 J Neurobiol. 61(2):250). In human acute lymphoblastic leukemia PEER cells, induction of HSP-70 inhibits cell death by preventing phosphorylation of JNK (Mosser et al. 1997 Mol Cell Biol. 17(17):5317). We have examined the phosphorylation of JNK in hair cells of utricles exposed to neomycin. Immunohistochemical results indicate that neomycin exposure results in dual phosphorylation of JNK on threonine 183 and tyrosine 185 in utricular hair cells. Heat shock treatment of utricles prior to exposure to neomycin does not significantly inhibit JNK phosphorylation. These results suggest that the protective effect of heat shock against aminoglycoside-induced hair cell death is mediated by a mechanism that is independent or downstream of JNK phosphorylation.

### **[830] Celastrol Protects the Vestibular Hair Cells Against the Ototoxicity of Aminoglycoside**

**Kazuma Sugahara<sup>1</sup>, Takefumi Mikuriya<sup>1</sup>, Tsuguyuki Arai<sup>1</sup>, Kuniyoshi Tanaka<sup>1</sup>, Tsuyoshi Takemoto<sup>1</sup>, Hiroaki Shimogori<sup>1</sup>, Hiroshi Yamashita<sup>1</sup>**

<sup>1</sup>*Department of Otolaryngology, Yamaguchi University, School of Medicine*

In the previous meeting, we reported that the heat shock response could protect the inner ear tissue against the stress. Recently, it was reported that the unique molecule: Celastrol could work as the heat shock inducer in many kinds of cells. The purpose of this study was to investigate the role of Celastrol in mammalian vestibular hair cell death induced by aminoglycoside. Cultured utricles of CBA/CaN mice were used. In this study, the reagent Celastrol was used as an inducer of heat shock response. Cultured utricles were divided to three groups (Control group, Neomycin group, Neomycin + Celastrol group). In the Neomycin group, utricles were cultured with neomycin (1 mM) to induce hair cell death. In Neomycin + Celastrol group, utricles were cultured with neomycin and Celastrol (3 µM). Twenty-four hours after exposure to neomycin, the cultured tissues were fixed with 4% paraformaldehyde. To label hair cells, immunohistochemistry were performed using anti-calmodulin antibody. The rate of vestibular hair cells was evaluated with the fluorescence microscope. The survival rate of hair cells in Neomycin + Celastrol group was significantly more than that in Neomycin group.

These data indicated that Celastrol protects sensory hair cells against neomycin-induced death in mammalian vestibular epithelium. These results show that Celastrol can be used as the inducer of heat shock response in the inner ear.

### **[831] Distribution and Noise Exposure Induced Activation of PARP-1 in Hair Cells**

**Weiju Han<sup>1,2</sup>, Xiao-Rui Shi<sup>1</sup>, Alfred L. Nuttall<sup>1,3</sup>**

<sup>1</sup>*Oregon Health & Science University*, <sup>2</sup>*Chinese PLA General Hospital, Dept of Otolaryngology Head/Neck Surgery*, <sup>3</sup>*Kresge Hearing Research Institute, The University of Michigan, Ann Arbor, MI, USA*

Poly (ADP-ribose) polymerase-1 (PARP-1) is a nuclear enzyme that responds to DNA damage and facilitates DNA repair and acts as a molecular switch between apoptosis and necrosis. Our previous study showed that PARP has a modulatory role in the mediation of the "inflammatory-like" proteins, such as intercellular adhesion molecule-1, P-selectin and Platelet-endothelial cell-adhesion molecule-1, and in the leukocyte migration in the cochlear lateral wall. In this study, we investigated the distribution of PARP-1 in the hair cells of organ of Corti and PARP-1 activation following noise exposure in guinea pigs, PARP<sup>+/+</sup> wild type mice and PARP knockout mice. Guinea pigs or mice were exposed to broadband noise at 120 dB SPL for 2 days (4h/d). The distribution of PARP-1, cleaved PARP-1 and Poly (ADP-ribose) (PAR), the product of PARP-1 activation, in organ of Corti was immunohistologically detected in control and noise exposure animals. The results showed that in the control condition, PARP-1 immunoreactivity was detected either inside or outside the nuclei of the hair cell (HCs) in both guinea pigs and PARP<sup>+/+</sup> mice, but not in the PARP<sup>-/-</sup> mice. Anti-PARP-1 antibody and MitoTracker double labeling showed PARP-1 distributed in mitochondria of HCs. No PAR was observed in the mitochondria or in the nuclei of all control cochleae. However, after noise stimulation, PAR was detected both in the nuclear area and cytosol in OHCs, which had apoptotic nuclear morphology. Cleaved PARP-1 was detected in the apical domain of OHCs that appeared to be necrotic. Taken together, these results suggest that PARP distributed not only in the nuclei but also in the mitochondria of hair cells of organ of Corti. Noise exposure induced PARP activation, production of PAR, in apoptotic hair cells.

**Acknowledgment** This work was supported by NIH NIDCD grant R01 DC00105.

### **[832] Auditory Brainstem Responses and Distortion Products of Oto-Acoustic Emission in Mouse Autoimmune Hearing Loss**

**Mohammad Habiby Kermany<sup>1</sup>, Michael Yoon<sup>1</sup>, Bin Zhou<sup>1</sup>, Tai June Yoo<sup>1</sup>**

<sup>1</sup>*University of Tennessee, College of Medicine, Department of Medicine*

Far field auditory brainstem responses (ABR) is used for detecting electrical signals of neural transmissions from the inner ear hair cells to central auditory nuclei in the brain, while distortion product of otoacoustic emission (DPOAE) is used for testing functional status of the cochlear hair cells. DPOAE tests the function of cochlear structures such as cochlear hair cell activity. The combination of ABR and DPOAE provide detailed information on physiological defects in auditory pathway.

Previous studies show that tubulin is a major constituent protein of microtubules, which are prominent structures in the sensory and supporting cells of the inner ear and is an auto-antigen to the inner ear. In current study, Balb/C mice presented autoimmune sensory neural hearing loss after immunization with high dose purified tubulin. Six weeks after the second booster, the sensorineural hearing loss was determined by elevation of ABR threshold in alternative polarity clicks and three different frequency levels: low (8KHz) middle (16KHz) and high (32KHz). ABR pick amplitude reductions show significant ( $P < 0.05$  mice# 28) as well as significant pick latencies. DPOAE also show significant elevation of threshold in low (8KHz) middle (16KHz) and high (32KHz) frequencies respectively ( $P < 0.05$  mice# 28). Degenerated spiral ganglion and cochlear hair cells were found in the inner ears under light microscopic assay. These results support studies which demonstrate that tubulin induces experimental autoimmune hearing loss in mice and the conclusion that tubulin is an autoantigen to inner ear. Electrophysiology data also reveals that this autoimmune damage affects the entire cochlea, from apical to basal turn (Low ~ High frequencies).

### **833 Ultrastructural and Confocal Localization of Calcium Store Channels in Cochlear and Vestibular Hair Cells**

**Anna Lysakowski<sup>1</sup>**, Steven Price<sup>1</sup>, Sophie Gaboyard<sup>1</sup>, Marcin Klapczynski<sup>1</sup>, Peter Cameron<sup>1,2</sup>

<sup>1</sup>University of Illinois at Chicago, <sup>2</sup>University of California, Berkeley

Ryanodine receptor (RyR) and inositol triphosphate (IP<sub>3</sub>) calcium store channels have been shown to be widely expressed in a variety of mammalian tissues. There have been few studies, however, on their localization in the vestibular periphery and cochlea. A functional model, put forth by Sridhar et al. (1997) for cochlea, where outer hair cells are contacted by efferent boutons opposite subsynaptic cisterns, is that the cistern creates a microdomain for  $\alpha 9$  nicotonic receptors to interact with calcium-gated potassium channels. They gave evidence for RyR involvement in this process. Other studies have provided functional evidence for IP<sub>3</sub> involvement.

We performed an initial screen with RT-PCR and found all six isoforms (RyR1, RyR2, RyR3, IP<sub>3</sub>R1, IP<sub>3</sub>R2, IP<sub>3</sub>R3) present in the vestibular and cochlear endorgans and ganglia (Cameron et al., ARO, 2004). In the present study, immunogold EM and confocal microscopy were used to ascertain which RyR and IP<sub>3</sub>R isoforms were expressed specifically within hair cells in the cristae, maculae, and cochlea, and vestibular and spiral ganglia. Western blots and preabsorption controls are used to confirm specificity of the antibodies.

With confocal microscopy, we have so far found IP<sub>3</sub>R1 to be a candidate for the subsynaptic cisternal isoform in outer hair cells (OHCs). In the crista and macula, IP<sub>3</sub>R1 is also found in type II hair cells and in calyces from the central/stricular zone. Confocal and electron microscopy confirmed the presence of RyR3 in Deiters cells, in inner hair cells (IHCs), and in some of their afferent endings, but not in OHCs, although RyR3 is present in efferent boutons

on OHCs. All 6 isoforms are found in ganglion cells. In summary, specific isoforms of RyR and IP<sub>3</sub> are both present in hair cells and ganglia in the rat inner ear, and may play a specific role in efferent neurotransmission.

Supported by NIH R01 DC2521.

### **834 The Effect of Subphysiological Temperature and Extracellular ATP on Apical Membrane Internalization in Guinea Pig Inner Hair Cells**

**Xiao-Rui Shi<sup>1</sup>**, Alfred L. Nuttall<sup>1,2</sup>

<sup>1</sup>Oregon Health & Science University, <sup>2</sup>Kresge Hearing Research Institute, The University of Michigan, Ann Arbor, MI, USA

Most cellular processes are known to be strongly temperature-dependent. Nevertheless, a large fraction of studies of mammalian hair cell function have been and are performed near room temperature (i.e., at least 10°C below physiological temperature). Here, we examined the effects of temperature on apical membrane internalization in the inner hair cells (IHCs) of the guinea pig cochlea. We used the annexin V-Alexa Fluor 488 to label the IHC apical membrane. We studied the change of this label and its internalization in IHCs at room temperature (~23°C) and ~37°C. At room temperature, we found that the pattern of annexin V label was punctuate and often confined along the marginal of the cuticular plate and at the site of the hair cell vestigial kinocilium within 10 min. The annexin V-labeled apical plasma membrane did not distributed further into the IHC even within 1-hour incubation. The punctuated annexin V label 'vesicles' co-labeled with an early endosome marker, Rab5. In isolated IHC, annexin V labeled vesicles were mobile, redium moving around the marginal of the cuticular plate. However, at ~37°C, we found that the annexin V labeled apical membrane extended further into cell. Annexin V labeled 'vesicles' in the cytosole wase found within up to 5  $\mu$ m from the surface of the cuticular plate. The vesicles were positioned along microtubules. Internalized vesicles with label were never seen in the basal lateral wall or at the base of the IHCs at up to 3 hours incubation. Dissemble of microtubules could prevent the 5  $\mu$ m internalization. In addition, blocking purinergic (P2X) receptors by PPADS (100  $\mu$ M) and activating P2X receptors by extracellular ATP (100  $\mu$ M) could reduce or increase the amount of the apical membrane internalization respectively. Our results suggest that internalized vesicles from the apical membrane in the IHCs are associated with microtubules and the movements is effected by temperature and extracellular ATP. Supported by NIH NIDCD DC 00105, DC 00141.

### **835 The Effect of Intracellular Camp and Endogenous Nitric Oxide on Slow Motility of Guinea Pig Outer Hair Cell**

**Xiao-Rui Shi<sup>1</sup>**, Alfred L. Nuttall<sup>1,2</sup>

<sup>1</sup>Oregon Health & Science University, <sup>2</sup>Kresge Hearing Research Institute, The University of Michigan, Ann Arbor, MI, USA

In this study, a strip of the organ of Corti from the second turn was freshly isolated from adult guinea pigs and into an artificial perilymph solution. Annexin V-alexa fluoro 488 was

used for the visualization of the hair bundle of hair cells using fluorescence microscopy. We found that there were no changes in orientation of the hair bundle of hair cells or any obvious OHC cell length or diameter change when tissues were bathed in the perilymph solution for up to three hours. However, after tissues were treated with 6-acetyl-7-deacetyl forskolin (forskolin), an adenylyl cyclases stimulator, at 10  $\mu$ M for 10 min, many (40%) first-row outer hair cells showed rotated hair bundles. The majority of hair bundles were rotated around between 30°~ 90°. For a smaller number of OHCs, hair bundles were rotated by up to 180°. Second- and third-row OHCs appeared normal in entire incubation or drug treated time. There was no rotation observed in the hair bundle of inner hair cells or of their 2<sup>nd</sup> and 3<sup>rd</sup> rows of the OHCs even at a high dose of forskolin (100  $\mu$ M). Also, we found that we found that forskolin initiates slow shortening of OHCs. This slow effect could be attenuated by a 10 min preincubation of the tissue cells with the nitric oxide synthase N(G)-nitro-L-arginine methyl ester hydrochloride, L-NAME (1mM) or the membrane-permeant cGMP antagonist, 8-bromo-guanosine 3':5'-cyclic monophosphate (1 mM). The slow shortening could also be diminished by pre-treated cells with PKA inhibitor, H89 (100  $\mu$ M) for 30 min. The decrease intracellular cAMP by membrane-permeant cAMP antagonist SQ-22536 at 1mM could cause OHC elongated contraction. Similarly, L-NAME (1mM) also induced length increases of guinea pig isolated OHCs. These results show that intracellular level of cAMP, as a second messenger, has a role in cell mechanics. The same can be said for NO stimulated cGMP as has been suggested by others. This experiment also demonstrated that activation of cAMP/PKA pathway can be modulated by nitric oxide/cGMP pathway. Supported by NIH NIDCD DC 00105, DC 00141.

### **[836] Mechanisms of Ca<sup>2+</sup> Homeostasis in Inner and Outer Hair Cells of the Mouse Cochlea**

**Rodrigue Nemzou<sup>1</sup>**, Matthias Ohlrogge<sup>1</sup>, Gaston Sendin<sup>1</sup>, Bruce Tempel<sup>2</sup>, Tobias Moser<sup>1</sup>

<sup>1</sup>University of Goettingen, <sup>2</sup>University of Washington, Seattle

Calcium (Ca<sup>2+</sup>) is a ubiquitous intracellular signal responsible for the control of many cellular processes including fertilization, proliferation, development, exocytosis and mechanoelectrical transduction. However, exceeding its normal concentration, Ca<sup>2+</sup> can be highly toxic and lead to cell death. Thus, it is very important for cells to tightly regulate the cytosolic Ca<sup>2+</sup> concentration [Ca<sup>2+</sup>]<sub>i</sub>. Mechanoelectrical transduction channels of hair cells allow entry of appreciable amounts of Ca<sup>2+</sup>, which regulates adaptation of transduction. The receptor potential then causes Ca<sup>2+</sup> entry through basolateral voltage-gated Ca<sup>2+</sup> channels, which are much more abundant in inner than in outer hair cells.

Here we studied hair cell Ca<sup>2+</sup> homeostasis following mechanoelectrical transduction in outer hair cells (OHCs) and patch-clamp depolarization in inner hair cells (IHCs). Most of the incoming Ca<sup>2+</sup> was buffered by cytosolic Ca<sup>2+</sup> binding proteins and mitochondria, then extruded by plasma membrane Ca<sup>2+</sup> ATPases (PMCA) in both OHCs

and IHCs as suggested by the effects of the PMCA inhibitor Carboxy-Eosin and changes of extracellular pH. Deafwaddler (dfw2j) mice harbor a mutation in the Atp2b2 gene that encodes the plasma membrane calcium ATPase type2 (PMCA2), leading to a complete lack of PMCA2. These mice are deaf and ataxic. Compared to controls, the OHCs of both the mutant and heterozygotes animals showed an elevated initial [Ca<sup>2+</sup>]<sub>i</sub> followed by a prolonged decay. In contrast, Ca<sup>2+</sup> clearance was undisturbed in IHCs lacking PMCA2, indicating that other PMCA isoforms, probably PMCA4 and PMCA1 apically (Wood et al., JARO 2004), and potentially the Na<sup>+</sup>/Ca<sup>2+</sup> exchanger in the basolateral membrane can support IHC Ca<sup>2+</sup> homeostasis.

Supported by a DFG grant (CMPB) and an EC grant (Eurohear) to T.M.

### **[837] In Vitro Differentiation of Mouse ES Cells Along the Inner Ear Hair Cell Pathway on Two-Dimensional and Three-Dimensional Culture Surfaces**

**Michelle G. de Silva<sup>1</sup>**, Andrea J. O'Connor<sup>2</sup>, Geoff W. Stevens<sup>2</sup>, Marisel Peverelli<sup>1,3</sup>, Ashley P.S. Robertson<sup>1</sup>, Hans-Henrik M. Dahl<sup>1,3</sup>

<sup>1</sup>Murdoch Childrens Research Institute, <sup>2</sup>Department of Chemical and Biomolecular Engineering, University of Melbourne, <sup>3</sup>Department of Paediatrics, University of Melbourne

By understanding the mechanisms that govern the genesis and regeneration of inner ear hair cells we believe we will be able to develop cell-based strategies to delay, prevent, or even reverse the hearing loss in individuals with hearing impairment. We hypothesise that identifying the key cytokines involved in hair cell commitment will promote differentiation of ES cells to inner ear hair cells. Several growth culture conditions, exposure to IGF-1, EGF, BDNF, NT-3, and bFGF both singly and in combination have been compared to cell culture in pre-conditioned media from hair cell precursor cell lines (UB/OC-1 and UB/OC-2) isolated from the Immortomouse. Expression of specific markers of early hair cell development (*Atoh1*, *Pou4f3*, *Myo6*) and differentiated cell types (*Chrna9*, *Myo7a*) have been assessed and it was shown that the most promising results arise when ES cultures are treated with the conditioned media from the hair cell precursor cell lines.

As terminally differentiated hair cells have not been grown on two-dimensional tissue culture plates, we are taking a tissue engineering approach using synthetic biodegradable polymers. We formed the copolymer, poly(lactic-co-glycolic acid) (PLGA) into 3D constructs using thermally induced phase separation, with morphology mimicking the key architectural features of the organ of Corti region of the inner ear, to encourage the growth and differentiation of stem cells into inner ear cell types. Our cell culture experiments showed that PLGA provides a favourable environment for the growth of our mouse ES cells. Taking the most promising culture conditions from our 2D work, we have successfully grown partially differentiated mouse ES cells on PLGA scaffolds and have shown that we can induce co-expression of the hair cell marker proteins Myosin 7a and Math1 in a proportion of the cells. This

approach provides encouraging results for the possibility of differentiating inner ear hair cells *in vitro*.

### **838 Temporal Gene Expression Profile in Murine Embryonic Stem Cells During Neural Differentiation**

**Jeffrey M. Clarke<sup>1</sup>**, Heather L. Aloor<sup>1</sup>, Rebecca J. Chan<sup>1</sup>, Eri Hashino<sup>1</sup>

<sup>1</sup>*Indiana University School of Medicine*

In spite of substantial evidence describing neural differentiation from embryonic stem cells (ESCs), the process by which ESCs acquire a neural phenotype is not well characterized. We have established a serum-free neural induction protocol and evaluated temporal changes in gene expression in mouse ESCs at various time points before and after the start of neural induction. Dissociated mouse ESCs were cultured first in defined medium containing Knockout Serum Replacement medium to allow formation of embryoid bodies (EBs). Thereafter, EBs were plated en bloc on poly-D-lysine/laminin substrates and grown in neural induction medium containing N2 supplement and brain derived neurotrophic factor (BDNF) for up to 15 days. Inclusion of fibroblast growth factor 2 (FGF2) in neural induction medium resulted in an increase of fibroblast-like cells. At day 7 after the start of neural induction, more than 80% of cells in an EB exhibited positive staining for HuC and TUJ1, validating the efficacy of our neural induction protocol. Our quantitative RT-PCR analysis revealed that Oct4 and Rex1, ESC marker genes, were down-regulated sharply in ESCs during EB formation and became barely detectable by day 3 during neural induction. In striking contrast, Musashi1 and HuC, early neuronal markers, were up-regulated markedly by day 3 during neural induction. Their expression levels reached plateau at day 3 and 10, respectively, after which they were down-regulated. Expression of mature neuronal markers, including nse, GluR4 and synaptophysin, displayed a steady increase throughout the progression of neural differentiation. Interestingly, expression levels of other neuronal markers, such as calretinin, tau and trkB, increased sharply between days 10 and 15 after the start of neural induction. The temporal changes in expression of the ESC- and neural-marker genes *in vitro* parallel essentially those during normal neural development *in vivo* and may serve as a reference to evaluate the progression of neuronal differentiation from ESCs.

Supported by NIH DC005507 and DC000012

### **839 Survival of Bone Marrow-Derived Stem Cells in the Mongolian Gerbil Cochlea**

**Akihiro Matsuoka<sup>1</sup>**, Richard Miyamoto<sup>1</sup>, Eri Hashino<sup>1</sup>

<sup>1</sup>*Department of Otolaryngology-Head and Neck Surgery, Indiana University School of Medicine*

The loss of spiral ganglion neurons (SGNs) is one of the major causes of profound sensorineural hearing loss. Cell replacement therapy holds a promise to treat this type of deafness and our previous study demonstrated that bone marrow-derived stem cells (MSCs) have the competence of differentiating into cells expressing a set of sensory neuron markers. The main purpose of this study is to evaluate the survival of mouse MSCs transplanted into the

Mongolian gerbil cochlea. Eight gerbils were used in this study and four of them were deafened with ouabain. Recent study has shown that exposure to ouabain selectively destroys most of the SGNs without damaging hair cells and thusly ouabain is a suitable reagent for studying interaction between newly transplanted stem cells and pre-existing hair cells. Under anesthesia, the animals were transplanted with 10,000 Green fluorescent positive (GFP+) MSCs. Seven days after the transplantation, MSC survival was evaluated by microscopic examination of frozen sections cut through the cochleae of the recipient animals. Transplanted MSCs survived in the perilymphatic space and modiolus in both the control animals and the ouabain-deafened animals. In animals with the scala-tympani injection, there was no surviving GFP+ MSC survival in the modiolus. The profile numbers in the modiolus in the ouabain-treated animals with the modiolar injection were greater than those in untreated animals. The profile numbers in the scala-tympani, the scala media, and the scala vestibule were similar between untreated and ouabain-deafened animals, suggesting that the injury caused by ouabain might have enhanced the survival of MSCs in the modiolus, but not in the perilymphatic space. These findings may have important clinical implications in establishment of MSC transplantation therapy in the cochlea.

Supported by NIH grant DC007390 and Biomedical Research Grant from Indiana University School of Medicine.

### **840 Stem Cell Antigen 1 (Sca1)-Positive Adipose Stromal Cells Exhibit Pluripotency and Neural Competence**

**Takako Kondo<sup>1</sup>**, Jamie Case<sup>1</sup>, Edward F. Srouf<sup>1</sup>, Eri Hashino<sup>1</sup>

<sup>1</sup>*Indiana University School of Medicine*

Our previous study and studies by others have shown that stromal cells isolated from adult bone marrow have the competence of differentiating into cells with phenotypic, genetic and biochemical characteristics of neurons when grown in neural induction medium. Adipose tissue, like bone marrow, is derived from the embryonic mesoderm and contains heterogeneous stromal cell populations. Because marrow and adipose stromal cells share ontogenic and morphological similarities, we sought to test whether adipose stromal cells express neural stem cell markers and are responsive to neural induction signals. In addition, we wished to identify among adipose stromal cells a phenotypically defined cell population that exhibits stem cell properties. Using florescent activated cell sorting (FACS), mouse adipose stromal cells were sorted out into two cell populations expressing Lin-CD45-CD117-CD90+ while differing for the expression of Sca1 (Sca1+ cells) or lack thereof (Sca1- cells). Sca1+ and Sca1- cells were plated separately on poly-D-lysine/laminin-coated culture dishes and grown in defined medium. All of neural stem cell markers examined, including nestin, Sox2, Egfr, Notch1 and FgfR, were constitutively expressed in Sca1+ cells, while Sca1- cells were devoid of Sox2 and Notch1. Cell proliferation assays showed that approximately 80% of both Sca1+/- cells were BrdU-positive in defined culture medium, but the majority of these cells became BrdU-



negative after being exposed to neural induction medium. Inclusion of Sonic hedgehog and retinoic acid in neural induction medium instructively promoted expression of GATA3, calretinin, GluR4 and NeuroD in Sca1+ cells, but not in Sca1- cells. These results reveal distinctive nature of Sca1+ and Sca1- adipose stromal cells, and suggest that Sca1+ cells identify an adipose stromal cell population with neural stem cell potential.

Supported by NIH DC005507 (EH) and HL069156 (EFS)

#### **[841] Canonical Wnt Signaling Promotes Glutamatergic Differentiation from Bone Marrow-Derived Stem Cells**

**Takako Kondo<sup>1</sup>**, Heather L. Aloor<sup>1</sup>, Raymond Romand<sup>2</sup>, Eri Hashino<sup>1</sup>

<sup>1</sup>Indiana University School of Medicine, <sup>2</sup>IGBMC

Our recent study (Kondo et al., PNAS 102:4789-94, 2005) demonstrated that Sonic hedgehog (Shh) and retinoic acid (RA) synergistically promote expression of several glutamatergic sensory marker genes in mouse bone marrow stromal cells (MSCs). However, Shh and RA failed to induce expression of the POU-domain transcription factor Brn3a. Surprisingly, conditioned medium prepared from E10 mouse hindbrain/somite/otocyst was able to induce expression of Brn3a as well as neuroD, which were not up-regulated by Shh and RA. Since many Wnt signaling components are constitutively expressed in MSCs, we hypothesized that Wnt(s) in the conditioned medium may instructively promote expression of these sensory neuron marker genes in MSCs. To test this hypothesis, we incubated MSCs with neural induction medium containing human recombinant Wnt1 or Wnt3a protein at various concentrations. Incubation of MSCs with Wnt1 for 7 days resulted in a more than 400-fold increase in the expression level of Brn3a, neuroD and neurogenin1. The up-regulation induced by Wnt1 was approximately 10-fold higher than that induced by hindbrain/somite/otocyst conditioned medium. Wnt3a had similar but lesser effects than Wnt1. In addition, several functional glutamatergic markers, including AMPA receptors (GluR1-4), VGLUT2, Synapsin1 and Nav1.7, became detectable in MSCs grown in the presence of Wnt1. Furthermore, the up-regulation of Brn3a by both Wnt1 and conditioned medium was suppressed by canonical Wnt inhibitors, such as Dkk1 and sFRP2, in a dose-dependent manner. Together, these results strongly suggest that in MSCs canonical Wnt signaling constitutes another sensory competence factor which is functionally distinguishable from Shh/RA.

Supported by NIH DC007390

#### **[842] Transplantation of Bone Marrow-Derived Stromal Cells Into Mouse Cochleae Damaged by Noise**

**Sadia Sharif<sup>1</sup>**, **Tsune-hisa Ohno<sup>1</sup>**, Takayuki Nakagawa<sup>1</sup>, Masahiro Matsumoto<sup>1</sup>, Tomoko Kita<sup>1</sup>, Takayuki Okano<sup>1</sup>, Shinpei Kada<sup>1</sup>, Ken Kojima<sup>1</sup>, Juichi Ito<sup>1</sup>

<sup>1</sup>Kyoto University Graduate School of Medicine

Bone marrow stromal cells (MSCs) are heterogeneous population of cells containing multipotent, mesenchymal progenitor cells that can differentiate into many lineages.

Neural progenitors can also be generated from MSCs. In addition, autologous MSCs are available from one's own bone marrows, which is great advance of MSCs as a source of transplants in cell therapy. Previously, we investigated the potential of autologous MSCs as transplants for the inner ear using chinchilla. The results indicate that MSCs can survive in the cochlea and have the ability to differentiate into neurons after settlement in the cochlear modiolus, although the number of neural differentiated grafted cells is very limited. However, details of fates of grafted MSCs are still undetermined. We then used mice as experimental animals because of convenience for immunohistochemical analyses. MSCs derived from GFP mice were used as transplants and adult C57BL/6 mice as recipients. C57BL/6 mice were deafened by intense noise exposure, and received an injection of GFP-positive MSCs through the cochlear lateral wall of the basal portion 3 days after noise exposure. The cochleae were collected on day 7 or 14 after transplantation for histological analyses. Grafted cells in the cochleae were identified by GFP signals. MSC-derived cells were mainly located in the perilymphatic spaces, and adhered to the cochlear lateral wall, modiolus, basal lamina or Reisner's membrane. Some grafted cells were settled within the stria vascularis, spiral ligament, spiral limbs and cochlear nerves. A few grafted cells were found in the sensory epithelium. Immunohistochemical analyses revealed the expression of CD34 and connexin 26 in the majority of grafted cells. Some of the grafted cells were positive for E-cadherin, indicating differentiation into epithelial cells. However, we have not found neural marker-positive cells. These findings indicate that MSCs may be a source of transplants to restore gap junction systems in the cochlea.

#### **[843] Expression of Hair Cell Markers in Cells Differentiated from Bone Marrow Stem Cells**

**Sang-jun Jeon<sup>1,2</sup>**, Stefan Heller<sup>3</sup>, Albert Edge<sup>1,2</sup>

<sup>1</sup>Department of Otolaryngology and Laryngology, Harvard Medical School, Boston, MA, <sup>2</sup>Eaton-Peabody Laboratory, Massachusetts Eye & Ear Infirmary, Boston, MA,

<sup>3</sup>Department of Otolaryngology and Head & Neck Surgery, Stanford University School of Medicine

Bone marrow contains mesenchymal stem cells that could be an alternative for cell-based treatment of hearing loss if these stem cells could be differentiated into hair cells. Bone marrow aspirate from C57BL/6 mice was cultured overnight in alpha MEM containing 9% FCS and 9% horse serum. When adherent cells were cultured for two passages (8 days) in serum-containing alpha MEM, they yielded CD44+ (13.8%), Sca1+ (5.7%) mesenchymal stem cells that were negative for CD34 and CD45. These cells gave rise to chondrocytes that expressed type IV collagen and type II collagen after culture in the presence of TGFβ, transferrin and insulin, demonstrating the chondrogenic differentiation capacity of the stem cells. In addition to CD44 and Sca1, the stem cells expressed otx2 and GATA3 based on RT-PCR but were negative for nestin, musashi, oct4, sox1 and math1.

Culture of mesenchymal stem cells in DMEM/F12 medium containing N2 and B27 without serum for 10 days in the presence of EGF, IGF and FGF gave rise to cells whose

proportion of CD44 (12.9%) and Sca1 (4.9%) remained similar but that were immunopositive for nestin (17.2%). The cells had been converted to neuroectoderm progenitors based on the expression of *musashi*, *oct4*, *sox1*, *BMP4*, *BMP7*, *math1* and *neurogenin1*, and the loss of *otx2* and *GATA3* expression. When mesenchymal stem cells from an *Atoh1*-GFP mouse were differentiated by co-culture with cells from a chick otocyst in medium containing IGF, EGF and FGF, they were converted from cells that lacked nuclear green fluorescence to cells that were positive for nuclear fluorescence, indicating expression of *math1*. Further analysis of these cells showed that they expressed myosin VIIa, parvalbumin 3 and *espin*, suggesting that they had differentiated into hair cell-like cells. Implantation into an intact otocyst demonstrated that these progenitors could develop characteristics of hair cells such as expression of hair cell markers and incorporation into the neuroepithelium of the embryonic chick inner ear.

#### **844 A New Method to Transplant Cells Into Spiral Ganglion Using Osteoclasts**

**Fukuichiro Iguchi<sup>1</sup>**, Hajime Nakamura<sup>1</sup>, Juichi Ito<sup>2</sup>

<sup>1</sup>*Department of Otolaryngology, Otsu Red Cross Hospital,*

<sup>2</sup>*Department of Otolaryngology, Head and Neck Surgery, Kyoto University Graduate School of Medicine*

We are attempting to regenerate spiral ganglion neurons using embryonic stem cells and neural stem cells. Cochleae receiving cell transplantation from the lateral semicircular canal exhibited robust survival of transplant-derived cells mainly in the scala tympani. But the transplanted cells do not reach spiral ganglion neurons easily, because of interruption by the bony wall of Rosenthal's canal. In this study, we examined the potential of osteoclastic resorption to perforate the bony wall. Osteoclasts are primarily responsible for bone resorption. The cells are formed from hematopoietic stem cells in the presence of macrophage colony stimulating factor (M-CSF) and a soluble form of receptor activator of NF- $\kappa$ B (sRANKL). Osteoclasts, obtained from SD rats, were propagated in media containing M-CSF, sRANKL. The cells were transplanted into SD rat cochlea *in vitro*. After 2 week-culture, histological analysis was performed. TRAP (tartate-resistant acid phosphatase) staining revealed osteoclast localization in the cochlea. Osteoclasts were further characterized by assessing their ability to form resorption pits on the bony wall (pit formation assay). We will discuss the possibility that osteoclastic resorption increase efficiency of cell transplantation to spiral ganglion.

#### **845 Expression of Nestin in Supporting Cell Subtypes from the Rat Crista Ampullaris Sensory Epithelia**

**Ricardo Cristobal<sup>1</sup>**, P. Ashley Wackym<sup>1</sup>, Joseph A. Cioffi<sup>1</sup>, Christy B. Erbe<sup>1</sup>, Paul Popper<sup>1</sup>

<sup>1</sup>*Medical College of Wisconsin*

Recent *in vitro* studies in dissociated sensory epithelia from the inner ear of mammals demonstrated the presence of stem cells with the ability to generate multiple cell types, including hair cells and supporting cells. These results

raised hope for developing new treatments for diseases resulting from inner ear hair cell loss. However, the identity of the stem cells remains unclear; they may be putative cells from the normal adult inner ear sensory epithelia or they may arise from *in vitro* transformation or dedifferentiation of epithelial cells. In previous studies we presented a method for evaluating the gene expression patterns of cell pools enriched in hair or supporting cells identified according to morphological criteria. Microarray gene expression profiling demonstrated multiple genes that are expressed in the hair or supporting cell-enriched pools alone. Furthermore some markers for neural derived precursors with proliferative capacity were identified in the supporting cell-enriched pool only, including the neuronal stem cell marker nestin. In the present study we demonstrated the expression of nestin in a subpopulation of supporting cells using immunofluorescent histological techniques. The experiments were carried out in fresh frozen tissue sections under RNase free conditions. Appropriate positive controls were conducted in brain histologic sections. In conclusion, the supporting cells from the rat crista ampullaris contain a subpopulation of cells that express specific progenitor cell markers. The techniques developed for this study may allow for future laser capture microdissection and gene expression profiling of individual cell types in the sensory epithelia.

Supported by R01DC02971 (PAW), and the Deafness Research Foundation and the American Academy of Otolaryngology-Head and Neck Surgery Foundation (RC)

#### **846 Reinnervation of Hair Cells in a De-Afferented Organ of Corti by Neurons Expressing Neuropilin 1**

**Rodrigo Martinez-Monedero<sup>1,2</sup>**, Li Luo<sup>1,2</sup>, Albert Edge<sup>1,2</sup>

<sup>1</sup>*Department of Otolaryngology and Laryngology, Harvard Medical School, Boston, MA,* <sup>2</sup>*Eaton-Peabody Laboratory, Massachusetts Eye & Ear Infirmary, Boston, MA*

Transplantation of stem cell-derived neural progenitors into the cochlea after denervation with  $\beta$ -bungarotoxin results in reinnervation of hair cells. We have used this *in vitro* explant system to investigate the role of guidance molecules in pathfinding by spiral ganglion neurons and neural progenitor cells obtained from stem cells.

Analysis of neuropilin 1 expression in the mouse cochlea during embryonic development indicated that the mRNA for the guidance receptor was present at early stages but its level decreased after birth. Immunohistochemistry revealed expression in statoacoustic ganglion cells during delamination from the otocyst at E10.5 and in later development at E12 and E15 but not at P5. RT-PCR revealed that semaphorin 3a, a guidance molecule often associated with repulsion of neurons expressing neuropilin 1, was expressed in the cochlea. The level of expression of neuropilin 1 was higher than that of neuropilin 2 at all developmental stages tested. When spiral ganglion neurons from newborn animals were transferred to a culture containing an organ of Corti denervated by  $\beta$ -bungarotoxin, immunohistochemical analysis showed that neuropilin 1 was expressed in the growing axons. Analysis of neural progenitors derived from stem cells also indicated expression of neuropilin 1 mRNA. Although the

neurons reinnervated hair cells, they approached the hair cells from peripheral locations rather than by the normal route through the spiral lamina, suggesting a repulsive interaction between the growing neuron and the extracellular environment.

We are currently testing the interaction between the growing neurons and CHO cells overexpressing semaphorin 3a to assess whether the guidance molecules are exerting a repulsive action on the growing neurites.

The identification of the molecular components of the guidance system will help to develop applications of cellular therapy in the inner ear.

Supported by NIDCD grants DC006789 and DC007174.

#### **[847] Expression of VEGF Receptor Flk-1 and Effects of VEGF on Cultures Derived from Mouse Inner Ear Tissue**

Juergen-Theodor Fraenzer<sup>1</sup>, Otto Gleich<sup>1</sup>, Frank-Peter Wachs<sup>2</sup>, Katharina Licht<sup>3</sup>, Jürgen Strutz<sup>1</sup>

<sup>1</sup>ENT-Department, University of Regensburg, <sup>2</sup>Department of Neurology, University of Regensburg, <sup>3</sup>Department of Voice, Speech and Hearing Disorders, UKE Hamburg

Recently we described successful cultures of cells derived from inner ear tissue (Licht et al., 2003, Abstr. 26th ARO Midwinter Meeting, p.259-260). Cells generated by proliferation in these cultures can differentiate in distinct types including those expressing the neural marker b-3-Tubulin and the glia marker GFAP (Gleich et al., 2005, 42nd workshop of IEB, Tuebingen). Here we show that cells in cultures from newborn mice are immunoreactive for the VEGF (vascular endothelial growth factor) receptor Flk-1 and VEGF added to the culture medium at an appropriate dose can increase cell density after a culture period of one week.

VEGF is a key regulator of angiogenesis and has been shown to have a broad spectrum of effects on neural cells, including neuroprotection and stimulation of proliferation. Here we show that the VEGF receptor Flk-1 is expressed in cell cultures derived from inner ear tissue. Positive Flk-1-immunoreactivity was observed in whole mounts of spheres as well as in adherent cells grown on chamber slides. Highly differentiated cells identified by the expression of b-3-Tubulin did not express Flk-1 suggesting that Flk-1 expression may dominate in less differentiated and potential stem cells.

VEGF added to cells derived from 2 week old primary cultures and seeded at a density of 50.000 cell per ml showed a dose-dependent effect on the cell number determined after one week. In controls without the addition of VEGF mean cell density (N = 11 cultures) increased by a factor of 3.9. With the addition of 10, 50 and 100 ng VEGF per ml the corresponding increase was 6.0, 4.6 and 3.7, respectively. Statistical analyses showed that cell density was significantly increased in the 10ng/ml condition compared to controls and 100ng/ml.

These in vitro results together with the Flk-1 expression analysis in the cultures suggest a role of VEGF in the development and regeneration of the inner ear.

Acknowledgments: We thank C. Woegerbauer for excellent technical and the ReForM-C project "Isolierung,

Differenzierung und Transdifferenzierung humaner Stammzellen" for financial support.

#### **[848] Multipotent Murine Cochlear and Vestibular Stem Cells After Protracted Postmortem Intervals** Pascal Senn<sup>1</sup>, Kazuo Oshima<sup>1</sup>, Stefan Heller<sup>1</sup>

<sup>1</sup>Dpts. of Otolaryngology and Molecular & Cellular Physiology, Stanford University School of Medicine

We performed a pilot study in newborn mice to assess viability and features of cochlear and vestibular stem cells as a function of the postmortem interval. The ultimate goal is to determine reasonable time limits for harvesting inner ear tissues from human autopsy cases.

Newborn Math1/nGFP mice were asphyxiated and kept at room temperature for 6 hours followed by storage at 4 degrees Celsius to simulate conditions found in autopsy cases. After 0, 6, 24, 48, 72, 96, 120, 240 and 360 hours postmortem, the temporal bones from 2 animals were removed for each time point. The utricles, organs of Corti, and spiral ganglia were isolated and dissociated to obtain single cell suspensions. Using Trypan blue staining, we found a considerable number of living cells directly after dissection in the suspension even after 360 hours postmortem. The single cell suspensions were then incubated for 7 days and inspected for the presence of free-floating spheres as an indication of stem cells (Li et al, Nature Med 9:1293-1299, 2003). We found significant numbers of spheres in cell suspensions harvested up to 240 hours postmortem. However, sphere numbers declined gradually for suspensions harvested later than 48 hours. As a proof for the presence of stem cells within the spheres, we propagated the spheres for more than 5 generations and found a stable increase in sphere numbers. In addition, we were able to obtain hair cell-like cells (Math1/GFP+, Myo7a+) and neuron-like cells (TUJ+) in a differentiation assay with secondary or tertiary spheres derived from tissues harvested up to 240 hours postmortem.

Our data show that stem cells in the inner ear of newborn mice are present, alive and functional up to 240 hours after death. Therefore we hypothesize that it should be possible to harvest human inner ear stem cells from autopsy cases within at least the first 2 days postmortem.

Supported by grants from the Swiss National Science Foundation PBBEB-105075 (PS) and NIDCD DC006167 (SH)

#### **[849] Cochlear Stem Cells Exist But Their Number Substantially Decreases During Postnatal Cochlear Maturation**

Kazuo Oshima<sup>1,2</sup>, Pascal Senn<sup>1,2</sup>, Eduardo Corrales<sup>3</sup>, Christian Grimm<sup>1,2</sup>, Jeffrey R. Holt<sup>4</sup>, Stefan Heller<sup>1,2</sup>

<sup>1</sup>Department of Otolaryngology, <sup>2</sup>Department of Molecular & Cellular Physiology, Stanford University School of Medicine, Stanford, CA, <sup>3</sup>Massachusetts Eye and Ear Infirmary, Boston, MA, <sup>4</sup>Department of Neuroscience, University of Virginia School of Medicine, Charlottesville, VA

Previously, we showed that the adult utricular sensory epithelium contains cells that display the characteristics

features of stem cells. Vestibular epithelial stem cells have the capacity for self-renewal and form spheres that express marker genes of the developing inner ear and the nervous system.

Here we show isolation and characterization of sphere-forming stem cells from the early postnatal organ of Corti, the spiral ganglion, and the stria vascularis as well as from the sacculus and the ampullae. Organ of Corti and vestibular sensory epithelial stem cells can give rise to cells that express multiple hair cell markers such as Myosin VIIa, espin, and parvalbumin 3, and express functional ion channels reminiscent of nascent hair cells. Spiral ganglion stem cells display features of neural stem cells and can give rise to neurons and glial cell types. Quantitative analysis of the number of stem cells per inner ear organ at different time points from birth to adulthood revealed that the ability for sphere formation in the mouse cochlea decreases approximately 100-fold during the second and third postnatal weeks; this decrease is substantially faster than the reduction of stem cells in vestibular organs, which robustly maintain their stem cell population also at older ages.

Our findings indicate that the lack of regenerative capacity of the adult mammalian cochlea is either a result of an early postnatal loss of stem cells or diminishment of stem cell features of maturing cochlear cells.

This work was supported by the National Organization for Hearing Research foundation (NOHR) (to KO) and by NIDCD DC006167 (to SH).

#### **[850] Survival and Stimulation of Neurite Outgrowth in a Serum-Free Culture of Adult Spiral-Ganglion Neurons**

**Richard Kollmar<sup>1</sup>**, Mauricio Vieira<sup>1</sup>, Barbara Christensen<sup>1</sup>, Bruce Wheeler<sup>1</sup>, Albert S. Feng<sup>1</sup>

<sup>1</sup>*Beckman Institute for Advanced Science and Technology, University of Illinois at Urbana-Champaign*

Regeneration of the auditory nerve in hearing-impaired adults has been difficult to investigate for lack of a convenient experimental system. *In vivo* studies are expensive and restricted by animal-use policies. *In vitro* studies have been conducted mostly with embryonic or neonate explants, which are easier to culture than those from mature animals; however, the active signalling pathways may well differ among these developmental stages. We therefore set out to establish an efficient system for the primary culture of adult auditory neurons. As our animal model we chose the CBA/CaJ mouse because it closely resembles humans in its physiology, offers extensive genetic tools, and does not suffer from age-dependent hearing loss. Cochleas were dissected from animals four to six weeks of age, at a time when hearing is fully developed. By adapting a protocol for the serum-free culture of hippocampal neurons, we were able to maintain dissociated spiral-ganglion neurons *in vitro* for at least seven days. The number of surviving neurons increased in the presence of brain derived neurotrophic factor (BDNF), leukemia inhibitory factor (LIF), neurotrophin 3 (NTF3 or NT-3), or a combination thereof. Similarly, neuritogenesis was enhanced by picomolar concentrations of these factors, with processes extending for up to 1.2 mm. This culture system can thus be used to

identify factors that promote survival of and neurite outgrowth from adult spiral-ganglion neurons, a critical step in restoring function to the damaged auditory nerve.

Support Contributed By: Beckman Institute for Advanced Science and Technology, University of Illinois at Urbana-Champaign.

#### **[851] Inhibition of Notch/RBP-J Signaling Induces Hair Cell Formation in Neonate Mouse Cochleas**

**Norio Yamamoto<sup>1,2</sup>**, Kenji Tanigaki<sup>3</sup>, Masayuki Tsuji<sup>2</sup>, Daisuke Yabe<sup>2</sup>, Juichi Ito<sup>1</sup>, Tasuku Honjo<sup>2</sup>

<sup>1</sup>*Department of Otolaryngology Head and Neck Surgery, Graduate School of Medicine, Kyoto University,*

<sup>2</sup>*Department of Medical Chemistry and Molecular Biology, Graduate School of Medicine, Kyoto University,* <sup>3</sup>*Research Institute, Shiga Medical Center*

Notch/RBP-J signaling is an evolutionally conserved signal pathway involved in binary cell fate specification through local interaction in various types of embryonic and even in some of postnatal mammalian organs. Several reports suggested that, in inner ear development, Notch/RBP-J signaling inhibits and promotes the specification of hair and supporting cell fates, respectively, from their common progenitor cells. But its function in postnatal inner ears is unknown.

In this study we showed that complete inhibition of Notch/RBP-J signaling in postnatal organs of Corti, by either conditional disruption of the *Rbpsuh* gene or treatment with a  $\gamma$ -secretase inhibitor, could give rise to ectopic hair cells in Hensen's cell region. Using quantitative RT-PCR we also showed that down-regulation of *Hes5* and up-regulation of *Math1* were associated with ectopic hair cell induction.

These results suggest that Notch/RBP-J signaling inhibits supporting cells from differentiation into hair cells in postnatal days, implying that inhibitors of Notch/RBP-J signaling can be used to help regenerating hair cells after birth. And thus administration of the inhibitors might serve for potential treatment of intractable sensorineural hearing impairment caused by loss of hair cells which have not been considered to regenerate after birth in mammals.

#### **[852] In Vivo Effects of Pharmacological Inhibition of Notch Signaling on Normal and Damaged Cochleae of Guinea Pigs**

**Takayuki Nakagawa<sup>1</sup>**, Yoshinori Matsuoka<sup>1</sup>, Tomoko Kita<sup>1</sup>, Shinji Takebayashi<sup>1</sup>, Koji Iwai<sup>1</sup>, Norio Yamamoto<sup>1,2</sup>, Juichi Ito<sup>1</sup>

<sup>1</sup>*Kyoto University,* <sup>2</sup>*NIH, Bethesda, MD*

The Notch signaling pathway is a key regulator for the specification of hair cell fate from progenitors during development and even after maturation. Among target genes of Notch signaling, *Atho1* has been paid particular attention because of its activity for hair cell regeneration in adult mammals. Raphael and his colleagues have demonstrated that *Atho1* overexpression in damaged cochleae of guinea pigs using virus vectors induces hair cell regeneration resulting in functional recovery. On the other hand, Yamamoto et al. have demonstrated that pharmacological inhibition of Notch signaling induces up-

regulation of *Atho1* and generation of ectopic hair cells in cochlear explants of postnatal mice. These findings suggest the possibility of in vivo hair cell regeneration in damaged cochleae by pharmacological inhibition of Notch signaling. To examine this hypothesis, we examined effects of local application of a gamma-secretase inhibitor (SI), a Notch signaling inhibitor, on guinea pig cochleae of the same model used in the experiments for *Atho1* overexpression. Local application was performed using an osmotic mini pump in the left cochlea for 14 days. Cochlear specimens were collected at day 14 or 28 after drug application following ABR measurements. Animals received local SI application without ototoxic treatment were used as controls. Control animals exhibited normal morphology and hearing. In damaged animals, local SI application induced generation of ectopic myosin VIIa-positive cells in the organ of Corti. However, no functional recovery was observed. These findings indicate that pharmacological inhibition of Notch signaling may have the potential of generation of new hair cells in vivo; however, further investigations to optimize conditions for local SI application are required for determination of the efficacy of this strategy.

### **853** p27 Antisense Oligonucleotides Stimulate Proliferation in the Organ of Corti, Spiral Ganglia and Stria Vascularis

Rende Gu<sup>1</sup>, Carol Pierce<sup>1</sup>, Eric Lynch<sup>1</sup>, Jonathan Kil<sup>1</sup>

<sup>1</sup>Sound Pharmaceuticals, Inc.

Ototoxic drugs, noise and aging typically cause an irreversible injury or loss of sensory and non-sensory cells in the organ of Corti, spiral ganglia and stria vascularis. Previous work from our lab indicates that cell proliferation can be induced with p27 Kip1 antisense oligonucleotides (AONs) (Kil et al., 2001, ARO, Gu et al 2001, ARO) at low doses (10-20 uM) following aminoglycoside ototoxicity in wildtype mice and Guinea pigs. Supporting cells of the organ of Corti appeared to be the most proliferative, although a corresponding analysis of the stria and spiral ganglia had not been performed. Here we report the infusion of high dose AONs (100-1000 uM) for 7-14 days following ototoxic lesion. Animals were allowed recovered for 0 and two weeks. Cell proliferation was determined using BrdU immunocytochemistry on whole mount tissues. Cochlea receiving AONs or vehicle only were analyzed histologically under light and fluorescence microscopy. P27 AONs at 100 uM induce proliferation in the organ of Corti, spiral ganglia and stria vascularis. Interestingly, at these doses, the stria vascularis contains the highest level of proliferating cells. Other non-sensory structures within the cochlea appear intact with no obvious signs of toxicity attributed to p27 AONs at this concentration. However, P27 AONs at 1000 uM induce significant inflammation and cell death. Since aminoglycoside ototoxicity has profound detrimental effects on the stria vascularis, it is reasonable to assume that its regeneration maybe necessary following ototoxic insult. P27 AONs can induce proliferation in this non-sensory structure that contributes to the sensory function of the organ of Corti.

Portions of this work have been supported by the Office of Naval Research

### **854** Expression Patterns Indicate Diverse Roles of Lim-Homeodomain Transcription Factors (LIM-HDs) in Mammalian Inner Ear

MingQian Huang<sup>1</sup>, Cyrille Sage<sup>1</sup>, Huawei Li<sup>2</sup>, Hideki Mutai<sup>3</sup>, Mengqing Xiang<sup>4</sup>, Stefan Heller<sup>5</sup>, Wei-Qiang Gao<sup>6</sup>, Zheng-Yi Chen<sup>1</sup>

<sup>1</sup>Massachusetts General Hospital and Harvard Medical School, <sup>2</sup>Massachusetts Eye and Ear Infirmary and Harvard Medical School, <sup>3</sup>Tokyo Medical Center, <sup>4</sup>UMDNJ-Robert Wood Johnson Medical School, <sup>5</sup>Stanford University, <sup>6</sup>Genentech, Inc

Mammalian inner ear development is regulated by concerted functions of a diverse group of transcription factors. However the expression and potential functional roles of Lim-homeodomain transcription factors (LIM-HD) in the inner ear are largely unknown.

LIM-HDs have two LIM domains for protein-protein interaction and one homeodomain to bind to DNA. Members of this family play critical roles in determining diverse neuronal cell types. To understand the potential involvement of LIM-HDs, we analyzed expression of most LIM-HDs during mouse inner ear development. The expression profiles of LIM-HDs can be classified by their tempo-spatial patterns that indicate their distinct yet overlapping roles. In otocyst at E10.5, *Lhx5* and *Lmx1b* are expressed ubiquitously in all cells and in neuroblasts, whereas *Lmx1a* expression is confined to the region of otocyst that is going to become non-sensory epithelium. Subsequently many LIM-HDs, including *Lhx2*, 3, 4, 8, 9 and *Isl2*, show expression in postmitotic neurons and sensory epithelia cells. *Lmx1a* continues expression in the non-sensory regions, including the transitional cells in vestibule and the stria of cochlea.

To further explore the pathways involved, we studied expression of selected LIM-HDs in hair cell-specific transcription factor *Pou4f3* knockout mice, in which hair cells display impaired differentiation and maturation. There was down-regulation of *Lhx3* and 9, and up-regulation of *Isl1*, suggesting that they are involved in the *Pou4f3* pathway. Transfection experiment with the cultured cochleas demonstrated that *Pou4f3* directly suppresses *Isl1* expression, and down-regulation *Lhx3* in *Pou4f3* hair cells is likely a secondary effect. Furthermore, over expression of *Lhx3* led to *Isl1* down-regulation, indicating their interaction at a transcriptional level. A subset of LIM-HDs therefore is linked to the *Pou4f3* pathway in the inner ear. The interplay of *Lhx3* and *Isl1*, controlled through *Pou4f3*, is likely to be important in hair cell differentiation and maturation.

### **855** Transcriptional Regulation of *Bmp4* in the Inner Ear

Beth Maisel<sup>1,2</sup>, John H. Greinwald<sup>1,2</sup>, Daniel Choo<sup>1,2</sup>, Valentina Pilipenko<sup>1</sup>

<sup>1</sup>Center for Hearing and Deafness Research, Pediatric Otolaryngology, Cincinnati Children's Hospital, <sup>2</sup>University of Cincinnati College of Medicine, Cincinnati, OH

*Bmp4* (bone morphogenic protein 4) is a member of the TGF- $\beta$  family that has been implicated in the regulation of inner ear development. Three different *Bmp4* transcripts,

1A, 1B and intron 2, were described. The *Bmp4* transcripts are regulated by three distinct promoters. *Bmp4* promoters have regions of the conserved sequence (5'-CAAG-3'), which is a core binding sequence for the Hmx transcription factor family. Two members of the Hmx transcription factor family, *Hmx2* and *Hmx3*, are known to control development of the inner ear. These two transcription factors have been reported to have similar patterns of expression. *Hmx3* was chosen for analysis in this study. *Bmp4* isoform expression was determined by RT-PCR analysis of RNA from the mouse inner ear at E9 and P2. At P2, only transcript 1A was detected, while at E9, both 1A and 1B transcripts were identified. To detect spatial expression of *Bmp4* and *Hmx3*, we performed *in situ* hybridization on the mouse inner ear cryosections. We found that *Bmp4* and *Hmx3* have overlapping patterns of expression. These data suggest that *Bmp4* isoform expression in the inner ear may be regulated by *Hmx3*. By studying the spatial expression of *Bmp4* isoforms in the inner ear at different stages, further insight into the molecules involved in inner ear development can be gained. Further studies are underway to delineate the regulation of *Bmp4* in inner ear development and the relationship between *Bmp4* and *Hmx3*.

#### **856 Integrin Expression in the Inner Ear**

Ivan Brunetta<sup>1</sup>, Andrew Forge<sup>1</sup>, Stefano Casalotti<sup>1</sup>

<sup>1</sup>University College London

Cellular Adhesion Molecules (CAMs) are a family of receptors that mediate the attachment to the extracellular matrix (ECM) and mediate cell-cell adhesion. CAMs include different subfamilies of transmembrane proteins such as cadherins, selectins, immunoglobulin (Ig-CAM), and integrins. Integrins are transmembrane glycoproteins which act as receptors for ECM proteins, and for cell-cell interactions. A functional integrin receptor is constituted by an  $\alpha$  and an  $\beta$  subunit which form a heterodimer complex. Integrins are involved in different cell processes such as development, maintenance and epithelial repair. We hypothesise that they play these roles in the inner ear. To date, 24 different integrin heterodimers have been characterized by the combinations of 18  $\alpha$  and 8  $\beta$  subunits.

We have focused our efforts to understand the roles of  $\alpha 1$ ,  $\alpha 3$  and  $\alpha V$  subunits in the inner ear sensory epithelia. Integrin subunits  $\alpha 1$  and  $\alpha 3$  were isolated by immunoprecipitation from OC-2 cell line and adult mouse cochlea. Total RNA was isolated from mature cochleae and OC-2 cells in order to amplify the mRNA of the integrin subunits  $\alpha 1$ ,  $\alpha 3$ ,  $\alpha V$ . Characterization of  $\alpha 1$ ,  $\alpha 3$  and  $\alpha V$  was also performed by immunostaining both cochlea and vestibular tissues of adult mice.

Results suggest that integrins  $\alpha 1$  and  $\alpha V$  are actively expressed in adult mouse cochlea as well as in the OC-2 cell line, whereas  $\alpha 3$  is mainly expressed in OC-2 cells. Further immunoprecipitations suggested that  $\alpha 1$  and  $\alpha V$  subunits do not aggregate to form a heterodimer receptor. Immunostaining results would suggest that  $\alpha V$  is expressed in the cells of the organ of Corti. In contrast  $\alpha 1$  is expressed in the basilar membrane.

This project is supported by Deafness Research UK.

#### **857 Slit Expression in the Developing Cochlea**

Wei Gao<sup>1</sup>, Ashish Shah<sup>1</sup>, Audra Webber<sup>1</sup>, Yael Raz<sup>1</sup>

<sup>1</sup>University of Pittsburgh School of Medicine

The process by which spiral ganglion neurites are guided to their hair cell targets is not well understood. The slit/robo signaling pathway has been implicated in axon guidance in other sensory systems including olfaction, vision and somatosensation. The aim of this study is to describe the detailed temporospatial expression of the slit genes in the developing mouse inner ear. *In situ* hybridization was performed using antisense RNA probes for the three slit genes. We have previously reported on the expression of slits and robos in whole-mount cochleae. This study was performed on sectioned tissue and reveals the expression of these genes at the individual cell level. Slit1 expression was not detected in the embryonic inner ear. Slit 2 expression was noted as early as E13 and continued through P3. At E16, slit2 expression was noted in the cells that separate the spiral ganglion from the greater epithelial ridge. A gradient of expression along the longitudinal axis of the cochlea was noted with stronger expression at the base. By P0, slit2 expression was also noted in the inner sulcus of the cochlear epithelium. Slit3 expression was also noted as early as E13 and continued through P3. Slit3 expression was also noted in the inner sulcus of the cochlear epithelium just neural to the slit2 expressing cells. Additionally, expression of slit3 was noted in the stria vascularis. The restricted expression of two slit genes in the developing inner ear suggests a role for this signaling pathway in auditory development. Functional studies are required in order to determine the significance of these expression patterns in shaping auditory connectivity.

#### **858 Development of a Voltage-Dependent Sodium Channel (Nav1.6) and Contactin-Associated Protein (Caspr) in the Cochlea and Cochlear Ganglion of the Mouse**

Waheeda A. Hossain<sup>1</sup>, Matthew N. Rasband<sup>1</sup>, D. Kent Morest<sup>1</sup>

<sup>1</sup>Dept. of Neuroscience, University of Connecticut Health Center

Neural excitability depends on appropriate expression and localization of voltage-dependent ion channels. We have previously demonstrated in adult mouse cochlea that Nav1.6 channels are clustered on the afferent endings, ganglionic initial segments, and nodes of Ranvier, where they may generate action potentials. Alongside Nav1.6, Caspr provides a lateral diffusion barrier and is considered essential for the formation and stability of the nodal spike generator. Here we trace the expression of Nav1.6 and Caspr during the development of cochlear ganglion and cochlea before onset of hearing. Immunostaining with specific antibodies showed the initial appearance of Nav1.6 in the ganglion cell bodies, in the afferent fibers of the organ of Corti, spiral lamina and 8th nerve, and in the hair cells as early as embryonic day 18 (E18). Nav 1.6 staining appeared in ganglion cells and all along the fibers from E18 to P1. By P7 the staining pattern resembled the mature form in that it clustered on both ganglionic initial

segments, the first heminodes, and nodes of Ranvier. Immunostaining for Caspr appeared already at E15 in ganglion cell cytoplasm and sparsely in the otic epithelium. By E18 it was also present in fibers in the spiral lamina but not in the otic epithelium. At P3, Caspr assumed its mature location in the paranodes and first heminode, but remained in the ganglion cell cytoplasm at P7 and P9. The lace-like network of Caspr, as seen around loosely myelinated Type I ganglion cell, in the adult, was not visible at this time point. Myelination, as assessed by immunostaining for myelin basic protein, first scarcely appeared at P1 but by P3 was present on the afferent fibers and surrounding the Type I ganglion cells. Our data suggest expression of Nav1.6 in a diffuse pattern during embryonic development, followed with formation of clusters flanked by Caspr after birth. Clustering of Nav1.6 and localization of Caspr precede hearing.

Supported by NIH grants from NIDCD(DKM, WAH) & NINDS(MNR).

### **859 Expression of Mouse PACT, a Gene Important in Otologic Development**

**Mark Rizzi<sup>1</sup>**, Keiko Hirose<sup>1</sup>, Gregory Peters<sup>1</sup>, Ganes Sen<sup>1</sup>

<sup>1</sup>*Cleveland Clinic Foundation*

PACT, or PKR activating protein, is known for its ability to bind double stranded RNA and for its ability to activate latent protein kinase R. Some double stranded RNA binding proteins have been shown to play a role in transport of mRNA during embryogenesis. We performed in situ hybridization in prenatal and postnatal mouse temporal bones to determine when and where PACT mRNA is expressed. In situ hybridization with antisense PACT mRNA probes was performed on temporal bone sections and on whole mount embryos. PACT expression is seen in the developing otocyst (E9), in Meckel's cartilage (E12) as well as in the developing bony anterior skull base. In adult mice, PACT is expressed in the spiral ligament, the marginal cells of the stria vascularis, sensory epithelium and the middle ear mucosa. How PACT exerts its effects on ear development is not yet understood. Examination of the PACT knockout mouse demonstrates that in the absence of PACT, the pinna is malformed, the middle ear cavity is shrunken and the ossicles are fused. This knockout mouse may provide a model for human microtia and may lend insight into the mechanism of normal outer and middle ear development.

### **860 Prosaposin in Organ of Corti Maturation and Outer Hair Cell Survival**

**Omar Akil<sup>1</sup>**, Lawrence Lustig<sup>1</sup>

<sup>1</sup>*Department of Otolaryngology - Head and Neck Surgery University of California, San Francisco*

Prosaposin, a precursor of four glycoprotein activators (Saposins) for lysosomal hydrolases, has been shown to have both lipid transfer properties and neuritogenic activity. Our previous studies have demonstrated that transgenic mouse (-/-) lacking the neuritogenic region of saposin C develop deafness between P16 and P21 and show abnormal afferent and efferent innervation patterns,

suggesting that prosaposin may be required for normal adult cochlear innervation.

In the present study, we sought to: 1) Extend these findings by examining the immunohistology expression of saposin D in normal rodent cochlea during development; and 2) determine outer hair cell (OHC) survival in prosaposin transgenic mice. From P1 to P10, the expression of saposin D was uniformly distributed throughout the organ of Corti, whereas from P15 to P30 saposin D expression became localized to the base of the OHCs, the supporting cells of the inner hair cells (IHC) (inner phalangeal cells and/or border cells) and the apex of the IHC. In addition, outer hair cell counts in adult prosaposin transgenic mice (wild, heterozygote and homozygote) using Rhodamine-Phalloidin stained surface preparations showed increased outer hair cells loss in the apical turn of the cochlea of the homozygote as compared to the wild and heterozygote mice, while the OHC counts in the mid- and basal-turns of the cochlea were identical in all animals tested. These results suggest an important role of prosaposin in the neuronal maturation processes of the organ of Corti and the maintenance of normal hearing.

### **861 CBP Expression in Mouse AVCN Neurons During a Developmental Critical Period**

**Xiao-Qing Tang<sup>1</sup>**, Lance Zirpel<sup>1</sup>

<sup>1</sup>*University of Minnesota*

Central auditory neurons are susceptible to removal of afferent activity from the eighth nerve during a developmental critical period. Substantial neuronal loss occurs in mouse anteroventral cochlear nucleus (AVCN) following afferent deprivation at ages younger than postnatal day (P)14. The surviving neurons remain healthy and continue normal development. The molecular events that lead to different neuronal fate in mouse AVCN after afferent removal are not fully understood. Calcium/CREB/CBP-dependent gene regulation is critical for neuronal survival in several systems. Our previous work indicated that activity deprivation induced intracellular calcium increase in all AVCN neurons, and CREB activation following calcium increase is essential for neurons to survive activity removal in chick nucleus magnocellularis, the avian homolog of mammalian AVCN. The role of the transcription coactivator CBP in this process is undetermined. In this study we examined CBP expression in mouse AVCN neurons at different developmental ages. We found that CBP expression decreases after the critical period of deafferentation-induced neuronal death, as the expression level at P21 drops by 30% compared to P7, indicating that CBP may be involved in the neuronal survival during this period of susceptibility. The change in CBP expression and CREB/CBP interaction at different times after deafferentation is being examined. This study aims to further delineate the molecular mechanism of neuronal survival following afferent deprivation within a developmental critical period.

Supported by DC05012



## **862 Identification of Guidance Molecules Necessary for the Formation of the Superior Olivary Complex**

**David M. Howell**<sup>1,2</sup>, Warren J. Morgan<sup>1,2</sup>, Albert S. Berrebi<sup>1,3</sup>, George A. Spirou<sup>1,4</sup>, Peter H. Mathers<sup>1,2</sup>

<sup>1</sup>*Sensory Neuroscience Research Center, Dept. of Otolaryngology, WVU School of Medicine,* <sup>2</sup>*Dept. of Biochemistry and Molecular Pharmacology, WVU School of Medicine,* <sup>3</sup>*Dept. of Neurobiology and Anatomy, WVU School of Medicine,* <sup>4</sup>*Dept. of Physiology and Pharmacology, WVU School of Medicine*

During development, neurons utilize guidance cues as they migrate from their birth place to their adult destination. However, the molecular factors directing cell migration and positioning in the lower auditory brainstem remain relatively unknown. We found that the medial nucleus of the trapezoid body (MNTB) and other superior olivary complex (SOC) neurons express RNA for the *DCC* and *robo1* cell surface receptors during their migration into the ventral brainstem. These receptors are known mediators of axonal guidance and neuronal migration throughout the central nervous system. As early as E13.5, *DCC* and *robo1* probes label cells in migratory streams that originate from the rostral-most extent of the brainstem and extend caudally on the ventral surface of the brainstem toward the future SOC. Expression of these molecules is maintained during the formation of discrete SOC nuclei. By E17.5, a gradient of *DCC* expression is present within the MNTB, with highest *DCC* levels medially. Secreted ligands for the *DCC* and *robo1* receptors, *netrin1*, *slit1* and *slit2*, are expressed along the brainstem midline, consistent with a potential role in neuronal cell guidance. The utilization of *netrin-DCC* signaling in MNTB migration is supported by the absence of MNTB neurons in mice carrying no functional *netrin1* or *DCC* genes. Mice carrying one functional *netrin1* or *DCC* gene have a laterally displaced MNTB at P0 that is maintained through adulthood. We find that the high frequency region of the displaced MNTB is disrupted, as determined by *cfos* immunoreactivity. We propose that *netrin-DCC* and *slit-robo* signaling is necessary for the migration and medial-lateral patterning of SOC neurons in a dose-dependant manner. Supported by NIH/NCRR grant P20 RR15574 and R01 EY012152.

## **863 Investigating the Mouse Auditory Brainstem in DCC Mutant Mice**

**Warren J. Morgan**<sup>1,2</sup>, David M. Howell<sup>1,2</sup>, Albert S. Berrebi<sup>2,3</sup>, George A. Spirou<sup>2,4</sup>, Peter H. Mathers<sup>1,2</sup>

<sup>1</sup>*Dept. of Biochemistry and Molecular Pharmacology, WVU School of Medicine,* <sup>2</sup>*Sensory Neuroscience Research Center, Dept. of Otolaryngology, WVU School of Medicine,* <sup>3</sup>*Dept. of Neurobiology and Anatomy, WVU School of Medicine,* <sup>4</sup>*Dept. of Physiology and Pharmacology, WVU School of Medicine*

Studies on the development of the central auditory system will provide a more comprehensive understanding of this particular system and neural development as a whole. The receptor Deleted in Colorectal Cancer (DCC) and its ligand Netrin-1 are known to be important factors in axon guidance and neuronal migration. Previous work from our

lab showed that mice deficient in one or both copies of *DCC* show perturbations in the medial nucleus of the trapezoid body (MNTB). In the pursuit of auditory cell-specific or region-specific markers to better understand the superior olivary complex (SOC) development, we have analyzed the expression of transcription and growth factors known to be active in the early hindbrain of the mouse. We found that the *Mafb* gene, which encodes the basic leucine zipper protein Kreisler, is specifically expressed in cell groups of the presumptive cochlear nucleus as well as the lateral superior olive (LSO), medial superior olive (MSO) and the lateral nucleus of the trapezoid body (LNTB) of the SOC, both at embryonic and postnatal stages. Further characterization of this gene expression will provide a marker for cell groups that can be utilized for investigation of the development of specific auditory nuclei. Preliminary data suggest a difference in the lateral nuclei of the SOC in *DCC*-knockout versus wild-type mice. By comparing the expression of *Mafb* and other genes that are specifically expressed in hindbrain auditory nuclei in *DCC*-mutant versus control mice, we can determine the importance of *DCC* in the formation of the SOC nuclei. Supported by NIH/NCRR grant P20 RR15574 and R01 EY012152

## **864 Spatiotemporal Expression Patterns of Otopetrin 1 and Otoconin-90 in Developing Quail at Normal and Hypergravity**

**Euysoo Kim**<sup>1</sup>, David Huss<sup>1</sup>, Elena Ignatova<sup>1</sup>, Ruediger Thalmann<sup>1</sup>, Isolde Thalmann<sup>1</sup>, Mark E. Warchol<sup>1</sup>, David Ornitz<sup>1</sup>, J. David Dickman<sup>1</sup>

<sup>1</sup>*Washington University*

Otoconia serve as mechanical inertial transducers for the detection of linear acceleration. Recently, we observed that otoconial formation was affected by different gravity conditions. The current study examined the effect of hypergravity on the biosynthesis and development of otoconia. We characterized the spatiotemporal expression patterns of two genes known to regulate otoconial formation, Otopetrin 1 (Otop 1) and Otoconin-90 (Oc-90) (Hurle, Hum Mol Genet 2003, Ignatova, Hear Res 2004) in embryonic *Coturnix japonica* at normal or 2G centrifugation. Similar to mice, *in situ* hybridization showed that starting at E4 Oc-90 mRNA was mainly present in the thin overlying non-sensory epithelium of the quail endorgans, whereas Otop1 mRNA was localized to the macular epithelium. Real-time quantitative PCR analysis showed that Oc-90 mRNA level reached its maximum at E10 and started to decrease as the embryo reached E12, resulting in significant reduction at hatching. Otop1 showed a slight delay in expression compared to Oc-90. Its expression level peaked at E10 and showed regression towards hatching. Embryos grown at 2G showed a change in expression of both Oc-90 and Otop1, where Oc-90 was reduced and Otop1 was increased. This effect was most prominent from E8 to E12 when increased packaging of otoconia occurred.

**865 Gene Expression Profiles and Pathway Analysis of Early Mouse Inner Ear Development**  
**Samin Sajan<sup>1</sup>**, Mark E. Warchol<sup>2</sup>, Michael Lovett<sup>1</sup>

<sup>1</sup>*Division of Human Genetics and Department of Genetics, Washington University School of Medicine,* <sup>2</sup>*Department of Otolaryngology, Washington University School of Medicine, St. Louis, MO*

We have analyzed the very early stages of mammalian inner ear development by large-scale gene expression profiling with the purpose of identifying new sets of inner ear genes and pathways. We micro-dissected inner ear tissues from mouse embryos beginning at E9 up to E15 at half-day intervals and obtained their gene expression profiles using Affymetrix MOE430Av2 chips. Two replicates per developmental stage were profiled, with each replicate being obtained from a different litter. From E9 to E10 whole inner ears were profiled, and from E10.5 to E12 the cochleae and the vestibular organs were separated and profiled individually. The cochleae, utricles, and saccules were profiled separately beginning at E12.5 and beyond. We identified 2,426 genes that were differentially expressed by at least 2-fold between two or more samples, of which 8% have previously been associated with the inner ear in one way or another, and approximately 11% of which currently have no known function. Moreover, 485 of the differentially expressed genes fall within one or more uncloned human deafness loci, thus serving as positional candidates for novel deafness genes. By creating self-organizing maps, we have identified genes with similar expression profiles across the developmental time-course, and compiled a list of genes that closely follow expression profiles of known hair cell and/or supporting cell-specific transcription factors such as *Atoh1* and *Hes5*. These genes serve as candidate downstream targets of these transcription factors. We also implemented a high-stringency statistical filter to identify genes that are only expressed in one tissue-type. We found 22 such genes in the cochlea (examples are *Rxrg*, *Capn6*, *Slco5a1* and *4631408O11Rik*), 8 in the utricle (such as *Kcnd2*, *D730039F16Rik*, *Ccnd2*, *Mitf*), and 9 in the saccule (*Dapk2*, *Adhfe1* and *Cdkn2b*, among others). The expression patterns of some of these genes were also validated by RNA in-situ hybridizations. Using informatics tools, we have compiled networks of gene interactions to identify discrete pathways that are active during early inner ear development. Finally, we have also measured the gene expression profiles of inner ear structures from various gene knock out mice. Specifically, we have focused upon transcription factor gene knock outs that result in inner ear defects (e.g. *Dlx5*) in order to identify candidate downstream targets of these transcriptional regulators.

**866 Differential Gene Expression in Kreisler Inner Ears**

Daniel Choo<sup>1,2</sup>, **Jaye Ward<sup>1</sup>**

<sup>1</sup>*Center for Hearing and Deafness Research, Pediatric Otolaryngology, Cincinnati Children's Hospital,* <sup>2</sup>*University of Cincinnati College of Medicine, Cincinnati, OH*

The *kreisler(kr)* mouse displays hindbrain and inner ear defects that arise from mutation of the *kr/mafBr* gene, a

zinc-finger transcription factor normally expressed in rhombomeres 5 and 6. The inner ear defects include failure of the endolymphatic duct and sac to differentiate and gross malformation of the cochlea and semicircular canals.

Our previous studies have shown that the molecular mechanisms underlying these inner ear defects involve *Gbx2*, *Dlx5* and *Wnt2b*-mediated processes. In order to identify additional candidate genes in this molecular pathway, we examined differential gene expression in *kreisler* inner ears using a microarray methodology validated by standard blotting and in situ hybridization techniques.

For these studies, RNA was harvested from mutant and control embryos at 2 developmental timepoints (E10, 25-30 somites and E15). Using standard Affymetrix MG-U74Av2 chips, array experiments were performed in independent triplicates. Genes that were differentially expressed >2-fold at E10 and >1.5 fold at E15 in *kreisler* inner ears compared to controls included *Gbx2*, *Gata3*, *Sox2*, *RaldH1*, *GJB2*, *Pou3f4*, *Ngn1*, *Nkx6.2* and *TectB*. At E15, *Gata3*, *TectB*, *GJB2* and *RaldH1* were shown on the array as being downregulated and *krt2-17* expression was up regulated. At E10, *Nkx6.2* and *Ngn1* showed significant up regulation, where as *Gbx2* and *RaldH1* were down regulated. Array data for these genes were corroborated by at least 2 other methodologies (RT-PCR, Northern, In situ hybridization, or Immunohistochemistry).

Further investigation of these genes will help identify additional components that regulate development of the *kreisler* inner ear. By focusing on the differentially expressed otic genes, we plan to develop a more refined hypothesis of the *kr* molecular pathway.

**867 Quantification Method for Spiral Ganglion Neurite Outgrowth In Vitro**

**Andre Gurr<sup>1</sup>**, Thomas Stark<sup>1</sup>, Dominik Brors<sup>1</sup>, Stefan Hansen<sup>1</sup>, Stefan Dazert<sup>1</sup>

<sup>1</sup>*Department of Otolaryngology Bochum, Germany*

In cell culture, the neurite outgrowth of spiral ganglion cells shows a polymorphic morphology which is difficult to analyse. To evaluate and compare this polymorphic growth pattern, special metrical methods are required to achieve comparable results. This becomes even more important if growth factors or solids like cochlea-implant electrode (MedEl, Austria) are introduced into culture.

Presently applied metrical methods compare data by geometrical calculation, but most of them do not consider form and appearance of the ganglion cell heaps. This concerns also solids which have been placed into the medium.

The here presented new method is based on surface oriented geometrical analysis. We use tangents to determine the neurites outgrowth angle and correlate a change of direction with the solids surfaces. The relationship of outgrowing neurites to solid surfaces are also determined by tangent based methods

We introduce this method that combines all possible morphological structures without a expanded simplification. With this method, spiral ganglion neurite

growth patterns in cell culture studies can be characterised more precisely and, thus it helps to better differentiate the action domain of different soluble factors or solids.

### **868 Early Dendritic Spine and Synapse Development in Auditory Cortical Pyramidal Neurons**

**Scott Schachte**<sup>1</sup>, Michael E. Dailey<sup>1</sup>, Steven H. Green<sup>1</sup>

<sup>1</sup>*University of Iowa*

In the rat auditory cortex, synaptogenesis precedes both the establishment of mature auditory hair cell thresholds and hearing-evoked activity in central auditory neurons, suggesting a correlation between hearing onset and synaptic reorganization in the auditory cortex. Indeed, previous studies have shown rapid change in auditory cortex pyramidal neuron dendritic structure and spine density concomitant with hearing onset as well as altered development of dendritic complexity and spine density following neonatal cochlear ablation. This research investigates synapse formation, via quantification of spine and synapse density, on dendrites of layer 2/3 and layer 5 pyramidal neurons in the auditory cortex of neonatal rats from postnatal day (P4), prior to hearing onset, through P42 when hearing is mature. The goal is to provide a baseline for comparison of synaptogenesis in auditory cortical slices to changes in neural activity and neurotrophin exposure. In vivo dendritic spine density was assessed using the lipophilic dye 1,1'-dioctadecyl-3,3,3',3'-tetramethylindocarbocyanine perchlorate (DiI) in P4, P9, P11, P14, P19, P21 and P42 rats. Spine density on apical and basal dendrites of layer 2/3 pyramidal neurons increases postnatally from <0.1 spine/μm to >1 spine/μm. Notably, most of the increase in spine density is between P14 and P19. Synapse density and distribution were assessed in organotypic cortical slices prepared from P4 rats and maintained for either 5 or 7 days in vitro (DIV), corresponding to the period of hearing onset in rats. Cortical neurons were transfected with PSD95-GFP, a fusion protein we have previously shown as a reliable postsynaptic marker, at either 3 or 5 days in vitro. We observed a small increase in synapse density from P4div5 to P4div7. Similar studies are now being performed on auditory cortical slices from P14 rats maintained 5 to 7 DIV, corresponding to the period where mature hearing thresholds are achieved in the rat CNS.

### **869 Spatiotemporal Pattern of Cholinergic Innervation in the Developing Mouse Cochlea**

**Dwayne Simmons**<sup>1</sup>, Adam Bergeron<sup>1</sup>, Helena Wotring<sup>1</sup>, Angela Schrader<sup>1</sup>

<sup>1</sup>*Washington University*

Acetylcholine (ACh) is the primary neurotransmitter for synaptic transmission between efferent olivocochlear (OC) axons and cochlear hair cells within the mammalian inner ear. Two enzymes and two transporters are required for ACh synaptic transmission at cholinergic synapses. Despite our knowledge of cholinergic neurotransmission at the NMJ, neither the temporal order of cholinergic enzyme expression nor the signals required for presynaptic cholinergic differentiation in the nervous system has been

elucidated. Neurons could develop a cholinergic phenotype either by up-regulating expression simultaneously or by undergoing a stereotyped pattern of expression. In this preliminary report, we investigated the spatiotemporal pattern of cholinergic differentiation in OC axons during the period of efferent synaptogenesis in the normal mouse cochlea. To test whether missing or degenerating hair cells alter cholinergic differentiation, the presence of cholinergic proteins was also examined in the adult cochlea of Bronx waltzer (bv) mutants.

Efferent axons first invade the organ of Corti in mid-basal regions as early as E18. Although acetylcholinesterase (AChE) histochemical staining was detected in the embryonic cochlea, it was initially associated with cells within the organ of Corti and not fibers. AChE mRNA was present in the organ of Corti from embryonic day (E)14 - postnatal day (P)6, but not in the adult. AChE-positive cochlear fibers were observed below inner hair cells (IHCs) at P0 and below outer hair cells (OHCs) between P4 and P6. The distribution of AChE-positive fibers mimicked fibers expressing growth-associated protein (GAP43) immunoreactivity. Vesicular acetylcholine transporter (VACHT) was detected below IHCs at P2 and OHCs by P6 and coincided with synapsin immunoreactivity. The high-affinity choline transporter (ChT1) was detected below IHCs by P4 and OHCs by P6. The adult bv mutant displayed larger VACHT- and ChT1-positive terminals below OHCs. Our data suggest that there are endogenous levels of AChE in the embryonic cochlea, that cholinergic enzymes and transporters are expressed sequentially, and that missing or degenerating hair cells in the bv mutant do not prevent cholinergic differentiation of OC terminals.

Research supported by NIDCD grants R01 DC004086 and P30 DC004665.

### **870 Regulation of Olivocochlear Innervation and Synaptogenesis by Cochlear Hair Cell Nicotinic Acetylcholine Receptors**

**Vidya Murthy**<sup>1</sup>, Douglas Vetter<sup>1</sup>

<sup>1</sup>*Tufts University School of Medicine*

The olivocochlear (OC) system enables the brain to influence hearing thresholds via synaptic contacts with the cochlear hair cells. The cochlear outer hair cells (OHCs) express α9 and α10 nicotinic acetylcholine receptor (nAChR) subunits and are contacted by cholinergic efferent fibers originating in the brainstem. Genetic ablation of α9 nAChR subunits has been previously shown to result in hypertrophy and a decrease in the number of efferent synaptic terminals at OHCs. A similar phenotype is also observed in whole mount preparation of cochlear tissue from α10 knock out mice. These studies indicate that loss of nAChR activity in hair cells results in dramatic rearrangement of the OC system. In addition, sectioned cochlear tissue from α9 knock out mice reveals an aberrant efferent synapse formation at OHCs in the mutant mice at earlier developmental stages (P7, before the onset of hearing). Together the adult and developmental data reveal an unconventional role for nAChRs in synapse stabilization,

counter to the well-known model of synapse formation at the neuromuscular junction, where synapse formation is not altered due to loss of cholinergic receptor activity. These abnormal innervation patterns in the mutant mice also correlate with changes in the expression levels of adhesion proteins that are implicated in processes such as target recognition and synaptogenesis in the cochlea. These results indicate that the nAChR subunits play a key role in regulating efferent synaptogenesis at OHCs possibly by regulating the expression of various synaptic adhesion molecules that provide the microenvironments in which synapses are formed. Thus these new findings provide insights into the molecular mechanisms by which post-synaptic receptor activity regulates efferent synapse formation and maturation in the inner ear. In addition these data will allow us to better understand the molecular mechanism by which the OC system affects hair cell physiology and modulates hearing.

### **871 Transmission Electron Microscopy of the Developing Mouse Outer Hair Cell Cuticular Plate and Associated Structures**

**Karen S. Pawlowski<sup>1,2</sup>**, Yayoi S. Kikkawa<sup>1</sup>, Charles G. Wright<sup>1</sup>, Kumar N. Alagramam<sup>3</sup>

<sup>1</sup>UT Southwestern Medical Center Department of Otolaryngology-Head and Neck Surgery, <sup>2</sup>University of Texas at Dallas Callier Center, <sup>3</sup>Case Western Reserve University

The bundles of stereocilia that reside at the apex of cochlear hair cells are essential to mechanotransduction in the auditory system. Recent mouse genetic studies have provided new insights into development of the stereocilia bundle. Immuno-fluorescent studies have demonstrated that many of the proteins associated with the development of the stereocilia bundle localize to the apical portion of the hair cell in the region of the cuticular plate, suggesting structures in the apex of the cell play a role in stereocilia bundle formation. Most ultrastructural studies of abnormal hair cells affected by genetic defects have utilized scanning electron microscopy (SEM), which can clearly show bundle disorganization at the hair cell surface. However, by SEM, observations are limited to changes observable at the cell surface. Transmission electron microscopy (TEM) is appropriate for detailed study of intracellular morphology. However, the majority of TEM studies published on these types of mutants, to date, have relied on longitudinal sectioning of the hair cells, which provides limited information on the spatial relationship of stereocilia within the bundle or on other more 2-dimensional structures that are present early in development, such as the early cuticular plate. TEM cross- or tangential sections of the apex of the hair cell can demonstrate bundle disorganization similar to that seen by SEM while allowing for detailed study of intercellular structures, but few studies have demonstrated normal developmental hair cell architecture by this method. This study utilized the cross sectional TEM method on wild type and control mice to investigate normal development of the region of cuticular plate in outer hair cells at ages P0, P2, P5, & P10, with emphasis on development of the stereocilia rootlets; the cuticle of the cuticular plate and the

fonticulus; the basal body, or centrosome and associated structures; the mesh within the cuticular plate; and the cellular junctions near the apex of the cell. This work was supported in part by NIDCD grant DC05385 to Kumar Alagramam

### **872 Genetic Analysis of Myosin XVa and Whirlin Interaction**

**Mirna Mustapha-Chaib<sup>1</sup>**, Lisa A. Beyer<sup>1</sup>, David Dolan<sup>1</sup>, Yehoash Raphael<sup>1</sup>, Sally Camper<sup>1</sup>

<sup>1</sup>University of Michigan

*Myo15a* encodes an unconventional myosin that is mutated in shaker 2 (*sh2*) mice and causes congenital deafness, circling behavior and short stereocilia in auditory and vestibular hair cells. Whirler (*wi*) mice have a similar phenotype caused by inactivation of a PDZ domain of whirlin. Myosin-XVa transports whirlin to the stereocilia tips via its carboxy-terminal PDZ-ligand. Considering this interaction and the similar phenotype of mutant mice, we explored the potential for overlapping functions using a classical genetic approach. Two month old double heterozygotes, *wi/+*, *sh2/+*, have normal ABR and no evidence of circling behavior. Double mutants, *wi/wi*, *sh2/sh2*, are viable, circle, and are deaf. All cell types of the inner ear are present in double mutant mice examined by SEM and light microscopy. The apical surfaces of double mutant cochlear hair cells are similar to *sh2*: the stereocilia are extremely short, and microvilli persist. At P21 we observe persistence of the kinocilium in cochlear inner hair cells (IHC) of the single mutants and double mutants, suggesting that these genes are necessary for kinocilium regression or general cellular maturation. At P12 vestibular and cochlear IHC of *sh2* mice have a cytocaud: an actin-rich tail-like structure extending from the basal aspect of the cell. Similar cytocauds appear as early as P0 in *wi* mice, although fewer *wi* cells have cytocauds than cells in *sh2* mice or double mutants. Our data suggest that both *Myo15a* and *Whrn* are necessary for kinocilium regression, although *Whrn* is not required for microvilli to be resorbed. Further exploration of the pathologies that distinguish double mutants and *sh2/sh2* and *wi/wi* will reveal processes unique to each protein and enhance our understanding of their roles in maintenance of normal hair cell structure.

Supported by NOHR and NIDCD RO1-DC05401, RO1-DC05053, P30-DC05188.

### **873 Whirlin Complexes with P55 at the Stereocilia Tip During Hair Cell Development**

P. Mburu<sup>1</sup>, Y. Kikkawa<sup>2</sup>, Rosario Romero<sup>1</sup>, S. Townsend<sup>1</sup>, H. Yonekawa<sup>2</sup>, **Steve D.M. Brown<sup>1</sup>**

<sup>1</sup>MRC Mammalian Genetics Unit, Harwell, UK, <sup>2</sup>Tokyo Metropolitan Institute of Medical Science (Rinshoken), Tokyo, Japan

Actin cytoskeleton remodelling is fundamental to a variety of cellular processes including morphological alterations at the cell surface. Hearing in mammals is dependent upon the proper development of actin-filled stereocilia at the surface of hair cells in the inner ear. Recent work has established that whirlin, a PDZ protein, localises to the

stereocilia tips and by virtue of mutations in the whirlin gene has been shown to play an important role in stereocilia development. Myosin XVa interacts with whirlin and is responsible for localising whirlin at the stereocilia tip. We have previously demonstrated that whirlin shows an extraordinary expression pattern that traverses the stereocilia bundle during its development. We now show using yeast 2-hybrid screening, in vitro and in vivo pull-down assays that whirlin interacts with the MAGUK protein p55. p55 is known in erythrocytes to form a trimeric complex with protein 4.1R and the transmembrane protein glycophorin C promoting actin cytoskeleton assembly. We find that both p55 and protein 4.1R are expressed in both the developing stereocilia bundle and in the shorter microvilli-like stereocilia surrounding the graded stereocilia. In the whirler mutant, expression of p55 and protein 4.1R in hair cell stereocilia fades out prematurely from around P5. In the shaker2 (myosin XVA) mutant, expression of both p55 and 4.1R is completely abolished. We propose that whirlin forms a complex with p55 and protein 4.1R at the stereocilia tip that mediates actin polymerisation in response to some as yet unidentified external signal.

#### **[874] Staurosporine-Induced Collapse of Developing Mouse Cochlear Hair Bundles**

Richard J. Goodyear<sup>1</sup>, Mark E. Warchol<sup>2</sup>, Guy P. Richardson<sup>1</sup>

<sup>1</sup>University of Sussex, UK, <sup>2</sup>Washington University School of Medicine

Whilst there are good morphological descriptions of sensory hair bundle development, the molecular mechanisms that underlie this complex process are only beginning to be elucidated. To evaluate some of the biochemical pathways that control this process we have examined how inhibitors of a number of signalling systems affect the morphology of the developing hair bundle. Cochlear cultures were prepared from 1-2 day old mice and after 1 day in vitro were grown for 5-48 hours in medium containing the inhibitor to be tested or the appropriate solvent as a control. Cultures were then fixed, stained with rhodamine-conjugated phalloidin and examined by confocal microscopy. Inhibitors of PI-3' kinase, LY-294002 and wortmannin, had no effect on bundle morphology at the highest concentrations tested (20  $\mu$ M and 2  $\mu$ M respectively), nor did the Rho-associated protein kinase inhibitor Y27632 at a concentration of 5  $\mu$ M, when applied for 48 h. The broad-spectrum protein kinase inhibitor, staurosporine, had a dramatic and rapid effect on hair bundles within 10 h at concentrations as low as 1 nM, with basal-coil outer hair cells being the most severely affected. For outer hair cells, effects included collapse, fragmentation and distortion of the hair bundles, and with inner hair cells the appearance of very long individual stereocilia was also observed. Inhibitors of potential staurosporine targets - myosin light chain kinase (ML7, 0.6  $\mu$ M), calmodulin dependent protein kinase II (KN-93, 0.74  $\mu$ M), protein kinases A (H89, 0.1  $\mu$ M), C (bis-indolylmaleimide I, 0.02  $\mu$ M) and G (KT-5823, 0.5  $\mu$ M) had no effect when tested in isolation or as a cocktail. A peptide inhibitor of c-Jun N-terminal kinase (JNK inhibitor

I, 5  $\mu$ M) also has very rapid effect and causes the distortion and collapse of hair bundles within 5 h. A scrambled form of this peptide is without effect. These results reveal a role for protein phosphorylation in the maintenance of hair-bundle structure in the developing organ of Corti.

Supported by The Wellcome Trust and the NIDCD.

#### **[875] Morphogenesis and Afferent Innervation During Development of the Avian Otolith System**

David Huss<sup>1</sup>, J. David Dickman<sup>1</sup>

<sup>1</sup>Washington University

We are interested in understanding otolith system development and the factors that regulate motion detection. In the present study, we examined the formation of receptor cells, stereocilia organization, and afferent innervation during embryogenesis (E6 – E15) and post-hatch development (P0 – P42, adult) in Japanese quails. We found that at E6, E8 and E10 hair cell densities (SEM) in the striolar region were significantly higher than in extra-striolar regions in both the saccule and utricle. By P7, however, this difference had reversed, with the striolar hair cell density falling significantly below that of the extra-striolar regions. The role of apoptosis in these hair cell number dynamics is currently being examined. Stereocilia planar polarity was examined and quantified across the macular surface using SEM micrographs. Prior to E7, we found that polarizations were diffusely arranged and chaotic, however by E8, adult-like polarity patterns were firmly established in both the utricle and saccule. At these early time points, the majority of the newly forming hair cells showed the kinocilia at the lateral edge of the stereocilia bundle. In a small percentage of new hair cells the kinocilia appeared in the center or near the center of the stereocilia bundle. Clear differences in stereocilia bundle morphology between type I and type II hair cells were first noted at E12. Afferent innervation of the otolith maculae was examined using HRP neural tracing, along with class III B-tubulin, neurofilament 200kDa, and tenascin immunohistochemistry. Only bouton afferents innervated the macular epithelium, from E6 – E10. At E12, the first dimorph afferents were observed, with calyx afferents forming from E14 and continuing through post-hatch development. In the utricle, the band of type II hair cells located within the striolar region was first observed at E14.

Supported in part by funds from NIH DC003286 and NASA NNA04CC52G.

#### **[876] Identification and Analysis of the Otoconial Protein Complex Reveals a Common Mechanism of Bio-Crystal Formation**

Yesha (Yunxia) Lundberg<sup>1</sup>, Xing Zhao<sup>1</sup>, Xiaona Huang<sup>1</sup>, Hua Yang<sup>1</sup>

<sup>1</sup>Boys Town National Research Hospital

Otoconia are dense bio-crystals that overlie the sensory epithelium of the utricle and saccule, the gravity receptors in the vestibule, and provide inertial mass to generate shearing forces that is essential for the sensation of gravity and linear acceleration. Such sensation is necessary for

spatial orientation and balance. These crystals are composed of CaCO<sub>3</sub> and glycoproteins (otoconins), and the major otoconin, OC90, has been identified. However, the low abundant otoconins remained elusive due to difficulties in obtaining sufficient quantity. Lack of information on these otoconins has hindered our understanding of the regulation of otoconia formation. Here we report the identification of low-abundance otoconial proteins. Immuno-co-precipitation and Western blotting assays show that some of these proteins forming a strongly interacting complex. This surprising protein complex suggests that otoconia formation is more intriguing than previously thought, and provides first evidence for the mechanistic similarity between otoconia and bone calcification.

### **877 Assessing the Contributions of Several Vestibular Cell Types to Otoconia Formation**

*Withdrawn*

### **878 Spontaneous Discharge Patterns in Mammalian Cochlear Spiral Ganglion Cells Before the Onset of Hearing**

**Timothy Jones<sup>1</sup>**, Patricia A. Leake<sup>2</sup>, Russell L. Snyder<sup>2</sup>, Ben Bonham<sup>2</sup>, Olga Stakhovskaya<sup>2</sup>

<sup>1</sup>CSDI, East Carolina University, <sup>2</sup>Epstein Lab, O-HNS, Univ. Cal. San Francisco

Spontaneous neural discharges have been recorded in the auditory nerve of cats as early as 2 days postnatal (P2) (Walsh and Romand, 1992), yet the nerve does not respond to ambient sound levels below 100 dB SPL from about P0 to P10. During this period, refinement of the central projections from the spiral ganglion to the cochlear nucleus has been described (Leake et al, 2002; J. Comp Neurol 448). Sound-evoked ganglion cell activity likely does not influence this refinement, but it may be dependent on peripheral spontaneous discharge activity.

To better understand the nature of cochlear spontaneous activity during this period, we recorded from single spiral ganglion cells in kittens aged P3 to P9 (total age postconception, 69 to 74 days). The Spiral ganglion was accessed via the round window and scala tympani. A small fenestration was made in the spiral lamina over the ganglion to allow microelectrode penetration. A total of 77 ganglion cells were isolated for study in 8 animals. Spike rates were very low, ranging from 0.06 to 23 sp/s with a mean of 2.4 +/- 3.8 sp/s. In contrast to the stochastic spontaneous discharge patterns of mature animals, the ganglion cells in neonatal animals demonstrated remarkable irregular and regular spontaneous bursting discharge patterns. The unusual patterns were evident in the large mean coefficient of variation (CV = 3.8 +/- 2.9) and burst factor (BF = 6.4 +/- 4.3; Jones et al, 2001, J Neurosci 21) across ganglion cells.

The spontaneous bursting patterns in these neonatal mammals are similar to those reported for cochlear ganglion cells of the embryonic chicken suggesting this may be a general phenomenon common across species. Rhythmic discharge of retinal ganglion cells has been

shown to be important in the development of normal binocular vision (Shatz, 1996, Proc Natl Acad Sci 93). Bursting rhythms in cochlear ganglion cells may play a similar role in the auditory system during pre-hearing periods.

Research supported by the NIH NIDCD Grant R01 DC000160.

### **879 Molecular Characterization of Stria Vascularis Degeneration in the Developing Inner Ear of the German Waltzing Guinea Pig**

**Zhe Jin<sup>1,2</sup>**, Mats Ulfendahl<sup>1,2</sup>, Leif Järlebark<sup>1,2</sup>

<sup>1</sup>Center for Hearing & Communication Research and Dept. of Clinical Neuroscience, Karolinska Institute, <sup>2</sup>Dept of Otolaryngology, Karolinska University Hospital, Stockholm, Sweden

The German waltzing guinea pig is a new strain of animals with recessively inherited cochleo-vestibular impairment. Cochlear morphological analysis of homozygous animals (*gw/gw*) indicates that the primary defect is located in the stria vascularis, although the underlying genetic substrate is yet unknown. Various functional proteins, e.g. ion channels, pumps, and intercellular junctions, are indispensable for structural integrity and ion homeostasis in the stria vascularis. Several markers for cellular functions were utilized to characterize the progressive degeneration of the stria vascularis in the developing inner ear of the German waltzing guinea pig.

Cochleae from guinea pigs (*gw/gw* and *+/+*; embryonic days E30, 35, 40, 45, 50 and 60, postnatal days 0 and 60; *n* ≥ 2) were harvested. Total RNA from micro-dissected cochlear lateral wall tissue served as templates, and guinea pig gene-specific primers were designed for semi-quantitative RT-PCR. Antibodies against KCNQ1, SLC12A2, KCNJ10 and CLDN11 were used in immunohistochemical assays.

We observed: 1) a significant reduction of *Dct* and *Cldn11* and slightly decreased expression of *Kcnj10*, *Kcnq1*, *Atp1a1*, and *Atp1b2* mRNA in the cochlear lateral wall of *gw/gw* inner ear; 2) a loss of SLC12A2, KCNJ10 and CLDN11 protein expression in *gw/gw* stria marginal cells, intermediate cells and basal cells, respectively; and 3) a persistent expression of the KCNQ1 channel protein in *gw/gw* stria marginal cells from E35 until the adult stage.

We suggest that dysfunctional intermediate cells (melanocytes) are involved in the mechanism underlying the type of stria vascularis degeneration found in German waltzing guinea pigs.

### **880 Visuospatial Attention Modulates the Amplitude of the Auditory Nerve Compound Action Potential and Cochlear Microphonics**

**Paul H. Delano<sup>1,2</sup>**, Diego Elgueda<sup>1</sup>, Carlos M. Hamame<sup>1</sup>, Luis Robles<sup>1</sup>

<sup>1</sup>Programa de Fisiologia y Biofisica, ICBM, Facultad de Medicina, Universidad de Chile, <sup>2</sup>Centro de Neurociencias Integradas, CENI.

Although the anatomical relevance of the efferent auditory system is well known, its function is still controversial. We

have tested the hypothesis that attention modulates cochlear afferent activity by recording cochlear electrical responses in chinchillas trained to perform a visuospatial discrimination task. Chinchillas in an operant mesh cage were presented a neutral cue (central light) followed by one of two lateral lights (target) to be discriminated by pressing the corresponding lever (placed below the light). Simultaneously, irrelevant auditory stimuli (clicks and tones) were delivered at rates of 1-4 Hz and intensities between 50-70 dB SPL. To study cochlear microphonic (CM) potentials we used compound stimuli, in which a tone followed a click with 40 ms delay. After chinchillas reached criterion (>80 % accuracy), they were chronically implanted with a round-window electrode (100  $\mu$ m). Round-window potentials were recorded daily (100-200 trials), in five successfully implanted chinchillas, while they were performing the visuospatial discrimination task. In all chinchillas, we found a reduction in amplitude of the auditory-nerve compound action potential (CAP) during the presentation of the neutral-cue light. We found, in two chinchillas, an increase in the magnitude of CM concomitant with the CAP reduction, but never a CM reduction during the neutral-cue. In one chinchilla we demonstrated that the observed CAP reduction and CM augmentation were not due to head or pinna movements, by recording the stimulus SPL with a microphone connected to a steel tube implanted in the same bulla in which the round-window electrode was placed. Finally, we trained chinchillas in a modified two-choice task, in which the neutral cue was presented just in 70% of the trials while the other 30% had no neutral cue before the target lights. In this modified task the CAP reductions and CM increments were delayed in the trials without neutral cue, compared with the same effects in the trials preceded by the neutral cue. These results show for the first time in awake animals that visuospatial attention reduces CAP amplitudes and concomitantly increases CM potentials. Thus, auditory afferent information is modulated by attention even at the level of sensory transduction.

Supported by FONDECYT 1020970, Fundacion Puelma, PG42-2004 & CONICYT to PD & CH.

### **[881] Characterization of Electrically Evoked Olivocochlear Fast and Slow Effects in Mice**

**Stéphane F. Maison<sup>1</sup>**, M. Charles Liberman<sup>1</sup>

<sup>1</sup>*Dept Otol & Laryngol, Harvard Med School and Eaton-Peabody Lab, Mass Eye & Ear Infirmary, Boston MA*

Electrical stimulation of the olivocochlear bundle (OCB) in guinea pig can modulate cochlear neural responses on several time scales including a fast inhibition ( $\tau \sim 100$  ms), a slow inhibition ( $\tau \sim 10$  s) and an even slower enhancement [Sridhar et al., J Neurosci 15:3667-78, 1995]. One way to dissect the mechanisms for these effects is via mutant mice with deletion or overexpression of ligands or receptors implicated in OC neurotransmission. However, to interpret mutant data, OC effects in wildtype mice must be well described.

Here, we characterize electrically evoked OC effects in 2 inbred strains (CBA/CaJ and C57Bl/6J) and a variety of C57Bl/6-129 hybrids (wildtypes from 17 mutant lines). Effects were studied at 6-8 wks, by obtaining DPOAE

and/or CAP measures every 4-6 sec before, during and after a 70-sec shock-train to the OCB.

In all strains, fast suppression was greatest for stimuli near 16 kHz, reflecting the apical-basal gradient of OC terminals on OHCs. Fast effects scaled with cochlear sensitivity, as expected given their shared reliance on OHC function. Slow suppressive effects were less common than in guinea pig data. However, slow post-shocks enhancement (i.e. "overshoot") was more consistent and robust in mouse. The slow overshoot was maximal for frequencies above 22 kHz; its magnitude was not well correlated with fast effect magnitudes, suggesting different mechanisms.

A challenge in interpreting OC effects from mutants is OHC dysfunction, seen as elevation of baseline DPOAE thresholds. Here we suggest a normalization procedure based on the wildtype relation between threshold and OC fast effects. The effectiveness of this procedure is demonstrated in data from 7 lines with deletion of GABA(A) receptor subunits: several lines showed moderate threshold elevations and several showed OC-effect reductions. After normalization, only one line showed an effect of genotype on OC effects, and only that line showed loss of OC terminals.

Supported by NIDCD RO1 DC0188

### **[882] Selective Removal of Lateral Olivocochlear Efferents Causes Increased Vulnerability to Acute Acoustic Injury**

**Keith Darrow<sup>1</sup>**, M. Charles Liberman<sup>1</sup>, Stéphane F. Maison<sup>2</sup>

<sup>1</sup>*MIT - Harvard Medical School*, <sup>2</sup>*Harvard Medical School*

The mammalian olivocochlear (OC) system has medial (MOC) and lateral (LOC) components. MOC cholinergic effects on OHCs, including protection from permanent noise damage, have been documented. The unmyelinated LOC system contains numerous neurotransmitters: effects on auditory nerve (AN) response include long-term excitation and inhibition. Pharmacological studies suggest that an LOC dopaminergic component controls excitotoxic effects of acoustic injury on AN synaptic terminals.

Here, we probe LOC function in mice by selective unilateral removal of LOC cell bodies in the brainstem via stereotaxic delivery of a neurotoxin. ABR and DPOAE measurements are made at 2 and 4 wks post surgery. At 5 wks, mice are exposed to 94dB at 8-16 kHz for 15 minutes; ABR and DPOAE threshold shifts are assessed at 6 hrs and 1 wk post-exposure. The lesion success in removing the LOC and sparing the MOC system is assessed by histological analysis of brainstem sections and cochlear whole-mounts. Based on this, mice are classified as LOC Hit (20), LOC Miss (18), or Uninjected (2). MOC effects of the neurotoxin are further assayed by comparing the magnitude of shock-evoked MOC suppression of DPOAEs in the two ears.

LOC Hit cases show interaural asymmetries in suprathreshold ABR amplitudes, with no effect on DPOAE amplitudes, suggesting that the LOC modulates AN excitability. In LOC Hit mice, noise-induced ABR threshold shifts were significantly greater on the injected side, while DPOAE shifts were symmetrical. In LOC Miss mice, ABR



and DPOAE shifts were symmetrical. These findings provide strong evidence that the LOC system protects the cochlea from acoustic injury. The increased vulnerability seen in ABR and not DPOAE measures is consistent with the hypothesis that the LOC system controls glutamate excitotoxicity at AN terminals.

Research supported by T32 DC 00038, RO1 DC00188 and P30 DC005209.

### **883 Localization and Function of Dopamine Transporter in the Mammalian Cochlea**

Jérôme Ruel<sup>1</sup>, Guy Rebillard<sup>1</sup>, Daniëlle Dememes<sup>1</sup>, Serge Gobaille<sup>2</sup>, Jing Wang<sup>1</sup>, Jean-Luc Puel<sup>1</sup>

<sup>1</sup>Inserm U. 583, and Université Montpellier I, Montpellier, France, <sup>2</sup>Laboratoire de Microtechnique Neurochimique, Faculté de médecine Strasbourg, France

Dopamine, one of the neurotransmitters released by the lateral olivocochlear efferents, has been shown to exert a tonic inhibition of the spontaneous and sound-evoked activity of auditory nerve fibers. This permanent inhibition probably requires the presence of an efficient transporter to remove dopamine from the synaptic cleft. Here we report that the dopamine transporter is localized within the lateral efferent fibers both below the inner hair cells and in the inner spiral bundle. Perilymphatic perfusions of dopamine transporter inhibitors, nimofensine and N-[1-(2-benzo[b]thiophenyl)cyclohexyl]piperidine into the cochlea caused a dose-dependent reduction of the spontaneous neural noise and the sound-evoked compound action potential of the auditory nerve, leading to a complete abolishment of both neural responses. Consistent with a selective action of dopamine transporter inhibitors on the auditory nerve activity, no significant change was observed neither on cochlear responses generated by sensory hair cells (cochlear microphonic, summing potential, distortion products otoacoustic emissions), nor on the endocochlear potential reflecting the functional state of the stria vascularis. Finally, HPLC measurements demonstrate that nomifensine-induced inhibition of auditory nerve responses was due to an increase of the extracellular dopamine level in the cochlea. Altogether, these results show that dopamine transporter is essential for the maintenance of spontaneous activity of auditory nerve neurons and their responsiveness to sound stimulation.

### **884 Onset and Adaptation of Distortion Product Otoacoustic Emissions in the Northern Leopard Frog, *Rana Phipps Phipps***

Sebastiaan Meenderink<sup>1</sup>, Peter M. Narins<sup>1</sup>

<sup>1</sup>Dept. of Physiological Science, University of California, Los Angeles

The frog inner ear consists of two anatomically-distinct papillae that are sensitive to airborne sound. These two papillae exhibit a number of physiological and anatomical differences, one being the presence/absence of efferent synapses. While anatomical studies have shown that the amphibian papilla (AP) is innervated by efferent nerve fibers, no such innervation has been found in the basilar papilla (BP). In mammals, distortion product otoacoustic emissions (DPOAEs) adapt after the onset of the two

primary tones. This is attributed to a primary-tone induced feedback from the brain to the cochlea via the efferent system. Given the apparent exclusive presence of efferent terminals in the frog AP, only DPOAEs elicited from this papilla are expected to show adaptation, while BP-DPOAEs are not expected to exhibit significant adaptation after the onset of the two primary tones.

Here, we present the time course of DPOAEs recorded from both the AP and the BP of the Northern leopard frog, *Rana pipiens pipiens*. We found a difference in the adaptation of DPOAEs from the two auditory papillae. Following the onset of the two primaries, AP-DPOAEs showed a systematic change (either an increase or a decrease) in their amplitudes before stabilizing at a constant level after approximately 500 ms. In contrast, the BP-DPOAEs reached a constant level almost immediately after primary onset. These results are in agreement with the idea that in the frog ear only the AP, and not the BP, is innervated by the efferent system. To our knowledge, these data provide the first physiological evidence for this disparity between the two papillae. As such, studying the onset of DPOAEs provides a tool that allows non-invasive investigation of the efferent system in the vertebrate ear.

### **885 Functional Role of the CRHR1 in the Mouse Inner Ear**

Christine Graham<sup>1</sup>, M. Charles Liberman<sup>2,3</sup>, Douglas Vetter<sup>1</sup>

<sup>1</sup>Tufts Univ. School of Medicine, <sup>2</sup>Mass. Eye and Ear Infirmary, <sup>3</sup>Eaton Peabody Labs

A corticotropin-releasing hormone (CRH)-related system is expressed in the inner ear of mammals, and includes both ligand (urocortin) and receptors (CRH-R1 and CRH-R2) (Vetter et al., 2002). Our previous results have shown that mice lacking urocortin show accelerated hearing loss with age and defects in outer hair cells. This neuroendocrine system may therefore protect the cochlea from noise-induced trauma given the stress-related role of the CRH system in other tissues. The goal of this project is to determine the functional significance of expression of one of the receptors of this system, CRH-R1. Mice lacking CRH-R1 exhibit hearing thresholds that are elevated approximately 20dB across all frequencies tested, but apparently normal iso-response distortion product amplitudes, indicating defects in inner, but not outer hair cell function. CRH-R1 could mediate its effects on hearing by activating signaling cascades that will modify phosphorylation states of neurotransmitter receptors and/or ion channels on hair cells and thus modify the function of these receptors. Additionally, given that CRH-R1 activity may regulate gene expression via these cascades, these signaling pathways may play a role in development of the inner ear. Western blotting experiments demonstrate that CRH-R1 null mice show enhanced phosphorylation of CREB (a known activator of transcription) and enhanced expression of CAMKinase IV compared to wild-type mice. Furthermore, morphological experiments demonstrate an efferent hyper-innervation of both inner and outer hair cells and ectopic positioning of terminals surrounding the inner spiral bundle. The present evidence thus suggests that the abnormal hearing thresholds observed in CRH-R1 null mice result from both

developmental defects and differential regulation of second messenger signaling cascades. The evidence confirms the importance of this neuroendocrine pathway for auditory function. *Supported by DC6258 (DEV)*

### **886 Functional Role of the CRHR2 in the Mouse Inner Ear**

**Johnvesly Basappa**<sup>1</sup>, M. Charles Liberman<sup>2,3</sup>, Douglas Vetter<sup>1</sup>

<sup>1</sup>Tufts Univ. School of Medicine, <sup>2</sup>Mass. Eye and Ear Infirmary, <sup>3</sup>Eaton Peabody Labs

A corticotropin-releasing hormone (CRH) system is expressed in the cochlea (Vetter et al., 2002) that, given its stress-related role in other tissues, may protect the cochlea from noise-induced trauma. Our goal is to determine the functional significance of expression of one of the receptors of this system, CRH-R2, and examine the biochemical responses of CRH-R2 null allele mice to sound.

The role of CRH-R2 in inner ear development and function was analyzed with standard immunostaining and ABR and DP protocols. Additionally, its role in modulating the activity states of various biochemical signaling pathways was evaluated by comparing cochlear lysates isolated from CRH-R2 null allele and littermate wildtype mice. Mice were raised in continuous exposure to moderate level noise and cochlear lysates immediately generated, or allowed to recover for 24 hrs. from such stimulation prior to lysate isolation. Preliminary immunostaining data indicate that mice lacking CRH-R2 exhibit a loss of efferent innervation in apical and high middle turn regions of the cochlea. The null mice exhibit normal hearing thresholds as assessed by ABR, but high iso-response distortion products. Since CRH-R2 is a G-protein coupled receptor, it may mediate its effects in the cochlea by activating signaling cascades that modify phosphorylation states, and thereby function, of neurotransmitter receptors and/or ion channels. Immuno-blotting for phospho-CREB, CaMKIV, and Akt/PKB (among others) were compared in wildtype and null allele mice under noisy or quiet conditions. pCREB was 70% up regulated in KO mice under quiet conditions and 78% down regulated in KOs under noisy conditions compared to wildtype mice exposed to similar sound conditions. CaMKIV was 36% up regulated in KOs in quiet conditions and 77% down regulated in KOs under noisy conditions. The Akt isoform 1 was 56% down regulated in KOs under quiet conditions, and 69% down regulated in KOs under noisy conditions.

Supported by DC6258 (DV)

### **887 Ultrastructural Study of the Neural Network Underneath Outer Hair Cells**

**Fabio A. Thiers**<sup>1,2</sup>, Barbara Burgess<sup>2</sup>, M. Charles Liberman<sup>1,2</sup>, Joseph B. Nadol, Jr.<sup>1,2</sup>

<sup>1</sup>Harvard-MIT Division of Health Sciences and Technology, Cambridge, MA, <sup>2</sup>Dept. of Otolaryngology, Harvard Med. School, and Eaton-Peabody Lab., Mass. Eye & Ear Infirmary.

Outer hair cells (OHCs) are innervated by type-II spiral ganglion neurons and olivocochlear (OC) efferent neurons.

Ultrastructural studies suggest these neurons form a complex neural network: type-II neurons interconnect neighboring OHCs through reciprocal synapses (with membrane specializations suggesting bidirectional signaling); OC neurons participate through axodendritic synapses on type-II neurons, as well as axosomatic synapses on OHCs. The present study provides an ultrastructural description of the connectivity patterns of individual type-II neurons.

Outer spiral bundles beneath 12 OHCs (2nd & 3rd rows) from the 500 Hz region of a normal adult cat were studied via electron microscopy of serial sections including reconstruction of all terminals and their parent fibers. Type-II & OC terminals (and parent fibers) were distinguished by size, vesicle content and neurofilament/tubule content. For either terminal type, synaptic complexes were classified as afferent, efferent or reciprocal according to the position and number of associated vesicles and the presence or absence of a sub-synaptic cistern.

Type II fibers gave rise to terminals (n=121) with different types of synapses on OHCs: reciprocal (88%), afferent (9%), or efferent (3%). Individual type-II fibers gave rise to a mixture of terminal types: two gave rise to an efferent terminal on one OHC and reciprocal terminals on others; one formed an afferent terminal on one OHC and a reciprocal on another. In 12 cases (6 in each row), type-II fibers gave rise to multiple reciprocal terminals on 2-4 of the six studied neighboring OHCs.

The sensory field of individual type II fibers is much larger than our limited area of study. Thus, extrapolating from present findings suggest that these neurons form an elaborate neural network which could modulate OHC state over extended cochlear regions.

Research Supported by NIDCD RO1; DC00188; National Organization for Hearing Research; Hugh Hampton Young Memorial Fellowship; and Amelia Peabody Foundation.

### **888 Expression Patterns of Metabotropic Glutamate Receptors and Associated Proteins in the Mouse Cochlea**

**Brian Manning**<sup>1,2</sup>, William F. Sewell<sup>1,2</sup>

<sup>1</sup>Massachusetts Eye and Ear Infirmary - Eaton-Peabody Laboratory, <sup>2</sup>Harvard Medical School - Program in Neuroscience

Expression Patterns of Metabotropic Glutamate Receptors and Associated Proteins in the Mouse Cochlea

Transmission of auditory signals from the hair cell to the spiral ganglion neuron relies predominately on ion-channel-linked glutamate receptors, though pharmacologic and molecular evidence also suggests the presence of G-protein-linked glutamate receptors (metabotropic, mGluR). We have examined the expression of mGluR proteins using a combination of SDS-PAGE/Western blotting and immunohistochemistry/confocal microscopy to detect possible expression pattern variability within the organ of Corti along the length of the cochlea. Western blotting successfully detected Group I mGluR1 and mGluR5 and Group II mGluR2/3 metabotropic glutamate receptors within cochlear homogenates, but did not detect Group III

mGluR6/7. mGluR1 was present immunohistochemically within both inner and outer hair cells, a subset of spiral ganglion neurons, and in modiolar nerve terminals, which were found in higher numbers in the basal turns of the cochlea. mGluR1 expression exhibited a basal to apical intensity gradient in the inner hair cells, whereas expression in the outer hair cells diminished from base to apex. In contrast, mGluR5 and mGluR2/3 expression demonstrated no marked gradient along the length of the cochlea, and labeling was comparable in pillar and modiolar nerve terminals. Within the spiral ganglion neurons, we also detected co-expression and co-localization of mGluR1 with Homer proteins that link the membrane-bound mGluR to intracellular calcium stores, and IP<sub>3</sub> receptors. mGluR1, Homer, and IP<sub>3</sub>R co-localization was also identified in nerve fibers and terminals within the organ of Corti. The presence of mGluR in modiolar nerve terminals and a subset of spiral ganglion neurons suggests that these receptors might function in afferent transmission at the high threshold, low spontaneous rate fibers. mGluR expression in the hair cells themselves suggests a possible autoreceptor role for these proteins, similar to that already described in frog vestibular organs.

**[889] Immunohistochemical Localization of Adrenergic Receptors in the Rat Organ of Corti**  
**Khalid M. Khan**<sup>1,2</sup>, Marian J. Drescher<sup>2</sup>, James S. Hatfield<sup>3</sup>, Dennis G. Drescher<sup>2,4</sup>

<sup>1</sup>*Department of Biological and Biomedical Sciences, Aga Khan University, Karachi, Pakistan,* <sup>2</sup>*Department of Otolaryngology, Wayne State University School of Medicine, Detroit, MI, USA,* <sup>3</sup>*Electron Microscopy Laboratory, Veterans Affairs Medical Center, Detroit, MI, USA,* <sup>4</sup>*Department of Biochemistry and Molecular Biology, Wayne State University School of Medicine*

We previously reported the existence of nerve fibers in the organ of Corti (OC) containing dopamine  $\beta$ -hydroxylase, an adrenergic marker (ARO Abstr. 28: 226, 2005), and the presence in the OC of norepinephrine itself (ARO Abstr. 26: 12, 2003). However, the identity and localization of adrenergic receptors (ARs) in the cochlea are uncertain. In the current study, we present the immunolocalization of  $\alpha$ 1,  $\beta$ 1, and  $\beta$ 2 AR subtypes in the cochlea of the adult ACI Black Agouti rat. For the  $\alpha$ 1 AR subtype, immunoreactivity was detected overlapping apical and basal sites of the inner hair cells (IHCs) in the basal turn, but no immunoreactivity was detected in relation to the IHCs in the middle and apical turns. Immunoreactivity was observed in close association with the outer hair cells (OHCs) in middle and apical turns, occasionally overlapping Deiters' cells. For the  $\beta$ 1 AR subtype, immunoreactivity was detected in close association with the IHCs in all turns. The immunoreactivity was also present in presumed nerve fibers at the base of the OHCs, overlapping Deiters' cells, but the OHCs themselves appeared devoid of immunoreactivity. Immunoreactivity for the  $\beta$ 2 AR subtype was strongly associated with IHCs. Immunoreactivity was detected around the basal poles of the OHCs in the middle and apical turns, possibly associated with nerve fibers, and in the region of Deiters'

cells in all three turns. Within the spiral ganglion, type I afferent cell bodies were immunoreactive for  $\alpha$ 1 and  $\beta$ 1 ARs, whereas a subpopulation of the cell bodies was immunoreactive for the  $\beta$ 2 AR. To our knowledge, this is the first report localizing  $\alpha$ 1 and  $\beta$ 2 AR immunoreactivity in the OC. The possible roles for ARs in the auditory periphery may be the modulation of afferent neural activity, control of OHC contractility, monitoring of intracellular Ca<sup>2+</sup>, and K<sup>+</sup> transport.

Supported by NIH RO1 grants DC000156, DC004076, and the Aga Khan University.

**[890] Localization of Beta 2 Adrenergic Receptors in the Gerbil Inner Ear**

**Claudius Fauser**<sup>1</sup>, Andrea Lohner<sup>1</sup>

<sup>1</sup>*Klinikum rechts der Isar, Technical University Munich*

The inner ear appears to be influenced by sympathetic stimulation via beta adrenergic receptors. In a previous study we demonstrated that functional beta 1 adrenergic receptors are located in various cells of the inner ear (Fauser et al., J.Membr.Biol. 201, 25-32, 2004). The purpose of the present study was to localize beta 2 adrenergic receptors ( $\beta$ <sub>2</sub> AR) in inner ear tissues. Therefore, immuno-histochemical-staining and RT-PCR were performed.

Paraffin sections were prepared from decalcified, formalin perfusion-fixed gerbil temporal bones.  $\beta$ <sub>2</sub> AR were detected by a polyclonal anti- $\beta$ <sub>2</sub> AR-antibody and visualized with biotinylated secondary antibody. RT-PCR for  $\beta$ <sub>2</sub> AR was performed on four microdissected fragments of the inner ear (modiolus including the organ of Corti, stria vascularis, non-strial lateral wall, and vestibular labyrinth).

Light microscopy examination revealed prominent and consistent immunostaining for  $\beta$ <sub>2</sub> AR in type I and II spiral ganglion cells, the organ of Corti, stria vascularis, and parts of the non-strial lateral wall, as well as sensory cells of utricle and ampullas. RT-PCR demonstrated the presence of  $\beta$ <sub>2</sub> AR RNA in all four inner ear fractions (modiolus, stria vascularis, non-strial lateral wall, and vestibular labyrinth).

Our findings are in accordance with previous studies that demonstrated functional  $\beta$ <sub>2</sub> AR in the vestibular labyrinth, where they stimulate the Cl<sup>-</sup> secretion, and in the nonstrial lateral wall, where its function is still unknown.

Our data demonstrate that  $\beta$ <sub>2</sub> AR are localized in sensory and non-sensory cells of the cochlea and the vestibular organ. Functional studies on the influence of  $\beta$ AR in the inner ear will follow.

Supported by KKF 8758168

**[891] Critical Role of Thiamine Transporter THTR1 in Auditory Function and Hair Cell Survival**

Simone Bertram<sup>1</sup>, Silvi Hoidis<sup>1</sup>, Jean W.T. Smolders<sup>1</sup>, Bruce Gelb<sup>2</sup>, Kimihiko Oishi<sup>2</sup>, **Marcus Mueller**<sup>1</sup>

<sup>1</sup>*University Frankfurt, Physiology II, Germany,* <sup>2</sup>*Department of Pediatrics and Human Genetics, Mount Sinai School of Medicine, New York, USA*

Thiamine (vitamin B1) is an important cofactor of enzymes essential for energy production including pyruvate

dehydrogenase, transketolase and  $\alpha$ -ketoglutarate dehydrogenase. Thiamine is transported into cells via thiamine transporters, THTR1 and THTR2, which are encoded by SLC19A2 and SLC19A3, respectively. A mouse model of thiamine-responsive megaloblastic anemia syndrome, which lacks Slc19a2 showed sensorineural hearing loss when they were on a thiamine-deficient diet. We investigated the effects of thiamine deficiency on peripheral auditory function using heterozygous and homozygous Slc19a2 knockout mice. Auditory-evoked brainstem response (ABR) thresholds to different acoustic stimuli ranging from 2 to 45 kHz were measured over several weeks. ABR thresholds of both Slc19a2<sup>-/-</sup> and Slc19a2<sup>+/-</sup> mice were normal when they were maintained on a normal diet. In Slc19a2<sup>-/-</sup> mice a low-thiamine diet resulted in a small increase of ABR threshold within three days and eventually in a total hearing loss after four weeks. Slc19a2<sup>+/-</sup> mice, in contrast, exhibited an increase of ABR threshold only in the high frequency range when placed on a low-thiamine diet within a week, without further deterioration. The hearing loss observed in the Slc19a2<sup>-/-</sup> and Slc19a2<sup>+/-</sup> mice was not reversible although they were re-fed with normal diet after 4 weeks of low-thiamine diet. Immunohistological analyses of cochlea were performed using DAPI, phalloidin and myosin 6 stainings at several time points during the treatment. In the homozygous animals, a complete loss of inner hair cells (IHC) was found, while only partial loss of outer hair cells (OHC) was observed. In the heterozygotes, IHC were preserved and OHC loss was occasionally noted at the cochlear apex. These results suggest the importance of thiamine and/or THTR1 for the function and survival of the hair cells. Sensitivity to thiamine deficiency in different types of hair cells may vary.

## **[892] Expression of Caveolin-1 in the Vestibulocochlear System of Mice**

**Masaaki Teranishi<sup>1</sup>**, Daniel Labbe<sup>2</sup>, Olaf Michel<sup>2</sup>, Wilhelm Bloch<sup>3</sup>, Tsutomu Nakashima<sup>1</sup>

<sup>1</sup>Department of Otorhinolaryngology, Nagoya University, Graduate School of Medicine, Japan, <sup>2</sup>Department of Otorhinolaryngology, University of Cologne, Germany, <sup>3</sup>Department of Anatomy, University of Cologne, Germany

**Introduction:** Caveolin is an intrinsic membrane protein with a molecular weight of approximately 25 kDa and it is involved in signal transduction mechanisms, including protein phosphorylation by protein kinases and G-protein-mediated signal transduction. Three types of the protein, caveolin-1, caveolin-2 and caveolin-3 have been identified and caveolin-1 is abundantly expressed in many tissues. The purpose of the present study is to investigate the expression of caveolin-1 in the vestibulocochlear system of mice.

**Materials/methods:** Seven 7-week-old C57BL/6 mice were used as experimental animals. Auditory brain stem responses (ABR) were measured to evaluate auditory function. The cochleae were fixed in 4% paraformaldehyde overnight after cardiac perfusion, decalcified in 10% EDTA and embedded in paraffin. Mid-modiolar sections were incubated with a primary antibody to caveolin-1 (mouse

monoclonal, Transduction Laboratories). A biotinylated secondary antibody was used for accentuation. Processing was ultimately performed by an HRP-streptavidin complex and nickel-enhanced DAB, with subsequent observation under a light microscope. **Results/conclusions:** All of the mice used in the present study showed normal hearing by ABR recordings. Immunohistochemical investigations revealed that caveolin-1 was expressed mainly in the neuroepithelium of macula and crista ampullaris and vestibular ganglion cells in the vestibule and in supporting cells of the organ of Corti, spiral ganglion cells and cells in the spiral ligament in the cochlea. These results suggest that caveolin-1 may be associated with signal transduction mechanisms in the vestibulocochlear system of mice.

## **[893] Expression and Localization of Chondromodulin-I in the Rat Cochlea**

**Kalpesh Vakharia<sup>1</sup>**, Omar Akil<sup>1</sup>, Lawrence Lustig<sup>1</sup>

<sup>1</sup>Department of Otolaryngology - Head and Neck Surgery, University of California, San Francisco

**Purpose:** Chondromodulin-I is a cartilage specific matrix protein that has been found to be a potent inhibitor of angiogenesis, a suppressor of T cell responses and of synovial cell proliferation and a promoter of proteoglycan synthesis and growth of chondrocytes. Its expression has been identified in rat articular cartilage and eyes, in the mouse thymus, in developing chick hearts and eyes, and in human intervertebral discs and tumors such as salivary pleomorphic adenomas and chondrosarcomas. To our knowledge, chondromodulin-I has not been reported in the mammalian cochlea.

**Methods:** Reverse transcription polymerase chain reaction (RT-PCR) and immunohistochemistry was used to examine the expression and localization of chondromodulin-I in the rat cochlea.

**Results:** RT-PCR analysis of the cochlea of 3-4 week old Sprague-Dawley rats revealed chondromodulin-I mRNA expression. Immunohistochemistry analysis of 3-4 week old rat cochleas revealed selective staining. Chondromodulin-I immunostaining was found to be greatest in the tectorial membrane as well in the spiral ganglion and supporting cells of the inner and outer hair cells.

**Conclusion:** This report documents the expression and localization of chondromodulin-I in cochlea of a rat. Further studies need to be completed in order to elucidate the function of this protein within the inner ear.

## **[894] Neural Refractoriness and Synchronization Determine the Reliability of Chick Cochlear Nerve Responses to Constant Pure Tones**

**Michael Avissar<sup>1</sup>**, Adam C. Furman<sup>2</sup>, James C. Saunders<sup>2</sup>, Thomas D. Parsons<sup>3</sup>

<sup>1</sup>Department of Neuroscience, University of Pennsylvania,

<sup>2</sup>Department of Otorhinolaryngology - Head and Neck Surgery, University of Pennsylvania, <sup>3</sup>Department of Clinical Studies - NBC, University of Pennsylvania

The chick cochlear nerve transmits information about acoustic stimuli with trains of all-or-none action potentials

(spikes). The response of a single cochlear neuron to repeated identical stimuli varies from trial-to-trial and limits the ability to transmit information. Characterizing this variability and understanding its source promises insights into both cellular mechanisms that generate the neural response and the ability of the nerve to encode acoustic stimuli.

We measured the response of single cochlear neurons in chicks responding to repeated identical 40 ms pure tones at their characteristic frequency (CF) and quantified the variability in spike patterns as the entropy of patterns (PE). PE progressively increased with higher CF across the frequencies studied (0.1 – 4 kHz). Variability in spike patterns can manifest as either fluctuations in spike count or timing. We measured the entropy of spike counts (CE) and interspike intervals (IE) to better understand the contribution of spike count and timing on response reliability. Both CE and IE were greatest at high CF's but IE showed a minimum at 350 – 450 Hz.

To better understand sources of variability, we modeled the response of each cochlear neuron as a stochastic point process in which the probability of spike occurrence at each time point depended only on the phase of the acoustic waveform at that time and the time elapsed since the last spike. Probability distributions were determined from the response of the real neuron. We found that this model fully mimicked the variability of spike counts, intervals, and patterns measured in real responses. Thus, we conclude that the process that generates variability can be sufficiently described as a combination of neural refractoriness and synchronization to the stimulus. Future studies are aimed at understanding the relative contribution of these two processes in producing this reliability.

### **[895] Estimating the Summed Post-Stimulus Time Histogram and Single Unit Action Potential from Human Compound Action Potentials**

**Jeffery Lichtenhan<sup>1</sup>, Mark Chertoff<sup>1</sup>**

<sup>1</sup>*University of Kansas Medical Center*

The convolution of a gamma function representing the post-stimulus time histogram [P(t)] with a decaying sine wave representing a single-unit action potential [U(t)] has been used to obtain an analytic expression of the compound action potential (CAP; Chertoff, JASA 116(5), 2004). Fitting the analytic CAP to physiologic CAPs recorded from the round window of normal hearing gerbils provided an estimate of the in vivo P(t) and U(t). We subsequently demonstrated that the analytic expression fit favorably to CAPs evoked from gerbils with permanent noise-induced hearing loss and could be used to characterize changes in P(t) and U(t) (Lichtenhan et al., ARO Abstracts, 2005). Here we provide a translational investigation from previous animal experiments to human application by characterizing attributes of P(t) and U(t) from normal human ears. The continuing objective of this research is to develop a clinical measure of anatomic and pathophysiologic consequences of cochlear damage.

Sound stimuli were clicks ranging in 10-dB increments from 125 to 95 dB pSPL, and 8kHz tone bursts ranging

from 105 to 95 dB pSPL. CAPs were recorded with a custom built electrode placed on the tympanic membrane (TM). Stimulus level and spectrum were monitored by attaching a microphone probe tube along side the TM electrode, with the probe tip resting approximately 8mm from the TM. CAPs were fit with the analytic expression using optimization software by TOMLAB. Changes in P(t) and U(t) were analyzed as a function of signal level.

The width and delay of P(t) varied inversely with stimulus level, while the height of P(t) increased with signal level. This indicates that the location and number of neurons contributing to the CAP changes with signal level. U(t) showed a decrease in decay at low signal levels, and an increase in decay at high stimulus levels. The frequency of U(t) oscillation, which is typically around 1 kHz, decreased at low and high signal levels. This suggests that the mechanism of action potential generation perhaps varies along the cochlear partition.

Supported by NIH Grant 2 RO1 DC02117

### **[896] Frequency Tuning in the Human Cochlea Is Not Exceptionally Sharp**

**Mario Ruggero<sup>1</sup>, Andrei Temchin<sup>1</sup>**

<sup>1</sup>*Northwestern University*

The responses to sound of auditory-nerve fibers are well known in many animals but are topics of conjecture for humans. Some investigators concluded that the auditory-nerve fibers of humans are more sharply tuned than those of various experimental animals [Shera, C. A., Guinan, J. J. & Oxenham, A. J. (2002) Proc. Natl. Acad. Sci. USA 99, 3318-3323; Harrison, R. V., Aran, J. M. & Erre, J. P. (1981) J. Acoust. Soc. Am. 69, 1374-1385] but others disputed that conclusion [Shofner, W. P., Sparks, K., Wu, Y. E. & Pham, E. (2005) ARLO - Acoustics Research Letters Online 6, 35-40]. Here we invalidate claims of much sharper cochlear frequency tuning in humans than in other species. Firstly, we show that forward-masking psychophysical tuning curves, which were used as the principal support for such claims [Shera et al., op. cit.], greatly overestimate the sharpness of cochlear tuning in experimental animals and, hence, also probably in humans. Secondly, we calibrate compound action potential tuning curves against the tuning of auditory-nerve fibers in experimental animals and use compound action potential tuning curves recorded in humans to show that the sharpness of tuning in human cochleae is not exceptional and that it is actually similar to tuning in all mammals and birds for which comparisons are possible.

Work supported by NIH Grant DC-00419.

### **[897] Spectral and Temporal Properties of the Auditory Nerve in Old-World Monkeys**

**Philip X. Joris<sup>1</sup>, Cherie L. Ramirez<sup>1</sup>, Myles Mc Laughlin<sup>1</sup>, Marcel van der Heijden<sup>1</sup>**

<sup>1</sup>*Lab. of Auditory Neurophysiology, K.U.Leuven, Leuven, Belgium*

Behavioral data suggest that spectral and temporal properties differ between humans and commonly used laboratory animals. Frequency selectivity seems sharper in

humans, while binaural data suggest that the upper frequency limit of phase-locking to pure tones is lower in humans than in cat. Monkeys are increasingly used as an experimental model in auditory physiology and can provide more insight into human functioning, but there is very little information on their peripheral physiology, especially in old-world monkeys.

We obtained responses of single neurons of the auditory nerve to pure tones, amplitude-modulated tones, broadband noise, and tonal non-harmonic complexes (zweis stimulus of van der Heijden & Joris, J. Neurosci. 2003 23:9194-9198) in barbiturate-anesthetized macaque monkeys, and compared their spectral and temporal properties to the auditory nerve of the cat.

The main results are as follows: 1) the range of spontaneous rates (SR) is comparable to the cat but its distribution is not bimodal, 2) the synchronization limits are very similar to those in the cat, both in the strength and the highest frequency extent of phase-locking, but there is a clearer relationship between SR and phase-locking in the monkey, 3) although there is much overlap, tonal tuning curves show sharper tuning in the monkey compared to the cat, resulting in higher Q10 and Q40 values, particularly so in the region of sharpest tuning around 10 kHz. "Low-frequency tails" were not observed in the monkey.

Supported by the Fund for Scientific Research – Flanders (G.0083.02 and G.0392.05), and Research Fund K.U.Leuven (OT/01/42 and OT/05/57).

#### **[898] Disruption of Lateral Olivocochlear Neurons Depresses Spontaneous Auditory Nerve Activity**

**Colleen Le Prell<sup>1</sup>**, David Dolan<sup>1</sup>, Karin Halsey<sup>1</sup>, Larry F. Hughes<sup>2</sup>, Sanford Bledsoe<sup>1</sup>

<sup>1</sup>University of Michigan, <sup>2</sup>Southern Illinois University

The neurons from the lateral olivocochlear (LOC) system project from the auditory brainstem to the cochlea, where they synapse on radial dendrites of auditory nerve fibers. Our understanding of the functional role of this pathway has been limited by the fact that it is difficult to selectively stimulate or disrupt this system. The chemical richness of the LOC neurons further complicates systematic manipulation. We recently developed two novel approaches to this problem, both resulting in the demonstration that LOC disruption depresses sound-evoked auditory nerve activity (Le Prell et al 2003, JARO, 4: 276-290; Le Prell et al 2005, JARO, 6: 48-62). Here, we report that selective LOC disruption also depresses spontaneous auditory nerve activity. Ensemble activity, estimated using round window noise, was depressed after LOC disruption. Recordings from single auditory nerve fibers revealed the population of auditory neurons was characterized by a smaller proportion of neurons with the highest spontaneous rates of firing, and an increase in the proportion of neurons with lower spontaneous firing rates. The shift in the distribution of spontaneous rates was statistically reliable. A decrease in neurons with the highest spontaneous rates, and thus the lowest thresholds, is consistent with the small elevations in threshold reported by us after selective LOC disruption, and by others who

have recorded from auditory neurons after disrupting the entire olivocochlear innervation. Although intact LOC neurons contain both excitatory and inhibitory transmitter substances, the extent to which individual transmitters are released tonically or in response to sound is not known. The observation of depressed auditory nerve spontaneous activity after LOC disruption could be produced by disrupting a tonic release of excitatory transmitter substances from the LOC terminals.

Supported by NIH-NIDCD P01-DC00078 (S. Bledsoe, D. Dolan), R01-DC004194 (D. Dolan), R03-DC007342 (C. Le Prell), and P30-DC05188.

#### **[899] Role of Glutamate Transporters in Glutamate-Induced Hearing Loss in the Mouse**

**Zhiqiang Chen<sup>1</sup>**, Sharon G. Kujawa<sup>1</sup>, William F. Sewell<sup>1</sup>

<sup>1</sup>Eaton Peabody Laboratory, Massachusetts Eye and Ear Infirmary, Harvard Medical School

In the cochlea, afferent transmission between inner hair cells and auditory neurons is mediated by glutamate receptors. Excess glutamate at the synapse, however, can interfere with transmission and induce excitotoxic auditory neuron damage. Glutamate transporters located near the synapse are thought to be important in maintaining low synaptic levels of glutamate. We investigated the roles of three different subtypes of glutamate transporters (GLT1, GLAST and EAAC1) on glutamate-induced hearing loss using intracochlear drug delivery in the mouse. Auditory nerve compound action potentials (CAPs) and outer hair cell-based distortion product otoacoustic emissions (DPOAEs) were stable with infusion of the control solution and vehicle for the drugs, artificial perilymph at 1  $\mu$ l/hr for 80 min. Infusion of glutamate (10  $\mu$ M; 210 min) alone produced ~5 dB CAP threshold shifts. Threo-beta-benzyloxyaspartate (TBOA) (200  $\mu$ M; 200 min), a broad spectrum transporter inhibitor, had little effect when infused alone, but produced 20-30 dB CAP threshold shifts across high frequencies when infused with 10  $\mu$ M glutamate. L-serine-O-sulfate (SOS), which preferentially inhibits GLAST and EAAC1, had little effect on its own (100  $\mu$ M, 180 min) but led to 10-20 dB CAP threshold shifts when infused in combination (100  $\mu$ M; 110 min) with 10  $\mu$ M glutamate. Dihydrokainate (1 mM; 90 min), a selective inhibitor of GLT1, was without effect on hearing when infused alone or in combination with 10  $\mu$ M glutamate. In all cases, DPOAEs were stable, suggesting the drugs did not act at outer hair cells. These results suggest that glutamate transporters, GLAST and/or EAAC1, but not GLT1, play an important role in the removal of glutamate at the synapse as indicated by the ability of their inhibitors to exacerbate glutamate-induced hearing loss.

#### **[900] Neurotrophic Regulation of Glutamate Receptor Subunit Distribution in Spiral Ganglion Neurons**

**Jacqueline Flores-Otero<sup>1</sup>**, Robin L. Davis<sup>2</sup>

<sup>1</sup>Rutgers University and UMDNJ, <sup>2</sup>Rutgers University

Postnatal spiral ganglion neurons *in vitro* display distinct electrophysiological firing patterns and voltage-gated ion

channel distributions that vary with cochlear location (Adamson et al., JCN, 2002). We have extended these findings by determining whether the frequency-dependent electrophysiological features of spiral ganglion neurons include their neurotransmitter receptors and whether the distribution of these neurotransmitter receptors can be regulated by neurotrophins.

We first investigated the distribution of antibodies against GluR2/3 and NR1 receptor subunits in apical and basal neuron cultures. Quantitative analysis of 6 separate experiments showed that anti-GluR2/3 antibody labeling intensity was significantly greater in basal spiral ganglion neurons ( $35.9 \pm 3.8$ ;  $N=169$ ) compared to apical neurons ( $19.0 \pm 1.5$ ;  $N=227$ ;  $P<0.01$ ). In contrast to this, anti-NR1 antibody labeling was significantly enriched in apical neurons ( $25.8 \pm 1.6$ ,  $N=955$ ) compared to basal neurons ( $21.8 \pm 1.8$ ;  $N=713$ ;  $P<0.05$ ), evaluated in 10 separate experiments.

The opposite distribution patterns observed for AMPA and NMDA receptor subunits suggested that they may be under differential regulatory control. We tested this hypothesis by examining the effects of neurotrophins on neurotransmitter receptor distribution. We found that brain-derived neurotrophic factor (BDNF) application significantly enhanced GluR2/3 antibody luminance in apical neurons ( $26.2 \pm 2.3$ ;  $N=354$ ;  $P<0.01$ ) but had little effect ( $38.0 \pm 2.7$ ;  $N=399$ ) on the already elevated level of GluR2/3 in basal neurons.

In conclusion, our results suggest that the AMPA glutamate receptors, which are enriched in the high frequency spiral ganglion neurons, may be specifically enhanced by exposure to BDNF. Additional experiments are currently underway to evaluate glutamate receptor distribution patterns after exposure to neurotrophin-3. Supported by NIH RO1 DC01856 (RLD) and Gates Millennium Scholarship (JFO).

### **[901] Rapid Regulation of Surface AMPA Receptor Expression in the Auditory Spiral Ganglion Neuron by Glutamate-Receptor Agonists**

**Zhiqiang Chen<sup>1</sup>**, William F. Sewell<sup>1</sup>

<sup>1</sup>*Harvard/MEEI*

Fast neurotransmission between inner hair cells and auditory neurons in the mammalian cochlea is mediated primarily by AMPA-type glutamate receptors. Work in the hippocampus suggests that synaptic strength can be regulated dynamically by movement of AMPA receptors in and out of the postsynaptic membrane following activation of NMDA and AMPA receptors. We have characterized this process in cultured spiral ganglion neurons by quantifying surface GluR2 receptor after immunolabeling the external portion of the receptor. Under basal conditions, ~75% of total GluR2 is present on the surface of auditory neuron. Incubation of neurons for 10 min with glutamate, NMDA, or AMPA, produced a decrease of 50-60% of surface GluR2 receptors. The surface GluR2 level began to recover partially at 20 min following stimulation and returned to basal levels at 1 h. AMPA application did not change the amount of total GluR2 receptor, while NMDA decreased total GluR2 by around 25%, implying

differential sorting of internalized AMPA receptor following NMDA and AMPA stimulation. APV, an NMDA receptor antagonist, inhibited NMDA- but not AMPA-induced surface GluR2 removal. Conversely, the AMPA receptor inhibitor, DNQX, specifically prevented AMPA-, but not NMDA-induced surface receptor removal. Neither glutamate, NMDA nor AMPA induced any change in surface GluR2 expression when incubated without calcium in the medium. AMPA- and NMDA-induced removal of surface GluR2 was blocked ~45% by the L-type calcium channel blocker, nifedipine, and ~60% by the N-type calcium channel blocker, omega conotoxin MVIIA. Combining the two calcium channel blockers inhibited ~80% of surface GluR2 removal. The robust dynamic regulation of surface AMPA receptor expression in auditory neurons implies a significant role for this process in regulating synaptic strength in auditory function, and suggests a role for the enigmatic NMDA receptors in auditory neurons.

### **[902] The Role of Ca<sup>2+</sup>-Activated K<sup>+</sup> Channel $\alpha$ and $\beta$ Subunits in Murine Spiral Ganglion Neuron Firing Patterns**

**Wei Chun Chen<sup>1</sup>**, Robin L. Davis<sup>1</sup>

<sup>1</sup>*Rutgers University*

Previous work has shown that the large conductance Ca<sup>2+</sup>-activated K<sup>+</sup> (BK) channels are important regulators of firing patterns in murine spiral ganglia. By contributing to the action potential afterhyperpolarization, these channel types are capable of exerting a powerful impact on firing rate and accommodation. We have found with immunocytochemistry that the apparent BK subunit density is differentially distributed such that neurons innervating the basal cochlea had significantly higher staining levels compared to those innervating the apical regions (Adamson et al., JCN, 2002). In order to characterize further the role of this channel type we have taken a multifaceted approach to define its interaction with  $\beta$  subunits, its expression pattern compared to other Ca<sup>2+</sup>-activated channel types, and its subcellular distribution.

Systematic gene expression profiling is currently underway to evaluate the expression patterns of the BK and BK $\beta$  subunits (BK $\beta$ 1-4), in addition to the small (SK1-3) and intermediate (IK1) conductance Ca<sup>2+</sup>-activated K<sup>+</sup> channels. Microarray and real-time quantitative RT-PCR showed that the BK and BK $\beta$ 4 subunits had the highest expression, with BK $\beta$ 2, SK2, and SK3 subunits also present but at lower levels. Immunocytochemical analysis of the highly expressed BK $\beta$ 4 subunit showed that the anti-BK $\beta$ 4 antibody luminance was similar in apical and basal neurons, and that it was specifically enriched in the cell soma and initial segments of the neurons. This regional specialization suggests that the BK $\beta$ 4 subunit may be particularly important for action potential conduction through the cell soma. Future studies will determine whether the BK and BK $\beta$ 4 subunits are co-localized, and ultimately we will examine the electrophysiological properties of BK channels in the spiral ganglion with single-channel patch clamp recordings. Supported by NIH R01 DC01856.



**903 Dendritic Voltage-Gated Ion Channels Shape Postsynaptic Potentials at the Inner Hair Cell Afferent Synapse**

Eunyoung Yi<sup>1</sup>, Elisabeth Glowatzki<sup>1</sup>

<sup>1</sup>Johns Hopkins University School of Medicine

Neurons in the auditory pathway are specialized in rapid and reliable signaling. Here we identify voltage-gated ion channels in afferent dendrites at the inner hair cell (IHC) afferent synapse and investigate their role in shaping postsynaptic activity.

Whole cell patch clamp recordings were done on IHC afferent dendrites in excised apical turns of the 7-12 day-old rat cochleae. First, we investigated outward K<sup>+</sup> currents that activated as low as -70 mV in voltage step protocols. These currents were completely blocked by 4 mM 4-aminopyridine (4-AP, n=6). 4-AP reversibly slowed down EPSP decay time constant by  $22 \pm 7\%$  while 10-90% rise time and EPSP amplitudes were not significantly changed (n=6). 4-AP had no effect on the EPSC waveform (n=3) suggesting that 4-AP did not affect the release machinery nor AMPA receptor kinetics *per se*. These results suggest that low-threshold activating K<sup>+</sup> channels play a significant role in shaping the EPSP waveform in afferent dendrites.

Secondly, we investigated a slowly activating inward current that activated during prolonged hyperpolarizing voltage steps to -90 or more negative. At voltage steps from -84 to -124 mV, this current was blocked ~60% by 2 mM CsCl and only ~20% by 2mM BaCl<sub>2</sub>. It was irreversibly blocked by ZD7288, a selective blocker for hyperpolarization-activated cyclic nucleotide-gated cation (HCN) channels (50  $\mu$ M, n=5). We are now investigating the effects of cAMP on HCN channels and EPSPs in afferent dendrites.

Supported by NICDC DC006476

**904 From Apex to Base: How Endogenous Neuronal Membrane Properties Are Distributed in the Spiral Ganglion**

Qing Liu<sup>1</sup>, Robin L. Davis<sup>1</sup>

<sup>1</sup>Dept. of Cell Biology and Neuroscience, Rutgers University, NJ

We have shown previously that electrophysiological features of postnatal spiral ganglion neurons differ between the apex and base of the cochlea (Adamson et al., *JCN*, 2002). To determine whether this represents a systematic gradient, we developed a novel preparation in which the entire ganglion is cultured as an explant, thus preserving the relative location of all surviving spiral ganglion neurons *in vitro*.

Interestingly, we found that some electrophysiological features were graded, whereas others were distributed non-monotonically along the cochlea. The most robust graded property was action potential latency at threshold. This parameter was brief in basal spiral ganglion neurons ( $10.7 \pm 0.7$  ms n=29), intermediate in middle neurons ( $11.6 \pm 0.8$  ms n=22), and prolonged in apical neurons ( $13.2 \pm 0.9$  ms n=28). This same general pattern was also observed for accommodation. In contrast, we found that threshold and inward rectification differed between middle

( $-49.3 \pm 0.7$  mV and  $64.6 \pm 2.0$  mV, respectively) and base ( $-43.4 \pm 1.0$  mV and  $57.5 \pm 1.5$  mV; respectively;  $P < 0.01$ ) but not between middle and apex ( $-49.0 \pm 0.7$  mV and  $66.9 \pm 1.5$  mV). The hyperpolarization-activated cationic channel (I<sub>h</sub>) responsible for the hyperpolarizing sag most likely contributes to threshold as evidenced by our finding that neurons with the greatest amount of inward rectification had the lowest thresholds.

In conclusion, our data suggest that timing-related parameters of spiral ganglion electrophysiology are graded along the tonotopic axis of the cochlea, whereas parameters related to threshold vary non-monotonically, with the lowest thresholds and highest inward rectification located in mid- and apical regions. The location-dependence, therefore, does not appear to reflect a simple gradient but instead may represent at least two levels of organization potentially related to coding of sound frequency and intensity.

**Supported by NIH R01 DC01856.**

**905 Patterned Electrical Stimulation Leads to CREB Phosphorylation in Neonatal Rat Spiral Ganglion Neurons *In Vitro***

Damon Fairfield<sup>1</sup>, Marlan Hansen<sup>1</sup>, Steven H. Green<sup>1</sup>

<sup>1</sup>Depts. of Biological Sciences and Otolaryngology, University of Iowa, Iowa City, IA, USA

Chronic depolarization of spiral ganglion neurons (SGNs) *in vitro* with elevated (25 mM) extracellular K<sup>+</sup> (25K), promotes SGN survival via multiple Ca<sup>2+</sup>-dependent signaling systems including activation of the transcription factor CREB by CaMKIV phosphorylation on Ser133. The ability of physiological neural activity, which occurs as patterned bursts of depolarization at various frequencies, to activate these intracellular signaling pathways and promote survival is unknown. We therefore assessed *in vitro* model systems for studying effects of more typically physiological patterns of electrical stimulation (ES) on SGN survival and intracellular signaling. Dissociated postnatal day 4-6 rat SGNs were cultured such that they could be exposed to electrical fields. Configurations included culture directly on conductive substrates, Au or indium tin oxide, or placing Pt wires in the culture well. CREB phosphorylated on Ser133 (pCREB) can be detected by immunofluorescence (IF) and was used as a reporter for SGN response to ES. SGNs were initially cultured in NT3 and BDNF (2 nM each) for 48 h. The medium was then replaced with control medium lacking trophic factors and, after 6 h, exposed to 45 min ES or 25K. Maximal pCREB IF was detected in SGNs cultured on a laminin-coated Au substrate with 2 msec biphasic pulses at 100 pulses/sec. ES at amplitudes of 100 mV or 500 mV, but not 20 mV, increased pCREB IF, although were less effective than 25K. Using this system, we are examining the ability of patterned ES at frequencies characteristic of physiological activity or of cochlear implants to promote SGN survival and modulate neurite outgrowth *in vitro*. This research was supported by NIDCD grants F32 DC007270 (DAF), K08 DC006211 (MRH) and R01 DC002961 (SHG).

## **906 Interaction of Spiral Ganglion Neurites with Cochlear Implant Settings**

**Thomas Stark<sup>1</sup>**, Stefan Hansen<sup>1</sup>, Andre Gurr<sup>1</sup>, Holger Sudhoff<sup>1</sup>, Stefan Dazert<sup>1</sup>, Dominik Brors<sup>1</sup>

<sup>1</sup>*Department of Otolaryngology Bochum, Germany*

The cochlear implant (CI), a major advance in the treatment of deafness, involves the introduction of alloplastic materials into the cochlea. The interaction between the host cells and the alloplastic material is essential for the adaptation and function of the new system. In cochlear and brainstem implants, a close contact between auditory neurons and the platinum electrodes embedded into a silicone array is desirable to optimize the function of the hearing devices. If, for example, the dendrites of surviving SG neurons could be stimulated to grow very close to the electrodes of a CI in a highly ordered manner, and contact between neurites and electrodes maintained, it might be possible to create hundreds of information channels.

To study the growth of auditory neurons on electrode settings, cochlear neurons of postnatal day 4 rats were cultured on platinum for 3 days and the resulting neurite growth was compared to control explants. On platinum, the average number of neurites extending from the spiral ganglion (SG) explants was significantly lower than in the control group. However, the length of the neurites was significantly higher in the explant group cultured on platinum (509µm) than in the control group (359µm). Additionally, rat SG explants were cultured together with a CI electrode array (MED EL, Innsbruck, Austria) in the same culture well for 96 hours. The explants were positioned at about 200 - 600 µm to the electrode and neurite extension was stimulated with NT-3 (10 ng/ml). The outgrowth patterns of the neurites towards the electrode and on its surface were studied under light and scanning electron microscopy. The outgrowing neurites readily approached the electrode and made contact with the CI materials. The neurites partially terminated, branched or turned at the electrode border. In some cases, neurites climbed the electrode and extended on the silicone surface.

These findings indicate that mammalian SG neurons can interact with and extend neurites on silicone materials used in CI electrode array manufacturing. Stimulation of SG neurite outgrowth to the perilymphatic space, e.g. by growth factor application via the electrode, might therefore result in a closer interaction of the neurites with the electrode array, leading to improved efficacy of cochlear implant systems.

## **907 Time Course of Glia-Like Cell Activation and Neurotrophic Factor Upregulation in a Gerbil Model of Auditory Neuropathy**

**Hainan Lang<sup>1</sup>**, Richard A. Schmiedt<sup>2</sup>, Ling Wei<sup>1</sup>, Nancy Smythe<sup>2</sup>, Samuel S. Spicer<sup>1</sup>, Liya Liu<sup>1</sup>, Bradley A. Schulte<sup>1,2</sup>

<sup>1</sup>*Department of Pathology and Laboratory Medicine, Medical University of South Carolina,* <sup>2</sup>*Department of Otolaryngology – Head & Neck Surgery, Medical University of South Carolina*

Transplantation of stem cells (SCs) into the injured inner ear offers a potential strategy for repairing or replacing

cells and restoring hearing. Application of ouabain to the round window niche of the gerbil cochlea results in the death of most spiral ganglion neurons and provides an excellent animal model for SC transplantation studies. A better understanding of the microenvironment of the injured auditory nerve following ouabain ototoxicity is important for optimizing transplant strategies in this model. Basic fibroblast growth factor (FGF2) plays an important role in regulating the proliferation, differentiation and survival of a wide variety of central and peripheral neurons. Expression of FGF2 is strongly upregulated after neuronal injury, with glial cells as the predominant source. In this study, degenerative changes in auditory nerve and immunohistochemical expression patterns of FGF2 were examined at 1 and 4 days, and 1, 2 and 4 weeks after ouabain treatment. At 4 days and 1 week after treatment, numerous elongated, spindled cells lacking myelin pigments, interpreted as glia-like cells, presented in the osseous spiral lamina, Rosenthal's canal and the modiolus. Two weeks after treatment, empty appearing vacuoles filled the cytoplasm of the glia-like cells. Between 2 and 4 weeks after treatment, a significant loss of the glia-like cells was seen in the osseous spiral lamina, but not in the modiolus. FGF2 immunoreactivity was present in the auditory neurons and glial cells in control ears. The intensity of immunolabeling for FGF2 in the glia cells in the modiolus decreased from control values at 1 day, increased above control values at 1 week, was strongest at 2 weeks, then decreased below control values again at 4 weeks after ouabain treatment. These data suggest that the period between 4 days and 2 weeks after trauma provides an optimal window for transplant survival.

Supported by R01AG14748, R01DC00713, R01NS45155 and R01NS045810.

## **908 Stem Cells for Auditory Nerve Replacement**

**Jeannie Hernandez<sup>1</sup>**, Noel Wys<sup>1</sup>, Diane Prieskorn<sup>1</sup>, Matt Velkey<sup>1</sup>, K. Sue O'Shea<sup>1</sup>, Josef Miller<sup>1</sup>, Richard Altschuler<sup>1</sup>

<sup>1</sup>*University of Michigan*

While interventions that can successfully and significantly enhance auditory nerve (spiral ganglion neuron – SGN) survival and regrowth following profound deafness are being developed, there remains a significant patient population in which these interventions would be too little, too late. This patient population presents a compelling target for stem cell research, since the primary treatment for deafness, cochlear prostheses, depends on remaining auditory nerve for its function. Studies from our lab and others have shown mouse embryonic stem cells (mESCs) will survive and differentiate following placement in the guinea pig cochlea, but without growth factor support the majority do not reach neuronal phenotypes and survival decreases over time. We are assessing if differentiation into a neuronal phenotype typical of SGN is improved by factors which mimic influences that guide SGN differentiation during normal development. Current studies examined the influence of transient induction of Neurogenin 1 (Ngn1), a proneural gene associated with early SGN differentiation induction and signaling molecules such as glial cell line derived neurotrophic factor (GDNF) implicated in SGN development, to affect

differentiation and survival. Studies used mESCs with Ngn1 under control of a doxycycline (dox)-inducible promoter. We find that transient expression of Ngn1 in vitro results in upregulation of downstream targets such as Brn3a that are also implicated in normal SGN development. Two weeks following placement in scala tympani with intrascler application of dox and GDNF as well as systemic cyclosporin, many stem cells differentiate into mature neurons based on expression of neuronal tubulin, TuJ1. In addition these cells have other characteristics of the SGN phenotype including vesicular glutamate transporter immunolabeling (glutamatergic) and immunolabeling for the calcium binding protein calretinin.

Supported by NIH / NIDCD grant DC03820 and core center grant P30 DC-05188

## **[909] Regeneration of the Human and Guinea Pig Auditory Nerve**

**Helge Rask-Andersen**<sup>1</sup>, Marja Boström<sup>1</sup>, Malin Anderson<sup>1</sup>, Kristian Pfaller<sup>2</sup>, Rudolf Glueckert<sup>3</sup>, Annelies Schrott-Fischer<sup>3</sup>

<sup>1</sup>Dept of Otorhinolaryngology, Uppsala University Hospital,

<sup>2</sup>Departments of Histology, Molecular Cell Biology and Otolaryngology, Medical University of Innsbruck, <sup>3</sup>Dept of otolaryngology, Innsbruck University Hospital

**Introduction:** It has been shown that neural stem cells (NSC) located at various sites of the CNS are able to proliferate in vitro and form neurospheres [Reynolds and Weiss, 1992]. A technique was developed to culture human spiral ganglion (hSG) cells obtained during petroclival meningioma surgery [Tylstedt et al., 1997]. Recently we reported, using in vitro-studies of the adult mammalian cochlea including man, that neural progenitors may exist that undergo proliferation and differentiation into mature elongating neurons [Rask-Andersen et al., 2005]. These results suggest that also selective areas of the adult PNS have the potential to undergo self-renewal and regeneration.

**Material and Methods:** Adult human and guinea pig SG cells were enzymatically treated and seeded on uncoated dishes. Spheres were expanded with EGF and bFGF and differentiated on fibronectin/collagen or poly-L-ornithine coated dishes with neurotrophic factors NT-3, BDNF and GDNF. BrdU was used as proliferate marker. Dissociated SG cells were also directly cultured on coated dishes together with neurotrophins. Nerve and neurite regeneration, [§ganglionization], GC morphology and plasticity were analysed in vitro using TLVM, immunocytochemistry and high resolution FE-SEM.

**Results and Conclusions:** This study indicates that the adult human inner ear contains neural progenitor cells, suggesting that the auditory nerve to a certain extent may undergo self-renewal and repair during life. Neurospheres showed expression of nestin and incorporation of 5<sub>i</sub>-Bromo-2-deoxyuridine (BrdU) and differentiated into cells expressing both GFAP/S-100 and f $\beta$ -tubulin, indicating multipotency. Differentiating neurons were immunopositive for both tyrosine kinase receptor B (Trk B) and C (Trk C) suggesting that they were inner ear specific. Human neuroblasts underwent cell division and formed mature f $\beta$ -tubulin positive neurites as verified with TLVM.

Auditory growth cone (GCs) steering was also analysed using high resolution SEM. This information may help to induce regeneration of the auditory dendrite and form future implant devices for electrical stimulation in the deaf.

## **[910] Effects of Cytokines and BMP4 on Neuronal Survival and Morphology in Cultures of Dissociated Newborn Mouse Spiral Ganglion**

**Donna S. Whitlon**<sup>1,2</sup>, May T. Coulson<sup>1</sup>, Tokoya Williams<sup>1</sup>, Mary Grover<sup>1</sup>

<sup>1</sup>Feinberg School of Medicine, Northwestern University,

<sup>2</sup>Institute for Neuroscience, Northwestern University

The mechanisms underlying the development, regeneration and maintenance of bipolar morphology of spiral ganglion neurons has not been well-studied. We recently developed a dissociated culture system that permits survival and analysis of a sizable fraction (20-30%) of the overall population of neurons in the newborn mouse spiral ganglion. The standard media includes BDNF, NT3 and 10% fetal bovine serum. Using this culture system, we examined the additional effects of cytokines leukemia inhibitory factor (LIF), oncostatin M (hOSM), ciliary neurotrophic factor (CNTF), interleukin 6 (IL6) or the bone morphogenic protein, BMP4, on neuronal survival and morphology. The number of neurons plated at 4 hours (approximately 30% of the total population of spiral ganglion neurons) was similar in all conditions. Without extra additions to the medium, 30% of the plated neurons died over the next 38 hours. The addition of BMP4 or any cytokine, except IL6, preserved 100% survival of the plated neurons. The increased survival by cytokines was due to a specific increase in the number of bipolar neurons, with little effect on the number of monopolar neurons. The increased survival by BMP4 was due to an increase in monopolar neurons and those with no processes, with little effect on the number of bipolar neurons. There was no change in the numbers of monopolar or bipolar neurons in the presence of IL6. These results suggest that a) cytokines, while preferentially preserving bipolar neurons, do not induce additional new neurites from monopolar neurons; b) cytokines act through the LIF-GP130 receptor, which is common to all tested cytokines except IL6; and c) BMP4, like cytokines, increases neuronal survival but does not reproduce the cytokine effect on bipolar morphology. (Supported by NIH grant #DC00653).

## **[911] Quantitative Analysis of Auditory Nerve Fibers and Synaptic Density on Hair Cells in Normal Canary and a Canary with Hereditary Hearing Loss**

**Brenda M. Ryals**<sup>1</sup>, Elena Sanovich<sup>2</sup>, Ron S. Petralia<sup>3</sup>, Nathan Havasy<sup>1</sup>, Robert J. Dooling<sup>2</sup>

<sup>1</sup>James Madison University, <sup>2</sup>University of Maryland,

<sup>3</sup>NIDCD, NIH, Rockville, MD

Belgian Waterslager canaries (BWS) have a severe, hereditary high frequency hearing loss accompanied by significant hair cell loss and stereocilia abnormalities but relatively insignificant changes in the total number of fibers in the auditory nerve (Gleich et al 2001). Studies in our

laboratories over the past several years have been aimed at determining the structure/function relationship between these anatomical characteristics and the ability of BWS to hear both simple and complex acoustic stimuli. We have shown that absolute hearing sensitivity is reduced in BWS but that some aspects of complex perception may actually be enhanced (Lauer and Dooling ARO 2004). In order to elucidate at least one potential underlying structural influence on hearing in BWS we are currently analyzing the neural consequences of this hereditary hearing loss in adult BWS canaries.

Quantitative TEM analysis of the synaptic density beneath hair cells in the distal, most abnormal appearing portion of the BWS basilar papilla (BP), reveals a slightly lower proportion of hair cells contacted by afferent terminals (60% in BWS and 79% in non-BWS) but a generally similar number of synapses per hair cell in both strains (Ryals et al ARO 2005). The purpose of the present study was to 1) determine the distribution of neural fibers below the habenula in the basal, middle and distal portions of the BWS and non-BWS and 2) determine synaptic density on hair cells at the basal and middle positions of the BWS and non-BWS BP.

Preliminary results indicate that the neural fiber distribution below the habenula in BWS canaries is similar to non-BWS at the base and middle of the BP but may be substantially reduced at the distal end of the BP. Preliminary analysis of TEM sections in the middle, 50% position, of the BP reveal fewer hair cells in BWS than in non-BWS. Nevertheless, the hair cells remaining do receive synaptic contact by both efferent and afferent fibers. These results continue our appreciation of the neural consequences of the hereditary inner ear abnormality in BWS and non-BWS BP and provide a first step toward understanding the potential mechanisms which may underlie auditory capacity in BWS.

(Supported by NIDCD R01DC001372 to RJD and BMR; RSP supported by NIH/NIDCD intramural program)

## **912 The Degree of Forward Masking Increases with Age in Gerbils**

Otto Gleich<sup>1</sup>, Ingo Hamann<sup>1</sup>, Malte C. Kittel<sup>1</sup>, Juegen-Theodor Fraenzer<sup>1</sup>, Georg M. Klump<sup>2</sup>, Jürgen Strutz<sup>1</sup>

<sup>1</sup>ENT-Department, University of Regensburg,

<sup>2</sup>Zoophysiology & Verhalten, University Oldenburg

Thresholds for a short signal following a preceding masker are elevated. This phenomenon is termed forward masking and has been studied in some detail for human subjects. Elevated forward-masking thresholds will degrade the comprehension of speech especially in a noisy environment. Here we characterize forward masking in gerbils and determined the effect of age. Detection threshold for a 20 ms probe tone at 2.85 kHz was first determined in quiet to evaluate a potential age dependent hearing loss. Then masked threshold was determined for the probe that was presented 2.5 ms following a 2.85 kHz masker with 400 ms duration and a level of 40 dB SPL. Presently we have both thresholds for a total of 20 gerbils varying in age between 4.9 and 46.7 months. Thresholds for the 20 ms probe in quiet exceeded 20 dB SPL only for 3 of the older gerbils while the 17 remaining animals with

thresholds below 20 dB SPL can be considered as evidence for normal hearing. A linear regression analysis for the 17 normal hearing animals demonstrates a significant effect of age on threshold in quiet ( $p < 0.038$ ), however, the slope of this function is quite shallow (0.18 dB hearing loss per month). Masked thresholds of these gerbils show a much more pronounced age dependent increase ( $p < 0.001$ ) with a slope of the regression line that is almost 0.6 dB per month, three times the value observed in the unmasked condition. A group comparison of data from 6 young animals in which both thresholds were collected before they reached 18 months of age, with those of 6 old animals that were older than 30 months revealed mean thresholds in quiet of 10.1 dB SPL (young) and 16.5 dB SPL (old) while masked thresholds were 32.3 dB SPL (young) and 49.6 dB SPL (old). Masked thresholds were increased by 22.2 dB for the young and 33.1 dB for the old gerbils. These data show that the forward masking paradigm efficiently detects auditory processing deficits in old gerbils with normal hearing in quiet.

We thank S. Kopetschek and C. Woegerbauer for animal care and help with the behavioral experiments. Supported by the DFG Str275/4-5.

## **913 Declines of Glutamate-Related Gene Expression in CBA Mouse Inferior Colliculus with Age**

Sherif F. Tadros<sup>1,2</sup>, Nicole Waxmonsky<sup>1,2</sup>, Mary D'Souza<sup>1,2</sup>, Xiaoxia Zhu<sup>1,2</sup>, Martha Lynch-Erhardt<sup>1,2</sup>, Robert D. Frisina<sup>1,2</sup>

<sup>1</sup>Univ. Rochester Med. Sch., <sup>2</sup>Int. Ctr. Hearing Speech Res.

The inferior colliculus (IC) is a prominent brainstem auditory processing center, and glutamate (Glu) is a primary excitatory neurotransmitter. This study investigates expression changes of glutamate-related genes with age in mouse IC, and examines their relation with degree of age-related hearing loss. CBA mice were divided, according to age, auditory brainstem responses (ABRs) and distortion product otoacoustic emissions (DPOAEs), into 4 groups: young adult (N=7), middle-aged (N=17), old-aged mild presbycusis (N=9) and old-aged severe presbycusis (N=5). Inferior colliculus cDNA was prepared from each mouse's IC RNA and analyzed using the Affymetrix<sup>TM</sup> *mus musculus* M430A GeneChipR (1 array/mouse). GeneTraffic RMA analysis and one-way analysis of variance were used to analyze the GeneChip results for 68 glutamate-related genes in the 4 subject groups. Significant differences in either signal log ratio or fold change (1.5 fold change or more) were found between mouse groups for 9 genes. These include solute carriers (transporters) *Slc1a2* (GLT1) and *Slc1a3* (GLAST) (family 1), *Slc17a6* (family 17); ionotropic glutamate receptors *Grik3* (kainate 3), *Grin3b* (NMDA3B), *Gria3* (AMPA3), *Grid2* (delta2); *pycs* (pyrroline-5-carboxylate synthetase) and *Mglap* (matrix gamma-carboxyglutamate protein). All genes expression showed down regulation with age except *Slc1a3* gene. The correlation between the gene expression data and the auditory phenotypes of mice (ABR thresholds and DPOAE amplitudes) were examined using linear regression analysis. Some significant

correlations were found for *Slc1a2*, *Grik3* and *pycs* gene expression. Currently, the GeneChip gene expression results are being validated by real-time PCR. The age-related *down-regulation* of glutamate transporters may play a role in glutamate excitotoxicity of age-related hearing loss (presbycusis), and contribute to the brainstem auditory processing problems previously reported in studies of the neural bases of presbycusis.

*Supported by NIH: NIA & NIDCD.*

#### **914 Age-Related Changes in the Rat Cochlear Lateral Wall**

**Steven K. Juhn<sup>1</sup>**, Ji-Eun Lee<sup>1</sup>, Min-Kyo Jung<sup>1,2</sup>, Vladimir Tsuprun<sup>1</sup>, Patricia A. Schachern<sup>1</sup>, George L. Adams<sup>1</sup>

<sup>1</sup>*Department of Otolaryngology, University of Minnesota Medical School, Minneapolis, Minnesota, U.S.A.,*

<sup>2</sup>*Department of Otolaryngology-HNS, College of Medicine, The Catholic University of Korea*

The blood labyrinth barrier (BLB) contributes to the maintenance of the specialized milieu of the inner ear by ensuring ion homeostasis by preventing the entry of unwanted substances from the systemic circulation into the inner ear fluids (Juhn et al, 2001). The proposed site of the BLB is the lateral wall of the cochlea, including the stria vascularis and spiral ligament. The spiral ligament plays an important role in potassium ion recycling. Furthermore, previous studies in C57BL/6 mice (Hequembourg and Liberman, 2001) and gerbils (Spicer et al, 1997) have implicated degeneration of the spiral ligament as an important factor in age-related hearing loss. In the present study, we evaluated age-related histopathological changes in the rat lateral wall. Three-month-old Fisher 344/Brown Norway Hybrid rats and twenty-four-month-old Fisher 344/Brown Norway Hybrid rats were used. Auditory brain stem response (ABR) from old rats showed an elevation of thresholds in all frequencies compared to the young animals. Hematoxylin and eosin staining showed age-related degeneration of spiral ligaments and TUNEL staining showed apoptotic cell death in spiral ligaments of aged rats. In addition, immunostaining for connexin 26, a protein involved in the formation of gap junctions, was also reduced in this region of aged rats. Electron microscopy showed age-related thickening of lamina densa in capillaries in spiral ligaments. Our results suggest that the cochlear lateral wall may be one of the regions responsible for age-related hearing loss.

(Supported by Minnesota Medical Foundation and Lions Research Foundation)

#### **915 Age-Related Changes on the Morphology of the Otoconia**

**Yoon Seok Jang<sup>1</sup>**, Chan-Ho Hwang<sup>1</sup>, Ji Young Shin<sup>1</sup>, Woo Yong Bae<sup>1</sup>, Jae Ryong Kim<sup>1</sup>, Yang Sun Cho<sup>2</sup>, Lee Suk Kim<sup>1</sup>

<sup>1</sup>*Dong-A University College of Medicine, <sup>2</sup>Sungyunkwan University School of Medicine*

Although there are numerous reports on otoconial morphology using field-emission scanning electron microscopy (FESEM), there are few reports regarding the changes of otoconial morphology according to aging *in*

*vivo*. We investigated age-related changes in otoconial morphology using FESEM in three groups of rats: young (1 week old), middle-aged (6 months old), and aged (23 months old). There was great size variation in utricular otoconia in the young and aged rats, but we found no clear regional separation of saccular otoconia in all groups based upon size. In the oldest rats, the bodies of many otoconia in both maculae were pitted, fissured, penetrated, and eventually broken into several fragments. However, the terminal facets were smooth and the lines of intersection of facets were sharp, despite the degenerated bodies of the otoconia in this group. Giant otoconia discovered frequently on the outer margin of the utricular macula in aged rats. We directly observed weakened or broken linking filaments and otoconial fragments in the aged group, and displacement of such fragments might cause idiopathic benign paroxysmal positional vertigo (BPPV). This study of age-related morphological changes in otoconia will help us understand the etiology of idiopathic BPPV.

#### **916 The Difference of Gene Expression by Aging in C57/BL6 Mouse Cochlea Nuclei and Inferior Colliculus with cDNA Microarray Analysis**

**Yasunori Osumi<sup>1</sup>**, Masao Yagi<sup>1</sup>, Seiji Shibata<sup>1</sup>, Kohei Kawamoto<sup>1</sup>, Mikiya Asako<sup>1</sup>, Hiromichi Kuriyama<sup>1</sup>, Toshio Yamashita<sup>1</sup>

<sup>1</sup>*Kansai Medical University*

Age-related hearing loss, presbycusis, is caused by degeneration and decudation of auditory neurons and cochlear hair cells, and it results in the changes in auditory brainstem activity. The molecular mechanisms of age-related hearing loss in auditory brainstem have been unknown. In this study, we aimed to investigate the changes in gene expression in cochlea nucleus (CN) and inferior colliculus (IC). C57/BL6 female mice were used in this study. Animals were underwent auditory brain stem response (ABR) testing to assess auditory functions. After ABR, we extracted the total RNA in CN and IC. The quality of the total RNA was checked with Agilent's Lab-on-a-Chip total RNA 6000 nano assay. The samples resulted in OD260/OD280  $\square$  1.8 were used in following protocols. The mRNA was amplified from the total RNA by amino-allyl amplification kit and hybridized on Intelligence Chip (Takara).

Slides were scanned by Affymetrix 428 Array scanner and analyzed with Image5.6 (Biodiscovery) software. We detected the downregulation of several genes including Protein kinase C  $\epsilon$  (Prkce) in CN and Glutamate receptor ionotropic NMDA1 (Grin1) in IC. Upregulation of several genes including glycine amidinotransferase (Gatm) was detected in CN and in IC. Both of them regulate neurotransmitters in the synaptic cleft, that may be relevant to the change in auditory brainstem activity. We made sure the result with real time PCR. The pathophysiological mechanisms of these findings are discussed.

**[917] Kv 3.1 Voltage-Gated Potassium Channels Involvement in the Mouse Medial Olivocochlear Efferent System and Its Age-Related Decline: An In Vivo Study**

Xiaoxia Zhu<sup>1,2</sup>, Jared R. Spencer<sup>1,2</sup>, Robert D. Frisina<sup>1,2</sup>

<sup>1</sup>Univ. Rochester Med. Sch., <sup>2</sup>Int. Ctr. Hearing Speech Res.

The medial olivocochlear (MOC) efferent system function may play a role in the development of presbycusis – age-related hearing loss. The contralateral suppression (CS) of distortion product acoustic emissions (DPOAEs) declines with age. We have previously discovered that CS age-related declines precede outer hair cell degeneration in both clinical cases and animal models. Delayed rectifier voltage-gated potassium channel (VGPCs) Kv 3.1 mRNA and protein is found in high expression in the mouse auditory brainstem, and declines with age. The aim of the present study was to investigate the involvement of VGPCs Kv3.1 in the functioning of the mouse MOC efferent system. Young adult mice (6-11 weeks old) were used: VGPCs Kv 3.1 +/+ (N=8), +/- (N=8), and -/- (N=5), developed on a mixed background of 3 strains, 129/Sv:C57Bl/6:ICR, (25:25:50). Auditory brainstem responses (ABRs), DPOAEs and CS of DPOAEs were measured for each mouse. The results revealed no differences in DPOAE amplitudes. ABR thresholds in the Kv 3.1 -/- group, at 24, 32 and 48 kHz were 5-10 higher than for the +/+ and +/- groups. Comparison of the Kv3.1 knockouts with the +/+ and +/- groups showed a lack of CS (5-48 kHz), for the Kv3.1 -/- group. These findings suggest that VGPCs Kv3.1 play an important role in auditory efferent system processing and may be involved the development of presbycusis as part of the middle age decline in the MOC system previously reported. Age-related changes in the efferent system, possibly mediated by declines in VGPC Kv3.1s, could occur in the auditory brainstem, superior olivary complex, and/or via changes in the outer hair cell efferent responses.

Work supported by NIH: NIA & NIDCD.

**[918] Calcium-Binding Protein Immunoreactivity in the Inferior Colliculus and Cochlear Nucleus Related to Changes in Auditory Periphery in Aging BALB/c Mice**

Esma Idrizbegovic<sup>1</sup>, Xianzhi Niu<sup>2</sup>, Agneta Viberg<sup>2</sup>, Barbara Canlon<sup>2</sup>

<sup>1</sup>Audiology, Karolinska University Hospital, <sup>2</sup>Physiology & Pharmacology, Karolinska Institutet

Quantification of calcium-binding proteins (calbindin D-28k, parvalbumin and calretinin) immunoreactivity in the aging BALB/c (BALB) mice inferior colliculus (IC), posteroventral (PVCN) and dorsal (DCN) cochlear nucleus was made and related to hair cell and spiral ganglion neuron loss. The BALB strain exhibits progressive cochlear pathology and severe sensorineural hearing loss at an early age. Young (1month) and old mice (24 months and 30 month) have been used. The quantification of the immunopositive neurons with calbindin, parvalbumin and calretinin has been performed on young (1month) and old mice (24 months and 30 month) using the stereological method, the optical fractionator. Calbindin immunoreactivity was high

only in the nucleus of the commissure of the IC. Parvalbumin immunoreactivity was evident in the central nucleus of the IC, while calretinin immunopositive neurons were dominant in the pericentral regions of the IC. The quantification of the immunopositive neurons of these calcium-binding proteins did not show any significant changes between 1, 24 and 30 months old mice, respectively. A correlation between loss in the auditory periphery and calcium binding protein expression in the PVCN and DCN and IC was also examined to determine how degenerative changes in the auditory periphery might influence the neuronal homeostasis and immunoreactivity of calcium-binding proteins in the cochlear nucleus and inferior colliculus.

**[919] Effect of Aging on the Otolith-Driven Cardiovascular Responses in Rats**

Hong Zhu<sup>1</sup>, Wu Zhou<sup>1</sup>, Xiaomei Zhu<sup>1</sup>

<sup>1</sup>Department of Otolaryngology University of Mississippi Medical Center

Our previous studies show that pure linear acceleration, which selectively activates otolith system, induces characteristic cardiovascular responses in rats. These studies established an awake rat model to study the neural mechanisms underlying the otolith-cardiovascular reflex. In the present study, we utilized this animal model to assess whether there is an effect of aging on the otolith-cardiovascular reflex. Conscious male Sprague-Dawley rats were stabilized on a linear sled by a surgically implanted head holder. Blood pressure was measured via a chronically implanted abdominal aortic catheter. The linear motions were in four directions (forward, backward, leftward and rightward) and consisted of an acceleration phase of 200ms (3m/s<sup>2</sup>) followed by a deceleration phase of 200ms (3m/s<sup>2</sup>). Our preliminary data show that changes in blood pressure in response to pure linear acceleration were significantly increased in older rats (18 month), indicating that the otolith-driven cardiovascular response is altered by aging. Supported by NIH R03 DA16440 and NIH R01 DC05785

**[920] Down-Regulation of Several Cochlear Genes with Age Determined by Microarray Expression Profile for Aging CBA Mice**

Martha Lynch-Erhardt<sup>1,2</sup>, Mary D'Souza<sup>1,2</sup>, Xiaoxia Zhu<sup>1,2</sup>, Robert D. Frisina<sup>1,2</sup>

<sup>1</sup>Univ. Rochester Med. Sch., <sup>2</sup>Int. Ctr. Hearing Speech Res.

Presbycusis - hearing loss that progresses with age, is the leading communication disorder affecting the elderly population. Investigation of the molecular mechanisms for cochlear sensory cell aging and development, and discovering therapeutic applications for hearing impaired and deaf people are topics of interest in the medical neuroscience and hearing research communities. In this study, Robust Multi-Chip Average Normalization and comprehensive analysis by one-way ANOVA was carried out on Affymetrix Gene Chip M430A microarray data composed of 22,600 distinct probe-sets. 40 CBA mice in Young adult (3.5 mon, N=8), Middle aged (12 mon, N=17), Old Mild (27 mon, N=9), and Severe Presbycusis (31 mon,

N=6), groups were subjected to distortion-product otoacoustic emission, and auditory brainstem response testing to measure hearing abilities. Tissue dissected from both left and right cochleae of each mouse was used for RNA extraction to assess the changes in gene expression during aging. Proliferation, differentiation and transcription factors play a major role in the process of regeneration of hair cells in the organ of Corti. We found upregulation in BMP-4, JAG-1, Brn3.1 and p27<sup>(Kip-1)</sup> genes, which are an important group of genes involved in inhibition and transcription of differentiation of inner hair cell regeneration. Subsequently, another group of genes, which might indirectly stimulate regeneration, were found at reduced levels in the cochleae of old mice. Some examples which were downregulated include SPARC (calcium binding protein), BMP-7 (differentiation), and Bcl-2 (apoptosis). To confirm these gene microarray findings, quantitative real time PCR validation is ongoing, along with assessment of possible correlations with functional hearing data from these same mice.

Work supported by NIH: NIA P01 AG09524, NIDCD P30 DC05409

## **[921] Age-Related Changes in GAD-67 Punctate Immunolabeling in Layer V of Rat Primary Auditory Cortex**

**Robert Helfert**<sup>1</sup>, Lynne Ling<sup>1</sup>, Aruna Weberg<sup>1</sup>, Deb L. Larsen<sup>1</sup>, Larry F. Hughes<sup>1</sup>, Donald M. Caspary<sup>1</sup>

<sup>1</sup>SIU School of Medicine

Recent studies revealed age-related functional declines in the primary auditory cortex (AI), and it is thought that impaired GABA function may be a cause. Levels of GAD expression are reduced in layer V neurons of AI, suggesting altered inhibitory neurotransmission at their synaptic targets. The focus of this study is to determine whether aging directly affects GABAergic input to layer V AI neurons.

GAD-immunolabeled sections through AI were available from a prior study. They were obtained from young (4-6 month), middle-aged (20-22 month) and old (30-32 month) FBN rats. Images of layer V fields were digitized and analyzed at a morphometric workstation running MCID Elite software. Perimeters of all identifiable somatic profiles were traced and GAD-immunolabeled puncta apposing each soma were counted. Densities of puncta in the layer V neuropil were measured using a counting grid. ANOVAs were used for statistical comparisons among age groups, along with Bonferroni corrections to adjust for multiple comparisons.

Two populations of layer V neurons were identified; one labeled intensely for GAD<sub>67</sub> (GAD+) and the other did not (GAD-). There were no changes in density of either cell type among the age groups. GAD- neurons were generally larger than GAD+ ones. Numbers of GAD+ puncta apposed to GAD- neurons in old rats were decreased relative to the young (-15.71%±3.15%,  $p=.002$ ). A drop in the number of GAD+ puncta contacting the perikarya of GAD+ neurons was observed in old groups relative to middle-aged (-11.63%±3.45%,  $p=.025$ ). No group differences in densities of GAD+ puncta were observed in the neuropil ( $p=.859$ ).

**Summary.** There is a moderate decline in the number of GABAergic endings impinging on somata of layer V neurons of aged rats. It appears that there are no changes in density or number of GABAergic endings in neuropil. Thus, alterations in inhibition in layer V neurons may be partially explained by reductions in GABAergic axosomatic input.

Supported by PHS DC-00151.

## **[922] Age-Related Declines in Kv3.1b Channel Protein Expression in the Medial Olivocochlear (MOC) Efferent System of CBA/CaJ Mice**

**Martha L. Zettel**<sup>1</sup>, Robert D. Frisina<sup>1</sup>

<sup>1</sup>Dept. of Otolaryngology, University of Rochester Sch. of Medicine & Dentistry

Kv3.1b channels have high thresholds and contribute to rapid repolarization of cells that phase-lock to high frequency stimuli. However Kv3.1b is widely distributed in the auditory brainstem implying additional functions. Previous work by our group examining age-related changes in Kv3.1b has shown a 26% decline in neuropil expression (probably presynaptic) in the medial nucleus of the trapezoid body (MNTB) in 15 month-old (mo) CBA mice (vs. 3 mo mice). To determine if declines are unique to high-frequency nuclei we examined relative optical density of Kv3.1b staining in various regions of cochlear nucleus, superior olivary complex, and inferior colliculus of 3-4 mo, 15 mo, 24-26 mo, and 31-34 mo CBA/CaJ mice (n=20). In addition to MNTB, age-related declines in neuropil expression were seen in high-frequency processing regions such as lateral superior olive (23%) and the globular bushy cell region of anteroventral cochlear nucleus (35%). No declines were seen in other CN regions or in IC. Of greater interest were significant declines seen in somatic expression of Kv3.1b in superior paraolivary nucleus (SPN; 19%), and ventral nucleus of the trapezoid body (22%). SPN is prominent in rodents and is analogous to the dorsal medial periolivary nucleus of other mammals. These nuclei are not critical for high frequency processing, but are the loci of projections for the MOC efferent system. Our group has shown declines in contralateral suppression of distortion product otoacoustic emissions (CS DPOAE) in CBA mice by 15 months, and current work by Zhu et al (ARO 2006) demonstrates a lack of CS DPOAEs in the KV3.1 knockout mouse. Thus Kv3.1b appears to play a critical role in CS DPOAE and its decline in the MOC system with age may be an important contributor to presbycusis.

NIA grant PO1 AG09524, NIDCD grant P30 DC05409, International Center for Hearing and Speech Research.

## **[923] Sinusoidal Amplitude-Modulated Signal Processing Across AI Layers in Young and Aged Rats**

**Larry F. Hughes**<sup>1</sup>, Jeremy G. Turner<sup>1</sup>, Deb L. Larsen<sup>1</sup>, Jennifer L. Parrish<sup>1</sup>, Donald M. Caspary<sup>1</sup>

<sup>1</sup>Southern Illinois University School of Medicine

Coding for amplitude modulation (AM) is an important component of the complex signal processing necessary for species survival and communication. Little is known about



how cortical processing of AM signals changes with age. Extra-cellular recordings were obtained with a single shank, 16-channel electrode (Neuronexus Technologies, Ann Arbor, MI). Unit responses were simultaneously recorded from all layers of the left primary auditory cortex (AI) of 10 young and 10 aged Fischer-Brown Norway rats. Three AI penetrations were attempted on each animal. A 20 kHz carrier was modulated at 2, 4, 8, 16, 32, 64, and 128 Hz and presented to the contralateral ear at 60 dB SPL. Modulation depths of 25, 50, and 100% were used at each modulation rate. Spontaneous activity was recorded for 2 minutes before and after the presentation of AM stimuli. Experimental protocols were executed by custom software (Hancock & Voigt) and data were recorded using a Plexon system. Power spectral densities, which provide an index of phase-locking by computing the relative energy present in the neural response at various modulation rates (2, 4 Hz, etc.), were determined for sorted responses on each channel. The channels were grouped into supragranular (layers 1-4) and infragranular (layers 5&6) for analysis. Preliminary findings suggest that supragranular layers exhibit significantly greater phase-locking than infragranular layers. In addition, increasing the modulation depth (from 25 to 50 and 100%) was associated with greater phase-locking for supragranular layers at 2 and 4 Hz modulation rates, but not for infragranular layers. Consistent with other cortical literature, phase-locking was not generally present at modulation rates above 16Hz. Preliminary results suggest similar patterns of AM coding in supra- and infragranular layers in young and aged rats. Supported in part by Grants (SIU Excellence in Academic Medicine grant to LFH, NIH DC00151 to DMC, NIH AG023910 to JGT).

#### **924 Age-Related Loss of Behavioral Ability to Track Ongoing But Not Initial SAM Envelope in CBA/CaJ Mice with Intact Modulation Transfer Functions**

**Paul Allen<sup>1</sup>**, Alaina Muldrow<sup>1</sup>, Peter Rivoli<sup>1</sup>, Alison St. John<sup>1</sup>, James Ison<sup>1</sup>

<sup>1</sup>*Department of Brain and Cognitive Sciences, University of Rochester*

Gap detection and amplitude modulation thresholds provide complementary metrics of temporal processing. Gap detection has been studied in mice using prepulse inhibition of the acoustic startle response (PPI) and here we use SAM onset as a prepulse to assess age-related changes in perceptual salience of SAM in CBA/CaJ mice. We hypothesize that mice will show an age-related reduction in the upper cut-off of their Modulation Transfer Function (MTF) analogous to their age-related increase in minimum gap threshold. Second we investigate the ability of these mice to encode the initial and ongoing SAM envelope, which depends on reliable phase-locking of neural responses to the stimulus. The prepulse was the onset of 100% sinusoidal amplitude modulation of an otherwise continuous 70dB SPL broadband noise. In Experiment 1, MTFs were measured for young (6mo, n=11) and old (24mo, n=10) mice for modulation frequencies 20-2000 Hz and SAM commencing 100ms prior to the startle stimulus (ES). There was no effect of

age on MTF with each group showing band-pass MTF maxima at 90Hz, 50% points at 400Hz, and no detection of 1400Hz SAM. In Experiment 2, SAM frequency was fixed at 100Hz, and the interstimulus interval (ISI) between onset of modulation and ES was systematically varied such that PPI was sampled at 4 different phases for the 1st, 7th, and 21st cycles. The PPI of Young (3 mo, n=7) and Middle-aged (12mo, n=17) mice modulates with SAM phase, even during the 21st cycle. For Old mice (24mo, n=16), only the 1st cycle yielded strong modulation. Sinusoidal curve fitting to the 7th and 21st cycle PPI data shows a modest age-related decline in the PPI baseline and Slope, and increase in phase (lag of response wrt stimulus) but a dramatic reduction in the amplitude of PPI modulation in the 24 mo mice compared to the 2 younger groups. Detection of very high MF is intact in the old mice yet phase-locking to moderate MF appears compromised. Age-related reduction of auditory temporal acuity is thought to contribute to age-related hearing loss, presbycusis. These results suggest that parallel mechanisms for modulation encoding are differentially affected by age, with implications for understanding the effects of presbycusis on human speech comprehension.

Support contributed by NIH/NIA PO1 AG09524. This research was conducted while Paul Allen was a Glenn/AFAR Postdoctoral Fellow

#### **925 Age-Related Differences in Intensity Discrimination Using Cortical Evoked Potentials** **Kelly C. Harris<sup>1</sup>**, John H. Mills<sup>1</sup>, Judy R. Dubno<sup>1</sup>

<sup>1</sup>*Medical University of South Carolina, Department of Otolaryngology-Head & Neck Surgery*

When measured behaviorally, older adults with normal hearing have poorer intensity discrimination than younger adults, but only at lower frequencies. Poor intensity discrimination at lower but not higher frequencies for older adults can be associated with an age-related decline in temporal processing. The current study was designed to assess age-related effects on intensity discrimination at 500 and 3000 Hz using the N1-P2 to determine if cortical evoked potentials may serve as an objective measure of intensity discrimination. Subjects were 10 younger and 10 older adults with normal hearing. The N1-P2 was elicited by a brief (150 msec) intensity increase, ranging from 0 dB to 5 dB at 500 Hz and from 0 dB to 8 dB in 1-dB steps at 3000 Hz, in an otherwise continuous pure tone presented at 70 dB SPL. Intensity discrimination threshold was defined as the smallest intensity change needed to evoke an N1-P2 response. Consistent with behavioral measures, N1-P2 response thresholds were significantly higher for older subjects than younger subjects at 500 Hz but did not differ significantly at 3000 Hz. In addition, N1 and P2 latencies for older subjects were significantly prolonged at 500 Hz, but not at 3000 Hz. Response amplitudes were not significantly different between the two groups. Similar intensity discrimination thresholds and age-related differences for behavioral and electrophysiological measures support the cortical N1-P2 as a neural correlate of intensity discrimination. [Supported by NIH/NIDCD]

## **926 Age-Related Differences in Identification and Discrimination of Temporal Cues in Speech Segments**

**Sandra Gordon-Salant<sup>1</sup>**, Grace Yeni-Komshian<sup>1</sup>, Peter Fitzgibbons<sup>2</sup>, Jessica Barrett<sup>1</sup>

<sup>1</sup>University of Maryland, <sup>2</sup>Gallaudet University

This study investigated age-related differences in sensitivity to temporal cues in discrete speech sounds. Listeners included young noise-masked subjects, elderly normal-hearing subjects, and elderly hearing-impaired subjects. Four speech continua were presented to listeners, with stimuli from each continuum varying in a single temporal dimension. The variable acoustic cue in separate continua was voice-onset time, vowel duration, silence duration, and transition duration. In separate conditions, the listeners identified the word stimuli, discriminated two stimuli in a same-different paradigm, and discriminated two stimuli in a 3-interval, 2-alternative forced-choice task. Results showed age-related differences in the identification function cross-over points for the continua that varied silence duration and transition duration. All listeners demonstrated shorter difference limens (DLs) for the three-interval paradigm than the two-interval paradigm, with older hearing-impaired listeners showing larger DLs than the other listener groups for the silence duration cue. The findings support the general hypothesis that aging can influence the processing of specific temporal cues that are related to consonant manner distinctions.

## **927 Age-Related Differences in Amplitude Modulation Detection**

Ning-ji He<sup>1</sup>, John H. Mills<sup>1</sup>, **Judy R. Dubno<sup>1</sup>**

<sup>1</sup>Medical University of South Carolina

In a previous study we observed that age-related differences in intensity and frequency discrimination were larger at low frequencies than at high frequencies (He et al., 1998). This frequency-dependent aging effect was explained in terms of temporal cues that may deteriorate with age. A tone with amplitude modulation (AM) carries temporal cues from both the carrier (phase locking) and modulator (envelope locking). In this study, AM detection as a function of modulation frequency was measured with 500- and 4000-Hz carriers. Increasing the modulation frequency increases the number of AM cycles, hence changing the temporal feature of the envelope. If AM detection is based on the temporal component of the envelope, a different functional dependence of AM thresholds on the modulation frequency between low and high carrier frequencies would be expected, as the temporal resolution of the auditory system degrades with increasing frequency. Subjects were younger and older normal-hearing adults. At a stimulus level of 75 dB SPL, AM thresholds plotted as a function of modulation frequency were generally in the shape of a lowpass filter with a corner frequency, or a critical modulation frequency (CMF; Zwicker and Fastl, 1990), of about 10% of the carrier frequency. For younger subjects, AM thresholds at modulation frequencies below the CMF remained relatively constant for the 500-Hz carrier and increased slightly with

increasing modulation frequency for the 4000-Hz carrier. In contrast, for older subjects, AM thresholds increased with increasing modulation frequency for both carrier frequencies. Age-related differences in AM thresholds were observed across modulation frequency for the 500-Hz carrier, but were restricted to modulation frequencies below the CMF for the 4000-Hz carrier. These results suggest that AM detection is largely based on temporal cues conveyed by the envelope, and that the ability to use temporal cues declines with age. [Supported by NIH/NIDCD]

## **928 The DPOAE Growth Function as a Peripheral Physiological Correlate of Auditory Temporal Resolution**

**Lauren Stack<sup>1</sup>**, Jennifer Lister<sup>1</sup>, Gabriel J. Pitt<sup>1</sup>

<sup>1</sup>University of South Florida

Older adults experience great difficulty understanding speech that is degraded by background noise and reverberation. Temporal resolution, the ability to follow rapid acoustic changes over time, deteriorates with age and/or hearing loss and is believed to be important for understanding speech, particularly degraded speech. The purpose of this study was to investigate a peripheral auditory explanation for temporal resolution deficits using the Distortion Product Otoacoustic Emission (DPOAE) growth function. It has been suggested that age- and hearing loss- related temporal deficits are associated with a loss of active cochlear compression that occurs due to outer hair cell loss or damage. Subsequently, temporal envelope fluctuations are enhanced and temporal cues (particularly silent gaps) are obscured. Otoacoustic emissions provide information about outer hair cell function and DPOAE growth functions provide information about the linearity of the cochlear response. We have examined the relationship between psychophysical gap detection thresholds (GDTs) for across and within channel conditions and the slope of the DPOAE growth function for two groups of adults: 1) 12 aged 21 to 40 with normal temporal resolution and 2) 12 aged 55 to 74 with varying temporal abilities. DPOAE growth functions were measured in 2 dB steps, with an F2/F1 ratio of 1.2, using the  $L1 = 0.4 \cdot L2 + 39$  dB equation, with L2 varying from 70 to 30 dB SPL at the frequencies of 1000, 1025, 1950, 2000, and 2050 Hz. As expected, there was a significant effect of age group ( $p = 0.001$ ) and stimulus condition ( $p < 0.0001$ ) for the behavioral GDTs and a significant interaction between age and stimulus condition ( $p = 0.016$ ) was observed. Overall, DPOAE amplitudes were lower for the older adults than for the young adults. Pearson Product Moment correlations between gap detection threshold and DPOAE growth function slope were not significant for either group. The results indicate that temporal deficits are not related to loss of peripheral auditory processes as measured by DPOAE growth functions.

## **929** Relations Between the Number of Pregnancies and Hearing in Aged Women

Patricia Guimaraes<sup>1,2</sup>, Susan Frisina<sup>1,2</sup>, Frances M. Mapes<sup>2</sup>, Robert D. Frisina<sup>1,2</sup>, Robert D. Frisina<sup>1,2</sup>

<sup>1</sup>Otolaryngology Dept., Univ. Rochester Medical School,

<sup>2</sup>Int. Ctr. Hearing Speech Res., Nat. Tech. Inst. Deaf, Rochester Inst. Tech.

Sex hormones may affect aging of the auditory system. We previously reported that hormone replacement therapy (HRT) can negatively impact the hearing of aged women (Guimaraes et al., ARO Abstr. 2004), and progesterone in HRT could be responsible for those effects (Guimaraes et al., ARO Abstr. 2005). The present study retrospectively analyzed hearing abilities among post-menopausal women, taking into consideration the number of pregnancies. Subjects were separated into two groups: those that had never been pregnant before (None) and those who had been pregnant one or more times (One+), with a total of 26 subjects (N=13, None, and N=16, One+). The criteria for subject selection were: age (57-83 years), relatively healthy medical history, negative history of hormonal replacement therapy (NHRT), absence of significant noise exposure, middle ear problems and current/heavy smoking. Subject groups were tested for pure tone audiometry, tympanometry, otoacoustic emissions, hearing-in-noise-test (HINT) and contralateral suppression of DPOAEs (distortion product otoacoustic emissions). Our results showed elevated pure tone thresholds in both ears for the One+ group relative to the None group in all frequency ranges for the right ear and a trend for the left ear. For DPOAE amplitudes, the "None" group presented with higher amplitudes than "One +" group in the right ear, and for the left ear the One+ group presented higher amplitudes for DP1, but not for DP2. The HINT results were similar across all background noise speaker locations, suggesting that the major effects were on the ear rather than the brain. Considering that the progesterone levels are elevated during pregnancy, the exposure to that hormone at greater levels during pregnancy could be partly responsible for the hearing deficits relative to women who were never exposed to endogenous administration of sex hormones in pregnancy. Supported by NIH grants NIA P01 AG09524, NIDCD P30 DC05409

## **930** Interaction Between Noise-Induced and Age-Related Hearing Loss: Effect of Military Service in Korean Male

SungHee Kim<sup>1</sup>, Soon Suck Jarng<sup>2</sup>, Jong Heon Shin<sup>1</sup>, Dong Ik Lee<sup>3</sup>

<sup>1</sup>Department of Otorhinolaryngology, Daegu Fatima Hospital, <sup>2</sup>Department of Information Control & Instrumentation Engineering, Chosun University,

<sup>3</sup>Department of Otolaryngology, University of Rochester, NY, USA

A lifetime of exposure to noise is likely to have negative effects on the hearing, but the interaction between noise-induced hearing loss (NIHL) and age-related hearing loss (ARHL) is difficult to determine. The most commonly accepted assumption is a simple accumulating effect of

noise and ageing on the hearing. This study investigates the effect of military service to age-related hearing loss in Korean male. Most Korean male spent at least two years in military service at their early twenties. Comparison between groups with- and without-military service could show the effects of noise in this otherwise similar groups. The subjects were the clients who visited Health Promotion Center in Daegu Fatima Hospital, since 2004 January to 2005 July. Total 1,684 data of male subjects were analyzed. The novel ARCISM, data management system, enables the assessment of the risk of past history of hearing impairment on the basis of known risk factors. We excluded any subjects who had (1) past history of ear drainage, (2) usage of known ototoxic drug, such as chemotherapeutic agent, parenteral antibiotics for serious illness such as tuberculosis, and parenteral diuretics, (3) head injury, and (4) working in noise environment. Finally, 998 subjects were included, 202 subjects without military service and 796 subjects with military service. There was a significant age-related hearing loss at each frequency in both groups. The higher frequency showed the steeper slope of hearing loss with age in both groups. The group of with-military-service showed significantly worse hearing levels at 4 and 8 kHz than that of without-military-service. However, there was no significant difference in the degree of slopes of hearing loss with age between two groups. Military service showed adverse effect on age-related hearing loss, especially in high frequency. However, it did not affect significantly to the slope of hearing loss with aging in this cross-sectional study. For the further research, the detailed quantification of noise exposure during military service may help to assess the effect of noise exposure in age-related hearing loss.

## **931** Alteration of Epithelial Water Loss in Human Nasal Mucosa in Health and Disease

Masato Miwa<sup>1</sup>, Noriyuki Nakajima<sup>1</sup>, Yoko Iwasaki<sup>1</sup>, Kensuke Watanabe<sup>1</sup>, Mayumi Matunaga<sup>2</sup>

<sup>1</sup>Dokkyo University, <sup>2</sup>Showa University

The epithelium of nasal mucosa displays two features that distinguish it from all other tissues; polarity and tightness. The barrier function of nasal epithelium is critical to the host defense. On the other hand, dry nose are common complaints among the older population. The regulation of barrier function of nasal epithelium seems to be involved in the pathogenesis of allergic rhinitis and aging. The measurement of transepidermal water loss has been already proved to be an important non-invasive method for assessing the efficiency of the skin as a protective barrier. In this study, we demonstrated the human nasal mucosal water loss as the transepithelial water loss both in the basal state in health and disease following topical application of various substances.

Japanese volunteers ranging from 10 to 75 years old were recruited for this study. Measurement of transepithelial water loss of nasal mucosa (TEWL, expressed in g/m<sup>2</sup>/h) was performed on the inferior nasal turbinate. TEWL was measured with an evaporation meter (Tewameter TM 210; Courage+Khazaka, Germany) with original probe during holding breath in a sitting position. After non-traumatic application of various substances on the mucosal surface

of the inferior turbinate for 5 minutes, the alteration of nasal mucosal water loss was studied.

Though the baseline TEWL of the human skin differs from regions, TEWL value of nasal mucosa in this study is much higher than those of skin. The value tends to be increasing in order of age. The values of patients with allergic rhinitis and/or chronic rhinosinusitis were higher than those of normal volunteers.

After application of physiological saline, TEWL decreased slightly but were not changed significantly. After application of 10% NaCl, TEWL were significantly increased compared with basal state. Hypertonic solutions such as 10% NaCl has been proved to increase the permeability of the tight junctions of the airway epithelium. Nasal cream (Hitachi Chemical, Japan) decreased TEWL significantly compared with basal state. After application of 10% glycerol, TEWL were also significantly decreased compared. These data would contribute to understand the pathogenesis of the upper airway diseases with the rupture of the barrier function including allergic and senile rhinitis.

### **932 Effects of Auditory Deprivation and Electrical Stimulation in the Developing Auditory System**

**Olga Stakhovskaya<sup>1</sup>**, Patricia A. Leake<sup>1</sup>, Gary Hradek<sup>1</sup>, Russell L. Snyder<sup>1</sup>

<sup>1</sup>*Dept. of Otolaryngology-HNS, Univ. of California San Francisco, CA, USA*

This study was designed to examine the effects of different deafening protocols on the cochlear spiral ganglion and cochlear nucleus (CN) and to explore the possible role of developmental "critical periods" in the effects elicited by electrical stimulation from a cochlear implant. Cats were deafened by daily neomycin injections for 18-26 days starting at 30 days of age and were studied either at 8-9 weeks of age or after several months of electrical stimulation (325 pps/60Hz AM) beginning at 8-9 weeks. Data from the stimulated and unstimulated groups were compared to neonatally deafened animals matched for age and duration of stimulation/deafness.

In both deafened groups studied at 8-9 weeks, spiral ganglion cell (SGC) survival was already significantly reduced, despite the fact that animals in the 30-day deafened group had a brief period of normal hearing before neomycin treatment was initiated and were studied only 1-2 weeks after deafening. Electrical stimulation delivered over 18-30 weeks significantly enhanced SGC survival in the group deafened at 30-days, maintaining 15-20% higher SG cell density in the stimulated ears. The neonatally deafened group showed a similar increase in SGC survival with no significant difference between the 30-day deafened and neonatally deafened groups.

Measurements of CN size, however, revealed significantly larger cross-sectional areas in animals deafened at 30-days as compared to neonatally deafened cats, in the two groups studied at 8-9 weeks of age. There was also a trend toward larger CN size in the 30-day deafened group studied after electrical stimulation, as compared to the neonatally deafened, stimulated group. These findings

suggest that even a brief period of normal auditory experience may be significant in lessening degenerative changes in the central auditory system after early-acquired deafness as compared to the effect of deafening at birth.

Work supported by NIDCD Contract N01-DC-3-1006 and R01 DC000160.

### **933 Local Dexamethasone Therapy Prevents the Progression of Hearing Loss in an Animal Model of Electrode Insertion Trauma**

**Thomas Van De Water<sup>1</sup>**, Adrien Eshraghi<sup>1</sup>, Jiao He<sup>1</sup>, Marek Polak<sup>1</sup>, Thomas Balkany<sup>1</sup>

<sup>1</sup>*University of Miami Ear Institute, University of Miami Miller School of Medicine*

**Hypothesis:** High dose corticosteroid therapy delivered locally to the cochlea immediately following electrode insertion and withdrawal will prevent the progression of electrode trauma-induced hearing loss.

**Background:** Corticosteroids are administered either systemically or locally to treat sudden idiopathic sensorineural hearing loss (SNHL) in the clinic. Local application of steroids to the round window membrane (RWM) is often used as a salvage procedure after systemic therapy is shown to be ineffective in treating SNHL. Treatment of animals with local application of low dose corticosteroids into the scala tympani have been modestly effective in preventing hearing loss caused by aminoglycoside ototoxicity and by exposure to a damaging level of noise (sound trauma).

**Methods:** a guinea pig model of electrode insertion trauma-induced hearing loss; electrode diameter at tip 0.14 mm; insertion depth 3 mm; insertion site-cochleostomy immediately above RWM niche; miniosmotic pump (Alzet 2001; flow rate-1  $\mu$ L/hr) delivery of dexamethasone (100 ug/mL); whole mount organ of Corti preparations; propidium iodide & FITC-phalloidin staining; hearing tests (i.e. ABR & DPOAE).

**Results:** High dose dexamethasone (total dose over 7 days was 20  $\mu$ g) delivered locally into the scala tympani immediately following electrode insertion and withdrawal prevented the progression of electrode insertion trauma-induced hearing loss in the guinea pig. This protection of hearing did not reverse and persisted even 2 months after the initial trauma.

**Conclusion:** Local delivery of a corticosteroid to the cochlea may prove to be part of an effective approach for the conservation of residual hearing during cochlear implantation.

Supported by a grant from MED-EL, Medical Electronics, Innsbruck, Austria.

### **934 Forward Masking of the Electrically Evoked Compound Action Potential in Animals with Residual Hair Cell Function**

**Kirill Nourski<sup>1</sup>**, Paul Abbas<sup>1</sup>, Charles Miller<sup>1</sup>, Barbara Robinson<sup>1</sup>, Fuh-Cherng Jeng<sup>1</sup>

<sup>1</sup>*The University of Iowa*

Previously, we described a non-monotonic recovery pattern of the auditory nerve electrically evoked compound

action potential (ECAP) following acoustic masking (Nourski et al., *Hear. Res.*, 2005, 202:141-153). We hypothesized that recovery from adaptation in the auditory nerve could be associated with changes in driven rate and firing synchrony. To achieve a better understanding of adaptation mechanisms in the hearing ear, the present study addressed the time course of ECAP recovery following electric stimulation before and after reversible deafening.

The auditory nerve in guinea pigs was stimulated with an intracochlear electrode. ECAPs were recorded from the nerve trunk. ECAP recovery from refractoriness was evaluated in a two-pulse forward masking paradigm. To address recovery from adaptation, 400 ms pulse trains (rate 5000 pps) were used as maskers, and single pulses, presented with delays relative to the masker offset, were used as probes. Masking was measured as a decrease in ECAP amplitude relative to an unmasked control. Data were obtained before and after systemic administration of furosemide.

Recovery from masking often featured a non-monotonic time course: a rapid recovery phase was followed by a transient depression in the ECAP amplitude. Such a pattern was observed both in hearing and temporarily deafened conditions. It was described by a three-component exponential function with two decaying and one rising component.

Forward masking functions suggest a multi-component process with refractory and adaptation effects contributing to the recovery time course. Refractory characteristics of the ECAP may be affected by hair cell-mediated responses. Post-stimulatory changes in synchrony likely contribute to the observed non-monotonicity of recovery. However, this study suggests that they cannot be attributed solely to the recovery of spontaneous activity, implying an additional mechanism unrelated to the hair cell-function.

Supported by NIH contract N01-DC-2-1005

### **[935] Long Term Effects of Growth Factor Upregulation and Electrical Stimulation on Hearing with Cochlear Implants**

**Jennifer A. Chikar**<sup>1,2</sup>, Deborah J. Colesa<sup>2</sup>, Donald L. Swiderski<sup>2</sup>, Yehoash Raphael<sup>1,2</sup>, Bryan E. Pfingst<sup>1,2</sup>

<sup>1</sup>*Neuroscience Graduate Program, University of Michigan,*

<sup>2</sup>*Kresge Hearing Research Institute, The University of Michigan, Ann Arbor, MI, USA*

In animal models of sensorineural hearing loss, the introduction of growth factors has been shown to promote spiral ganglion cell (SGC) survival, which is thought to play a key role in the performance of cochlear implants. Electrical stimulation (ES) of the cochlea has also been shown to enhance SGC survival. Previous studies have concentrated on morphological and electrophysiological measures to evaluate acute or short-term effectiveness of these treatments on auditory nerve survival. The current study assessed the psychophysical effects of growth factors in conjunction with ES in a long-term experiment (80 days). BDNF and CNTF, or BDNF alone, were upregulated via adenovirus inoculation in the cochlea and animals were stimulated with a multi-channel cochlear

implant. Psychophysical detection thresholds were tested daily using 6 combinations of electrode locations and configurations. At the beginning of the experiment (at the peak of growth factor expression), treated groups showed lower (better) detection thresholds when compared to control groups for 5 of the 6 ES combinations tested. At the end of the experimental period, treated groups had lower thresholds for all 6 combinations. The treatment group that received both BDNF and CNTF showed no significant difference in detection thresholds between the beginning and the end of the study in 4 conditions, indicating stable hearing levels over time. Two additional testing combinations showed a significant improvement in thresholds over time. In the treatment group that received only BDNF, a similar pattern of thresholds changes over time was seen, with 4 conditions stable and 2 conditions improved. Supporting data for the long-term benefits of this treatment was also seen in EABR thresholds and SGC counts. This study provides support for the feasibility of adenovirus-mediated growth factor upregulation in aiding long-term cochlear implant performance by enhancing/improving the cochlear environment.

### **[936] Cytoprotection with Systemic Steroids During Cochlear Implantation**

Alan Micco<sup>1</sup>, Claus-Peter Richter<sup>1</sup>, Sarah Russell<sup>2</sup>

<sup>1</sup>*Northwestern University,* <sup>2</sup>*Oklahoma University*

Preservation of residual hearing during cochlear implantation can potentially improve the patient's performance with the device. Typically, residual hearing is lost during the surgical procedure when the cochleostomy is created. Surgical techniques have been developed to minimize trauma while creating the cochleostomy. These techniques all utilize intracochlear perfusion of either steroids or Healon. This study evaluates the effect of systemic steroids on hearing preservation in gerbil model after cochlear implantation. Ten animals, (5 study and 5 control) were utilized. All animals underwent cochlear implantation with a custom-made silicone dummy-electrode. The study group was given systemic dexamethasone one hour prior to surgery. The cochleostomy was created just above the round window through a trans-bullar approach. Auditory evoked potentials were measured in all animals preoperatively, and post-operatively at two and four weeks. The animals were then sacrificed and the cochleae were plastic embedded and serial sectioned at 5µm for histopathologic examinations. In particular, spiral ganglion cell survival was examined. The results and possible clinical implications will be discussed.

### **[937] Local D-JNKI-1 Therapy Prevents the Progression of Electrode Trauma Induced Hearing Loss in the Guinea Pig**

**Adrien Eshraghi**<sup>1</sup>, Elam Adir<sup>1</sup>, Jiao He<sup>1</sup>, Brian Gibson<sup>1</sup>, Ried Graves<sup>1</sup>, Fred Telischi<sup>1</sup>, Marek Polak<sup>1</sup>, Thomas Balkany<sup>1</sup>, Thomas Van De Water<sup>1</sup>

<sup>1</sup>*University of Miami Ear Institute*

The JNK binding peptide D-JNKI-1 has been shown to prevent both hearing and hair cell loss in guinea pigs subjected to either aminoglycoside ototoxicity or a

damaging level of noise. The current study is focused on testing the ability of D-JNKI-1 in preventing cochlear implant electrode trauma induced hearing loss.

Guinea pigs were tested before and after electrode insertion trauma by pure tone evoked ABR and DPOAE recordings. D-JNKI-1 peptide in artificial perilymph (AP) was delivered locally to the cochlea immediately following electrode trauma and over 7 days. Controls consisted of the contralateral ears of untreated electrode trauma animals, animals perfused with D-JNKI-1 peptide that were not exposed to electrode trauma and electrode trauma animals treated with AP only. There was no increase in the hearing thresholds of either the control, contralateral ears of the untreated-electrode insertion trauma animals or in the ears of the animals perfused with D-JNKI-1 peptide without trauma. There was also no change in the amplitudes of the DPOAEs of either of these two groups of control animals. There was a progressive increase in hearing thresholds following electrode insertion trauma in the untreated animals and in electrode insertion animals that received AP only. This progressive increase in hearing thresholds following electrode insertion trauma was prevented in animals that were treated by scala tympani perfusion of a 10  $\mu$ M solution of D-JNKI-1 in AP. There was a progressive decrease in the amplitudes of the DPOAEs after electrode insertion trauma in the untreated animals and in animals treated with AP for 1 week following electrode trauma. D-JNKI-1 perfusion of electrode trauma animals did not have a decrease of amplitudes of the DPOAE responses. The one month follow up of these animals found that the hearing preserved by D-JNKI-1 treatment was stable over this long period of time post trauma. The results of double stained surface preparations of organ of Corti specimens suggest a pattern of trauma induced hair cell loss that involves both necrosis and apoptosis.

Research supported by grants from NOHR and MED-EL.

### **[938] Do Corticosteroids Preserve Hearing in Cochlear-Implanted Guinea Pigs?**

**Susanne Braun**<sup>1,2</sup>, Qing Ye<sup>3</sup>, Jan Kiefer<sup>4</sup>, Wolfgang Gstöttner<sup>1</sup>, Jochen Tillein<sup>2,5</sup>

<sup>1</sup>J.W.Goethe University Frankfurt/Main, Germany, ENT Dept., <sup>2</sup>J.W.Goethe University Frankfurt/Main, Germany, Dept. of Physiology II, <sup>3</sup>Hospital Fujian China, ENT Dept., <sup>4</sup>Technical University Munich, Germany, ENT Dept., <sup>5</sup>MedEl Austria

For patients with a profound hearing loss using combined electric and acoustic stimulation (EAS) preserving of their residual hearing is an important issue for the success of EAS. Steroids are used in the treatment of inner ear disorders and were recently applied to EAS patients to reduce insertion trauma. In a previous animal study threshold shifts caused by electrode implantation could be diminished by a local administration of a crystalline suspension of the steroid triamcinolone into the cochlea (Ye et.al, ARO 2005, Abstr. 1198). In the present study the effect of non-crystalline triamcinolone and dexamethasone on the physiology of implanted guinea pig cochleae was investigated.

Three groups of guinea pigs were implanted with a guinea pig electrode (MedEl) through a cochleostomy in the basal turn of the cochlea. 3  $\mu$ l of triamcinolone (1st group), dexamethasone (2nd group) or artificial perilymph (AP) as a control (3rd group) was carefully infused with a microsyringe before implantation. In each group the second ear received the same treatment omitting implantation (additional controls). Hearing loss (HL) was tested before and after drug/AP application for 4 weeks postoperatively by measuring click-evoked compound action potentials (CAPs) and frequency-specific CAP-audiograms via electrodes implanted near the round window.

Click-evoked CAPs revealed a HL between 10-50 dB after electrode insertion in all groups. 7-14 days post-implantation a recovery of thresholds to values close to the pre-implantation status with no difference between steroid and control groups was observed. Frequency-specific CAP-audiograms showed highest HL in the high frequency range (>11 kHz) while the middle frequency range (1-8 kHz) was less affected. Recovery was found in all groups but was more pronounced in the steroid groups. The results indicate that the two steroids are not toxic when applied to the inner ear but may be helpful in reducing the progressive hearing loss caused by electrode insertion trauma.

Supported by DFG & MedEl

### **[939] Spatial Selectivity in Cat Inferior Colliculus Is Degraded Following Long-Term Deafness**

**Maïke Vollmer**<sup>1</sup>, Russell L. Snyder<sup>1</sup>, Ralph E. Beitel<sup>1</sup>, Stephen J. Rebscher<sup>1</sup>, Patricia A. Leake<sup>1</sup>

<sup>1</sup>Otolaryngology-HNS, University of California, San Francisco

Selective neural activation is an important factor for maintaining functional independence of channels in a multichannel cochlear implant. This study examines the effects of neonatally induced deafness on spatial selectivity of intracochlear electrical stimulation (ICES) in the central auditory system. Electrically evoked auditory brainstem response (EABR) thresholds and neural response thresholds in the inferior colliculus (IC) were estimated in cats after varying durations of deafness. Acutely deafened, implanted adult cats served as controls. Threshold distributions to ICES were analyzed across the tonotopic gradient of the IC to determine the spread of excitation (spatial selectivity/tuning) and the dynamic range, i.e., difference between minimum IC threshold and the higher threshold at the border between external (ICX) and central (ICC) nuclei of the IC. At the conclusion of study, spiral ganglion cell (SGC) densities were analyzed in each cat.

Long-deafened animals (LD cats; duration of deafness >2.5 yr) with severe cochlear pathology (mean SGC density <6% of normal) had significantly higher EABR and IC thresholds than animals deafened <1.5 yr (MLD cats; mean SGC density ~45% of normal). The spatial extent of electrical excitation was significantly broader and the dynamic range significantly reduced in LD animals compared to MLD and control animals. However, a

cochleotopic organization was maintained in both the ICX and the ICC regardless of the duration of deafness.

These data suggest that long-term auditory deprivation results in a significant degradation of spatial selectivity of ICES in the central auditory system. Similar changes likely contribute to poorer speech discrimination performance in prelingually deafened human cochlear implant users who are implanted as adults.

Supported by NIH NIDCD Contract N01 DC-3-1006.

#### **940 Neural Net for Long-Term Auditory Cortical Plasticity Elicited by Fear Conditioning: Model**

**Nobuo Suga<sup>1</sup>, Xiaofeng Ma<sup>1</sup>, Weiqing Ji<sup>1</sup>**

<sup>1</sup>*Washington University in St. Louis*

Auditory fear conditioning evokes long-term cortical and short-term collicular best frequency (BF) shifts in the big brown bat. Gao and Suga (1998) hypothesized the neural net model for the production of these BF shifts. The Gao-Suga model is different from the Weinberger model (1998). This model states that small and short-term cortical and collicular BF shifts specific to CS (tone bursts) are evoked by the neural net of the auditory cortex (AC) and corticofugal feedback activated by CS, and this tone-specific cortical BF shift is augmented and changed into long-term by acetylcholine released into the AC by the cholinergic basal forebrain which is activated by the auditory and somatosensory cortices through the association cortex and the amygdala. Accordingly, the change caused by the CS-US association occurs in the AC after the amygdala. The collicular BF shift is increased by the augmented cortical BF shift through the corticofugal system and contributes to the development of the large, long-term cortical BF shift. The data that have been accumulated after 1998 support the Gao-Suga model. It is particularly important that the large, long-term cortical BF shift can be evoked by focal electric stimulation and acetylcholine applied to the AC, without the CS-US association by the multi-sensory thalamic nuclei (MGBm/PIN). It should be noted that the CS-US association appears to occur first in the lateral amygdala rather than the MGBm/PIN, that the lateral amygdala receives both the cortical and thalamic inputs, and that conditioned behavioral responses can be acquired by animals whose AC is inactivated or removed, i.e., without the cortical BF shift. To extend the Gao-Suga model, we hypothesize that the cortico-amygdala projection is essential for eliciting the tone-specific cortical BF shift, whereas the thalamo-amygdala projection is essential for eliciting tone-nonspecific cortical changes. Supported by NIDCD DC-00175.

#### **941 Effect of Serotonin on Auditory Cortical Plasticity Elicited by Fear Conditioning**

**Weiqing Ji<sup>1</sup>, Nobuo Suga<sup>1</sup>**

<sup>1</sup>*Washington University in St. Louis*

In the big brown bat, 30-min-long auditory fear conditioning with tone bursts (CS) followed by electric leg-stimulation (US) causes the best frequency (BF) shifts of cortical auditory neurons toward the frequency of the tone bursts.

These BF shifts develop slowly to a plateau after the conditioning and last long. Serotonin (5-HT), an important neuromodulator extensively distributed in the cerebral cortex, including the auditory cortex (AC). We, therefore, studied the effects of 5-HT,  $\alpha$ -methyl-5-HT (an agonist of 5-HT 2A receptors), and ritanserin (an antagonist of 5-HT 2A receptors) applied to the AC on the development of the cortical BF shift caused by the conditioning in awake bats. We found: (1) 5-HT applied to the AC prior to the conditioning reduced the auditory responses of cortical neurons by 29% as well as the development of the long-term cortical BF shift caused by the conditioning and made it short-term. (2) 5-HT applied immediately after the conditioning reduced the BF shift by 38% and changed it into short-term in 4 out of the 12 neurons, but kept it long-term in the remaining 8. (3) 5-HT applied to the AC 70 min after the conditioning had no effect on the wholly developed cortical BF shift. (4)  $\alpha$ -methyl-5-HT applied to the AC prior to the conditioning increased the auditory responses of cortical neurons by 35%, and accelerated the development of the cortical BF shift. (5) Ritanserin applied to the AC prior to the conditioning reduced the auditory responses of cortical neurons by 41% and temporarily shifted the cortical BF "away" from the frequency of the conditioning tone. Our data show that the serotonergic system can modulate the reorganization of the frequency map of the AC caused by auditory learning. (Supported by NIDCD DC-00175)

#### **942 Effect of Task Difficulty on Receptive Field Plasticity in A1**

**Serin Atiani<sup>1</sup>, Pingbo Yin<sup>1</sup>, Mounya Elhilali<sup>1</sup>, Shihab Shamma<sup>1</sup>, Jonathan Fritz<sup>1</sup>**

<sup>1</sup>*University of Maryland*

What is the role of attention in auditory processing? In order to approach this question we developed an auditory detection task with variable levels of difficulty that may require corresponding variable levels of attention for successful task performance. In the simplest version of the task the animal learned to distinguish between a set of similar background noise stimuli (temporally orthogonal ripple combinations or TORCs) and pure tone target stimuli. In more difficult versions of the task, the pure tone was embedded in noise with variable ratios of tone signal-to-noise. In order to successfully perform the task the animal needed to detect the presence of the tone, and extract the narrowband stimulus from the broadband noise. We trained two ferrets on this task using conditioned avoidance behavioral techniques and measured threshold performance for frequencies between 125Hz to 16kHz. We recorded neural responses from primary auditory cortex in the ferret in non-behaving and behaving states with different levels of task difficulty. We computed the on-line spectrotemporal receptive fields (STRF) of single neurons in A1 in multiple passive and behaving states. It has been previously reported that there are task related dynamic spectral changes in STRF shape at target frequency during performance of the simple version of this task (Fritz et al. 2003). We asked whether there were enhanced changes in the STRF at target frequency during performance of the more complex



versions of the task. We discuss our results in the context of the general problem of signal extraction in background noise.

#### **943 How Faithfully Does Cortical Receptive Field Plasticity Follow the Spectral Profile of Multi-Tonal Targets During Detection Tasks?**

**Jonathan Fritz<sup>1</sup>**, Serin Atiani<sup>1</sup>, Pingbo Yin<sup>1</sup>, Kevin Donaldson<sup>1</sup>, Mounya Elhilali<sup>1</sup>, Shihab Shamma<sup>1</sup>

<sup>1</sup>*University of Maryland*

We have previously demonstrated task-related dynamic spectral changes in auditory cortical receptive field shape at tone target frequency during performance of a single-tone detection task (Fritz et al., 2003). In this task, ferrets learned to discriminate between a set of thirty similar background noise stimuli (temporally orthogonal ripple combinations or TORCs) and foreground isoamplitude single-tone target stimuli. The ferrets were trained on the single-tone target detection task using conditioned avoidance behavioral techniques (Heffner and Heffner, 1995) and quickly generalized to respond to random single-tone targets of any frequency between 125Hz-16kHz and ignore background noise. After mastering this version of the task, the ferrets also learned to selectively respond to multiple-tone targets (in which the target consisted of several tones presented simultaneously). In this multi-tonal version of the task, the target contained additional, redundant spectral information as compared to the single-tone version. We recorded neural responses from primary auditory cortex in the ferrets in non-behavioral (passive) and behavioral (multi-tonal detection) states. Using standard reverse correlation techniques, we computed the on-line spectrotemporal receptive fields (STRF) of single neurons in A1 in a sequence of successive passive and behavioral states. We compared the passive and active STRFs and asked whether the resulting STRF changes arising during task performance were faithful to the spectral profile of multi-tonal targets (suggesting redundant information storage during task-related plasticity) or whether the STRF changes only reflected single tonal components of the multi-tonal target complex (sparse information storage during task-related plasticity). We shall discuss the implications of our results for auditory object recognition.

#### **944 Differential Gene Expression of Glutamate Receptor Subunits in Auditory Cortex After Bilateral Cochlear Ablation**

**Yilei Cui<sup>1</sup>**, Avril Genene Holt<sup>1</sup>, Catherine Lomax<sup>1</sup>, Ling Tong<sup>1</sup>, Richard Altschuler<sup>1</sup>

<sup>1</sup>*Kresge Hearing Research Institute, Dept. Otolaryngology, Univ. Michigan, Ann Arbor, MI, USA*

There is increasing evidence of plasticity in the adult auditory pathways. We have previously shown deafness related changes in glutamate receptor subunit expression in the rat auditory brainstem and inferior colliculus. Recently Sun et al (2005) have shown changes in NMDAR2A and 2B receptor subunit expression in the rat auditory cortex following learning. We therefore examined deafness-related changes in glutamate receptor subunits

in the rat auditory cortex using quantitative real time PCR. Male Sprague-Dawley rats, 250-300g, with normal hearing, were bilaterally deafened by cochlear ablation and assessed at 3 days and 3 weeks following deafening. In each experimental group (normal hearing, 3 day deaf, and 3 week deaf) twelve rats were randomly divided into three sub-groups (pools) each consisting of three-four rats. Three different pools of total RNA from the auditory cortex (AC) were generated for each group. Changes in the expression of AMPA (GluR1, 2, 3, 4) and NMDA (NMDAR1, NMDAR2A-2D and NMDAR3) receptor subunits were determined. There were significant decreases from normal expression in NMDAR2A, 2C and 3A at 3 days following deafening that were no longer significant by 3 weeks. Future studies will address changes in AMPA and NMDA receptors at an earlier time point following deafening with RT-PCR and cellular localization of these changes with immunocytochemistry. Interestingly, we did not see changes in NMDAR2B receptor subunit as Sun et al (2005) found with learning. This suggests that

there may be differences in the plastic responses to changes in activity levels resulting from hearing loss versus changes in neuronal activity resulting from learning.

**Acknowledgements** -This research was supported by research grant DC00383 to RAA and core center grant P30 DC-05188 from the NIDCD, NIH

#### **945 Deafness Disrupts Long-Term Excitatory Synaptic Plasticity in the Auditory Cortex**

**Vibhakar Kotak<sup>1</sup>**, Andrew Briethaupt<sup>1</sup>, Dan Sanes<sup>1</sup>

<sup>1</sup>*Center for Neural Science, New York University*

In vivo and in vitro electrophysiological experiments have established that sensorineural or conductive hearing loss modifies cellular properties and processing in the auditory CNS (Kitzes and Semple, 1985; Reale et al., 1987; McAlpine et al., 1997; Kotak and Sanes, 1998; Mossop et al., 2000; Vale and Sanes, 2000; Syka, 2002; Wang et al., 2002; Rajan, 2001, 2003). However, virtually nothing is known on whether excitatory or inhibitory long-term potentiation or depression (LTP, LTD) in the developing auditory cortex (A1) relies on normal hearing experience. In this study, sensorineural hearing loss (SNHL) was induced at P10 by surgical extirpation of both cochleae, and excitatory synaptic plasticity was examined in A1 neurons at P14-20. Whole cell current-clamp recordings were obtained from infragranular pyramidal neurons in the auditory thalamocortical brain slices, and extracellular stimuli were applied at the Layer 6-white matter junction. Such extracellular stimulation evoked EPSPs in the recorded neurons; the stimulus intensity was then adjusted to elicit a 50% of maximum amplitude EPSP. Baseline L6-evoked EPSPs were recorded for 10 mins, followed by the plasticity conditioning protocol (5 pulses at 100 Hz x 5 trains, 5 repetitions every 30). EPSPs were then acquired for an additional hour. In slices from normal gerbils, this conditioning protocol induced either LTP or LTD. For LTP, the pre-conditioning mean EPSP amplitude was  $6.0 \pm 0.4$  mV that increased to  $10.5 \pm 0.7$  1 h after the conditioning ( $\pm$ SEM; t-test,  $p=0.0002$ ,  $N=10$ ). For LTD, the preconditioning mean EPSP amplitude was  $7.3 \pm 0.3$  that

decreased to  $3.8 \pm 0.3$  mV 1 h after the conditioning (t-test,  $p=0.0001$ ,  $N=12$ .) In contrast, SNHL neurons displayed only LTD. Their mean EPSP amplitude was  $7.2 \pm 1.6$  mV before conditioning, that decreased to  $4.4 \pm 1.9$  mV 1 h after the conditioning protocol (t-test,  $p=0.004$ ,  $N=11$ ). Preliminary data from pre-hearing animals ( $N=11$ ) showed induction of LTD but not LTP. One possible explanation for these results is that deafness increases excitability in infragranular neurons, as has been previously demonstrated for layer 2/3 pyramidal neurons in A1 (Kotak et al. 2005). If so, then further use-dependent strengthening of excitatory synapses may be hindered. Supported by the NIDCD grant DC006864 to DHS and VCK.

#### **[946] Unilateral Conductive Hearing Loss Results in Disparate Changes in Neuronal Activity in Inferior Colliculus and Auditory Cortex**

**Ken Hutson<sup>1</sup>**, Dianne Durham<sup>2</sup>, Thomas Imig<sup>3</sup>, Debara L. Tucci<sup>1</sup>

<sup>1</sup>*Dept Otolaryngology, Duke Univ Med Ctr*, <sup>2</sup>*Dept Otolaryngology, Univ of Kansas Med Ctr*, <sup>3</sup>*Dept Physiology, Univ of Kansas Med Ctr*

We have used unilateral malleus removal in the young gerbil as a model to study the effects of conductive hearing loss (CHL) on central auditory system (CAS) function. Previous studies have shown a marked decrease in CAS activity and metabolism in the major afferent projection from the manipulated ear (Tucci et al., 1999, 2001; Hutson et al., 2005). In contrast, Stuermer and Scheich (2000) demonstrated contralateral enhanced 2-deoxyglucose (2-DG) uptake in auditory cortex subsequent to unilateral CHL. To help reconcile these differences, we studied these effects at the level of the inferior colliculus (IC) and primary auditory cortex (AC; AI and AAF). CAS activity was assessed using the 2-DG method following CHL, cochlear ablation (CA) or a sham procedure (SH) in postnatal day 21 gerbils. Three weeks after surgery, animals were injected with 2-DG, and then exposed to tones of 1 and 2 kHz, alternating at 4 Hz, for 45 minutes prior to sacrifice. Brains were sectioned in the horizontal plane and processed using standard 2-DG procedures (Tucci et al., 1999). From the 2-DG exposed film, optical density (OD) measurements were taken from AI and AAF of both the right and left hemispheres and from the right and left IC using NIH Image software. Mean OD values for each structure were then corrected for background using OD of the corpus callosum, yielding a relative OD (OD rel) value. OD rel values were then SH-corrected, and analyzed across the experimental conditions. Preliminary results (three animals per condition) show that activity in the IC was significantly altered by both CHL and CA procedures, consistent with previous findings. At the level of primary auditory cortex, an opposite pattern was seen, with an increase in 2-DG uptake contralateral to the CHL/CA ear, although these differences did not reach significant levels. Results confirm previous findings, and confirm that 2-DG activity patterns following hearing loss differ between the IC and AC. Supported by DC 005416

#### **[947] Physiological Response to Sound, and Auditory-Cued Learning, May Require Functioning Nicotinic Acetylcholine Receptors in Auditory Cortex**

**Raju Metherate<sup>1</sup>**, Kevin Liang<sup>1</sup>, Bonnie Poytress<sup>1</sup>, Norman Weinberger<sup>1</sup>, Yiling Chen<sup>1</sup>, Frances Leslie<sup>1</sup>

<sup>1</sup>*University of California, Irvine*

Nicotinic acetylcholine receptors (nAChRs) are concentrated in layers 3-4 of rat sensory cortex, where they are thought to regulate sensory inputs. We found that systemic administration of nicotine (2 mg/kg nicotine tartrate) in adult rats resulted in decreased thresholds and increased magnitudes of tone-evoked local field potentials (LFPs) in layer 4 of primary auditory cortex (stimuli at characteristic frequency). Conversely, microinjection of the nAChR antagonist mecamylamine (10  $\mu$ M, 1  $\mu$ l) into layer 4 raised thresholds and strongly reduced amplitudes of tone-evoked LFPs. These results indicate that cortical nAChRs regulate cortical responsiveness to sound. Moreover, since mecamylamine was delivered alone—without nicotine—its effect suggests that endogenous acetylcholine acting at cortical nAChRs may be necessary for cortical neurons to respond to sound.

However, brief nicotine exposure during a neonatal critical period (2 mg/kg twice a day from P8-12; Aramakis et. al., J. Neuroscience, 2000) largely prevented in adult rats the effects of systemic nicotine and intracortical mecamylamine, although it did not affect pre-drug tone-evoked responses. Neonatal exposure also impaired auditory learning in adults, determined using an auditory-cued active avoidance task. Neonatal exposure did not affect nAChR density and binding affinity in adult auditory cortex, suggesting that any disruption in nAChR function occurred downstream to receptor binding. Thus, whereas activation of cortical nAChRs apparently can sustain and enhance auditory function in adults, developmental exposure to nicotine produces a long-lasting nAChR hypofunction and learning deficit. The results are consistent with the hypothesized role of cortical acetylcholine in cognitive function, and may be a model for auditory-cognitive deficits observed in the children of smokers.

Supported by NIDCD (DC02967, DC02398, DC05592), NIDA (DA12929, DA10612, DA07318) and the Irvine Research Unit for Hearing and Speech Sciences.

#### **[948] Development of Auditory Cortical Responses to Complex Sounds**

**Martin Pienkowski<sup>1</sup>**

<sup>1</sup>*Karolinska Institutet*

We recently reported [J Neurophysiol. 93: 454-66] that neurons in newborn chinchilla core auditory cortex were much less likely to have complex tuning properties than those in adult animals. The question is whether the developmental increase in receptive field complexity reflects specialization for the detection of spectrotemporal features characteristic of important natural sounds (e.g., communication calls).

I have begun recording cortical neuron responses to simple (tonal), random complex (chord train) and structured complex (conspecific call) stimuli in newborn and mature (anesthetized) chinchillas. Preliminary data will be presented. It will be interesting to see whether the strength and robustness of the newborn responses to random complex sounds compare favourably with those of adults (as do responses to simple tones). If so, then a strong indication of specialization for call detection will be the finding of more vigorous responses to the set of call stimuli in adult than in newborn animals. It is further hypothesized that spectrotemporal receptive fields (STRFs) estimated from random stimuli will be better predictors of responses to conspecific calls in newborns than in adults, again suggesting that less specialized, more linear neurons are giving way to increasingly nonlinear circuitry.

#### **[949] Mild Noise Induced Hearing Loss Affects the Temporal Modulation Transfer Functions in Cat Primary Auditory Cortex**

**Naotaka Aizawa<sup>1</sup>, Jos Eggermont<sup>1</sup>**

<sup>1</sup>*University of Calgary*

We investigated the neural temporal resolution in cat primary auditory cortex at least four weeks after a 2-4 hr. noise exposure (N=35) with 120 dB SPL narrow-band noise or tones of 5-6 kHz and in 23 normal hearing control cats. The average hearing loss in the 6-10 kHz range was around 20 dB and about 10 dB for higher frequencies. We used periodic click trains and amplitude modulated (AM) noise stimuli presented at 65 dB SPL and calculated the temporal Modulation Transfer Function (tMTF). The one-second duration click trains and AM noise bursts were followed by two seconds of silence. Twenty-one different repetition rates or modulation frequencies, equally spaced logarithmically between 2 and 64 Hz were randomly presented and repeated ten times. Multi-electrode arrays were used for recording from 256 unit clusters in the control group and 218 in the noise trauma group. Best modulating frequencies were on average between 9.2 and 9.9 Hz and not significantly different between stimuli and experimental groups. Limiting rates, defined as the highest rates that produced a clear response to the second click/modulation period at the appropriate interval, were not significantly different ( $p > 0.01$ ) for click trains between the control and noise trauma group. However, the limiting rate for AM noise for the noise trauma group (21.9 Hz) was significantly ( $p < 0.0005$ ) larger than in the control group (18.8 Hz). In addition, for the control group the limiting rates for click trains (15.3 Hz) and AM noise (18.8 Hz) were significantly different ( $p < 0.0001$ ). The same difference was found for the noise trauma group (click trains: 16.4 Hz; AM noise: 21.9 Hz), which was also significant ( $p < 0.0001$ ). Model studies suggest that this can be explained by a reduced post-activation inhibition for AM noise compared to click train stimulation in the control cats, and a further reduction in post-activation inhibition following mild noise-induced hearing loss.

#### **[950] Noise-Induced Developmental Delay of Auditory Cortex - Physiology and Gene Expression Changes**

**Wei Sun<sup>1</sup>, Liyan Zhang<sup>1</sup>, Guang Yang<sup>1</sup>, Edward Lobarinas<sup>1</sup>, Richard Salvi<sup>1</sup>**

<sup>1</sup>*University at Buffalo*

Early auditory experiences play an important role in the acquisition of language and the lack of appropriate auditory experiences can lead to severe language disability. Since the auditory cortex (AC) plays a crucial role in processing and interpreting complex sound, there is growing interest in the physiological and molecular mechanisms that underlie experience dependent AC plasticity. Recent studies have shown that long-term exposure to a static noise environment in early life can completely suppress the development of neural tuning and tonotopy in rat AC. However, normal tuning and tonotopy can be reinstated if rats are put back into a dynamic acoustic environment. To begin to identify the mechanisms that suppress the development of AC tuning and tonotopy induced by long-term static noise, we implanted chronic microwire electrodes into AC to monitor its functional development and used focused gene microarrays and quantitative real time PCR to identify changes in AC gene expression associated with cortical plasticity. When newborn rats were raised in a static noise environment for two months to suppress tonotopy and then shifted to a normal environment to restore tonotopy, the best frequency (BF) of many neurons shifted from high to low frequencies consistent with previous results. Gene analysis showed significant changes in gene expression of growth-associated protein 43 kD (GAP-43), a protein closely associated with axonal outgrowth. GAP-43 expression decreased with age when animals were raised in a normal acoustic environment. However, GAP-43 expression remained high in older rats raised in a static noise environment, but then declined when the animals were placed back into their normal sound environment. Other genes related with nerve synaptic function (e.g., NMDA receptors) also showed significant time-dependent changes in expression when rats shifted from a static noise environment back into their normal acoustic environment. These results are the first to identify a molecular basis for the noise-induced developmental delay of AC tonotopy and tuning. (Supported by NIH R01 DC06630-01 and DRF)

#### **[951] Primary Auditory Corticocortical Connections in Hearing and Deaf Shaker-2 Mice**

**Noah E. Meltzer<sup>1</sup>, David K. Ryugo<sup>1,2</sup>**

<sup>1</sup>*Johns Hopkins University School of Medicine, Department of Otolaryngology - Head & Neck Surgery,* <sup>2</sup>*Department of Neuroscience*

Human functional imaging studies show that prelingually-deaf adult cochlear implant (CI) recipients, who were implanted after the language acquisition period, demonstrate cortical activation limited to primary auditory cortex contralateral to the CI. We hypothesized that this limited pattern of cortical activation reflected changes in cortical input to primary auditory cortex due to deafness.

Using electrophysiology, electrical stimulation, cytochrome oxidase histochemistry, and neural tracing methods, we studied hearing and congenitally deaf shaker-2 (sh-2) mice to show inputs to primary auditory cortex. We observed no difference in these inputs. These observations do not demonstrate an anatomic basis for the functional imaging data, but support use of the sh-2 mouse as a model for further studying the effects of congenital deafness on cortical development and function.

### **[952] Effects of Memantine and Scopolamine on the Tinnitus Induced by Salicylate**

**Guang Yang<sup>1</sup>**, Wei Sun<sup>1</sup>, Edward Lobarinas<sup>1</sup>, Liyan Zhang<sup>1</sup>, Salvi Richard<sup>1</sup>

<sup>1</sup>*University at Buffalo*

Memantine (MM), an antiglutamatergic drug that acts on NMDA receptors, and scopolamine (SC), an anticholinergic drug, have been proposed as possible pharmacologic treatments for tinnitus. To determine if MM and SC could block the effects of sodium salicylate (SS), behavioral and physiological assessments were carried out on rats. Behavioral assessment of tinnitus was carried out with Schedule Induced Polydipsia Avoidance Conditioning. Rats were trained to lick for water during quiet intervals and to avoid licking when a real sound was present. The number of lick-in-quiet remained high and within the normal range when rats were injected with saline or low-doses of SS (<150 mg/kg). Treatment with 150 mg/kg SS significantly decreased in licks-in-quiet, results consistent with the presence of tinnitus. MM alone in the range of 1.5-3 mg/kg had no adverse effect on licks-in-quiet. Co-administration of MM (1.5-3 mg/kg) plus SS caused a slight increase in licks-in-quiet, but the effect was not dose-dependent and failed to completely block tinnitus-like behavior. To identify the physiological effects of SS and MM, microwire electrode arrays were implanted into the auditory cortex and the local field potentials evoked by tone bursts were recorded from awake-animals before and after drug treatment. Tone burst evoked field potentials increased in amplitude (hyperactive) after SS treatment; however, co-administration of MM or SC failed to block the SS-induced amplitude increase. Behavioral assessment of SC on SS-induced tinnitus is currently underway. (Supported in part by American Tinnitus Association)

### **[953] Noise-Induced Physiological and Molecular Changes in Auditory Cortex-Potential Substrates for Tinnitus**

**Liyan Zhang<sup>1</sup>**, Wei Sun<sup>1</sup>, Guang Yang<sup>1</sup>, Edward Lobarinas<sup>1</sup>, Richard Salvi<sup>1</sup>

<sup>1</sup>*University at Buffalo*

Acoustic overstimulation, which frequently induces tinnitus with a pitch near the region of maximum hearing loss, reduces the neural output of the cochlea. Paradoxically, recent studies suggest that the reduced cochlear output triggers an increase in spontaneous activity in the central auditory system. Changes in spontaneous activity, both increases and decreases, have been observed at many sites along the auditory pathway following acoustic overstimulation; however, most of these measurements are confounded by anesthetics which have a profound

effect on the rate and pattern of spontaneous activity. To circumvent this problem, we implanted 16-channel microwire electrodes into rat auditory cortex (AC) and recorded spontaneous and sound evoked activity from single or multi-unit clusters in awake-animals before and after acoustic overstimulation (110 dB SPL, narrow band noise at 12 kHz, 2 h). Spontaneous and stimulus induced spike rates near the region of maximum threshold shift were reduced significantly immediately after the exposure and only partially recovered after 1 day. The reductions in neural activity seen immediately after acoustic trauma are likely to lead to changes in gene expression in the auditory cortex. To identify these changes, we used focused gene microarrays to search for significant changes in gene expression in the auditory cortex induced by noise-induced cochlear damage. Several members of the heat shock protein (HSP) gene family, that regulate stress related proteins, increased significantly in the noise exposure group. Although acoustic overstimulation directly damages the cochlea, stress responses are expressed as far centrally as the auditory cortex, possibly due to a high level of neural activity bordering on excitotoxicity. Some genes related with cell proliferation (cyclin-dependent kinase inhibitor 1A) and cell death (cathepsin D) are also been found increased after noise exposure.

Supported by the Tinnitus Research Consortium

### **[954] Auditory Object Normalisation in the Echolocating Bat *Phyllostomus Discolor***

**Maïke Schuchmann<sup>1</sup>**, Lutz Wiegrebé<sup>1</sup>

<sup>1</sup>*Ludwig-Maximilians-Universität*

Echolocating bats identify real, three-dimensional objects exclusively through the auditory analysis of echoes. They do so despite the variability of their emissions and the echoes from one occurrence to the next. Object information is encoded in its acoustic impulse response (IR), and much of the echo variability relates to the size of the object. For reliable object recognition, the auditory system must segregate information about object size from information about object structure. This results in a size-invariant object representation; the auditory object is normalised.

In this study, 5 individuals of the echolocating bat *Phyllostomus discolor* are trained to discriminate two IRs of virtual objects in a phantom-object playback experiment. When the animals had learned this task, scaled versions of the two IRs are presented. The bats' spontaneous classification of the scaled IRs as either IR1 or IR2 is assessed. Simulations based on the similarity of the auditory spectrograms suggest that these scaled IRs cannot be reliably classified as one of the trained IRs. Preliminary data indicate, however, that the bats tend to classify the scaled IRs correctly.

### **[955] Dynamic Object Analysis in Echo Imaging: Spectral Envelope Modulation Detection**

**Daria Genzel<sup>1</sup>**, Lutz Wiegrebé<sup>1</sup>

<sup>1</sup>*Ludwigs-Maximilians-Universität*

Bats can recognize three-dimensional objects by analyzing the echoes of their ultrasonic emissions. Most of the

information about object size is encoded in the impulse response. One impulse response of a three-dimensional object will only reflect the depth dimension unambiguously. Bats acquire more detailed information about an object by moving around the object and scanning it with a series of echolocation calls. When moving around the object, the magnitude spectra of the impulse responses and therefore the magnitude spectra of the echoes change dependent from which angle the object is ensonified. Stringing together object related information from the echoes will produce a three-dimensional image of the object. Our goal is to analyze the basic mechanisms with which the bat, *Megaderma lyra*, is able to reconstruct the three-dimensional shape of complex objects by perceptual integration of the information acquired through these echoes. We therefore are examining the detection threshold of *M. lyra* for variations in the spectral content of echoes. In a two-alternative-forced-choice procedure bats were trained to discriminate synthesized echolocation calls with time variant spectral envelope modulations from calls with time invariant spectral envelope modulations. The calls were filtered with a time invariant band pass filter (center frequency = 60 kHz) or with a band pass filter whose center frequency was sinusoidally modulated. The detection threshold of the spectral envelope modulations was measured by varying the modulation rate and depth of the time variant filtered calls. The results show that, at a modulation rate of 2 Hz, the bats were able to detect a frequency modulation depth of 13 kHz. Further results are still being acquired.

#### **[956] Perceptual Compensation of Spectral-Envelope Distortion in the Echolocating Bat *Phyllostomus Discolor***

**Holger R. Görlitz<sup>1</sup>, Mathias Hübner<sup>1</sup>, Lutz Wiegrebe<sup>1</sup>**

<sup>1</sup>Neurobiologie, Dept. Biologie II, Ludwig-Maximilians-University München, Germany

Echolocating bats live in an acoustically complex and highly variable environment. They use the temporal and spectral properties of the echoes of their calls for orientation and foraging. Yet, the spectral envelope of the echoes is altered by reverberation and interference, by atmospheric attenuation or masking by surrounding sounds. To assess the spectral envelope of an echo correctly, the bat's auditory system has to compensate for spectral effects of the environment's transfer function, but should retain spectral envelope changes caused by the reflector. We investigated the ability of bats to compensate for spectral envelope distortions of transient foreground stimuli superimposed on background noise of variable spectral shape. Perceptual compensation of the background-noise spectrum was assessed both in a passive-acoustic paradigm, where the foreground signals are filtered impulses, and in an active-acoustic paradigm, where the foreground consists of filtered versions of the bats' sonar emissions.

In a 2AFC paradigm, the bat *Phyllostomus discolor* learned to discriminate highpass- (+6 dB/oct.) from lowpass- (-6 dB/oct.) filtered impulses or echoes superimposed on white background noise (0 dB/oct.). In randomly interspersed test-trials, where the background

was either white or pink (-3 dB/oct.), bats were asked to spontaneously classify stimuli of variable intermediate spectral-envelope slopes as low- or high-pass.

With pink-noise background, bats classified impulses more often as being high-pass than with white-noise background. Thus, the bats perceptually compensated for the spectral envelope of the background, i.e., they evaluated the stimuli's spectral envelope relative to the background. Currently, we investigate the bats' perceptual compensation during active echolocation where the bats do not evaluate filtered impulses but filtered versions of their sonar emissions.

#### **[957] Phase Sensitivity in Bat Sonar Revisited**

**Sven Schoernich<sup>1</sup>, Lutz Wiegrebe<sup>1</sup>**

<sup>1</sup>LMU Munich

Whenever a bat echolocates, the echo it perceives consists of a convolution of the echolocation call and the impulse response (IR) of the ensonified object. An ongoing discussion in the investigation of echolocation regards the question if bats are able to extract this IR from the echo. In the time domain the IR is extracted by cross-correlating the echolocation call and the time-inverted echo. In the frequency domain, the IR is extracted by multiplying the magnitude spectra of echo and echolocation call and summing the phase spectra. Unfortunately, in the auditory system of the bat, the echo is represented neither solely in the time nor in the frequency domain, but as an auditory spectrogram. This means that the bat would have to use a combination of the two mentioned procedures. Here it is investigated to which extent the bat *Phyllostomus discolor* has access to the phase of a virtual-object's IR.

In a two-alternative, forced-choice playback setup, bats were trained to discriminate two IRs with identical magnitude spectra but different phase spectra. The adaptive parameter was the duration of the fft window over which the phase manipulation was applied. Preliminary results indicate that the fft window must be at least 250 µs for successful phase discrimination. These results and their numerical simulation suggest that phase sensitivity is limited by the temporal resolution of the peripheral auditory system, specifically, the inner-ear band-pass filtering and mechano-electrical transduction.

#### **[958] Auditory Sensitivity and Its Morphological Correlates in the Grasshopper Sparrow (*Ammodramus Savannarum*)**

**Bernard Lohr<sup>1</sup>, Otto Gleich<sup>2</sup>, Brenda M. Ryals<sup>3</sup>, Robert J. Dooling<sup>1</sup>**

<sup>1</sup>Department of Psychology, University of Maryland, College Park, MD, <sup>2</sup>ENT Department, University of Regensburg, Regensburg, Germany, <sup>3</sup>Department of Communication Sciences and Disorders, James Madison University, Harrisonburg, VA

The present study examined auditory sensitivity in a songbird with unusually high frequency vocalizations. Grasshopper sparrows (*Ammodramus savannarum*) produce little acoustic energy below 6 kHz, and have songs centered in the region of 7 – 9 kHz, higher than the

upper auditory limit of some other small passerines. We determined thresholds in this species using operant conditioning for frequencies between 0.5 and 13 kHz tested in 0.5 octave steps and measured basic morphological characteristics of the basilar papilla. Audiogram parameters were derived from a best-fit third-order polynomial of the raw data. Estimates of the frequency of best hearing and high frequency auditory limit for this species (based currently on data from 2 individuals) indicate that grasshopper sparrows hear best between 4 – 5 kHz and have an upper auditory limit (30 dB above best threshold) near 10 kHz. They thus have extended high frequency hearing compared to other songbirds. Neither the length of the basilar papilla (~ 2.3 mm), nor the number of hair cells (~ 3300) were unusual for birds of this size (16 –18 g). Our results suggest that while high frequency hearing in the grasshopper sparrow extends beyond that of typical passerines, papillar morphology is not fundamentally different from that of other songbirds. [Work supported by NIH].

### **959** Relative Saliency of Auditory vs. Visual Cues to Contact Call Production in Budgerigars

Michael Osmanski<sup>1</sup>, Robert J. Dooling<sup>1</sup>

<sup>1</sup>University of Maryland College Park

Humans are known to use both auditory and visual cues when perceiving speech sounds and that cross-modal integration of these cues results in enhanced performance. Here we examined the relative salience of auditory and visual cues in operant-controlled vocal learning in the budgerigar, a small Australian parrot. Previous experiments have shown that budgerigars can be easily trained to associate different contact calls with specific visual cues (e.g., a specific LED reliably elicits a particular call from the animal). We asked whether these birds can associate different contact calls with specific auditory cues (e.g., contact calls). Birds were first trained to produce two different contact calls, each one associated with a different auditory-visual cue (e.g., simultaneous presentation of one of the bird's own contact calls and one LED). Training was complete when the birds' percent correct exceeded 80%. We then removed the visual cue so that, on each trial, only one of the two auditory stimuli (i.e., one contact call) was presented. With the visual stimuli removed as cues, the birds had to rely on the auditory cue alone. Performance dropped to chance levels (i.e., 50%) under these conditions, suggesting that the birds had attended only to the visual cue. Budgerigars trained using only auditory cues (i.e., presentation of either contact calls or short-duration tones) could not be trained to produce a specific contact call to each cue; performance never exceeded chance levels. This striking, modality-specific, difference in learning ability appears to support previous evidence that the combination of auditory and visual experience (i.e., face-to-face social interaction) is a more powerful cue for call-learning in budgerigars compared to auditory experience alone. These findings will be the focus of future work. Supported by NIH DC-04664-01 A2 and NIH DC-006766 to MSO.

### **960** Masking of Songbird Communication

#### **Signals by Environmental Noise**

Nina Broel<sup>1</sup>, Ellouise Leadbeater<sup>2</sup>, Hans Slabbekoorn<sup>3</sup>, Georg M. Klump<sup>1</sup>, Ulrike Langemann<sup>1</sup>

<sup>1</sup>Oldenburg University, <sup>2</sup>University of London, <sup>3</sup>Leiden University

The detection of communication signals is influenced by masking environmental noise. Thus, communication signals can be expected to be optimally adapted for sound transmission and for the receiver's sensory system. Naturally occurring environmental noise in Middle Europe may be the wind induced noise of woodland habitats or the dawn chorus of song birds in temperate forests. The anthropogenic noise (e.g., traffic noise) mainly found in urban environments may hamper acoustic communication and therefore potentially influence species density (Slabbekoorn, Peet, 2003, *Nature* 424: 267). In the present study a song bird was used as a model species to test specific signal characteristics for their detectability in different kinds of environmental background noise.

Seven great tits (*Parus major*) were trained in a Go/NoGo paradigm to report the detection of test signals in a continuous noise background. The background matched the natural sound pressure level and spectral distribution of either urban or woodland environmental noise or consisted of a natural dawn chorus. Test signals were either great tit song elements (phrases of 2 or 3 elements) or consisted of synthetic elements that represented isolated features of natural song elements (sinusoids, multi-tone signals, FM sweeps, noise bands). Signal detection theory was applied to determine the level of the test signal at detection; threshold criterion was a *d'* of 1.8.

Repeated measures ANOVAs of preliminary data revealed that detection thresholds of song elements were significantly dependent on the background noise and song type presented. Thresholds for song signals with 3 elements were on average about 3 dB lower than for signals with 2 elements. Detection thresholds of synthetic elements did not differ for sinusoids and FM sweeps. Detection of signals with the acoustic energy spread over a wider frequency range was on average slightly worse than for signals of smaller bandwidth.

(Supported by the DFG, SFB/TRR 31)

### **961** Characteristics of the Illusory Franssen Effect in Birds

Micheal Dent<sup>1</sup>, Elizabeth McClaine<sup>1</sup>

<sup>1</sup>University at Buffalo, SUNY

The properties of the auditory illusion known as the Franssen Effect (FE) have been characterized in humans and also more recently in cats. It was not known, however, whether this illusion would occur in non-mammals, and if it did occur, if the characteristics would be similar. To elicit the FE, listeners are presented with a signal which has been split into two components and presented from symmetrically-placed lateral speakers. One of the components is known as the transient portion of the signal and contains an abrupt onset and immediately ramping offset, with a 50 ms total duration. The other component is the sustained portion of the signal and has a 50-ms

ramped onset, 350 ms steady-state portion, and 100 ms ramped offset. When these two signals are played to human and cat listeners simultaneously, under certain conditions (where the FE is said to be operating) the perception is that of a long-duration steady state tone at the location of the transient component only. In humans and cats, the conditions where this illusion is found include echoic listening environments and stimuli that are difficult to localize when presented singly. Here, we examined the FE in two species of birds: budgerigars and zebra finches. The spatial hearing abilities of these birds are well known and reveal that neither bird can be considered a localization "specialist". The birds were trained using operant conditioning methods on a categorization task to peck a left key when presented with a sound from a left speaker and to peck a right key when presented with a sound from a right speaker. Once training was completed, paired FE stimuli as described above were presented. Both species of birds exhibited the FE, although to varying degrees across conditions. These results show that a non-mammalian animal experiences the FE illusion in a manner similar to mammals, suggestive of similar auditory processing mechanisms for complex stimuli in confusing listening situations.

**[962] In Unpredictable Listening Conditions Lead-Exposed Chicks Respond Similarly to Children with Attention-Deficit Disorders**  
**Lincoln Gray<sup>1</sup>**

<sup>1</sup>*James Madison University*

Lead poisoning is a risk factor for attention deficits in children. Recent results show that children with ADHD are more affected by background sounds than control children (Gray et al. 2002 *Int J Ped Otorhinolaryngol* 66:265). To explore a possible parallel in an animal model, normal and lead-exposed chicks were tested for their ability to detect a 250 Hz tone in the presence of a 500-800Hz masker. Since all components of the masker are at least an octave away from the signal, any masking would be of the non-sensory or distraction type rather than energetic masking at a cochlear level. Lead-exposed birds needed a higher signal level for a given level of responsiveness in the presence of this masker (Gray, ARO, 2005). Thus, lead-exposed chicks are detrimentally affected by background sounds in a way that is similar to children with ADHD.

Chicks had blood lead levels of 20µg/dl, a level considered safe by the CDC in 1991 and a level experienced by many American children and even more worldwide (mean levels in India are 18 µg/dl, for example).

If listening conditions become sufficiently unpredictable, normal children behave as if they had an attention deficit. That is, there is no effect of ADHD under highly unpredictable masking conditions. To explore further parallels in the animal model, normal and lead-exposed chicks were tested under unpredictable listening conditions. The test was the same as above except the sampling rate of the digital-to-analog converter was randomly changed (70-110% of base) twice per second. Both the masker and signal thus varied randomly in frequency by up to 50% every 500 ms. Under these

conditions there was no difference between normal and lead-exposed birds. The unpredictable listening conditions made the normal birds behave as if they were "lead-ed". This is conceptually similar to the effect of informational masking, which makes normal children behave as if they had an attention deficit.

Supported by NIH Grant RO1-DC4303.

**[963] Behavioral Studies of Tinnitus in Domestic Cats**

**Stephanie Brown<sup>1</sup>, Brad May<sup>1</sup>**

<sup>1</sup>*Dept. of Otolaryngology-HNS, Johns Hopkins University*

Prior studies have confirmed behavioral correlates of tinnitus in animal models as a context for exploring the physiological basis of the impairment. Behavioral tinnitus is manifested by changes in the discrimination of stimulus parameters such as silent intervals in background noise. Experimentally induced discrimination deficits are assumed to indicate the masking of objective acoustic information by subjective tinnitus percepts. This presentation introduces a variant of the animal psychophysical approach that has been adapted for the longterm assessment of tinnitus-like behaviors in domestic cats. Because tinnitus is induced in our subjects by sound exposure, procedural controls are offered as quantifiable measures of tinnitus loudness and to distinguish the subjective perception of 'phantom sounds' from noise-induced hearing loss. Our related neurophysiological studies suggest that the physiological consequences of tinnitus are not conveyed by global changes in brain activity, but rather by discrete neural populations that may be identified by their sharpness of tuning, temporal response patterns or proximal relationship to the exposure stimulus. From this perspective, domestic cats represent an ideal preparation for linking well characterized physiological response types in the central auditory system to the currently unknown mechanisms of tinnitus generation.

Funded by a grant-in-aid from the Tinnitus Research Consortium.

**[964] Comodulation Masking Release Determined in the Mouse (*Mus Musculus*) Using a Band-Narrowing Paradigm**

**Verena Weik<sup>1</sup>, Karin Klink<sup>1</sup>, Georg M. Klump<sup>1</sup>**

<sup>1</sup>*Oldenburg University*

Hall et al. (1984, *JASA* 76: 50) described an improved detection of a signal in a band-limited noise masker that exhibits correlated amplitude fluctuations (i.e., comodulation) over a wide range of frequencies compared to the detection of the signal in an unmodulated masker of the same bandwidth. They introduced the term "Comodulation Masking Release" (CMR) for this effect. There is some debate whether within-channel cues that can be extracted from a single auditory filter centered on the signal frequency or across-channel cues that are computed by the auditory system comparing the excitation across separate auditory filters contribute to this effect (e.g., Verhey et al. 1999, *JASA* 106: 2733). Using the psychoacoustic paradigm developed by Hall et al. (1984),



we determined the amount of CMR in the house mouse, a species that has its best hearing at frequencies of 10 kHz and above and has an auditory-filter bandwidth that is much larger than the bandwidth above which CMR usually is observed.

We determined psychophysical thresholds for detecting an 800-ms 10-kHz tone in noise with a bandwidth ranging from 0.1 to 20 kHz that was either comodulated or unmodulated in four NMRI mice and three C57BL/6 mice. At a frequency of 10 kHz, the auditory filter bandwidths of the NMRI mouse and the C57BL/6 mouse were 3.3 kHz and 5.1 kHz, respectively. In both mouse strains we found a considerable CMR (range 5.7 to 12.8 dB) for masker bandwidth of 0.4 kHz and above. CMR was reduced considerably for bandwidths of 0.2 kHz. At a masker bandwidth of 0.1 kHz no significant difference was observed between the signal-detection threshold in comodulated and unmodulated noise indicating no masking release at this bandwidth. The data suggest that within-channel cues are sufficient to explain CMR in the mouse which is consistent with a model that was used to explain CMR in humans in this paradigm (Verhey et al. 1999).

Supported by the Deutsche Forschungsgemeinschaft

### **965 The Effect of Stimuli Variables on Infants' Perceptions of Transposed Melodies**

**Daniella Kim<sup>1</sup>, Lynne Werner<sup>1</sup>**

<sup>1</sup>*University of Washington*

Musical pitches are defined by both frequency and chroma (note name). Demany and Armand (1984) suggested that infants, like adults, perceive octave-separated notes as having the same chroma. Previously, we reported replication data based on Demany and Armand's original experiment (Kim & Werner, 2004). We tested infants' and adults' perceptions of 7<sup>th</sup> and 9<sup>th</sup> chroma transpositions of a 3-note melody. We reported generally no difference between infants and adults in the way that they responded to 7<sup>th</sup>, 9<sup>th</sup> and octave transpositions, confirming Demany & Armand's original results. Changing stimulus variables or the "structure of the input" has been shown to affect subjects' perceptions of musical pitch (Saffran, et al, 2005). To further explore the effect of stimuli variables on subjects' perceptions of pitch, we systematically tested infants and adults as before, using a new melody. We also tested effect of major or minor key (mode) on perception of pitch. All subjects were tested using an observer-based psychoacoustic procedure. As before, all subjects were tested in 2 conditions. In the MELODY condition, subjects heard the new standard 3-note melody randomly played in 1 of 4 octaves. In the NOTE condition, subjects heard each note of the new 3-note melody randomly transposed to 1 of 4 octaves. This manipulation created a "scrambled melody" with notes the same chroma (octave) as the original melody, but with new frequencies. Target stimuli were transposed either a 7<sup>th</sup> or 9<sup>th</sup>. In both conditions, subjects were trained to respond to only chroma changes, and not octave transpositions. The number of trials that were needed to learn to respond to chroma changes were recorded. As before in the replication study, there was again no difference between infants' and adults'

performance in both conditions. 65% of the infants and 90% of the adults tested reached an 80% correct criterion in 19 trials. Infants and adults performed surprisingly similarly in this perceptual test of octave equivalence, although the melody was new and we introduced mode. We conclude, based on these data and the data from the 1<sup>st</sup> replication study, that infants and adults can identify chroma changes and ignore octave transpositions in a similar fashion, even with stimulus manipulations. These data are in agreement with Demany and Armand's original data.

### **966 The Effect of Frequency on Reaction Time for Listeners with Normal Hearing**

**Michael Epstein<sup>1,2</sup>, Mary Florentine<sup>1,2</sup>**

<sup>1</sup>*Northeastern University - Dept. of Speech-Language Pathology and Audiology*, <sup>2</sup>*Institute for Hearing, Speech, and Language*

Because reaction time (RT) is correlated with loudness, RTs have been used to study Softness Imperception (Florentine et al., 2004), which is the inability to hear soft sounds. Measures of RT near threshold are used to indicate whether some listeners with hearing losses of primarily cochlear origin experience greater loudness at elevated thresholds than at normal thresholds. These measurements have been based on the assumption that RTs near threshold are not affected by stimulus frequency. In order to test this assumption and to gain an understanding of how RT is affected by frequency, RTs to 1-kHz and 4-kHz tones for 16 normal listeners were measured across a wide range of sensation levels (SLs). Statistical analyses indicate that RTs are affected by frequency in some listeners. This effect is most common at low SLs, but also may be present at other SLs. Learning effects could not account for the observed differences between RTs at the two frequencies. Although RT--especially at low levels--is affected by stimulus frequency in some listeners in the 1- to 4-kHz range, the effect is not large enough to account for the differences in RTs measured in some impaired listeners.

### **967 Desynchronizing Effects of Noise on Cortical Evoked Potentials in Normals and in Individuals with Auditory Neuropathy (AN)**

**Henry J. Michalewski<sup>1</sup>, Tin Toan Nguyen<sup>1</sup>, Arnold Starr<sup>1</sup>**

<sup>1</sup>*University of California, Irvine*

Understanding speech in a noisy environment is a major problem in individuals with disordered hearing, and in particular, for auditory neuropathy (AN) subjects. Noise masking can cause a reduction in both the number of neurons responsive to signals due to a 'line busy' and to a desynchronization of activity in the population of remaining to respond. We studied 12 normal hearing subjects and 8 individuals with auditory neuropathy using both behavioral measures (reaction times, accuracy) and cortical evoked potentials. Tones (1 kHz, 100 ms duration, ranging between 100 – 40 dB SPL in 10 dB steps) were presented in silence or in continuous broadband noise (90 dB SPL) in separate conditions. Cortical N100 potentials from midline scalp sites (Fz, Cz, and Pz) were recorded and processed;

averages to tones in silence and in noise were computed. Measures of peak latency were analyzed and only the results of N100 from Cz are described here. In normals, N100 latencies to tones in silence were gradually prolonged from 100 ms (100 dB) to 135 ms (40 dB) with the largest latency increases occurring at 50 dB and 40 dB levels. The addition of broadband noise masked cortical responses so that only the tones between 100 dB (S/N ratio +10) to 70 dB (S/N ratio -20) could still be identified. N100 latencies were significantly delayed in noise compared to silence at all levels between 100 dB (115 ms) and 70 dB (165 ms). The function relating N100 latency and dB level was fitted by a quadratic polynomial ( $r = .99$ ) in each condition. In AN subjects, N100 latencies to tones in silence were prolonged in latency compared to normals and the extent of the delay was similar to normals in noise. These results suggest that auditory cortical activity in AN in silence has latency delays similar to auditory cortical events in normal subjects in the presence of broadband noise. Both desynchrony and deafferentation are candidate mechanisms for these latency delays. Supported by: NIH DC-02618

### **[968] The Influence of Level on Spectral Weighting Functions** **Jennifer Lentz<sup>1</sup>**

<sup>1</sup>*Indiana University*

This experiment tested whether the different spectral weighting functions measured in normal-hearing and hearing-impaired listeners (Lentz and Leek, 2003; JASA) were related different strengths of the cochlear nonlinearity. Spectral weights for a profile-analysis task were measured in normal-hearing listeners at three stimulus levels: 35, 60, and 85 dB SPL per component. Stimuli were the sum of six tones spaced equally on a logarithmic frequency scale ranging from 200 to 5000 Hz. Listeners detected a spectral change in which the three low-frequency components decreased in level and the three high-frequency components increased in level. Spectral weights that reflect the relative importance of each frequency component on a decision variable were estimated using a correlation technique. Results indicated that stimulus level influenced the pattern of weights across frequency. The weighting functions showed that the weights at the edge of the spectral change (components 3 and 4) were enhanced at the 60-dB stimulus level when compared to the 35- and the 85- dB stimulus level. The enhancement of weights at the spectral edge at a moderate stimulus level is consistent with the level-dependent activity of the cochlear nonlinearity. [Work supported by NIH (DC005835).]

### **[969] Melody Recognition with Binaural-Pitch Stimuli in Normal-Hearing and Hearing-Impaired Listeners**

**Sébastien Santurette<sup>1</sup>**, Torsten Dau<sup>1</sup>

<sup>1</sup>*Centre for Applied Hearing Research, Technical University of Denmark*

When two white noises differing only in phase in a particular frequency range are presented simultaneously

each to one of our ears, a pitch sensation may be perceived inside the head. This phenomenon, called 'binaural pitch' or 'dichotic pitch', can be produced by frequency-dependent interaural phase-difference patterns. The evaluation of these interaural phase differences depends on the functionality of the binaural auditory system and the temporal fine-structure information at its input. Several experiments were performed including the detection and discrimination of binaural pitch, and melody recognition using different types of binaural pitches. Normal-hearing listeners and hearing-impaired listeners with different kinds of hearing impairment participated in the experiments. For the normal-hearing listeners, all types of binaural pitches could be perceived immediately and were musical. The hearing-impaired listeners could be divided into three groups based on their results: a) some perceived all types of binaural pitches, but with decreased salience or musicality compared to normal-hearing listeners; b) some could only perceive the strongest pitch types; c) some were unable to perceive any binaural pitch at all. The performance of the hearing-impaired listeners was not correlated with audibility. The experimental results were only to some extent consistent with predictions from the modified equalization-cancellation model (Culling et al., 1998), suggesting that different mechanisms might be involved in the perception of different types of binaural-pitch signals. Overall, binaural pitch stimuli could be very useful within clinical diagnostics for detecting auditory deficits that are linked to temporal processing of sounds. Temporal fine-structure information has also been demonstrated to play a major role in speech intelligibility.

### **[970] Spectral Weights for Level Discrimination in Quiet and in Noise**

**Lori Leibold<sup>1</sup>**, Hongyang Tan<sup>1</sup>, Samar Khaddam<sup>1</sup>, Walt Jesteadt<sup>1</sup>

<sup>1</sup>*Boys Town National Research Hospital*

Doherty and Lutfi (1996) examined the perceptual weights listeners assign to the individual components of a multi-tone complex during a level discrimination task and reported that hearing-impaired listeners consistently gave the most weight to frequency components in the region of their high-frequency hearing loss. In contrast, weighting patterns obtained in listeners with normal hearing varied. In the current study, the relation between perceptual weight and sensation level was examined by measuring weights from normal-hearing listeners in quiet, in the presence of high-pass noise, and in the presence of low-pass noise. Following Doherty and Lutfi, stimuli were 300-ms, multi-tone complexes consisting of the 6 octave frequencies between 250-8000 Hz. Levels of the individual components in the signal and nonsignal complexes were selected at random on each trial from a normal distribution with a range of 25 dB. The complexes were identical except for a level increment added to each component in the signal complex. A signal and a nonsignal complex were presented in random order on each 2IFC trial. Listeners were instructed to indicate the interval containing the more intense complex. The mean level of each component for the signal and nonsignal complexes was 65 and 62.5 dB SPL, respectively, in the quiet condition

compared with 80 and 75 dB SPL in the noise conditions. Listeners were also tested in quiet at the more intense levels used the noise conditions. Ten 100-trial blocks were run for each condition. Weights were estimated using a conditioned-on- single-stimulus (COSS) analysis based on the trial-by-trial data. Consistent with Doherty and Lutfi, subjects assigned roughly equal weight to all components in the quiet condition but assigned more weight to the 4000-Hz component in the high-pass noise condition. Weights in the other two conditions, however, resembled those obtained in the high-pass noise. This suggests that neither the degree of hearing loss nor the sensation level of the tones was the primary cause of the effect that Doherty and Lutfi observed.

Supported by the NIH

### **971 Processing of Intensity in Children**

**Emily Buss<sup>1</sup>**, Joseph Hall<sup>1</sup>, John Grose<sup>1</sup>

<sup>1</sup>UNC Chapel Hill

There are several studies in the literature suggesting that children have elevated thresholds for both intensity discrimination and for amplitude modulation detection. Previous work on intensity discrimination for gated stimuli suggests that thresholds may be elevated due to higher levels of internal noise in children. One of the current experiments investigated whether a factor contributing to the high thresholds of the children was memory for loudness. In one condition stimuli were gated, such that intensity increment detection relied on memory for loudness across intervals. In another condition stimuli were continuous, such that intensity increment detection could be based on detecting a dynamic change in level. Results suggest that memory did not play a substantial role in children's performance. Further conditions compared performance for intensity increment detection for a continuous pure tone carrier to modulation detection thresholds (10-Hz AM) for a continuous tone. Preliminary data suggest that there may be a smaller developmental effect for modulation detection than for increment detection, a result which will be discussed in terms of a multiple looks hypothesis.

[This work was supported by NIH, RO1 DC00397.]

### **972 Spectral Envelope Perception as a Function of Age and Degree of Hearing Loss**

**David A. Eddins<sup>1,2</sup>**, Robert D. Frisina<sup>2</sup>, Frances M. Mapes<sup>2</sup>, Patricia Guimaraes<sup>2</sup>

<sup>1</sup>Department of Otolaryngology, University of Rochester,

<sup>2</sup>International Center for Hearing & Speech Research, Rochester Institute of Technology, Rochester, NY

Spectral envelope perception was investigated using a spectral modulation detection task in which sinusoidal spectral modulation was superimposed upon a noise carrier. The principle goal of this study was to characterize spectral envelope perception in terms of listener age and hearing sensitivity as estimated using the pure-tone audiogram. The spectral modulation detection task involved discrimination of a noise carrier with a flat spectral envelope from a noise having a sinusoidal spectral envelope across a logarithmic audio frequency scale. The

noise carrier had a bandwidth of 3 octaves (400 – 3200 Hz), a spectrum level of 40 dB SPL, and a duration of 400 ms including 10-ms cosine-squared rise-fall envelopes. Modulation detection thresholds were estimated by varying the modulation depth (peak-to-valley difference in dB) required to discriminate modulated from unmodulated noise using a cued, two-interval, forced-choice paradigm with a three-down, one-up adaptive tracking strategy.

Plotting spectral modulation threshold as a function of modulation frequency (cycles/octave) results in a spectral modulation transfer function (SMTF). SMTFs for young-normal hearing listeners were bandpass in nature, with a minimum modulation detection threshold between 2 and 4 cycles/octave. SMTFs for elderly listeners with normal hearing were remarkably similar to those of the young, normal hearing listeners. SMTFs for listeners with mild and moderate hearing loss had a low-pass rather than a bandpass shape. This change in shape of the transfer function resulted from elevated modulation detection thresholds for modulation frequencies greater than 1 cycle/octave. The differences in spectral modulation detection observed among listener groups will be considered in terms of predictions based on changes in frequency selectivity and subsequent computations of excitation patterns for the spectrally modulated noises used in this study.

### **973 Spatial-Temporal Processing as a Function of Age and Hearing Loss**

**Robert D. Frisina<sup>1</sup>**, David A. Eddins<sup>1,2</sup>, Frances M. Mapes<sup>1</sup>, Patricia Guimaraes<sup>1</sup>

<sup>1</sup>International Center for Hearing & Speech Research, Rochester Institute of Technology, Rochester, NY,

<sup>2</sup>Department of Otolaryngology, University of Rochester

This project was designed to identify any changes in the ability to perceive temporal gaps marked by acoustic signals distributed across auditory space as a function of age and/or hearing loss and to examine possible relationships among these measures and speech perception in noise. The main experiment used noise stimuli presented in sound field in which the spatial location of the pre-gap burst was fixed at 90 degrees (left ear) while the spatial location of the post-gap burst was systematically varied (90 degrees left, 90 degrees right, or both) resulting in conditions termed left/left, left/right, and left/both. The spectrum of the noise was shaped by the audiogram such that the sensation level of the stimulus delivered to the loudspeakers was fixed across frequency and across listeners. The pre-gap noise burst duration was 40 ms and the post-gap burst duration was 140 ms. The offset of the pre-gap burst and the onset of the post-gap burst were shaped with linear ramps 1-ms in duration. The overall stimulus was shaped by a 5-ms cosine squared window. To further limit the possible perception of transients associated with the temporal gap, a low-pass (10,000 Hz) background noise was presented at a spectrum level of 30 dB below the peak level of the stimulus carrying the gap. For normal hearing listeners, gap-detection thresholds were shortest for the left/left and left/both conditions and were slightly higher in the left/right condition. Gap-detection thresholds for elderly listeners were significantly longer in the left/right and left/both

conditions than young listeners regardless of the presence or degree of hearing loss. Data will be compared to measures of the recognition of NU-6 monosyllabic words presented in multi-talker babble at a signal-to-noise ratio of 8 dB as well as to data from the HINT test.

#### **974 Analysis of B Cells in Murine Cervical Lymph Node**

**Seung Geun Yeo**<sup>1</sup>, Moo-Jin Baek<sup>1</sup>, Jae Yong Byun<sup>1</sup>, Chang Il Cha<sup>1</sup>, Dong Choon Park<sup>2</sup>

<sup>1</sup>Department of Otolaryngology, <sup>2</sup>Department of Obstetric and Gynecology

This study was aimed to investigate the characteristic feature of cervical lymph node B cells and the possibility that cervical lymph node B cells located there behave differently than B cells located elsewhere because they may be subjected to continual antigenic stimulation from naso- or oropharynx. We obtained cervical lymph node, spleen and peritoneal fluid of mice. Isolated B cells were cultured in medium and after the addition of several stimuli. The expression of various surface molecules to characterize lymphoid B cells were analyzed by flow cytometry. Immunoglobulin secreted into the culture supernatants was evaluated by enzyme-linked immunosorbent assay. B220+ cells cultured for 5 days with medium alone, or LPS. Entering of S phase in response to stimuli was measured by proliferative assay. Identifying phenotypic characteristics of B cells of lymph node include CD5low, CD23high, CD43low, B220high, slg Mlow, slgDhigh, B7.1low, B7.2low, and Syndecam-1low. Spontaneous Immunoglobulin production did not occur in lymphoid B cells. When stimulation, IgM secretion was increased more than that of IgA and IgG. In thymidine incorporation, B cells were entered actively S phase after 48hours stimulation. Our results show that B cells in cervical lymph node are conventional B cells(B2) like splenic B cells.

#### **975 EP2/EP4-Receptor-Mediated PGE2 Inhibition of Upper Airway Fibroblast Migration and Contraction In Vitro**

**P.A. Hebda**<sup>1</sup>, A. Parekh<sup>1</sup>, V.C. Sandulache<sup>1</sup>, A.C. Palbus<sup>2</sup>, J.E. Dohar<sup>1</sup>

<sup>1</sup>Children's Hospital of Pittsburgh/University of Pittsburgh, <sup>2</sup>Chatham College

Prostaglandin E2 (PGE2) is an important inflammatory mediator that has been linked to the inhibition of lower airway fibrosis following injury. PGE2 exerts a wide variety of cellular effects by binding to four E-prostanoid (EP) receptors coupled to intracellular secondary messengers Ca<sup>2+</sup> and cyclic AMP (cAMP). PGE2 has been shown to regulate the migratory and contractile properties of lower airway fibroblasts via EP2 and/or EP4 cAMP-dependent alterations of the actin cytoskeleton. This study was designed to, for the first time, address the mechanisms by which PGE2 regulates upper airway fibroblast migration and contraction. These two properties are crucial components of proper fibroblast activity during tissue repair (wound healing). The hypothesis is that PGE2 will inhibit upper airway fibroblast migration and contraction. Migration was tested using a standard in vitro cell

monolayer scratch assay while contraction ability was evaluated using a free floating collagen gel model. The effects of PGE2 and specific EP receptor agonists were tested on primary cultures of upper airway fibroblasts derived from fetal and adult human mucosa as well as pathological tissue from three cases of subglottic stenosis. PGE2 was found to inhibit migration in all cell types; this effect was mimicked by EP2 and EP4 agonists and by a direct pharmacological activator of adenylate cyclase, indicating a cAMP-dependent process. The effects of PGE2 on fibroblast contractility of free floating collagen gels was consistent with its effects on two dimensional fibroblast migration. Inhibition of fibroblast migration and collagen gel contraction coincided with a disruption of the actin cytoskeleton. The conclusion of this study is that PGE2 can inhibit upper airway fibroblast migration and contraction, essential components of fibroblast activity in a wound bed. As such, it is likely that modulation of levels of PGE2 in the upper airway may alter the course of mucosal wound healing and scar formation.

#### **976 Comprehensive Analysis of the Expression of Cancer-Testis Antigens as Possible Targets for Antigen-Specific Immunotherapy in Patients with Head and Neck Squamous Cell Carcinoma**

Inga Blum<sup>1</sup>, Sören Wenzel<sup>1</sup>, Yanran Cao<sup>1</sup>, Katrin Bartels<sup>1</sup>, Christiane Faltz<sup>1</sup>, Kai Dikta<sup>2</sup>, Susanna Hegewisch-Becker<sup>1</sup>, Carsten Bokemeyer<sup>1</sup>, Djordje Atanackovic<sup>1</sup>, Rudolf Leuwer<sup>2</sup>

<sup>1</sup>Hamburg University Medical School, <sup>2</sup>Klinikum Krefeld

**Background:** Cancer-Testis (CT) antigens are by definition expressed in tumor but not in healthy tissue except testis. These genes might, therefore, represent ideal targets for antigen-specific immunotherapy. Here, we present the first comprehensive analysis of CT antigen expression in patients with head and neck squamous cell carcinoma (HNSCC).

**Methods:** Tumor samples and adjacent healthy tissue from 54 patients with HNSCC were analyzed for the expression of 26 genes previously designated CT antigens using rt-PCR.

**Results:** According to their expression pattern antigens were divided into four groups. ADAM2, TPTE, LDHC, SPO11, MORC, TPX1 were expressed neither in tumor samples nor in adjacent healthy tissue. SCP-1, AKAP-3, CTAGE, ZNF165, CAGE, FTHL17, SLLP1 were expressed in both tumor samples and adjacent healthy tissue at comparable levels. NY-TLU-57, GAGE1, SAGE were overexpressed in tumor samples in the sense that numbers of positive samples were at least 50% higher among tumorous than among healthy tissues. 10 CT antigens were expressed only in the tumor tissue and thus should represent ideal candidates for active immunotherapy: MAGE3 was expressed in 67%, SSX1 in 40%, MAGEE1 in 37%, MAGEC1 in 30%, SSX2 in 16%, BAGE in 15%, ESO-1 in 9%, CSAGE in 8%, HOM-TES-85 in 7%, and LIPI in 2% of cases. 83% of the tumor samples expressed at least one of the latter 10 CT antigens, 64% expressed at least two, and 42% expressed at least three CT antigens.

**Conclusions:** In this first comprehensive analysis, we demonstrate that patients with HNSCC show a frequent

expression of CT antigens. Furthermore, a relatively high percentage of patients expressed more than one CT antigen opening the perspective for polyvalent vaccination therapy. Since, in the case of HNSCC local recurrences following surgery/radiotherapy are common, antigen-specific immunotherapy using CT antigens as targets could, in these patients, represent a promising adjuvant therapy without significant side effects.

### **[977] Auditory Brainstem Implants in Profound Hearing Loss Associated to Post Meningitis Cochlear Ossification**

**Alexis Bozorg Grayeli**<sup>1,2</sup>, Michel Kalamarides<sup>3</sup>, Didier Bouccara<sup>1</sup>, Evelyne Ferrary<sup>1,2</sup>, Emmanuelle Ambert-Dahan<sup>1</sup>, Martine Smadja<sup>1</sup>, Olivier Sterkers<sup>1,2</sup>

<sup>1</sup>Beaujon Hospital, Otolaryngology department, <sup>2</sup>Inserm, EMI-U 0112, <sup>3</sup>Beaujon Hospital, Neurosurgery Department

**Objective:** The aim of this study was to evaluate the performances of auditory brainstem implants (ABI) in patients with profound hearing loss associated to bilateral cochlear ossification after bacterial meningitis

**Material and method:** Between 1999 and 2004, 3 adult patients with profound hearing loss and totally ossified cochleas secondary to a bacterial meningitis underwent auditory brainstem implantation. The ABI (Nucleus 22, Cochlear, Lane Cove, Australie) was placed through a retrosigmoid approach in 2 cases and a translabyrinthine approach in one case. The placement of the electrode array was verified by electrically evoked auditory brainstem response and the intraoperative monitoring of the cranial nerves 7, 9 and 11. The postoperative follow-up is 5 years, 2 years and 6 months for these 3 patients. The discrimination of open-set dissyllabic words and sentences was assessed in lip-reading (LR), LR and ABI, and ABI alone conditions.

**Results:** No technical problem was encountered during the implantation and the postoperative course was uneventful. With LR alone the word recognition score was 0, 70, and 30% in our 3 patients. The number of activated electrodes was 11, 14 and 15 respectively. The word recognition with ABI alone was 40, 70 and 0%. LR combined to ABI increased this performance to 90, 90, and 50% respectively. Sentence recognition scores followed a similar trend.

**Conclusion:** ABI is an efficient mean of profound hearing loss associated to total cochlear ossification secondary to bacterial meningitis. These functional are comparable to those of cochlear implants in postmeningitis hearing loss with patent cochleae.

### **[978] Round Window Mechanical Stimulation for Severe Mixed Hearing Loss**

**Vittorio Colletti**<sup>1</sup>, M. Carner<sup>1</sup>, L. Sacchetto<sup>1</sup>, L. Colletti<sup>1</sup>, N. Giarbini<sup>1</sup>

<sup>1</sup>University of Verona

Middle ear implantable (MEI) devices may be indicated to restore hearing in patients with sensorineural hearing loss (SNHL) who fail to benefit from hearing aids. The first available MEI devices were designed for unresolved middle ear conductive/mixed hearing losses (Suzuki et al,

1985). Subsequently, the indications shifted to patients with well functioning ossicular chains (OCs) and pure SNHL. We believe that the MEI prostheses may still be indicated in patients with mixed congenital or acquired hearing loss with defects of the OC or without OC after unsuccessful operations. The floating mass transducer (FMT) of the MEI prosthesis should be placed on the round window membrane (RWM). Thus, the classic cochlear stimulation mechanism is inverted, with a similar or even better final outcome on the cochlear partition.

This study considers seven patients with severe mixed hearing loss due to congenital or acquired external and/or middle ear defects previously treated unsuccessfully with reconstructive surgery; and one patient with SNHL previously treated with the Vibrant Soundbridge (VSB) with the traditional technique.

A transmastoid approach with posterior tympanotomy in non operated patients and a revision of the radical mastoidectomy or tympanoplasty was performed in operated patients. Reshaping of the RW area was necessary for fitting the transducer, placed in front of the RWM and covered with temporalis fascia. No complications were observed; all patients were discharged 1-2 days after surgery. Activation was performed during surgery under local anaesthesia in 1 patient and from 1-3 days postoperatively in the 7 patients operated on under general anaesthesia.

The improvements in threshold and speech testing indicate that this approach is ideal for patients with mixed hearing losses due to congenital or acquired defects of the external and middle ear, if the cochlea has not been damaged and in patients obtaining limited benefit from a VSB applied on the incus.

### **[979] Inner Ear Anomalies in Korean Cochlear Implantees: Classification by Computed Tomography Measurements**

**Hyun Joon Shim**<sup>1</sup>, Jung Eun Shin<sup>2</sup>, Jong Woo Chung<sup>1</sup>, Kwang Sun Lee<sup>1</sup>

<sup>1</sup>Department of Otolaryngology, Asan Medical Center, University of Ulsan College of Medicine,

<sup>2</sup>Department of Otolaryngology, Kunkuk University College of Medicine

**Objective:** The objective of this study was to classify the inner ear anomalies of cochlear implantees with profound sensorineural hearing loss (SNHL). To classify anomalous cochleovestibular anatomy, predetermined designated areas of the inner ear structures were numerically measured in ears with normal bone-conduction thresholds and in ears with profound SNHL.

**Material and Methods:** The normative data of the inner ear structures were measured in 120 ears with normal bone-conduction threshold (<15 dB) and were applied to 570 ears of cochlear implantees with profound SNHL. Predesignated inner ear structures were measured in temporal bone computed tomography (TBCT) images from the normal and cochlear-implantation groups using a computer-based caliper that formed part of a picture archiving and communication system. Six identifiable structures were measured in axial and coronal TBCT images. The inner ear anomalies were defined when the

structures presented visually obvious malformations or the measurements deviated 2 standard deviations from the means in the normative data. The data were analyzed using the chi-square test and Fisher's exact test.

**Results:** The application of normative data to 570 profound-SNHL ears resulted in the identification of 293 individual anomalies in 127 anomalous ears. An enlarged vestibular aqueduct was the most common individual anomaly (49 cases), followed by vestibular enlargement (38 cases), other semicircular canal dysplasia (37 cases), and shortened cochlea (34 cases). When the individual anomalies were re-accounted according to the more prominent anomaly where multiple anomalies were present in each ear, incomplete partition type II was the most common (34 ears), followed by cochlear hypoplasia (22 ears) and incomplete partition type I (20 ears).

**Conclusion:** We established a method of deriving normative measurements of the inner ear structures using computed tomography. Using these normative data, we classified the inner ear anomalies of profound SNHL ears in cochlear implantees.

### **980** **Diagnosis of Congenital Cytomegalovirus Infection in Patients with Sensorineural Hearing Loss Using Preserved Umbilical Cords**

**Terukazu Mizuno**<sup>1</sup>, Saiko Sugiura<sup>1</sup>, Hiroshi Kimura<sup>2</sup>, Yukihiko Nishiyama<sup>3</sup>, Tsutomu Nakashima<sup>1</sup>

<sup>1</sup>Department of Otorhinolaryngology, Nagoya University,

<sup>2</sup>Department of Pediatrics and Virology, Nagoya

University, <sup>3</sup>Department of Virology, Nagoya University

Cytomegalovirus (CMV) is the most frequent congenital infection in humans. Congenital CMV infection has been identified as one of the leading causes of sensorineural hearing loss (SNHL) in children. The large majority of infected newborns are asymptomatic, although they are at risk for developing SNHL. In most asymptomatic infants the diagnosis of congenital CMV infection is missed during the neonatal period. Retrospective diagnosis of congenital CMV infection is difficult. There is a Japanese tradition to dry and store the umbilical cord of newborns. We investigated whether CMV DNA exists in the preserved umbilical cords from patients with SNHL using real-time polymerase chain reaction method. Thirty seven patients with SNHL were enrolled. The study population consisted of 5 groups (group A, 10 patients with bilateral SNHL, onset under 7 years old; group B, 11 patients with unilateral SNHL, onset under 7 years old; group C, 3 patient with bilateral SNHL, onset over 7 years old; group D, 9 patients with unilateral SNHL, onset over 7 years old; group E, 4 patients with enlarged vestibular aqueducts). Umbilical cords had been preserved for 2 months to 52 years (mean, 16.7 years). To examine whether analyzable DNA exists in preserved umbilical cords, detection of human actin DNA by real-time PCR was done at the same time. Out of 37 umbilical cords, actin DNA could be detected in 34. CMV DNA was detected in 3 patients in group A. CMV DNA was not detected in other groups. These results suggest that detection of CMV DNA from preserved umbilical cords is useful for the retrospective diagnosis of congenital CMV infection.

### **981** **Randomized, Double-Blind, Placebo-Controlled, Dose-Titration Study with Latanoprost Salt in Meniere's Disease**

**Helge Rask-Andersen**<sup>1</sup>, Ulla Friberg<sup>1</sup>, Dan Bagger-Sjöbäck<sup>2</sup>, Ann-Charlotte Hessén-Söderman<sup>2</sup>, Johan Bergenius<sup>2</sup>, Esma Idrizbegovic<sup>3</sup>, Anna Granath<sup>3</sup>, Leif Hergils<sup>4</sup>, Dag Hydén<sup>4</sup>, Marianne Johansson<sup>5</sup>, Johan Stjernschantz<sup>5</sup>

<sup>1</sup>Uppsala University Hospital, <sup>2</sup>Karolinska Hospital,

<sup>3</sup>Karolinska University Hospital Huddinge, <sup>4</sup>Linköping University Hospital, <sup>5</sup>Synphora AB Sweden

**Objective:** Latanoprost, a PGF2 $\alpha$  analogue which is widely used for glaucoma treatment, was recently shown to alleviate symptoms of Meniere's disease in a short-term, double-blind, placebo-controlled study (Otolaryngology-Head and Neck Surgery 133; 441-443). The purpose of the present study was to investigate whether a dose-response relationship can be obtained with latanoprost salt in the inner ear.

**Methods:** 34 patients with unilateral Meniere's disease were enrolled in the study. Preservative-free latanoprost salt solution (50, 150 and 450  $\mu$ g/ml) was administered once daily during three consecutive days by intratympanic injection. A small control group in which the patients received latanoprost (ester) was also included. On days 5, 15 and 29 the patients underwent a thorough audiological examination. The study was randomized, double-blind and followed a parallel group design with respect to the dose groups. In each group, however, the patients received both latanoprost salt and placebo in random order according to a crossover protocol.

**Results:** Best effect was always obtained with the 450  $\mu$ g/ml dose in the primary variables; speech discrimination, PTA, tinnitus and vertigo (mean value of days 15 and 29). The two lower doses appeared to have no effect. Speech discrimination increased by 11.4%-units ( $p=0.05$ ), PTA was reduced by 2.6 dB ( $p=0.08$ ), and tinnitus loudness was reduced by 12.9 dB ( $p=0.04$ ). The number of vertigo attacks was 7 in the high dose group compared to 13 and 26 in the other groups. The effect was seen for up to 29 days.

**Conclusion:** A dose-response relationship appears to exist with latanoprost salt in the inner ear of patients with Meniere's disease. The most prominent effect was obtained in tinnitus loudness and speech discrimination. The results indicate that latanoprost salt exerts pharmacologic effect in the inner ear that could be beneficial in the treatment of Meniere's disease.

### **982** **High Rate Transtympanic Electrocochleography in Meniere's Patients Using Continuous Loop Averaging Deconvolution (CLAD)**

**Jorge Bohorquez**<sup>1</sup>, Krzysztof Morawski<sup>2</sup>, Ozcan Ozdamar<sup>1,3</sup>, Kazimierz Niemczyk<sup>2</sup>

<sup>1</sup>University of Miami, Department of Biomedical Engineering, <sup>2</sup>Medical University of Warsaw, <sup>3</sup>University of Miami, Department of Otolaryngology

Using the new Continuous Loop Averaging Deconvolution (CLAD) acquisition technique, it is now possible to record

evoked potentials at very high stimulation rates. CLAD uses less jittered sequences than the Maximum Length Sequence (MLS) technique thus reducing adaptation problems. In this study CLAD was applied to record Transtympanic (TT) Electrocochleograms (ECochG) at conventional and high rates in Meniere's and vertigo patients. ECochG was measured directly from the promontory using a needle electrode. Alternating clicks were delivered thorough an ER2 (Etymotic) insert earphone placed in the external ear canal. CLAD sequences corresponding to average stimulation rates of 19/s, 59/s, 98/s, 137/s, 234/s, 293/s and 391/s were used to acquire ECochG. Rarefaction and condensation responses were separately averaged and deconvolved. They were processed to separate Cochlear Microphonics (CM) from Summating Potential (SP) and compound Action potential (AP). ECochGs elicited from rarefaction and condensation clicks showed different patterns as the stimulation rate increases. Amplitudes of SP and CM were little affected by the stimulus rate while the AP amplitude was reduced differently at high rates for both rarefaction and condensation clicks. Separation of AP and SP components were enhanced at high stimulus rates. The acquisition of high rate ECochG using CLAD revealed physiological patterns not previously observed at conventional rates. The use of high rate ECochG has the potential to improve the diagnosis of cochlear diseases by providing more information not available in conventional ECochG.

### **[983] Measurements of Human Inner-Ear Function with Superior Semicircular Canal Dehiscence (SCD)**

**Michael E. Ravicz**<sup>1</sup>, Wade Chien<sup>1,2</sup>, Jocelyn E. Songer<sup>1,3</sup>, John J. Rosowski<sup>1,2</sup>, Saamil N. Merchant<sup>1,2</sup>

<sup>1</sup>Eaton-Peabody Lab., Mass. Eye & Ear Infirmary,

<sup>2</sup>Department of Otolaryngology and Laryngology, Harvard Medical School, Boston, MA, <sup>3</sup>SHBT Program, Harvard-MIT Division of Health Science and Technology

Superior semicircular canal dehiscence (SCD) syndrome is a recently-described clinical condition that offers an opportunity to investigate basic inner-ear fluid dynamics in human temporal bones and patients. Patients with SCD show a break in the bony superior semicircular canal and frequently have sound- and/or pressure-induced vertigo, oscillopsia, and a 0–50 dB low-frequency conductive hearing loss. It has been hypothesized that a dehiscence provides a "third window" into the inner ear that shunts acoustical energy away from the cochlea at low frequencies, causing a hearing loss. Such a shunt might also be expected to produce (1) sound-induced fluid velocity within the open dehiscence, (2) a reduction in sound-induced round-window velocity by reducing fluid motion across the cochlear partition, and (3) an increase in sound-induced umbo and stapes velocity by reducing inner-ear input impedance.

Middle- and inner-ear mechanics in SCD were explored in a human temporal-bone preparation: stapes, umbo, and round-window velocities were measured in response to air-conducted sound: (a) with the inner ear intact, (b) with a dehiscence in the superior canal, and (c) with the dehiscence patched. Sound-induced fluid velocity in the

open dehiscence was also measured. Dehiscences larger than 1 mm<sup>2</sup> caused 10–22 dB reductions in round window velocity below 200 Hz (implying a 10–22 dB hearing loss) and small but statistically significant increases in stapes and umbo velocities at low frequencies. The computed volume velocity of the fluid in the dehiscence increased as dehiscence size increased. These results help to define, constrain, and test a mechano-acoustic model of SCD in the human and are consistent with both patient data and the "third window" hypothesis.

Supported by NIDCD.

### **[984] Comparative Study on the Risk Factors and Clinical Features of Fungal Rhino-Sinusitis**

**Gehua Zhang**<sup>1</sup>, Yuan Li<sup>1</sup>, Hong Zhang<sup>2</sup>

<sup>1</sup>The Third Affiliated Hospital of Sun Yat-Sen University,

<sup>2</sup>The First Affiliated Hospital of Jinan University

[Abstract]Objective To investigate the risk factors and clinical features of fungal rhino-sinusitis. Methods The clinical data of all 110 patients with fungal rhino-sinusitis which were operated and another group of 110 patients with chronic rhino-sinusitis which were sampled randomly between January 1999 and June 2004 in our hospital were retrospectively compared. The risk factors and the clinical features of fungal rhino-sinusitis were investigated by using the multiple factor Logistic regression analysis and chi-square test. The pathological types of 110 cases fungal rhino-sinusitis were classified by using Gomori methenamine silver staining which is special for fungi. Results The Logistic regression predictive equation for fungal rhino-sinusitis was:  $y = -8.713 - 0.496X_1 - 4.575X_2 - 1.190X_3 - 4.119X_4 - 1.199X_5 - 2.698X_6 - P = \exp(y) / [1 + \exp(y)]$ , in which the concomitant variables were course of the disease $X_1$ , haem-nasal discharge $X_2$ , headache $X_3$ , calcified plaque in CT scan $X_4$ , age $X_5$  and unilateral / bilateral sinus lesion $X_6$ , respectively. The P value means the probability of suffering fungal rhino-sinusitis. By comparing with chronic rhino-sinusitis, the clinical features of fungal rhino-sinusitis were female, over 40-year-old, course of disease < 3 years, headache, haem-nasal discharge, unilateral sinus lesion and calcified plaque in CT scan. Among the 110 fungal rhino-sinusitis patients, 34 cases were non-invasive and 76 were invasive. Conclusions Fungal rhino-sinusitis can be predicted by using the suitable Logistic regression predictable equation. The clinical features of fungal rhino-sinusitis are significant for the diagnosis.

### **[985] Identification of Adenoid Biofilms in Children with Chronic Rhinosinusitis**

**Michael Carron**<sup>1</sup>, Giancarlo Zuliani<sup>1</sup>, Crystal Coleman<sup>1</sup>, Jose Gurrola, II<sup>1</sup>, Michael Haupt<sup>2</sup>, Richard Berk<sup>3</sup>, James Coticchia<sup>1</sup>

<sup>1</sup>Wayne State University School of Medicine Division of Pediatric Otolaryngology Head and Neck Surgery,

<sup>2</sup>Childrens Hospital of Michigan, <sup>3</sup>Wayne State University School of Medicine Department of Microbiology Immunology

Purpose: Chronic rhinosinusitis (CRS) in the pediatric population is a complex disease which is poorly



understood. CRS has been demonstrated to be resistant to standard antimicrobial therapy. It is well established that adenoidectomy is useful in the treatment of CRS resistant to antibiotics. It is thought that microorganisms on the adenoid surface may be a nidus for infection. Microorganisms are known to form biofilm colonies on mucosal surfaces that may shed planktonic bacteria. Biofilms have altered resistance to antibiotics because of incomplete penetration of the drug, altered chemical microenvironments, and an inactive state of bacterial growth in these microenvironments.

**Methods:** Adenoids removed from patients with CRS were fixed in glutaraldehyde and treated with osmium tetroxide, sequentially dehydrated with ethanol, washed with HMVS, gold sputter coated, and imaged using scanning electron microscopy (SEM).

**Results:** These specimens imaged at 500, 1000, and 2000x demonstrated confluent biofilms covering the entire field. These electron micrographs depicted an amorphous matrix with embedded rods and cocci. This cytoarchitecture is consistent with the literature and our previous images of adenoids removed from children with recurrent acute otitis media.

**Conclusions:** As stated, previous work in our lab has demonstrated biofilms in adenoids recovered from patients with recurrent acute otitis media. Other studies have shown biofilms in the sinus mucosa of adult patients with CRS. Resistant biofilms in the nasopharynx of children with CRS may act as a chronic reservoir for bacterial pathogens resistant to antimicrobial therapy. Also, the mechanical debridement of the nasopharyngeal biofilms may explain the observed clinical benefit associated with adenoidectomy in this subset of pediatric patients.

### **986 The History of the Glomus Tumor: A Glimpse of a Bio-Medical Camelot** **Robert Ruben<sup>1</sup>**

<sup>1</sup>*Albert Einstein College of Medicine*

The glomus tumor has had a number of different names, including glomus jugulare, glomus tympanicum, nonchromaffin paraganglioma and carotid body tumor. This poster will use the term glomus to include all of the nonchromaffin paraganglioma which arise in the ear. Although having occurred throughout the ages, glomus tumors were neither recognized nor understood until Harry Rosenwasser read Stacy Guild's report of 1941 report. Stacy Guild's pursuit of basic scientific knowledge laid the foundation for a chain of clinical and scientific advances that continue to the present and will continue to have positive effects into the future. Guild's brief basic science note of 1941 was used through the scholarship of Rosenwasser to define a clinical entity that had not been recognized. The new nosology, rapidly adopted worldwide, provided a biological basis for the rational grouping of patients and analysis of their ills. Subsequent to this, it was noted that many of these tumors occurred in families, apparently transmitted as an autosomal dominant but occurring primarily in the males. Further study based on these observations led to the identification of a genetic mechanism of inheritance: Genomic Imprinting. A further

advance of the synergetic relationship between the environment – oxygen tension/altitude – and the mutation explains Guild's 1953 observations that all patients, without any sexual predominance, have glomus bodies but not all have tumors. Guild's initial 231 word report was the source of a stream of positive consequences; the glomus story is a paradigm of the utility of basic science.

### **987 Dissemination/Validation of Virtual Simulation Temporal Bone Dissection: A Project Update**

**Gregory Wiet<sup>1</sup>, Donald Stredney<sup>2</sup>, Thomas Kerwin<sup>2</sup>, Dennis Sessanna<sup>2</sup>**

<sup>1</sup>*Children's Hospital/The Ohio State University, <sup>2</sup>Ohio Supercomputer Center*

We report on continuing progress in the refinement and development of a virtual environment for simulating temporal bone dissection. The purpose of this research is to develop an adjunct to the traditional temporal bone dissection laboratory for learning otologic surgery. Key to this effort is to provide open-source data, software, and hardware configurations that facilitate dissemination and adoption of the technology to multiple institutions both nationally and internationally. Progress in the following areas will be addressed:

1. Conversion of the system to a cost-effective PC-based configuration. The currently suggested system will be defined and discussed, with recommendations for future extensions.
2. Development of a refined data acquisition protocol, that includes multi-modal (i.e., computed tomography, magnetic resonance) and multi-scale (i.e., clinical or macro, and micro) data.
3. Investigations into the processing and integration of histological sections, such as those available in the national temporal bone registry.
4. Development of open-source software that facilitates the structural and functional segmentation of the data.

This research, Validation/Dissemination of Virtual Temporal Bone Dissection, is supported by a grant from the National Institute on Deafness and Other Communication Disorders, of the National Institutes of Health, 1 R01 DC06458-01A1

### **988 Intraoperative Monitoring of Hearing During Cerebellopontine Angle Surgery Using On-Line Analyzed Electrocochleography. An Animal Model and Clinical Study**

**Krzysztof Morawski<sup>1</sup>, Fred Telischi<sup>2,3</sup>, Jorge Bohorquez<sup>3</sup>, Rafael Delgado<sup>4</sup>, Ozcan Ozdamar<sup>2,3</sup>, Kazimierz Niemczyk<sup>1</sup>**

<sup>1</sup>*Medical University of Warsaw, <sup>2</sup>University of Miami, Department of Otolaryngology, <sup>3</sup>University of Miami, Department of Biomedical Engineering, <sup>4</sup>Intelligent Hearing Systems*

**Methods and Measures:** Young rabbits were used in experimental part of this study. The round window and the VIII nerve complex were surgically visualized. Laser-Doppler cochlear blood flow and electrocochleography (ECochG) were applied to monitor reversible cochlear

ischemic episodes. In the human clinical study, ECoChG was measured directly from the promontory (TT-ECoChG) and auditory brainstem responses (ABR) were monitored intraoperatively during cerebellopontine angle tumor (CPAT) removal. In both animal model and clinical study, click and tone-bursts were used to stimulate the hearing pathway.

**Results:** The cochlea showed different susceptibility at the base, middle and apical areas after reversible cochlear ischemia. An animal model of various intraoperative hearing insults was developed and applied to the clinical situations occurring during CPAT surgery. Tone bursts were found to have limited application during clinical IM of hearing, though they could be used during experimentally-induced ischemia in the animal model. ECoChG derived by click was more sensitive and reproducible during CPAT surgery. Stretching the eighth nerve, drilling close to the labyrinth, and application of bipolar cautery near the internal auditory canal contents were critical factors affecting hearing status during CPAT removal.

**Conclusions:**

1. ECoChG was a sensitive tool for detection of even minimal changes in hearing organ activity occurring during CPAT surgery.
2. A strategy of on-line evoked electrophysiological analysis to monitor peripheral auditory function intraoperatively in real time was developed.
3. ECoChG should be simultaneously recorded with direct eighth nerve potentials and ABR to provide comprehensive intraoperative monitoring of auditory function in real time.
4. A combined ECoChG/ABR strategy of intraoperative monitoring may serve as an effective tool to significantly improve the surgeon's ability to identify events detrimental to auditory function during CPAT removal.

### **[989] Amplification via "Compression Waves" in the Cochlea – A Parable**

**Egbert de Boer<sup>1</sup>, Alfred L. Nuttall<sup>2,3</sup>**

<sup>1</sup>Academic Medical Center, <sup>2</sup>Oregon Hearing Research Center, <sup>3</sup>Kresge Hearing Research Center

Most of cochlear mechanics is concerned with the component of the fluid pressure that is anti-symmetrical in the two channels of a cochlear model. This is the component that can give rise to propagating waves, also called 'slow waves'. And it is the component assumed to be involved in cochlear amplification ('activity'). Another component, symmetrical in the two channels, has become important of late. This component can give rise to 'fast waves', or 'compression waves', which propagate with a very large velocity through the fluid. Although generally both types of wave are involved in cochlear functioning, this paper delves into the properties of a cochlear model in which only compression waves and their reflections at the stapes are involved in the amplification process. It will be shown that this mechanism by itself is not capable of creating the type of mechanical response that we know from the mechanical response of the viable cochlea. A model in which too great a part is dedicated to compression waves or fast waves cannot be a realistic model. A related topic discussed in this contribution is

wave interference of fast waves as opposed to that of slow waves.

### **[990] The Backward Propagation of Basilar Membrane Vibration in a Temporal Bone Preparation**

**Fangyi Chen<sup>1</sup>, Tianying Ren<sup>1</sup>, Alfred L. Nuttall<sup>1,2</sup>**

<sup>1</sup>Oregon Hearing Research Center / Oregon Health and Science University, <sup>2</sup>Kresge Hearing Institute, University of Michigan

Recent work from Ren (Ren, 2004) cast doubts on the long-believed existence of backward traveling wave (BTW). However, the narrow span of measured locations in Ren's experiments offers possibilities for some other explanations (Shera, 2005), instead of Ren's claim of no BTW. In this work, a temporal bone preparation of a guinea pig cochlea is used to verify the existence of the BTW in a much wider range along the BM. Post-mortem preparation has long been used to study the cochlear macro- (von Békésy, 1960) and micro- (Ulfendahl et al., 1989) mechanics. Since the BTW was mostly related to the macro-mechanics, the stiffness gradient and fluid channel, the fresh post-mortem preparation is proper for our study. This preparation gives us accessibility to a relatively wide range on BM, which is not possible in an in vivo preparation. A window of about 3 mm long 1 mm wide was opened on the bony wall of the basal turn of the scala timpani (ST). The fluid in the ST was carefully lowered using wicks, still retaining the BM under the fluid to preserve its mechanical features. A glass probe with a tip of 10  $\mu$ m was positioned to contact the BM for the stimulation. Reflective beads were placed on different locations along the exposed BM. Using the LDV system and lock-in amplifier, we measured and recorded the frequency responses at those locations. During the experiments, we first applied the probe on the most basal location. The expected forward traveling wave was indicated by both the magnitude and phase response of the vibration at different locations. After that, we moved the probe to the most apical location. No significant phase difference was observed from different locations along the BM in an about 3 mm span.

Supported by NIH-NIDCD grants DC00141 and DC4554.

### **[991] Active Hair-Bundle Motility**

**Pascal Martin<sup>1</sup>, Jean-Yves Tinevez<sup>2</sup>, Frank Jülicher<sup>3</sup>**

<sup>1</sup>Institut Curie/CNRS, <sup>2</sup>Institut Curie, <sup>3</sup>Max-Planck-Institut für Physik Komplexer Systeme

The vertebrate inner ear must produce active mechanical work to boost the ear's sensitivity, sharpen its frequency discrimination, extend its dynamical range of responsiveness and sustain the mechanical oscillations that underlie oto-acoustic emissions. The hair bundle, the mechanical antenna of the sensory hair cells, displays correlates of these four essential properties and could thus embody at least part of the aural amplifier. The dynamical behaviours of a hair bundle are rich. A hair bundle can oscillate spontaneously, "twitch" or simply relax in response to a force step. Using iontophoresis to affect the  $\text{Ca}^{2+}$  concentration near a hair bundle from the bullfrog's

sacculus and displacement-clamp measurements of the bundle's force-displacement relation, we were able to reconcile these contrasting manifestations of active hair-bundle motility. We used  $\text{Ca}^{2+}$  and offsets of the bundle's mean position to control the fraction of open transduction channels at steady state and thus the bundle's operating point. In the case of non oscillatory hair bundles, we found that the polarity and kinetics of active hair-bundle movement evoked by a step stimulus depended on the bundle's operating point in the nonlinear force-displacement relation. When the force-displacement relation displayed a region of negative stiffness, spontaneous hair-bundle oscillations arose when the hair bundle was required to operate within this unstable region. Only two ingredients are necessary to account for the various incarnations of active hair-bundle motility: nonlinear gating compliance of the transduction apparatus and the  $\text{Ca}^{2+}$ -regulated activity of the myosin-based adaptation motor. Numerical simulations successfully reproduced a wide range of observations from different laboratories and animal species, thereby suggesting that only one force-generating mechanism is needed to describe the seemingly unrelated active movements that a hair-bundle can produce.

## **[992] Traveling-Wave Delays in the Human Cochlea Are Not Exceptionally Long**

Mario Ruggero<sup>1</sup>, Andrei Temchin<sup>1</sup>

<sup>1</sup>Northwestern University

The first, and still the only, direct measurements of basilar-membrane (BM) traveling-wave delays in humans were carried out by George von Békésy in cadaveric temporal bones [J.A.S.A. 21, 245-254, 1949; J.A.S.A. 21, 233-245, 1949]. All subsequent estimates of BM delays for humans have been performed using indirect methods in-vivo. Two of the longest estimates, namely those based on stimulus-frequency otoacoustic emissions (SFOAEs) [C. A. Shera et al., P.N.A.S. USA 99, 3318-3323, 2002] and brainstem evoked responses (BSERs) to tone bursts [S. T. Neely et al., J.A.S.A. 83, 652-656, 1988], have been presented as evidence that BM delays are much longer in humans than in experimental species. Here we dispute those claims. First, we note that a recent study [J. H. Siegel et al., J.A.S.A. 118: 2434-2443, 2005] showed that the assumption on which the estimates from SFOAEs are based, i.e., that SFOAE group delays amount to twice the BM group delays [Shera et al., op. cit.], does not apply to experimental animals and therefore its validity for humans is at best questionable. Second, we show that the putative derivation of BM delays on the basis of BSERs to tone bursts [Neely et al., op. cit.] was flawed, leading to gross overestimation of BM traveling-wave delays. Third, we argue that delay estimates based on "derived-band" compound action potentials (e.g., [J. J. Eggermont, J.A.S.A. 65, 463-470, 1979]) or BSERs stimulated by masked clicks (e.g., [R. Schoonhoven et al., J.A.S.A. 109, 1503-1512, 2001]) correctly approximate BM delays in humans and show that the latter are very similar to BM delays in other mammals.

Work supported by NIH Grant DC-00419.

## **[993] Images and Motion Measurements of the Intact Mammalian Cochlea Using Doppler Optical Coherence Microscopy**

Stanley Hong<sup>1</sup>, Dennis M. Freeman<sup>1</sup>

<sup>1</sup>Research Laboratory of Electronics, Massachusetts Institute of Technology, Cambridge, MA

Three-dimensional images and motion measurements have been obtained in an in vitro preparation of the gerbil cochlea using Doppler optical coherence microscopy (DOCM). The high optical sensitivity and coherence-gating capability of DOCM enable images and motion measurements to be obtained without the use of contrast agents and without wide optical access. The images possess sufficient dynamic range to image transparent structures such as the tectorial membrane and sufficient spatial resolution to image cellular structures such as outer hair cells. In addition, every pixel in the images yields a motion measurement comparable to that obtained using laser Doppler velocimetry. Consequently, motion measurements using DOCM are not restricted to reflective surfaces such as the basilar membrane and reticular lamina; the motions of all visible structures in the cochlea are measured including the tectorial membrane, tunnel of Corti, and outer hair cells.

## **[994] Blockage of Forward Transduction Alters Cochlear Amplification**

Jiefu Zheng<sup>1</sup>, Alfred L. Nuttall<sup>1,2</sup>

<sup>1</sup>Oregon Hearing Research Center, Oregon Health & Science University, Portland, OR, <sup>2</sup>Kresge Hearing Research Institute, The University of Michigan, Ann Arbor, MI, USA

In mammals cochlear sensitivity and frequency selectivity depend on the function of cochlear amplifier. Prestin-based outer hair cell (OHC) somatic motility is well accepted as the major source of the cochlear amplification that provides mechanical feedback to the basilar membrane motion. Recently, hair bundle or stereocilia motility has also been proposed to be an alternative source of mammalian cochlear amplification. However, direct evidence is still not available. In this study, we investigated the presence of hair bundle motility in vivo by manipulating the somatic motility and the mechanotransducer channel activity in the stereocilia. Endolymphatic perfusion was performed to apply NMDG<sup>+</sup> and d-tubocurarine into the scala media of guinea pig cochlea. Elimination of potassium current through the OHCs by infusing NMDG<sup>+</sup> endolymph substantially reduced the magnitude of cochlear microphonics (CM) and distortion product otoacoustic emissions (DPOAE). Addition of d-tubocurarine (a mechanotransducer channel blocker) resulted in further reduction of CM. A residual DPOAE decreased to a level of noise floor. The inhibitive effect of d-tubocurarine was reversible after washout. These preliminary data may provide evidence in support of the presence of stereocilia motility in production of otoacoustic intermodulation distortion.

Supported by NIH NIDCD R01 DC 00141

### **995 Control of Mammalian Basilar Membrane Amplification by Chloride Anions**

**Joseph Santos-Sacchi<sup>1</sup>**, Lei Song<sup>1</sup>, Jiefu Zheng<sup>2</sup>, Alfred L. Nuttall<sup>2</sup>

<sup>1</sup>*Otolaryngology and Neurobiology, Yale University School of Medicine*, <sup>2</sup>*Oregon Hearing Research Center, Department of Otolaryngology, Oregon Health & Science University*

Chloride ions have been shown to directly interact with the integral membrane outer hair cell (OHC) motor protein, prestin, on its intracellular domain. Thus, we had previously hypothesized that transmembrane chloride movements via the cell's lateral membrane conductance, GmetL, could serve to underlie cochlear amplification in the mammal. Here we report on experimental manipulations of chloride-dependent OHC motor activity, in vitro and in vivo. In vitro, we focused on the motor's signature electrical characteristic, the cell's nonlinear capacitance. Using the well known ototoxicant, salicylate, which competes with prestin's anion binding site, to assess level-dependent interactions of chloride with prestin, we determined that the resting level of chloride in OHCs is near or below 10 mM, while perilymphatic levels are known to be about 140 mM. With this observation in hand we sought to determine the effects of perilymphatic chloride level manipulations of basilar membrane amplification in the living guinea pig. By either direct basolateral perfusion of the OHC with altered chloride content perilymphatic solutions or by the use of tributyltin, a chloride ionophore, we find alterations in OHC electromechanical activity and cochlear amplification which are fully reversible. Since these anionic manipulations do not impact on the cation selective stereociliary process or the endolymphatic potential, our data lend additional support to the argument that prestin activity dominates the process of mammalian cochlear amplification.

(Supported by NIH NIDCD DC 00141 (ALN) and DC 00273 (JSS))

### **996 A Multi-Compartment, Nonlinear Cochlear Model with Piezo-Electric Outer Hair Cells**

**Shan Lu<sup>1</sup>**, David Mountain<sup>1</sup>, Alllyn Hubbard<sup>1,2</sup>

<sup>1</sup>*Boston University, Biomedical Engineering*, <sup>2</sup>*Electrical and Computer Engineering*

A linear, multi-compartment model of the cochlea has previously been shown to create a slow-traveling pressure wave inside the organ of Corti, which is principally responsible for amplified response of the basilar membrane (BM). This was accomplished using an active force generation mechanism that produced outer hair cell (OHC) force as a function of reticular lamina (RL) displacement. This model has been shown generally to mimic experimental data [Ren, T., Nuttall, A., Basilar membrane vibration in the basal turn of the sensitive gerbil cochlea, *Hearing Research* 151 2001, 48-60] using physiologically-realistic parameters.

In the present version of the model, cochlear electroanatomy has been included. The (OHCs) consist of apical and basal membrane portions, which have a membrane conductance and capacitance in parallel. The

apical conductance varies nonlinearly as a function of the stereocilia displacement. Scala media (SM) fluid resistance creates a longitudinal electrical coupling, as does the scala vestibule (SV) and scala tympani (ST). SM also has membrane conductances and capacitances to ST and SV. Intracellular and stria vascularis batteries were also included in this model. At high frequencies, the basolateral membrane voltage produced by RL displacement is substantially reduced due to low pass filtering. In order to overcome this reduction, the basolateral membrane capacitance was shunted with a piezo-electric element, which translates mechanical loading seen by the OHC into an electrical impedance seen by the OHC cell membrane.

The simulation results of this model were compared with low-frequency cochlear microphonic (CM) data from the gerbil and BM motion data whose characteristic frequencies are in the vicinity of 14 kHz. The model's CM data compare favorably in magnitude and nonlinear aspects with experimental data.

This work was supported by NIH.

### **997 Influence of Electrically-Induced Somatic Mobility of Outer Hair Cells on the Organ of Corti Motion**

**Manuela Nowotny<sup>1</sup>**, Anthony W. Gummer<sup>1</sup>

<sup>1</sup>*Department Otolaryngology, University Tuebingen, Tuebingen, Germany*

For a better understanding of the amplification process in the mammalian inner ear the electrically-induced transverse vibration patterns of the organ of Corti (OC) were investigated at different radial and longitudinal locations: i) on the reticular lamina (RL) ii) lower and upper surface of the tectorial membrane (TM) and iii) on the basilar membrane (BM). Velocity was measured using a laser-interferometer (Polytec OFV 302) with a depth resolution of  $\pm 1.8 \mu\text{m}$  from the focus plane (at -10 dB).

The results derived from an in-situ preparation of 81 pigmented guinea-pig (250- 500 g) cochleae. The in-vivo characteristic frequency (CF) associated with a given longitudinal position was calculated from the tonotopic map of Tsuji and Liberman [*J.Comp.Neurol.* 381, 1997]. Investigated were the basal turn (CF = 24 kHz), medial turn (CF = 3.0 kHz) and apical turn (CF = 0.8 kHz). The turn of interest was isolated by removal of the lateral part of all other turns. Reissner's membrane was left intact, allowing better preservation of the tectorial membrane. For electrical stimulation, two platinum electrodes and one gold electrode were used; the latter also served as a mirror for illumination from the tympanic side of the organ. The stimulus frequency was between 480 Hz and 70 kHz.

A complex vibration pattern of the organ of Corti was found. The amplitudes of the transversal BM motion in the region of the pars arcuata exhibited a resonance. In the basal part of the cochlea (in-vivo CF = 24 kHz), at the frequency of the resonance on the BM motion below the outer hair cells (OHCs), the vibration pattern of the RL and TM exhibited an antiresonance. This was located at  $16.6 \pm 0.9 \text{ kHz}$  ( $n = 5$ ). This data suggests a resonance in the radial motion of the TM at this frequency.

The results support earlier suggestions that cochlear amplification involves resonant TM motion.

Supported by the German Research Council, DFG Gu 194/7-2.

### **998 Lateral Wall Protein Content Modulates OHC Stiffness Before and After the Onset of Hearing**

Heather Jensen-Smith<sup>1</sup>, Richard Hallworth<sup>1</sup>

<sup>1</sup>Creighton University, Omaha, NE

Electromotile length change and force generation by OHCs are essential for a sensitive and sharply-tuned cochlea. OHC stiffness is in turn important for effective transmission of force from OHCs to other cells in the organ of Corti. Maturation of stiffness in OHCs during development may therefore be an important factor in the onset and maturation of electromotility and hearing in mammals. The mechanical properties of developing and adult gerbil OHCs were compared using calibrated glass fibers. The deformability of OHCs increased immediately before the onset of hearing. Around the onset of hearing OHC deformability dramatically decreased.

Cochlear OHCs have a specialized lateral wall consisting of a plasma membrane, in which the motor protein prestin is densely packed, an actin-spectrin cortical lattice and subsurface cisternae. Developmental alterations in the protein content of each of these structures were examined to assess their potential to influence OHC mechanics before and after the onset of hearing. Dramatic F-actin reorganization coupled with low prestin content in the lateral wall resulted in an increase in OHC compliance immediately before the onset of hearing. A dramatic increase in spectrin and prestin content at the onset of hearing was associated with a decrease in compliance. These results suggest a role for the actin-spectrin cortical lattice and prestin in modulating the mechanical properties of cochlear OHCs before and after the onset of hearing. Such dramatic alterations in OHC mechanics clearly indicate that the mammalian OHC acquires specific mechanical properties in concert with electromotility resulting in a sharply tuned cochlea.

### **999 Modeling the Mechanics of Cetacean Hearing**

Brian Miller<sup>1</sup>, Aleks Zosuls<sup>1</sup>, Seth Newburg<sup>1</sup>, Darlene R. Ketten<sup>2</sup>, David Mountain<sup>1</sup>

<sup>1</sup>Boston University Hearing Research Center, <sup>2</sup>Woods Hole Oceanographic Institution

There are many cetacean species for which it is not currently possible to obtain a behavioral audiogram. In this study, mechanical and anatomical properties of ears harvested from stranded animal cadavers are used to predict general hearing capabilities for the bottlenose dolphin, *Tursiops truncatus*. Stiffness measurements of the middle ear and cochlear partition were made using piezoelectric force probes in fresh, fixed and frozen/thawed specimens. The acoustic stiffness of the dolphin middle ear was measured at the stapes to be  $1.04 \times 10^{17}$  Pa/m<sup>3</sup>. In terrestrial mammals, the correlation between middle ear acoustic stiffness and low frequency cutoff of hearing threshold can be fit by the function  $f_c =$

$1.02 \times 10^{-6} \cdot k^{0.58}$  where  $f_c$  is the 20 dB cutoff frequency and  $k$  is the acoustic stiffness of the middle ear.

Using the middle ear stiffness value measured for bottlenose dolphin in the above equation yields  $f_c$  of approximately 7.56 KHz, which is close to value of 8 KHz obtained from the behavioral audiogram. Stiffness gradients along length of basilar membrane in bottlenose dolphin were measured. Point stiffness was converted to volume compliance for comparison to terrestrial species. Our results indicate that the volume compliance of the bottlenose dolphin basilar membrane is similar to that of terrestrial species with good high frequency hearing. Preliminary results for *Phocoena phocoena* (harbor porpoise) will also be presented. The measured values for middle ear and basilar membrane stiffness were then used, along with anatomical measurements to create an integrated model of the dolphin auditory periphery.

Funded by the National Oceanographic Partnership Program (award #N00014-04-1-0708)

### **1000 Encoding Additional Information via Variable Stimulation Rates in Cochlear Implants: Investigating Potential Benefits to Music Appreciation Using Acoustic Models**

Joshua Stohl<sup>1</sup>, Leslie Collins<sup>1</sup>

<sup>1</sup>Duke University

Current cochlear implant strategies present an amplitude-modulated constant-rate pulse train on each electrode, relying on the place of stimulation to communicate pitch information. While these strategies have proven to be sufficient for speech recognition, familiar melody recognition test results demonstrate a significant divide between normal-hearing listeners and implant users. Nie et al. (2005) proposed the Frequency Amplitude Modulation Encoding (FAME) algorithm, which contains a slowly varying frequency envelope in addition to the commonly used amplitude envelope in order to include fine structure information. Kucukoglu et al. (2005) proposed the Multi-Carrier Frequency Algorithm (MCFA), which uses peak-picking methods to map spectral information to predefined frequencies on each of 22 electrodes. Both of these algorithms have been implemented experimentally in acoustic models and suggest that variable pulse rate stimulation could improve speech perception in noise. Fearn (2001) implemented two variable pulse rate algorithms with the express intent of improving music perception, namely Voc-L and Inst-L. These algorithms use variable pulse rates extracted from overlapping fast Fourier transforms to stimulate apical electrodes, while stimulating basal electrodes at a constant pulse rate of 1000 pps. In order to show the potential benefit of variable pulse rate strategies to music appreciation, we implemented each of these four algorithms in acoustic models and had subjects perform a qualitative comparison of the strategies to the currently implemented ACE strategy. In three out of four cases, variable pulse rate stimulation demonstrated a significant ( $p < 0.05$ ) improvement over the ACE strategy with respect to music perception. This result justifies the implementation of variable pulse rate strategies in actual implant users for further investigation of the possible benefit to music appreciation.

## **1001 A Wavelet-Based Speech Processing Strategy for Cochlear Implants**

Alessia Paglialonga<sup>1</sup>, **Gabriella Tognola**<sup>1</sup>, Giuseppe Baselli<sup>2</sup>, Marta Parazzini<sup>1</sup>, Paolo Ravazzani<sup>1</sup>, Ferdinando Grandori<sup>1</sup>

<sup>1</sup>CNR Inst. Biomedical Engineering, Milan, Italy, <sup>2</sup>Dept. Biomedical Eng., Polytechnic of Milan, Milan, Italy

An innovative approach is proposed for speech processing in cochlear implants (CI) in order to overcome the limitations that traditional strategies demonstrate in consonant coding. Differently from the usual filterbank spectral analysis strategies (i.e., CIS and ACE), this new method decomposes the speech signal by means of the wavelet transform (WT). The traditional numeric filters are inadequate to localize fast patterns, whereas the WT performs a multiresolution analysis of speech providing a highly accurate decomposition of transient signals in the time-frequency domain.

Yao and Zhang (IEEE Trans. Biomed. Eng., 48(8), pp. 856-863) used the WT to build an analysis algorithm that accurately models cochlear properties. They asserted that it could be useful for CIs. In our study the problem was considered from an innovative point of view, focusing on the applicability of WT to real cochlear implants and trying to insert the transform in a realistic framework. The WT processing here proposed is slightly different from the classical one because some modifications were needed to fit the operative conditions of a CI. Information loss relevant to the limited pulse rate allowed by real implants and the necessary log compression were inserted, as well. In particular the Nucleus® 24 system by Cochlear Corporation was considered as a reference.

Preliminary analyses were conducted to examine the behaviour of the WT in the new context. The proposed strategy was then tested on speech material and compared with traditional algorithms.

Results showed that the WT is a robust transform able, unlike traditional methods, to efficiently capture extremely rapid transitions in speech (i.e., plosive consonants) [Tognola G., Baselli G., Parazzini M., Paglialonga A., Grandori F. (2005): "Wavelet speech processing for cochlear implants: a preliminary study", in IFMBE Proceedings of the 3rd European Medical & Biological Engineering Conference, November 20-25 2005, Prague (Czech Republic)]. With respect to filterbank methods, WT strategy better preserves speech features, giving a coding that retains most of the information present in the original signal. Thus it would be possible, on a real implant, to obtain a stimulation pattern that accurately reproduces the speech signal hence facilitating the patient perception and comprehension.

## **1002 Frequency Modulation Detection with Simultaneous Amplitude Modulation in Cochlear Implant Users**

**Xin Luo**<sup>1</sup>, Qian-Jie Fu<sup>1</sup>

<sup>1</sup>Department of Auditory Implants and Perception, House Ear Institute

Studies have shown that understanding speech in noise and appreciating music are extremely difficult with current

cochlear implants (CI's), because of insufficient temporal and spectral fine structure cues. Among various attempts to overcome these defects, it has been proposed to change the stimulation rates to encode the frequency modulation (FM) information in input acoustic signals, as a complement to the amplitude modulation (AM) information encoded by varying the stimulation levels. Such a strategy requires users to detect FM, which, however, may be greatly affected by simultaneous AM. As an extension to the experiments conducted by Chen and Zeng (2004), the present study investigated the abilities of CI users to detect FM when different amounts of AM exist. Five adult CI subjects using Nucleus-22 or -24 devices participated in this study. Detection thresholds for upward sweep FM

were measured as a function of the standard frequency (from 75 Hz to 1000 Hz). The stimulation position was fixed at the middle of the electrode array (10, 12). In the baseline condition, the stimulation level was fixed at 50 % of the estimated dynamic range, thus there was no AM; while in other conditions, 20 Hz sinusoidal AM (SAM) with 10 %, 20 %, and 30 % relative modulation depths, as well as noise AM (NAM) with 1 dB, 2 dB, and 3 dB roving ranges were tested; note that both the SAM and NAM stimuli were loudness-balanced to 50 % of the estimated dynamic range. Results showed that FM detection thresholds increased significantly and monotonically with the standard frequency for all AM conditions, consistent with previous studies; FM detection thresholds also significantly increased when the amount of AM was increased, and when NAM was used instead of SAM. Such findings that FM detection in electric hearing became worse with stronger simultaneous AM and higher standard frequencies should be taken into account when designing the FM+AM strategies.

## **1003 Alternative Methods for Frequency Selection in a Frequency Encoding Algorithm for Cochlear Implant Speech Processors**

**M. Selin Kucukoglu**<sup>1</sup>, Leslie Collins<sup>1</sup>

<sup>1</sup>Duke University

Recent work by Nie et al. (2005), among others, has suggested that the addition of finer resolution spectral cues may improve speech recognition in cochlear implant subjects. In order to encode additional frequency information that could be linked to psychophysical data and thus tuned for the individual, we proposed the multiple carrier frequency algorithm (MCFA) (Kucukoglu et al., 2005). The listening experiments on normal hearing subjects in the previous study revealed that significant improvement could be gained by providing information via a discrete set of carrier frequencies in each analysis band. MCFA utilized a short time Fourier transform (STFT) applied in 2ms windows and a peak picking strategy to determine the most prominent frequency within the window, and then mapped the dominant frequency to one of the predefined carrier frequencies. Even though the preliminary results were promising, this methodology could be further developed, particularly since the accuracy of the STFT-based frequency selection is limited in the lower frequency analysis bands. Therefore, in this current work, a variety of frequency selection strategies, including

vocoders and overlapping FFTs, are compared. In the first stage of this new analysis, the errors incurred using the various frequency selection techniques are analyzed on a band-by-band basis. In addition, the impact of providing more accurate frequency information on speech recognition is evaluated with a listening experiment. This study suggests mechanisms by which to enhance MCFA so that frequency information can be presented more accurately.

#### **1004 Modulation Rate Difference Limens Using Different Waveforms in Electrical Hearing**

**David Landsberger<sup>1,2</sup>**, Colette McKay<sup>1,2</sup>

<sup>1</sup>University of Melbourne, Department of Otolaryngology, Australia, <sup>2</sup>Aston University, School of Life and Health Sciences, Birmingham, UK

The fundamental frequency is important for hearing pitch in music, interpreting tones of speech, and understanding speech in background noise. Listeners with cochlear implants are poor at perceiving the fundamental frequency using current commercial speech processing strategies. It is known that modulations of the amplitude of the current on a high rate pulse train can elicit a pitch perception. Experimental strategies have been developed that use modulations of the amplitude of the current to deliver fundamental frequency information. However, the most appropriate waveform to be used for the modulations is debated. A sinusoidal waveform is most similar to a natural acoustic stimulation. Sawtooth waveforms are hypothesized to elicit a less stochastic response from the neurons. In the presented experiment the minimum discriminable modulation rates are measured for four different waveforms and three different electrodes. The waveforms used are sinusoid, a sawtooth, a sharpened sawtooth, and a square waveform. Preliminary results suggest that there are not large differences between the rate difference limens for the different waveforms. Variability across electrodes and subjects seems to be larger than the variability between waveforms. It is likely that the choice of waveform used for an experimental speech processing strategy will not make a large difference on pitch discrimination. The most appropriate choice for a waveform would likely be determined by the technical requirements of the specific speech processing strategy.

#### **1005 Evidence for Fine Structure Encoding by a Cochlear Implant User**

**Chad V. Ruffin<sup>1</sup>**, Ward R. Drennan<sup>1</sup>, Jong Ho Won<sup>1</sup>, Jay T. Rubinstein<sup>1</sup>

<sup>1</sup>Virginia Merrill Bloedel Hearing Research Center - University of Washington

Cochlear implant simulations are often used with normal-hearing listeners to predict the best results available to cochlear implantees. However, they fail to account for positive outliers in speech and music perception if envelope is the sole source of temporal information. Drennan et al. (2005) demonstrated that inclusion of even small amounts of temporal fine-structure in a six-channel vocoder could account for improvements in speech

understanding in noise, lateralization and binaural unmasking. We test the hypothesis that speech processing strategies discard fine structure. The spondee reception threshold (SRT) was measured for a cochlear implantee presented with stimuli in competing speech noise processed by 12-channel vocoder. The Hilbert envelope of stimuli outputs from each bandpass filter were used to modulate the products of the extracted fine structure and a randomized Hilbert phase shift:  $X_{FS}(t) = \text{abs}[H(x(t)) \cdot \cos(\phi(H(x(t))) + 2\pi nr)]$ , where  $r$  is a uniformly distributed random number between -0.5 and +0.5 and noise factor,  $n$ , varies from 0 to 1.0, fractionally randomizing the fine structure. Thus, psychophysical performance with fine structure randomization,  $n = 1$ , recreates a traditional cochlear implant vocoder. If no fine-structure is delivered, either condition will sound identical to a cochlear implantee. In this user, a  $t$ -test indicated a significant difference ( $t_{14} = 2.35$ ,  $p \leq 0.02$ ) between a random presentation of 8 SRT trials of  $n = 0$  (SRT = -16.10  $s_e = 0.47$ ) and  $n = 1.0$  (SRT = -14.03  $s_e = 0.82$ ). Learning may have occurred in the  $n = 1.0$  condition. Interestingly, this user could also qualitatively identify the randomized versus original signals. To summarize, our pilot study suggests that cochlear implants may allow some encoding of temporal information beyond envelope.

[Work was supported by the University of Washington; Ruffin is a Howard Hughes Medical Institute Medical Research Training Fellow]

#### **1006 Delayed Pseudomonophasic Pulses in Cochlear Implants: Effects of Phase Duration and Polarity**

**Olivier Macherey<sup>1</sup>**, Astrid van Wieringen<sup>1</sup>, Robert P. Carlyon<sup>2</sup>, John M. Deeks<sup>2</sup>, Jan Wouters<sup>1</sup>

<sup>1</sup>Lab Exp ORL, KULeuven, Kapucijnenvoer 33, Belgium,

<sup>2</sup>MRC Cognition and Brain Sciences Unit, Cambridge, UK

Existing cochlear implants stimulate the auditory nerve with trains of symmetric biphasic (BP) pulses. Behavioral, physiological and modeling data have shown that modifying the pulse shape, while maintaining charge balance, may be beneficial in terms of reducing power consumption, increasing dynamic range and/or limiting channel interactions. In a previous study, we introduced a "delayed pseudomonophasic (DPS)" stimulus which is identical to a pseudomonophasic one except that the long/low phase is delayed to be mid-way between the big/short phases of two subsequent pulses. The DPS stimulus was shown to give lower threshold and lower maximum comfort level (MCL) than a BP one (more than 6 dB at suitable parameter values for a speech processing strategy). It remains however unclear which part of the DPS stimulus contributes to these low levels of stimulation. Is it the big/short phase of the pulse, the long/low one or both? Is it the anodic phase, the cathodic one or both?

Users of the Clarion CII and HiRes implants participated in three experiments designed to tease out the relative effects of the DPS phases. Experiment 1 compared threshold and MCL of three 813 pps stimuli: ALT-DPS (identical to DPS except that leading polarity alternates from pulse to pulse), ALT-DPS with the big/short phases



removed and ALT-DPS with the long/low phases removed. Experiment 2 was a pitch discrimination experiment in which the pitch of a 76 pps DPS stimulus was compared to several 152 pps BP stimuli where the amplitude of one pulse out of two was varied. In experiment 3, several masking period patterns were measured. The masker was either a 76 pps DPS anodic first or a 76 pps DPS cathodic first stimulus. The signal was a 76 pps biphasic pulse train that was either presented 1 ms after the big/short phase or 1 ms after the long/low phase.

Results suggest that both phases of DPS have an effect on neural activation but that the big/short phase dominates slightly at threshold and more clearly at MCL. Applications for speech processing strategies will be discussed.

### **1007 Activation of the Auditory Pathway with an Auditory-Nerve Electrode Array**

**John C. Middlebrooks<sup>1</sup>**, Russell L. Snyder<sup>2,3</sup>

<sup>1</sup>University of Michigan, <sup>2</sup>UCSF, <sup>3</sup>Utah State University

The present state of the art for auditory prosthesis is a cochlear implant consisting of an array of electrodes inserted in the scala tympani. Although effective at stimulating the auditory nerve, the sensitivity and frequency resolution of a scala tympani array is limited by its position within a volume of conductive perilymph, separated from the auditory nerve by a bony wall (the osseous spiral lamina). We are exploring arrays of electrodes inserted directly in the auditory nerve as an alternative means of electrical stimulation for auditory prosthesis.

We recorded unit activity from 32 sites along the tonotopic axis of the central nucleus of the inferior colliculus (ICC) in anesthetized cats. In each animal, we compared the tonotopic spread of ICC activation in response to 3 modes of stimulation: (1) acoustic stimulation in normal-hearing conditions; (2) electrical stimulation using a conventional scala-tympani implant (after deafening the cochlea); and (3) electrical stimulation using a 16-site intra-neural electrode array (also in deafened conditions). The intra-neural array was inserted through the osseous spiral lamina into the modiolar portion of the auditory nerve.

Monopolar intra-neural stimulation showed the following characteristics compared to conventional scala-tympani stimulation: (1) Thresholds were as much as 30 dB lower. (2) Tonotopic spread of activation was substantially more restricted than that for monopolar scala-tympani stimulation, comparable to the most restricted patterns observed with bipolar scala-tympani stimulation. (3) The topographic map of intra-neural stimulation site onto ICC recording site was precise, but was non-monotonic in keeping with the spiral trajectory of auditory nerve fibers. (4) Intra-neural stimulation provided access to the entire frequency representation, from <1 kHz to 32 kHz.

These early results offer encouragement for development of intra-neural stimulation as a mode of auditory prosthesis.

Supported by NIDCD NO1 DC-5-0005

### **1008 Bilateral Comparison of Auditory Brainstem Implants with a Cochlear Implant or Acoustic Hearing**

**Robert V. Shannon<sup>1</sup>**, John J. Galvin, III<sup>1</sup>, Qian-Jie Fu<sup>1</sup>

<sup>1</sup>House Ear Institute

Auditory Brainstem Implants (ABIs) produce hearing sensations by electrical stimulation of the human cochlear nucleus. However the level of speech understanding with an ABI is considerably poorer than that obtained with cochlear implants. One possible cause of this poor performance is the uncertain connection of the electrodes to the tonotopic dimension of the cochlear nucleus. In cochlear implants the electrodes are positioned along the tonotopic axis of the cochlea and pitch produced by stimulation typically decreases in a reliable fashion from base to apex. In the ABI however, it is not possible to align the electrode array with the tonotopic dimension and so pitch sensations produced by the ABI are not as orderly as in a cochlear implant. Here we report on three ABI patients who had hearing in the contralateral ear; two with normal acoustic hearing and one with a cochlear implant. In all cases the hearing ear had a large tumor (vestibular schwannoma) that will eventually eliminate the hearing on that side. Frequency and amplitude discrimination was measured across ears using the method of constant stimuli. Listeners heard one sound from the ABI and another sound from the contralateral ear and were asked to judge which was higher in pitch (or loudness). For each ABI electrode a sigmoidal curve was fit to the pitch (or loudness) judgements as a function of acoustic frequency (or acoustic dB). ABI speech processors were then programmed so that the appropriate pitch-matched frequency region was assigned to each electrode. Unfortunately, no improvement in speech understanding was observed. This failure to obtain improved speech understanding, even with the appropriate frequency-to-electrode mapping, raises important theoretical issues about peripheral physiological mechanisms that contribute to speech recognition. [Funded by NIDCD]

### **1009 Event-Related fMRI Evaluation of Adaptation to Acoustic Simulation of Cochlear Implant Electrical Stimulation**

**Javier Gonzalez Castillo<sup>1</sup>**, Angela Hoffa<sup>1</sup>, Thomas Talavage<sup>1,2</sup>, Mario Svirsky<sup>2,3</sup>, Eri Haneda<sup>1</sup>, Heidi Neuburger<sup>2</sup>

<sup>1</sup>Purdue University, <sup>2</sup>Indiana University School of Medicine, <sup>3</sup>New York University School of Medicine

Functional magnetic resonance imaging (fMRI) has been used to study longitudinal changes in cortical activity arising from exposure to acoustic simulations of cochlear implant (CI) electrical stimulation. Previously a block-paradigm experiment revealed notable changes in cortical activity as a function of training. Normal-hearing (NH) subjects were exposed to 15 hours of speech perception training using an 8-channel, noiseband-based real-time simulator. At three times during training (0, 7 and 15 hours), subjects underwent fMRI while exposed to forward and time-reversed words in an unaltered (NS) state, and after alteration by a CI simulator modeling either a 3.25mm

(HS) or a 6.5mm basalward shift (FS). When contrasting forward and time-reversed FS stimuli, cortical differentiation was initially limited. Activation observed for this contrast shifted over 15 hours of training into normal language activation patterns. Minimal forward vs. time-reversed contrast was observed for the NS and HS stimuli. However, these experiments involved presentation of blocks of 20 words, each with like modification, over a 40s period. Therefore, it was possible that subjects anticipated if late presentations in a block would be comprehensible, potentially affecting attention. Such confounds would bias the resulting activation in favor of the forward presentations.

To eliminate the aforementioned confounds, an event-related fMRI experiment was conducted in which subjects were presented with the same word stimuli, but with the state of successive stimuli being uncorrelated. Results of this new study confirm our previously obtained results. These new results eliminate the possibility that previous preferential activation to forward stimulus presentations was an artifact of adaptation of subjects to stimuli and/or lack of attention to time-reversed stimulus presentations, demonstrating that fMRI of NH subjects has potential as a tool for the study of CI speech perception.

#### **1010 Electrical Stimulation of Hearing Ears: How the ECAP Reflects Single-Fiber Responses**

**Charles Miller<sup>1</sup>**, Barbara Robinson<sup>1</sup>, Kirill Nourski<sup>1</sup>, Fuh-Cherng Jeng<sup>1</sup>, Paul Abbas<sup>1</sup>

<sup>1</sup>*University of Iowa*

Auditory prostheses are being implanted in cochleae of ears with residual acoustic hearing. This leads to the possibility of complex auditory-nerve response patterns resulting from both electrically induced and hair-cell mediated responses to electric stimuli. Our laboratory has been collecting auditory nerve responses from animal subjects with cochlear implants that have significant acoustic sensitivity. We typically run parallel studies of single-fiber responses and the electrically evoked compound action potential (ECAP) in order to provide a link to measures that can be obtained from humans.

Single-fiber responses have indicated several unique response patterns not observed in deafened animals. These include electrophonic responses, enhanced and degraded synchrony, "build-up" responses to electric pulse trains, and acoustically enhanced responses to electric stimuli.

In this presentation, we examine both single-fiber and ECAP responses with the goal of determining the degree to which ECAP response patterns can reflect single-fiber response properties in hearing ears. Such connections to the ECAP are useful for assessing various animal models and possibly for clinical assessments of implantees with residual hearing.

Specifically, we will show that the ECAP can demonstrate electrophonic activity, "build up" responses, and enhanced responses. Our working hypothesis is that altered response to electric stimuli (relative to those observed in deafened ears) are due, in part, to the modulation of spontaneous spike activity. We will also briefly discuss the

relationship between the responses observed in animal subjects and cochlear-implant users and suggest reasons why the two may yield different results.

This research was supported by the U.S. National Institutes of Health (Contract N01-DC-2-1005).

# Author Index

(Indexed by abstract number)

- Abbas, Paul 100,934,1010  
Abe, Kousuke 175  
Abe, Takahisa 369  
Abel, Cornelius 698  
Abraira, Victoria E. 296  
Abrashkin, Karen 571  
Abu Sa'ed, Judeh 352  
Adachi, Tsunemichi 428  
Adams, Brittany 217  
Adams, George L. 914  
Adams, Joe 26,354  
Adany, Istvan 127  
Adelman, John 260  
Adir, Elam 937  
Adler, Henry J. 809  
Afghan, Muhammad K.N. 154,162  
Agrawal, Smita S. 97,444  
Agterberg, Martijn 550  
Ahmad, Shoab 594,595,796,797  
Ahmed, Bashir 94,155,157,695  
Ahmed, Zubair M. 344,348,349,606  
Ahn, Jin-Chul 816  
Ahn, Joong Ho 561  
Ahrens, Misha 514  
Aizawa, Naotaka 949  
Akil, Omar 860,893  
Alagramam, Kumar N. 284,532,539,871  
Alais, David 435  
Alexandrov, Vladimir 654  
Alexandrova, Tamara 654  
Alkhatib, Ala 702  
Allen, Jont 386,635,738,740,741  
Allen, Kachina 435  
Allen, Paul 177,665,924  
Allen, Stanley 226,227  
Alliston, Tamara 787  
Allport, Johanna 493  
Aloor, Heather L. 838,841  
Al-Shurbaji, Ayman 489  
Altschuler, Richard 252,556,699,806,908,944  
Alván, Gunnar 489  
Alvarado, David 286  
Ambert-Dahan, Emmanuelle 977  
Ambrosetti, Umberto 492  
Amitay, Sygal 184  
Anderson, Charles T. 370,393  
Anderson, lee-Ching W. 9,727  
Anderson, John 469,610  
Anderson, Lucy 144  
Anderson, Malin 909  
Andoni, Sari 775  
Angelaki, Dora S. 194,208  
Angeli, Simon 231  
Antonioni, Robert 223  
Anvari, Bahman 384  
Arai, Andrew 341  
Arai, Tsuguyuki 820,830  
Aranyosi, A.J. 79  
Armstrong, David 567,821  
Arnold, Wolfgang 600  
Aronow, Bruce 345  
Aronson, Peter 265  
Arruda, J. 366  
Art, Jonathan 780  
Asako, Mikiya 916  
Ashida, Go 175  
Ashmore, Jonathan 262,266  
Askew, Charles 42,598  
Aso, Sadamitsu 823  
Atanackovic, Djordje 976  
Atiani, Serin 942,943  
Atiba-Davies, Margaret 290  
Atkin, Graham 46,794  
Atzori, Marco 512  
Auer, Manfred 381  
Avan, Paul 261  
Avissar, Michael 894  
Avraham, Karen B. 27,302,351,352  
Azeredo, William 66  
Babaria, Hitendra 465  
Babb-Clendenon, Sherry 305  
Bacon, Sid 211  
Bae, Woo Yong 915  
Baek, In-Young 816  
Baek, Moo-Jin 974  
Bagger-Sjöbäck, Dan 981  
Bahmad, Fayeze, Jr. 649  
Bai, Jun-Ping 265,377,630  
Bajo, Victoria 168,703,704  
Baker, Kim 275  
Baker, Suzanne 605  
Balaban, Carey 195,197,209  
Balakrishnan, Uma 445  
Baldridge, Mandi 493  
Balkany, Thomas 933,937  
Ball, Geoffrey 101  
Balooch, Guive 787  
Bance, Manohar 647,650  
Bandyopadhyay, Sharba 681  
Barald, Kate 294,305  
Barbour, Dennis L. 161  
Barnett-Johnson, Rachel 367  
Barrese, James 782  
Barrett, Jessica 926  
Barroso, Margarida 270  
Barta, Patrick 425  
Bartels, Katrin 976  
Bartho, Peter 707  
Bartles, James R. 45,258,547  
Bartlett, Edward 711  
Bartolome, Marivi 536  
Basappa, Johnvesly 886  
Baselli, Giuseppe 1001  
Bashiardes, Stavros 286  
Basta, Dietmar 476,519,798  
Batts, Shelley 320  
Baucom, Jessica 292  
Bauer, Carol 38  
Baumann, Ingo 275  
Bebak-Williams, Julie 41  
Becker-Lenzian, Ursula 791  
Bedrosian, Jeffrey 484,611  
Beirowski, Bogdan 791  
Beisel, Kirk W. 28,49,329,378,612,634  
Beitel, Ralph E. 655,939  
Belyantseva, Inna A. 348,547  
Bendor, Daniel 156  
Bengani, Prity 714  
Bennett, Jean 611  
Benson, Christina 148,771  
Ben-Yosef, Tamar 344  
Bergenius, Johan 981  
Berger, Rachel 296  
Bergeron, Adam 869  
Bergevin, Christopher 70  
Berk, Richard 985  
Berninger, Erik 489  
Bernstein, Leslie 760  
Berrebi, Albert S. 108,136,498,862,863  
Bertram, Simone 891  
Best, Virginia 188,714  
Bettinelli, Matteo 492  
Beurg, Maryline 631  
Beyer, Lisa A. 294,303,322,546,547,872  
Bhagat, Shaum 211  
Bhattacharya, Gautam 25,48,289  
Bhonagiri, Veena 286  
Bian, Lin 59  
Bibas, Thanos 648  
Biebel, Ulrich W. 702  
Biedenapp, Désirée 702  
Bielefeld, Eric 399  
Biesecker, Leslie 300  
Billig, Isabelle 122  
Billings, Curtis 420  
Billings, Peter 31  
Birck, Jon 465  
Bird, Jonathan 333  
Bitsche, Mario 355  
Bizley, Jennifer 703,704  
Black, Owen 471,579  
Blauwkamp, Marsha 294  
Bajo, Victoria 168,703,704  
Bleek, Stefan 107,109  
Blikas, Athanasios 122  
Bloch, Wilhelm 892  
Blum, Inga 976  
Blumenthal, Kenneth 573  
Boahen, Kwabena 77,769  
Bodmer, Daniel 804  
Boettcher, Flint 103  
Boger, Erich T. 627  
Bohne, Barbara A. 32,33  
Bohorquez, Alex 692  
Bohorquez, Jorge 427,982,988  
Bok, Jinwoong 295  
Bokemeyer, Carsten 976  
Bolanthur, Anitha 792  
Bolz, Steffen-Sebastian 600  
Bonabi, Sharouz 804  
Bond, Chris T. 260  
Bonham, Ben 413,878  
Boo, Sung Hyun 580  
Borina, Frank 152  
Boström, Marja 909  
Botta, Laura 776  
Bouccara, Didier 977  
Boulter, Jim 609  
Boutet de Monvel, Jacques 92  
Boyle, Richard 389  
Bozorg Grayeli, Alexis 977  
Bozorg, Sara 396  
Bozovic, Dolores 47,256  
Bradford, Yvonne 304  
Bradley, Schulte 593  
Brahmer, Tobias 281  
Braig, Claudia 257,607,629  
Brandon, Carlene S. 829  
Brandt, Niels 257,607  
Braun, Allen 418  
Braun, Susanne 771,938  
Breneman, Kathryn 389  
Brew, Helen 177  
Brewer, Carmen 341  
Briethaupt, Andrew 945  
Brittan-Powell, Elizabeth F. 809  
Broel, Nina 960  
Brooker, Rachael 525  
Brors, Dominik 867,906  
Brough, Douglas 325  
Brown, M. Christian 114,121,664  
Brown, Stephanie 963  
Brown, Steve D.M. 20,873  
Brown, Trecia 198  
Brownell, William E. 380,383,384,385  
Brownstein, Zippora 351  
Brozoski, Thomas 38  
Bruce, Ian 772  
Brugaud, Aurore 779  
Brunet, Lisa 295  
Brunetta, Ivan 856  
Brungart, Douglas 758  
Brunso-Bechtold, Judy K. 694  
Buchman, Craig 223,224  
Bui, Huyen 512  
Buran, Bradley Nicholas 616  
Burgess, Barbara 354,359,887  
Burkard, Robert 399,577  
Burmeister, Margit 546  
Burrows, Amy 229  
Buschermöhle, Michael 186  
Buss, Emily 971  
Bussey, Rhiannon R. 661  
Butman, John 341  
Byrapureddy, Rajasekhar 512  
Bystrom, Cory 254  
Byun, Jae Yong 974  
Cafaro, Jon 335  
Cai, Chun 274,486  
Cai, Hongxue 639  
Cai, Qing 274,487  
Calabrese, Daniel 448  
Cameron, Peter 833  
Campbell, Kathleen C.M. 819  
Camper, Sally 302,303,872  
Camps, Reyna 348  
Canlon, Barbara 395,532,535,802,803,918  
Cant, Nell 148,771  
Cao, Juyang 343  
Cao, Xiaojie 677  
Cao, Yanran 976  
Carey, John P. 8,9,726,727,728  
Carlile, Simon 435  
Carlyon, Robert P. 757,1006  
Carner, M. 978  
Carninci, Piero 634  
Carr, Catherine E. 135,172,768  
Carron, Michael 134,985  
Carson, Matt 533  
Casalotti, Stefano 856  
Case, Jamie 840  
Caspary, Donald M. 395,921,923  
Casseday, John H. 689  
Centonze, V. E. 268  
Ceranica, Borka 494  
Cervantes, Blanca 454  
Cha, Chang Il 974  
Chabbert, Christian 779  
Chadwick, Richard S. 82,83,88,366  
Chait, Maria 422  
Chan, Rebecca J. 838  
Chandrasekaran, Bharath 520  
Chang, Catherine 430  
Chang, Jolie 787  
Chang, Qin 312  
Chang, Qing 594,595,796,797  
Chang, Sun-O 599  
Chang, Weise 11  
Chapla, Marie 447  
Chatlani, Shilpa 785  
Chatterjee, Monita 416  
Chavez, Eduardo 536  
Cheatham, Mary Ann 24,379  
Cheeseman, Michael 20  
Chen, Fangyi 990  
Chen, Ganling 517  
Chen, Guang-Di 34,577  
Chen, Lin 735  
Chen, Ping 312,316,594,595,797  
Chen, Wei Chun 902  
Chen, Xinxin 595,797  
Chen, Yiling 947  
Chen, Zheng-Yi 314,854  
Chen, Zhiqiang 899,901  
Cheney, Paul 127  
Cheng, Genhong 749  
Cheour, Marie 427  
Cherian, Neil 87  
Chertoff, Mark 390,895  
Chien, Wade 641,642,983  
Chikar, Jennifer A. 935  
Chin, Ling 239  
Chinchilla, Sherol 408  
Chiu, Chen 442  
Cho, Byung-Han 578  
Cho, Yang Sun 915  
Cho, Yang-Sun 580  
Choi, Byung-Min 815  
Choi, Chul-Hee 390  
Choi, Ho-Suk 578  
Choi, Kwang Dong 723  
Choi, Sung-Min 815  
Choo, Daniel 855,866  
Choung, Yun-Hoon 228,466  
Chow, Lionel 605  
Christensen, Barbara 850  
Christensen-Dalsgaard, Jakob 135,139,172,640  
Christison, Joe 306  
Christova, Peka 469  
Chu, Eugene 727,728  
Chung, Jong Woo 561,979  
Chung, Won-Ho 580,750  
Chung, Yoojin 178  
Chung, Yunju 225  
Church, Michael 217  
Cioffi, Joseph A. 229,455,458,845  
Clarey, Janine 102  
Clarke, Jeffrey M. 838  
Clarke, Maria 94  
Clifford, Sarah 781  
Coffey, Lauren 289  
Coffin, Allison B. 337,367  
Coffin, J. Douglas 327  
Cohen, Bernard 193,205,206,207  
Cohen, Helen 477  
Cohen, Mazal 219  
Cohen, Yale 510  
Colburn, H. Steven 178,761  
Coleman, Crystal 985  
Colesa, Deborah J. 935  
Coling, Donald 399,573  
Colletti, L. 978  
Colletti, Vittorio 978  
Colligon, Lynda 40  
Collins, Leslie 656,754,1000,1003  
Comeau, Jonathan 271  
Cone-Vesson, Barbara 216,347  
Connell, Sara 231  
Coomes, Diana 143  
Cooper, Nigel 78  
Corbett, Mary 605  
Corbett, Scott 533  
Cordero, Joehassin 432  
Corey, David P. 313,314  
Corfas, Gabriel 457  
Cornforth, Theodore 693  
Corrales, Eduardo 849  
Corwin, Jeffrey T. 293  
Cosgrove, Dominic 25,48,49,289  
Cosme, Furlong 644

- Costa, Candice 210  
Cotanche, Douglas 330,331,336  
Coticchia, James 985  
Cotton, John 451  
Coulson, May T. 910  
Covey, Ellen 145,146,689  
Cowan, Justin 755  
Cox, Stephanie 345  
Cramer, Karina 529,666,667  
Cramer, Michele 825  
Crane, Benjamin 784  
Crawford, Andrew 43  
Cristaudo, Salvatore 145,146,701  
Cristobal, Ricardo 845  
Crumling, Mark 320,321,322,571  
Cui, Yilei 944  
Cullen, Kathleen E. 4,729  
Cunningham, Lisa L. 829  
Cureoglu, Sebahattin 361,790  
Cusack, Rhodri 757  
Cushing, Sharon 407  
Cyr, Janet L. 291,293,543  
D'Souza, Mary 920  
Dabdoub, Alain 526  
Dade, Monica 416  
Dagan, Orit 351  
Dahl, Hans-Henrik M. 347,837  
Dai, Chenkai 645  
Dai, Chunfu Dai 473  
Dailey, Michael E. 868  
Dalhoff, Ernst 62  
Dallender, S. 44  
Dallos, Peter 24,51,370,376,379  
Danilov, Yuri 200  
Darbon, Pascal 259  
Darland, Tristan 336  
Darr, Stacy 395  
Darrow, Keith 882  
Dasika, Vasant 182  
Dau, Torsten 718,969  
David, Amelyne 314  
David, Stephen 163  
Davidson, John 41  
Davis, James 456  
Davis, Kevin 142  
Davis, Rickie 532  
Davis, Robin L. 634,900,902,904  
Day, Mitchell 176  
Dazert, Stefan 867,906  
Dazet, Stefan 536  
de Boer, Egbert 989  
de Cheveigné, Alain 191  
De Groot, John 550  
de La Rochefoucauld, Ombeline 71  
De Lisle, Robert C. 592  
de Silva, Michelle G. 837  
de Venecia, Ronald K. 121  
Deak, Levente 376  
Dean, Isabel 106,773  
Deane-Pratt, Adenike 164,166  
Deeks, John M. 1006  
DeGagne, Jacqueline 280,483  
Dehmel, Susanne 679,684  
Del Bo, Luca 492  
Delano, Paul H. 880  
Delgado, Rafael 988  
Delgutte, Bertrand 93  
Deligeorges, Socrates 653  
Delimont, Duane 289  
Della Santina, Charley C. 9  
Dememes, Daniëlle 779,883  
Demer, Joseph 784  
Dent, Micheal 961  
Depireux, Didier 154,162  
Derr, Adam 290  
Desai, Anuradha 485  
Devore, Casey 601  
DeYoe, Edgar 731  
Diaz-Molina, Nancy 654  
Dickman, J. David 7,194,208,317,459,864,875  
Dietrich, Susanne 65  
Dikta, Kai 976  
Dimitriadis, Emiliós K. 88,366  
Ding, Dalian 287,400,573,574,575,576,799,828  
Divenyi, Pierre 737  
Dobbins, Heather 154,162  
Dobie, Robert 579  
Doetzelhofer, Angelika 15  
Dohar, J.E. 975  
Doi, Katsumi 308,346,817  
Doi, Takashi 710  
Doiron, Brent 176  
Dolan, David 130,294,303,320,806,826,872,898  
Doleviczényi, Zoltán 812  
Domenichetti, Emanuela 492  
Donaldson, Kevin 943  
Donato, Roberta 104  
Donepudi, Sreekrishna 567,821  
Dong, Wei 72  
Donnelly, Neil 648  
Dooling, Robert J. 809,911,958,959  
Dootz, Gary 303,398,806  
Doucet, John 128  
Downing, John 336  
Downing, Mark 99  
Drabo, Melissa 475  
Drayton, Meghan 542  
Drennan, Ward R. 1005  
Drescher, Andrew J. 310  
Drescher, Dennis G. 621,624,889  
Drescher, Marian J. 621,624,889  
Driver, Elizabeth 300  
Dror, Amiel A. 27,302  
D'Sa, Chrystal 327  
D'Souza, Mary 401,913  
Du, Bo 799  
Du, Guo-Guang 370,376  
Du, Li Lin 285  
Du, Xiaoping 527,567,821  
Duan, Maoli 22,586  
Dubno, Judy R. 925,927  
Duchen, Michael 810  
Dufort, Daniel 523  
Duggan, Anne 258  
Duifhuis, Hendrikus 125  
Dulon, Didier 631  
Duncan, Luke 330,331  
Duncan, R. Keith 626  
Durham, Dianne 671,946  
Dziewit, J. Andrew 633  
Eatock, Ruth Anne 2,452,453  
Ebert, Jonathan 345  
Ebmeier, Joerg 750  
Eckert, Mark 430  
Eddins, Ann 117  
Eddins, David A. 437,972,973  
Edge, Albert 843,846  
Edge, Roxanne 370,379  
Edsman, Katarina 281  
Eernisse, Rebecca 455,663  
Eggermont, Jos 949  
Ehrlich, Garth 229  
Ehrsson, Hans 281,585  
Eickhoff, Simon B. 423,431  
Eisen, Marc 411  
Eisner, Frank 734  
Ekbom, Andreas 281,585  
Elgoyhen, Ana Belén 372,609  
Elgueda, Diego 880  
Elhilali, Mounya 942,943  
Elliott, Taffeta 139  
Ellison, John C. 61  
Ellison, William 41  
Ellsworth, Buffy S. 302  
Elsabbagh, Mayada 219  
Emadi, Gulam 99  
Endo, Tsuyoshi 282,827  
Engel, Jutta 257,607,629  
Englitz, Bernhard 110,684  
Engmör, Cecilia 281  
Epley, John 465  
Eppard, Holly 342  
Epstein, Michael 753,966  
Erbe, Christy B. 455,458,845  
Erenberg, Sheryl 412  
Ergonul, Zuhai 590  
Ernst, Arne 476,519,798  
Erra, Gouthami 214  
Erven, Alexandra 614  
Escabi, Monty A. 150,151,709  
Eshraghi, Adrien 933,937  
Esterberg, Robert 10  
Eulitz, Carsten 733  
Euteneuer, Sara 319  
Evans, Alan 626  
Evans, Michael G. 43,44,259  
Fagnani, Enrico 492  
Fahey, Paul 58,386  
Fairfield, Damon 905  
Faltz, Christiane 976  
Fan, Yun-Hui 639  
Fang, Jie 374  
Fang, Qing 303  
Farahbakhsh, Nasser 388  
Farrell, Brenda 383  
Farris, Hamilton 392  
Fathman, Garrison 274  
Faulkner, Andrew 98,409  
Fauser, Claudius 890  
Fechter, Laurence 35  
Feeney, M. Patrick 646  
Fekete, Donna 13  
Felsheim, Christian 756  
Feng, Albert S. 149,673,850  
Feng, Feng 301,329,500  
Feng, Guoyin 343  
Feng, Weihong 612  
Feng, Yanmei 516  
Ferguson, Melanie 755  
Fernandez-Perez, Antonio J. 467  
Feroze-Merzouk, Farhana 526  
Ferraro, John 214  
Ferrary, Evelyne 586,977  
Ferrieri, Patricia 225  
Fettilplace, Robert 43,747  
Feudel, Ulrike 186  
Fink, Stefan 275  
Fiolka, Katharina 302  
Firszt, Jill 731  
Fishman, Yonatan 159,160  
Fitzgerald, Matthew B. 179  
Fitzgibbons, Peter 926  
Fitzpatrick, Denis F. 61  
Fleming, Carrie 19  
Fletcher, Kenneth 342  
Florentine, Mary 183,210,753,966  
Flores-Otero, Jacqueline 900  
Flynn, Eric 151  
Folowosele, Fopefolu 67  
Fong, Karen 482  
Ford, Fred 41  
Forge, Andrew 317,856  
Forsythe, Ian 251  
Fraenzer, Juergen-Theodor 847, 912  
Franchini, Lucia 372  
Francis, Howard 404  
Franck, Kevin 411  
Frangulov, Anna 345  
Frankel, Adam 41  
Franklin, Samuel R. 694  
Franzoni, Claudia 405  
Freeman, Dennis M. 70,79,80,81,993  
Freeman, Nancy 239  
French, J. Courtney 226,227  
Frenz, Dorothy 309  
Freund, Jan A. 186  
Freyman, Richard 445,760  
Friberg, Ulla 981  
Fridberger, Anders 92  
Fridman, Gene Yevgeny 658  
Friederici, Angela 213  
Friedland, David 663  
Friedman, Thomas B. 302,339,344  
348,349,547,606,627  
Friedrich, Victor L., Jr. 781  
Frisina, Robert D. 396,397,401,537,913  
917,920,922,929,929,972,973  
Frisina, Susan 929  
Fritz, Andreas 10  
Fritz, Jonathan 942,943  
Fritzsch, Bernd 14,28,298,301,329,500,530  
Froemke, Robert 508  
Frolenkov, Gregory I. 627  
Froud, Karen 435  
Frydman, Moshe 351  
Fu, Qian-Jie 408,417,1002,1008  
Fuchs, Helmut 27  
Fuchs, Paul 260,503  
Fujioka, Masato 36,558  
Fujiwara, Keizo 428  
Fukuda, Hitoshi 307  
Fullerton, Lynne 806  
Funabiki, Kazuo 175  
Funahashi, Jun-ichi 311  
Funnell, W. Robert J. 636  
Furman, Adam C. 620,894  
Furman, Joseph 461,462,463,474  
Furness, David N. 44,45  
Furst, Miriam 436  
Furukawa, Masayuki 750  
Furukawa, Shigeto 169  
Fuzessery, Zoltan 518,774  
Gaboyard, Sophie 833  
Gaboyard-Niay, Sophie 619  
Gaddam, Anupa 214  
Gaese, Bernhard 756  
Gaggl, Wolfgang 731  
Gagnon, Patricia M. 538  
Galazyuk, Alexander 143,147  
Gale, Jonathan 333,810  
Gallun, Frederick J. 190,714,717  
Galvin, John J., III 408,417,1008  
Gambino, Ashley 577  
Gamiz, Maria Jose 467  
Gan, Rong 645  
Gandon, Clément 191  
Gandour, Jackson 112,520  
Ganesh, Vidya 115  
Gans, Donald 143,691  
Gantz, Bruce 412  
Gao, Jiangang 23,24,379  
Gao, Wei 857  
Gao, Wei-Qiang 854  
Garadat, Soha 660,715  
Garcia Lazaro, Jose Alberto 695  
Garcia-Anoveros, Jaime 258  
Garell, P. Charles 419  
Gasiewicz, Thomas A. 583  
Gassmann, Max 804  
Gastaldi, Giulia 776  
Gaur, Ashmita 415  
Gea, Myung-Ryong 815  
Gelb, Bruce 891  
Genzel, Daria 955  
Georgopoulos, Christina 379  
Gerber, Michael Todd 819  
Getnick, Geoffrey S. 84  
Ghaffari, Roozbeh 80  
Ghose, Kaushik 441  
Ghosh, Manju 348  
Giampola, Matthew 625  
Giabini, N. 978  
Gibson, Brian 231,937  
Giersch, Anne 548  
Gill, Ruth 363,587  
Gillespie, Peter 254  
Girod, Douglas A. 671  
Glattfelder, Jerry, Jr. 563  
Gleich, Otto 847,912,958  
Glickstein, Jonathon 486  
Glowatzki, Elisabeth 615,617,903  
Glueckert, Rudolf 362,909  
Gobaille, Serge 883  
Goldberg, Jay M. 506,785,786  
Goldfarb, Abraham 351  
Golding, Nace 683,688  
Goldowitz, Daniel 527,540  
Golenbock, Douglas 748  
Gomez, Christopher 469  
Gómez-Casati, María Eugenia 609  
Gomez-Fiñana, Manuel 467  
Gong, Siew-Ging 807  
Gong, Tzy-Wen 303,571,806,807  
Gong, Wangsong 202,203  
Gonzalez Castillo, Javier 1009  
Goodman, Shawn S. 61  
Goodrich, Lisa V. 296  
Goodyear, Richard J. 48,874  
Gooler, David 700,741  
Gopal, Kamakshi 493  
Gordon, Karen 407  
Gordon-Salant, Sandra 926  
Gorga, Michael 56  
Görlitz, Holger R. 956  
Gottshall, Kim 472  
Gould, Herbert 567,821  
Goutman, Juan 615,617  
Graham, Christine 885  
Granath, Anna 981  
Grandori, Ferdinando 405,1001  
Grant, John 451  
Grant, Lisa 264  
Grati, M'hamed 261  
Gratton, Michael Anne 25,42,289,484,598,611  
Graves, Ried 937  
Gray, Lincoln 962  
Graydon, Cole 450  
Grazioli, Monica 776  
Green, Glenn 350  
Green, Steven H. 551,552,553,868,905  
Green, Tim 409  
Greeson, Jennifer 368  
Greicius, Michael 430  
Greinwald, John H. 345,855  
Griesinger, Claudius 262  
Griffith, Andrew 300,301,339,341,349,544,545  
Griffiths, Timothy 164  
Grimm, Christian 849  
Grose, John 971

Gross, Julia 327,328	Harvey, Michael 242	Holt, Avril Genene 252,699,944	Izquierdo, Marco A. 133,145,146,701	Kadner, Alexander 108,498
Gross, Manfred 488	Hasegawa, Mamoru 279	Holt, Jeffrey R. 342,778,849	Izumikawa, Masahiko 303,320,321,322,571	Kaga, Kimitaka 315
Gross, Oliver 791	Hashimoto, Makoto 565	Holt, Joseph C. 504,785,786	Izzo, Agnella 96	Kahng, Hison 228,466
Grothe, Benedikt 171,719,767	Hashino, Eri 838,839,840,841	Hong, Stanley 993	Jabba, S.V. 795	Kai, Chikatashi 634
Grover, Mary 910	Hashisaki, George T. 342	Hong, Sung Hwa 100,221,580	Jackie Hunter, A. 20	Kaiser, Christina L. 671
Groves, Andrew 12,15,523	Hatch, Ekaterina 521	Honjo, Tasuku 307,851	Jacob, Rolf 461,462,463	Kakazu, Yasuhiro 682,766
Grube, Manon 165,720	Hatfield, James S. 621,889	Hoogduin, Hans 125	Jacques, Bonnie 299	Takehata, Seiji 369
Gstoettner, Wolfgang 938	Hauptert, Michael 985	Horiuchi, Timothy 686	Jajoo, Sarvesh 572	Kalamirides, Michel 977
Gu, Jianwen 81	Hauser, Marc 510	Horton, Nicholas 67	Jakkamsetti, Vikram 512	Kaliner, Federico 387
Gu, Rende 326,563,853	Havasy, Nathan 911	Horváth, Tamás 812	Jang, Yoon Seok 915	Kalluri, Radha 53
Guan, Bing-Cai 581,604	Hawkins, David 286	Hosoi, Hiroshi 495,497	Jansen, E. Duco 96	Kaltenbach, James 134,765
Guerrero, Willi 654	Hayashi, Hideo 361	Hossain, Waheeda A. 858	Janssen, Thomas 63,65	Kamdar, Nirav 430
Guha, U. 44	Hayashizaki, Yoshihide 634	Hotra, John 217	Jaquish, Dawn 485	Kampalli, Suresh B. 592
Guimaraes, Patricia 929,972,973	Hayes, Jonathan 567,821	Howard, Omar 295	Järleback, Leif 39,632,879	Kanaan, Moien 351,352
Guinan, John J., Jr. 78,121,478,479,505	He, David Z.Z. 23,24,253,329	Howell, David M. 862,863	Jarnig, Soon Suck 930	Kandler, Karl 662
Guipponi, Michel 18	He, Jiao 933,937	Hozumi, Katsuto 525	Jastreboff, Margaret 490,569	Kang, Eunjo 423,431
Gummer, Anthony W. 50,62,997	He, Lin 343	Hrabé de Angelis, Martin 27	Jastreboff, Pawel 490,569	Kang, Hun Hee 561
Gundelfinger, Eckart 616,617	He, Ning-ji 927	Hradek, Gary 932	Jeffcoat, Ben 204	Kang, Hyejin 423,431
Guo, Chao 807	He, Wenxuan 74,91	Hsieh, Candace 667	Jen, K.-L. Catherine 217	Kang, Xiaojian 426
Guo, Yun-Kai 540	Healy, Eric W. 746	Hsu, Chi 325	Jeng, Fuh-Cherng 934,1010	Kanicki, Ariane 806
Gurr, Andre 867,906	Hebda, P.A. 975	Htut, Alvin 670	Jensen, Marianne E. 441	Kanwal, Jagmeet 511,706
Gurrola, Jose, II 985	Hegewisch-Becker, Susanna 976	Hu, Bo-Hua 399,560,577	Jensen, Patricia 527	Kanzaki, Sho 36,279,491,541,558
Gutschalk, Alexander 513	Heid, Silvia 95	Huang, Jie 552	Jensen-Smith, Heather 998	Karasawa, Takatoshi 582
Guzman, Miguel 456	Heil, Peter 181	Huang, MingQian 854	Jeon, Hyunah 764	Karino, Shotaro 721
H.B., Shi 682,766	Hein, Sarah 398	Huang, Rong 190	Jeon, Sang-jun 843	Karlsson, Kjell K. 489
Habiby Kermany, Mohammad 540,832	Helfer, Karen 445	Huang, Xiaona 530,876	Jesteadt, Walt 61,970	Karmali, Faisal 192
Haburcakova, Csilla 202,203	Helfert, Robert 921	Hubbard, Allyn 996	Jeung, Changmo 55	Karmiloff-Smith, Annette 219
Hacker, Terry 20	Hellberg, Victoria 585	Hübner, Mathias 956	Ji, Weiqing 940,941	Karmody, Collin 643
Hackney, Carole M. 44,45	Heller, Stefan 17,843,848,849,854	Hudspeth, A.J. 47,256,292	Ji, Yadong 154,162	Karolyi, Jill 303
Haft, Ervin 446	Helyer, Rich 264	Hughes, Larry F. 395,805,819,898,921,923	Jia, Shuping 253	Kash, Jacob 317
Hagino, Tomotaka 440	Henderson, Donald 399,577	Huh, Jeong-Wha 599	Jia, Xuebin 89	Kashino, Makio 739
Haider, Neena 289	Henkel, Craig K. 694	Hullar, Timothy 447,448,777,783	Jiang, Dan 648	Kashio, Akinori 823
Hajduk, Agata 218	Henkemeyer, Mark 666	Hultcrantz, Malou 22,230,281,788	Jiang, Haiyan 400,575,576,799,828	Kasper, Anne 548
Halberstadt, Adam 195,197	Hennies, Hans Christian 798	Hultman, David 365	Jiang, Hao 403	Kato, Toshihiko 220
Hale, Shane 60,587,588	Henshall, Katherine 406	Hunker, Kristina L. 546,547	Jiang, Hongyan 570	Katsura, Koji 439
Hall, Joseph 971	Hergils, Leif 981	Hurley, Karen 453	Jiang, Ming 278	Katz, Eleonora 609
Hallworth, Richard 273,378,998	Herman, B. 268	Hurley, Laura 692	Jiang, Yuehua 610	Kawai, Jun 634
Halmos, György 812	Hermann, Joachim 767	Husnain, Tayyab 349	Jiang, Zhi-Gen 581,602,603,604	Kawamoto, Kohei 916
Halpa, Gonzalo 654	Hermesh, Orit 27	Huss, David 7,317,864,875	Jin, Shanxue 688	Keefe, Douglas H. 61
Halsey, Karin 130,294,826,898	Hernandez, Jeannie 908	Hutson, Ken 946	Jin, Yong-Ming 136	Keirnes, Hannah 296
Hama, Takemitsu 238	Hernández, Olga 146	Huynh, Kristin 24,379	Jin, Zhe 632,879	Keithley, Elizabeth 31
Hamame, Carlos M. 880	Herrmann, Barbara S. 478,479	Hwang, Chan-Ho 297,915	Jin, Zhen-Hua 541	Kelley, Darcy 139
Hamann, Ingo 912	Herron, Tim 426	Hydén, Dag 981	Johansson, Marianne 981	Kelley, Matthew W. 16,299,300,301,302,317,526
Hamard, Ghislaine 261	Hertzano, Ronna 27,302	Hyun, Naomi 296	Johansson, Peter 802,803	Kelly, Jack 138
Hamilton, Nicholas 409	Hess, Mailee 357,358	Ichbangase, Takashi 220	John, Earnest O. 226,227	Kempe, G. Steven 328
Hamish, Scott 18	Hessén-Söderman, Ann-Charlotte 981	Idrizbegovic, Esma 489,918,981	Johnson, Jacob 787	Kempler, Richard 488
Hamre, Kristin 527,567,821	Hetherington, Alexander 413	Ifediba, Marytheresa 464	Johnson, Kenneth R. 232,285,287	Kempton, Beth 280,481,482,483
Han, Dongyi 343	Hibino, Hiroshi 346	Ignatova, Elena 864	Johnson, Matthew 283	Kenjale, Himanshu 127
Han, Gyu 460	Higaki, Megumu 827	Iguchi, Fukuichiro 844	Johnson, Stuart 608,614	Kenna, Margaret A. 345
Han, WeiJu 29,831	Higgins, Jake 351	Ihlefeld, Antje 763	Johnson, Tiffany 56	Kennedy, Helen 43,264
Hand, Beth 398	Higgins, Nathan 709	Iizuka, Takashi 68,541	Johnson, Tim 533	Kent, Raymond 233
Haneda, Eri 1009	Highstein, Stephen M. 6,389,780,781	Ikeda, Katsuhisa 68,541	Johnstone, Patti 759	Kenworthy, Anne 269
Hans, Stefan 306,522	Hill, Brandon D. 237	Imamura, Akihide 220	Joho, Rolf 665	Kermany, Mohammad Habiby 274
Hansen, Marlan 551,905	Hill, Patrick 300	Imig, Thomas 946	Jones, Chonnetia 316	Kerschner, Joseph 229
Hansen, Stefan 867,906	Hillman, Dean 670	Ingham, Neil 109	Jones, Diane 354	Kerwin, Thomas 987
Hansson, Anita C. 802	Hind, Sally 755	Inoue, Makoto 279	Jones, Gary L. 97,444	Kesser, Bradley W. 342
Haque, Asim 7,208,459	Hirai, Shigeo 361	Irons-Brown, Shunda 633	Jones, Jennifer 526	Ketten, Darlene R. 366,999
Hara, Akira 549,559	Hirose, Keiko 30,800,859	Irving, Samuel 438	Jones, Sherri M. 284,730	Khaddam, Samar 970
Hara, Hirotaka 568	Hiroya, Sadao 739	Irwin, Amy 184	Jones, Simon J. 705	Khan, Aaysha M. 360
Harada, Tamotsu 361	Hirose, Keiko 30,800,859	Isaacson, Brandon 477	Jones, Timothy 449,878	Khan, Khalid M. 621,889
Harasztosi, Csaba 50	Hirya, Sadao 739	Ishida, Ieda Maria 499	Joris, Philip X. 85,897	Khan, Shahid 348
Harding, Gary W. 32,33	Hirschberg, Koret 352	Ishihara, Tsutomu 827	Josephson, Ron 367	Khandwala, Vivek 142
Hardisty-Hughes, Rachel E. 20	Hiryu, Shizuko 439,440	Ishikawa, Kazuo 340,468	Jost, Jürgen 110,684	Khimich, Darina 617
Hardy-Bruce, Karen 657,659	Hisa, Yasuo 238,596	Ishikawa, Kotaro 544	Juhasz, Ondrej 192	Khurana, Sukant 688
Hargunani, Christopher 280,483	Ho, Calvin C.K. 167	Ishimoto, Shin-ichi 326	Juhn, Steven K. 225,914	Kidd, Gerald, Jr. 189,190,717
Harland, Richard 295	Hoang Dinh, Emilie 631	Ishiyama, Akira 356	Juiz, Jose 133,699	Kiefer, Jan 938
Harms, Michael 424	Hoeffe, Teresa 719	Ishiyama, Gail 356	Jülicher, Frank 991	Kiernan, Amy E. 27
Harper, Nicol 106	Hoffa, Angela 1009	Ison, James 177,665,924	Jung, Jae-Yun 816	Kikkawa, Y. 873
Harrington, Ian A. 174	Hoffer, Michael 243,472	Ito, Juichi 276,277,282,307814,827,842,844,851,852	Jung, Min-Kyo 914	Kikkawa, Yayoi S. 284,539,871
Harris, Belinda S. 232	Hoffman, Howard J. 470	Ito, Ken 721	Jung, Timothy T.K. 226,227	Kikuchi, Masahiro 428
Harris, Jeffrey 31	Hoffpauir, Brian 132	Iwai, Koji 282,852	Kabahuma, Rosemary 353	Kil, Jonathan 326,563,853
Harris, Kelly C. 925	Hoidis, Silvi 891	Iwamoto, Lynn 215	Kabara, Lisa 294	Kilgard, Michael 512
Harris, Kenneth 707	Holbrook, Brenda 341	Iwasa, Kuni 374	Kabra, Madulika 348	Kim, Ana H. 725
Hartley, Douglas 94	Holmberg, Raena 660	Iwasaki, Yoko 931	Kacelnik, Oliver 434	Kim, Bok-Ryang 815
Hartmann, Rainer 95	Holstein, Gay R. 780,781	Iyer, Nandini 758	Kach, Jacob 310	Kim, Chong-Sun 423,431,599
			Kaczmarek, Leonard 250	Kim, Daniella 965
			Kada, Shinpei 814,842	

Kim, Duck O. 173	Kristiansen, Arthur 26	Leibold, Christian 171	Lomax, Margaret 303,806,807	Marquardt, Torsten 164
Kim, Euysoo 864	Kros, Cornelis 255,608,614	Leibold, Lori 970	Lombardini-Parker, Lowell 334	Marriage, Josephine 219
Kim, Hyungjin 818	Krumbholz, Katrin 716	Leight, William 223,224	Long, Glenis 55	Marriott, Gerard 374
Kim, In Young 100,221	Kubo, Takeshi 308,346,817	Lemort, Nicole 314	Longnion, Jeff 182,651	Marrone, Nicole 189
Kim, Jae Ryong 915	Kucukoglu, M. Selin 1003	Lenarz, Thomas 554,555	Longo-Guess, Chantal 285	Marrs, James 305
Kim, Ji Soo 723	Kudo, Motoi 710	Lendvai, Balázs 812	Lopez, Ivan 356	Martin, Donna M. 350,546
Kim, Jinkyung 818	Kuenzel, Thomas 119	Lenihan, Nicole 128	Lopez-Escamez, Jose A 467	Martin, Glen 57,58
Kim, Jong-Seung 556	Kuhn, Stephanie 257,607,629	Lentz, Jennifer 968	Lovett, Michael 286,865	Martin, Pascal 991
Kim, Joung Uk 561	Kujawa, Sharon G. 478,479,789,899	Leong, Francis 403	Lovitt, Andrew 738,740	Martinelli, Giorgio 781
Kim, Jun Woo 237,274	Kulesza, Randy 124	Leong, U-Cheng 117	Low, Walter 610	Martinez-Monedero, Rodrigo 846
Kim, Kyu-Sung 578	Kumar, Gagan 258	LePage, Eric 75	Loyzaga, Pablo 536	Maruta, Jun 205
Kim, Lee Suk 915	Kumpik, Daniel 434	LePrell, Colleen 131	Lu, Shan 996	Maruya, Shin-ichiro 369
Kim, Patrick 274	Kunin, Mikhail 193,206	Leslie, Frances 947	Lu, Tao 675	Marvit, Peter 154,162
Kim, SungHee 930	Kuo, Min-Wen 532	Leuwer, Rudolf 976	Lu, Xiaowei 528	Masaki, Kinuko 80,81
Kim, Tae-Soo 276,282,827	Kuramasu, Toshihiro 346,817	Levi, Jessica 51,84	Luczak, Artur 707	Mason, Christine R. 189,190,717
Kim, Young Jin 561	Kurima, Kiyoto 544	Levine, Stephen 642,643,650	Ludwig, Alexandra 213	Massing, Thomas 791
Kim, Youngki 225	Kurita, Akihiro 491	Lewandoski, Mark 299	Luebke, Anne E. 583,661,696	Masuda, Masatsugu 36,558
Kim, Yunha 818	Kuriyama, Hiromichi 916	Lewis, Julian 525	Luethke, Lynn 239	Mathers, Peter H. 862,863
Kimura, Hiroshi 980	Kuwabara, Nobuyuki 123	Lewis, Richard 202,203	Luisi, John C. 574	Matsui, Jonathan 330,336
King, Andrew 94,157,168,170,434,703,704	Labay, Valentina 545	Li, Guiyuan 278	Luksch, Harald 119	Matsumoto, Masahiro 842
King, Isabella 756	Labbe, Daniel 892	Li, Huawei 854	Lundberg, Yesha (Yunxia) 530,876	Matsumoto, Nozomu 387
King, Mary-Claire 351,352	Ladrech, Sabine 562	Li, Jian-Dong 752	Luo, Hao 735	Matsunami, Tatsuya 596
King, W.M. 294,725	Lafien, J. Brandon 657,659	Li, Lijun 309	Luo, Huan 421	Matsuoka, Akihiro 839
Kirkegaard, Mette 39	Laforenza, Umberto 776	Li, Na 775	Luo, Li 846	Matsuoka, Yoshinori 282,852
Kirkpatrick, Katie 650	LaGasse, James 326,563	Li, Qingzhong 793	Luo, Xin 1002	Matunaga, Mayumi 931
Kishida, Tsunao 238	Lagziel, Ayala 606	Li, Xingqi 89	Lustig, Lawrence 245,787,860,893	Mavoori, Hareesh 215
Kisley, Lauren 539	Lahiri, Aditi 733	Li, Yan 46,794	Lutfy, Justyn 636	Maxfield, Nathan 429
Kita, Tomoko 276,277,282,827,842,852	Lai, Eseng 297	Li, Yi 626	Luxon, Linda 494	May, Brad 963
Kitahara, Tadashi 346	Laitman, Jeffrey 235	Li, Yuan 984	Ly, Derick 226,227	Mazda, Osam 238
Kitajiri, Shin-ichiro 301,339	Lalanne, Zuzanna 20	Liang, Chengya 601	Lyford-Pike, Sofia 728	Mburu, P. 873
Kitani, Rei 369	Lally, Brent 498	Liang, Fenghe 593,822	Lynch, Eric 326,563,853	Mc Elveen, John 231
Kittel, Ágnes 812	Lalwani, Anil K. 46,787,794	Liang, Guihua 632	Lynch-Erhardt, Martha 401,913,920	Mc Laughlin, Myles 897
Kittel, Malte C. 912	Landau, Jessica 611	Liang, Jianning 792	Lysakowski, Anna 502,619,782,833	McAlpine, David 104,106,164,166,773
Klapczynski, Marcin 833	Landsberger, David 1004	Liang, Kevin 947	Ma, Jie 116	McArthur, Kimberly 194
Klein, Reinhild 480	Lang, Hainan 533,907	Liao, Amy 25	Ma, Wei-Li 105	McCandless, Cyrus 209
Klink, Karin 964	Langemann, Ulrike 960	Liao, Isaac 426	Ma, Xiaofeng 708,940	McCarty, Christopher M. 232,285
Klis, Sjaak 550	Langner, Gerald 771	Liao, Zhijie 385	MacArthur, Carol 481	McClaine, Elizabeth 961
Klug, Achim 767	Larsen, Deb L. 819,921,923	Lieberman, M. Charles 457,501,616,622 881,882,885,886,887	MacDougall, Hamish 205	McCormack, Stephen 826
Klump, Georg M. 719,912,960,964	Larue, D.T. 140	Licht, Katharina 847	Macherey, Olivier 1006	McDermott, Brian 292
Knipper, Marlies 257,531,607,629	Lasker, David 460	Lichtenhan, Jeffery 895	MacLeod, Katrina 686	McDonald, Kent 381
Knirsch, Martina 607	Latz, Eicke 751	Lidington, Darcy 600	Macpherson, Ewan A. 174	McGee, JoAnn 48
Ko, Chia-wen 470	Laurell, Göran 22,281,585,586	Lim, Insook 7	Madeo, Anne 341	McGettigan, Carolyn 743
Ko, Jennifer 772	Lawal, Adeshola 657,659	Limb, Charles 418	Maganti, R.J. 795	McGuire, Ryan 375
Kobayashi, Toshimitsu 311	Layman, Erynn 299,526	Limón, Agenor 454	Magezi, David 716	McKay, Colette 406,1004
Kobayasi, Kohta 116	Le Gall, Morgane 261	Lin, Jizhen 225,610	Maghnouj, Abdel 46	McKenna, Michael 26
Koch, Dawn Burton 99	Le Goff, Loïc 47	Lin, Liang-Kong 439,440	Mahendrasingam, Shanthini 44,45	McMillan, D. Randy 48
Koehler, Seth 113,131	Le Prell, Colleen 898	Lin, Wen-Yu 149	Maier, Julia 719	McMillen, Debra 254
Koehn, Fred 485	Le, Jun-Ho 599	Lin, Xi 312,594,595,796,797	Maisel, Beth 855	McNamara, Rachel 349,545
Koenig, Ovidiu 488	Leadbeater, Ellouise 960	Lindblad, Ann-Cathrine 222	Maison, Stéphane F. 622,881,882	Meddis, Ray 676,678
Koenig, Ronald 294	Leake, Patricia A. 414,878,932,939	Linden, Jennifer 514	Majdalawieh, Osama 647	Meech, Robert 819
Koepl, Christine 768	Leal, Suzanne M. 793	Ling, Feng 610	Maki, Katuhiro 169	Meehan, Daniel 289
Kohrman, David C. 546,547	Lechere, Aurelie 292	Ling, Lynne 921	Makishima, Tomoko 341,349,545	Meenderink, Sebastiaan 884
Koike, Takuji 68	Kohrman, David C. 546,547	Lipán, Michael 235	Mallery, Robert 783	Meinke, Deanna 57
Kojima, Ken 276,307,842	Koike, Takuji 68	Lipovsek, Marcela 609	Malmierca, Manuel S. 133,145,146,246,701	Melcher, Jennifer 424,513
Kollmar, Richard 850	Kojima, Ken 276,307,842	Lis, Maciej 573	Manabe, Tomoko 428	Meltzer, Inna 802,803
Komori, Masahiro 610	Kollmar, Richard 850	Lisowska, Grazyna 218	Mancilla, Jaime 685	Meltzer, Noah E. 951
Komune, Shizuo 682,766	Komori, Masahiro 610	Lister, Jennifer 429,928	Mangiardi, Dominic 330,331	Mendolia-Loffredo, Sabrina 455
Kondo, Kenji 315,319	Komune, Shizuo 682,766	Litovsky, Ruth Y. 97,444,660,715,759	Manis, Paul 113,248,685,687	Menon, Vinod 430
Kondo, Takako 840,841	Kondo, Kenji 315,319	Litvak, Leonid 658	Manley, Geoffrey 640	Merchán, Miguel A. 133,701
Kong, Jee-Hyun 260	Kondo, Takako 840,841	Liu, Dong 306,522	Mann, Zoë 810	Merchant, Saamil N. 354,359,641,642,649,983
Koo, Ja-Won 723	Kong, Jee-Hyun 260	Liu, Feng 15	Manning, Brian 888	Merfeld, Daniel M. 199,202,203
Kopelovich, Jonathan 411	Koo, Ja-Won 723	Liu, Haiying 380	Manoussaki, Daphne 88,366	Mersel, Marcel 562
Kopperman, Jacob 51	Kopelovich, Jonathan 411	Liu, Liang-Fa 141,144	Mansour, Suzanne 521	Merzenich, Michael 508,712
Kopp-Scheinflug, Cornelia 110,679,684	Kopperman, Jacob 51	Liu, Liya 907	Mapes, Frances M. 929,972,973	Mesgarani, Nima 163
Köpschall, Iris 531	Kopp-Scheinflug, Cornelia 110,679,684	Liu, Qin 305	Marcario, Joanne 127	Metherate, Raju 947
Kopun, Judy 56	Köpschall, Iris 531	Liu, Qing 904	Marcotti, Walter 255,608,614	Metzner, Walter 116
Kopyar, Beth 764	Kopun, Judy 56	Liu, Wei 309	Marcus, Daniel C. 589,590,591,592	Meurling, Lennart 489
Kössl, Manfred 69,698	Kopyar, Beth 764	Liu, Wenxia 274	Margolis, Robert 225	Mey, Jörg 119
Kotak, Vibhakar 945	Kössl, Manfred 69,698	Liu, Xue Zhong 285,343	Marguet, Stephan 707	Meyer-zum-Gottesberge, Angela-Maria 791
Kothiyal, Prachi 345	Kotak, Vibhakar 945	Lobarinas, Edward 574,950,952,953	Mark, Sharayne 312	Mhatre, Anand N. 46,794
Kral, Andrej 95	Kothiyal, Prachi 345	Lobdell, Bryce 740	Marler, Jeffrey 789	Micco, Alan 936
Krieg, Edward 532	Kral, Andrej 95	Lobl, Tom 826	Marozeau, Jeremy 753	Michaels, Leslie 792
Krips, Ram 436	Krieg, Edward 532	Loebach, Jeremy 744,745		Michalewski, Henry J. 967
Krishnan, Ananthanarayan 112,115,520	Krips, Ram 436	Lohner, Andrea 890		Michel, Olaf 892
Krishnan, R.V. 268	Krishnan, Ananthanarayan 112,115,520	Lohr, Bernard 958		
	Krishnan, R.V. 268	Lomakin, Oleg 142		
		Lomax, Catherine 699,944		

Micheyl, Christophe 185,187,513	Mullan, Lina 319	Northrop, Clarinda 359,642,643,650	Palbus, A.C. 975	Pollak, George 770,775
Middlebrooks, John C. 174,413,1007	Müller, Barbara 50	Nourski, Kirill 100,934,1010	Palma, Maria Jose 467	Pollard, Hilary J. 543
Middleton, Alice 20	Muller, Yves A. 543	Nouvian, Regis 261	Palmer, Alan R. 141,144,705	Polley, Daniel 712
Migliaccio, Americo A. 9,726	Muly, Emil C. 594	Nowotny, Manuela 997	Palmer, Lawrence 590	Polony, Gábor 812
Migunov, Sergei 654	Mun, Ga Hee 808	Noyes, Albert 521	Palmer, Rachel E. 313	Pondugula, Satyanarayana 589,590,591
Mihara, Masahiko 558	Munirathinam, Subramani 328	Nozomu, Matsumoto 682,766	Paloski, William 471	Popel, Aleksander 385
Mikiel-Hunter, Jason 266	Münkner, Stefan 257,607,629	Nuttall, Alfred L. 29,90,91,602,604 831,834,835,989,990,994, 995	Paolini, Antonio 102	Popelka, Gerald 233
Miko, Ilona 666	Murai, Norihiko 39	Oas, John 87	Paparella, Michael M. 361,790	Popper, Arthur N. 41,337,367
Mikuriya, Takefumi 565,566,722,724,820,830	Murashita, Hidekazu 549,559	Obleser, Jonas 733	Papsin, Blake 407	Popper, Paul 229,458,663,845
Milenkovic, Ivan 669	Murata, Junko 308	Ochiai, Atsushi 721	Parazzini, Marta 405,1001	Popratiloff, Anastas 196
Mileski, Adam 807	Murdoch, Jennifer 317	Murphy, Emily 477	Parekh, A. 975	Porsov, Edward 91
Miller, Antonio 637	Murofushi, Toshihisa 721	Murray, Narelle 75	Parent, Pierre 635	Portfors, Christine 111
Miller, Brian 999	Murthy, Vidya 870	Murthy, Vidya 870	Park, Byung-Rim 578	Portis, Denise 241
Miller, Charles 100,934,1010	Murtie, Joshua 457	Musiek, Frank 212	Park, Chan-Il 564	Portis, Terry 240
Miller, Darla 540	Mustapha-Chaib, Mirna 303,872	Mutai, Hideki 854	Park, Channy 818	Post, J. Christopher 229
Miller, Diane L. 337,367	Myers, Kristin 38	Myers, Kristin 38	Park, Dong Choon 974	Poston, Amanda 224
Miller, Josef 556,826,908	Mynatt, Robert 587,588	Nadol, Joseph B., Jr. 359,360,887	Park, Hong Ju 9,201,460	Potashner, Steven J. 680
Miller, Katharine 370	Nabi, Hani A. 574	Nadler, Jacob 194	Park, Keehyun 228,466	Poulakis, Zeffie 216,347
Miller, Lloyd S. 749	Nadler, Jacob 194	Nadol, Joseph B., Jr. 359,360,887	Park, Min-Hyun 723,808	Pouyatos, Benoit 35
Miller, Michael 425	Nadol, Joseph B., Jr. 359,360,887	Nagashima, Reiko 36	Park, Raekil 818	Powder, Kara 286
Miller, Roger 239	Minor, Lloyd B. 1,3,9,460,726,729	Nagata, Keiichi 258	Park, So Yean 580	Poynton, Clare 425
Mills, John H. 925,927	Minowa, Osamu 541	Nagato, Tsuyoshi 439	Park, Sungyeol 818	Poytress, Bonnie 947
Minekawa, Akira 68	Mitchell, Alice 556	Nagy, Ivana 804	Park, Yong-Ho 564	Praetorius, Mark 275,325,480
Minor, Lloyd B. 1,3,9,460,726,729	Miwa, Masato 931	Naillat, Florence 526	Parker, Lisan 540,622	Preciado, Diego 225
Minowa, Osamu 541	Miyagi, Morimich 220	Naito, Yasushi 428	Parmentier, François 191	Pressimone, Vanessa J. 498
Mitchell, Alice 556	Miyamoto, Richard 839	Nakagawa, Takashi 682,766	Parrish, Jennifer L. 395,923	Pressnitzer, Daniel 191
Miyazaki, Hiromitsu 311	Miyazawa, Toru 320,322	Nakagawa, Takayuki 276,277,282,814,827,842, 852	Parsons, Thomas D. 618,620,625,633,894	Price, Steven 619,833
Miyazawa, Toru 320,322	Mizukoshi, Akifumi 827	Nakahata, Tatsutoshi 276	Paschall, Dwayne 432,433	Prieskorn, Diane 556,826,908
Mizuno, Terukazu 499,980	Mo, Jiling 612	Nakajima, Noriyuki 931	Patel, Amit H. 9	Prolla, Tomas 534
Mizuno, Terukazu 499,980	Mo, Zhicheng 680	Nakamura, Hajime 844	Patel, Nimisha 403	Prost, Robert 731
Mo, Jiling 612	Mochida, Takemi 739	Nakamura, Harukazu 311	Pathria, Jyoti 96	Pryor, Shannon 300
Mo, Zhicheng 680	Mock, Bruce E. 730	Nakashima, Tsutomu 86,499,811,892,980	Paul, Asit K. 574	Puel, Jean-Luc 562,779,883
Mochida, Takemi 739	Möckel, Doreen 69	Nakmali, Don 645	Pauley, Sarah 14,298	Pujol, Remy 584
Mock, Bruce E. 730	Modlin, Robert L. 749	Nam, Jong-Hoon 451	Paulovicks, Jennifer 212	Puligilla, Chandrakala 301
Möckel, Doreen 69	Mohamed, Othman 523	Nam, Jong-Hoon 451	Pawlowski, Karen S. 284,539,871	Puranik, Sachin 618
Modlin, Robert L. 749	Moiseff, Andrew 173	Nannapaneni, Naveen 668	Peake, William 642	Purdy, John 364
Mohamed, Othman 523	Molina, Maria I. 467	Narayan, Opendra 127	Pedemonte, Marisa 515	Puria, Sunil 76
Moiseff, Andrew 173	Molitor, Scott 118	Narins, Peter M. 149,167,388,884	Peng, Shu-Chen 410	Qi, Li 636
Molina, Maria I. 467	Moncho, Jose 133	Narui, Yuya 68,541	Penn, Claire 353	Qian, Dong 312,316
Molitor, Scott 118	Monge, Arianne 804	Nasser, Sigrid 762	Pereira, Fred A. 323,368,375,380	Qian, Feng 384
Moncho, Jose 133	Montcouquiol, Mireille 302,317	Navaratnam, Dhasakumar 265,369,377,630	Perez, Amaya 442	Qian, Jinyu 437
Monge, Arianne 804	Moon, Jeong-Hwan 816	Nayagam, David 102	Pérez-González, David 146,689	Qin, Wei 343
Montcouquiol, Mireille 302,317	Moore, David R. 168,184,438,755	Nayak, Gowri D. 543	Perfettini, Isabelle 261	Qiu, Anqi 425
Moon, Jeong-Hwan 816	Moore, Robert 472	Neadar, Sarah 715	Periasamy, Ammasi 270	Qiu, Qiang 149
Moore, David R. 168,184,438,755	Morales Garcia, José 531	Neelon, Michael 419	Perin, Paola 776	Qu, Chunyan 593,822
Moore, Robert 472	Moravec, William 452	Neely, Stephen 56	Pesavento, Michael 142	Qu, Yan 595
Morales Garcia, José 531	Morawski, Krzysztof 982,988	Neil, Segil 12	Pesznecker, Susan 579	Quesnel, Alicia M. 84
Moravec, William 452	Morell, Robert J. 606	Nemzou, Rodrigue 836	Peter, Bernhard Friedrich 600	Quirk, Wayne 403
Morawski, Krzysztof 982,988	Morest, D. Kent 327,328,858	Neubauer, Heinrich 181	Peters, Gregory 859	Raibla, David W. 21,584,824
Morell, Robert J. 606	Morgan, Warren J. 862,863	Neuburger, Heidi 657,659,1009	Peters, Linda M. 606	Raiguru, Suhurd 464
Morinaka, Yuichi 440	Morizono, Tetsuo 220	Newburg, Seth 999	Peterson, Ellengene 450,452	Ramakrishnan, Neeliyath A. 621,624
Morizono, Tetsuo 220	Mörby, Tarik 302	Ng, Philip 323	Petit, Christine 261	Ramaswamy, Rajesh 50
Morris, David P. 650	Morris, David P. 650	Nguyen, Jerry 226,227	Petralia, Ron S. 911	Ramirez, Cherie L. 897
Morris, Ken 612,634	Morse, Susan A. 20	Ni, Jing-Tian 735	Peusner, Kenna 196	Ramkumar, Vickram 572,805
Morse, Susan A. 20	Morton, Cynthia 548	Nichols, Justin 512	Peverelli, Marisel 837	Ramsay, Michele 353
Morton, Cynthia 548	Morton, Kenneth 656	Nicosia, Mark 226,227	Pfaller, Kristian 362,909	Randell, Scott 223,224
Morton, Kenneth 656	Moser, Tobias 261,615,616,617,836	Nie, Liping 598,612,613	Pfingst, Bryan E. 935	Ransohoff, Richard 30,800
Moser, Tobias 261,615,616,617,836	Motts, Susan D. 126	Niemczyk, Kazimierz 982,988	Pham, Liem 31	Rao, Shaohui 793
Motts, Susan D. 126	Mou, Kewa 626	Nishimura, Tadashi 495,497	Pham, Tammy 226,227	Rao, Velidi 25
Mou, Kewa 626	Mountain, David 331,653,996,999	Nishiyama, Yukihiro 980	Phatak, Sandeep 738	Raphael, Robert M. 272,368,371,375,381,597
Mountain, David 331,653,996,999	Mridha, Zakir 194,459	Niu, Xianzhi 535,918	Phillips, Kelli R. 291	Raphael, Yehoash 283,294,303,320,321,322 398,546,547,571,725,872, 935
Mridha, Zakir 194,459	Mueller, Joerg 65	Noben-Trauth, Konrad 290,542	Pickles, Raymond 223,224	Raphan, Theodore 193,205,206,207
Mueller, Joerg 65	Mueller, Marcus 891	Noda, Tetsuo 541	Pienkowski, Martin 948	Rapson, Ian 364,365
Mueller, Marcus 891	Mukherjea, Debashree 572,805	Nodal, Fernando 168,170,703,704	Pierce, Carol 326,563,853	Rasband, Matthew N. 858
Mukherjea, Debashree 572,805	Muldrow, Alaina 177,665,924	Nogaki, Geraldine 408	Pignol, Bernadette 562	Rask-Andersen, Helge 362,909,981
Muldrow, Alaina 177,665,924	Mulheisen, Michael 297	Noh, Heil 100	Pilipenko, Valentina 855	Ratnanather, J. Tilak 425
Mulheisen, Michael 297		Nordmark, Jan 489	Pilling, Michael 736	Ratzlaff, Kerstin 480
			Pingault, Veronique 313,314	
			Pitson, Stuart M. 600	
			Pitt, Gabriel J. 429,928	
			Platt, Christopher 239	
			Plinkert, Peter K. 275,480	
			Plontke, Stefan 587,588	
			Poeppel, David 421,422	
			Pohl, Ulrich 600	
			Polak, Marek 933,937	



Rauch, Steven D. 244,478,479	Rubel, Edwin W. 21,120,584,824	Schachtele, Scott 868	Shim, Hee Yeon 221	Spirou, George A. 132,862,863
Ravazzani, Paolo 405,1001	Ruben, Robert 986	Schaechinger, Thorsten 267	Shim, Hyun Joon 979	Sridhar, Divya 414
Raveendran, Nithya 589,590,591	Rubin, Jeffrey 526	Schaette, Roland 488	Shimogori, Hiroaki 565,566,568,722,724,820, 830	Srivastava, Arth 496
Ravicz, Michael E. 641,644,983	Rubinstein, Jay T. 182,651,1005	Scheffer, Deborah 313	Shin, Dong Hoon 808	Srour, Edward F. 840
Rawool, Vishakha 40	Rubio, Maria 247	Scheper, Verena 554	Shin, Hyang Ae 201	St. John, Alison 177,665,924
Raz, Yael 122,857	Rübsamen, Rudolf 110,165,213,669,679,684	Scherer, Elias Q. 600	Shin, Ji Young 915	Stack, Lauren 429,928
Razak, Khaleel 518	Ruckenstein, Michael 484	Schick, Bernhard 275	Shin, Jong Heon 930	Staecker, Hinrich 325
Razavi, Babak 443	Rudolf, Glueckert 355	Schmiedt, Richard A. 533,907	Shin, Jung Eun 201,979	Stafferton, Tina 217
Read, Heather L. 150,151,709	Ruebsamen, Rudolf 720	Schnneider, Daniel 453	Shin, Jung-Bum 254	Stagner, Barden 57,58
Rebibo, Annie 344	Ruel, Jérôme 562,883	Schnupp, Jan W.H. 94,155,157,434,695	Shin, Yu Ri 466	Stakhovskaya, Olga 414,878,932
Rebillard, Guy 883	Ruettiger, Lukas 531	Schoernich, Sven 957	Shinden, Seiichi 491	Stallings, Valerie 579
Rebscher, Stephen J. 413,939	Ruffin, Chad V. 1005	Schofield, Brett R. 126	Shinkawa, Hideichi 369	Stamataki, Sofia 404
Redfern, Mark 461,462,463,474	Ruggiero, Mario 639,896,992	Scholes, Chris 697	Shinn-Cunningham, Barbara G. 188,714,757,762,763	Stankovic, Konstantina 26
Regehr, Keil 601	Rupert, Angus 471	Schrader, Angela 869	Shinohara, Shogo 428	Stanton, Susan 532
Rehm, Heidi 345	Russ, Brian 510	Schreiner, Christoph 508	Shiomi, Yosaku 428	Stark, Thomas 867,906
Reidenberg, Joy 235	Russell, Sarah 936	Schrott-Fischer, Annelies 355,362,909	Shiotani, Akihiro 279	Starr, Arnold 967
Reiss, Lina 412	Rüther, Ulrich 300	Schubert, Claudia 165,720	Shoelson, Brett 82,366	Stecker, G. Christopher 174,426
Remus, Jeremiah 754	Rutherford, Mark 263	Schuchmann, Maike 954	Shore, Susan 113,130,131,668	Steel, Karen P. 27,288,614
Ren, Tianying 73,74,90,91,990	Rüttiger, Lukas 629	Schug, Nicola 607	Shoshani, J. 366	Steele, Charles 76
Renken, Remko 125	Ryals, Brenda M. 789,911,958	Schuller, Gerd 152	Shub, Daniel 761	Steinbach, Heidi M. 746
Répásky, Gábor 812	Ryan, Allen F. 319,536,750	Schulte, Bradley A. 623,822,907	Siciliano, Catherine 98	Steinschneider, Mitchell 159,160
Rha, Ki-Sang 564	Rybak, Leonard 572,805	Schultz, Julie M. 344	Siddiqui, Shazia 529	Stenberg, Annika 788
Rhee, Chung-Ku 816	Ryugo, David K. 404,951	Schulz, Andreas 170	Siegel, Jonathan 54	Stepanyan, Ruben 627
Rhodes, Charlotte R. 27	Rzadzinska, Agnieszka K. 27,288	Schvartz, Kara 416	Sigalovsky, Irina 424	Sterkers, Olivier 586,977
Riazi, Mariam 127,214	Sabin, Andrew T. 179,180	Scott, Luisa 683	Sigudla, Jerry 353	Stern, Ryan 787
Riazuddin, Sheikh 348,349	Sacchetto, L. 978	Scott, Sophie K. 732,733,734,743	Silva, Ikaro 183,210	Stevens, Geoff W. 837
Ricci, Anthony 392,628	Sachdev, Vandana 341	Scotti, Alberto 492	Silvius, Derek 524	Stewart, Christopher C. 179
Rice, Ann C. 129	Sadeghi, Soroush G. 729	See Youn, Kwon 221	Simmler, Marie-Christine 261	Steyger, Peter 581,582
Richard, Salvi 952	Safe, Theresa M. 583	Seeber, Bernhard 446	Simmons, Dwayne 388,869	Stjernschantz, Johan 981
Richards, Christopher 262	Safieddine, Saaïd 261	Segil, Neil 15	Simon, Jonathan Z. 421,422	Stocks, Rose Mary 567,821
Richards, Virginia 190	Sage, Cyrille 854	Seidl, Armin 120	Simonis, Claudia 771	Stofko, Elizabeth 573
Richardson, Dustin 774	Sahani, Maneesh 514	Seidman, Michael 403	Simonoska, Rusana 788	Stohl, Joshua 1000
Richardson, Guy P. 48,80,81,291,293,332,543, 874	Sahlin, Lena 788	Semple, Malcolm 509	Simpson, Brian 758	Stone, Jennifer 334,335
Richter, Claus-Peter 51,84,96,936	Sajan, Samin 865	Sen, Ganes 859	Simpson, Ivra 204	Stong, Benjamin 594,796
Rickards, Field W. 347	Sakaguchi, Donald 378	Senda, Michio 428	Simpson, John 205	Stöver, Timo 554,555
Riley, Alison 755	Sakaguchi, Takefumi 495,497	Sendin, Gaston 615,836	Singer, Wibke 531	Stredney, Donald 987
Rinne, Teemu 426	Sakai, Shuhei 549,559	Senn, Pascal 848,849	Singh, Ameet 397	Strutz, Jürgen 847,912
Rinzel, John 176	Sakamoto, Takashi 823	Sessanna, Dennis 987	Singh, R. 795	Sturm, Angela K. 380
Riquimaroux, Hiroshi 439,440,710,742	Sakata, Shuzo 707	Seth, Rahul 397	Sinha Ray, Saumitra 427	Sudhoff, Holger 906
Risling, Mårten 39	Sakata, Tomoyo 374	Sewell, William F. 507,888,899,901	Sivaramakrishnan, Shobhana 153	Suga, Nobuo 708,940,941
Risner, Jessica R. 778	Salm, Adrienne K. 498	Seyfarth, Ernst-August 69	Siveke, Ida 171	Sugahara, Kazuma 236,565,566,724,820,830
Rivoli, Peter 665,924	Salt, Alec 60,363,587,588	Seymour, John 75	Skinner, Kim 200	Sugamura, Mayumi 220
Rizel, Leah 344	Salvi, Richard 287,400,573,574 575,576,799,828,950,953	Sha, Su-Hua 37,402,570,801	Sklare, Daniel A. 239,470	Sugiura, Makoto 499
Rizzi, Mark 859	Sampedro-Castaneda, Marisol 266	Shabbir, Imran 348	Slabbekoorn, Hans 960	Sugira, Saiko 980
Roberts, Brock 21	Samson, Frank 127	Shackleton, Trevor M. 141,144	Slabu, Lavinia 125	Suh, Eul 96
Roberts, Patrick 111	Samuel, Erica 458	Shah, Ashish 857	Slonismky, John D. 296	Suh, Myung-Whan 808
Roberts, William 263,304	Samuels, Tina 455,458	Shaha, Steven 215	Smadja, Martine 977	Summerfield, A. Quentin 438
Robertson, Ashley P.S. 837	Sanchez, Jason 691	Shahin, Hashem 27,352	Smith, Michael E. 41,337,367	Sumner, Christian 697
Robinson, Barbara 100,934,1010	Sandulache, V.C. 975	Shalit, Ella 27	Smith, Sonya 83	Sun, Hanjun 343
Robinson, Benjamin 773	Sanes, Dan 318,509,945	Shamma, Shihab 163,942,943	Smith, Zachary 93	Sun, Hong 278
Robles, Luis 639,880	Sanford, Chris A. 646	Shang, Jia Lin 334	Smolders, Jean W.T. 702,891	Sun, Hongyu 137,690
Rocha-Sanchez, Sonya M.S. 28,49,634	Sanovich, Elena 809,911	Shannon, Robert V. 415,1008	Smotherman, Michael 116	Sun, Wei 950,952,953
Rodgers, Matthew T. 644	Santos, Felipe 824	Shapiro, Steven M. 129	Smullen, Jennifer 359	Sun, Xiao-Ming 64
Rodríguez Campos, Francisco 150,151	Santos-Sacchi, Joseph 265,369,377,382,630,995	Sharif, Sadia 842	Smythe, Nancy 907	Suneja, Sanoj K. 680
Roehm, Pamela 551	Santulli, Carlo 648	Shashanka, Madhusudana 762	Snyder, Russell L. 413,655,697,878,932,939, 1007	Surlykke, Annemarie 441
Rohbock, Karin 531	Santurette, Sébastien 969	Shaver, Mark D. 64	So, Hongseob 818	Surowitz, Joshua 223,224
Romand, Raymond 841	Saoji, Aniket 658	Shechter, Barak 154,162	Someya, Shinichi 534,813	Suzukawa, Keigo 823
Romero, Rosario 20,873	Sato, Eisuke 499	Sheih, Mengkai 430	Sone, Michihiko 811	Suzuki, Ryuji 114
Rommel, Sentiel 447	Sato, Takashi 346,817	Song, Jae-Jun 723,808	Song, Jung-whan 228,466	Suzuki, Toshihiro 596
Roof, Bryan 512	Sato, Teruyuki 340,468	Song, Lei 382,995	Songer, Jocelyn E. 638,983	Svirskis, Gytis 176
Rosen, Stuart 98,219,409,734	Satou, Minako 491	Song, Sava 792	Soto, Enrique 454,654	Svirsky, Mario 657,659,1009
Rosenhall, Ulf 222	Saul, Lucinda 98	Soucek, Garrett 28	Soucek, Sava 792	Swaminathan, Jayaganesh 112,520
Rosing, Douglas 341	Saunders, James C. 42,620,894	Sounders, Thom 544	Souza, Pamela 420	Swanson, D.J. 540
Rosner, Thomas 63	Sautter, Nathan 800	Souza, Anthony J. 658	Spahr, Patrick 474	Swiderski, Donald L. 283,320,322,571,935
Rosowski, John J. 638,641,644,983	Savino, Jessica 609	Sparto, Patrick 474	Spector, Alexander 385	Tabata, Yasuhiko 282
Rostaing, Philippe 261	Saxon, Eugene 364	Spelman, Francis 533	Spencer, Jared R. 537,917	Tabucchi, Taronne 67
Roux, Isabelle 261	Schachern, Patricia A. 361,790,914	Spencer, Linda J. 410	Spicer, Samuel S. 623,907	Tabuchi, Keiji 549,559
Rozanski, Michael T. 443	Schacht, Jochen 37,402,570,801	Shick, Elizabeth 30	Spindel, Jonathan 101	Tachibana, Ryosuke 742
		Shim, Dae Bo 201		Tadros, Sherif F. 913
				Tahera, Yeasmin 802,803
				Takahashi, Terry 693
				Takaiwa, Kazutaka 682,766
				Takaso, Hideki 732
				Takebayashi, Shinji 307,852
				Takemoto, Tsuyoshi 236,565,566,722,820,830

Takemura, Keiji 294,725	Tsuprun, Vladimir 790,914	Wang, Kevin 794	Wood, Scott 471	Yoon, Yang-soo 741
Takeno, Kenji	Tubis, Arnold 52	Wang, Ping 400,576	Woods, Charles 66	Yoon, Yongjin 76
565,566,568,722,724	Tucci, Debara L. 130,946	Wang, Qi 581,582	Woods, David 426	Yoshimoto, Momoko 276
Taketo, Makoto 523	Tucker, Andrew 296	Wang, Qiong 553	Woodward Dyrstad, Sara 819	Yoshino, Takahiko 499
Talaska, Andra 402,801	Tucker, James 781	Wang, Qiuju 793	Woolf, Nigel 485	Young, Eric D. 105,681
Talati, Ronak 270	Turcanu, Diana 62	Wang, Rong 89	Wooltorton, Julian 453	Young, Lucy 622
Talavage, Thomas	Turnbull, Daniel H. 318	Wang, Tao 427	Wotring, Helena 869	Young, Rebeccah 573
657,659,1009	Turner, Christopher 412	Wang, Xiang 23,24,329	Wouters, Jan 1006	Yu, Gonggiang 660,715
Talmdage, Carrick L. 52,55	Turner, Jeremy G. 395,923	Wang, Xiaoqin 156,158,711	Wright, Anthony 792	Yu, Heping 232,285,287
Tamayo, Rosa 654	Turner, Joyce 300	Wang, Yadong 421	Wright, Beverly A. 179,180	Yu, Hu 284,539
Tamura, Manabu 308	Tyler, Mitchell 200	Wang, Yan 468	Wright, Charles G.	Yu, Ning 19,373,394
Tamura, Tetsuya 276,827	Tzounopoulos, Thanos 249	Wang, Yong 248,687	284,539,871	Yu, Xin 318
Tan, Hongyang 970	Uemaetomari, Isao 559	Wangemann, Philine 601,795	Wright, Daniel 259	Yu, Zu-Lin 149
Tan, Justin 18,557	Ueno, Tetuko 220	Warchol, Mark E.	Wright, Tracy 521	Yuan, Huijun 343
Tan, Z. Tina 140	Ulfendahl, Mats 39,92,879	286,293,310,317	Wu, Doris K. 11,295,297	Yue, Qi 689
Tanaka, Kuniyoshi	Ulmer, John 731	332,333,864,865,874	Wu, Qingyu 18	Yuge, Isamu 491
565,566,722,830	Upile, Tao 792	Ward, Jaye 866	Wu, Shu Hui 137,690	Yund, E. William 426
Tang, Lauren 620	Urban, Zsolt 789	Ward-Bailey, Patricia 232	Wu, Tao 592	Zafar, Ahmad Usman 349
Tang, Wenxue 594,595,797	Urness, Lisa 521	Waryah, Ali 348	Wu, Xudong 23,24,273	Zakir, Mridha 7,208
Tang, Xiao-Qing 861	Vainio, Seppo 526	Washington, Jesse 539	Wys, Noel 908	Zalewski, Christopher 341
Tang, Xuehui 204	Vakharia, Kalpesh 893	Washington, Stuart 511,706	Wysocki, Lidia E. 41	Zapata, Cristobal 467
Tang, Yezhong 135,172	Valli, Paolo 776	Wasserman, Stephen I. 750	Xia, Anping 323	Zelles, Tibor 812
Tang, Yong 356	Van De Water, Thomas	Watanabe, Kensuke 931	Xian, Wei 442	Zeng, Fan-Gang 660,715,735
Tanigaki, Kenji 851	231,933,937	Watanabe, Yoshiaki	Xiang, Mengqing 854	Zettel, Martha L. 401,922
Tanokura, Masaru 534,813	van der Heijden, Marcel	439,440,497	Xie, Ruili 770	Zhang, Da-Ren 735
Tao, Ran 343	85,897	Watkins, Paul V. 161	Xoinis, Konstantine 215	Zhang, Duan Sun 313
Taranda, Julián 609	van Hoesel, Richard 97,444	Watson, Bracie 239	Xu, Chun-He 149	Zhang, Fawen 103
Tarner, Ingo 274	Van Netten, Sietse 255	Waxmonsky, Nicole 913	Xu, Jin 94	Zhang, Gehua 984
Tateossian, Hilda 20	van Wieringen, Astrid 1006	Webber, Audra 857	Xu, Ningyong 551	Zhang, Hong 984
Taylor, N. Ellen 657,659	Van Wijhe, Rene 647,650	Weber, Manfred 791	Xu, Pin-Xian 524	Zhang, Huiming 138
Teixeira, Marie 586	Vasilyeva, Olga 696	Weber, Thomas 605	Xu, Sheng 158	Zhang, J-H 268
Tekin, Mustafa 352	Vavasour, Emilie 184	Weberg, Aruna 921	Xu, Tonghui 612	Zhang, JiangPing 232
Telischi, Fred 937,988	Vazquez, Ana 612	Wefstaedt, Patrick 554,555	Xu, Youguo 204	Zhang, Jinsheng 134,765
Temchin, Andrei 639,896,992	Vega, Rosario 454	Wei, Lei 576	Xu, Zhi-Min 149	Zhang, Liqun 223,224
Tempel, Bruce 177,836	Veile, Rose 286	Wei, Ling 907	Xue, Jingbing 450	Zhang, Liyan 950,952,953
Teranishi, Masaaki 811,892	Velkey, Matt 908	Weihing, Jeffrey 212	Yabe, Daisuke 307,851	Zhang, Mei 825
Ter-Mikaelian, Maria 509	Velluti, Ricardo A. 515	Weik, Verena 964	Yagi, Masao 916	Zhang, Ming 432,433
Terry, Caitlin 330,331	Ventura, Ulderico 776	Weinberger, Norman 947	Yakovlev, Andrei 401	Zhang, Quang-An 225
Thalmann, Isolde 864	Verfaillie, Catherine 610	Weirather, Yushita 215	Yakushin, Sergei B. 207	Zhang, Xiaohui 316
Thalmann, Ruediger 864	Verhey, Jesko L. 186	Weisend, Stacy 475	Yamada, Chikako 813	Zhang, Yi 612
Thiers, Fabio A. 887	Versnel, Huib 550	Weisman, Rony 618	Yamamoto, Akira 710	Zhang, Ying 89
Thomas, Naumann 706	Vetter, Douglas	Wells, Gregg 392	Yamamoto, Hiroshi 86,811	Zhang, Ying 89
Thomas, Sharon 736	609,664,870,885,886	Wen, Bo 77	Yamamoto, Norio	Zhao, Hong-Bo 19,373,394
Thompson, Eric R. 718	Viberg, Agneta 918	Wenstrup, Jeffrey 143,691	307,851,852	Zhao, Xing 530,876
Thompson, Felisa 345	Vicente-Torres, Maria	Wenthold, Robert 317	Yamano, Takafumi 220	Zheng, Duan Sun 314
Thompson, Jerome 567,821	Angeles 37,801	Wenzel, Gentiana 323	Yamanoi, Koichi 742	Zheng, Jiefu 90,994,995
Thompson, Sarah 164	Vidal, Corina 660	Wenzel, Sören 976	Yamasaki, Aigo 236	Zheng, Jing
Thompson, Tres 512	Vieira, Mauricio 850	Werner, Lynne 182,764,965	Yamashita, Hiroshi	24,258,370,376,393
Tian, Junru 784	Viirre, Erik 465	Wesolowski, Karolina 626	236,565,566,568,722,724,	Zheng, Lili 258,547
Tian, Yong 605	Vizi, E. Sylvester 812	Westerfield, Monte 306,522	820,830	Zheng, Qing 284,539
Tiefenau, Andreas 181	Vogelheim, Casey 728	Weston, Michael D. 28,48,49	Yamashita, Toshio 916	Zheng, Qing Ying
Tillein, Jochen 95,938	Voie, Arne 357,358,363,364	Wheeler, Bruce 850	Yamasoba, Tatsuya	225,232,285,287
Timmer, Ferdinand C.A. 478	Voigt, Herbert 674	White, John 652	326,534,813,823	Zheng, Xiaohan 674
Tinevez, Jean-Yves 991	Vollmer, Maïke 655,939	White, Judith 475	Yamauchi, Daisuke 591	Zheng, Yi 151
Tobin, Sherryn E. 216,347	von Cramon, D. Yves 165,720	White, Patricia 15	Yamoah, Ebenezer	Zhou, Bin 274,486,832
Tobita, Tadamichi 559	von der Behrens, Wolfer 756	White, Perrin C. 48	598,612,613	Zhou, Guangwei 478,479
Todt, Ingo 476,798	von Kriegstein, Katharina 164	Whitley, Chester 790	Yan, Denise 285,343	Zhou, Jian 118
Tognola, Gabriella 405,1001	von Unge, Magnus 230	Whitlon, Donna S. 910	Yan, Jun 517	Zhou, Jianxun 668
Tokita, Joshua 356	Voss, Susan 67,637	Whitney, Susan 474	Yang, Guang 950,952,953	Zhou, Wu 204,919
Tokunaga, Akinori 308	Voytenko, Sergiy 143,147	Whitworth, Craig 572,805	Yang, Hua 530,876	Zhu, Hong 919
Tolnai, Sandra 110,684	Wachs, Frank-Peter 847	Wickesberg, Robert 744,745	Yang, Kuo-Hsiung 319	Zhu, Meng-Lei 373
Tomaszewska, Renata 218	Wackym, P. Ashley	Wiegrobe, Lutz	Yang, ShuZhi 343	Zhu, Saihong 278
Tomblin, J. Bruce 410	455,458,845	152,713,954,955,956,957	Yang, Sungchil 673	Zhu, Xiaomei 919
Tomlinson, R.D. 198	Wada, Tetsuro 559	Wiersinga-Post, J. Esther C.	Yang, Weiyang 343	Zhu, Xiaoxia
Tomo, Igor 92	Wagner, Hermann 119	125	Yang, Yu-Qin 602,603	396,397,401,537,913,917,
Tong, Busheng 22	Waguespack, Jessica 628	Wiet, Gregory 987	Yankova, Maya 328	920
Tong, Ling 699,944	Waixing, Tang 611	Williams, Campbell 447	Ye, Qing 938	Ziegenbein, Sylvia 634
Tornabene, Stephen 31	Wake, Melissa 216,347	Williams, Joanne 347	Yeager, Matthew S. 122	Zimmermann, Ulrike 531
Townsend, S. 873	Walker, Kerry 157	Williams, Justin 419	Yee, Kathleen 672	Zirpel, Lance 861
Trahiotis, Constantine 760	Wall, Michael 227	Williams, Tokoya 910	Yeni-Komshian, Grace 926	Zosuls, Aleks 999
Tran, Huy 326,563	Wallace, Mark 144	Wilson, Courtenay 513	Yeo, Seung Geun 974	Zou, Dan 524
Travo, Cécile 779	Wallin, Inger 585	Winer, J.A. 140	Yi, Eunyoung 903	Zou, Jing 318
Tremblay, Kelly 420	Wallrabe, Horst 270	Winter, Harald 257	Yin, Pingbo 942,943	Zou, Yuan 90
Triffo, William 381	Walsh, Edward J. 48	Winter, Ian 109	Yin, Shankai 516	Zuliani, Giancarlo 985
Trifunovic, Aleksandra 535	Walsh, Joseph T., Jr. 96	Wise, Richard J.S. 732,734	Yokota, Yoshifumi 314	Zuo, Jian
Triller, Antoine 261	Walsh, Tom 351,352	Wiseman, Paul 271	Yonekawa, H. 873	23,24,273,379,540,605,62
Tritto, Simona 776	Walton, Joseph 696	Wittig, John, Jr. 618,769	Yoo, Donald 380	2,696
Trune, Dennis	Wang, Haobing 359	Won, Jong Ho 1005	Yoo, Jin Suk 201	Zupan, Lionel H. 199
280,481,482,483	Wang, Jian 516	Wong, Patrick 496	Yoo, Tai June	Zupancic, Steven 432,433
Trussell, Larry 675	Wang, Jie 765	Wong, Weng Hoe 468	237,274,486,487,540,832	
Tsuji, Masayuki 851	Wang, Jing 562,883	Woo, Jihwan 100	Yoon, Michael 832	
Tsuji, Shigeki 559		Wood, Mark 645	Yoon, Tae Hyun 561	